



GEOLOGICAL SURVEY OF CANADA
COMMISSION GÉOLOGIQUE DU CANADA

PAPER
ÉTUDE 79-1B

This document was produced
by scanning the original publication.

Ce document est le produit d'une
numérisation par balayage
de la publication originale.

CURRENT RESEARCH
PART B

RECHERCHES EN COURS
PARTIE B



Energy, Mines and
Resources Canada

Énergie, Mines et
Ressources Canada

1979

Notice to Librarians and Indexers

The Geological Survey's thrice-yearly *Current Research* series contains many reports comparable in scope and subject matter to those appearing in scientific journals and other serials. All contributions to the Scientific and Technical Report section of *Current Research* include an abstract and bibliographic citation. It is hoped that these will assist you in cataloguing and indexing these reports and that this will result in a still wider dissemination of the results of the Geological Survey's research activities.

Avis aux bibliothécaires et préparateurs d'index

La série Recherches en cours de la Commission géologique paraît trois fois par année; elle contient plusieurs rapports dont la portée et la nature sont comparable à ceux qui paraissent dans les revues scientifiques et autres périodiques. Tous les articles publiés dans la section des rapports scientifiques et techniques de la publication Recherches en cours sont accompagnés d'un résumé et d'une bibliographie, ce qui vous permettra, nous l'espérons, de cataloguer et d'indexer ces rapports, d'où une meilleure diffusion des résultats de recherche de la Commission géologique.

Technical editing and compilation *Rédaction et compilation techniques*

R.G. Blackadar
P.J. Griffin
H. Dumych
E.R.W. Neale

Production editing and layout *Préparation et mise en page*

Leona R. Mahoney
Lorna A. Firth
Michael J. Kiel

Typed and checked by *Dactylographie et vérification*

Debby Busby
Janet Gilliland
Sharon Parnham
Susan Gagnon



**GEOLOGICAL SURVEY
PAPER 79-1B
COMMISSION GÉOLOGIQUE
ÉTUDE 79-1B**

**CURRENT RESEARCH
PART B**

**RECHERCHES EN COURS
PARTIE B**

1979

©Minister of Supply and Services Canada 1979

Available in Canada through

authorized bookstore agents
and other bookstores

or by mail from

Canadian Government Publishing Centre
Supply and Services Canada
Hull, Québec, Canada K1A 0S9

and from

Geological Survey of Canada
601 Booth Street
Ottawa, Canada K1A 0E8

A deposit copy of this publication is also available
for reference in public libraries across Canada

Cat. No. M44-79/1B Canada: \$7.50
ISBN - 0-660-10251-X Other countries: \$9.00

Price subject to change without notice

Geological Survey of Canada – *La Commission géologique du Canada*

D.J. McLAREN
Director General
Directeur général

J.O. WHEELER
Deputy Director General
Sous-directeur général

E. HALL
Scientific Executive Officer
Agent exécutif scientifique

M.J. KEEN
Director, Atlantic Geoscience Centre, Dartmouth, Nova Scotia
Directeur du Centre géoscientifique de l'Atlantique, Dartmouth (Nouvelle-Écosse)

J.A. MAXWELL
Director, Central Laboratories and Administrative Services Division
Directeur de la Division des laboratoires centraux et des services administratifs

PETER HARKER
Director, Geological Information Division
Directeur de la Division de l'information géologique

D.F. STOTT
Director, Institute of Sedimentary and Petroleum Geology, Calgary,
Directeur de l'Institut de géologie sédimentaire et pétrolière, Calgary (Alberta)

J.E. REESOR
Director, Regional and Economic Geology Division
Directeur de la Division de la géologie économique et régionale

A.G. DARNLEY
Director, Resource Geophysics and Geochemistry Division
Directeur de la Division de la géophysique et de la géochimie appliquées

J.S. SCOTT
Director, Terrain Sciences Division
Directeur de la Division de la science des terrains

ERRATUM

Current Research, Part A

Geological Survey of Canada, Paper 79-1A

New data on unnamed $\text{CaZrSi}_2\text{O}_7$ from Kipawa, Quebec;
A.G. Plant and A.C. Roberts; Paper 79-1A, p. 391.

Some of the Miller indices in Table 1 were incorrectly presented.
The correct version of the table follows.

Table 1
X-ray powder data for unnamed $\text{CaZrSi}_2\text{O}_7$ **

	I_{est}	$d_{\text{meas}}^{\text{\AA}}$	$d_{\text{calc}}^{\text{\AA}}$	hkl
*	6	5.31	5.31	110
*	4	4.59	4.58	001
*	1	4.34	4.33	020
*	2	3.79	3.79	111
*	8	3.225	3.221	111
*	10	3.151	3.148	021
*	7	3.023	3.021	201
	7	2.655	{ 2.656	220
			{ 2.654	130
	1	2.478	{ 2.479	201
			{ 2.479	221
	$\frac{1}{2}b$	2.387	2.382	131
	$\frac{1}{2}$	2.296	2.291	002
*	5	2.221	2.220	131
	$\frac{1}{2}$	2.169	{ 2.170	310
			{ 2.167	040
*	2	2.153	2.152	221
*	1	2.130	2.131	311
*	1	2.105	2.104	202
	$\frac{1}{2}$	2.027	2.025	022
	$\frac{1}{2}$	2.001	1.990	112
	$\frac{1}{2}$	1.958	1.959	041
*	3	1.892	1.893	222
	$\frac{1}{2}$	1.823	{ 1.826	311
			{ 1.821	240
	$\frac{1}{2}$	1.808	1.808	132
	$\frac{1}{2}$	1.767	1.771	330
	$\frac{1}{2}$	1.757	1.759	312
	$\frac{1}{2}$	1.746	1.749	331
*	1	1.735	1.735	202
	$\frac{1}{2}$	1.692	1.694	401
	1b	1.677	{ 1.681	400
			{ 1.679	150
*	3	1.668	1.669	132
	$\frac{1}{2}$	1.630	1.631	241
	$\frac{1}{2}$	1.610	1.611	222
	$\frac{1}{2}$	1.599	1.603	151
	$\frac{1}{2}$	1.581	1.579	421
	$\frac{1}{2}b$	1.573	1.574	042
	$\frac{1}{2}b$	1.564	1.567	420
	$\frac{1}{2}$	1.546	1.551	151

** Guinier camera, $\text{Co K}\alpha_1$ radiation ($\lambda = 1.7889\text{\AA}$).
Intensities estimated visually. Diffraction lines
belonging to apophyllite have been deleted.

b = broad line
* = lines used in unit cell refinement.
Indexed with $a = 6.869\text{\AA}$, $b = 8.667\text{\AA}$, $c = 4.681\text{\AA}$,
 $\beta = 101.82^\circ$

SCIENTIFIC AND TECHNICAL REPORTS RAPPORTS SCIENTIFIQUES ET TECHNIQUES

ECONOMIC GEOLOGY/GÉOLOGIE ÉCONOMIQUE

Metallic Mineral Deposits/Gîte minéral métallique

R.V. KIRKHAM: Copper in iron formation	17
A.J. SINCLAIR: Preliminary evaluation of summary production statistics and location data for vein deposits, Slocan, Ainsworth and Slocan City camps, southern British Columbia	173
J.W. LYDON, R.D. LANCASTER, and P. KARKKAINEN: Genetic controls of Selwyn Basin stratiform barite/sphalerite/galena deposits: an investigation of the dominant barium mineralogy of the Tea deposit, Yukon	223

Nonmetallic Mineral Deposits/Gîte minéral non métallique

R.L. CHRISTIE: Phosphorite in sedimentary basins of Western Canada	253
--	-----

Uranium/Uranium

J.A. KERSWILL and J.W. McCONNELL: The Grenville of Labrador: A possible target for uranium exploration in light of recent geological and geochemical investigations	329
---	-----

GEOCHEMISTRY/GÉOCHIMIE

B.W. SMEE and D.J. KOOP: The stability of some anions in natural water samples ...	137
Y.T. MAURICE and A.G. PLANT: Some mineralogical and geochemical characteristics of uranium occurrences in the Nonacho Lake area, District of Mackenzie	179
W.B. COKER and R.N.W. DiLABIO: Initial geochemical results and exploration significance of two uraniferous peat bogs, Kasmere Lake, Manitoba	199

GEOCHRONOLOGY/GÉOCHRONOLOGIE

V.E. CHAMBERLAIN, R. ST. J. LAMBERT, H. BAADSGAARD, and N.H. GALE: Geochronology of the Malton Gneiss Complex of British Columbia	45
---	----

GEOPHYSICS/GÉOPHYSIQUE

J.G. CONAWAY: Computer processing of gamma-ray logs: A program for the determination of radioelement concentrations	27
K.L. FORD and B.W. CHARBONNEAU: Investigation and regional significance of airborne gamma ray spectrometry patterns in the Sharbot Lake area, eastern Ontario	207
A.K. SINHA: Maxiprobe EMR-16: A new wide-band multifrequency ground E.M. system..	23

MARINE GEOSCIENCE/ETUDES GÉOSCIENTIFIQUE DU MILIEU MARIN

C.L. AMOS and K.W. ASPREY: Geophysical and sedimentary studies in the Chignecto Bay system, Bay of Fundy – a progress report	245
C.T. DALE and R.T. HAWORTH: High resolution reflection seismology studies on Late Quaternary sediments of the northeast Newfoundland continental shelf	357
E.M. LEVY: Further chemical evidence for natural seepage on the Baffin Island Shelf ...	379
B. MacLEAN and R.K.H. FALCONER: Geological/geophysical studies in Baffin Bay and Scott Inlet-Buchan Gulf and Cape Dyer-Cumberland Sound areas of the Baffin Island Shelf.....	231
R.V. WAHLGREN: Ice-scour tracks in eastern Mackenzie Bay and north of Pullen Island, Beaufort Sea	51

MINERALOGY/MINÉRALOGIE

H.J. GREENWOOD: Thermodynamic properties of edenite	365
J. RIMSAITE: Petrology of basement rocks at the Rabbit Lake deposit and progressive alteration of pitchblende in an oxidation zone of uranium deposits in Saskatchewan	281

PALEONTOLOGY/PALÉONTOLOGIE

T.E. BOLTON: Some Late Ordovician colonial corals from eastern Canada	1
H.J. HOFMANN, J. HILL and A.F. KING: Late Precambrian microfossils, southeastern Newfoundland	83
D.C. MCGREGOR: Devonian spores from the Barrandian region of Czechoslovakia and their significance for interfacies correlation	189
R.S. TIPNIS and B.D.E. CHATTERTON: An occurrence of the apparatus of " <u>Prooneotodus</u> " (Conodontophorida) from the Road River Formation, Northwest Territories	259
E.T. TOZER: Latest Triassic ammonoid faunas and biochronology, Western Canada.....	127

PETROLOGY/PÉTROLOGIE

H.L. GIBSON and D.H. WATKINSON: Silicification in the Amulet "Rhyolite" formation, Turcotte Lake section, Noranda area, Quebec	111
--	-----

QUATERNARY GEOLOGY/GÉOLOGIE DU QUATERNAIRE

Engineering and Environmental Geology Studies/Géologie de l'ingénieur et de l'environnement

J.J. CLAGUE: An assessment of some possible flood hazards in Shakwak Valley, Yukon Territory	63
A.S. DYKE: Radiocarbon-dated Holocene emergence of Somerset Island, central Canadian Arctic	307
W.A. MORRIS and J-S. VINCENT: Magnetostratigraphy of Pleistocene sediments of Banks Island, Northwest Territories: A feasibility study.....	301

Inventory Mapping and Stratigraphic Studies/Inventaire cartographique et stratigraphique

T.W. ANDERSON: Stratigraphy, age, and environment of a Lake Algonquin embayment site at Kincardine, Ontario	147
J. BÉLAND et G. VENNAT: Notes sur les groupes d'Honorat et de Matapédia dans la région de Carleton-St-Omer, Gaspésie, Québec	13
A.S. DYKE: Glacial geology of northern Boothia Peninsula, District of Franklin	385
R.C. GAUTHIER: Aspects of the glacial history of the north-central Highlands of New Brunswick	371

Paleoecology and Geochronology/Paléoécologie et géochronologie

S. LIČHTI-FEDEROVICH: Contributions to the diatom flora of Arctic Canada: Report 1. Scanning electron micrographs of some freshwater species from Ellesmere Island	71
--	----

Sedimentology and Geomorphology/Sédimentologie et géomorphologie

P.A. EGGINTON: Mudboil activity, central District of Keewatin	349
---	-----

REGIONAL GEOLOGY/GÉOLOGIE RÉGIONALE

Arctic Islands/Archipel Arctique

H.P. TRETTIN, C.R. BARNES, J.W. KERR, B.S. NORFORD, A.E.H. PEDDER, J. RIVA, R.S. TIPNIS, and T.T. UYENO: Progress in Lower Paleozoic stratigraphy, northern Ellesmere Island, District of Franklin	269
--	-----

Cordilleran Region/Région de la Cordillère

W.H. FRITZ: Cambrian stratigraphic section between South Nahanni and Broken Skull rivers, southern Mackenzie Mountains	121
W.H. FRITZ: Cambrian stratigraphy in the northern Rocky Mountains, British Columbia ..	99
L.C. STRUIK: Stratigraphy and structure of the Barkerville-Cariboo River area, central British Columbia	33

Precambrian Shield/Bouchier précambrien

A. DAVIDSON, J.M. BRITTON, K. BELL, and J. BLENKINSOP: Regional synthesis of the Grenville Province of Ontario and western Quebec	153
J. DIXON: Comments on the Proterozoic stratigraphy of Victoria Island and the Coppermine area, Northwest Territories	263
I. ERMANOVICS and M. RAUDSEPP: Geology of the Hopedale Block of eastern Nain Province, Labrador Report 1	341
A.N. LeCHEMINANT, R.W. LEATHERBARROW, and A.R. MILLER: Thirty Mile Lake map area, District of Keewatin	319
P. MORTON: Volcanic stratigraphy in the Shebandowan Ni-Cu Mine area, Ontario	39

SCIENTIFIC AND TECHNICAL NOTES NOTES SCIENTIFIQUES ET TECHNIQUES

T.A. RICHARDS and R.D. GILCHRIST: Groundhog coal area, British Columbia	411
A. OVERTON: Seismic reconnaissance survey of the Dubawnt Group, districts of Keewatin and Mackenzie	397
D.D. PICKLYK: Data entry and validation for the CANMINDEX project	401
M.L. MORRISON: Structure and petrology of the southern portion of the Malton gneiss, British Columbia	407
C.A. KASZYCKI and W.W. SHILTS: Average depth of glacial erosion, Canadian Shield ...	395
M.P. CECILE and L.D. JONES: Note on a radioactive barite sinter, Bonnet Plume map area, District of Mackenzie	416
U. MAYR and C.D.S. DE VRIES: Biostratigraphic significance of a Lower Cambrian trilobite in the Hazen Formation, Judge Daly Promontory, Ellesmere Island.....	415
S. ABBEY and others: Studies in reference samples of rocks	418
J.-L. BOUVIER and S. ABBEY: An improved method for total carbon and total water determination in rocks	417
G.R. LACHANCE: Theoretical aspects of alpha coefficients used in X-ray fluorescence analysis.....	416

DISCUSSIONS AND COMMUNICATIONS DISCUSSIONS ET COMMUNICATIONS

M. PAGEL and R.E. OPENSHAW: The paleolatitude and paleomagnetic age of the Athabasca Formation, northern Saskatchewan. Discussion	419
Note to Contributors	ix
Author Index	420

Note To Contributors

Submissions to the *Discussion* section of *Current Research* are welcome from both the staff of the Geological Survey and from the public. Discussions are limited to 6 double-spaced typewritten pages (about 1500 words) and are subject to review by the Chief Scientific Editor. Discussions are restricted to the scientific content of Geological Survey reports. General discussions concerning branch or government policy will not be accepted. Illustrations will be accepted only if, in the opinion of the editor, they are considered essential. In any case no redrafting will be undertaken and reproducible copy must accompany the original submissions. Discussion is limited to recent reports (not more than 2 years old) and may be in either English or French. Every effort is made to include both *Discussion* and *Reply* in the same issue. *Current Research* is published in January, June and November. Submissions for these issues should be received not later than November 1, April 1, and September 1 respectively. Submissions should be sent to the Chief Scientific Editor, Geological Survey of Canada, 601 Booth Street, Ottawa, Canada, K1A 0E8.

Avis aux auteurs d'articles

Nous encourageons tant le personnel de la Commission géologique que le grand public à nous faire parvenir des articles destinés à la section discussion de la publication Recherches en cours. Le texte doit comprendre au plus six pages dactylographiées à double interligne (environ 1500 mots), texte qui peut faire l'objet d'un réexamen par le rédacteur en chef scientifique. Les discussions doivent se limiter au contenu scientifique des rapports de la Commission géologique. Les discussions générales sur la Direction ou les politiques gouvernementales ne seront pas acceptées. Les illustrations ne seront acceptées que dans la mesure où, selon l'opinion du rédacteur, elles seront considérées comme essentielles. Aucune retouche ne sera faite aux textes et dans tous les cas, une copie qui puisse être reproduite doit accompagner les textes originaux. Les discussions en français ou en anglais doivent se limiter aux rapports récents (au plus de 2 ans). On s'efforcera de faire coïncider les articles destinés aux rubriques discussions et réponses dans le même numéro. La publication Recherches en cours paraît en janvier, en juin et en novembre. Les articles pour ces numéros doivent être reçus au plus tard le 1^{er} novembre, le 1^{er} avril et le 1^{er} septembre respectivement. Les articles doivent être renvoyés au rédacteur en chef scientifique: Commission géologique du Canada, 601, rue Booth, Ottawa, Canada, K1A 0E8.

Separates

A limited number of separates of the papers that appear in this volume are available by direct request to the individual authors. The addresses of the Geological Survey of Canada offices follow:

601 Booth Street,
OTTAWA, Ontario
K1A 0E8

Institute of Sedimentary and Petroleum Geology,
3303-33rd Street N.W.,
CALGARY, Alberta
T2L 2A7

British Columbia Office,
100 West Pender Street,
VANCOUVER, B.C.
V6B 1R8

Atlantic Geoscience Centre,
Bedford Institute of Oceanography,
P.O. Box 1006,
DARTMOUTH, N.S.
B2Y 4A2

When no location accompanies an author's name in the title of a paper, the Ottawa address should be used.

Tirés à part

On peut obtenir un nombre limité de "tirés à part" des articles qui paraissent dans cette publication en s'adressant directement à chaque auteur. Les adresses des différents bureaux de la Commission géologique du Canada sont les suivantes:

*601, rue Booth
OTTAWA, Ontario
K1A 0E8*

*Institut de géologie sédimentaire et pétrolière
3303 N. - O., 33rd, ST. N.W.,
CALGARY, Alberta
T2L 2A7*

*Bureau de la Colombie-Britannique
100 West Pender Street
VANCOUVER, Colombie-Britannique
V6B 1R8*

*Centre géoscientifique de l'Atlantique
Institut océanographique de Bedford
B.P. 1006
DARTMOUTH, Nouvelle-Écosse
B2Y 4A2*

Lorsque l'adresse de l'auteur ne figure pas sous le titre d'un document, on doit alors utiliser l'adresse d'Ottawa.

SCIENTIFIC AND TECHNICAL REPORTS

RAPPORTS SCIENTIFIQUES ET TECHNIQUES

1. SOME LATE ORDOVICIAN COLONIAL CORALS FROM EASTERN CANADA

Project 740084

Thomas E. Bolton
Director General's Office, Special Projects

Bolton, Thomas E., *Some Late Ordovician colonial corals from eastern Canada; in Current Research, Part B, Geological Survey of Canada, Paper 79-1B, p. 1-12, 1979.*

Abstract

The colonial corals *Favistina honoratensis* n. sp. and *Saffordophyllum* sp. A date the Honorat Group rocks of the Mount Saint Joseph area, Gaspé, Québec as Late Ordovician. The close relationship between *Palaeophyllum*, *Favistina*, and *Cyathophylloides* is demonstrated by a series of gradually developing Late Ordovician loosely fasciculate to cateniform growth forms of *Palaeophyllum vaurealensis* Twenhofel from the Vauréal Formation of Anticosti Island through tightly fasciculate colonies of *P. clion* n. sp. and cerioid *Cyathophylloides lyterion* n. sp. from the overlying Ellis Bay Formation.

1. *Favistina* and *Saffordophyllum* from the Honorat Group, Gaspé, Québec

The Honorat Group (Skidmore, 1965) as defined in the Honorat-Riboul area, southeastern Gaspé, comprises some 4.2 km. of dark grey, noncalcareous to very slightly calcareous, mudstone or argillite and siltstone. Argillaceous to silty limestone, calcareous slaty shale, coarse calcarenite and fine conglomerate are present locally. Poorly sorted sandstone and conglomerate alternate with siltstone, mudstone and slaty shale in the more easterly exposures. The Honorat sequence farther west in the Mount Saint Joseph area has been described by St. Julien et al. (1972), and Béland and Vennat (1979).

Fossils are rare in the Honorat Group, with only a few coral fragments (*Calapoecia* sp.) being reported from the greywacke unit at the base in the Mount Saint Joseph area (St. Julien et al., 1972, p. 87). M.J. Copeland and G.S. Nowlan, Geological Survey of Canada, and J.E. Béland and G. Vennat, Université de Montréal, in 1978 collected several well preserved coral colonies, some in living position, from GSC locality 96048 in a fine conglomerate near the base of the Honorat sequence exposed on the north side of the road leading to the shrine on Mount Saint Joseph north of Carleton, Québec (Béland and Vennat, 1979, fig. 2.2). The taxa *Favistina honoratensis* n. sp. and *Saffordophyllum* sp. A are described herein from these collections.

Both genera have been found in Middle and Upper Ordovician rocks of North America and U.S.S.R.; the greatest development of each was in the Late Ordovician. Such an age is suggested for the Honorat coral-bearing beds. According to G.S. Nowlan (Fossil Report 02-GSN-1979), among the few, black, fragmentary conodont specimens obtained from 2.8 kg of rock, "The representatives of *Ambalodus* and *Ligonodina*, together with a fragmentary platform element, probably constitute part of an apparatus referable to the multi-element genus *Amorphognathus* Branson and Mehl. The ligonodiniform element is reasonably well preserved and is closely similar to *L. delicata* (Branson and Mehl) s.f., and the ambalodiform element closely resembles *A. triangularis* Branson and Mehl s.f. Both these form species belong in *Amorphognathus ordovicicus* Branson and Mehl, however similar forms belong in other species of the genus of Middle and Upper Ordovician age. Earlier representatives of the genus (e.g. *A. variabilis* Sergeeva) have distinctly different ambalodiform elements.

"The representatives of *Oistodus* and *Panderodus* cannot be identified at the species level. Thus, on the basis of the elements of *Amorphognathus*, the sample is probably of Caradocian-Ashgillian age (Blackriveran-Richmondian)".

Anthozoa, Rugosa

Genus *Favistina* Flower, 1961

Type species. *Favistella undulata* Bassler, 1950

Discussion. Because of nomenclatorial confusion associated with the name *Favistella* Dana, 1846, Flower (1961, p. 77) proposed *Favistina* as a new name for the group of Ordovician colonial corals formerly included in that genus. As diagnosed by him, the taxon consists of ceroid corals with simple fibrous walls and axial plates. There are eight to ten or more major septa commonly not reaching a corallite centre, although their tips may join in small irregular groups, short but common minor septa, and generally horizontal tabulae some with edges narrowly downturned, some with slight median depressions, and some faintly arched upward. In addition to the type species *Favistina undulata* (Bassler) (a junior synonym of *F. stellata* (Hall) by Browne, 1965), Flower included in *Favistina* the other Middle Ordovician species *F. discreta* (Foerste), *F. minima* (Foerste), *F. minor* (Bassler), *F. paleophylloides* Flower and the Late Ordovician species *F. calicina* (Nicholson), *F. crenulata* Flower, *F. magister* (Bassler), *F. stellaris* (Wilson) and *F. stellata* (Hall). He indicated that although there was some degree of intergradation between *Favistina* and *Cyathophylloides*, the two were better retained as distinct genera.

Cyathophylloides Dybowski, 1873 was reserved by Flower (1961) for those cerioid corals with simple fibrous walls and axial plates, twelve or more major septa that join and slightly twist at a corallite centre, long minor septa, and upward arching tabulae. In addition to the type species *C. kassariensis* Dybowski, Flower included in *Cyathophylloides* the Late Ordovician form *C. burksae* Flower. Browne (1965) recognized within the Richmond Group of north-central Kentucky two species that had features common to both *Cyathophylloides* and *Favistina*, and accordingly retained only the former genus, describing an additional species *C. wellsi* Browne. This new species was subsequently considered by Jull (1976, p. 458) as synonymous with *F. calicina* (Nicholson) following the establishment of a lectotype for that species. In a review of blastogeny in Paleozoic rugose corals (Fedorowski and Jull, 1976, p. 55, 58), corallite development through lateral increase was described for *F. stellata* and *F. calicina*.

The retention of both genera as distinct taxa is advocated in the present study. Cerioid corals with tabulae edges narrowly downturned and major septa not uniting at the centre of a corallite are included in the genus *Favistina*. The length of the major septa range from short, extending halfway or slightly more to the centre (*F. stellata*: Pl. 1.1, fig. 6; Pl. 1.2, fig. 5) to longer, extending close to the axis with some uniting of septal tips but no twisting (*F. stellata*: Pl. 1.1, fig. 3; *F. honoratensis*: Pl. 1.2, fig. 1, 2). The genus *Cyathophylloides* is restricted to those cerioid corals in which the major septa meet in the corallite centre with some fusion, and the tabulae are arched; it is essentially a Silurian taxon, but species as old as late Middle Ordovician are known. A new species common in the latest Ordovician bioherms of member 6, Ellis Bay Formation, Anticosti Island, Québec, is described in the second part of this note. The species illustrates the morphological relationship between *Cyathophylloides*, *Favistina*, and *Palaeophyllum*. Phylogenetic relationships of these genera have been discussed by Flower and Duncan (1975, p. 176, text-fig. 1) and Ivanovsky (1969, p. 96, 97).

Favistina honoratensis n. sp.

Plate 1.1, figures 1, 2, 5, 8, 9; Plate 1.2, figures 1, 2

Coralla cerioid, with the largest colony 15 by 9 cm; corallites meandering, subpolygonal, ranging in diameter from 2.5 to 3 mm. In transverse section, walls are thick with no axial plate apparent, thinner walls slightly crenulate; 12 major septa extend nearly to the centre of a corallite, tips rarely uniting in pairs; minor septa are short but distinct, regularly present. In longitudinal section, tabulae are uniformly spaced, 8 to 10 in 5 mm corallite length, transverse with edges downturned, rarely depressed centrally.

Discussion. The Honorat form is quite distinct from the more common and widespread North American Late Ordovician species, *F. calicina* and *F. stellata* in which the corallite diameters range from 5 to 9 mm, major septa vary from 12 to 18, and tabulae are more closely spaced. The only other species with corallite diameters of 2.5 to 3 mm are *F. minor* and *F. minima* from the Middle Ordovician of Tennessee and Kentucky. The latter closely resembles a *Cyathophylloides* species according to Flower (1961, p. 74). The Lake Timiskaming, Ontario, form from the Liskeard Group assigned to *Columnaria alveolata* var. *minima* Foerste by Hume (1925, p. 60), although composed of corallites 2.5 to 3 mm in diameter, has from 15 to 18 major septa uniting in the centre and closely spaced arched tabulae. Accordingly, it is a late Middle-early Upper Ordovician *Cyathophylloides* species (hypotype, GSC 9091), but not *C. burksae* as suggested by Browne (1965, p. 1189). The other form in the Liskeard Group, *Columnaria alveolata* var. *discreta* Foerste (Hume, 1925, p. 60), was assigned by Sinclair (1961, p. 12) to *Palaeophyllum humei* Sinclair (hypotype, GSC 14597). The former species, *Favistina minor*, differs from *F. honoratensis* in that the 12 major and minor septa are short, and the tabulae are more widely spaced, 5 to 9 in 5 mm length.

Types. Holotype, GSC 61611; paratypes, GSC 61612-61619. GSC locality 96048; Honorat Group, Upper Ordovician.

Anthozoa, Tabulata

Genus *Saffordophyllum* Bassler, 1950

Type species. *Saffordophyllum deckeri* Bassler, 1950

Saffordophyllum sp. A

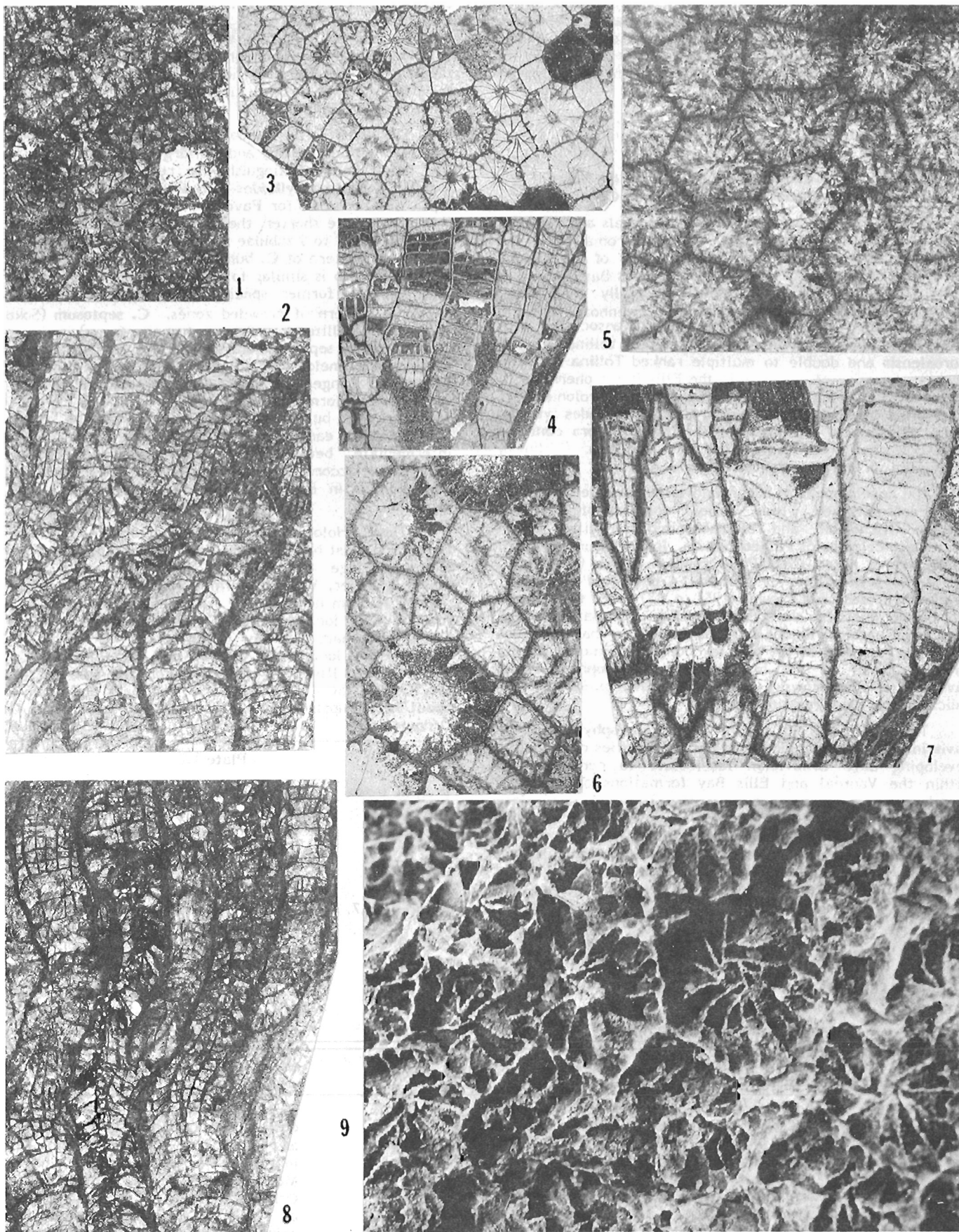
Plate 1.2, figures 3, 6, 7

Coralla cerioid, variable in size with the largest 250 by 170 mm. In transverse section, corallites are irregularly pentagonal, rarely hexagonal, 1.8 to 2.0 mm in diameter ranging from 1.6 to 2.4 mm, walls straight to slightly curved, 0.01 mm thick, undulating into short, broad, wedge-like septal spines, 14 to 17 per corallite; rare pore at corallite angle (Pl. 1.2, fig. 7). In longitudinal section, tabulae are complete, flat to slightly convex, normally 6 to 8 or 9 in 5 mm corallite length but 12 to 16 in crowded zones.

Discussion. Bassler (1950, p. 267) assigned five North American species to his new taxon (*S. deckeri*, *S. tabulatum*, *S. franklini*, *S. undulatum*, *S. kiaeri*) and Flower (1961, p. 58, 59) considered at least eight species belonged in this genus (adding *S. crenulatum*, *S. newcombae*, *S. goldfussi*). Nelson (1963) described *S. (?) portagechutense* (= *Calapoecia coxi* Bassler) relating it to *S. franklini*; Browne (1965) erected *S. floweri*; and Scrutton (1975) confirmed that *S. franklini* was not a *Saffordophyllum* and established *S. troedssoni*. Recently, Bolton (Bolton and Nowlan, in press) included *S. churchillensis* (Nelson) in the taxon. In the U.S.S.R., *S. sibiricum* Sokolov, 1955 occurs in the Upper Ordovician of the Siberian Platform, and *S. kasachstanicum* Poltavzeva, 1973 is characteristic of the Upper Ordovician of the Urals.

Plate 1.1

- Figures 1,2,5,8,9. *Favistina honoratensis* n. sp. Honorat Group, road-cut on road from Carleton to shrine on Mount Saint Joseph, Québec (GSC locality 96048).
- 1,2,8. Transverse section showing major septa extending nearly to centres of corallites, and longitudinal sections showing uniformly spaced downturned tabulae, X5. Holotype, GSC 61611.
5. Transverse section showing major septa slightly withdrawn from centres of corallites, X5. Paratype, GSC 61612.
9. Corallum surface showing variation in lengths of major septa, X14. Paratype, GSC 61613.
- Figures 3,4,6,7. *Favistina stellata* (Hall)
- 3,4. Transverse section showing major septa not quite reaching the centres of corallites and short minor septa, and longitudinal section showing flat to downturned widely spaced tabulae, X2. Georgian Bay Formation (Kagawong beds), Upper Ordovician, road-cut 6 km northwest of Kagawong Village, Manitoulin Island, Ontario. Hypotype, GSC 61620.
- 6,7. Transverse section showing major septa of varying lengths and longitudinal section showing downturned tabulae, X4. Georgian Bay Formation, Upper Ordovician, Streetsville, Ontario. Hypotype, GSC 48692.



Saffordophyllum sp. A is most nearly similar to *S. tabulatum* Bassler from the Middle Ordovician of Tennessee but the latter has 6 to 10 tabulae in 5 mm length and 18 to 20 septa. *S. churchillensis* from the Upper Ordovician of northern Manitoba differs from *S. sp. A* in the uniformly greater number of tabulae.

Types. Figured specimens, GSC 61623, 61624. GSC locality 96048; Honorat Group, Upper Ordovician.

2. *Cyathophylloides* and *Palaeophyllum* from the Vauréal and Ellis Bay formations, Anticosti Island, Québec

Well preserved rugose and tabulate corals are the most abundant faunal elements in the biostromal-biohermal complexes present in both the upper member of the Vauréal Formation and at the base of member 6, Ellis Bay Formation (Bolton, 1972, p. 5, 8). Fasciculate, locally cateniform, colonies of *Palaeophyllum vaurealensis* Twenhofel are the most dominant coral form in the Vauréal; associated with these are small colonies of subcerioid tollinaform *P. vaurealensis* and double to multiple ranked *Tollina* sp. The greatest diversity of corals is in the Ellis Bay bioherms with large hemispherical, closely fasciculate colonies of *Palaeophyllum clio* n. sp., cerioid *Cyathophylloides lyterion* n. sp., *Calapoecia anticostiensis* Billings, *Propora conferta* Milne-Edwards and Haime and *P. speciosa* (Billings), *Catenipora* sp. and *Paleofavosites* spp.

The development of subcerioid to fasciculate structures has been described within cerioid colonies of *Favistina calicina* (Nicholson) and of subcerioid corallites within fasciculate colonies of *Palaeophyllum*. In fact, Duncan (1956, Pl. 24 legend) noted that "*Palaeophyllum thomi* (Hall) from the Montoya limestone of Texas is a phaceloid version of *Cyathophylloides*" and Flower (1961, p. 88) noted that "There can be no question that *Palaeophyllum* is related to the *Favistina-Cyathophylloides* lineage; enough so that questions have been raised as to the best taxonomic treatment of these forms". Study of the blastogeny in *Palaeophyllum* and *Favistina* by Fedorowski and Jull (1976, p. 68) further indicated this close relationship.

The difficulty of separating *Palaeophyllum* from *Favistina-Cyathophylloides* is evident in a series of gradually developing Late Ordovician fasciculate to cerioid forms within the Vauréal and Ellis Bay formations of Anticosti Island. The species range from 1) simple fasciculate *Palaeophyllum vaurealensis*; to 2) complex fasciculate *P. vaurealensis* with *Tollina*-like and *Favistina*-like morphological growth forms; 3) closely packed fasciculate to rarely cerioid *Palaeophyllum clio* n. sp.; and 4) cerioid *Cyathophylloides lyterion* n. sp.

Anthozoa, Rugosa

Genus *Cyathophylloides* Dybowski, 1873

Type species. *Cyathophylloides kassariensis* Dybowski, 1873

Cyathophylloides lyterion n. sp.

Plate 1.4, figures 1, 4, 6, 7

1972. *Cyathophylloides* sp. Bolton, Pl. 3, fig. 2, 10

Coralla cerioid, rarely closely semi-fasciculate, variable in size, with the largest colony 150 mm high. In transverse section, corallites are polygonal, four to six sided, with walls straight to slightly curved, ranging in diameter from 1.5 (juvenile) to 7.5 (adult) mm with mature corallites commonly 4.5 to 5.5 mm; displaying considerable variation both within and between colonies, 16 to 18 thin, curving major septa either almost reach the centre, frequently their tips joining in groups of two or three, or actually reach the

centre of a corallite where the tips meet and twist slightly; a few pores occur in walls and/or near the corners of a corallite; minor septa are well developed, extending up to half the length of the major septa. In longitudinal section, tabulae are strongly arched, downturned at edges and frequently concave centrally, uniformly 5 or rarely 6 in 5 mm corallite length.

Discussion. The greater variability in corallite diameter within a colony and the larger number of long major and minor septa distinguish this new species from other species of *Cyathophylloides-Favistina*. A similar number of septa are recorded for *Favistina calicina*, but the septa in that species are shorter, the corallites are uniformly larger, and there are 7 to 9 tabulae present in 5 mm corallite length. The septal pattern of *C. burksae* from the Upper Ordovician of New Mexico is similar to *C. lyterion* but there are fewer septa in the former species and the tabulae display a rhythmic pattern of crowded zones. *C. septosum* (Sokolov, 1950) has corallites 4 to 8.5 mm (usually 6 mm) in diameter, 26 to 28 major septa and abundant, close tabulae, whereas *C. aktshaulicus* Smelovskaja, 1963 from the Upper Ordovician of Tarbagatai Range, southeastern Alma-Ata, Kazakhstan, has corallites uniformly 5 to 7 mm in diameter with 15 to 16 major septa but more abundant domed tabulae. *C. kiaeri* Spjeldnaes, an early Upper Ordovician species from Norway intermediate between *Cyathophylloides* and *Favistella* (= *Favistina*) according to Spjeldnaes (1964, p. 2) has corallites about 3 mm in diameter, 13 to 16 major septa, and flat tabulae.

Types. Holotype, GSC 61625 (member 4, Ellis Bay Formation, east bank Vauréal River, second bend above main highway bridge - GSC loc. 92401); paratypes, GSC 29588 (upper member, Vauréal Formation, main highway approximately 16.8 km northeast of Port Menier east of Lake Anne road - GSC loc. 36141), GSC 61626 (member 6, Ellis Bay Formation, main highway 4.8 km south of Vauréal River bridge - GSC loc. 91448), GSC 61627-61629 (member 6, south bank Salmon River 12 km upstream from mouth - GSC loc. 33642), GSC 61630 (member 6, east bank of Salmon River about 9.6 km upstream from mouth - GSC loc. 33685); Upper Ordovician.

Plate 1.2

- Figures 1,2. *Favistina honoratensis* n. sp. Transverse sections showing long major septa, X5. Honorat Group, road-cut on road from Carleton to shrine on Mount Saint Joseph, Québec (GSC locality 96048). Paratypes, GSC 61614, 61615.
- Figures 3,6,7. *Saffordophyllum* sp. A. Honorat Group, same locality as figs. 1, 2.
3. Longitudinal section showing zonation of tabulae, X5. Fig. spec., GSC 61623.
- 6,7. Longitudinal section showing regular, widely spaced tabulae, and transverse section showing undulating corallite walls and mural pore at corallite corner (upper edge), X10. Fig. spec., GSC 61624.
- Figures 4,5. *Favistina stellata* (Hall). Longitudinal section showing flat to slightly downturned tabulae and lateral budding, and transverse section showing variable length major septa, X5. Bardstown Member, Drakes Formation, Upper Ordovician, road-cut along southwest side of U.S. Highway 150, about 1.6 km northwest of Fredericktown, Kentucky, U.S.A. Hypotypes, GSC 61621, 61622.

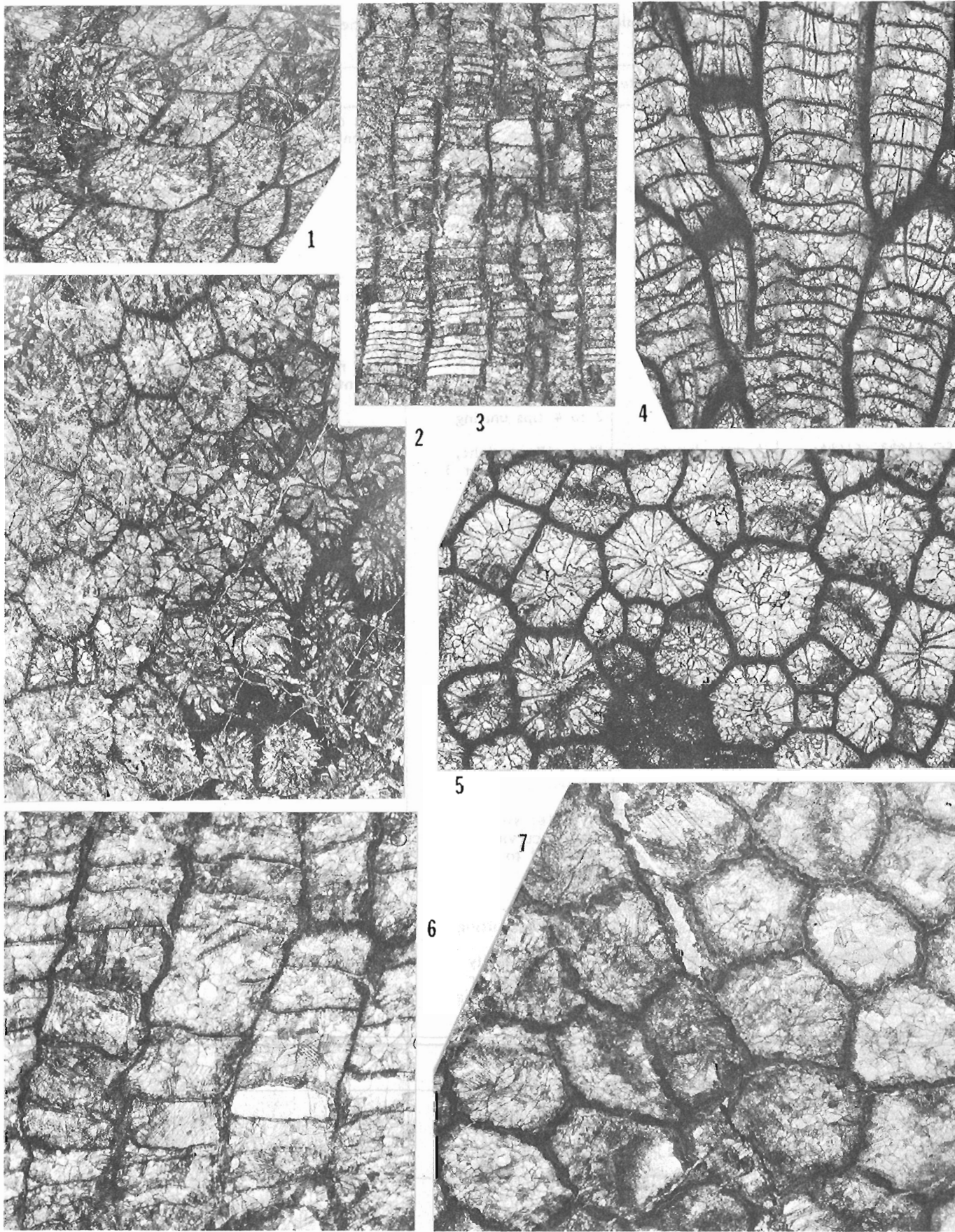


Table 1.1
Corallite-septa-tabulae features for *Palaeophyllum* species with cateniform growth

Taxon	Corallite diameter	Major septa	Minor septa	Tabulae
<i>P. vaurealensis</i> Twenhofel GSC 61631; GSC loc. 36146	1.5-2.5 mm, mainly 2 mm	13 or 14, rarely 15 or 16; straight, to centre, 2 or 3 tips uniting	short nodes when present	platformal, axial depression, 9 in 5 mm
GSC 61635; GSC loc. 36269	2-3 mm, lacunae narrow	15, rarely 13, 14 or 16; straight to curving, to centre, 2 or 3 tips uniting	short	platformal, axial depression, 8 in 5 mm
GSC 61632, 61636, 61637; GSC locs. 36146, 36313, 36262	3 mm, lacunae wide	15 to 16, rarely 13, 14, 17 to 19; straight to curving, to centre, 2 to 4 tips uniting	short to 1/4 major length	platformal, strongly arched to axial depression, 8 to 12 in 5 mm
GSC 61642, 61638, 61633; GSC locs. 36353, 36262, 36146	3-4 mm	14 to 16, with 19 maximum; straight to curving, near centre, 2 to 4 tips uniting	short nodes when present	platformal, axial depression, 8 to 10 in 5 mm
GSC 61643, 61644; GSC locs. 36157, 36329	4 mm, lacunae narrow	16 to 18; straight, near centre, 2 or 3 tips uniting	short to 1/4 major length	platformal, axial depression, 6 to 8 in 5 mm
GSC 61645; GSC loc. 33722	5 mm, lacunae narrow	17; near centre	short	platformal, axial depression, 4 in 5 mm
<i>P. halysitoides</i> (Wilson)	3-5 mm	20; very fine, to centre with slight union	1/4 to 1/2 major length	platformal
<i>P. halysitoides</i> (Troedsson)	3-6 mm	20; nearly to centre	—	platformal, 5 to 7 in 5 mm
<i>P. pasense</i> Stearn	3-4.5 mm	15; thin, just to centre, unjoined	septal ridges	arched, 7 to 8 in 5 mm
<i>P. pasense parvum</i> Stearn	1.7 to 2 mm	10; thin, straight, to centre, untwisted, unfused	septal ridges	arched, 10 in 5 mm
<i>P. radugini</i> (Cherepnina)	2.9-3, to 4 mm	14 to 16, straight to slightly curving, to centre, 2 to 3 tips uniting	very short	flat to low platformal, 4 to 6 per 5 mm
<i>P. radugini</i> Nelson	2.5-3.5 mm	16 to 18; to centre, 2 to 4 tips uniting	very short	platformal, 10 in 5 mm
<i>P. proliferum</i> Webby	2.5-5 mm, averaging 3.6- 3.9 mm	12 to 22, usually 15 to 19; to near or sometimes meeting at centre	very short	flat to platformal, axial depression, 6 to 10 in 5 mm
<i>P. humei</i> Sinclair	4-6 mm	18; thin, almost to centre	short	flat to low platformal, shallow axial depression, 6 in 5 mm
<i>P. cateniforme</i> Flower	6-9 mm	22 to 26; tips fused near centre into groups of 4	short	platformal, axial depression, 6 to 7 in 5 mm

Genus *Palaeophyllum* Billings, 1858

Type species. *Palaeophyllum rugosum* Billings, 1858

Diagnosis. As revised by Hill (1961) but with Webby's (1972) recognition of both non-parricidal and parricidal budding.

Discussion. The genus has been reviewed by Ivanovsky (1969), Webby (1972), McLean and Webby (1975), and McLean (1975; 1977). Hill (1961, p. 2) described the corallum of the type species "to be in part cerioid and in part phaceloid; in much of the corallum the corallites are in contact and polygonal through mutual pressure, but on the outside of the colony cylindrical corallites are commoner though close together". Loosely cerioid or cateniform corallites are characteristic of *P. halysitoides* (Wilson), *P. cateniforme* Flower, *P. humei* Sinclair, *P. radugini* Nelson, *P. pasense* Stearn, *P. pasense parvum* Stearn, and *P. proliferum* Webby. In the extreme development, coral forms could exist that "could be considered either as cerioid colonies in which cavities exist between many of the corallites, or as a cateniform coral in which lacunae are small and irregular, and the colony is a network of closely joined ranks" (Flower, 1961, p. 23). All such form variance is displayed by various morphological growth forms of one species, *Palaeophyllum vaurealensis* Twenhofel, collected from coral biostromes-bioherms within the upper member of the Vauréal Formation of Anticosti Island, Québec. The extreme forms could be mistaken as different species if isolated specimens were collected.

Palaeophyllum vaurealensis Twenhofel, 1928

Plate 1.3, figures 1-10

1928. *Columnaria*(?) (*Palaeophyllum*) *vaurealensis*
Twenhofel, p. 122, Pl. 4, fig. 1

1972. *Palaeophyllum vaurealensis* Twenhofel. BOLTON, Pl. 3,
fig. 6, 11

1976. *Palaeophyllum* cf. *vaurealensis* Twenhofel.
FEDOROWSKI and JULL, p. 61, Pl. 8, fig. 3a, b; Pl. 10,
fig. 1a-s; text-fig. 7, 8

1976. *Palaeophyllum vaurealensis* Twenhofel, 1928 *sensu*
Bolton, 1972. FEDOROWSKI and JULL, p. 64, Pl. 8,
fig. 4a-c; Pl. 9, fig. 1a-p; text-fig. 9

1976. *Palaeophyllum* sp. FEDOROWSKI and JULL, p. 66,
Pl. 8, fig. 5a, b; Pl. 9, fig. 2a-g; text-fig. 10

Coralla are dendroid to cateniform to tollinaform to phacelo-cerioid; holotype 75 mm wide by 95 mm high by 45 mm thick, other coralla at least 120 mm high and Twenhofel records colonies several feet in diameter; corallites sinuous, usually well spaced and cylindrical, flattening into more angular shapes where in contact with others in a single or multi-corallite chain; no suggestion of connecting processes; epitheca with strong longitudinal septal grooves and low, wide, interseptal ridges, and fine, crowded growth lines. In transverse section, corallites are round to four to five sided with walls slightly curving and crenulate when tollinaform or phacelo-cerioid, 2.9 to 3.3 mm in diameter in holotype and ranging between 2.5 and 4.4 mm in other colonies; 13 to 16 thick major septa extend into centre of a corallite with some loosely uniting and others slightly withdrawn leaving centre void; minor septa 0.2-0.4 mm long; cut tabulae (dissepiment-like) in some sections are present in one to three rows with the outermost usually occurring at the

ends of minor septa. In longitudinal section, corallites increase both as lateral offsets which rapidly attain maturity and freedom, and more rarely peripherally (Fedorowski and Jull, 1976); tabulae are abundant, thin, complete, strongly convex, forming wide platformal zones, peripherally horizontal or downturning sharply, 0.6 to 1 mm apart (6 to 8 in 5 mm corallite length).

Discussion. The major structural variations within a series of cateniform *P. vaurealensis* colonies of increasing diameter along with comparable data for other species with similar growth form is documented in Table 1.1. The major differences in the description of *P. vaurealensis* are in the growth form — Twenhofel (1928) stated that the corallites were not connected except at the places of origin whereas cateniform growth is evident even in the holotype — and the uparching of tabulae rather than sagging as believed by Twenhofel. No tertiary septa (Fedorowski and Jull, 1976) were observed during the present study.

P. vaurealensis is distinct. The closest Ordovician species, *P. radugini* Nelson (= *P. radugini* (Cherepnina, 1960)) and *P. proliferum* Webby, both have very short minor septa.

Types. Holotype, Yale Peabody Museum 20495, 'zone 6', Vauréal River; paratype, Yale Peabody Museum 7845, 'zone 12', MacDonald River; hypotypes, GSC 29592, 61643, 61645 (main highway approximately 10.4 km northeast of Port Menier — GSC locs. 36157, 33722), GSC 61631-61634 (main highway 77 km from Port Menier — GSC loc. 36146), GSC 61635 (Jupiter River road (1958) 0.8 km south of main highway — GSC loc. 36269), GSC 61636 (main highway 48 km from Port Menier — GSC loc. 36313), GSC 61637-61639 (main highway 57.6 km from Port Menier — GSC loc. 36262), GSC 61642 (Jupiter River road 76.8 km from Port Menier, 2.24 km south of main highway — GSC loc. 36353), GSC 61644 (main highway 68.8 km from Port Menier — GSC loc. 36329), GSC 61640, 61641 (second and third exposures on east bank Oil River, upriver from East Branch junction — GSC loc. 36305, 36341). Upper member, Vauréal Formation, Upper Ordovician.

Palaeophyllum clion n. sp.

Plate 1.4, figures 2, 3, 5

Coralla spherical, at least 150 mm wide and 9 mm high. In transverse section, corallites are close together, round to subpolygonal when compressed, 5.5 to 5.8 mm in diameter although mature corallites range between 5.2 and 6.5 mm; 18 or rarely 19 thin, curving major septa extend to near centre of a corallite, tips either uniting in groups of two or three or individually twisting slightly; minor septa are well developed, 0.7 mm long but ranging between 0.5 and 1.2 mm. In longitudinal section, tabulae thin, complete, flat to slightly arched with some axially depressed, 4.5 to 5 per 5 mm corallite length; reproduction through lateral increase.

Discussion. The most closely similar species to *P. clion* is the late Middle Ordovician cateniform *P. humei* which has closer and flatter tabulae and persistently shorter minor septa. Compact forms display a close relationship with the associated cerioid *Cyathophylloides lyterion*.

Types. Holotype, GSC 61646; paratypes, GSC 61647, 61648. Ellis Bay Formation, Upper Ordovician, basal bioherm member 6, north bank Salmon River 12 km upstream from mouth (GSC loc. 92404) and member 5, haulage road opposite east end of lakes north of Parkland road (GSC loc. 84368), Anticosti Island, Québec.

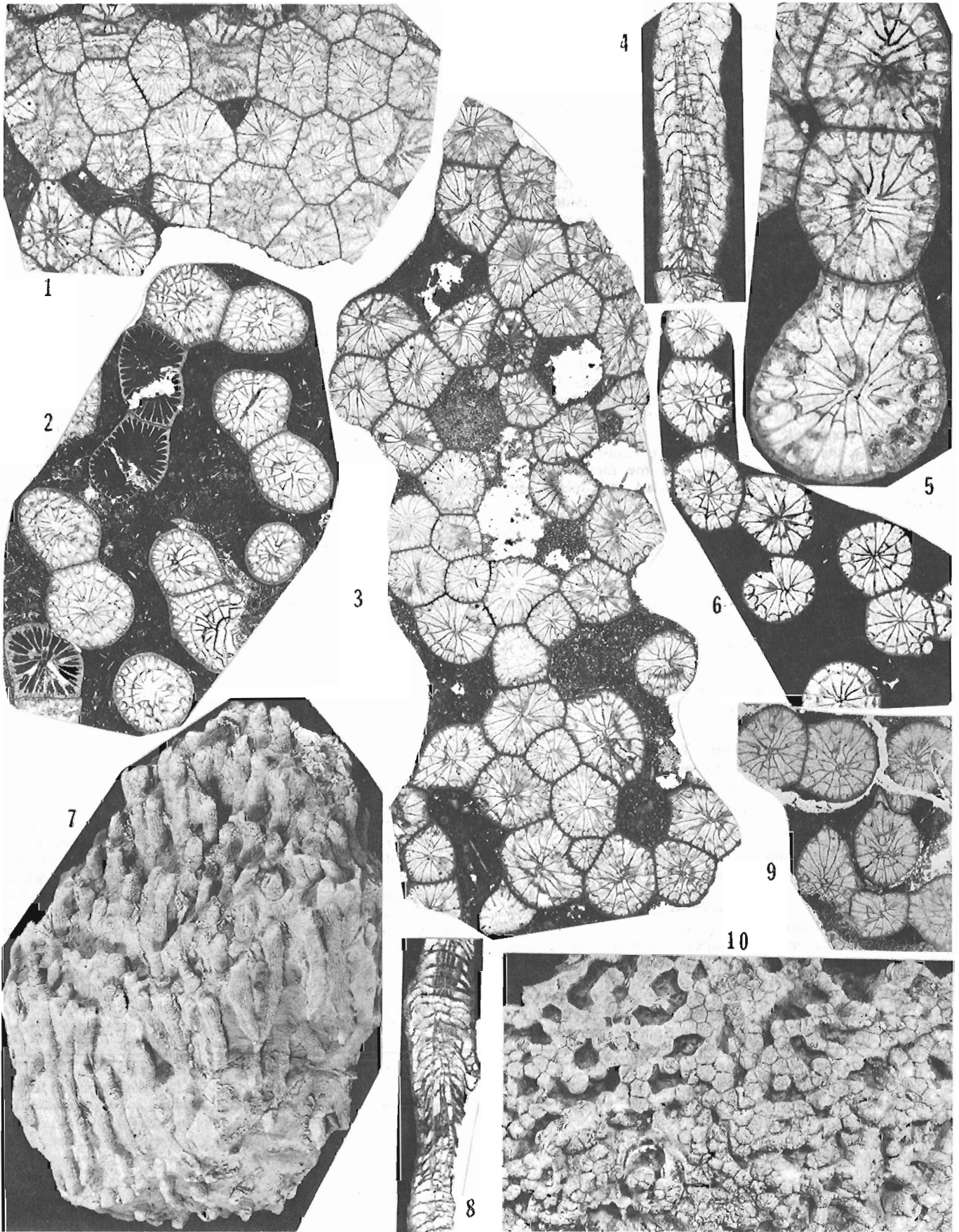


Plate 1.3

- Figures 1-10. **Palaeophyllum vaurealensis** Twenhofel. Upper member, Vauréal Formation, Upper Ordovician, Anticosti Island, Québec.
1. Transverse section displaying sub-ceriod corallite development, X4. Main highway 57.6 km from Port Menier (GSC loc. 36262). Hypotype, GSC 61639.
 2. Transverse section displaying simple cateniform growth, lacunae narrow, X4. Second exposure on east bank upriver from East Branch junction, Oil River (GSC loc. 36305). Hypotype, GSC 61640.
 - 3,10. Transverse section displaying tollinaform growth, X4, and surface of colony, X1. Same locality as figure 1. Hypotype, GSC 61638.
 - 4,9. Longitudinal and transverse sections, X4. 'Zone 12', MacDonald River. Paratype, Yale Peabody Museum 7845.
 5. Transverse section displaying loosely cateniform growth, X10. Third exposure on east bank upriver from East Branch junction, Oil River (GSC loc. 36341). Hypotype, GSC 61641.
 6. Transverse section displaying isolated and loosely cateniform growth, X4. Main highway 77 km from Port Menier (GSC loc. 36146). Hypotype, GSC 61634.
 - 7,8. Side view of colony (X1) and longitudinal section of one corallite, X4. 'Zone 6', Vauréal River. Holotype, Yale Peabody Museum 20495.

References

- Bassler, R.S.
1950: Faunal lists and descriptions of Paleozoic corals; Geological Society of America, Memoir 44.
- Béland, J.E. and Vennat, G.
1979: Notes sur les Groupes d'Honorat et de Matapédia dans la région de Carleton-St-Omer; Commission géologique du Canada, Recherche en cours, partie B, rapport 2.
- Bolton, T.E.
1972: Geological map and notes on the Ordovician and Silurian litho- and biostratigraphy, Anticosti Island, Québec; Geological Survey of Canada, Paper 71-19.
- Bolton, T.E. and Nowlan, G.S.
A late Ordovician fossil assemblage from an outlier north of Aberdeen Lake, District of Keewatin; Geological Survey of Canada, Bulletin 321. (in press)
- Browne, R.G.
1965: Some upper Cincinnati (Ordovician) colonial corals of north-central Kentucky; Journal of Paleontology, v. 39, no. 6, p. 1117-1191.
- Cherepnina, S.K.
1960: Subclass Tetracoralla (Rugosa); in Paleozoic Biostratigraphy of the Sayano-Altai Mountains, v. I Lower Paleozoic, Transactions of the Siberian Scientific Research Institute of Geology, Geophysics and Mineral Raw Materials (SNIIGGIMS) of the USSR Ministry of Geology and Conservation of Mineral Resources, no. 19, p. 387-393.
- Duncan, H.
1956: Ordovician and Silurian corals of western United States; United States Geological Survey, Bulletin 1021-F.
- Dybowski, W.N.
1873: Monographie der Zoantharia sclerodermata rugosa aus der Silur-formation Estlands, Nord-Livlands und des Insel Gotland; Dorpat, p. 257-532.
- Fedorowski, J. and Jull, R.K.
1976: Review of blastogeny in Paleozoic corals and description of lateral increase in some Upper Ordovician rugose corals; Acta Palaeontologica Polonica, v. 21, no. 1, p. 37-78.
- Flower, R.H.
1961: Part I, Montoyan and related colonial corals; New Mexico Bureau of Mines and Mineral Resources, Memoir 7, p. 3-97.
- Flower, R.H. and Duncan, H.
1975: Some problems in coral phylogeny and classification; Bulletin American Paleontology, v. 67, no. 287, p. 175-189.
- Hill, D.
1961: Part I — On the Ordovician corals **Palaeophyllum rugosum** Billings and **Nyctopora billingsi** Nicholson; Geological Survey of Canada, Bulletin 80, p. 1-7.
- Hume, G.S.
1925: The Palaeozoic outlier of Lake Timiskaming, Ontario and Quebec; Geological Survey of Canada, Memoir 145.

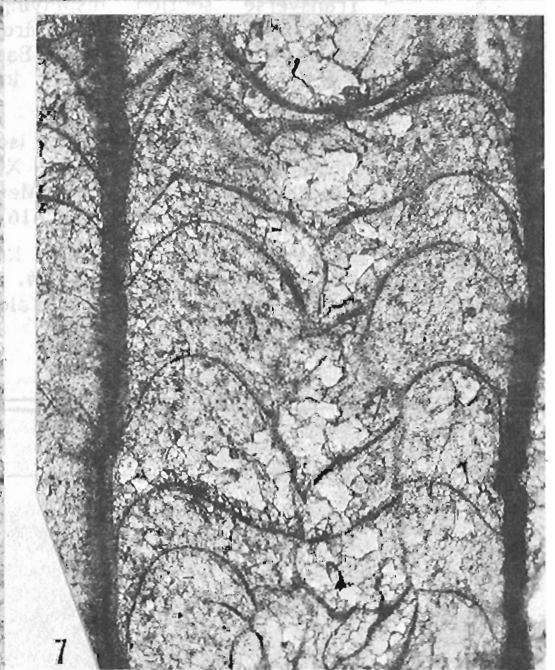
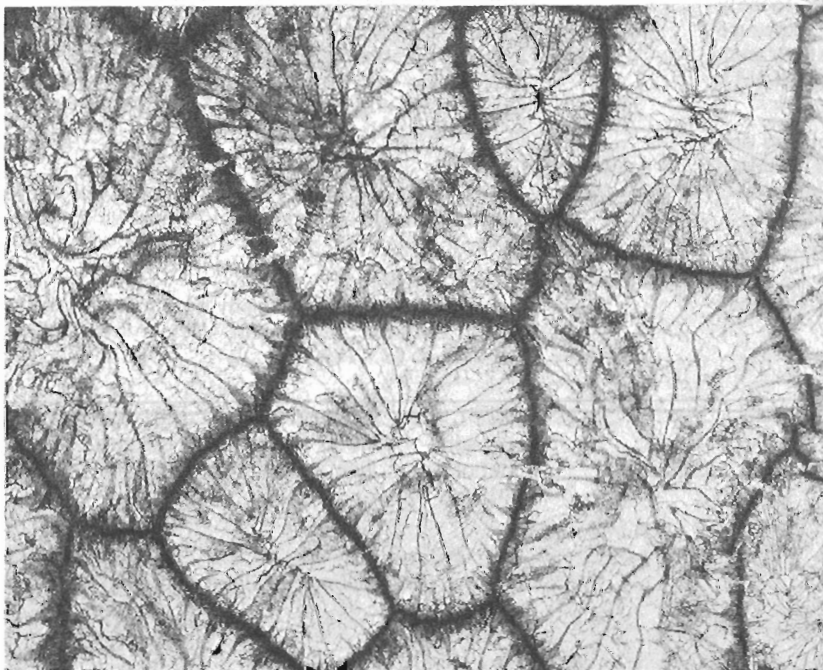
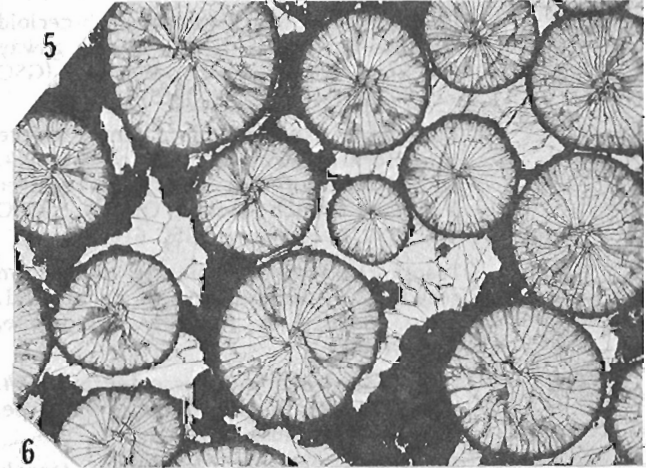
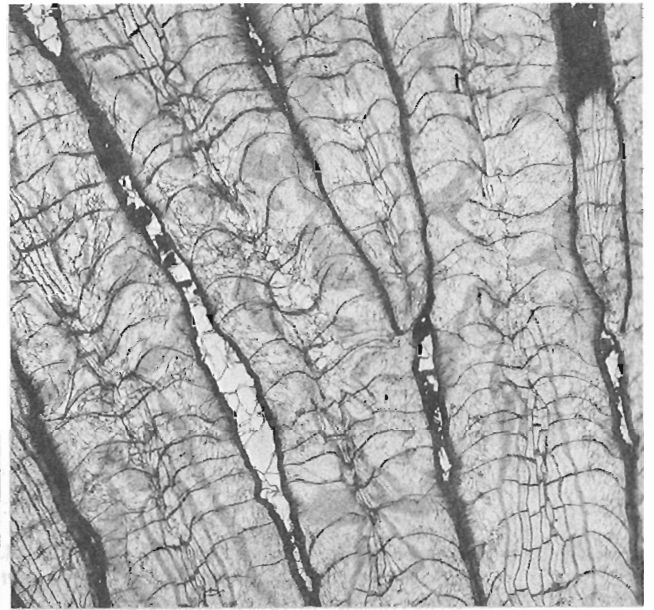
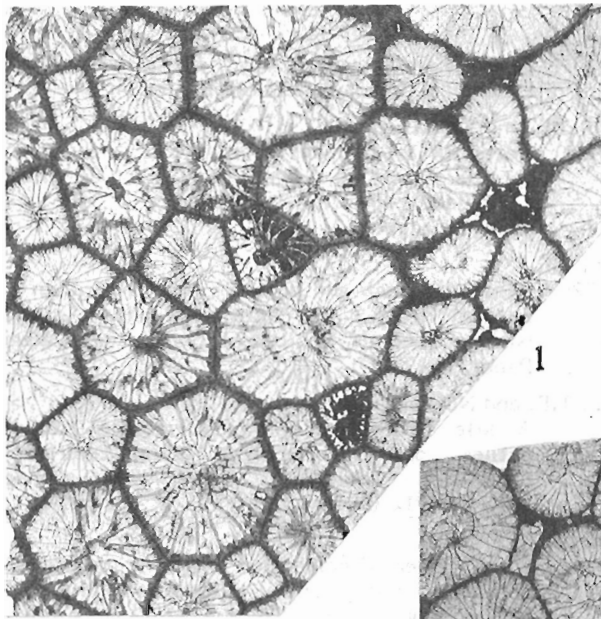


Plate 1.4

- Figures 1,4,6,7. **Cyathophylloides lyterion** n. sp. Ellis Bay Formation, Upper Ordovician.
- 1,4. Transverse and longitudinal sections displaying lateral budding, X4. Small bioherm in member 4, east bank, second bend above main highway bridge, Vauréal River (GSC loc. 92401). Holotype, GSC 61625.
6. Transverse section displaying central union of major septa, X10. Bioherm base of member 6, main highway 4.8 km south of Vauréal River bridge (GSC loc. 91448). Paratype, GSC 61626.
7. Longitudinal section displaying strongly arched tabulae with axial depression, X10. Bioherm base of member 6, south bank Salmon River 12 km upstream from mouth (GSC loc. 33642). Paratype, GSC 61627.
- Figures 2,3,5. **Palaeophyllum clien** n. sp. Bioherm base of member 6, Ellis Bay Formation, Upper Ordovician. Same locality as figure 7 (GSC loc. 92404).
- 2,5. Longitudinal section with two buds and transverse section, displaying isolated round mature corallites, X4. Holotype, GSC 61646.
3. Transverse section displaying abundant buds and crowded mature corallites, X4. Paratype, GSC 61647.

- Ivanovsky, A.B.
1969: Corals of the families Tryplasmataceae and Cyathophylloideae (Rugosa); Akademya Nauk SSSR, Sibirskoe Otdelenie Institut Geologii i Geofiziki, Moscow.
- Jull, R.K.
1976: Review of some species of *Favistina*, *Nyctopora*, and *Calapoecia* (Ordovician corals from North America); Geological Magazine, v. 113, no. 5, p. 457-467.
- McLean, R.A.
1975: Silurian rugose corals from the Mumbil area, central New South Wales; Proceedings of the Linnean Society of New South Wales, v. 99, pt. 4, p. 181-196.
1977: Early Silurian (Late Llandovery) rugose corals from western North Greenland; Grønlands Geologiske Undersøgelse, Bulletin 121.
- McLean, R.A. and Webby, B.D.
1975: Upper Ordovician rugose corals of central New South Wales; Proceedings of the Linnean Society of New South Wales, v. 100, pt. 4, p. 231-244.
- Nelson, S.J.
1963: Ordovician paleontology of the northern Hudson Bay Lowland; Geological Society of America, Memoir 90.
- Poltavzeva, N.V.
1973: New species of Ashgillian tabulates of southern Kazakhstan; Materials for the Middle Paleozoic paleontology of the Ural-Tienscham region, Collection of twelve papers on the problems of stratigraphy, no. 18, editors V.P. Sapellnikov and B.F. Chuvashkev, Transactions of the Institute of Geology and Geochemistry, USSR Academy of Science, no. 99, p. 48-53.
- St-Julien, P., Hubert, C., Skidmore, W.B., and Béland, J.
1972: Appalachian structure and stratigraphy in Quebec; XXIV International Geological Congress, Field Excursion A56-C56.
- Scrutton, C.T.
1975: Corals and stromatoporoids from the Ordovician and Silurian of Kronprins Christian Land, Northeast Greenland; Meddelelser om Grønland, v. 171, no. 4.
- Sinclair, G.W.
1961: Part II — Notes on some Ordovician corals; Geological Survey of Canada, Bulletin 80, p. 9-18.
- Skidmore, W.B.
1965: Honorat-Reboul area, Bonaventure County; Québec Department of Natural Resources, Geological Report 107.
- Sokolov, B.S.
1950: Silurian corals of the western Siberian platform; Voprosy paleontologii, Leningrad State University, v. 1.
1955: Tabulata of the Paleozoic of the European part of the USSR; Trudy Vsesoyuznogo Neftyanogo Nauchno — Issledovatel'skogo Geologo-Razvedochnogo Instituta, Novaya Seriya, v. 85.

Smelovskaja, N.M.

1963: Corals of the Upper Ordovician Subclass Tetracoralla (Rugosa); Stratigraphy and fauna of the Paleozoic deposits of the Tarbagatai Range (Ordovician, Silurian, Devonian, Lower Carboniferous), editor A.A. Bogdanov, Moscow, p. 178, 179.

Spjeldnaes, N.

1964: Two compound corals from the **Tretaspis** beds of the Oslo-Asker District; Norsk Geologisk Tidsskrift, v. 44, pt. 1, p. 1-10.

Twenhofel, W.H.

1928: Geology of Anticosti Island; Geological Survey of Canada, Memoir 154.

Webby, B.D.

1972: The rugose coral **Palaeophyllum** Billings from the Ordovician of central New South Wales; Proceedings of the Linnean Society of New South Wales, v. 97, pt. 2, p. 150-156.

Béland, J. et Vennat, G., Notes sur les groupes d'Honorat et de Matapédia dans la région de Carleton – St-Omer, Gaspésie, Québec; en Recherche en cours, partie B, Commission géologique du Canada, Etude 79-1B, p. 13-15, 1979.

Résumé

La cartographie d'une région de 100 km² sur le flanc sud-est de l'anticlinorium d'Aroostook-Matapédia, montre que le groupe d'Honorat et le groupe de Matapédia sus-jacent constituent une séquence concordante.

La transition entre les deux groupes se fait par une unité rattachée au Matapédia et qui s'apparente au faciès de Pabos de l'Est de la Gaspésie.

Près de la base de la partie visible du groupe d'Honorat, un conglomérat, dont l'épaisseur maximum est de 650 m, délimite en partie une dépression structurale.

Un relevé systématique des éléments structuraux indique qu'il y a eu au moins deux phases de déformation. A un premier plissement d'orientation nord-ouest – sud-est et sans clivage a succédé un deuxième plissement nord-nord-est – sud-sud-ouest accompagné d'un clivage bien développé.

Le Siluro-Dévonien qui appartient au groupe de Restigouche est dans la partie orientale de la région étudiée en contact de faille avec l'assemblage Honorat-Matapédia.

Introduction

La structure générale de la zone d'Aroostook-Matapédia est celle d'un anticlinorium bordé au nord-ouest par le synclinorium de Gaspé-Connecticut Valley et au sud-est par celui de la baie des Chaleurs. L'intérêt de cette zone est qu'elle est constituée de formations accumulées au moment ou peu après la déformation taconienne pré-silurienne.

Le projet en cours vise à une meilleure compréhension de la succession stratigraphique, de la structure et du lieu de provenance des diverses lithologies reconnues dans cette zone.

Au cours de l'été de 1978 les travaux de terrain ont porté sur la région de Carleton – St-Omer sise en bordure de la baie des Chaleurs (fig. 2.1). La surface cartographiée à l'échelle 1:10 000 couvre environ 100 km carrés et longe le flanc sud-est de l'anticlinorium. Elle chevauche le contact entre deux assemblages lithologiques bien distincts, l'un appartenant au groupe d'Honorat (au nord) et l'autre à celui de Matapédia (au sud).

L'objectif poursuivi était double: préciser les relations structurales et stratigraphiques entre ces deux assemblages lithologiques et déterminer le style tectonique des formations du groupe d'Honorat. On escomptait utiliser à cette fin les horizons-repères de conglomérat et de grès qui caractérisent ce dernier groupe.

Il nous était apparu, lors des travaux de l'été de 1977, concentrés le long des rivières Restigouche et Matapédia dans les formations du groupe de Matapédia (Hubert et Béland, 1978) qu'il était difficile d'arriver à un schéma tectonique élaboré en l'absence de niveaux-repères permettant de contrôler la validité des géométries obtenues à partir de mesures d'orientation de stratifications, schistosités et linéations. A ce point de vue le travail exécuté dans le groupe d'Honorat du secteur de Carleton – St-Omer a été plus fructueux même si les niveaux-repères cartographiables se sont avérés peu nombreux. Nous avons pu délimiter le contact entre les deux groupes (Honorat et Matapédia) et établir qu'il s'agissait d'une relation de concordance et en outre suivre dans l'Honorat une épaisse zone de conglomérat et quelques niveaux de grès. Grâce à ces marqueurs et un

relevé systématique de tous les éléments d'informations structurales nous avons pu établir qu'il s'agissait d'une tectonique polyphasée comprenant au moins deux plissements majeurs dont les axes sont quasiment à angle droit l'un de l'autre. Nous pensons que la forme lobée de l'affleurement d'Honorat telle que délimitée sur la carte de McGerrigle et Skidmore (1967) est grandement contrôlée par la disposition de ces axes de plissement.

Stratigraphie

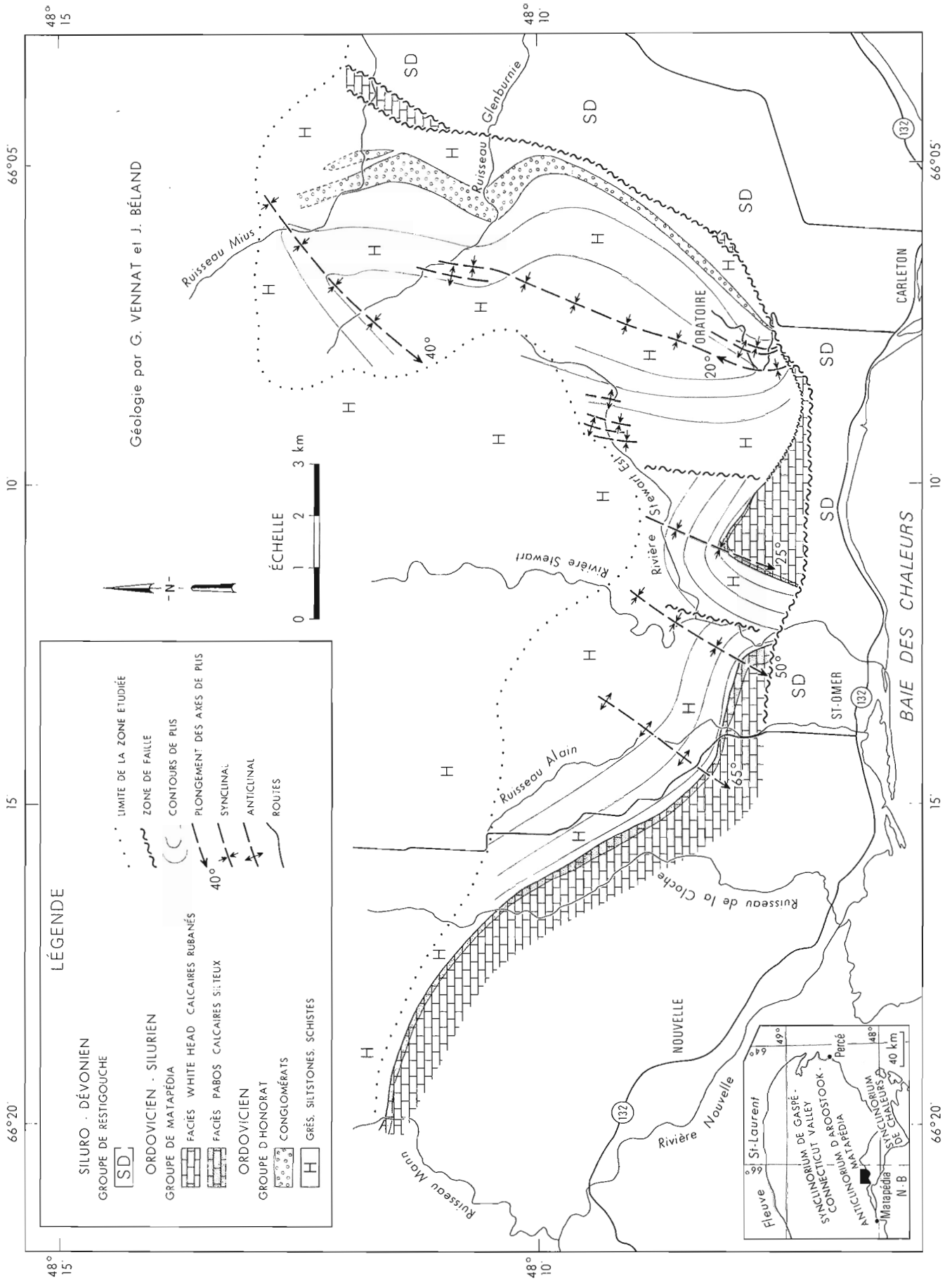
L'utilisation des noms de groupe d'Honorat et groupe de Matapédia que nous faisons dans ce texte est conforme à celle de Skidmore (1965). Honorat désigne l'assemblage de conglomérat, grès et pélites sous-jacents aux roches calcaires regroupées sous le terme Matapédia. Dans le groupe de Matapédia nous avons reconnu deux faciès appelés "Pabos" et "Whitehead" conformément à la nomenclature de Kindle (1936). Diverses données paléontologiques antérieures donnent un âge ordovicien supérieur (Ashgillien) et silurien inférieur (Llandovérien) au Matapédia. L'âge du groupe d'Honorat plus incertain se situerait entre l'Ordovicien moyen (Caradocien?) et l'Ashgillien. On ne sait pas encore très bien sur quoi reposerait l'Honorat.

Le groupe d'Honorat

Le groupe d'Honorat dans la région de Carleton – St-Omer est un assemblage de turbidites bien caractérisées allant du conglomérat grossiers à la fine pélite.

Les pélites, qui prédominent sont généralement noires laminées et par endroit fortement calcaires. Elles contiennent même parfois quelques niveaux calcaires. Le conglomérat et les grès sont étroitement associés et affleurent surtout dans la partie est du secteur cartographié. Le conglomérat en particulier forme une épaisse zone sinieuse que l'on peut suivre sur une dizaine de kilomètres depuis la route de l'oratoire (angle sud-est de la carte). L'épaisseur maximum est d'environ 650 m. Cette zone de conglomérat, localement très grossier et constitué en grande partie de matériel volcanique, se situe près de la base de l'Honorat cartographié mais repose sur d'autres pélites ou

¹Département de géologie, université de Montréal, C.P. 6128, Montréal, Québec. H3C 3J7.



semi-pélites assez semblables à celles situées au-dessus du conglomérat. Les pélites sous-jacentes s'aboutent contre une faille les mettant en contact avec les formations volcano-sédimentaires siluro-dévonienne appartenant au synclinorium de Chaleurs.

Le groupe de Matapédia

Nous avons pu reconnaître dans le groupe de Matapédia deux faciès distincts que nous avons appelés "Pabos" et "Whitehead" à la suggestion du Dr. W.B. Skidmore qui étudie présentement ces faciès dans la région de Percé et les environs (l'Est de la Gaspésie).

Dans le secteur de Carleton — St-Omer le faciès "Pabos" constitué principalement de siltstones calcaires finement lités se situe entre l'Honorat et des calcaires rubanés du type attribué au "Whitehead". Le tout forme une succession graduée et concordante indiquant un changement rapide du milieu de sédimentation. Le faciès "Pabos" ne dépasse que rarement quelques dizaines de mètres d'épaisseur.

Le "Whitehead" en plus des calcaires rubanés contient tout aussi typiquement des lentilles de grès calcaires à débris organiques et des niveaux restreints de shale calcaireux.

Structure

Le grain tectonique prédominant, c.-à-d., la direction des axes de plis, est dans la partie est de la carte nord-nord-est — sud-sud-ouest mais, dans la partie ouest, il est nord-ouest — sud-est. La schistosité par contre, de direction plus constante, correspond assez bien aux plans axiaux des plis nord-nord-est — sud-sud-ouest ce qui laisse entendre que le plissement de direction nord-nord-est — sud-sud-ouest est superposé à un plissement antérieur d'orientation nord-ouest — sud-est. Les plis de deuxième phase (nord-nord-est — sud-sud-ouest) sont serrés, droits et en partie tronqués par des failles ou zones de failles directionnelles. L'épaisse zone de conglomérat affleure sur le flanc d'une structure

synclinale ayant l'allure d'une dépression tectonique. Vers l'ouest les plis nord-nord-est — sud-sud-ouest s'estompent et le contact entre les deux assemblages lithologiques (Honorat et Matapédia) plonge abruptement vers le sud-ouest. Nous attribuons ce plongement au plissement antérieur.

Le contact entre les formations volcano-sédimentaires siluro-dévonienne et les unités sous-jacentes (Honorat et Matapédia) doit être, dans la partie sud-est du secteur étudié, un contact de faille. Nous avons interprétés les petites plages de Matapédia, apparaissant le long de ce contact, comme des écaillés coincées le long d'une cassure majeure. D'autres travaux (Bourque, 1975) ont déjà établi que ce même siluro-dévonien ou l'équivalent repose ailleurs en concordance sur le groupe de Matapédia.

Références

Bourque, P.A.

1975: Stratigraphie du Silurien et du Dévonien de l'Est de la Gaspésie, Complexe de la baie des Chaleurs; min. Rich. nat., Qué., Rapport prélim., D.P. 315.

Hubert, C. et Béland, J.

1978: Stratigraphy of the Upper Ordovician-Lower Silurian sequence in the Aroostook-Matapédia anticlinorium, Gaspé Peninsula, Québec; in Current Research, Part B, Geol. Surv. Can., Paper 78-1B, p. 89-90.

Kindle, C.H.

1936: A geological map of southeastern Gaspe; The Eastern Geologist No. 1.

McGerrigle, H.W. et Skidmore, W.B.

1967: Carte géologique, Péninsule de Gaspé; min. Rich. nat., Qué., carte n°. 1642.

Skidmore, W.B.

1965: Région d'Honorat-Reboul, Cté Bonaventure; min. Rich. nat., Qué., Rapport géol. 107.

Kirkham, R.V., *Copper in iron formation; in Current Research, Part B, Geological Survey of Canada, Paper 79-1B, p. 17-22, 1979.*

Abstract

Chalcopyrite is a conspicuous component of some oxide-sulphide-silicate facies iron formations that occur in mafic volcanic terranes. Although these occurrences have not been important sources of copper, the environment and processes of ore formation are such that large amounts of copper and/or other base and precious metals might have been concentrated in this type of deposit.

Cupriferous iron formations are probably products of submarine, volcanic exhalative activity. Most known occurrences are conformable, well bedded, and probably were deposited at some distance from their exhalation vents. Exhalative, feeder alteration zones under or near known deposits have not been recognized but with some searching they eventually may be found at some localities.

Introduction

Most major iron formations¹ of the world do not contain important amounts of copper or other base metals and no significant copper production has come from bedded iron formation. Nevertheless, interesting amounts of copper occur in some iron formations and conceivably significant copper and other base metal production might eventually be obtained from them. In this report some occurrences in Canada are described briefly and aspects of their genesis and possible economic potential are discussed.

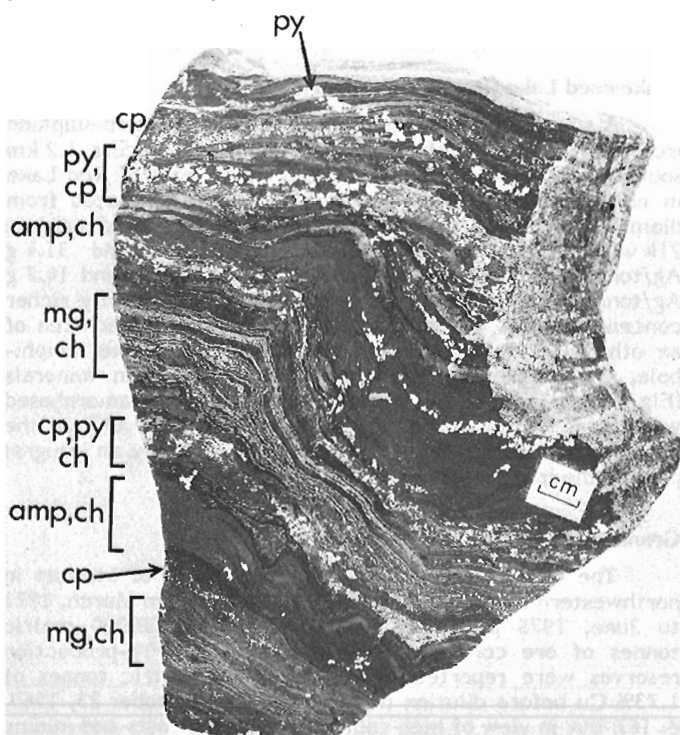
Exploration for volcanogenic base-precious metal deposits in Canada has been concentrated on the poly-metallic, massive sulphide deposits that occur in felsic parts of submarine volcanic piles (i.e., "Noranda"-or "Kuroko"-type) (see Hutchinson et al., 1971; Sangster, 1972; Hutchinson, 1973; and Sangster and Scott, 1976). At many localities this type of deposit has thin iron and/or manganese formation overlying or laterally equivalent to the massive sulphides (e.g., Brown et al., 1960; and Sangster and Scott, 1976, Manitouwadge area; Watson and Sangster, 1977, Eastern Townships; and Davies, 1972, Bathurst Camp) but the base metal ore does not occur directly in the bedded iron formation. Exploration models for these base metal sulphide deposits are well documented but little attention has been given to those occurrences where the base metals are an integral part of iron formation. The general nature and setting of these occurrences are sufficiently different from typical "Noranda"-type deposits to suggest that the environments and processes of ore deposition were not the same and that, therefore, other criteria should be established for exploration and evaluation of these deposits.

Copper, zinc, and lead are reported to occur in minor amounts in iron formation in many parts of the Canadian Shield but because the writer's studies have been directed towards copper deposits and because the occurrences examined contain negligible amounts of sphalerite and galena, the discussions in this paper are weighted heavily towards copper.

J.M. Franklin kindly read this paper and made many useful comments.

Pacaud Township, Ontario

Near Boston Creek in Pacaud Township about 20 km southeast of Kirkland Lake, two thin, 1 m- to 3 m-thick, bedded, cherty magnetite iron formation units with pyrite and chalcopyrite have been traced intermittently approximately 4 km along strike (Lawton, 1959, p. 24). The iron formation is in the Pacaud Tuff which Ridler (1970) stated is at the base of the volcanic succession in the Kirkland Lake area. Lawton (1959) suggested that these tuffs are felsic but Ridler (1970; and pers. comm., 1978) indicates that they are basaltic. According to Bell (1929), Lawton (1959), and Savage (1964) shafts were sunk and small amounts of copper ore were shipped from the Amity, Patterson, and Tretheway-Ossian properties in the late 1920s and narrow zones a few tens of



cp = chalcopyrite
ch = chert

mg = magnetite
py = pyrite

Figure 3.1. Typical well bedded, tuffaceous (?), cherty (recrystallized), oxide-sulphide iron formation, Amity dump, Boston Creek, Ontario. (GSC 203283-S)

¹ The generally accepted definition of an iron formation as a chemical sedimentary rock containing at least 15 per cent iron (James, 1954, p. 239) is used in this paper but it is important to point out that typical iron formation in many areas grades into similar and genetically related chemical sedimentary rocks that do not contain 15 per cent iron. Ridler (1973) and Ridler and Shilts (1974) have proposed the term "exhalite" for sediments, regardless of their composition, formed by volcanic exhalative processes.

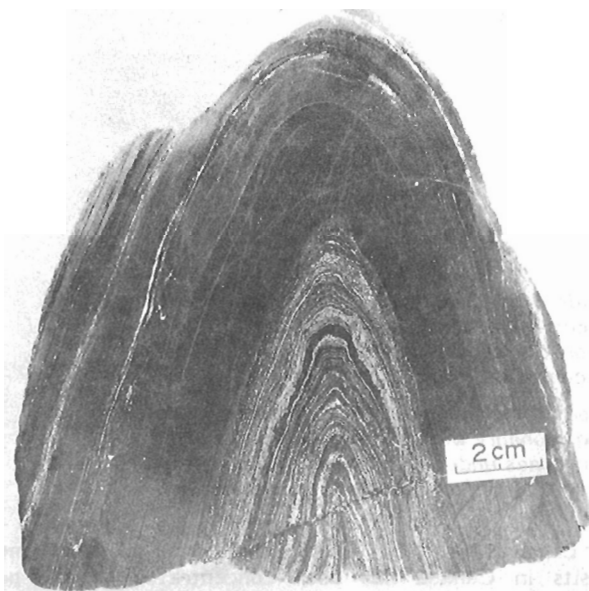


Figure 3.2. Typical folded, interbedded amphibolitic tuff (?) and chalcopyrite-pyrite-magnetite exhalite, Amity dump, Boston Creek, Ontario. (GSC 203283-L)

centimetres to a few metres thick grading several per cent copper and minor silver have been traced for a few tens of metres along strike. Although the amount of copper-bearing material that has been indicated in this area is not large, reported grades of over 1 per cent are interesting and the geological nature of the occurrences is such that, given an environment where a greater thickness of iron formation could have accumulated, sizable orebodies might have formed.

Based on megascopic examination of specimens, the main components of the iron formation appear to be bedded amphibolitic tuff (?), recrystallized chert, magnetite, pyrite, chalcopyrite, and carbonate (Fig. 3.1 to 3.4). Both chemical and volcanoclastic sedimentation were important during iron formation deposition.

Atikokan Iron Formation, Ontario

The Atikokan iron formation occurs intermittently in a 20 km-long east-west belt along the Atikokan River and under Sabawi Lake about 6 to 26 km east of Atikokan in northwestern Ontario. The main properties from east to west are the old Atikokan iron mine, Cross, Iron Lands, Archibald, Pattison Roberts, and the Hanna Mining Company Limited property.

At most localities the iron formation consists of a narrow, highly deformed and metamorphosed zone ranging from 10 to 80 m wide and containing variable amounts of magnetite, pyrrhotite, pyrite, chalcopyrite, and silicate minerals (Fig. 3.5). At some localities the iron formation is dominated by magnetite, whereas, at others it consists of essentially massive sulphides. The iron formation occurs in a belt of mafic metavolcanic rocks and minor metasedimentary rocks a few tens to a few hundreds of metres north of the Quetico fault and as a result deformation has been intense. Small bodies of amphibolitic ultramafic rocks occur near the iron formation. Grabowski (1975, p. 17) has documented extensive carbonate alteration in certain units near the old Atikokan iron mine.

About 21 800 000 metric tonnes containing approximately 35% Fe, 0.40% Cu, and low values in Ni and Co have been indicated to a depth of about 300 feet in the area. Of

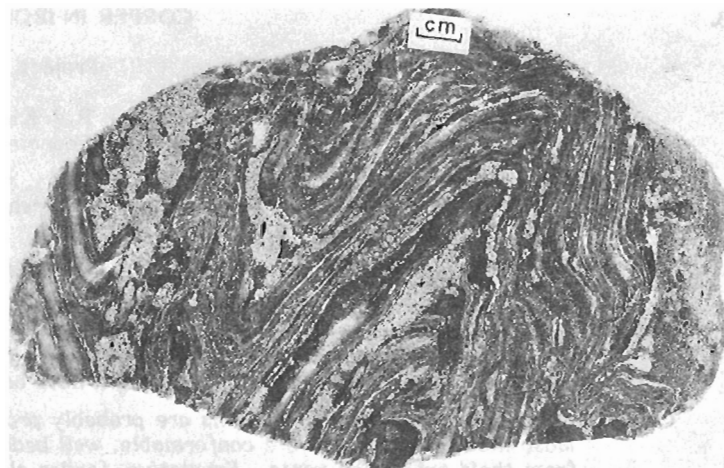


Figure 3.3. Typical folded, well bedded, chert (recrystallized)-pyrite-chalcopyrite exhalite, Amity dump, Boston Creek, Ontario. (GSC 203283-M)

this amount about 10 900 000 tonnes occur at the old Atikokan iron property, 2 725 000 on Iron Lands, 2 725 000 on Archibald, and 5 450 000 tonnes on Pattison Roberts ground (Northern Miner, October 26, 1972, p. 1 and 17). A small amount of iron ore was produced from the Atikokan mine in the early 1900s (Hawley, 1929). Although copper contents are low, the iron formation is narrow, and diamond drill data are incomplete, given the tremendous strike length of the iron formation, reasonable speculations indicate that large amounts of copper are contained in this formation.

Snakeweed Lake (Rexdale Property), Ontario

A small copper (silver) deposit in silicate-oxide-sulphide iron formation in mafic metavolcanic rocks occurs 1.2 km southeast of Snakeweed Lake, about 60 km east of Red Lake in northwestern Ontario. Archibald (1970) estimated from diamond drill information that the deposit could contain 214 480 metric tonnes containing 1.94% Cu and 31.4 g Ag/tonne or 774 742 tonnes containing 1.01% Cu and 14.7 g Ag/tonne. This small zone might represent a slightly richer concentration of chalcopyrite in a complexly folded area of an otherwise lean, thin iron formation. Magnetite, amphibole, pyrrhotite, and chalcopyrite are the main minerals (Fig. 3.6). The ore has been deformed and metamorphosed with some mobilization of chalcopyrite (Fig. 3.6) but the chalcopyrite is premetamorphic and was probably an integral part of the iron formation.

Granduc Mine, British Columbia

The Granduc Mine is about 40 km north of Stewart in northwestern British Columbia. It operated from March, 1971 to June, 1978 producing approximately 13 000 000 metric tonnes of ore containing about 1.27% Cu. Pre-production reserves were reported to be 39 320 106 metric tonnes of 1.73% Cu before dilution (Northern Miner, October 23, 1969, p. 16), but in view of high capital and mining costs and mining problems these "reserves" could not be extracted.

The geology of the area has been described by Bacon (1956), Davidson (1960), Norman (1962), Norman and McCue (1966), and Dudas and Grove (1970). The deposit consists of a number of conformable pyrite-pyrrhotite-chalcopyrite-magnetite lenses in highly deformed metasedimentary rocks near a regional contact between underlying mafic metavolcanic rocks and overlying fine grained clastic sedimentary rocks. Extensive local mobilization of sulphides occurred during regional deformation yet in many places the original

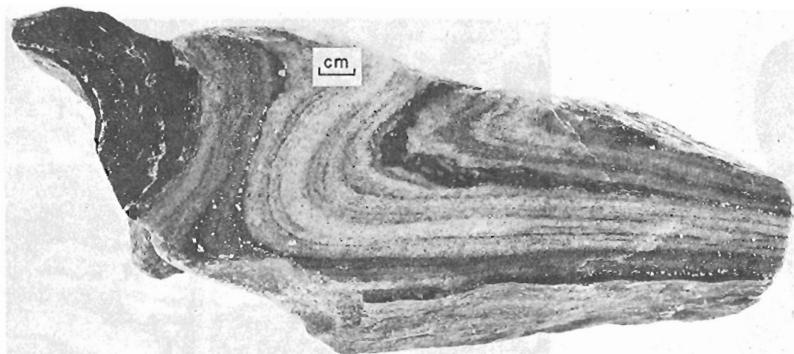


Figure 3.4. Typical folded interbedded calcite exhalite and amphibolitic tuff (?) with disseminated chalcopyrite and pyrite, Amity dump, Boston Creek, Ontario. (GSC 203283-P)

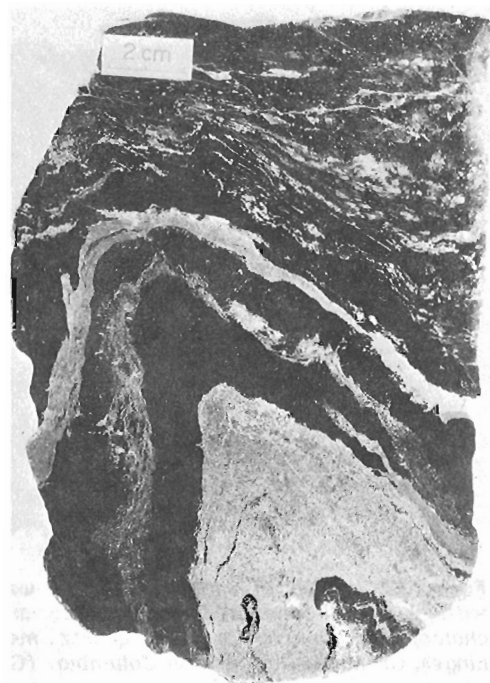


Figure 3.6. Typical, folded, interbedded amphibolitic tuff (?) and magnetite iron formation with wispy veins and disseminations of chalcopyrite and pyrite, Rexdale property, Snakeweed Lake, Ontario. (GSC 203283-I)

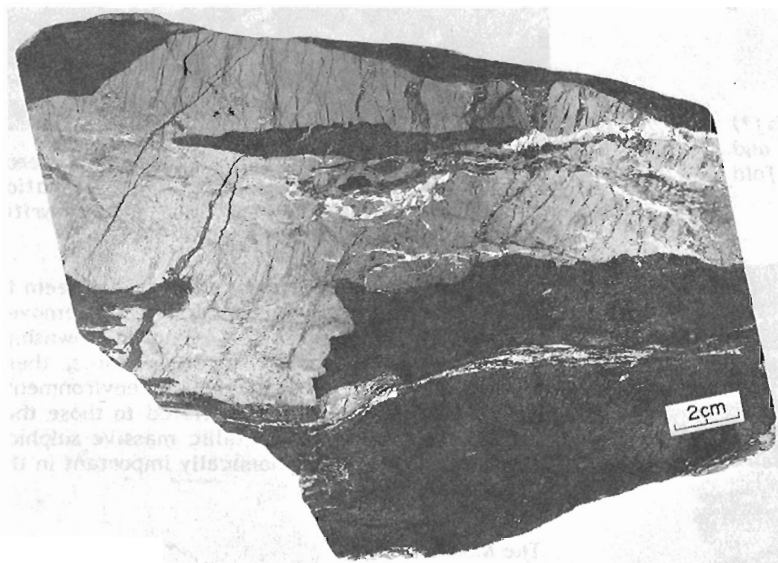


Figure 3.5. Typical, intensely deformed, interbedded amphibolite and magnetite with pyrrhotite, chalcopyrite, and pyrite in wispy and "pull-apart" veins, Atikokan iron mine, Ontario. (GSC 203283-T)

bedded nature of the ore is still apparent (Fig. 3.7 and 3.8). Amphibolitic layers in the ore, which are probably metamorphosed mafic tuff beds, suggest that volcanic activity had not stopped completely at the time of ore formation.

The mill-head iron content of the ore averaged about 12% (mine personnel, pers. comm., 1978) which is slightly low to refer to the entire deposit as an iron formation. Nevertheless, sections of the deposit graded into zones with abundant magnetite layers (Fig. 3.8) which in a traditional sense could be considered as typical bedded magnetite-sulphide iron formation. The regional distribution of bedded sulphide relative to oxide material has not been documented.

The Granduc deposit is not a typical massive sulphide deposit but rather consists primarily of thin massive and disseminated sulphide beds intricately interlayered with silicate and oxide chemical and volcaniclastic sediments. Chemical precipitation of sulphides, oxides, and other components probably took place in hot, quiescent, layered brine pools on the seafloor and was periodically interrupted by clastic sedimentation and/or volcanic eruptions.

Other Occurrences

References to minor base metal sulphide occurrences in iron formation, especially in the Superior Province of the Canadian Shield, are abundant in the literature. For instance, Thurston et al. (1977, p. 231) in reference to the Chapleau

area in Ontario, stated that 20 per cent of all known base metal and sulphide occurrences in the area are in iron formation. Thurston et al. (1977, p. 234-240) report that on the Consolidated Shunsky Mines Limited property in Cunningham township 281 313 metric tonnes of material grading 1.2% Cu and 1.3% Zn "occur over a broad area in lean, brecciated, siliceous iron formation with minor associated greywacke". Mafic metavolcanic rocks occur near the sulphides.

Pyke (1978b, p. 45) mentioned that "minor and trace amounts of copper are associated with the siliceous sulphide-bearing iron formations throughout much of English Township and the central part of Bartlett Township" south of Timmins, Ontario. Pyke (1978a, p. 29) also mentioned the presence of similar minor disseminated copper in iron formation in McArthur Township north of Bartlett Township. The writer has observed disseminated pyrite and chalcopyrite in siliceous sideritic iron formation (Fig. 3.9) in the southwestern corner of Whitney Township about 3 km south of South Porcupine, southeast of Timmins, Ontario.

Harris (1974, p. 42-43) stated that minor copper occurrences in Algoma-type iron formation are common in the Rainy Lake area of northwestern Ontario and Fenwick (1976, p. 43) stated that massive pyrrhotite, nodular pyrite, and minor chalcopyrite are associated with cherty iron formation in the Finlayson Lake area of northwestern Ontario. These examples serve to illustrate that in the Superior Province minor base metal occurrences are reasonably abundant in some Algoma-type iron formations (Gross, 1965, p. 90) or those iron formations that show an intimate association with volcanic rocks.

Discussion

Copper is not an important component of iron formation in most localities but it occurs in enough areas to suggest that under favourable conditions it can be concentrated in

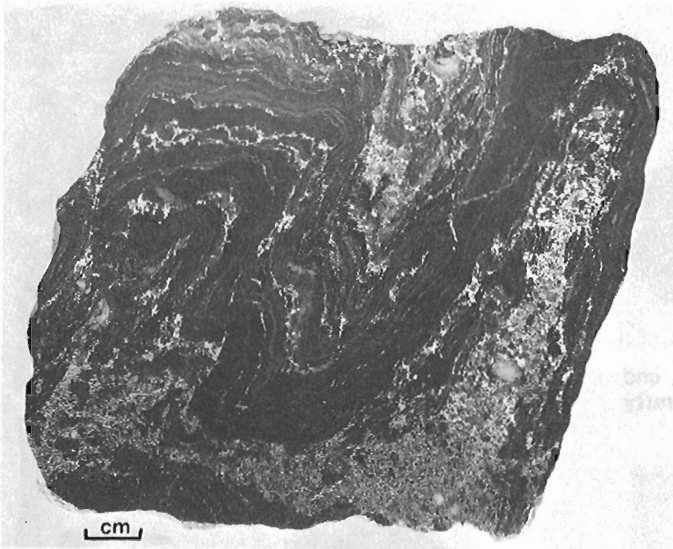


Figure 3.7. Typical, highly contorted, well bedded tuffs (?) with wispy disseminated chalcopyrite and pyrrhotite and chalcopyrite, pyrrhotite, and quartz mobilized into fold hinges, Granduc Mine, British Columbia. (GSC 201963-R)

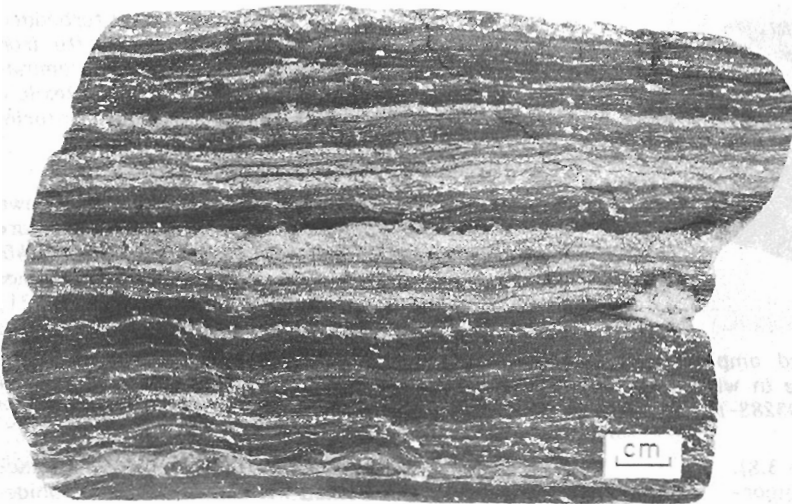


Figure 3.8. Typical interbedded amphibolitic tuff (?), chalcopyrite, pyrite, and magnetite, Granduc Mine, British Columbia. (GSC 203283-R)

some Algoma-type iron formations. Algoma-type iron formations in the greenstone belts of the Canadian Shield seem to be of two basic varieties: 1) those that occur in successions that are dominantly volcanic, and 2) those that occur in successions that are dominantly sedimentary (i.e. greywackes) (R.H. Ridler and J.M. Franklin, pers. comm., 1978). Only those that occur in successions with a high component of volcanic rocks seem to be favourable for the occurrence of copper.

The close proximity to volcanic rocks suggests that volcanic processes, such as exhalative activity, were probably important in ore genesis. Nevertheless, exhalative feeder alteration zones that would support an exhalative origin have not been recognized at any of the localities mentioned in this paper. Such feeder systems eventually may be found at some localities or they might be too far removed from the cupriferous iron formations to be demonstrated as the hydrothermal feeder systems.

In many localities cupriferous iron formations, unlike the typical polymetallic massive sulphide deposits, do not show a close association with felsic, subaqueous volcanic



Figure 3.9. Typical well bedded, siliceous (recrystallized chert), sideritic iron formation with disseminated pyrite and chalcopyrite, Whitney Township, Ontario. (GSC 202516-V)

rocks. In fact many of these occurrences seem to be well down in the volcanic piles far removed from any felsic centres (e.g., Pacaud Township, see Ridler, 1970, p. 34). In other words, these deposits have formed apparently in environments and by processes that are unrelated to those that formed the typical polymetallic massive sulphide deposits that are so economically important in the Canadian Shield.

The Model

Sato (1972) has evaluated the behaviour of brines of various temperatures and densities as they are expelled onto the seafloor. He has identified three basic types (Fig. 3.10). Type I is characterized by ore solutions that have relatively low temperature and high salinity. When the Type I ore fluid is expelled onto the seafloor it will flow down the slope because of its high salinity. The brine should become layered and remain stable for some time in the depression, where ore deposition should occur. Type II brines pass through a density maximum before they mix completely with seawater. Type IIa brine is initially more dense than seawater but as it mixes with seawater it becomes even denser and sinks below the freshly expelled solution. Type IIb brine is initially less dense than seawater but as it rises and mixes with seawater a density maximum is reached at which point it will sink to the bottom. Type III brines, which might be very hot, are less dense than seawater and continuously increase in density as they mix with seawater but never exceed its density. In this case any mineral deposition from the brine will be dispersed over a large area forming a thin blanket that conforms to the seafloor topography. Turner's and Gustafson's (1978) experimental studies indicate that submarine volcanic exhalations are probably even more complex than envisaged by Sato and they caution against the over extension of simple experimental results to complex natural situations.

Sato (1972, 1976) suggested that the "Kuroko" deposits formed from IIb brine. The typical polymetallic Cu-Zn massive sulphide deposits (i.e., "Noranda"-type), so

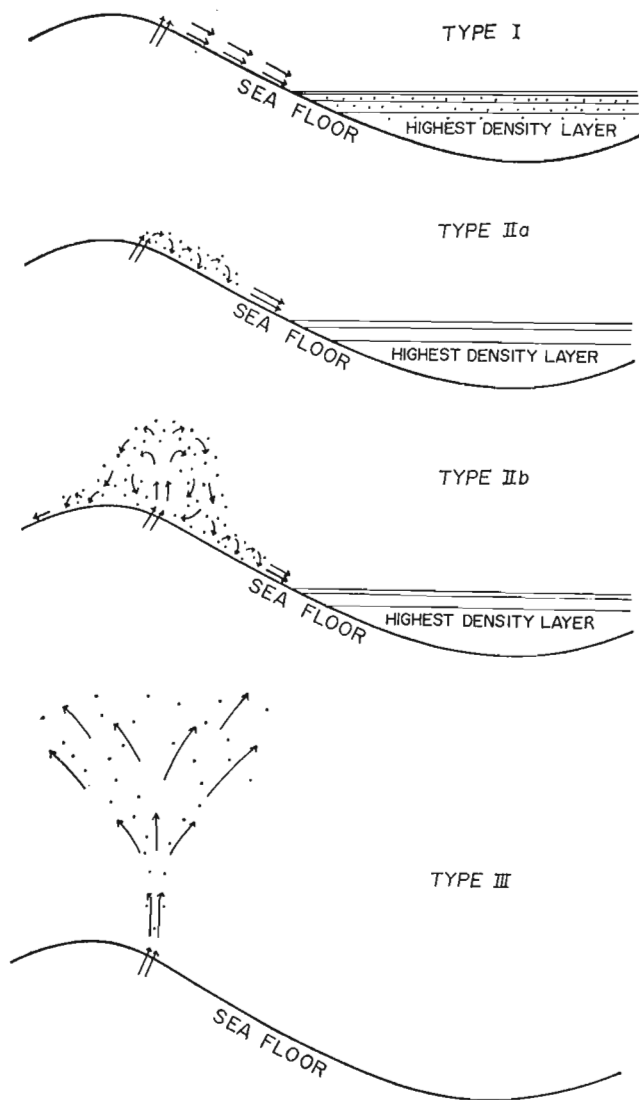


Figure 3.10. Probable behaviours of ascending ore-forming solutions welling up onto seafloor, according to four basic types of initial temperature-salinity relations. Dotted areas are sites of mineral precipitated at early stages of mixing (after Sato, 1972).

characteristic of subaqueous felsic volcanic centres of the Canadian Shield, probably also formed from this type of brine. The copper occurrences in iron formation might be products of Type I or III exhalative solutions or some even more complex exhalative process. The geological features at Granduc are permissive for chemical precipitation in paleotopographic depressions from layered brines with periodic interruption by volcanoclastic sedimentation, suggesting that this deposit might have formed from Type I brines. Sato (1976) suggested that the Red Sea deposits, Besshi-type deposits in Japan, Mt. Isa, McArthur River, Sullivan, and possibly sulphide deposits of the Bathurst Camp also formed from Type I brines. The Red Sea deposits could be reasonable modern analogues for the occurrences discussed in this paper, inasmuch as both bedded iron oxide and base metal sulphides are present (Degens and Ross, 1969; Hackett and Bischoff, 1973).

Assuming that these cupriferous iron formations formed from some sort of Type I low temperature-high density brines, Figure 3.11 illustrates a model for their formation. In Case A the brines are expelled from exhalative vents near the

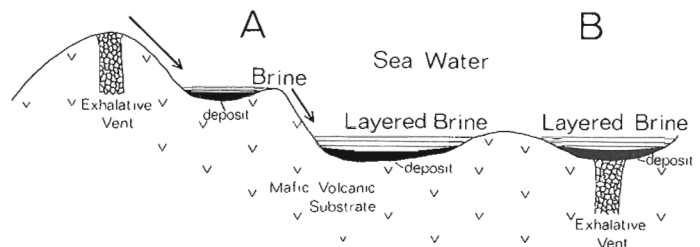


Figure 3.11. Model for the formation of volcanic-exhalative, cupriferous iron formations.

crest of a hill on the seafloor. In this case the brines would migrate to the closest depression, become layered, and mineral deposition would occur. If the depression became filled with brine, it would spill over into the next depression. Such a mechanism could lead to "decantation" of light brine and result in strong mineral zonation. In Case B the exhalative vent is in a topographic depression which, if large enough, would restrict the movement of the brine. In either case the deposits should be well bedded and should conform to the shapes of depressions. The grades and tonnages of deposits would be controlled by the morphology of the basin, the amount of brine expelled, its copper, iron and other metal content, availability of reduced sulphur, and the amount of dilution by clastic sediments and volcanic debris. Reduced sulphur might come from the ore solution or from seawater. If the exhalative activity is long-lived, the morphology of the depositional basins will change with time, perhaps as a result of volcanism, tectonism or sedimentation, giving a possible irregular en echelon pattern of ore zones.

Conclusions

Copper occurrences in certain Algoma-type iron formations are sufficiently abundant and extensive to suggest that cupriferous iron formations might eventually become economic sources of copper. These occurrences appear to be of a syngenetic, subaqueous, volcanic-exhalative origin but to have formed at times and places very different from typical polymetallic, Cu-Zn, massive sulphide deposits. At most localities they appear to be related to mafic volcanism and to occur towards the base of the volcanic sequence. Granduc, which contains some ore that could be classified as iron formation, is an exception to this rule. It occurs at the top of a thick mafic volcanic pile beneath an extensive sequence of fine grained clastic sedimentary rocks.

The environment of formation and controls on metal deposition are sufficiently different from those of many of the economically important massive sulphide deposits to suggest that quite different exploration models and methods are necessary for the discovery and evaluation of this type of deposit. Recognition of this type of occurrence as a reasonable exploration target for copper makes the extensive mafic parts of the volcanic piles in Archean greenstone belts in Canada more attractive for copper exploration.

References

- Archibald, C.W.
1970: Summary report on Copper-lode Mines Limited, Red Lake-Uchi Lake area; Ontario Department of Mines Assessment Files, 10 p.
- Bacon, W.R.
1956: The Granduc area; Canadian Mining Journal, p. 90-91.
- Bell, L.V.
1929: Boston-Skead gold-copper area, District of Timiskaming; Ontario Department of Mines, v. 37, pt. 6, p. 86-113.

- Brown, W.L., Bray, A.C.E., and Mine Staff
1960: The geology of the Geco Mine; Canadian Institute of Mining and Metallurgy, Transactions, v. 63, p. 1-9.
- Davidson, D.A.
1960: Surface geology at the Granduc Mine; unpublished M.A.Sc. thesis, University of British Columbia.
- Davies, J.L.
1972: Geology and geochemistry of the Austin Brook area, Gloucester County, New Brunswick with special emphasis on the Austin Brook iron formation; unpublished Ph.D. thesis, Carleton University, Ottawa.
- Degens, E.T. and Ross, D.A. (eds.)
1969: Hot brines and recent heavy metal deposits in the Red Sea; New York, Springer-Verlag, 600 p.
- Dudas, B.M. and Grove, E.W.
1970: Granduc Mine; in Geology, Exploration, and Mining in British Columbia, p. 67-73.
- Fenwick, K.G.
1976: Geology of the Finlayson Lake area, District of Rainy River; Ontario Division of Mines, Geoscience Report 145, 86 p.
- Grabowski, G.P.B.
1975: The geology and geochemistry of the Atikokan iron mine; unpublished B.Sc. thesis, Lakehead University, Thunder Bay, Ontario, 83 p.
- Gross, G.A.
1965: Geology of iron deposits in Canada: Volume 1 – General geology and evaluation of iron deposits; Geological Survey of Canada, Economic Geology Report no. 22, 181 p.
- Hackett, J.P., Jr. and Bischoff, J.L.
1973: New data on the stratigraphy, extent, and geologic history of the Red Sea geothermal deposits; Economic Geology, v. 68, p. 553-564.
- Harris, F.R.
1974: Geology of the Rainy Lake area, District of Rainy River; Ontario Division of Mines, Geological Report 115, 94 p.
- Hawley, J.E.
1929: Geology of the Sapawe Lake area with notes on some iron and gold deposits of Rainy River District; Ontario Department of Mines, v. 38, p. 1-58.
- Hutchinson, R.W.
1973: Volcanogenic sulfide deposits and their metallogenic significance; Economic Geology, v. 68, p. 1223-1246.
- Hutchinson, R.W., Ridler, R.H., and Suffel, G.G.
1971: Metallogenic relationships in the Abitibi belt, Canada: a model for Archean metallogeny; Canadian Institute of Mining and Metallurgy Transactions, v. 74, p. 106-115.
- James, H.L.
1954: Sedimentary facies of iron formation; Economic Geology, v. 49, p. 235-293.
- Lawton, K.D.
1959: Geology of Boston Township and part of Pacaud Township; Ontario Department of Mines, v. LXVI, pt. 5, 55 p.
- Norman, G.W.H.
1962: Faults and folds across Cordilleran trends at the headwaters of Leduc River, northern British Columbia; in Petrologic studies: a volume in honour of A.F. Buddington, Geological Society of America, p. 313-326.
- Norman, G.W.H. and McCue, J.
1966: Relation of ore to fold patterns at Granduc, B.C.: in Tectonic history and mineral deposits of the western Cordillera; Canadian Institute of Mining and Metallurgy, Special Volume 8, p. 305-314.
- Pyke, D.R.
1978a: Geology of the Redstone River area, District of Timiskaming; Ontario Division of Mines, Geoscience Report 161, 55 p.
1978b: Geology of the Peterlong Lake area, Districts of Timiskaming and Sudbury; Ontario Division of Mines, Geological Survey Report 171, 53 p.
- Ridler, R.H.
1970: Relationship of mineralization to volcanic stratigraphy in the Kirkland-Larder Lakes area, Ontario; Geological Association of Canada Proceedings, v. 21, p. 33-42.
1973: Exhalite concept a new tool for exploration; Northern Miner, November 29, p. 59-61.
- Ridler, R.H. and Shilts, W.W.
1974: Exploration for Archean polymetallic sulphide deposits in permafrost terrains: an integrated geological/geochemical technique, Kaminak Lake area, District of Keewatin; Geological Survey of Canada, Paper 73-34, 33 p.
- Sangster, D.F.
1972: Precambrian volcanogenic massive sulphide deposits in Canada: a review; Geological Survey of Canada, Paper 72-22, 44 p.
- Sangster, D.F. and Scott, S.D.
1976: Precambrian, stratabound, massive Cu-Zn-Pb sulfide ores of North America: in Handbook of strata-bound and stratiform ore deposits, v. 2, Regional studies and specific deposits; Elsevier, Amsterdam, p. 129-222.
- Sato, T.
1972: Behaviours of ore-forming solutions in seawater; Mining Geology, v. 22, p. 31-42.
1976: Origins and classification of exhalative-sedimentary mineral deposits (abstract); 25th International Geological Congress, Abstracts, v. 1, p. 187.
- Savage, W.S.
1964: Mineral resources and mining properties in the Kirkland Lake-Larder Lake area; Ontario Department of Mines, Mineral Resources Circular 3, 108 p.
- Thurston, P.C., Siragusa, G.M., and Sage, R.P.
1977: Geology of the Chapleau area, Districts of Algoma, Sudbury, and Cochrane; Ontario Division of Mines, Geoscience Report 157, 293 p.
- Turner, J.S. and Gustafson, L.B.
1978: The flow of hot saline solutions from vents in the sea floor – some implications for exhalative massive sulfide and other ore deposits; Economic Geology, v. 73, p. 1082-1100.
- Watson, D.M. and Sangster, D.F.
1977: A preliminary study of iron oxide and manganese oxide units associated with volcanogenic sulphide deposits, Sherbrooke area, Quebec; in Report of Activities, Part A, Geological Survey of Canada, Paper 77-1A, p. 13-14.

Sinha, A.K., *Maxiprobe EMR-16: A new wide-band multifrequency ground E.M. system; in Current Research, Part B, Geological Survey of Canada, Paper 79-1B, p. 23-26, 1979.*

Abstract

The Maxiprobe EMR-16 multifrequency ground electromagnetic sounding system provides 123 discrete frequencies from 1 Hz to 40 kHz with coil separations from 50 m to 1 km or more. The transmitter loop is laid on the ground along any closed-loop geometry and the receiver measures the ratio of the total vertical and the horizontal magnetic fields. The method is ideal for deep sounding over layered or quasi-layered ground.

Graphical techniques of interpreting field data have been devised which involve comparison of the field data with theoretically computed response plots in order to get some characteristic values which depend on the depth of the various interfaces. The technique has been applied to a sounding curve obtained from the Meager Creek area of British Columbia. The error in depth interpretation is usually less than five per cent whereas the error may be somewhat greater in conductivity estimates.

Introduction

Maxiprobe EMR-16 is a new multifrequency dipole-dipole ground electromagnetic sounding system that has been available to the industry since 1977. The system was originally developed by McPhar Geophysics Ltd., Toronto, for deep exploration surveys. But the initial prototype was bulky and could hardly be used for routine geophysical surveys in remote areas. After McPhar Geophysics was sold by its owners, the system was developed further by Geoprobe Ltd., Toronto. The development, which resulted in a semi-portable system was supported by the Geological Survey of Canada under a DSS Contract. The first prototype of the system, called the Maxi-Probe EMR-16¹ was ready in January 1977. As per the agreement with Geoprobe Ltd., the first prototype was delivered to the Geological Survey for research purposes.

Since then, the system has been tested and used by the author and by the staff of Geoprobe Ltd. for deep sounding over quasi-layered ground. The system has been used successfully for mapping the continuity of coal beds and bedded mineral deposits in U.S.A., for looking for geothermal resources in British Columbia, and for uranium exploration in Saskatchewan. Because most of the contract work by Geoprobe Ltd. involved proprietary data, they have been unable to publish anything on the method or its technique of interpretation.

At the Geological Survey of Canada, field studies have been carried out and theoretical investigations on the interpretation of Maxiprobe field data have been done based on layered earth models. The unit has been used over several types of terrain to understand the advantages and limitations of the system in different conditions. The present paper is devoted mainly to a description of the system and the methods of interpreting the data. A field example is also included in the paper to clarify the interpretation procedure.

Acknowledgment

The author is thankful to M.K. Ghosh of Geoprobe Ltd., Toronto, for many discussions regarding interpretation techniques and field procedures for the Maxiprobe EMR-16 System.

Maxiprobe System

The factor that distinguishes the system from most other existing geophysical sounding systems employing artificial sources is its large potential depth of penetration.

This wide-band, multifrequency ground system can use up to 123 frequencies from 1 Hz to about 40 kHz. There are 16 coarse frequency settings and for each coarse setting, there are 8 fine settings, thus making it possible to obtain a maximum of 128 discrete frequencies. However, in the present system, the five highest frequencies are not operational because they are too high for induction sounding purposes.

The large range of available frequency values enables a trained geophysicist to select the range of frequency he deems appropriate at any particular site after a preliminary test. It is feasible, therefore, to obtain a complete sounding of the ground at a station with, say, 20 to 30 frequencies which are appropriate. The separation of the transmitter and the receiver dipoles is selected after a trial survey; this may be to 1 km or more under special circumstances. The minimum coil separation is dictated by the diameter of the transmitter coil loops, which is 28 feet (8.53 m). To be sure

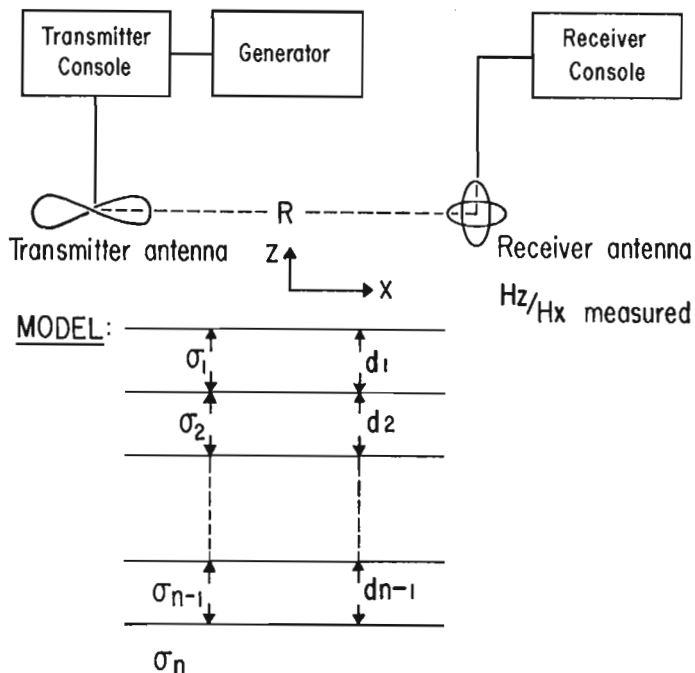


Figure 4.1. Schematic diagram of the Maxiprobe System and the multilayer earth model assumed in the interpretation of data.

¹ EMR stands for Electro Magnetic Resistivity and 16 stands for the 16 coarse frequency settings in the instrument.

that the loop sources behave as dipoles, the transmitter-receiver separation should be at least five times the diameter of the transmitter loops. Hence, a coil separation of 50 m seems to be the minimum with the present transmitter coil size. As the penetration of the wave is controlled by the conductivity of the ground, coil separation, and frequency, it is possible to probe deeper inhomogeneities by using this system by appropriate selection of coil separation and frequencies for various ground conductivity values.

Figure 4.1 shows the Maxiprobe system schematically. The generator has a 2-stroke gasoline powered engine with 2.5 kW power output. The power is fed from the generator to the transmitter loops via the transmitter console. The transmitter console is used to select the desired frequencies. The current is fed into two identical transmitter loops connected in parallel which form a figure eight as shown. The total current is divided into two parts and channelled into the two loops such that the inducing field from these loops reinforce each other. The loops with nominal diameter of 28 feet (8.53 m) are laid flat on the ground. The transmitter therefore behaves like a vertical magnetic dipole.

The receiver consists of a pair of orthogonal ferrite cored coils wound on the same frame. The coil assembly is placed inside a spherical shell which reduces the effect of wind noise and provides a convenient multi-axis orientation with respect to the gravitational vertical and the direction of the transmitter. The ball antenna is placed on a tripod stand for stability. The ball has an arrow which is pointed toward the transmitter coil and the bubble level is centred which ensures that the receiver coils are horizontal and vertical. The output from the receiver antenna is transmitted to the receiver console via about 5 m of cable. A preamplifier inside the spherical shell is used for adjusting the signals to a level and impedance suitable for transmission to the receiver console. The receiver console has the same frequency switches as the transmitter console and when they are tuned to the same frequency, the in-phase and quadrature parts of the total vertical and horizontal fields may be read from four meters in the console.

One of the advantages of this system is that there is no need for a connecting cable between the transmitter and the receiver. This simplifies field operations tremendously especially for large transmitter-receiver separations. The receiver employs a stable internal frequency source (crystal clock) and the in-phase and quadrature parts of the vertical and horizontal fields are measured with reference to this stable source. Thus, the measured in-phase and quadrature components are not absolute but relative to this stable source.

But, if the amplitudes of the fields are computed from the in-phase and quadrature components, they will be true amplitudes, so long as the internal clock remains stable. As a matter of fact, the parameter that is used in the interpretation is the ratio of the amplitudes of the vertical and the horizontal magnetic fields, i.e., $|H_z/H_x|$. Because the ratio values are used, no knowledge about the transmitter dipole moment is needed. Another advantage of the ratio measurement is that the loops may be placed on the ground in any fashion, not necessarily along any predetermined geometry. Also, in ratio measurement, information regarding the current flowing into the transmitter dipole, the pick-up factors of the receiver dipoles, or the number of turns of either coil need not be known since these factors cancel out when the ratios are taken.

Theory of the Method

The theory of the method is similar to published theories on dipole-dipole electromagnetic systems over layered earth (Frischknecht, 1967; Sinha and Collett, 1973). Let us assume that we have a vertical magnetic dipole

carrying a current $I \exp(i\omega t)$ and placed at a height 'h' over an n-layer earth as shown in Figure 4.1. The electrical conductivities and the thicknesses of the different layers are given by σ_m and d_k where m varies from 1 to n and k varies from 1 to (n-1). The permeabilities of all the layers are taken to be the same as that of vacuum and designated by $\mu(4\pi \times 10^{-7} \text{ H/m})$. The point of observation may be taken to be any point along the X-axis at a distance of R_1 and at a height of 'z' over the surface.

The horizontal and the vertical components of the magnetic field recorded at the receiver may be written down as (Sinha and Collett, 1973):

$$H_z = \frac{IdA}{4\pi\delta_1^3} \cdot T_0(A, B, D_j, k_j) - \frac{IdA}{4\pi R_1^3} \quad (1)$$

$$H_x = \frac{IdA}{4\pi\delta_1^3} \cdot T_1(A, B, D_j, k_j) \quad (2)$$

where

$$T_0(A, B, D_j, k_j) = \int_0^\infty R_{TE}(g) g^2 \exp(-gA) J_0(gB) dg \quad (3)$$

$$T_1(A, B, D_j, k_j) = \int_0^\infty R_{TE}(g) g^2 \exp(-gA) J_1(gB) dg \quad (4)$$

and $R_{TE}(g)$ is the reflection coefficient for the TE mode (Sinha and Collett, 1973).

Here, dA is the area of the transmitting dipole and,

$$A = (h+z)/\delta_1,$$

$$B = R/\delta_1,$$

$$D_j = 2d_j/\delta_1,$$

$$k_j = \sigma_j/\sigma_1,$$

$$\delta_1 = (2/\omega \mu \sigma_1)^{1/2}$$

where R is the horizontal separation between the points and

$$j = 1, 2, 3, \dots \dots n \quad (5)$$

To compute the response of the Maxiprobe system over a layered earth, one has to evaluate the infinite integrals T_0 and T_1 by numerical integration. However, the integrals converge only when the parameter A is finite, i.e. either z or h or both have finite values. In this system the coils are in general placed on the surface (the receiver loop is actually slightly above the ground since it is placed over a tripod stand), therefore, the integrals T_0 and T_1 are divergent. To obtain the integrals when both are on the surface, a method suggested by Frischknecht (1967) is used.

When $A = 0$, we may write

$$T_0 = T_0' + T_0'' = \int_0^\infty [R_{TE}(g) - R_{TE}(g)] g^2 J_0(gB) dg + \int_0^\infty R_{TE}(g) g^2 J_0(gB) dg \quad (6)$$

$d_1 = \infty$

$$T_1 = T_1' + T_1'' = \int_0^\infty [R_{TE}(g) - R_{TE}(g)] g^2 J_1(gB) dg + \int_0^\infty R_{TE}(g) g^2 J_1(gB) dg \quad (7)$$

$d_1 = \infty$

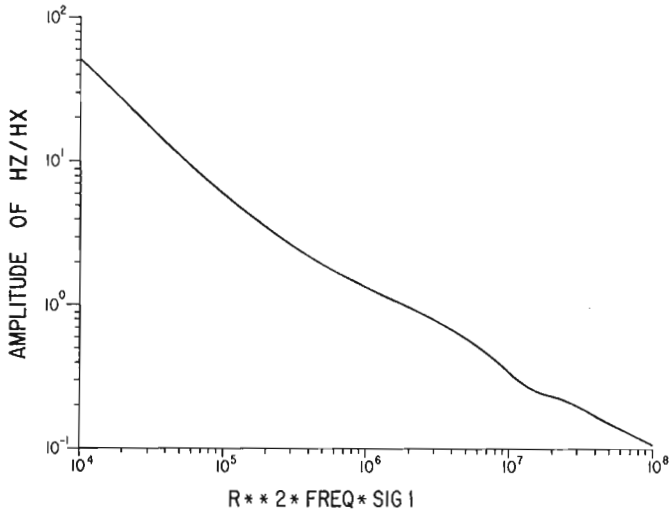


Figure 4.2. Response of a homogeneous medium to the Maxiprobe System.

The first integrals T_0' and T_1' containing the difference of R_{TE} values are now convergent. The second integrals T_0'' and T_1'' represent the secondary fields at the surface of a homogeneous ground and expressions are available for them in closed forms.

Therefore, the ratio of the vertical to the horizontal magnetic field at the receiver may be expressed by

$$\frac{H_z}{H_x} \Big|_{\substack{h=0 \\ z=0}} = \frac{(Z/Z_0)_1' - B^3 T_0'}{(Z/Z_0)_2' - B^3 T_1'} \quad (8)$$

where $(Z/Z_0)_{1,2}$ are the mutual coupling ratio values for the horizontal coplanar and perpendicular loop systems over a homogeneous earth given by:

$$(Z/Z_0)_1' = \frac{2}{\gamma_1^2 R^2} \left[9 - (9 + \gamma_1 R + 4\gamma_1^2 R^2 + \gamma_1^3 R^3) \exp(-\gamma_1 R) \right] \quad (9)$$

$$(Z/Z_0)_2' = \gamma_1^2 R^2 (I_1 K_1 - I_0 K_0) + 4\gamma_1 R (I_1 K_0 - I_0 K_1) + 16 I_1 K_1 \quad (10)$$

$$\text{Here, } \gamma_1^2 R^2 = i\omega\mu\sigma_1 R^2 = 2iB^2 \text{ where } i = \sqrt{-1}. \quad (11)$$

I_1, K_1, I_0 and K_0 are modified Bessel functions with arguments $(\gamma_1 R/2)$. Thus, using equations (8), (9), (10) and (11), it is possible to evaluate the ratio of the vertical to the horizontal magnetic fields over a layered earth. Figure 4.2 shows the response of the system over a homogeneous earth where the amplitude of the ratio of the fields is plotted along the ordinate and the product of R^2 , frequency and conductivity of the top layer (σ_1) is plotted along the abscissa. The curve shows a monotonous decrease with increasing abscissa values. That may be explained easily by the following reasoning.

At low values of the product parameter, i.e., at low frequency values, since R and σ_1 remain constant during a set of readings at any position, the field is mainly vertical. The total vertical field consists of a small induced field and a much larger primary field. The horizontal field, on the other hand, consists only of a small induced field. Hence, the ratio is quite large. As the frequencies are increased, the increasing induced fields become polarized more and more in the horizontal plane and the influence of the vertical primary

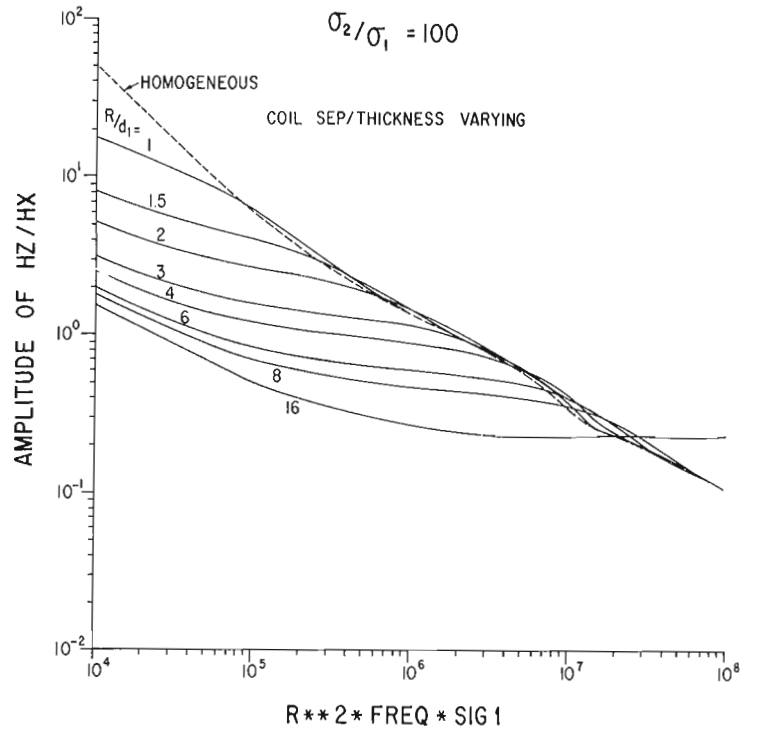


Figure 4.3. Response of the Maxiprobe EMR-16 System over a 2-layer model with constant conductivity contrast and varying R/d_1 values.

field diminishes. Therefore, at high abscissa values, the horizontal field becomes greater than the vertical field resulting in ratio values less than 1.

Figure 4.3 illustrates the response of a 2-layer earth where the conductivity ratio σ_2/σ_1 is taken as 100. The homogeneous response is plotted as a dashed line and the solid lines represent the response of the 2-layer earth with different values of the ratio R/d_1 , where d_1 is the thickness of the top layer. The point to note in this curve is that the curves with different R/d_1 , or different d_1 if R is constant, intersect the homogeneous curve at different points. The higher the R/d_1 value, the greater the abscissa value is and the less the ordinate value is at the point of intersection. This indicates that it is possible to obtain the thickness of the top layer from the positions of either the abscissa or the ordinate of the intersection point. At high abscissa values (high frequencies), however, all the curves merge with the homogeneous response curve since the skin depth at higher frequencies makes the influence of the bottom layer insignificant. In Figure 4.3, the line with $R/d_1 = 16$ does not merge with the homogeneous curve even at the highest frequency plotted since the layer is so thin that the bottom layer still has some influence on the response.

Figure 4.4 shows the response of a 2-layer earth where the parameter R/d_1 (or d_1 since R is kept constant for all frequencies) is kept constant and taken to be 2.0 and the curves are plotted for different conductivity ratios σ_2/σ_1 from 0.1 to 100.0. Interestingly enough, the intersection of the different lines with that for the homogeneous earth ($\sigma_2/\sigma_1 = 1.0$) take place at one point only, indicating thereby that the position of the intersection point is independent of the conductivity contrasts, but depends only on the depth of the second layer. Similarly, for a 3-, or 4-layer earth, the response breaks away from the homogeneous response curve at 2 or 3 positions which depend only on the depths of the interfaces from the surfaces. The interpretation technique of the Maxiprobe data is mainly based on these two conclusions.

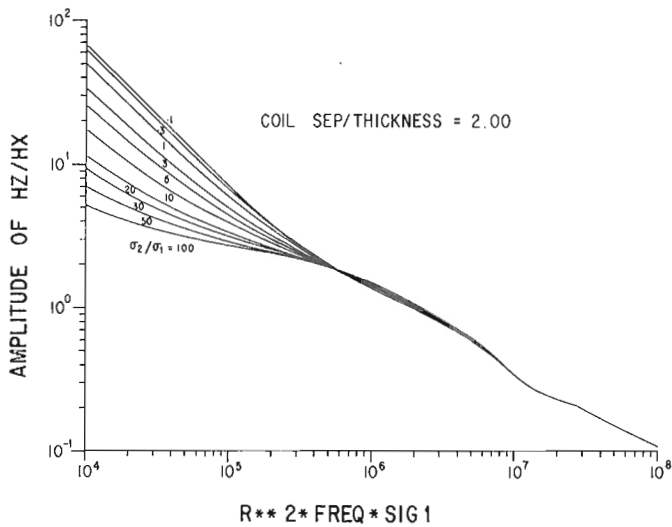


Figure 4.4. Response of the Maxiprobe EMR-16 System over a 2-layer model with constant R/d_1 value and varying conductivity contrast values.

Interpretation of Maxiprobe Data

Interpretation of the Maxiprobe EMR-16 field data, as in the case of all geophysical field data, may be performed in two ways. In the graphical approach, the field curve is plotted with the field amplitude ratios on the ordinate and the frequency in Hertz on the abscissa on a log-log graph sheet with identical cycle lengths (2.5 inch) as the ones on which the theoretical master-charts are plotted. The homogeneous response master curve is placed over the field curve so that the starting ordinate values are matched. Then the master-curve is moved sideways (changing the abscissa values) until the right sides of the field and theoretical curves match. Then, if at a common point, the $R^2 \sigma_1$ has a value of X and the frequency has a value of F , the conductivity σ_1 of the top layer is given by

$$\sigma_1 = X/R^2F \quad (12)$$

Since R is known from field data, σ_1 may be determined. Next, the point where the first break takes place is noted down either along the ordinate or along the abscissa. Using master charts derived from computer generated theoretical Maxiprobe response over layered ground, the depth d_1 may be determined in terms of the coil separation. To obtain the conductivity of the next layer, 2-layer master charts similar to Figure 4.4 are used for the appropriate value of R/d_1 ratio. From a match of the theoretical and field curves, the value of σ_2 may be derived. The same procedure is followed if more than two layers are present.

Maxiprobe data may also be interpreted by direct inversion on a computer. Studies in that direction have been initiated and will be reported later. In order to explain the interpretation procedure, a field example will now be discussed. Figure 4.5 illustrates the Maxiprobe EMR-16 sounding curve over one station in the Meager Creek area of British Columbia. There are several hot springs in the area and geological and geophysical studies have indicated the probable presence of a geothermal source in the area. In the test, the coil separation was kept at 300 m and the frequencies were varied from 150 Hz to 39 kHz. There are three distinct breaks in the field curve corresponding to depth values of 200 m, 246 m and 411 m from the surface yielding thickness values of 200 m, 46 m and 165 m for the three layers. The resistivity values of the media are derived by comparison of the field curve with theoretical master curves and are shown in the diagram.

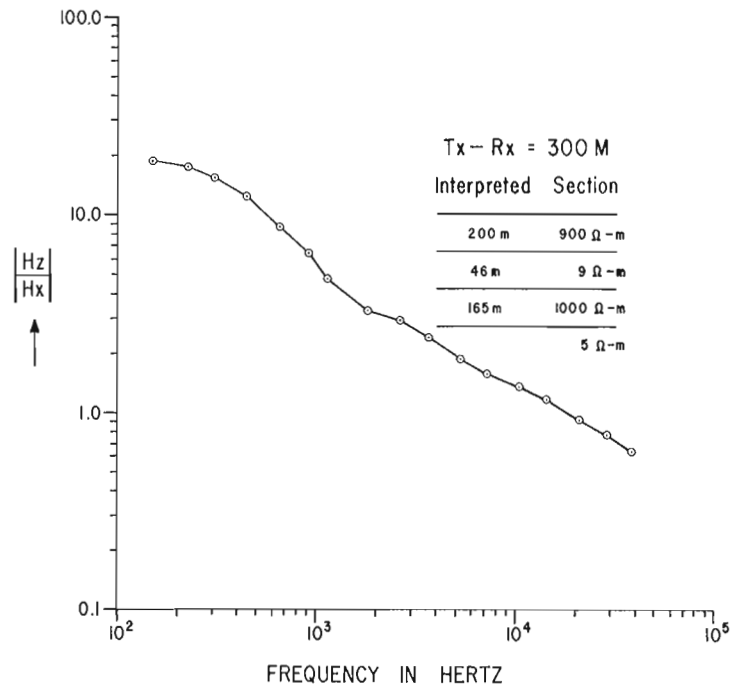


Figure 4.5. Field response of the Maxiprobe EMR-16 System in the Meager Creek area, British Columbia, for a coil separation for 300 m.

Concluding Remarks

The Maxiprobe EMR-16 System has proved to be useful for deep exploration in areas with quasi-parallel layering. The large number of available frequencies and coil separation values from 50 m to 1 km or more makes this system most versatile. At present, the system (EMR-16) consists of five different components. Thus, it is not very portable compared to some existing e.m. sounding systems. But this system should be used only where information is needed at greater depths, say from 150 m down. Because it is possible to have coil separation values of 1 km or more, it has the potential for sounding up to 2 km from the surface under favourable circumstances.

The main advantages of the system are (i) large depth penetration, (ii) no need for cable connection between the transmitter and the receiver, (iii) no need to put the transmitter loops along any predetermined geometry, and (iv) no need to know the transmitter loop area, loop current, number of turns of the loops or the pick-up factors of the receiver loops. The present instrument is capable of performing 10-15 soundings per day with a 3 or 4 man crew. The time taken at each sounding varies from 30-45 minutes. Using a hand-held programmable calculator it is possible to plot the data as they are being measured so that any suspicious looking readings may be repeated, if needed. Interpretations are also easy and may be carried out in the field itself using the master-charts. The error in the interpretation of depth values is usually less than 5 per cent while the error is somewhat higher for conductivity determination.

References

- Frischknecht, F.C.
 1967: Fields about an oscillating magnetic dipole over a two-layer earth, and applications to ground and airborne electromagnetic surveys; Colorado School of Mines, Quarterly, v. 62, no. 1, 326 p.
- Sinha, A.K. and Collett, L.S.
 1973: Electromagnetic fields of oscillating magnetic dipoles placed over a multilayer conducting earth; Geological Survey of Canada, Paper 73-25, 48 p.

**COMPUTER PROCESSING OF GAMMA RAY LOGS:
A PROGRAM FOR THE DETERMINATION OF RADIOELEMENT CONCENTRATIONS**

Project 740085

John G. Conaway
Resource Geophysics and Geochemistry Division

Conaway, J.G., *Computer processing of gamma ray logs: A program for the determination of radioelement concentrations; in Current Research, Part B, Geological Survey of Canada, Paper 79-1B, p. 27-32, 1979.*

Abstract

The accuracy of ore grade information from gamma ray logs may be improved by computer processing the raw data. A simple technique for accomplishing this utilizes a combined digital inverse and smoothing filter which is applied to the data using an open-ended discrete convolution algorithm. Such an algorithm is on the order of 20 times more efficient in terms of computation time than the iterative technique currently in common use in the gamma ray logging industry. A Fortran program which utilizes the inverse filter technique is given here; this program may be used either with data from a digital logging system or with digitized data from an analog logging system having an exponential ratemeter impulse response. The data may be either total count data, or the output of a specified energy window of a spectral log. If proper procedure has been used in the logging operation the processed log will have resolution improved over the raw log, and will more accurately represent the true ore grades along the borehole.

Introduction

If the distribution of radioactive material along a borehole is to be determined as accurately as possible on the basis of a gamma ray log, it is necessary that the raw data be enhanced. This may be accomplished easily by applying a combined digital inverse and smoothing filter to the data using a discrete convolution routine (Conaway and Killeen, 1978a). The processed log will have improved accuracy and resolution, especially in the vicinity of thin beds and complex sequences. A computer program which utilizes such a technique is given in Appendix A. This program, called RALOG (for Radiometric Assay log), is written in Fortran-IV. A simplified flow chart is shown in Figure 5.1. RALOG may be used with data from a digital logging system, or with digitized data from an analog logging system having an exponential ratemeter impulse response, although in the latter case some degradation of the log quality must be expected because of the loss of accuracy inherent in analog recording.

RALOG requires relatively little core memory (CM), and thus may be used with a minicomputer or microprocessor, although translation into machine language may be necessary. The data are processed sequentially with only a few data values in core at any one time; thus the processing of a 1 km log requires no more CM than a 10 m log. Studies show that the inverse filter technique is on the order of 20 times more efficient in terms of computation time than the standard iterative program used commonly in the gamma ray logging industry today (Conaway and Killeen, 1978b).

RALOG makes use of a combined digital inverse and smoothing filter as described by Conaway and Killeen (1978a). The smoothing term is composed of a sinc function tapered by a Blackman window (see Oppenheim and Schafer, 1975). The deconvolution term is a 3-point approximate inverse filter of the form

$$\left(-\frac{1}{(\alpha \Delta z)^2}, 1 + \frac{2}{(\alpha \Delta z)^2}, -\frac{1}{(\alpha \Delta z)^2} \right)$$

which is designed to remove the effect of the geologic impulse response (GIR), the response of an ideal logging system to a thin bed of radioactive material. The constant α is easily determined in a model borehole as described by Conaway and Killeen (1978a); Δz is the sampling interval (cm).

In the case of analog logs obtained at a logging velocity V (cm/s), a second 3-point approximate inverse filter of the form

$$\left(\frac{\sqrt{T}}{2\Delta z}, 1, -\frac{\sqrt{T}}{2\Delta z} \right)$$

is used to compensate for the effect of the ratemeter with exponential time constant T (seconds). These separate deconvolution and smoothing terms are computed by subroutine FILGEN, and combined into a single filter by subroutine COMBIN, a simple convolution subroutine.

Input Parameters

Program RALOG requires a total of 7 input parameters on 3 cards in the formats given in Table 5.1.

These parameters are:

NPTS — the number of points in the combined smoothing and deconvolution filter. The optimum value of NPTS depends on the logging system characteristics, sampling interval, whether a digital or analog system was used, etc., and therefore requires some experience on the part of the user. NPTS must be odd, and should be less than 100 to avoid exceeding the array dimensions; generally NPTS will be much less than 100. The shorter the sampling interval, the larger the value of NPTS generally required for smoothing the data. If no smoothing is desired, use NPTS = 3 for a digital logging system, or NPTS = 5 for an analog system with exponential time constant; these are the lengths of the inverse filters alone. For sampling intervals shorter than about 10 cm, some degree of smoothing will probably be required.

A good way to determine the optimum value of NPTS under particular logging conditions is to run two or more logs past a complex ore zone using the same logging speed, detector, etc. Process the individual logs using RALOG with no smoothing, and compare the logs for repeatability. Increase the smoothing as required to give a good compromise between resolution and repeatability. The resulting value of NPTS may then be used under logging conditions similar to those in the test.

ALPHA — the constant α which controls the shape of the approximate geologic impulse response. Generally ALPHA will be on the order of $0.1-0.2 \text{ cm}^{-1}$ (see Conaway and Killeen, 1978a, for more information).

Table 5.1

Data Card Number	Parameters	Format
1	NPTS	I5
2	ALPHA, CALCON, DT	3F10.3
3	V, ST, TC	3F10.3

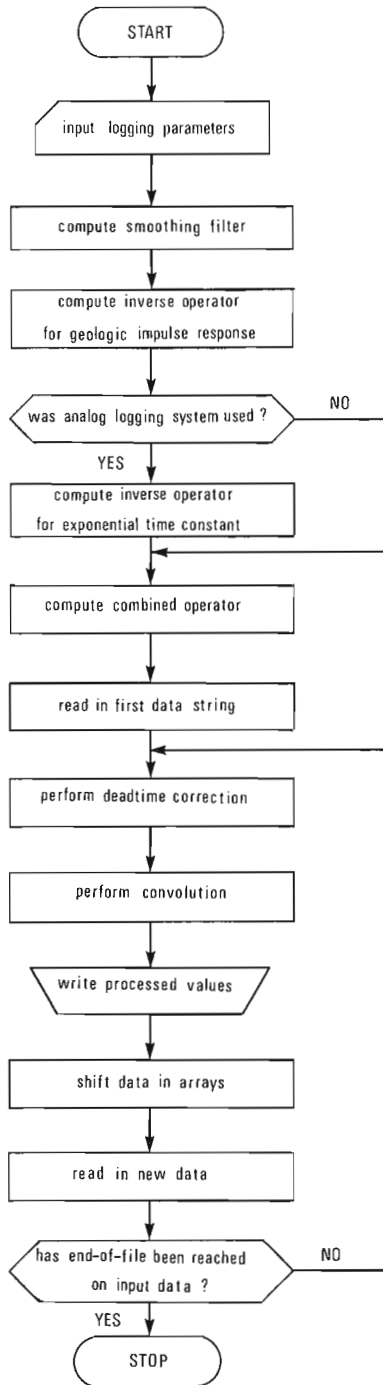


Figure 5.1. A simplified flow chart of the RALOG program.

CALCON – the system calibration constant in $\%eU_3O_8 / (\text{count/s})$, or ppm/(count/s) where ppm is parts per million equivalent uranium (or other radioelement).

DT – the system dead time (or resolving time) in microseconds. If no dead time correction is desired, specify DT = 0.

V – logging velocity in m/min.

ST – the sampling time in seconds. For an analog system $ST = 60\Delta z/V$, where Δz is the sampling interval along the borehole in metres, and V is the logging velocity in m/min.

TC – the time constant in seconds of an analog logging system having an exponential ratemeter impulse response. If a digital system is used specify TC = 0. The values of the time constant specified by the manufacturer should be verified experimentally.

In order that the data processing technique be valid it is necessary that certain conditions be met (see Conaway and Killeen, 1978a). The following conditions are important with respect to the input parameters:

- (A) Logging speed and ratemeter time constant should be constant throughout the entire log. If either of these is altered, then a new filter must be computed.
- (B) Sampling interval must be constant, and fairly short. For good results the data should be sampled at least every 10 cm of depth; in general a shorter sampling interval is recommended.
- (C) CALCON and ALPHA for the particular probe used must have been determined in model holes under conditions similar to those in the logged borehole (i.e. similar borehole diameter, casing, fluid content, and so forth).

Data Input and Output

The data are read by RALOG in pairs of COUNT and DEPTH values. COUNT is the number of counts per sampling interval in the case of the digital logging system, and gamma ray intensity (counts per second) in the analog case. The data may be either from a Total Count log, or may represent the counts from one energy window of a spectral log. DEPTH may be in any units. The program is set up to read data pairs in Format (2F10.2) from Device 1, which has previously been assigned by the user according to the procedure required by the computer manufacturer. The format and device may be altered as required. Device 1 may generally be assigned to either disk or magnetic tape. If the data are on punched cards, Device 5 (card reader) should be specified in the program rather than Device 1.

The output data are written on Device 2 (generally assigned to disk or magnetic tape) as pairs of ore grades and depths, in Format (2F10.2). Once again the format and device may be changed as required; if the processed data are to be printed, Device 6 should be specified.

The Convolution Algorithm

In subroutine CONVOL raw COUNT and DEPTH values are read and the combined smoothing and inverse filter is applied using an open-ended convolution algorithm. New data pairs are read in 'N' at a time, where N may be specified as anything from 1 to 100 without changing the current array dimensions. The last group of data values less than N in number will not be processed. The convolution process continues until the end of the input data file is reached. Generally it is a good idea to record data for a minute or two at both the top and the bottom of the borehole with the probe stationary; this allows some data for the filter to 'run out on' at both ends of the log.

Subroutine CONVOL utilizes an end-of-file test of the form

```
IF(EOF(NDEV))I,J
```

where NDEV is the input device number, and I and J are the statement numbers to which control is transferred if an end-of-file is encountered, or is not encountered, respectively. Although this is a non-standard statement, most computer systems have a similar end-of-file test which can be substituted. An alternate approach is to terminate the input data file with a unique character string (say, a DEPTH value of 9999.99) that can be recognized with a logical IF statement, which then replaces the EOF test statement.

Before processing, each gamma ray reading is corrected for instrument dead time, since this is a non-linear correction. The dead time correction is performed by subroutine LAZAR. The dead time correction used in this program is an approximation; see Chase and Rabinowitz (1968) for a discussion of dead time corrections.

Strictly speaking, in the case of analog logs the dead time correction should be performed after the effect of the ratemeter time constant is removed but before the effect of the GIR is removed. For simplicity here the dead time correction is made before the combined inverse filters are applied. If the ratemeter time constant is kept short the two methods should give equivalent results. The program may, of course, be modified if it is deemed desirable to do so.

Conclusion

If RALOG is to be used with a minicomputer or microprocessor for on-line processing of the gamma ray data, the parameter N in subroutine CONVOL should be set to 1. Thus, the procedure will be as follows. As the logging operation begins, the first NPTS raw gamma ray readings (where NPTS is the filter length) are entered into CM. The filter is then applied to those values, and the resulting processed ore grade value goes to output (plot, print, magtape, etc.). Now the first raw gamma ray reading is ejected, the remaining (NPTS-1) readings are shifted by one position in memory, and the computer is then ready for the next gamma ray reading. Clearly the computation-and-shift operation must be accomplished in less time than the sampling time (ST seconds). If the data are to be recorded on magnetic tape it is always advisable that the raw data be recorded for reprocessing if desired.

It should be pointed out that the effect of the analog ratemeter is direction dependent. The program is designed to process the data in the same order in which they were obtained in the field. If the data are processed in reverse order, then the first and third terms of the ratemeter inverse filter must be interchanged.

The basic computer program given in Appendix A may be modified easily to suit individual requirements. As an example, the program may be modified in the case of a digital logging system to monitor the depth interval Δz on the basis of successive DEPTH values. If Δz varies by more than a preselected amount (e.g. due to a slow variation in cable speed), the filter can be recomputed before continuing the processing. The filter may also be recomputed when a depth is reached at which the borehole conditions are known to change significantly. Parameters such as borehole diameter, casing thickness, and borehole fluid all affect the calibration constant CALCON, and in some cases the shape of the geologic impulse response (and therefore ALPHA). A change in one of these parameters may introduce significant error into the processed results unless the filter is adjusted accordingly.

Acknowledgments

The author thanks John Carson and P.G. Killeen of the Radiation Methods Section, Resource Geophysics and Geochemistry Division of the Geological Survey of Canada for helpful discussions regarding the text of this report.

References

- Chase, G.D. and Rabinowitz, J.L.
1968: Principles of radioisotope methodology; 3rd ed., Burgess Publishing Company, Minneapolis.
- Conaway, J.G. and Killeen, P.G.
1978a: Quantitative uranium determinations from gamma-ray logs by application of digital time series analysis; Geophysics, v. 43, p. 1204-1221, 1978.
- 1978b: Computer processing of gamma-ray logs: iteration and inverse filtering; in Current Research, Part B, Geological Survey of Canada, Paper 78-1B, p. 83-88.
- Oppenheim, A.V. and Schafer, R.W.
1975: Digital signal processing; Prentice-Hall, Englewood Cliffs.

APPENDIX A

```

PROGRAM RALOG(INPUT,OUTPUT,TAPE1,TAPE2,TAPE5=INPUT,TAPE6=OUTPUT)
C THE PRECEDING PROGRAM CARD IS MACHINE DEPENDENT.
C READ INPUT PARAMETERS FROM FUNCHED CARDS
C NPTS - THE DESIRED NUMBER OF POINTS IN THE COMBINED
C SMOOTHING AND INVERSE OPERATOR (ODD)
  READ(5,1000)NPTS
C ALPHA - THE GEOLOGIC IMPULSE RESPONSE SHAPE CONSTANT
C CALCON - THE SYSTEM SENSITIVITY
C DT - THE SYSTEM DEADTIME IN MICROSECONDS
  READ(5,1100)ALPHA,CALCON,DT
  DENOM=10.**6.
  DT=DT/DENOM
C V - THE LOGGING VELOCITY IN M/MIN
C ST - THE SAMPLE TIME IN SECONDS. FOR ANALOG SYSTEMS ST=60H/V
C WHERE H IS SAMPLING INTERVAL ALONG THE BOREHOLE IN METERS,
C AND V IS LOGGING VELOCITY IN M/MIN.
C TC - THE EXPONENTIAL TIME CONSTANT OF AN ANALOG SYSTEM
C IN SECONDS. FOR DIGITAL SYSTEMS TC=0.
  READ(5,1100)V,ST,TC
  CALL CONVOL(NPTS,ALPHA,CALCON,DT,V,ST,TC)
1000  FORMAT(I5)
1100  FORMAT(3F10.3)
      STOP
      END

```

```

SUBROUTINE LAZAR(DT,ST,C)
C THIS IS AN APPROXIMATE DEADTIME CORRECTION
  C=(C*ST)/(ST-(C*DT))
  RETURN
  END

```

```

SUBROUTINE COMBIN(LA,A,LB,B,LC,C)
DIMENSION A(LA),B(LB),C(LC)
DO 10 I=1,LC
10  C(I)=0.
DO 20 I=1,LA
DO 20 J=1,LB
  K=I+J-1
20  C(K)=C(K)+A(I)*B(J)
  RETURN
  END

```

```

      SUBROUTINE CONVOL(NPTS,ALPHA,CALCON,DT,V,ST,TC)
      DIMENSION COUNT(300),FILT(200),OREGRD(100),DEPTH(300)
C   OREGRD - OUTPUT RADIOELEMENT CONCENTRATION
C   COUNT - INPUT GAMMA-RAY COUNTS (NUMBER OF GAMMA-RAYS DETECTED
C           PER TIME INCREMENT ST).
C   FILT - THE COMBINED INVERSE AND SMOOTHING FILTER
C   N - NUMBER OF POINTS PROCESSED AT A GO
C   THIS PROGRAM WRITES N VALUES EACH TRIP THROUGH
      N=1
C   GENERATE THE COMBINED SMOOTHING AND DECONVOLUTION OPERATOR
      CALL FILGEN(NPTS,ALPHA,TC,CALCON,V,ST,FILT)
      NA=NPTS-1
      NB=NA+N
      DTMIN=1./(10.**7.)
C   READ IN FIRST DATA STRING
      DO 30 I=1,NB
      READ(1,1000) DEPTH(I),COUNT(I)
      IF(EOF(1))9999,10
10    CONTINUE
      IF(DT-DTMIN)30,30,20
20    CALL LAZAR(DT,ST,COUNT(I))
30    CONTINUE
C   PERFORM CONVOLUTION
40    CONTINUE
      DO 60 J=1,N
      OREGRD(J)=0
      JA=J-1
      DO 50 K=1,NPTS
      KA=K+JA
      KB=NPTS+1-K
      OREGRD(J)=OREGRD(J)+FILT(KB)*COUNT(KA)
50    CONTINUE
      JZ=J+(NA/2)
      WRITE(2,1000)DEPTH(JZ),OREGRD(J)
60    CONTINUE
C   SHIFT DATA IN ARRAYS
      DO 70 I=1,NA
      DEPTH(I)=DEPTH(I+N)
      COUNT(I)=COUNT(I+N)
70    CONTINUE
C   READ IN N NEW DATA POINTS
      DO 100 I=NPTS,NB
      READ(1,1000) DEPTH(I),COUNT(I)
C   TEST FOR END OF INPUT DATA FILE
      IF(EOF(1))999,80
80    CONTINUE
      IF(DT-DTMIN)100,100,90
90    CONTINUE
      CALL LAZAR(DT,ST,COUNT(I))
100   CONTINUE
      GO TO 40
999   CONTINUE
      RETURN
9999  CONTINUE
      WRITE(6,1100)
1000  FORMAT(2F10.2)
1100  FORMAT(///38HERROR - TOO FEW DATA VALUES TO PROCESS///)
      RETURN
      END

```

```

      SUBROUTINE FILGEN(NPTS,ALPHA,TC,CALCON,V,ST,FILT)
      DIMENSION FSMOO(200),FILT(200),FGIR(3),FTC(3),HOLD(5)
C   COMPUTE SMOOTHING FILTER
C   NSMOO - NUMBER OF POINTS IN SMOOTHING OPERATOR.
      NSMOO=NPTS-2
      IF(TC.GT.0.01)NSMOO=NPTS-4
      N2=(NSMOO+1)/2
      NSMOO2=(NSMOO*2)+1
      PI=4.*ATAN(1.)
      R   RAT=4./FLOAT(NSMOO2+1)
      A2=PI*RAT
      NN=(NSMOO2+1)/2
      AXE=0.
      DO 30 I=1,NSMOO2
      A1=PI*FLOAT(I)/FLOAT(NSMOO2+1)
      FBLACK=.42-.5*COS(2.*A1)+.08*COS(4.*A1)
      A3=FLOAT(I-NN)*A2
      IF(NN.NE.I)GO TO 10
      FSINC=A2
      GO TO 20
10     FSINC=A2*SIN(A3)/A3
20     CONTINUE
      FSMOO(I)=FSINC*FBLACK
30     CONTINUE
      DO 40 I=1,NSMOO
      FSMOO(I)=FSMOO(I+N2)
      AXE=AXE+FSMOO(I)
40     CONTINUE
      DO 45 I=1,NSMOO
      FSMOO(I)=FSMOO(I)/AXE
45     CONTINUE
C   COMPUTE DECONVOLUTION FILTER FOR GEOLOGIC IMPULSE RESPONSE
C   THIS FILTER INCLUDES THE SYSTEM CALIBRATION CONSTANT
      DENOM=(ALPHA*ST*V*100./60.)**2.
      IF(TC.LT.0.01)CALCON=CALCON/ST
      FGIR(1)=-CALCON/DENOM
      FGIR(2)=CALCON-(2.*FGIR(1))
      FGIR(3)=FGIR(1)
      IF(TC.GT.0.01)GO TO 50
      CALL COMBIN(3,FGIR,NSMOO,FSMOO,NPTS,FILT)
      RETURN
C   COMPUTE DECONVOLUTION FILTER FOR RATEMETER TIME CONSTANT IF AN
C   ANALOG LOGGING SYSTEM WAS USED
50     CONTINUE
      FTC(1)=TC/(ST*2.)
      FTC(2)=1.
      FTC(3)=-FTC(1)
      CALL COMBIN(3,FTC,3,FGIR,5,HOLD)
      CALL COMBIN(5,HOLD,NSMOO,FSMOO,NPTS,FILT)
      RETURN
      END

```

**STRATIGRAPHY AND STRUCTURE OF THE BARKERVILLE-CARIBOO RIVER AREA,
CENTRAL BRITISH COLUMBIA**

E.M.R. Research Agreement 1113-4/79

L.C. Struik¹

Regional and Economic Geology Division

Struik, L.C., Stratigraphy and structure of the Barkerville-Cariboo River area, central British Columbia; in Current Research, Part B, Geological Survey of Canada, Paper 79-1B, p. 33-38, 1979.

Abstract

The Cariboo River area of central British Columbia was remapped at a scale of 1:50 000. Several conclusions of local and regional significance are: 1) The upper Black Stuart Formation is apparently lithologically and chronologically equivalent to the Guyet Formation excluding the Greenberry Limestone Member; 2) The combined Black Stuart and Guyet formations represent Middle Ordovician to Lower Pennsylvanian deposition; 3) The Antler Formation is at least partly of Early Pennsylvanian age; 4) No evidence was found for a Mississippian Cariboo Orogeny; and 5) Four or more stages of faulting, including east to west thrusting, are present. Thrust faults formed in the first stage have been folded.

Introduction

The Barkerville area of central British Columbia has been of continued geologic interest since the first discovery of placer gold about 1861. The area has been mapped several times by geologists of the Federal and British Columbia governments. Recent mapping by Campbell et al. (1973) has initiated controversy over stratigraphy and the structural history. Major points of disagreement with previous workers are repeated here, as they are investigated in this project.

1. Campbell et al. (1973) found no evidence for a Late Paleozoic orogeny as described by Sutherland Brown (1957) and named the Cariboo Orogeny by White (1959). In brief Campbell et al. (1973) did not find foliated clasts of various orientation (representing an orogenic event) within a non-foliated matrix of Guyet Formation conglomerate which unconformably overlies the Cariboo and Kaza groups. Rather, they found a penetrative cleavage indicating one deformation phase postdating deposition of the conglomerate. The difference in intensity of folding between the Slide Mountain Group and older rocks was thought to be due to lithological differences and not to two folding events.
2. The Guyet Formation was speculated by Campbell et al. (1973, p. 80) to be a mélange deposited in front of a possible advancing thrust sheet of Antler Formation volcanics and cherty sediments. This is contrary to the earlier view (Sutherland Brown, 1957) of the Guyet Formation as a fluvial deposit resulting from an orogenic uplift involving pre-Slide Mountain Group strata.
3. The clasts of the Guyet Formation conglomerate were suggested by Campbell et al. (1973) not to be derived from underlying strata, whereas Uglow (Johnston and Uglow, 1926) set forth the idea that the clasts were derived from older underlying formations.
4. The stratigraphy established by Campbell et al. (1973) in the Cariboo Mountains did not correspond to that established by Holland (1954) and Sutherland Brown (1957, 1963) in the Cariboo River area to the west. A new formation was described by Mansy (1970). This formation, the Black Stuart, had been previously incorporated as part of the Midas Formation of Sutherland Brown (1963) and Campbell (1961). Figure 6.1 contrasts the stratigraphic interpretations of Sutherland Brown (1963) and Campbell et al. (1973).

Field work in the summers of 1977 and 1978 has yielded answers to some of these problems. It has also made it necessary to redefine the stratigraphy of the Slide Mountain Group and the Black Stuart Formation.

Acknowledgments

I wish to thank R.B. Campbell for the introduction to Cariboo geology, B.E.B. Cameron and B.S. Norford for their fossil identification and continued interest, R.B. Campbell, P.S. Simony, and L. Hills for reviewing the material and providing gratefully accepted comments, and P.S. Simony for providing a stimulating and highly appreciated learning experience.

Stratigraphy

Present mapping has essentially confirmed the stratigraphic interpretation of the Cariboo Group presented by Campbell et al. (1973). A composite section of the Isaac to Mural formations can be demonstrated in the area south of Waverly Mountain. This includes Roundtop Mountain, one of the type localities used by Holland (1954) to establish the stratigraphy of the Cariboo Group.

A well exposed composite section from Isaac Formation to Mural Formation exists on Kimball Mountain. Lithologic transitions from one formation to the next are distinctive. However, in isolated exposures it is difficult to distinguish Midas from Yankee Belle or Cunningham from Mural.

The transition between the Isaac and Cunningham formations is gradational over 30 m or more. This is in strong contrast to the rapid gradation from the Midas to Mural formations. The upper Isaac Formation consists of calcareous, grey to black, thinly laminated pelites. These are interbedded with brown to dark grey-brown weathering, grey to dark grey limestone beds near the Cunningham Formation contact. The limestone becomes the predominant constituent with its bedding defined by lamellae of dark grey to black carbonaceous pelite.

The transition from the Cunningham Formation to Yankee Belle Formation is also gradational, but the thickness of the transition interval is not constant. At the base of the Yankee Belle Formation grey to orange-brown weathering, grey limestone members of 6 to 20 m are separated by grey to green-grey pelite, siltstone, and sandstone of similar thicknesses. Limestone-sandstone contacts are generally gradational across zones of sandy limestone and calcareous sandstone. The presence of limestone beds at the base of the Yankee Belle Formation provides a distinction from the Midas Formation which is devoid of limestone.

Where present the coarse white to dark grey, clean quartzite of the Yanks Peak Formation is a good marker. Where the quartzite is absent the Yankee Belle-Midas contact is difficult to define.

¹ Geology Department, University of Calgary, Calgary, Alberta T2N 1N4.

The base of the Mural Formation is marked by a sharp contact on Midas Formation green and purple pelites. The uppermost 2 to 6 m of Midas Formation commonly contain 1 to 2 cm thick lenses of limestone which thicken upsection to 2 to 8 cm beds directly below the massive limestone of the Mural Formation.

Two previously unreported archeocyathid localities were found in the Black Stuart Mountain area. These establish the limestone from which they were taken as Mural Formation, thus confirming the mapping by Mansy (1970), and providing further evidence that the stratigraphy of the Cariboo River area is the same as that determined by Campbell et al. (1973) for the Cariboo Mountains.

Holland (1954) described feldspathic micaceous quartzite and assigned it to the Snowshoe Formation, which he believed to overlie the Midas Formation. If this were correct, the Snowshoe Formation would apparently be equivalent to the Mural which Campbell et al. (1973) suggested overlies the Midas (see Fig. 6.1). Campbell et al. (1973) suggested instead that the Snowshoe is equivalent to the Kaza Group. Poor exposure, and the complexity of the structure has made resolution of the stratigraphic position of the feldspathic micaceous quartzite particularly difficult. For the purposes of this report the Snowshoe is considered to be a western facies of the Kaza Group as proposed by Campbell et al. (1973).

	Sutherland Brown (1963)		Campbell et al. (1973)			
Mississippian	Slide Mtn Gp.	Antler Fm.	pillow basalt, chert arg., diabase	Antler Fm.	pillow basalt, brx. tuff, chert, arg.	Lower Mississippian and/or younger
		Guyet Fm.	conglomerate, grwke., vol., crinoidal lst.	Guyet Fm.	conglomerate, sst., arg., basalt, lst.	Lower Mississippian and (?) older
Guyet Fm. not in contact with Snowshoe Fm.						
	Cariboo Group	Proserpine dykes		Black Stuart Fm.	argillite, chert, lst. sandstone, dolostone breccia	Lower Devonian and (?) younger
		Snowshoe Fm.	micaceous quartzite phyllite, lst.	Dome Ck. Fm.	shale, siltstone, arg., minor lst.	Lower and Upper Cambrian
		Midas Fm.	phyllite, metasilstone minor dark lst.	Mural Fm.	lst., dst., shale, minor siltstone	Lower Cambrian
		Yanks Peak Quartzite	quartzite, rare lst.	Midas Fm.	shale, siltstone, minor sandstone	Lower Cambrian and Hadrynian
Ordovician(?)		Yankee Belle Fm.	phyllite, metasilstone quartzite, minor lst.	Yanks Peak Fm.	quartzite, minor silty shale	
Early and (?) Middle Cambrian		Cunningham Limestone	lst., pelletal lst., dst., minor phyllite	Yankee Belle Fm.	shale, siltstone, sst. lst., minor sst & dst.	Hadrynian (Windermere)
		Isaac Fm.	phyllite, calcareous phyllite, lst.	Cunningham Fm.	lst., shale, dst near Rocky Mtn. Trench	
Windermere		Kaza Group	gritty feldspathic micaceous quartzites and green schists	Isaac Fm.	phyllite, shale, minor silstone, sst & lst.	
				Kaza Group (incl. Snowshoe Fm.)	feldspathic grit, phyllite or schist, minor lst. and cong.	

Figure 6.1. Stratigraphic interpretations of Cariboo Mountain area by Sutherland Brown (1963) and Campbell et al. (1973).

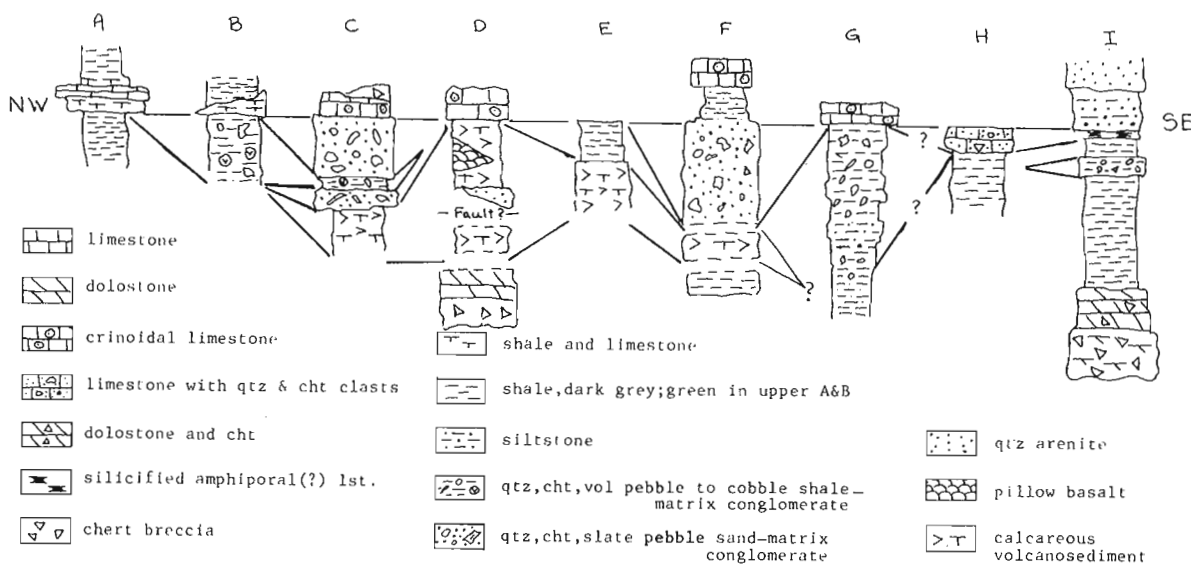
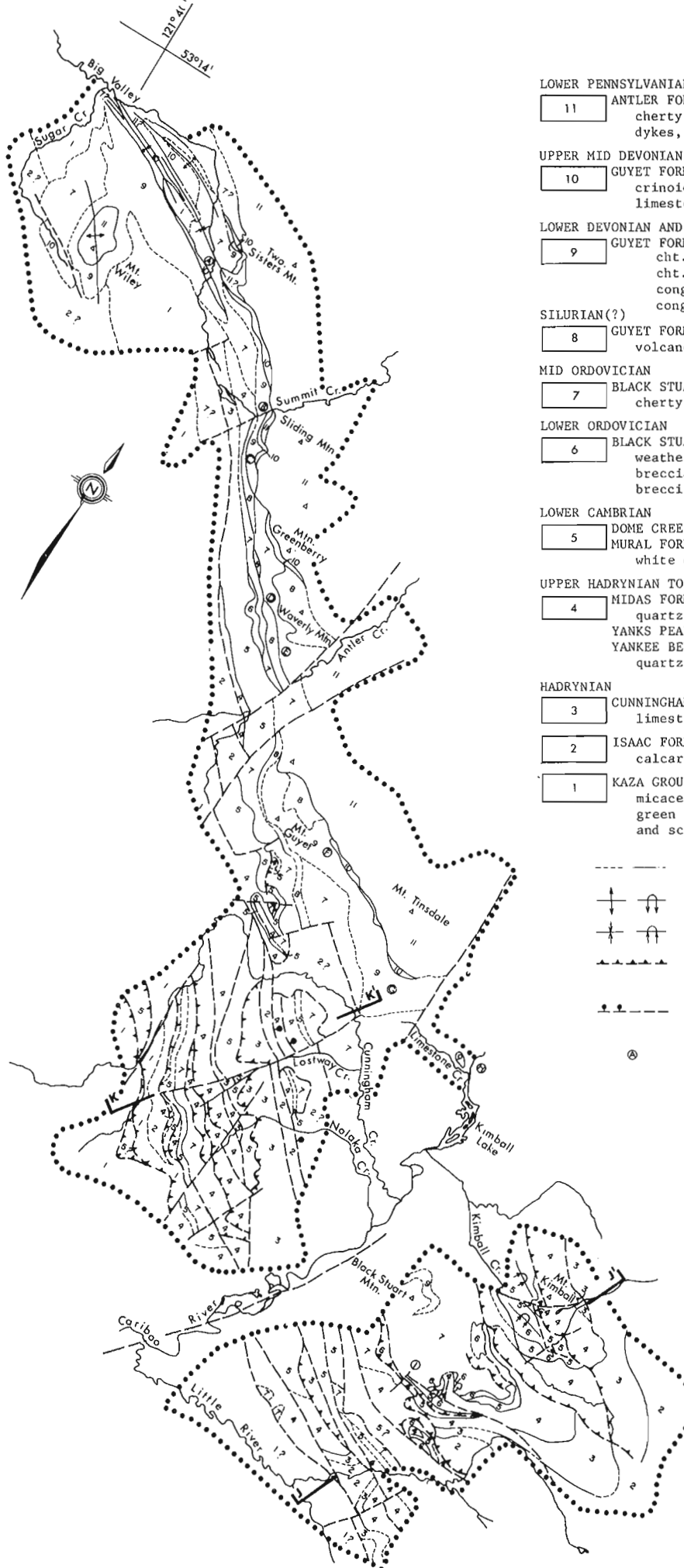


Figure 6.2. Sections showing variations of major lithologies within combined Black Stuart and Guyet formations. Locations of sections shown on Figure 6.3.



LEGEND

LOWER PENNSYLVANIAN

11 ANTLER FORMATION: pillow basalts, green and maroon cherty argillite and siltstone, diabase sills and dykes, chert, minor gabbro

UPPER MID DEVONIAN TO LOWER PENNSYLVANIAN

10 GUYET FORMATION, GREENBERRY LIMESTONE MEMBER: crinoidal limestone, dark grey micritic limestone (1P)

LOWER DEVONIAN AND(?) LOWER MID DEVONIAN

9 GUYET FORMATION, CONGLOMERATE: qtz.,cht.,sand-matrix cht. pebble conglomerate, shale-matrix slate, cht., qtz., vol., lst. granule to cobble conglomerate, light brown quartzite, qtz. cht. conglomerate, limestone

SILURIAN(?)

8 GUYET FORMATION, VOLCANIC: calcareous green volcanosediment, pyroclastics, pillow basalt

MID ORDOVICIAN

7 BLACK STUART FORMATION, SLATE: dark grey to black cherty slate to argillite

LOWER ORDOVICIAN

6 BLACK STUART FORMATION, BASAL CHERT: light grey weathering dark grey dolostone and dolostone breccia, light and dark grey chert and chert breccia, minor dolostone cobble conglomerate

LOWER CAMBRIAN

5 DOME CREEK FORMATION: dark grey shale and slate
MURAL FORMATION: dark grey to light grey limestone white dolostone, dark grey slate

UPPER HADRYNIAN TO LOWER CAMBRIAN

4 MIDAS FORMATION: grey slate, siltstone, fine quartzite
YANKS PEAK FORMATION: dark grey to white quartzite
YANKEE BELLE FORMATION: grey-green slate to quartzite

HADRYNIAN

3 CUNNINGHAM FORMATION: dark grey to light grey limestone, white dolostone

2 ISAAC FORMATION: grey and dark grey phyllite and calcareous phyllite, dark grey limestone

1 KAZA GROUP: grey and green-brown feldspathic micaceous quartzite, olivegreen and grey-green slate and phyllite, minor white quartzite and schist

--- Stratigraphic contact (approx., assum.)

↑ Anticline (upright, overturned)

↓ Syncline (upright, overturned)

▲ Thrust fault (approx. and assum., teeth in dip direction)

• Fault (approx. and assum., dot on the downthrown side)

⊗ Location of stratigraphic sections of figure 2



Figure 6.3.
Geology of study area.

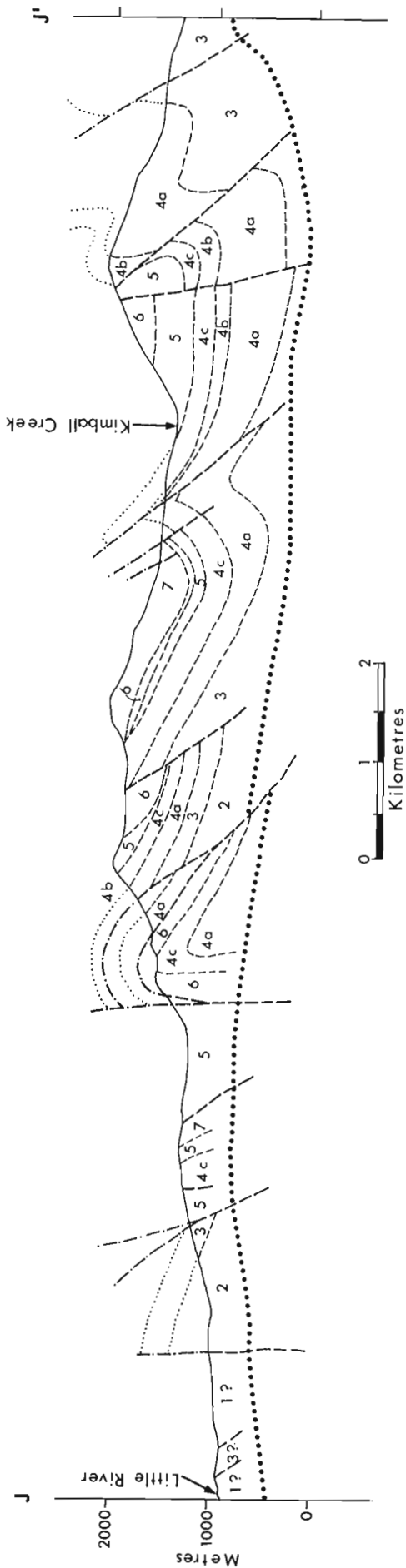


Figure 6.4. Cross-section JJ' in the Black Stuart Mountain area. Stratigraphic units and location of section is described in Figure 6.3.

The Cariboo and Kaza groups are unconformably overlain by the Black Stuart Formation and the Slide Mountain Group. The Guyet Formation was thought to overlie the Black Stuart Formation (Campbell et al., 1973). Several lines of evidence, however, suggest that the Guyet Formation is a time and lithological correlative of a portion of the Black Stuart Formation

1. The Greenberry Limestone Member of the Guyet Formation has yielded conodonts. Preliminary age determinations by B.E.B. Cameron (pers. comm. 1978) of the Geological Survey of Canada indicate that the ages range from late Eifelian (late lower-middle Devonian) to early Pennsylvanian. Apparently a hiatus separates lower Mississippian and lower Pennsylvanian rocks (no fossils with intermediary ages were found).

The Upper Eifelian to Lower Mississippian Greenberry limestone is a light grey crinoidal wackestone to mudstone. The time span associated with this part of the Greenberry limestone is not thought to represent continuous deposition but rather sporadic influxes of carbonate debris flows. In contrast, the overlying lower Pennsylvanian Greenberry Limestone is a dark grey mudstone (micritic limestone). The Guyet Formation conglomerate underlies the Greenberry Limestone Member and therefore part at least must be older than late Eifelian suggesting correlation with a portion of the Black Stuart Formation, assigned an early Devonian age by Mansy and Campbell (1970).

2. The limestone from which early Devonian macrofossils and conodonts were taken to date the Black Stuart Formation is from an outcrop near the mouth of the Limestone Creek (Mansy and Campbell, 1970). This limestone contains abundant clasts which resemble those in the Guyet Formation conglomerate. Correlation between the Limestone Creek limestone outcrop (early Devonian) and part of the Guyet Formation conglomerate (pre-late Eifelian) is possible from considerations of their ages and the similarity of their clasts. However, the Limestone Creek rocks are similar in some ways to a common Lower Devonian calcareous quartzite in northern British Columbia and Yukon (H. Gabrielse, pers. comm. 1978). Nowhere is a sand matrix conglomerate associated with calcareous quartzite known within the typical Guyet Formation assemblage.
3. A section of fine grained quartzite near the top of the Black Stuart Formation in the type area is underlain by 1.5 m of black silicified carbonate containing possible *Amphipora* (J.E. Klován, F. Stoakes, pers. comm. 1978), indicating a Late Silurian or Devonian age.
4. Guyet Formation shale matrix conglomerate found on the southeastern slope of Mount Tinsdale is also found on the east slope of Black Stuart Mountain. The conglomerate lies beneath the upper quartzite of the Black Stuart Formation referred to in (3) above.

These four points indicate that the upper portion of the Black Stuart Formation in the type area may be equivalent to the Guyet Formation.

Graptolites (GSC loc. no. C-53427) were found at one locality near the base of the Black Stuart Formation (52°52'27"-1/2"N, 121°06'59"W). They were examined by B.S. Norford and identified as *Climacograptus?* sp. *Dicellograptus?* sp. and *Orthograptus?* sp., indicating a Late Middle or Late Ordovician age (Caradoc or Ashgill). The collection was taken from dark grey slate which overlies the basal dolostone and chert of the Black Stuart Formation. This dates the unconformity at the base of the Black Stuart Formation as pre-Middle Ordovician.

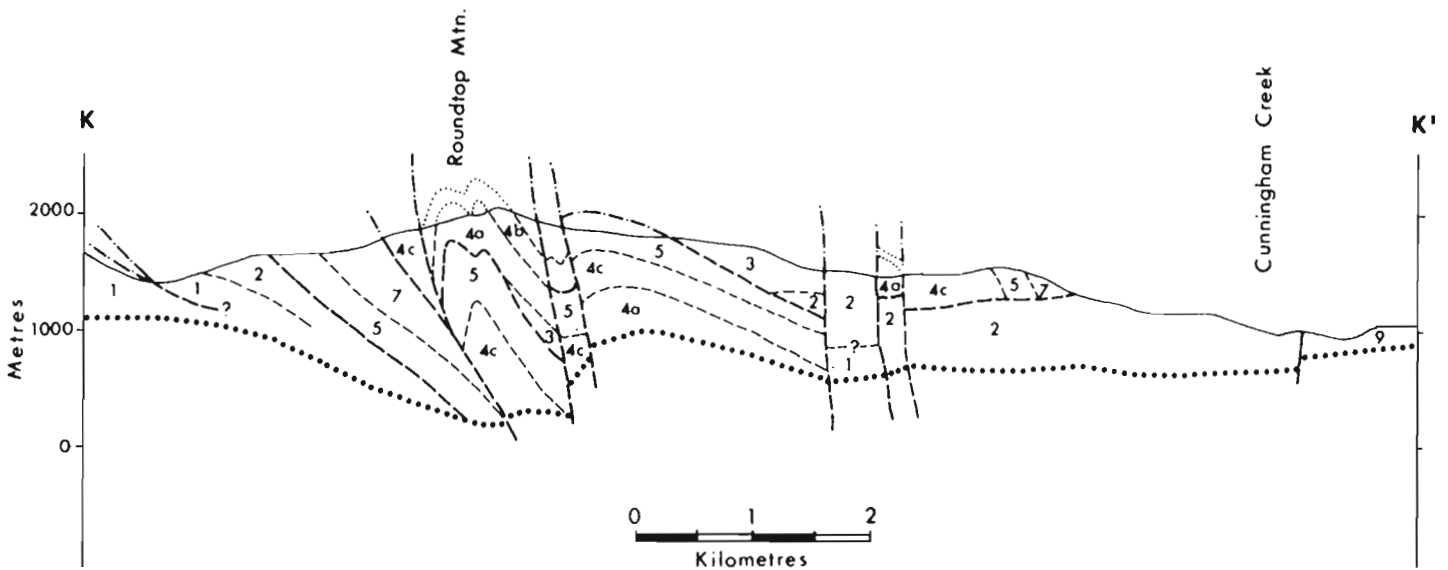


Figure 6.5. Cross-section KK' in Lostway Creek area. Stratigraphic units and location of section is described on Figure 6.3.

Sutherland Brown (1957) described occurrences of a volcanic member within the Guyet Formation on the hill between Waverly and Greenberry mountains and on North Cunningham Mountain. These localities were visited by the author and were found to consist of volcanic bombs set in carbonate or to have interstitial carbonate. The Waverly Mountain locality also has associated pyroclastics and minor pillow basalt. Both of the volcanic outcrops can be traced and/or projected under the Guyet Formation conglomerate and Greenberry Limestone Member. A similar schistose calcareous volcanic sediment occurs at the base of the Guyet Formation at Alex Allan Creek and can be traced to Antler Creek. Campbell et al. (1973) mapped this rock near Antler Creek as possible Black Stuart Formation. The present work supports this correlation and suggests that the volcanic sediment is possibly Silurian in age. Silurian pyroclastics are found in the north section of McBride map sheet on the McGregor Plateau.

Figure 6.2 is a diagrammatic section from northwest to southeast showing variations of major lithologies within the combined Black Stuart and Guyet formations.

The majority of the clasts in the Guyet Formation conglomerate are not from underlying units. The source of the clasts can be from either western or possibly eastern pre-Lower Devonian (probably oceanic) volcanic terranes.

The Guyet Formation cannot be a mélangé deposited in front of an advancing Antler Formation thrust sheet, because the Guyet Formation was deposited prior to the deposition of the Antler Formation. The Antler Formation is Early Pennsylvanian in age as opposed to the Early Devonian to Early Pennsylvanian age (excluding the Silurian(?) volcanogenic sediments) of the Guyet Formation. The Early Pennsylvanian age of the Antler Formation is from preliminary examination of conodonts (B.E.B. Cameron, pers. comm., 1978) derived from cherty argillites of that formation.

The Guyet Formation was not thrust onto older formations. It is a part of the Black Stuart Formation which unconformably overlies the Cariboo and Kaza groups. The Black Stuart and Guyet formations have been observed in unconformable contact with the Mural, Midas, Yanks Peak, and Isaac and/or Kaza formations. The unconformity represents a period of extensive erosion, possibly involving regional tilting.

Campbell et al. (1973) described the Lower and Upper Cambrian Dome Creek Formation conformably above the Lower Cambrian Mural Formation in the Cariboo Mountains. The relationship between the Dome Creek and Black Stuart formations is unknown in the field area, however Campbell et al. (1973) described the Dome Creek Formation as being truncated below an unconformity at the base of the Black Stuart Formation. This unconformity may represent the pre-Black Stuart erosional event. The erosional event, however, may be associated instead with the Middle Cambrian hiatus of the Dome Creek Formation. Although ambiguity may remain as to the exact timing of the major erosional event which has cut down through the entire Cariboo Group and into the Kaza Group, it must be pre-Late Middle Ordovician.

If the Guyet Formation conglomerate demonstrated an orogenic event prior to its deposition (it does not) that orogenic event would then have to be pre-Late Middle Ordovician. This is in contrast to the Mississippian age assigned to the unconformity below the Guyet Formation as described by Sutherland Brown (1957). The Mississippian Cariboo Orogeny was invoked to account for this unconformity. As originally defined, the Cariboo Orogeny cannot be real, since the unconformity is actually of pre-Late Middle Ordovician age.

The nature of the lower Antler Formation contact is unknown for it has not been observed in outcrop. No unequivocal evidence has been found to substantiate or refute tectonic emplacement of the Antler Formation.

Detailed redefinition of the Ordovician to Lower Pennsylvanian strata of the Barkerville-Black Stuart Mountain area is continuing.

Structure

Hadrynian to Lower Pennsylvanian strata have been folded about northwest and west-northwest plunging axes. The major folds are westward verging and relatively open, however, parasitic minor folds are usually tighter and may occasionally be isoclinal. Cleavage is predominantly axial planar and within the field area has a predominantly steep northeast dip. The cleavage fans in the area of Cunningham Creek and exhibits a steep southwestward dip. Only the most competent of the Yanks Peak Formation quartzites do not

display this cleavage. The cleavage within the Guyet Formation conglomerate is penetrative through clast and matrix. No case can be made for deformation of the clast material prior to deposition. This substantiates the conclusion of Campbell et al. (1973).

Folding of the major cleavage by second generation deformation is evident only as minor near-co-axial crinkles in phyllites occurring at the greatest stratigraphic depth. Only in the biotite zone of metamorphism along the Little River are there minor folds which fold the predominant cleavage. There is an axial plane cleavage developed through these folds and it is essentially parallel to the first cleavage as measured in the higher stratigraphic levels.

At least four phases of faulting have been identified. The first and second consist of major thrust faults and minor reverse faults respectively. Larger displacement thrusts such as the one in Lostway Creek (Fig. 6.3) which puts Cunningham on Mural Formation, cut bedding at low angles and follow bedding planes for distances of 1 to 3 km. This type of thrust is folded in the Black Stuart Mountain area (Fig. 6.4). The Lostway Creek thrust is surmised to be folded as shown in Figure 6.5.

Most reverse faults of small displacement are due to competency differences between strata. An example of these are the faults associated with the Yanks Peak Formation quartzites in the Roundtop Mountain area. These faults are relatively steep (40 to 55°) and cut bedding at high angles. These low displacement faults are not folded, nor are they observed to cut the larger displacement thrusts, which are folded. The low displacement faults are assumed to be younger because they are not folded. Both the thrust and reverse faults cut down-section to the northeast and east and postdate the Black Stuart Formation.

The third set of faults consist of high angle reverse and normal faults which strike parallel to the thrust faults. These offset the thrusts although they were not observed to intersect the low displacement reverse faults.

The three sets of faults are cut by transverse steep faults which down-drop the southeastern side. These may be displaced along northerly and east-northeasterly right lateral strike-slip faults.

No evidence has been found of fold structure or cleavage development prior to deposition of the Black Stuart Formation or during the Middle to Upper Mississippian hiatus. Structures formed during the Columbian Orogeny are continuous throughout the entire stratigraphic section. Fold style outlined by the Greenberry Limestone Member of the Guyet Formation in the Two Sisters Mountain area is consistent with that in older formations. This contradicts the impression given by Sutherland Brown (1957) that the formations unconformably above the Cariboo Group do not display the same deformational style as those below the unconformity. In general no structural evidence has been found in support of a Mississippian or Early(?) Ordovician orogeny.

References

- Campbell, R.B.
1961: Quesnel Lake (west half) British Columbia; Geological Survey of Canada, Map 3-1961.
- Campbell, R.B., Mountjoy, E.W., and Young, F.G.
1973: Geology of McBride map-area, British Columbia; Geological Survey of Canada, Paper 72-35.
- Gordey, S.P.
1978: Stratigraphy and structure of the Summit Lake area, Yukon and Northwest Territories; in Current Research, Part A, Geological Survey of Canada, Paper 78-1A, p. 43-48.
- Holland, S.S.
1954: Yanks Peak-Roundtop Mountain area, British Columbia; British Columbia Department of Mines, Bulletin 34.
- Johnston, W.A. and Uglow, W.L.
1926: Placer and vein gold deposits of Barkerville, Cariboo District, British Columbia; Geological Survey of Canada, Memoir 149.
- Mansy, J.L.
1970: Etude geologique d'un secteur des Monts Cariboo: Le Black Stuart Synclinorium, B.C., Canada; These, Docteur 3e Cycle L'Universite de Lille, France.
- Mansy, J.L. and Campbell, R.B.
1970: Stratigraphy and structure of the Black Stuart Synclinorium, Quesnel Lake map-area, British Columbia (93A); in Report of Activities, April to October, 1969, Geological Survey of Canada, Paper 70-1, pt. A, p. 38-41.
- Sutherland Brown, A.
1957: Geology of the Antler Creek Area, Cariboo District, British Columbia; British Columbia Department of Mines, Bulletin 38.
1963: Geology of the Cariboo River area, British Columbia; British Columbia Department of Mines and Petroleum Resources, Bulletin 47.
- White, Wm. H.
1959: Cordilleran Tectonics in British Columbia, American Association of Petroleum Geologists Bulletin, v. 43, p. 60-100.

EMR Research Agreement 2239-4-181/77

Penelope Morton¹

Regional and Economic Geology Division

Morton, Penelope, *Volcanic stratigraphy in the Shebandowan Ni-Cu Mine area, Ontario; in Current Research, Part B, Geological Survey of Canada, Paper 79-1B, p. 39-43, 1979.*

Abstract

The Shebandowan Mine area, northwestern Ontario, is underlain by two series of tholeiitic basalts and related volcanoclastic rocks. They are divided into a younger and older succession. A thick andesitic tuff breccia separates these successions. The older series is composed of pillowed basalts, mafic pyroclastic rocks and feldspar phyric flows. The younger volcanic succession can be subdivided into a) older high Mg basalts and picrites with intercalated mafic tuffs and b) younger pale green subaqueous pillowed basalts, pillow breccia and hyaloclastite. Associated with each series are peridotitic and gabbroic sills; peridotites within the younger rocks have related black-white, banded magnetite-chert iron formations, those within the older do not. Later intrusions are the Shebandowan Lake Stock and the Peewatai Lake Stock, respectively a synkinematic granodiorite and a high level quartz monzonite.

INCO's Ni-Cu mine occurs at the contact between an ultramafic body and the younger series of high Mg basalts. Structural data indicate that the orebody is at the top of the ultramafic. Cu/Cu+Ni (0.36) ratios of the orebody show that the sulphides separated from a basaltic magma or that after formation from a peridotitic magma, metamorphism and deformation caused remobilization of the orebody separating the Cu-rich part of the orebody from the Ni-rich.

Introduction

Detailed geological mapping (scale: 1:4800) of meta-volcanic and volcanoclastic rocks in the vicinity of Shebandowan Ni-Cu Mine (INCO Ltd.) was carried out in the summers of 1976 and 1977. This work serves as the basis for the author's Ph.D. thesis. The purpose of the study was to determine volcanic stratigraphy and geological structure of the area, which would, in turn, lead to an understanding of the volcanic environment and the potential for other Ni-Cu deposits in the area.

Shebandowan Mine is situated on the south shore of Lower Shebandowan Lake some 80 km west of Thunder Bay, Ontario. Access is via Highway 11 and a paved mine road built by INCO in 1969. The area mapped extends from Loch Maclean, in the west, to approximately 6.5 km east of the mine and south to Peewatai Lake.

History of the Shebandowan Mine area

Ni-Cu sulphides from the Shebandowan area were described by Cross (1920) and Tanton (1922). The initial discovery was made by Benner in 1913 and Cross in 1914 detected Ni in pits west of Discovery Bay. INCO purchased the property in 1936 and brought the mine into production in the early 1970s.

The area was originally mapped by Tanton (1922) and has been studied by Ontario Geological Survey geologists (Hodgkinson, 1968; Morin, 1973; and Srivastava and Fenwick, 1973). Unfortunately, the mine is located close to the junction of Hagey, Lamport, Haines and Begin townships, and correlation among map sheets is not readily made. The structural geology of the Shebandowan Belt has not been clearly understood, but the present study, and a regional study of the structural geology of the Shebandowan Belt being carried out by Greg Stott, University of Toronto, may help to elucidate the problem.

Watkinson and Irvine (1964) did a regional study of the petrography and chemistry of some of the ultramafic bodies within the Shebandowan Belt, including the ultramafic body associated with the Shebandowan Mine.

General Geology

Figure 7.1 depicts the general geology of the Shebandowan Mine area. Mapping was facilitated by access to INCO's drill core and their ground magnetometer surveys. The area is underlain by two series of tholeiitic metabasalts; the older is coeval with a volcanoclastic suite of rocks exposed in the southeast part of the map area. Grade of metamorphism varies from greenschist in the west to epidote-amphibolite facies in the southeast. The area has undergone at least two periods of folding. The first deformation resulted in isoclinally folded rocks with an east-west trend and vertical dip; the second caused gentle warping of the previous structures in a north-south direction. A major east-west fault (the Crayfish Creek Fault) and numerous northeast-southwest cross faults transect the area.

Older Succession of Metabasalts

The older basalt series strikes east-west and dips vertically. It has an apparent thickness of 1800 m in the west and thins to 300 m in the central part of the area. Stratigraphic cross-sections indicate that the true thickness is probably between 800 and 900 m. The unit is composed of tuffaceous sediments of basaltic composition interlayered with massive basalt flows which grade upwards into pillowed basalts. Towards the top of the sequence, basalts contain up to 25 per cent phenocrysts (1 to 3 cm) of plagioclase, which are concentrically zoned; these are opaque in thin section because of saussuritization and alteration to chlorite. Several distinct iron-rich carbonate rocks occur within the unit. They are composed of quartz, ankerite, pyrite and minor fuchsite and are easy to trace because of their unique mineralogy and their resistance to erosion.

Intrusive into this succession are small subround to lenticular bodies of gabbro which weather whitish grey and were initially mapped as diorite. Thin section studies showed that they are composed of plagioclase and pyroxene; they have between 45 and 47 per cent SiO₂ and thus have been reclassified as gabbro. Plagioclase and pyroxene of the gabbro have been saussuritized and altered to an opaque mixture of albite and chlorite and quartz, probably during regional metamorphism.

¹ Department of Geology, Carleton University, Ottawa, Canada.

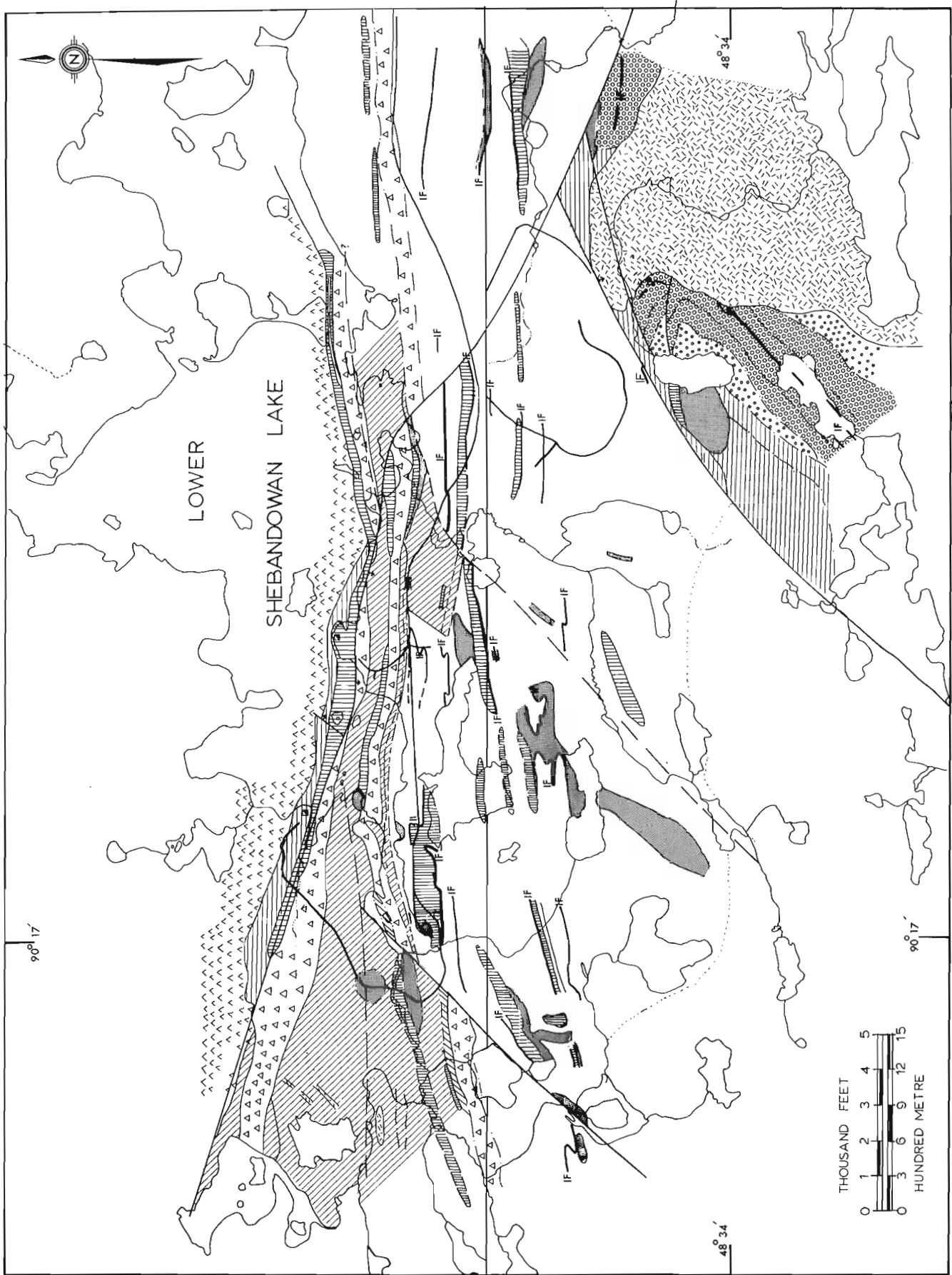


Figure 7.1. Geology of the Shebandowan Mine Area.

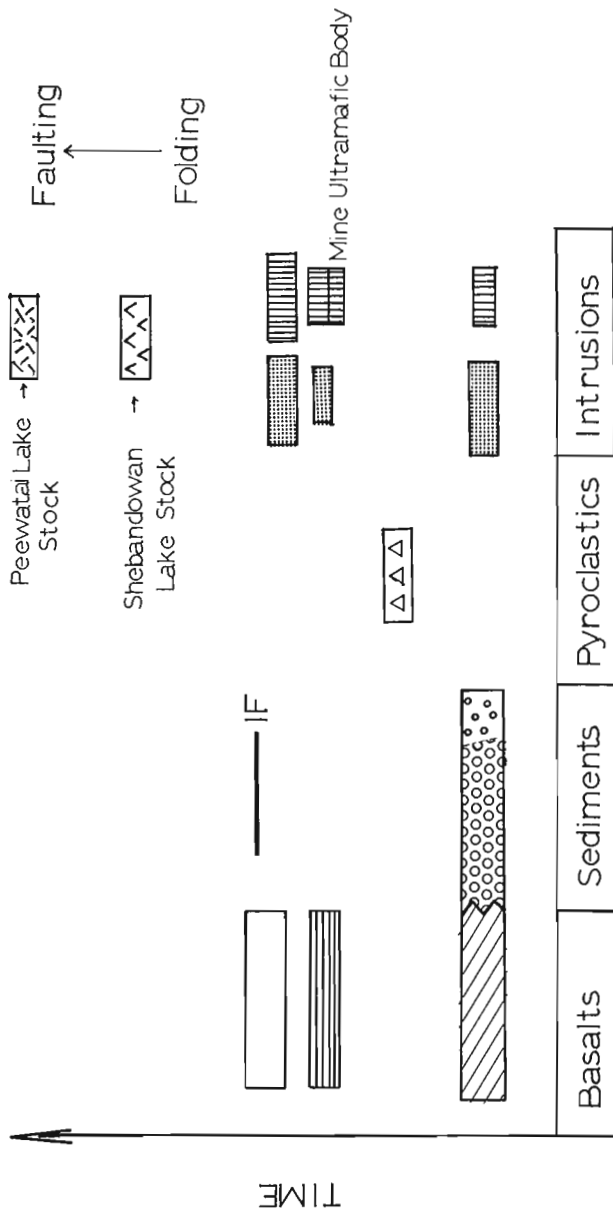
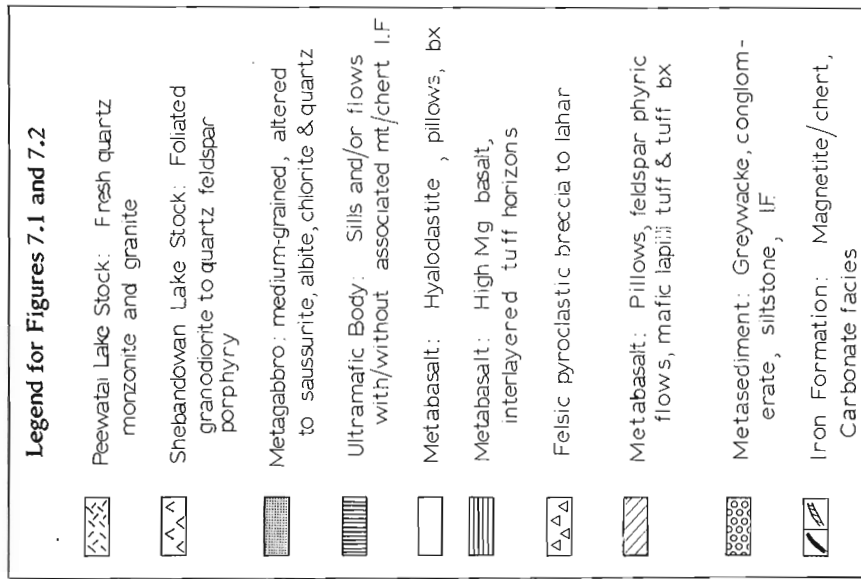


Figure 7.2. Temporal evolution of the Shebandowan Mine area.

About 5 to 10 per cent of the older succession is composed of ultramafic bodies that are conformable with the overall stratigraphy. In most cases they show relict textures indicating that they were dunites to peridotites. Primary mineralogy shows that olivines are usually poikilitically enclosed by clino- or orthopyroxene. No spinifex or pseudospinifex textures have been seen in any of these ultramafic rocks. Relict bladed pyroxenes and olivines, along with swallow-tail and hollow-core plagioclases have been found in the contact zone of one ultramafic body, which could have occurred by quenching upon intrusion into cold rocks.

Mineralogy is now a) lizardite-talc, c) talc-ankerite, and d) lizardite-talc-chlorite with minor ankerite. Antigorite is rarely seen. Secondary magnetite and disseminated primary chromite are present in all assemblages. Sulphides, where present, are usually pyrite-chalcopyrite, pyrite-chalcopyrite-millerite, pyrite-millerite, chalcopyrite-pyrrhotite-pentlandite, or pyrrhotite-pentlandite. Ilmenite is rare.

Unconformably overlying the older series of basalts is a felsic pyroclastic unit which strikes east-west, dips vertically and is repeated within the succession by folding (Fig. 7.1). In general, the southerly limb of the unit is grey-green, whereas the northern limb is red-green due to pervasive hematite alteration. The unit consists of green fragments in a red, feldspar-rich matrix or red feldspar-rich fragments in a green matrix. Maximum diameter of fragments varies from 1 cm to greater than 1 m, the majority being approximately 10 cm. Fragments consist of broken crystals of feldspar, quartz and hornblende, although hornblende seems to have grown across the fragments matrix boundaries and may in fact be metamorphic. Both matrix and fragments are andesitic in composition, although the redder fragments are slightly more siliceous.

In the west, the unit is composed of approximately 60-70 per cent tuffaceous material (tuff-breccia and lapilli tuff) and 30 per cent bedded sediments. The northern limb has up to 5 per cent magnetite with minor pyrite, whereas the southwestern limb has 2-3 per cent pyrite as well as a little magnetite. In the central part of the map area and toward the northeast, the unit is extremely sheared and altered; the fragments have been stretched and flattened into pancake-like and sometimes bomb-shaped fragments. Because of this, mine geologists have called this unit felsic agglomerate. In the eastern part of the area, only the southern limb of the unit is exposed and the rock is light grey and remarkably fresh. There is no hematite staining; fragments contain 10-20 per cent hornblende phenocrysts and broken crystals, as elsewhere in the unit. It is for this reason, as well as its chemical similarity to the felsic pyroclastic in the west, that this has been mapped as part of the same red-green pyroclastic unit.

Coeval with the older series of basalts is a group of metasediments mapped as Windigokan by Tanton (1922). These grade from greywackes with associated sedimentary magnetite-chert

iron formations, through greywacke-conglomerate to fine grained mafic siltstone. Siltstone shows crossbedding, graded bedding and channel scours. Channel scours were used in preference to cross and graded bedding for top determinations.

This group of rocks is exposed southeast of the Tinto Lake Fault. They strike northeast to southwest and dip approximately 70 degrees to the northwest and wrap around the Peewatai Lake Stock.

Clasts in the greywacke-conglomerate unit are matrix-supported and are half granitic and half basaltic. Clasts of granite are generally round to subround whereas basalt clasts are subround to subangular. Approximately 50-60 per cent of the basaltic clasts have large (1 cm) plagioclase phenocrysts and appear to be similar to the basalt flows that occur at the top of the older volcanic sequence.

Numerous felsic dykes are intrusive into the older volcanic sequence, the felsic pyroclastic unit, and the volcanoclastic rocks. They vary in thickness from 2 cm to several metres and from aphanitic to quartz and feldspar phyrific in texture. They weather pink or pinkish grey but most of the feldspar is hematite-stained albite. Less numerous and thick are diabasic dykes and sills. In some cases, these have been completely metamorphosed to actinolite, and were mapped as hornblende dykes.

Younger Volcanic Succession

Younger metabasalts overlie the felsic pyroclastic unit and compose half the stratigraphic section. They are divisible into two distinct types based on texture, mineralogy and chemistry. The earliest and least abundant are high Mg basalts (8-16% MgO) and interlayered fine grained tuffs, exposed north of the northern limb of the felsic pyroclastic unit and northwest of the previously described sedimentary package. These basalts compose 15 per cent of the younger volcanic succession.

Intercalated with this series of rocks are thin (0.5 to 3.3 m) olivine rich rocks that in thin section show relict textures indicating olivine cumulation zones (20% MgO). These zones are now composed of actinolite with minor talc and serpentine, primary chromite and secondary magnetite. They are conformable with the basalts and are interpreted to be picrites from their normative mineralogy, and the presence of pseudomorphs after olivine in thin section.

Intrusive into the Mg-rich basalts and sediments in the southeast part of the map area is a gabbro-ultramafic stock which is approximately 600 m in diameter. Relict garnets (now chlorite and carbonate) are recognizable in the more mafic part of the body. These have not been recorded in any other ultramafic body in the map area.

The rest of the younger volcanic succession is characterized by pale green, amygdaloidal pillowed basalt, pillow breccia and hyaloclastite with minor amounts of hornblende-bearing basalts. Within this succession are minor quantities of cherty tuff and black-white banded magnetite-chert iron formations (3-10 m thick) and thin red-black banded jasper-magnetite (1-6 m thick) iron formations. Thin graphitic pyrite-rich shales occur within this unit and can be traced using geophysical techniques. This shale has been intersected in numerous diamond-drill holes, but no outcrops have been discovered.

High-level sills of peridotite to dunite are intrusive into these basalts; ninety-five per cent of them have a black-white, magnetite-chert iron formation at the top. These are readily traced because of their high magnetic expression and known rock associations. The ultramafic bodies are usually 20 to 200 m thick and have fresh olivine, orthopyroxene and clinopyroxene in their cores, in strong

contrast to other ultramafic bodies in the area where no original minerals remain. Associated with these peridotites are light grey, medium grained gabbros that both conform to and crosscut the volcanic stratigraphy.

Later Intrusions

Intrusive into both series of metabasalts and volcanoclastic sediments are two felsic plutons. The Shebandowan Lake Stock, in the north is a medium grained, pinkish grey, highly foliated granodiorite with associated quartz feldspar porphyries. The Peewatai Lake Stock is a porphyritic quartz monzonite to granite which is pink on both weathered and fresh surfaces. Feldspars in the latter show very little alteration to sericite whereas those in the Shebandowan Lake Stock are either saussuritized or metamorphosed to albite. Mafic minerals in Peewatai Lake Stock are fresh hornblende and biotite whereas chlorite is the predominant mafic mineral in Shebandowan Lake Stock. The Shebandowan Lake Stock is interpreted to be synkinematic with folding whereas intrusion of the Peewatai Lake Stock represents the last igneous activity in the area.

A schematic diagram (Fig. 7.2) shows the temporal evolution of the volcanic and associated rocks in the Shebandowan Mine area.

Economic Geology

Mineralogy and Description

INCO's Ni-Cu mine is located at the northern contact of an ultramafic body (herein called the mine ultramafic) and the southern contact of a series of high Mg basalts with intercalated picrites (younger succession). Structurally, the facing direction is toward the north, indicating that the orebody occurs at the top of the mine ultramafic.

Ore is composed of pyrite-pyrrhotite-pentlandite-chalcopryite and magnetite with minor chromite and Pd minerals (Watson, 1928; Watkinson et al., 1978). The overall Cu/Cu+Ni ratio is 0.36. The ore is generally massive or breccia sulphide and there is essentially no net-textured or disseminated ore in the mine ultramafic. Contacts are usually sharp and the orebody contains numerous inclusions which have been mapped underground as peridotite, basalt and feldspar porphyry dyke material. Preliminary studies of the inclusions indicate that most of them are now hornblende, peridotite and porphyry dyke material. No distinctive basalt inclusions have been recognized. Minor chalcopryite with pentlandite and pyrrhotite is commonly found in the inclusions.

Genesis

Initially this orebody was interpreted to be an immiscible sulphide melt that separated from and then settled toward the bottom of the mine ultramafic. Magmatic and synvolcanic orebodies of this type generally have Cu/Cu+Ni ratios less than 0.1 (Naldrett and Cabri, 1976). Because the Shebandowan orebody is interpreted to be on top of the mine ultramafic, and has a high Cu/Cu+Ni ratio, this explanation does not seem tenable.

If the orebody is a result of a sulphide flow that lagged behind a peridotite intrusion, and intruded (or extruded) above the ultramafic the high Cu/Cu+Ni ratio still has to be explained. The average MgO content of the mine ultramafic is 37.8 per cent MgO (anhydrous). Sulphide liquids separating from a magma of this composition would have Cu/Cu+Ni ratios less than 0.1 (Naldrett and Cabri, 1976). This is not the case at Shebandowan. If the orebody is an exhalative Ni-Cu deposit (Lusk, 1976) the same arguments concerning Cu/Cu+Ni ratios might still apply.

Alternatively, remobilization of sulphides may have occurred during metamorphism and deformation, leaving behind the nickel-rich portion of the ore. Either this part has not been discovered or it has been eroded away. Where sulphides have been remobilized on a small scale within the mine, they are always chalcopyrite-rich. Alternatively, the sulphides of the Shebandowan orebody may have separated from a magma of basaltic composition; and the sulphides were extruded as a flow or settled from a basalt flow or series of flows. The Cu/Cu+Ni ratio in the high Mg basalts north of the orebody have Cu/Cu+Ni ratios very close to that of the orebody. It is hoped that detailed work on the inclusions in the orebody, as well as a re-evaluation of facies directions within the mine sequence (mine ultramafic and high Mg basalts), will lead to a better understanding of the genesis of this orebody.

Conclusions

The Shebandowan Mine area is underlain by two series of tholeiitic basalts and related volcanoclastic sediments. They are divided into a younger and older succession. The older succession is composed of pillowed basalts, mafic pyroclastic rocks and feldspar phyric flows. Unconformably overlying these older rocks is an andesitic tuff breccia, probably a submarine pyroclastic flow deposit. The younger succession itself can be subdivided into a) older high Mg basalts and picrites, and b) younger pale green subaqueous pillowed basalts with a large percentage of pillow breccia and hyaloclastite. Intrusive into each succession are ultramafic bodies; within the older rocks they have no related chert-magnetite iron formations whereas within the younger group, 95 per cent have related iron formations.

Coeval with the older succession are volcanoclastic conglomerates, greywackes and mafic siltstones. These are exposed in the southeast portion of the map area.

The Shebandowan Ni-Cu orebody seems to occur at the top of the mine ultramafic, at the contact with the high Mg basalts. Its Cu/Cu+Ni ratio indicates that the sulphides were in equilibrium with a basaltic magma when they formed or that after separating from a peridotitic magma, remobilization occurred causing metamorphic segregation within the sulphide body.

Acknowledgments

This study is part of the author's Ph.D. thesis, concerning a study of the different ultramafic bodies and related rocks in the Shebandowan Mine Area. Discussions with G. Skippen, J. Franklin and D. Watkinson as well as INCO geologists B. Osborne and D. Moses have proved to be very helpful. INCO Ltd. kindly gave permission to map and sample the mine property, sample diamond-drill core and gave access to INCO geology and aeromagnetic surveys.

References

- Cross, J.C.
1920: Lake Shebandowan nickel deposit; Ontario Department of Mines, v. 29, pt. 1, p. 225-234.
- Hodgkinson, J.M.
1968: Geology of the Kashabowie area; Ontario Department of Mines Geological Report 53, 35 p.
- Lusk, J.
1976: A possible volcanic-exhalative origin for lenticular nickel sulfide deposits of volcanic association, with special reference to those in western Australia; Canadian Journal of Earth Sciences, v. 13, p. 451-458.
- Morin, J.A.
1973: Geology of the Lower Shebandowan Lake area, District of Thunder Bay; Ontario Department of Mines Geological Report 110, 45 p.
- Naldrett, A.J. and Cabri, L.J.
1976: Ultramafic and related mafic rocks: Their classification and genesis with special reference to the concentration of nickel sulfides and platinum-group elements; Economic Geology, v. 71, p. 1131-1158.
- Srivastava, P. and Fenwick, K.G.
1973: Lamport Township, District of Thunder Bay; Ontario Division of Mines, Preliminary Map P826, Geological Series, scale 1 inch to 1/4 mile.
- Tanton, T.L.
1922: Geological Survey of Canada Summary Report, Pt. D, p. 1-8.
1938: Shebandowan area; Geological Survey of Canada Map 338A.
- Watkinson, D.H. and Irvine, T.N.
1964: Peridotitic intrusions near Quetico and Shebandowan, Northwestern Ontario: A contribution to the petrology and geochemistry of ultramafic rocks; Canadian Journal of Earth Sciences, v. 1, p. 63-98.
- Watkinson, D.H., Hak, J., Morton, P., and Johan, Z.
1978: Merenskyite from the Shebandowan Ni-Cu Mine, Northwestern Ontario; Canadian Mineralogist, v. 16, p. 659-663.
- Watson, B.J.
1928: Platinum-bearing nickel copper deposit on Lower Shebandowan Lake, district of Thunder Bay; Ontario Department of Mines, v. 37, Pt. 4, p. 128-149.

E.M.R. Research Agreement 2239-4-84/78

V.E. Chamberlain¹, R. St J. Lambert¹, H. Baadgaard¹ and N.H. Gale²

Chamberlain, V.E., Lambert, R. St J., Baadgaard, H., and Gale, N.H., *Geochronology of the Malton Gneiss Complex of British Columbia; in Current Research, Part B, Geological Survey of Canada, Paper 79-1B, p. 45-50, 1979.*

Abstract

A distinctive horizon of garnetiferous siliceous gneiss in the Malton Gneiss Complex, near Valemount, British Columbia, yields a whole rock rubidium strontium date of 3235 ± 258 Ma (initial $^{87}\text{Sr}/^{86}\text{Sr}$ 0.7001 ± 32); and episodic discordant uranium-lead zircon dates of close to 2500 Ma and 1200-1300 Ma. Hornblende gneiss structurally concordant with the Archean siliceous gneiss yield a rubidium-strontium "errorchron" of 996 ± 395 Ma (initial $^{87}\text{Sr}/^{86}\text{Sr}$ 0.7067 ± 18). Intrusive sheets of alkaline granite gneiss give rubidium-strontium whole rock dates of 887 ± 24 Ma (I.R. 0.7023 ± 7) and 533 ± 12 Ma (I.R. 0.7111 ± 2).

Introduction

The Malton Gneiss Complex is exposed over an area of approximately 1000 km² in the Malton, Monashee, and Selwyn mountain ranges, centred at approximately 119°W, 52°30'N near Valemount, British Columbia (Fig. 8.1). It occurs as an enigmatic block or blocks of amphibolite facies gneiss surrounded by metasediments of presumed Proterozoic age, and

is located to the west of a longitudinal culmination in the Rocky Mountains which brings Proterozoic rocks to the surface in the area between Mount Robson and Jasper.

The gneiss have attracted interest because they are unlike any other rocks found in the region, they occur in close proximity on both sides of a major fault, the Rocky Mountain Trench (Fig. 8.1), and they may be shield rocks and hence have some bearing on the vexing question of the western limit of the Canadian Shield. Campbell (1973) has argued the case for basement involvement in the Omineca Crystalline Belt.

The area was first mapped by Campbell (1968) and he, Giovanella (1967) and Wheeler et al. (1972) described the gneisses as fault bounded, although in The Cherries area, to the east of the Rocky Mountain Trench, Wheeler et al. (1972) suggested that a metamorphic "aureole" surrounds the gneiss.

The metasediments surrounding the gneisses to the west of the Rocky Mountain Trench are known as the Kaza Group. They consist of phyllite and muscovite-garnet-schist with psammitic and calc-silicate bands, reaching staurolite-kyanite grade in the north of the area and garnet grade in the south. The Kaza Group has been equated with the Horsethief Creek Group of the Selkirk Mountains (Campbell, 1968), and unmetamorphosed "equivalents" of this group in the Rocky Mountains have yielded a detrital mica potassium-argon date of 1535 Ma (Wanless et al., 1967).

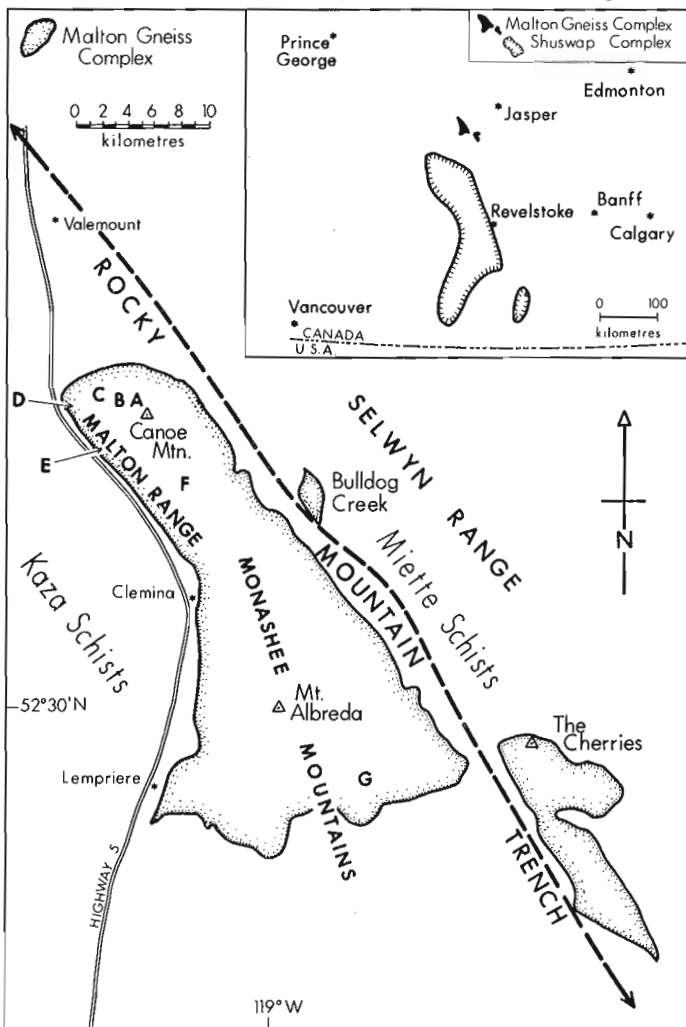


Figure 8.1. Outline map to show location of Malton Gneiss outcrop and specimen localities for the isotopically analyzed samples.

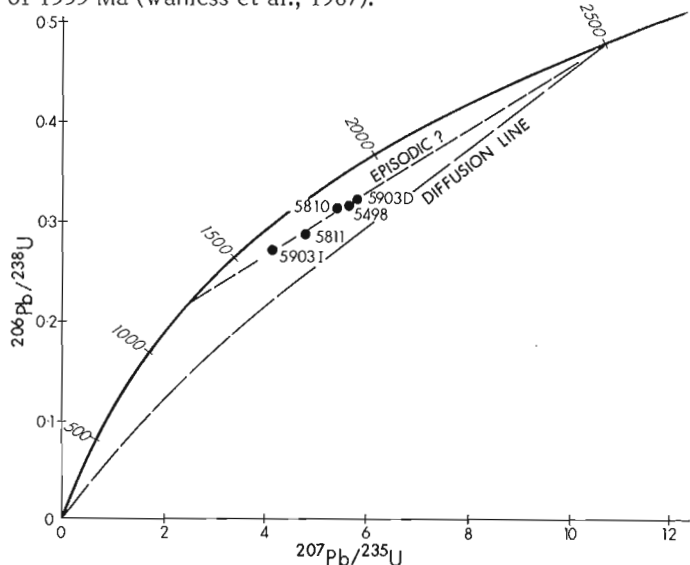


Figure 8.2. U-Pb isotopic analyses of bulk zircon populations from group 2 gneiss.

¹ Department of Geology, University of Alberta, Edmonton, Alberta, Canada T6G 2E3

² Department of Geology and Mineralogy, University Museum, Parks Road, Oxford, England OX1 3PR

Table 8.1
Rb-Sr analyses on Malton Gneiss whole-rock samples

Sample	Location and Grid reference	Lithology	Rb ppm	Sr ppm	Rb/Sr	$^{87}\text{Rb}/^{86}\text{Sr}$ $\pm 2\%$	$^{87}\text{Sr}/^{86}\text{Sr}$ $\pm 2\sigma\bar{x}$	Group
5502	Canoe Mt. 499 418	hornblende gneiss	12	430	0.029	0.0839 ± 17	0.70793 ± 9	1
5803	Canoe Mt. 530 420	hornblende gneiss	38	394	0.097	0.281 ± 6	0.71029 ± 8	1
5804	Canoe Mt. 530 420	hornblende gneiss	56	363	0.154	0.446 ± 9	0.71216 ± 10	1
5805	Canoe Mt. 530 420	hornblende gneiss	44	352	0.125	0.362 ± 7	0.71229 ± 8	1
5806	Canoe Mt. 530 420	hornblende gneiss	19	358	0.053	0.153 ± 3	0.70932 ± 15	1
5807	Canoe Mt. 524 422	hornblende gneiss	42	270	0.156	0.452 ± 9	0.71335 ± 9	1
5808	Canoe Mt. 5235 4225	hornblende gneiss	30	265	0.113	0.327 ± 7	0.71362 ± 10	1
5809	Canoe Mt. 523 423	hornblende gneiss	82	350	0.235	0.680 ± 14	0.71444 ± 13	1
5812	Canoe Mt. 515 426	hornblende gneiss	43	365	0.117	0.339 ± 7	0.71075 ± 6	1
5819B	Malton Rge. 477 420	biotite amphibolite	67	230	0.290	0.840 ± 17	0.71156 ± 8	1
5498	Canoe Mt. 520 421	granodiorite gneiss	69	340	0.202	0.586 ± 12	0.72750 ± 10	2
5810	Canoe Mt. 520 420	granite gneiss	99	309	0.320	0.929 ± 19	0.74547 ± 7	2
5811	Canoe Mt. 520 420	tonalite gneiss	104	274	0.382	1.111 ± 22	0.75158 ± 14	2
5903I	Canoe Mt. 519 419	leucocratic tonalite gneiss	86	344	0.250	0.722 ± 14	0.72629 ± 14	2
5893C	Malton Rge. 578 363	cataclastic tonalite gneiss	117	247	0.474	1.375 ± 28	0.77397 ± 10	2
5897C	Monashee Mts. 707 132	leucocratic granite gneiss	48	134	0.358	1.037 ± 21	0.74771 ± 12	2
5499	Canoe Mt. 503 426	alkaline granite gneiss	62	157	0.395	1.130 ± 23	0.71891 ± 10	3
5500	Canoe Mt. 500 422	mesocratic olig-qz-gneiss	50	188	0.27	0.782 ± 16	0.71168 ± 15	3
5501	Canoe Mt. 500 419	alkaline granite gneiss	128	126	1.01	2.93 ± 6	0.74072 ± 6	3
5814	Canoe Mt. 514 430	alkaline bi-granite gneiss	51	30	1.71	4.96 ± 10	0.74791 ± 16	3
5817	Canoe Mt. 491 422	hololeucocratic-alkaline granite gneiss	66	69	0.95	2.77 ± 6	0.73933 ± 17	3

Table 8.1 (cont.)

Sample	Location and Grid reference	Lithology	Rb ppm	Sr ppm	Rb/Sr	$^{87}\text{Rb}/^{86}\text{Sr}$ $\pm 2\%$	$^{87}\text{Sr}/^{86}\text{Sr}$ $\pm 2\sigma$	Group
5820	Malton Rge. 477 420	hololeucocratic-alkaline bi-granite gneiss	69	34	2.03	5.93 ± 12	0.77878 ± 16	3
5821	Malton Rge. 477 4195	alkaline granite gneiss	63	22	2.82	8.21 ± 16	0.77395 ± 11	3
5822	Malton Rge. 477 4195	alkaline tonalite gneiss	97	175	0.56	1.61 ± 3	0.72328 ± 7	3
5823	Malton Rge. 477 4195	alkaline granite gneiss	61	33	1.88	5.46 ± 11	0.75498 ± 7	3
AC 11	Canoe Mt. 533 412	alkaline granite gneiss	104	56	1.87	5.44 ± 11	0.75310 ± 6	4
5803X	Canoe Mt. 532 415	alkaline tonalite gneiss	37	388	0.095	0.275 ± 6	0.71339 ± 8	4
5815	Canoe Mt. 509 531	alkaline granite gneiss	92	33	2.78	8.12 ± 16	0.79518 ± 7	4
5816	Canoe Mt. 508 430	alkaline bi-granite gneiss	64	89	0.72	2.10 ± 4	0.72912 ± 14	4
5845B	Malton Rge. 509 377	alkaline granite gneiss	187	51	3.67	10.8 ± 5	0.82174 ± 14	4

The metasediments surrounding the gneisses to the east of the Rocky Mountain Trench, the Middle Miette Group, have also been tentatively correlated with the Kaza Group (Campbell, 1967). This correlation is based largely on stratigraphic thicknesses, lithological similarities and possible equivalence of carbonate beds. The Middle Miette Group consists of Precambrian phyllite and psammite of staurolite-kyanite grade, overlain conformably in turn by the Upper Miette Group and Lower Cambrian quartzite of the Gog Group.

About 100 km south of the Malton Gneiss Complex lies the much larger Shuswap Metamorphic Complex (insert Fig. 8.1), but the two differ fundamentally in that the Malton Gneiss Complex consists almost entirely of meta-igneous rocks (Chamberlain et al. in press) whereas the Shuswap Complex is apparently of mostly metasedimentary origin with igneous rocks forming only a small proportion of the cores of mantled gneiss domes (Wanless and Reesor, 1975) and in a few localities elsewhere in the Complex. Zircons from one of these Shuswap meta-igneous rocks (a biotite-hornblende augen granodiorite gneiss from the Thor Odin dome) have yielded U-Pb discordant dates of 1960^{+35}_{-45} Ma and 175^{+73}_{-81} Ma, which are interpreted by Wanless and Reesor as being the age of formation of the igneous rock and the age of metamorphism and deformation respectively. Wanless and Okulitch (1976) have reported a minimum U-Pb date on zircons from granitic gneiss within the Shuswap Complex; and Duncan (1978) has obtained imprecise Rb-Sr isochrons of 3000 Ma, 2000 Ma, and 935 Ma on whole rocks from various localities in the Shuswap. The Clachnacudainn Salient, a wedge of meta-igneous granodiorite gneiss tectonically or intrusively "emplaced between two contrasting panels of amphibolite facies metasedimentary rocks" (Gilman, 1972),

has provided an imprecise 750 Ma Rb-Sr isochron (Blenkinsop, 1972) and a 372 Ma U-Pb date on zircons (Wanless and Okulitch, 1976). Okulitch et al. (1975) have reported discordant U-Pb zircon ages of 372 Ma and 50-175 Ma for the Mount Fowler Batholith, a large granitic body intruding Paleozoic sediments on the western margin of the Shuswap Complex. They interpret the Devonian date as being the age of intrusion and the younger date as being the time of most recent deformation in the area.

Petrology and Geochemistry

Chamberlain et al. (in press) have described the petrology and geochemistry of the Malton Gneiss Complex. In the Canoe Mountain area, four distinct petrological/geochemical groups have been defined.

The most common rock type (designated group 1 gneiss) in that area is a lineated hornblende gneiss of dioritic or basaltic composition, enriched in potassium and depleted in aluminum. It frequently contains up to 10 per cent biotite, which is often concentrated on shear surfaces. The yttrium-niobium ratio of this rock is variable, the yttrium values being consistently low (< 50 ppm) and the niobium varying from 10 to 80 ppm. Amphibolites, some of which have been extensively biotitized, are also included in the group 1 gneiss.

Group 2 gneiss is rare and quite distinctive; it consists of garnetiferous granitic and tonalitic gneiss; again enriched in potassium, but low in aluminum and calcium. It has a characteristic yttrium-niobium ratio of 2, distinguishing it from any of the other gneissic units in the complex. The rocks are equigranular, non-porphyroblastic, lineated or foliated quartz oligoclase biotite gneiss, some also containing

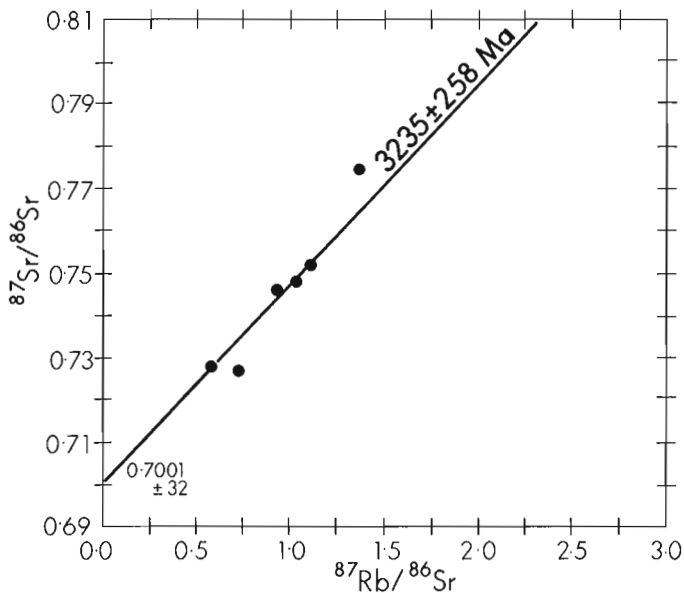


Figure 8.3. Rb-Sr isochron diagram for group 2 gneiss samples. These samples come from comparatively inert tonalitic gneiss with a low range of Rb-Sr compared with the group 2 gneiss samples of Figure 8.5.

microcline, muscovite, or a green-brown hornblende. Zircon and sphene are typical accessories, with rare apatite, oxide, and allanite. It is a normal siliceous gneiss showing no evidence of unusual metamorphic history or of greatly disturbing metasomatism. The only visible sign of retrogression is epidotisation of the garnets many of which are hollow or spongy, some with epidote cores. Their texture however is occasionally cataclastic with deformed plagioclase, granulated quartz and bent biotite. Group 2 gneiss occurs at one horizon on Canoe Mountain (B in Fig. 8.1), where it appears to be structurally concordant with group 1 gneiss. It also occurs at a few other localities in the Malton Range and Monashee Mountains.

Gneisses of groups 3 and 4 occur as intrusive sheets and are similar petrologically. Both are peralkaline leucocratic or hololeucocratic granite gneiss, slightly low in alumina; their geochemistries differ, group 3 being characteristically lower in yttrium and rubidium (resulting in lower Y/Nb and higher K/Rb) than group 4 gneiss. They are composed of quartz, microcline, oligoclase (rarely albite), biotite and a deep green almost opaque amphibole. Sphene is common; apatite, zircon and oxide rare. They are banded on a microscopic and megascopic but not a mesoscopic scale. Field observations suggest that the normal hand specimen is representative of 1 m³, that is, any other hand specimen within such a volume from the same locality would give the same result.

Analytical Methods

Rock samples weighing 2-4 kg were collected for rubidium-strontium analyses and aliquots taken from about 100 g of fine powder representative of each whole rock sample. The analytical methods used were that of Pankhurst and O'Nions (1973) for rubidium and strontium concentrations, using a Phillips 1200 XRF spectrometer, and that described by Galet et al. (1975) for ⁸⁷Sr/⁸⁶Sr, using a V.G. Micromass 30 mass spectrometer. Analyses performed in Oxford and Edmonton by the same operator give good agreement, the Oxford isotope analyses being standardized by subtracting an Eimer and Amend correction of 1 x 10⁻⁴ and

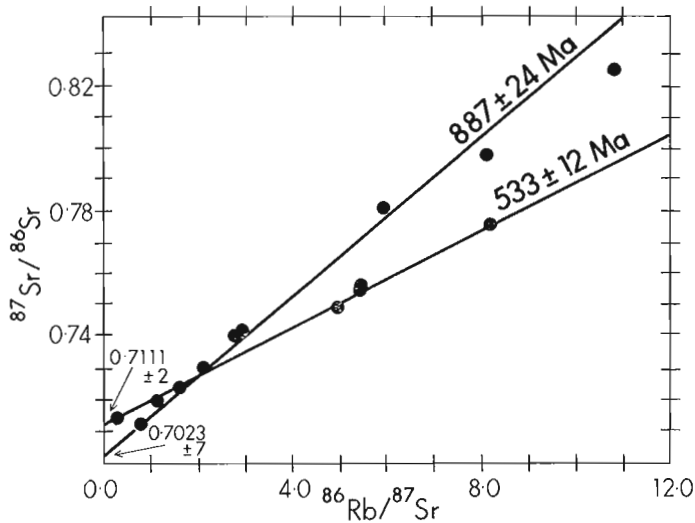


Figure 8.4. Rb-Sr isochron diagram for the mildly peralkaline discordant granite-gneiss sheets. Two distinct populations are present, consistent with intrusion at about 887 Ma and partial re-setting at about 533 Ma.

those performed in Edmonton by subtracting a SRM 987 correction of 7 x 10⁻⁵, assuming a value of 0.70800 for Eimer and Amend and 0.71014 for SRM 987. Rubidium and strontium analyses are given in Table 8.1 and the whole rock rubidium-strontium plots in Figures 8.2-8.4.

Five whole rock samples weighing 10-20 kg from the group 2 gneiss on Canoe Mountain were crushed and zircons separated. The bulk zircon samples were analyzed for lead and uranium, using the method described by Krogh (1973). These analyses are given in Table 8.2 and shown on a concordia plot in Figure 8.2.

Throughout this paper, the internationally recommended decay constants have been used (Steiger and Jäger, 1977).

Discussion

Rubidium-strontium analyses for six group 2 gneiss samples are given in Table 8.1 and plotted on Figure 8.3. A least-squares regression line drawn through four of these points yields a date of 3235 ± 258 Ma and an initial strontium ⁸⁷/⁸⁶ ratio of 0.7001 ± 32, at the 95 per cent confidence level (MSWD = 2.25). Three of the samples included in the date calculation came from the distinctive garnetiferous horizon on Canoe Mountain (B on Fig. 8.1), and one from the Windfall Creek area in the Monashee Mountains, about 30 kilometres to the south (G on Fig. 8.1). Of the two samples not included in the calculation, one was from the same garnetiferous horizon on Canoe Mountain (B on Fig. 8.1) and one from the Malton Range (F on Fig. 8.1). These two samples were not included in the isochron calculation because they would have produced an impossibly low initial ⁸⁷/⁸⁶ strontium ratio; but they are both obviously older than gneiss from any of the other groups and are probably Archean, their position off the isochron being due to disturbance by later events. (5893C has a cataclastic texture, with granulated quartz grains and bent mica flakes. 5903I is banded on the microscopic scale with abundant green hornblende in some bands.) It is difficult to see how the isochron itself could have been produced by a disturbance of the rubidium-strontium systematics, since rubidium/strontium

abundance disturbances of a factor of 3 would be required to bring these samples in line with results from the other units and there is no evidence that such large changes have occurred. The rocks are neither abnormally rich in strontium or strontium acceptor minerals, nor abnormally poor in rubidium. Amphibole, which in other units has been extensively biotitized, with a possible concomitant influx of rubidium, is typically absent in these rocks. Furthermore, these group 2 rocks are of a distinctive lithology, easily differentiated from the other units on mineralogical, petrological, and geochemical criteria, and on Canoe Mountain they occur in a small identifiable horizon.

Five rocks (four of which had previously been analyzed for rubidium and strontium) from this same horizon had zircons separated and analyzed for lead and uranium. These bulk zircon analyses are given in Table 8.2 and plotted on Figure 8.2. The uranium-lead systematics of the zircons are discordant, and in Figure 8.2 the data points appear to lie on an episodic lead loss line cutting the concordia at about 2500 Ma and 1200-1300 Ma. The older date appears to confirm the Archean nature of this gneiss, but a ~1200 Ma event has not yet been detected by Rb-Sr.

Rubidium-strontium whole rock analyses on nine group 3 gneiss samples (from areas C and D on Figure 8.1) and five group 4 gneiss samples (areas A, C and E on Figure 8.1) are shown in Table 8.1 and on Figure 8.4. Two sets of least squares regressions (with one point being used in both calculations) produced isochrons giving dates of 887 ± 24 Ma and 533 ± 12 Ma at the 95 per cent confidence level. Gneisses from both groups and from the various parts of the complex plot on both lines, suggesting two separate intrusive events. The initial ratios are consistent with the younger event being a reworking of material intruded 350 Ma earlier.

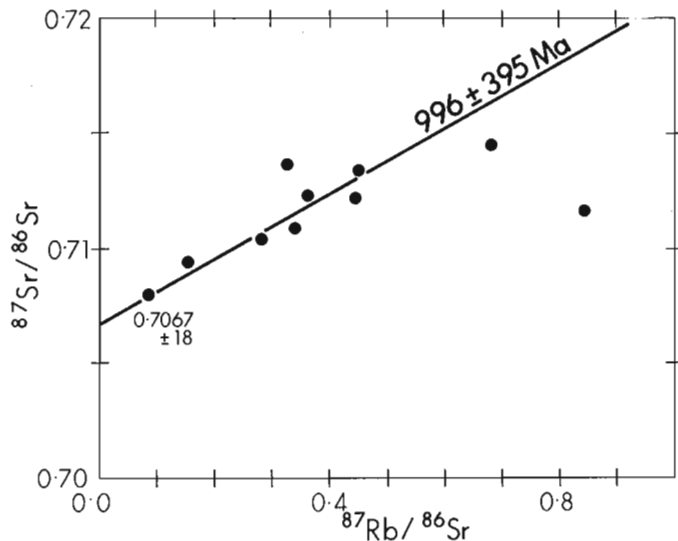


Figure 8.5. Rb-Sr isochron diagram for group 1 gneiss samples. The best-fit line at 996 Ma has little age significance, but the initial ratio of 0.7067 ± 0.0018 is consistent with the re-setting of Rb-Sr systems originally generated in the Archean and disturbed in the later Proterozoic.

Table 8.2
U-Pb analyses on Malton Gneiss Zircons

Sample	Measured lead ratios			ppm U	ppm ²⁰⁶ Pb
	206/204	207/204	208/204		
5498	15500	2042	1500	403.7	109.8
5810	45400	5730	4994	670.2	180.8
5811	19150	2352	2009	380.1	93.7
5903D	33380	4406	2931	604.8	167.7
5903I	16300	1824	1772	599	140.2
Errors at 1σ level	± 1%	± 0.1%	± 0.1%	± 3 ppm	± 0.5 ppm

The scatter of points on the rubidium-strontium plot for the group 1 gneiss samples (Fig. 8.5) is an indication of modification of these rocks by a later event or events. Of the ten points shown on Figure 8.5, nine are hornblende gneiss samples from Canoe Mountain (areas A, B and C) and these were used to calculate the least-squares regression line shown. The date computed from the slope of this line has no real meaning, except to show that the rocks have been partially reset, possibly during a Proterozoic event. The hornblende gneisses may be Archean since, on Canoe Mountain, they appear to be concordant with the group 2 Archean unit. The tenth point, plotting to the right on Figure 8.5, was not included in the isochron calculation. It is a biotitized amphibolite and appears to be recording a mineral age.

Modification of this group 1 unit is apparent from its petrology. These rocks produce an unusual trend on a calcium-yttrium plot, they have high and variable alkali content, abnormally high potash content, and have suffered extensive biotitization (Chamberlain et al., in press). A period of metasomatism involving the exchange of alkalis and lime, possibly during the intrusion of the group 3 and 4 units, could explain the scatter on this rubidium-strontium plot.

Conclusions

The Malton Gneiss Complex contains felsic rocks of Archean age occurring in an identifiable garnetiferous horizon or horizons, and having a distinctive mineralogy, petrology and geochemistry. Results from the hornblende gneiss, which forms the major part of the complex on Canoe Mountain, scatter widely on a rubidium-strontium plot, but a least-squares regression suggests that the gneiss may have been modified during a Proterozoic event; and its structural conformity with Archean gneiss suggests that it may be of Archean age. Peralkaline granite sheets were intruded into the complex in the Late Proterozoic (c. 900 Ma) and were remobilized during Cambrian times. These sheets may be responsible for the widespread potash metasomatism apparent in all the rocks of the complex.

The dates recorded by the rocks of the Malton Gneiss Complex differ markedly from most other dates recorded in the region. The nearest exposures of Archean rocks are 200 km away in the Shuswap Complex, 1150 km away in the Slave Province, or 1000 km away in Montana. The Archean ages support the interpretation of fault contacts with the Kaza and Miette groups and confirm basement involvement in the Malton Gneiss Complex.

References

- Blenkinsop, J.
1972: Computer assisted mass spectrometry and its application to Rb/Sr geochronology, Ph.D. thesis, University of British Columbia, Vancouver.
- Campbell, R.B.
1967: McBride (93H) map area; in Report of Activities, Geological Survey of Canada, Paper 67-1, pt. A., p. 53-55.
1968: Canoe River, British Columbia; Geological Survey of Canada, Map 15-1967.
1973: Structural cross-section and tectonic model of the southeastern Canadian Cordillera; Canadian Journal of Earth Sciences, v. 10, p. 1607-1620.
- Chamberlain, V.E., Lambert, R. St J., and Holland, J.G.
The Malton Gneiss: Archean Gneisses in British Columbia; Precambrian Research (in press).
- Duncan, I.J.
1978: Rb/Sr whole rock evidence for three Pre-Cambrian events in the Shuswap Complex, S.E. BC; in Abstracts with Programs, Geological Association of Canada, Mineralogical Association of Canada, Geological Society of America Annual Meeting, Toronto, p. 392-393.
- Gale, N.H., Arden, J.W., and Hutchinson, R.
1975: The chronology of the Nakhla achondritic meteorite; Earth Planetary Science Letters, v. 26, p. 195-206.
- Gilman, R.A.
1972: Geology of the Clachnacudainn Salient near Albert Canyon, British Columbia; Canadian Journal of Earth Sciences, v. 9, p. 1447-1454.
- Giovanella, C.A.
1967: Structural studies of the metamorphic rocks along the Rocky Mountain Trench at Canoe River, British Columbia; in Report of Activities, Part A, Geological Survey of Canada, Paper 68-1, pt. A., p. 27-31.
- Krogh, T.E.
1973: A low contamination method for hydrothermal decomposition of zircon and extraction of U and Pb for isotopic age determinations; Geochimica et Cosmochimica Acta, v. 37, p. 485-494.
- Okulitch, A.V., Wanless, R.K., and Loveridge, W.D.
1975: Devonian plutonism in south-central British Columbia; Canadian Journal of Earth Sciences, v. 12, p. 1760-1769.
- Pankhurst, R.J. and O'Nions, R.K.
1973: Determination of Rb/Sr and $^{87}\text{Sr}/^{86}\text{Sr}$ ratios of some standard rocks and evaluation of X-ray fluorescence; Chemical Geology, v. 12, p. 127-136.
- Steiger, R.H. and Jäger, E.
1977: Subcommission on geochronology: convention on the use of decay constants in geo- and cosmo-chronology; Earth and Planetary Science Letters, v. 36, p. 359-362.
- Wanless, R.K. and Okulitch, A.V.
1976: Geochronologic studies of the Shuswap Metamorphic Complex, Southern B.C.; in Program with Abstracts, Vol. 1, Geological Association of Canada, Annual Meeting, Edmonton, Alberta, p. 47.
- Wanless, R.K. and Reesor, J.E.
1975: Precambrian zircon age of orthogneiss in the Shuswap Metamorphic Complex, British Columbia; Canadian Journal of Earth Sciences, v. 12, p. 326-332.
- Wanless, R.K., Stevens, R.D., Lachance, G.R., and Edmonds, C.M.
1967: Age determinations and geological studies, K-Ar isotopic ages. Report 7; Geological Survey of Canada, Paper 66-17, p. 76 (GSC sample 65-94).
- Wheeler, J.O., Campbell, R.B., Reesor, J.E., and Mountjoy, E.W.
1972: Structural style of the southern Canadian Cordillera. Field Excursion X01-A01; 24th International Geological Congress, Montreal.

Project 700092

R.V. Wahlgren¹
Terrain Sciences Division

Wahlgren, R.V., *Ice-scour tracks in eastern Mackenzie Bay and north of Pullen Island, Beaufort Sea; in Current Research, Part B, Geological Survey of Canada, Paper 79-1B, p. 51-62, 1979.*

Abstract

Ice-scour tracks are created by ice pressure-ridge keels and ice islands scraping the seabed. Tracks visible on echosounding and side-scan sonar records obtained in water depths of 25 to 50 m are analyzed quantitatively in order to understand the relationship between track form and the processes that created the tracks. A system of classification and methods for analyzing data on ice-scour tracks are presented. Seabed morphology affects the length of ice-sonar tracks that can be left by a grounding keel but does not deflect the keel. In water depths less than 45 m, ice keels that are being driven upslope usually do not penetrate deeper into the seabed sediment (silty clay or clay) but rise along the seabed slope.

Introduction

Ice-scour tracks found on the continental shelf of the Beaufort Sea at depths to 80 m are unique evidence that ice keels scraped across the seabed. Organizations in government and industry concerned with offshore hydrocarbon exploration, development, and production in the region wish to understand the magnitude of the hazard that grounding ice keels pose to wellhead and pipeline installations in the seabed. Ice-scour tracks in the Canadian Beaufort Sea have been researched by Shearer et al. (1971), Pelletier and Shearer (1972), Shearer and Blasco (1975), Hnatiuk and Brown (1977), and Lewis (1977a, b). This report is based mainly upon data from echograms and side-scan sonographs collected in 1974 by the Geological Survey of Canada. The analyses described below were carried out as part of a Master of Arts thesis at the Department of Geography, Carleton University, Ottawa (Wahlgren, 1979) to which the reader is referred for additional detailed information.

The data was analyzed in order (1) to determine the relative importance of winds, ocean currents, tidal currents, and ice pressure in driving the ice masses which eventually scour the seabed; (2) to determine the frequency distributions of ice-scour depth and ice-keel depth from seabed information obtained on an areal, rather than a linear basis; (3) to determine the relative importance of large-scale bathymetric features in deflecting ice keels that are scouring the seabed; (4) to account for the various planimetric forms of ice-scour tracks; (5) to investigate the influence of ice zonation upon the degree of seabed disturbance caused by ice keels in an area; (6) to develop a model of the processes involved in the formation of ice-scour tracks based upon the results of (1) to (5). These goals could not be achieved as fully as desired because of the variable quality of the sonographs and echograms.

Acknowledgments

I am indebted to the Geological Survey of Canada and the Arctic Petroleum Operators' Association for making the original ice-scour track data and sonograph mosaics available for analysis. The data were collected in 1974 with the co-operation of the officers and crew of the **M.V. Pandora II**. Dr. C.F.M. Lewis of the Atlantic Geoscience Centre facilitated the completion of the thesis project in numerous ways as did Professor J.P. Johnson (thesis supervisor), Carleton University. Dr. B.R. Pelletier kindly critically reviewed this report.

Methods of Study

The echograms and sonographs which form most of the data base for this report were collected in late August and early September of 1974 by scientists from the Geological Survey of Canada working onboard the vessel, **M.V. Pandora II**. The echo-sounder used was a Krupp Atlas-Deso 10 operated mainly at 30 kHz (beam angle between half-power points: 20° longitudinal; 30° transverse). An EG&G Mark 1B side-scan sonar system (105 kHz, 1.2° horizontal beam angle between half-power points) produced the sonographs.

Two seabed mosaics (Fig. 9.1) were constructed from the sonographs by means of a process of anamorphic photography by Bureau d'Etudes Industrielles et de Cooperation de l'Institut Français du Pétrole. The mosaic of the east Mackenzie Bay study area (8 x 32 km or 256 km²) is at 1:20 000 scale and that for Pullen Island (14 x 9 km or 126 km²) is at 1:10 000 (Fig. 9.1).

Bathymetric charts were made on transparent film to overlay the two mosaics. The bathymetric information was obtained from the echograms which had been recorded onboard the survey vessel at the same time that the sonographs were collected. With the addition of the bathymetric overlays, the seabed mosaics give a generalized three-dimensional representation of the seabed. The ice-scour tracks themselves are not represented by bathymetric contours; the intent was rather to represent a seabed surface undisturbed by ice impacts. The direction of motion of an ice keel that is scouring the seabed is likely to be upslope in nearly all cases; therefore, use of the bathymetric overlays in conjunction with the pattern of ice-scour tracks on the seabed allows one to infer the direction of the ice-keel movement associated with the creation of each track.

Most of the quantitative results in this study are based on the east Mackenzie Bay area (Fig. 9.1). Regrettably, the quality of data in the Pullen Island mosaic area was too variable to permit much quantitative study.

All tracks are within the northernmost 15 km² of the east Mackenzie Bay mosaic area (referred to as the east Mackenzie (north) area; water depths 40 to 50 m) were outlined in ink on a second plastic overlay that was placed over the mosaic and its bathymetric overlay. Information on each individual track was then recorded. Most information was readily computer-coded and could be analyzed using a statistical program.

¹ Box 86188, North Vancouver, British Columbia. V7L 4J8

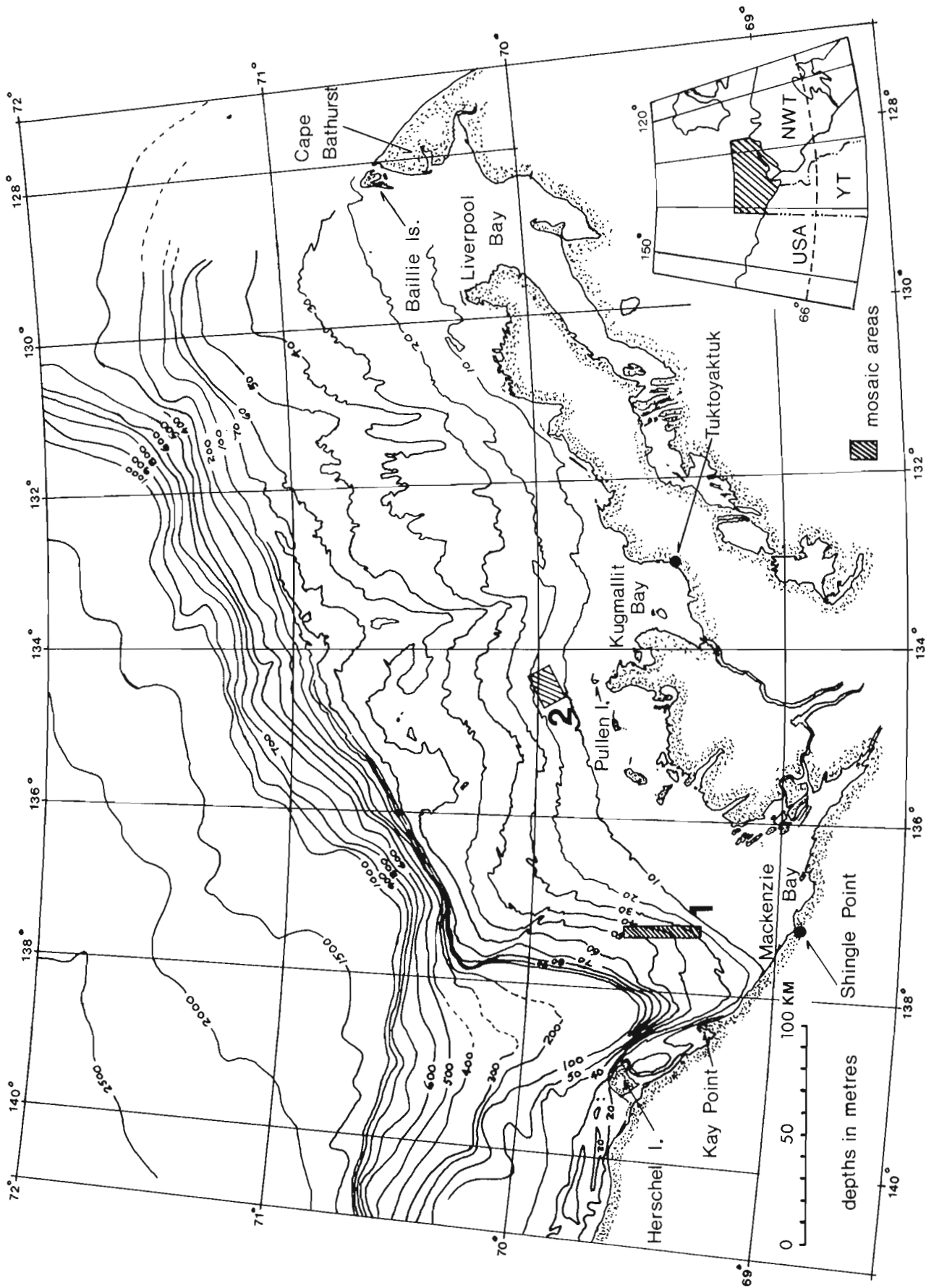


Figure 9.1. Bathymetry of the continental shelf of the Canadian Beaufort Sea (from the Canadian Hydrographic Service Beaufort Sea plotting base). Side-scan sonar mosaic areas are labelled: (1) east Mackenzie and (2) Pullen Island.

Classification System of Ice-Scour Tracks

A classification system was designed based on observations of ice-scour tracks in three different environments, namely the St. Lawrence estuary mudflats (Dionne, 1969, 1971), the eastern continental shelf of Canada (Harris and Jollymore, 1974; van der Linden et al., 1976), and the Beaufort Sea. Ice-scour tracks are classified according to type (single, multiple, broad, and flat-bottomed), planimetric form (straight, arcuate, sinuous, ice-scour crater), and some secondary characteristics (unmodified, abrupt change in direction, crater at one end). Some examples of forms of ice-scour tracks are illustrated in Figures 9.2A-F. Table 9.1 shows the manner in which the form of a track might be related to the processes occurring during the scouring event; Table 9.2 outlines a suggested classification code.

Measurement of Ice-Scour Tracks

The information collected on individual ice-scour tracks includes the following:

1. Length of track:
Each measurement made from the sonograph mosaic had an uncertainty of ±100 m.

2. Planimetric width of track:
This measurement was made with an uncertainty of ±10 m on the 1:20 000 scale mosaic. The planimetric width is defined as the minimum distance between the ridge lines of the two lateral embankments which usually run parallel to an ice-scour track (Fig. 9.3).
3. Mean depth of track:
This measurement (see Fig. 9.3) was made from the echograms; the uncertainty depended upon the vertical scale of the echogram but was usually ±0.2 m.
4. Azimuth of track:
This is defined as the direction from which an ice keel came (following the convention of naming winds according to the direction from which they blow). This measurement was made from the seabed mosaic with an uncertainty of ±1°.
5. Angle of approach of ice to a slope:
The angle of approach (θ_{app}) is the angle between the normal to the bathymetric contour and the long axis of the ice-scour track (Fig. 9.4). This measurement was made using the seabed mosaic and the bathymetric overlay with an uncertainty of ±1°.

Table 9.1

Scheme of relationships between form and processes on which the classification of ice-scour track form (Table 9.2) is based. This scheme is not specific to the Beaufort Sea but can be applied to tracks on lakebeds and on other continental shelves.

ORIGIN OF ICE KEEL	ICE KEEL MORPHOLOGY	TYPE OF ICE-SCOUR TRACK	PROCESSES/ FORCES ON GROUNDING ICE IN MOTION	STATE OF FORCES ON ICE MASS	PLANIMETRIC FORM OF TRACK	MODIFICATION OF PLANIMETRIC FORM	
						PROCESSES	FORM
pressured sea or lake ice ↗ first year ↘ multi-year	angular blocks of ice projecting from keel, one or several penetrate seabed ↗ one keel ↘ multi keel	single track	wind stress	constant	straight	nil	unmodified
		multiple track	currents - ocean - tidal		arcuate		
pressured ice → ablation rounds profile	bowl-shaped, smooth	broad, flat-bottomed track	rise and fall of tide	one force steadily increasing or decreasing or effect of Coriolis force dominates		interaction with other ice?	abrupt change in direction
ice shelf → ice island	flat-bottomed		ice flow interaction	variable forces	sinuous	sediment resistance changes?	
glacier → iceberg	angular or flat-bottomed ↗ single keel ↘ multi keel	single track	Coriolis force	zero		change in direction of driving force?	crater at end of track
		multiple track	seabed friction (above based on Pounder, 1965, p. 40)		crater	settling of ice mass; consolidation of sediment?	

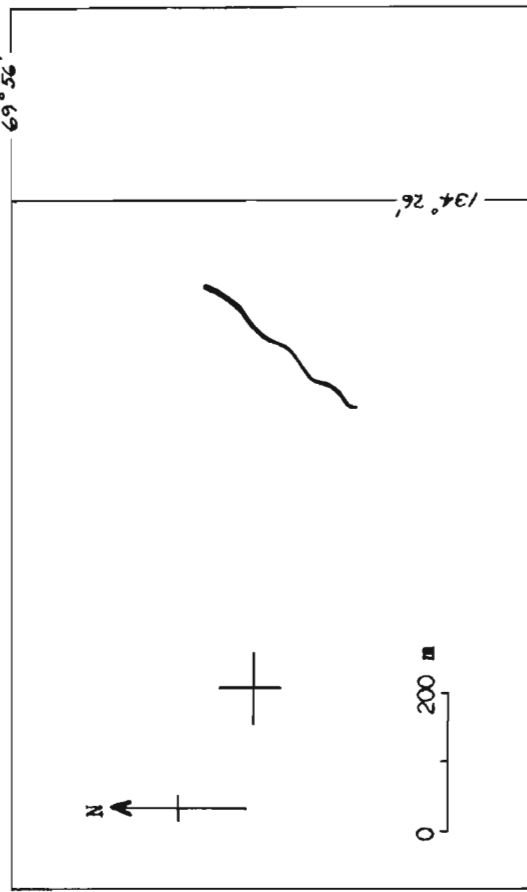
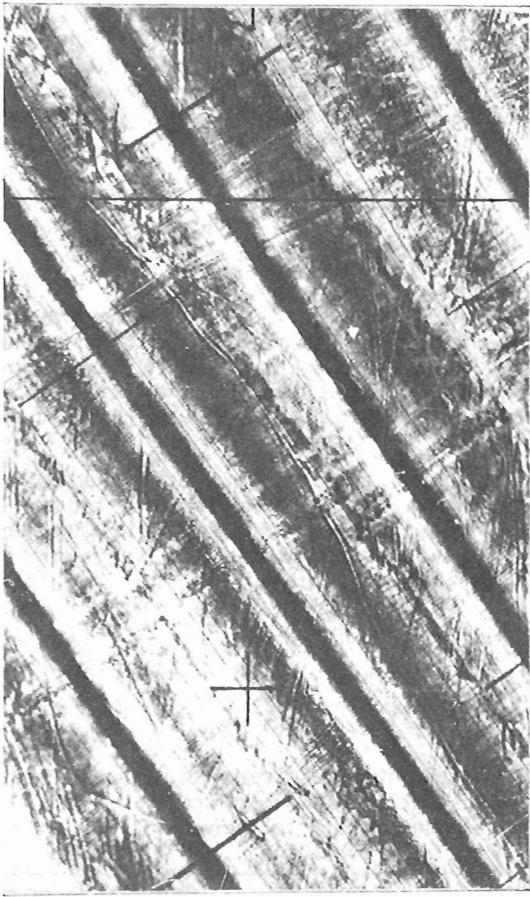


Figure 9.2B. Single, sinuous, unmodified ice-scour track observed in 12.5 to 13 m water depth in the Pullen Island survey area, 1974. Classification code for track is S si u (see Table 9.2).

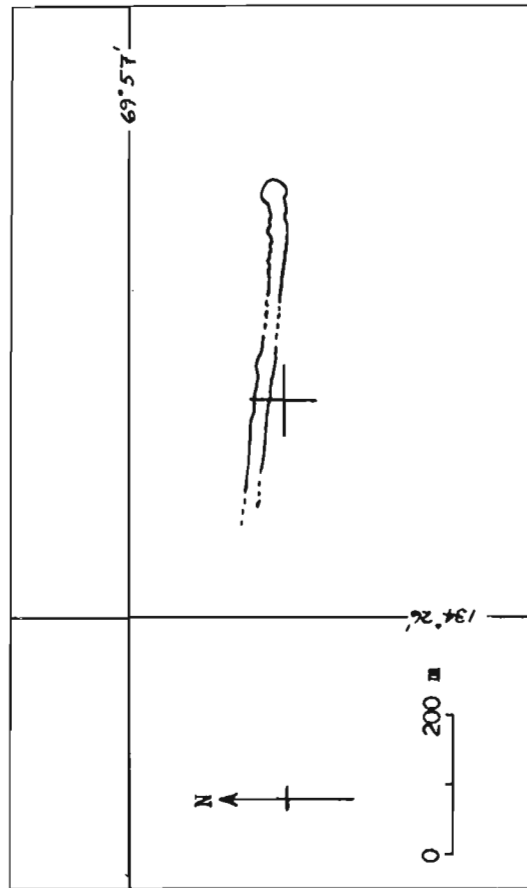
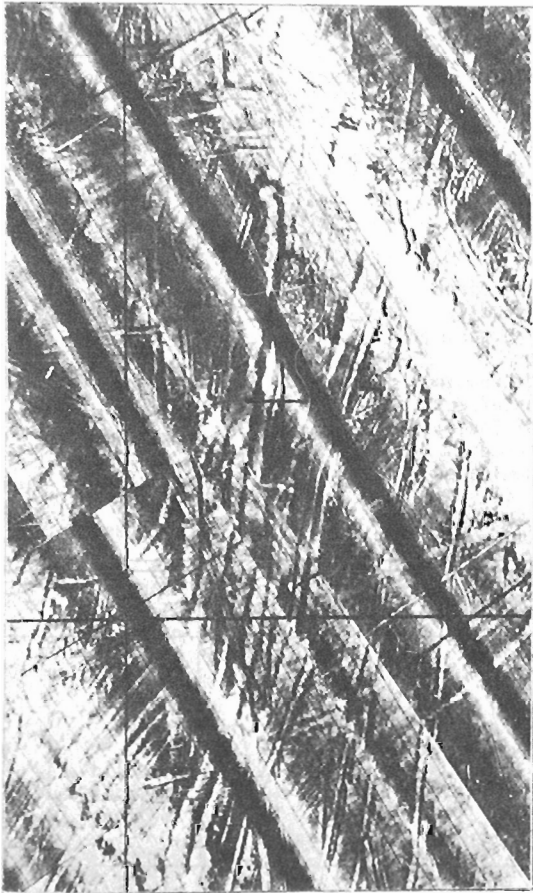


Figure 9.2A. Single, straight ice-scour track with pronounced crater on east end observed in 13.5 to 14 m water depth in the Pullen Island survey area, 1974. Classification code for outlined track is S st d (see Table 9.2).

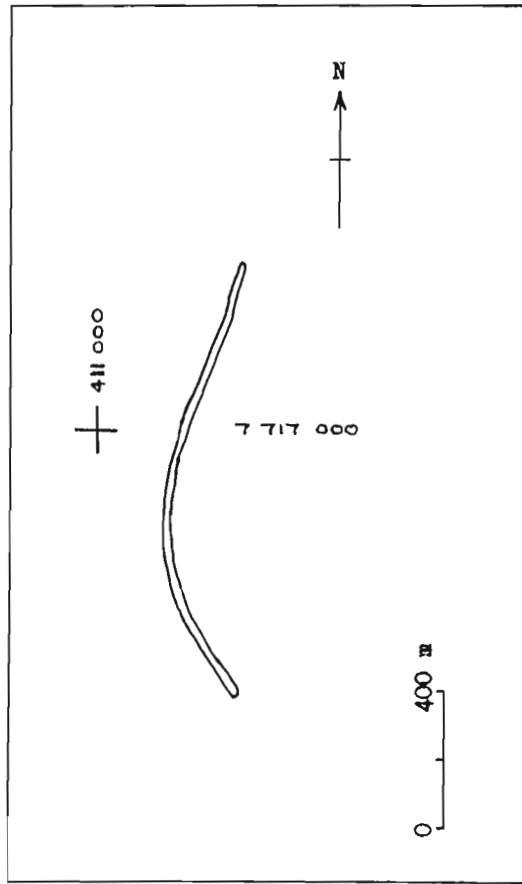


Figure 9.2C. Single, arcuate, unmodified ice-scour track observed in 44 to 45 m water depth in the east Mackenzie survey area, 1974. Classification code is S a u (Table 9.2).

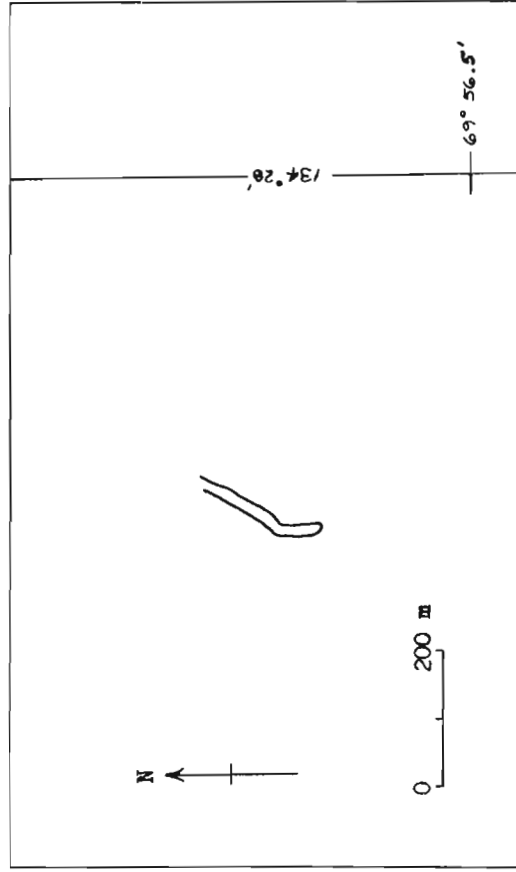


Figure 9.2D. Single, straight ice-scour track showing evidence of a relatively abrupt change in direction of the moving ice mass. This feature occurs in 13.5 to 14 m water depth in the Pulten Island mosaic area, 1974. Classification code is S st z (Table 9.2).

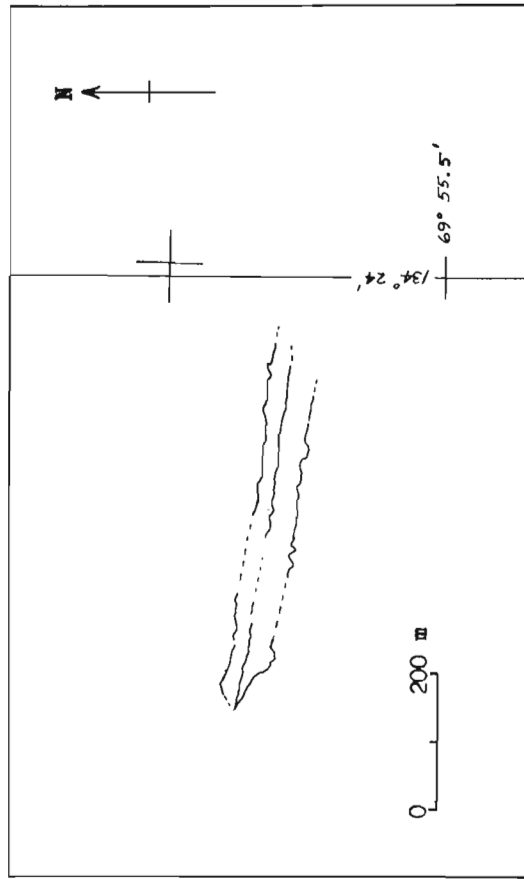
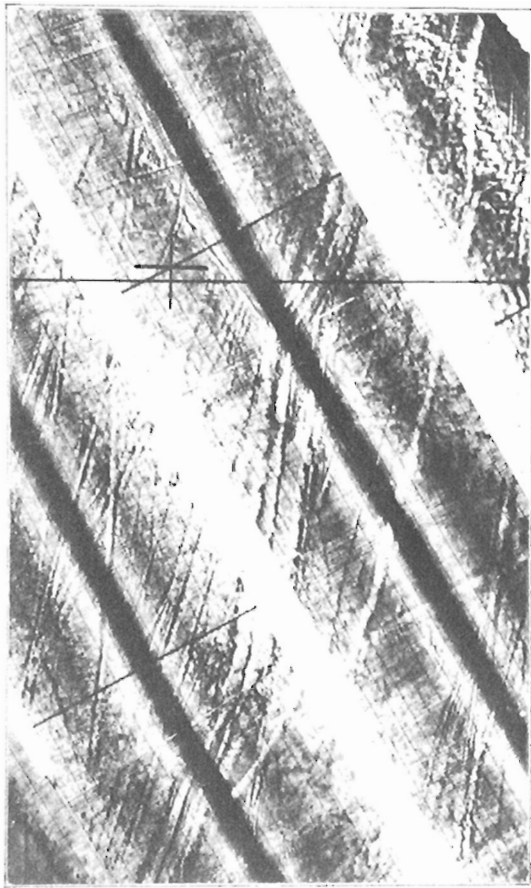


Figure 9.2F. Broad, flat-bottomed ice-scour tracks, which appear to be straight and unmodified, observed in 12.5 to 13 m water depth in the Pullen Island mosaic area, 1974. The irregularities along the lateral embankments may be a result of towfish yaw. Classification code is B st u (Table 9.2).

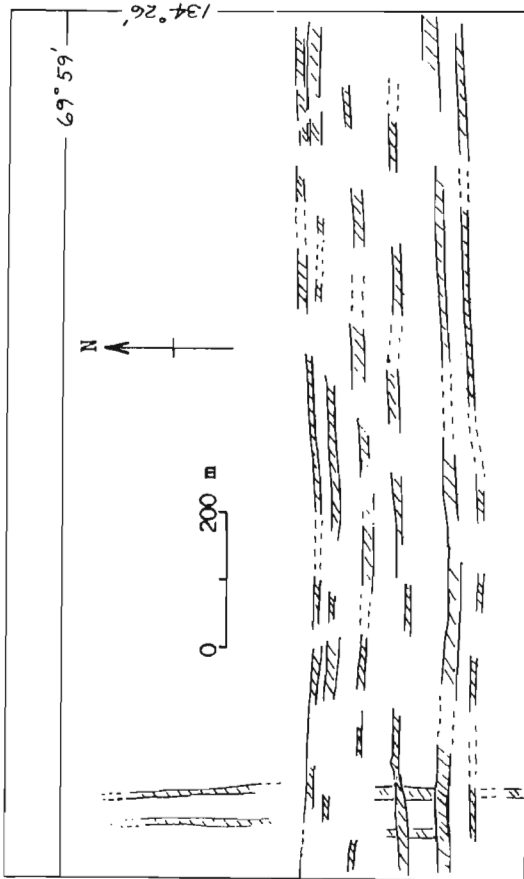
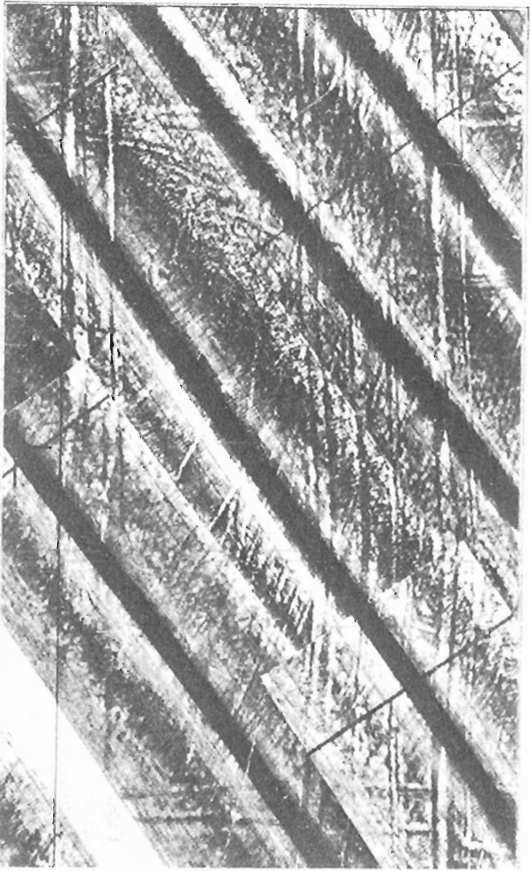


Figure 9.2E. Part of a multiple, straight, unmodified ice-scour track several kilometres long from the Pullen Island mosaic area, 1974. Classification code is M st u (Table 9.2).

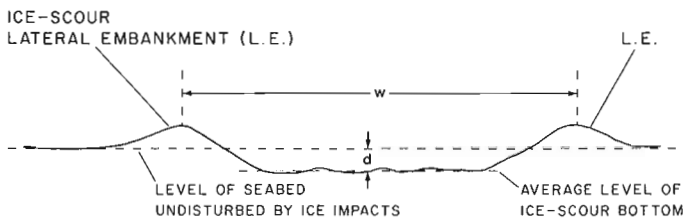


Figure 9.3. Idealized cross-section of an ice-scour track showing the definitions for planimetric width (w) measurements made from sonograph mosaics and ice-scour depth (d) measurements made from echograms.

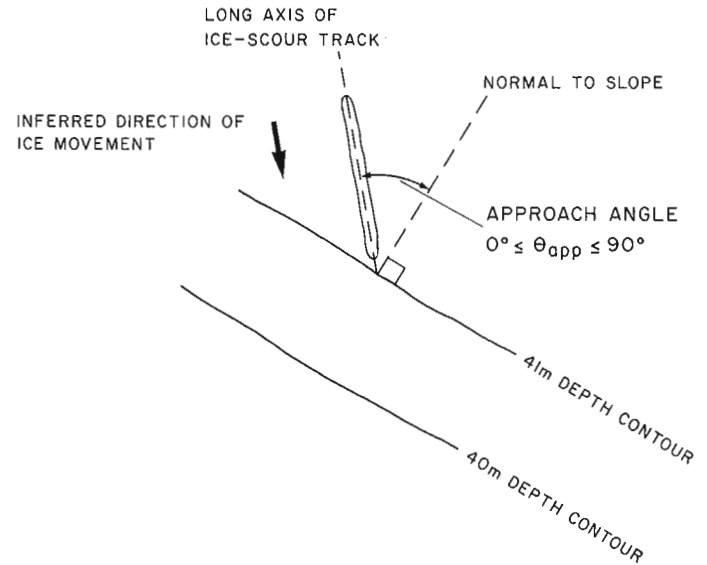


Figure 9.4. Illustration of the measurement of the approach angle (θ_{app}) of an ice keel to a slope.

Table 9.2
Classification code for ice-scour tracks

Type of ice-scour	Symbol	Computer code
Single	S	1
Multiple	M	2
Broad, flat-bottomed ¹	B	3
<u>Planimetric form of ice-scour track</u>		
straight	st	4
arcuate	a	5
sinuous	si	6
ice-scour crater	c (this symbol always stands alone)	7
<u>Modifications to planimetric form</u>		
unmodified	u	8
abrupt change in direction	z	9
crater at one end	d	0

¹ This cross-sectional shape is listed as a type of track because of its association with ice islands and mature ice pressure-ridge keels (see Table 9.1). Refinement of the classification scheme given here is possible by considering cross-sectional shape in a similar manner as planimetric form.

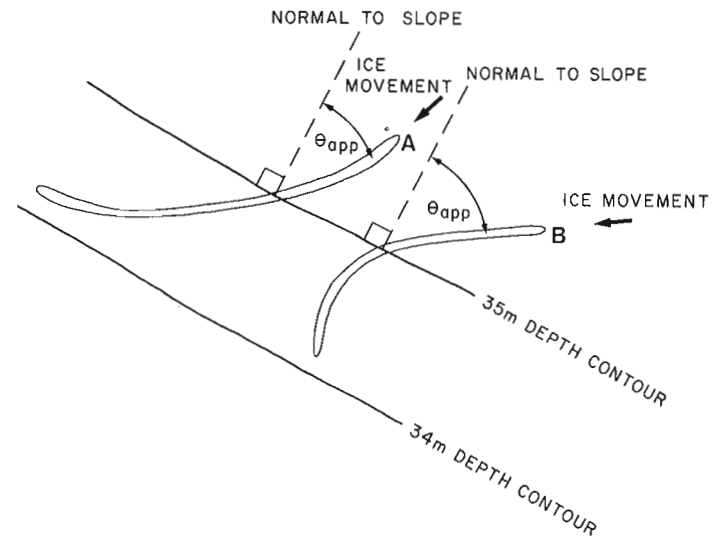


Figure 9.5. This illustration shows two single arcuate ice-scour tracks. The direction of ice keel movement is presumed to be upslope in both examples. Arcuate track A is turning to the right of the direction of ice movement, and track B is turning to the left. Furthermore, it can be postulated that the turning to the right of track A is consistent with the angle of approach of the ice keel to the slope; in contrast, the turning to the left of track B can be regarded as being inconsistent. Hence, for arcuate tracks, data can be collected on direction of turning (left, right) and on consistency or inconsistency of turning with the angle of approach to a slope.

6. Net rise of an ice keel:
The vertical distance that the bottom of an ice keel was raised or lowered as it traversed a seabed slope could be determined for those ice-scour tracks that were crossed by at least two survey lines. This variable is defined by the expression:

$$\text{net rise} = \Delta W.D. - \Delta d \quad (1)$$

where $\Delta W.D.$ is the difference in water depth (measured to level of non-scoured seabed) between the locations of two cross-sections on an ice-scour track

and Δd is the difference in depth of an ice-scour track from two locations on the track. The downslope ice-scour depth is subtracted from the upslope ice-scour depth.

7. Direction of curvature of arcuate tracks:
This characteristic was investigated in order to determine the importance of Coriolis force in influencing the motion of a grounding ice keel and to determine the importance of seabed slope in deflecting an ice keel (see Fig. 9.5).

The problem of making measurements of ice-scour tracks that have been infilled or buried by sediment (apparent from the echograms) is discussed in Wahlgren (1979).

Energy Cascade Model for the Ice-Scouring Process

A mathematical model describing energy flow from atmosphere to seabed was developed to demonstrate the processes involved in the creation of ice-scour tracks. Input to the model consists of information on the length, width, and depth of an ice-scour track as well as the water depth at the inferred origin of the track. The model reconstructs the dimensions of the ice mass that created the track. Estimates of the magnitude of the forces required to drive the ice keel can be made by giving the model information on the net rise per unit length of the bottom of the ice-scour track, the submerged unit weight of the seabed sediment, and the sediment shear strength. An equation derived by Chari (1975, 1978) was used to calculate the energy transfer from ice keel to seabed. The model discussed in Wahlgren (1979) has not yet been converted to a computer simulation model which will

enable large quantities of ice-scour track measurements to be handled and the soundness of the model to be tested thoroughly.

Physical Environment and Creation of Ice-Scour Tracks

Winds and Currents

An ice mass having a fairly deep draft will be acted upon by winds and currents. In the relatively shallow waters over the Beaufort Shelf (water depth less than 100 m) the current directions throughout the water column are usually similar (i.e. within the same 45° sector) to the surface wind direction (cf. MacNeill and Garrett, 1975; Wahlgren, 1979). A comparison of directional frequency distributions for ice-scour track azimuth (from the east Mackenzie (north) area) and for strong winds (speed greater than 14 m/s or 28 knots) over the Beaufort Sea shows some similarity with regards to the predominance of the northwest azimuth (Fig. 9.6). The wind distribution shown in Figure 9.6 (from Berry et al., 1975) is generalized with respect to both location and season. Local prevailing wind directions as measured by Wilson (1974) at Shingle Point (see Fig. 9.1) help to explain the strong southwest peak in the distribution of the ice-scour track azimuths. It is noted that even though strong easterly winds are common, hardly any ice-scour tracks have an easterly azimuth due to the bathymetric configuration of the mosaic area; tracks are only expected to be formed in the seabed when an ice keel moves upslope.

Floating Ice

During periods of northwest (onshore) winds, the concentration of ice floes usually increases. An individual ice floe, acted upon by wind and currents, can have its path through the water modified by interaction with other ice floes; if an ice floe has a keel which penetrates into the seabed, the planimetric form of the ice-scour track should show evidence of the interaction. It is suggested (Wahlgren, 1979) that straight ice-scour tracks occur when ice floe concentration is high and an individual flow does not have much lateral freedom of movement. Arcuate and sinuous tracks could develop in pack ice when a grounding keel is at the leading edge of the pack and the individual floes, having more lateral freedom of movement, are constantly shifting position in relation to each other.

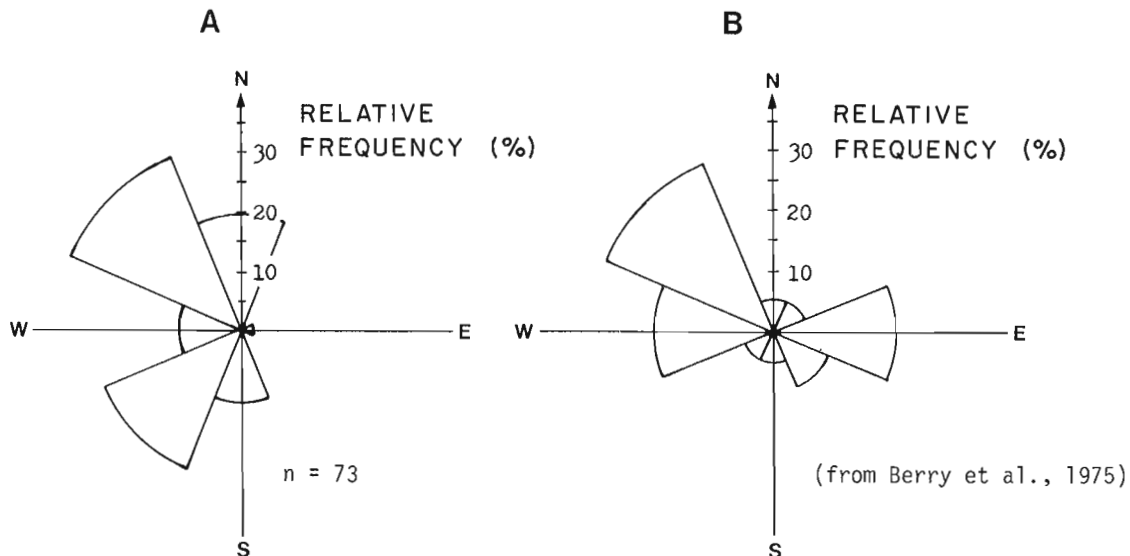


Figure 9.6. Frequency distributions for ice-scour track azimuths (A) and for strong (speed greater than 14 m/s or 28 knots) winds (B) over the Beaufort Sea.

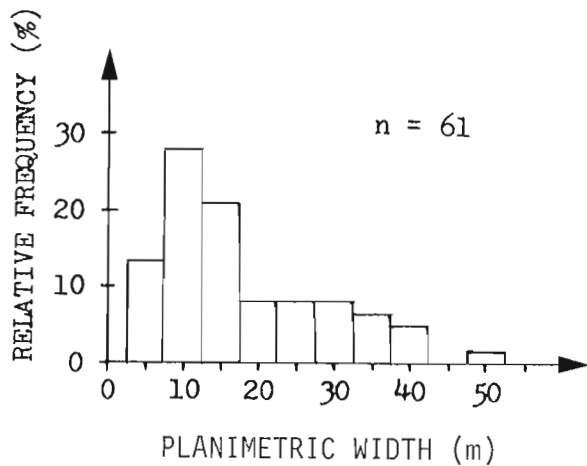


Figure 9.7. Frequency distribution of the planimetric width of a sample of discrete ice-scour tracks in the east Mackenzie (north) area.

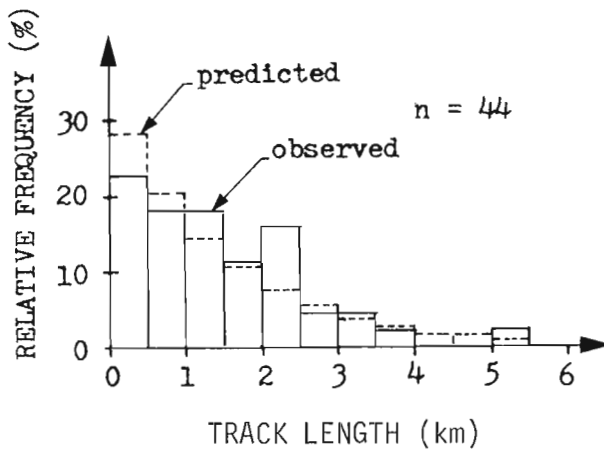


Figure 9.8. Frequency distribution of a sample of ice-scour track lengths from the east Mackenzie (north) area.

In the east Mackenzie (north) mosaic area (water depth 40 to 50 m), more than 80 per cent of the ice-scour tracks are single tracks, with the remainder being broad and flat-bottomed or multiple tracks. The proportions suggest that most ice floes which contain pressure ridges and which pass across the area have only one portion of the ice mass in contact with the seabed at any one time. Measurements of track widths (Fig. 9.7) indicate that the majority of ice keels are 20 m or less in width at the point at which they scrape the seabed. Large-scale systems of pressure ridges or large ice islands are responsible for only about 20 per cent of the ice-seabed interactions in the study area.

The east Mackenzie mosaic area is occupied by either fast ice or ice of the transition zone; the transition zone lies between the zone of fast ice and the pack ice of the Beaufort Sea Gyre (Marko, 1975). The time of year that the ice-scour tracks were formed is uncertain. One method of determining the season of formation of ice-scour tracks is to survey the same area of seabed at least once each year. No repetitive mosaic surveys have been done successfully in the east

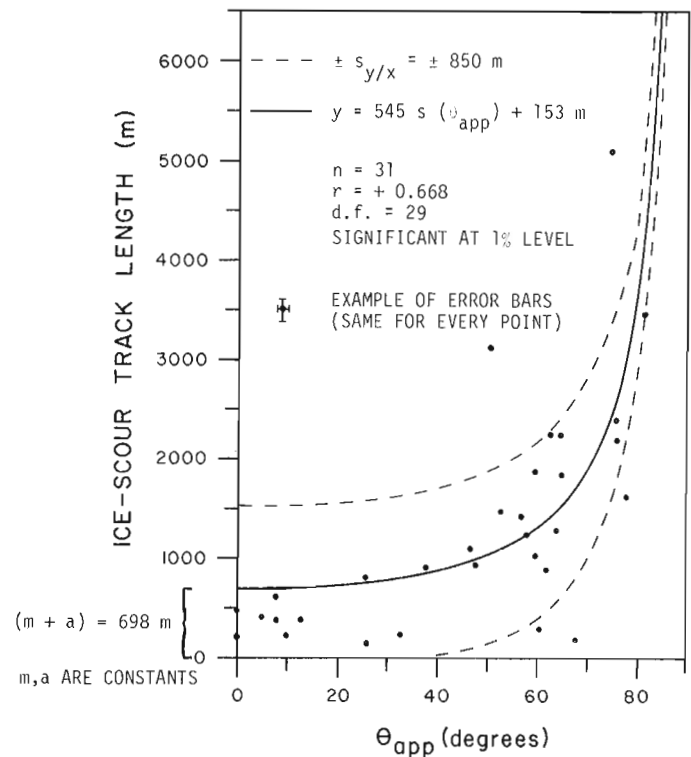


Figure 9.9. Ice-scour track length versus approach angle for 31 single tracks in the east Mackenzie (north) mosaic area. The one standard error limit about the regression line is shown.

Mackenzie Bay area, but repetitive surveys in the Pullen Island area show that new tracks have been formed in the past decade (Lewis, 1977a, 1977b). The surveys, however, were not carried out on an annual basis; therefore, the season of track formation remains unknown. The tracks provide a cumulative record of grounding ice over a period of perhaps hundreds of years. Favourable conditions for substantial ice movement and scraping of keels across the seabed could have occurred at any time during the year over such a long span of time.

Tracks several kilometres long probably could be formed any time that a wide lead or polynya opens in the ice pack and subsequently increases the potential for lateral movement of discrete ice floes. Lengths of ice-scour tracks may be partly related to the degree of lateral freedom of movement of an ice floe. Because the frequency distribution of a sample of ice-scour lengths (Fig. 9.8) has a decaying exponential distribution, it implies that for a given approach angle, driving force magnitude and duration are the most important influences on track length. If the lateral freedom of movement of keels was the dominant influence on track length, it is more likely that a normal distribution of track lengths would result.

Effect of Coriolis Force

Coriolis force is not a driving force but rather a deflecting force which must be taken into account for objects travelling across the Earth's surface. Arcuate tracks that curve to the right of the direction of ice movement may be showing evidence of this effect rather than of ice floe interaction; that is, these tracks may have been formed during times of fairly low ice concentrations. Calculations by Wahlgren (1979) indicate that the degree of track curvature

agrees with the assumption that Coriolis force has affected the form of these tracks. The fact that sinuous tracks and leftward turning arcuate tracks occur, however, suggests that ice floe interaction is commonly an important part of the ice scouring process. A statistical test showed that in a sample of 24 arcuate tracks from the east Mackenzie area, there was an equal probability of a track curving to the right or to the left of the direction of ice movement (see also Fig. 9.5). More data must be obtained before the relative importance of the Coriolis force effect on the planimetric form of ice-scour tracks is known.

Bathymetric Control on the Motion of Grounding Ice

The seabed gradient in the east Mackenzie mosaic area is relatively constant at about 1/400 to 1/500. The seabed sediment is saturated silty clay or clay (cf. Pelletier, 1975) with a surface shear strength of about 1.7 to 6 kN.m⁻² (Lewis, 1977a).

A relationship was found between ice-scour track length and the approach angle of an ice keel to the seabed slope for 31 tracks from the northern part of the study area (Fig. 9.9). For a given driving force and seabed gradient, the relationship is:

$$L = m \secant(\theta_{app}) + a \quad (2)$$

where L is ice-scour track length,

θ_{app} is the approach angle of an ice keel to the seabed slope,

m and a are constants.

Ice keels heading directly into a slope ($\theta_{app} = 0^\circ$) are likely to create shorter tracks than keels travelling parallel to a slope ($\theta_{app} = 90^\circ$). Of course, a driving force of unusually large magnitude could result in the formation of a long track even at a low approach angle. The scatter in the relationship between track length and approach angle is probably a result of variability in the magnitude of the driving force which caused each track.

The relatively gentle gradient of the seabed does not appear to have deflected ice keels from the course that they had when they first struck the seabed. Arcuate tracks analyzed as to their consistency of turning (see Fig. 9.5)

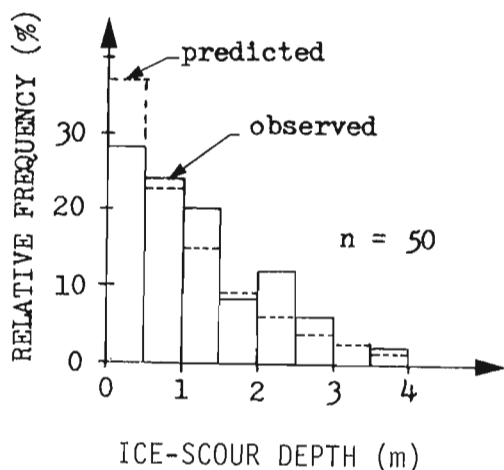


Figure 9.10. Frequency distribution of a sample of ice-scour depths from the east Mackenzie (north) area; the data set includes information from 16 buried tracks.

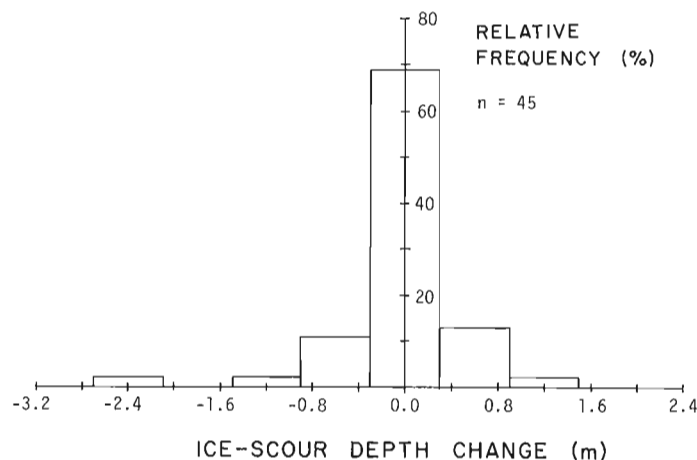


Figure 9.11. Frequency distribution of changes in ice-scour depth along 45 tracks observed in the east Mackenzie Bay area; the data set includes information from 5 buried tracks.

showed that there is an equal chance for turning to be consistent or inconsistent. The lack of a significant bias towards consistent turning suggests that a seabed gradient of 1/400 to 1/500 fails to influence the direction of motion of ice keels. Other influences on ice-keel motion, such as interaction between ice floes, must be more important.

Ice Keel Interaction with Seabed Sediment

Ice-Scour Depth

The sample frequency distribution for ice-scour track depths in the east Mackenzie (north) area follows a decaying exponential distribution (Fig. 9.10). A similar type of distribution was found by Lewis (1977a, 1977b) in his analyses of ice-scour track data from other regions of the Beaufort Sea. Deep penetrations of ice keels into the seabed appear to be rarer events than shallow penetrations.

Ice-Scour Depth Changes Along Tracks

The depths along an ice-scour track can vary significantly over distances of several hundred metres. For example, one track in the east Mackenzie area was 0.2, 0.8, and 0.4 m deep (± 0.2 m) at its first, second, and third cross-sections, respectively, spaced about 1 km apart.

Figure 9.11 shows the frequency distribution of a sample of 45 ice-scour depth changes that were observed between cross-sections (400 to 2800 m apart) of tracks in the east Mackenzie area. Uncertainty in the calculated changes of ice-scour depth was ± 0.3 m as represented by the width of the bars in the histogram. About 70% of the cases fail to show a significant depth change between cross-sections; 15% show an increase and 15% show a decrease in ice-keel penetration into the seabed with upslope movement. It is remarkable that about 85% of the cases show no tendency for the ice keel to plough deeper into the seabed slope as the keel moved forward. This is significant in terms of the ice impact hazard for objects buried beneath the seabed. Figure 9.11 indicates that even a gentle gradient of the seabed appears to minimize the likelihood of ice keels creating extremely deep tracks. Unusually deep tracks can still occur, however, but these appear to be the result of rare events for which the probability is less than 0.2 in the study area.

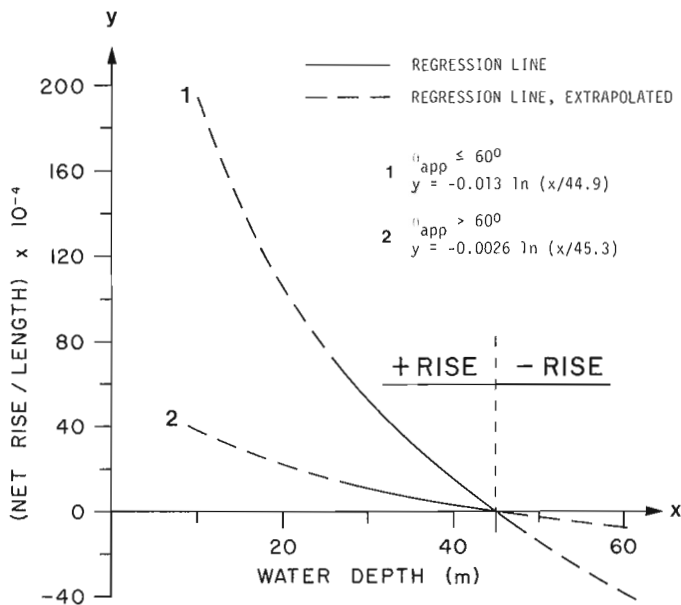


Figure 9.12. Extrapolation of the relationships between net rise per unit length of track and water depth. At water depths exceeding 45 m, negative rises (i.e., ice keel scours deeper into the seabed as the keel moves upslope) are predicted.

Net Rise of Ice Keels Grounding on a Seabed Slope

Kovacs and Mellor (1974, p. 143) stated that grounded ice islands commonly have been uplifted by as much as 4 m when driven aground by the force of pack ice. A study of grounded floebergs near Prudhoe Bay (Kovacs and Gow, 1976) indicated an uplift of 1.85 m in one case where pack ice, again, had been the main driving force.

The net rise phenomenon is not believed to be a result of the temporary rises in sea level (up to 3 m; Kovacs and Mellor, 1974) that accompany storm surges in the area. This possibility largely can be eliminated because many tracks with a southwest azimuth also exhibit a net rise of the bottom of the ice-scour track in the upslope direction. Although positive storm surges (increases in sea level) are associated with storm winds from the northwest (Henry, 1975), negative storm surges (decreases in sea level) should occur with southwest winds.

A general relationship between the net rise per unit length of track and water depth (Fig. 9.12) is suggested by data obtained from the east Mackenzie area. The relationship has the form:

$$(\text{net rise/length}) = -m \ln(\text{water depth}/b) \quad (3)^*$$

where m and b are constants.

As seen in Figure 9.12, the relationship between net rise per unit length and water depth was clarified when the data set was partitioned into those tracks with θ_{app} greater than 60° and those with θ_{app} less than or equal to 60° . The success of this partitioning must be related to the pronounced change in character of the relationship between track length and θ_{app} at approach angles exceeding 60° (see Fig. 9.9).

In water depths less than 45 m, ice-scour depth in a track usually decreases with distance upslope (positive net rise) whereas in water depths exceeding 45 m, ice-scour depth in a track usually increases with distance upslope (negative net rise). The physical basis for the relationship between net

rise and water depth is not understood fully, but some possible explanations can be offered.

An exploratory calculation (Wahlgren, 1979) indicated that excess pore-water pressure developed in the saturated clay on the seabed beneath a scouring ice keel could support any negative buoyancy that the ice keel might develop. This effect would enable an ice keel to be uplifted as it moved into shallower water.

Another explanation for the relationship between net rise and water depth involves the relationship between the speed of an ice keel and the rate of dissipation of excess pore-water pressure in the sediment on which the ice keel acts as a load. If an ice keel is moving extremely slowly, it may consolidate the sediment beneath it because the excess pore-water pressure has time to dissipate. This process could cause depths of ice-scour tracks to increase as the ice keel moves upslope.

Sediment permeability and shear strength are likely to be important factors in the two above-mentioned hypotheses. Detailed geotechnical studies of the seabed must be carried out before these hypotheses can be tested.

A third explanation given in Wahlgren (1979) involves the moment of inertia of the grounding ice mass. Ice masses with a sufficiently shallow draft to enter waters inshore of 45 m have a relatively low moment of inertia. The floating ice mass would be rotated slightly from its original vertical axis as the keel tip encountered the seabed; the effective draft of the ice keel would then be decreased. Hence, the amount of penetration of the keel into the seabed would remain constant or decrease as the ice keel moved upslope. Those keels with a draft exceeding 45 m have a relatively large moment of inertia; little or no rotation of the floating ice mass about its metacentre would occur upon impact. As the ice keel moved upslope, the keel tip would necessarily penetrate farther into the seabed as long as forward motion continued.

It is possible that uplift, varying degrees of sediment consolidation, and moments of inertia of ice keels all may be influencing the observed distribution of changes in ice-scour depth along tracks (Fig. 9.11) and the relationship between net rise per unit length and water depth (Fig. 9.12).

Summary

Ice-scour tracks in eastern Mackenzie Bay were studied quantitatively using information from echograms and sonograph mosaics. A system of classification that relates the form of the ice-scour tracks to the processes involved in their creation was devised to aid in the study; various types of measurements on ice-scour tracks were outlined. An energy cascade model was found to be useful for developing an understanding of the processes creating the tracks. Winds, currents, and ice pressure are the main driving forces causing ice keels to scour the seabed. The forms of the tracks may be influenced by the Coriolis force effect and ice floe interaction. It was found that the length of an ice-scour track is related to the angle of approach of an ice keel to a seabed slope. A keel heading directly into a slope is likely to create a shorter track than a keel moving parallel to a slope; however, no deflection of ice keels by the seabed slope was evident. In most cases, particularly in water depths of less than 45 m, ice keels moving upslope failed to penetrate deeper into the seabed. The net rise phenomenon does not appear to be related to the storm surges that accompany strong northwest winds. Rather, a combination of a pore-water reaction force on the base of grounding ice keels, rate of sediment consolidation, and rotation of the keels about their metacentres may be responsible for the phenomenon.

* $\ln x = \log_e x$

It is hoped that the techniques and methods involved in this study can be applied to similar studies using data from other regions of the Beaufort Sea or other continental shelves. A sound theoretical knowledge of the processes creating ice-scour tracks must be developed so that empirical analyses of ice-scour data can be applied safely to seabed engineering problems.

References

- Berry, M.O., Dutchak, P.M., Lalonde, M.E., McCulloch, J.A.W., and Savdie, I.
1975: Weather, waves, and icing in the Beaufort Sea; Department of Fisheries and the Environment, Beaufort Sea Technical Report 21, Beaufort Sea Project, Victoria.
- Chari, T.R.
1975: Some geotechnical aspects of iceberg grounding; unpublished Ph.D. thesis, Memorial University of Newfoundland, 181 p.
1978: Model studies of iceberg scouring; (preprint) Proceedings of the Fourth International Conference on Port and Ocean Engineering under Arctic Conditions; Memorial University of Newfoundland, 9 p.
- Dionne, J.C.
1969: Tidal flat erosion by ice at La Pocatière, St. Lawrence Estuary; *Journal of Sedimentary Petrology*, v. 39, no. 3, p. 1174-1181.
1971: Erosion glacielle de la slikke, estuarie du Saint-Laurent; *Revue de géomorphologie dynamique*, vol. 20, n°1, p. 5-21.
- Harris, I. McK. and Jollymore, P.G.
1974: Iceberg furrow marks on the continental shelf northeast of Belle Isle, Newfoundland; *Canadian Journal of Earth Sciences*, v. 11, p. 43-52.
- Henry, R.F.
1975: Storm surges; Department of Fisheries and the Environment, Beaufort Sea Technical Report 19, Beaufort Sea Project, Victoria, 41 p.
- Hnatiuk, J. and Brown, K.D.
1977: Sea bottom scouring in the Canadian Beaufort Sea; (preprint) 9th annual Offshore Technology Conference (Houston, Texas), May 2-5.
- Kovacs, A. and Gow, A.J.
1976: Some characteristics of grounded floebergs near Prudhoe Bay, Alaska; *Arctic*, v. 29, no. 3, p. 169-173.
- Kovacs, A. and Mellor, M.
1974: Sea ice morphology and ice as a geologic agent in the southern Beaufort Sea; in *The Coast and Shelf of the Beaufort Sea*, ed. J.C. Reed and J.E. Sater; Arctic Institute of North America, Arlington, Va., p. 113-161.
- Lewis, C.F.M.
1977a: Bottom scour by sea ice in the southern Beaufort Sea; Department of Fisheries and the Environment, Beaufort Sea Technical Report 23 (draft), Beaufort Sea Project, Victoria, 88 p.
1977b: The frequency and magnitude of drift ice groundings from ice-scour tracks in the Canadian Beaufort sea; in *Proceedings of the Fourth International Conference on Port and Ocean Engineering under Arctic Conditions*, Memorial University of Newfoundland, v. 1, p. 568-576.
- MacNeill, M.R. and Garrett, J.F.
1975: Open water surface currents; Department of Fisheries and the Environment, Beaufort Sea Technical Report 17, Beaufort Sea Project, Victoria, 113 p.
- Marko, J.
1975: Satellite observations of the Beaufort Sea ice cover; Department of Fisheries and the Environment, Beaufort Sea Technical Report 34, Beaufort Sea Project, Victoria, 137 p.
- Pelletier, B.R.
1975: Sediment dispersal in the southern Beaufort Sea; Department of Fisheries and the Environment, Beaufort Sea Technical Report 25a, Beaufort Sea Project, Victoria, 80 p.
- Pelletier, B.R. and Shearer, J.M.
1972: Sea bottom scouring in the Beaufort Sea of the Arctic Ocean; 24th International Geological Congress (Montreal), Section 8, p. 251-261.
- Pounder, E.R.
1965: *The Physics of Ice*; Pergamon Press, London, 151 p.
- Shearer, J.M. and Blasco, S.M.
1975: Further observations of the scouring phenomena in the Beaufort Sea; in *Report of Activities, Part A, Geological Survey of Canada, Paper 75-1A*, p. 483-493.
- Shearer, J.M., MacNab, R.F., Pelletier, B.R., and Smith, T.B.
1971: Submarine pingos in the Beaufort Sea; *Science*, v. 174, p. 816-818.
- van der Linden, W.J., Fillon, R.H., and Monahan, D.
1976: Hamilton Bank, Labrador margin: Origin and evolution of a glaciated shelf; *Canadian Hydrographic Service, Marine Sciences Paper 14*, 31 p.; *Geological Survey of Canada, Paper 75-40*.
- Wahlgren, R.V.
1979: Ice-scour tracks on the Beaufort Sea Continental Shelf - their form and an interpretation of the processes creating them; unpublished M.A. thesis, Department of Geography, Carleton University, Ottawa, 183 p.
- Wilson, H.P.
1974: Winds and currents in the Beaufort Sea; in *The Coast and Shelf of the Beaufort Sea*, ed. J.C. Reed and J.E. Sater; Arctic Institute of North America, Arlington, Va., p. 13-23.

**AN ASSESSMENT OF SOME POSSIBLE FLOOD HAZARDS IN SHAKWAK VALLEY,
YUKON TERRITORY**

Project 780037

J.J. Clague
Terrain Sciences Division, Vancouver

Clague, J.J., An assessment of some possible flood hazards in Shakwak Valley, Yukon Territory; in Current Research, Part B, Geological Survey of Canada, Paper 79-1B, p. 63-70, 1979.

Abstract

Potential flood hazards in Shakwak Valley, the proposed site of a pipeline which would transport Alaskan gas to the midwestern United States, include: (1) ponding of water in Dezadeash Valley due to damming of Alsek River by Lowell Glacier, (2) jökulhlaups (i.e., glacier outburst floods) in White, Donjek, and Slims river valleys, and (3) floods of high-gradient streams entering Shakwak Valley from the bordering Kluane Ranges.

Neoglacial Lake Alsek has occupied parts of Dezadeash Valley many times during late postglacial time, the most recent major ponding event having occurred about 125 years ago. It is possible that the lake may form again in the future as a result of a surge of Lowell Glacier. If such a lake extended into Dezadeash Valley, it might cause extensive damage to man-made structures and might disrupt ground transportation.

Existing glacier-dammed lakes in the Saint Elias Mountains are only capable of producing jökulhlaups with peak discharges similar to or less than normal summer peak ice-melt and snowmelt events. Much larger, potentially catastrophic floods might result if Klutlan or Donjek glaciers advanced to block streams and thus form new glacier-dammed lakes. Under existing climatic conditions, however, it is unlikely that Klutlan Glacier could advance sufficiently to create such lakes.

High-gradient streams flowing from the Kluane Ranges across alluvial fans and aprons at the edge of Shakwak Valley are capable of producing localized flooding along the Alaska Highway.

Introduction

In response to a proposal by a group of companies to construct a natural gas pipeline from Prudhoe Bay, Alaska through Canada to the midwestern United States, the Geological Survey of Canada in 1978 initiated a study of some of the potential terrain hazards in southwest Yukon Territory. This study includes an investigation of the Quaternary displacements of the Denali Fault System, a reconnaissance survey of mass movement features and processes, and an assessment of potential flood problems. Results of the investigation of the Denali Fault System were presented by Clague (1979). The following is a preliminary summary and assessment of potential flood hazards within the Shakwak Valley portion of the Alaska Highway corridor.

Possible flood hazards discussed below include: (1) ponding of water in Dezadeash Valley due to the damming of Alsek River by Lowell Glacier, (2) jökulhlaups (i.e., floods resulting from the rapid draining of glacier-dammed lakes) in White, Donjek, and Slims valleys, and (3) floods of high-gradient streams entering Shakwak Valley from the bordering Kluane Ranges.

Acknowledgments

This program is part of joint studies, partially funded by Foothills Pipe Lines (South Yukon) Ltd., concerning environmental aspects relating to pipeline concerns in southern Yukon Territory. V.N. Rampton accompanied me in the field, provided information on Neoglacial Lake Alsek, and reviewed a draft of the manuscript.

Neoglacial Lake Alsek

Several times during late postglacial time, Lowell Glacier, a large surging glacier in the Saint Elias Mountains, advanced across Alsek Valley and blocked south-flowing Alsek River (McConnell, 1905; Kindle, 1952; Johnson and Raup, 1964; Hughes et al., 1972; Rampton, in press). The resulting

lake, termed "Recent Lake Alsek" by Kindle (1952), occupied portions of Alsek, Dusty, Kaskawulsh, and Dezadeash valleys (Fig. 10.1), and at its maximum extent was at least 200 m deep at the glacier dam. Large areas in Dezadeash Valley, including what are now the community of Haines Junction and portions of the Alaska Highway and Haines Road, were inundated.

Although the future history of Lowell Glacier cannot be predicted, it is possible that the glacier might surge, block Alsek River, and thus again form Lake Alsek. If the resulting lake was large enough to reach Haines Junction, it of course would inundate buildings and other structures. There is the additional possibility of damage caused by forces exerted on structures by water draining rapidly out of Dezadeash Valley following failure of the Lowell Glacier dam. The chronology and characteristics of Neoglacial Lake Alsek are reviewed briefly below in order to place these hazards in perspective.

Evidence for Multiple Fillings

Beaches, wave-cut benches, and accumulations of driftwood occur throughout the Lake Alsek basin (Fig. 10.2). These were subdivided by McConnell (1905, p. 4A) and Kindle (1952, p. 22) into an older higher group and a younger lower group. More recently Johnson and Raup (1964, p. 30-32) have proposed that there were three phases of Neoglacial Lake Alsek. Work by Rampton (in press) and myself, however, indicates that Lake Alsek has had many ponding phases, each separated by an interval during which the present southward drainage pattern in Alsek Valley prevailed. The evidence for this is the occurrence of major driftwood horizons and coincident breaks in the density and maximum size of lichens on gravelly and rubbly beach deposits at various levels within the basin.

Each major driftwood layer probably accumulated when Lake Alsek filled to the upper limit of a phase. The alternative explanation, that the driftwood beaches and

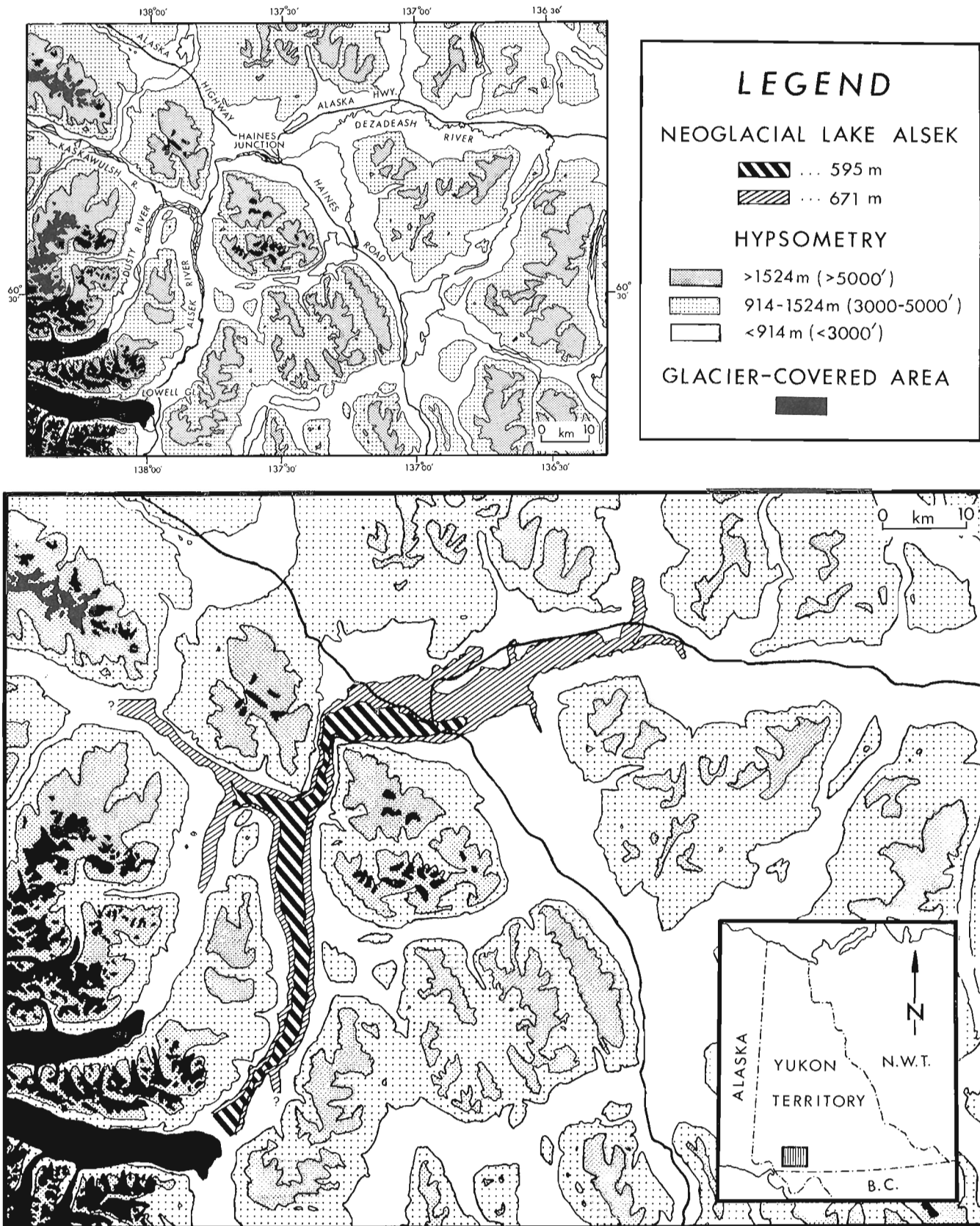


Figure 10.1. Extent of Lake Alsek about 125 years ago (595 m phase) and earlier during Neoglacial time (671 m). The index map at the top shows place names referred to in the text. At its Neoglacial maximum Lake Alsek reached an elevation equal to or greater than 678 m, higher than the 671 m (2200') contour delineated on the diagram. The extent of older phases of the lake in Kaskawulsh Valley is unknown because there has been extensive aggradation in the valley near the toe of Kaskawulsh Glacier during the past several hundred years.

related differential lichen development were produced during long-term stillstands of a single, progressively shrinking Neoglacial lake, is untenable for the following reasons. (1) Beaches associated with lichen breaks and having abundant driftwood are no better developed than beaches lacking such features and thus apparently took no longer to form. Each strandline, whether it has driftwood or not, probably formed during a relatively short period of time; the driftwood-laden beaches are unique only in that they represent filling limits which separate lake phases of different ages. (2) Glacier-dammed lakes are characteristically unstable, emptying and filling rapidly and repeatedly (e.g., Post and Mayo, 1971). (3) Lake Alsek deposits in general are thin or absent, an observation compatible with relatively brief lacustrine occupation of Alsek Valley.

Each of the major lake phases perhaps consisted of many short-lived cyclic filling and draining events, as is common for present day, self-dumping, glacier-dammed lakes (e.g., Stone, 1963; Mathews, 1965, 1973; Post and Mayo, 1971). The major driftwood filling event of each of these phases. Individual events within a phase probably were too brief and too closely spaced in time to give rise to differences in lichen density and to the accumulation of substantial driftwood below the maximum level attained during the phase.

Phases of Neoglacial Lake Alsek

Using the above discussed criteria, Rampton (in press) proposed the existence of at least five phases of Neoglacial Lake Alsek, the maximum elevations of ponding being about 595, 623, 637, 640, and 678+ m (Table 10.1). The highest beaches that may be confidently assigned to Lake Alsek, largely on the basis of their youthful appearance, are 678 m in elevation. There are, however, higher strandlines in Dezadeash Valley; although some of these are possibly of Neoglacial age, it is considered more likely that they formed at the close of the Pleistocene when a large proglacial lake, Glacial Lake Champagne, occupied the low-lying parts of the area (Kindle, 1952; Hughes et al., 1972).

The details and chronology of the various Lake Alsek ponding phases have not been completely worked out. This in part results from the fact that lacustrine sediments deposited in the lake are lacking in most areas, thus conventional stratigraphic analysis cannot be undertaken in a satisfactory manner. In addition, with the exception of driftwood, datable material which can be related definitely to Lake Alsek ponding or drainage events is rare. Furthermore, radiocarbon dates on driftwood may themselves be of limited value in that they are only maximum limiting dates, the wood possibly having been dead prior to the flooding event.

Table 10.1
Recognized phases of Neoglacial Lake Alsek

Phase	Highest level of lake (m)	Recognition criteria*	Approximate age (a)
1	678+		?
2	640	L,W	300-500
3	637	L	300-500
4	623	L,W	200-300
5	595	L,W	125

* Criteria used to identify a particular strandline as the uppermost formed during the specified lake phase:

L = lichen density difference above and below strandline,
W = major driftwood line.

Ages of Phases

In spite of the above disclaimers, there is good evidence that most of the recognized Lake Alsek ponding events occurred recently (Table 10.1). The beaches and wave-cut benches in many places are unmodified by erosion, even on steep slopes; driftwood is not decomposed; and vegetation is not yet fully established at lower elevations of the lake basin. The oldest trees on the gravelly floor of Alsek Valley are about 80 years old. Kindle (1952) estimated that 50 or 60 years would be required for trees to seed in this area and thus concluded that the last phase of Lake Alsek occurred about 1850 A.D. Rampton (in press) determined a similar age for the 595 m strandline on the basis of lichen growth-rate estimates and tree ring counts. Support for this age assignment is provided by Indian legends of a catastrophic flood on the Alsek River delta in southeast Alaska in 1852 A.D. or shortly before (de Laguna, 1972, p. 276). Indians attributed this flood to the "breaking of a glacier" that crossed Alsek Valley.

The youthfulness of the last major Lake Alsek ponding is emphasized by the discovery in 1978 of a crudely hewed wood paddle in driftwood in Alsek Valley. The paddle, which appears to have been shaped with a metal tool, was found at an elevation of 561 m, 28 m above the level of Alsek River, and about 21 km north-northeast of Lowell Glacier. The paddle may have been stranded on the valley wall during a draining event of the 595 m phase of Lake Alsek. Alternatively it may have been deposited during a separate younger phase when the lake was of relatively small size and restricted to Alsek Valley. Although there is at present no direct evidence for the latter possibility, it is worth noting that a major flood on the Alsek River delta which occurred in August 1909 (Tarr and Martin, 1914, p. 158) tentatively has been attributed to the draining of Lake Alsek (Post and Mayo, 1971). Eyewitness accounts of this flood clearly indicate that it was caused by the rapid emptying of a glacier-dammed lake. It is conceivable, however, that this lake may have been impounded behind Tweedsmuir, Alsek, Fisher, or some other large glacier, rather than behind Lowell Glacier.

Kindle estimated that the earlier of his two periods of Lake Alsek ponding occurred about 1725 A.D. This is within the estimated age range of the 623 m phase determined from lichen growth-rate estimates and radiocarbon dates on driftwood (Rampton, in press). Higher beaches in turn are older. The 637 and 640 m phases tentatively are thought to be about 300 to 500 years old, also on the basis of lichen growth rates and radiocarbon dates. Earlier Lake Alsek events have not yet been adequately dated.

It is possible that there was more than one lake phase preceding the 640 m event. Although there are no major driftwood layers or lichen differences which directly support this, Rampton (in press) has suggested that thin lacustrine (?) units northwest of Haines Junction were deposited during early Lake Alsek ponding events. Additional work is required to substantiate these possible early high-level phases of Lake Alsek.

Drainage Phenomena and Potential for Future Damming

Each lacustrine event probably terminated with the breaching of the ice dam at Lowell Glacier and the rapid emptying of the lake. The failure of the ice dam at the close of the most recent Lake Alsek phase is documented by the presence of flood bedforms on the floor of Alsek Valley both upstream and downstream from the terminus of Lowell Glacier (Fig. 10.3). Giant bars and dunes attest to the rapidity with which the lake drained and to the forces exerted on the valley floor by the moving water.

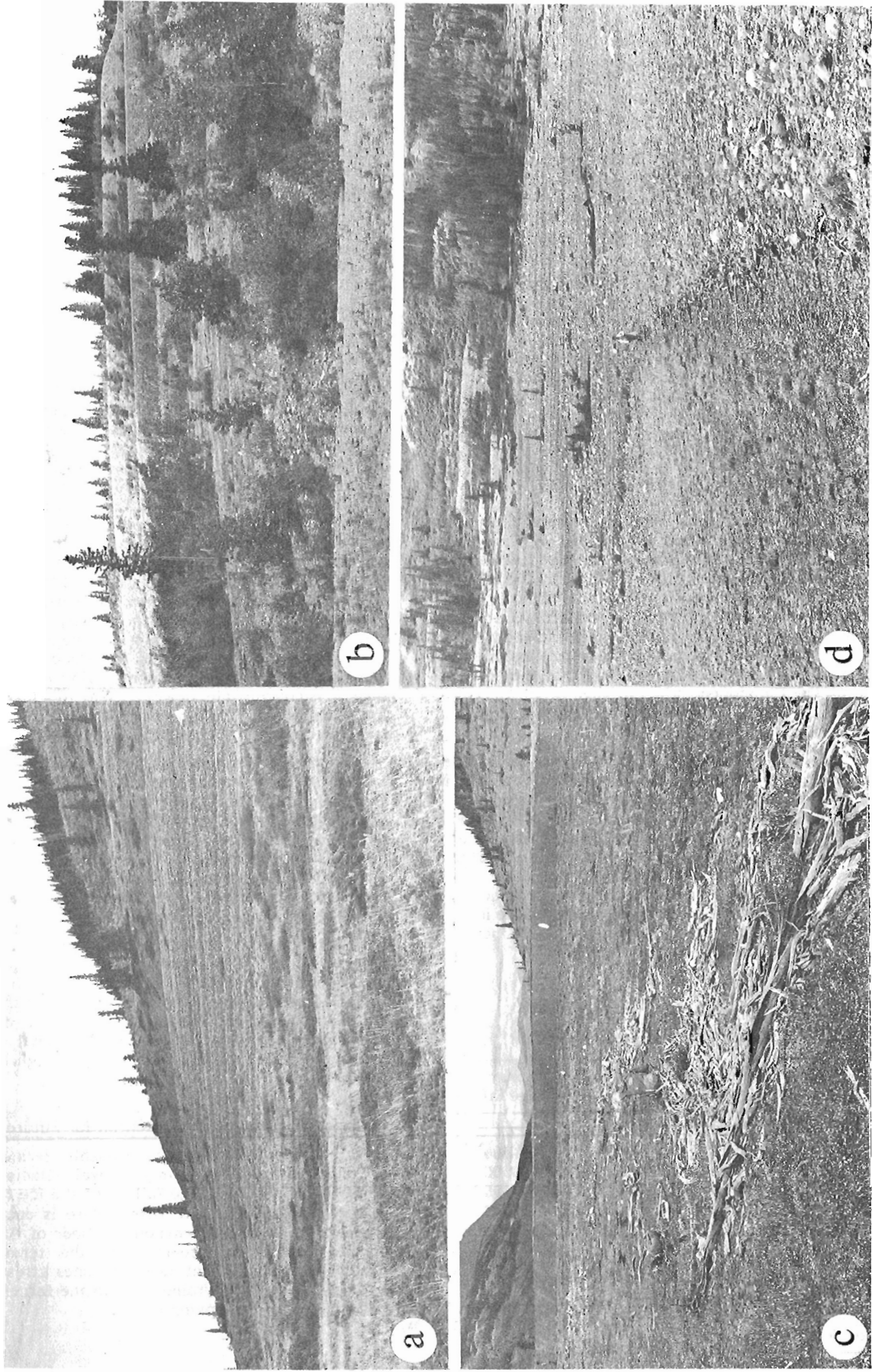


Figure 10.2. Beaches (a), wave-cut benches (b), and driftwood accumulations (c,d) of Neoglacial Lake Alsek.

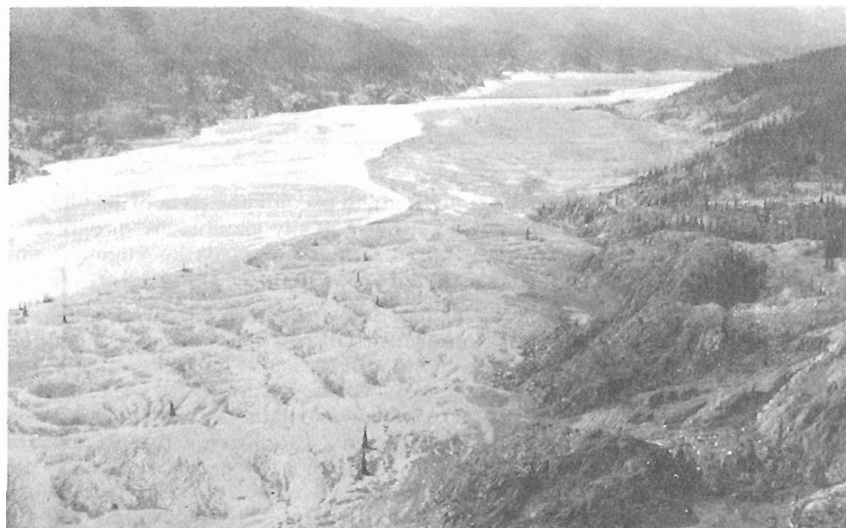
The past history of Neoglacial Lake Alsek suggests that future ponding events are likely. The terminus of Lowell Glacier is presently less than 2 km from the east wall of Alsek Valley; thus during a major surge the glacier probably would block the river and create a new lake. It is not known, however, how large the resulting lake might grow. This depends in part on the present and future regimen of Lowell Glacier and on the magnitude of the surge blocking the valley. Because Lowell Glacier has receded and thinned somewhat during the past few centuries (Rampton, in press), it is unlikely that it could impound a lake comparable in size to the large lakes existing in Alsek Valley prior to the ca. 1850 A.D. phase.

Jökulhlaups

Rivers and streams fed by large glaciers in the Saint Elias Mountains flow into and across Shakwak Valley (Fig. 10.4). The largest of these are White, Donjek, and Slims

ivers. While these rivers exhibit large diurnal and seasonal variations in discharge, which themselves may be important in the assessment of flood periodicity and magnitudes (Table 10.2), of perhaps greater importance are the unusually large floods which might result from the rapid draining of glacier-dammed lakes. The catastrophic effects of such floods, or jökulhlaups, have been documented extensively for other glacierized areas (e.g., Mason, 1935; Ström, 1938; Thorarinnsson, 1939, 1957; Arnborg, 1955; Liestøl, 1955; Rist, 1955; Aitkenhead, 1960; Stone, 1963; Mathews, 1965, 1973; Post and Mayo, 1971; Björnsson, 1974; Tomasson, 1974; Nye, 1976).

In the following section an assessment is made of flood hazards related to existing and potential glacier-dammed lakes in the White, Donjek, and Slims-Kaskawulsh drainage basins in Yukon Territory. "Potential" lakes are those which might form during a glacier advance. The data on which this short summary is based were collected by the Glaciology Division of the Inland Waters Directorate (Glaciology Division, 1977).



White River Basin

Within the White River drainage in Yukon Territory there are at least four sites where large ($>10 \times 10^6 \text{ m}^3$), ice marginal lakes might form during an advance of Klutlan Glacier (Fig. 10.4, Table 10.2; Glaciology Division, 1977). However, these lakes would form only if Klutlan Glacier advanced to positions it last attained about 300 years ago (Klutlan V moraine of Rampton, 1970) and, in some cases, to its maximum Neoglacial position, attained 850 to 1100 years ago (Harris Creek moraines). Although Klutlan Glacier is a surging glacier, minor surges probably would not affect the position of the terminus because movement would be damped by the massive ice-cored Neoglacial moraines extending downvalley from the active glacier (Rampton, 1970, p. 1254). Although a large surge might cause a significant advance of the Klutlan terminus, the past history of Neoglacial fluctuations of the glacier indicates that an advance large enough to pond ice marginal lakes at the sites shown in Figure 10.4 is unlikely to occur under existing climatic conditions. Thus, although the potential floods from such lakes are very large indeed (Fig. 10.4, Table 10.2), the likelihood of their occurring in the next several decades is remote.

Small ($<10 \times 10^6 \text{ m}^3$) glacier-dammed lakes are common on the debris-covered terminus of Klutlan Glacier. None of the existing lakes, however, are capable of producing jökulhlaups in excess of about $270 \text{ m}^3/\text{s}$, which is smaller than peak summer ice-melt and snowmelt discharges of White River.* There might be flood damage in the vicinity of the Alaska Highway, however, if a jökulhlaup of this size occurred simultaneously with high snowmelt discharge or during a period when river channels were constricted or plugged with ice.

Figure 10.3. Dunes on the floor of Alsek Valley north of the Lowell Glacier terminus. Slip faces of the dunes are up to 5 m high.

* Peak discharge estimates were made using an empirical equation relating lake volume and maximum instantaneous flood discharge (Clague and Mathews, 1973). Because all existing glacier-dammed lakes in the White River basin are more than 50 km from the Alaska Highway, jökulhlaups from these lakes would be attenuated before reaching the highway. There, peak discharges might be less than those calculated using this equation.

Table 10.2

Comparison of normal discharge range of White, Donjek, and Slims rivers and possible maximum jökulhlaup discharges in the valleys of these rivers.

River	Normal discharge (m ³ /s)			Largest existing lake in basin**		Largest potential lake in basin**	
	Max.	Min.	Mean	Max. jökulhlaup (m ³ /s)†	Distance to Alaska Hwy. (km)	Max. jökulhlaup (m ³ /s)†	Distance to Alaska Hwy. (km)
White	1126	14	112	270	76	2186	49
Donjek	—	—	—	440	67	2268	64
Slims	320	<1	—	440	60	776	14

* Data for White River from Water Survey of Canada records, 1975-1978. No streamflow records are available for Donjek River, but discharge values are probably somewhat lower than those of White River (Glaciology Division, 1977, p. 20-22). Data for Slims River from miscellaneous measurements reported by Fahnestock (1969).
 Max. = maximum instantaneous discharge;
 Min. = minimum daily discharge;
 Mean = mean discharge for period of record.

** Data from Glaciology Division (1977).

† Jökulhlaup discharges determined from empirical equation of Clague and Mathews (1973):
 $Q = 75V^{0.67}$, where
 Q = maximum instantaneous discharge,
 V = lake volume.

Donjek River Basin

Within the Donjek River basin upstream from the Alaska Highway, one existing glacier-dammed lake and one potential glacier-dammed basin exceed $10 \times 10^6 \text{ m}^3$ in volume (Fig. 10.4). The former, Hazard Lake ($14 \times 10^6 \text{ m}^3$), drained abruptly in July 1975, in July or August 1977, and again in late summer 1978 (Collins and Clarke, 1977; R. May, pers. comm., 1978). In each case there was no apparent flooding of the Alaska Highway at the Donjek River crossing. This is perhaps due to the fact that Hazard Lake is 67 km from the highway crossing, thus a jökulhlaup probably would attenuate as it progressed down Donjek Glacier and the broad Donjek River floodplain. Furthermore, Hazard Lake theoretically is capable of producing a maximum flood discharge of $440 \text{ m}^3/\text{s}$, which is within the range of normal summer discharge maxima of Donjek River.

An advance of the toe of Donjek Glacier of less than 1 km might block Donjek River and form a lake with a maximum volume of about $162 \times 10^6 \text{ m}^3$. Theoretically, a flood with a peak discharge of about $2270 \text{ m}^3/\text{s}$ might result from the failure of the resulting ice dam (Table 10.2), although the flood would attenuate somewhat as it passed down Donjek Valley. Shorelines in Donjek Valley near the terminus of Donjek Glacier indicate that such a lake has existed at least once since the glacier reached its Neoglacial maximum 300 to 440 years ago (Denton and Stuiver, 1966).

Because a relatively minor advance of Donjek Glacier might form a large unstable lake capable of draining rapidly due to breaching of the ice dam, the possibility of catastrophic flooding should be considered in the future development of Shakwak Valley in the vicinity of Donjek River.

Slims-Kaskawulsh Basin

Meltwater flow issuing from the snout of Kaskawulsh Glacier is in part funnelled north via Slims River into Shakwak Valley and Kluane Lake and in part south via Kaskawulsh River into Alsek Valley. The proportion of the total meltwater discharge of Kaskawulsh Glacier transmitted by Slims and Kaskawulsh rivers varies seasonally and

annually, thus it is difficult to predict the path of jökulhlaups originating in the glacier basin. Only jökulhlaups progressing down Slims Valley might damage the Alaska Highway and other structures on the subaerial delta of Slims River.

Two glacier-dammed lakes and one potential lake basin associated with Kaskawulsh Glacier have or are capable of water volumes in excess of $10 \times 10^6 \text{ m}^3$ (Fig. 10.4; Glaciology Division, 1977). The potential lake basin ($33 \times 10^6 \text{ m}^3$) has a small probability of refill under existing climatic conditions, and its jökulhlaup flow path is into Kaskawulsh River. The two existing lakes (each $14 \times 10^6 \text{ m}^3$) are located so far upglacier from the Kaskawulsh terminus that jökulhlaups would be damped significantly before the floodwaters left the glacier.

Future changes in the regimen of Kaskawulsh Glacier likely will affect the apportionment of meltwater between Slims and Kaskawulsh rivers. This in turn will affect jökulhlaup flow paths. For example, if Kaskawulsh River progressively "pirates" water now channeled down Slims Valley, jökulhlaups increasingly will flow into Kaskawulsh Valley.* An additional consequence of the long-term diversion of Slims River water into Kaskawulsh River would be a decrease in the mean level of Kluane Lake by at least 1 m (short-term diversions of Slims River in the past 25 years have caused fluctuations in lake levels of this magnitude). A lengthy stand of Kluane Lake at a lower level might result in streams flowing into the lake incising their channels. The design of bridge footings and the determination of pipeline burial depths at stream crossings should be made with this in mind.

Stream Flooding

High-gradient streams enter Shakwak Valley from the rugged Kluane Ranges to the southwest. Most of these cross large alluvial fans and alluvial aprons built from the mountain front into the valley.

Although there are no long-term water discharge records for any of these streams, field observations indicate that there are very large discharge variations, probably caused by summer storms and by large seasonal differences in the supply of meltwater from snowpack and glaciers. Extreme

* Although the headwaters of the two rivers issue from opposite sides of the snout of Kaskawulsh Glacier and are only about 6 km apart, Kaskawulsh River heads at a lower elevation than Slims River. It is likely that only the glacier itself prevents the capture of the latter by the former.

discharge variability is reflected geomorphically by multiple braided distributary channels on alluvial fans and aprons. During periods of high discharge, a stream entering Shakwak Valley may shift its course from one part of the alluvial surface on which it is flowing to another. Although attempts have been made to constrain the flow of the most unruly of these streams to single channels, the possibility of serious localized flooding still remains.

Conclusions

Neoglacial Lake Alsek formed and drained repeatedly in the past several hundred years as a result of the damming of Alsek River by Lowell Glacier. At the maximum of each of the major lake phases, water backed up into Dezadeash Valley. Parts of what are now the Alaska Highway and Haines Road, the site of the town of Haines Junction, and part of the

proposed Alaska Highway gas pipeline route were inundated during high stands of the lake. Lowell Glacier presently terminates in Alsek Valley and may be capable during a surge of blocking Alsek River and forming a new lake. The maximum size of the resulting lake cannot be predicted, but under existing conditions it is unlikely that it would exceed that of the ca. 1850 A.D. lake.

In addition to floods caused by excessive precipitation and snow and ice melt, jökulhlaups may occur in White, Donjek, and Slims valleys. Jökulhlaups from existing glacier-dammed lakes would have peak discharges no larger than maximum summer ice-melt and snowmelt discharges in these valleys. Much larger, potentially catastrophic floods might result however if either Klutlan or Donjek glaciers advanced to block streams near their termini. Although the possibility that Klutlan Glacier might advance far enough to create large ice marginal lakes is remote in the foreseeable future, Donjek Glacier probably is capable under present climatic conditions of advancing across Donjek Valley to impound a potentially dangerous lake.

High-gradient streams flowing from the Klauane Ranges across alluvial fans and aprons into Shakwak Valley may periodically flood, with resultant damage to the Alaska Highway and other man-made structures.

References

Aitkenhead, N.
1960: Observations on the drainage of a glacier-dammed lake in Norway; *Journal of Glaciology*, v. 3, p. 607-609.

Arnborg, L.
1955: Hydrology of the glacier river Austurfljot; *Geografiska Annaler*, arg 37, p. 185-201.

Björnsson, H.
1974: Explanation of jökulhlaups from Grimsvatn, Vatnajökull, Iceland; *Jökull*, ar. 24, p. 1-26.

Clague, J.J.
1979: The Denali Fault System in southwest Yukon Territory - A geologic hazard?; in *Current Research, Part A Geological Survey of Canada, Paper 79-1A*, p. 169-178.

Clague, J.J. and Mathews, W.H.
1973: The magnitude of jökulhlaups; *Journal of Glaciology*, v. 12, p. 501-504.

Collins, S.G. and Clarke, G.K.C.
1977: History and bathymetry of a surge-dammed lake; *Arctic*, v. 30, p. 217-224.

Denton, G.H. and Stuiver, M.
1966: Neoglacial chronology, north-eastern St. Elias Mountains, Canada; *American Journal of Science*, v. 264, p. 577-599.

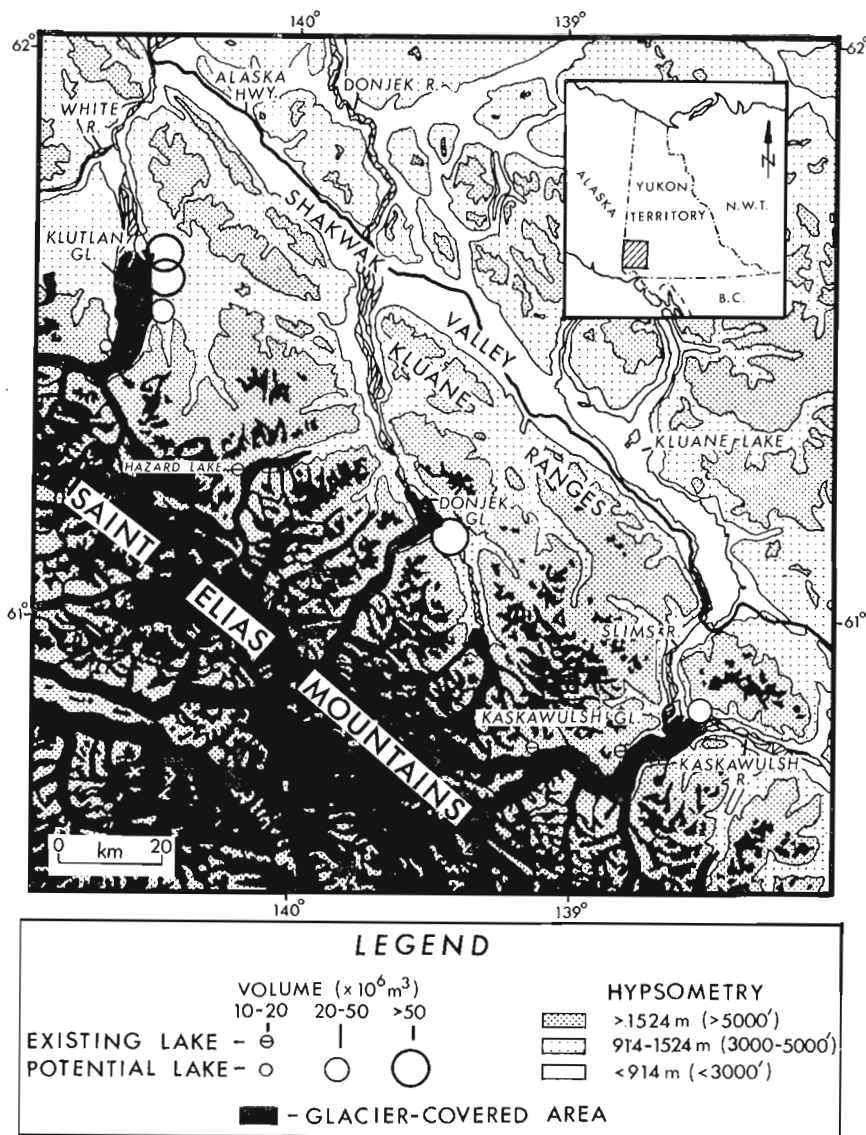


Figure 10.4. Existing and potential glacier-dammed lakes larger than $10 \times 10^6 \text{ m}^3$ within the White, Donjek, and Slims-Kaskawulsh basins in Yukon Territory. Potential lakes are basins in which water would be ponded in the event of a major glacier advance. Basins near the termini of Klutlan and Kaskawulsh glaciers have not held water for several centuries and are not likely to do so in the foreseeable future.

- Fahnestock, R.K.
1969: Morphology of the Slims River; in Icefield Ranges Research Project: Scientific Results, Volume 1, ed. V.C. Bushnell and R.H. Ragle; American Geographical Society, Arctic Institute of North America, New York, Montreal, p. 161-172.
- Glaciology Division
1977: Report on the influence of glaciers on the hydrology of streams affecting the proposed Alcan pipeline route; Canada Department of Fisheries and Environment, Inland Waters Directorate, Vancouver, British Columbia, unpublished report, 38 p.
- Hughes, O.L., Rampton, V.N., and Rutter, N.W.
1972: Quaternary geology and geomorphology, southern and central Yukon (northern Canada); 24th International Geological Congress (Montreal), Guidebook, Field Excursion All, 59 p.
- Johnson, F. and Raup, H.M.
1964: Investigations in southwest Yukon: geobotanical and archaeological reconnaissance; Robert S. Peabody Foundation, Archaeological Papers, v. 6, no. 1, p. 3-198.
- Kindle, E.D.
1952: Dezadeash map-area, Yukon Territory; Geological Survey of Canada, Memoir 268, 68 p.
- Laguna, F. de
1972: Under Mount Saint Elias: the history and culture of the Yakutat Tlingit; Smithsonian Contributions to Anthropology, v. 7 (3 pt.), 1395 p.
- Liestøl, O.
1955: Glacier dammed lakes in Norway; Norsk Geografisk Tidsskrift, bd. 15, p. 122-149.
- Mason, K.
1935: The study of threatening glaciers; Geographical Journal, v. 85, p. 24-41.
- Mathews, W.H.
1965: Two self-dumping ice-dammed lakes in British Columbia; Geographical Review, v. 55, p. 46-52.
1973: Record of two jökullhlaups; in Symposium on the Hydrology of Glaciers; International Association of Scientific Hydrology, Publication no. 95, p. 99-110.
- McConnell, R.G.
1905: The Kluane mining district; in Summary Report on the Operations of the Geological Survey for the Year 1904; Geological Survey of Canada, Annual Report (New Series), v. 16, p. 1A-18A.
- Nye, J.F.
1976: Water flow in glaciers: jökulhlaups, tunnels and veins; Journal of Glaciology, v. 17, p. 181-207.
- Post, A. and Mayo, L.R.
1971: Glacier dammed lakes and outburst floods in Alaska; United States Geological Survey, Hydrologic Investigations Atlas, no. HA-455, map and explanatory text.
- Rampton, V.N.
1970: Neoglacial fluctuations of the Natazhat and Klutlan Glaciers, Yukon Territory, Canada; Canadian Journal of Earth Sciences, v. 7, p. 1236-1263.
Surficial deposits and landforms of Kluane National Park; Geological Survey of Canada, Paper (in press).
- Rist, S.
1955: Skeidarárhlaup 1954 (in Icelandic) ; Jökull, ár. 5, p. 30-36.
- Stone, K.H.
1963: The annual emptying of Lake George, Alaska; Arctic, v. 16, p. 26-40.
- Ström, K.M.
1938: The catastrophic emptying of a glacier-dammed lake in Norway 1937; Geologie der Meere und Binnengewässer, bd. 2, p. 443-444.
- Tarr, R.S. and Martin, L.
1914: Alaskan glacier studies of the National Geographic Society in the Yakutat Bay, Prince William Sound and lower Copper River regions; National Geographic Society, Washington, D.C., 498 p.
- Thorarinsson, S.
1939: The ice dammed lakes of Iceland with particular reference to their values as indicators of glacier oscillations; Geografiska Annaler, bd. 21, p. 216-242.
1957: The jökulhlaup from the Katla area in 1955 compared with other jökulhlaups in Iceland; Jökull, ár. 7, p. 21-25.
- Tomásson, H.
1974: Grimsvatnahlaup 1972, mechanism and sediment discharge; Jökull, ár. 24, p. 27-39.

Project 720078

Sigrid Lichti-Federovich
Terrain Sciences Division

Lichti-Federovich, S., *Contributions to the diatom flora of Arctic Canada: Report 1. Scanning electron micrographs of some freshwater species from Ellesmere Island; in Current Research, Part B, Geological Survey of Canada, Paper 79-1B, p. 71-82, 1979.*

Abstract

Scanning electron micrographs of the diatoms *Achnanthes flexella*, *Amphora veneta*, *Ceratoneis arcus*, *Cyclotella antiqua*, and *Navicula tuscula* are presented, together with a description of their respective ecological and environmental characteristics. This report represents the first contribution to a comprehensive illustrated floristic account of the diatoms of the Canadian Arctic.

Introduction

This paper is the first contribution to a comprehensive illustrated account of the diatom flora of the Canadian Arctic. This larger endeavour is designed to enumerate the diatom taxa of arctic regions, to characterize their respective ecologies, and to delineate their climatic/geographic affinity. The extensive use of scanning electron micrographs is aimed principally to aid in the description of new taxonomic entities, to clarify phylogenetic relationships, and specifically to facilitate and assist in critical identification since the effectual application of diatom analysis as a paleoecological tool and the validity of paleoenvironmental interpretations rest foremost upon the ability to identify correctly the various taxa present.

Acknowledgments

I extend my appreciation to W. Blake, Jr. for collecting the sample material, to D.A. Walker for his technical skill in taking the scanning electron micrographs, and to the members of the Photographic Section for preparation of the photographic prints. The manuscript has been read critically, and helpful comments provided as to the distribution of the species reported, by M.R. Sreenivasa, University of New Brunswick, Fredericton.

Materials and Methods

The diatoms illustrated in this report (Plates 11.1-11.5 on following pages) were obtained from samples collected by W. Blake, Jr. during glacial geological studies in eastern and southern Ellesmere Island in July and August 1977.

Preparation of the samples followed the conventional methods employed by most diatomists. Plankton samples were treated with concentrated sulphuric acid and potassium dichromate; diatoms in sediment samples were cleaned with cold 15% hydrogen peroxide. Variations in the treatment as to its duration, application of heat, strength of acid, etc. depend on the organic content of the sample material. After several washings with distilled water to remove any trace of acid or oxidizing agent, a small amount of the diluted diatom-bearing suspension was filtered using a 0.45 μm polycarbonate filter. Preparation for electron-microscopic studies (Walker, 1978) consisted in mounting a 1/2 inch disc of the diatom-bearing 'Nuclepore' filter onto a SEM stub covered with a thin layer of carbon paint to eliminate heat build up, and coating it with gold/palladium. All electron micrographs were taken with the Geological Survey's ETEC Autoscan at 20 kV, and the light micrographs were obtained with a Leitz Ortholux x90 oil immersion objective and the Wild Photoautomat MPS50.

References

- Cleve-Euler, A.
1953: Die Diatomeen von Schweden und Finnland, III; Kungliga Svanska Vetenskaps-akademiens Handlingar, Fjärde Serien, v. 4, no. 5, p. 1-255.
- Cholnoky, B.J.
1968: Die Ökologie der Diatomeen in Binnengewässern; Verlag J. Cramer, 699 p.
- Florin, M.B.
1944: En sensubarktisk transgression i trakten av södra Kilsbergen enligt diatomacésucceSSIONEN i områdets högre belägna fornsjölagerföljder; Stockholm, Geologiska Förening i Stockholm Förhandlingar, v. 66, p. 417-448.
- Foged, N.
1953: Diatoms from West Greenland; Meddelelser om Grønland, v. 4, no. 6, p. 1-86.
1954: On the diatom flora of some Funen lakes; Folia Limnologica Scandinavica, no. 6, p. 1-75.
1955: Diatoms from Peary Land, North Greenland; Meddelelser om Grønland, v. 128, no. 7, p. 1-90.
1958: The diatoms in the basalt area and adjoining areas of Archean rock in West Greenland; Meddelelser om Grønland, v. 156, no. 4, p. 1-146.
1964: Freshwater diatoms from Spitsbergen; Tromsø Museums Skrifter, v. 11, 204 p.
1973: Diatoms from Southwest Greenland; Meddelelser om Grønland, v. 194, no. 5, p. 1-84.
- Gandhi, H.P.
1966: The freshwater diatom flora of the Jog-Falls, Mysore State; Nova Hedwigia, v. 11, p. 89-197.
- Halme, E. and Mölder, K.
1958: Planktologische Untersuchungen in der Pojo-bucht und angrenzenden Gewässern. III. Phytoplankton; Annales Botanici Societatis "Vanamo", v. 30, no. 3, p. 1-70.
- Haworth, E.Y.
1972a: The recent diatom history of Loch Leven, Kinross; Freshwater Biology, v. 2, p. 131-141.
1972b: Diatom succession in a core from Pickerel Lake, northeastern South Dakota; Geological Society of America Bulletin, v. 83, p. 157-172.
1974: Some problems of diatom taxonomy in Scottish lake sediments; British Phycological Journal, v. 9, p. 47-55.

(References continue p. 82)

***Achnanthes flexella* (Kützing) Brun**

Diat. des alpes, p. 29, 1880.

Synonymy: See Van Landingham, 1967, p. 26-28.

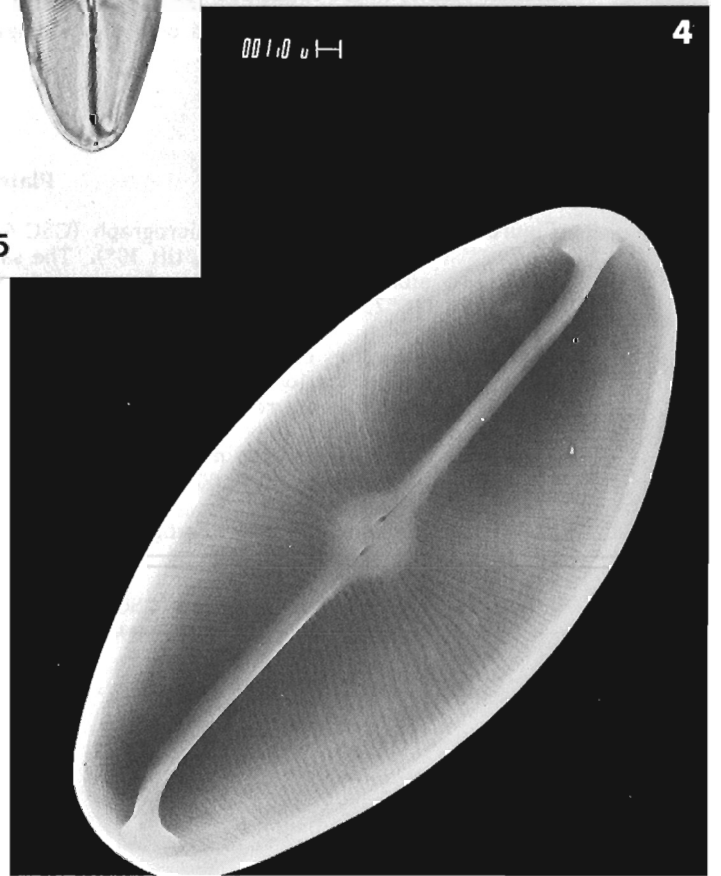
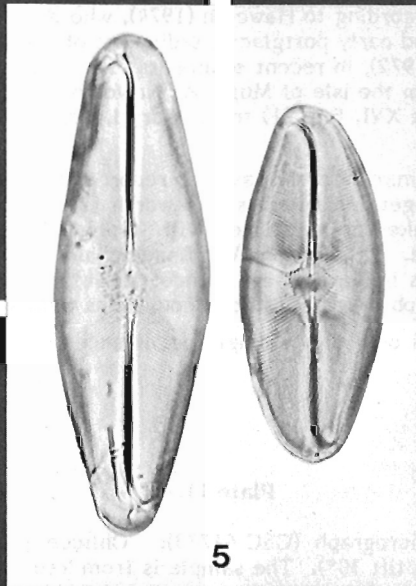
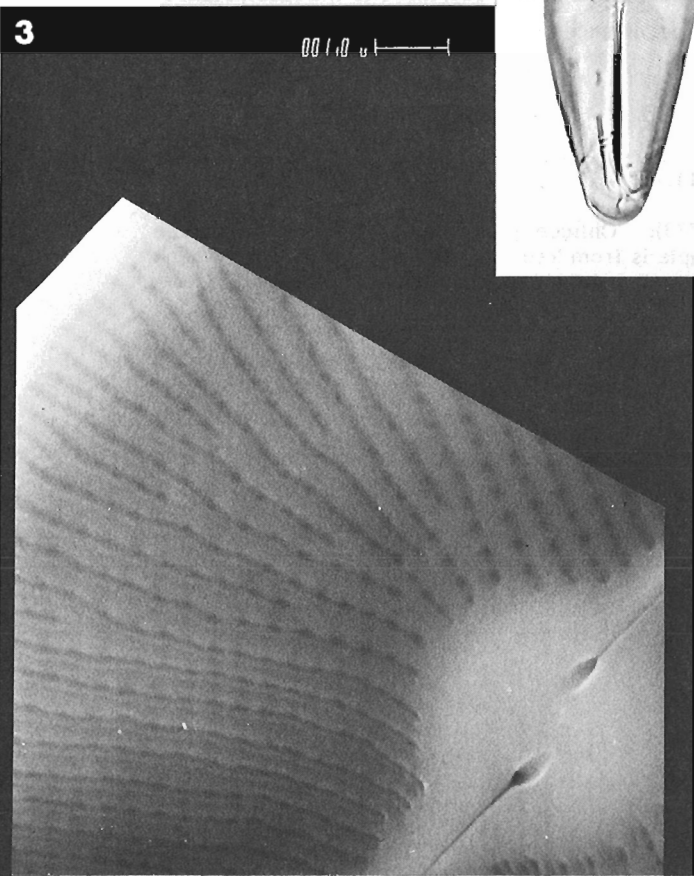
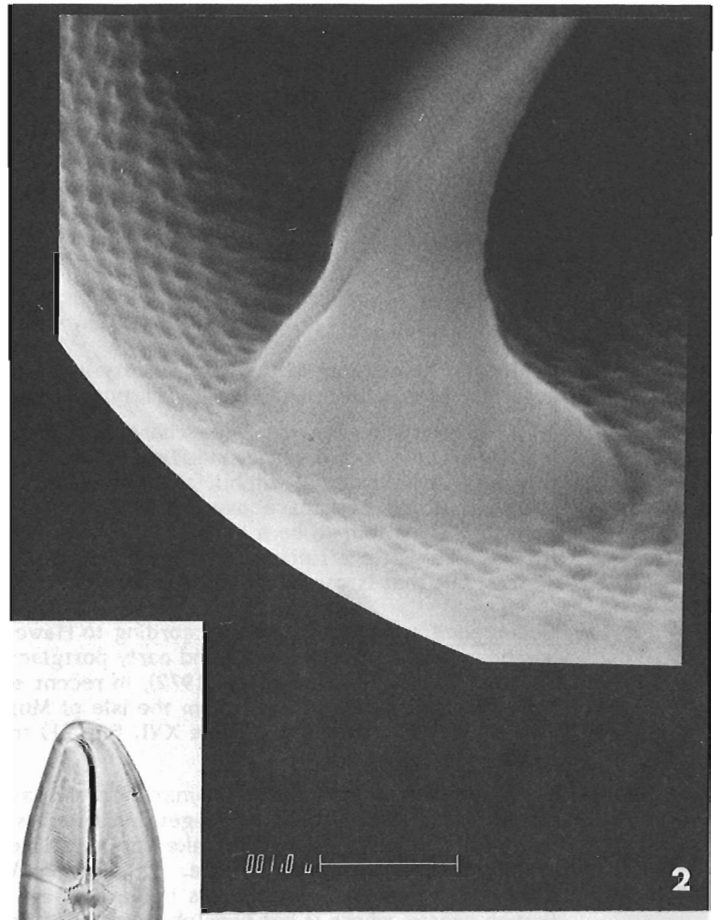
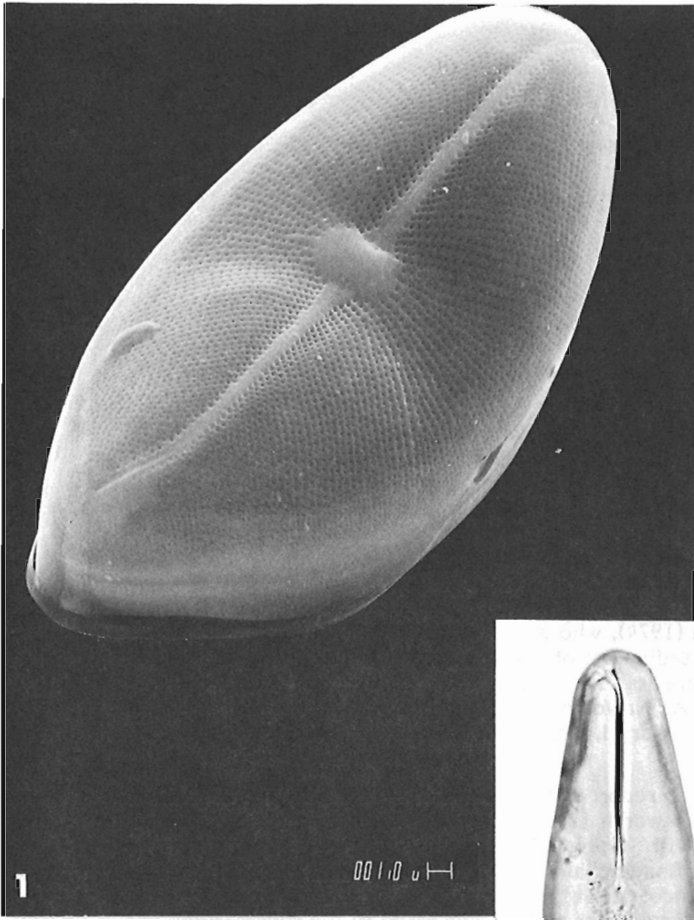
Ecology: Foged (1954) characterized this boreal cold water form as being limnophilous and indifferent to salinity and pH, whereas Jørgensen (1948) and Round (1957) considered the species to be acidophilous. Cholnoky (1968) assigned *Achnanthes flexella* a pH optimum of about 6.0; he also included this taxon in the list of indicator species for high oxygen concentration. Hustedt (1942) listed a pH range of 6.2 to 9.0 with maximum abundance at pH 6.3 as well as pH 7.0.

Occurrence and Distribution: *Achnanthes flexella* was reported from northern Sweden by Hustedt (1942) and Cleve-Euler (1953), from Finnish lakes by Mölder and Tynni (1972), and from Greenland and Spitsbergen by Foged (1955, 1958, 1964, 1973).

In eastern Ellesmere Island, *Achnanthes flexella* occurs as common co-dominant or attendant species in many freshwater diatom associations from arctic ponds.

Plate 11.1

- Figure 1. Scanning electron micrograph (GSC 61769): Frustule in valve view (magnification x3000, tilt 30°). The sample is from the water of some moss collected along the shore of the largest low-level lake in the northwestern part of the Cape Herschel Peninsula (78°37.6'N, 74°43'W).
- Figure 2. Scanning electron micrograph (GSC 61770): Higher magnification of inner marginal zone illustrating the deflected polar raphe fissure ending (magnification x19 000, tilt 30°). Figures 2 to 5 are of diatoms from the mud-water interface in a pond on raised beaches north of the head of Herschel Bay (78°36.3'N, 74°45'W).
- Figure 3. Scanning electron micrograph (GSC 61770): Magnified central area of inner valve surface showing the expanded central raphe fissure ending (magnification x10 000, tilt 30°).
- Figure 4. Scanning electron micrograph (GSC 61770): Inside view of valve (magnification x900, oil immersion, Hyrax mount).
- Figure 5. Light photomicrographs (GSC 61771 and GSC 61772): General picture. Valvar view (magnification x900, oil immersion, Hyrax mount).



***Amphora veneta* Kützing**

Die Kieselchal. Bacill. od. Diat., Nordhausen, p. 108, Pl. 3, Fig. 24, 1844.

Synonymy: See Van Landingham, 1967, p. 276-277.

Var. **capitata** Haworth
Br. phycol. J., v. 9, p. 48, Fig. 6, 19, 1974

Ecology: The ecology of this new variety is insufficiently known; however, it may be assumed that it is similar to that of the nominate variety.

Amphora veneta has been characterized by Hustedt (1957) as oligohalobous (indifferent), pH indifferent, meso-oxybiontic, indifferent to current rate but not limnobiontic. Foged (1953) regarded this form as halophil, alkaliphil, and limnophil, and Cholnoky (1968) assigned ***Amphora veneta*** a pH optimum at or perhaps above pH 8.5. Whereas Hustedt (1930) and Halme and Mölder (1958) considered this diatom to be a littoral form of fresh as well as brackish water, Cholnoky (1968) negated its brackish water affinity and stated that ***Amphora veneta*** occurs as an inhabitant of highly alkaline waters, but that it cannot tolerate changes in osmotic pressure.

Occurrence and Distribution: According to Haworth (1974), who described and named this variety, it has been found in late-glacial and early postglacial sediments of Loch Borrelan and Loch Sionascaig, Scotland (cf. Pennington et al., 1972), in recent sediments of Loch Leven (cf. Haworth, 1972a), and in collections of algal material from the Isle of Mull. As Haworth stated, and I agree, the specimen of Foged's (1955) drawing (his Table XVI, Fig. 21) from Peary Land, North Greenland is likely to belong to var. **capitata**.

The occurrence of the nominate variety has been recorded by Gandhi (1966) in ditches and pools and in marked abundance on vegetable detritus. Haworth (1972b) reported ***Amphora veneta*** as a benthic form from Minnesota lakes or associated with ***Typha***. Hustedt (1957) found it on stones, mosses, ***Hydrocharis***, and ***Lemna***. In addition, Van Landingham (1966) indicated its rare to locally abundant occurrence in dry lakes in Nevada, and Hendey (1964) stated its common occurrence on all British coasts, where it has been observed as "flat mucous films tightly adpressed to the substratum".

In eastern Ellesmere Island only a few single occurrences of ***Amphora veneta*** and its variety **capitata** have been noted to date.

Plate 11.2

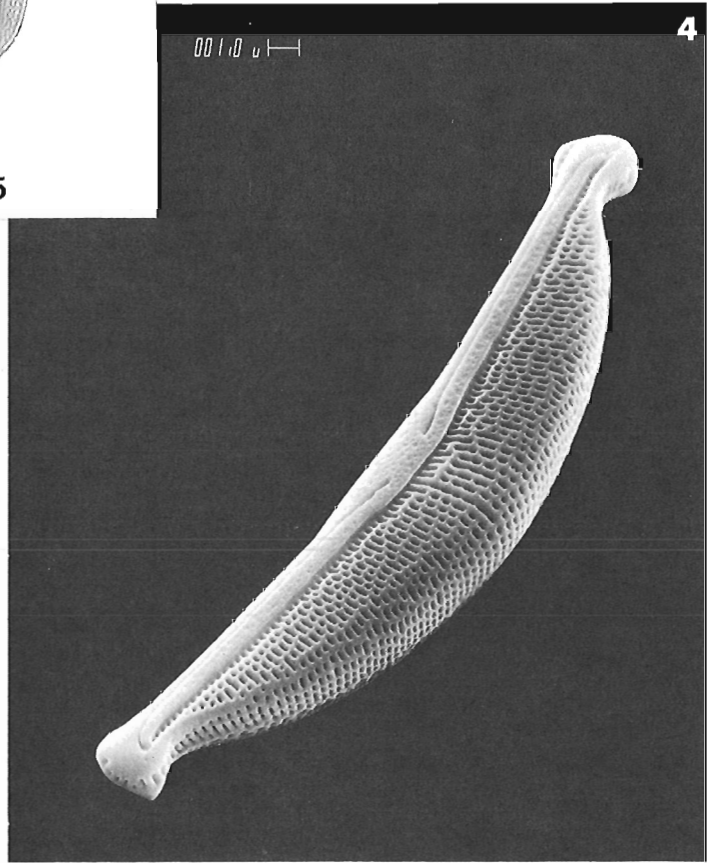
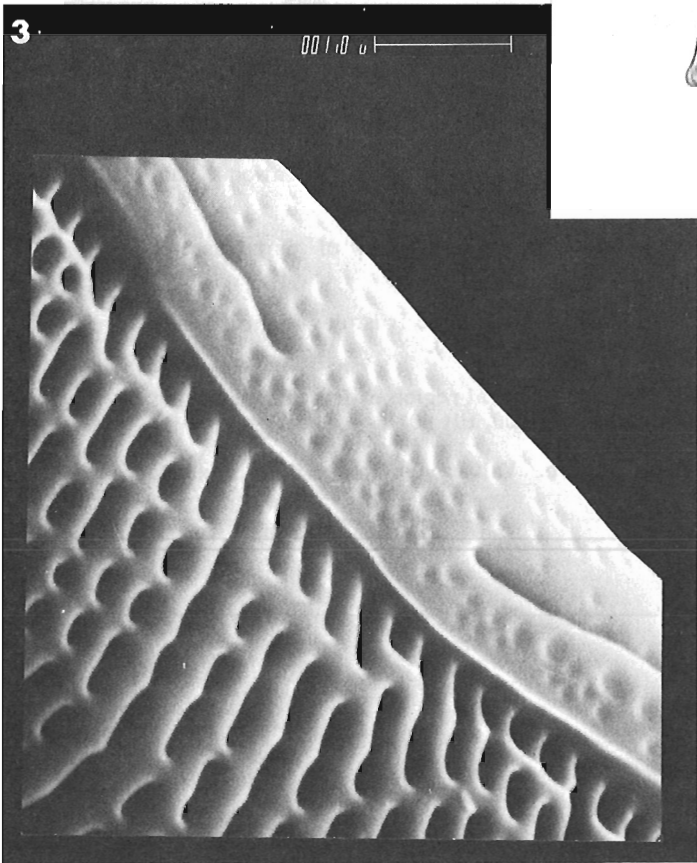
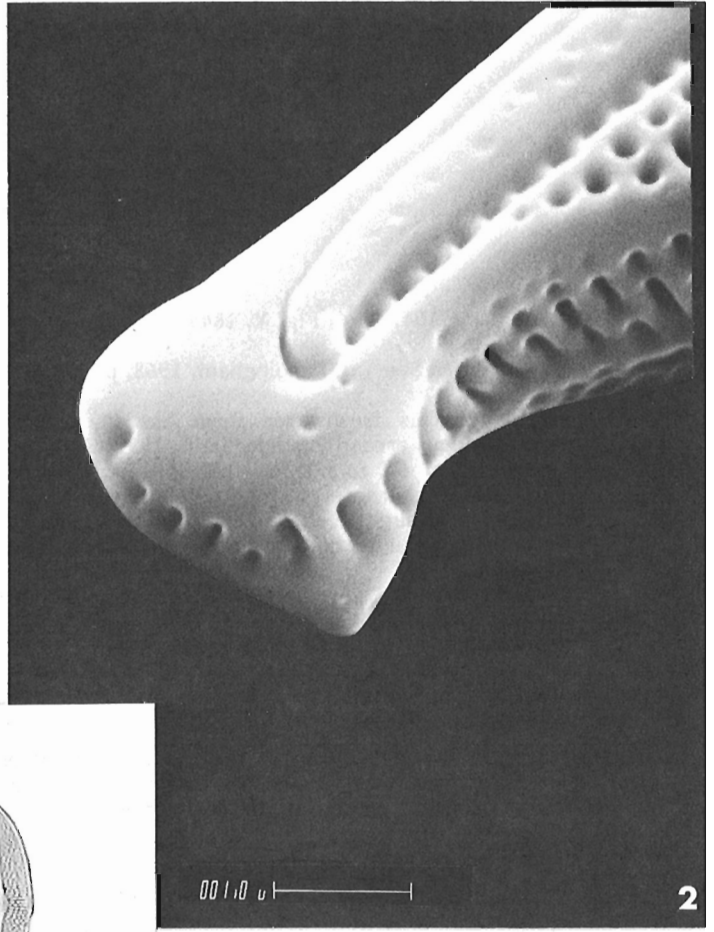
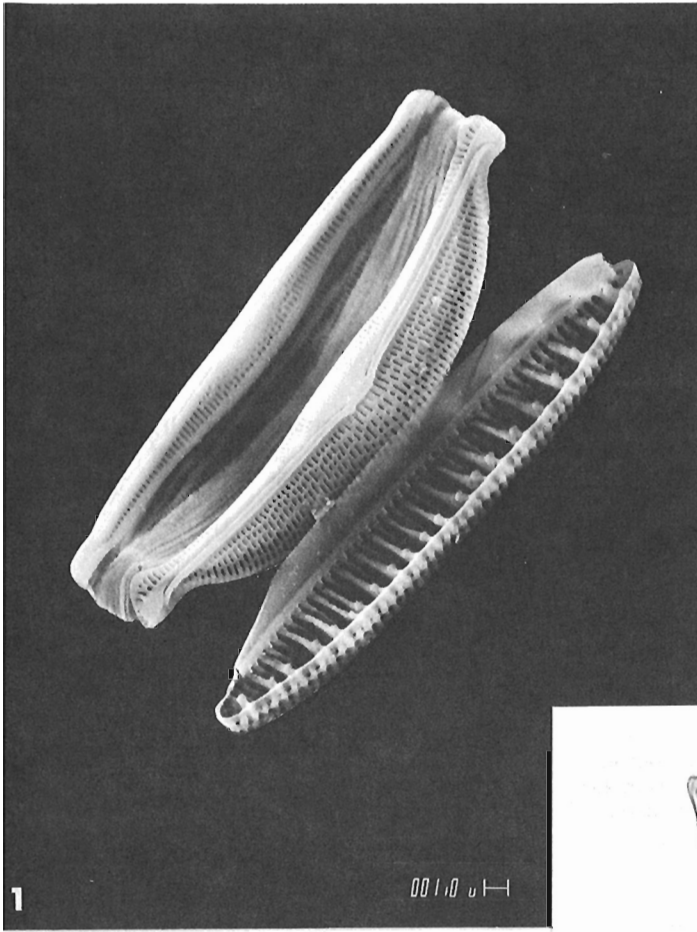
Figure 1. Scanning electron micrograph (GSC 61773): Oblique internal view of entire frustule (magnification x3000, tilt 30°). The sample is from 'red snow' collected from a snowbank along the north side of a river valley, ca. 6.5 km north-northeast of Cape Storm (76°23.9'N, 87°32'W).

Figure 2. Scanning electron micrograph (GSC 61774): Valve end showing structural detail (magnification x19 000, tilt 30°). Figures 2 to 5 are from the same mud-water interface sample as figures 2 to 5, Plate 11.1.

Figure 3. Scanning electron micrograph (GSC 61774): Enlarged central area of outer valve surface (magnification x90 000, tilt 30°).

Figure 4. Scanning electron micrograph (GSC 61774): Outside view of valve (magnification x4000, tilt 30°).

Figure 5. Light photomicrograph (GSC 61775): General picture. Valvar view (magnification x900, oil immersion, Hyrax mount).



Ceratoneis arcus (Ehrenberg) Kützing

Bacill., p. 104, Pl. 6, Fig. X, 1844.

Synonymy: See Van Landingham, 1968, p. 687-688.

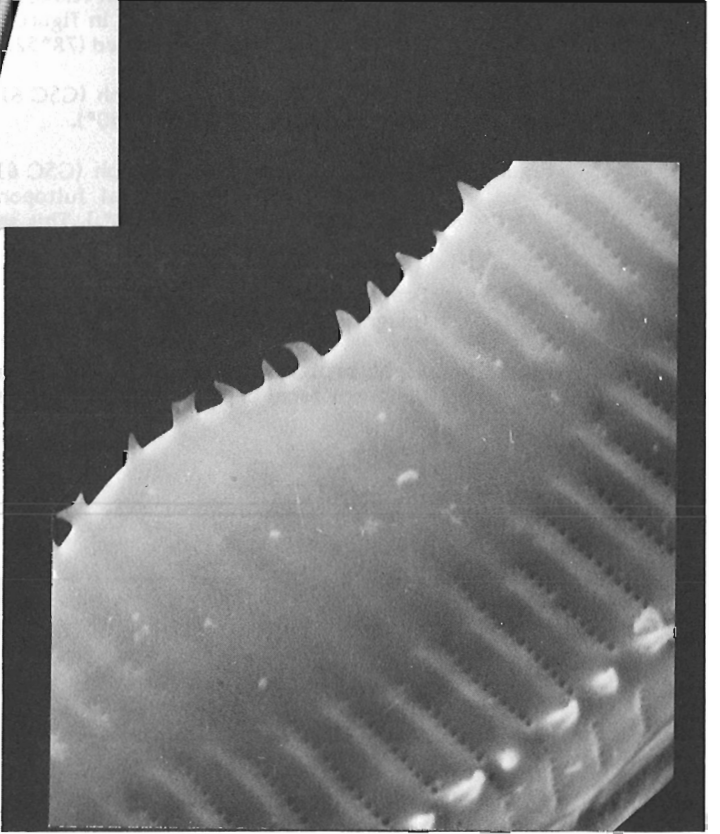
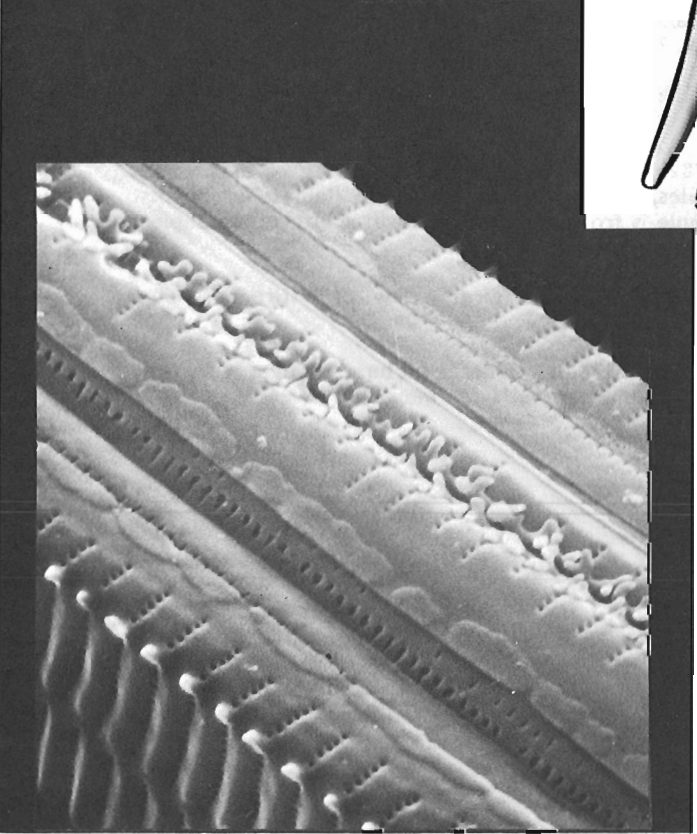
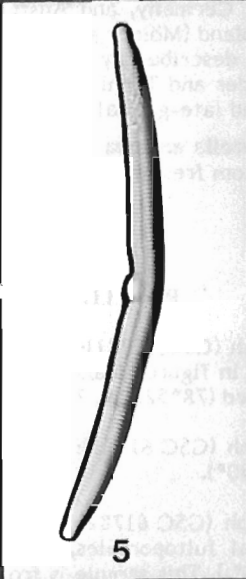
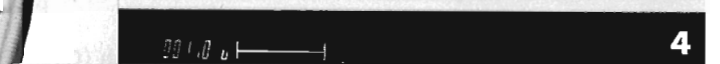
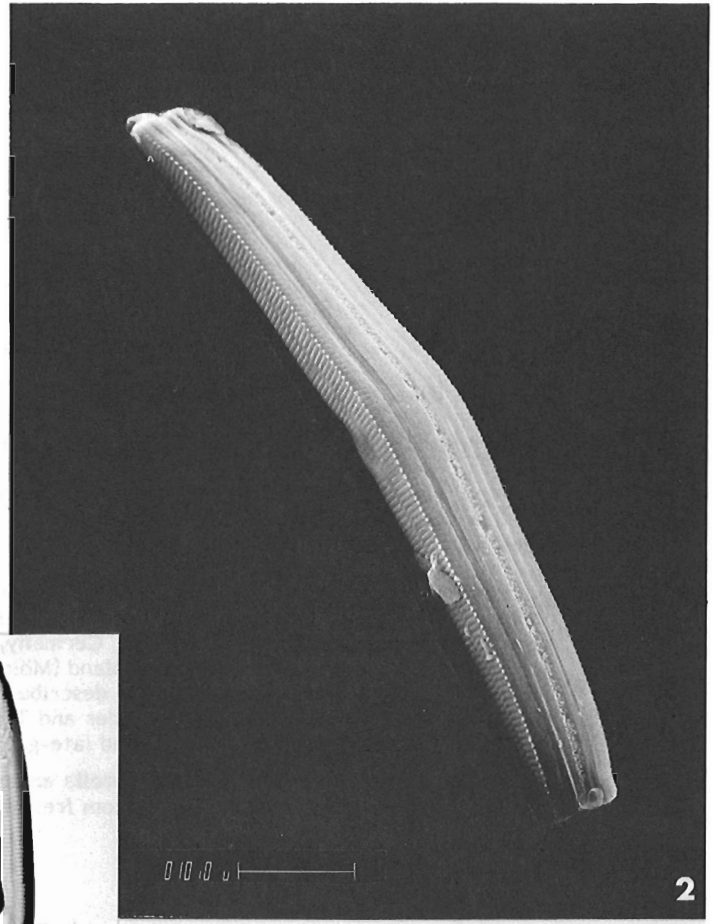
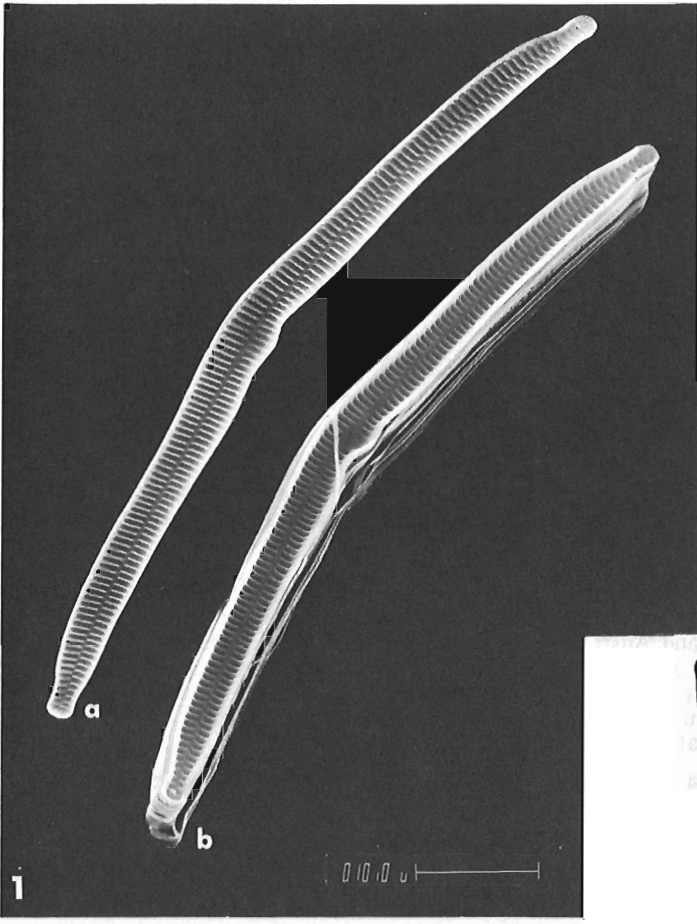
Ecology: This freshwater form has its optimal development in cold flowing water, especially mountainous areas (Hustedt, 1930, 1959; Patrick and Reimer, 1966). Sovereign (1958) suggested a pH range from 6.0 to 8.0 for this species. Hustedt (1957) assigned **Ceratoneis arcus** the following ecological characteristics: alkaliphilous (alkalibiontic?), oligohalobous, and rheobiontic. A pH optimum of slightly above pH 7.0 (at about pH 7.2 to 7.3) has been cited by Cholnoky (1968). He also stated that this taxon is unable to withstand changes in osmotic pressure.

Occurrence and Distribution: According to Hustedt (1959) **Ceratoneis arcus** is common in flowing water throughout Europe where it occurs in great abundance in mountain streams and springs. Mölder and Tynni (1970) reported it as a frequent inhabitant of clear water lakes and fast flowing streams in northern Finland, and Sovereign (1958) stated its frequent occurrence in mountain streams of the Pacific Northwest. Additional distribution of this species in the United States has been listed by Patrick and Reimer (1966).

In eastern Ellesmere Island, the marked preponderance of **Ceratoneis arcus** in stream water samples, its less frequent occurrence in collections from lakes with fluvial influx, and its absence from floristic enumerations of pond samples clearly denote the highly specific autecology of this rheobiontic form.

Plate 11.3

- Figure 1a. Scanning electron micrograph (GSC 61776): Exterior view of a valve (magnification x1800, tilt 30°). The sample is from stream water on the north side of the northernmost tidal glacier on the west side of Bentham Fiord, Makinson Inlet (77°10.5'N, 80°10'W).
- Figure 1b. Scanning electron micrograph (GSC 61777): Interior view of a valve (magnification x1700, tilt 30°).
- Figure 2. Scanning electron micrograph (GSC 61778): Oblique dorsal girdle view of joint frustules (magnification x1600, tilt 30°).
- Figure 3. Scanning electron micrograph (GSC 61778): Detail of two joined frustules in girdle view with marginal and linking spines (magnification x12 000, tilt 30°).
- Figure 4. Scanning electron micrograph (GSC 61779): Enlarged central region of frustule displaying structureless area of ventral margin (magnification x13 000, tilt 30°).
- Figure 5. Light photomicrograph (GSC 61780): General picture. Valvar view (magnification x900, oil immersion, Hyrax mount).



Cyclotella antiqua W. Smith

Syn. Brit. Diat., v. I, p. 28, Pl. V, Fig. 49, 1853.

Synonymy: See Van Landingham, 1969, p. 1099-1100.

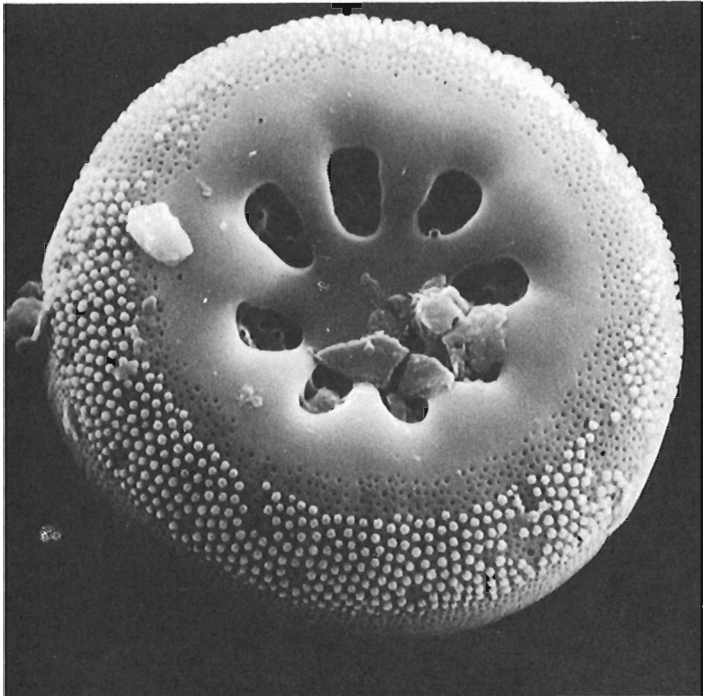
Ecology: Foged (1953) considered **Cyclotella antiqua** a halophob and an acidophil. Hustedt (1942) listed a pH range of 6.3 to 8.4, but stated that the taxon always occurs most abundantly at a pH below 7.0.

Occurrence and Distribution: The general distribution of this boreal cold water species is limited to northern or mountainous regions (Hustedt, 1930). **Cyclotella antiqua** has been found in northern Russia, Fennoscandia, the British Isles, Germany, and Austria. It also has been recorded from the littoral zone of oligotrophic lakes in Lapland (Mölder and Tynni, 1968), and its frequent occurrence as a benthic form in Peary Land has been described by Foged (1955). The subfossil occurrence of this boreal species has been reported by Mölder and Tynni (1968). Round (1957) characterized this form as important indicator species of glacial and late-glacial sediments.

In eastern Ellesmere Island **Cyclotella antiqua** occurs as frequent but never abundant floristic component of the diatom associations from freshwater collections.

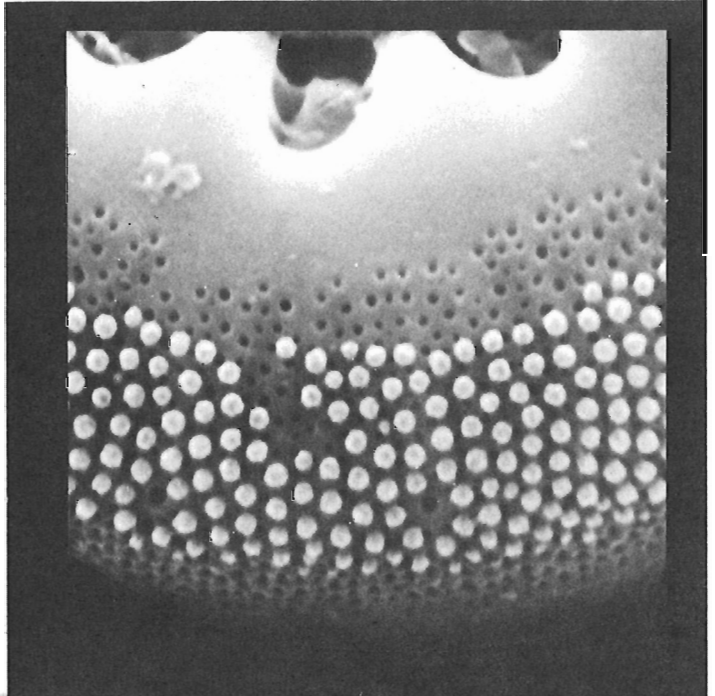
Plate 11.4

- Figure 1. Scanning electron micrograph (GSC 61781): Exterior view of valve (magnification x7000, tilt 30°). The sample shown in figures 1 and 2 is from the water of a pond adjacent to the RCMP post at Alexandra Fiord (78°52.9'N, 75°47'W).
- Figure 2. Scanning electron micrograph (GSC 61781): Enlarged part of outer marginal valve zone (magnification x17 000, tilt 30°).
- Figure 3. Scanning electron micrograph (GSC 61782): Inside view of valve showing poroids with cribra, central and marginal fultoportules, and a single rimoportule (labiate process). (Magnification x6000, tilt 30°.) This sample is from the same mud-water interface sample as figures 2 to 5, Plates 11.1 and 11.2.
- Figure 4. Scanning electron micrograph (GSC 61783): Oblique girdle view of entire frustule (magnification x6000, tilt 30°).
- Figure 5. Light photomicrograph (GSC 61784 and GSC 61785): General picture. Valvar view at different focal depth (magnification x900, oil immersion, Hyrax mount).



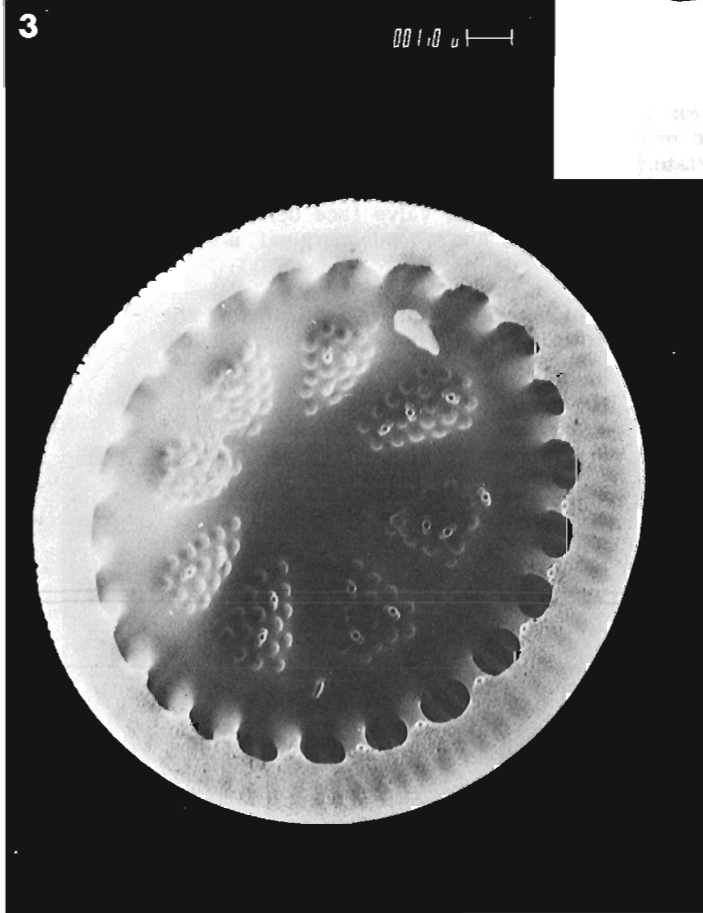
1

001.0 μm



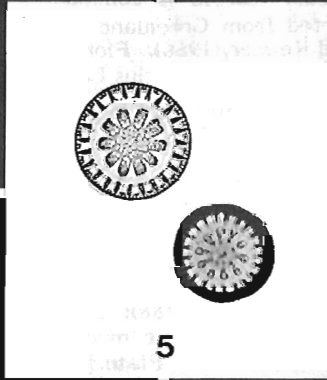
2

001.0 μm

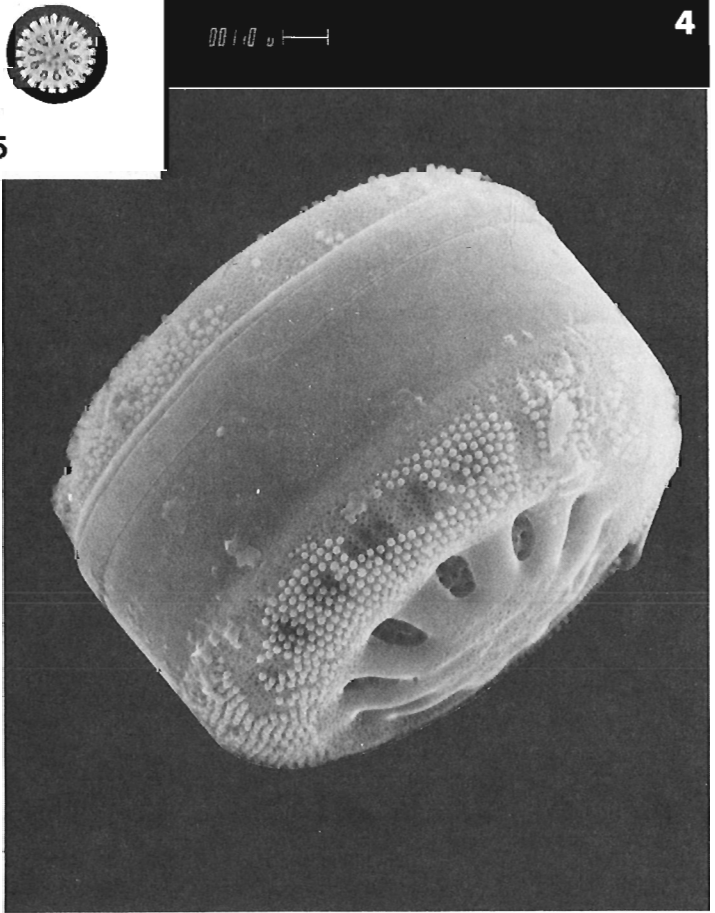


3

001.0 μm



5



4

001.0 μm

Navicula tuscula Ehrenberg

Ber. Akad. Wiss. Berlin for 1840, p. 215.

Synonymy: See Van Landingham, 1975, p. 2861-2863.

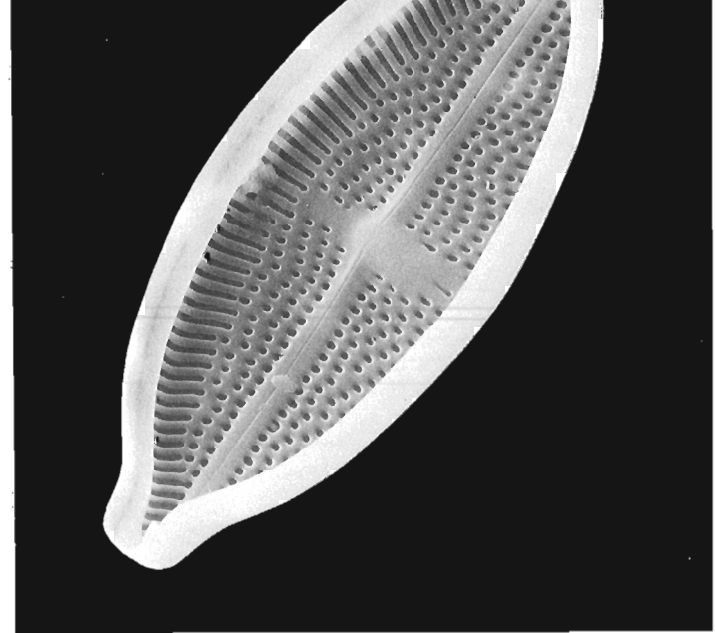
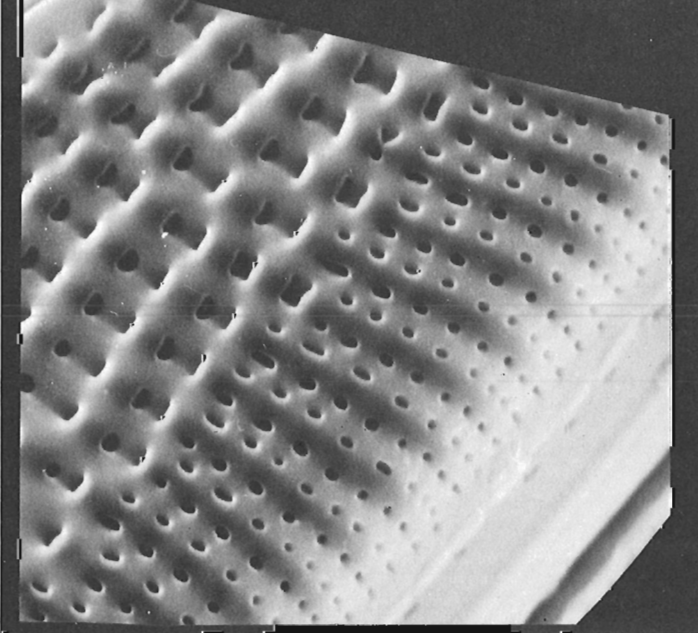
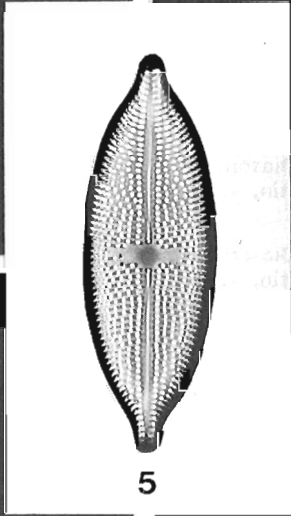
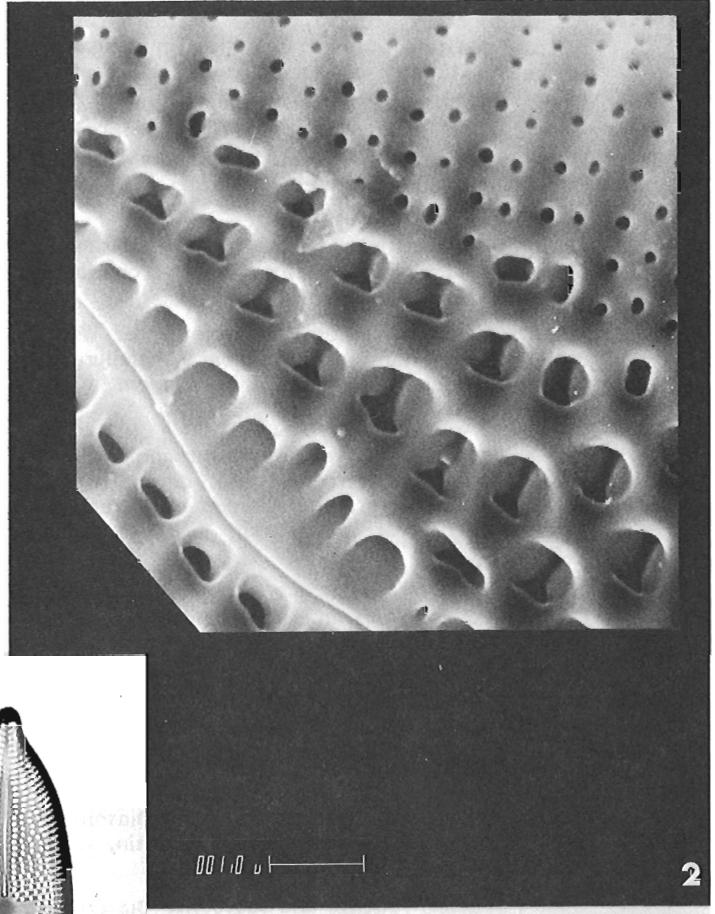
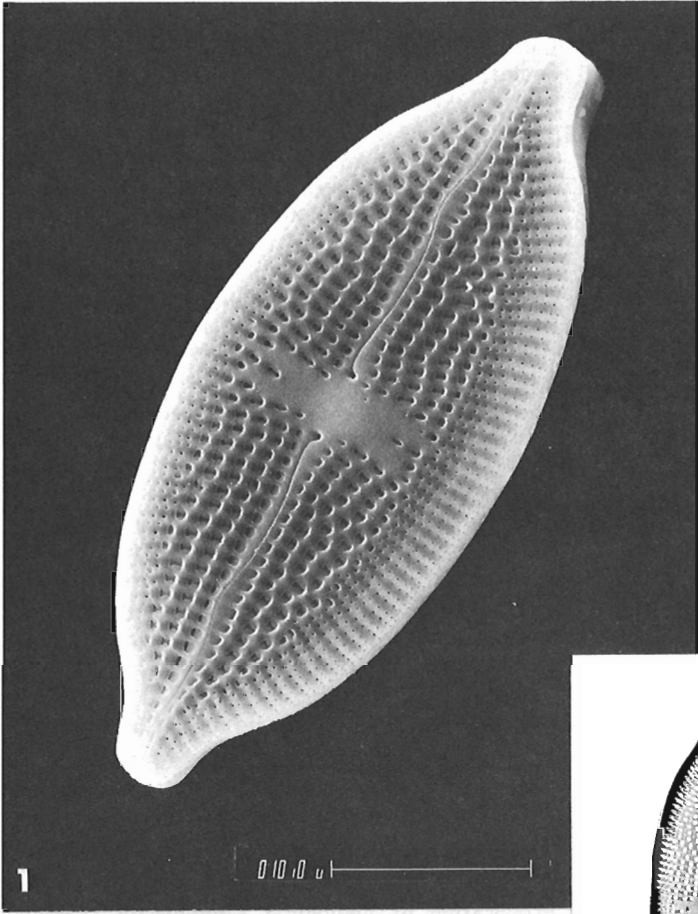
Ecology: This taxon is listed as halobion indifferent (Foged, 1954; Hustedt, 1957; Simonsen, 1962), alkalibiontic (Jørgensen, 1948; Foged, 1954; Hustedt, 1957), and limnobiontic (Foged, 1954). Jørgensen (1948), in his investigations of the diatom flora of Danish lakes and ponds, stated a pH range of 7.7 to 8.5 for this species; Hustedt (1957), as a result of his researches in Swedish Lapland, suggested a range of pH 6.1 to 9.0; and Cholnoky (1968) assigned **Navicula tuscula** a pH optimum at or slightly below pH 8.0. According to Cleve-Euler (1953) this clear water form is found in fresh to slightly brackish or calcium-rich water, and Jørgensen (1948) limited its occurrence to eutrophic lakes and ponds.

Occurrence and Distribution: **Navicula tuscula** is common in the Baltic region and in Germany (Hustedt, 1930). It has been reported from Greenland (Foged, 1953, 1955, 1958, 1973) and from several American states (Patrick and Reimer, 1966). Florin (1944) cited fossil occurrences in central Swedish deposits from both the Yoldia Sea and Ancylus Lake.

In eastern Ellesmere Island, **Navicula tuscula** represents a significant floristic element of the recent diatom population of lakes and ponds.

Plate 11.5

- Figure 1. Scanning electron micrograph (GSC 61786): External view of valve (magnification x2800, tilt 30°). The sample is from the same mud-water interface sample as figures 2 to 5, Plates 11.1 and 11.2, and figures 3 to 5, Plate 11.4.
- Figure 2. Scanning electron micrograph (GSC 61786): Enlarged part of valve face denoting the raphe fissure undulation, the sunken slit-like central and round marginal areolae. (magnification x13 000, tilt 30°).
- Figure 3. Scanning electron micrograph (GSC 61787): Part of outer valve margin illustrating the structural difference between marginal and central areolae (magnification x10 000, tilt 30°).
- Figure 4. Scanning electron micrograph (GSC 61788): Internal view of valve (magnification x3000, tilt 30°).
- Figure 5. Light photomicrograph (GSC 61789): General picture. Valvar view (magnification x900, oil immersion, Hyrax mount).



- Hendey, I.N.
 1964: An introductory account of the smaller algae of British coastal waters; Fisheries Investigation Series IV, Ministry of Agriculture, Fisheries and Food, London, 317 p.
- Hustedt, F.
 1930: Die Süßwasser — Flora Mitteleuropas; Heft 10: Bacillariophyta (Diatomeae), Verlag G. Fisher, Jena, 466 p.
 1942: Diatomeen aus der Umgebung von Abisko in Schwedisch-Lapland; Archiv für Hydrobiologie, v. 39, no. 1, p. 82-174.
 1957: Die Diatomeenflora des Flusssystemes der Weser im Gebiet der Hansestadt Bremen; Abhandlungen. Naturwissenschaftlicher Verein, Bremen, v. 34, no. 3, p. 181-440.
 1959: Die Kieselalgen. 2. Teil; in Kryptogamen-Flora von Deutschland, Österreich und der Schweiz, Bd. II, L. Rabenhorst, ed.; Akademische Verlagsgesellschaft Geest und Portig K.-G., Leipzig, 845 p.
- Jørgensen, E.G.
 1948: Diatom communities in some Danish lakes and ponds; Det Kongelige Danske Videnskabernes Selskab. Biologiske Skrifter, v. 5, no. 2, p. 1-140.
- Mölder, K. and Tynni, R.
 1968: Über Finnlands rezente und subfossile Diatomeen II; Geological Society of Finland Bulletin, v. 40, p. 151-170.
 1970: Über Finnlands rezente und subfossile Diatomeen IV; Geological Society of Finland Bulletin, v. 42, p. 129-144.
 1972: Über Finnlands rezente und subfossile Diatomeen VI; Geological Society of Finland Bulletin, v. 44, p. 141-149.
- Patrick, R. and Reimer, C.W.
 1966: The diatoms of the United States; Academy of Natural Sciences, Philadelphia, v. 1, Monograph no. 13, 688 p.
- Pennington, W., Haworth, E.Y., Bonny, A.P., and Lishman, J.P.
 1972: Lake sediments in northern Scotland; Royal Society of London, Philosophical Transactions, Series B, v. 264, p. 191-294.
- Round, F.E.
 1957: The late-glacial and post-glacial diatom succession in the Kentmere Valley deposit. Part I. Introduction, methods and flora; New Phytologist, v. 56, p. 98-126.
- Simonsen, R.
 1962: Untersuchungen zur Systematik und Ökologie der Bodendiatomeen der westlichen Ostsee; Akademie-Verlag, Berlin, p. 1-144.
- Sovereign, H.E.
 1958: The diatoms of Crater Lake, Oregon; American Microscopical Society, Transactions, v. 77, p. 96-134.
- Van Landingham, S.L.
 1966: Diatoms from dry lakes in Nye and Esmeralda counties, Nevada, U.S.A.; Nova Hedwigia, v. 11, p. 221-241.
 1967: Catalogue of the Fossil and Recent Genera and Species of Diatoms and their Synonyms. Part I. **Acanthoceras** through **Bacillaria**; J. Cramer, Lehre, 493 p.
 1968: Part II. **Bacteriastrum** through **Coscinodiscus**; J. Cramer, Lehre, p. 494-1086.
 1969: Part III. **Coscinophaena** through **Fibula**; J. Cramer, Lehre, p. 1087-1756.
 1975: Part V. **Navicula**; J. Cramer, Lehre, p. 2386-2963.
- Walker, D.A.
 1978: Preparation of geological samples for scanning electron microscopy; Scanning Electron Microscopy, v. 1, p. 185-192.

H.J. Hofmann¹, J. Hill², and A.F. King²
Regional and Economic Geology Division

Hofmann, H.J., Hill, J., and King, A.F., *Late Precambrian microfossils, southeastern Newfoundland; in Current Research, Part B, Geological Survey of Canada, Paper 79-1B, p. 83-98, 1979.*

Abstract

A palynological study of 294 samples from almost all Precambrian stratigraphic units in southeastern Newfoundland was made. Less than half of the samples (121) yielded carbonaceous debris, but only 40 of these, from 11 different formations, contain organic-walled microfossils. The units containing organic-walled microfossils are the Connecting Point and Musgravetown groups, and the Mall Bay, Drook, Fermeuse, Renews Head, Cappahayden, Gibbett Hill, Halls Town, Snows Pond, and Random formations. The Mistaken Point Formation that contains the important Hadrynian metazoan fauna has not yielded a microbiota.

Although geographically widespread on the Avalon Peninsula, the microfossils in any one sample are generally rare, poorly preserved, and taxonomically restricted. Included are acritarchs and nonseptate filaments, preserved as highly degraded brown to dark grey compressions. They are assigned to the taxa *Trachysphaeridium* sp., *Trematosphaeridium holtedahlii* Timofeev 1966, *Eomicrhystridium?* sp., and *Taeniatum* sp. All are forms with a long stratigraphic range and worldwide geographic distribution. No comparatively more complex forms typically restricted to the Vendian were observed. Thus the microbiota obtained does not provide a firm basis for biostratigraphic conclusions. If anything, the composition and type of preservation of the Avalon assemblage compares with the Late Precambrian biotas described from the Lower Dalradian succession of Scotland and the Brioverian of the Armorican Massif in France.

Introduction

A reconnaissance sampling program was started in June 1977 to locate Precambrian units and sections with microfossils on the Avalon Peninsula for assessment of their biostratigraphic potential. This program was continued during the 1978 field season. Altogether 294 localities were sampled, representing 24 stratigraphic units of formation rank or higher. Although amorphous carbonaceous matter is abundant in many samples, the yield of structurally preserved microfossils is, on the whole, very low. Microfossils were successfully recovered by HF treatment of samples from only 11 of the Precambrian units at 40 localities (Fig. 12.1-12.3; Appendixes 1 and 2). Advanced levels of organic metamorphism and the crushed nature typically exhibited by the Avalon fossil remains present major problems in the identification of taxa. Specimens are generally dark brown to dark grey and black, although in several localized areas of more moderate metamorphism outlined in Figure 12.1, microfossils of medium brown colour are found.

Included in the study for comparison were a small number of samples from the Lower Cambrian units (Bonavista Formation, Smith Point Formation). These have yielded tubular and spheroidal microfossils of somewhat lighter colour, indicating that these rocks have possibly undergone a lesser degree of burial or deformation.

The purpose of this report is to provide identifications, descriptions, and illustrations of the Precambrian microfossils of the Avalon Peninsula, and to interpret them in terms of biostratigraphy and paleoenvironmental setting.

General Geological Setting

The area under study (Fig. 12.1) is part of the Avalon Zone in eastern Newfoundland, one of the most continuous and best defined zones in the Appalachian - Caledonide Orogen (Williams et al., 1974; Williams, 1978). Three separate northerly trending belts of late Precambrian (Hadrynian) clastic and volcanic rocks, locally overlain by Cambrian and Ordovician sediments, are present in the region

and are included in the A, B, C, zones of Figure 12.1. These sequences are separated by faults exposed along the zone boundaries. Generalized lithostratigraphic subdivisions, based on the maps and reports of Rose (1952), Hutchinson (1953), Jenness (1963), McCartney (1967) and Williams and King (1975, 1976), are shown in Figure 12.2.

Williams and King (1976) divided the 3 to 5 km thick Conception Group of southeastern Avalon Peninsula (zone C) into five formations. Studies in progress by A.F. King suggest these formations have wide areal extent and are also present in zone B. A distinctive 300 m diamictite unit, the Gaskiers Formation, present in eastern St. Mary's Bay, is provisionally correlated with "tillite" at Bacon Cove, southwestern Conception Bay, and Red Head, 20 km north of St. John's (Brückner and Anderson, 1971; King and Brückner, 1972; King et al., 1974). Precambrian metazoan fossils (Anderson and Misra, 1968; Misra, 1969; Anderson, 1972; Williams and King, 1976) are well preserved in a number of stratigraphic levels above the diamictite, especially in the green and red tuffaceous sandstones of the Mistaken Point Formation, chosen by Williams and King (1976) to define the top of the Conception Group. The Hibbs Hole Formation (Hutchinson, 1953) has been traced from its type locality in southwestern Conception Bay southeast to St. Mary's Bay, where medusoid forms (cf. Fig. 6D of King et al., 1974) were discovered during the 1978 field season; this unit appears to be a correlative with the Mistaken Point Formation. None of the formations established in the Conception Group (zones B and C) have been recognized in the predominantly argillaceous Connecting Point Group (zone A) and it is not possible at present to make a direct correlation between them.

The 8 km thick Hodgewater Group (zone B) and the 8 to 9 km thick St. John's - Signal Hill groups (zone C) are similar and conformably overlie the Conception Group. Each zone contains an upward coarsening sequence. Black shales of the Carbonear and Fermeuse formations gradually pass upwards into grey sandstones of the Halls Town and Gibbett Hill formations, through red sandstone, to red conglomerate of the Bay de Verde and Cuckold formations. Variegated shale and sandstone define the top of the Hodgewater and Signal

¹Department of Geology, University of Montreal, Montreal, Que. H3C 3J7.

²Department of Geology, Memorial University of Newfoundland, St. John's, Nfld. A1B 3X5.

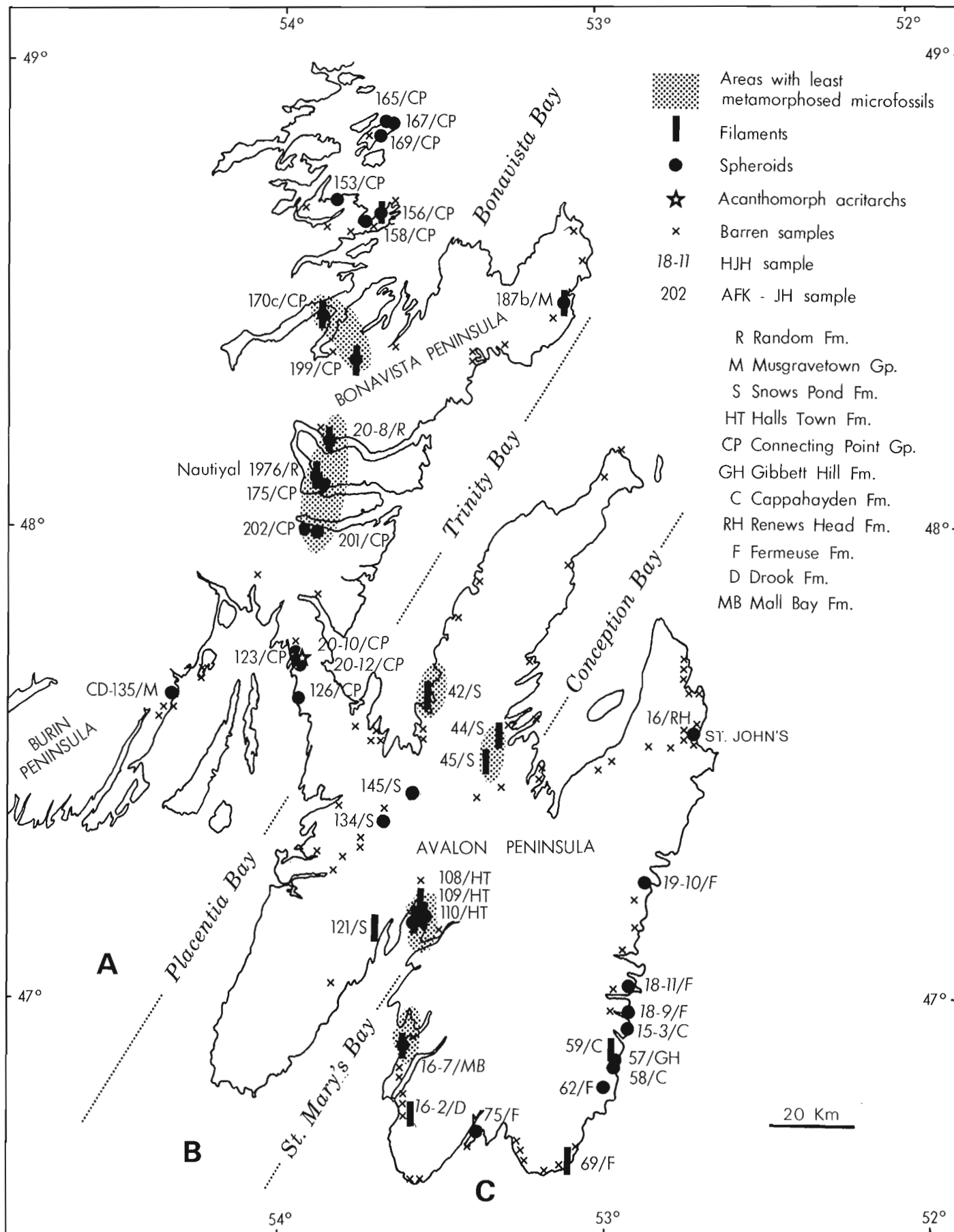


Figure 12.1. Map showing Precambrian microfossil localities in southeastern Newfoundland. Three zones characterized by different lithostratigraphic assemblages are outlined by the major bays and are marked A to C. For more detail on sample location see Appendix 1.

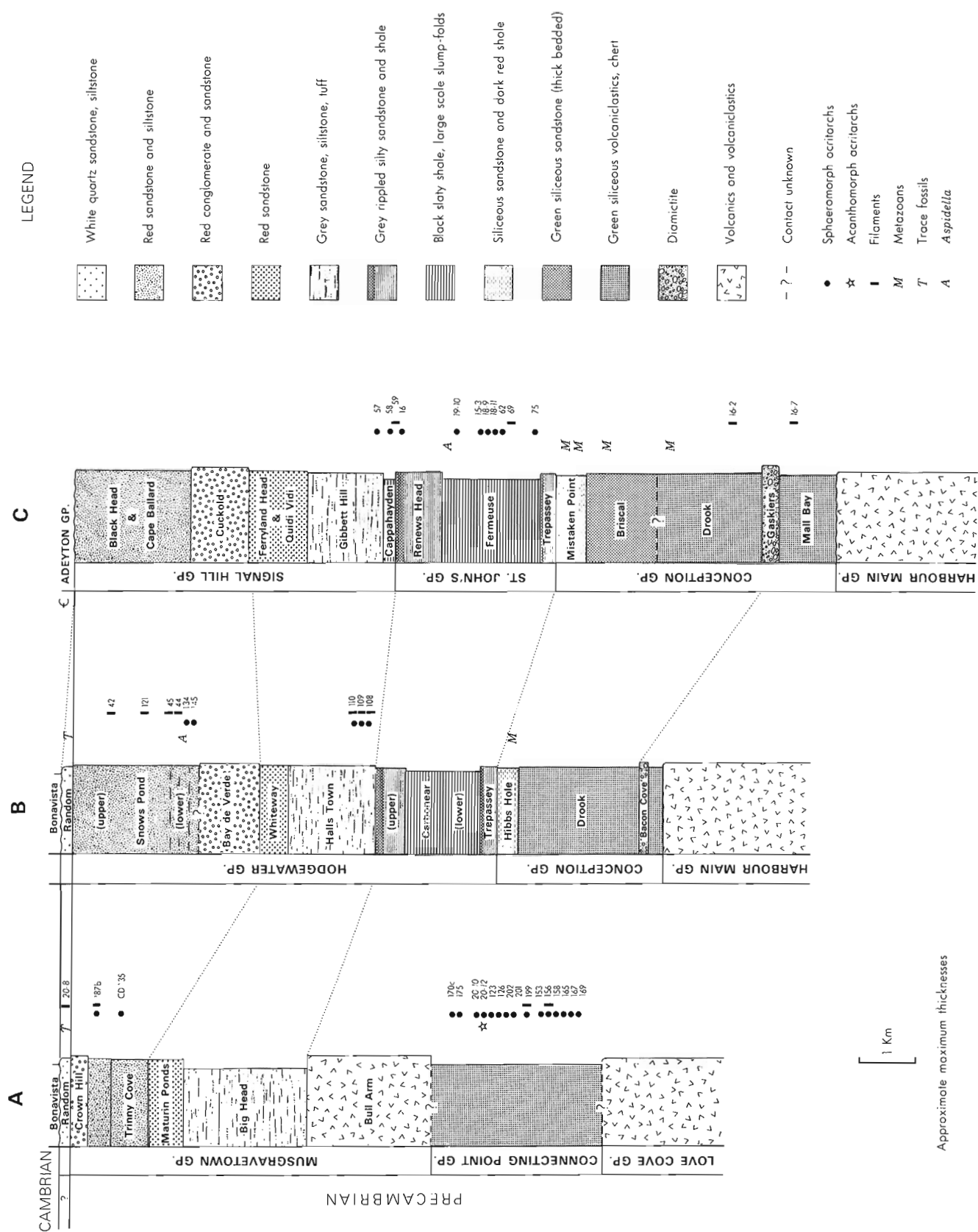


Figure 12.2. Generalized Precambrian stratigraphic sections showing the vertical distribution of microfossil occurrences in southeastern Newfoundland. Sections A to C correspond to the 3 zones outlined in Figure 12.1.

Hill groups. The Snows Pond (lower) and Fermeuse formations contain *Aspidella terranovica* Billings, 1872; this form is thought to be inorganic although some of the larger varieties may be medusoid impressions. Musgravetown Group sandstones, siltstones, and volcanic rocks form a substantial part of the Bonavista Peninsula (zone A) and are also present along the east coast of Placentia Bay (zone B). Provisional correlations are indicated in Figure 12.2 as follows: (1) Big Head Formation is equivalent to the grey sandstone of Halls Town Formation and, (2) Maturin Ponds Formation corresponds with red sandstone of Whiteway Formation (Jenness, 1963; McCartney, 1967). Trinny Cove sandstone, overlain by undivided coarse – fine clastics and Crown Hill conglomerate of the Musgravetown Group, has no precise correlatives in the Hodgewater and Signal Hill groups. A thin quartzite unit, the Random Formation, overlies the latter units in zones A and B and underlies fossiliferous Cambrian beds.

The Late Precambrian rocks of the region are folded about north-northwesterly trending axes. The folds are open to tight with steeply dipping axial plane cleavage especially prominent in argillaceous formations such as the Trepassey and Fermeuse. Fault sets trend northeast and northwest.

Stratigraphic and sedimentologic relationships indicate an early history of widespread marine deposition (Connecting Point – Conception) around an active volcanic archipelago (Harbour Main). The Carboniferous – St. John's units record a shoaling of the marine basin, and then southward prograding deposition of deltaic sands of the Big Head-Halls Town and Gibbett Hill formations. Intermittent deposition of volcanic ash continued. Alluvial plain conditions developed and a rising mountain front on the northern periphery of the system gave rise to red sandstones (Maturin Ponds, Whiteway, Ferryland Head and Quidi Vidi formations) and conglomerates (Bay de Verde – Cuckold). Latest Hadrynian (Random – Cape Ballard) and Cambro-Ordovician sediments accumulated as tidal and offshore deposits.

The Avalon Zone may represent a wide distentional belt and partly marine basin and range domain, which developed as a precursor to the actual opening of the Early Paleozoic proto-Atlantic.

Previous Micropaleontological Investigations

The only previously published account of Precambrian microfossils is by Nautiyal (1976), from the questionably Precambrian (or Cambrian) Random Formation of the Random Island area. These comprise 6-12 μm wide filaments that he attributed to the genera *Siphonophycus*, *Gunflintia*, and *Heliconema*, and sphaeromorph acritarchs identified as *Leiosphaeridia*, *Leiovalia*, *Nucellosphaeridium*, and *Huronospora*. Although reported to be both septate and nonseptate, the filaments could be assigned to a single taxon on the basis of the illustrations and descriptions, considering their poorly preserved nature, and allowing for diagenetic distortion. The purported septa and primary helical coiling are not convincing and appear to be degradational artifacts of nonseptate tubes. The identifications of the sphaeromorphs were not supported by descriptions or illustrations.

Knoll has found specimens of *Bavlinella* from the Gaskiers Formation at Red Head (47°43'20"N, 52°42'23"W) (A.H. Knoll, pers. comm., April 7, 1977 and November 1, 1978).

Types of Microfossils

The microfossils here newly reported fall into two broad categories: compressions of nonseptate filaments 2-15 μm wide, and isolated, flattened spheroids 9.7-340 μm across, including spinose forms. The spheroids are referred to the acritarchs. None are three-dimensionally preserved.

Both types are interpreted to be the remains of microorganisms of algal affinities. Based only on morphology and size ranges, the spheroids are considered as the remains of mainly planktonic eucaryotes, and the filaments as the evacuated sheaths of cyanophytes, possibly washed in from benthic habitats. However, other affinities are not excluded. Also present in many samples is framboidal pyrite, whose biological significance is still debated (e.g., see Volkova, 1974).

Distribution

The widespread geographic distribution of Precambrian microfossil occurrences is shown in Figure 12.1. No pronounced systematic trends are evident, although the apparent abundance of localities with filaments in the Halls Town and Snows Pond formations in the western part of the Avalon Peninsula (zone B) is noteworthy. Spheroids predominate in the western part of the map area (zone A), reflecting the predominance of samples from the older Connecting Point Group, and in the east (zone C) in rocks of the St. John's and Signal Hill groups which are considered correlatives of the Hodgewater Group.

Despite the widespread occurrences, the yield at all localities is extremely low, possibly due to low population densities, rapid sediment accumulation, and other factors. The highest yield of any sample was from the Fermeuse Formation at Mobile (sample 19-10), which provided 49 spheroids in one slide. Most samples with microfossils had less than 5 specimens per slide.

Figure 12.2 summarizes the stratigraphic distribution of the observed microfossils. While both spheroids and filaments occur throughout the late Precambrian (Hadrynian) interval in eastern Newfoundland, certain units, as shown, are characterized by the predominance of one type over the other. These compositional differences may reflect differences in environmental settings, including depth and distance from shoreline. Although the search for microfossils in the Connecting Point Group was relatively successful, the Conception Group, generally assumed to be its lateral equivalent, is barren except for a few specimens from the Mall Bay and Drook formations.

Systematic Paleontology

Two principal factors make specific identification of the microfossils difficult: 1) Most specimens are poorly preserved; the organic matter has undergone advanced stages of degradation (carbonization), and surface features of potential taxonomic significance have been modified or obliterated. 2) The taxonomy of the spheroidal and filamentous microfossils is in a state of disorder. The systematics of both categories is plagued by synonyms, frequent lack of adherence to the provisions of international codes of nomenclature, and the lack of appreciation for diagenetic modification of morphologic features (see also Volkova, 1974). A major, up-to-date, treatise-like synthesis with standardized nomenclature, taxonomic keys and superior illustrations, particularly for sphaeromorph acritarchs, is not yet available.

Apart from specimens of original material, photographs provide the most efficient way to communicate and assimilate morphologic information. Juxtaposed illustrations of several specimens of one taxon, reproduced with identical magnifications, will assist in visualizing the degree of morphologic variability to be expected, as well as any overlap with similar taxa.

The identifications of the Avalon microfossils are provisional, pending clarification of the acritarch nomenclature. The fossils are amply illustrated, to facilitate future studies and to support comparisons with specific illustrations from other publications.

All slides containing the specimens illustrated in this report are deposited in the National Type-Fossil Collection, Geological Survey of Canada, Ottawa, under catalogue numbers 61571 – 61610. Particulars are cited in the respective figure captions. The stage co-ordinates cited in the captions refer to distances in millimetres from the upper right reference corner formed by the intersection of the distal margin (x-axis) and right margin (y-axis) of the slide; the slide is oriented with the label to the right of the observer.

Plate 12.1

Phylum CYANOPHYTA
Genus *Taeniatum* Sin ex Sin & Liu 1973

Taeniatum sp.

Plate 12.1, figures 1-22, ?23, 24-29

Siphonophycus kestron Nautiyal, 1976, p. 609, Fig. 10-11.

Siphonophycus sp. A Nautiyal, 1976, p. 609, Fig. 1-9.

Heliconema sp. A Nautiyal, 1976, p. 609, Fig. 12-16.

Gunflintia sp. A Nautiyal, 1976, p. 610, Fig. 17.

Description: Flattened fragments of simple, nonseptate filaments, sometimes twisted, dark brown to medium grey, 2-15 µm wide, averaging 9 µm (62 specimens from 9 formations at 15 localities); up to 140 µm long. Surface diagenetically modified, psilate to irregularly granulated or reticulate, sometimes perforated, originally apparently smooth; faint transverse markings in some places.

Occurrence: Connecting Point Group: localities 156, 170c, 199.

Drook Formation: locality 16-2.

Mall Bay Formation: locality 16-7.

Fermeuse Formation: locality 69.

Cappahayden Formation: locality 59.

Halls Town Formation: localities 108, 109, 110.

Snows Pond Formation: localities 44, 45, 121.

Musgravetown Group: locality 187b.

Random Formation: locality 20-8; Nautiyal, 1976.

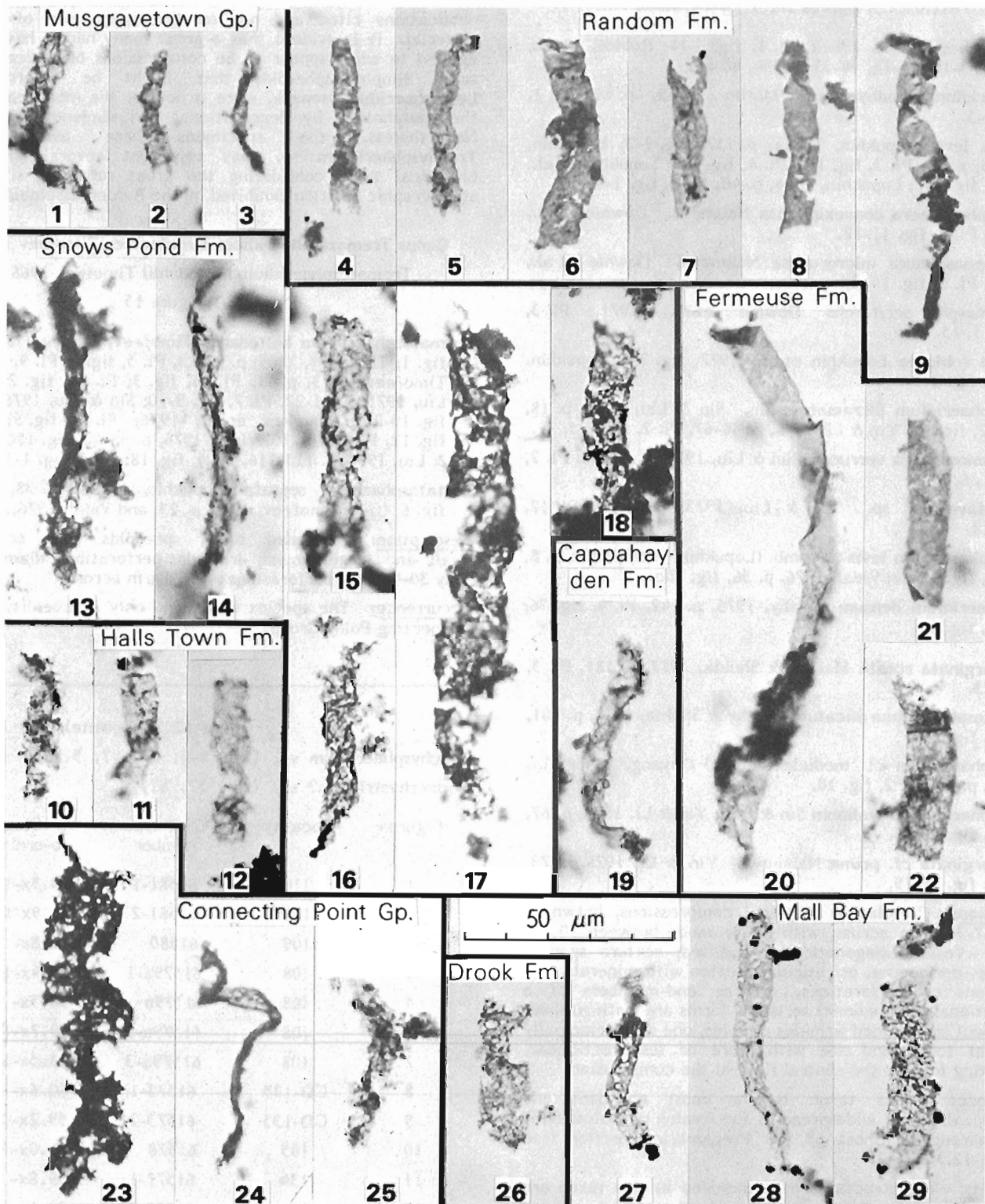
Comments: Nautiyal (1976) described and illustrated filamentous microfossils from the Random Formation and referred them to 4 taxa: *Siphonophycus kestron*, S. sp. A, *Heliconema* sp. A, and *Gunflintia* sp. A. All these filaments are between 6 and 12 µm wide and less than 115 µm long, and thus of the same size as the new material here referred to *Taeniatum*. It is most likely that some of the morphologic characteristics (twisted thallus, "septa") used in attributing the earlier reported material to different genera and species are preservational artifacts, and that only a single filamentous form genus is represented. Twisted and untwisted filaments also occur in our material, and similar compressed structures are found in many mid- and late Proterozoic marine clastic sequences in Eurasia (e.g., Timofeev, 1969, 1973; Timofeev et al., 1976, Sin and Liu, 1973). Elsewhere in North America they have been reported from the Helikian Belt Supergroup of Montana (Horodyski and Bloeser, 1978) and the Little Dal Group of the Mackenzie Mountains (Hofmann and Aitken, 1979).

Faint transverse markings in some of our filaments are suggestive of cell impressions, but these markings are not sufficiently well developed or preserved, nor numerous enough to allow definite conclusions. The filaments are here interpreted to be the remains of tubular sheaths of cyanophytes.

Taeniatum sp. (fig. 1-22, 23?, 24-29)

Linear fragment of *Trachysphaeridium* sp. (fig. 23?)

Figure	Locality	GSC type number	Stage co-ordinates
1	187b	61572-1	28.5x-12.6y
2	187b	61572-2	23.1x 5.3y
3	187b	61572-3	21.4x-12.9y
4	20-8	61571-1	19.8x-20.8y
5	20-8	61571-2	20.8x-11.3y
6	20-8	61571-3	22.8x-17.5y
7	20-8	61571-4	19.6x-19.5y
8	20-8	61571-5	20.8x-17.0y
9	20-8	61571-6	31.4x- 6.7y
10	109	61580-1	21.1x- 5.1y
11	109	61580-2	28.7x-16.9y
12	110	61581	29.4x- 6.4y
13	45	61575-1	32.8x- 8.7y
14	45	61575-2	27.8x-10.9y
15	44	61574-1	19.9x-14.8y
16	44	61574-2	27.0x- 3.5y
17	44	61574-3	28.7x- 7.8y
18	44	61574-4	27.8x- 6.4y
19	59	61585	36.0x-15.0y
20	69	61591-1	19.6x-17.5y
21	69	61591-2	26.6x-13.2y
22	69	61591-3	19.0x-14.8y
23	20-10	61592	26.4x-16.3y
24	170c	61599	18.9x- 5.5y
25	199	61601	19.4x-15.3y
26	16-2	61603	32.8x- 5.0y
27	16-7	61604-1	24.1x-16.6y
28	16-7	61604-2	29.4x-18.9y
29	16-7	61604-3	46.6x-20.2y



Group ACRTARCHA Evitt 1963

Subgroup Sphaeromorphitae Downie et al. 1963

Genus *Trachysphaeridium* Timofeev ex Timofeev 1966

Trachysphaeridium sp.

Plate 12.2, figures 1-2, 3?, 4?, 5-14;
Plate 12.3, figures 1-2, 3?, 4-14, 18-28

Sporomorphes Roblot, 1964a, Pl. 1, fig. 6-14; Roblot, 1964b, Fig. 1, 3-10, 15-16, 18-33, 45-54, 60-63.

Retisphaeridium vindhyanensis Maithy, 1969, p. 49, Pl. 1, fig. 4-5.

Menneria levis Lopukhin, 1971a, p. 157, fig. 1-2; Lopukhin, 1971b, p. 85, Pl. 3, fig. 1-3; Pl. 4, fig. 1-3; Lopukhin et al., 1972, fig. 2-1; Lopukhin, 1974, p. 40, Pl. 2, fig. 1-4.

?*Leisosphosphaera convexiplicata* Naumova. Downie et al., 1971, Pl. 3, fig. 11-12.

?*Leiopsosphosphaera microrugosa* Naumova. Downie et al., 1971, Pl. 3, fig. 14, 16.

Sphaeromorph acritarchs Downie et al., 1971, Pl. 3, fig. 13, 15.

Menneria roblotae Lopukhin et al., 1972, fig. 2-2; Lopukhin, 1974, fig. 2-5.

Trachysphaeridium incrassatum Sin. Sin & Liu, 1973, p. 18, Pl. 12, fig. 17; Yin & Li, 1978, p. 66-67, Pl. 2, fig. 2-5, 11.

Pseudozonosphaera verrucosa Sin & Liu, 1973, p. 19, 56, Pl. 2, fig. 1, 6, 7.

Archaeofavosina? sp. Sin & Liu, 1973, p. 23-24, Pl. 12, fig. 18.

Trachysphaeridium levis n. comb. (Lopukhin) Vidal, 1974, p. 8, Pl. 1, fig. 13-14; Vidal, 1976, p. 36, fig. 20c.

Vavosphaeridium densum Maithy, 1975, p. 142, Pl. 4, fig. 36; Pl. 5, fig. 39.

Granomarginata rotata Maithy & Shukla, 1977, p. 181, Pl. 3, fig. 23.

Orygmato-sphaeridium plicatum Maithy & Shukla, 1977, p. 181, Pl. 3, fig. 26.

Trachysphaeridium cf. *mediale* (Schep.) Ouyang, Yin et Li, 1978, p. 67, Pl. 2, fig. 10.

Trachysphaeridium hyalinum Sin & Liu. Yin & Li, 1978, p. 67, Pl. 2, fig. 12-18.

Granomarginata cf. *prima* Naumova. Yin & Li, 1978, p. 73, Pl. 3, fig. 16-19.

Description: Circular to elliptical compressions, brown to black, 9.7-340 µm across, with major mode between 20 and 50 µm. Vesicle diagenetically modified; texture spongy, granulate, coriaceous, or reticulate, often with mineral grain impressions or perforations. Three end-members of a preservational (taphonomic) series of forms are distinguished: one without pronounced wrinkles or folds, one with principally peripheral folds, and one with more or less rectilinear, intersecting folds in the central field of the compression.

Occurrence: This taxon is the most abundant and geographically most widespread of the Avalon microfossils; it ranges throughout most of the Precambrian section (see Fig. 12.1-12.3).

Comments: The structures here included in this taxon are highly variable in size and morphology, and could be assigned to several different taxa. For instance, the preservational type with rectilinear intersecting folds (Pl. 3, fig. 13, 28) might be attributed to *Kildinella* Timofeev. However,

because of the presence of intermediate stages, the morphological variation is continuous between the three main types, and the folds are here considered to be accidental features resulting from differences in the compaction and the sedimentary matrix of each individual spheroid.

The synonymy given above is based on comparison of our material with illustrations and descriptions in the publications cited and not on the comparison of actual material. It is evident that a great many names have been applied to what appear to be compressions of basically the same simple spheroids that might be referred to *Leiosphaeridia* Eisenack, were it not for the modification of the morphology by degradational and diagenetic effects. Nevertheless, the specimens here assigned to *Trachysphaeridium* sp. may represent several different biological taxa, considering the great range in size and stratigraphic position exhibited by the Avalon assemblage.

Genus *Trematosphaeridium* Timofeev ex Timofeev 1966

Trematosphaeridium holtedahlii Timofeev 1966

Plate 12.3, figure 15

Trematosphaeridium holtedahlii Timofeev, 1966, p. 28, Pl. 5, fig. 1; Timofeev, 1969, p. 22-23, Pl. 5, fig. 1; Pl. 9, fig. 10; Timofeev, 1973, p. 11, Pl. 10, fig. 5; Pl. 21, fig. 2; Sin & Liu, 1973, p. 21-22, Pl. 7, fig. 9-10; Sin & Liu, 1976, Pl. 3, fig. 19-20; Timofeev et al., 1976, Pl. 1, fig. 9; Pl. 3, fig. 12, Pl. 4, fig. 10; Vidal, 1976, p. 38-40, fig. 18C-E; Sin & Liu, 1978, p. 115-116, Pl. 4, fig. 18; Pl. 5, fig. 1-3.

Costatosphaerina septata Lopukhin, 1966, p. 38, Pl. 1, fig. 6 (*vide* Timofeev, 1969, p. 23, and Vidal, 1976, p. 39).

Description: Flattened black spheroids with scattered small and large, round, irregular perforations; diameter of body 30-40 µm, perforations up to 6 µm across.

Occurrence: The species was found only at Locality 20-10, Connecting Point Group.

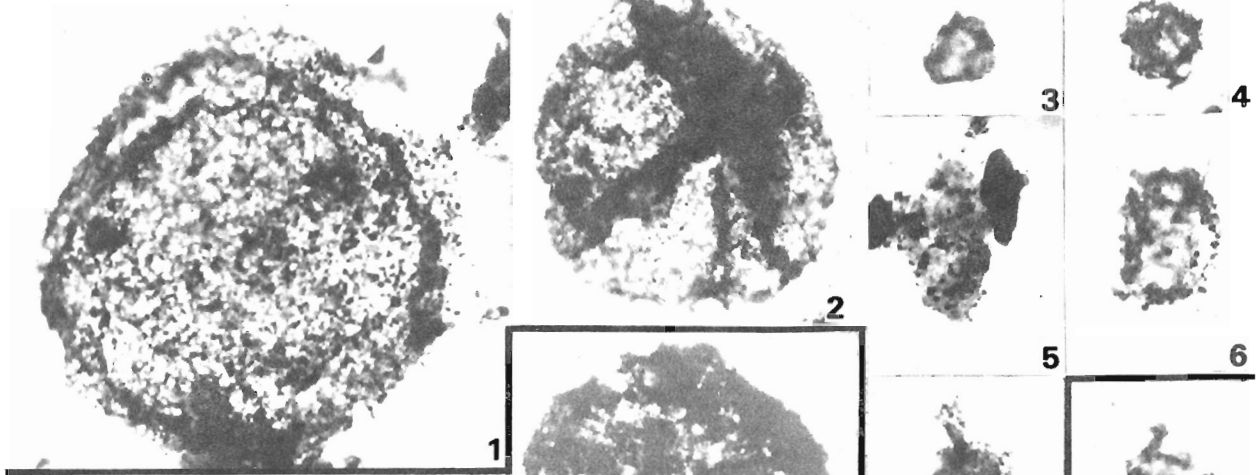
Plate 12.2 (opposite)

Trachysphaeridium sp. (fig. 1-2, 3?, 4?, 5-14)

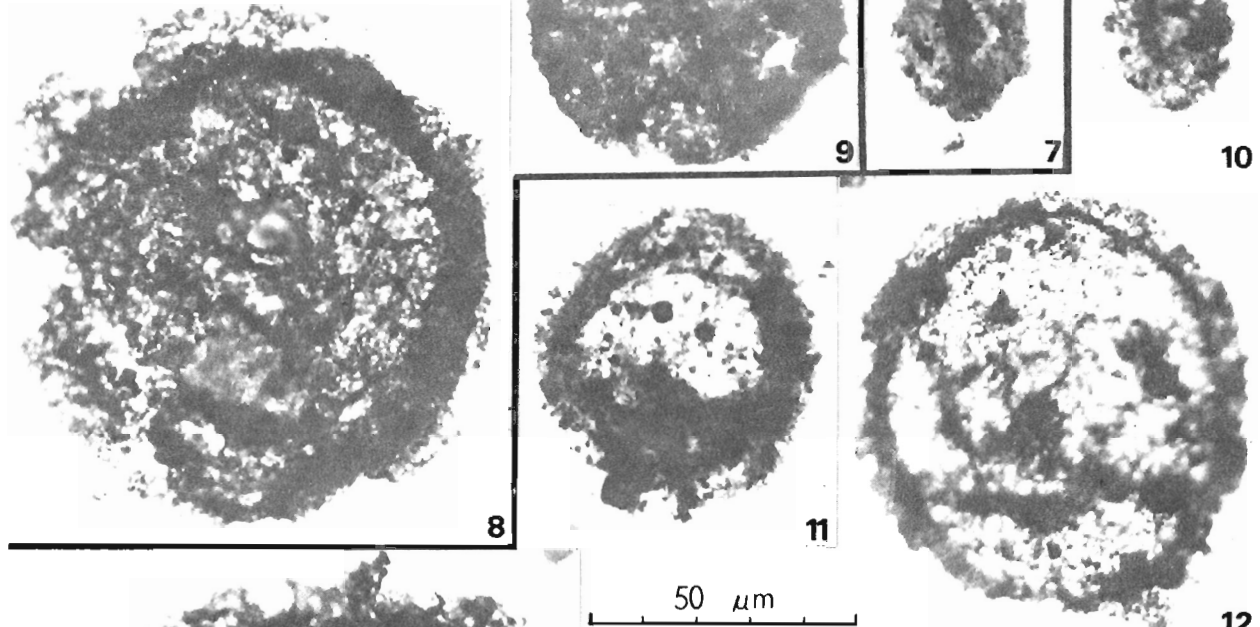
Eomichystridium? sp. (fig. 3?, 4?)

Figure	Locality	GSC type number	Stage co-ordinates
1	110	61581-1	23.5x-15.8y
2	110	61581-2	27.9x-18.5y
3	109	61580	16.8x- 6.5y
4	108	61579a-1	26.4x-10.1y
5	108	61579b	30.5x- 6.9y
6	108	61579a-2	29.7x-13.0y
7	108	61579a-3	25.5x-10.7y
8	CD-135	61573-1	60.6x- 9.5y
9	CD-135	61573-2	59.2x-10.5y
10	145	61578	26.0x-13.5y
11	134	61577-1	59.8x- 8.0y
12	134	61577-2	29.4x-16.2y
13	134	61577-3	24.4x-15.7y
14	134	61577-4	58.3x-19.6y

Halls Town Fm.

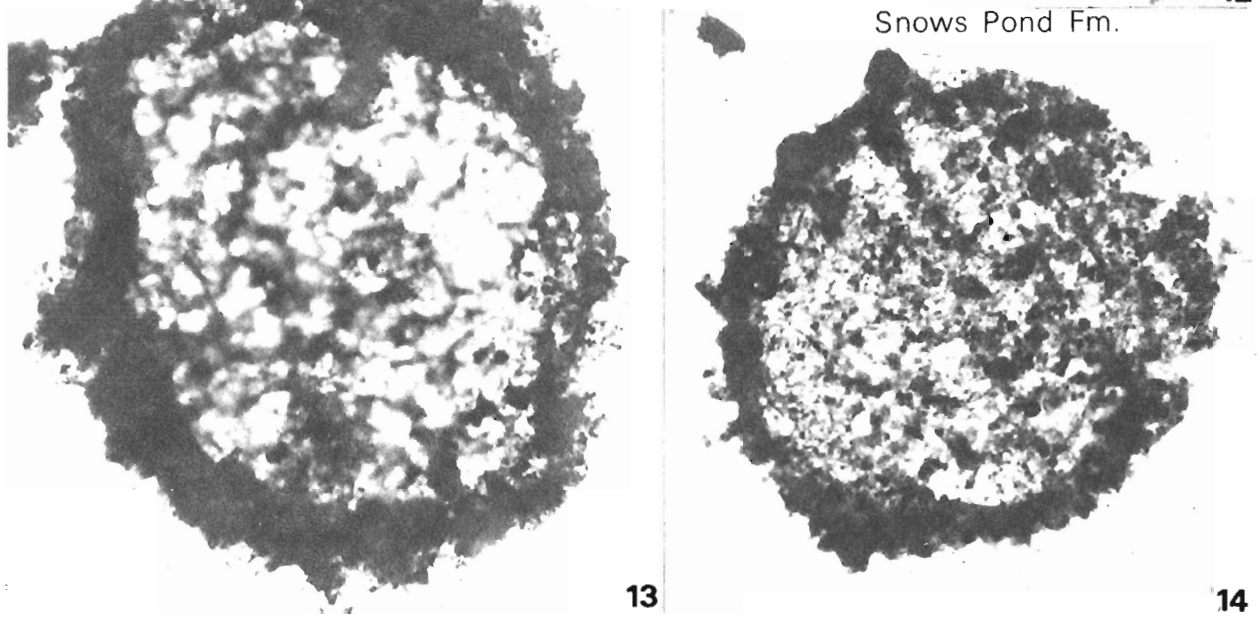


Musgravetown Gp.



50 μ m

Snows Pond Fm.



Comments: This microfossil has the morphological characteristics of specimens of *T. holtedahlia* reported from a great many Late Riphean and Vendian horizons in Asia and Europe (for a long list see Vidal, 1976, p. 40).

According to Timofeev (1959, p. 27), the genus was erected in 1956. This reference could not be located. In the 1959 publication the name of the genus was qualified by the notation "gen. n.", and the species *T. decoratum* was described as a new species, but no type species was designated; the genus thus was invalid then. It was subsequently validated by the selection of *T. holtedahlia* Timofeev as the type species (Timofeev, 1969, p. 22).

Subgroup Acanthomorpha Downie et al., 1963

Genus *Eomicrhystridium* Deflandre 1968

Eomicrhystridium? sp.

Plate 12.2, figures 3?, 4?; Plate 12.3, figures 3?, 16, 17

Description: Small flattened echinate spheroids, 10-15 µm across; spines and cones simple, less than 1 µm long.

Occurrence: Connecting Point Group. Locality 20-12. Questionably present in Cappahayden Formation at Locality 15-3 and in Halls Town Formation at Localities 108 and 109.

Comments: The structures are too poorly preserved to permit more definite identifications. Specimens identified with a query in the plate captions may be badly deformed small sphaeromorphs rather than acanthomorphs.

Comparable forms are found in the Brioverian of the Armorican Massif of France (Roblot, 1964b, fig. 55, 57; Deflandre, 1968, Pl. 1, fig. 4-5), the Late Precambrian of Bohemia (Konzalová, 1974, Pl. 1, fig. 4-6), and the Aphebian Gunflint Formation of Ontario (Hofmann, 1971, Pl. 25, fig. 8).

Summary and Conclusion

The small microbiota recovered from Precambrian units in the Avalon Peninsula is of low abundance, low diversity, and of very poor preservation. It includes compressions of simple, allogenic spheroidal and filamentous forms with long stratigraphic range, similar to elements in assemblages found in other Proterozoic fine grained clastic rocks in many parts of the world. These include the Riphean and Vendian of the Soviet Union (Timofeev, 1969, 1973; Lopukhin, 1976; Timofeev et al., 1976), the Sinian of China (Sin and Liu, 1973, 1976, 1978; Yin and Li, 1978), the Vindhyan of India (Maithy, 1969; Maithy and Shukla, 1977), the Late Precambrian of Africa (Lopukhin et al., 1972; Maithy, 1975), the Visingsö Beds of Sweden (Vidal, 1976), and the Helikian of North America (Horodyski and Bloeser, 1978; Hofmann and Aitken, 1979). However, based on the very low variety of taxa present, morphologic similarity of spheroids, and state of preservation, there is a relatively closer resemblance to the assemblages in the Brioverian of France (Roblot, 1964a, b; Deflandre, 1968) and the Lower Dalradian of Scotland (Downie et al., 1971). No further elaboration on the biostratigraphic utility of the Avalon microbiota is contemplated at this time.

Acknowledgments

Samples from the initial collection made in 1977 were processed and slides prepared at INRS-Pétrole, Quebec City; subsequent samples were processed at Memorial University. We thank M.S. Barss and B. Crilley for explaining to one of us (JH) various palynological preparation techniques employed at

the Atlantic Geoscience Centre. A.H. Knoll provided information on a microfossil locality. We also thank E. Hussey, C.F. O'Driscoll, and V.S. Papezik for providing additional samples for our investigations.

The study was financed under EMR Research Agreements 2239-4-264-77 and 2239-4-107-78, and also supported in part by the National Research Council of Canada under Grant A-7484 to Hofmann and A-7052 to King. We thank A.H. Knoll, D.C. McGregor, and G. Vidal for critical review of an early draft of the manuscript.

Plate 12.3

Trachysphaeridium sp. (fig. 1-2, 3?, 4-14, 18-28)

Trematosphaeridium holtedahlia (fig. 15)

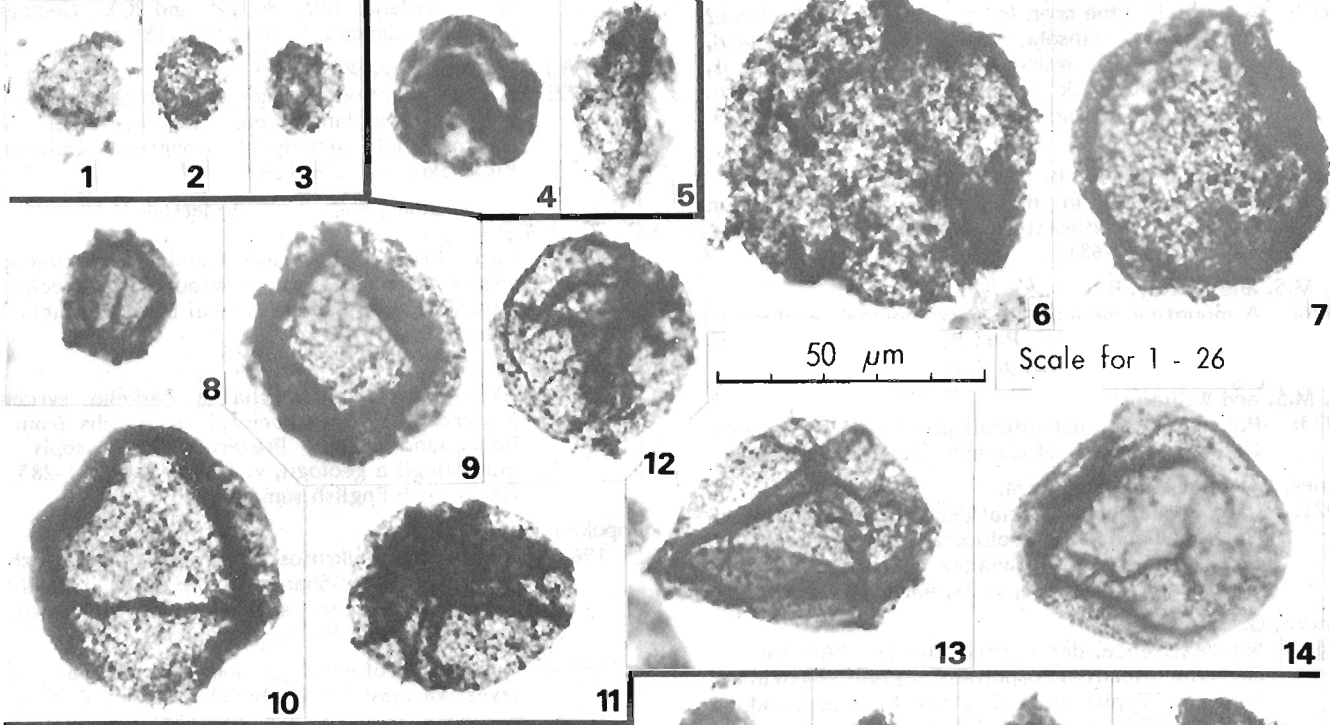
Eomicrhystridium? sp. (fig. 3?, 16-17)

Figure	Locality	GSC type number	Stage co-ordinates
1	58	61584	16.5x-12.6y
2	15-3	61583-1	29.4x- 2.5y
3	15-3	61583-2	35.7x- 9.7y
4	57	61582-1	30.2x-17.6y
5	57	61582-2	17.8x- 6.7y
6	18-11	61589	40.0x- 5.7y
7	19-10	61587-1	26.4x- 5.2y
8	19-10	61587-2	33.0x-10.8y
9	19-10	61587-3	22.5x- 6.7y
10	19-10	61587-4	38.8x-10.5y
11	19-10	61587-5	22.5x- 7.8y
12	19-10	61587-6	22.4x- 6.7y
13	19-10	61587-7	23.7x- 8.0y
14	19-10	61587-8	27.9x- 4.6y
15	20-10	61592	35.2x-12.2y
16	20-12	61593a-1	34.6x- 8.6y
17	20-12	61593a-2	30.5x- 6.5y
18	170c	61599	18.8x-17.8y
19	175	61600	31.3x-16.4y
20	123	61594	28.8x- 8.4y
21	199	61601	20.7x-13.4y
22	165	61598	19.8x- 9.5y
23	20-12	61593b-1	41.4x-15.8y
24	20-12	61593b-2	26.0x-16.3y
25	153	61596	24.9x-19.9y
26	126	61595	19.8x-12.9y
27	202	61602	36.5x-11.5y
28	16	61586	60.1x-10.9y

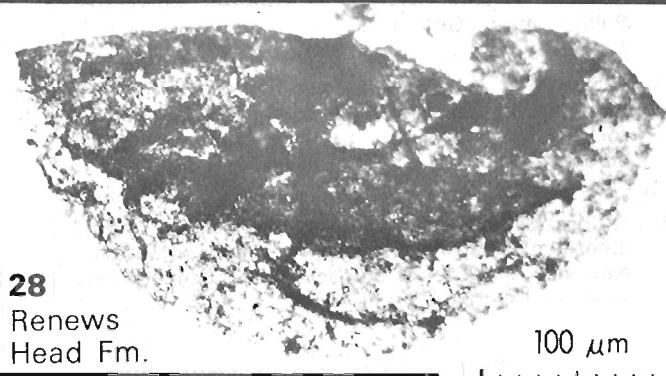
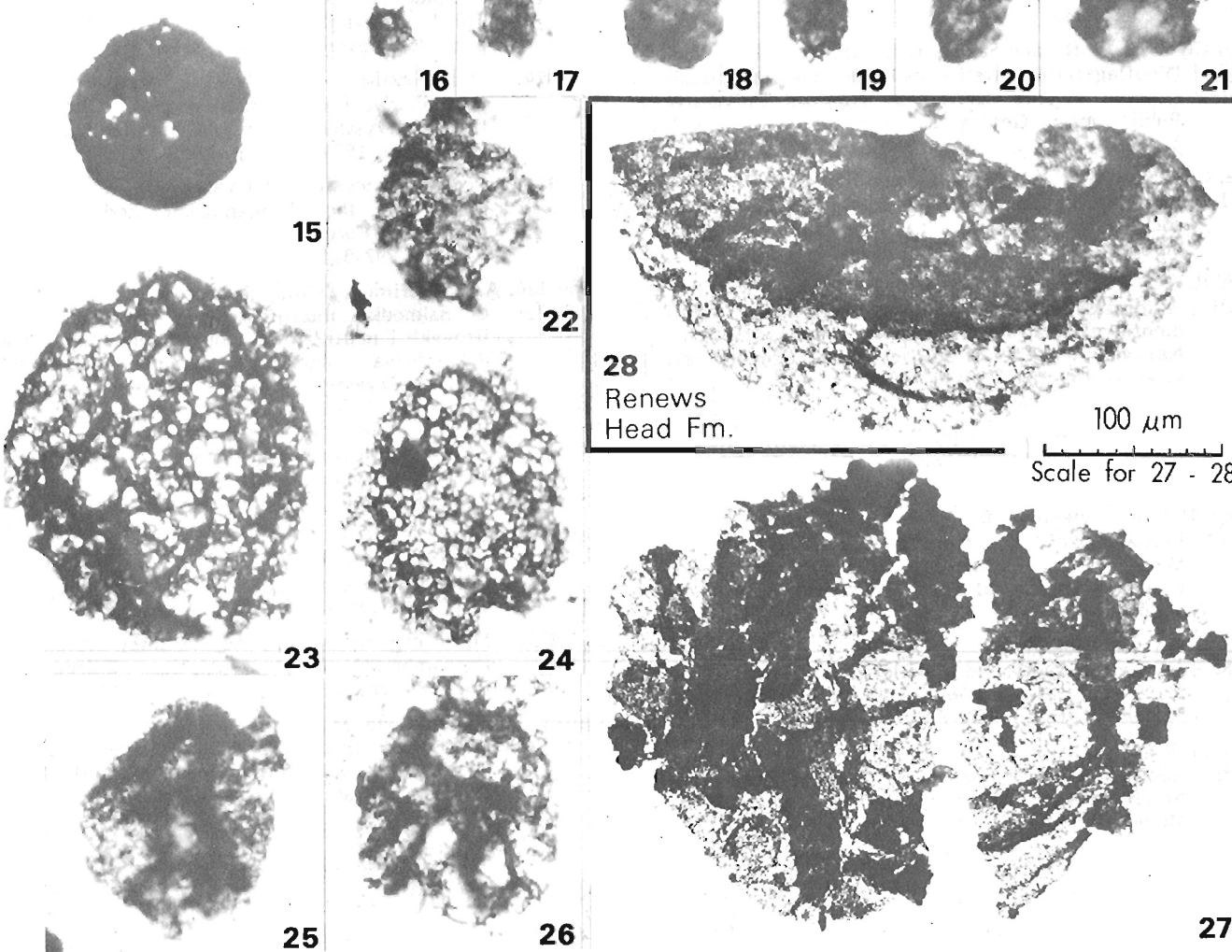
Cappahayden Fm.

Gibbett Hill Fm.

Fermeuse Fm.



Connecting Point Gp.



References

- Anderson, M.M.
1972: A possible time span for the Late Precambrian of the Avalon Peninsula, southeastern Newfoundland, in the light of worldwide correlation of fossils, tillites and rock units within the succession; *Canadian Journal of Earth Sciences*, v. 9, p. 1710-1726.
- Anderson, M.M. and Misra, S.B.
1968: Fossils found in the Precambrian Conception Group of southeastern Newfoundland; *Nature*, v. 220, p. 680-681.
- Barss, M.S. and Crilley, B.
1976: A mounting medium for palynological residues; in *Report of Activities, Part B, Geological Survey of Canada, Paper 79-1B*, p. 131-132.
- Barss, M.S. and Williams, G.L.
1973: Palynology and nanofossil processing techniques; *Geological Survey of Canada, Paper 73-26*, 25 p.
- Brückner, W.D. and Anderson, M.M.
1971: Late Precambrian glacial deposits in southeastern Newfoundland — a preliminary note; *Geological Association of Canada, Proceedings, A Newfoundland Decade*, v. 24, no. 1, p. 95-192.
- Deflandre, G.
1968: Sur l'existence, dès le Précambrien, d'Acritarches du type Acanthomorpha: *Eomicrhystridium* nov. gen. Typification du genre *Palaeocryptidium* Defl. 1955; *Comptes Rendues, Académie des Sciences, Paris*, v. 266, sér. D, no. 26, p. 2385-2389.
- Downie, C., Evitt, W.R., and Sarjeant, W.A.S.
1963: Dinoflagellates, hystrichospheres, and the classification of the acritarchs; *Stanford University Publications, Geological Sciences*, v. 7, no. 3, p. 1-16.
- Downie, C., Lister, T.R., Harris, A.L., and Fettes, D.J.
1971: A palynological investigation of the Dalradian rocks of Scotland; *Institute of Geological Sciences, Report 71/9*, 29 p., London.
- Evitt, W.R.
1963: A discussion and proposals concerning fossil dinoflagellates, hystrichospheres and acritarchs; *National Academy of Sciences (U.S.) Proceedings*, v. 49, p. 158-164, 298-302.
- Hofmann, H.J.
1971: Precambrian fossils, pseudofossils, and problematica; *Geological Survey of Canada, Bulletin 189*, 146 p.
- Hofmann, H.J. and Aitken, J.D.
1979: Precambrian biota from the Little Dal Group, Mackenzie Mountains, northwestern Canada; *Canadian Journal of Earth Sciences*, v. 16, no. 1, p. 150-166.
- Horodyski, R.J. and Bloeser, B.
1978: 1400-million-year-old shale-facies microbiota from the lower Belt Supergroup, Montana; *Science*, v. 199, p. 682-683. Washington.
- Hutchinson, R.D.
1953: Geology of Harbour Grace map-area, Newfoundland; *Geological Survey of Canada, Memoir 275*, 43 p.
- Jenness, S.E.
1963: Terra Nova and Bonavista map-areas, Newfoundland (2D, E 1/2 and 2C); *Geological Survey of Canada, Memoir 327*, 184 p.
- King, A.F. and Brückner, W.D.
1972: A Cross Section through the Appalachian Orogen in Newfoundland, ed. E.R.W. Neale; 24th International Geological Congress, Guidebook, Field Excursion A62-C62, p. 27.
- King, A.F., Brückner, W.D., Anderson, M.M., and Fletcher, T.P.
1974: Late Precambrian and Cambrian sedimentary sequences of eastern Newfoundland; *Geological Association of Canada Annual Meeting, Field Trip Manual B-6*.
- Konzalová, M.
1974: Akantomorfní akritarcha z českého svrchního proterozoika (Acanthomorph acritarchs from the Bohemian Upper Proterozoic); *Časopis pro mineralogii a geologii*, v. 17, no. 3, p. 281-285. (In Czech with English summary.)
- Lopukhin, A.S.
1966: Rastitel'nyia mikrofosilii drevneishikh otlozhenii Severnogo Tyan'-Shanya in the book: "Znachenie palinologicheskogo analiza dlya stratigrafii i paleofloristiki"; *Nauka*. (not seen)
- 1971a: Novye mikrofosilii iz dokembriya Tyan'-Shana; *Izvestiya vysshikh uchebnykh zavedenii, Geologiya i razvedka*, 1971, no. 3, p. 156-158.
- 1971b: Fitoplankton proterozoya i paleozoya Evrazii; *Third Palynological Congress, Novosibirsk*, p. 80-90. Novosibirsk. (not seen)
- 1974: Mikrofosilii rifeya Severo-Vostochnogo Priabar'ya (nizov'e r. Leny, pos. Chekurovka); *Izvestiya vysshikh uchebnykh zavedenii, Geologiya i razvedka*, 1974, no. 7, p. 37-44.
- 1976: Probable ancestors of Cyanophyta in sedimentary rocks of the Precambrian and Paleozoic; *Geologiska Föreningens i Stockholm Förhandlingar*, v. 98, p. 297-315.
- Lopukhin, A.S., Trofimov, D.M., and Borovskiy, V.V.
1972: O nakhodke mikrofosilii v tillitakh, podtillitovykh i nadtillitovykh otlozheniyakh verkhnego dokembriya sineklizy Taoudeni (Zapadnaya Afrika); *Izvestiya vysshikh uchebnykh zavedenii, Geologiya i razvedka*, 1972, no. 11, p. 141-143. (Discovery of microfossils in Upper Precambrian tillites, sub-tillitic and supratillitic deposits of the Taoudeni syncline (West Africa); *International Geology Review*, v. 16, no. 1, p. 80-82.)
- Maithy, P.K.
1969: On the occurrence of microorganisms from the Vindhyan formations of India; *The Palaeobotanist*, v. 17, no. 1, p. 48-51.
- 1975: Micro-organisms from the Bushimay System (Late Precambrian) of Kanshi, Zaire; *The Palaeobotanist*, v. 22, no. 2, p. 133-149.
- Maithy, P.K. and Shukla, M.
1977: Microbiota from the Suket Shales, Rampura, Vindhyan System (Late Pre-Cambrian), Madhya Pradesh; *The Palaeobotanist*, v. 23, no. 2, p. 176-188.

- McCartney, W.D.
1967: Whitbourne map-area, Newfoundland; Geological Survey of Canada, Memoir 341, 135 p.
- Misra, S.B.
1969: Late Precambrian (?) fossils from southeastern Newfoundland; Geological Society of America Bulletin, v. 82, p. 979-988.
- Nautiyal, A.C.
1976: First record of filamentous algal remains from the Late Precambrian rocks of Random Island (Trinity Bay), eastern Newfoundland, Canada; Current Science, v. 45, no. 17, p. 609-611.
- Roblot, M.M.
1964a: Sporomorphes du Précambrien armoricain; Annales de Paléontologie, v. 50, no. 2, p. 105-110. Paris.
1964b: Sporomorphes du Précambrien normand; Revue de Micropaléontologie, v. 7, no. 2, p. 153-156. Paris.
- Rose, E.R.
1952: Torbay map area, Newfoundland; Geological Survey of Canada, Memoir 265, 64 p.
- Sin Yu-sheng and Liu Kui-zhih
1973: On Sinian micro-flora in Yenliao region of China and its geological significance; Acta Geologica Sinica, no. 1, p. 1-64. (In Chinese, with English abstract and diagnoses of taxa.) A complete English translation is: Hsing-Yü-sheng and Liu Kuei-chih, 1975, Sinian microflora in the Yenliao region of China and its geological significance. (Available from Plenum Publishing Corporation, 227 West 17th Street, New York, N.Y. 10011. \$15.00.)
- Sin Yu-sheng and Liu Kui-chi
1976: Micropalaeoflora from the Sinian Subera of W. Hupeh and its stratigraphic significance; Preprint, 23 p. Peking.
1978: Sinian microplant and algal fossils, p. 109-126; in the book: "Stratigraphy and paleontology, Sinian to Permian, East Gorge Area"; Shanshia Stratigraphic Division, Hubei Geological Survey, 381 p., 113 plates.
- Timofeev, B.V.
1959: Drevneishaya flora Pribaltiki i ee stratigraficheskoe znachenie; Trudy vsesoyuznogo neftyanogo nauchno-issledovatel'skogo geologo-razvedochnogo instituta (VNIGRI), no. 129, 320 p. Leningrad.
1966: Mikropaleofitologicheskoe issledovanie drevnikh svit (Micropalaeophytological research into ancient strata); Akademiya nauk SSSR, laboratoriya geologii dokembriya, Nauka, 240 p. Leningrad. (An English translation is available from British Library - Lending Division, Boston Spa, Wetherby Yorks. L523 7BQ, United Kingdom. £5.)
- Timofeev, B.V. (cont'd.)
1969: Sferomorfidy proterozoya; Akademiya nauk SSSR, Institut geologii i geokhronologii dokembriya, Nauka, 146 p. Leningrad.
1973: Mikrofitofossilii dokembriya Ukrainy; Akademiya nauk SSSR, Institut geologii i geokhronologii dokembriya, Nauka, 58 p. Leningrad.
- Timofeev, B.V., Hermann, T.N., and Mikhailova, N.S.
1976: Mikrofitofossilii dokembriya, kembriya i ordovika; Akademiya nauk SSSR, Institut geologii i geokhronologiya dokembriya, Nauka, 106 p. Leningrad.
- Vidal, G.
1974: Late Precambrian microfossils from the basal sandstone unit of the Visingsö beds, south Sweden; Geologica et Palaeontologica, v. 8, p. 1-14. Marburg.
1976: Late Precambrian microfossils from the Visingsö Beds in southern Sweden; Fossils and Strata, no. 9, p. 1-57. Oslo.
- Volkova, N.A.
1974: Tipy povrezhdeniy obolochek dokembriyskikh i kembriyskikh akritarkh; Paleontologicheskii Zhurnal, 1974, no. 4, p. 101-108. (Types of damage to the body of Precambrian acritarchs. Paleontological Journal, 1974, no. 4, p. 530-536.)
- Williams, Harold (Compiler)
1978: Tectonic lithofacies map of the Appalachian Orogen; Memorial University of Newfoundland, Map No. 1.
- Williams, Harold and King, A.F.
1975: Southern Avalon, Newfoundland: Trepassey map-area (1K); in Report of Activities, Part A, Geological Survey of Canada, Paper 75-1A, p. 11-15.
1976: Southern Avalon Peninsula, Newfoundland: Trepassey map-area (1K); in Report of Activities, Part A, Geological Survey of Canada, Paper 76-1A, p. 179-182.
- Williams, Harold, Kennedy, M.J., and Neale, E.R.W.
1974: The northeastward termination of the Appalachian Orogen; in The Oceans Basins and Margins, eds. A.E.M. Nairn and F.G. Stehli; v. 2, p. 79-123, Plenum Publishing Corporation, New York.
- Yin Leiming and Li Zaiping
1978: Precambrian microfloras of southwest China, with reference to their stratigraphical significance; Memoirs of Nanjing Institute of Geology and Paleontology, Academia Sinica, 1978, no. 10, p. 41-102. (In Chinese, with summary and diagnoses of new taxa in English.)

Appendix 1

Localities yielding Precambrian microfossils

No.	Location	
HJH Samples		
15-3	46°56'27"N 52°53'44"W	<u>Bear cove point:</u> ca. 200 m west-northwest of lighthouse
16-2	46°46'00"N 53°35'45"W	<u>Peter's River:</u> roadcut on east side of Highway 5, ca. 1 km east-northeast of bridge
16-7	46°54'22"N 53°36'51"N	<u>La Haye Point:</u> ca. 220 m north of lighthouse
18-9	46°58'11"N 52°55'00"W	<u>Port Kirwan:</u> roadcut at western outskirts of village
18-11	47°00'40"N 52°53'35"W	<u>Ferryland:</u> coastal exposure opposite Crow Island
19-10	47°14'51"N 52°50'41"W	<u>Mobile:</u> uppermost (most southern) bed in roadcut opposite NLPG transformer station
20-8	48°11'20"N 53°50'18"W	<u>White Rock:</u> coastal exposure 750 m east-northeast of Smith Point, ca. 100 m east of quartzite beds at water level
20-10	47°44'09"N 53°56'05"W	<u>Trans Canada Highway:</u> west side of roadcut 0.2 km south of junction of Southern Harbour road; 40 cm thick rusty weathering, recessive unit near middle of section
20-12	47°43'53"N 53°56'03"W	<u>Trans Canada Highway:</u> west side of roadcut 0.9 km south of junction of Southern Harbour road; upper part of shaly unit in middle part of section
C.F. O'Driscoll sample		
CD-135	47°38'30"N	<u>Davis Cove:</u> 1.5 km east of Davis Cove
AFK — JH samples		
16	47°33'12"N 52°42'54"W	<u>St. John's:</u> Southside Road, outcrop on south side of road, opposite Gordon Forwarders and below overpass foundations
42	47°39'00"N 53°31'00"W	<u>Green Harbour:</u> west side of Green Harbour Aspidella level
44	47°31'12"N 53°22'00"W	<u>Halls Town:</u> 4 km southwest of Halls Town, 0.4 km northeast of The Pond that Feeds the Brook
45	47°30'30"N 53°22'17"W	<u>Halls Town:</u> 4.8 km southwest of Halls Town, 1.5 km east of The Pond that Feeds the Brook
57	46°51'45"N 52°56'23"W	<u>Cappahayden:</u> 1.2 km north of Cappahayden at end of road, Burnt Point
58	46°51'45"N 52°56'23"W	<u>Cappahayden:</u> 1.2 km north of Cappahayden at end of road, Burnt Point
59	46°51'45"N 52°56'23"W	<u>Cappahayden:</u> 1.2 km north of Cappahayden at end of road, Burnt Point
62	46°50'00"N 52°59'20"W	<u>Cappahayden:</u> 6.5 km south of Cappahayden, outcrop in gravel pit on east side of highway
69	46°38'30"N 53°06'36"W	<u>Cape Race:</u> 3.5 km southwest of Cape Race, outcrop on west side of Gripple Cove, near small brook
75	46°43'30"N 53°22'00"W	<u>Mutton Bay:</u> outcrop on beach point southeast of causeway to Powles Peninsula
108	47°09'30"N 53°33'24"W	<u>Harricott:</u> 2 km southwest of Harricott, outcrop on beach below road
109	47°09'30"N 53°33'24"W	<u>Harricott:</u> 2 km southwest of Harricott, outcrop on beach below road
110	47°09'30"N 53°33'24"W	<u>Harricott:</u> 2 km southwest of Harricott, outcrop on beach below road

Appendix 1 (cont'd.)

121	47°08'00"N 53°41'24"W	<u>North Harbour:</u>	2.5 km southwest of North Harbour on east side of road
123	47°44'00"N 54°55'24"W	<u>Trans Canada Highway:</u>	1.5 km southwest of junction of Southern Harbour road, outcrop on east side of road
126	47°38'30"N 54°56'20"W	<u>Little Harbour East:</u>	outcrop at roads end, southwest side of harbour
134	47°23'24"N 53°36'14"W	<u>Placentia Highway:</u>	8 km south of Trans Canada Highway junction, outcrop on north side of road
145	47°27'00"N 53°34'24"W	<u>Trans Canada Highway:</u>	0.5 km west of junction to Placentia-Argentia
153	48°43'00"N 53°48'12"W	<u>Burnside:</u>	outcrop of black shale next to ferry wharf, diabase dyke cross-cuts the unit
156	48°40'48"N 53°40'43"W	<u>Wild Cove:</u>	3 km southwest of Salvage outcrop on northwest side of road
158	48°39'53"N 53°42'36"W	<u>Dark Cove:</u>	7 km southwest of Salvage, rock cut on south side of road
165	48°53'33"N 53°39'55"W	<u>Cottel Island:</u>	1.5 km northwest of St. Brendan's beside northernmost wharf (end of road)
167	48°52'12"N 53°39'00"W	<u>Cottel Island:</u>	west side of Hayward's Cove
169	48°50'24"N 53°41'15"W	<u>Cottel Island:</u>	outcrop next to ferry wharf, Shalloway Cove
170c	48°26'45"N 53°50'40"W	<u>Canning's Cove:</u>	0.5 km south of Cutwater Head, blue-black cherty nodules
175	48°06'25"N 53°46'30"W	<u>Random Island:</u>	3.5 km west of Hickman's Harbour, outcrop on the northwest side of road beside Long Pond
187b	48°29'30"N 53°04'58"W	<u>Melrose:</u>	1.5 km north of Melrose, shale band
199	48°22'00"N 53°42'00"W	<u>Lethbridge:</u>	2 km west of Southern Bay Station on north side of Cabot Highway
201	48°00'07"N 53°51'00"W	<u>Leonard's Cove:</u>	Road to Little Heart's Ease, outcrop on south side of road
202	48°00'40"N 53°56'00"W	<u>Queen's Cove:</u>	outcrop on south side of road on east side of brook

Appendix 2

Preparation Technique

Samples were collected from coastal exposures and roadcuts. Because of the reconnaissance nature of the project the sampling interval was often large and irregular. Rock samples that were as fresh as possible were collected. Sample numbers were assigned in the field and maintained throughout laboratory processing.

Laboratory procedures followed those of Barss and Williams (1973). Small amounts (15-20 g) of finely crushed sample (1-4 mm size) were placed in a 600 mL polyethylene beaker and covered with concentrated HCl acid. The contents of each beaker were agitated using a stirring rod. When the reaction was complete the sample was diluted with distilled water, the contents were allowed to settle and the excess liquid was decanted. This rinsing step was repeated three times to ensure a neutral solution before the addition of other acids.

Enough concentrated HF acid was added to each beaker to cover the sample. Agitation of the beaker contents was continued and with completion of the reaction the sample was rinsed three times. Concentrated HCl acid was added to the samples which were then placed on an oscillating hotplate for 1.5 hours. The oscillator was turned off and the contents of the beakers were allowed to settle. The HCl acid was then decanted and the samples rinsed three times.

The remaining contents of the beaker were poured through a 90 μm and 20 μm mesh sieve and each of these residue fractions was bottled in a 1 dram glass vial with a screw cap. Permanent slides were made of the two size fractions, following methods outlined in Barss and Williams (1973) and Barss and Crilley (1976). Slides of unsieved macerates were also prepared for about 30 samples collected by Hill and King, and all samples collected by Hofmann.

When preparing permanent slides of the residues, two drops of Cellosize were placed on a 20 x 20 mm coverslip. A drop of residue was then placed on the Cellosize drop and, using a toothpick, the two were thoroughly mixed and evenly spread to the edges of the coverslip. The coverslip with the mixture was placed in a dust free chamber and allowed to set at 25°C. When dried the coverslip was inverted and secured to a glass slide with Elvacite and allowed to set at 25°C.

Project 650024

W.H. Fritz

Regional and Economic Geology Division

Fritz, W.H., *Cambrian stratigraphy in the northern Rocky Mountains, British Columbia; in Current Research, Part B, Geological Survey of Canada, Paper 79-1B, p. 99-109, 1979.*

Abstract

Six stratigraphic sections are presented from in and near the Ware (94F, east half) map area. Lower Cambrian quartzite is widespread and contains interbedded shale and carbonate to the west. Rapid facies changes are noted in the Middle Cambrian and are believed to have taken place in a north(?) -trending trough (three facies) and in the basin to the west (one facies). Clastics of various sizes including conglomerate continually filled the trough immediately north of the map area, whereas within the map area the trough received fine sand and siltstone deposited in relatively deep water. At the same time, carbonate in medium and thick beds was deposited in the trough to the south. Middle Cambrian basin deposits are generally thin and comprise mainly dark shale and platy limestone, but are locally displaced by large bioherms of light coloured limestone. During the Late Cambrian, platy limestone and shale were deposited over three of the Middle Cambrian facies and possibly the fourth. Erosion has erased the Upper Cambrian record above the conglomerate-bearing facies.

Introduction

In 1978 the writer assisted G.C. Taylor with his regional mapping (project 630017) by studying five stratigraphic sections (Fig. 13.1a, b, 13.2) in and near the Ware (east half) map area in northeastern British Columbia. The present paper is an attempt to organize data from these sections and to relate them to previous work in nearby areas. An adjacent section of particular importance (Gabrielse, 1975, Fig. 3, Section 1) has been redrafted and is refigured here (Fig. 13.1a, Section 1; Fig. 13.2, Section 1) for ease of correlation.

Taylor et al. (1979) have recognized four Cambrian facies in and near the Ware (east half) map area that are given here in a rearranged order to fit the present discussion. The four facies are as follows: (1) in the northwest part of the area (west of the Gataga Fault), Lower Cambrian quartzite overlain by either Middle Cambrian shale or by undated massive limestone; (2) in the northern part of the map area, basal Cambrian quartzite overlain by undated dolomite, Middle Cambrian siliceous siltstone, calcareous siltstone, and finally by Upper Cambrian platy limestone; (3) immediately north of the map area, basal Cambrian quartzite overlain by interbedded sandstone, dolomite, and coarse conglomerate; (4) near the southwestern boundary of the area, Lower Cambrian quartzite, dolomite, and shale overlain by Upper Cambrian platy limestone and nodular limestone. The Upper Cambrian in facies 4 was assigned to the Lynx Group.

The sections figured in this paper lie within three of the above mentioned facies, and the sections to be cited (Gabrielse, 1975) lie within and near the fourth. As the limited number of sections presented here represent only a start in documenting the facies, they are organized so that data can be extracted and added to future work. Attention is given to accurately locating the sections, to briefly describing numbered lithologic units, and to giving unit thicknesses. All fossil localities are shown on the sections, and their GSC numbers given for rapid retrieval and review.

Facies 1

Sections 1 and 2 (Fig. 13.1, 13.2) lie within the first facies and at both localities the Cambrian can be separated into a Lower Cambrian quartzite, an overlying undated carbonate, and a Middle and Upper Cambrian succession of dark shale and platy limestone. At both sections the Lower Cambrian is underlain by a succession of Precambrian

diamictite, dark shale, and dolomite that will be discussed later. At Section 1 the oldest exposed Cambrian strata (unit 6) consist of 176 m of light brown to rust weathering, fine grained quartzite in thick to thin beds. Above the quartzite is 157 m (unit 7) of shale and siltstone that contain limestone in sparse nodules and in thin, wavy beds in the upper half. A Lower Cambrian *Nevadella* Zone faunule is present at three GSC localities (88750-88752) near the top of the unit. The next overlying unit (8) is composed of 310 m of light brown weathering, thick bedded quartzite and a subordinate amount of mainly orange weathering dolomite. Fossils belonging to the late Lower Cambrian *Bonnia-Olenellus* Zone are present near the middle of the unit (GSC loc. 88753) and near the top (GSC loc. 88754, 88755). No fossils were found in the overlying unit (unit 9, 128.3 m) of medium and thick bedded, cream weathering dolomite, except for the uppermost beds (GSC loc. 88156) which contain an early Middle Cambrian *Albertella*(?) Zone faunule. The youngest Cambrian unit (10) is composed of 40.2 m of dark siltstone and shale interbedded with platy limestone. Within the unit are fossils belonging to the Middle Cambrian *Albertella*(?) Zone (GSC loc. 88762, 88763), *Bathyriscus-Elrathina* Zone (GSC loc. 88764), and *Bolaspidella* Zone (GSC loc. 88765-88769) and to the Upper Cambrian *Dunderbergia* Zone (GSC loc. 88770, 88771). The close spacing of the zones indicates a history of slow deposition and/or intermittent removal of strata.

At Section 2 (Pl. 13.1, fig. 1) the Cambrian is indirectly underlain by the Helikian Aida Formation (unit 1) and directly underlain by a 130 m succession of diamictite, black shale, and dolomite (units 2, 3) that correlates with units 1 to 5 in Section 1. At Section 2 the Precambrian-Cambrian boundary is placed at an angular unconformity (Pl. 13.1, fig. 1), and the basal Cambrian unit (4) consists of 112.5 m of white weathering, medium- to very thick-bedded quartzite. The quartz grains are poorly sorted and are fine to coarse. Above the quartzite is a 295-m unit (5) of very fine grained sandstone and silty sandstone that weathers medium light brownish grey to rust and locally contains burrowed beds. Orange weathering, fine- to medium-grained quartzite in medium to very thick beds with a sparse amount of dolomite near the top (unit 6, 136.5 m) overlies the sandstone. The quartzite in turn is overlain by a 32.5 m carbonate unit (7) containing some (2/5) orange weathering dolomite that resemble the dolomite of unit 9 in Section 1. However, at Section 2 the dolomite is in irregular pods that interfinger with thin to thick beds of light grey limestone (3/5). At the

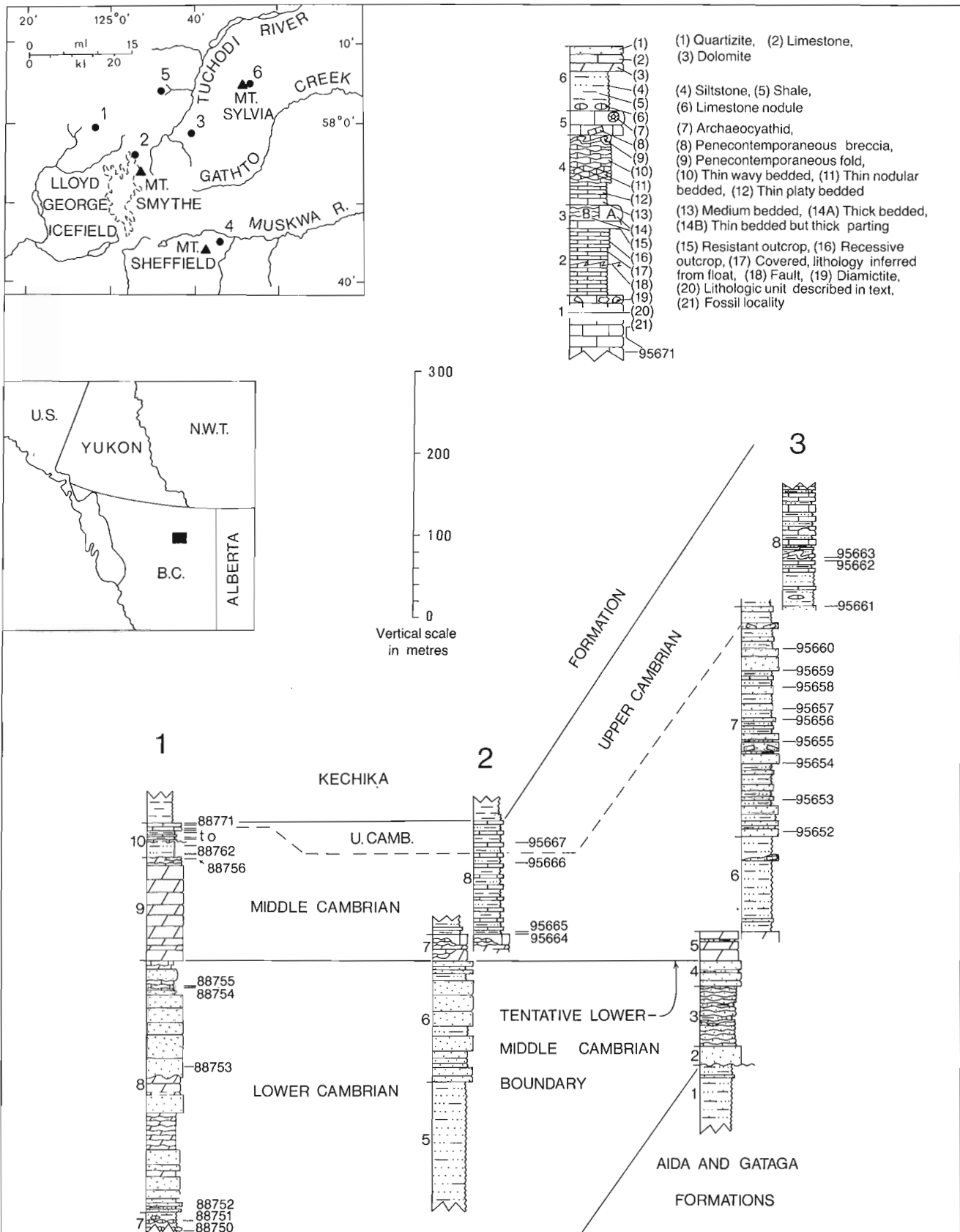


Figure 13.1. Stratigraphic sections from the northern Rocky Mountains. The index map covers only part of the Ware (94F) map area (north boundary is 58°) and extends northward into adjacent Tuchodi (94K) map area. Sections near the southern boundary of the Ware map area have been published by Gabrielse (1975) and are mentioned in the text, but are not shown on index map. The symbol for conglomerate (Section 5, unit 5) has been omitted from the legend. The lower part of Sections 1 and 2 could not be shown in this figure because of space limitations; all of these sections are shown on Figure 13.2.

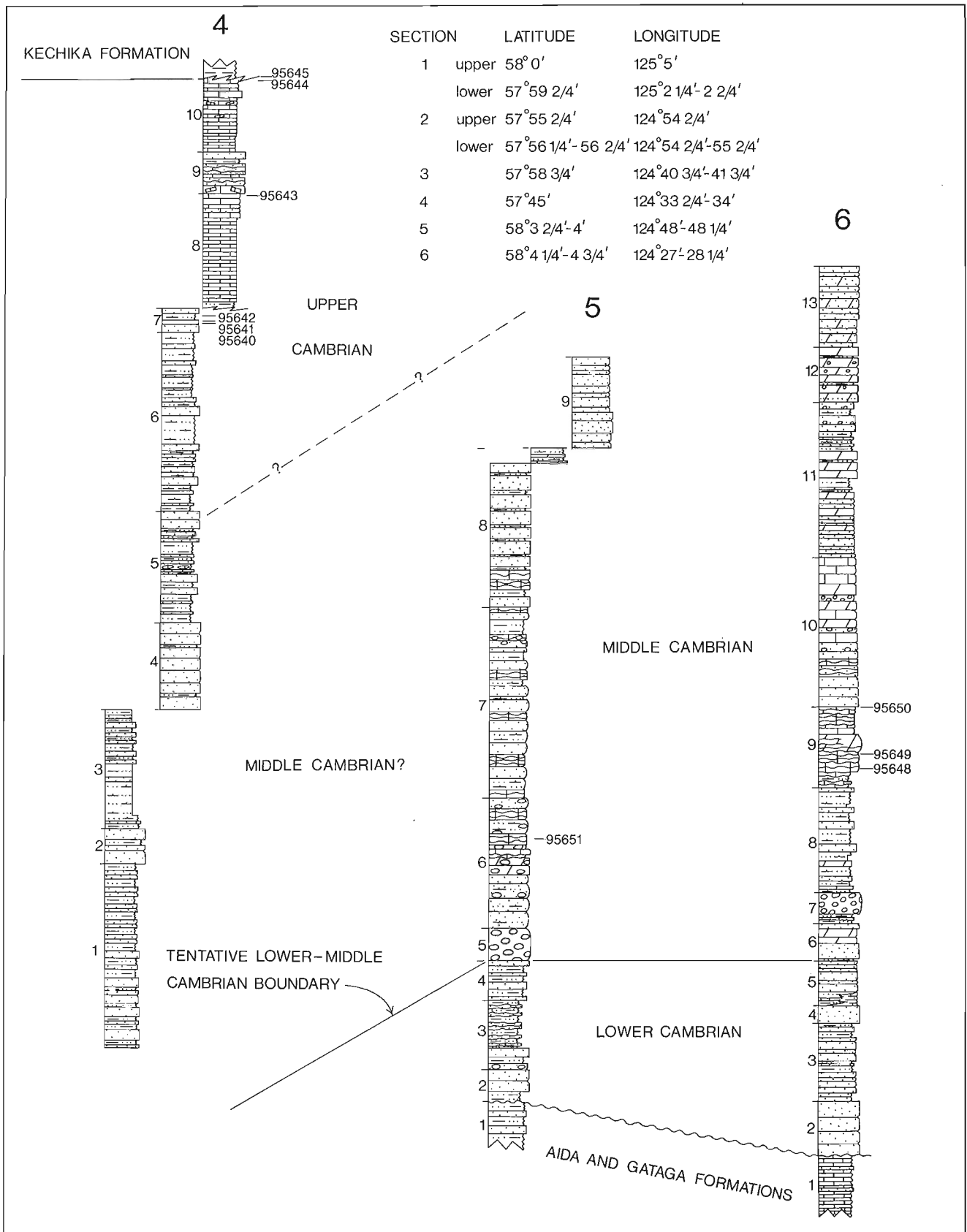


Figure 13.1b

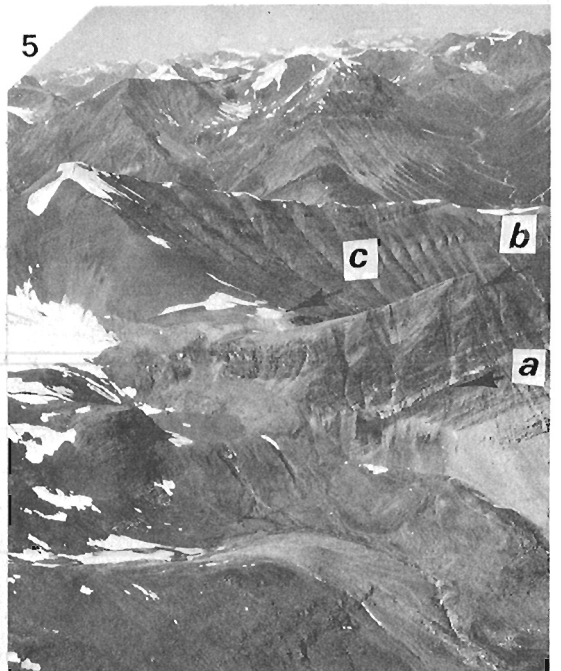
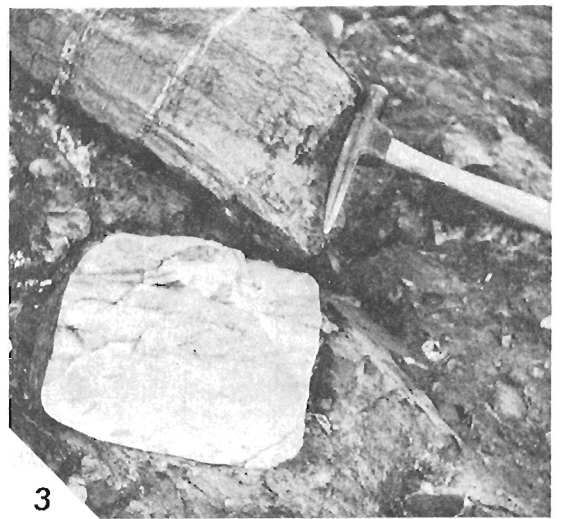
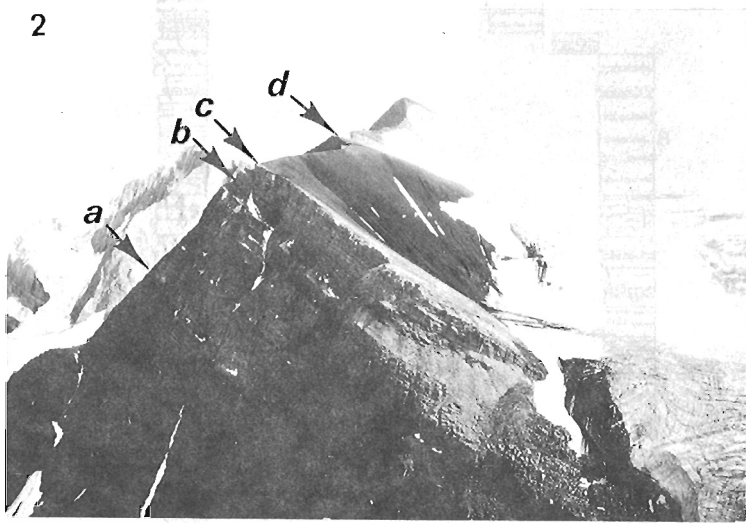
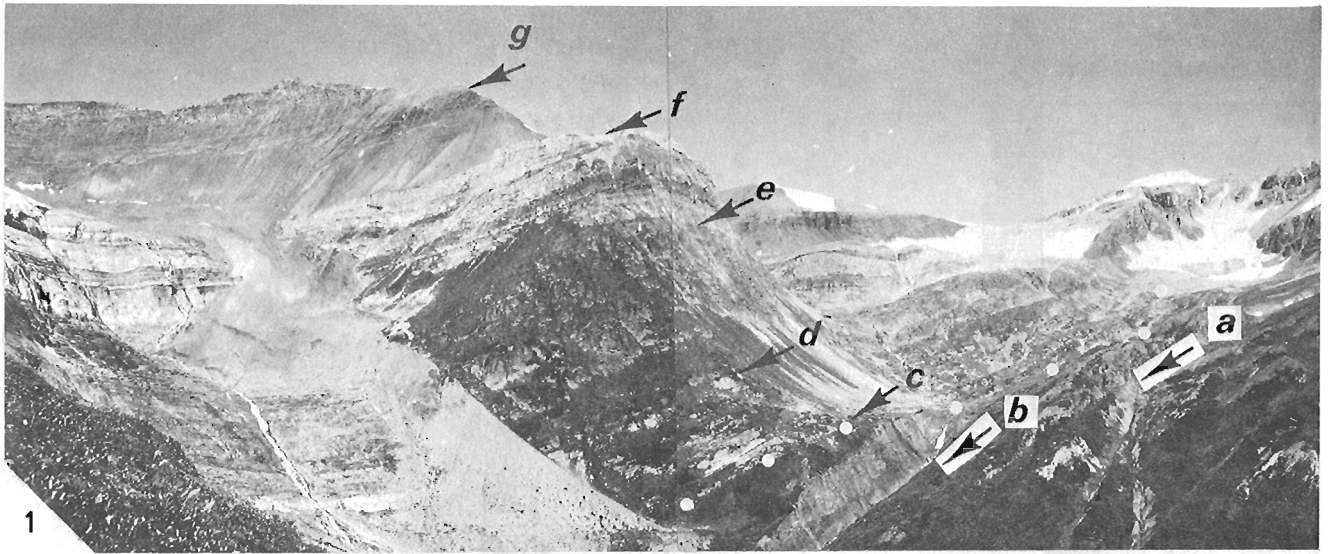


PLATE 13.1 (opposite)

Figure 1. View looking north at lower segment of Section 2. Contact between Aida Formation and diamictite-bearing succession is at (a), top of diamictite (unit 2) is at (b), Precambrian-Cambrian angular unconformity is marked by white dots at (c), top of basal Cambrian white quartzite (unit 4) is at (d), top of unit 5 is at (e), top of unit 7 and of lower segment of the section is at (f). Base of Kechika Formation is at (g). Composite from GSC photos 203472-B and 203473-Y.

Figure 2. View looking south at upper segment of Section 2. Top of unit 5 is at (a), base and top of unit 7 is at (b) and (c), base of Kechika Formation is at (d). GSC photo 203472-T.

Figure 3. Diamictite from near point (a) in figure 1 and located 38.5 m above base of unit 2. Large white clast is composed of fine grained quartzite and large clast touching hammer head is composed of dense limestone. GSC photo 203472-A.

Figure 4. Coarsely crystalline diorite clast (at base of rock sample) in medium brownish grey weathering diamictite. Float sample from unit 2, Section 2, diorite clast is 12 cm long. GSC photo 202029-G.

Figure 5. View looking northwest at Section 3. Base of Cambrian is at (a), base and top of dolomite unit 5 is at (b) and (c). Note recessive weathering of Cambrian above level of (c). GSC photo 203472-J.

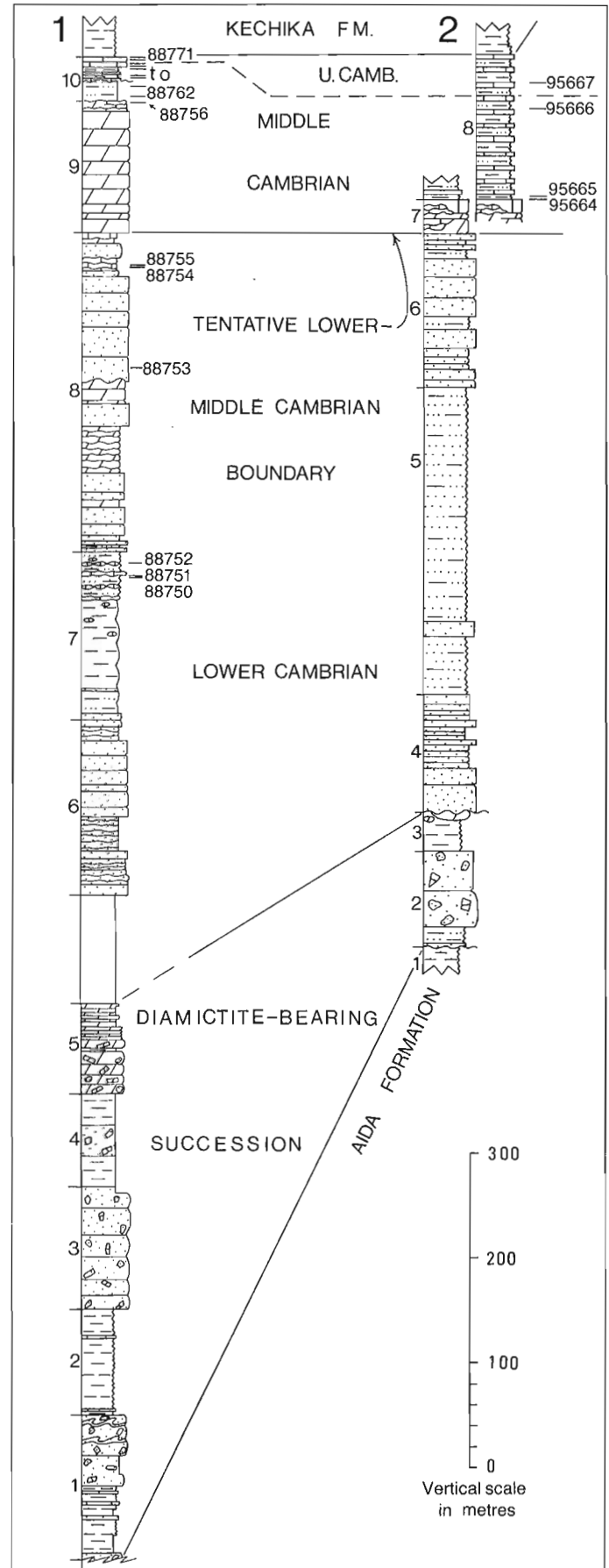
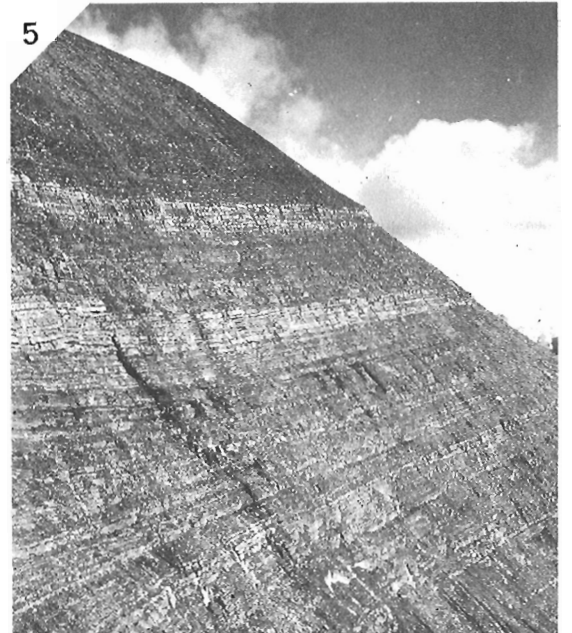
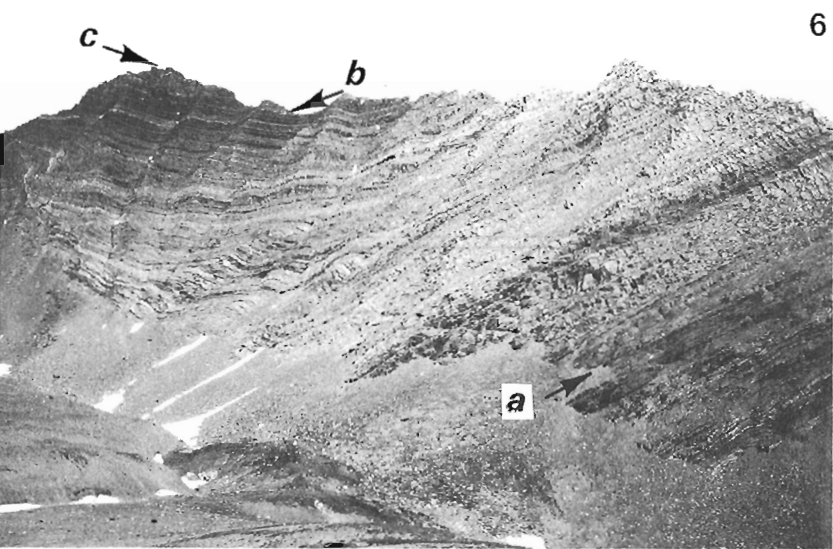
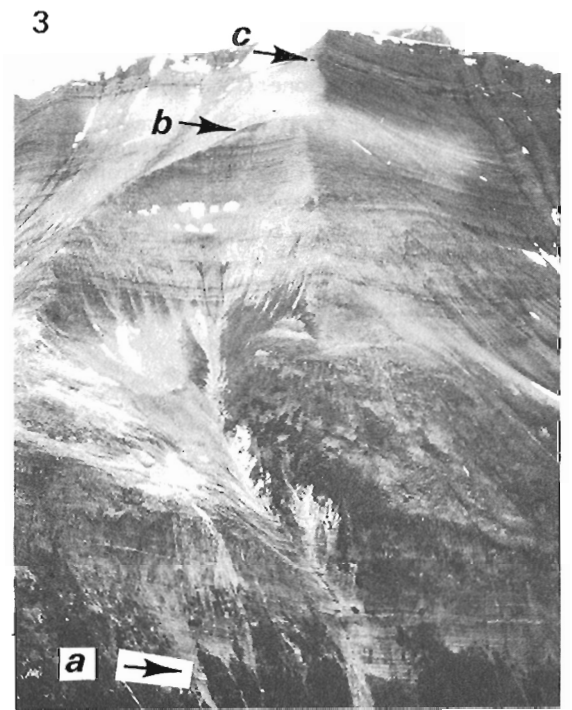
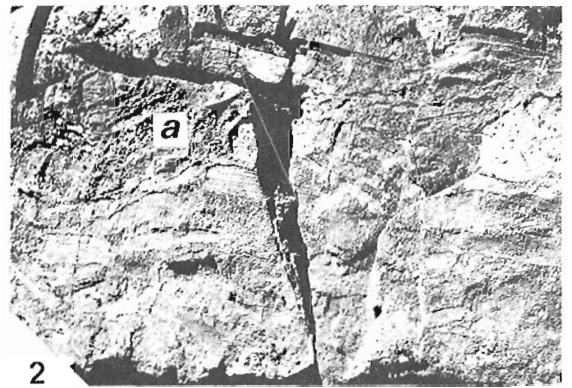
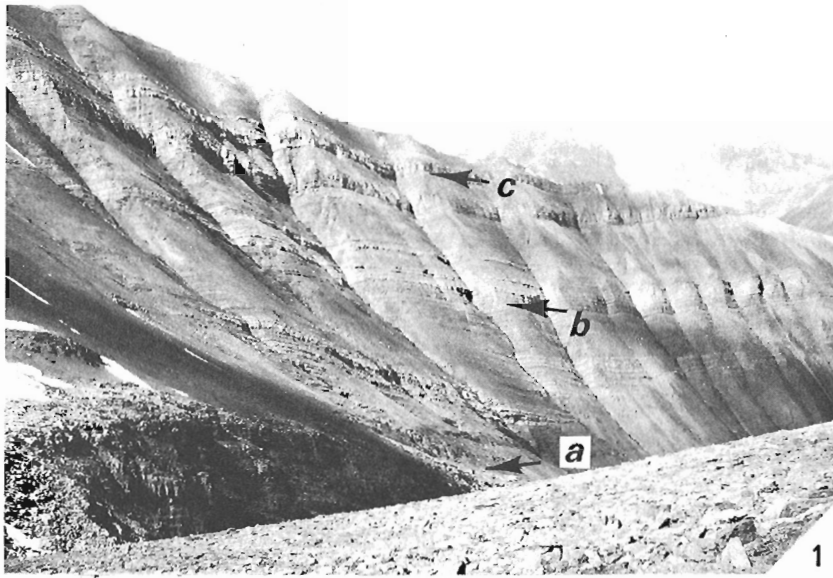


Figure 13.2

Stratigraphic sections from the northern Rocky Mountains. The upper part of these two sections is shown in Figure 13.1.



top of the Cambrian succession is a recessive unit (unit 8, 147 m) of black weathering siltstone and shale that contains interbedded platy limestone. Fossils from this unit belong to the Middle Cambrian *Albertella*(?) Zone (GSC loc. 95664, 95665), *Bolaspidella* Zone (GSC loc. 95666), and to the Upper Cambrian *Aphelaspis* Zone (GSC loc. 95667).

Section 3 (Pl. 13.1, fig. 5; Pl. 13.2, fig. 1) lies near the boundary between facies 1-3 and lithologically belongs in a transition zone between Facies 1 and 2. At Section 3 yellow to light greenish grey weathering Aida siltstone indirectly underlies the Cambrian and is followed by Helikian orange brown weathering siltstone belonging to the Gataga Formation (unit 1). An unconformity with little or no angularity separates the Gataga from a 23 m Cambrian unit of white, thick bedded quartzite (unit 2). This quartzite is followed by 76.5 m of light brown weathering, irregularly bedded and burrowed quartzite (unit 3) that in turn is overlain by 31 m (unit 4) of medium and thick bedded, light brown to rusty weathering quartzite. The upper and lower quartzite units are fine to very fine grained and the medial quartzite is poorly sized, ranging between fine to coarse grained. Above the quartzite succession is a 36.5 m unit (5) of medium and thick bedded dolomite, the lower 28.5 m of which weathers dark brownish orange (almost terra cotta) and the upper 8 m weathers bright orange to pink. The dolomite and the underlying quartzites are highly resistant (Pl. 13.1, fig. 5) relative to the overlying succession of interbedded siltstone, quartzite, and limestone. The first unit (6) in the overlying recessive succession is composed of light brownish grey (base to 22.5 m) and dark grey to rust (22.5 to 11.5 m) weathering siltstone with minor interbedded quartzite. The thickest of the quartzite interbeds contains penecontemporaneous slump breccia. The next unit (unit 7, 290 m) is in part (2/3) composed of dark grey to rust weathering siltstone and in part (1/3) composed of interbedded light brown weathering, limy quartzite. Some penecontemporaneous breccia (Pl. 13.2, fig. 2) is visible in the quartzite beds, but because both breccia and matrix are composed of fine to very fine grained

quartzite, the breccia is inconspicuous. Fossils collected from this unit belong to the late Middle Cambrian *Bolaspidella* Zone (GSC loc. 95652 to 96660) and to the early Upper Cambrian *Cedaria-Crepicephalus* Zone (GSC loc. 95661). The youngest unit (8) in the Cambrian succession is composed of 125.5 m (section ends at ridge top) of dark grey to rust weathering siltstone and platy limestone. Some penecontemporaneous folds are present and two fossil localities (GSC loc. 95662, 95663) just below the middle contain faunules belonging to the *Cedaria-Crepicephalus* Zone.

Facies 2

Strata in the second facies were studied at Section 4, which is located near Mt. Sheffield and just south of the Muskwa River. There the Lower Cambrian quartzites and the overlying dolomite (equivalent to units 2 to 4 and unit 5 respectively in Section 3) are exposed in the nearby hills, but are separated from Section 4 by a covered interval and were not measured. Section 4 begins with the next younger units 1 to 7 (unit 1, 225.5 m; unit 2, 43 m; unit 3, 145 m; unit 4, 107 m; unit 5, 135.5 m; unit 6, 218.5 m; unit 7, 30 m) consisting of 904.5 m of siltstone and interbedded quartzite that probably continues down section below the cover for an additional several hundred metres. Typical exposures (Pl. 13.2, fig. 4) consist of medium light brown weathering quartzite in thin to thick beds and interbedded rust to light brown weathering siltstone. The quartzite is fine to very fine grained and is medium grey to medium brownish grey on fresh surfaces. Throughout most of the succession siltstone predominates over the quartzite except in units 2, 4, and 7 where the reverse is true. Siltstone below the base of unit 6 is not limy (except in rare beds) whereas siltstone above is. From a distance strata below the base of unit 6 have a slight reddish or rusty hue as compared to the more neutral greys of the Cambrian above. GSC localities 95640 to 95642 in unit 7 contain *Crenulimbus?* sp., *Dunderbergia* sp., *Dytremacephalus?* sp. and *Pseudagnostus* sp. that belong to the Upper Cambrian *Dunderbergia* Zone. Above the siltstone and shale succession the Cambrian is composed mainly of limestone. Units 8 and 10 (140 m, 90+ m respectively) contain medium grey weathering, platy limestone that is planar laminated and is dark grey on fresh surface. Some penecontemporaneous breccia is present in unit 10, and the presence of *Pseudagnostus* sp. and *Wilbernia* sp. (GSC loc. 95643) indicates that at least the upper strata in unit 8 belongs to the Upper Cambrian *Conaspis* Zone or to the *Ptychaspis-Prosaukia* Zone. Unit 9 (49.5 m) weathers into three prominent ribs of light brown, fine grained quartzite and contains a subordinate amount of shale and limestone. Penecontemporaneous breccia is abundant at several horizons within the unit. A fault at the top of the section marks the contact between unit 10 and the overlying Kechika Formation. Two fossil localities (GSC loc. 95644, 95645) in limestone float scattered over the concealed contact contain the early Lower Ordovician index genus *Sympysurina*. Although the fossils could not be traced to outcrop, it is believed that they originated close to the lower boundary of the Kechika Formation.

Facies 3

Sections 5 and 6 are within the third facies and are located a short distance north of the Ware (east half) map area. At Section 5 the Cambrian is unconformably underlain by rust weathering siltstone and interbedded light orange brown weathering quartzite mapped by Taylor and Stott (1973) as the Helikian Gataga Formation. The overlying Cambrian (unit 2) begins with maroon siltstone (base to 13.5 m) followed by coarse grained, white quartzite in thick beds (13.5 m to 23.5 m). The next unit (unit 3, 85 m) is

PLATE 13.2 (opposite)

Figure 1. View looking northwest at Section 3, top of dolomite unit 5 is at (a), GSC loc. 95654 is at (b), base of cliff at (c) is 254.5 m above base of unit 7 and 25.5 m above GSC loc. 95660. GSC photo 203473-A.

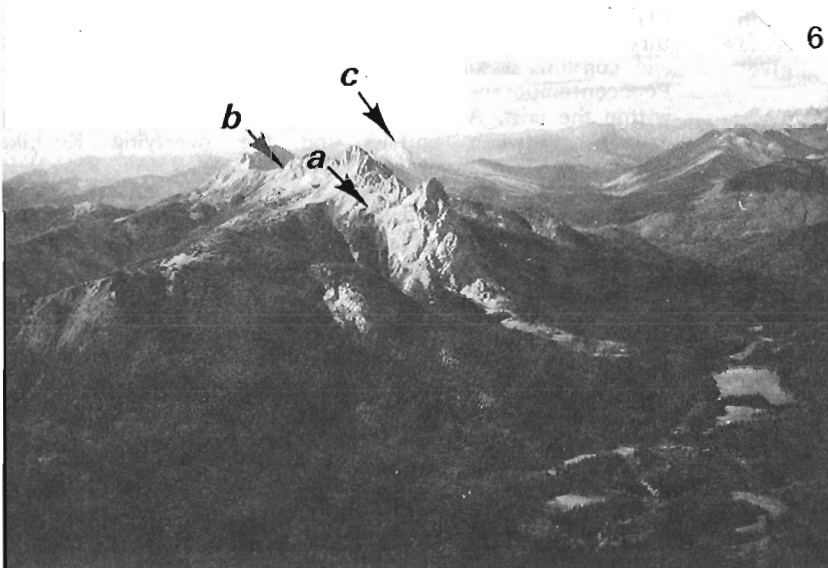
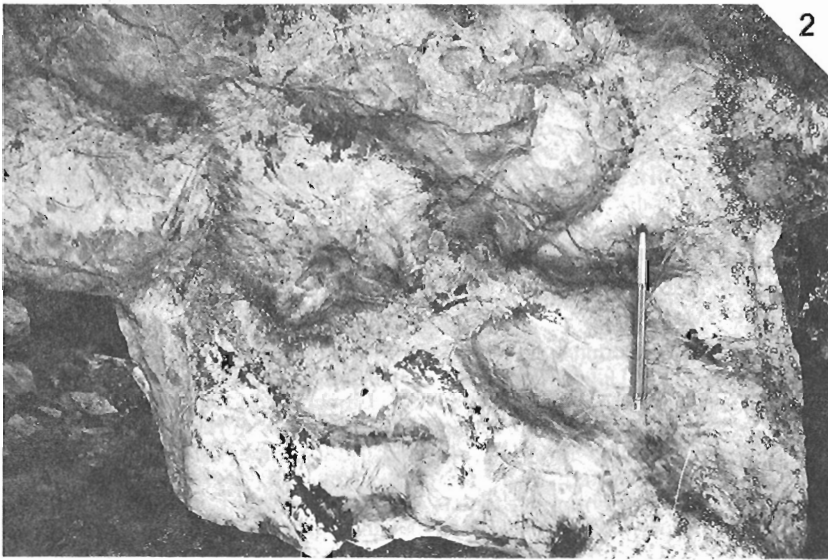
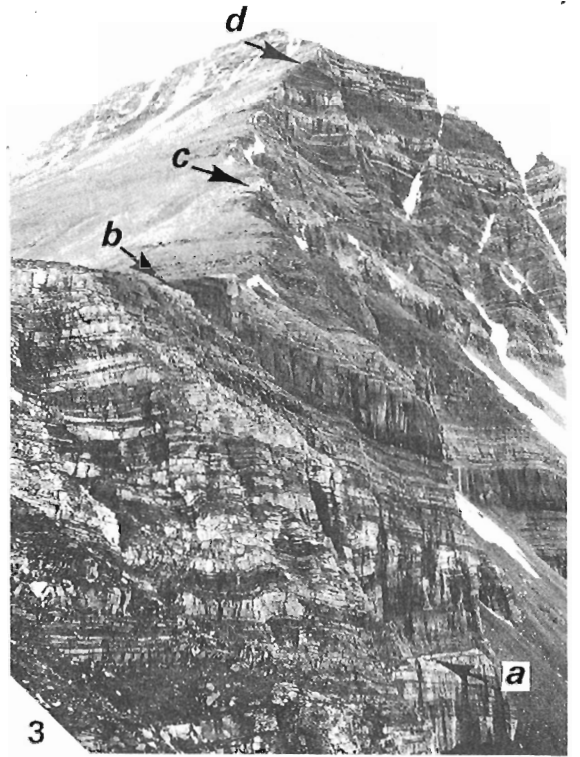
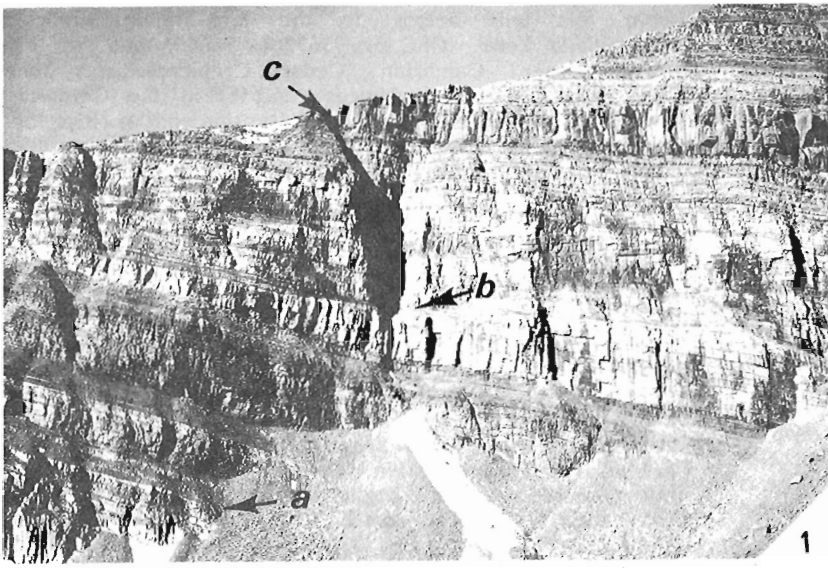
Figure 2. Penecontemporaneous breccia in Section 3, both clast and matrix are fine grained quartzite; breccia is 103.5 m above base of unit 7. Pencil at (a) gives scale. GSC photo 203473-C.

Figure 3. View looking west at Section 4 located on east slope of Mt. Sheffield. Base of section is at (a), GSC loc. 95640-95642 are at (b), base of unit 9 is at (c). GSC photo 203472-G.

Figure 4. Thin- to thick-bedded, fine to very fine grained quartzite with subordinate amount of interbedded siltstone. Head of hammer (a) is 0.7 m below top of unit 2 in Section 4. GSC photo 203472-P.

Figure 5. Siltstone with subordinate interbeds of thin- to thick-bedded quartzite in unit 6 of Section 4. View looking north at steep slope below point (b) in figure 3. GSC photo 203472-Q.

Figure 6. View looking northeast at Section 5. Base of unit 5 is at (a), top of lower segment of section is at (b) (arrow "b" also points to bright orange dolomite interbeds near top of unit 8). Top of section is at top of peak (c). GSC photo 203472-H.



composed of rust weathering siltstone interbedded with irregular thin to thick bedded quartzite that is very fine grained and burrowed. Fresh surfaces of the siltstone and quartzite are dark grey and greenish grey, respectively. The uppermost unit in the quartzite succession (unit 4, 45.5 m) contains very fine grained, light brownish grey weathering quartzite in thick to thin beds, and interbedded rust weathering siltstone. The Lower-Middle Cambrian boundary is tentatively placed at the base of an overlying maroon weathering conglomerate (unit 5, 42.5 m). The mainly quartzite clasts within this unit are angular and poorly sorted (Pl. 13.3, fig. 5), the largest seen being 0.5 m in greatest dimension. Above the conglomerate is 160 m (unit 6) of light grey brown weathering, very fine grained sandstone to sandy siltstone with interbedded, impure, light grey weathering limestone in the upper half. Sparse layers and isolated pebbles are scattered throughout the interval. From a distance this unit has a slight greenish cast. A species of *Fieldaspis* located (GSC loc. 95651) 110.5 m above the base of the unit is tentatively placed in the upper part of the early Middle Cambrian *Plagiura-Poliella* Zone. The overlying unit 7 (233 m) resembles unit 6, but pebbles are very rare and, in the upper, half recessive weathering, medium brown siltstone constitutes one fourth of the thickness. Sandstone beds in both units 6 and 7 weather with a rounded profile as opposed to the blocky weathering quartzite about unit 7. Unit 8 (192 m) is mainly composed of orange brown weathering, very fine grained quartzite in thick beds, some recessive weathering siltstone as in unit 7, and a few bright orange weathering dolomite beds near the top. Between the top of unit 8 and the top of the section (top of mountain) is 113 m (unit 9) of white and maroon quartzite in thick to thin beds, and some (1/6) dolomite and sandy dolomite in orange weathering beds.

Section 6, the second section within Facies 3, is located on the southeast flank of Mt. Sylvania. Here the Cambrian overlies medium light grey to medium brownish grey shaly limestone (unit 1) that has been mapped (Taylor and Stott, 1973) as the Helikian Aida Formation. Unconformably above

PLATE 13.3 (opposite)

Figure 1. View looking southwest of Section 6 located on southeast slope of Mt. Sylvania. Top of basal Cambrian quartzite unit 2 is at (a), channeled top of white quartzite unit 4 is at (b) in this figure and at (a) in figure 3, base of thick conglomerate bed in unit 7 is at (c). GSC photo 203472-C.

Figure 2. Fossil trace markings in unit 3 of Section 6. GSC photo 203472-N.

Figure 3. View looking northwest at Section 6. Channeled top of unit 4 is at (a), note giant crossbeds in overlying unit 5, base of large conglomerate bed (see also figure 4) in unit 7 is at (b), GSC loc. 95648 and 95649 are just below (c) and GSC loc. 95650 is just above, top of thick maroon band and top of unit 11 is at (d). GSC photo 203472-M.

Figure 4. Thick conglomerate bed, unit 7, Section 6, GSC photo 203472-L.

Figure 5. Angular to rounded clasts in conglomerate of unit 5, Section 5. Hammer head is 26 m above base of unit. GSC photo 203472-G.

Figure 6. View looking northwest at white limestone ridge with Spectre Peak at far end. This ridge and distant ridge (c) are believed to represent two of many large Middle Cambrian bioherms. GSC loc. 95646 is at (a) (base of bioherm?), GSC loc. 95647 is at northeast side of pass at (b). GSC photo 203472-O.

the Aida is 238.5 m of Cambrian quartzite that is subdivided into 4 stratigraphic units, the lowest (unit 2, 66 m) of which consists of white to light brown weathering, fine- to coarse-grained quartzite in thick beds. The next unit (unit 3) contains greenish brown (base to 36 m) and brownish grey (36 to 96 m), very fine grained quartzite in thin and medium beds. Burrows and fossil traces (Pl. 13.3, fig. 2) are common. Two layers of dark maroon, hematite rich siltstone totalling 9 m in thickness are also present. This unit is overlain by light coloured quartzite (unit 4, 21.5 m) similar to that in unit 2. The uppermost quartzite unit (unit 5, 55 m) consists of light brown weathering, very fine grained quartzite in thin to thick beds and dark grey siltstone. Giant crossbeds (Pl. 13.3, fig. 1), channels (Pl. 13.3, fig. 2), and burrows are well displayed. The Lower-Middle Cambrian boundary is tentatively placed at the top of the quartzite succession, and immediately above this horizon (base of unit 6) is 3 m of light brown weathering, sandy, limy siltstone with "floating" quartzite pebbles up to 1.5 cm in diameter. Overlying the siltstone is 18.5 m of pink to light brick red weathering sandstone followed by 18 m of cream to pink dolomite, and finally by 6 m of light brown quartzite. Unit 7 (38.5 m) contains a very thick bed of conglomerate (Pl. 13.3, fig. 4) that resembles the conglomerate bed (unit 5) above the basal quartzite succession in Section 5, except at Section 6 the clasts are better sorted and more highly rounded. Clasts in Section 6 average 7.5 cm in diameter and the largest seen is 33 cm in greatest dimension. At the base of unit 7 is 12 m of interbedded limy siltstone, brick red quartzite, and cream to pink weathering dolomite. The next overlying unit (unit 8, 128 m) contains medium light brownish grey weathering, limy siltstone, a subordinate amount (1/4) of interbedded, light brown weathering, very fine grained sandstone, and some sparse "floating" quartzite pebbles up to 1.25 cm in diameter. Some light grey limestone and orange weathering dolomite are also present in the lower 38 m of the unit. Unit 9 (98.5 m) contains the greatest carbonate concentration in the section, most of which consists of medium grey weathering limestone in thin, wavy beds. Near the middle of the unit is 35.5 m of light brown to cream weathering dolomite. Three fossil localities (GSC loc. 95648 to 95650) within this unit contain a species of *Fieldaspis* that is tentatively assigned to the upper part of the early Middle Cambrian *Plagiura-Poliella* Zone. Unit 10 contains mainly light brownish grey, limy sandstone in its lower part (77.5 m), a mixture of limestone, dolomite, and sandstone in its medial part (58.5 m), and mottled (burrowed?) medium light grey to light brown weathering dolomite and limestone in its upper part (46 m). Lenticular conglomerate interbeds are present in the medial part, the thickest being 8 m thick and the largest clast seen being 40 cm in greatest dimension. Strata in overlying unit 11 consist of medium brown weathering sandstone and light orange weathering dolomite in thin to thick interbeds (80 m) followed by maroon siltstone and cream weathering dolomite in thick beds (49.5 m), and finally by maroon siltstone with subordinate conglomerate interbeds (61 m). Cream weathering dolomite with laminae of quartz sand predominate in unit 12 (66.5 m), and rare beds of quartz pebbles are also present. Between unit 12 and the top of Mt. Sylvania is 99 m (unit 13) of white quartzite that is fine and very fine grained and interbedded dolomite and dolomitic sandstone that are orange weathering.

Facies 4

South of the map area, one section (Pesika Creek) within Facies 4 and three nearby sections (Ospika River) have been published by Gabrielse (1975, p. 7-9, 19-24, Fig. 3). The Pesika Creek section begins above complexly faulted Cambrian strata and the lowest measured unit (1) consists of medium grey to medium brownish grey weathering shale (178.3 m) overlain by medium light brown weathering, very fine grained quartzite and interbedded medium brown to

medium grey weathering siltstone (41.4 m). The next unit (unit 2, 112.5 m) is composed of medium light grey weathering, medium bedded, oolitic limestone that locally grades into bright orange weathering dolomite. Fossil localities near the top of the unit 1 (GSC loc. 88887, 88888) and near the middle of unit 2 (GSC loc. 88889) belong to the Lower Cambrian **Nevadella** Zone. Unit 3 (316.7 m) contains mainly light grey weathering siltstone with abundant interbeds of light brown weathering, fine grained sandstone and orange weathering dolomite. No fossils were found in this unit, but equivalent strata in sections to the southeast (Gabrielse, 1975, Sections 3-5) contain fossils belonging to the late Lower Cambrian **Bonnia-Olenellus** Zone. Undated black shale (unit 4, 48.8 m) with interbedded (1/7) light orange weathering, platy limestone overlies the Lower Cambrian succession. The dark shale is in turn overlain by brownish grey weathering shale (unit 5, 88.4 m) with a subordinate amount of interbedded light grey weathering, platy limestone. Fossils (GSC loc. 88890) from the upper one-third of this unit belong to the Upper Cambrian **Cedaria-Crepicephalus** Zone. The next overlying unit (unit 6, 127.7 m) is almost wholly composed of medium grey weathering limestone in thin platy beds. Between unit 6 and the overlying Kechika Formation is a unit (unit 7, 371.5 m) composed of limestone as in unit 6 and interbedded light silvery brown shale. Fossils from the top of unit 6 and the base of unit 7 (GSC loc. 88891, 88892) are of an unknown zone and the remaining fossils from unit 7 (GSC loc. 88893 to 88901) belong to the Upper Cambrian **Ptychaspis-Prosaukia** Zone and/or to the **Saukia** Zone.

Southeast of the Pesika Creek section and on the nearby Ospika River are three sections (Gabrielse, 1975, Sections 3-5) containing a thick succession of Middle Cambrian dolomite. As this dolomite is not present at the Pesika Creek section, it is possible that it has been removed at the Pesika site by pre-Late Cambrian erosion, but more probable that the Pesika Creek section contains Middle Cambrian shale (unit 4) that is the lateral equivalent of the Ospika River dolomite.

The above suggested correlation of the Pesika Creek shale (unit 4) with the Ospika River Middle Cambrian dolomite brings the Facies 4 concept as stated by Taylor et al. (1979) into question, as the Middle? Cambrian shale at Pesika Creek closely resembles the Middle Cambrian shale in Facies 1 at Sections 1 and 2. It might also be added that the Lower Cambrian at Pesika Creek resembles that at Section 1, and that there is a partial similarity in the Upper Cambrian, however most of these latter strata at Sections 1 and 2 have probably been removed by a sub-Kechika unconformity, and therefore a full comparison cannot be made. Given the mentioned close similarities, it seems logical that the Pesika Creek Section should be placed in Facies 1 with Sections 1 and 2. This change would allow the reference area for Facies 4 to be changed from Pesika Creek to the Ospika River (Gabrielse, 1975, Sections 3-5) where a thick Middle Cambrian dolomite succession in the Cambrian represents a striking change from the other three facies.

Precambrian (Hadrynian?) Strata

At Section 1 a succession of diamictite, shale, and dolomite underlies the Cambrian. This succession begins above a fault with a unit (unit 1, 136.5 m) containing light brown shale in the lower half and diamictite in the upper half. The second unit (102.7 m) consists of rust weathering, black shale which in turn is overlain by diamictite (unit 3, 119.2 m) with sparse granite boulders near the base. Unit 4 (90.8 m) contains black shale and interbedded diamictite similar to that below. The uppermost unit (unit 5, 64.9 m) is composed

of bright orange weathering dolomite in thick beds that grade upward into light grey dolomite in thin beds. A covered interval separates unit 5 from the overlying Cambrian quartzite.

At Section 2 the unconformity between the Hadrynian(?) succession and the underlying light orange brown to silvery brown weathering Aida Formation is exposed. Above the unconformity is a succession (unit 2) that begins with 5.5 m of fine grained, thin bedded sandstone followed by 24.5 m of light brown weathering shale, which is abruptly overlain by 62.5 m of diamictite. The only igneous boulder found in this unit is a diorite with a high pyrite content (Pl. 13.1, fig. 4). The uppermost unit in this succession (unit 3, 38.5 m) is composed of rust weathering, black shale with large dolomite (slump?) blocks up to 7.5 m thick at the top. The Hadrynian(?) succession at Section 2 terminates at a sub-Cambrian unconformity that cuts through unit 3 to the north and into unit 1 (Pl. 13.1, fig. 1).

The position of the Hadrynian(?) strata below a thick succession of Lower Cambrian strata at Section 1 led the writer to place the diamictite bearing sequence in the Precambrian in 1972. The sharp lithologic change across the unconformity at Section 2 and the angularity of this unconformity are viewed as additional reasons to retain the Precambrian assignment. The diamictite-bearing succession has been mapped as Cambrian by Taylor and Stott (1973), returned to the Precambrian by Gabrielse (1975), and placed in the "(?)Hadrynian" or "possibly Cambrian" by Taylor et al. (1979, p. 227). No new evidence was found by the writer that might resolve the question as to the origin of the diamictite. In 1972 the writer suggested that it might be a tillite or a turbidite (Fritz, 1972, p. 211), and in 1979 Taylor et al. (p. 229) offered the alternative suggestion that it might be "mass flows originating from scarps and triggered by active faults".

Related Observation

Isolated ridges of white Cambrian limestone were observed in the adjacent (Ware west half) map area. These ridges are aligned and are considered to be large bioherms, the largest of which are Spectre Peak (Pl. 13.3, fig. 6), Mt. McCrae, and Mt. Lavoie. Two fossil collections were made from near the southeastern end of Spectre Peak, which is located 100 km west of the present map area and 32 km north of the village of Ware. The first collection (GSC loc. 95646) from the southwest (lower?) side of the bioherm contains **Elrathina?** sp., **Kootenia** sp., **Spencella** sp., and the second collection (GSC loc. 95647) from the northeast side contains **Modocia** sp. These collections indicate that part of the bioherm belongs to the Middle Cambrian **Bolaspidella** Zone, and may contain some strata as old as the underlying **Bathyriscus-Elrathina** Zone. The bioherms resemble a smaller limestone mound that occurs in Middle Cambrian shale south of Section 1 and the large limestone mound south of Section 2. Taylor et al. (1979, p. 230) have described the latter mound as "300 m of massive limestone lithologically similar to the Atan".

Speculations on Mode of Deposition

The present investigation suggests that the rapid Cambrian facies changes reported by Taylor et al. (1979) took place mainly during Middle Cambrian time. The Lower Cambrian is predominantly composed of quartzite and siltstone deposited over a deeply eroded surface and shows no striking change over the area, except for the expected basinal increase of shale and carbonate in Section 1, and at Pesika Creek. During Middle Cambrian time a (north-trending?)

trough developed in which sporadic but generally rapid deposition took place. Within the trough and just north of the map area (Sections 5, 6) subsidence was rapid enough to trap a significant proportion of the fine and most of the coarse clastics from a nearby uplift. The trough in the northern part of the map area was farther from the clastic supply and received mainly fine quartz sand and siltstone deposited in deeper and quieter waters (Section 4). South of the map area near Ospika River (Gabrielse, 1975, Sections 3-5) the water in the trough was clear enough to permit the deposition of a thick succession of carbonate. At the basinward edge of the trough (Section 3) the supply of clastics diminished, the deposition rate was generally slower, and still farther seaward (Sections 1 and 2; Gabrielse, 1975, Pesika Creek Section) only very fine clastics and thin bedded, platy carbonates were deposited. However, here too vertical movement related to the Middle Cambrian movements to the east may have taken place allowing bioherms to develop on strata uplifted into shallow waters.

During Late Cambrian time widespread, platy limestone and dark shale were deposited (Sections 1-4; Gabrielse, 1975, Pesika Creek and Ospika River Sections), indicating uniform deposition in relatively deep water.

More published sections are needed to test and expand the above speculations and new formations should be erected for control. The present data are interpreted by the writer as reinforcing his (Fritz, 1978, p. 15) previous suggestion that the Atan Group should not be used in this region. They also suggest that the recent extension of the Lynx Group into the map area (Taylor et al., 1979, p. 229) should be discouraged, as Upper Cambrian strata near the type Lynx (Burling, 1928, p. 367) are not lithologically similar to the Upper Cambrian described here.

References

- Burling, L.D. in Walcott, C.D.
1928: Pre-Devonian Paleozoic Formations of the Cordilleran provinces of Canada; Smithsonian Miscellaneous Collections, v. 75, n. 5.
- Fritz, W.H.
1972: Cambrian biostratigraphy, western Rocky Mountains, British Columbia (83E, 94C, F); in Report of Activities, Part A, Geological Survey of Canada, Paper 72-1A, p. 209-211.
1978: Upper (carbonate) part of Atan Group, Lower Cambrian, north-central British Columbia; Current Research, Part A, Geological Survey of Canada, Paper 78-1A, p. 7-16.
- Gabrielse, H.
1975: Geology of Fort Grahame E 1/2 map area, British Columbia; Geological Survey of Canada, Paper 75-33.
- Taylor, G.C. and Stott, D.F.
1973: Tuchodi Lakes map area, British Columbia; Geological Survey of Canada, Memoir 373.
- Taylor, G.C., Cecile, M.P., Jefferson, C.W., and Norford, B.S.
1979: Stratigraphy of Ware (east half) map area, northeastern British Columbia; Current Research, Part A, Geological Survey of Canada, Paper 79-1A, p. 227-231.

SILICIFICATION IN THE AMULET "RHYOLITE" FORMATION,
TURCOTTE LAKE SECTION, NORANDA AREA, QUEBEC

Contract OST 78-00081

H.L. Gibson¹ and D.H. Watkinson¹
Regional and Economic Geology Division

Gibson, H.L. and Watkinson, D.H., *Silicification in the Amulet "Rhyolite" formation, Turcotte Lake section, Noranda area, Quebec*; in *Current Research, Geological Survey of Canada, Paper 79-1B*, p. 111-120, 1979.

Abstract

The Amulet "rhyolite" formation, within the central Noranda volcanic complex, northwestern Quebec, is divided into two members. The lower member consists of a rhyolite flow-dome that is underlain by a felsic pyroclastic breccia, and overlain by chloritic flows. The upper member is a succession of variably silicified andesite flows.

Silicification within the upper Amulet "rhyolite" is of two types. The first, a conformable, widespread, mottled alteration, is controlled by the original permeability of the flows. The second type is discordant, occurring as crosscutting zones of white-fragment breccia at or near the top of the Amulet "rhyolite" formation.

Introduction

The Amulet "rhyolite" formation has been mapped and described by Wilson (1941) and De Rosen-Spence (1976). Striking slightly west of north, and dipping gently east (30-40°), the Amulet "rhyolite" is sandwiched between the

Flavrian tonalite complex to the west, and the Lac Dufault granodiorite to the east (Fig. 14.1). The formation is interpreted as the third cycle of felsic volcanism (Spence and De Rosen-Spence, 1975) within the central Noranda volcanic complex (Goodwin and Ridler, 1970) and directly underlies three volcanogenic massive sulphide deposits.

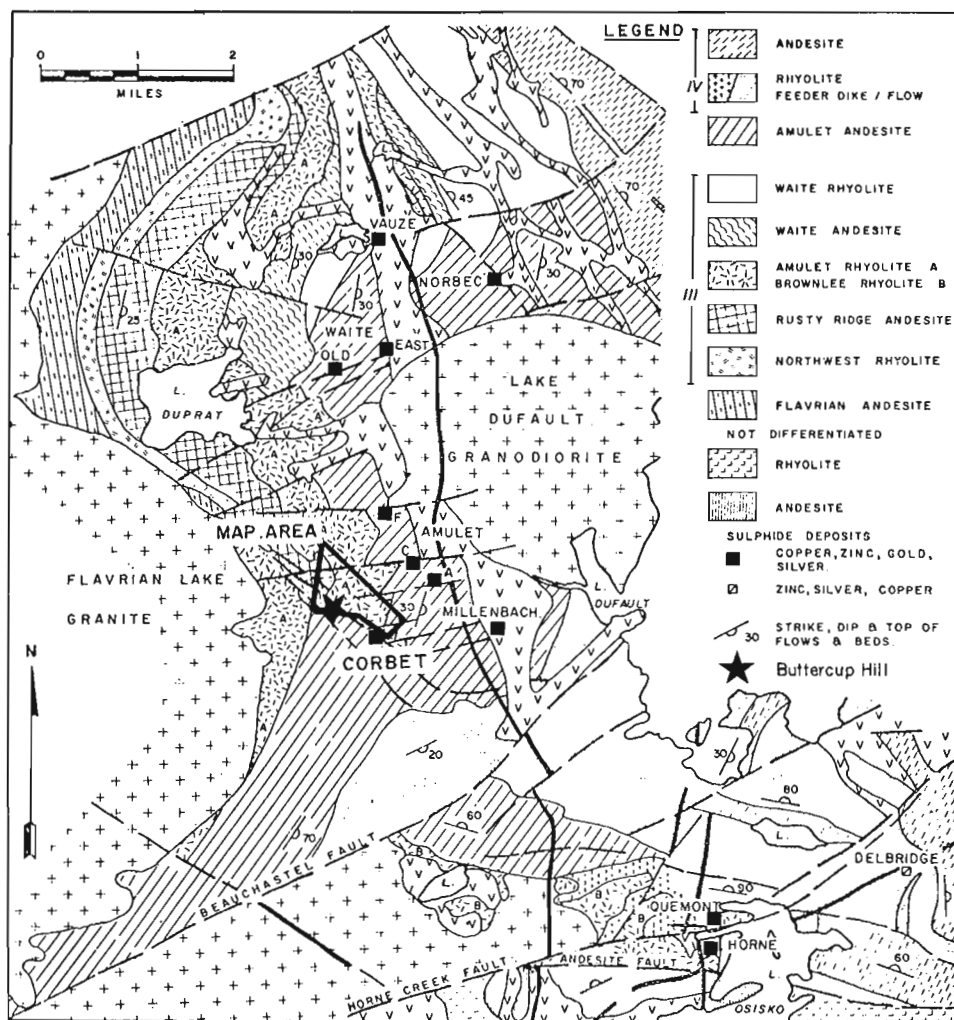


Figure 14.1. Geology of the Noranda area after Spence and De Rosen-Spence, 1975.

¹Department of Geology, Carleton University, Ottawa, Canada.

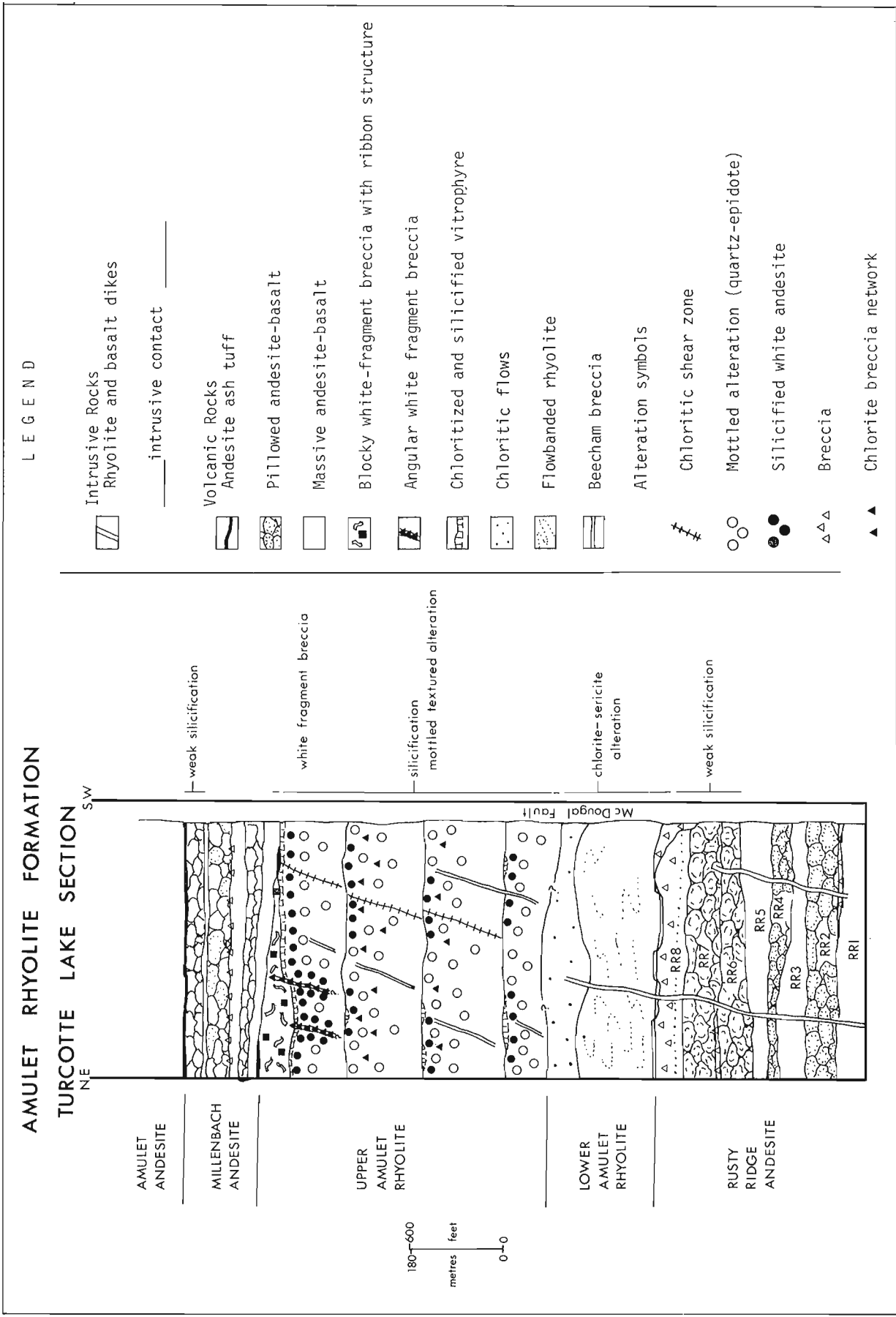


Figure 14.2. Reconstructed stratigraphic section of Amulet "rhyolite" formation.

Table 14.1
Analyses of samples from Buttercup Hill

Sample	BC 13	BC 14	BC 11	BC 12	BC 16	BC 7A	BC 7B	600	1	2
Symbol	○	○	◐	◑	●	▲	▼			
SiO ₂	65.06	63.33	68.32	66.53	68.10	79.00	79.04	73.76	58.30	76.26
Al ₂ O ₃	13.62	16.40	13.61	14.11	14.44	10.28	10.51	10.98	15.32	12.54
Fe ₂ O ₃	10.39	6.23	6.49	7.70	5.33	2.04	1.81	9.21	8.85	3.20
MgO	2.66	1.19	1.79	1.91	2.29	0.17	0.24	2.48	4.51	0.69
CaO	2.04	4.94	3.28	3.30	2.21	3.92	3.03	0.05	6.12	1.49
Na ₂ O	3.36	5.52	4.34	3.13	5.12	3.49	3.90	0.08	4.20	4.07
K ₂ O	0.11	0.21	0.15	0.55	0.18	0.23	0.35	1.44	0.69	1.03
TiO ₂	0.91	0.98	0.82	0.86	0.85	0.63	0.62	0.25	1.26	0.31
P ₂ O ₅	0.27	0.28	0.23	0.23	0.23	0.18	0.18	0.04	—	—
MnO	0.20	0.11	0.15	0.13	0.10	0.04	0.04	0.15	—	—
TOTAL	98.62	99.19	99.18	98.45	98.85	99.98	99.72	98.44	99.25	99.59
Samples BC-13 and 14, massive andesite Samples BC-11 and 12, mottled andesite Sample BC-16, white andesite					Samples BC-7A and 7B, white fragments Sample 600, massive rhyolite from lower Amulet rhyolite Samples 1 and 2, from De Rosen-Spence (1976), average Noranda andesite and rhyolite respectively					

Detailed geologic mapping was conducted through a complete and relatively undisturbed stratigraphic section of Amulet rhyolite, along the McDougal Fault, northwest of the Corbet Mine (Fig. 14.1). In the map area, Rusty Ridge andesite and Amulet andesite conformably underlie and overlie the Amulet rhyolite formation respectively.

The purpose of the study is twofold: to outline, as well as chemically and mineralogically define, zones of silicification, and to develop a model to explain silicification and its relationship to volcanic stratigraphy. The scope of this paper is to summarize briefly the work done to date. A detailed discussion of silicification, its geochemistry, and relationship to mineralization will be provided at a later date.

Acknowledgments

This paper benefits from discussions with J.M. Franklin, M.B. Lambert, and J.W. Lydon of the Geological Survey of Canada, and C.D.A. Comba and D.H. Watkins of Falconbridge Copper Ltd. A.D. Hunter, Carleton University, and S. Perry, University of Western Ontario, working on similar problems west of central Noranda, shared ideas. J.M. Franklin critically reviewed a draft of the paper. The project was financially supported by a contract to D.H. Watkinson from the Geological Survey of Canada. Assistance was also provided by Falconbridge Copper Ltd.

Geology of the Amulet "Rhyolite" Formation

A stratigraphic column of the map area is shown in Figure 14.2, which relates the important geologic features from Figure 14.1. The Amulet "rhyolite" formation may be divided into two members, the upper and lower Amulet "rhyolite". Comba (1977) in mapping the Amulet "rhyolite" similarly divided the formation into two stratigraphic sections.

The lower member consists of a volcanic breccia unit locally referred to as Beecham breccia, overlain by a flow banded, spherulitic rhyolite flow-dome that is mantled by chloritic flows.

Beecham breccia is thick- to thin-bedded, consisting of variably silicified volcanic fragments in a fine grained quartz-rich matrix, interlayered with finely laminated felsic ash tuff. The unit is graded, both normally and reversely, and crossbedded, and has been interpreted as a reworked felsic pyroclastic (C.D.A. Comba, pers. comm., 1978). Beecham breccia is a distinct, mappable unit, defining the base of the Amulet "rhyolite" formation.

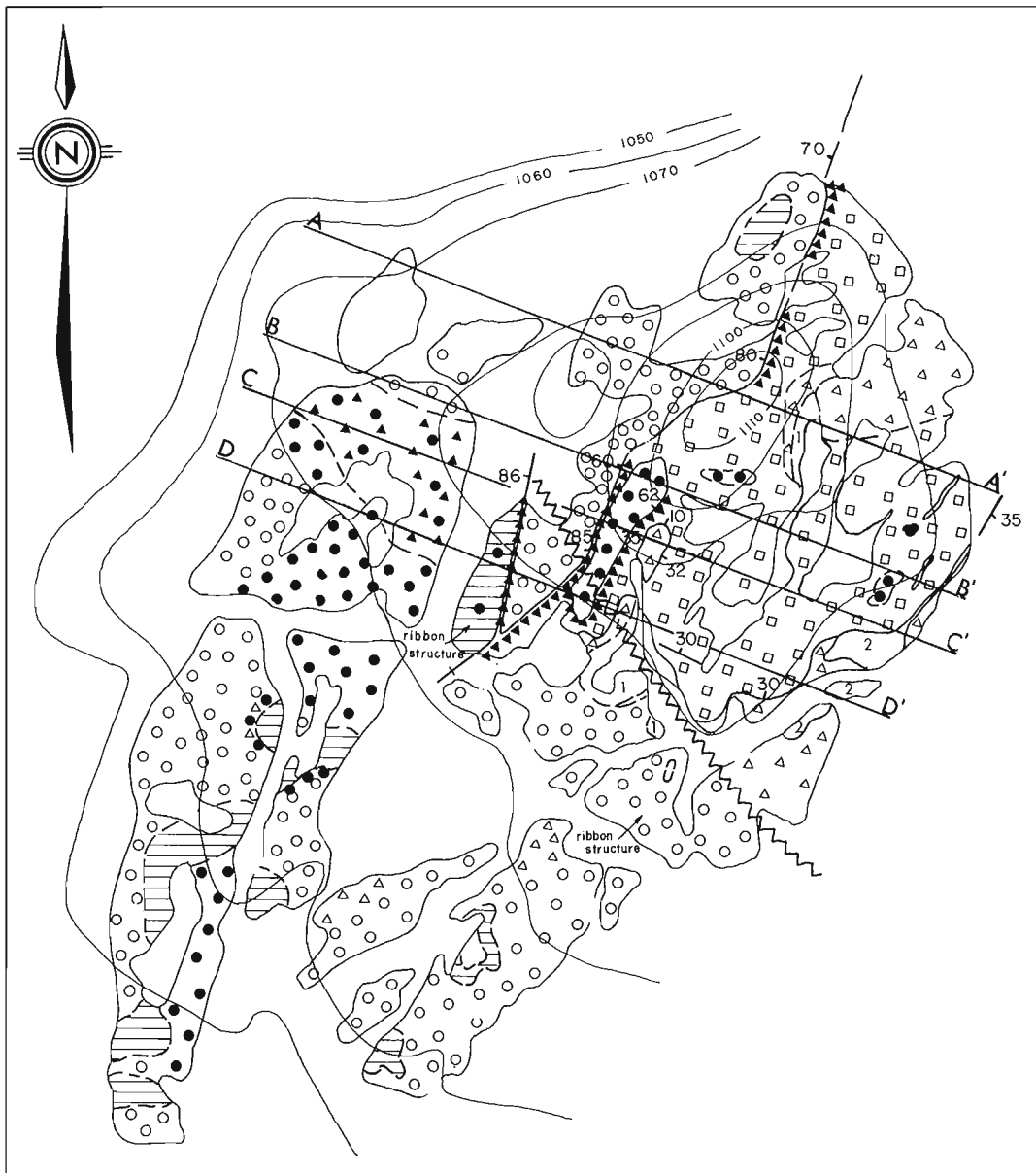
A rhyolite flow-dome conformably overlies the breccia. The rhyolite is typically microspherulitic, quartz-amygdaloidal, and massive to flow-banded. Intraflow breccia dykes crosscut flow-banded rhyolite, with both massive and flow-banded rhyolite locally brecciated and sericitized. The flow is grey-green on weathered surface, a result of sericite and chlorite alteration. A distinctive feature of this rhyolite is its amygdaloidal nature and absence of quartz phenocrysts. Thin (0.2 to 0.5 m) zones of amygdules within the flow parallel contorted flow-banding, and contain up to 25 per cent elliptical quartz amygdules.

In thin section the rhyolite has spherulites which display all stages of recrystallization and replacement by quartz. The rhyolite matrix is a mosaic of quartz and potassic feldspar with minor chlorite and sericite. Quartz pseudomorphs after feldspar phenocrysts are rare.

Chemically the rhyolite resembles De Rosen-Spence's (1976) average Noranda rhyolite (Table 14.1). The anomalously low Na₂O values and high MgO and FeO content are attributable to chlorite-sericite alteration and feldspar breakdown.

Brown weathering, chloritic intermediate flows overlie the rhyolite. The flows are massive, except for chlorite-quartz amygdules that increase in size and number towards altered flow tops.

The upper member of the Amulet "rhyolite" formation consists of variably silicified andesite flows that (chemically) are similar to De Rosen-Spence's (1976) low-silica rhyolite. Where not affected by silicification the flows are brown to green, massive to laminated, and feldspar-porphyrific.



LEGEND		SYMBOLS	
	Pyritic, andesitic ash tuff, minor chert		Strike and dip of bed or geologic contact
	Conformable, blocky breccia with ribbon texture		Shear
	Discordant, angular white-fragment breccia		Breccia
	Chloritized and silicified autobrecciated vitrophyre		Silicified white andesite
	Brown andesite		Mottled alteration
	Massive amygdaloidal, feldspar porphyritic andesite		"Vent" zone, chlorite - quartz alteration
			Contour interval in feet (Wilson, 1941)

Figure 14.3. Geology of Buttercup Hill.

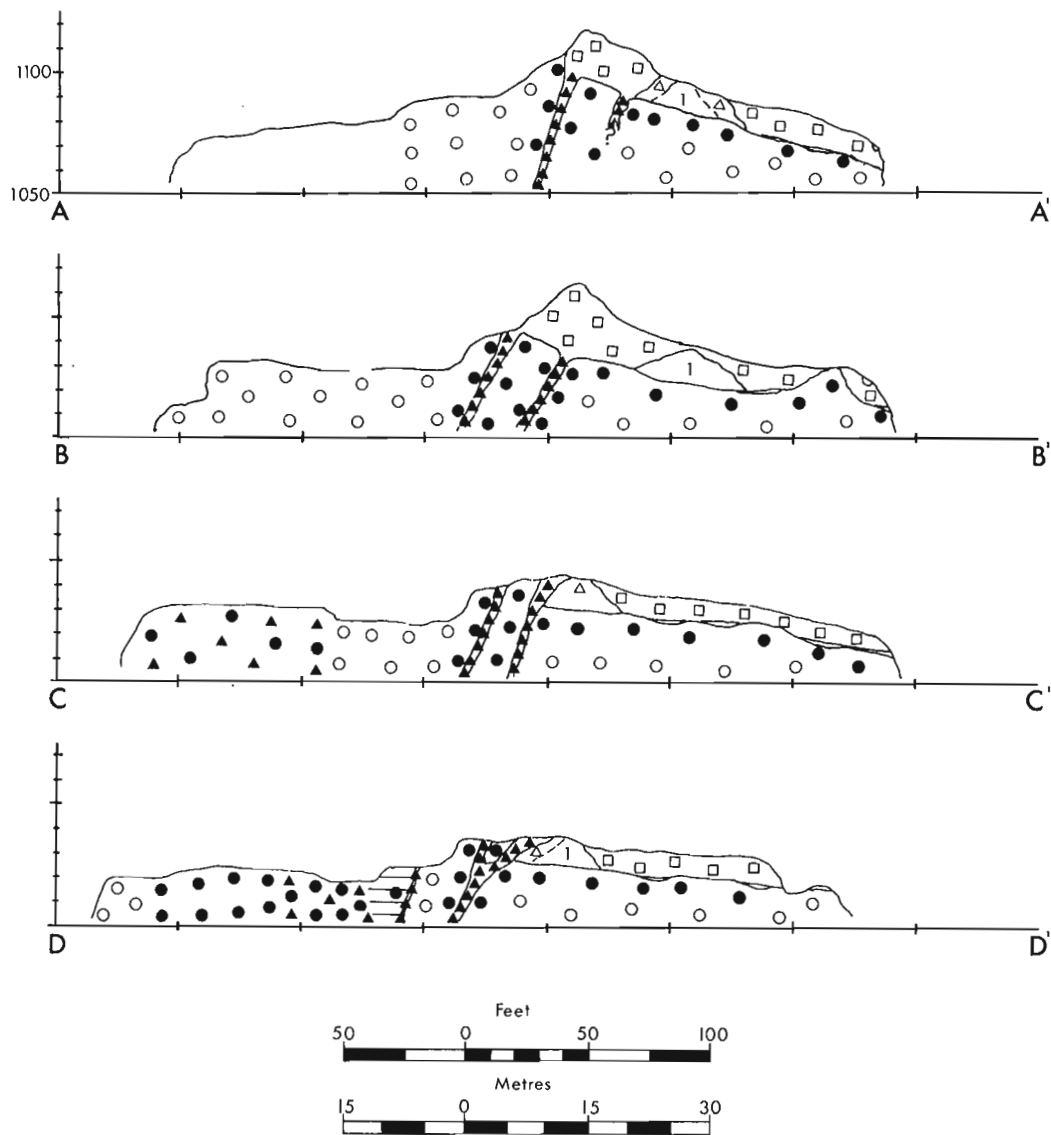


Figure 14.4. Cross-section of Buttercup Hill. For legend see Figure 14.3.

Massive flows rarely contain more than 3 per cent chlorite-actinolite amygdules. Adjacent to flow contacts the andesite is increasingly amygdaloidal, with an average amygdule content of 15 to 20 per cent. At the flow top, andesite weathers lighter brown-green, is finer grained, and is crosscut by fine chlorite fractures.

In thin section andesites are typically microglomeroporphyritic, containing up to 10 per cent albite phenocrysts. The matrix is a felted network of albite microlites (25 to 35 per cent), chlorite, actinolite, quartz, and minor epidote.

The flows are capped by a chloritized and silicified, autobrecciated vitrophyre. The once glassy flow-top is silicified, usually white to dark green, and hosts amoeboid ribbon forms up to 1.5 m long. Spherulitic and perlitic textures show various degrees of replacement by quartz. Feldspar phenocrysts and microlites are rare and are always replaced by polygonal quartz.

The flows of upper Amulet "rhyolite" dip 30 to 40° to the east and are transected by northeast-striking, steeply dipping (70° to 80°) shear-fracture zones of two types. The

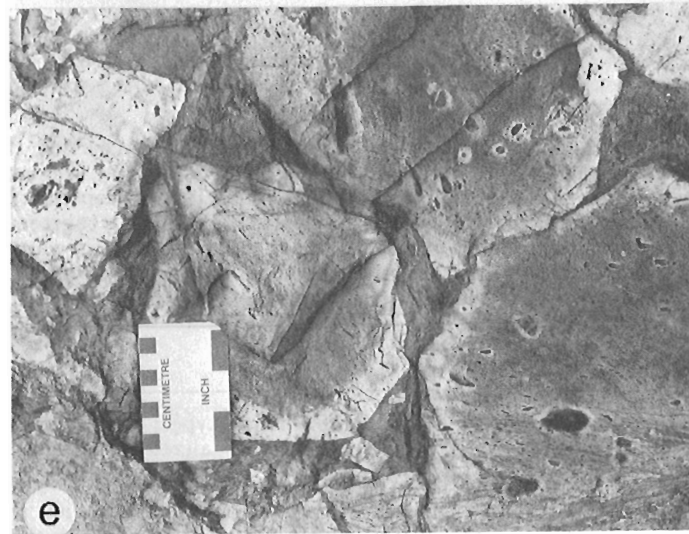
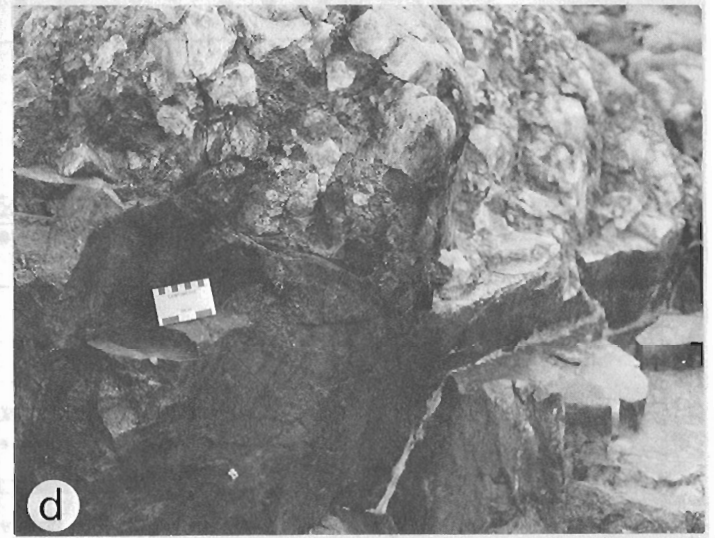
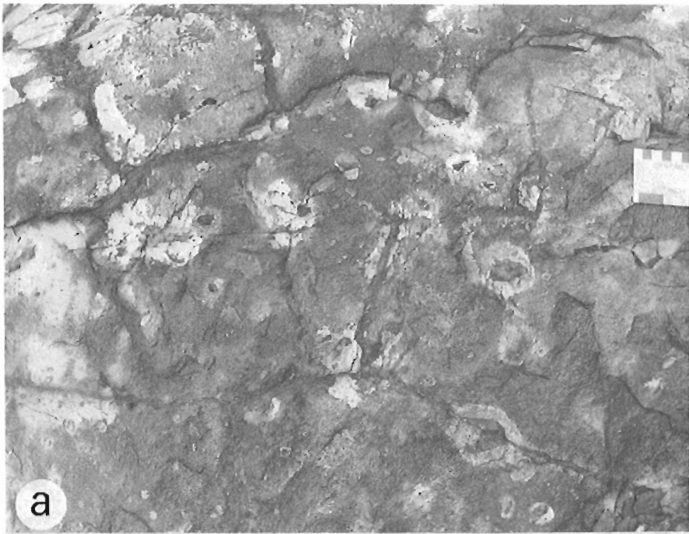
first are dyke-like zones of angular white-fragment breccia, whereas the second are chloritic shear zones with attendant pyrite, quartz, and chalcopyrite.

The top of the Amulet "rhyolite" formation is characterized by a conformable, blocky, white-fragment breccia with ribbon texture. The breccia fills depressions within the underlying mottled andesite (Fig. 14.2). Fragments within the breccia resemble those of crosscutting white-fragment breccia dykes; the ribbon forms are interpreted to be an in situ alteration texture. The matrix is massive or brecciated andesite.

Silicification

Silicification is of two main types; conformable widespread, patchy alteration and localized crosscutting alteration.

Conformable silicification manifests itself in the development of a mottled textured alteration, controlled primarily by vesicles and fractures within the andesites (Fig. 14.2). In upper Amulet rhyolite, the proportion of



mottled alteration increases sympathetically with percentage of amygdules and degree of chlorite-filled fractures. Consequently, the upper portions of flows are characterized by mottling which consists of irregular white patches and white envelopes around amygdules and chlorite fractures. The vitrophyric flow-top breccias are silicified and represent conformable zones of intense silicification.

Glomeroporphyritic albite microphenocrysts and albite microlites are preserved in the altered andesite except within 1-2 cm of, and within, mottled patches and envelopes. Mottled alteration is a fine intergrowth of quartz and epidote, with variable actinolite and carbonate. Similar alteration patches have been described from the Watson Lake volcanics, Matagami District, northwestern Quebec by Harrigan and MacLean (1976).

Angular white-fragment breccia dykes are linear zones of crosscutting silicification located at or near the top of the upper Amulet rhyolite. These linear zones of silicification strike approximately 070°. The breccia consists of variably silicified, white, quartz-amygdaloidal, feldspar-porphyrific andesite fragments in a finer grained fragmental matrix cut by chlorite veins. In many cases fragments appear to be derived from adjacent wall rock. The breccia zones are surrounded by an envelope of intensely silicified white andesite up to 13 m wide. Preserved glomeroporphyritic albite microphenocrysts and albite microlites in the fragments and adjacent white andesite attest to the original andesitic nature of the rocks.

Flow-banded to massive, spherulitic rhyolite and basalt dykes crosscut the Amulet "rhyolite" formation. The dykes are high-level synvolcanic intrusions that are not affected by silicification. Medium- to coarse-grained diorite dykes cut all rock types in the map area.

Buttercup Hill

Buttercup Hill is located in the northwest corner of the map area (Fig. 14.1). This outcrop is thought to be upper Amulet "rhyolite" displaced along the McDougal fault. Buttercup Hill is a unique exposure and is representative of all rock types and alteration within the upper Amulet "rhyolite" member.

A geologic map and accompanying cross-sections of Buttercup Hill are shown in Figures 14.3 and 14.4. Andesite flows form the base of the Buttercup Hill section. They display flow lamination, are feldspar porphyritic, and have ellipsoidal amygdules that parallel flow direction. The andesite flows are commonly mottled (Fig. 14.5a) and capped by patches of altered vitrophyre (Fig. 14.3).

Figure 14.5 (opposite)

- a. Columnar jointed, mottled andesite. White envelopes developed around amygdules.
- b. Discordant white-fragment breccia dyke.
- c. Fragments within breccia dyke. White, flow-banded andesite fragments in a chlorite matrix.
- d. Gently dipping (30°) contact of blocky, white-fragment breccia and underlying andesite.
- e. Blocky white-fragment breccia. Andesite fragments have silicified borders, and halos around amygdules.
- f. Pyritic ash tuff intercalated with blocky white-fragment breccia.

Andesite flows consist of albite phenocrysts in a felted matrix of albite microlites, chlorite, actinolite, quartz, and minor epidote. Angular vesicles are filled by chlorite, quartz, and actinolite.

Three parallel zones of discordant angular, white-fragment breccia cut the andesite flows (Fig. 14.3, 14.5b). Discordant white-fragment breccia grades vertically into a conformable blanket of blocky white-fragment breccia (Fig. 14.4). Adjacent to discordant white-fragment breccia dykes, mottled andesite is white and intensely silicified. Fragments within the dykes appear to have been plucked from the surrounding white andesite host (Fig. 14.5c).

A second zone of intense chlorite-quartz alteration transects the outcrop (Fig. 14.3) parallel to a local shear direction and the larger scale McDougal fault. Spring (1976) referred to this alteration as a "vent zone".

Ribbon textured, blocky-breccia conformably overlies the andesite flows (Fig. 14.5d). The breccia is characterized by white fragments in a mottled andesitic matrix (Fig. 14.5e). Fragments are angular blocks with bleached borders and are weakly feldspar-porphyrific and quartz-amygdaloidal. In thin section the fragments are characterized by albite phenocrysts in a fine grained felted matrix of albite microlites and quartz, similar texturally to the underlying andesite.

A pyritic andesitic ash tuff rests conformably upon and within the blocky white fragment breccia (Fig. 14.5f). The tuff is well bedded and laminated, typical of the Noranda-camp exhalative sediments.

Buttercup Hill is interpreted as an extremely altered silicified andesite. The alteration was produced by submarine hot spring activity at and near the seafloor.

Chemistry of the Silicified Andesites

Representative chemical analyses of massive andesite, mottled andesite, and white-fragment breccia from Buttercup Hill are presented in Table 14.1. A comparison of the weight per cent oxides shows that SiO₂ increased and FeO, MgO, MnO and TiO₂ decreased with silicification. Constant volume calculations, using molecular proportions, confirm the above chemical change (Babcock, 1973; Gresens, 1967).

Silicified andesite samples BC-16, 7A, and 7B resemble rhyolite in chemistry, but not in texture. In the field, silicified andesite is extremely difficult to distinguish from rhyolite, especially where the two rock types are associated. Table 14.1 shows that the TiO₂ contents of true rhyolites are low (0.2 to 0.3 weight per cent) and are significantly less than that of silicified andesite (0.82 to 0.62 weight per cent). The range in TiO₂ values for altered andesite and rhyolite stated above may apply only to the Noranda area.

Chemical analyses of massive and silicified andesite from Buttercup Hill are plotted on three variation diagrams (Fig. 14.6, 14.7, 14.8). Trends shown on the diagrams are representative of the entire upper Amulet "rhyolite". Depletion of FeO and especially MgO, in white fragments from Buttercup Hill, results in the analyses lying outside the boundaries of Figures 14.7 and 14.8.

Data for Buttercup Hill are shown in Figure 14.6, an alkali ratio diagram developed by Hughes (1973) to distinguish the spectrum of igneous rocks from spilites and keratophyres. The dashed lines in Figure 14.6 enclose the field in which igneous rocks lie. All but one of the Buttercup Hill samples lie in the spilite field.

Miyashiro (1974) proposed that SiO₂ - FeO/MgO and FeO-FeO/MgO diagrams would distinguish rocks of calc-alkaline and tholeiitic affinity. Data from Buttercup Hill are shown in Figures 14.7 and 14.8. Massive andesite lies in

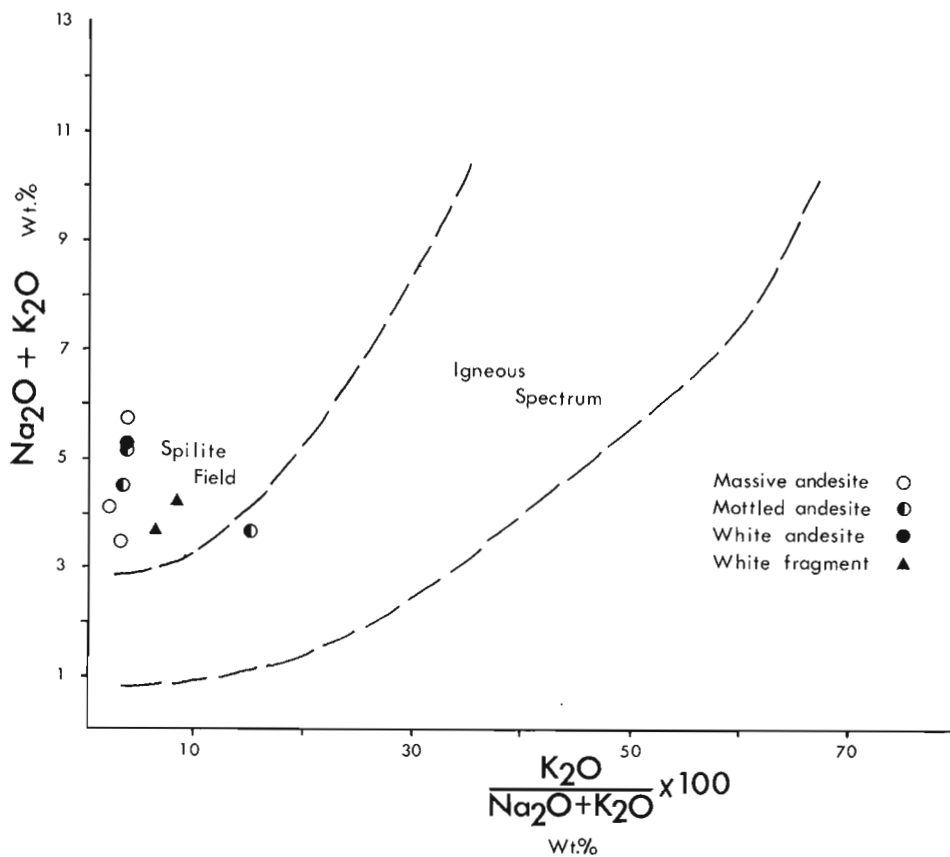


Figure 14.6

Spilitic character of andesite from Buttercup Hill. Symbols and sample numbers are presented in Table 14.1.

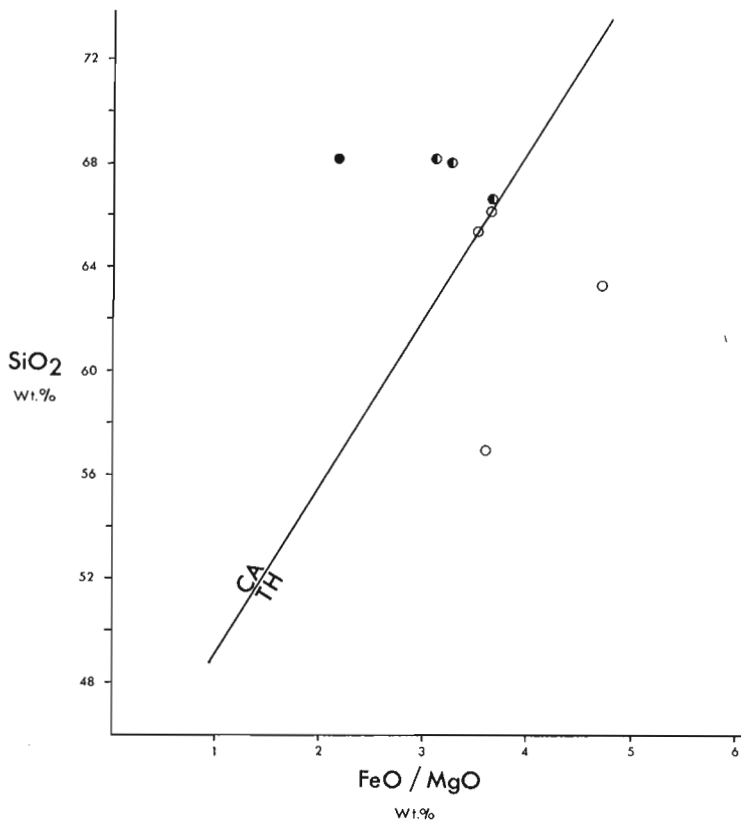


Figure 14.7. *SiO₂ - FeO/MgO diagram. Tholeiitic and calc-alkaline character of andesite and silicified andesite respectively. Total iron as FeO. See Table 14.1 for sample numbers.*

Miyashiro's tholeiitic field, whereas mottled andesite lies in the calc-alkaline field of both diagrams. Data from Buttercup Hill and upper Amulet rhyolite plotted on an AFM diagram (Irvine and Baragar, 1971), and a cation plot, developed by Jensen (1976), also show tholeiitic to calc-alkaline trends.

A tholeiitic to calc-alkaline trend with progressive silicification was recognized in volcanic rocks at Matagami, Quebec by MacGeehan (1978), and in volcanic rocks from the Aldermac area, west of Noranda by A.D. Hunter (pers. comm., 1979). It is important to note that silica metasomatism produces an apparent tholeiitic to calc-alkaline trend indistinguishable from a magmatic trend on existing chemical variation diagrams.

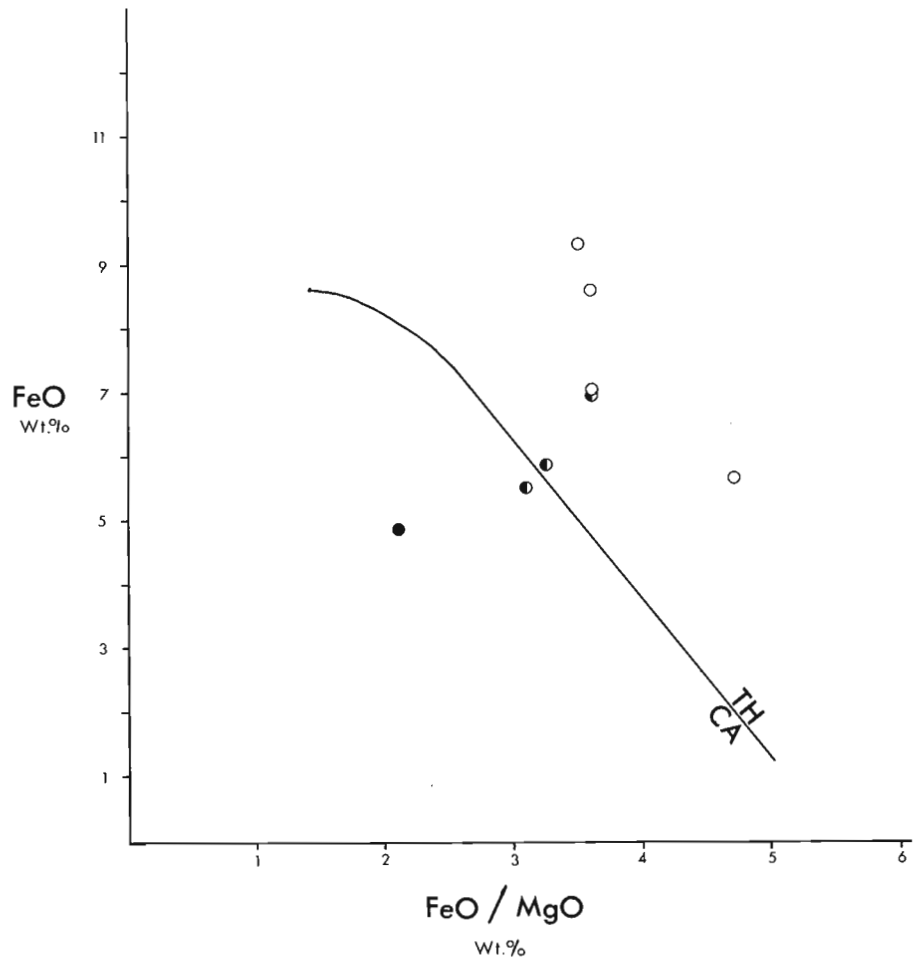
Summary and Conclusions

The Amulet "rhyolite" formation may be divided into two sections. The lower Amulet "rhyolite" consists of a rhyolite flow-dome underlain by a pyroclastic marker horizon, the Beecham breccia. The upper portion is a succession of variably silicified andesite flows.

Silicification is of two types. The first, a conformable, pervasive, mottled alteration, is characterized by the development of epidote-quartz patches and envelopes mantling amygdules, fractures, and flow laminations in andesite. Mottled silicification is controlled by the original permeability of the unit and is interpreted to be the result of hot water-rock interaction during submarine volcanic activity. Its widespread nature and its preferential development along permeable horizons within flows indicate primary stratigraphic control of a large volume of fluid in a probable aquifer. Considering the volume of fluid required for alteration, and the submarine volcanic setting, circulating sea water is favoured as a source for such a fluid.

Figure 14.8

FeO - FeO/MgO diagram. Tholeiitic to calc-alkaline trend with silicification. Total iron as FeO. See Table 14.1 for sample numbers.



The second type of silicification occurs as crosscutting zones of white-fragment breccia at or near the top of the Amulet "rhyolite" formation. White-fragment breccias are fault or fracture controlled zones of white, silicified quartz amygdaloidal andesite fragments in a fine grained chloritic matrix. The discordant breccias are interpreted as discharge zones: conduits that fed submarine hot springs at the seafloor. Deposition of silica within channelways by cooling, ascending silica-saturated solutions would eventually seal the discharge zone (Facca, 1967), and hydrothermal activity would cease.

With self-sealing, fluid pressure of the hydrothermal solution would increase. Where the fluid pressure exceeded load pressure by an amount equal to the tensile strength of the silicified cap rock, a hydrothermal or steam-blast explosion would result (Muffler et al., 1971). The explosion would clear the conduit, fracture the cap rock, re-establish permeability, and scatter silicified blocks peripheral to the hot spring vent. The brecciated cap rock and ejected fragments might be incorporated into later flows or mud flows forming conformable blocky and ribbon textured breccias as proposed at Buttercup Hill (Fig. 14.3, 14.4) and the top of the Amulet "rhyolite" (Fig. 14.2). The size of hydrothermal explosion craters is variable. Muffler et al. (1971) described hydrothermal explosion craters at Yellowstone National Park, with diameters from tens of metres to about 1500 m.

The net chemical exchange that occurred with silicification, assuming constant volume metasomatism, was an increase in SiO₂ and a decrease in MgO, FeO, TiO₂ and MnO.

Silicified andesite chemically resembles rhyolite, and has a calc-alkaline affinity. The relatively unsilicified massive andesite on the other hand is tholeiitic.

Silicified rocks are interpreted to have been products of a geothermal system, generated during circulation and discharge of hot silica-saturated solutions in a submarine volcanic pile.

References

- Babcock, R.S.
1973: Computational models of metasomatic processes; *Lithos*, v. 6, p. 279-290.
- Comba, C.D.A.
1977: Summary report on the Waite Dufault Mines Ltd. option, Duprat Township, Noranda, Quebec; Falconbridge Copper Ltd., unpubl. internal report, 44 p.
- De Rosen-Spence, A.F.
1976: Stratigraphy, development and petrogenesis of the central Noranda volcanic pile, Noranda, Quebec; unpubl. Ph.D. thesis, University of Toronto, Toronto, 166 p.
- Facca, G.
1967: Self sealing geothermal field; *Bulletin Volcanologique*, v. 30, p. 1-3.

- Goodwin, A.M. and Ridler, R.
1970: The Abitibi orogenic belt; in *Symposiums on Basin and Geosynclines of the Canadian Shield*, A.J. Baer (ed.); Geological Survey of Canada, Paper 70-40, p. 1-24.
- Gresens, R.L.
1967: Composition-volume relationships of metasomatism; *Chemical Geology*, v. 2, p. 47-65.
- Harrigan, D.B. and MacLean, W.H.
1976: Petrography and geochemistry of epidote alteration patches in gabbro dykes at Matagami, Quebec; *Canadian Journal of Earth Sciences*, v. 13, p. 500-511.
- Hughes, C.J.
1973: Spilites, Keratophyres, and the igneous spectrum; *Geological Magazine*, v. 6, p. 513-527.
- Irvine, T.N. and Baragar, W.R.A.
1971: A guide to the chemical classification of the common volcanic rocks; *Canadian Journal of Earth Sciences*, v. 8, p. 523-548.
- Jensen, L.S.
1976: A new cation plot for classifying subalkalic volcanic rocks; Ontario Geological Survey, Misc. Paper 66, 22 p.
- MacGeehan, P.J.
1978: The geochemistry of altered volcanic rocks at Matagami, Quebec: a geothermal model for massive sulphide genesis; *Canadian Journal of Earth Sciences*, v. 15, p. 551-570.
- Miyashiro, A.
1974: Volcanic rock series in island arcs and active continental margins; *American Journal of Science*, v. 274, p. 321-355.
- Muffler, L.J.P., White, D.E., and Truesdell, A.H.
1971: Hydrothermal explosion craters in Yellowstone National Park; *Geological Society of America Bulletin*, v. 82, p. 723-740.
- Spence, C.D. and De Rosen-Spence, A.F.
1975: The place of sulphide mineralization in the volcanic sequence at Noranda, Quebec; *Economic Geology*, v. 70, p. 90-101.
- Spring, R.M.
1976: Study of alteration textures on Buttercup Hill, Noranda area, Quebec; unpubl. B.Sc. thesis, Queen's University, Kingston, 67 p.
- Wilson, M.E.
1941: Noranda district, Quebec; Geological Survey of Canada, Memoir 229, 162 p.

**CAMBRIAN STRATIGRAPHIC SECTION BETWEEN SOUTH NAHANNI AND
BROKEN SKULL RIVERS, SOUTHERN MACKENZIE MOUNTAINS**

Project 650024

W.H. Fritz
Regional and Economic Geology Division

Fritz, W.H., *Cambrian stratigraphic section between South Nahanni and Broken Skull rivers, southern Mackenzie Mountains; in Current Research, Geological Survey of Canada, Paper 79-1B, p. 121-125, 1979.*

Abstract

Unnamed siltstone and fine grained quartzite (map unit 3, 231⁺ m) underlie the Lower Cambrian Sekwi Formation (674 m) at the site of the section. In the lower part of the Sekwi, siltstone and thin bedded carbonate exhibit penecontemporaneous folds and breccias, suggesting deposition on an unstable slope. In the upper part of the formation orange and purple weathering siltstone and dolomite record an abrupt change to very shallow water and supratidal conditions. The overlying Rockslide Formation (452.5 m) contains mostly thin bedded limestone with penecontemporaneous breccia indicating a return to unstable slope conditions during most of the Middle Cambrian. At the top of the Rockslide, light coloured, medium and thick bedded limestone and dolomite register shallow water conditions near the end of Middle Cambrian time. An unconformity at the top of the Rockslide interrupts the stratigraphic record. No fossils were found in the overlying basal sandstone and succeeding light coloured dolomite belonging to the Broken Skull and Sunblood formations (undivided).

Introduction

In 1978 the writer assisted S.P. Gordey with his geological mapping (Project 730069) in the Nahanni map area by measuring a stratigraphic section located (Fig. 15.1) northeast of the South Nahanni River in the southern Mackenzie Mountains. Except for a slight difference in the route, the section presented here was measured along a course followed by Green et al. (1968), who plotted the section on their map, and gave a generalized description of the strata in their map legend and marginal notes. Gordey (1979, Fig. 2.1, "c") drew a generalized stratigraphic column based on his observation of the section in 1978, and published the column as part of a regional stratigraphic cross-section. In view of the recent economic activity in this area, and growing appreciation of the complex structural and stratigraphic problems related to the ore deposits, it was decided that more stratigraphic details should be published. To help make this possible, Gordey and his assistant, K.B. Heather, provided the necessary field support to maintain the writer on the section and assisted with the measuring of the lower part.

The presentation of the present section follows the procedure used by Fritz (1979b) for the description of sections in the northern Rocky Mountains.

Pre-Sekwi (Lower Cambrian?) strata, upper map unit 3, 231 m

The oldest stratigraphic unit (unit 1) in the section starts above valley alluvium (Pl. 15.1, fig. 5) and consists of siltstone (base to 120 m) and silty sandstone (120 m to 181.5 m) that weather medium greenish grey and rust, and are medium greenish grey on fresh surfaces. Rare thin to thick interbeds of quartzite are present, and are either the colour of the adjacent strata or are light brown on weathered and fresh surfaces. Both the quartzite and the sand in the silty sandstone are very fine grained. The second unit (unit 2) contains very fine grained quartzite in thick, light orange-brown to rust weathering beds (base to 37.5 m) and in thick to thin, greenish yellow to rust weathering beds (37.5 to 49.5 m). Fresh quartzite surfaces on the former beds are light brown, whereas those on the latter are greenish grey. The transition between unit 2 and unit 3 of the overlying Sekwi Formation takes place in an interval that is 1 or 2 m thick. Thus the boundary between the two map units, map unit 3 and the

Sekwi Formation, was placed at the horizon where limy siltstone (above) predominates over very fine grained quartzite (below).

Sekwi Formation (Lower Cambrian) 674 m

The basal unit in the Sekwi Formation (unit 3, 39.5 m) contains medium brown to light orange weathering siltstone (1/2) that is limy and is light brown to medium grey on fresh surface, and orange to medium grey weathering limestone (1/2) in thin wavy beds and nodules. Fresh limestone surfaces are medium dark grey and finely crystalline. Fossils located (GSC loc. 95668) 6.5 m above the base of the unit are questionably assigned to the Lower Cambrian **Fallotaspis** Zone. The next unit (unit 4, 28 m) consists of limestone in thin (average 3.75 cm), broadly wavy beds that weather medium grey and have light yellow to pink parting surfaces. Fresh surfaces are medium dark grey and finely crystalline. Sparse layers containing "floating", medium grained quartz sand are present. Unit 5 (64.5 m) resembles unit 3 in that it contains similar limestone and siltstone in approximately the same ratio. However, penecontemporaneous folds (Pl. 15.1, fig. 2) and breccia are abundant at various horizons in unit 5. Rare, "exotic" blocks are also present in this unit, such as a large (2 m wide) limestone boulder that is medium grey on fresh and weathered surfaces and contains coarse "floating" clasts of quartz sand. **Holmiella** sp. and **Nevadella faceta** located (GSC loc. 95669) 38 m above the base of unit 5 belong to the **Nevadella** Zone.

Light grey to cream weathering dolomite in thin (0.6 to 1.2 cm) beds and lenses predominate in unit 6. In the lower 114 m the bedding is distinct, and locally small penecontemporaneous folds and pods of breccia are present. In the upper 64.5 m large scale slumping has fused the thin beds to give the dolomite a thick bedded to massive appearance (Pl. 15.1, fig. 4). Most of the dolomite is medium grey on fresh surface and finely crystalline, but the uppermost 10.5 m is light grey on fresh surface, finely to coarsely crystalline, and contains fine to coarse "floating" quartz grains. A concentration of quartz sand near the middle of the Sekwi Formation provides a reliable criterion for the recognition of unit 7. The lower part (base to 31.5 m) contains light orange weathering, thin to thick sandstone beds that are intercalated with beds of medium brown weathering siltstone. The sandstone is medium grey on fresh surface and is mainly very

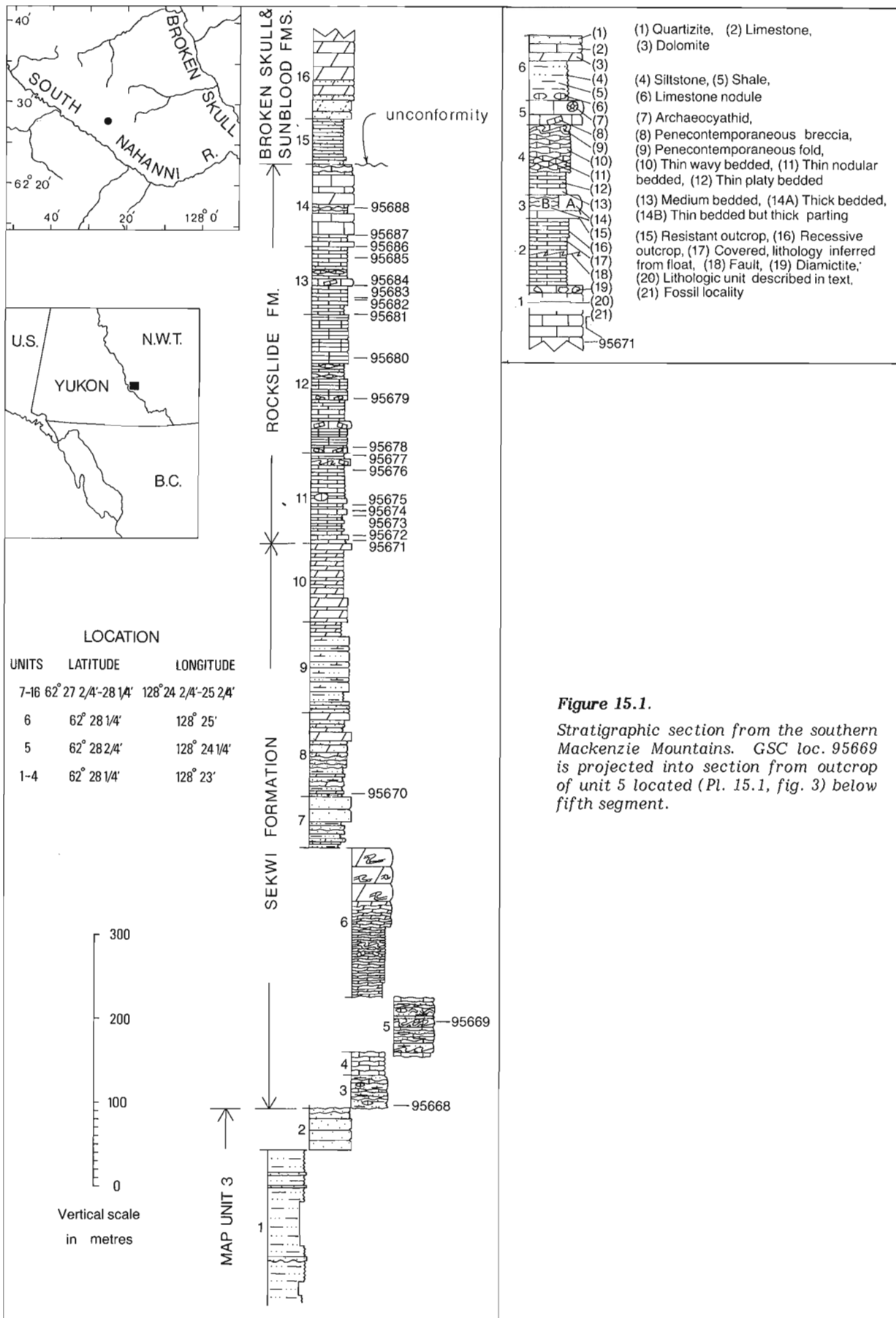


Figure 15.1.

Stratigraphic section from the southern Mackenzie Mountains. GSC loc. 95669 is projected into section from outcrop of unit 5 located (Pl. 15.1, fig. 3) below fifth segment.

fine grained. The upper part of the unit (31.5 to 61.5 m) is composed of quartzite in thick, resistant beds that are light grey on weathered and fresh surfaces, and contains the trace fossil *Skolithos*. Unit 8 (100 m) contains a mixture of thin to thick bedded quartzite and orange weathering dolomite, and, in the lower part, brownish grey weathering siltstone. Burrows and mud cracks are present, and fossils belonging to the *Bonnia-Olenellus* Zone were located (GSC loc. 95670) 3 m above the base of the unit.

Purple grey is the dominant weathering colour of strata in unit 9 (108 m). Brownish grey and purple-grey siltstone (base to 13 m) and brownish grey weathering siltstone (13 to 25 m) with mud cracks are in the lower part of the unit. Dolomitic(?) siltstone in thick to thin, blocky beds occupy most (25 to 90.5 m) of the unit. This siltstone is medium dark purple grey on fresh and weathered surfaces. Recessive weathering, thin bedded dolomite at the top of unit 9 (90.5 to 108 m) weathers to bands of orange, medium dark grey, and purple. The uppermost unit (unit 10, 94 m) in the Sekwi Formation is composed of bright orange weathering dolomite in thin to thick beds that provide a sharp contrast to the overlying grey weathering strata of the Rockslide Formation.

Rockslide Formation, 452.5 m

The basal unit (unit 11, 108.5 m) of this formation is composed of medium and medium dark grey weathering limestone that is dark grey and finely crystalline on fresh surfaces. The lower half weathers to chips with some thin and medium beds of platy, planar laminated limestone, whereas in the upper half of the unit the platy limestone predominates. A limestone pod (3 m diameter, Pl. 15.1, fig. 6) is present 67 m above the base of the unit, and a scoured surface at least 2 m deep is located 76.5 m above the base. Fossils from this unit belong to the Middle Cambrian *Albertella* and/or *Glossopleura* Zone (GSC loc. 95671-95673), *Bathyriscus-Elrathina* Zone (GSC loc. 95674, 95675), and *Bolaspidella* Zone (GSC loc. 95676, 95677). Unit 12 (166 m) is composed of limestone weathering to plates with a medium brownish grey surface. Although the plates are thin and planar laminated, the parting is thick to thin, and fresh surfaces are dark grey and finely crystalline. Several thick beds containing penecontemporaneous breccia are present in the lower half of the unit and bright orange weathering limestone interbeds are located in the top 7.5 m of the unit. Limestone in thin plates that weather medium brown to orange on parting surfaces predominate in unit 13 (81 m). Fresh surfaces are dark grey and finely crystalline. Two beds containing penecontemporaneous breccia were noted, and 2.5 m of very fine grained sandstone is present. The uppermost unit (unit 14, 97 m) of the Rockslide Formation is mainly composed of medium light to medium grey limestone in medium and thick beds. Fresh surfaces are medium grey and fine to coarse grained. Cream weathering dolomite containing abundant fine quartz sand is present 50.5 to 64.5 m above the base. Fossil localities in this unit (GSC loc. 95686-95688) and in the two units below (units 12, 13; GSC loc. 95678-95685) belong to the late Middle Cambrian *Bolaspidella* Zone.

Broken Skull and Sunblood Formation (undivided), 101.5⁺ m

Overlying the Rockslide Formation at the Nahanni River Section are strata which Gordey (1979, Fig. 2.1) has placed in the Broken Skull and Sunblood formations (undivided). He showed a regional unconformity separating the Rockslide Formation from the overlying formations. The first unit (unit 15, 55.5 m) above the unconformity is composed of medium light brownish grey and light grey weathering sandstone in thin, platy beds. On a fresh surface the sandstone is light brown and light grey, and very fine

grained. Some bright orange weathering interbeds of sandy dolomite are also present. Only the lower part of the next unit (unit 16, 46⁺ m) was inspected. The basal beds (base to 22.5 m) contains cream to light orange weathering dolomite in medium and thick beds. Fresh surfaces are light brownish grey, and abundant very fine quartz grains (some up to coarse in size) are visible. Higher beds (22.5 to 46 m) contain cream weathering dolomite that is light grey on a fresh surface and finely crystalline. Dolomite above the 46 m level is light and medium light grey weathering and fresh, thick bedded, and finely crystalline.

Correlations

Units 1 and 2 of the present section represent the upper part of map unit 3 of Green et al. (1968). These strata were later correlated by Gordey (1979, Fig. 2.1) with the Backbone Ranges Formation that has its type section (Gabrielse et al., 1973, p. 33) in the adjacent map area to the east. Gordey's correlation is consistent with the Backbone Ranges-Sekwi Formation relationship to the east as illustrated by Gabrielse et al. (1973, Fig. 7). They showed the Backbone Ranges in that area as both underlying the Sekwi and laterally interfingering with it. However, to the north of the present area the writer (Fritz, 1979a) has shown that the Sekwi Formation possibly lies unconformably above the Backbone Ranges Formation (there called map unit 12). Sections basinwards and near these northern sections have a dark siltstone map unit (map unit 13) between the Sekwi and the Backbone Ranges Formation. Until the seemingly contradictory relationships to the east and north of the present area are resolved, the writer prefers to retain the designation by Green et al. (1968) of map unit 3 for stratigraphic units 1 and 2 in the present section.

The next eight stratigraphic units in the present section (units 3-10) represent Green et al. (1968) map units 4 and 5, and have rightly been recognized by Gordey (1979, Fig. 2.1) as belonging to the Sekwi Formation. Correlation with the grand cycles recognized (Fritz, 1979a) within the Sekwi Formation to the north can also be made. Units 3 through 6 can be correlated with the uppermost part of grand half-cycle A1 and all of grand half-cycle A2. Unit 4 may correlate with a thin tongue of outer detrital strata within the *Nevadella* Zone (within A2) that penetrates eastwards into middle carbonate strata in numerous sections (Fritz, 1979a, Fig. 5) to the north. It is believed that during deposition of grand half-cycle A2 strata in the present section were located on an unstable slope, as is suggested by the lithology and by abundant penecontemporaneous folds and breccias. At nearby localities Gordey (1978, p. 43; 1979, p. 13) has noted conglomerates and debris flows in the Lower Cambrian strata that may also have been deposited on this slope.

Units 7 through 10 are correlated with grand cycle B, which occupies the upper part of the Sekwi Formation to the north. In the present section, the lower (clastic) grand half-cycle (B1) is represented by unit 7 and the lower part of unit 8. These strata are believed to have been deposited during a regional regression and in the present section the concentration of quartz sand, the presence of mud cracks, and the abundance of *Skolithos* suggest a shallow depositional environment. A very shallow water to supratidal, lower energy environment is envisioned for the upper half of the grand cycle (B2), which is represented by the upper half of unit 8 through unit 10. This environment is suggested by the abundance of brightly coloured, planar laminated dolomite and dolomitic(?) siltstone, and by the lack of fossils. The lack of fossils below the top of the formation leaves the possibility of an unconformity (Gordey, 1979, Fig. 2.1) between the Sekwi Formation and the base of the overlying Rockslide Formation open to speculation. The questionable presence of

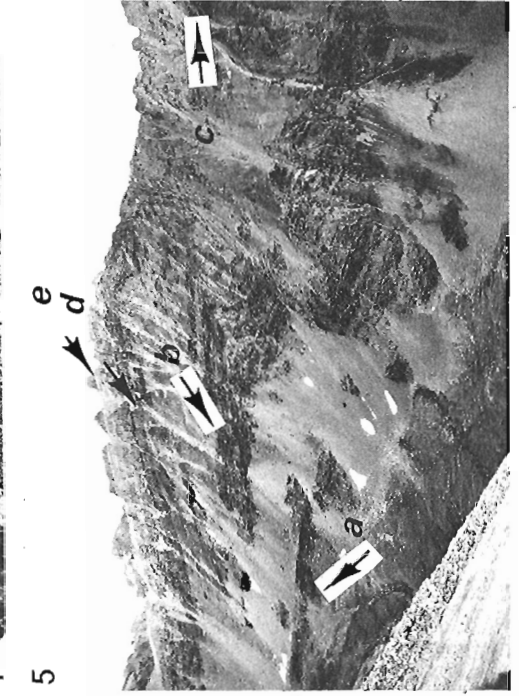
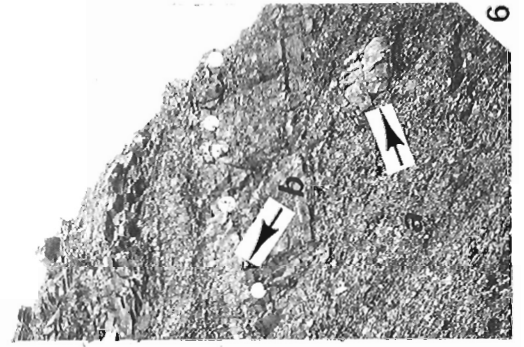
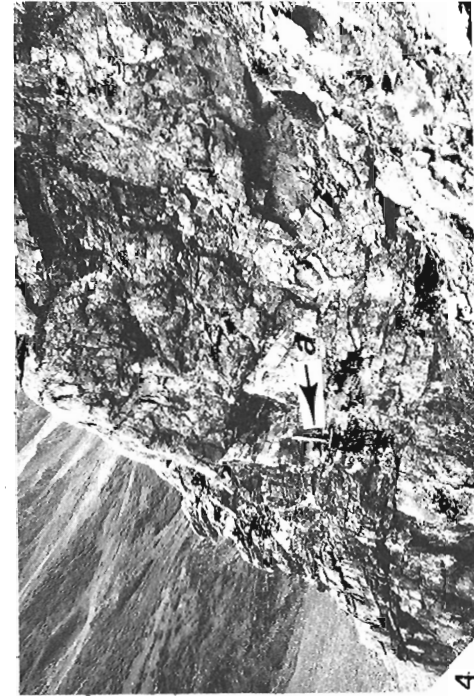
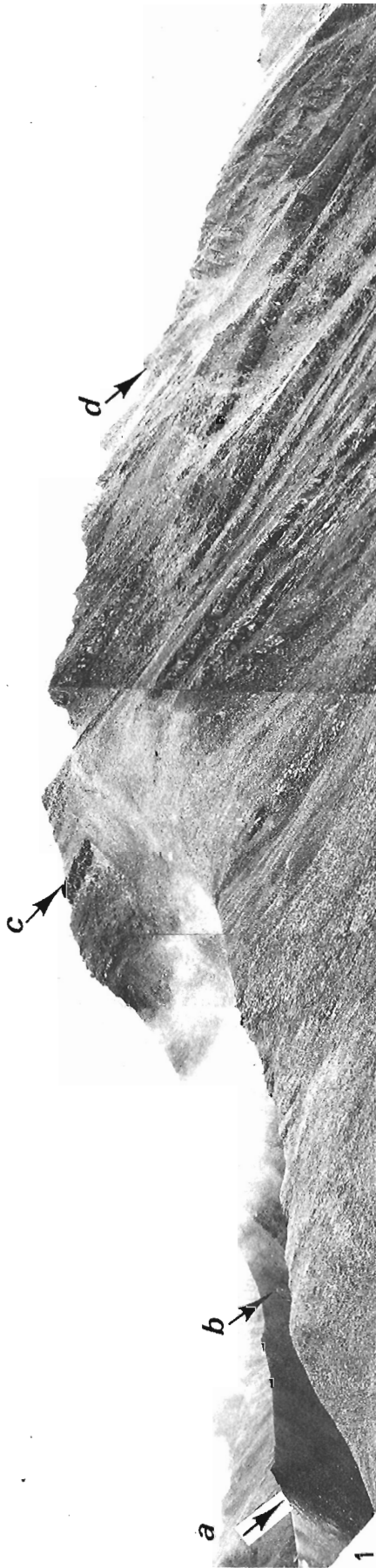


Plate 15.1 (opposite)

- Figure 1. View looking south at Rockslide Formation. Base and top of formation are at "a" and "d", "b" marks limestone pod at level of point "a" in figure 6, and point "c" marks point 3 m above fossil locality 95680 and 50 m below top of unit 12. Composite from GSC photos 203472-R, 203472-V, 203472-Z.
- Figure 2. Penecontemporaneous folds in unit 5, Sekwi Formation. Folds are located 13 m down section from point "b" in figure 3. Orange brown weathering limy siltstone has "Swiss cheese" appearance caused by recessive weathering limestone in nodules and wavy beds. GSC photo 203473.
- Figure 3. View looking south at fifth and sixth segments of measured section. GSC locality 95669 is at "a", base and top of unit 6 are at "b" and "c", base and top of unit 7 are at "d" and "e". GSC photo 203472-W.
- Figure 4. Light grey weathering dolomite in unit 6, Sekwi Formation, near measured section. View of section shown in figure 3 was photographed from this outcrop. Note in present figure that thin beds to left of hammer ("a") can be traced into "thick" beds to right. Beds to right have undergone penecontemporaneous folding and brecciation which has fused thin beds to give thick bedded appearance. GSC photo 203472-X.
- Figure 5. View looking east at lower segments of measured section. Unit 1 (basal segment) was measured between points "a" and "b", base of unit 2 (second segment) is at "c" (measuring route continues to right and beyond margin at figure), and units 3 and 4 (third segment) were measured between points "d" and "e". View is from ridge just below point "d" in figure 3. GSC photo 203473-D.
- Figure 6. Thin bedded, platy limestone of Rockslide Formation. Base of limestone pod (3 m in diameter) at "a" is 67 m above base of unit 11. Scour surface (located by white dots) is overlain by bed of penecontemporaneous breccia. GSC photo 203473-B.

Parafallotaspis (Fallotaspis Zone?) near the base of the Sekwi Formation (GSC loc. 95668) in the present section suggests that the base here is as old as it is to the north, and therefore does not indicate a diachronous (interfingering?) relationship with underlying map unit 3.

Units 11 through 14 have been correctly identified by Gordey (1979, Fig. 2.1) as belonging to the Rockslide Formation. These strata were earlier mapped by Green et al. (1968) as map unit 6. The abundance of platy, laminated limestone with interbeds of penecontemporaneous breccia at various horizons suggest a slope environment for most of the formation. The uppermost unit (unit 14) was probably deposited under shallow platform conditions as is suggested by the light coloured, medium and thick bedded limestone, interbedded dolomite, and interbeds rich in quartz sand. The formation contains fossils belonging to the Middle Cambrian **Albertella** and/or **Glossopleura** Zone through the **Bolaspidella** Zone, and therefore a close agreement in both age and lithology exists between the present strata and those at the type section for the Rockslide Formation (Gabrielse et al., 1973, p. 37).

Gordey's (1979, Fig. 2.1) assignment of the strata in the uppermost stratigraphic units (units 15, 16) to the undivided Broken Skull and Sunblood formations will not be commented upon here, as the writer is unfamiliar with the physical distribution of these formations, and no fossils were found for faunal correlation.

References

- Fritz, W.H.
1979a: Eleven stratigraphic sections from the Lower Cambrian of the Mackenzie Mountains, northwestern Canada; Geological Survey of Canada, Paper 78-23.
1979b: Cambrian stratigraphy in the northern Rocky Mountains, British Columbia; in Current Research, Part B, Geological Survey of Canada, Paper 79-1B, report 15.
- Gabrielse, H., Blusson, S.L., and Roddick, J.A.
1973: Geology of Flat River, Glacier Lake, and Wrigley Lake map-areas, District of Mackenzie and Yukon Territory; Geological Survey of Canada, Memoir 366.
- Gordey, S.P.
1978: Stratigraphy and structure of the Summit Lake area, Yukon and Northwest Territories; in Current Research, Part A, Geological Survey of Canada, Paper 78-1A, p. 43-48.
1979: Stratigraphy of southeastern Selwyn Basin in the Summit Lake area, Yukon Territory and Northwest Territories; in Current Research, Part A, Geological Survey of Canada, Paper 79-1A, p. 13-16.
- Green, L.H., Roddick, J.A., and Blusson, S.L.
1968: Nahanni map area, District of Mackenzie and Yukon Territory; Geological Survey of Canada, Map 8-1967.

Project 670576

E.T. Tozer

Institute of Sedimentary and Petroleum Geology, Ottawa

Tozer, E.T., *Latest Triassic ammonoid faunas and biochronology, Western Canada; in Current Research, Part B, Geological Survey of Canada, Paper 79-1B, p. 127-135, 1979.*

Abstract

A new division of the latest Triassic is proposed with the definition, in ascending order, of the **Gnomohalorites cordilleranus**, **Cochloceras amoenum** and **Choristoceras crickmayi** zones filling the interval between the Columbianus Zone (late Middle Norian) and the Hettangian (earliest Jurassic). New ammonoids significant for correlation are described. Eight are new species, one each of **Metasibirites** and **Choristoceras**, the remainder of new genera **Nassichukites** (one species), **Lissonites** (one), **Gnomohalorites** (three), **Paraguembelites** (one). Classification of Choristocerataceae is revised with inclusion of **Cycloceltites** and the introduction of **Vandaites** new genus, for **Peripleurites stuerzenbaumi** Mojsisovics.

Introduction

This report provides a revised biochronological scale for the interval between the Upper Triassic Columbianus Zone and the Jurassic (Table 16.1). It also provides descriptions of new ammonoid taxa significant for the recognition and correlation of the chronostratigraphic divisions and a revised classification of the Superfamily Choristocerataceae.

The interval with which this report is concerned is one for which it has been difficult to devise a satisfactory zonal scheme, not only in North America, but everywhere. Faunas representing parts of the interval have long been known wherever marine Triassic rocks occur – in the Arctic, around the Pacific and in Tethys. It has been generally recognized that a succession of three faunas occurred, but sections which objectively demonstrate the sequence are rare.

The succession of zones now recognized, compared with the previous scheme (Tozer, 1967) is given in Table 16.1. The informal divisions of the Suessi Zone are now replaced with two zones defined at type localities, thus providing an unambiguous basis for their recognition. Use of the Marshi Zone, defined in the Kössen Beds of Kendelbachgraben, Austria, is discontinued in order that the highest zone be defined in a section where the relationship to the underlying zone is demonstrable. This is not so at Kendelbachgraben. The species from Canada formerly identified as **Choristoceras marshi** is now identified as **C. crickmayi** n. sp. which becomes index species for the highest zone. **Choristoceras marshi** and **C. crickmayi** are probably about the same age. Although closely similar they can be distinguished on the basis of sutural differences.

Rhabdoceras suessi is unknown at the type locality of the Crickmayi Zone but occurs in the fauna of the Sutton Formation which is now regarded as representative of the Crickmayi Zone. According to this interpretation **Rhabdoceras suessi** is present in all three zones and the Suessi Zone serves no purpose in the subdivision of the interval.

For the time being the Cordilleranus, Amoenum and Crickmayi zones are grouped as the three components of the Upper Norian (Sevatian) Substage. The possibility that Rhaetian (interpreted with the whole of the Kössen Beds as stratotype) may be synonymous with Upper Norian (Sevatian), considered by Kittl (1903) and Zapfe (1968) gained impetus with the discovery by Ulrichs (1972) of **Rhabdoceras suessi** in the type section of the Kössen Beds, at and below the level of **Choristoceras**. This does not necessarily establish equivalence of Sevatian and Rhaetian for, to my knowledge, ammonoids indicative of the Cordilleranus and Amoenum zones have not been found in the Kössen. Nevertheless, if the Zlambach beds that yielded **Choristoceras haueri**

Mojsisovics and **C. nobile** Mojsisovics are regarded as typical Sevatian, then Sevatian and Rhaetian at least overlap in scope. The question of appropriate substage nomenclature for these beds is a matter of applying legal and historical principles and will not be dealt with here.

Kozur (1973) refers the Columbianus Zone to the Sevatian, but he does not appear to have attracted adherents (cf. Tatzreiter, 1978).

Definition of Zones

Cordilleranus Zone (Index species: **Gnomohalorites cordilleranus** n. gen., n. sp., Pl. 16.1, fig. 18a,b)

Type locality: Pardonet Formation, Mount Ludington, northeastern British Columbia where it overlies the Columbianus Zone (Tozer, 1967, p. 54, 55).

The fauna known from the type locality comprises: **Placites symmetricus** (Mojsisovics), **Sagenites** sp. indet., **Metasibirites columbianus** n. sp. (Pl. 16.1, fig. 20a-c), **Nassichukites dimidiatus** n. gen., n. sp. (Pl. 16.1, fig. 17a-d), **Gnomohalorites cordilleranus** n. gen., n. sp. (Pl. 16.1, fig. 18a,b), **Paraguembelites ludingtoni** n. gen., n. sp. (Pl. 16.1, fig. 21-23), **Rhabdoceras suessi** Hauer (Pl. 16.1, fig. 8a-c), **Peripleurites roemeri** Mojsisovics (Pl. 16.1, fig. 7a-c), **Rhacophyllites occultus** (Mojsisovics), **Monotis ochotica** (Keyserling) (sensu lato).

Lissonites canadensis n. gen., n. sp. (Pl. 16.1, fig. 16a-d) is associated with **Monotis ochotica** and is accordingly regarded as representative of the Cordilleranus Zone.

Monotis subcircularis Gabb and **M. ochotica** occupy the same stratigraphic position within the Pardonet Formation (Westermann and Verma, 1967, p. 802). Beds with these species of **Monotis**, which are known worldwide, are interpreted as correlatives of the Cordilleranus Zone. **Gnomohalorites southeri** n. sp. (Pl. 16.1, fig. 19a,b) and **G. yukonensis** n. sp. are from the level of **Monotis subcircularis**.

Amoenum Zone (Index species: **Cochloceras amoenum** Mojsisovics, Pl. 16.1, fig. 12)

Type locality: **Cassianella** Beds of Tyaughton Group, Tyaughton Creek valley, southern British Columbia, which overlie beds with **Monotis subcircularis** (Cordilleranus Zone) (Tozer, 1967, p. 76, 77). In addition to the index species the ammonoid fauna of the **Cassianella** Beds includes **Placites polydactylus** (Mojsisovics), **Rhabdoceras suessi** Hauer (Pl. 16.1, fig. 10), also arcestids, cladiscitids and **Rhacophyllites**.

Cochloceras has never been found in the lower beds of the Upper Norian nor is it known from the uppermost Triassic. The genus evidently characterizes the middle part of the substage. This is the view of Kozur (1973) who recognizes a **Cochloceras suessi** Zone (type locality, Zlambach Beds, Austria) in this position. As far as the writer can determine, the exact position of the **Cochloceras** beds of Tethys, in relation to older beds, has not been established. The **Cochloceras** bearing strata of North America and Tethys are nevertheless presumably correlative. Possibly also correlative are beds with **Rhabdoceras suessi** above those with **Monotis** but without **Cochloceras**, e.g. those in the Pardonet Formation of Peace River (Tozer, 1967, p. 55).

Crickmayi Zone (Index species: **Choristoceras crickmayi** n. sp., Pl. 16.1, fig. 4-6)

Type locality: Green sandstone and conglomerate unit of Tyaughton Group, which overlies the **Cassianella** Beds (Amoenum Zone), Tyaughton Creek, southern British Columbia (Tozer, 1967, p. 75, 76). **Psiloceras** ex aff. **P. planorbis** (Sowerby), indicating the Planorbis Zone (Hettangian, basal Jurassic), is also known from the green sandstone and conglomerate unit (Frebold, 1967, p. 9), but not from the sections that have provided **Choristoceras**.

The only ammonoids known from the type locality are **Arcestes** sp. indet. and **Choristoceras crickmayi**. True **Choristoceras** (as defined below), of which **C. crickmayi** is an example, appear to be restricted to the topmost Triassic zone (Crickmayi Zone and correlatives). Apparently there are no undoubted occurrences of **Choristoceras** in beds that are demonstrably older than the Crickmayi Zone. This seems to be the case everywhere. Statements to the contrary based on North American occurrences (e.g. Tozer, 1974, p. 204) have never been fully documented and my own examination of material from Canada and the United States suggests that these records refer to species of **Peripleurites**. **Choristoceras suttonense** Clapp and Shimer (Pl. 16.1, fig. 1-3), from the

Sutton Formation of Cowichan Lake, Vancouver Island, clearly shows the characters of the genus. The Sutton fauna is accordingly now considered representative of the uppermost Triassic Zone (Crickmayi), not the penultimate zone ("Upper Suessi"), as in Tozer (1967). The ammonoid fauna comprises: **Megaphyllites** sp. (Pl. 16.1, fig. 13a,b), **Placites** sp., **Cladiscites** sp., **Cyclocelmites** cf. **C. arduini** Mojsisovics (Pl. 16.1, fig. 14, 15), **Rhabdoceras suessi** Hauer (Pl. 16.1, fig. 9a,b), **Choristoceras suttonense** Clapp and Shimer (Pl. 16.1, fig. 1-3). **Myophoria suttonensis** Clapp and Shimer occurs at the type locality for the Crickmayi Zone and in the Sutton Formation, which supports the correlation.

According to this interpretation of the biochronological significance of **Choristoceras**, **Rhabdoceras suessi** ranges up into the latest Triassic zone.

Some authors (Kozur, 1973; Mostler et al., 1978) recognize two **Choristoceras** zones, **Choristoceras haueri**, followed by **C. marshi**, at the top of the Triassic. These two zones have their type localities in different formations (Zlambach Beds and Kössen Beds respectively) and are not known in sequence. They are here regarded as correlative, as by Kuehn (1962, p. 87). Wiedmann's remarks (1972, p. 602) on the difficulty (or impossibility) of separating Rhaetian and Late Norian **Choristoceras** are germane in this context.

The following are thus taken to be correlatives of the Crickmayi Zone: Upper Gabbs and possibly also the Middle Gabbs of Nevada; Modin Formation of California; **Choristoceras**-bearing parts of the Kössen and Zlambach Beds of the Austrian and Bavarian Alps. **Vandaites** n. gen. is a genus of Choristoceratidae known at present only from the fauna of Drnava, Czechoslovakia, the exact age of which has long been a subject of debate. **Vandaites** and **Choristoceras** are evidently closely related and are probably about the same age. The Drnava fauna is probably correlative with the Crickmayi Zone. Unfortunately the Drnava fauna, like that from the Sutton, is in a situation where the relationship to the Amoenum and Planorbis zones cannot be demonstrated.

Table 16.1

PREVIOUS SCHEME (TOZER, 1967, 1971, 1974; SILBERLING & TOZER, 1968)				PROPOSED SCHEME			
OVERLYING: JURASSIC (HETTANGIAN STAGE)				OVERLYING: JURASSIC (HETTANGIAN STAGE)			
UPPER TRIASSIC SERIES (PART)	RHAETIAN STAGE	MARSHI ZONE (<i>Choristoceras marshi</i>)		UPPER TRIASSIC SERIES (PART)	NORIAN STAGE (PART)	UPPER NORIAN (=SEVATIAN) (≈RHAETIAN)	CRICKMAYI ZONE (<i>Choristoceras crickmayi</i>)
	NORIAN STAGE (PART)	UPPER NORIAN SUBSTAGE	SUESSI ZONE (<i>Rhabdoceras suessi</i>)			UPPER SUESSI ZONE	AMOENUM ZONE (<i>Cochloceras amoenum</i>)
			LOWER SUESSI ZONE			CORDILLERANUS ZONE (<i>Gnomonhalorites cordilleranus</i>)	
UNDERLYING: COLUMBIANUS ZONE (<i>Himavatites columbianus</i>) LATE MIDDLE NORIAN (ALAUNIAN)				UNDERLYING: COLUMBIANUS ZONE (<i>Himavatites columbianus</i>) LATE MIDDLE NORIAN (ALAUNIAN)			

Descriptions of New Ammonoid Taxa

Order CERATITIDA

Superfamily CLYDONITACEAE (Mojsisovics 1879)

Family METASIBIRITIDAE Spath 1951

Genus *Nassichukites*, Tozer n. gen.

Type species: *Nassichukites dimidiatus* n. sp.

Named for W.W. Nassichuk, who discovered the type locality in northeastern British Columbia.

Diagnosis: Inner whorls with arched periphery, smooth siphonal band and feeble projection of ribs. Outer whorl with distinct ventral shoulders and tabulate periphery. Ribs simple or with branching or intercalation on the inner flank, projected at the margin where they terminate abruptly adjacent to a smooth band on the periphery. Umbilical and marginal tuberculation absent. External rib-terminations prominent, more or less tuberculate. Suture line goniatitic; external lobe with median saddle.

Discussion: The outer whorl section, lateral ribbing and suture line suggest affinity with *Helictites*, from which *Nassichukites* is distinguished by the interruption of the ribs on the periphery.

Composition of the genus: Known only from the type species.

Age and distribution: Late Norian, Cordilleranus Zone, British Columbia.

Nassichukites dimidiatus n. sp.

Plate 16.1, figures 17a-c. Figure 16.1H

1967. *Ceratites* aff. *riezingeri* Mojsisovics, Tozer, 1967, p. 54.

Diagnosis: *Nassichukites* about 20 mm in diameter with about 40 ribs at the periphery and about 25 at the umbilicus.

Registered material: Holotype, GSC 28941, GSC locality 68300.*

Discussion: In addition to the holotype, two other specimens (GSC 28942, 28943) collected from talus at the type locality, are known. GSC 28942 shows the inner whorls and a septal surface with 8 lobes (i.e. a 5-lobe formula), confirming assignment to Clydonitaceae rather than Choristocerataceae. The new species is appreciably more evolute than *Ceratites riezingeri*; the affinities of the latter species are not clear due to incomplete knowledge of the suture line. Resemblance to *Hesperites clarae* Pompeckj in external characters is remarkable, but the ammonitic suture line of *Hesperites* is quite unlike that of *Nassichukites*.

Genus *Metasibirites* Mojsisovics 1896

Type species. *Ammonites spinescens* Hauer

Metasibirites columbianus n. sp.

Plate 16.1, figures 20 a-c, Figure 16.1G

Registered material: Holotype GSC 28972, GSC locality 68300.

Diagnosis: Phragmocone with depressed whorls. Inner flank with simple bullate ribs (about 15 on half a whorl) from which stem two ribs which pass uninterrupted, with slight projection, across the periphery. Suture line with indented lateral lobe.

Discussion: This species is known only from the holotype. Resemblance to *Metasibirites spinescens* (Hauer) is obvious but the new species is distinguished by having bullate ribs rather than spines on the flanks. The suture line is not

perfectly preserved but there is no doubt that the first lateral lobe is indented and it is virtually certain that there is no median saddle in the external lobe. The indented lateral lobe is evidently a diagnostic character. Suture lines of the Alpine *Metasibirites* are imperfectly known but are probably goniatitic. Those of the species from Bulgaria, the Himalayas and Indonesia are goniatitic.

Genus *Lissonites*, Tozer, n. gen.

Type species: *Lissonites canadensis* n. sp.

Named for C.I. Lissón who was the first to describe ammonoids referable to the genus.

Diagnosis: Whorl section ovoid, quadrangular or sub-hexagonal. Ribs simple and branched, crossing or interrupted at the periphery. Low bullate swellings may be present where the ribs meet on the inner flank; low marginal and external tubercles may or may not be present. Suture line goniatitic, external lobe without a median saddle.

Discussion: The marginal and external tuberculation, which although not present on all individuals, but nevertheless present on some variants in each population, invites comparison with that of Middle Norian species such as "*Sandlingites*" *archibaldi* Mojsisovics. F. Tatzreiter (pers. comm.) will propose a new genus for "*Sandlingites*" *archibaldi*. Representatives of true *Sandlingites* of Carnian age differ from both "*S.*" *archibaldi* and *Lissonites* in their ontogeny, having, at an early stage strong marginal tuberculation. *Lissonites* is distinguished from Tatzreiter's new genus by having much more subdued sculpture and also by the simple external lobe. The sculpture of some *Lissonites* resembles that of *Helictites* but that genus is distinguished by having a median saddle in the external lobe. The suture line of *Lissonites* resembles that of some *Metasibirites* (e.g. *M. protractus* Mojsisovics as described by Sacharjeva-Kovatscheva, 1967, p. 85) but the lateral tuberculation of *Lissonites* is much more subdued than that of all *Metasibirites*. Both *Metasibirites* and *Helictites* lack the marginal and external tuberculation characteristic of sculptured *Lissonites* variants.

Composition of the genus: *Lissonites canadensis* n. sp., *L. lissoni* (Jaworski), *L. sutanensis* (Jaworski).

Age and distribution: Late Norian, Cordilleranus Zone, British Columbia and Peru. Cordilleranus Zone (or possibly Amoenum Zone), Kotel, Bulgaria.

Lissonites canadensis n. sp.

Plate 16.1, figures 16a-d. Figure 16.1J

Registered material: Holotype GSC 28932, 4 paratypes (GSC 28929, 28930, 28931, 28933), all from GSC locality 83818.

Diagnosis: *Lissonites* attaining a diameter of about 22 mm. Sculpture very variable. Ribs simple, branched or intercalated crossing periphery with or without interruption. Some variants have thickened bullate ribs on the inner flank; some (e.g. the holotype) have faint marginal and external tuberculation.

Discussion: More than 50 specimens of this species are known and no two are exactly alike. Tuberculation is never prominent. The holotype best shows the marginal and external tuberculation. GSC 28931 shows a trace of lateral as well as marginal and external tuberculation. The sculpture and suture line of *Lissonites canadensis* undoubtedly indicates affinity with "*Sibirites*" *eichwaldi* var. *peruana* Lisson (1911), a taxon in which Jaworski (1923) named two species, *Nevadites lissoni* Jaworski and *Nevadites sutanensis* Jaworski. (See also Sacharjeva-Kovatscheva, 1967, p. 78). Virtually all

* Detailed descriptions for the GSC localities are given at the end of this article.

the characters encountered in the population of *Lissonites canadensis* can be matched in specimens illustrated by Lisson and Jaworski, the only difference being that none is as evolute as the holotype of *L. canadensis*. The suture lines of all these taxa clearly exclude them from the Anisian genus *Nevadites*, as implied by Spath (1934, p. 37).

Superfamily TROPITACEAE (Mojsisovics 1875)

Family HALORITIDAE Mojsisovics 1893

Subfamily HALORITINAE (Mojsisovics 1893)

Genus *Paraguembelites*, Tozer, n. gen.

Type species: *Paraguembelites ludingtoni* n. sp.

Diagnosis: Haloritin with last quadrant of body chamber smooth. Phragmocone with nodose to almost smooth ribs. Siphonal line with smooth band bordered by nodes. These nodes, at the external extremity of the ribs, are more prominent than those on the ribs. Suture line with weakly indented saddles.

Discussion: The excentric umbilicus and nodose ribs clearly indicate affinity with Haloritinae (sensu Tozer 1971, p. 1004, 1028), in particular *Halorites* Mojsisovics, from which *Paraguembelites* is distinguished by having regular, paired external nodes, recalling those of *Guembelites*. *Guembelites*, a much older genus (Juvavitinae) lacks an excentric umbilicus and is probably not closely related.

Composition of the genus: *Paraguembelites ludingtoni* n. sp., probably also "*Miltites*" *pauli* Mojsisovics.

Age and distribution: Late Norian, Cordilleranus Zone, British Columbia; probably also Hallstatt Limestone, Austria.

Paraguembelites ludingtoni n. sp.

Plate 16.1, figures 21-23. Figure 16.1N

Indoclionites ? sp., McLearn, 1960, p. 45, Pl. 21, fig. 2-4.

Halorites ? n. sp., Tozer, 1967, p. 39, 54.

Registered material: Holotype GSC 32279, 7 paratypes (GSC 32280-32286) all from GSC locality 68304.

Diagnosis: *Paraguembelites* with about one quarter of a whorl excentric. Body chamber outline angular, with obtuse elbow bend at start of excentricity of umbilicus. Phragmocone ribs branch at inner and outer flank with some tertiary ribs. Ribs provided with barely perceptible to moderately prominent spirals of nodes, about 6 spirals between the umbilicus and the external nodes.

Discussion: The nodose sculpture on the periphery of "*Miltites*" *pauli* Mojsisovics suggests that it is congeneric with *Paraguembelites ludingtoni* despite the fact that Mojsisovics' species is not known to be excentrumbilicate. In terms of specific differences, "*Miltites*" *pauli* is appreciably more inflated than *Paraguembelites ludingtoni*.

Genus *Gnomohalorites*, Tozer, n. gen.

Type species: *Gnomohalorites southeri* n. sp.

Diagnosis: Small haloritin with slightly clavate tubercles on the ribs. Tuberculation in no way differentiated on the siphonal line; reduced on body chamber, at least on the inner flank. Suture line with very weakly indented saddles.

Plate 16.1

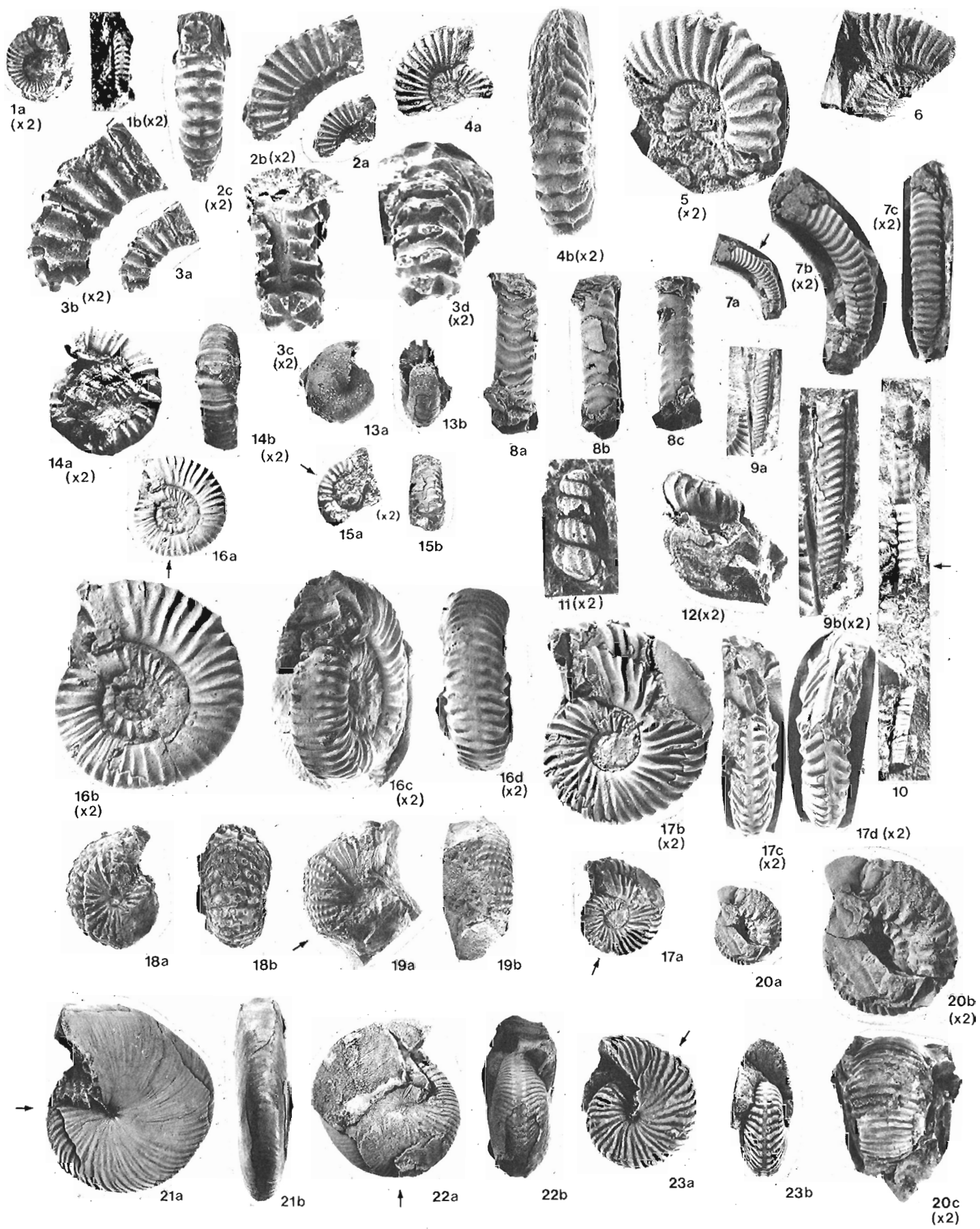
Figures are natural size unless otherwise indicated.

Arrows indicate position of last septum.

Numbers in parentheses are of GSC localities.

Figures

- 1-3. *Choristoceras suttonense* Clapp and Shimer. 1a,b, GSC 32326 (23379). 2a-c, GSC 32322 (23370). 3a-d, GSC 32325 (23372). All from Sutton Formation, Vancouver Island.
- 4-6. *Choristoceras crickmayi* n. sp. 4a,b, holotype, GSC 18912 (56395). 5, paratype, GSC 32327 (10095). 6, paratype, GSC 34608 (10095). All from Tyaughton Group, Tyaughton Creek, British Columbia.
- 7a-c. *Peripleurites roemeri* Mojsisovics. GSC 32320 (68300), Pardonet Formation, Mount Ludington, British Columbia.
- 8-10. *Rhabdoceras suessi* Hauer. 8a-c, GSC 32314 (68304), Pardonet Formation, Mount Ludington, British Columbia. 9a,b, GSC 32317 (23370), Sutton Formation, Vancouver Island. 10, GSC 32318 (56415), Tyaughton Group, north of Tyaughton Creek, British Columbia.
11. *Cochloceras canaliculatum* Hauer. GSC 32329, Bonanza Group, Julian Cove Vancouver Island, collected by J.A. Jeletzky.
12. *Cochloceras amoenum* Mojsisovics. GSC 32328 (56405), Tyaughton Group north of Tyaughton Creek, British Columbia.
- 13a,b. *Megaphyllites* sp. GSC 28275 (23374), Sutton Formation, Vancouver Island.
- 14,15. *Cycloclitites* cf. *C. arduini* Mojsisovics. 14a,b, GSC 17015 (23372). 15a,b, 28944 (23372). Sutton Formation, Vancouver Island.
- 16a-d. *Lissonites canadensis* n. gen., n. sp. Holotype, GSC 28932 (83818). Pardonet Formation, British Columbia.
- 17a-d. *Nassichukites dimidiatus* n. gen., n. sp. Holotype GSC 28941 (68300) Pardonet Formation. Mount Ludington, British Columbia.
- 18a,b. *Gnomohalorites cordilleranus* n. gen., n. sp. Holotype, GSC 32277 (68300) Pardonet Formation. Mount Ludington, British Columbia.
- 19a,b. *Gnomohalorites southeri* n. gen., n. sp., Holotype, GSC 32292 (40429) Sinwa Formation, Tulsequah Area, British Columbia.
- 20a-c. *Metasibirites columbianus* n. sp. Holotype, GSC 28927 (68300), Pardonet Formation, Mount Ludington, British Columbia.
- 21-23. *Paraguembelites ludingtoni* n. gen., n. sp. 21a,b, paratype, GSC 32281 (68304). 22a,b, holotype GSC 32279 (68304). 23a,b, paratype GSC 32282 (68304). All from Pardonet Formation, Mount Ludington, British Columbia.



Discussion: As no complete specimens of *Gnomohalorites* are known all characteristics of the body chamber have not been determined. However mature characters are known for the type species, indicating that a small genus of Haloritinae is represented. The nodose sculpture indicates affinity with some species that have been referred to *Halorites*, a genus which up to now has been very broadly interpreted. Mojsisovics (1893) distinguished two main groups, *acatenati* and *catenati*, based on the extent of nodose sculpture. On the type species of *Halorites* [*H. ramsaueri* (Hauer)] nodes are apparently absent entirely making the distinction between *Gnomohalorites* and *Halorites* obvious. More comparable are the nodose *Halorites* (*catenati*), which F. Tatzreiter suggests represent a distinct genus. Typical *catenati* [e.g. *Halorites catenatus* (von Buch)] are much larger than *Gnomohalorites*. The more significant difference between *Gnomohalorites* and both *acatenate* and *catenate Halorites* is in their suture lines. The suture of *Gnomohalorites* is much less deeply indented than that of *Halorites ramsaueri* and *H. catenatus*.

Composition of the genus: *Gnomohalorites southeri* n. sp., *G. cordilleranus* n. sp., *G. yukonensis* n. sp., *G. americanus* (Hyatt). *Halorites bufonis* Mojsisovics and *H. pomponii* Diener are possibly referable (see below).

Age and distribution: Late Norian, Cordilleranus Zone, Yukon, British Columbia, California, Tethys (?).

Gnomohalorites southeri n. sp.

Plate 16.1, figures 19a-b

Halorites cf. *H. americanus* Hyatt; Tozer, 1967, p. 77; Souther, 1971, p. 79. Named for J.G. Souther, who collected the type specimen.

Registered material: Holotype GSC 32292, GSC locality 40429.

Diagnosis: *Gnomohalorites* with relatively dense tuberculation (about 8 nodes on each rib).

Discussion: See that for *G. yukonensis* n. sp.

Gnomohalorites cordilleranus n. sp.

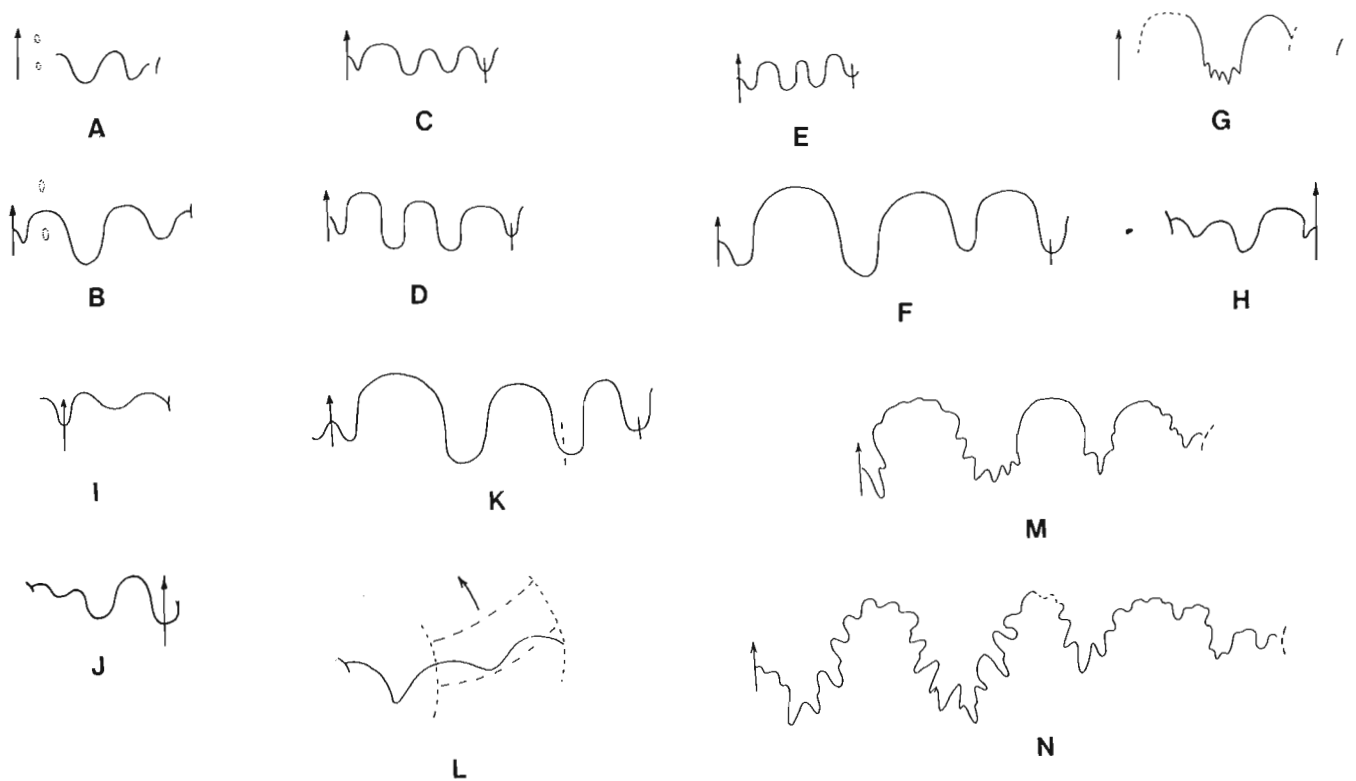
Plate 16.1, figures 18a,b. Figure 16.1M.

Halorites cf. *H. americanus* Hyatt; Tozer, 1967, p. 54.

Registered material: Holotype GSC 32277, paratype, GSC 32278, both from GSC locality 68300.

Diagnosis: *Gnomohalorites* with moderately dense tuberculation (about 6 nodes on each rib).

Discussion: See that for *G. yukonensis* n. sp.



- A. *Choristoceras crickmayi* n. sp. GSC 18912
- B. *Choristoceras crickmayi* n. sp. GSC 32327
- C. *Peripleurites roemerii* Mojsisovics GSC 32320
- D. *Rhabdoceras suessi* Hauer GSC 32318
- E. *Rhabdoceras suessi* Hauer GSC 32317
- F. *Rhabdoceras suessi* Hauer GSC 32314
- G. *Metasibirites columbianus* GSC 28927

- H. *Nassichukites dimidiatus* GSC 28941
- I. *Cycloceltites* cf. *C. arduini* Mojsisovics GSC 28944
- J. *Lissonites canadensis* n. gen., n. sp. GSC 28933
- K. *Choristoceras suttonense* Clapp and Shimer. GSC 32325
- L. *Cochloceras amoenum* Mojsisovics GSC 32328
- M. *Gnomohalorites cordilleranus* n. gen., n. sp. GSC 32278
- N. *Paraguembelites ludingtoni* n. gen., n. sp. GSC 32285

Figure 16.1. Suture lines. All X 4.

Gnomohalorites yukonensis n. sp.

Halorites sp. indet., Tozer, 1958, p. 15.

Halorites cf. **H. americanus** Hyatt; Tozer, 1962, Pl. 12, fig. 17a,b; Tozer, 1967, p. 80 (part).

Registered material: Holotype, GSC 14262 (illustrated in Tozer, 1962), GSC locality 23457.

Diagnosis: **Gnomohalorites** with three or four large distant nodes on each rib.

Discussion: **Gnomohalorites southeri**, **G. cordilleranus** and **G. yukonensis**, judging from their phragmocones and suture lines, are closely related, differing only in tuberculation. **Gnomohalorites southeri** is the most densely tuberculate, **G. yukonensis** the least, and **G. cordilleranus** intermediate. **Halorites americanus** Hyatt is probably congeneric with these species and might even be conspecific with **G. cordilleranus**. This cannot be satisfactorily determined because both the body chamber characters and suture line of **H. americanus** are not revealed by the holotype and there are no descriptions of any other material. The sculpture of **Halorites bufonis** Mojsisovics and **H. pomponii** Diener resembles that of **Gnomohalorites** but the suture lines of these two species are not known and accordingly the relationship cannot be positively established. The suture line of **Halorites gemmatus** Mojsisovics is apparently comparable with that of **Gnomohalorites** species, but **H. gemmatus** differs in having the sculpture interrupted on the siphonal line.

Superfamily CHORISTOCERATACEAE (Hyatt 1900)

Choristocerataceae are interpreted to comprise four families in which the number of lobes on the adult septal surface is 6 (4-lobe formula) (Cycloceltitidae, Rhabdoceratidae, Choristoceratidae) or 4 (3-lobe formula) (Cochloceratidae) instead of 8 (5-lobe formula) or more, as in all other Ceratitida. Coiling is serpenticone or heteromorph, sculpture is of ribbing (almost invariably simple), with external tuberculation in Choristoceratidae. Suture lines are generally goniatitic, some have an indentation in the lateral lobe. Thus defined, Choristocerataceae are exclusively Upper Norian. No fully documented occurrences of ammonoids meeting the above diagnosis have been provided for older Triassic ammonoids.

Family CYCLOCELTITIDAE Tozer, n. fam.

Diagnosis: Serpenticone ribbed Choristocerataceae with goniatitic suture lines. External lobe without median saddle.

Composition of family: **Cycloceltites** Mojsisovics 1893, Upper Norian, North America, Tethys.

Discussion: The admirable descriptions and illustrations provided by Kollárová-Andrusovová (1973) show that **Cycloceltites**, like **Choristoceras**, has a septal surface with only 6 lobes. This has been confirmed on a specimen from Canada (Pl. 16.1, fig. 15).

Family RHABDOCERATIDAE Tozer, n. fam.

Diagnosis: Heteromorph (baculicone or criocone), planispiral or twisted Choristocerataceae, ribbed on flank and periphery but not tuberculate. Suture line goniatitic.

Composition of family: **Rhabdoceras** Hauer 1860, Upper Norian (Cordilleranus, Amoenum and crickmayi zones), worldwide (= **Rhabdoceras** (**Cyrtorhabdoceras**) Wiedmann 1973); **Peripleurites** Mojsisovics 1893, Upper Norian (Cordilleranus Zone, probably also Amoenum Zone, not certainly known from Crickmayi Zone and its correlatives), North America, Peru, Tethys.

Discussion: The study of the Triassic heteromorph ammonoids is handicapped by the generally fragmentary nature of the material and it is commonly difficult or impossible to determine the exact nature of the coiling. Suture line and sculpture are fairly well known and for the time being one must rely principally on these characters for the discrimination of taxa. Most, if not all of the heteromorphs of the two earlier Upper Norian zones, have ribbing on the periphery and no tuberculation. This is a feature of the type species of both **Rhabdoceras** and **Peripleurites**. To group these two in a family serves to separate the earlier Triassic heteromorphs, the later, characterized by external nodes, now being separated as Choristoceratidae. The two families are not mutually exclusive however, both definitely being present in the Sutton Formation of Vancouver Island.

Rhabdoceras suessi var. **curvata** Mojsisovics is here interpreted as a variety of **R. suessi**, as by Mojsisovics, not as the type species of the subgenus **Cyrtorhabdoceras**, as by Wiedmann (1973).

Family COCHLOCERATIDAE Hyatt 1900

Diagnosis: Sinistral turricone Choristocerataceae. Ribs strong, on early whorls commonly if not invariably interrupted anteriorly by a smooth band – the canal.

Composition of family: **Cochloceras** Hauer 1860, Late Norian (Amoenum Zone), Yukon, Western British Columbia, Nevada, Tethys. (= **Cochloceras** (**Paracochloceras**) Mojsisovics 1893.)

Discussion: **Cochloceras fischeri** Hauer, the type species, which lacks a canal on the ultimate whorl, is provisionally interpreted as indicating the mature characters; those with a canal (i.e. **Paracochloceras**), as immature. Mojsisovics (1893, p. 573) describes the **Cochloceras** septal surface as having a total of 4 lobes. Diener (1925, p. 93) gives a similar description, although he expressed it differently (i.e. as a 3-lobe formula). Wiedmann (1973, figure 1F) has given a drawing, derived from one of the specimens described by Mojsisovics, which he interprets as showing the **Cochloceras** has a suture line comparable with that of **Choristoceras**, i.e. with a 4-lobe formula. The specimens from Canada show only parts of the suture line and septal surface but what they do show seems to agree with the descriptions of Mojsisovics and Diener, i.e. there appears to be one lobe on each side of the quadrangular whorl, 4 in all. I erred (Tozer, 1971, p. 1004) in stating that all Choristocerataceae have a suture line with a 4-lobe formula. Wiedmann has apparently made the same mistake.

Family CHORISTOCERATIDAE Hyatt 1900

Diagnosis: Planispiral or helicoid Choristocerataceae. Generally criocone although much of the phragmocone may be serpenticone. Body chamber commonly (invariably ?) has non-tuberculate ribs crossing the periphery (as in Rhabdoceratidae) but part or all of the phragmocone has peripheral interruption of sculpture with distinct external nodes at the ends of the ribs. Suture line goniatitic or with one indentation in the lateral lobe.

Composition of family: **Choristoceras** Hauer 1865, Late Norian (Crickmayi Zone) British Columbia, Nevada, California, Tethys; **Vandaites** n. gen. Late Norian; (Crickmayi Zone ?), Tethys (Czechoslovakia).

Discussion: Choristoceratidae are distinguished from other Choristocerataceae by having interruption of the sculpture on the periphery and the development of external nodes, at least on the phragmocone.

Genus *Choristoceras* Hauer 1865

Type species: *Choristoceras marshi* Hauer.

Diagnosis: Choristoceratidae coiled in plane spiral; inner whorls serpenticone or criocone, outer whorl detached. Suture line with or without indentation in lateral lobe.

Age and distribution: Late Norian, Crickmayi Zone, British Columbia, Nevada, California, Tethys.

Genus *Choristoceras* Hauer 1865

Choristoceras crickmayi n. sp.

Plate 16.1, figures 4a,b, 5, 6. Figure 16.1A,B.

Choristoceras marshi Hauer; Tozer, 1967, p. 42, 70, Pl. 10, fig. 8a-c, 9 (?); (not of Hauer, 1865, p. 654). Named for C.H. Crickmay, who discovered the type locality.

Registered material: Holotype GSC 18912, GSC locality 56395, paratypes GSC 32327, 34608, GSC locality 10094.

Diagnosis: *Choristoceras* like *Choristoceras marshi* but with a relatively shallow external lobe and without an indentation in the lateral lobe.

Discussion: The holotype and paratype GSC 32327 show whorls in contact and closely resemble *Choristoceras marshi* at a comparable size. GSC 34608, although slightly crushed, definitely seems to show detachment of the outer whorl. GSC 18913 (Tozer, 1967, Pl. 10, fig. 9) which is from a different locality, is definitely criocone, being coiled like *Choristoceras nobile* Mojsisovics, *Choristoceras ammonitiforme* (Gümbel) and some variants of *Choristoceras marshi* Hauer. GSC 18913 is possibly an unusually loosely coiled variant of *Choristoceras crickmayi*.

Choristoceras suttonense Clapp and Shimer

Plate 16.1, figures 1-3. Figure 16.1K.

Choristoceras suttonensis Clapp and Shimer, 1911, p. 434, Pl. 40, fig. 4, 6; Smith, 1927, p. 98, Pl. 105, fig. 5, 6; Tozer, 1967, p. 39, 79.

Registered material: Holotype, GSC 7813, GSC locality 13703. GSC 32322, GSC locality 23370; GSC 32324, 32325, GSC locality 23372; GSC 32326, GSC locality 23379.

This species is known only from well preserved fragments, none of which shows whorls in contact. Their curvature suggests that the species is criocone, like *Choristoceras haueri* Mojsisovics, to which *C. suttonense* is probably very closely related. Specimens that preserve the test show that ribs extend across the dorsum although those with the test removed are smooth in this area (Pl. 16.1, fig. 3c). The ribbed dorsum presumably confirms that the species was criocone.

Genus *Vandaites* Tozer, n. gen.

Type species: *Peripleurites (Choristoceras) stuerzenbaumi* Mojsisovics. Named for Vanda Kollárová-Andrusovová.

Diagnosis: Choristoceratidae coiled openly, in a helicoid spiral, with sculpture distinctly interrupted, at the periphery, with more or less nodose rib terminations on the early formed part of the conch. On the later formed part the ribs cross the periphery, without conspicuous nodes. Suture line goniatic.

Discussion: Thanks to the work of Kollárová-Andrusovová (1973) the suture line of the type species is now known,

leaving no doubt as to the affinity with *Choristoceras*, from which *Vandaites* is distinguished by being coiled in a helicoid instead of plane spiral.

Age and distribution: Late Norian, in beds probably correlative with the Crickmayi Zone, Czechoslovakia.

GSC Localities

- 10095 Tyaughton Group, Tyaughton Creek 1500 m above Spruce Lake Creek, NTS Tyaughton Creek 92 O/2W. C.H. Crickmay, 1939 (Tozer, 1967, p. 76).
- 13703 Sutton Formation, Cowichan Lake 4.8 km northwest of mouth of Sutton Creek, NTS Cowichan Lake 92 C/16E. C.H. Clapp 1908, 1909 (Clapp and Shimer, 1911).
- 23370, 23372, 23374, 23379 } Sutton Formation, as 13703, E.T. Tozer, 1953 (Tozer, 1967, p. 79).
- 23457 Lewes River Group, Formation D, 5.6 km northeast of Povoas Mountain, NTS Lower Laberge 105 E/6. E.T. Tozer, 1953 (Tozer, 1958, p. 15).
- 40429 Sinwa Formation, elevation 1350 m, 7.4 km north of west end of King Salmon Lake, NTS Tulsequah 104 K. J.G. Souther (Souther, 1971, p. 79).
- 56395 Tyaughton Group, Tyaughton Creek, 1500 m above mouth of Spruce Lake Creek, NTS Tyaughton Creek 92 O/2W. E.T. Tozer 1963 (Tozer, 1967, p. 76).
- 56405 Tyaughton Group, on ridge 1700 m northwest of Castle Peak, NTS Tyaughton Creek 92 O/2W. E.T. Tozer, 1963 (Tozer, 1967, p. 77).
- 56415 Tyaughton Group, head of Last Creek, tributary of Tyaughton Creek, NTS Warner Pass 92 O/3. E.T. Tozer, 1963 (Tozer, 1967, p. 77).
- 68300, 68304 } Pardonet Formation, west side Mount Ludington, NTS Nabesche River 94 B/6W. E.T. Tozer, 1965. (Tozer, 1967, p. 54).
- 83818 Pardonet Formation, about 1.5 m below contact with Bocock Formation, upper part of unit 34, section 7 (Gibson, 1971, p. 74), near summit of ridge between Ducette and Eleven Mile creeks, NTS Carbon Creek 93 O/15W. E.T. Tozer, 1969.

References

- Clapp, C.H. and Shimer, H.W.
1911: The Sutton Jurassic of the Vancouver Group, Vancouver Island; Proceedings of the Boston Society of Natural History, v. 134, p. 425-438, Pl. 40-42.
- Diener, C.
1925: Leitfossilien der Trias; Berlin, Borntraeger.
- Frebald, Hans
1967: Hettangian Ammonite Faunas of the Taseko Lakes area, British Columbia; Geological Survey of Canada, Bulletin 158.
- Gibson, D.W.
1971: Triassic Stratigraphy of the Sikanni Chief River-Pine Pass Region, Rocky Mountain Foothills, Northeastern British Columbia; Geological Survey of Canada, Paper 70-31.

- Hauer, F. v.
1865: **Choristoceras**. Eine neue Cephalopodensippe aus den Kössener Schichten; Sitzungberichte Akademie der Wissenschaften in Wien, Bd. 52, p. 654-660.
- Jaworski, E.
1923: Die marine Trias in Südamerika; Neues Jahrbuch für Mineralogie, Geologie und Paläontologie, Beilage-Band 47, p. 93-200.
- Kittl, E.
1903: Salzkammergut; Guide IV, IX International Geological Congress, Vienna.
- Kollárová-Andrusovová, V.
1973: in Kollárová-Andrusovová, V. and Kochanová, M., Molluskenfauna des Bleskový Prameň bei Drnava - Nor, Westkarpaten; Verlag der Slowakischen Akademie der Wissenschaften, Bratislava.
- Kozur, H.
1973: Beiträge zur Stratigraphie von Perm and Trias; Geologische Paläontologische Mitteilungen Innsbruck, Bd. 3, p. 1-31.
- Kuehn, O.
1962: Autriche; Lexique Stratigraphique International, v. 1 (Europe), Fasc. 8.
- Lissón, C.I.
1911: Determinación de Algunos Fósiles del Museo de la Escuela de Ingenieros; Boletín de Minas Industrias y Construcciones, Series II, v. 3, p. 1-6.
- McLearn, F.H.
1960: Ammonoid Faunas of the Upper Triassic Pardonet Formation, Peace River Foothills, British Columbia; Geological Survey of Canada, Memoir 311.
- Mojsisovics, E. v.
1893: Die Cephalopoden der Hallstätter Kalke; Abhandlungen der Kaiserlich-Königlichen Geologischen Reichsanstalt, Bd. 6, 2 Hälfte.
- Mostler, H., Scheuring, B., and Urlichs, M.
1978: Zur Mega-, Mikrofauna and Mikroflora der Kössener Schichten (alpine Obertrias) vom Weissloferbach in Tirol unter besonderer Berücksichtigung der in der **suessi-** and **marshi-**Zone auftretenden Conodonten; Österreichische Akademie der Wissenschaften Schriftenreihe der Erdwissenschaftlichen Kommissionen, Bd. 4, p. 141-174.
- Pompeckj, J.F.
1895: Ammoniten des Rhät; Neues Jahrbuch für Mineralogie, Geologie und Paläontologie, II Bd., p. 1-46.
- Sacharjeva-Kovatcheva, K.
1967: Norische Ammoniten von der Trias bei Kotel; Annuaire de L'Université de Sofia, Faculté de Géologie et Géographie, Livre I, Géologie, v. 60, p. 75-106. (Bulgarian with German summary.)
- Silberling, N.J. and Tozer, E.T.
1968: Biostratigraphic Classification of the Marine Triassic in North America; Geological Society of America Special Paper 110.
- Smith, J.P.
1927: Upper Triassic marine invertebrate faunas of North America; U.S. Geological Survey, Professional Paper 141.
- Souther, J.G.
1971: Geology and mineral deposits of Tulsequah map-area, British Columbia; Geological Survey of Canada, Memoir 362.
- Spath, L.F.
1934: The Ammonoidea of the Trias; British Museum (Natural History), London.
- Tatzreiter, F.
1978: Zur Stellung der **Himavatites columbianus** Zone (höheres Mittelnor) in der Tethys; Österreichische Akademie der Wissenschaften Schriftenreihe der Erdwissenschaftlichen Kommissionen, Bd. 4, p. 105-139.
- Tozer, E.T.
1958: Stratigraphy of the Lewes River Group (Triassic), central Laberge area, Yukon Territory; Geological Survey of Canada, Bulletin 43.
1962: Illustrations of Canadian Fossils, Triassic of Western and Arctic Canada; Geological Survey of Canada, Paper 62-19.
1967: A Standard for Triassic Time; Geological Survey of Canada, Bulletin 156.
1971: Triassic Time and Ammonoids: Problems and Proposals; Canadian Journal of Earth Sciences, v. 8, p. 989-1031.
1974: Definitions and limits of Triassic stages and substages: Suggestions prompted by comparisons between North America and the Alpine-Mediterranean region; Österreichische Akademie der Wissenschaften Schriftenreihe der Erdwissenschaftlichen Kommissionen, Bd. 2, p. 195-206.
- Urlichs, M.
1972: Ostracoden aus der Kössener Schichten und ihre Abhängigkeit von der Ökologie; Mitteilungen der Gesellschaft der Geologie- und Bergbaustudenten in Österreich, Bd. 21, p. 661-710.
- Westermann, G.E.G. and Verma, H.
1967: The Norian Pine River Bridge section, British Columbia and the succession of **Monotis**; Journal of Paleontology, v. 41, p. 798-803.
- Wiedmann, J.
1972: Ammoniten-Nuklei aus Schlammproben der nordalpinen Obertrias - ihre strammesgeschichtliche und stratigraphische Bedeutung; Mitteilungen der Gesellschaft der Geologie- und Bergbaustudenten in Österreich, Bd. 21, p. 561-622.
1973: Upper Triassic Heteromorph Ammonites, in Atlas of Palaeobiogeography (A. Hallam, Editor), p. 235-249, Elsevier, Amsterdam, London, New York.
- Zapfe, H.
1968: Fragen und Befunde von allgemeiner Bedeutung für die Biostratigraphie der alpinen Obertrias; Verhandlungen der Geologischen Bundesanstalt (Wien), 1967, Heft 1/2, p. 13-27.

Project 770023

Barry W. Smee and David J. Koop¹
Resource Geophysics and Geochemistry Division*Smee, B.W. and Koop, David J., The stability of some anions in natural water samples; in Current Research, Part B, Geological Survey of Canada, Paper 79-1B, p. 137-146, 1979.***Abstract**

Tests on anion stability were conducted over a pH range from 3 to 9 and anion concentrations encompassing three orders of magnitude. Synthetic solutions containing sulphate, chloride, fluoride, nitrate, and phosphate and various concentrations of clay-size particles (<2 µm) or humic acid were analyzed over a period of time to ascertain changes in sample equilibrium conditions for these anions. The concentration of anions in natural water samples appears to be stable for up to 170 hours over the pH range studied. Low concentrations of clay-size particles or humic acid do not significantly affect the concentration of anions in aqueous solutions, but clay concentrations of 10 000 mg/L significantly alter phosphate and chloride concentrations, while 1000 mg/L of a humic acid suspension at pH 5 adsorb fluoride and phosphate from the solutions examined.

Introduction

The stability of inorganic anions in aqueous solutions has not been adequately studied by applied geochemists. Little is known about the effect of pH and anion concentration on the shelf life of a water sample. Likewise, the presence of suspended solids or organic compounds in a water sample will alter the equilibrium conditions from those present in the natural environment. The development of ion chromatography as a rapid and sensitive analytical technique for the halogens, nitrate and sulphate in natural waters (Small et al., 1975; Smee et al., 1978) has permitted the study of a number of these parameters.

This communication summarizes the findings of a research program designed to measure the equilibrium changes of anions in both natural and artificial aqueous solutions. The complete study has been released as Geological Survey of Canada Open File 613.

Method

That portion of the study which examined the equilibrium and stability of anions under various conditions was subdivided into four separate analytical programs: inter-anion interferences and the effect of pH on sample solutions; a time stability study of natural groundwater samples; the effect of various concentrations of clay-sized particles such as might be found in stream bank or overburden water samples; and the effect of humic acids similar to those found in swampy environments. All stability studies were undertaken at a temperature of 22°C ± 2°C.

The inter-anion interference study involved three sets of solutions, analyzed for each of five anions: fluoride, chloride, phosphate, nitrate, and sulphate. One set of five solutions consisted of the subject anions only, the next set of the interferent anions only (to determine any blank contribution), and the last set of five solutions comprised the subject anions with interferent anions present. Subsequent to the analysis of the fifteen mixtures, each solution was adjusted with 0.1% NaOH from a pH of 3.0 or their unaltered pH (whichever was greater) to a pH of 9.0, by integral values. At each integral pH, the solutions were allowed to equilibrate for a day, then analyzed for the five anions.

Samples used in the time stability study were collected from wells near Milton, Ontario and stored in clear polyethylene screw-top bottles. At each of four sites, four samples of filtered and four of unfiltered water was obtained. One sample of each of the filtered and unfiltered splits was adjusted to pH 9.0 with 1% NaOH, one adjusted to pH 5.0

with HCl, one adjusted to pH 5.0 with H₂SO₄, and one sample set was unaltered. The resulting set of 32 solutions were analyzed the same day as collected, and again after 1 day, 3 days, 1 week, and 3 weeks.

Four solutions varying over two orders of magnitude in anion concentrations plus a blank solution containing distilled water only were each mixed with four clay concentrations of between 10 and 10 000 mg/L to determine the effect of suspended particles on anion equilibrium. A similar set of anion solutions plus a blank for each anion was combined with four humic acid suspensions varying between 1 and 1000 mg/L concentration. The natural glaciolacustrine clay sample was collected from Glacial Lake Iroquois sediments near Milton, Ontario. The clay was washed twice with distilled water and filtered through a type HA 0.45 µm Millipore filter prior to use. The cation exchange capacity of this clay was 13.0 meq/100g. The humic acid was obtained from K&K Laboratories Ltd., Plainview, N.Y.

Results

No appreciable effect of varying the anion concentrations or the pH was found with fluoride, chloride, nitrate, or sulphate. Data obtained for phosphate in the inter-anion interference study could not be interpreted because of a poisoned chromatographic column.

The time stability study using natural water samples showed that there was little difference between filtered and unfiltered sample sets. Adjustment of the pH of these natural samples did not alter the concentration of any anion, thus verifying the results found in the previous study. All data for all four samples lay within a previously established experimental error of less than ±10 per cent at the 95 per cent confidence level throughout the 20 day test period, suggesting that anion concentrations in these groundwater samples are stable for at least three weeks from the time of collection, and that polyethylene bottles are satisfactory for use in routine geochemical water sampling programs.

Results obtained from the addition of clay-sized particles to synthetic aqueous solutions indicated that only at the higher concentrations of clay does an appreciable change in anion concentration occur. Table 17.1 shows the anion contribution to the blank with time for each of the clay concentrations. For fluoride, clay concentrations up to 100 mg/L had a negligible effect. However at the 1000 mg/L and 10 000 mg/L concentrations of clay, a release of fluoride from the clay to solution was observed. This release and the new equilibrium was achieved in approximately 10 hours.

¹GEO ANALYTICAL SERVICES (WESTERN) LTD., Calgary, Alberta.

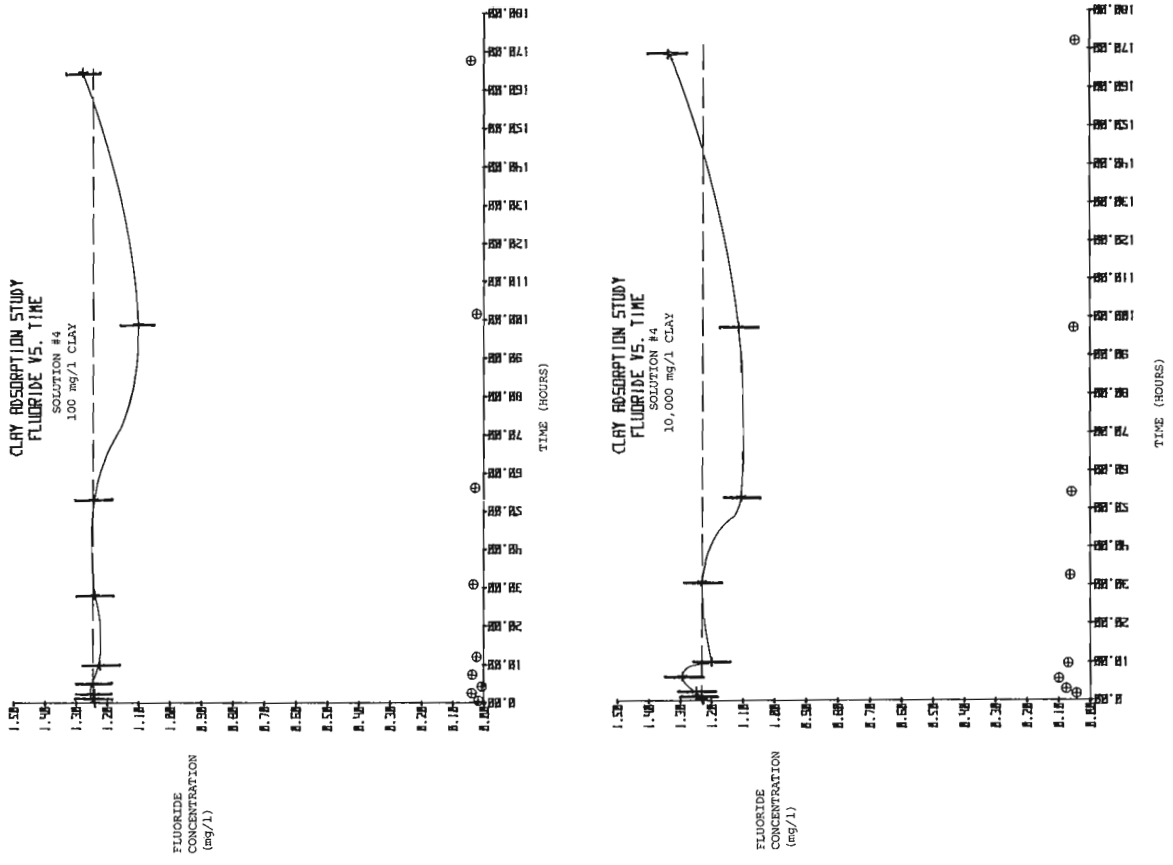


Figure 17.1. The effect with time of various concentrations of clay-sized particles on a solution containing 1.2 mg/L fluoride.

Table 17.1

Change of concentration of anions in control blank solution with time

Time Hours	F ⁻ mg/L	Cl ⁻ mg/L	NO ₃ ⁻ mg/L	PO ₄ ³⁻ mg/L	SO ₄ ²⁻ mg/L
CLAY CONCENTRATION OF 10mg/L					
1	0.006	0.002	0.0	0.0	0.0
2	0.002	0.06	0.0	0.0	0.0
6	0.019	0.04	0.0	0.0	0.0
11	0.009	0.09	0.0	0.0	0.0
25	0.0	0.08	0.0	0.0	0.0
58	0.0	0.0	0.0	0.0	0.0
98	0.02	0.0	0.04	0.0	0.04
176	0.006	0.0	0.0	0.0	0.0
CLAY CONCENTRATION OF 100 mg/L					
1	0.005	0.04	0.0	0.0	0.04
2	0.0	0.06	0.0	0.0	0.04
6	0.015	0.08	0.0	0.0	0.0
11	0.005	0.04	0.0	0.0	0.04
28	0.006	0.09	0.0	0.0	0.04
55	0.007	0.06	0.0	0.0	0.04
100	0.005	0.01	0.0	0.0	0.04
165	0.018	0.10	0.0	0.0	0.04
CLAY CONCENTRATION OF 1000 mg/L					
1	0.008	0.05	0.0	0.0	0.0
2	0.005	0.04	0.0	0.0	0.0
5	0.058	0.04	0.0	0.0	0.0
35	0.01	0.10	0.0	0.0	0.0
52	0.01	0.04	0.0	0.0	0.0
95	0.005	0.06	0.0	0.0	0.0
171	0.02	0.05	0.0	0.0	0.0
CLAY CONCENTRATION OF 10 000 mg/L					
1	0.038	0.28	0.04	0.0	0.04
2	0.048	0.35	0.11	0.0	0.08
5	0.088	0.39	0.11	0.0	0.12
10	0.059	0.32	0.10	0.0	0.12
30	0.058	0.26	0.08	0.0	0.18
55	0.055	0.16	0.08	0.0	0.26
95	0.069	0.13	0.08	0.0	0.31
168	0.065	0.28	0.08	0.0	0.38

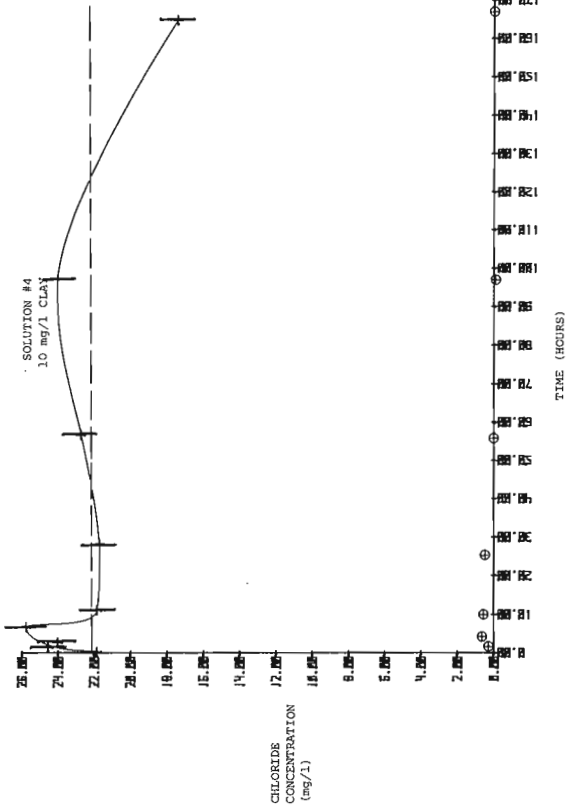
Chloride, nitrate, and sulphate were desorbed almost immediately only at the highest clay concentration, however only the sulphate exhibited a continuous release to solution with time but only at clay concentrations of 10 000 mg/L.

Examples of equilibrium changes for each anion at each of the clay concentrations studied are presented in Figures 17.1 and 17.5. Dashed lines represent the initial anion concentration before the addition of clay, solid lines depict the actual concentrations found at various times after the clay addition. Vertical bars represent the error limits of the analyses (Smee et al., 1978). The circled crosses represent the blank contribution. Fluoride, nitrate, and sulphate all exhibited a rapid shift in equilibrium within the first 10 hours of the experiment, then returned to values that fall close to experimental limits of the pre-clay concentrations. The shift in chloride concentration in the 10 000 mg/L clay sample suggests that a complex equilibrium condition exists between the particles and the anion in solution probably involving both surface and interlayer bonding sites.

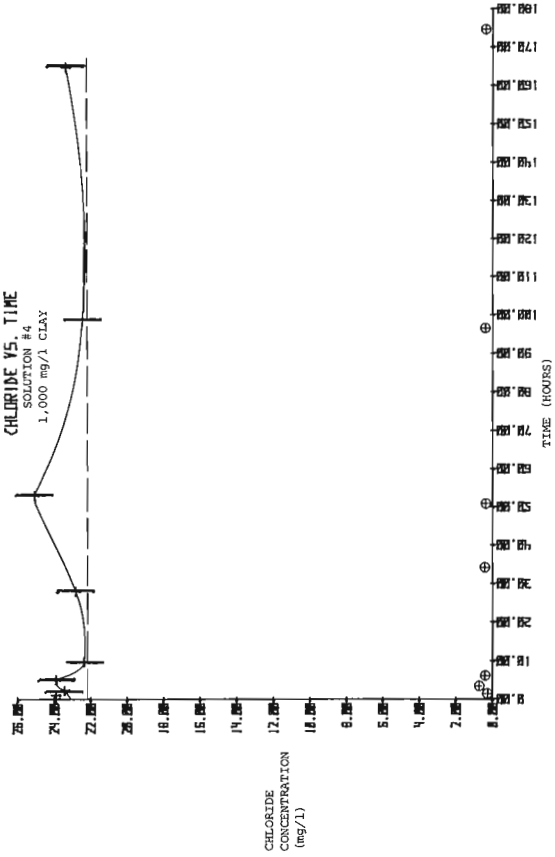
Phosphate, in the presence of 10 mg/L and 100 mg/L of clay did not exhibit significant changes in concentration. At higher clay concentrations a rapid adsorption of phosphate from solution was observed; equilibrium being achieved within 10 hours of the initiation of the experiment. The adsorption of phosphate by clay minerals has been noted by other workers (Wada, 1959) and appears to be related to interaction with Al-OH₂⁺ groups (Hingston et al., 1967).

The humic acid study revealed a small contribution to the blank solution for fluoride and sulphate. No contribution from the humic acid was measured for chloride, phosphate or nitrate. A significant adsorption of fluoride by the humic acid suspension was noted only at the 1000 mg/L clay concentration; the reduction in fluoride being 0.2 mg/L in the 1.0 mg/L fluoride solution (Fig. 17.6). Phosphate was also adsorbed from solution, with 0.25 mg/L phosphate being lost when in the presence of 1000 mg/L humic acid (Fig. 17.7). Analogous to the clay study, all equilibrium shifts occurred within the first 10 hours of the study.

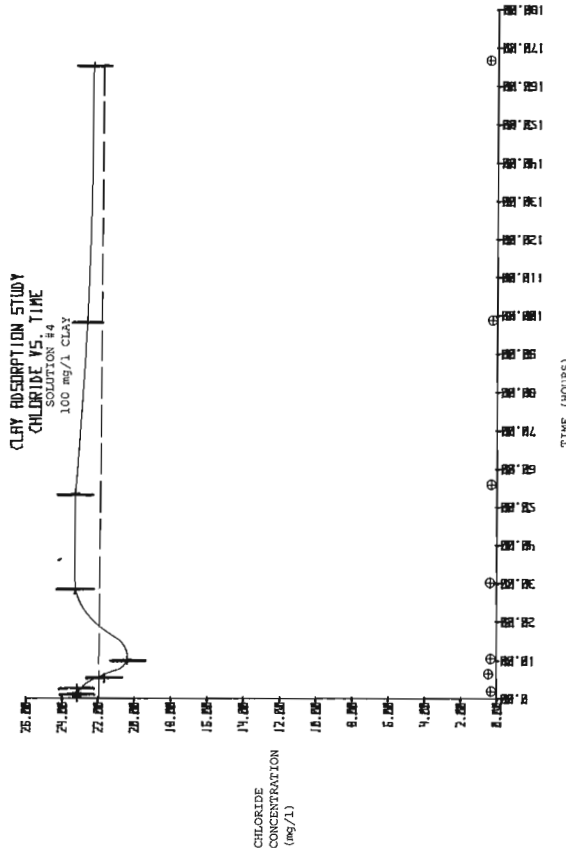
CLAY ADSORPTION STUDY
CHLORIDE VS. TIME



CLAY ADSORPTION STUDY
CHLORIDE VS. TIME



CLAY ADSORPTION STUDY
CHLORIDE VS. TIME



CLAY ADSORPTION STUDY
CHLORIDE VS. TIME

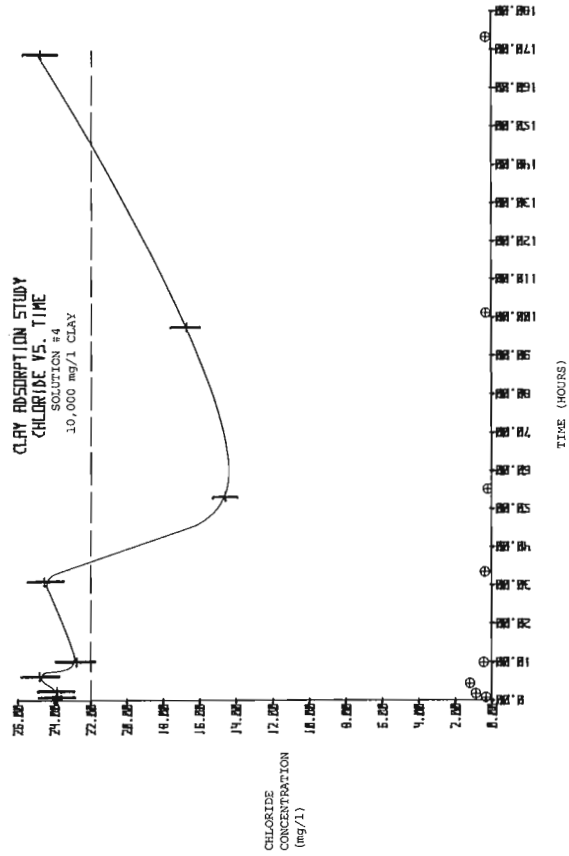


Figure 17.2. The effect with time of various concentrations of clay-sized particles on a solution containing 22 mg/l chloride.

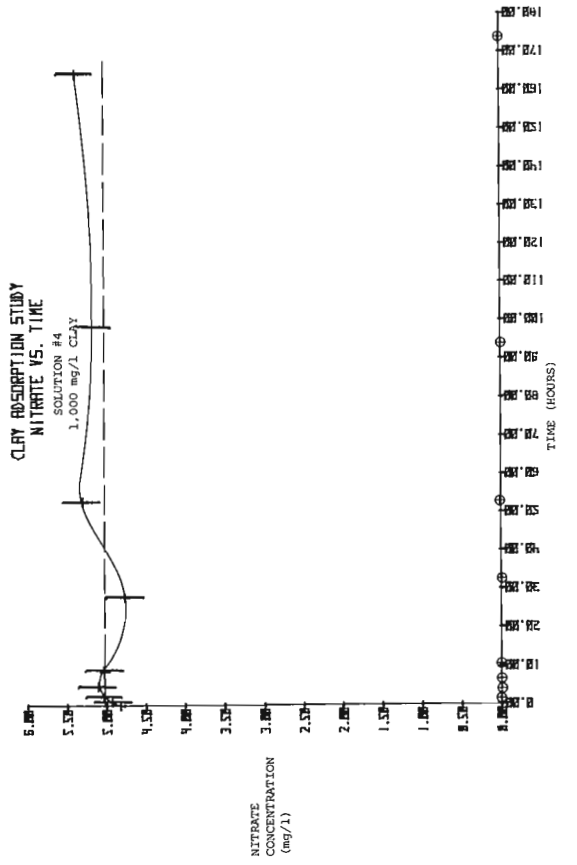
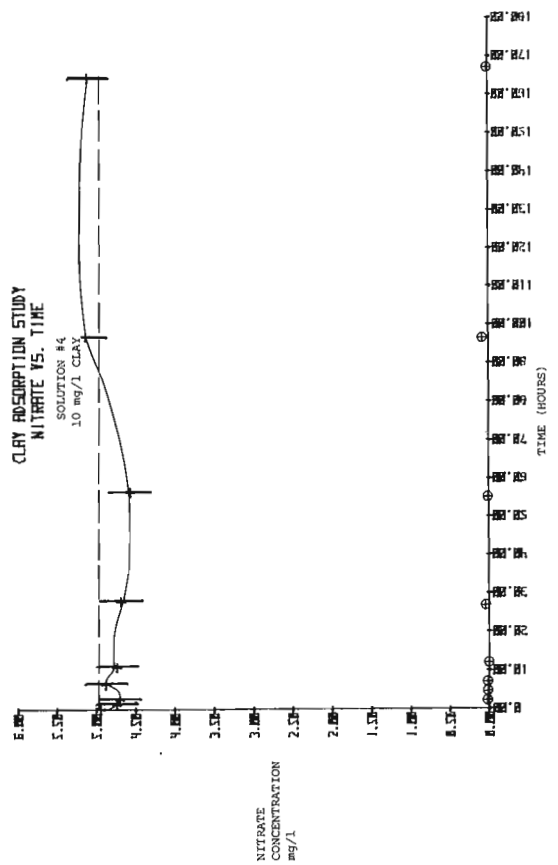
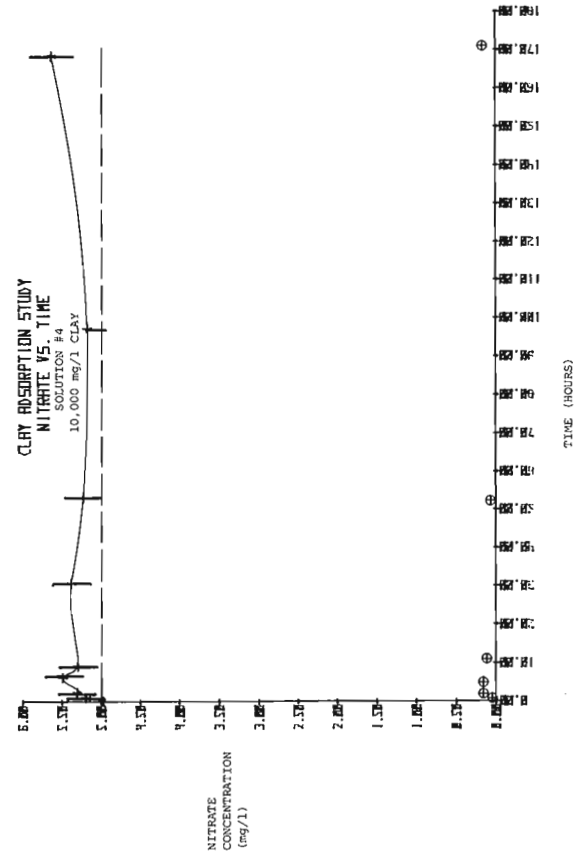
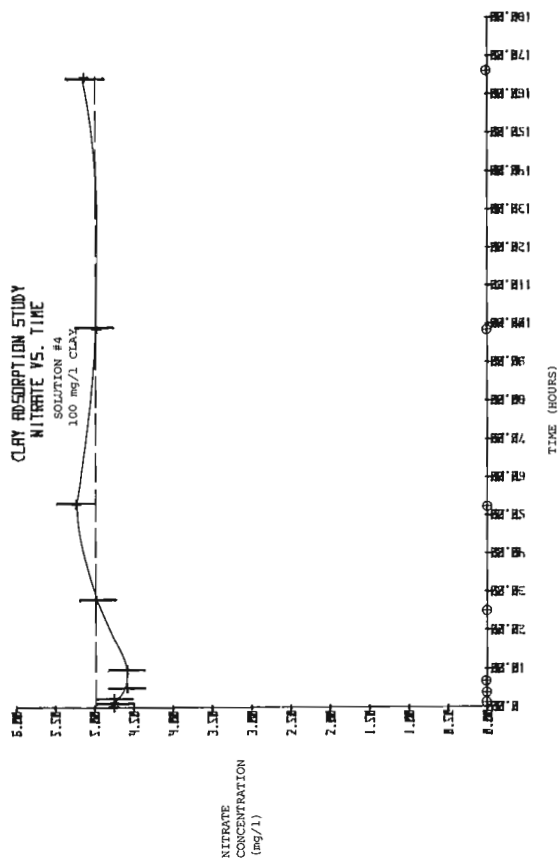


Figure 17.3. The effect with time of various concentrations of clay-sized particles on a solution containing 5 mg/L nitrate.

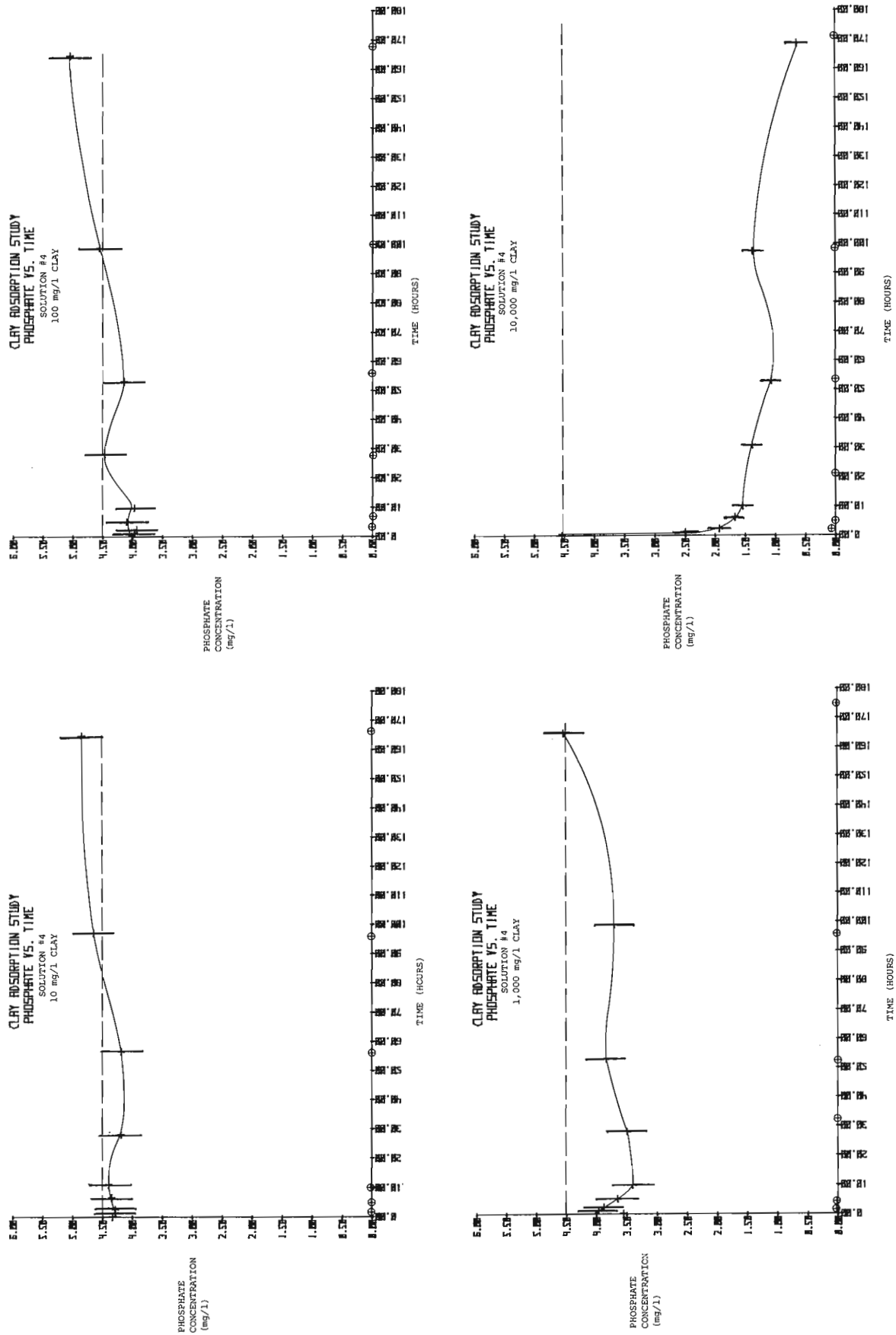


Figure 17.4. The effect with time of various concentrations of clay-sized particles on a solution containing 4.5 mg/L phosphate.

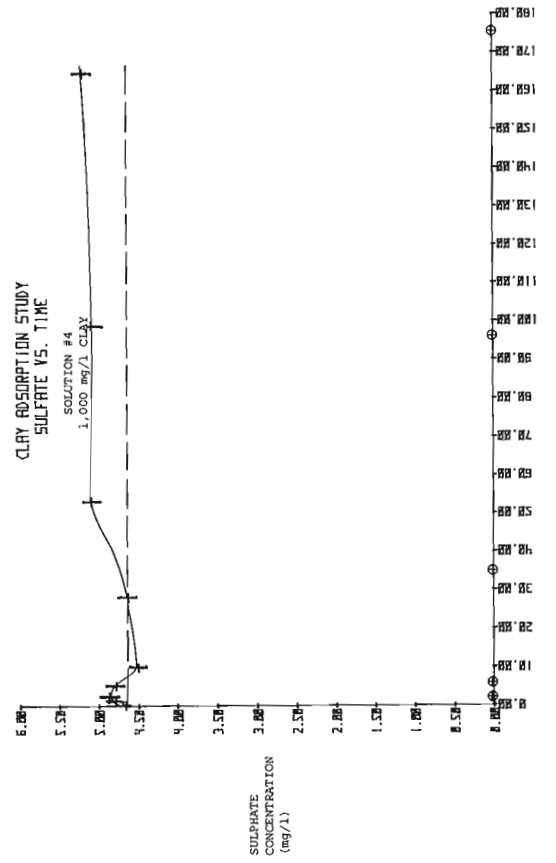
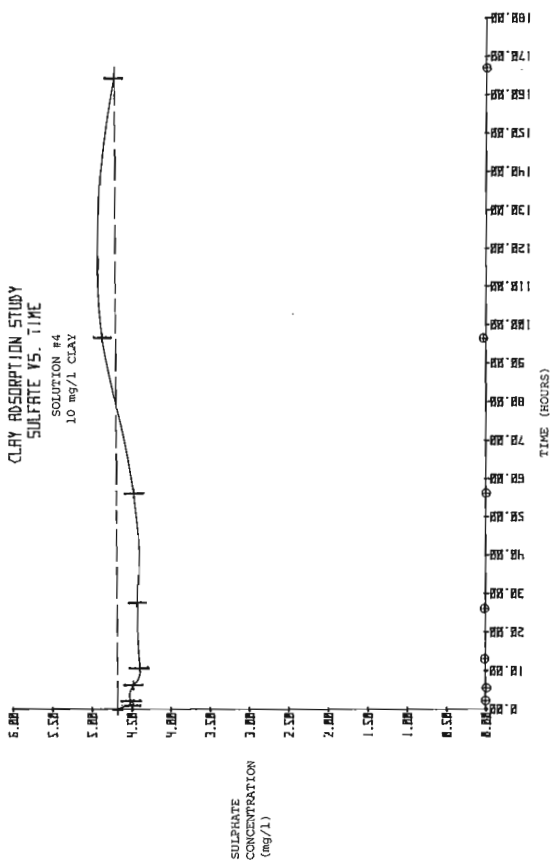
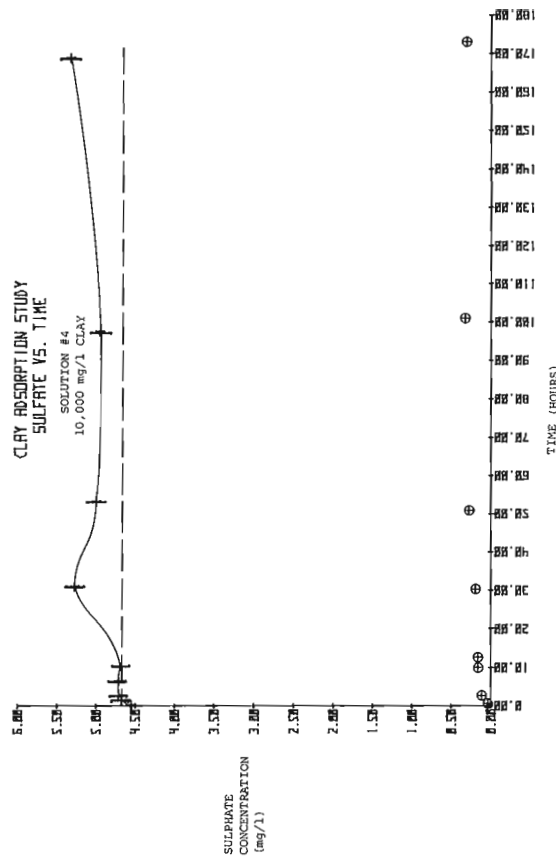
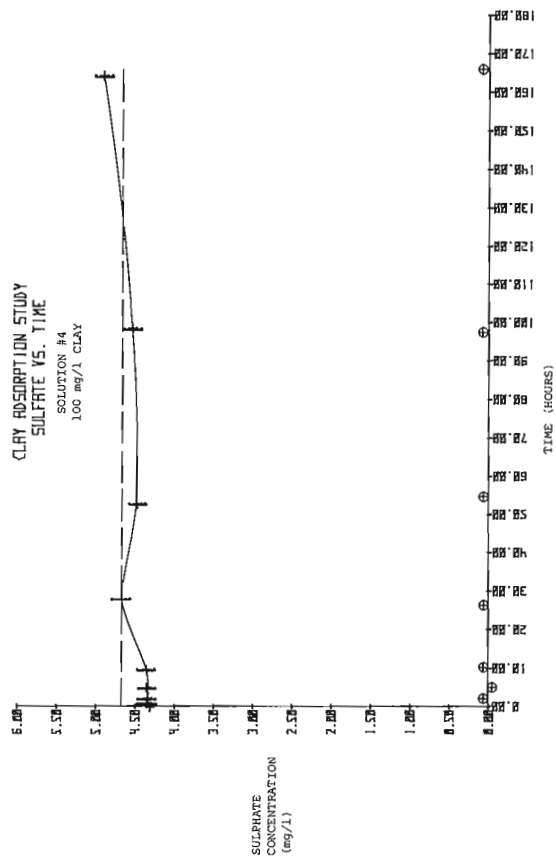
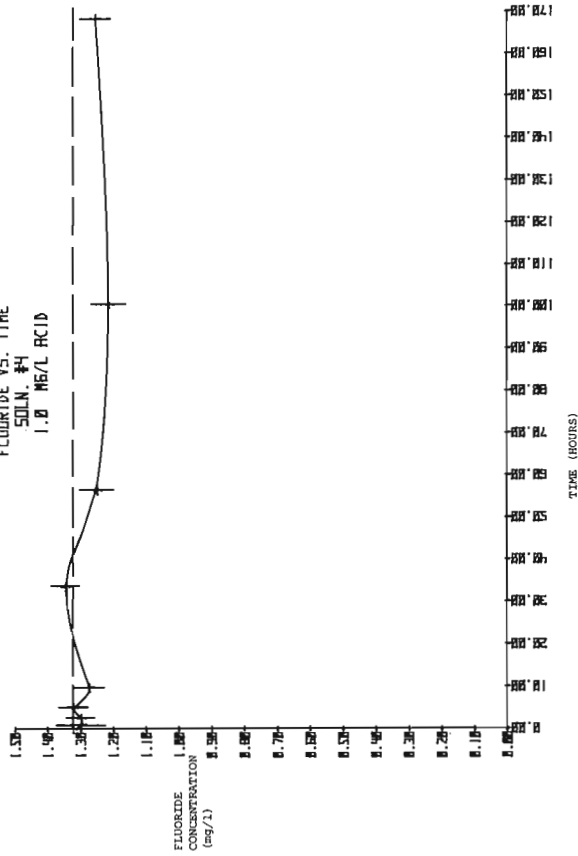
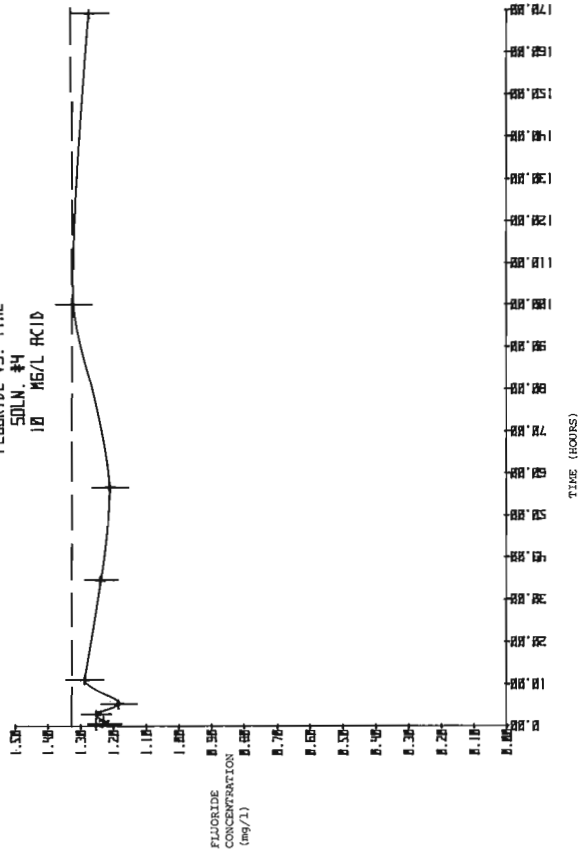


Figure 17.5. The effect with time of various concentrations of clay-sized particles on a solution containing 4.6 mg/L sulphate.

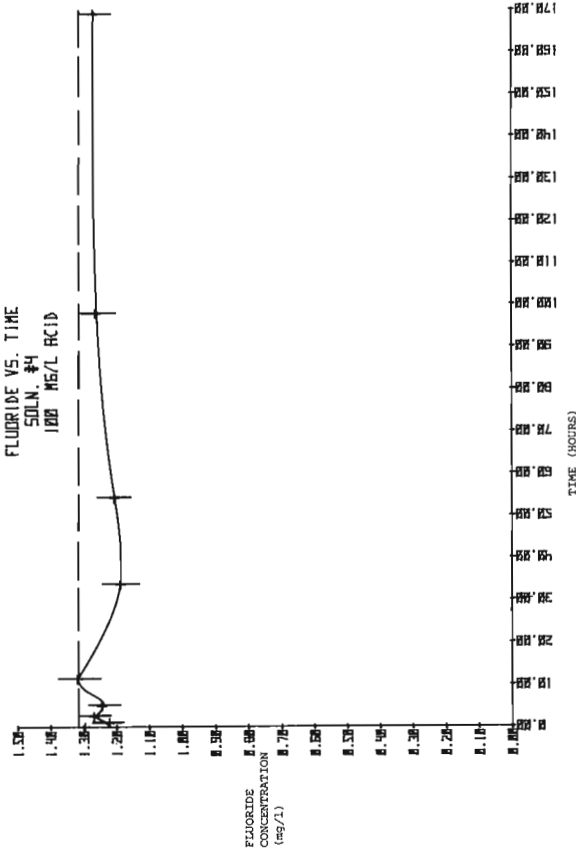
HUMIC ACID EFFECT STUDY
FLUORIDE VS. TIME
SOLN. #4
1.0 MG/L ACID



HUMIC ACID EFFECT STUDY
FLUORIDE VS. TIME
SOLN. #4
10 MG/L ACID



HUMIC ACID EFFECT STUDY
FLUORIDE VS. TIME
SOLN. #4
100 MG/L ACID



HUMIC ACID EFFECT STUDY
FLUORIDE VS. TIME
SOLN. #4
1000 MG/L ACID

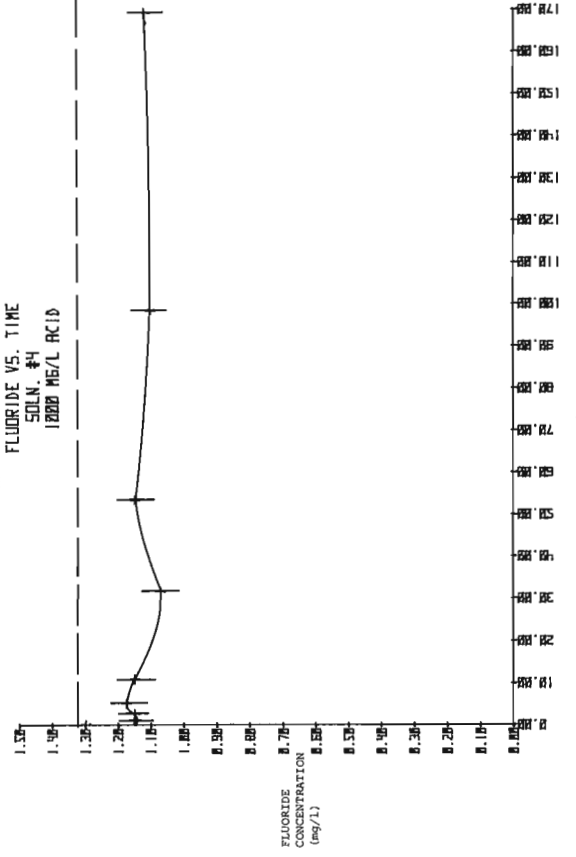


Figure 17.6. The effect with time of various concentrations of humic acid suspensions on a solution containing 1.32 mg/L fluoride.

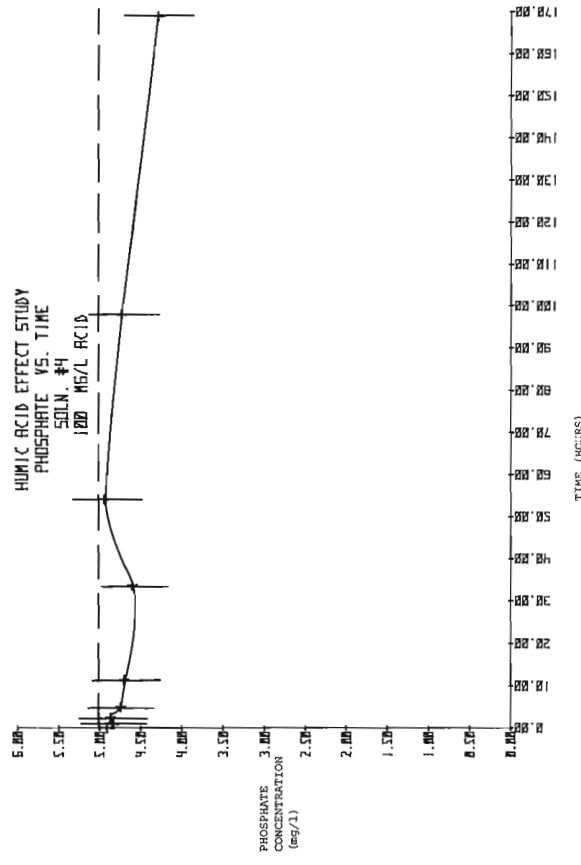
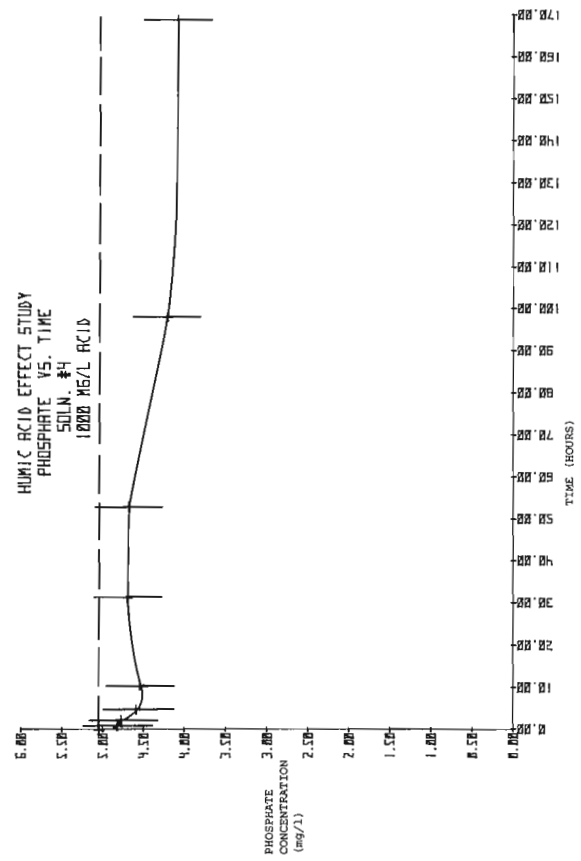
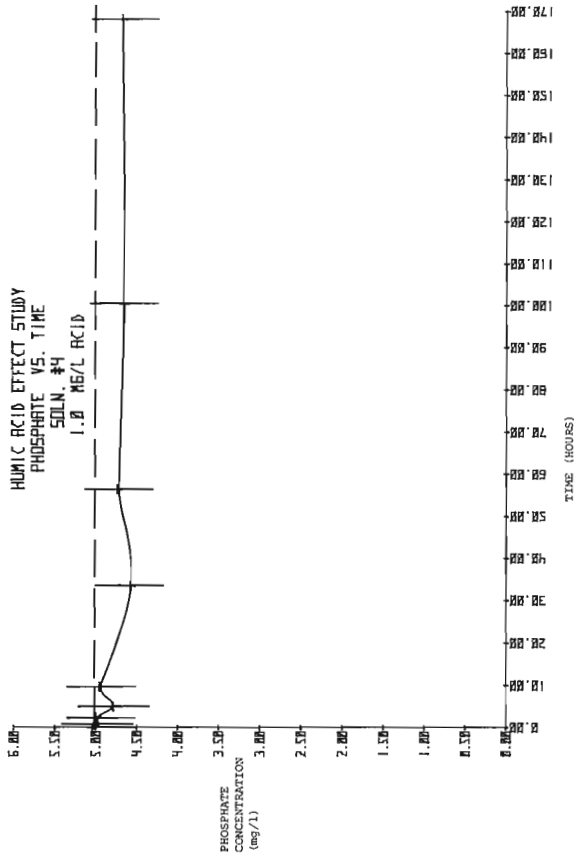
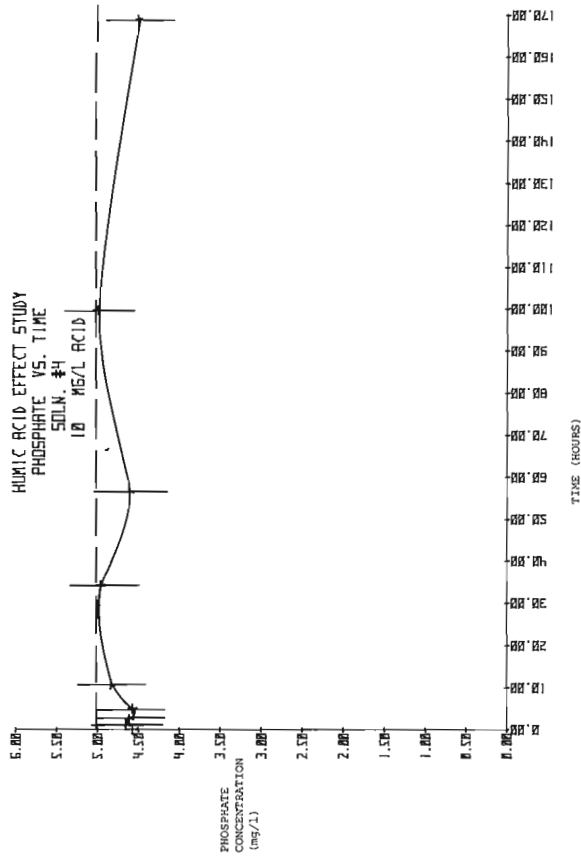


Figure 17.7. The effect with time of various concentrations of humic acid suspensions on a solution containing 5.00 mg/L phosphate.

Conclusions

The concentration of anions in natural water samples is stable with time over a wide range of pH conditions. Low concentrations of clay-sized particles or humic acid do not significantly affect the concentration of anions in aqueous solutions. Only at high concentrations of a humic acid suspension is fluoride adsorbed, and at high concentration of both clay and humic acid is there a decrease from solution in the phosphate concentration.

These results indicate that the anionic components of natural waters can be incorporated on a routine basis into geochemical surveys to either serve as direct guides to mineralization, or to aid in delineating the origin of cationic components.

References

Smee, B.W. and Koop, D.J.

- 1979: Evaluation of the ion chromatographic analytical technique for the determination of inorganic anions in natural waters exhibiting a wide range of pH, organic content and suspended load conditions; Geological Survey of Canada, Open File Report 613, 126 p.

- Hingston, F.J., Atkinson, R.J., Posner, A.M., and Quirk, J.P.
1967: Specific adsorption of anions; *Nature*, v. 215, p. 1459-1461.
- Small, H., Stevens, T.S., and Bauman, W.C.
1975: Novel ion-exchange chromatographic method using conductimetric detection; *Analytical Chemistry*, v. 47, no. 11, p. 1801-1809.
- Smee, B.W., Hall, G.E.M., and Koop, D.J.
1978: Analysis of fluoride, chloride, nitrate and sulfate in natural waters using ion chromatography; *Journal of Geochemical Exploration*, v. 10, p. 245-258.
- Wada, K.
1959: Reaction of phosphate with allophane and halloysite; *Soil Science*, v. 87, p. 325-330.

Project 780033

T.W. Anderson
Terrain Sciences Division

Anderson, T.W., *Stratigraphy, age, and environment of a Lake Algonquin embayment site at Kincardine, Ontario; in Current Research, Part B, Geological Survey of Canada, Paper 79-1B, p. 147-152, 1979.*

Abstract

Terrace sediments along North Penetangore River contain fossiliferous, silty clay over till and under sand and interbedded sand, silt, and clay. The clay bed and pollen, plant macrofossils, molluscs, and ostracodes extracted from it are interpreted as having accumulated in a lagoonal-alluvial environment behind a baymouth bar of Lake Algonquin. Wood in the clay bed dates $11\,300 \pm 140$ years. Since the lagoonal-alluvial habitat existed contemporaneously with main Lake Algonquin, the date provides an age for the high-water stand of main Lake Algonquin in the Lake Huron basin. The overlying interbedded sand-silt-clay sequence is believed to be a post-Algonquin floodplain deposit. The top of the terrace sediments is the surface of the floodplain deposits modified by postglacial alluvial activity.

Introduction

Reconnaissance studies carried out along the eastern shore of Lake Huron from 1968 to 1975 have revealed several terrace exposures in many river and stream valleys entering Lake Huron. These valley terraces have evolved as a result of changing lake levels accompanied by stream dissection from the time of Lake Algonquin to the Nipissing stage (Karrow, 1978).

Two such terrace sections along Eighteen Mile River have been discussed previously by Karrow et al. (1975) and Ashworth (1977). The tops of the terraces correspond to the Lake Algonquin terrace occurring along the Lake Huron shore. An estuarine-alluvial sequence yielded wood, peat layering, pollen, plant macrofossils, molluscs, ostracodes, and insect remains. The wood was radiocarbon-dated at $10\,500 \pm 150$ and $10\,600 \pm 160$ years (GSC-1126, -1127). The fossil assemblages provide evidence that the sequence accumulated in an estuarine environment at the time main Lake Algonquin stood in the Lake Huron basin.

At nearby Kincardine Bog (Fig. 18.1), fossiliferous, organic-bearing, fine grained sediments indicate that a lagoonal habitat existed $11\,200 \pm 170$ years ago (GSC-1374) (Karrow et al., 1975). The lagoonal habitat was interpreted as a low-level environment brought about when early Lake Algonquin drained via the Kirkfield opening into the Lake Ontario basin.

This paper deals with another valley terrace section exposed along the south bank of North Penetangore River, 1.6 km upstream at Kincardine, Ontario (Fig. 18.1). The section was first visited in 1972, and sediment samples were collected for pollen analysis and wood for radiocarbon dating. The site was revisited in 1977, and bulk samples were collected for shell and plant macrofossil determinations. In this paper, the stratigraphy is described and interpreted, the paleoenvironment is reconstructed, and the sequence of events is compared to those at Eighteen Mile River and Kincardine Bog.

Acknowledgments

P.F. Karrow drew my attention to the North Penetangore River exposure and provided elevation data for the terrace section and Lake Algonquin baymouth bar. M.F.I. Smith and L.D. Delorme kindly identified the molluscs and ostracodes, respectively. J.V. Matthews, Jr. helped to identify some of the seeds. W. Blake, Jr. reviewed the manuscript.

Physiographic Setting and Stratigraphy

The North Penetangore River site falls within the Huron Slope and Huron Fringe physiographic regions of Chapman and Putnam (1966). The prominent features of the area are the shorelines of glacial lakes Warren and Algonquin and the

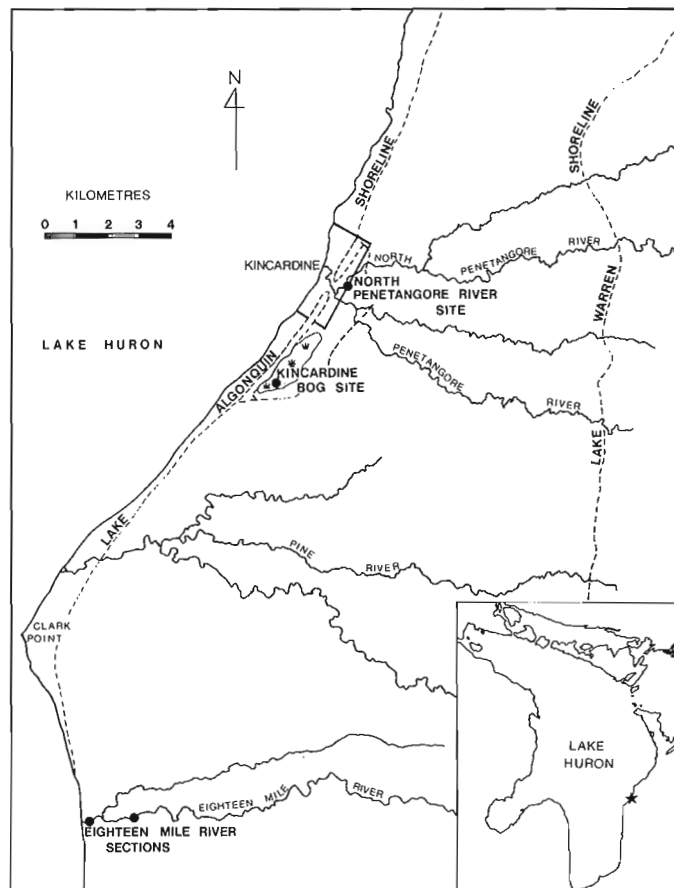


Figure 18.1. Map of the Kincardine district of Ontario showing the shoreline positions of glacial lakes Warren and Algonquin and locations of sites discussed in the text. The stippled area represents a massive baymouth bar of Lake Algonquin.

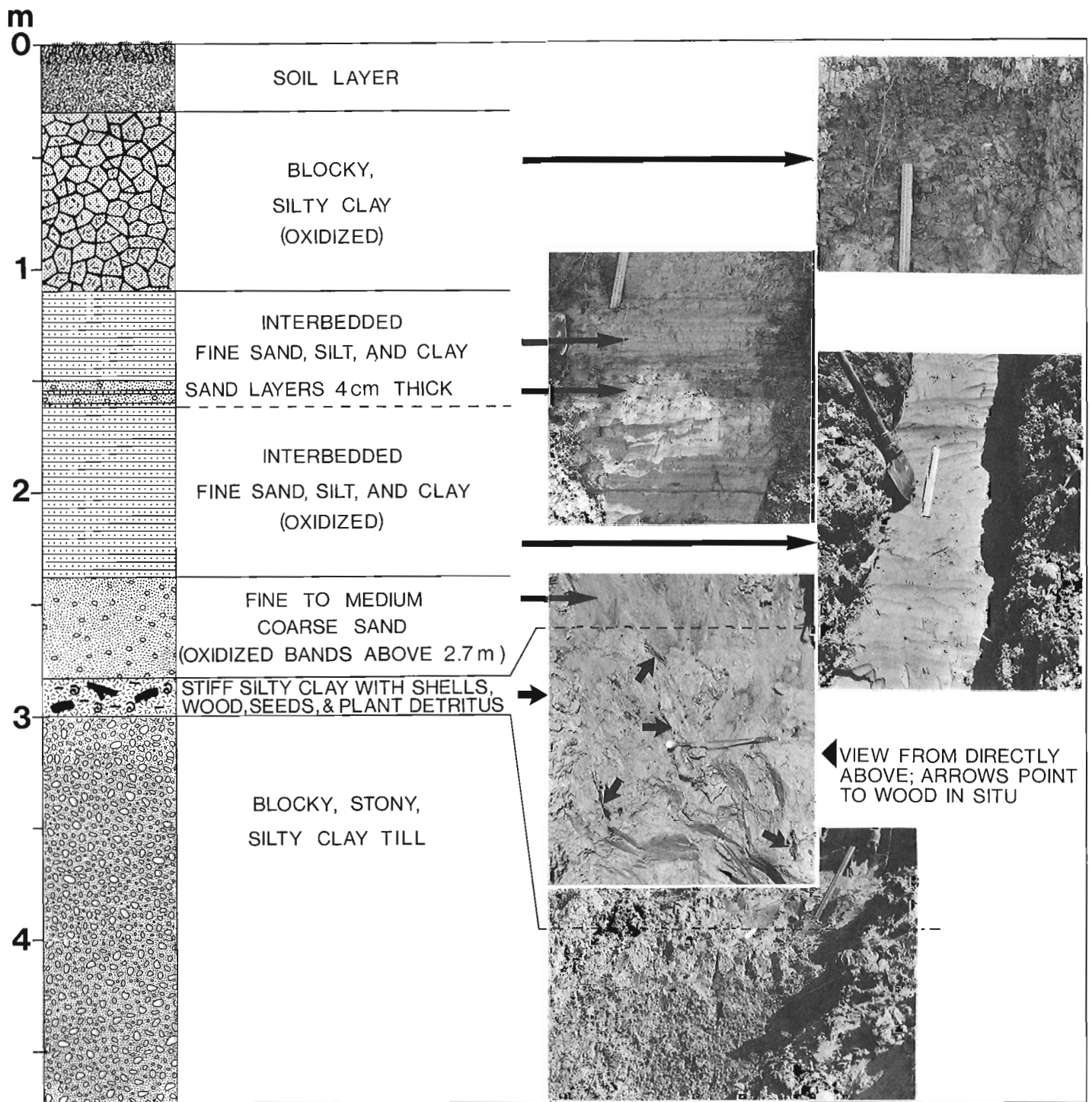


Figure 18.2. Stratigraphic sequence at the North Penetangore River section. GSC 175478, -80, -82, -88, -94.

wave-cut terrace of Lake Nipissing. The upland topography is characterized by the Warren clay plain which slopes gently towards Lake Huron. The clay plain and Algonquin shore bluff are dissected by several streams and rivers entering into Lake Huron, most notably, the North Penetangore, Penetangore, Pine, and Eighteen Mile River systems.

The Lake Algonquin shoreline is well developed from Clark Point northward (Fig. 18.1). South of Kincardine it swings inland from Lake Huron and parallels the lake east of

Kincardine Bog and the North Penetangore River site, and curves towards the lake again north of Kincardine. A massive baymouth gravel beach bar was built by Lake Algonquin across the mouth of Penetangore River west of the north branch (Fig. 18.1). The crests of the baymouth bar and inner beach ridge lie at 200 and 200.9 m elevation, respectively, in the Kincardine Bog area (P.F. Karrow, pers. comm., 1972).

The stratigraphic sequence at the site is shown in Figure 18.2. Till extends from river level up to within 3 m

Table 18.1

Relative pollen percentages from three horizons in the North Penetangore River exposure

Pollen Taxa	Per cent of tree and shrub pollen		
	273 cm	303 cm	308 cm
TREES			
<i>Picea</i>	78.8	31.7	83.5
<i>Pinus</i>	7.6	5.6	3.8
<i>Larix</i>		1.1	
<i>Betula</i>		1.4	0.8
<i>Populus</i>		0.4	0.8
<i>Quercus</i>	4.3	3.3	1.2
<i>Carpinus-Ostrya</i>	1.6	1.6	0.4
All other trees	2.6	2.2	0.8
SHRUBS			
<i>Juniperus</i>	2.1	1.4	0.4
<i>Alnus</i>	0.5	0.4	
<i>Salix</i>	1.6		
<i>Elaeagnus commutata</i>		12.3	1.6
<i>Shepherdia canadensis</i>	0.5	38.0	6.3
HERBS			
Cyperaceae	35.3	7.2	8.0
Gramineae	3.8	1.1	
Tubuliflorae	2.1	3.7	1.6
Liguliflorae		0.2	
Ambrosieae	1.6	0.7	
<i>Artemisia</i>	1.0	2.1	1.2
Chenopodiineae		0.2	0.8
<i>Dryas integrifolia</i>	0.5	0.2	
<i>Thalictrum</i>	1.0	0.2	
Saxifragaceae		0.2	0.4
Cruciferae	0.5		
<i>Urtica</i>			0.4
<i>Humulus</i>		0.2	
Pteridophyta	0.5	2.3	1.2
<i>Equisetum</i>	1.0	0.7	
<i>Selaginella Selaginoides</i>	8.1		
Indeterminable - Unknown	10.8	17.0	7.1
Pollen sums	184	428	237
Total grains counted	311	598	288

from the top of the section. Stony, silty clay till grades into compact, silty clay containing many wood fragments, plant detritus, and invertebrate shells. The clay layer is approximately 20 cm thick and is overlain by 173 cm of interbedded, waterlain fine sand, silt, and clay and 45 cm of fine to medium-coarse sand. The fine sand-silt-clay sequence contains coarse sand layers up to 4 cm thick and is highly oxidized in the lower half. Less than 1 m of blocky (oxidized) silty clay overlies the interbedded sequence, and a soil layer is developed at the top of the section.

Methods

The upper part of the exposure was cleared of slump debris, and a fresh surface was described and sampled for pollen and megafossils. Samples for pollen generally were taken at 10 cm intervals, but at the top of the till and in the overlying, compact silty clay samples were collected at 5 cm intervals. Bulk samples and 5 cm-increment samples of the silty clay were removed for fossil determinations, and large pieces of wood were collected for radiocarbon dating.

Samples for pollen were treated according to the acetolysis/HF procedure of Faegri and Iversen (1964). Up to approximately 425 tree and shrub pollen counts were made, upon which all taxa were calculated as percentages.

Plant macrofossils, molluscs, ostracodes, and insect remains were extracted from the bulk samples after the sediment was soaked in water and washed through a 100 mesh (149 μ m) sieve. Oven drying followed by wet sieving facilitated disintegration of the clay matrix.

Results

Pollen

Pollen is generally lacking and poorly preserved, especially in the oxidized sediments. In three samples (from 273, 303, 308 cm depth) from the top of the till and overlying sediments, however, pollen is well preserved and is of sufficient concentration for percentage calculations as shown in Table 18.1.

All three samples are characterized by relatively high percentages of *Picea* and Cyperaceae and low percentages of *Pinus*, hardwood, and upland herb pollen. Pollen percentages of the shrubs, *Elaeagnus commutata* and *Shepherdia canadensis* are unusually high, as much as 12.3 and 38%, respectively. Microspores of *Selaginella Selaginoides* are also abundant (8.1%) in one sample.

Wood and Plant Macrofossils

The wood was compressed and lignified, and so detailed identification was not possible. One large piece, identified as either *Picea* or *Larix* sp. by L.D. Farley-Gill (unpublished Wood Identification Report No. 73-9), gave a radiocarbon date of $11\ 300 \pm 140$ years (GSC-1842).

Table 18.2 lists the plant macrofossils extracted from the silty clay bed. The assemblage is characterized by (undifferentiated) spruce needles (amounting to as many as 20 per 100 g of sediment), seeds of *Potentilla anserina* and *Juncus* sp., and oogonia of the Characeae. Shrub and herb seeds identified include *Rumex fenestratus* type, *Arctostaphylos Uva-ursi*, *Ranunculus Cymbalaria*, *Potentilla nivea* type, *Fragaria vesca*, and *F. virginiana*. Of the aquatics, Characeae (over 200 oogonia per 100 g of sediment), *Zannichellia palustris*, and *Juncus* sp. predominate. Least common are leaves of *Myriophyllum* cf. *verticillatum*, seeds of *Carex aquatilis*, *Potamogeton filiformis*, *P. alpinus*, and macrospores of *Selaginella Selaginoides*.

Invertebrate Shells

Table 18.3 shows the taxa and numbers of molluscs and ostracodes extracted from the silty clay bed. Numbers of molluscs range from 32 and 36 specimens per 100 g of sediment in the upper increments of the clay bed to only 6 in the lowest increment; numbers of ostracodes are also highest in the upper increment, amounting to as many as 267 valves per 100 g of sediment.

Terrestrial molluscs predominate, but the majority of the specimens are juveniles (M.F.I. Smith, pers. comm., 1978). The more abundant molluscs are identifiable only to the family Succineidae and to the genus *Pupilla*. Only seven freshwater species of molluscs occur; *Fossaria parva*, *Gyraulus deflectus*, and *Pisidium compressum* dominate.

The ostracode fauna consists of 13 species (Table 18.3). The fauna is characterized by a predominance of the shallow stream species, *Ilyocypris bradyi*, and by only minor occurrences of lacustrine species.

Table 18.2

Taxa and numbers of plant macrofossils extracted from the fossiliferous silty clay bed at the North Penetangore River exposure. Relative numbers in overall sample represent an analysis of several bulk samples plus the three 100 g-increment samples

Plant Macrofossil Taxa	Relative numbers in overall sample	Numbers per 100 g of sediment		
	283-300 cm	Increment 283-289 cm	Increment 289-295 cm	Increment 295-300 cm
TREES				
<i>Picea</i> (needles)	109	14	20	1
<i>Picea</i>	1		1	
<i>Larix</i> (needles)	3		1	
SHRUBS AND HERBS				
<i>Rumex fenestratus</i> type	1			
<i>Viola</i> sp.	6		1	
<i>Arctostaphylos Uva-ursi</i>	1			
<i>Ranunculus Cymbalaria</i>	2			1
<i>Potentilla anserina</i>	60	3	8	1
<i>Potentilla nivea</i> type	2			
<i>Fragaria vesca</i>	2			
<i>Fragaria virginiana</i> cf. v. <i>platypetals</i>	1			
cf. <i>Veronica</i> sp.	5		1	3
AQUATICS				
Characeae (oogonia)	Numerous	Numerous	250+	4
<i>Myriophyllum</i> cf. <i>verticillatum</i> (leaves)	6		6	
<i>Zannichellia palustris</i>	12	5	4	
<i>Potamogeton filiformis</i> type	1			
<i>Potamogeton alpinus</i> type	1			
<i>Potamogeton</i> sp.	2	1	1	
<i>Carex aquatilis</i>	6	1		1
<i>Juncus balticus</i> type	23	10	11	
<i>Juncus</i> sp.	13	1	11	1
<i>Selaginella Selaginoides</i> (macrospores)	3	2	1	
Indeterminable -- Unknown	60	40	2	1

Interpretation

Stratigraphy

The exposed terrace section indicates a sequence of events beginning at least 13 000 years ago. The upper part of the till sequence is characterized by a stony, silty clay till which is the St. Joseph Till (P.F. Karrow, pers. comm., 1979) as mapped by Cooper and Clue (1974) farther to the south. The till was deposited by an advance of the Huron lobe during the Port Huron Stadial and is radiocarbon-dated at $13\,100 \pm 110$ years (GSC-2213; Lowdon and Blake, 1976).

Fossiliferous, compact silty clay unconformably overlies the till. The unconformity is thought to represent the time interval from about 13 000 years ago up to the time of main Lake Algonquin in the sequence of glacial events. The till had been eroded and reworked during this interval as pollen, plant detritus, and shell fragments extend about 10 cm into the till. Thus any trace of the high-level glacial lakes, Warren to early Algonquin, and the subsequent Kirkfield low-level stage, is missing here, although the inner gravel bar (Fig. 18.1) is believed to represent an embayment shoreline of early Lake Algonquin.

The fossiliferous, silty clay bed is interpreted as a lagoonal deposit, the origin of which is related to the return to high lake levels (main Lake Algonquin) in the Lake Huron basin. Main Lake Algonquin built a baymouth bar across the mouth of the modern Penetangore River, and lagoonal sedimentation commenced inside of the bar about 11 160 to 11 440 years ago according to the radiocarbon date (GSC-1842) on wood recovered from the silty clay bed.

Fine to medium-coarse sand on top of the fossiliferous clay bed presumably was deposited by streams entering the lagoon, by erosion of the baymouth bar, or by offshore winds. The lagoonal habitat became progressively shallower, and lagoonal sedimentation ceased completely when main Lake Algonquin, which would have acted as the headwater for the lagoon, dropped to the Stanley low-stage (Hough, 1963) in the Lake Huron basin.

The interbedded, waterlain, fine sand-silt-clay sequence, interrupted by discontinuous sand layering, is interpreted as a post-Algonquin floodplain deposit. The sequence is horizontally bedded and is strongly oxidized towards the base, presumably as a result of postdepositional groundwater seepage.

Table 18.3

Taxa and numbers of mollusc and ostracode specimens extracted from bulk samples of the silty clay bed at the North Penetangore River exposure

MOLLUSCS	Relative numbers
Gastropoda	
Terrestrial species	
Succineidae	
Succineidae	80
Pupilla(?) sp. (too small to identify)	38
Columella alticola (Ingersoll)	17+fragments
Pupilla muscorum (L)	14+fragments
Catinella avara (Say)	5±
Oxyloma retusa (Lea)	3±
Vallonia cf. albula Sterki	3
Freshwater species	
Fossaria parva (Lea)	8
Gyraulus deflectus (Say)	5
Fossaria sp. (juv.)	3
Valvata tricarinata Say	2
Valvata sincera (juv.) Say	2
Amnicola limosa Say	1
Pelecypoda	
Pisidium compressum Prime	5 values
OSTRACODES	
Ilyocypris bradyi Sars	92
Limnocythere itasca Cole	32
Limnocythere pseudoreticulata Staplin	22
Candona caudata Kaufmann	18
Cypridopsis vidua Muller	11
Candona parahoensis Staplin	8
Cyclopypris laevis (Muller)	7
Ilyocypris gibba (Ramdohr)	6
Cytherissa lacustris (Sars)	3
Lymnocythere sp.	3
Candona candida (Muller)	2
Cyclopypris sharpei Furtos	2
Cyprinotus sp.	2

The blocky, silty clay at the top is believed to represent alluvium derived from erosion upstream and possibly also from the upland Warren lake plain during postglacial time. The top of the terrace section, at 193.8 m elevation (P.F. Karrow, pers. comm., 1979), represents the surface of the older floodplain deposit modified by postglacial alluvial activity.

Paleoenvironment

Fossil remains were recovered only from the top of the (reworked) till and from the lagoonal clay bed. Paleoenvironmental conditions therefore are inferred for the lagoonal clays which are interpreted as being contemporaneous with main Lake Algonquin in offshore Lake Huron.

Vegetation. The high percentages of spruce pollen and the presence of spruce needles imply that a spruce forest formed the upland vegetation at the time that lagoonal clays were being deposited. *Elaeagnus commutata* and *Shepherdia canadensis* are abundantly represented by pollen. Occurring

in smaller quantities are pollen of the grasses, composites (Tubuliflorae, Liguliflorae, *Artemisia*), chenopods, saxifragas, *Dryas integrifolia*, and *Thalictrum*, and seeds of *Arctostaphylos Uva-ursi*, *Potentilla nivea*, *Fragaria vesca*, *F. virginiana*, and *Veronica* sp. These plant taxa commonly favour calcareous barks and open, dry shoreline sites (Fernald, 1950) and, thus, presumably formed a major part of the shoreline vegetation around the lagoon. A distinctly wetter shoreline flora is inferred from pollen of the Cyperaceae, *Equisetum*, and pteridophytes, from seeds of *Potentilla anserina*, *Rumex fenestratus*, *Ranunculus Cymbalaria*, and from macrospores of *Selaginella Selaginoides*. *Chara*, *Myriophyllum*, *Zannichellia palustris*, *Potamogeton filiformis*, and *P. alpinus* formed much of the submersed vegetation in the deep parts of the lagoon; *Carex aquatilis* and *Juncus* sp. were part of the emergent vegetation in the littoral zone.

With the exception of some species within the Gramineae, Scrophulariaceae and Saxifragaceae, none of the plant taxa are true arctic types. *Elaeagnus commutata*, *Arctostaphylos Uva-ursi*, *Potentilla nivea*, *Carex aquatilis*, and *Selaginella Selaginoides* have arctic distributions which extend from Greenland and Labrador to Alaska and south to Newfoundland and the upper Great Lakes region; all the other taxa have low arctic to boreal-temperate distributions from Newfoundland and Labrador to Alaska and southward into United States (Fernald, 1950).

Fauna. The molluscs are dominated by several terrestrial species which normally inhabit the moist to wet banks adjacent to ponds, lakes, and rivers. They presumably lived at the edge of the lagoon or along streams entering the lagoon contemporaneously with the aquatic species.

All seven species of freshwater molluscs are characteristic of most freshwater gastropod faunas and are associated with eutrophic habitats. *Fossaria parva* is known to inhabit mud flats at the water's edge but is generally found out of water (Baker, 1928). *Gyraulus deflectus*, *Valvata tricarinata*, *V. sincera*, and *Amnicola limosa* are especially indicative of quiet, relatively deep bodies of water in which soft sediments accumulate (Baker, 1928) and where the submersed vegetation varies from sparse to thick (Clarke, 1973). Although *Pisidium compressum* can also be found in relatively deep water, it has a preference for sandy bottoms with vegetation in shallow water (Herrington, 1962).

The ostracode fauna has a strong fluvial element shown by the predominance of *Ilyocypris bradyi* and a weak, nearshore lacustrine element; the latter is thought to have been derived in place (L.D. Delorme, pers. comm., 1979, unpublished Ostracoda Report No. 79-0-143). Like the molluscs, the ostracode assemblage implies a shallow-pond or lagoonal environment strongly influenced by streams nearby.

All the molluscs are widely distributed throughout the Boreal Forest and southward into United States (Baker, 1928; Clarke, 1973). *Gyraulus deflectus* is common north of the treeline while *Amnicola limosa* and *Pisidium compressum* have ranges that extend into southern United States and Mexico (Clarke, 1973). At least five of the ostracodes (*Limnocythere itasca*, *Cypridopsis vidua*, *Cyclopypris laevis*, *Cyclopypris sharpei*, and *Candona candida*) extend into the arctic region today (Delorme et al., 1977).

Summary and Conclusions

Fossiliferous, silty clay unconformably overlies till (St. Joseph Till) deposited by Port Huron ice about 13 000 years ago and underlies sand at North Penetangore River. The fossiliferous clay bed is interpreted as having been deposited in a lagoonal environment brought about when lake

levels in the Lake Huron basin rose to the main Lake Algonquin level and built a barrier beach bar across the mouth of the present-day Penetangore River. Pollen, plant macrofossils, molluscs, and ostracodes extracted from the clay bed indicate that the lagoon may have been at least 3 m deep, eutrophic, and that it probably resembled a modern sheltered embayment behind a beach bar with shallow streams entering it. Many of the floral and faunal taxa found as fossils presently are distributed throughout the Boreal Forest and commonly into the temperate zone; however, some have ranges that extend well into the arctic region. Thus climatic conditions at the time of deposition were probably not unlike those prevailing throughout the northern parts of the Boreal Forest today.

Wood from the lagoonal sediments was radiocarbon dated at $11\,300 \pm 140$ years (GSC-1842). Since the lagoon existed contemporaneously with main Lake Algonquin, the radiocarbon date provides an age for the main Lake Algonquin phase in the Great Lakes sequence of events. Records of earlier high-level lake stages (Warren to early Algonquin) as well as the Kirkfield low-level outlet stage are missing here. An age of about 11 500 years is suggested for the Kirkfield low-level stage when early Lake Algonquin is thought to have drained eastward into the Lake Ontario basin.

The lagoonal sediments correspond to similar fossiliferous (low-level) sediments dated at $11\,200 \pm 170$ years (GSC-1374) at the base of Kincardine Bog (Anderson, 1971; Karrow et al., 1975). They are also, in part, time correlative with the estuarine-alluvial sequence dated $10\,500 \pm 150$ and $10\,600 \pm 160$ years (GSC-1126, -1127) at Eighteen Mile River (Karrow et al., 1975). The fossil assemblages are not too dissimilar to the assemblages found in the low-level sediments at Kincardine Bog. A predominance of terrestrial molluscs and stream species of ostracodes at North Penetangore River, however, indicates that there was more fluvial influence at this locality than in the Kincardine Bog area.

The Kincardine Bog sediments previously had been related to the Kirkfield low-level stage (Anderson, 1971; Karrow et al., 1975); an origin associated with the development of the baymouth bar of main Lake Algonquin, as at North Penetangore River, is now preferred.

The lagoonal sediments are buried by sand believed to be equivalent to the fossiliferous sand layer, radiocarbon dated at $10\,300 \pm 200$ and $10\,600 \pm 150$ years (GSC-1644, -1366) at Kincardine Bog (Anderson, 1971; Karrow et al., 1975). Overlying the sand is the interbedded, waterlain fine sand-silt-clay sequence which is interpreted as a floodplain deposit. A floodplain environment thus existed inside the barrier bar after main Lake Algonquin drained, i.e. shortly after 10 400 years B.P. (Karrow et al., 1975), and it persisted well on into postglacial time. Concurrent with this floodplain environment was a small, inland lake habitat in the area covered by present-day Kincardine Bog. A radiocarbon date of 7620 ± 70 years (GSC-1816) from near the top of the basal gyttja in Kincardine Bog indicates the small lake habitat existed until shortly after this time and then changed into a rich fen environment.

Postglacial alluvium rests on top of the fine sand-silt-clay sequence. The top of the valley terrace section is the surface of the floodplain deposits modified by postglacial alluvial activity.

References

- Anderson, T.W.
1971: Postglacial vegetative changes in the Lake Huron-Lake Simcoe district, Ontario, with special reference to Glacial Lake Algonquin; unpublished Ph.D. thesis, University of Waterloo, Waterloo, 246 p.
- Ashworth, A.C.
1977: A late Wisconsinan Coleopterous assemblage from southern Ontario and its environmental significance; *Canadian Journal of Earth Sciences*, v. 14, p. 1625-1634.
- Baker, F.C.
1928: The fresh water Mollusca of Wisconsin. Part 1, Gastropoda; Wisconsin Geological and Natural History Survey, Bulletin 70, 507 p.
- Chapman, L.J. and Putnam, D.F.
1966: The Physiography of Southern Ontario; University of Toronto Press, Toronto, 386 p.
- Clarke, A.H.
1973: The freshwater molluscs of the Canadian Interior Basin; *Malacologia*, v. 13, 509 p.
- Cooper, A.J. and Clue, J.
1974: Quaternary geology, Grand Bend area, southern Ontario; Ontario Division of Mines, Preliminary Map 974.
- Delorme, L.D., Zoltai, S.C., and Kalas, L.L.
1977: Freshwater shelled invertebrate indicators of paleoclimate in northwestern Canada during late glacial times; *Canadian Journal of Earth Sciences*, v. 14, p. 2029-2046.
- Fægri, K. and Iversen, J.
1964: Textbook of Modern Pollen Analysis; Scandinavian University Books, Copenhagen, 237 p.
- Fernald, M.L.
1950: Gray's Manual of Botany; American Book Company, New York, 8th edition, 1632 p.
- Herrington, H.B.
1962: A revision of the Sphaeriidae of North America (Mollusca:Pelecypoda); Michigan University Museum of Zoology, Miscellaneous Publication 118, 74 p.
- Hough, J.L.
1963: The prehistoric Great Lakes of North America; *American Scientist*, v. 51, p. 84-109.
- Karrow, P.F.
1978: The relationship of valley terraces and glacial lake levels east of Lake Huron, Ontario, Canada; *Geological Society of America, Abstracts with Programs*, v. 10, p. 258.
- Karrow, P.F., Anderson, T.W., Clarke, A.H., Delorme, L.D., and Sreenivasa, M.R.
1975: Stratigraphy, paleontology, and age of Lake Algonquin sediments in southwestern Ontario, Canada; *Quaternary Research*, v. 5, p. 49-87.
- Lowdon, J.A. and Blake, W., Jr.
1976: Geological Survey of Canada radiocarbon dates XVI; *Geological Survey of Canada, Paper 76-7*, 21 p.

**REGIONAL SYNTHESIS OF THE GRENVILLE PROVINCE OF
ONTARIO AND WESTERN QUEBEC**

Project 760061

A. Davidson¹, J.M. Britton², K. Bell³, and J. Blenkinsop³

Davidson, A., Britton, J.M., Bell, K., and Blenkinsop, J., Regional synthesis of the Grenville Province of Ontario and western Quebec; in Current Research, Part B, Geological Survey of Canada, Paper 79-1B, p. 153-172, 1979.

Abstract

Data on the nature of deformation and metamorphism and on the continuity of rocks units, obtained during 24 traverses across the southwesternmost 450 km of the Grenville Front, are summarized and discussed. Observations on metamorphism and plutonic rocks within the southwestern Grenville Province indicate that granulite facies metamorphism is more widespread in Ontario than formerly reported, and confirm that nondeformed plutonic rocks are rare indeed northwest of the Central Metasedimentary Belt. Progress reports are presented on plutonic rocks within the Central Metasedimentary Belt and on Rb-Sr isotope studies in southeastern Ontario, the subjects of subsidiary projects being carried out under contract. Late-tectonic plutonic rocks are shown to be divisible into several suites. Tentative Rb-Sr whole rock isochron ages of 1180 ± 90 Ma and 1072 ± 22 Ma have been obtained respectively for tonalite-granodiorite and granite plutons, both of which belong to suites that intrude the Grenville Supergroup but are older than the Flinton Group, and are pre-tectonic with respect to Grenvillian Orogeny. Analytical results suggest that Rb-Sr isotope systems have been disturbed even in the Hastings Basin where Grenvillian metamorphism is relatively low grade.

Introduction

This project is concerned with the geology of the Grenville Province in Ontario and Quebec west of longitude 74°W (approximately west of a line between Montreal and Chibougamau), an area of about 175 000 km² and covering one third of the exposed part of the Province. According to Wynne-Edwards' (1972) classification, this area encompasses all or parts of the following subdivisions: Grenville Foreland Belt, Grenville Front Tectonic Zone, the Ontario and Quebec Gneiss Segments of the Central Gneiss Belt, Central Metasedimentary Belt, and Central Granulite Terrain. These are outlined in Fig. 19.1 with only minor modifications from Wynne-Edwards (1972, Fig. 1). The purposes of this project are to assess the current state of knowledge of the geology and economic potential of the southwestern Grenville Province, to identify areas where knowledge is lacking or where controversies may be resolved, and to initiate corrective studies and ultimately to derive a better synthesis than can be made at present.

The southwestern Grenville Province has a long history of geological study. Among the earliest works is that of Logan; he was the first to use the term 'Grenville series' for marbles and gneisses now included in the Grenville Supergroup (Logan, 1863, p. 839). Later works include such classics as 'Geology of the Haliburton and Bancroft areas, Ontario' (Adams and Barlow, 1910) and 'The disappearance of the Huronian' (Quirke and Collins, 1930). Primary acquisition of knowledge through systematic mapping, however, is still incomplete; mapping to date is at various scales and of varying quality, and much of the older work requires revision. Parts of the Ontario Grenville Province, for example south of latitude 46°N and west of the well known 'Grenville marbles' (the Central Metasedimentary Belt), have never been mapped other than at reconnaissance scale of 1:1 000 000 (Baer et al., 1977), even though close to the most heavily populated part of eastern Canada. Although mining has been active in parts of this region for more than one hundred years, it has never reached the status of a major industry. Its economic potential has not been judged as favourable as that of other regions of the Shield, and the slow progress of mapping by government agencies can no doubt in large part be attributed to this.

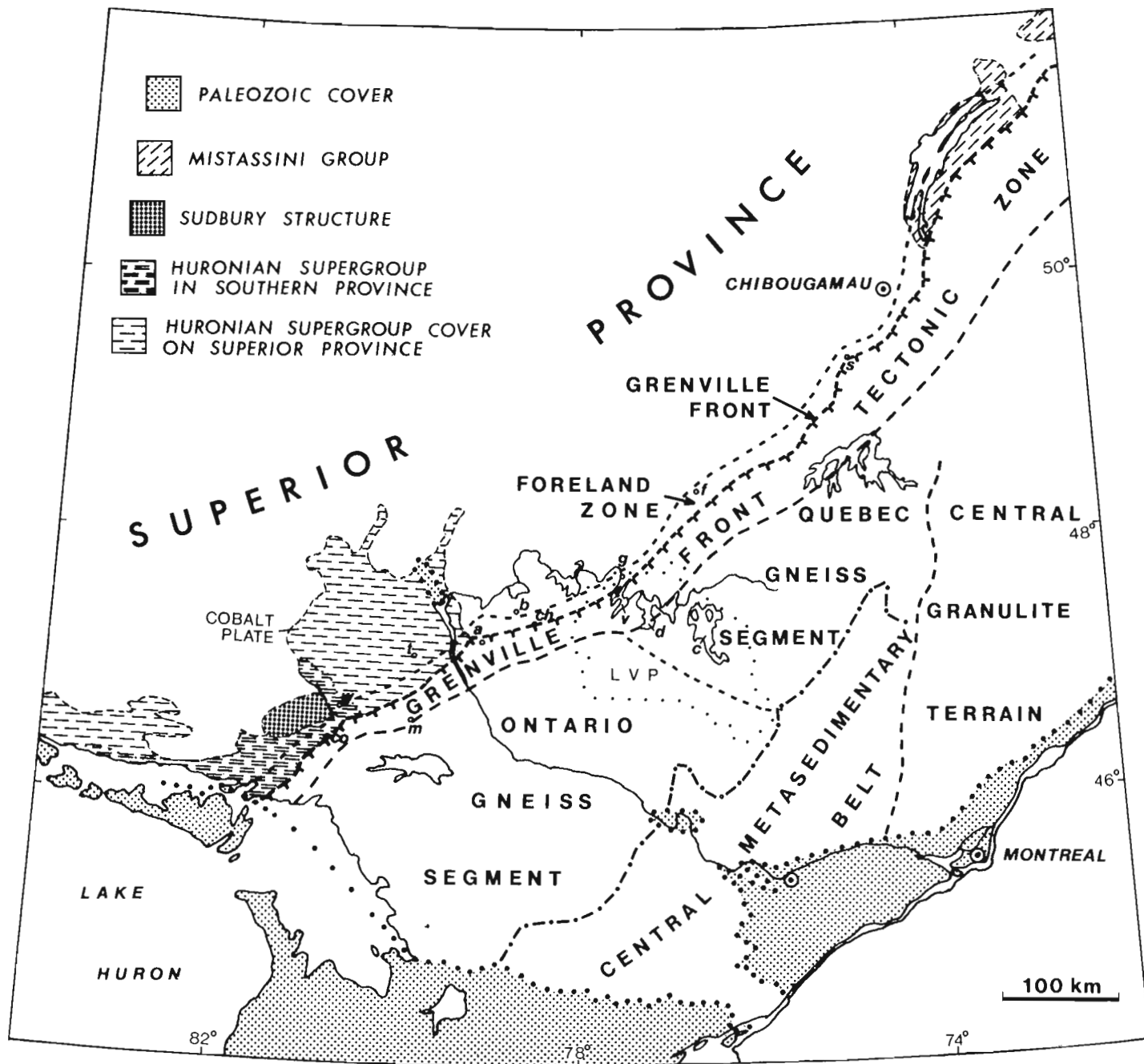
Resource requirements change, however, and with added interest in the environment and land utilization, it is timely that the immediate backyard of half of Canada's population should receive due attention.

An excellent summary of the status of knowledge of the Grenville Province as a whole and of the problems associated with the interpretation of its geology is given by Baer (1974). He states (p. 54) that the Grenville Province, "An extremely complex and poorly known region, . . . symbolizes to many the unfathomable mysteries of the Canadian Shield. No other part of the Shield possesses such an aura of legend, accumulated over more than a hundred years of frustrated efforts at understanding its evolution." After reviewing recent data and models, however, he states (p. 61) that "It may be that the Grenville problem will not be one very much longer." Resolution of the Grenville problem revolves around determining what evolutionary model best explains a major orogenic event whose main expression is one of extreme deformation, culminating almost everywhere in high grade metamorphism about 1 Ga ago, yet for most parts of which evidence for directly related sedimentation, volcanism and plutonism appears to be lacking. Current geochronological evidence, for example, suggests a time span of between two and three hundred million years between deposition of the Grenville Supergroup and the peak of the so-called Grenvillian Orogeny, and also that a considerable part of the Province contains rocks older than the Grenville Supergroup, yet abuts, with marked contrast in structural style, against older Shield provinces to the northwest. Despite Baer's prophetic optimism, several major problems of local or topical nature must be resolved before the larger picture can become clear, among them: 1) What is the nature of the Grenville Front in its entirety? 2) What elements of adjacent provinces can be recognized southeast of the Front, and how far do they extend into the Grenville Province? 3) To what orogenic systems do the various recognizable metasedimentary and volcanic rock packages within and peculiar to the Province belong, what are their age relationships, and on what basement were they deposited? 4) What is the rôle, if any, of the 'anorthosite suite' in the development of the Grenville Province? It appears that controversies surrounding the answers to these and other

¹ Regional and Economic Geology Division

² Department of Geology, University of Toronto, Toronto M5S 1A1

³ Department of Geology, Carleton University, Ottawa K1S 5B6



- | | |
|------------------------------------|-------------------------|
| LVP - La Vérendrye Provincial Park | f - lac Faillon |
| a - lac St.-Amand | g - lac Granet |
| b - Belleterre | m - Marten River |
| c - Cabonga Reservoir | s - Surprise Lake |
| ch - lac Chenon | t - Temagami |
| co - Coniston | v - Grand Lake Victoria |
| d - Dozois Reservoir | w - Wanapitei Lake |

Figure 19.1. Subdivisions of the southwestern Grenville Province, after Wynne-Edwards (1972).

questions arise from factors such as: 1) the difficulty inherent in mapping and in consistently classifying rocks and rock units in large terranes of gneiss and migmatite whose origins are mostly speculative and at best uncertain; 2) the existence of unresolved disagreement concerning some interpretations that have been and are being made, even to the extent that identical rocks in adjacent areas are ascribed different origins, ages and histories; 3) the currently unavoidable necessity of having to use inadequate or unevenly distributed data to support interpretations, correlations, extrapolations and hypotheses, both for different parts within the Province and across the Grenville Front. In any terrane where controversy becomes a stimulus for discussion and further endeavour, it goes without saying that fact must be distinguished rigorously from interpretation, and, as Baer stated (*ibid.*, p. 61), "More field information is urgently needed." It is intended that this project will contribute toward filling this need.

To date, two field seasons have been spent in the southwestern Grenville Province. Emphasis has been placed on examination of sections across the Grenville Front, and on metamorphism and plutonic rocks northwest of the Central Metasedimentary Belt. The senior author was ably assisted in the field by W.N. Houston in 1977 and by P. Erdmer in 1978, and is indebted to S.B. Lumbers, Royal Ontario Museum, J.M. Moore, Jr., Carleton University, M. Rive, Ministère des Richesses naturelles du Québec, and W.M. Schwerdtner, University of Toronto, for stimulating discussions during excursions in their respective field areas. In addition, two subsidiary projects, a study of late-tectonic plutons in the Central Metasedimentary Belt, and Rb-Sr isotope studies in southeastern Ontario, are being carried out on contract; progress reports for these projects are included as the second and third parts of this paper.

PART I

SOME OBSERVATIONS ON THE GRENVILLE FRONT, AND ON METAMORPHISM AND PLUTONIC ROCKS IN THE SOUTHWESTERN GRENVILLE PROVINCE

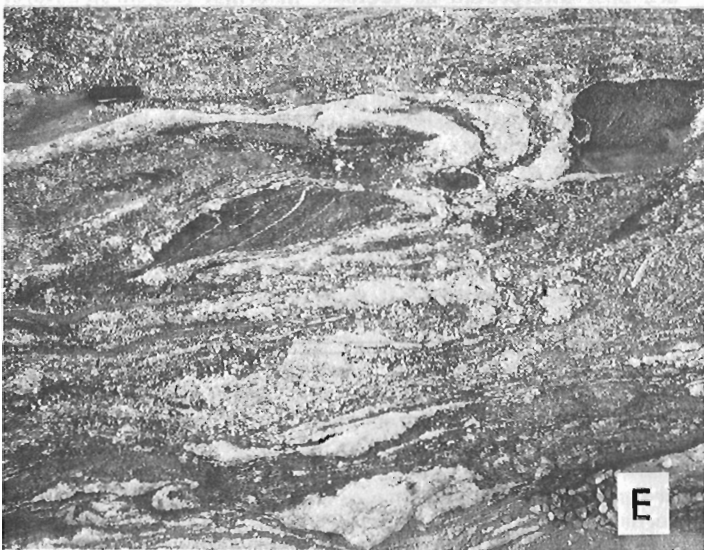
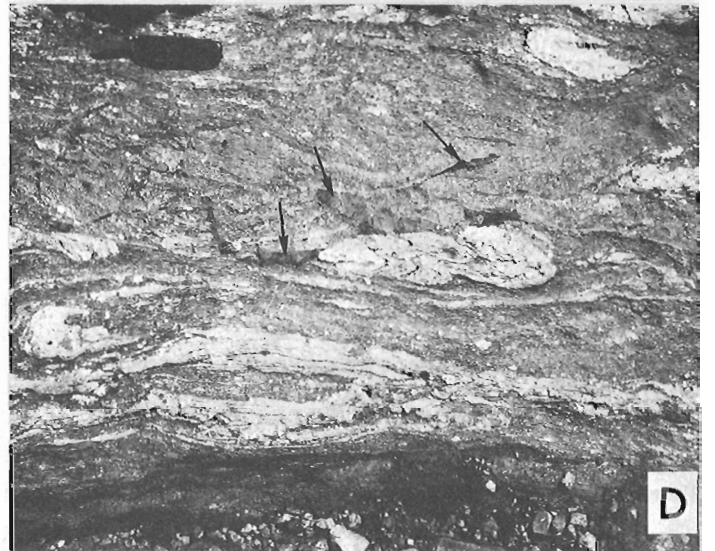
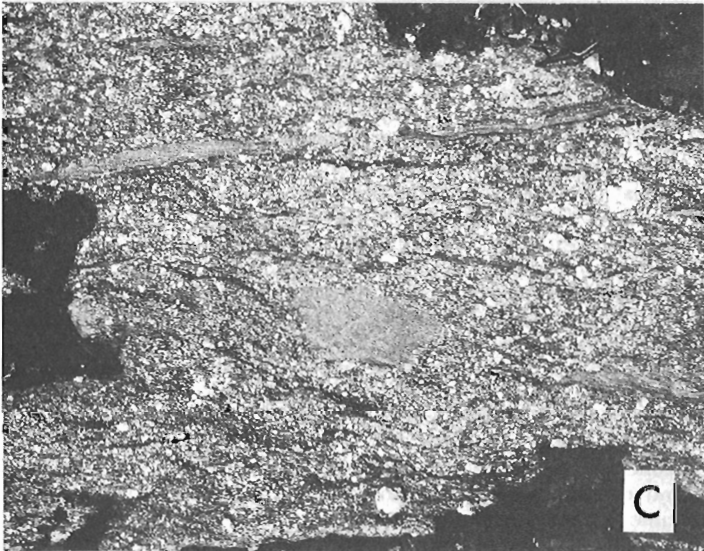
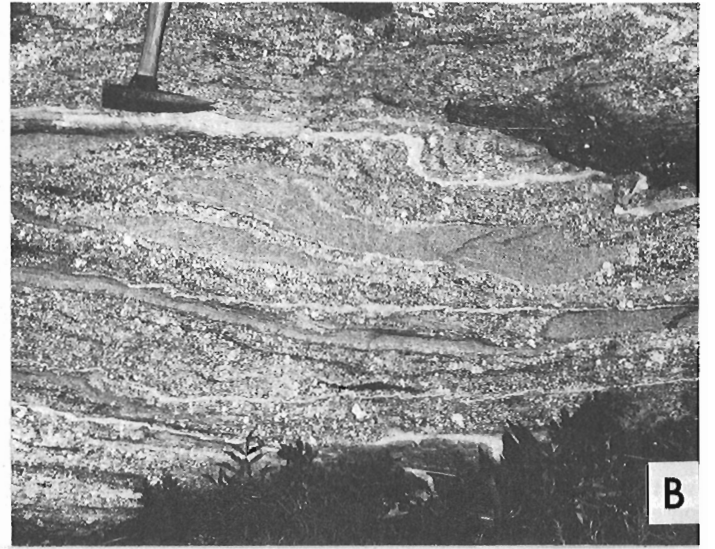
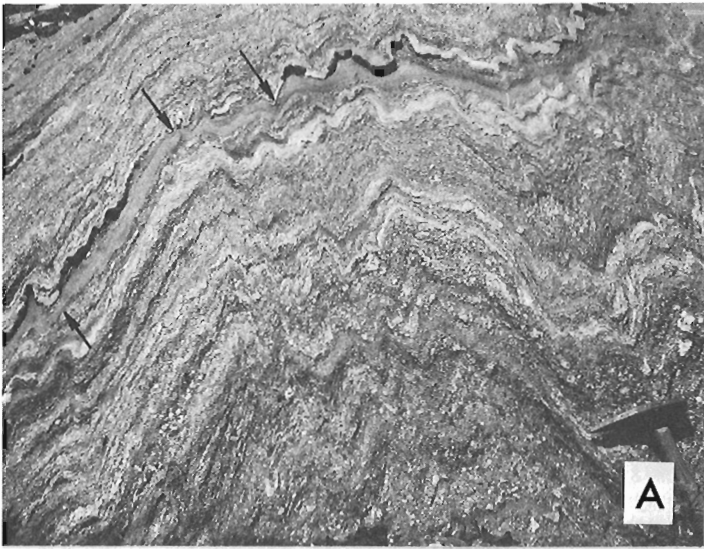
A. Davidson

Remarks on Features Associated with the Grenville Front

The Grenville Front is generally accepted as marking the northwest margin of the Grenville Province. It does not, however, mark the most northwesterly limit of the deformation and metamorphism which characterizes that Province. Wynne-Edwards (1972) has outlined the Grenville Foreland Belt to include that region northwest of the Front in which features that can be related to orogeny in the Grenville Province are recognizable. He uses the Front, "... a fault zone, a belt of mylonite, or a broad zone of metamorphic transition..." (*ibid.*, p. 265), to separate the Foreland Belt and the Grenville Front Tectonic Zone (Fig. 19.1). On the other hand, Lumbers (1978, Fig. 1) distinguished all of the Front in Ontario as a fault, which he referred to as the Grenville Front Boundary Fault, lying within the Grenville Front Tectonic Zone. The limit of mesoscopic cataclasis and prominent, southeast plunging lineation in rocks of the Superior and Southern provinces marks the northwest boundary of his Tectonic Zone, some 5 to 10 km northwest of the Front, and much closer to it than the northwest boundary of Wynne-Edwards' Foreland Belt. In Figure 19.1, the Foreland Zone corresponds more closely to that part of Lumbers' Tectonic Zone which lies northwest of the Front than to Wynne-Edwards' Foreland Belt. During the last two field seasons, twenty-four sections across the Grenville Front were examined along its 450 km extent from Lake Huron to south of lac Faillon, Quebec. Rocks northwest of the Foreland Zone of Figure 19.1 do not show any noticeable features, except perhaps for discrete faults, that can be unequivocally related to orogeny within the Grenville Province.

The Grenville Front Boundary Fault can only rarely be specifically located, as south of Coniston, Ontario, where it is identified as a fault characterized by "... a zone of extreme cataclasis and mylonitization up to 100 feet (30 m) wide..." (Lumbers, 1975, p. 122). At several of the sections examined, however, it can be located to within a few hundred metres, and is commonly marked by a linear, swamp- or lake-filled valley that separates outcrops of recognizable Superior or Southern Province rocks on one side from gneisses, usually cataclastic, of less certain or indeterminate parentage on the other. In many places, however, there are several subparallel faults or linears in the vicinity of the Front, both within the Foreland and the Tectonic zones, and it is not everywhere easy to specify which, if any, should be regarded as the Grenville Front Boundary Fault. In other places, for example just east of Lake Timiskaming, what appears to be a well defined Boundary Fault linear swings north-northeast away from the Grenville Province so that it has Superior Province rocks on both sides (M. Rive, J. van der Leeden, pers. comm., 1978). There is evidence, too, that the Boundary fault not only cuts pre-existing faults but is itself offset by north-northeast trending faults (see maps by Rive, 1976, and by Card and Lumbers, 1977).

Some workers have concluded that the Grenville Front was a long-lived feature whose history may have begun well back in Proterozoic time. It has been suggested, for example, that an important paleogeographic boundary existed in the region of the Grenville Front during the time of deposition of the Huronian sedimentary formations, controlling changes in their facies and thicknesses, and subsequently becoming the locus for late Aphebian granite plutonism (Card, 1978). Lumbers (1978) correlated certain gneisses in the Tectonic Zone in Ontario, the Red Cedar Lake formation, with lower Huronian formations, suggesting that they were deep water facies equivalents deposited in a continental margin trough which subsequently influenced the location and development of the Tectonic Zone. On the other hand, those who favour some form of collision model (e.g. Irving et al., 1972; Dewey and Burke, 1973) imply that the Front may have formed late in the history of the Province. Evidence from various localities along the Front and within the Tectonic Zone in the southwestern Grenville Province suggests that movement causing cataclasis has occurred at more than one time, although what time span may have been involved is not directly known. Many gneisses have internal structures that are best interpreted as tectonic in origin (augen structure, detached and rotated fold hinges, etc.), yet contain porphyroblasts of garnet and/or plagioclase formed during subsequent metamorphism. Other gneisses contain these minerals as distinct porphyroclasts, formed during post-metamorphic cataclasis. The respective roles of cataclasis and metamorphic recrystallization are illustrated by photographs of outcrop surfaces in Plate 19.1. In Plate 19.1A, small scale compositional layers, possibly of sedimentary origin, have been accentuated by cataclasis; certain layers have tended to pull apart at necking points, forming elongate boudins, but in much of the rock cataclasis is fully penetrative. Plate 19.1A,B show completely detached layer segments in a blastocataclastic matrix. Once formed, these tectonic clasts appear to have survived continued cataclasis, which was subsequently confined to their matrix. Mesoscopic folding followed cataclasis and was accompanied and outlasted by preferential metamorphic mineral growth in the cataclastic matrix. In places where rocks with layers of markedly different composition have been subjected to this process, clasts and matrices in the tectonic breccias so formed, illustrated by Plate 19.1D, E and F, retain these compositional differences. In D, postmetamorphic cataclasis has formed cataclasite and ultracataclasite layers and pseudotachylite veinlets in previously formed blastocataclastic tectonite with quartzofeldspathic clasts; this example is from a broad, late-formed cataclastic zone



lying parallel to the Front but well within the Tectonic Zone. In Plate 19.1E, amphibolite and quartz-feldspar clasts with 'tails' are enclosed in a foliated biotite-quartz-plagioclase matrix with plagioclase porphyroblasts. This outcrop does not show postmetamorphic cataclasis, but similar rocks are progressively reduced to dark, homogeneous cataclasite as the Grenville Front Boundary Fault, a mere 300 m to the northwest, is approached. Outcrops 200 m beyond the Boundary Fault at this locality are composed of weakly foliated and metamorphosed hornblende diorite containing easily recognized relict igneous texture and only slightly flattened xenoliths, part of a suite of mafic to intermediate plutons common to the Belleterre region of the Superior Province in Quebec. The rock shown in Plate 19.1F is essentially identical to that of 19.1E except that the metamorphic growth of matrix minerals is more pervasive. This rock is part of the Red Cedar Lake formation (Lumbers, 1978); similar rocks are found in the Tectonic Zone to the northeast at least as far as Grand Lake Victoria.

Along some segments of the Grenville Front in the southwestern Grenville Province there does not appear to be a single, well defined Boundary Fault. This is the case in the Surprise Lake area southwest of Chibougamau (Déland and Grenier, 1959), and Baer suggested that displacement along the Front was minimal in this region, and that "... movement of the (southwest part of the Grenville Province) relative to the North American craton seems to have decreased from southwest to northeast, as if this part of the Front moved like giant scissors pivoting around Chibougamau." (Baer, 1976, p. 512). The absence of an easily defined or unique Boundary Fault, however, may have another correlative, namely the juxtaposition of the Grenville Province against metagreywackes of relatively high metamorphic grade, commonly migmatized and associated with granite and pegmatite, in the Superior Province. In this regard, it is worthwhile recording the nature of the Grenville Front from north of La Vérendrye Provincial Park southwest to Lake Timiskaming. Archean

metavolcanic rocks and associated diorite, tonalite and granodiorite plutons of the Abitibi greenstone belt lie north of the Pontiac Group metagreywacke schist belt, and both about the Grenville Province east of Val d'Or. Between Grand Lake Victoria and lac Faillon, slivers of metagreywacke separate the greenstone belt and high grade gneisses of the Grenville Province. Across a narrow zone of cataclastic rocks that here defines the Front, metamorphic grade changes from lower amphibolite facies (staurolite schist) in the Superior Province to lower granulite facies (hypersthene-garnet-biotite gneiss) in the Grenville Province. This grade change occurs within a distance of as little as 3 km, suggesting very steep isograds, or alternatively upward displacement of the crust to the southeast. Whether or not the staurolite grade metamorphism in the Pontiac schists in the Superior Province close to the Front in this region is a product of Grenvillian metamorphism is open to question; farther northeast, near Surprise Lake, micas in similar schists with prograde metamorphism toward the Grenville Province retain Archean Rb-Sr ages (Krogh et al., 1970). Just west of Quebec Highway 117, in Mink Passage at the northeast end of Grand Lake Victoria, the Front is a zone of intense mylonitization that separates staurolite schist with southeast structures from upper amphibolite (muscovite absent) biotite-garnet gneiss with northeast structures. But staurolite schist occurs north of this locality 9 km from the Front, and farther west, at the north end of lac Granet, identical staurolite schist is at least 15 km from the Front. This metamorphism, therefore, does not relate to the Grenville Front, and is part of the east-west oriented southward rise in late Archean regional metamorphism that has affected the Pontiac Group south of the Abitibi greenstone belt. South along the shores of lac Granet, metamorphic grade continues to rise toward the Grenville Province, staurolite schist giving way to sillimanite-bearing migmatitic schist and gneiss that still retain southeasterly structure. Farther to the south, along the northeast oriented arms of lac Gaotanaga and Grand Lake Victoria, several parallel zones of intense cataclasis, including rocks with pseudotachylite, cut across these gneisses, turning their structures southwesterly and demonstrating a dextral sense of movement (see preliminary map by Rive, 1977a). Possibly the northwesternmost cataclastic zone should be accepted as the Grenville Front in this region, but none of these zones seems to have opposing features that set it apart from the rest.

The southern side of the late Archean metamorphic 'high' in the Pontiac schist belt is reached in the Belleterre area, where greenstones with diorite-tonalite-granodiorite intrusions reappear (the Belleterre-Temagami greenstone belt). Here the grade of Archean regional metamorphism has decreased to lower amphibolite facies, and the Grenville Front is locally well defined (as noted in the foregoing description of Grenville Front relationships for Plate 19.1E). Farther southwest again, metagreywackes flank the southern side of the Belleterre-Temagami greenstone belt, metamorphic grade again rises southward, and the position of the Grenville Front is hard to define (van der Leeden, in prep., 1978, pers. comm.). Trondhjemite and greenstone are once more the dominant Archean rocks adjoining the Grenville Province in the vicinity of Lake Timiskaming, where the Front is defined by a single fault zone.

If the Grenville Front Tectonic Zone represents a zone of crustal uplift with respect to the Superior Province, as northwest verging structures and the generally high rank of metamorphism on the Grenville side suggest, then it seems that movement was concentrated along one particular fault zone in some places, but was accomplished by less severe movement on each of several fault zones in others, especially where the Grenville Province abuts originally higher grade metagreywacke terranes. The nature of the adjacent crustal blocks in the Superior Province may therefore have

PLATE 19.1

- A. Mesoscopic folds in cataclastic biotite gneiss. Arrows indicate necking points at which certain layers tend to pull apart. Highway 101, 4 km south of Laniel, Quebec; 15 km southeast of the Grenville Front. (GSC 175505)
- B and C. Same outcrop as A. Progressive stages in the development of tectonic clasts formed from pulled-apart layers. Blastocataclastic matrices contain biotite and plagioclase porphyroblasts. (GSC 175506, 175507)
- D. Tectonic breccia developed from layered cataclastic gneiss. Quartzo-feldspathic clasts are detached fold hinges or rolled-up segments of layers. Matrix contains plagioclase augen, and arrows indicate patches and veinlets of pseudotachylite. Approximately 9 km from the Grenville Front southeast of lac Chenon, Quebec. (GSC 175521)
- E. Migmatite developed by recrystallization of tectonic breccia. Both quartzo-feldspathic and amphibolitic clasts lie in a foliated matrix of biotite, quartz and feldspar. 300 m south of intensely cataclased rocks exposed at the Grenville Front 3 km west of lac Chenon, Quebec. (GSC 175526)
- F. Advanced recrystallization of tectonic breccia in which matrix structure is partly obliterated by plagioclase blastesis. Highway 11, Marten River, Ontario; 10 km southeast of the Grenville Front. (GSC 175529)

influenced the expression of the Grenville Front. Although few would deny that metamorphic grade in the Grenville Foreland Zone rises toward the Front, it must be cautioned that much of the higher grade metamorphism close to the Front on the Superior side may be Archean in age and nothing to do with Grenvillian events. The same holds true for the Southern Province, where late Aphebian metamorphism related to the Penokean Orogeny is not spatially related to the Grenville Front. It is noted that where Huronian rocks of the Cobalt Plate, not affected by Penokean metamorphism, are preserved as cover on the Superior Province (northeast of Wanapitei Lake to east of Lake Timiskaming), metamorphism is barely discernible in the argillaceous rocks of the Gowganda Formation at localities as close as 4 km to the Front, immediately south of which metamorphism is middle amphibolite grade. If, where the Front cannot be identified as a specific zone of faulting, a metamorphic isograd is chosen to represent the Front, it must be unequivocally shown that such an isograd is related to orogeny peculiar to the Grenville Province. If an isograd chosen for this purpose is subsequently found to give, say, an Archean age for metamorphism, it does not necessarily follow that the Grenville Front existed as long ago as Archean time. An alternative explanation is that "... the progression of higher isograds towards the Grenville Front is due to uplift of pre-existing metamorphic zones in the Foreland Zone during the Grenvillian Orogeny." (Wynne-Edwards, 1972, p. 319).

Regarding identification of Superior Province rock units south of the Grenville Front, mapping by Rive (1977a) indicates that migmatitic garnet-biotite gneisses in the Grand Lake Victoria region cannot be separated from Pontiac Group gneisses and schists to the north. The same is likely true in the region southwest of Belleterre. These probable Pontiac Group correlatives in the Tectonic Zone contain metamorphosed tectonoclastic features like those illustrated in Plate 19.1, have minor structures suggesting a dominant right lateral component of movement, can be traced a long way to the southwest, parallel to the Front, and may be correlative with the strikingly similar rocks of the Red Cedar Lake formation in Ontario. If this correlation proves valid, then the Red Cedar Lake formation may be interpreted to have an Archean parentage rather than being a facies equivalent of lower Huronian formations.

Large units of mafic gneiss that might be equated with Superior Province greenstones have not so far been identified from La Vérendrye Provincial Park to the southwest within the Tectonic Zone, but tracts of fine grained, layered mafic granulites north of Cabonga Reservoir may have been derived from mafic volcanic rocks.

Among the plutonic rocks of the Superior Province, some have distinctive textures and compositions (Rive, pers. comm., 1978), and tectonically detached lensoid bodies of these rocks might be expected to have survived the intense cataclasis that characterizes the Tectonic Zone. For example, a northeasterly-trending lenticular mass of distinctive hornblende quartz monzonite orthogneiss with flattened xenoliths is incorporated within recrystallized cataclastic gneiss 4 km south of the Front south of lac St. Amand, 22 km east of Lake Timiskaming. Very little imagination is needed to equate this rock with nondeformed xenolithic hornblende quartz monzonite north of the Front in the same region. Radiometric isotope studies may be of further assistance; they have already indicated that Archean ages can survive in the Tectonic Zone (Krogh and Davis, 1968; Doig, 1975; Frith and Doig, 1975). It remains to be shown, however, that rocks of Archean age are present southeast of the Tectonic Zone in this part of the Grenville Province.

Notes on Metamorphism

Metamorphism within the Grenville Province is for the most part recognized to be of high rank (Bourne, 1978). In the western part of the Province lower amphibolite and greenschist rank metamorphism is restricted to the Central Metasedimentary Belt of Ontario. Metamorphism west of this Belt is mainly of upper amphibolite rank, judging by the fact that muscovite is not usually encountered except in late pegmatites or in altered rocks related to late movement, such as where shearing and cataclasis have occurred in the Grenville Front Tectonic Zone. Muscovite is present, however, locally with kyanite, in quartzofeldspathic gneiss and quartzite in the region between North Bay and Lake Kipawa, and may extend east as far as La Vérendrye Provincial Park in Quebec.

Granulite facies metamorphism has been recognized northwest of the Central Metasedimentary Belt in the Kempt Lake map area (Wynne-Edwards et al., 1966), and farther west it is known north of Cabonga Reservoir (Otton, 1972) and in the Dozois Reservoir area (Gillies, 1952; Chagnon, 1976). In Fréville County near the northern boundary of La Vérendrye Park, hypersthene-garnet-biotite gneiss is found within 3 to 6 km of the Grenville Front, on the northwest side of which staurolite-muscovite-biotite schist occurs. Both of these metamorphic rocks are likely derived from sediments of the Pontiac Group, Archean in age, that form a large tract of the Superior Province south of the Abitibi greenstone belt. Sporadic occurrences of hypersthene-bearing gneiss, charnockite and 'green rock' have been noted in Quebec south of this region, all lying northwest of but close to the northwest margin of the Central Metasedimentary Belt; examples are found in La Vérendrye Park 27 km from the southeast gate on Quebec Highway 117, just west of Pythonga Lake (Bourne, 1970), and 5 km west of Waltham Station on the north side of the Ottawa River. The last locality is southeast of granulite facies rocks reported by Katz (1969), indicated as an area of upper amphibolite to granulite transitional facies on the recently published Metamorphic Map of the Canadian Shield (Fraser et al., 1978). This map also shows an area of upper amphibolite to granulite transitional facies in the Algonquin Provincial Park region of Ontario, as well as scattered occurrences of orthopyroxene in neighbouring areas. Based as it is on limited reconnaissance mapping in a very poorly known area (Bell, 1971; Hewitt, 1967; Baer et al., 1977), this distribution will remain ill-defined until mapping in greater detail is accomplished.

If the presence of metamorphic hypersthene is accepted as an indicator of granulite facies metamorphism, then present studies show that rocks in granulite facies (the regional hypersthene zone of Winkler, 1976) are more widespread in this part of the Grenville Province, particularly in Ontario, than is commonly recognized. Orthopyroxene, confirmed as hypersthene in thin sections, has been identified in the field in many places from the vicinity of Parry Sound on Lake Huron to Barry's Bay east of Algonquin Park, and is particularly prevalent in the southwestern part of Algonquin Park and adjacent areas. Other 'nodes' of hypersthene-bearing rocks occur between Port Carling and Bracebridge, and east of Parry Sound (Fig. 19.2). Hypersthene occurs in both layered (paragneiss) and homogeneous (orthogneiss) metamorphic rocks, both of which types are characterized by reddish brown weathering rinds and the dark colour of fresh feldspars (olive-green plagioclase and pinkish brown K-feldspar).

Rocks that may be termed granulites in the strictest sense, by any definition, do occur in places. For example, slabby gneisses east of Huntsville, considered meta-sedimentary by Hewitt (1967), and east of Parry Sound, the

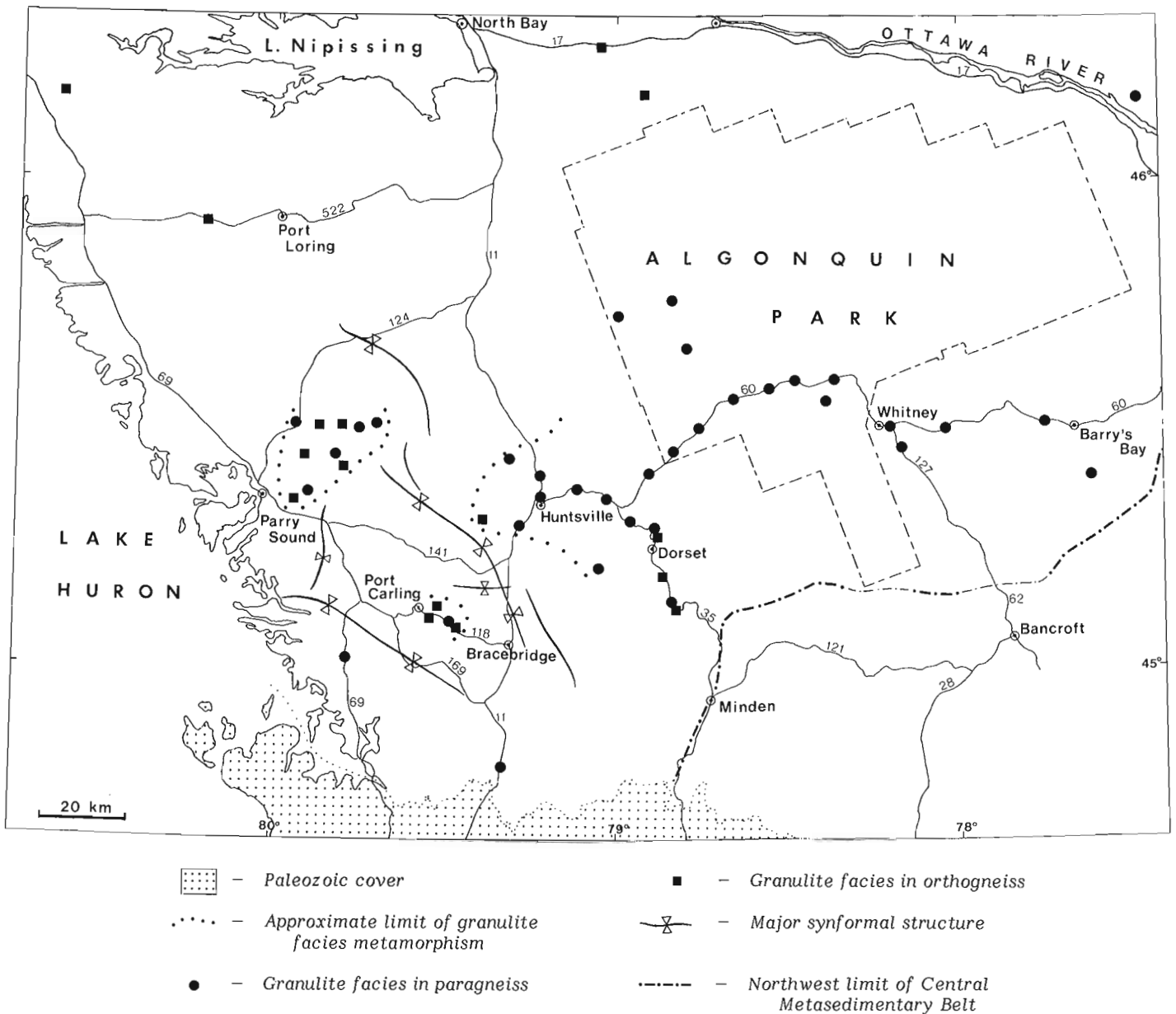


Figure 19.2. Observations on the occurrence of granulite facies metamorphism in the Ontario Gneiss Segment of the Grenville Province in Ontario. Numbered lines are main highways.

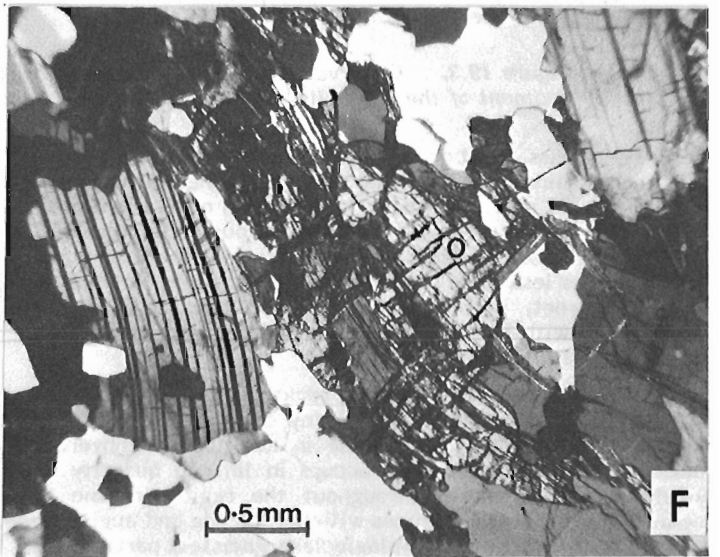
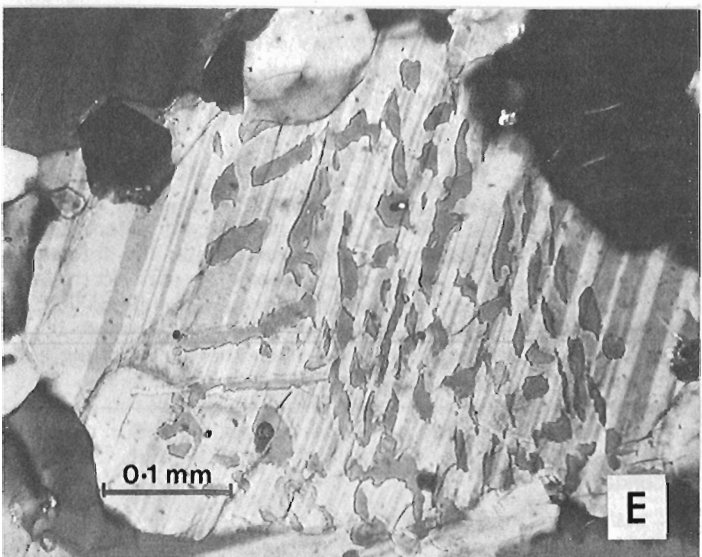
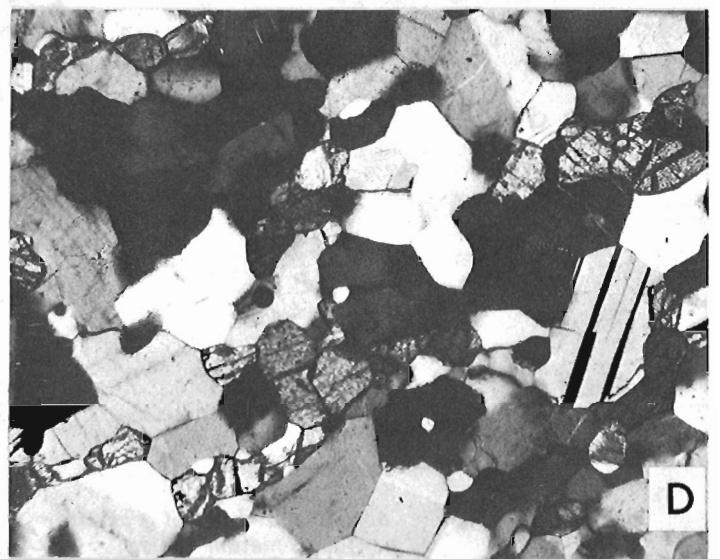
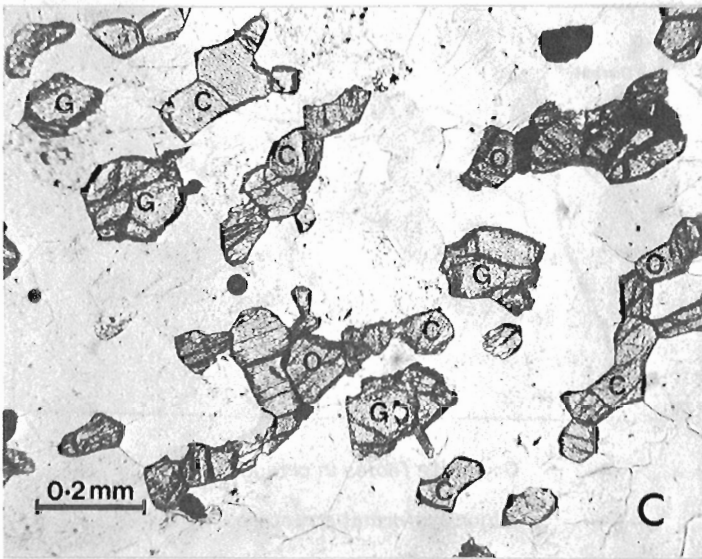
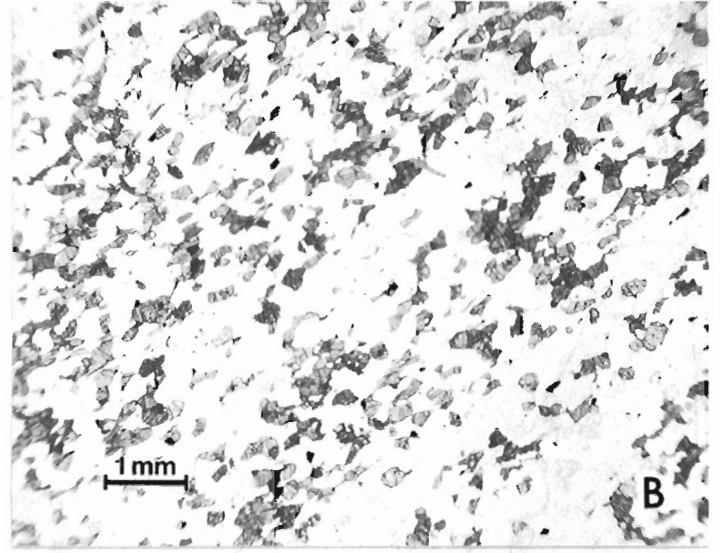
McKellar gneiss of Lacy (1960), contain layers of rock composed dominantly of feldspar and quartz that has uniform, very fine grain size (less than 0.5 mm), thin quartz lenticles, polygonal granoblastic texture, and anhydrous mafic minerals. Despite their dark appearance, these rocks commonly have colour indices less than 15; the mafic minerals are combinations of garnet, pyroxenes and opaque oxides. They are interlayered with darker gneisses of equally fine grain, such as are illustrated in Plate 19.2A to D.

Not all hypersthene-bearing rocks by any means fit the category of classic granulite. Many fine grained gneisses contain biotite and/or hornblende in addition to anhydrous mafic minerals. Hypersthene occurs in limited quantity at widely scattered places throughout the region in fine to medium grained mafic gneisses with hornblende and augite, in some garnet-biotite-quartz-plagioclase gneisses, particularly those rich in quartz, and with or without garnet in small, irregular plagioclase-quartz veins or swaths within these

rocks. It is a major mafic constituent of various types of orthogneiss, for example: quartz diorite to granodiorite orthogneiss bodies east of Parry Sound (Lacy, 1960) and near Port Carling (Hewitt, 1967), charnockitic rocks at and south of Dorset and west of Port Loring, and parts of the deformed and metamorphosed monzonitic plutons in the North Bay (Lumbers, 1971) and Burwash map areas (Lumbers, 1975). Metamorphic mineral assemblages, judged to be stable from thin section examination of rocks from the Port Carling and Huntsville - Algonquin Park regions are listed below. All assemblages contain plagioclase and opaque oxides in addition to the minerals listed; biotite and amphibole are omitted from assemblages in which it is obvious that they are secondary.

1. with quartz and K-feldspar:

- hypersthene - augite - almandine
- hypersthene - augite - hornblende
- hypersthene - augite - biotite
- hypersthene - almandine - biotite



2. with quartz, without K-feldspar:
 - hypersthene – augite – almandine
 - hypersthene – almandine – hornblende – biotite
 - augite – almandine – hornblende – scapolite
3. without quartz and K-feldspar:
 - hypersthene – augite – almandine – hornblende

The assemblage hypersthene – augite – biotite in the presence of quartz and K-feldspar is incompatible according to Reinhardt and Skippen (1970, Fig. 1), but is admissible at relatively high temperature according to Froese and Jen (1979, Fig. 16.1).

Toward the margins of the centres of granulite facies metamorphism, rocks of 'non-granulite facies' aspect, that is to say, pink and dark to light grey rather than greenish to brownish grey gneisses, become increasingly abundant, although hypersthene-bearing assemblages may be present locally in certain rock types. Such rocks are not so fine grained and in places are more obviously migmatitic in the sense that they contain an appreciable mobilisate component. The granulite facies rocks of the Port Carling and Huntsville – Algonquin Park areas, for example, are separated by a broad, northwest-trending synformal zone of migmatitic hornblende and biotite gneisses in places containing garnet and clinopyroxene but apparently devoid of any hypersthene-bearing assemblages. South and east of the Algonquin Park metamorphic 'high', upper amphibolite facies gneisses predominate as far as the edge of the Central Metasedimentary Belt (Wynne-Edwards, 1972), and lower amphibolite to greenschist facies rocks are not encountered before reaching the Hastings – Arnprior metamorphic 'trough' (see Fig. 19.4) (Carmichael et al., 1978). It is possible, judging by a limited thin section study, that the disappearance of granulite facies assemblages toward the Central Metasedimentary Belt is a retrogressive effect, conceivably due to a subsequent metamorphic event. The following petrographic observations may be evidence for this contention. K-feldspar in the 'highest grade' hypersthene-bearing rocks in the Port Carling and Algonquin Park areas is

cryptoperthitic and shows no evidence of microcline twinning, plagioclase in some rocks is strongly antiperthitic (Pl. 19.2E), and hypersthene is stable in contact with K-feldspar and lacks overgrowths of biotite or hornblende. Hypersthene-bearing rocks near Dorset and Whitney, however, contain perthitic microcline and nonantiperthitic plagioclase, and cores of relict hypersthene within aggregates of hornblende and biotite; both plagioclase and hypersthene may be bent (Pl. 19.2F), but hornblende and biotite show straight extinction. It is stressed, however, that a great deal more work must be done before even the pattern, let alone the history of metamorphism in this part of the Grenville Province can be properly evaluated.

Observations on Plutonic Rocks

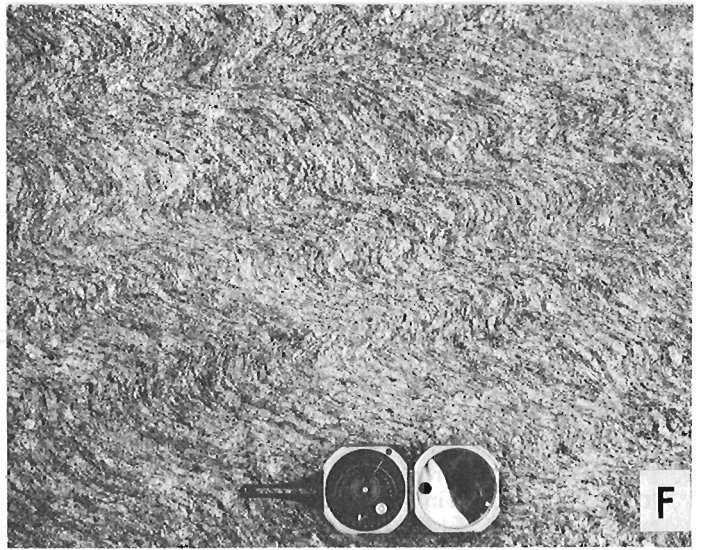
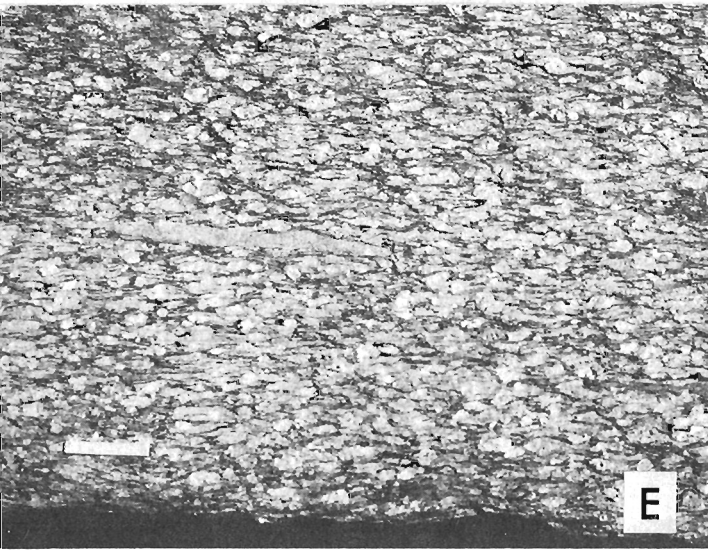
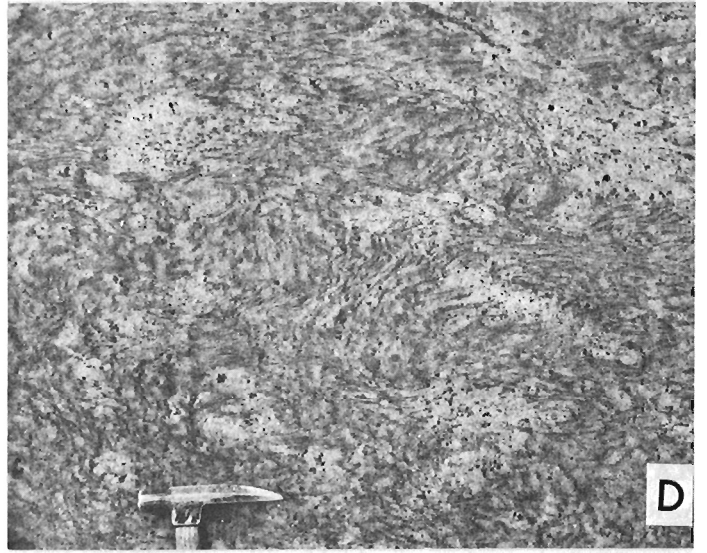
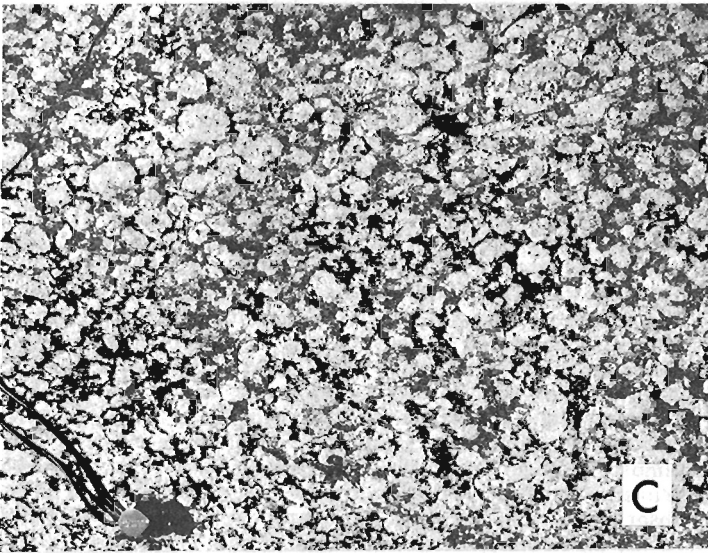
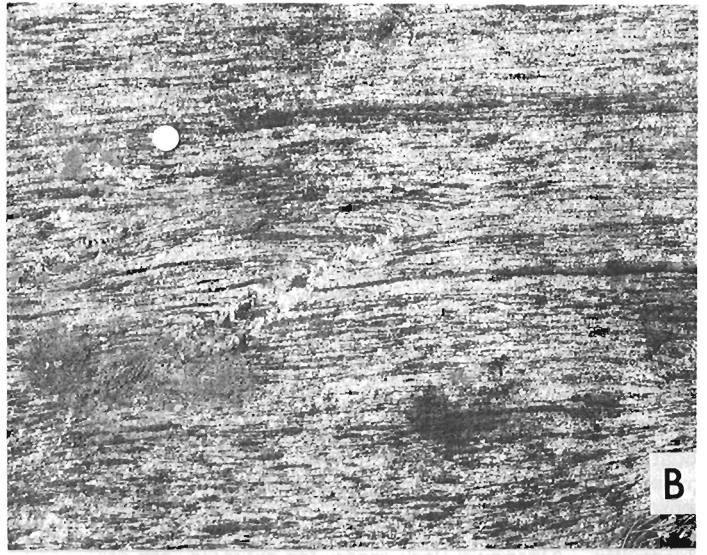
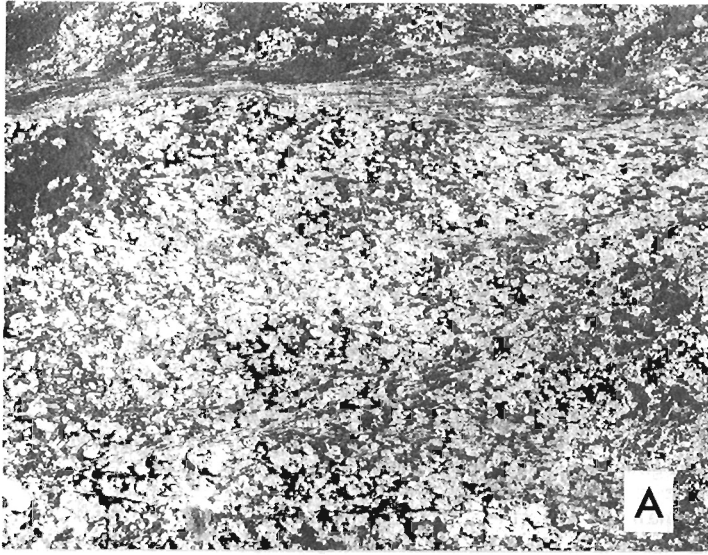
During geological reconnaissance in the Ontario Gneiss Segment, the southwest part of the Grenville Front Tectonic Zone, and the southwesternmost part of the Quebec Gneiss Segment, particular attention was paid to existing map-units designated as plutonic. None of the many examined, large and small and regardless of composition, has wholly escaped some degree of deformation and metamorphic recrystallization, with the exception of the small alkaline intrusions of early Paleozoic age associated with post-Grenville rifting (Lumbers, 1971, p. 47-54). Many plutons, perhaps originally more equidimensional, are now elongate masses of orthogneiss lying within the regional structural grain and folded with the enclosing gneiss and migmatite. In some plutonic masses, however, primary igneous texture, although deformed, can be recognized, and in a few, nondeformed primary texture and mineralogy is preserved locally, giving the impression that parts of some plutons behaved as rigid blocks during deformation. This phenomenon is most commonly exhibited by mafic plutonic rocks, and has been observed at scales ranging down from regions many square kilometres in area to domains a few metres across within otherwise deformed plutonic rocks, or in detached, boudin-like masses within heterogeneous gneiss. Examples of little-deformed plutonic rocks, contrasted with their highly deformed equivalents, are illustrated in Plate 19.3A to D. It is noted that granitoid plutonites, even where massive, are almost invariably recrystallized. Although vestiges of gross primary igneous features may be preserved, textures observed in thin sections are metamorphic. Some granitic rocks, particularly felsic members of the 'anorthosite suite' (Lumbers, 1975), contain garnet and a few contain either or both clino- and orthopyroxene. The same minerals occur in nearby highly deformed equivalents of these rocks and in their enveloping gneisses, where they are undoubtedly of metamorphic origin.

Evidence of superimposed deformations, generally folded or transposed foliation, is common in some orthogneiss units, particularly where orthogneiss can be traced across the boundary region between the Ontario Gneiss Segment and the Grenville Front Tectonic Zone. For example, southeast of this boundary and east of Ontario Highway 11, granite orthogneiss has uniformly northwest trending foliation and a well-developed lineation that plunges gently southeast. Xenoliths in this rock are highly flattened, with dimensions as distended as 1:12:30, and could be useful as strain indicators (Pl. 19.3E). In the boundary region, this northwest-trending foliation has been folded about northeasterly axial planes (Pl. 19.3F), parallel to the main foliation trend in the Tectonic Zone and to the Grenville Front itself.

Observations that some plutonic rocks are more deformed than others, and that the state of deformation may be related to time of emplacement, could prove useful in the task of temporally ordering plutonic events within this part of the Grenville Province. Before this task can be accomplished, however, more information must be obtained on the way in

PLATE 19.2

- A. Roadside outcrop, 22 km east of Highway 11 on Highway 60, Ontario. Layered, very fine grained granulite gneiss displays sub-isoclinal folds with gently dipping axial planes. (GSC 175556)
- B. Photomicrograph of granulite from the same outcrop illustrating grain size of less than 0.5 mm in the assemblage quartz-K-feldspar-plagioclase-hypersthene-augite-almandine-magnetite-ilmenite with traces of biotite; plane light. (GSC 203511)
- C. Photomicrograph (plane light) of the same granulite facies assemblage from roadside outcrop at the intersection of Highways 11 and 60, Huntsville, Ontario. O – hypersthene, C – augite, G – almandine. (GSC 203511-A)
- D. Photomicrograph (crossed polarizers) of the same field as C. Note polygonal grain outlines. (GSC 203511-B)
- E. Photomicrograph (crossed polarizers) of antiperthitic plagioclase in hypersthene- and garnet-bearing metagranodiorite, east side of Rosseau Lake, 1.5 km northwest of Brackenrig, Ontario. (GSC 203511-C)
- F. Photomicrograph (crossed polarizers) of bent hypersthene (O) and plagioclase in olive-brown gneiss interlayered with pelitic gneiss, 6 km north of Dorset, Ontario, on Highway 35. Hypersthene is partly surrounded by a younger generation of non-deformed hornblende. (GSC 203511-D)



which different plutonic rock types of the same age behaved during succeeding orogeny, and in which similar rock types behaved when subjected to different conditions or histories of deformation and metamorphism. It may well not be correct to interpret that a particular plutonic rock is young relative to the Grenvillian Orogeny just because it does not appear to have been deformed.

A large variety of stocks and batholiths has been recognized within the Central Metasedimentary Belt. Most have been modified by later deformation and metamorphism, ascribed to the Grenvillian Orogeny, and they are therefore either pre- or syntectonic with respect to this orogeny. The least modified plutons lie in the region of lowest metamorphic grade, the Hastings Basin (Fig. 19.4). Also found here are possible examples of post-tectonic plutons, the Mount Moriah (Thivierge, 1977) and Deloro stocks (Saha, 1959; Kuehnbaum, 1977), although some thin sections of rocks from the latter show alteration that may be metamorphic (stilpnomelane and/or biotite developed from primary amphibole) along with evidence of strain in quartz and some recrystallization of feldspar and amphibole. Away from the Hastings Basin, most of the plutonic rocks appear to be thoroughly recrystallized with development of secondary foliation and metamorphic texture. Some plutons exhibit granulite facies characteristics (quartz lenticles, mesoperthite, hypersthene and garnet), as for example in the Frontenac Axis and east of the Gatineau River. In the region north of Peterborough, Ontario, domes of gneissic and granitoid rocks, associated with anatectic granite, are interpreted as basement to the Grenville Supergroup (Bright, 1977; Morton, 1978). Some gabbros, syenites and granites in the higher grade terrains, however, seem relatively well preserved, and are tentatively classified as late- or even post-tectonic (Wynne-Edwards, 1972, p. 314; see Britton, J.M., Part II of this report).

Important aspects of plutonism in the Central Metasedimentary Belt involve the age relationships between the various plutonic rock types and between plutonic and orogenic activity. Recent detailed mapping has shown, for example, that certain plutons pre-date part of the Grenville Supergroup. A major stratigraphic unconformity has been identified at the base of the Flinton Group (Moore and Thompson, 1972) which lies both on folded rocks of the older

PLATE 19.3

- A. Relict primary texture in anorthositic gabbro. 11 km north of Highway 17 at Markstay, Ontario. (GSC 175538)
- B. Same outcrop as A. Streaky garnet-hornblende-plagioclase orthogneiss derived from anorthositic gabbro. (GSC 175537)
- C. Massive quartz monzonite with K-feldspar megacrysts. East side of Powassan batholith (Lumbers, 1971), 9 km south-southeast of Callander, Ontario. (GSC 175550)
- D. Swirly folds and feldspar-rich patches developed by recrystallization in quartz monzonite orthogneiss. Powassan batholith, Highway 11, 5 km south of Trout Creek, Ontario. (GSC 175552)
- E. Granite orthogneiss with K-feldspar augen and flattened xenoliths. Mulock batholith in the Ontario Gneiss Segment, 3.5 km east of Highway 11 at Tilden Lake, Ontario. (GSC 175499)
- F. Foliation in granite orthogneiss is refolded in southern part of the Grenville Front Tectonic Zone. New folds trend northeast, parallel to the Grenville Front 16 km to the northwest. Probable extension of the Mulock batholith, 10 km east of Marten River, Ontario. (GSC 175545)

Hermon Group and on granodioritic and tonalitic plutons (Northbrook and Elzevir, Fig. 19.4) that intrude the Hermon. The Flinton Group, not known to have been intruded by plutonic rocks, was nevertheless strongly deformed and metamorphosed during the Grenvillian Orogeny. Pre-Flinton deformation and plutonism must consequently be ascribed to an earlier orogenic event.

Any attempt at classifying plutonic rocks into pre-, syn-, late-, or post-tectonic categories must relate them to specific tectonic events. To do this requires knowledge of the age relationships between plutonism, deformation and metamorphism. An extensive geochronological study, using whole rock Rb-Sr isotope analysis, is currently being undertaken to help place constraints on the timing of plutonism in the Central Metasedimentary Belt in southeast Ontario (see Bell, K. and Blenkinsop, J., Part III of this report). It is hoped that this study will contribute toward answering questions such as: 1) What has been the effect of the latest (Grenvillian) deformation and metamorphism on earlier Rb-Sr isotope equilibria? 2) Can it be shown that plutons of different type have significantly different ages or initial $^{87}\text{Sr}/^{86}\text{Sr}$ ratios? 3) Do plutonic rocks of similar type but from different plutons and/or in different structural states have similar ages? 4) Is it possible to obtain reliable ages for volcanic rocks in the Grenville Supergroup and for metamorphism of the Flinton Group? 5) Do supposed basement rocks in the Ontario Gneiss Segment retain older Rb-Sr ages?

PART II

LATE-TECTONIC SYENITE AND GRANITE PLUTONS OF THE GRENVILLE PROVINCE OF SOUTHWEST QUEBEC AND SOUTHEAST ONTARIO

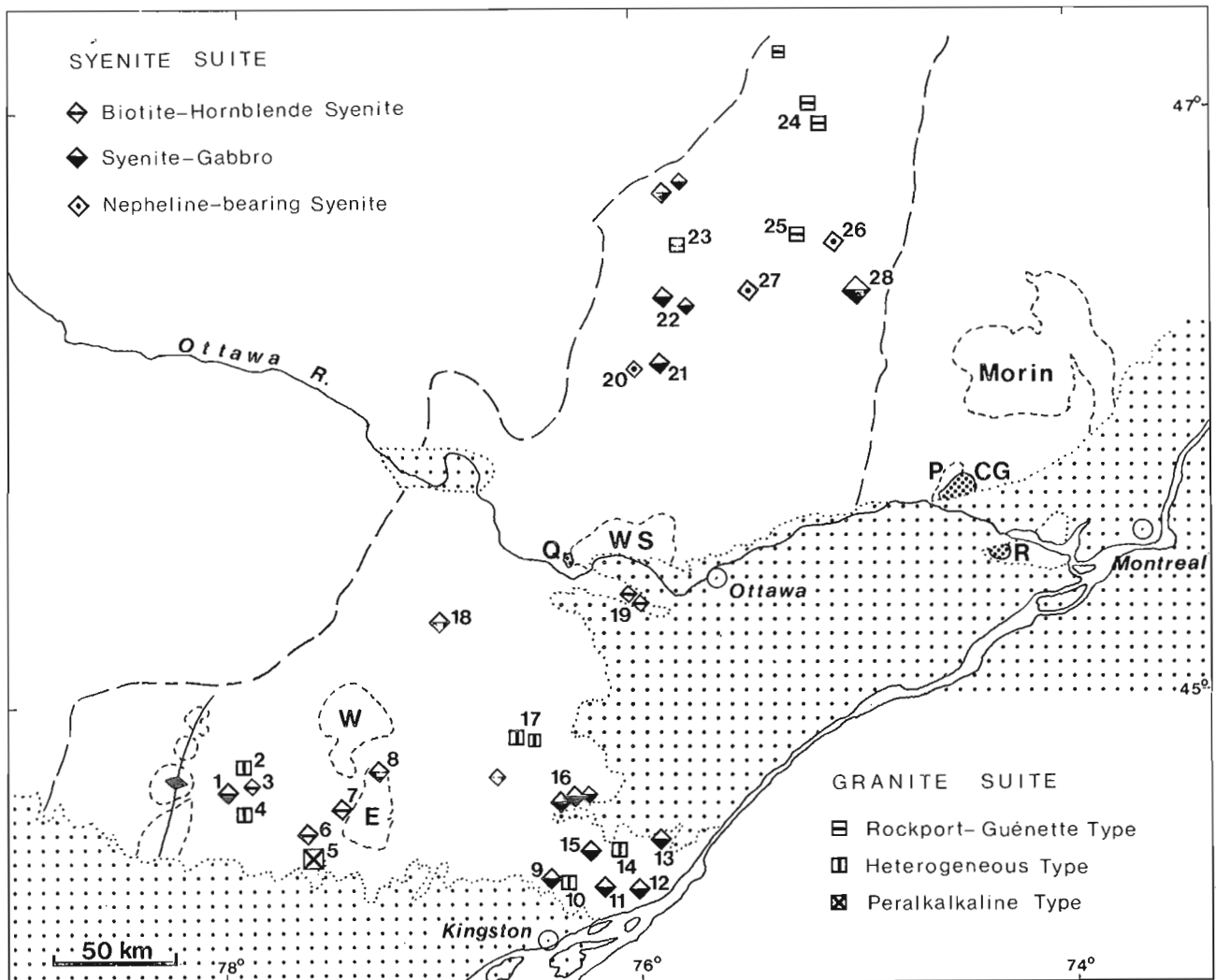
J.M. Britton (Contract 94736)

Introduction

During the 1978 field season, some thirty discrete granitic and syenitic plutons, generally considered to represent late-tectonic igneous activity associated with the Grenvillian Orogeny, were examined with a view to improving knowledge and understanding of the geology, inter-relationships and economic potential of these rocks. Some of the plutons, particularly those in Ontario, have already been studied separately, either during mapping by Federal or Provincial Surveys or through university thesis research. However, except for the Frontenac Axis region (e.g. Sauerbrei, 1966; Currie and Ermanovics, 1971; Shieh, 1978) and the Bancroft-Madoc area (Saha, 1959; Lumbers, 1967), comparative studies of more than a few plutons have not been undertaken.

Syntheses of regional mapping, particularly those by Hewitt (1964), Lumbers (1967) and Wynne-Edwards (1969) have identified several plutonic and metaplutonic associations within which syenitic and granitic rocks occur. Certain of these associations have been omitted from this study on the basis that they do not fit the late-tectonic category with respect to Grenvillian Orogeny. These are: metaplutonic suites such as the deformed Wakefield and Pine Hill syenites, syenitic gneisses in the Perth, Carleton Place and Renfrew areas, nepheline syenites and gneisses that are distributed along the northwest edge of the Central Metasedimentary Belt, mangerites and charnockites related to the anorthosite massifs such as the Morin Anorthosite, and deformed granites such as the Addington and Mazinaw plutons (Fig. 19.4). Syenitic and granitic phases of the pre-Flinton Group, $1226 \pm 25 \text{ Ma}^*$ biotite diorite series of Lumbers (1967) are excluded, with the exception of the Deloro pluton which is younger (Stockwell, 1972), chemically distinct, and may not belong to this association. Post-Grenvillian intrusions such as

* This and subsequent U-Pb ages quoted are recalculated using U decay constants of Jaffey et al. (1971).



- | | | | |
|-----------------|------------------|-----------------------|--------------------|
| 1. Lòn Lake | 8. Skootamatta | 15. Crow Lake | 22. Kensington |
| 2. Wollaston | 9. Perth Road | 16. Westport | 23. Aumond |
| 3. Coe Hill | 10. Battersea | 17. Elphin | 24. Leman |
| 4. Ridge | 11. South Lake | 18. Mount St. Patrick | 25. Guénette |
| 5. Deloro | 12. Gananoque | 19. Carp | 26. Ste.-Véronique |
| 6. Gawley Creek | 13. Beales Mills | 20. Gracefield | 27. Lac Rouge |
| 7. Mount Moriah | 14. Lyndhurst | 21. Cameron | 28. Loranger |
- Pre-Grenvillian plutons:
- W - Weslemkoon
E - Elzevir
WS - Wakefield Syenite
P - Pine Hill Syenite
- Post-Grenvillian plutons:
- Q - Quyon
CG - Chatham-Grenville
R - Rigaud

Figure 19.3. Location of syenitic and granitic plutons in the Central Metasedimentary Belt. Paleozoic cover is stippled.

the Onslow syenite, Chatham-Grenville and Rigaud stocks (Doig and Barton, 1968) are also excluded. Gabbroic rocks are widespread within the study area; some in Ontario are part of the biotite diorite series, others are considered to be younger (Lumbers, 1967). Although the association of syenite and gabbro has been noted by many authors, plutons that are predominantly gabbro have not been included in this study.

It is not possible in every case to assign individual plutons, especially small or poorly exposed ones, to a particular association because similarities exist between associations. The study area is outlined in Figure 19.3

plutons examined during the course of this study are assigned numbers and are identified in the text by these numbers in parentheses following numbers.

General Geological Characteristics

All the plutons examined and, according to existing geological maps, all similar plutons, appear to be confined to the northeast-trending Central Metasedimentary Belt. Country rocks for the most part belong to the Grenville Supergroup, characterized by abundant marbles and also including less regularly distributed quartzofeldspathic,

feldspathic and pelitic gneiss, quartzite and metavolcanic rocks. Massive to gneissic gabbroic to granitoid rocks, and possibly some older gneisses, are also present. The plutons comprise a group of circular to elliptical-plan bodies ranging in size from small stocks with as little as 2 km² exposed area, such as the Carp Stocks (19)*, to bodies approaching batholithic size, such as the Loranger Syenite (28) at 105 km². Shape and size do not appear to correlate either with degree of deformation or with geological complexity. Structure within plutons ranges from virtually massive to strongly gneissose and conformable. This variation appears to be generally related to the degree of regional metamorphism and deformation in the host rocks. The syenitic plutons, less so the granitic ones, that lie outside the very high grade metamorphic terranes (e.g. the Frontenac Axis) and show the least evidence of deformation and recrystallization tend to have well-developed, coincident, positive aeromagnetic anomalies.

Reported radiometric ages have been mainly K-Ar determinations and are characteristically 'Grenville' ages – from 822 Ma for the lac Rouge Syenite (27) to 1005 Ma for a mafic phase of the Ste.-Véronique pluton (26) (Doig and Barton, 1968). Isotopic studies of U-Pb systems in zircons (Silver and Lumbers, 1966; Lumbers, 1967) from rock associations in the Bancroft – Madoc area have defined two principal age groups for plutonic rocks. The biotite diorite series, including tonalite-granodiorite batholiths such as the Elzevir, Northbrook and Weslemkoon plutons, has an age of 1226 ± 25 Ma**, whereas a granite group, including the Addington, Mazinaw and Methuen plutons, has an age of 1104 ± 25 Ma**. No specific ages are given for late-tectonic syenitic plutons, but in a diagram (Lumbers, 1967, p. 20) they are shown to be as old as or slightly younger than the youngest of the granite group.

Rb-Sr isotope data for the Ridge Granite (4), Westport Monzonite (16), Gananoque Syenite (12) and Lyndhurst Granite (14) with well-defined isochrons have been reported by Krogh and Hurley (1968). Wanless and Loveridge (1972) have reported a poorly-defined Rb-Sr isochron for the Deloro pluton (5). Because different ⁸⁷Rb decay constants have been used, ages have been recalculated using the currently favoured ⁸⁷Rb decay constant of 1.42 x 10⁻¹¹ a⁻¹ to facilitate comparison, and are presented in Table 19.1. Rb-Sr isotope studies of igneous rocks of the Central Metasedimentary Belt currently underway (see Bell and Blenkinsop, part III of this paper) should yield further age determinations for late-tectonic plutons.

Granite Suite (2, 4, 5, 10, 14, 17, 23-25)

Most of the granite plutons fall into two categories: leucocratic, allotriomorphic-granular granites that lie in the granite-B field of the IUGS classification scheme (Streckeisen, 1973), and inequigranular, leuco- to mesocratic biotite-hornblende granites of the granite-A or alkali-feldspar granite fields. The first category (23-25 and parts of 2 and 17) is referred to as the Rockport or Guénette type (Wynne-Edwards, 1962; Wynne-Edwards et al., 1966). These are fine to medium grained subsolvus granites with subequal amounts of quartz, microcline and sodic plagioclase, with minor biotite and accessory hornblende, chlorite, epidote, magnetite, apatite, fluorite, zircon, tourmaline, sphene and muscovite. The second category (2, 4, 5, 10, 14, 17) is compositionally less homogeneous, richer in mafic minerals (primarily hornblende and biotite), more coarse grained, has alkali feldspar/plagioclase ratios greater than 2:1, and contains from 10 to 35 per cent quartz (Currie and Ermanovics, 1971). In most places, particularly in the

Frontenac Axis region, the textures of the rocks resemble those of spatially related monzonitic and syenitic rocks far more closely than those of the Rockport-Guénette type.

Syenite Suite (1, 3, 6-9, 11-13, 15, 16, 18-22, 26-28)

Syenitic rocks, including monzonitic and related mafic phases, constitute the greater proportion of the plutons examined. Despite the fairly wide range in lithologies represented by these plutons, they can be grouped into two secondary categories, based on whether or not they are associated with mafic plutonic rocks. It is not yet certain whether the presence of nepheline-bearing rocks in the Gracefield (20), Ste.-Véronique (26) and lac Rouge (27) syenites (Currie, 1976) is sufficiently distinctive to warrant a third category.

In plutons lacking associated mafic phases (1, 3, 6, 7, 12, 19, 20, 27), the dominant syenitic phase contains either or both biotite and hornblende, although clinopyroxene is locally abundant. Subordinate phases range from monzodiorite to granite. Limited magmatic differentiation is suggested for at least the Mount Moriah Syenite (7) (Thivierge, 1977) because later phases tend to be more siliceous. Other evolutionary trends are hydration of clinopyroxene to hornblende and biotite, and a change from hypersolvus to subsolvus alkali-feldspar relationships (ibid., and P.A. Brown, pers. comm., 1978).

In plutons distinguished by the presence of a mafic phase, characteristically monzogabbro to monzodiorite (8, 9, 11-13, 15, 16, 18, 21, 22, 26, 28), gradations between mafic and felsic phases are known, but more commonly discrete bodies of each phase are present. The mafic and felsic phases appear to be genetically related, but evidence from both the literature and the field suggests that relationships are complex. In the Loughborough Lake area of southeastern Ontario, detailed studies show clearly that the gabbroic rocks are tectonically included enclaves that behaved buoyantly in hot anatectic melts (Currie and Ermanovics, 1971). On the other hand, field evidence in the Skootamatta Syenite (8) suggests that monzogabbro and monzonite have gradational contacts but that both are enveloped by later felsic phases which themselves grade to quartz syenite and microgranite. At Mount St. Patrick (18) the syenite has been intruded by mafic dykes that appear to be genetically related to a central mafic plug. In most cases, however, poor exposure of definitive outcrops precludes subdivision of this group of plutons into two subgroups on the basis of relative ages of the constituent rock phases. It should be borne in mind that the biotite-hornblende syenites of the former category may also be associated with mafic phases at levels not currently exposed.

Table 19.1

Ages of Late-tectonic plutons in southeast Ontario

Pluton	Whole rock Rb-Sr isochron age ¹
Ridge Granite (4) Westport Monzonite (16)	995 ± 38 Ma
Gananoque Syenite (12) Lyndhurst Granite (14)	1073 ± 49 Ma
Deloro Granite (5)	1096 ± 48 Ma
¹ Recalculated using $\lambda^{87}\text{Rb} = 1.42 \times 10^{-11} \text{ a}^{-1}$	

*Numerals in brackets refer to Figure 19.3

**Recalculated using U decay constants of Jaffey, et al. (1971).

Dykes

Most plutons examined have a variety of associated minor syenitic, granitic, lamprophyric and pegmatitic dykes. These are usually found only within the plutons themselves, although some dykes have been observed to intrude the country rocks for short distances away from the contacts. Field evidence suggests that these dykes are cogenetic with the magmatic activity responsible for the spatially related plutons. Late diabase dykes are present locally; these invariably postdate the syenite dykes and are not considered related to the plutons.

Structure and Metamorphism

A striking feature of all the plutons is their lack of chilled margins and their apparent concordance with regional structure, suggesting passive emplacement into relatively warm rocks. Only a few of the plutons (e.g., Loranger Syenite (28)) have such discordant features as dykes or apophyses cutting the country rocks. In general there appears to be a positive correlation between the extent of internal deformation, the degree of recrystallization, and regional metamorphic grade. The plutons intruding greenschist facies rocks of the Hastings Basin (5-8) are more or less massive, showing only minor recrystallization haloes around some feldspar crystals or mild marginal deformation such as is found along the eastern side of the Skootamatta Syenite (8). Thermal aureoles around these plutons are narrow, but locally reach pyroxene hornfels facies (Thivierge, 1977). In contrast, in high grade metamorphic terranes such as the Loughborough Lake area, recrystallization is widespread, cataclasis is a pervasive feature, and migmatites are common to the extent that, for example, the Crow Lake pluton (15) "... fades imperceptibly into its surroundings." (Currie and Ermanovics, 1971, p. 53).

There are, however, many exceptions to this general pattern, suggesting that within any given area, suite, or even polyphase pluton, emplacement was episodic and was commonly accompanied by deformation, perhaps spanning a substantial period of tectonic activity. As Wynne-Edwards (1969, p. 165) noted for plutons in Quebec, "... intrusions might be further divided into late and early tectonic categories depending on the nature of their foliation and degree to which they are discordant, but they are all manifestly not metamorphic rocks." It is on this point that all authors appear unanimous: that these plutons are indeed products of orogenesis extant 1.0 Ga ago. The following reasons are commonly cited as support for a syn- to late-tectonic origin: the plutons are relatively more massive than the enclosing metamorphic rocks, including metaplutonites; they are little enough deformed that parts of them have primary igneous textures preserved, contrasting strongly with neighbouring orthogneisses; they post-date all other intrusive rocks except diabase dykes (latest Precambrian and early Paleozoic plutons postdate these dykes). Field evidence therefore points to a relatively limited participation in the dynamothermal metamorphism of the Grenvillian Orogeny.

Outside the low metamorphic grade Hastings Basin, contact metamorphic effects are difficult to distinguish from those of regional metamorphism. A common feature of all the syenite plutons in Quebec and of several in Ontario outside the Frontenac Axis region, is the development of large biotite porphyroblasts in monzonitic to dioritic rocks, apparently due to late-stage autometamorphism. These biotites generally occur as large, very thin plates, do not have preferred orientation, and appear to have grown at the expense of clinopyroxene and hornblende.

Genesis

The existence of geologically diverse plutons apparently confined to the Central Metasedimentary Belt has for some time stimulated speculation concerning their origins. On the basis of trace element geochemistry, Dostal (1975, p. 1344) considered that the monzonite and quartz monzonite of the Loon Lake pluton (1) were "... formed from a magma that was generated by partial melting of lower crustal/upper mantle rocks, probably followed by fractional crystallization." Partial melting of higher-level crustal rocks induced by the intrusions may have contaminated the initial melt. Currie and Ermanovics (1971, p. 67) considered that the Perth Road (9), Battersea (10) and Crow Lake (15) plutons "... originated by anatexis of quartz-poor feldspathic rock ..." more or less in situ, at the same time involving processes of desilication and ion diffusion through gradients of pressure, temperature and concentration of a volatile phase. Wynne-Edwards (1963, 1967) has suggested that the Westport plutons (16) originated by replacement processes and/or remobilization of anhydrous basement rocks at structurally favourable sites, and that the Rockport-type granites formed by anatexis or metasomatism of hydrous metasedimentary rocks. Most recently, Shieh (1978) has suggested on the basis of oxygen isotope studies that the source rocks of the Westport plutons are Grenville basement gneisses and that those of the Perth Road (9), Battersea (10), South Lake (11), Gananoque (12), Lyndhurst (14), and Crow Lake (15) plutons are Grenville Supergroup metasediments. In interpreting their Rb-Sr and Pb-Pb isotope data, Krogh and Hurley (1968), Zartman (1969), and Wanless and Loveridge (1972) suggested that for at least the Ridge Granite (4), Westport Monzonite (16), Gananoque Syenite (12), Lyndhurst Granite (14) and Deloro Granite (5), derivation from an ancient sialic basement source is unlikely. Projected initial $^{87}\text{Sr}/^{86}\text{Sr}$ ratios are too low to support such a hypothesis. For the Ridge and Westport plutons the initial ratio is 0.7040; for the Gananoque and Lyndhurst plutons it is 0.7054; for the Deloro pluton it is 0.7036. Zartman (1969, p. 201) stated that "... two feldspar leads (from the Westport pluton) have isotopic compositions which lie right in the main spectrum of ordinary lead for 1.0 b.y.-old igneous rocks ...", and that "... certainly no peculiarity in the lead from this pluton exists which can be definitely used as evidence for the pluton's having been derived from remobilized old basement rock."

Economic Geology

Many plutons in the Bancroft - Madoc area, including some of the late-tectonic ones, have small contact metamorphic or metasomatic ore deposits associated with them. These tend to be small bodies rich in magnetite or talc (Lumbers, 1967; Hewitt, 1968). Gold-bearing arsenopyrite has been mined in quartz veins around the Deloro Granite (5). The veins are thought to be genetically related to the intrusion (Wilson, 1965). Within alkaline rocks of the Intermontane Belt of British Columbia (Barr et al., 1976), porphyry Cu-Mo mineralization is well known. However, apart from the once-mined molybdenite deposit in syenite of late Precambrian (post-Grenvillian) age (Doig and Barton, 1968) near Quyon, Quebec, Cu-Mo mineralization has not been reported and none was observed during field work. Very few scintillometer surveys have been conducted over the plutons. Results so far have not been encouraging (e.g., Rive, 1977b).

Guénette-type granite has been quarried extensively in Quebec and Ontario, and makes excellent dimension stone. Most of the syenite plutons could also produce attractive facing material, access and economic conditions permitting.

PART III

RUBIDIUM-STRONTIUM ISOTOPE STUDIES IN THE GRENVILLE PROVINCE OF SOUTHEAST ONTARIO

K. Bell and J. Blenkinsop (DSS Contract No. OSU78-00052)

Introduction

The Central Metasedimentary Belt in southeastern Ontario contains some of the best preserved, albeit highly deformed, supracrustal rocks within the Grenville Province. Assigned to the Grenville Supergroup, these rocks range from greenschist facies metamorphism in the Hastings Basin to two-pyroxene granulite facies in the Frontenac Axis. To the northwest, granulite facies assemblages are found sporadically in the Ontario Gneiss Segment as close as 10 km beyond the northwestern limit of 'Grenville-type' marbles that is taken to define the edge of the Central Metasedimentary Belt (Fig. 19.1, 19.2). Basement to the Grenville Supergroup has not been positively identified in the area of Figure 19.4, but it may be present in the area of complex migmatites referred to as the Radcliffe Hybrid Gneiss in the Combermere area (Appleyard, 1974). West of the Hastings Basin, basement has been identified in the Harvey-Cardiff Arch (Bright, 1977).

Several distinct suites of plutonic rocks are present in this region, and can be divided into the following petrologic groups: 1) gabbro and diorite, 2) tonalite and granodiorite, 3) granite, 4) syenite, and 5) peralkaline granite and granophyre. Plutons of the second group and some plutons of the first group are combined to form the so-called biotite diorite series of Lumbers (1967). Within and adjacent to the Hastings Basin metamorphic 'low' these plutonic rocks are well preserved, commonly having primary igneous textures. Away from the Hastings Basin their state of preservation deteriorates with increasing deformation and metamorphism, although rocks of some of the plutonic suites appear to have been less affected than others, suggesting perhaps that there may have been more than one period of magmatic activity.

For the sake of consistency in the following discussion, all Rb-Sr and U-Pb ages quoted have been recalculated from those reported using the decay constants: $\lambda^{87}\text{Rb} = 1.42 \times 10^{-11} \text{ a}^{-1}$ (Steiger and Jäger, 1977), $\lambda^{238}\text{U} = 1.55125 \times 10^{-10} \text{ a}^{-1}$ and $\lambda^{235}\text{U} = 9.84850 \times 10^{-10} \text{ a}^{-1}$ ($^{238}\text{U} : ^{235}\text{U} = 137.88$) (Jaffey et al., 1971). Radiometric ages reported to date from the area shown in Figure 19.4 range from approximately 1300 to 850 Ma. In general, U-Pb and Rb-Sr ages are significantly older than K-Ar ages, most being in excess of 1000 Ma. K-Ar ages from the Hastings Basin region are listed by MacIntyre et al. (1967), and range from 1070 to 843 Ma. More recently determined K-Ar ages lie within the same range. Pertinent U-Pb and Rb-Sr ages reported in the literature are given in Table 19.2.

Two periods of magmatism are recognized by Silver and Lumbers (1966): an earlier biotite diorite series, represented by the Elzevir pluton (1226 Ma), to which group also belong the Weslemkoon, Northbrook, probably the Mellon Lake and possibly the Hinchinbrooke (1254 Ma, Wallach, 1974) plutons (see Fig. 19.4) a granitic ('quartz monzonite') group, represented by the Addington pluton (1104 Ma), to which the Mazinaw pluton likely belongs. Lumbers (1967, p. 20, Fig. 3) postulated that certain mafic and nepheline syenite plutons have ages intermediate between these two, and that potassic syenite and monzonite intrusions may slightly postdate the granitic group. Although Lumbers includes the Deloro peralkaline granite stock in his biotite diorite series, its chemistry is distinctive and it may belong to the younger potassic group. It is important to note that the age determined on zircon from the Flinton Group conglomerate is a maximum age, and that pebbles of Addington-like granite

are present in the Flinton conglomerates (P.H. Thompson, 1978, pers. comm.). The geological age relationship of the Flinton Group to the Deloro stock is not certain. The variously younger K-Ar ages obtained on these units presumably reflect thermal overprinting and uplift related to the post-Flinton Grenvillian deformation and metamorphism.

The overall aims of the present geochronological project are to attempt to define intrusive ages for each of the plutonic suites mentioned, to evaluate the rôle and extent of crustal reworking, and to investigate rock units considered to be possible basement to the Grenville Supergroup.

Results and Discussion

Suites of large, fresh samples suitable for Rb-Sr isotopic analysis have been collected, mainly from blasted roadside outcrops, from the Elzevir, Weslemkoon, Northbrook, Mellon Lake, White Lake, Addington, Mazinaw, Skootamatta, Deloro and Moira Lake plutons, and also from the Radcliffe Hybrid Gneiss (Fig. 19.4). An additional suite was collected from the Loranger syenite pluton in Quebec (Fig. 19.3). Table 19.3 gives the ranges of Rb-Sr ratios for seven of the suites that have been or are currently being processed. The value ranges are broadly consistent with the rock types that make up each of the rock units. The three tonalite-granodiorite suites (Elzevir, Northbrook, Mellon Lake), for example, all have Rb-Sr ratios less than 0.3, whereas the samples of the Addington granite pluton have significantly higher ratios. The highest ratios are from the Deloro stock. Syenite samples from the Skootamatta stock have surprisingly low ratios.

Three of the suites are from plutonic units that flank the Clare River Synform, a major northeast trending structure containing Grenville Supergroup formations and including probable correlatives of the Flinton Group. This structure is interpreted to have formed by early recumbent folding followed by coaxial, tightly closed to isoclinal folding. The Addington pluton structurally underlies the supracrustal succession on both sides of the synform and is supposedly separated from it by a zone of décollement (Chappell, 1978).

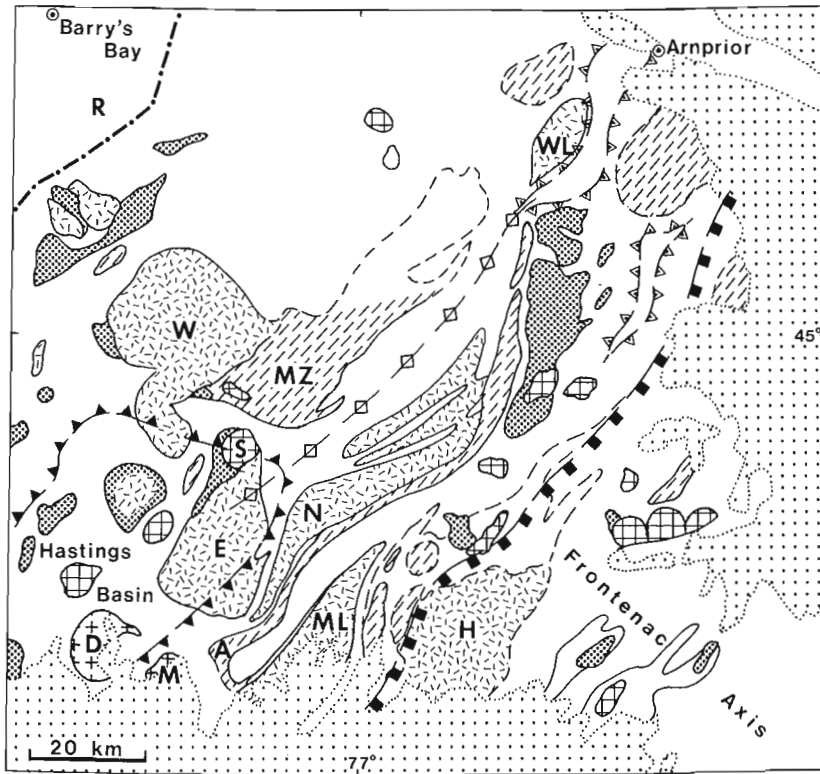
Table 19.2

Recalculated U-Pb and Rb-Sr ages previously reported for rocks of the Hastings Basin region

Rock Unit	U-Pb age	Rb-Sr age Reference ¹
Pegmatites	1030 ± 20 Ma	1
Deloro stock		1096 ± 48 Ma 2
Conglomerate, Flinton Group	1118 ± 30 Ma	3
Addington pluton	(1104 ± 25 Ma) ²	1013 ± 59 Ma 1,4
Elzevir pluton	1226 ± 25 Ma	1
Hinchinbrooke pluton	1254 ± ? Ma	5
Volcanic rocks, Tudor Formation	1286 ± 15 Ma	1

¹ 1 - Silver and Lumbers, 1966; 2 - Wanless and Loveridge, 1972; 3 - Boutcher et al., 1965; 4 - Krogh and Hurley, 1968; 5 - Wallach, 1974.

² Age reported for 'quartz monzonite' group to which the Addington pluton is assigned (Lumbers, 1967).



- | | | |
|--|--|---|
| | Paleozoic cover | |
| | Peralkaline granite, granophyre | D - Deloro, M - Moira Lake |
| | Syenite | S - Skootamatta |
| | Granite, gneissic granite | A - Addington, M - Mazinaw |
| | Tonalite, granodiorite | ML - Mellon Lake, N - Northbrook, E - Elzevir, H - Hinchinbrooke, W - Weslemkoom, WL - White Lake |
| | Gabbro, diorite | |
| | Grenville Supergroup, undifferentiated gneiss | R - Radcliffe Hybrid Gneiss |
| | Northwest margin of Central Metasedimentary Belt | |
| | Boundary of greenschist facies metamorphism | } Symbols on high grade side |
| | Boundary of 'relatively low grade' metamorphism | |
| | Boundary of granulite facies metamorphism | |
| | Axis of Hastings - Arnprior metamorphic 'trough' | |

Figure 19.4. Distribution of plutonic rocks in part of the Central Metasedimentary Belt of the Grenville Province in Ontario.

It is composed of pink, fine grained leucogranite and is strongly deformed. In most places it has a well-defined linear fabric parallel to that in the supracrustal rocks. Evidence is preserved locally that its quartz has been highly flattened, but for the most part it is composed of equant polygonal quartz and feldspar that form a fine mosaic within which only the micas display orientation. Relict igneous texture and xenoliths can be recognized locally in its westernmost parts. The Northbrook and Mellon Lake plutons lie on the northwest and southeast sides of the Clare River Synform respectively, beyond the Addington pluton. A narrow septum of marble, calc-silicate gneiss and pegmatite separates the Mellon Lake and Addington plutons. The Northbrook and Addington plutons are separated in part by Grenville Supergroup metasediments, including the 'Kaladar conglomerate', tentatively correlated with the Flinton Group (Moore and Thompson, 1972), but are in contact northeast of Kaladar where Psutka (1976) interpreted Addington granite to intrude Northbrook granodiorite. It is possible that the Northbrook and Elzevir plutons are continuous beneath the infolded Flinton Group (Moore and Thompson, 1972). The amount of penetrative deformation and recrystallization in these granodiorite plutons increases southeastward, commensurate with rise in regional metamorphic grade (Carmichael et al., 1978). Both the Northbrook and the Mellon Lake granodiorites are well foliated, but whereas in the Northbrook relicts of primary texture are preserved in the form of elongate domains of recrystallized quartz and plagioclase, in the Mellon Lake advanced recrystallization has completely destroyed all microscopic evidence of primary texture. The Mellon Lake granodiorite is locally permeated by leucocratic mobilisate which was avoided during sampling.

The preliminary results of Rb-Sr isotope analysis of samples from these three units are summarized in Table 19.4. The ages listed were computed using $\lambda^{87}\text{Rb} = 1.42 \times 10^{-11} \text{ a}^{-1}$. The large uncertainties, of the order of 8 per cent, attached to the Mellon Lake and Northbrook ages are due mainly to the restricted spread in Rb/Sr ratios. The ages obtained for these two plutons agree within the limits set by analytical uncertainty. The age for the Northbrook pluton, however, is controlled mainly by a single sample that has the highest Rb/Sr ratio. Sericitization of the plagioclase and sheaves of muscovite intimately associated with calcite in this sample may indicate some potash metasomatism, and therefore it is considered that the $1100 \pm 100 \text{ Ma}$ age is perhaps a minimum age for the emplacement of the pluton. On the basis of their modal mineralogy, geological setting, and similarity in initial $^{87}\text{Sr}/^{86}\text{Sr}$ ratios, it is preferable, at present, to consider both the Mellon Lake and Northbrook plutons to be the same age. Data from both suites can be plotted on one isochron (ten points), and this results in an age of $1180 \pm 90 \text{ Ma}$, and initial $^{87}\text{Sr}/^{86}\text{Sr}$ ratio of 0.7017 ± 0.0005 , and a MSWD of 3.6. For the time being, this is considered to be a fair

estimate of the age of intrusion for both plutons. The low initial $^{87}\text{Sr}/^{86}\text{Sr}$ ratio implies that most of the Sr within these granodiorites was derived from a source region with fairly low Rb/Sr ratio, unlikely to have been typical continental crust.

Seven samples from the Addington pluton were analyzed, although only five analyses were used to compute the age of $1072 \pm 22 \text{ Ma}$ given in Table 19.4. Two samples that fall significantly off the isochron were excluded from the calculation because they contain fluorite, chlorite and carbonate, suggestive of secondary alteration and open-system behaviour.

On the basis of these results, it seems safe to say that the Addington pluton is younger than the Mellon Lake and Northbrook plutons, a finding which supports Psutka's (1976) contention that granite dykes which cut the southern part of the Northbrook pluton are related to the Addington granite. The determined age and the initial $^{87}\text{Sr}/^{86}\text{Sr}$ ratio of 0.7067 ± 0.0007 , significantly higher than those of the Mellon Lake and Northbrook plutons, lead to the conclusion that the Addington pluton is both different in age and in origin to the granodioritic plutons examined so far. A Rb-Sr age of $1013 \pm 59 \text{ Ma}$, with a high initial $^{87}\text{Sr}/^{86}\text{Sr}$ ratio of 0.711, has been reported for the Addington pluton (Kaladar gneiss) by Krogh and Hurley (1968) who consider, however, that this age represents a minimum value for the time of formation of the pluton.

The Mellon Lake and Northbrook plutons belong to the biotite diorite series of Lumbers (1967) and the Addington pluton to his younger 'quartz monzonite' group. The ages reported here can be interpreted as consistent with the U-Pb ages of $1226 \pm 25 \text{ Ma}$ and $1104 \pm 25 \text{ Ma}$ reported by Silver and Lumbers (1966) for these two plutonic suites, but because the uncertainties on the Rb-Sr ages are quite large, nothing can at present be added to their conclusions. On a cautionary note, it should be pointed out that, because no detailed account of their work has been published, it is difficult to compare in any way their data with those obtained during the present study.

In addition to the plutons already discussed, samples from the Deloro stock, a high-level, composite pluton of predominantly peralkaline granite and granophyre, were also analyzed. Although the results to date are only preliminary, the pronounced scatter of the data on an isochron plot would suggest that either the Rb-Sr system was disturbed during regional metamorphism or that the composite pluton did not have a uniform Sr isotope composition at the time of its formation. The isochron obtained by Wanless and Loveridge (1972) for this pluton shows a similar scatter.

In all of the plutons examined in this study so far, a scatter of data has been encountered which cannot be attributed solely to analytical uncertainty, a feature that is reflected in the high MSWD values given in Table 19.4. In almost all the plutonic units it would seem that the Rb-Sr

Table 19.3

Range of whole rock Rb-Sr weight ratios

Rock Unit	No. of samples	Range of Rb-Sr ratios ¹
Deloro stock	9	6.4 - 8.6
Skootamatta stock	10	0.01 - 0.29
Addington pluton	11	1.2 - 6.3
Elzevir pluton	8	0.08 - 0.11
Northbrook pluton	8	0.07 - 0.26
Mellon Lake pluton	8	0.09 - 0.28
Radcliffe Hybrid Gneiss	11	0.01 - 0.41

¹ All samples analyzed in duplicate by X-ray fluorescence. Analytical uncertainty $\pm 1\%$ at the 1σ level.

Table 19.4

Preliminary whole rock Rb-Sr isochron data

Rock Unit	Preferred age	Initial $^{87}\text{Sr}/^{86}\text{Sr}$ ratio	MSWD	No. of points
Addington pluton	$1072 \pm 22 \text{ Ma}$	0.7067 ± 0.0007	3.5	5
Northbrook pluton	$1100 \pm 100 \text{ Ma}$	0.7023 ± 0.0006	4.0	5
Mellon Lake pluton	$1250 \pm 130 \text{ Ma}$	0.7012 ± 0.0007	4.0	5

systems have almost been disturbed, and as a consequence have become 'leaky'. It had been hoped that this problem would have been avoided by choosing the Hastings Basin region for this study because it is one of the areas of lowest metamorphic grade in the whole Grenville Province.

References

- Adams, F.D. and Barlow, A.E.
1910: Geology of the Haliburton and Bancroft areas, Ontario; Geological Survey of Canada, Memoir 6, 419 p.
- Appleyard, E.C.
1974: Basement/cover relationships within the Grenville Province in eastern Ontario; Canadian Journal of Earth Sciences, v. 11, p. 369-379.
- Baer, A.J.
1974: Grenville geology and plate tectonics; Geoscience Canada, v. 1, no. 3, p. 54-61.
1976: The Grenville Province in Helikian times: a possible model of evolution; Philosophical Transactions of the Royal Society of London, ser. A, v. 280, p. 499-515.
- Baer, A.J., Poole, W.H., and Sanford, B.V.
1977: Rivière Gatineau; Geological Survey of Canada, Map 1334A.
- Barr, D.A., Fox, P.E., Northcote, K.E., and Preto, V.A.
1976: The alkaline suite porphyry deposits – a summary; in Porphyry Deposits of the Canadian Cordillera, ed. A. Sutherland Brown; Canadian Institute of Mining and Metallurgy, Special Volume 15, p. 359-367.
- Bell, R.T.
1971: A Geological survey of Algonquin Provincial Park and recommendations for Park Master Plan; report 1; unpublished manuscript report, 25 p.
- Bourne, J.H.
1970: Geology of Pythonga Lake area; Ministère des Richesses naturelles du Québec, Preliminary Report, Open File GM 28638, 22 p.
1978: Metamorphism in the eastern and southwestern portions of the Grenville Province; in Metamorphism in the Canadian Shield, eds. J.A. Fraser and W.W. Heywood; Geological Survey of Canada, Paper 78-10, p. 315-328.
- Boutcher, S.M.A., Davis, G.L., and Moorehouse, W.W.
1965: Potassium-argon and uranium-lead ages from two localities; Canadian Mineralogist, v. 10, p. 198-203.
- Bright, E.G.
1977: Regional structure and stratigraphy of the Eels Lake area, Haliburton and Peterborough Counties; in Summary of Field Work, 1977, Ontario Geological Survey, Miscellaneous Paper 75, p. 110-117.
- Card, K.D.
1978: Geology of the Sudbury – Manitoulin area, Districts of Sudbury and Manitoulin; Ontario Geological Survey, Report 166, 238 p.
- Card, K.D. and Lumbers, S.B.
1977: Sudbury – Cobalt; Ontario Geological Survey, Map 2361.
- Carmichael, D.M., Moore, J.M., Jr., and Skippen, G.B.
1978: Isograds around the Hastings metamorphic "low"; in Toronto '78, Field Trips Guidebook, eds. A.L. Currie and W.O. Mackasey; Geological Association of Canada, p. 325-346.
- Chagnon, J.-Y.
1976: Membre – Chalifoux area, Abitibi-East and Gatineau Counties; Ministère des Richesses naturelles du Québec, Geological Report 175, 102 p.
- Chappell, J.F.
1978: The Clare River structure and its tectonic setting; unpublished Ph.D. thesis, Carleton University, Ottawa, 184 p.
- Currie, K.L.
1976: The alkaline rocks of Canada; Geological Survey of Canada, Bulletin 239, 228 p.
- Currie, K.L. and Ermanovics, I.F.
1971: Geology of Loughborough Lake region; Geological Survey of Canada, Bulletin 199, 85 p.
- Déland, A.-N. and Grenier, P.-E.
1959: Hazeur – Druillettes area, Abitibi-East Electoral District; Quebec Department of Mines, Geological Report 87, 71 p.
- Dewey, J.F. and Burke, K.C.A.
1973: Tibetan, Variscan and Precambrian basement reactivation: products of continental collision; Journal of Geology, v. 81, p. 683-692.
- Doig, R.
1975: A syenitic pluton of Archean age within the Grenville Province of Quebec; Canada Journal of Earth Sciences, v. 12, p. 890-893.
- Doig, R. and Barton, J.M., Jr.
1968: Ages of carbonatites and other alkaline rocks in Quebec; Canadian Journal of Earth Sciences, v. 5, p. 1401-1407.
- Dostal, J.
1975: Geochemistry and petrology of the Loon Lake pluton, Ontario; Canadian Journal of Earth Sciences, v. 12, p. 1331-1345.
- Fraser, J.A., Heywood, W.W., and Mazurski, M.A.
1978: Metamorphic map of the Canadian Shield; Geological Survey of Canada, Map 1475A.
- Frith, R.A. and Doig, R.
1975: Pre-Kenoran tonalitic gneisses in the Grenville Province; Canadian Journal of Earth Sciences, v. 12, p. 844-849.
- Froese, E. and Jen, L.S.
1979: A reaction grid for biotite-bearing mafic granulites; in Current Research, Part A, Geological Survey of Canada, Paper 79-1A, p. 83-85.
- Gillies, N.B.
1952: Canimite River area, Pontiac County; Quebec Department of Mines, Geological Report 52, 46 p.
- Hewitt, D.F.
1964: Geological notes for maps nos. 2053 and 2054, Madoc – Gananoque area; Ontario Department of Mines, Geological Circular 12, 33 p.
1967: Geology and mineral deposits of the Parry Sound – Huntsville area; Ontario Department of Mines, Geological Report 52, 65 p.

- Hewitt, D.F. (cont.)
 1968: Geology of Madoc Township and the north part of Huntingdon Township, Hastings County; Ontario Department of Mines, Geological Report 73, 45 p.
- Irving, E., Park, J.K., and Roy, J.L.
 1972: Palaeomagnetism and the origin of the Grenville Front; *Nature*, v. 236, p. 344-346.
- Jaffey, A.H., Flynn, K.F., Glendenin, L.E., Bentley, W.C., and Essling, A.M.
 1971: Precision measurement of half-lives and specific activities of ^{235}U and ^{238}U ; *Physical Review*, ser. C, v. 4, p. 1889-1906.
- Katz, M.
 1969: Geology of the Saint-Patrice Lake and Portage-du-Fort areas; Quebec Department of Natural Resources, Preliminary Report 578, 27 p.
- Krogh, T.E., Brooks, C., Hart, S.R., and Davis, G.L.
 1970: The Grenville Front in the Chibougamau - Surprise Lake area, Quebec; *Carnegie Institute of Washington, Yearbook* 68, p. 313-314.
- Krogh, T.E. and Davis, G.L.
 1968: Geochronology of the Grenville Province; *Carnegie Institute of Washington, Yearbook* 67, p. 224-230.
- Krogh, T.E. and Hurley, P.M.
 1968: Strontium isotope variations and whole rock isochron studies in the Grenville Province of Ontario; *Journal of Geophysical Research*, v. 73, p. 7107-7125.
- Kuehnbaum, R.M.
 1973: Petrology of the Deloro pluton and associated country rocks, near Madoc, Ontario; unpublished M.Sc. thesis, University of Toronto, 173 p.
- Lacy, W.C.
 1960: Geology of the Dunchurch area, Ontario, Canada; *Geological Society of America Bulletin*, v. 71, p. 1713-1718.
- Logan, Sir W.E.
 1863: Report on the geology of Canada; *Geological Survey of Canada, Report of Progress from its Commencement to 1863*, 983 p.
- Lumbers, S.B.
 1967: Geology and mineral deposits of the Bancroft - Madoc area; in *Guidebook - Geology of Parts of Eastern Ontario and Western Quebec*, ed. S.E. Jenness; Geological Association of Canada, p. 13-29.
 1971: Geology of the North Bay area, Districts of Nipissing and Parry Sound; Ontario Department of Mines and Northern Affairs, Geological Report 94, 104 p.
 1975: Geology of the Burwash area, Districts of Nipissing, Parry Sound, and Sudbury; Ontario Division of Mines, Geological Report 116, 158 p.
 1978: Geology of the Grenville Front Tectonic Zone in Ontario; in *Toronto '78, Field Trips Guidebook*, eds. A.L. Currie and W.O. Mackasey; Geological Association of Canada, p. 347-361.
- MacIntyre, R.M., York, D., and Moorehouse, W.W.
 1967: Potassium-argon age determinations in the Madoc - Bancroft area in the Grenville Province of the Canadian Shield; *Canadian Journal of Earth Sciences*, v. 4, p. 815-828.
- Moore, J.M., Jr. and Thompson, P.H.
 1972: The Flinton Group, Grenville Province, eastern Ontario, Canada; in *Precambrian Geology*, section 1, 24th International Geological Congress, p. 221-229.
- Morton, R.L.
 1978: Harvey Township, Peterborough County; in *Summary of Field Work, 1978*, Ontario Geological Survey, Miscellaneous Paper 82, p. 128-130.
- Otton, J.K.
 1972: Geology of the Bouchette Lake area, Montcalm and Pontiac Counties; Ministère des Richesses naturelles du Québec, Preliminary Report, Open File GM 27780, 13 p.
- Psutka, J.F.
 1976: Provenance of the plutonic pebbles in the Kaladar metaconglomerate and geology of associated metasediments; unpublished B.Sc. thesis, Carleton University, Ottawa, 62 p.
- Quirke, T.T. and Collins, W.H.
 1930: The disappearance of the Huronian; *Geological Survey of Canada, Memoir* 160, 129 p.
- Reinhardt, E.W. and Skippen, G.B.
 1970: Petrochemical study of Grenville granulites; in *Report of Activities, Part B, November 1969 to March 1970*, Geological Survey of Canada, Paper 70-1B, p. 48-54.
- Rive, M.
 1976: Géologie des lacs Simard, Winawash et Décelles (Comté de Témiscamingue et de Pontiac); Ministère des Richesses naturelles du Québec, Rapport préliminaire DP-338, 16 p.
 1977a: Région des lacs Cawasachouane et Otanabi; Ministère des Richesses naturelles du Québec, Rapport préliminaire DPV-491, 7 p.
 1977b: Sainte-Véronique area, Electoral District of Laurentide-Labelle; Ministère des Richesses naturelles du Québec, Geological Report 182, 68 p.
- Saha, A.K.
 1959: Emplacement of three granitic plutons in southeastern Ontario, Canada; *Geological Society of America Bulletin*, v. 70, p. 1293-1326.
- Sauerbrei, A.
 1966: The granitic rocks of the Frontenac Axis; unpublished M.Sc. thesis, Queen's University, Kingston, 141 p.
- Shieh, Y.-N.
 1978: High ^{18}O granitic plutons from the Frontenac Axis, Grenville Province of Ontario; *Geological Association of Canada, Abstracts with Programs*, v. 10, no. 7 (Annual Meeting), p. 491.
- Silver, L.T. and Lumbers, S.B.
 1966: Geochronological studies in the Bancroft - Madoc area of the Grenville Province, Ontario; *Geological Society of America, Special Publication* 87, p. 156.
- Steiger, R.H. and Jäger, E.
 1977: Subcommission on Geochronology: Convention on the use of decay constants in geo- and cosmochronology; *Earth and Planetary Science Letters*, v. 36, p. 359-362.

- Stockwell, C.H.
1972: Deloro stock, southeastern Ontario: geological setting and interpretation; in Wanless, R.K., and Loveridge, W.D., Rubidium-strontium isochron age studies, report 1; Geological Survey of Canada, Paper 72-23, p. 49-52
- Streckeisen, A.
1973: IUGS Subcommittee on the Systematics of Igneous Rocks, classification and nomenclature of plutonic rocks. Recommendations; Neues Jahrbuch fuer Mineralogie, Monatshefte, h. 4, p. 149-164.
- Thivierge, R.H.
1977: The geology of the Mount Moriah syenite, Grenville Province, southeast Ontario; unpublished B.Sc. thesis, Carleton University, Ottawa, 64 p.
- van der Leeden, J.
The geological history of the Grenville Front in western Quebec; Ph.D. thesis, University of Ottawa. (in prep.)
- Wallach, J.L.
1974: Origin of the Hinchinbrooke gneiss and its age relationship to the Grenville Group rocks of southeastern Ontario; Geological Association of Canada, Annual Meeting 1974, Program of Abstracts, p. 96.
- Wanless, R.K. and Loveridge, W.D.
1972: Rubidium-strontium isochron age studies, report 1; Geological Survey of Canada, Paper 72-23, 77 p.
- Wilson, M.E.
1965: The Deloro stock and its mineralized aureole; Economic Geology, v. 60, p. 163-167.
- Winkler, H.G.F.
1976: Petrogenesis of metamorphic rocks; Springer-Verlag New York Incorporated, 4th ed., 334 p.
- Wynne-Edwards, H.R.
1962: Gananoque map-area, Ontario; Geological Survey of Canada, Map 27-1962.
1963: Brockville - Mallorytown area, Ontario; Geological Survey of Canada, Map 7-1963.
1967: Westport map-area, Ontario, with special emphasis on the Precambrian rocks; Geological Survey of Canada, Memoir 346, 142 p.
1969: Tectonic overprinting in the Grenville Province, southwestern Quebec; in Age relations in high-grade metamorphic terrains, ed. H.R. Wynne-Edwards; Geological Association of Canada, Special Paper 5, p. 163-182.
1972: The Grenville Province; in Variations in tectonic styles in Canada, eds. R.A. Price and R.J.W. Douglas, Geological Association of Canada, Special Paper 11, p. 263-334.
- Wynne-Edwards, H.R., Gregory, A.F., Hay, P.W., Giovanella, C.A., and Reinhardt, E.W.
1966: Mont Laurier and Kempt Lake map-areas, Quebec; Geological Survey of Canada, Paper 66-32, 32 p.
- Zartman, R.E.
1969: Lead isotopes in igneous rocks of the Grenville Province as a possible clue to the presence of older crust; in Age relations in high-grade metamorphic terrains, ed. H.R. Wynne-Edwards; Geological Association of Canada, Special Paper 5, p. 193-205.

PRELIMINARY EVALUATION OF SUMMARY PRODUCTION STATISTICS AND
LOCATION DATA FOR VEIN DEPOSITS, SLOCAN, AINSWORTH AND SLOCAN CITY CAMPS,
SOUTHERN BRITISH COLUMBIA

EMR Research Agreement 2239-4-62/78

A.J. Sinclair¹
Regional and Economic Geology Division

Sinclair, A.J., *Preliminary evaluation of summary production statistics and location data for vein deposits, Slocan, Ainsworth and Slocan City camps, southern British Columbia*; in *Current Research, Part B, Geological Survey of Canada, Paper 79-1B, p. 173-178, 1979.*

Abstract

Summary production statistics (total production and average grades) and location data for vein deposits in a large area in the West Kootenay district of southern British Columbia are examined. These data appear to have useful applications in providing value measures for mineral deposits, in regional zonation studies, in comparative studies of several mining camps, in establishing empirical limits to mineralized centres, and in studying spatial density of productive mineral deposits.

Introduction

Production data for present and past producing mineral deposits in British Columbia are being prepared in a computer file that can be merged both with MINFILE (computerized mineral deposits file of the British Columbia Ministry of Energy, Mines and Petroleum Resources) and MINDEP (computerized mineral deposits file of the Department of Geological Sciences, University of British Columbia). This so-called PRODUCER FILE, in preparation, also contains a variety of geological information. Here we confine our attention to locations of producers and summary production statistics.

Information available is derived principally from records of the Ministry of Energy, Mines and Petroleum Resources extending back to the latter part of the 19th century. Three types of information are available – tonnage (tons of ore produced), metal grades, and deposit locations. Tonnage and grades can be combined to determine metal contents which represent fundamental value measures of a mineral deposit.

Some reasons these data are important are:

- they provide a quantitative base for measuring value of a mineral deposit, a mining camp, etc.;
- they provide a data base for statistical modelling of mineral deposits, with a view to improving resource estimation procedures and exploration success ratios;
- they have potential application to metallogenic studies, especially with regard to regional zonation, definition of centres of mineralization, etc.

Location Data

Locations of mineral deposits that have produced, generally are known accurately. Some exceptions exist in the case of very small deposits with insignificant production records but as a rule such uncertainties are rare. Depending on the scale at

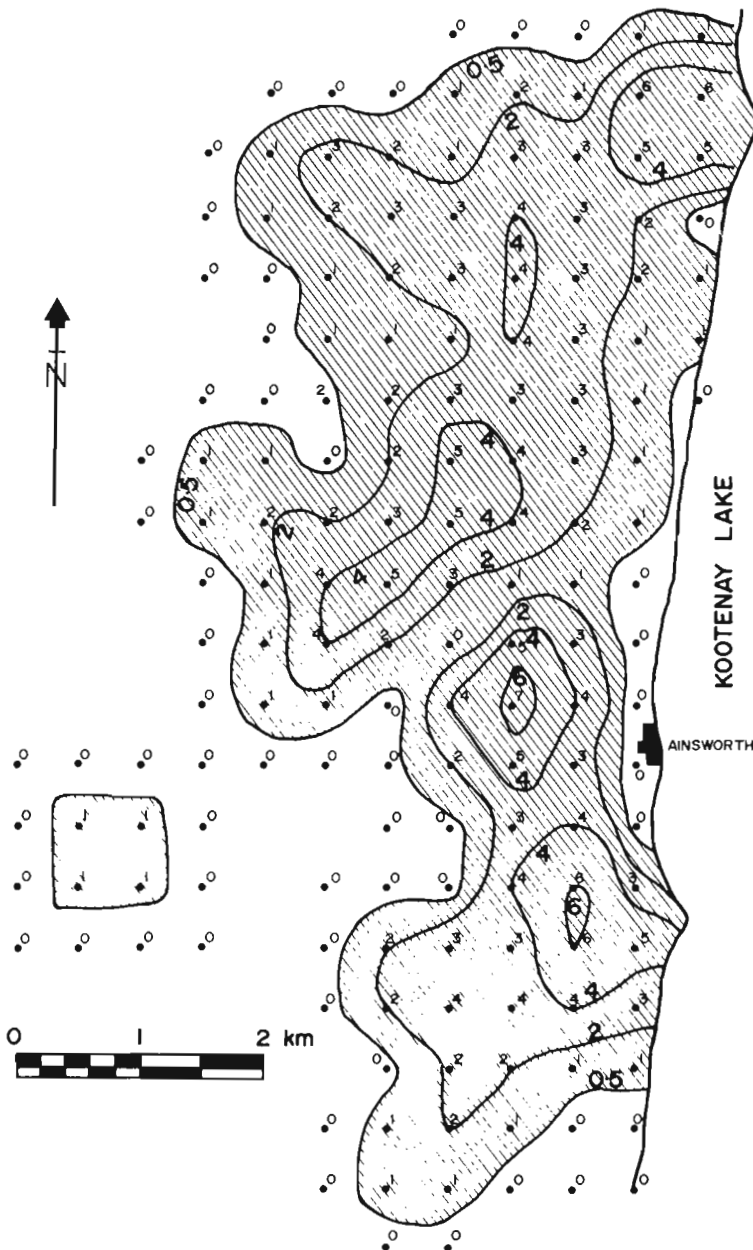


Figure 20.1. Hand-contoured spatial density map of vein deposits in Ainsworth camp, southern British Columbia. Contours are drawn arbitrarily at 0.5, 2, 4 and 6 deposits per km². Cross hatching defines the area of the camp based on the hypothetical contour at 0.5 deposit per km². Note the five local highs; the southern four contain the five largest deposits known in the camp.

¹Department of Geological Sciences, University of British Columbia.

which locations are being considered it may be much more important to be aware of what part of a deposit has been located. Normally we deal with horizontal co-ordinates for deposits about 200 m or less from the surface. Ideally it is desirable to locate the centroid and to have some appreciation of shape, extent, and, where applicable, orientation of each deposit. As a rule geological information provides a general guide to these features for mineral occurrences in a given camp. For some past producers, particularly those that produced during the nineteenth century, it is difficult to determine the relation of published co-ordinates to the centroid of the deposit. On a regional scale this source of uncertainty rarely presents a problem, but one should be aware that such uncertainty exists. In rare cases deposits are located incorrectly on maps or, as described, in the literature. This source of error is extremely difficult to detect without thorough familiarity with an area.

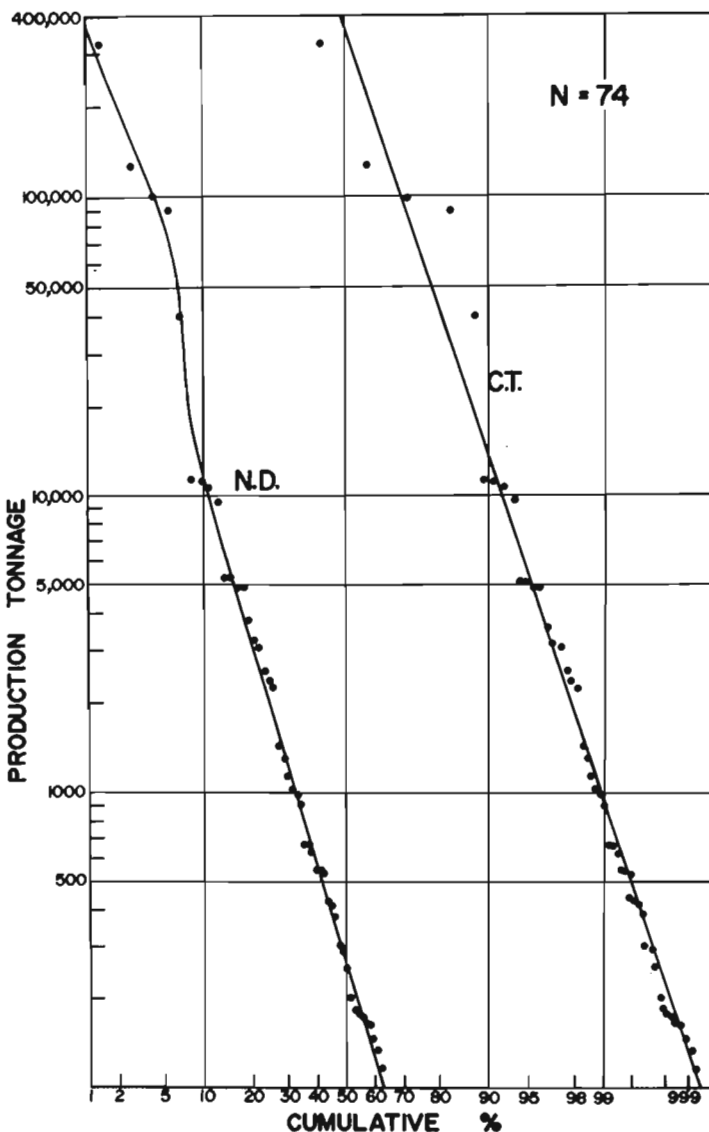


Figure 20.2. Probability graphs of tonnage (ND) and cumulative production tonnage (CT) for Ainsworth camp. Data are in short tons. That part of the plot below a size of 100 short tons is not reproduced because it includes more than 35 per cent of deposits in the camp which account for significantly less than one per cent of total production tonnage.

Table 20.1

Mean spatial density of productive vein deposits in Ainsworth camp

	area (km ²)	number of deposits	mean spatial density (deposits/km ²)
Ainsworth Camp	26	73	2.8

An appreciation of the "quality" of location information is important because such information is the basis for estimates of spatial density of mineral occurrences, a variable whose use in evaluating regional metal distribution patterns has been emphasized recently by Sinclair et al. (1978).

Figure 20.1 is a moving average of spatial density of vein deposits in the Ainsworth camp of southern British Columbia. Numbers of deposits per square kilometre have been counted by superimposing overlapping square grids (unit cell 2 x 2) over the figure; counts are assigned to the centre of each cell position. Adjacent cells were overlapped by 50 per cent. The resulting regular data grid was hand contoured to produce a spatial density map. This type of contoured plot provides an empirical means of defining arbitrary but unbiased and reproducible boundaries of centres of mineralization and can be used as one means of defining physical limits of mining camps. For example, the 0.5 spatial density contour provides a sensible demarcation between mineralized and unmineralized ground, recognizing, of course, the likelihood that new deposits might be found to change spatial density contours to some extent.

The foregoing procedure has been used to define Ainsworth camp and to calculate area and average spatial density of mineral deposits (Table 20.1). The single "outlying" deposit and associated area (one counting cell) has not been included in the tabulated estimates. Internal structure of spatial density within individual camps can also be studied. In Figure 20.1, five "highs" with spatial densities of four deposits or more per square kilometre are apparent. The five largest known deposits in the camp occur in the southernmost four highs. In some cases it might be necessary to use more detailed contours and/or a smaller counting "window" to examine internal structure. It is apparent that the area of the counting "window" or grid cell can be important.

This discussion of spatial density of mineral occurrences illustrates the obvious immediate practical applications of the procedures. Another advantage to a reproducible method of characterizing the lateral extent, shape, average spatial density and structure of spatial density in mineral camps is that some of these features may be useful as standards in various approaches to resource modelling.

Production Tonnages

Ore production tonnages represent a measure of size of a mineral deposit. It is apparent that such estimates are a "minimum" except in rare cases where a deposit has been mined completely. Many past producers, for example, stopped production with some known reserves left in the ground. Furthermore, continued exploration of a past producer invariably results in location of new reserves, however large or small. Production tonnages for some deposits are based on selective mining and/or hand picking. Such procedures decrease the apparent size of a mineral deposit and increase apparent grades as indicated by metal contents of production tonnages. To some extent this difficulty can be overcome by considering metal contents themselves rather than either tonnage or grades.

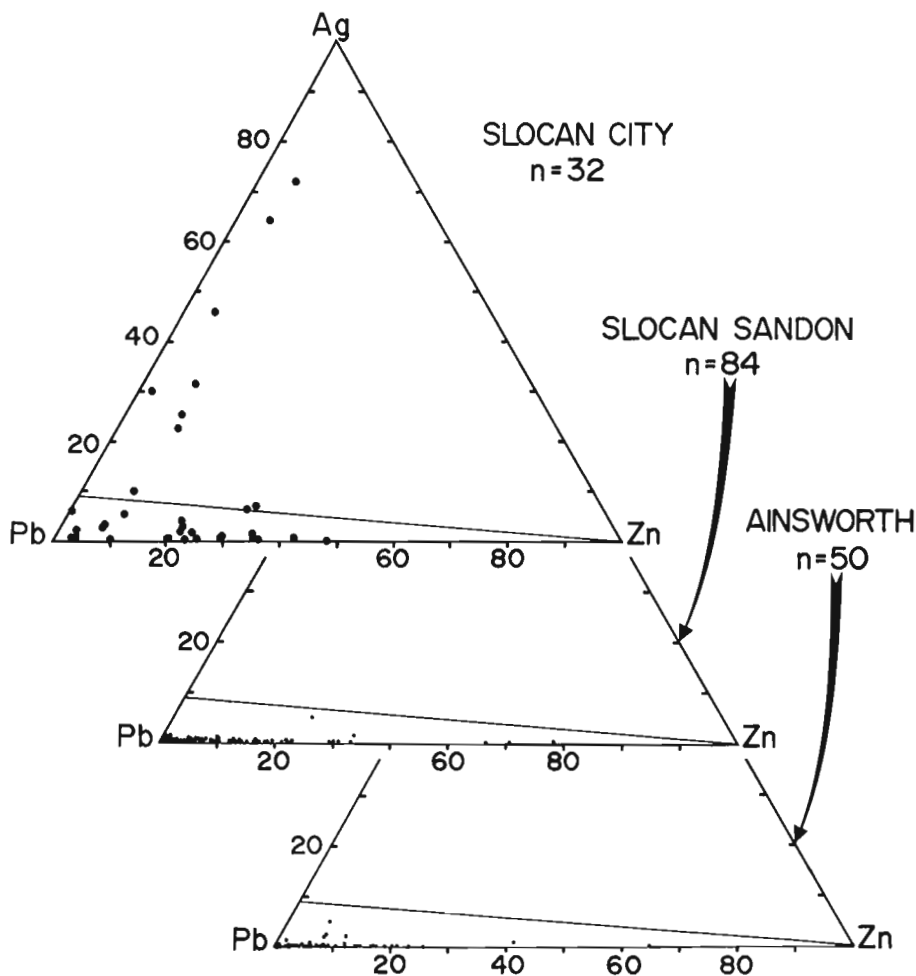


Figure 20.3. Triangular graphs of average Ag, Pb and Zn grades for deposits in Slocan City, Slocan and Ainsworth mining camps (Fig. 20.4) plotted as atomic percentages. The line extending from about 9 atomic per cent Ag to the Zn apex represents a Ag/Pb atomic ratio of 0.1, that is, a Ag(oz/ton)/Pb(%) ratio of roughly 15. Differences in metal ratios among the three camps are apparent.

In some cases ore production tonnages define more than a single population and recognition of this may provide insight into size ranges of the exploration targets in a particular mining camp (Sinclair, 1974). Production tonnages for Ainsworth camp are presented as a probability graph in Figure 20.2 where two separate log probability plots are shown. Those not familiar with probability plots are referred to Sinclair (1976). In brief, they are simply a cumulative histogram plotted to a particular cumulative percentage scale (probability scale) which is arranged so that a cumulative normal distribution will plot as a straight line. A cumulative lognormal distribution plots as a straight line if a logarithmic scale forms one co-ordinate and a probability scale the other. Two or more populations combined in a single data set totalling 100 cumulative per cent will plot on appropriate probability paper as sinuous curves with interpretable patterns if the form of the density distribution is known for each of the individual populations. Generally, tonnage as a size estimator is lognormally distributed. In the curve labelled ND, deposits have been accumulated and plotted individually from high production tonnages to low. Examination of the ND curve (accumulated number of deposits) indicates the possible presence of two size populations, an upper population represented by the five largest deposits known in the camp, and a lower population

consisting of all remaining deposits. This type of plot allows particular deposits to be assigned to high or low tonnage populations, although the possibility exists that some of the smaller deposits might well be high tonnage deposits not yet explored sufficiently to be recognized as such. In fact, the ability to isolate examples of a high tonnage population may lead to the recognition of other geological features by which such deposits can be identified and thus provide greater confidence in evaluation of prospects during exploration (Orr, 1971; Orr and Sinclair, 1971). By the same token, this evaluation process may lead to the recognition of apparent low tonnage procedures with high tonnage potential.

Production tonnages are recognized as a biased measure of size of a mineral deposit, i.e., they are mostly an underestimate. Despite this limitation tonnages generally are closely approximated by one or more lognormal populations. If substantial new ore reserves were found in a few cases the general arguments pertaining to size populations would remain unchanged although specific parameters for the lognormal population(s) would change somewhat.

Note in Figure 20.2 that a second curve labelled CT refers to cumulative ore production tonnage cumulated in order of decreasing deposit size and for individual deposits. The possible existence of two populations is somewhat vaguer than for the ND curve. The ND and CT plots jointly provide a comprehensive summary of production in Ainsworth camp. For example, it is a simple matter to read at a tonnage level corresponding to the smallest deposit in the upper population (40 000 tons) that

the five largest deposits have accounted for about 87 per cent of all the tons of ore produced in the camp. Such statistics provide a realistic basis for appraising the relative importance of the two populations.

Production Grades

Grades for production tonnages are in many cases slightly high estimates of the grade of an entire mineralized body. For many small deposits grades are substantial overestimates of the grade of a mineralized mass because of selective mining and/or hand picking of ore. A practical problem with grade data is that they are commonly relatively incomplete for many deposits in a mining camp. Early production may have avoided zinc and cadmium, for example. Byproduct metals may or may not be recorded depending on smelter agreements. Nevertheless, data are commonly adequate to examine some variations within and between individual mining camps. Figure 20.3 shows Ag-Pb-Zn triangular plots for the three mining camps shown in Figure 20.4 and emphasizes the Ag-rich nature of Slocan City camp relative to the other two.

Production grades can be used, in a manner analogous to grade distribution maps of a single deposit, to test for the presence of systematic variations on the scale of a mining



Figure 20.4. Machine-contoured plot of average Pb grades for about 340 vein deposits in and near the northern end of the Nelson batholith (patterned). Triangles are control points (deposits). Three principal concentrations of deposits (Slocan camp on the north, Slocan City camp on the southwest and Ainsworth camp on the southeast) stand out with centrally located pronounced Pb highs. Closed contours lacking control points on both sides or with very few control points are not considered significant.

camp. As an example consider the contoured distribution map for mean Pb grade of more than 300 past producers about the northern end of the Nelson batholith (Fig. 20.4). Crude but definite systematic patterns are apparent and the three major mining camps stand out as having Pb-rich cores. Silver (not shown) has a more-or-less antithetic distribution pattern. The apparently truncated pattern of the Ainsworth camp might lead one to speculate that a roughly comparable number of deposits lie beneath Kootenay Lake to the east.

It is interesting that average grades can also be examined as probability plots in a manner analogous to tonnage as illustrated in Figure 20.1.

Grade Versus Tonnage

Informal statements are common regarding the general tendency for average grades to decrease as deposit-size increases. While there may be some basis in fact for this generalization in dealing with a single deposit there seems to be no foundation for it in a group of deposits from a single mining camp. Figure 20.5 shows the disposition of Ag grades as a function of size (production tonnage) for vein deposits in Slocan City camp (cf. Orr and Sinclair, 1971). Average grades for each order of magnitude of production are itemized in Table 20.2. These average grades are indistinguishable statistically over five orders of magnitude

of size. Variabilities, however, as measured by the standard deviation do appear to differ as a function of size. Small deposits show a relatively high variation in average grades whereas larger deposits show much lower variability. In all likelihood if a large deposit were divided arbitrarily into smaller units, these units would also show a much higher variability. Thus, the observed decrease in variability of average grade of mineral deposits as a function of increasing size is an expected result of smoothing of small scale variability in large mineral deposits and is comparable to regularization in geostatistics (Matheron, 1971).

Table 20.2

Ag grade (oz/ton) as a function of deposit size: summary statistics for Slocan City camp

Size Range (short tons)	n	Mean (\bar{x})	Dispersion (s)
>10 000	3	73.1	19.4
1000-10 000	3	112.6	39.2
100-1000	14	107.8	123.2
10-100	27	97.5	96.3
1-10	14	103.9	104.6

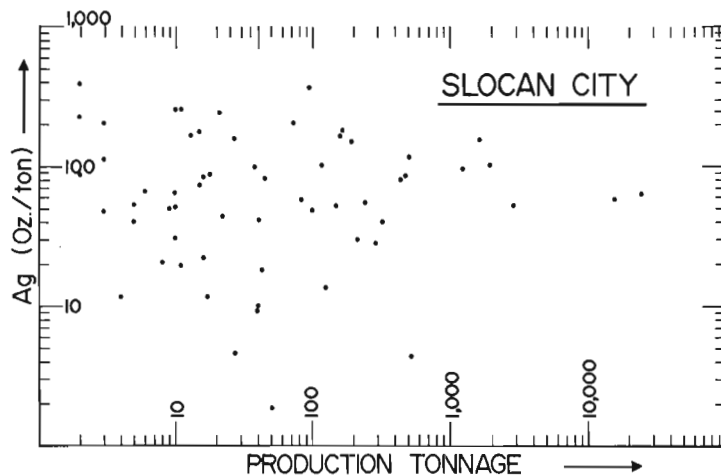


Figure 20.5. Silver grade (oz/ton) vs. total production tonnage (short tons) for vein Ag deposits in Slocan City mining camp. Note that size ranges over five orders of magnitude but mean silver values do not vary greatly as a function of size. See also Table 20.2.

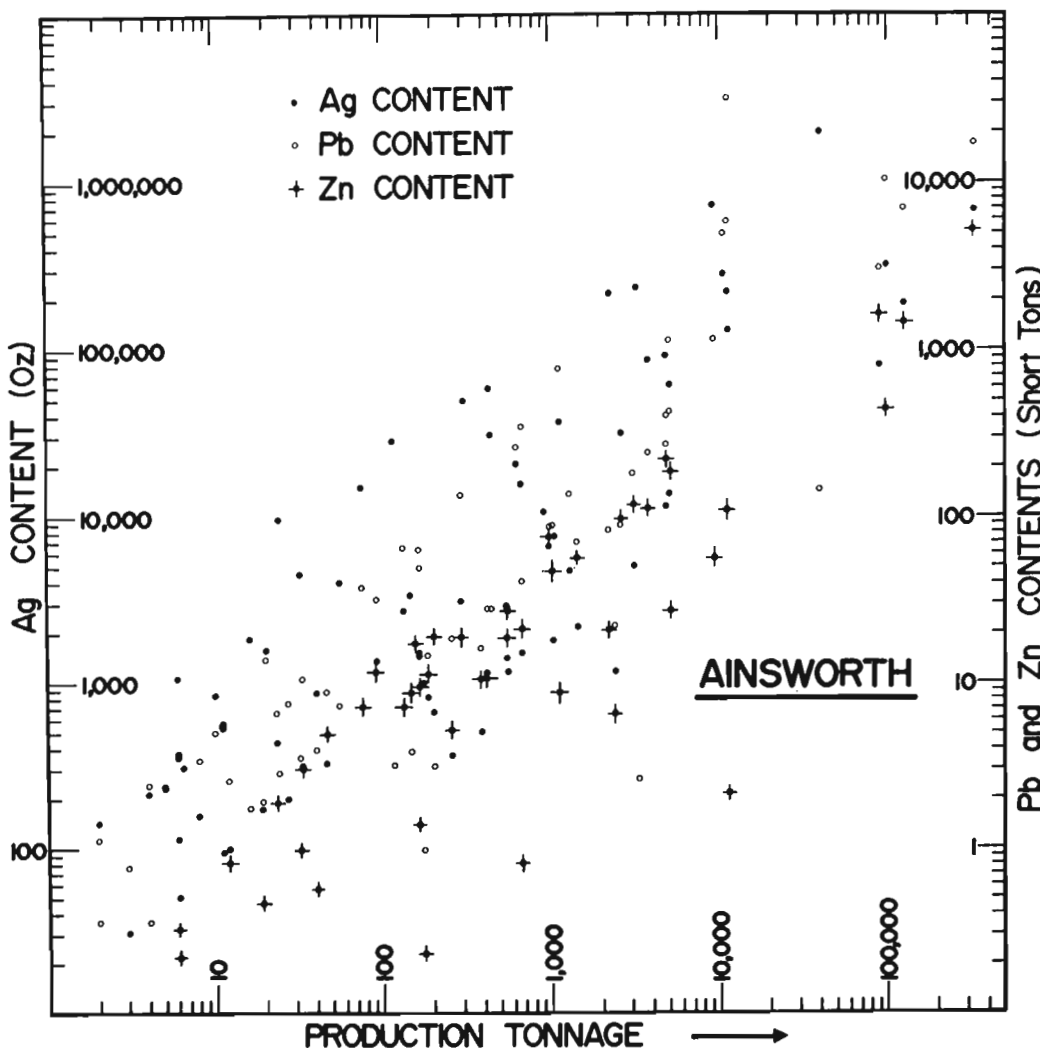


Figure 20.6. Graph of metal contents (average grades x ore tonnage produced) versus ore tonnage produced (short tons) for vein deposits in Ainsworth mining camp. Lead and zinc contents are tons of contained metal; silver contents are ounces of contained silver.

Value of a Mineral Deposit

In simplest terms gross value of a mineral deposit can be expressed by the relationship:

$$V = T \cdot (g_1 p_1 + g_2 p_2 \dots + g_i p_i \dots + g_n p_n)$$

or

$$V = T \sum_{i=1}^n g_i p_i$$

where V is monetary value, T is a tonnage or volume measure, g_i is mean grade of the i^{th} commodity, and p_i is unit price of the i^{th} commodity. Many economic factors can affect the ultimate values of T, g_i and p_i and these detailed aspects will not be considered here. It is apparent, however, that of these three particular types of variables (size, grade and price) only price is unrelated in any obvious way to geological features. Consequently, it is of some interest to examine more closely those components of a value measure that have geological significance – tonnage (size) and average grades.

From a practical point of view the fundamental value of a mineral deposit is determined by the metal contents, that is, by the products of grades and tonnages. Where a single commodity is important, metal content provides a single value measure for individual deposits. However, it is impossible or inconvenient in many practical cases to require value of a mineral deposit to be expressed as several metal contents. This necessity of a single value measure for single polymetallic deposits has led many authors to combine all metal contents in terms of their respective dollar values, a procedure that seems unjustified from a geological point of view because of the arbitrary and variable nature of metal prices. An alternative approach is to use a single estimator whose relationships to all metal contents are known.

Figure 20.6 shows Ag, Pb and Zn contents plotted against production tonnage for more than 70 vein deposits from Ainsworth mining camp. It is apparent that \log_{10} (tons) is directly proportional to \log_{10} (metal content) for all three metals according to the following relationship.

$$\log_{10} (\text{metal content}) = K \log_{10} (\text{tons}) \pm e$$

where K is a constant for each metal and e is a random error term. The important observation from this set of data is that tonnage can be used as a reasonable single measure of value in the case of a mining camp characterized by polymetallic deposits. Such a value measure can be important in modelling studies involving mineral resources or mineral exploration (e.g. Orr and Sinclair, 1971).

Conclusions

These preliminary analyses lead to the following general conclusions regarding location data and quantitative production statistics for vein deposits in three mining camps in southern British Columbia.

- (1) Spatial density of procedures appears to be a useful procedure for delimiting mining camps and describing the nature of "structure" of concentrations of mineral deposits, despite the fact it is a biased estimator which is generally less than reality.
- (2) Average grades of producers seem to be useful on a regional scale in that systematic distribution patterns help define the zonal structure of mineralized fields. Quantitative grade data also provide a useful means of comparing and contrasting several camps, as for example by comparing Ag-Pb-Zn proportions using triangular plots.

(3) Tonnage is a measure of size of deposit and on the average is strongly biased on the low side. Despite this biased nature tonnage provides an important value measure of a deposit and may have a significant relationship to structures and/or lithologies that have a close association with mineralization.

(4) Metal contents of a mineral deposit are fundamental value measures that appear to correlate strongly with tonnage. Where several metals are involved tonnage provides a useful single measure of value. Consequently, tonnage appears to be a likely candidate for value measure in quantitative approaches to resource evaluation and exploration modelling. A somewhat comparable conclusion is implicit for massive sulphide deposits (Sangster, 1977) and porphyry-type deposits (Singer et al., 1975).

The foregoing conclusions are generalities relative to production data. It seems likely that results based on such data will be greatly improved as the data themselves are improved, for example, by the addition of updated reserve information.

References

- Matheron, G.
1971: The theory of regionalized variables and its application; Les cahiers du Centre de Morphologie Mathematique, Fontainebleau, 211 p.
- Orr, J.F.W.
1971: Mineralogy and computer-oriented study of mineral deposits in Slocan City camp, Nelson Mining Division, British Columbia; unpublished M.Sc. thesis, Department of Geological Sciences, University of British Columbia, Vancouver, 143 p.
- Orr, J.F.W. and Sinclair, A.J.
1971: A computer-processable file for mineral deposits in the Slocan and Slocan City areas of British Columbia; *Western Miner*, v. 44, p. 22-34.
- Sangster, D.F.
1977: Some grade and tonnage relationships among Canadian volcanogenic massive sulphide deposits; in Report of Activities, Part A, Geological Survey of Canada, Paper 77-1A, p. 5-12.
- Sinclair, A.J.
1974: Probability graphs of ore tonnages in mining camps – a guide to exploration; *Canadian Institute of Mining and Metallurgy Bulletin*, v. 67, no. 750, p. 71-75.
1976: Applications of probability graphs in mineral exploration, Special Volume 4, Association of Exploration Geochemists, 95 p.
- Sinclair, A.J., Wynne-Edwards, H.R., and Sutherland Brown, A.
1978: An analysis of distribution of mineral occurrences in British Columbia; *British Columbia Ministry of Energy, Mines, and Petroleum Resources, Bulletin* 68, 125 p.
- Singer, D.A., Cox, D.P., and Drew, L.J.
1975: Grade and tonnage relationships among copper deposits; U.S. Geological Survey Professional Paper 907-A, 11 p.

Projects 760047 and 620308

Y.T. Maurice¹ and A.G. Plant²

Maurice, Y.T. and Plant, A.G., *Some mineralogical and geochemical characteristics of uranium occurrences in the Nonacho Lake area, District of Mackenzie; in Current Research, Part B, Geological Survey of Canada, Paper 79-1B, p. 179-188, 1979.*

Abstract

Ten radioactive occurrences, in and around the Nonacho sedimentary basin, representing a variety of geological settings, were examined and sampled during the summer of 1976. Grab samples were analyzed for major, minor and trace elements and their mineralogy was studied by autoradiography, optical microscopy, X-ray diffraction, and microprobe analysis.

Several occurrences in the Nonacho Basin have syndimentary characteristics. The host rocks are: (1) basal conglomerates where radioactive minerals were deposited clastically and (2) pyritiferous siltstones in which uranium was chemically precipitated during sedimentation. Other occurrences in the basin are fracture-controlled, but these may be associated with stratiform mineralization at depth. One showing occurring in a basement fracture may be supergene and related to processes at the Nonacho-basement unconformity.

Radioactivity is high in the basement rocks surrounding the Nonacho Basin. Some occurrences are associated with acid intrusives, others with diorites or highly metamorphosed sediments. These basement rocks are believed to be the major source of uranium and thorium in the Nonacho sediments although the association Sn-Au-Nb-Ta identified in the basal conglomerates may indicate sediment contribution from the Slave Province.

Introduction

The Nonacho Lake area, in the northwestern Canadian Shield, contains favourable geological settings for the occurrence of uranium mineralization. Several prospects were found as a result of intensive prospecting during the 1950s but none resulted in economic deposits. The region has recently experienced a resurgence of activity and it may be that a better understanding of ore forming processes and the application of modern exploration techniques will result in more significant discoveries.

Ten radioactive occurrences were visited in and around the Nonacho Basin during the summer of 1976. This work was preliminary to the geochemical follow-up campaign (Maurice, 1976, 1977) undertaken to examine in detail the results of a reconnaissance lake sediment survey carried out in an area extending from the East Arm of Great Slave Lake to the Saskatchewan border (Hornbrook et al., 1976). The main objective was to recognize characteristic element associations in these occurrences to help interpret the lake sediment results. This report concentrates on the mineralogical and geochemical data obtained from the study of the mineralization. A brief discussion on possible genetic processes and a few guidelines for uranium exploration are also presented. Other applications of these results to mineral exploration in the area is the subject of another paper (Maurice, in press).

General Geology

The Nonacho Basin (Fig. 21.1) is composed of essentially unmetamorphosed Lower Proterozoic continental sediments that unconformably overlie undifferentiated Archean and Proterozoic basement rocks. The Nonacho Group comprises a clastic sequence of basal conglomerates overlain by arkoses, quartzites, greywackes, siltstones and shales. These sediments were deposited in a fault-controlled intracratonic basin of not much greater extent than the area now underlain by the sediments (Henderson, 1937). The finer sediments were probably deposited in the deeper parts of the basin while the coarser material most likely represents shallow, largely fluvial deposits. The total thickness of the sedimentary pile was estimated at 3000 m (Burwash and Baadsgaard, 1962).

The basement rocks on either side of the Nonacho Basin consist mostly of granitic gneiss and intensely metamorphosed sediments intruded by granitoid bodies, many of which are coarsely porphyroblastic. Most basement rocks have undergone postmetamorphic cataclastic deformation and many are mylonitized (Fraser, 1978).

The age relation between the Nonacho Group and some of the younger basement granites is the subject of debate. Henderson (1937), who mapped the Nonacho Basin, described intrusive contacts and thermal metamorphic features in the Nonacho sediments. McGlynn (1971, 1978), working in the southern part of the Basin, found no such evidence; he maintains that all granitic rocks in the region are older than the Nonacho Group (J.C. McGlynn, pers. comm., 1978).

Sampling and Analytical Techniques

All the occurrences visited, except locality A (Fig. 21.1), were previously known, most having been discovered in the 1950s. Uranium mineralization at locality A was discovered as a result of the follow-up campaign of 1976.

Grab samples, mostly from old trenches, were collected at each of the showings visited. These samples were generally selected from the zones of maximum radioactivity so that the analytical results presented here should not be considered as representative of the overall concentrations in the mineralized rocks. For U and Th, the values reported may, in certain cases, be close to the maximum concentrations for these elements at the surface, if not at depth.

Analytical data from selected samples for major, minor and trace elements are given in Tables 22.1 and 22.2. The major elements, Th and Ta were determined by X-ray fluorescence. CO₂ and H₂O were obtained using an infrared analyzer. Uranium was determined by neutron activation/delayed neutron counting. Of the trace elements, Zn, Cu, Pb, Ni, Co, and Mo were obtained by atomic absorption spectrophotometry following HF sample digestion. Fluorine was determined by selective ion electrode using a Na₂CO₃/ZnO fusion and Au was obtained by fire assay.

¹Resource Geophysics and Geochemistry Division

²Central Laboratories and Administrative Services Division

The remaining twelve elements, Ag, Ba, Bi, Ce, La, Nd, Nb, Sn, V, Y, Yb, and Zr were determined by emission spectrographic techniques. The accuracy of the latter determinations is believed to be better than $\pm 15\%$, except for Ag, Bi, and Sn which are accurate to within $\pm 30\%$. For certain determinations by emission spectrography, the presence of interfering elements in the samples may have affected the accuracy of the results. These cases are identified as semiquantitative in Table 21.2.

Autoradiographs of rock slabs and polished thin sections were used to study the general distribution of U and Th minerals and to select samples for more detailed studies. The mineralogy was studied using a combination of optical microscopy and X-ray diffraction supplemented by electron microprobe analysis. Quantitative microprobe analyses of some uraninites are given in Table 21.3. A scanning electron microscope was used to examine fine grained mineral intergrowths that were not resolved with the electron microprobe.

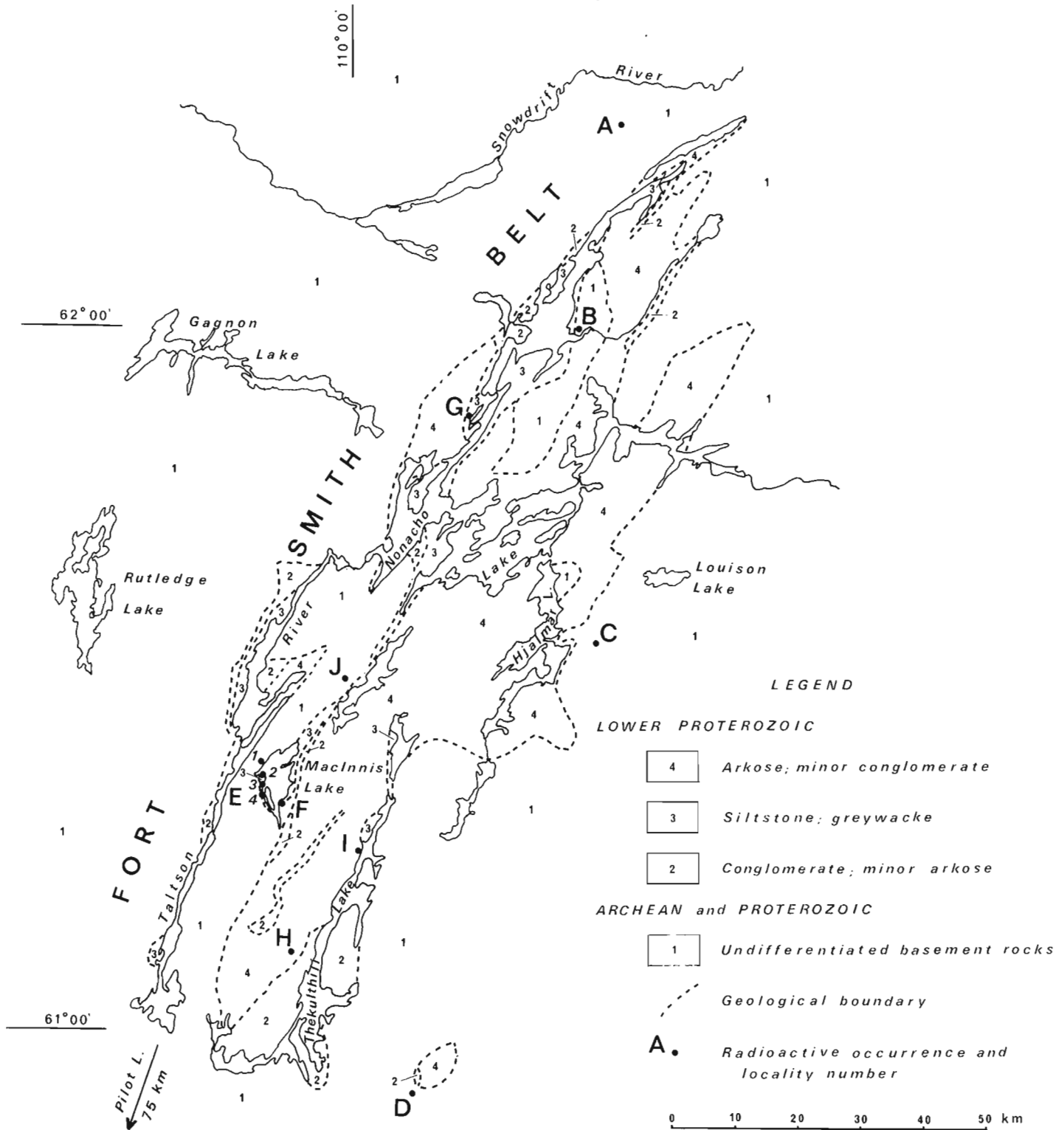


Figure 21.1. Geology of the Nonacho Basin (after Henderson, 1937) and location of radioactive occurrences.

Table 21.1

Major element content of selected rock samples from various radioactive occurrences in the Nonacho Lake area (in per cent)

Locality	Sample No.	SiO ₂	Al ₂ O ₃	K ₂ O	CaO	Na ₂ O	MgO	FeO	Fe ₂ O ₃	MnO	TiO ₂	P ₂ O ₅	CO ₂	H ₂ O	Totals	Description
A	K-9004	65.5	17.8	3.21	0.29	1.3	1.66	4.7	2.4	0.06	0.23	0.08	0.1	2.2	99.53	Metasediment
A	K-9023	53.9	9.8	3.20	5.43	0.0	3.74	10.5	3.7	0.29	2.49	3.78	0.2	2.1	99.13	Mafic band
A	K-9003	68.3	14.6	5.74	0.62	2.2	0.85	3.1	0.8	0.03	0.52	0.40	0.1	0.9	98.16	Porphyry
B	F-9019	79.0	7.0	2.19	0.57	0.3	2.26	2.8	2.3	0.07	0.80	0.00	0.2	1.2	98.69	Quartz-biotite paragneiss
C	F-9008	68.0	17.0	0.10	0.30	11.0	0.20	0.1	0.5	0.00	0.10	0.00	0.3	0.5	98.10	Pegmatite - Acid phase
C	F-9006	38.0	18.2	1.63	9.09	0.6	7.39	8.2	6.8	0.17	2.31	0.00	2.1	5.9	100.39	Pegmatite - Mafic phase
C	F-9001	64.6	17.4	0.18	3.18	8.8	0.76	0.4	1.9	0.03	0.27	0.08	0.9	1.0	99.50	Diorite boulder
D	C-9001	52.1	16.6	4.39	3.42	2.8	7.02	2.5	6.1	0.18	1.37	0.79	0.1	1.8	99.17	Wall-rock biotite schist
D	C-9004	60.0	10.0	2.00	3.00	0.0	5.00	2.5	5.0	0.20	0.20	0.10	1.5	6.0	95.50	Vein material
E ₁	E-9027	39.4	11.1	1.14	12.50	1.5	3.74	9.5	7.0	0.28	2.39	0.19	8.0	3.2	99.94	Basic intrusive
E ₂	E-9002	51.8	14.7	2.15	0.16	3.5	4.52	7.2	8.3	0.29	1.67	0.11	0.1	4.3	98.80	Acid intrusive
E ₃	E-9017	79.0	8.7	2.35	0.00	1.0	0.70	3.4	0.2	0.02	0.22	0.09	0.1	2.5	98.28	Sediment
F	E-9006	56.9	8.6	3.87	0.12	0.0	0.21	0.6	25.8	0.00	1.36	0.33	0.1	1.0	98.89	Basal conglomerate
G	F-9011	65.4	13.5	5.92	3.08	0.7	1.36	1.0	2.1	0.06	0.43	0.13	2.3	2.1	98.08	Siltstone
H	E-9011	66.8	5.6	2.46	2.03	0.0	0.95	0.8	13.3	0.03	2.13	1.27	0.3	1.4	97.07	Boulder in basal conglomerate
I	F-9029	57.3	19.1	6.39	0.84	3.2	2.58	0.5	4.6	0.11	0.51	0.12	0.7	3.8	99.75	Arkose
J	F-9024	77.8	11.0	5.86	0.26	1.6	0.24	1.9	0.0	0.02	0.11	0.00	0.4	0.0	99.19	Acid gneiss

Analyses by Analytical Chemistry Section, Geological Survey of Canada.

The state of enrichment of the mineralization with respect to the various elements was estimated by comparing the results with published average concentrations for the corresponding types of host rocks. Because only few samples were collected at each locality, this estimate is only qualitative; however, this information is useful to establish the nature of the element associations present. Table 2 of Granier (1973, p. 2, 3 and 4) was used in this comparison.

Description of Selected Occurrences

The localities referred to in the text are shown in Figure 21.1.

Locality A

Uranium mineralization was found in the basement to the north of the Nonacho Basin within a porphyroblastic granitoid intrusion. The discovery was made during the follow-up of the reconnaissance lake sediment data in 1976. The intrusive rock appears to be similar to the radioactive rocks seen by B.W. Charbonneau (pers. comm., 1979) along the axis of the Fort Smith Belt. It is composed essentially of sericitized K-feldspar porphyroblasts in a matrix of K-feldspar > quartz > sericite-biotite > plagioclase. The rock is generally pink and shows signs of severe cataclastic deformation. It intrudes granitic gneiss and quartz-biotite schist; the latter are locally sulphide-bearing and a few rock analyses indicate that they are slightly enriched in Cu and Mo (Table 21.2, K-9004). Sulphide mineralization may be present in the area because reconnaissance and detailed lake sediment data show strong enrichment in Cu, Pb and Zn and, to a lesser extent, in Ni, Co, As and Mo in this region (Maurice, 1977).

Several zones of high radioactivity were found within a 15 km² area. Secondary uranium minerals were locally seen on outcropping porphyry, but the highest radioactivity was encountered in dyke-like mafic bands, a few centimetres thick and several metres in length. The material forming these bands is schistose and its modal composition (biotite ≈ 60%, quartz ≈ 20%, garnet ≈ 10%) strongly suggests metasedimentary inclusions in the igneous mass. Their elongated and narrow structure, however, make it appear as

though they intrude the porphyry. Perhaps more significant is the fact that these narrow bands were generally found near the margins of the porphyries and that they resemble the surrounding metasediments. The latter, however, were not found to be radioactive.

Table 21.2 (K-9023) gives analytical data for one of the mafic bands. The radioactivity is due to thorium monazite and uraninite. The thorium monazite grains are present as inclusions in the biotite where they show haloes of radiation damage. The uraninite occurs as disseminated rounded grains, often surrounded by a thin, discontinuous ring of galena (Fig. 21.3a). It contains considerable amounts of Pb and is relatively low in Th (Table 21.3, K-9023). Other minerals present in accessory amounts in the mafic bands include: ilmenite, zircon, rutile, apatite, fluorite, sphalerite, pyrite, pyrrhotite and chalcocopyrite. The last two generally occur intergrown. Fluorite is associated with the biotite in the mafic bands; in the porphyry, purple fluorite often occurs along joints, but it is also found disseminated in the rock.

Locality B

Several zones of high radioactivity occur within a basement inlier in the northern part of the Nonacho Basin. The predominant mineralization consists of disseminated uraninite in a quartz-biotite paragneiss. The uraninite (Fig. 21.3b) occurs as large hypidiomorphic grains, generally associated with the biotite. This mineral is often accompanied by sulphur-bearing (5-10% S) uraniferous hydrocarbon. Galena is generally found in cracks within the uraninite grains. The uraninite itself is a high-Th variety and contains substantial amounts of radiogenic Pb (Table 21.3, F-9019).

Other minerals identified in the host rock include manganian ilmenite rimmed by sphene and occasionally rutile, zoned zircons containing minor Ca, molybdenite, pyrrhotite, and minor chalcocopyrite. Table 21.2 (F-9019) shows relatively low rare-earth content but high concentrations of F (0.16%) and V (0.11%). Uranothorite mineralization in brecciated fault zones has also been reported in this area; these occurrences, however, have not been investigated in the present study.

Table 21.2

Minor and trace element content of selected rock samples from various radioactive occurrences in the Nonacho Lake area (all values in ppm except when marked %)

Locality	Sample No.	Ag	Ba	Bi	Ce	Co	Cu	F	La	Mo	Ni	Pb
A	K-9004	0.3	360	<0.5	<200	<10	510*	700	<100	52+	25	62*
A	K-9023	0.2	430	<0.5	1100+	28	100	1.35%+	620+	32+	46	262+
A	K-9003	0.08	740	<0.5	<200	<10	18	1100	<100	4	3	36
B	F-9019	0.1	210	NF	<200	21	59	1600*	<100	258+	32	420+
C	F-9008	<0.05	26	NF	<200	<10	11	100	<100	3	2	6
C	F-9006	<0.05	320	NF	<200	16	15	600	<100	4*	29	58*
C	F-9001	0.2	120	NF	340+	<10	12	300	270*	4+	2	335+
D	C-9001	1.7*	2800+	34+	<200	44	2900+	1800*	<100	49+	38	1240+
D	C-9004	ND	1500*	700(s)+	8200+	230*	4068+	800	1100+	18+	8	3927+
E ₁	E-9027	0.6	1200*	1.7	450+	40	87	385	NF	5*	32	588+
E ₂	E-9002	0.7	4900+	28*	<200	64	57	500	<100	4	46	520+
E ₃	E-9017	17+	1300*	700(s)+	290+	<10	205	420	160*	5*	18	2.5%+
F	E-9006	0.1(s)	390	6(s)	770+	35	17	600	420+	9*	4	107*
G	F-9011	1.7	2100	2.8	<200	<10	14	800	<100	4	17	560+
H	E-9011	0.5	7200+	<0.5	590+	11	95	1390*	<100	18+	7	1571+
I	F-9029	25+	1700	23+	220*	17	500*	575	<100	5	27	1286+
J	F-9024	0.3	790	<0.5	<200	<10	27	182	<100	27+	5	246+

* > 3x average abundance in host rock; + > 10x average abundance in host rock (Granier, 1973)

(s) - Semi-quantitative (possible interference from other elements)

NF - No detectable signal found

ND - Not determined

Locality C

A large number of radioactive diorite boulders occur near Hjalmar Lake, about 4 km east of the Nonacho-basement unconformity. The bedrock source of these boulders has not been discovered but is considered to be nearby. The rock is medium-grained, composed essentially of sodic plagioclase, chlorite, epidote, and secondary amphibole with accessory sphene and zircon. Its major element composition (Table 21.1, F-9001) is very similar to that of sodic diorite reported by Johannsen (1937, v. 3, Table 52).

Radioactive pegmatites outcrop in the same area; they are composed mostly of coarse pink albite grains with variable amounts of chloritized ferromagnesian minerals in irregular patches. Table 21.2 gives trace element data for the chloritized and feldspathic phases of the pegmatite (F-9006 and F-9008 respectively). The trace element assemblage of the chloritized phase is due to the presence of yttracolumbite (Y, U, Ti, Fe)(Nb, Ta)O₆. Some grains of this mineral were found to exceed one centimetre in diameter. They gave an X-ray diffraction pattern similar to yttrantalite (PDF11-116, JCPDS, 1974) but they contain higher concentration of Nb than Ta as shown by a semi-quantitative X-ray fluorescence analysis.

The diorite boulders contain disseminated colloform pitchblende in epidote (Fig. 21.3c). Due to the delicate texture of these grains, they were not suitable for microprobe

analysis. However, a few subhedral uraninite grains were analyzed and the results are given in Table 21.3 (F-9003). These data do not account for the relatively high Th content of the rock; this element was not detected in the epidote, sphene or zircon, and no Th-bearing mineral was identified in the thin sections.

Locality D

An interesting occurrence is found in basement rocks about 4 km south of a Nonacho sedimentary outlier situated southeast of the Nonacho Basin. Concentrated uranium mineralization occurs in veins, up to 20 cm in width, that fill north-south oriented fractures in granites and schistose metasediments. To date, three veins have been reported; the longest measured 20 m in length.

The vein material is black with a resinous, pitch-like lustre containing a yellow secondary mineral identified as uranophane. The black material is composed essentially of uraninite grains, up to 3 mm in diameter (averaging ≈ 0.5 mm), in a biotite-chlorite-quartz groundmass. These grains are partly altered showing remnants of uraninite in a Si-rich, Pb-deficient matrix (Fig. 21.3d). Table 21.3 (C-9006) gives microprobe analyses of both phases.

Table 21.2 (cont'd.)

Sn	Nd	Nb(s)	Th	U	V	Y	Yb	Zn	Zr	Description
<0.5	NF	NF	51*	16*	70	<20	<4	60	230	Metasediment
2.5	980+	150*	515+	418+	210	270+	15+	506*	1700+	Mafic band
1.4	NF	<50	147+	14*	35	<20	<4	56	340	Porphyry
<0.5	NF	<50	170+	1310+	1100*	44	4	72	610*	Quartz-biotite paragneiss
NF	NF	NF	14	46+	28	<20	<4	4	24	Pegmatite - Acid phase
12	NF	300+	24*	116+	220	390+	24+	162	610	Pegmatite - Mafic phase
<0.5	<150	NF	120+	925+	61	<20	<4	14	240	Diorite boulder
3.2	<150	150*	14*	2430+	1100*	72*	<4	193	130	Wall-rock biotite schist
NF	3900+	300+	73+	6.8%+	3400+	1900+	180+	96	ND	Vein material
0.9	NF	50	NF	1632+	550	46	7*	313	270	Basic intrusive
1.0	NF	100*	8	2130+	540*	78*	<4	253	150	Acid intrusive
6(s)	<150	NF	716+	2.0%+	41	25	6*	23	170	Sediment
2100+	340+	300+	311+	1090+	320	210*	7*	19	840*	Basal conglomerate Au=1.9+
4.8	NF	70*	18	1550+	620*	<20	<4	34	200	Siltstone Ta=139+
11	NF	1000+	1300+	320+	790*	49	24(s)+	46	7500+	Boulder in basal conglomerate
1.5	<150	NF	55+	9630+	97	23	6	100	300	Arkose
2.1	NF	<50	NF	333+	89	43	<4	19	430	Acid gneiss

U: by Atomic Energy of Canada Limited

Th, Ta, Au: by Bondar-Clegó and Company Limited

Zn, Cu, Pb, Ni, Co, Mo: by Geochemistry Section, Geological Survey of Canada

Other elements: by Analytical Chemistry Section, Geological Survey of Canada

Stringers of calcite cut the veins lengthwise. Copper sulphides including chalcopyrite, bornite and chalcocite, often intergrown, are abundant in the veins and in the metasedimentary wall rock. Tables 21.1 and 21.2 give the composition of selected samples from one of the veins (C-9004) and from the wall rock (C-9001). Note the low levels of Th and the high rare-earth content of the vein material. Besides uraninite, the veins also contain stringers of a mineral with an X-ray diffraction pattern similar to that of boltwoodite but which contains considerably more Ca than boltwoodite. More detailed study of this mineral is being carried out and complete X-ray and chemical data are expected to be published at a later date.

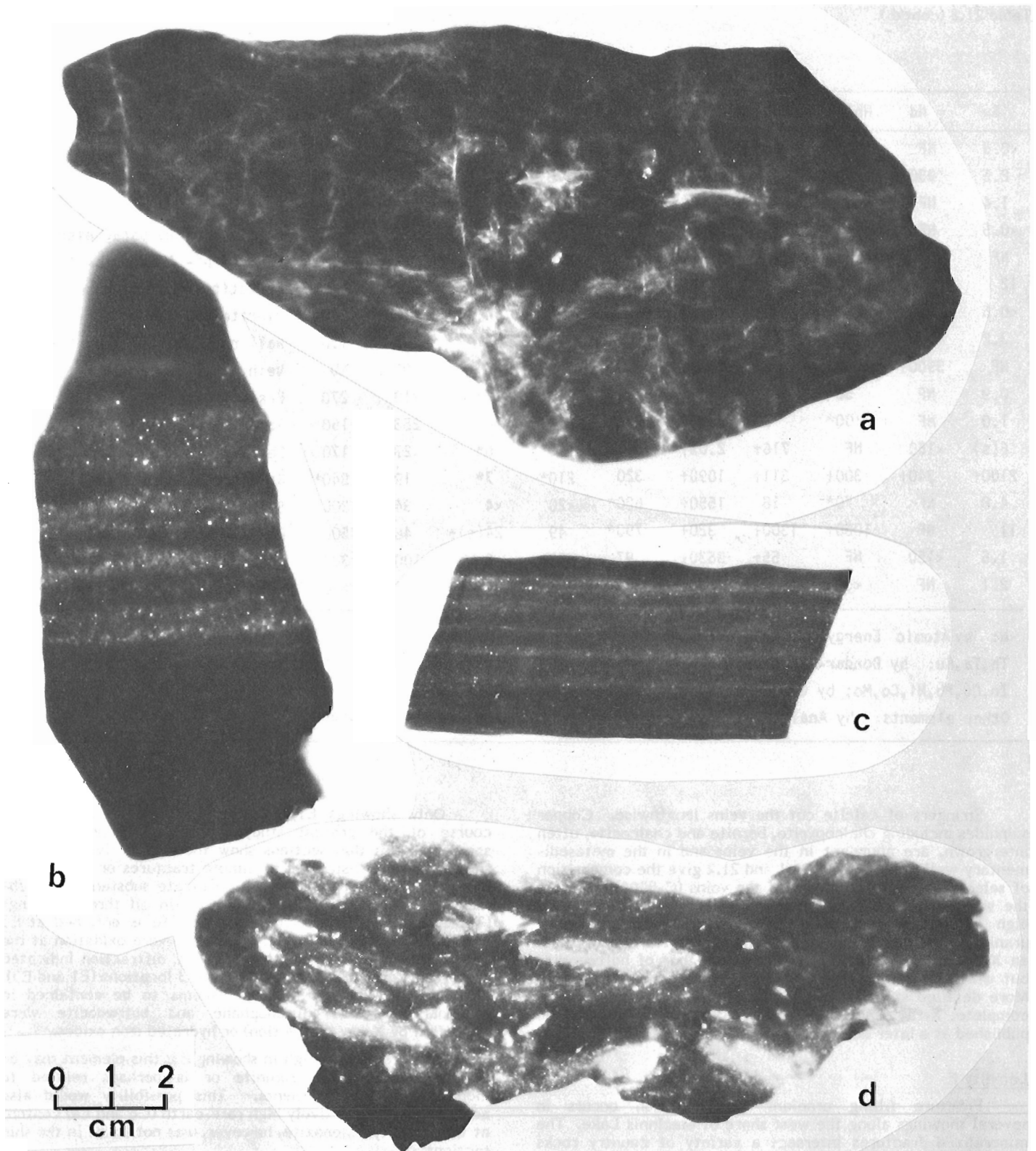
Locality E

Fracture filling uranium mineralization occurs in several showings along the west shore of MacInnis Lake. The mineralized fractures intersect a variety of country rocks including arkosic sediments (at E3 and E4), granitic rocks (at E2) and basic intrusives (at E1). In all cases, the radioactive mineralization is accompanied by heavy chloritization which darkens the surrounding wall rock. The distribution of the showings along a north-south trend suggests that the mineralizing activity may have occurred along a single fracture system.

Only showings E1, E2, and E3 were sampled in the course of the present study. Autoradiographs of hand specimens and thin sections show the radioactivity in these showings to be restricted to minute fractures or shear zones (Fig. 21.2a). Selected specimens indicate substantial enrichment in Pb and Ba in addition to U in all three showings (Table 21.2, E-9027, E-9002, E-9017). Bi is enriched at E3 and to a lesser extent at E2. Despite severe oxidation at the surface and along the fractures, X-ray diffraction indicated the presence of uraninite at 2 of the 3 locations (E1 and E3). Most of the uranium however, seems to be contained in secondary minerals (uranophane and boltwoodite were identified by X-ray diffraction) or hydrated iron oxides.

Th is relatively high in showing E3; this element may be incorporated in the uraninite or is perhaps related to monazite in the sediments. This possibility would also account for the relatively high rare-earth (Ce and La) content at this locality. Monazite, however, was not found in the thin sections.

There is abundant galena, particularly at E3 accounting for the very high Pb (and possibly the high Ag) contents. A Cu-Pb-Bi sulphide was also detected in thin section by microprobe analysis but the quantity was insufficient for identification. Minor chalcopyrite is also present.



- a Radioactivity in minute fractures in chloritized granitic host rock, locality E2.
 b Stratiform radioactivity in sandy layer within basal conglomerate, locality F.
 c Stratiform radioactivity in siltstone, locality G.
 d Radioactivity in intra-formational breccia in siltstone, locality G.

Figure 21.2. Autoradiographs of rock slabs.

Table 21.3
Microprobe analyses of uraninite, in weight per cent

Sample No.	K-9023		F-9019		F-9003			C-9006	
Grain No.	1*	2*	1*	2*	1	2	3	(uraninite)	(matrix)
Ca	0.4	1.3	0.6	1.3	2.3	2.4	2.4	1.3	1.9
Pb	11.8	7.0	13.0	8.5	18.2	18.0	18.0	14.6	1.3
U	67.3	70.1	57.8	61.1	62.5	62.4	62.0	67.7	63.7
Th	2.7	4.0	7.0	7.5	NF	NF	NF	NF	NF
Si	0.1	0.0	0.2	0.3	0.2	0.3	0.2	0.7	4.4
Fe	0.3	0.6	0.1	0.3	0.1	0.1	0.1	NF	NF
S	0.3	0.3	0.9	0.8	NF	NF	NF	NF	NF

* - Average of two analyses
NF - Not found

Analyses by G.J. Pringle, Mineralogy Section, Geological Survey of Canada.

Locality F

A radioactive showing occurs in the basal conglomerates of the Nonacho Group near the southeast shore of MacInnis Lake. The radioactivity is stratiform (Fig. 21.2b) and is concentrated in layers of heavy minerals that contain an abundance of dark iron oxide grains. These layers are particularly well developed in the more sandy facies of the formation.

The most radioactive grains in the sections examined are uranophane; thorium monazite is also present. The bulk of the uranium, however, seems to occur in a very soft, fine grained mineral phase, interstitial to the clastic sand grains. On the autoradiographs, this phase produces a poorly defined haze. Its very small grain size precluded identification by X-ray diffraction. However, using the microprobe, and by comparison with a uranium standard, its U content was estimated at between 55 and 60%. Most grains also contain Ti, P, Fe, and Si. About 87% of the U in the rock was found to be extractable using a cold, weak acid (1M HCl) leach. Assuming that the uranium contained in the clastic heavy minerals was not extracted by this leach, this test indicates that a large proportion of the uranium in this rock is present in the interstitial phase.

The iron oxide is mostly hematite containing small quantities of exsolved ilmenite. Remnants of magnetite in the hematite grains were observed occasionally. Other heavy minerals identified in the conglomerate include zircon, tourmaline, cassiterite and native gold. The Sn and Au content of the radioactive sample analyzed are respectively 2100 ppm and 1.9 ppm (Table 21.2, E-9006). According to R.W. Boyle (pers. comm., 1979) the concentrations of Nb (300 ppm) and Ta (139 ppm) are unusually high for a conglomerate. The minerals containing these elements, however, have not been identified in the thin sections.

Locality G

Stratiform radioactivity (Fig. 21.2c) occurs in a siltstone in the northwestern part of the Nonacho Basin. The rock is greenish grey to pink and is composed essentially of quartz and feldspar grains in a micaceous/chloritic or carbonate cement. The carbonate content of the cement appears to vary stratigraphically but its effect on the distribution of the radioactivity is not apparent. The bedding is often well marked by concentrations of small pyrite cubes and the radioactivity tends to follow these pyritiferous zones.

Occasionally, radioactive minerals are found along fractures, probably from local remobilization. Intraformational breccias have been found, and in these, the angular fragments are often more radioactive than the matrix (Fig. 21.2d).

The samples analyzed from this showing have a very high U/Th ratio and show considerable enrichment in Pb and, to a lesser extent, in V (Table 21.2, F-9011). Under the microscope, the radioactive grains are usually very small with a pitted surface and appear to be composed of an assemblage of different phases. X-ray diffraction shows uraninite and galena to be the major components of these grains but microprobe analyses also indicate the presence of a U-Ti phase (Fig. 21.4). By comparison with uranium and titanium standards this phase contains 35 to 40% U and about 20% Ti. The U/Ti ratio appears fairly constant.

Other Areas

At locality H, the Nonacho basal conglomerate contains sparingly distributed boulders of an altered intermediate or basic igneous rock now composed essentially of sericitized feldspar with irregular bands of an acicular Ti-bearing iron oxide. These oxides probably derive from the alteration of the original mafic minerals. Accessories include sphene, zircon and apatite. Thorite was also tentatively identified in thin sections in association with the apatite. It is possible that some of the Th is also present in the accessory minerals. Several grains of niobian rutile were also identified. Major and trace element content of these boulders are given in Tables 21.1 and 21.2 (E-9011).

Fracture-controlled radioactivity occurs in arkosic Nonacho sediments near the west shore of Thekulthili Lake (locality I). The samples collected at this locality are altered extensively so that most of the radioactive elements in them are now in the form of secondary minerals. Remnants of uraninite grains, however, were identified in the thin sections. Enrichment in some elements, viz. Pb, Ba, Ag, Bi, Cu, Th and Ce (Table 21.2, F-9029) makes this occurrence somewhat similar to those of locality E, particularly E3.

Fracture controlled radioactivity also occurs at locality J. Here, the host rocks are basement gneiss and schist. The main radioactive phase was tentatively identified as secondary kasolite. No primary uranium minerals were seen. Chemical analyses indicate enrichment in U, Pb, and Mo, but low Th and rare-earths (Table 21.2, F-9024).

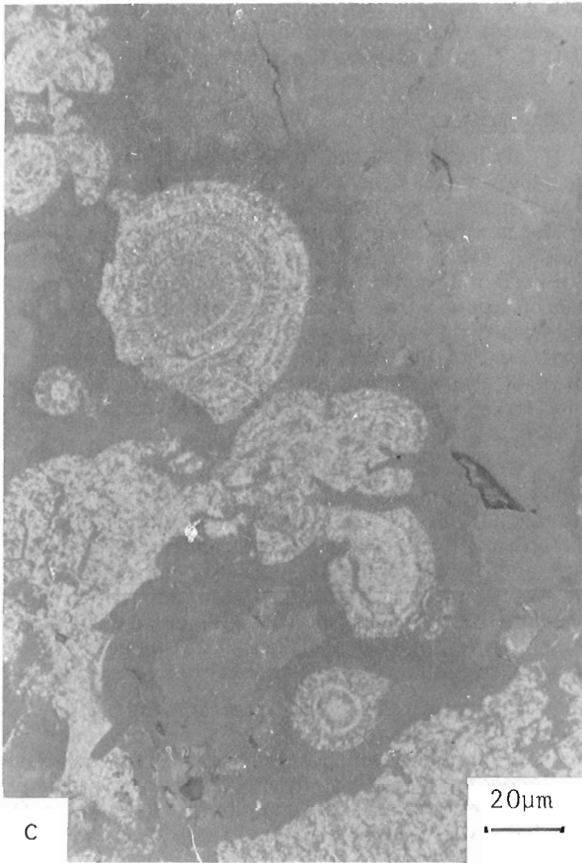
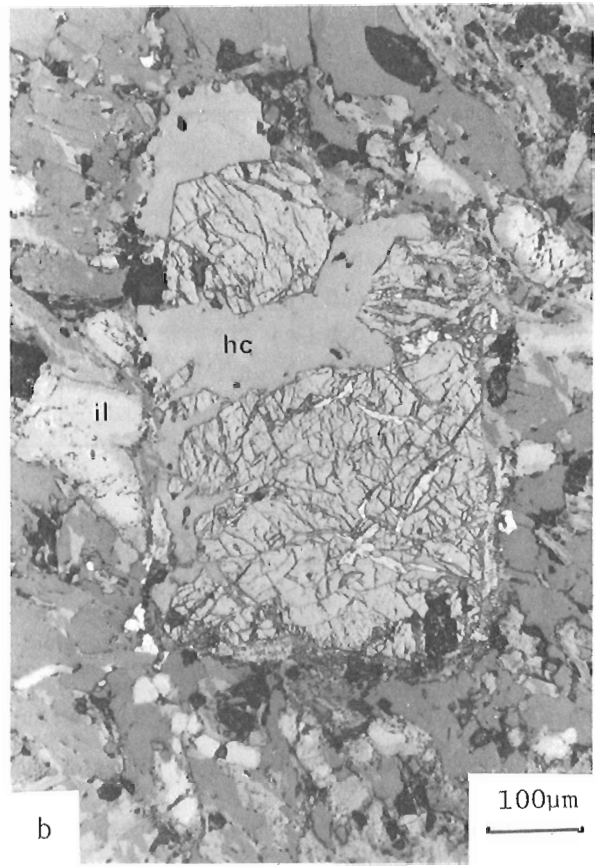
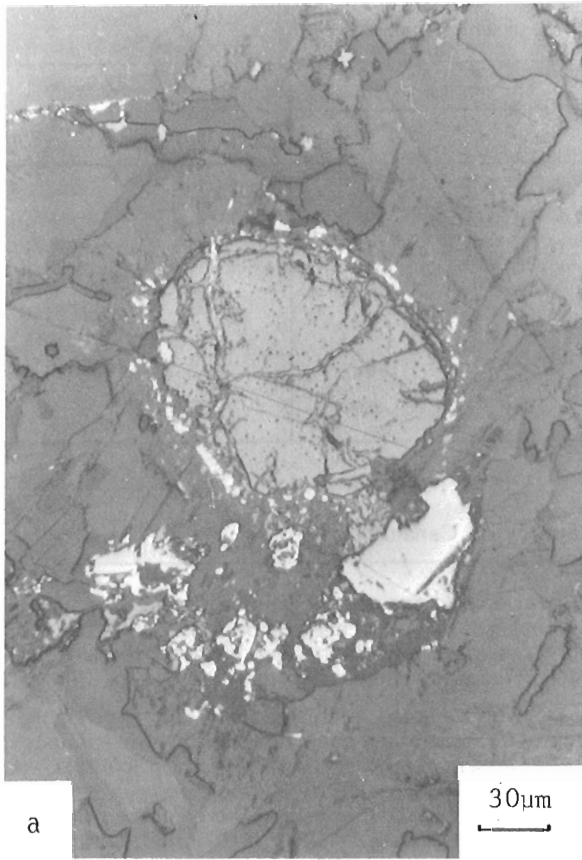


Figure 21.3 (opposite)

Photomicrographs in reflected light.

- a *Locality A (K-9023). Rounded, fractured uraninite surrounded by a discontinuous ring of galena grains in biotite. Associated sulphides are pyrite (large grain), chalcocopyrite and sphalerite.*
- b *Locality B (F-9019). Hypidiomorphic, fractured uraninite with hydrocarbon (hc). Stringers of galena are present as fracture fillings in the uraninite. Ilmenite (il) is rimmed by sphene.*
- c *Locality C (F-9003). Colloform pitchblende in epidote.*
- d *Locality D (C-9006). Part of large fractured uraninite grain composed of unaltered phase (higher reflectivity) in Pb-deficient, Si-rich matrix (lower reflectivity). Small granules of galena (white) are present within the uraninite and around its perimeter.*

Genetic Interpretation

Three of the radioactive occurrences examined in the Nonacho Basin have syngenic characteristics: (1) the heavy mineral concentrations in the basal conglomerate at locality F; (2) the stratiform mineralization in siltstone at locality G; and (3) the rounded boulders in the basal conglomerates at locality H. These occurrences testify to the fact that radioactive minerals were undergoing erosion from rocks in proximity to the Nonacho Basin at the time the Nonacho sediments were being deposited. The uranium and thorium minerals in the Nonacho sediments may have originated from radioactive rocks in the Fort Smith Belt and/or from sources of the type found at localities B or C.

Radioactivity in the Fort Smith Belt is widespread (B.W. Charbonneau, pers. comm., 1979) and is of the type found at locality A. Its close association to intrusive rocks suggests a magmatic origin for the U and Th. Cape (1977), however, describing biotite-rich pods near Pilot Lake (Fig. 21.1) that are similar to the mafic bands at locality A, suggests that the radioactive minerals were initially present in placer-type sedimentary strata that were caught as inclusions in an intruding granitic magma. He believes that the radioactivity of the intrusive rocks derives from the assimilation of radioactive sediments by the magma.

The radioactivity in the Nonacho sediments originates either from the transportation and deposition of clastic mineral species as in the basal conglomerate at locality F, or from the precipitation of uranium under reducing conditions during sedimentation as in the case of the pyritiferous siltstone at locality G. The unidentified interstitial uranium phase, which is closely associated with the clastic radioactive minerals at locality F, may derive from the alteration of uranothorite during diagenesis. According to Frondel (1958), this mineral alters to a glass-like metamict phase; this alteration may have allowed local redistribution of the uranium in the rock.

The abundance of certain elements in the conglomerate (locality F) suggests a contribution from sources other than the Fort Smith Belt. The Sn-Au-Nb-Ta assemblage in the conglomerate is strikingly similar to assemblages found in the southern Slave Province (Mulligan, 1975). Such a distant source, however, may be problematic; these elements may in fact have originated from as yet unidentified but much nearer sources. In the case of Nb and Ta, these elements occur at locality C.

The fracture-controlled occurrences in the Nonacho sediments (localities E and I) probably reflect late remobilization from an underlying source, possibly of syngenic origin. S.S. Gandhi (pers. comm., 1979), from the

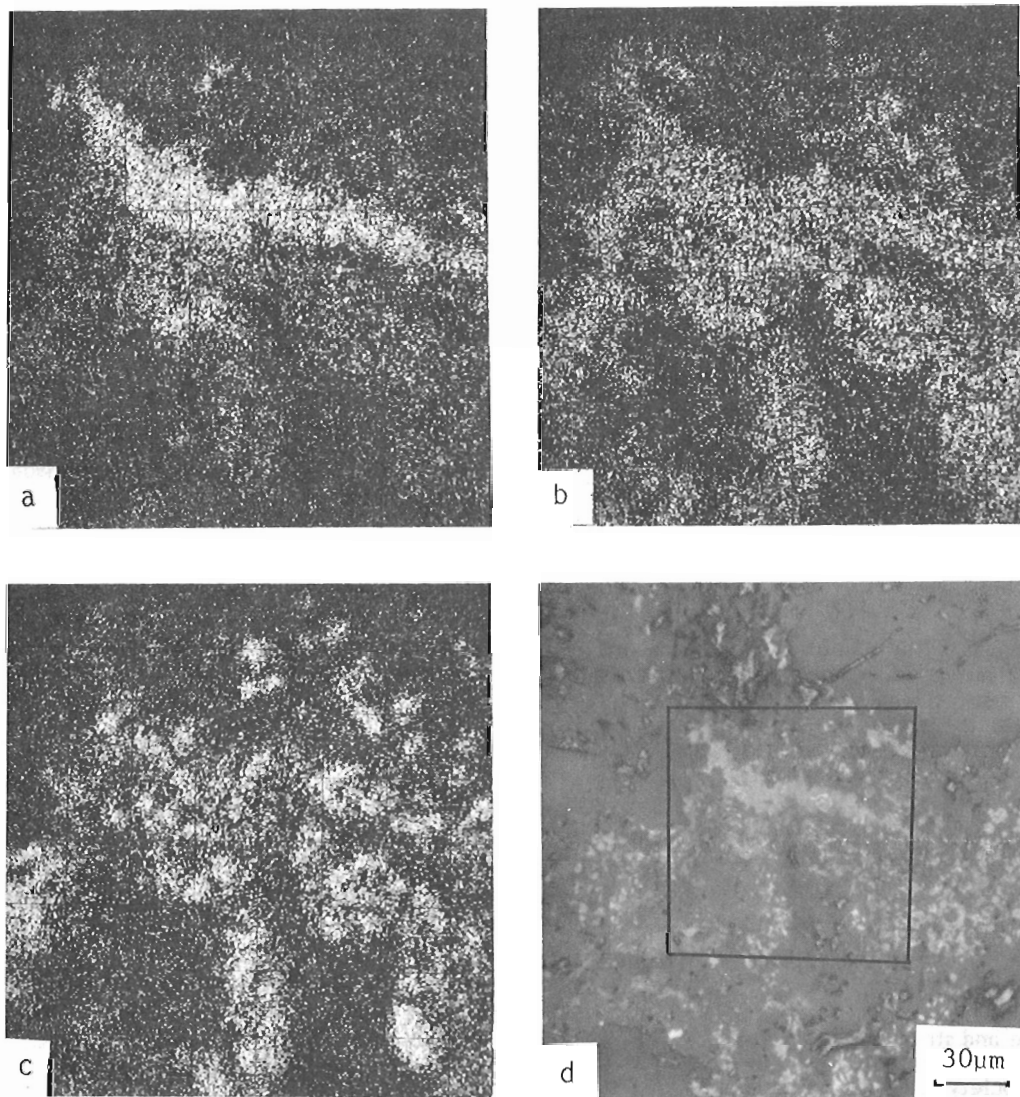


Figure 21.4. X-ray scanning images showing the distribution of a) titanium, b) uranium, and c) lead in the small area of photomicrograph (d).

examination of drill core from the MacInnis Lake area (locality E), found evidence of stratiform mineralization at depth.

The mineralization at locality D may call for a different genetic process: the occurrence of uranium minerals in a basement fracture in proximity to the Nonachobasement unconformity and the very high U/Th ratio suggest a supergene, unconformity-related origin. Although it may be advocated that the complex assemblage of metals present is more in line with a hydrothermal origin, Langford (1977) pointed out that such assemblages are not necessarily incompatible with supergene processes.

Exploration Guidelines

On the basis of the proposed genetic model, the pyritiferous siltstones, such as those hosting uranium minerals at locality G, may represent the most favourable lithology for uranium mineralization in the Nonacho Basin. A zone of these rocks extends along the western margin of the basin from MacInnis Lake (locality E) to the northern end of the Nonacho Basin (Fig. 21.1). Other smaller zones have been mapped along the shores of Thekulthili Lake, north of locality I. Although the radioactive rocks may occur at surface, as is the case at locality G, their surface expression in other areas may be restricted to later remobilization along fractures that intersect the mineralization at depth. Possible examples of this are found at localities E and I.

The basal conglomerate should also be examined closely. According to Boyle (in press), the Au concentration found in one sample is in the order of one hundred times greater than the average concentration for Au in other conglomerates and well within the range of values of productive auriferous quartz-pebble conglomerates in various parts of the world. The Sn content of the conglomerate is also of interest; the distribution of this element in the conglomerate as well as its provenance should be investigated.

Basement fractures at or near the unconformity should be examined for possible supergene uranium concentrations, particularly in the vicinity of U-enriched basement rocks. The basement rocks themselves may be of interest. For example, the source of the highly radioactive diorite boulders that occur at locality C may be of economic significance. In the Fort Smith Belt, B.W. Charbonneau (pers. comm., 1979) recommended exploration in the areas of high U/Th ratio, as outlined by airborne radiometric data.

Acknowledgments

Summer students Sandy Denton, Roy Smith and Catherine Crosby assisted the senior author in the field and with the optical microscopy studies respectively. In addition to the analytical staff referenced in the tables, we thank A.C. Roberts for careful X-ray diffraction measurements. Dr. S.S. Gandhi is acknowledged for drawing our attention to the presence of gold in the basal conglomerate.

References

- Boyle, R.W.
The geochemistry of gold and its deposits; Geological Survey of Canada, Bulletin 280. (in press)
- Burwash, R.A. and Baadsgaard, H.
1962: Yellowknife-Nonacho age and structural relations; in J.S. Stevenson (Editor), *Tectonics of the Canadian Shield*, Royal Society of Canada, Special Publication 4, p. 22-29.
- Cape, D.F.
1977: An investigation of the radioactivity of the Pilot Lake area, N.W.T.; M.Sc. thesis, University of Alberta, Edmonton, 156 p.
- Fraser, J.A.
1978: Metamorphism in the Churchill Province, District of Mackenzie; in J.A. Fraser and W.W. Heywood (Editors), *Metamorphism in the Canadian Shield*, Geological Survey of Canada, Paper 78-10, p. 195-202.
- Frondel, C.
1958: Systematic mineralogy of uranium and thorium; U.S. Geological Survey, Bulletin 1064, 400 p.
- Granier, C.L.
1973: Introduction à la prospection géochimique des gîtes métallifères; Masson et cie, Paris, 143 p.
- Henderson, J.F.
1937: Nonacho Lake area, Northwest Territories; Geological Survey of Canada, Paper 37-2, 22 p.
- Hornbrook, E.H.W., Garrett, R.G., and Lynch, J.J.
1976: National geochemical reconnaissance, N.W.T., NTS 75C, F, and K; Geological Survey of Canada, Open Files 324, 325, and 326.
- Johannsen, A.
1937: The intermediate rocks; in *A descriptive petrography of the igneous rocks*; University of Chicago Press, Chicago, Illinois, v. 3, 360 p.
- Joint Committee on Powder Diffraction Standards
1974: Selected powder diffraction data of minerals, Search Manual; Publication M-1-23, Berry, L.G. (Editor), 262 p.
- Langford, F.F.
1977: Surficial origin of North American pitchblende and related uranium deposits; American Association of Petroleum Geologists, Bulletin, v. 51, no. 1, p. 28-42.
- Maurice, Y.T.
1976: Detailed geochemical investigations for uranium and base metal exploration in the Nonacho Lake area, District of Mackenzie; in Report of Activities, Part C, Geological Survey of Canada, Paper 76-1C, p. 259-262.
1977: Follow-up geochemical activities in the Nonacho Lake area (75F, K), District of Mackenzie; Geological Survey of Canada, Open File 489.
Methods of interpretation and follow-up of reconnaissance lake sediment data in the northern Canadian Shield; 7th International Geochemical Exploration Symposium, Denver, 1978. (in press)
- McGlynn, J.C.
1971: Stratigraphy, sedimentology and correlation of the Nonacho Group, District of Mackenzie; in Report of Activities, Part A, Geological Survey of Canada, Paper 71-1A, p. 140-142.
1978: Geology of the Nonacho Basin, District of Mackenzie; Geological Survey of Canada, Open File 543.
- Mulligan, R.
1975: Geology of Canadian tin occurrences; Geological Survey of Canada, Economic Geology Report no. 28, 155 p.

**DEVONIAN SPORES FROM THE BARRANDIAN REGION OF CZECHOSLOVAKIA AND
THEIR SIGNIFICANCE FOR INTERFACIES CORRELATION**

Project 750036

D.C. McGregor
Regional and Economic Geology Division

McGregor, D.C., Devonian spores from the Barrandian region of Czechoslovakia and their significance for interfacies correlation; in Current Research, Part B, Geological Survey of Canada, Paper 79-1B, p. 189-197, 1979.

Abstract

Spores similar to those of Canada and western Europe occur in strata of Pragian, Zlichovian, and Dalejan age in the classic Lower Devonian sequence of the Barrandian region, Czechoslovakia. The spore assemblages are associated with zonally significant conodonts and/or tentaculites, and are therefore calibrated precisely with marine faunal zones. Marine palynomorphs (acritarchs, chitinozoans, and scolecodonts) of potential stratigraphic significance, but not useful for direct marine-nonmarine correlation, occur with the spores. Spores are at this time the only fossils available for directly correlating parts of the offshore Hercynian facies of the Barrandian area with the nearshore Rhenish facies, and for correlating both of these marine magnafacies directly with continental strata of Europe and North America. Spores are especially abundant in the Daleje Shale and lower Třebotov Limestone, from which conodont recovery is poor. Comparisons with the Eifelian Hills indicate that the lower Daleje Shale is older than the Wiltz Schichten, the upper Daleje Shale at Císařská rokle is equivalent to the lower Wiltz, and the middle part of the Třebotov Limestone at Praha-Hlubočepy is older than the upper Wetteldorf Schichten. Spores have not yet been found in Czechoslovakia in the interval between the middle of the Třebotov Limestone and the middle of the overlying Choteč Limestone, i.e. from any of the three levels now being considered for the Lower-Middle Devonian boundary stratotype. In view of the demonstrated presence of spores in older and younger strata of the Barrandian region, a diligent search should be made for them within this interval.

Introduction

Biostratigraphic correlations between offshore, nearshore, and continental strata are limited by the facies-dependence of the commonly used index faunas. These limitations are well known, and have been summarized and illustrated by many authors. Spores, on the other hand, are in theory practicable for direct correlation among all of these facies. Their recognition as index fossils has however been inhibited by a lack of established and tested zonal standards, and possibly by the "conventional wisdom" that spores are of plant origin and therefore a priori unsuited for precise correlation. Recent work has shown that spores are practicable for long distance correlation, and in those parts of the Devonian in which they are most thoroughly studied they rival the more traditional fauna-based orthochronologies for correlation of both continental and marine strata (see summary in McGregor, in press, a).

Spores of Rhenish and Old Red Sandstone type are common in the Lower Devonian rocks of eastern, central, and northern Canada (McGregor, in press, b). For the most part they occur in strata deficient or lacking in zonally significant marine faunas (e.g. the Gaspé Sandstone) or in which bed by bed correlation with marine faunal sequences has not been attained (e.g. the subsurface of the Hudson Bay region). Precise correlation of Canadian Devonian spores with faunal zones, and their use for long distance interfacies correlations, can only be achieved by means of reference sections in Canada and abroad in which spores, conodonts, tentaculites, ostracodes, and other zonal fossils occur together.

The purpose of this preliminary report is to note the presence of Lower Devonian spores in strata of Hercynian magnafacies in the Barrandian Basin of Czechoslovakia. The Barrandian spores are virtually identical to those from continental and Rhenish facies in Canada and the Eifel region, and occur with a rich and varied marine fauna.

Stratigraphic Significance of the Barrandian Region

In North America, some biostratigraphers advocate abandonment of the traditional western European (Rhenish) Standard Stages for the Lower Devonian in favour of the Barrandian (Hercynian) stages, i.e. Lochkovian, Pragian, Zlichovian, and Dalejan. The use of Hercynian stages is particularly attractive for western and arctic North America because the widespread pelagic faunas of these regions are readily correlatable with the predominantly pelagic faunas of the Hercynian facies. If the Hercynian stages become more widely accepted, the Barrandian Devonian will achieve considerable significance as a world reference standard. The Lower-Middle Devonian sequence of the Barrandian area is considered by the Subcommittee on Devonian Stratigraphy to be a leading contender for the location of the world stratotype of the Lower-Middle Devonian Series boundary. The stratotype of the boundary between the Silurian and Devonian systems already has been established in the Barrandian region.

Correlations between the major Devonian magnafacies, Rhenish, Hercynian, and continental, commonly have been indirect or unattained because of marked difference in biofacies. Only recently, detailed direct correlations have been established by means of conodonts between the upper Dalejan of the Barrandian region and the latest Emsian, Eifelian, and Couvinian Rhenish facies of the Eifelian Hills and the Ardennes (Klapper et al., 1978). Older, Pragian to mid Dalejan rocks of the Barrandian region cannot yet for the most part be correlated directly by faunas with either the western European Rhenish facies or the Old Red continental facies.

EIFELIAN HILLS		BARRANDIAN REGION			Palynomorph samples	Tentaculite zones	Conodont zones	
EIFELIAN	JUNKERBERG	CHOTEČ LS		•	sulcata	kockelianus		
	AHRDORF			•		australis		
	NOHN			•		costatus costatus		
	LAUCH			▽				
U	HEISDORF	DALEJAN	TŘEBOTOV LS		holynensis	u		
	WETTELDORF					1	patulus	
	WILTZ					•	serotinus	
	BERLE			DALEJE SH		•	1	richterii
						•		
EMSIAN	KLERF	ZLICHOVIAN	ZLÍCHOV LS	•	barrandei	gronbergi		
							•	
							•	
							•	
L	STADTFELD		KAPLIČKA CORAL HOR	•	praecursor	dehiscens		
				•	zlichovensis			
				•				
SIEGENIAN		PRAGIAN	DVORCE-PROKOP LS	•	G. strangulata	acuaria		
				•				
GEDINNIAN (part)	LOCHKOVIAN (part)	RADOTÍN LS (part)		•	P. intermedia			

Closed circles = spores and marine palynomorphs;
open circles = marine palynomorphs only;
triangles = no palynomorphs.

Figure 22.1. Location of palynomorph samples in the Lower and Middle Devonian of the Barrandian region. Correlation with the Eifelian Hills and with tentaculite and conodont zones after Chlupáč (1976) and Klapper et al. (1978). Dashed lines indicate uncertain correlation of conodont and tentaculite zones, and of the Eifelian sequence. Numbers are GSC locality numbers.

PLATE 22.1 (opposite)

All figures X500.

Figures 1-11, GSC locality 9553, Dvorce-Prokop Limestone, Upper Pragian.

1. *Retusotriletes* sp. GSC 61649.
2. *Retusotriletes* sp. cf. *R. actinomorpha* Chibrikova. GSC 61650.
3. ?*Apiculiretusispora* sp. GSC 61651.
4. ?*Dibolisporites* sp. GSC 61652.
5. *Dictyotriletes* sp. GSC 61653.
6. *Emphanisporites micronatus*? Richardson and Lister. GSC 61654.
- 7,8. *Emphanisporites rotatus* McGregor. 7, GSC 61655; 8, GSC 61656.
9. *Emphanisporites decoratus* Allen. GSC 61657.
10. *Synorisporites* sp. GSC 61658.
11. ?*Dibolisporites wetteldorfensis* Lanninger. GSC 61659.

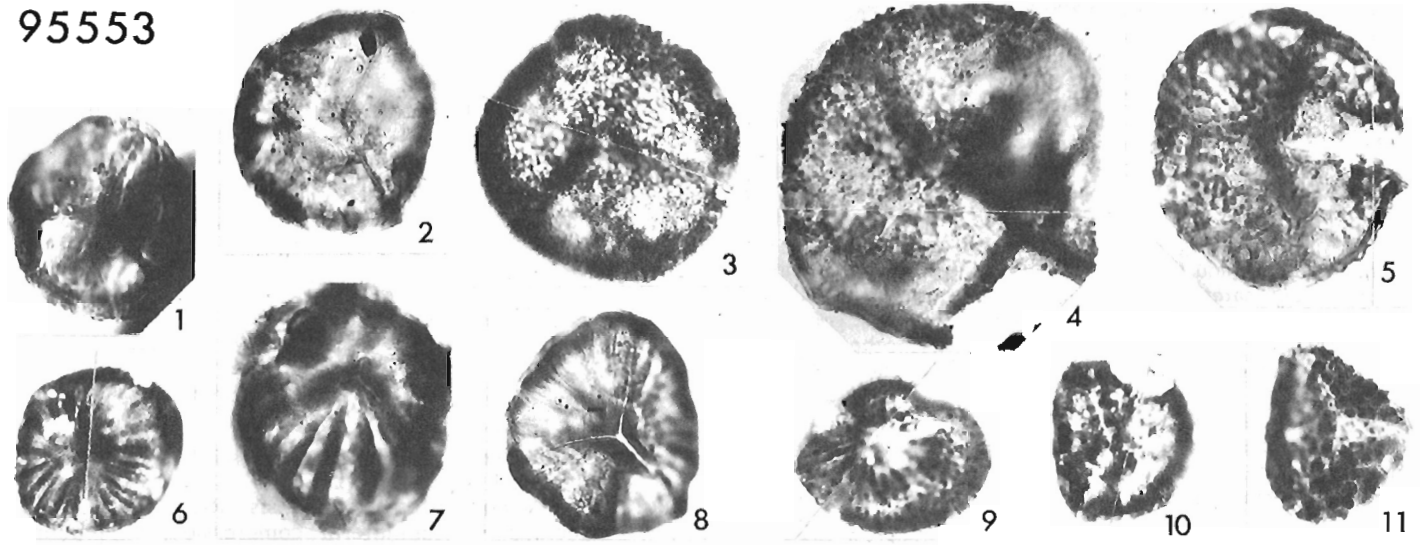
Figures 12-28, GSC locality 9558, Zlíčov Limestone, Upper Zlichovian.

12. *Retusotriletes* sp. GSC 61660.
13. *Retusotriletes psychovii*? Naumova. GSC 61661.
14. *Retusotriletes* sp. GSC 61662.
15. ?*Dibolisporites* sp. cf. *D. echinaceus* (Eisenack) Richardson, *gibberosus* type. GSC 61663.
16. *Apiculiretusispora* sp. GSC 61664.
17. *Dictyotriletes* sp., same species as fig. 5. GSC 61665.
18. *Apiculiretusispora* sp. GSC 61666.
19. *Apiculatasporites* sp. cf. *A. perpusillus* (Naumova) McGregor. GSC 61667.
- 20,25. *Dibolisporites wetteldorfensis* Lanninger. 20, GSC 61668; 25, GSC-61669.
21. *Dictyotriletes emsiensis*? (Allen) McGregor. GSC 61670.
22. *Streelispora* (?=*Aneurospora*) sp. GSC 61671.
23. *Emphanisporites rotatus* McGregor. GSC 61672.
24. ?*Dictyotriletes* sp. GSC 61673.
26. ?*Kraeuselisporites* sp. GSC 61674.
27. ?*Dibolisporites* sp. GSC 61675.
28. *Dictyotriletes favosus*? McGregor and Camfield. GSC 61676.

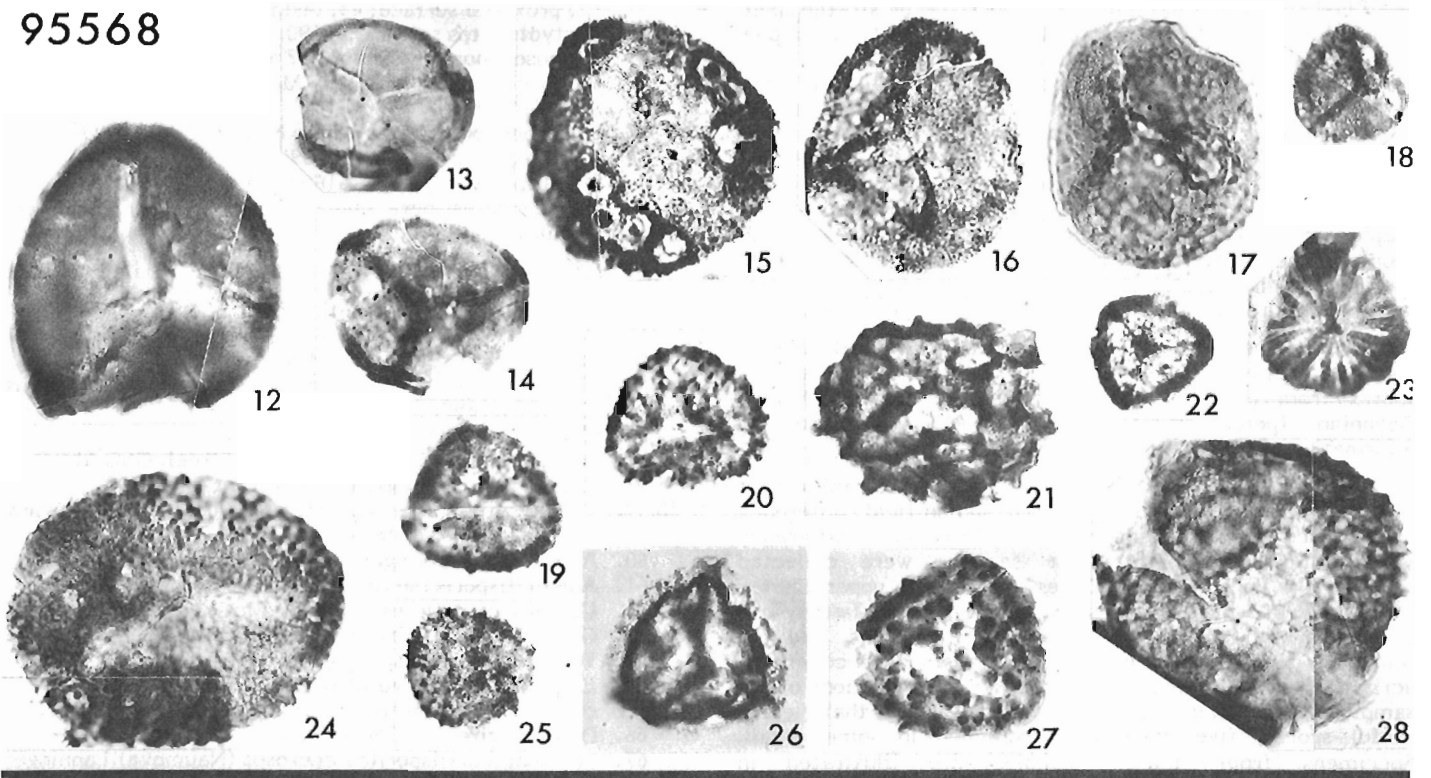
Figures 29-37, GSC locality 9558, lower Daleje Shale, lower Dalejan.

29. *Retusotriletes rotundus* Streele. GSC 61677.
30. *Calamospora pannucea* Richardson. GSC 61678.
31. *Deltoidospora* sp. GSC 61679.
- 32,33. *Retusotriletes* sp. 32, GSC 61680; 33, GSC 61681.
34. *Retusotriletes psychovii*? Naumova. GSC 61682.
35. *Apiculiretusispora* sp. GSC 61683.
36. *Apiculiretusispora plicata* (Allen) Streele. GSC 61684.
37. *Apiculiretusispora* sp., same species as fig. 16. GSC 61685.

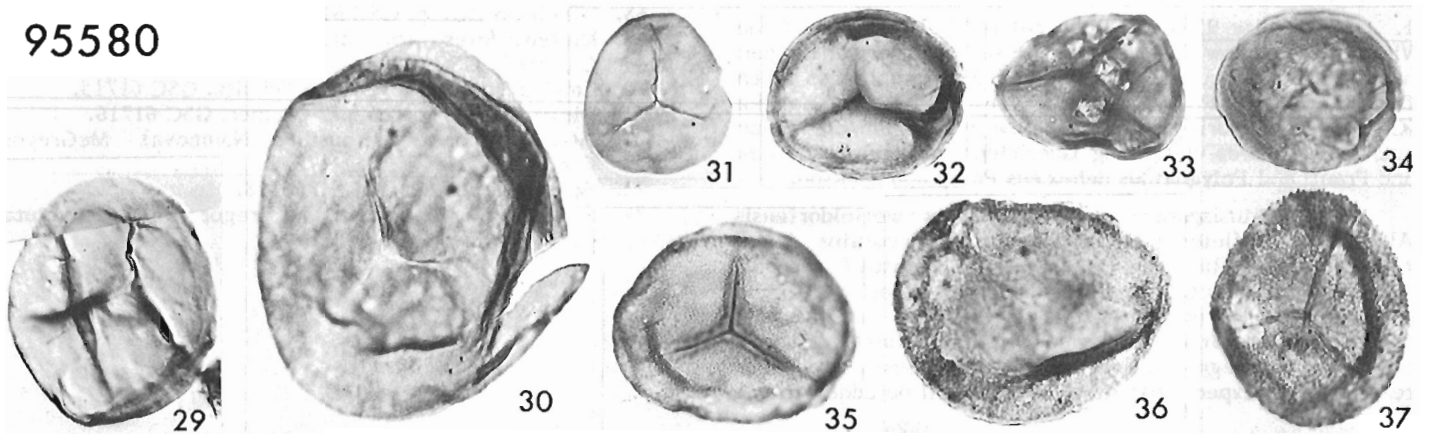
95553



95568



95580



Spores from the Barrandian Devonian

Obrhel (1959) was the first to report the presence of spores in the Barrandian Devonian, when in the course of paleobotanical studies he found spores in sporangia of *Barrandina dusliana* (Krejčí) Stur and *Protopteridium hostinense* Krejčí from the Kacák Member of the Givetian Srbsko Formation. In 1968 he reported sporangia filled with spores, possibly of *P. hostinense*, in the Roblín Member of the Srbsko Formation. In 1961 he sent the present author five rock samples bearing plant specimens from the Kačák and Roblín members and from the Choteč Limestone. Fragments cut from each sample were analyzed for spores, and only two of them, one each from the Kačák and Roblín beds, contained rare, poorly preserved spores. Subsequently, other samples from the Choteč, Kačák, and Roblín beds, some of them without visible plant remains, have proved to contain spores in a better state of preservation (see below). In the Barrandian Basin, as elsewhere, it seems that plant-bearing beds may not always contain the best assemblages of dispersed spores, even when the plants themselves bear in situ spores.

Lele (1972) found spores in the Daleje Shales, then thought to be lower Eifelian. He neither illustrated nor described them, and did not give geographic or stratigraphic details beyond stating (ibid., p. 131) that the "... samples were collected from a section near Srbsko." He identified fourteen genera, of which eleven are long ranging and provide no clue as to age. *Samarisporites* and cf. *Grandispora* suggest late Emsian or later age, and *Ancyrospora*, if correctly identified, would not be older than the upper Wetteldorf Schichten, much younger than the age now ascribed to the Daleje Shale. Lele's report, too generalized to be biostratigraphically useful, nevertheless did signal the presence of spores in the Daleje Shale. In the same paper, Lele reported spores from the Givetian Srbsko Formation, but included few details of location and no illustrations of the specimens.

J.B. Richardson of the British Museum (Natural History) and W. Riegel of the University of Göttingen have extracted spores from parts of the Barrandian Lower and Middle Devonian (pers. comm., 1977). Both have provided information useful in the preparation of this report.

The samples that are the major basis for this paper were collected in 1977 during the Barrandian field conference of the International Subcommittee on Devonian Stratigraphy led by I. Chlupáč. Thirty-four samples were collected between the upper Radotín Limestone and the upper Choteč Limestone, of which all but six were productive. Twenty-one contained both spores and marine palynomorphs, and the remainder contained only marine forms, most commonly acritarchs and chitinozoans. The stratigraphic positions of the samples are shown in Figure 22.1. Of the samples that yielded useful spores, five have been examined in some detail. Specimens from these samples are illustrated in Plates 22.1-22.3.

1. GSC locality 95553: Road cut on the west side of the Vltava River below Barrandov in the southern part of Prague, north of the old quarry "U Kapličky". The sample was taken from the Dvorce-Prokop Limestone, 1 m below the Kaplicka (Chapel) Coral Horizon, i.e. 1 m below the Pragian-Zlichovian boundary, in beds containing *Guerichina strangulata* Bouček and Prantl and *Polygnathus dehiscens* Philip and Jackson.

Apiculiretusispora sp., ?*Dibolisporites wetteldorfensis* Allen, *Dictyotriletes* sp., *Emphanisporites decoratus* Allen, *E. microratus*? Richardson and Lister, *E. rotatus* McGregor, *Retusotriletes* sp. cf. *R. actinomorpha* Chibrikova, and *Synorisporites* sp. occur at this level. Other species are present but cannot be identified owing to exinal corrosion, pitting, and fragmentation of the specimens. It seems reasonable to expect that other species will be added to the

list when late Pragian assemblages from the Barrandian region are examined more thoroughly. Even at this preliminary stage of the investigation the Siegenian to early Emsian character of the assemblage is evident, i.e. distally sculptured *Emphanisporites*, rare zonate spores, and small *Dibolisporites*. *Emphanisporites decoratus* occurs in the Eifelian Hills, Vestspitsbergen, eastern Canada, northwestern United States, and possibly the Ardennes.

PLATE 22.2 (opposite)

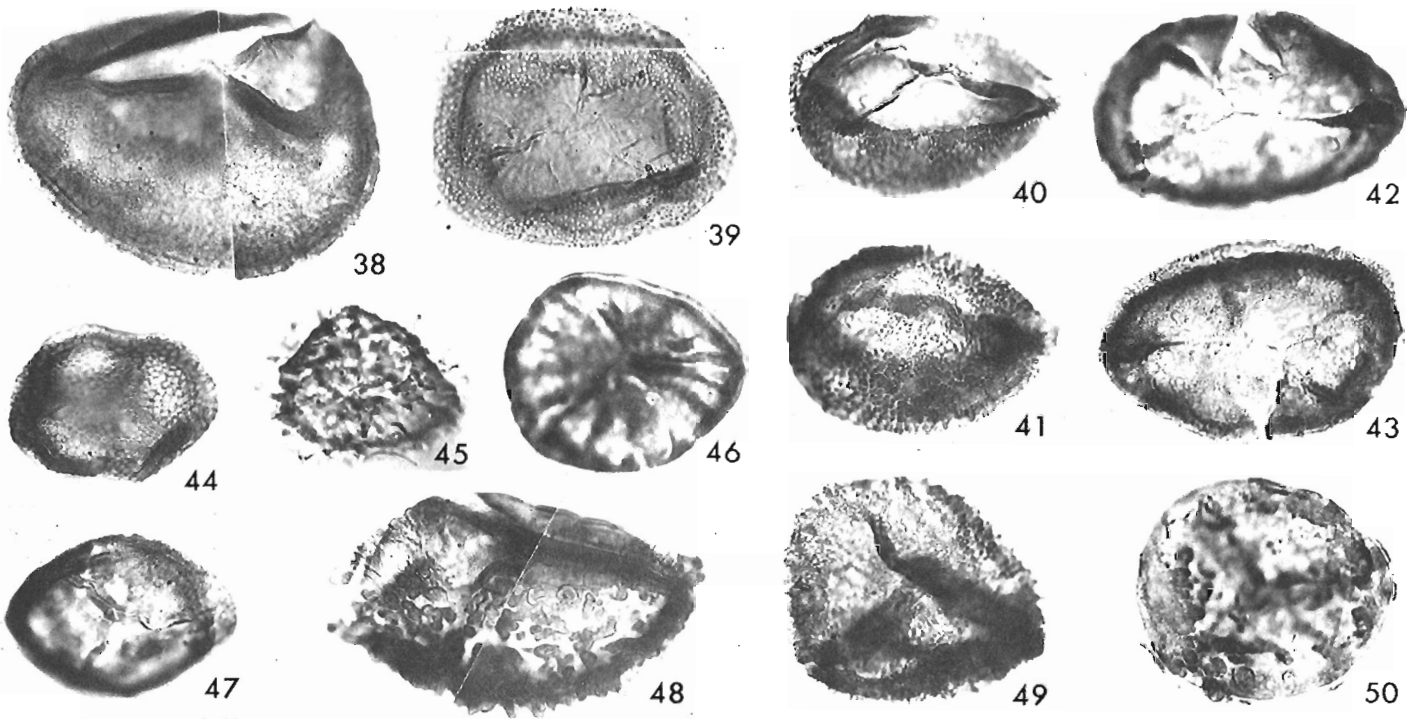
All figures X500.

Figures 38-50, GSC locality 95580 (continued).

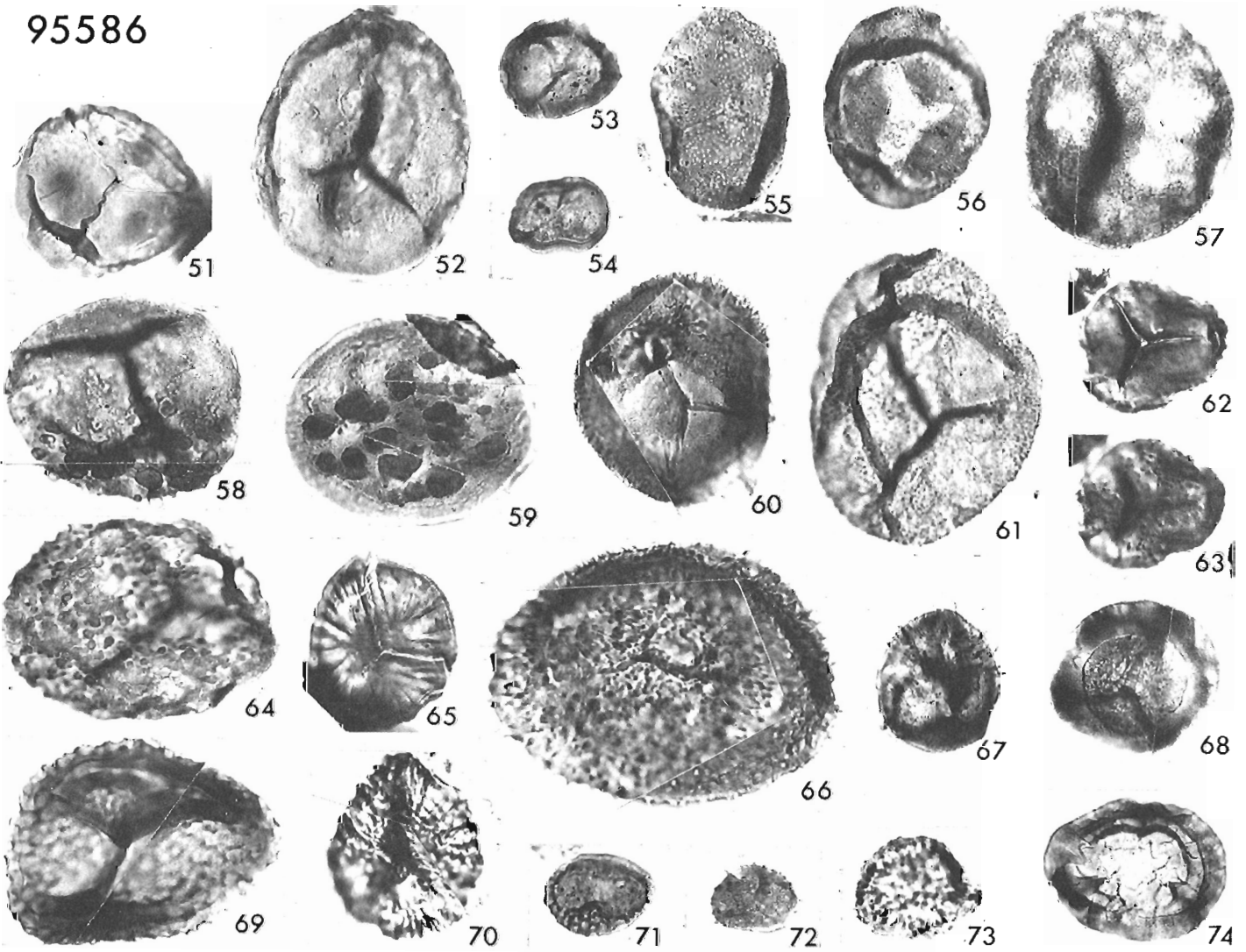
38. ?*Apiculiretusispora* sp. GSC 61686.
39. *Dibolisporites echinaceus* (Eisenack) Richardson, *gibberosus* type. GSC 61687.
- 40,41. cf. *Acinosporites lindlarensis* Riegel. GSC 61688, specimen in semilateral compression; 40, proximal-equatorial view; 41, distal view.
- 42,43. ?*Hymenozonotriletes asper* Chibrikova. GSC 61689; 42, proximal surface; 43, distal surface.
44. *Dictyotriletes* sp. GSC 61690.
45. *Kraeuselisporites gaspiensis*? McGregor. GSC 61691.
46. *Emphanisporites rotatus* McGregor, *robustus* type. GSC 61692.
47. ?*Archaeozonotriletes varius* Nadler. GSC 61693.
48. ?*Acinosporites* sp. GSC 61694.
49. *Dibolisporites* sp. GSC 61695.
50. ?*Verruciretusispora dubia* (Eisenack) Richardson and Rasul. GSC 61696.

Figures 51-74, GSC locality 95586, upper Daleje Shale, Dalejan.

51. *Retusotriletes ocellatus* McGregor. GSC 61697.
52. *Retusotriletes* sp. GSC 61698.
- 53,54. *Tholisporites chulus* (Cramer) McGregor var. *nanus*. 53, GSC 61699; 54, GSC 61700.
55. *Cyclogranisporites* sp. GSC 61701.
56. *Apiculiretusispora plicata* (Allen) StreeL. GSC 61702.
57. ?*Retusotriletes biornatus* Schultz. GSC 61703.
- 58,59. *Verruciretusispora* sp. 58, GSC 61704, lateral view; 59, GSC 61705, distal view.
60. *Apiculiretusispora gaspiensis* McGregor. GSC 61706.
61. *Apiculatisporis microconus* Richardson. GSC 61707.
- 62,63. *Camarozonotriletes sextantii* McGregor and Camfield. GSC 61708, 62, proximal view; 63, distal view.
64. *Verrucosporites* sp. GSC 61709.
65. *Emphanisporites rotatus* McGregor, GSC 61710, rib conformation transitional to *E. schultzii* McGregor.
66. *Dibolisporites* sp. GSC 61711.
67. cf. *Anapiculatisporites acerosus* (Naumova) Lanninger. GSC 61712.
68. ?*Tholisporites* sp. GSC 61713.
69. *Dictyotriletes* sp. cf. *D. favosus* McGregor and Camfield. GSC 61714.
70. *Emphanisporites foveolatus* Schultz. GSC 61715.
71. *Dictyotriletes gorgoneus*? Cramer. GSC 61716.
72. *Apiculatisporites perpusillus* (Naumova) McGregor. GSC 61717.
73. *Apiculatisporites* sp. GSC 61718.
74. *Clivosispora verrucata* McGregor var. *convoluta*. GSC 61719.



95586



2. GSC locality 95568: Near Pekárek Mill west of the village of Solopysky, in the southern part of a small outcrop at the dam of the pond. The sample was obtained from the upper Zlíčov Limestone, 3 m below the boundary between the *Nowakia barrandei* and *N. elegans* tentaculite zones, 4.4 m below *Latericriodus beckmanni* (Ziegler) and 2.7 m below *Polygnathus perbonus* (Philip) in shale 40 cm below bed 5 of Chlupáč et al. (1977, fig. 5).

Spores are relatively common at this level. Most of the small-sculptured forms, such as *Apiculiretusispora* and *Dibolisporites*, are specifically unidentifiable because exinal sculpture, which is a basic criterion for identification of species, has been altered diagenetically. However, some species, especially those with grosser structural and sculptural features, were identified: *Apiculatasporites* sp. cf. *A. perpusillus* (Naumova) McGregor, *?Dibolisporites* sp. cf. *D. echinaceus* (Eisenack) Richardson (*gibberosus* type), *D. wetteldorfenis*, *Dictyotrilletes* sp. (as at 95553), *D. emsiensis?* (Allen) McGregor, *D. favosus?* McGregor and Camfield, *Emphanisporites rotatus*, *?Kraeuselisporites* sp., and *Retusotrilletes pychovii?* Naumova.

On spore evidence, the age range can be bracketed with some confidence between early Emsian and early late Emsian (pre-Wiltz) by relatively large spores suggestive of the *Dibolisporites echinaceus*-*Apiculatisporis microconus* complex, and the absence of prominent-sculptured zonate-camerates such as *Grandispora*.

3. GSC locality 95580: Near Karištejn, 1 km north of Budnany in the Hluboké Valley, in small roadside outcrop at sharp bend of road opposite house no. 130. The sample was taken from the left side (base) of the outcrop, low in the Daleje Shale in the uppermost *N. elegans* zone.

Spores are more numerous in the Daleje Shale than lower in the sequence, and in some samples, such as this one, they are better preserved than any found in older rocks of the Barrandian region. This sample contains the first specimens of species similar to *Hymenozonotrilletes asper* Chibrikova from the Takata beds of Bashkiria, and *Archaeozonotrilletes varius* Nadler from the Krasnogorsk beds of Altai-Sayan. The following are also present at this level: cf. *Acinosporites lindlarensis* Reigel, *Apiculiretusispora plicata* (Allen) StreeI, *Calamospora pannucea* Richardson, *Dibolisporites echinaceus* (*gibberosus* type), *Emphanisporites rotatus*, *Kraeuselisporites gaspiensis?* McGregor, *Retusotrilletes pychovii?*, *R. rotundus* StreeI, and *?Verruciretusispora dubia* (Eisenack) Richardson and Rasul. *Grandispora*, common high in the Daleje Shale and in the Trebotov Limestone, was not found among several hundred specimens examined, which suggests that the lower Daleje Shale is older than the base of the Wiltz Schichten of the Eifel.

4. GSC locality 95586: Upper part of southeast slope of Císařská rokle, southeast of Srbsko. The sample was taken 9.5 m above the base and 1.5 m below the top of the Daleje Shale, 1 m below the highest recorded *Nowakia cancellata*, 1.5 m below *Polygnathus laticostatus* Klapper and Johnson.

This sample contains the most diversified spore assemblage discovered so far in the Barrandian Basin. Most of the species found at this level also occur in nearshore marine and continental strata elsewhere in the Old Red Sandstone region: cf. *Anapiculatisporites acerosus* (Naumova) Lanninger, *Apiculatasporites perpusillus*, *Apiculatisporis microconus*, *Apiculiretusispora brandtii?* StreeI, *A. gaspiensis* McGregor, *A. plicata*, *Camarozonotrilletes sextantii* McGregor and Camfield, *Clivosispora verrucata* McGregor var. *convoluta*, *?Dibolisporites echinaceus* (*echinaceus* type), *Dictyotrilletes* sp. cf. *D. favosus*, *D. gorgoneus?* Cramer, *D. subgranifer?* McGregor, *Emphanisporites foveolatus* Schultz, *E. rotatus*, *?Hymenozonotrilletes asper*,

Retusotrilletes biornatus Schultz, *R. ocellatus* McGregor, and *Tholisporites chulus* (Cramer) McGregor var. *nanus*. Based on these spores, the age may be placed confidently in the early to mid-late Emsian range.

A more precise direct correlation with the Eifelian Hills is possible based on the incoming at this level of the first specimens of *Grandispora*, i.e. *G. (Endosporites) biornata* (Lanninger, 1968) n. comb. (*?Hymenozonotrilletes aculeatus* Nadler, nomen nudum in Chibrikova and Nadler, 1971) and *G. ?macrotuberculata* of McGregor, 1973. The appearance of large, prominent-spined zonate/camerates (*Grandispora*) is a geographically widespread event that has been recognized in Central Asia, the southwest Urals, western Europe, and eastern, central and arctic Canada. This event has been regarded as synchronous in all regions, and coincident with the incoming of bifurcate exinal processes, at the level of the upper Wetteldorf Schichten of the Eifelian Hills. However, it now seems that the first, rare grandisporites appeared somewhat before bifurcate spines. *G. biornata* begins in the lower Wiltz in the Eifel (W. Riegel, pers. comm. 1977); *G. ?macrotuberculata* begins before the first bifurcate spined spores in Gaspé; and "*H. aculeatus*" occurs in central Asia in the Krasnogorsk beds, which do not contain bifurcate-spined

PLATE 22.3 (opposite)

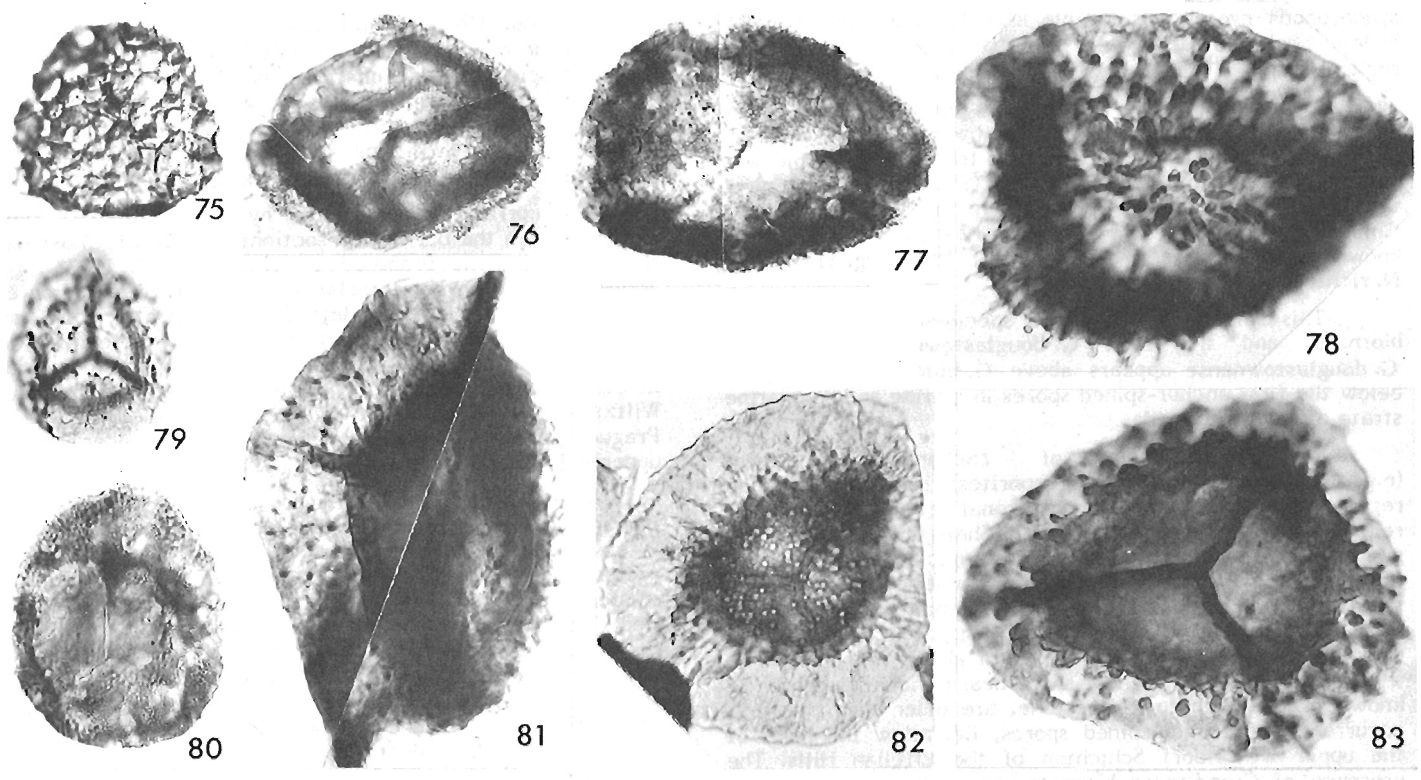
All figures X500.

Figures 75-83, GSC locality 95586 (continued).

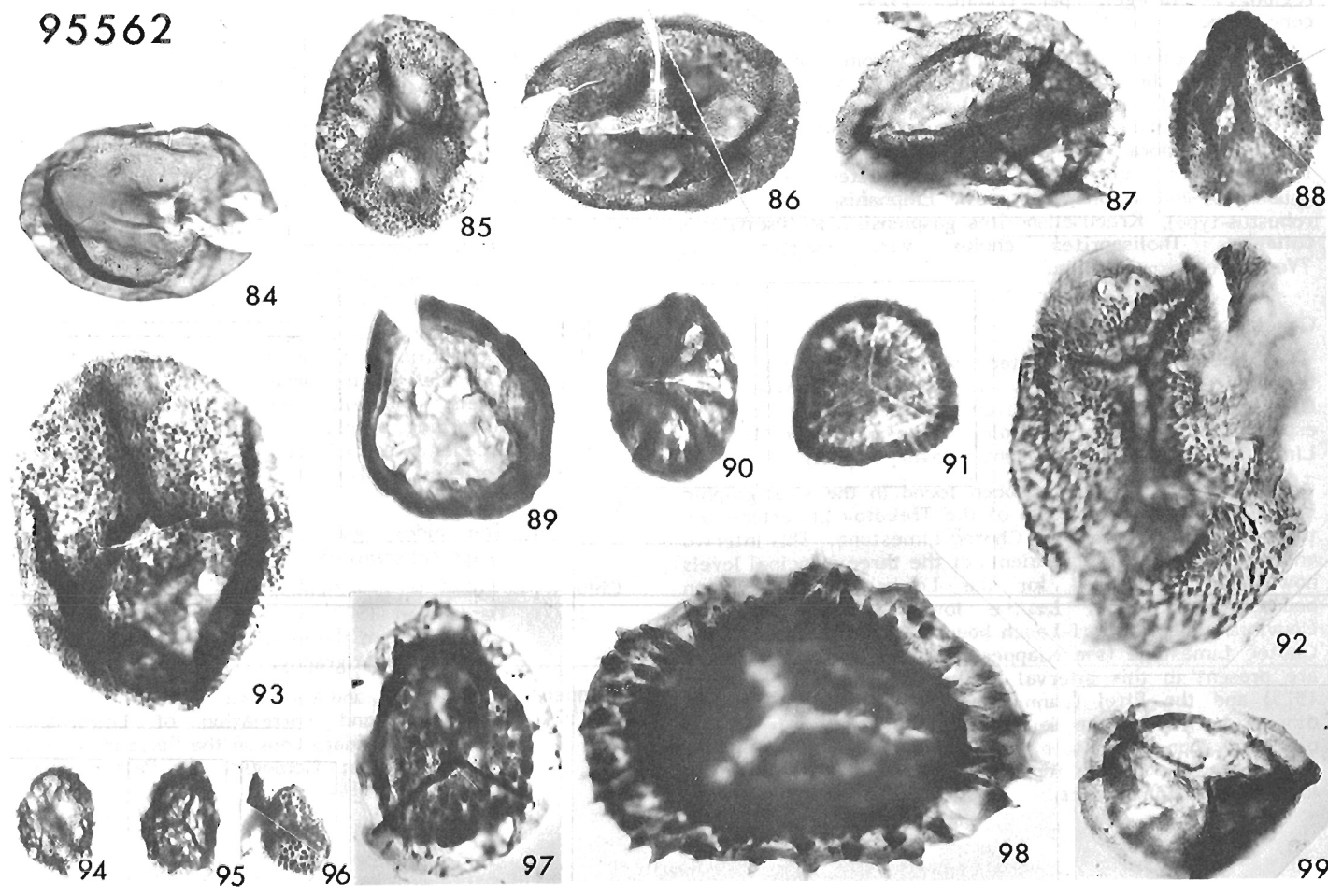
75. *Dictyotrilletes subgranifer?* McGregor. GSC 61720.
- 76, 77. *?Hymenozonotrilletes asper* Chibrikova. 76, GSC 61721; 77, GSC 61722.
78. *?Dibolisporites echinaceus* (Eisenack) Richardson, *echinaceus* type. GSC 61723.
79. *Kraeuselisporites* sp. GSC 61724.
80. *Apiculiretusispora brandtii?* StreeI. GSC 61725.
81. *Grandispora* sp. GSC 61726.
82. *Grandispora ?macrotuberculata* (Archangelskaya) McGregor, of McGregor (1973). GSC 61727.
83. *Grandispora biornata* (Lanninger) McGregor. GSC 61728.

Figures 84-99, GSC locality 95562, Trebotov Limestone, Dalejan.

84. *Retusotrilletes rotundus* StreeI. GSC 61729.
85. *Apiculiretusispora brandtii* StreeI. GSC 61730.
86. *Apiculiretusispora arenorugosa* McGregor. GSC 61731.
87. *Rhabdosporites* sp. GSC 61732.
88. *Dibolisporites* sp. GSC 61733.
89. *Tholisporites chulus* (Cramer) McGregor var. *magnus*. GSC 61734.
90. *Emphanisporites rotatus* McGregor, *robustus* type. GSC 61735.
91. *Emphanisporites rotatus* McGregor. GSC 61736.
92. *Dibolisporites echinaceus* (Eisenack) Richardson, *echinaceus* type, GSC 61737.
93. *Dibolisporites echinaceus* (Eisenack) Richardson, *gibberosus* type. GSC 61738.
94. *Dictyotrilletes gorgoneus?* Cramer. GSC 61739.
95. *Brochotrilletes* sp. GSC 61740.
96. *Apiculatasporites perpusillus* (Naumova) McGregor. GSC 61741.
97. *Kraeuselisporites gaspiensis?* McGregor. GSC 61742.
98. *Grandispora douglstownense* McGregor. GSC 61743.
99. *?Rhabdosporites* sp. GSC 61744.



95562



spores. Therefore, based on this preliminary study, and assuming that the first appearance of *Grandispora* is a synchronous event, this sample and the upper beds of the Daleje Shale correlate with the basal Wiltz of the Eifel region.

5. GSC locality 95562: North side of the Prokopské Valley at Hlubočepy near Prague, on northwest side of railway, northwest of abandoned quarry "Nad trati". The sample was collected about 18 m above the base (24 m below the top) of the Třebotov Limestone, 40 cm above the base of unit 4 of Chlupáč et al. (1977, Fig. 3), about 12 m below the lowest known conodonts (see Klapper et al., 1978, fig. 1), in the *N. richteri* zone.

This sample contains rare specimens of *Grandispora biornata*, and the first *G. douglastownense* McGregor. *G. douglastownense* appears above *G. biornata* but slightly below the first anchor-spined spores in marine and nonmarine strata of eastern Canada.

The appearance of anchor-spined spores (e.g. *Ancyrospora* and *Hystricosporites*) in the Barrandian region would be a significant zonal event. Lele (1972) reported *Ancyrospora* in the Daleje Shale but did not supply geographic, stratigraphic, or paleontologic details in support of the record. I have not found any anchor-spined spores in samples of the Daleje Shale or the Třebotov Limestone, in spite of an intensive search. I can only conclude that the samples from locality 95562 and 8 m above it in the same section, which is the highest spore-bearing locality presently known in the Třebotov Limestone, are older than the first occurrence of anchor-spined spores, i.e. below the level of the upper Wetteldorf Schichten of the Eifelian Hills. The presence of *Grandispora biornata*, which "... is essentially restricted to the Wiltz and Wetteldorf beds in the Eifel region..." (Riegel, pers. comm., 1979), supports this conclusion.

The other species identified from locality 95562 characterize the middle to late Emsian transition from assemblages of "Lower Devonian" to "Middle Devonian" type in the Eifel and in Canada: *Apiculatasporites perpusillus*, *Apiculiretusispora arenorugosa* McGregor, *A. brandtii*, *Dictyotriletes gorgoneus?*, *Dibolisporites echinaceus* (gibberosus- and echinaceus-types), *Emphanisporites rotatus* (robustus-type), *Kraeuselisporites gaspiensis?*, *Retusotriletes rotundus*, *Tholisporites chulus* var. *magnus*, and *Verruciretusispora dubia*.

Conclusions

Spores are associated with zonally significant tentaculites and conodonts in Pragian, Zlichovian, and Dalejan strata of the Barrandian Devonian. They are especially abundant in the Daleje Shale and lower Třebotov Limestone, from which conodont recovery is poor.

Spores have not yet been found in the stratigraphic interval between the middle of the Třebotov Limestone and the middle of the overlying Choteč Limestone. This interval encompasses the age equivalents of the three principal levels now being considered for the Lower-Middle Devonian boundary stratotype, i.e. the lower boundary of the Couvinian, the Heisdorf-Lauch boundary, and the base of the Choteč Limestone (see Klapper et al., 1978, p. 107). Spores are present in this interval in the Ardennes (Streef et al., 1975) and the Eifel (Lanninger, 1968; Riegel, 1973; and others). In view of the demonstrated presence of spores in older and younger strata of the Barrandian region, a diligent search should be made for them in the upper Třebotov and lower Choteč Limestones.

An added advantage to be gained by thorough search for spores in the Barrandian Devonian is the recovery of marine palynomorphs. Methods employed for extraction of spores from marine rocks commonly result in recovery of a variety of other acid resistant microfossils (palynomorphs) such as acritarchs, chitinozoans, graptolite and arthropod fragments, and scolecodonts, that also have biostratigraphic value. In the Barrandian region, marine palynomorphs occur with and without spores at most of the localities so far investigated.

The correlations suggested by the preliminary spore evidence from the Barrandian sections corroborate those with the Eifelian Hills proposed by Klapper et al. (1978). In addition the following correlations with the Eifel region are indicated: 1. The lower Daleje Shale at locality 95580 and most of the Daleje Shale at its type locality ("Ke hřbitovu") are older than the Wiltz Schichten; 2. The upper Daleje Shale at Císařská rokla (locality 95586) is correlated with the lower Wiltz; 3. The middle part of the Třebotov Limestone at Prague-Hlubočepy, 8 m above locality 95562, is older than the upper Wetteldorf Schichten.

The Lower Devonian spore assemblages from the Barrandian region resemble those already known from the Eifel, the Ardennes, southern England, Spitsbergen, and eastern, central, and northern Canada. This fully supports the existence of a strikingly uniform flora in and around the Old Red Sandstone continent (cf. Banks, 1975). It seems reasonable to expect that when study of the spores of the Barrandian area is completed, detailed direct correlations will be attainable with these regions. Eventually the correlations may extend to the southern Urals and central Asia, as there are evidently some species in common in these regions as well.

Acknowledgments

M.J. Copeland, A.W. Norris, and T.T. Uyeno of the Geological Survey of Canada, W. Riegel of the University of Göttingen, and I. Chlupáč of the Geological Survey of Czechoslovakia critically read the manuscript.

References

- Banks, H.P.
1975: Palaeogeographic implications of some Silurian-Early Devonian floras; in *Gondwana Geology*, ed. K.S.W. Campbell; Australian National University Press, Canberra, p. 75-97.
- Chibrikova, E.V. and Nadler, Yu.S.
1971: Correlation and age of the lower horizons of the Devonian of the western slope of the southern Urals, Priuralia and Kuznetsk Coal Basin according to plant microfossils; *Bulletin of the Academy of Sciences of the USSR, Geological Series*, v. 1971, no. 1, p. 101-109. (In Russian.)
- Chlupáč, I.
1976: The oldest goniatite faunas and their stratigraphical significance; *Lethaia*, v. 9, p. 303-315.
- Chlupáč, I., Lukeš, P., and Zikmundová, J.
1977: Barrandian 1977, a field trip guidebook; *Field Conference of the International Subcommittee on Devonian Stratigraphy*, Prague, 23 p.
- Klapper, G., Ziegler, W., and Mashkova, T.V.
1978: Conodonts and correlation of Lower-Middle Devonian boundary beds in the Barrandian area of Czechoslovakia; *Geologica et Palaeontologica*, v. 12, p. 103-116.

- Lanninger, E.-P.
 1968: Sporen-Gesellschaften aus dem Ems der SW-Eifel; Palaeontographica, B, v. 122, p. 95-170.
- Lele, K.M.
 1972: Observations on Middle Devonian microfossils from the Barrandian Basin, Czechoslovakia; Review of Palaeobotany and Palynology, v. 14, p. 129-134.
- McGregor, D.C.
 1973: Lower and Middle Devonian spores of eastern Gaspé, Canada, I, systematics; Palaeontographica, B, v. 142, p. 1-77.
 Spores in Devonian stratigraphic correlation; Palaeontological Association, Special Paper 22 (in press, a).
 Devonian miospores of North America; Palynology, v. 3 (in press, b).
- Obrhel, J.
 1959: Neue Pflanzenfunde in den Srbsko-Schichten (Mitteldevon); Věstník Ústředního Ústavu Geologického, v. 34, p. 384-388.
 1968: Die Silur- und Devonflora des Barrandiums; Paläontologische Abhandlungen, Paläobotanik, v. 2, p. 661-706.
- Riegel, W.
 1973: Sporenformen aus den Heisdorf-, Lauch- und Nohn-Schichten (Emsium und Eifelium) der Eifel, Rheinland; Palaeontographica, B, v. 142, p. 78-104.
- Streef, M., Demaret-Fairon, M., and Otazo, N.
 1975: Siegenian and Emsian spores from the Dinant Basin (Belgium); Commission Internationale de Microflore du Paléozoïque, Newsletter 10, p. 7.

Projects 760044 and 780016

W.B. Coker¹ and R.N.W. DiLabio²

Coker, W.B. and DiLabio, R.N.W., *Initial geochemical results and exploration significance of two uraniferous peat bogs, Kasmere Lake, Manitoba; in Current Research, Part B, Geological Survey of Canada, Paper 79-1B, p. 199-206, 1979.*

Abstract

Detailed examination of surficial sediments was initiated in a restricted area of northwestern Manitoba, identified by anomalous airborne eU and eU/eTh patterns and elevated uranium levels in lakes. The sampling program was designed to determine the provenance, pathways, and depositional sites of uranium and other metals in surficial sediments in an area of discontinuous permafrost. Specifically, emphasis was placed on evaluation of peat as a sampling medium for detailed exploration in areas of little outcrop. Two peat bogs sampled contained elevated contents of uranium and low contents of Zn, Cu, Pb, Ni, Co, Mo, As, Fe, and Mn. The highest uranium contents found were in the most humified basal peat sections.

Introduction

Surficial organic and inorganic materials were sampled within a 2 km² area of the Kasmere Lake map area (64N), Manitoba. The two peat bogs which were sampled (Fig. 23.1; U.T.M. reference: 375000E, 6593000N, zone 14) were selected because they lie within a drainage system where modern lake sediments and lake waters are enriched in uranium and where airborne eU and eU/eTh radiometric anomalies are marked (Coker, 1976). Two deep peat cores were recovered from Bog 1 (Line 72+00N, 5+70E and 7+50E) which was expected to have background concentrations of uranium. One deep peat core recovered from Bog 2 (CD Grid 0+00, 6+00W), located about 2500 m west of Bog 1, was expected to contain significant concentrations of uranium.

Peat in both bogs was found to be highly enriched in uranium. Although uraniferous peat bogs have been described in California (Bowes et al., 1957) and Sweden (Armands, 1967), the bogs described here are perennially frozen at depth.

General Geology

Bedrock Geology

Geological mapping was first carried out in the Kasmere Lake area of Manitoba by the Geological Survey of Canada (Fraser, 1962). Further geological mapping (Fig. 23.1) was done by the Government of Manitoba (Weber et al., 1975).

Bedrock exposures average one to two per cent and seldom exceed five per cent of the surface area of parts of this region. The bedrock is Precambrian and forms part of the Churchill structural province. Weber et al. (1975) divided the bedrock into three main groups: Archean igneous rocks, Aphebian metamorphic rocks mainly of sedimentary origin, and igneous and metamorphic rocks emplaced during the Hudsonian orogeny.

The Archean rocks consist of foliated granitoid bodies, ranging in composition from quartz diorite to alaskite (Weber et al., 1975). The Aphebian rocks in the northern part of the area are considered to be correlative with the Hurwitz Group sediments in the southern part of the District of Keewatin. The remainder of the Aphebian rocks lie in the extension of the Wollaston fold belt, as defined by Money (1968), in Saskatchewan. The igneous and metamorphic rocks produced during the Hudsonian orogeny include migmatite, plugs and stocks of anatexite, and syn- and late-orogenic batholiths. Most are massive and many truncate Hudsonian trends.

Recent exploration activity, initiated as a result of the release of Federal-Provincial Uranium Reconnaissance geochemical maps (Hornbrook et al., 1976) and radiometric data (Geological Survey of Canada, 1976), has resulted in the discovery of several new mineral occurrences, primarily uranium but also base metal and molybdenum, in addition to those previously known and described by Weber et al. (1975).

Geochemical follow-up studies (Coker, 1976), closely spaced airborne radiometric surveys (Geological Survey of Canada, 1977), and detailed geological mapping by the mineral exploration industry have contributed a considerable amount of new geological data, particularly within the Wollaston Metasedimentary Belt. More recently, detailed gradiometer surveys (Geological Survey of Canada, 1978) have aided interpretation of the geology in this region of abundant overburden and scarce outcrop.

The specific nature of the bedrock geology in the area of the peat bogs is unknown, due to absence of outcrop. However, airborne geophysical data and some nearby drilling (W. Nielsen, United Siscoe Mines, pers. comm.) indicate that the peat bogs are probably situated within the Wollaston Metasedimentary Belt.

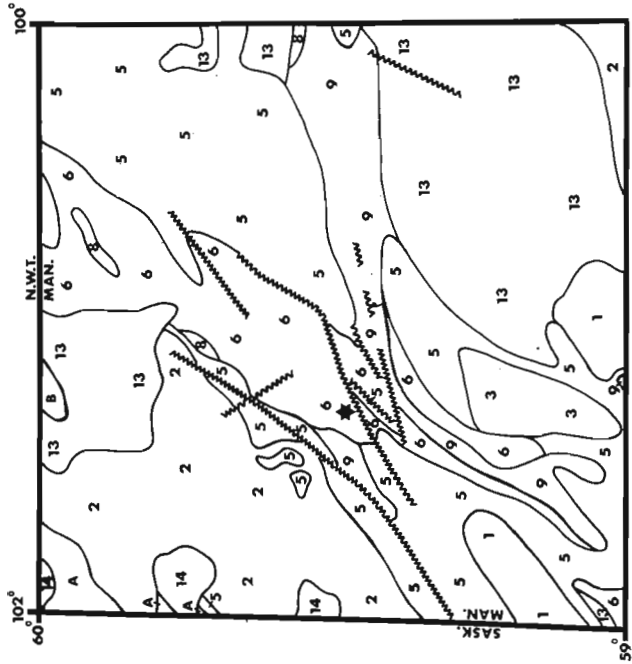
Surficial Geology

Glaciation of the area has produced a landscape composed of drumlinoid ridges, ribbed moraine, eskers, and lakes; bedrock outcrops are rare. A southwestward direction of glacial transport is indicated by the orientation of drumlinoid ridges and by the position of erratics.

The two peat bogs sampled lie in separate poorly drained valleys between drumlinoid ridges. The ridges are cored with sandy till and veneered with angular boulders that may represent a lag deposit or ablation till. Till thicknesses of up to 20 m have been measured by overburden drilling in this region (H. Veerman, United Siscoe Mines, pers. comm.). Up to 1 m of poorly sorted sand mantles the lower slopes and overlies till in the valley bottoms. This sand is believed to be fluvial sand or colluvium winnowed from till in the drumlinoid ridges by stream and slope erosion. Low-centred bogs, dominated by sedge growing around ponds and sluggish streams, are surrounded by raised bogs of *Sphagnum* spp. supporting stunted *Picea mariana* (black spruce) and *Ledum groenlandicum* (Labrador tea) growth. The peat is up to 2.5 m thick and overlies fluvial and colluvial sand and till. Organic-rich silt is present as alluvium in stream beds.

¹Resource Geophysics and Geochemistry Division

²Terrain Sciences Division



GENERAL GEOLOGY

LEGEND

Rocks of uncertain affinity

- B Migmatite
- A Hurwitz Group, Great Island Group metasedimentary rocks

Hudsonian Intrusive Rocks

- 14 Fluorite-bearing quartz monzonite
- 13 Quartz monzonites

Archean Metasedimentary Rocks

- 9 Meta-arkose, arkosic gneiss
- 8 Calc-silicate rock, marble, albite - pyroxene rock
- 6 Psammitic gneiss, meta-greywacke
- 5 Pelitic, semi-pelitic gneiss, impure quartzite and calc-silicate lenses

Archean

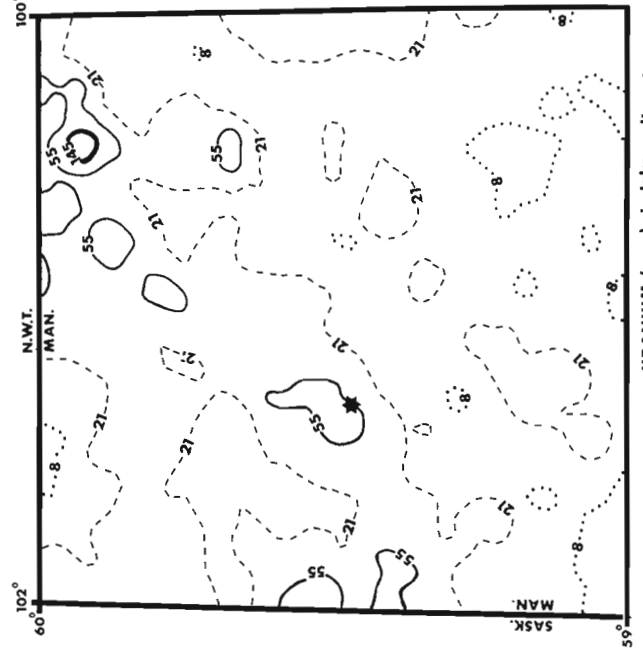
- 3 Foliated pink quartz monzonite
- 2 Foliated grey quartz monzonite and grey quartz monzonite gneisses
- 1 Hypersthene-bearing quartz monzonite, quartz diorite, hypersthene gneisses

www Fault proposed

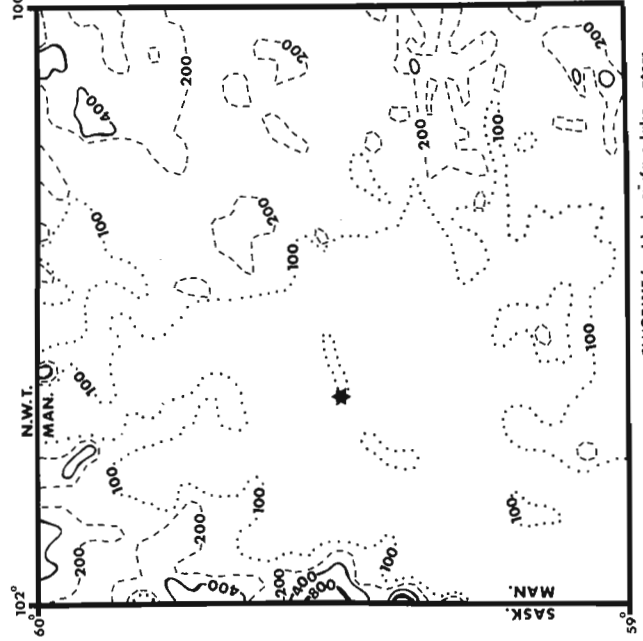
— Geologic contact proposed

(after Weber et al., 1975)

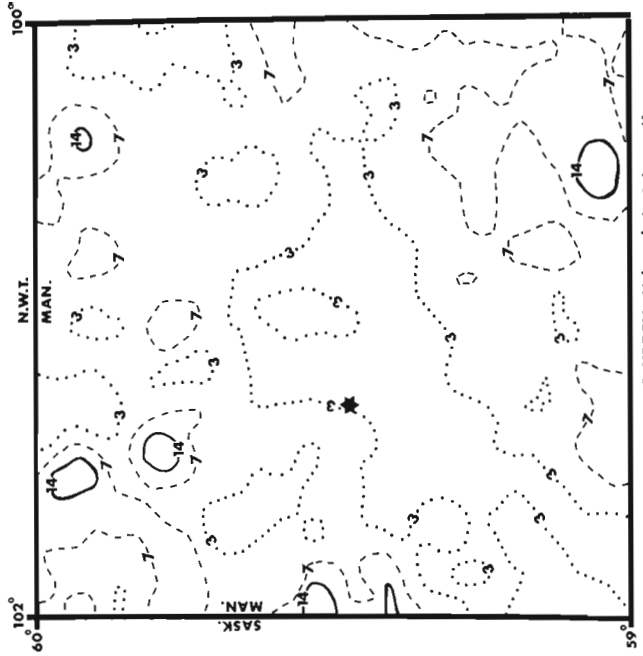
Figure 23.1. General geology (after Weber et al., 1975) and the distributions of U and Mo in lake sediments, and F in surface lake waters, northwestern Manitoba. (Approximate location of the peat bogs under study is indicated by the star.)



URANIUM (ppm) in lake sediments



FLUORINE (ppb) in surface lake waters



MOLYBDENUM (ppm) in lake sediments

Permafrost

The area is within the zone of discontinuous permafrost (Brown, 1967). Frozen ground was encountered at depths of 0.2-0.4 m in test pits and drill holes where *Sphagnum* spp. formed a continuous cover. Frozen ground was not encountered at depths of 2 m in wet sedge peat or at depths of 1 m in till and colluvium where insulating *Sphagnum* spp. cover was thin.

Regional Geochemical and Radiometric Trends

The regional distributions of U and Mo in lake sediments and of F in lake waters (contoured at the geometric mean (\bar{x}) and the geometric mean plus one ($\bar{x} + 1\sigma$), two ($\bar{x} + 2\sigma$), and three ($\bar{x} + 3\sigma$) geometric standard deviations) within the Kasmere Lake area are illustrated in Figure 23.1. A definite relationship exists between elevated contents of U, Mo, and F in lakes and the Hudsonian granitoid bodies. A pattern of elevated contents of U is also observed in sediments from lakes situated along the trend of the Wollaston Metasedimentary Belt, wherein the peat bogs under study most probably lie (Fig. 23.1).

The regional airborne radiometric survey of the Kasmere Lake area revealed a trend similar to the regional geochemistry with elevated eU and eU/eTh values outlining the Wollaston Metasedimentary Belt (Geological Survey of Canada, 1976).

Detailed geochemical studies (Coker, 1976) have shown coincident elevated U contents in both surface lake water and modern lake sediments, and some instances of elevated As levels in modern lake sediments, in the region of the peat bogs under study. The detailed airborne radiometric survey gave a eU/eTh ratio of 1.10 near the same peat bogs (Geological Survey of Canada, 1977).

Sampling Techniques and Analytical Procedures

Sample Collection

In the grid sampling program carried out in the two peat bogs, three continuous deep (>2 m) cores were collected. At each site a pit was first dug to the permafrost table (0.2 to 0.4 m). Below the permafrost table materials were recovered using a frozen ground coring kit consisting of a Stihl 4308, hand-held gas-powered auger adapted to a modified CRREL (3 inch inside diameter) barrel sampler (Veillette, 1975; Veillette and Nixon, 1976).

The surface *Sphagnum* spp. and cored frozen materials comprising *Sphagnum* spp., humic materials, and inorganic clastic sediments (alluvium, colluvium, fluvial sand, till) were collected from the three deep cores and classified and separated on the basis of textural, compositional and colour differences. A sample of *Ledum groenlandicum* (Labrador tea) was collected from growing plants at each site. All samples were sealed in plastic bags and shipped to Ottawa for later preparation and analyses.

Sample Preparation

On receipt of the samples in Ottawa, the interstitial waters of the thawed materials from the three deep cores were squeezed out and filtered (0.45 μm). Both filter papers and filtered waters, stored in polyethylene bottles, were retained for analyses.

All samples were transferred to kraft paper bags and air dried. Organic-rich materials were ground with a mortar and pestle to approximately 80-mesh (180 μm) size. The inorganic clastic sediments were sieved through an 80-mesh sieve to obtain the minus 80-mesh fraction.

Clay-sized (<2 μm) material was extracted from samples, where possible, by centrifugation and decantation. Heavy mineral concentrates were prepared on selected samples.

The relative organic content of the samples after being dried overnight at 105°C, was estimated by loss-on-ignition (L.O.I.) during a three hour time-temperature controlled rise to 450°C. The ashed residue was retained for selected analyses.

Analyses

Analyses of samples for Cu, Pb, Zn, Co, Ni, Mo, Mn, Fe, and As were carried out by Bondar-Clegg and Co. Ltd., Ottawa and for U by Atomic Energy of Canada Ltd., Ottawa.

The contents of Cu, Pb, Zn, Co, Ni, Mo, Mn, and Fe in the minus 80-mesh fraction of organic material or inorganic clastic sediment were determined by atomic absorption spectroscopy. Arsenic in the minus 80-mesh sample materials was determined colorimetrically using silver diethyl-dithiocarbamate. Colorimetric measurements were made at 520 nm.

The neutron activation delayed neutron counting method of analysis, whereby the minus 80-mesh and ashed materials were analyzed for total uranium, was developed by Atomic Energy of Canada Ltd., Commercial Products Division, and is described in detail by Boulanger et al. (1975).

The interstitial waters were analyzed for major, minor and trace cation components by inductively coupled plasma emission and for the common anions, F^- , Cl^- , PO_4^{3-} , NO_3^- and SO_4^{2-} , by liquid ion chromatography (e.g. Smeed et al., 1978). These analyses were performed by Barringer Magenta Ltd., Toronto.

All other analytical work was carried out in the laboratories of the Geochemistry Subdivision, Resource Geophysics and Geochemistry Division, Geological Survey of Canada.

The fluorometric method of analysis for acid extractable uranium, by which the minus 80-mesh materials, clay-sized (<2 μm) materials, and interstitial waters were analyzed, was based on that described by Smith and Lynch (1969).

The pH, conductivity, F^- content (by selective-ion electrode), alkalinity (Thomas and Lynch, 1960), and organic carbon content (estimated using the Pye Unicam Spectrophotometer-1800 at 254 nm) of the interstitial waters were also measured.

Radium was determined on the ashed residue of samples from the three deep peat cores. Digested material was stored in bottles where radon accumulated and equilibrated with radium in the sample (ca., 2 weeks). The amount of radon present was determined as described by Dyck (1969). With sample weight, volume of solution, and time all known the amount of radium (and also equivalent uranium) present in the sample can be determined.

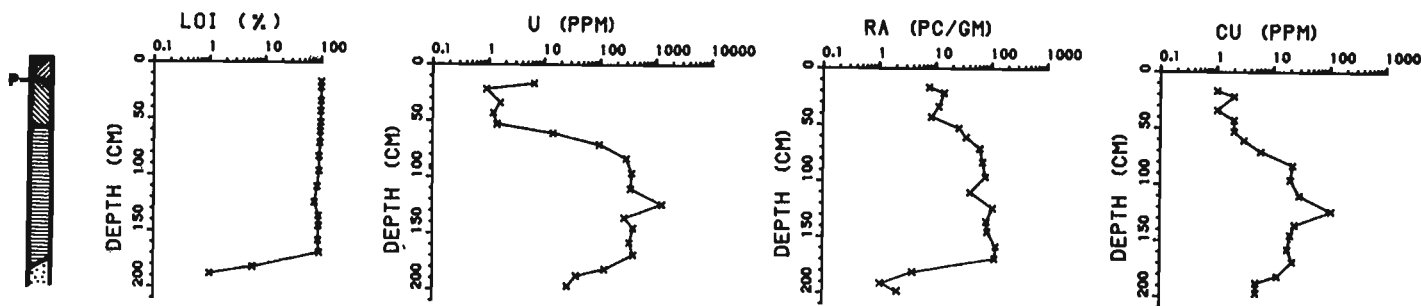
Physical and Chemical Characteristics of the Peat Bogs

Bog 1

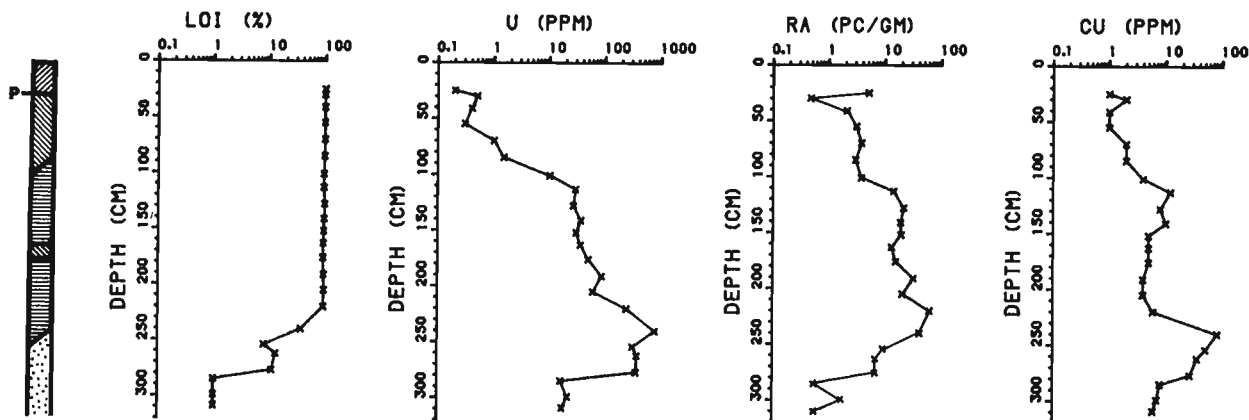
In this bog, expected to have background concentrations of uranium, two deep peat cores were recovered (Line 72+00N, 5+70E and 7+50E).

The material recovered at 5+70E (Fig. 23.2) consists of 22 cm of *Sphagnum* moss (permafrost table at 22 cm), above 50 cm of relatively fresh light brown fibrous peat, overlying 115 cm of compressed, dark brown, humified (visual scale, Korpijaakko and Woolnough, 1977) peat which in turn overlies

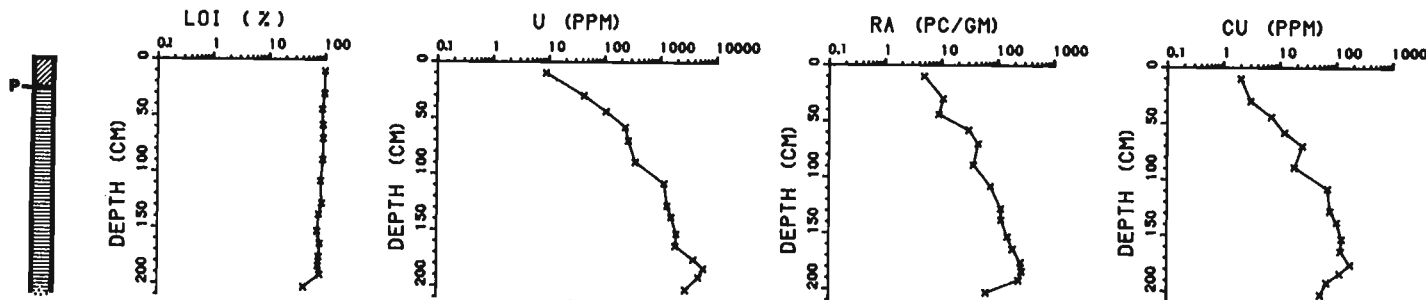
LINE 72+00N - 5+70E PEAT BOG PROFILE



LINE 72+00N - 7+50E PEAT BOG PROFILE



CD GRID 0+00 - 6+00W PEAT BOG PROFILE



LEGEND





-  SPHAGNUM MOSS
-  LIGHT BROWN FIBROUS PEAT
-  DARK BROWN HUMIFIED PEAT
-  SAND
- P** PERMAFROST TABLE

Figure 23.2. The vertical distribution of organic matter (as estimated by loss-on-ignition (450 C)), U (by neutron activation), Cu, Zn, Ni, Mo, Mn, and Fe (by atomic absorption techniques), of minus 80-mesh materials, and the Ra content of ash in the three peat cores, Kasmere Lake area, Manitoba.

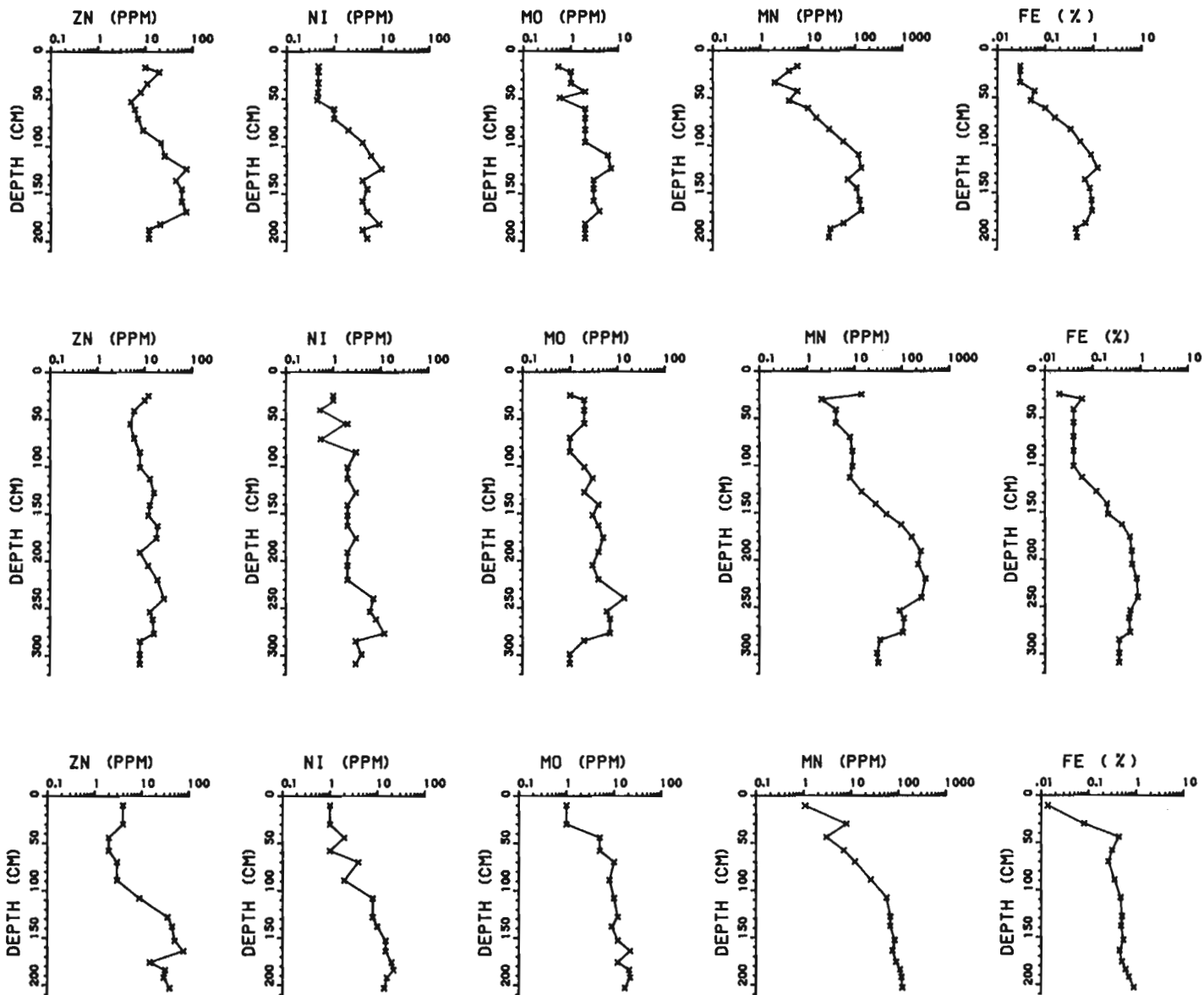


Figure 23.2 (cont'd.)

at least 25 cm of sand (colluvium?). Uranium (Line 72+00N, 5+70E - Fig. 23.2) is concentrated to a level of 6.5 ppm in the surface *Sphagnum* moss, falls in content to values ranging from 0.9 to 1.6 ppm in the light brown fibrous peat before rising markedly to values ranging from 278 to 1290 ppm in the dark brown humified peat in the lower part of the core. The maximum accumulation of uranium (1290 ppm), three times greater than any other value in this core, occurs in the most humified section (L.O.I. lowest, i.e. 76%) of the dark brown humified peat. Sandy material underlying the peat contains 26.4 to 38.5 ppm uranium in the minus 80-mesh material. In order of decreasing strength of correlation, the following elements vary sympathetically with uranium: Cu(.98), Mo(.84), Fe(.80), Mn(.77), Zn(.76), Ni(.72), As(.72) and Ra(.70). The actual distributions and levels of concentration of these elements are illustrated in Figure 23.2. Cobalt and lead were detectable (up to 2 and 3 ppm, respectively) in only a few samples, primarily the basal sands, whereas the maximum concentration of arsenic (3 ppm), from the few samples with detectable arsenic, coincides with the maximum

concentration of uranium (1290 ppm) in the humified peat. The loss-on-ignition of the peat generally decreases with depth, the inverse of the levels of concentration of uranium and the other elements.

The cored material from 7+50E (55 m (180 ft) east of 5+70E) is composed of 30 cm of *Sphagnum* moss (permafrost table at 30 cm), above 65 cm of relatively fresh light brown fibrous peat, overlying 150 cm of compressed, dark brown, humified peat (with a lens of light brown fibrous peat at 163 to 176 cm depth) which overlies at least 75 cm of sand (colluvium?). The uranium concentration of the organic materials (Line 72+00N, 7+50E - Fig. 23.2) increases in a logarithmic manner with depth: surface *Sphagnum* moss contains 0.2 ppm uranium, light brown fibrous peat from 0.3 to 1.0 ppm uranium, and dark brown humified peat from 10.1 to 786 ppm uranium. The upper 40 cm of the basal sand (L.O.I.'s - 8 to 13%) contains 316 to 377 ppm uranium whereas the lower 35 cm of sand (L.O.I.'s of 1%) contains 16.3 to 21.7 ppm uranium in the minus 80-mesh fraction. In order of decreasing strength of correlation, the following

elements vary sympathetically with uranium: Mo(.94), Cu(.94), As(.92), Pb(.84), Ni(.73), Zn(.71), Fe(.71), Co(.70), Mn(.60) and Ra(.37). The actual distribution and levels of concentrations of these elements are illustrated in Figure 23.2. Cobalt and lead were detectable (up to 2 and 4 ppm, respectively) in only a few samples, primarily the basal peat and sand, with the maximum lead value (4 ppm) correlating with the maximum uranium value (786 ppm) at the base of the humified peat. Arsenic was present in detectable levels in only the basal portion of the dark brown humified peat and the upper 40 cm of the basal sand. The maximum level of arsenic (3 ppm) correlates with the maximum level of uranium (786 ppm) at the base of the humified peat. As at the first site, loss-on-ignition decreases with depth, varying inversely with uranium and associated elements in the peat and directly in the basal sands (Fig. 23.2).

Radiocarbon ages of 5990 ± 80 years (GSC-2759) and 4450 ± 60 years (GSC-2803) were determined on dark brown humified peat (240 to 254 cm and 128 to 141 cm respectively) and an age of 1040 ± 50 years (GSC-2798) was determined on light brown fibrous peat immediately below the permafrost table (30 to 40 cm) in this core.

Bog 2

Only one deep peat core (CD Grid 0+00, 6+00W) was recovered from Bog 2, which is located approximately 2500 m west of Bog 1. This bog was expected to contain significant concentrations of uranium, based on analyses of surface and spring waters and of surficial materials collected by United Siscoe Mines Ltd. (pers. comm., H. Veerman and W. Nielsen, United Siscoe Mines). Nine surface waters collected as part of this study had uranium concentrations ranging from 0.38 to 13.8 ppb and a water sample from a flowing spring on the edge of the bog contained 50 ppb uranium.

The cored material recovered at 6+00W (Fig. 23.2) consists of 30 cm of *Sphagnum* moss (permafrost table at 30 cm) overlying 180 cm of compressed, dark brown, humified peat. The bottom 10 cm of core contains about 2 cm of the underlying sand (colluvium and/or alluvium?). The uranium content of the cored materials increases logarithmically with depth from a concentration of 8.8 ppm in the surface *Sphagnum* moss to 42.3 ppm in the upper dark brown humified peat to a maximum of 5840 ppm in the lower, most humified, dark brown peat. The lower metre of dark brown humified peat averages 2800 ppm uranium (9 samples from 1170 to 5840 ppm uranium). In order of decreasing strength of correlation, the following elements vary with uranium: Ni(.92), Ra(.91), As(.90), Mn(.88), Mo(.81), Co(.80), Fe(.70), Cu(.69) and Zn(.43). The actual distributions and levels of concentration of these elements are illustrated in Figure 23.2. Cobalt and arsenic were detectable (both up to 4 ppm) in only the basal samples of the dark brown humified peat with the maximum contents (4 ppm) being coincident with the maximum level of accumulation of uranium (5840 ppm). Loss-on-ignition of the peats generally decreases with depth and thus varies inversely with the uranium content of the peats.

Discussion

It is well known that peat can concentrate metals to significant levels, due to its high cation exchange capacity (i.e. 150 to 220 me/100g; Walmsley, 1977). Many examples of metalliferous peat bogs have been described (Salmi, 1967; Armands, 1967; Boyle, 1977; and Toverud, 1977). However, few such studies have dealt with peat in a permafrost environment.

The two peat bogs sampled in this study are significantly enriched in uranium, maximum concentrations occurring in the most humified (based on a visual scale, Korpijaakko and Woolnough, 1977) basal parts of the peat. Positive correlations exist between ash content (100 - L.O.I. = per cent ash), relative degree of humification, and uranium content. Humification includes the following processes: compaction, dewatering, and organic decomposition. These processes result in a decrease in organic matter content and a buildup of the amount of mineral grains and inorganic compounds (as indicated by increased ash contents), as well as increased concentrations of organically fixed trace and minor elements, per unit volume. The onset of permafrost will stop humification.

The peat bogs of northwestern Manitoba contain low contents of the other trace and minor elements examined, compared to the high uranium levels (Fig. 23.2). Similar low metal contents are not entirely unknown for peat (Smith and Gallagher, 1975). Whatever the ultimate source of the uranium, the source either contains low contents of the trace and minor elements determined or these elements have undergone some form of geochemical separation from uranium during transport between the source and the peat bogs. The other metals examined are all highly correlated with uranium indicating that the controls on their distribution and adsorption are similar, and probably related to diagenetic organic phenomena.

Although autoradiography and scanning electron microscopy have yet to be carried out on samples, comparative uranium data obtained from analyses of clay-sized (fluorometry) and minus 80-mesh (fluorometry and neutron activation) materials are available. The clay-sized fractions generally contain higher levels of uranium, consistent with an interpretation that the uranium has been transported hydromorphically and is present as adsorbed ions on the peat and clastic sediments. Because the interstitial waters contain up to 400 ppb uranium and show uranium distribution patterns highly correlative with those in the minus 80-mesh materials, it seems probable that a state of uranium equilibrium was established between the interstitial waters and the peat, after thawing and before separation of the waters from the peat. The acid interstitial waters (pH 3.5-6.5, but as low as 2) contain a representative portion of the total uranium in the peat itself, illustrating the loosely bound nature of the uranium (i.e. readily exchangeable; Szalay, 1964).

Reconstructions by Nichols (1974) of the location of the northern limit of continuous forest and of changes in mean July temperatures in the southern District of Keewatin and northwestern Manitoba provide scales against which the geochemistry of the peat cores can be compared. Nichols estimated that from 5500 to 3500 years B.P. the northern limit of forest was about 200 km north of its present position and the mean July temperature was about 3°C warmer than at present. About 3500 years B.P., estimated conditions approached present day ones, with minor variations. Based on the radiocarbon dates determined on the core from Line 72+00N, 7+50E, the uranium-rich, most humified lower portions of the peat bogs examined date from a warmer episode characterized by more successful vegetation, and probably more intense weathering, than at present. During that warmer episode, it is possible that no near-surface permafrost existed in this area, which would allow peat diagenesis and uranium enrichment to proceed. The much lower levels of uranium found in the upper light brown fibrous peat date from a period when the temperature and vegetation conditions were similar to those at present.

Potential mechanisms for the enrichment of uranium in the peat bogs under study can be advanced. One possibility assumes a decreased delivery of uranium into the bogs with time. Relatively strong weathering and leaching of glacial drift, bedrock and/or uranium mineralization during the warm episode at the time of the onset of peat accumulation, may possibly have made relatively high concentrations of uranium available in surface waters and groundwaters. Humification could have resulted in an increased exchange capacity in the peat, as long as the peat was in the active layer of the permafrost profile. This may account for the uranium maxima in the basal (oldest), most humified dark brown peats. Lower levels of uranium in the light brown fibrous peat in the upper portions of the cores may have resulted from a depletion of available uranium at source, or from partial or total removal of the source from the zone of active weathering by burial and/or by permafrost aggradation.

A second possibility assumes a more or less constant delivery of uranium into the peat bogs through time. Surface streams and ponds in Bog 2 contain uranium concentrations ranging from 0.38 to 13.8 ppb and a spring at the bog contains approximately 50 ppb uranium. According to this model it is proposed that similar contents of uranium in surface waters and groundwaters delivered to the unfrozen peat bogs and organically adsorbed by the peats could be upgraded, solely by humification, to presently observed levels. A constraint on this model is that the basal portions of the peats would have had to remain unfrozen for a considerable length of time in order for humification to proceed to a high degree. Based on the lower two radiocarbon dates from the core in Bog 1 at Line 72+00N, 7+50E, at least 1500 years were available for humification to occur. It is not known if 1500 years is enough time to account for the observed degree of humification or enrichment of uranium. According to this model it is possible to envisage a drift and/or bedrock source consisting of a large volume of material containing relatively low to medium concentrations of uranium.

Possible sources for the uranium contained within the peat bogs under study consist of any one or combinations of:

- a. Glacial drift containing low level uranium concentrations (in general located upslope from the peat bogs as preliminary indications show that the drift below the peat bogs is not the source (Fig. 23.2)).
- b. Bedrock containing low to medium level concentrations of uranium.
- c. Bedrock containing high level (economic or sub-economic) concentrations of uranium.
- d. Drift containing glacially dispersed grains of uranium-bearing minerals and mineralized boulders.

None of the above potential sources of uranium have been thoroughly investigated to date. Further sampling and analyses of vegetation, peat, surficial clastic sediments, and underlying bedrock as well as surface waters, groundwaters and interstitial waters is planned. This will include additional sampling within the peat bogs currently under study as well as in other peat bogs related to known uranium mineralization, located within one of the Hudsonian granitoid plutons, and at a site selected to represent background levels of uranium within northwestern Manitoba.

Acknowledgments

The co-operation and logistical support of United Siscoe Mines, in particular from M.E. Holt, H. Veerman, and W. Nielsen, are gratefully acknowledged. Computer graphics were prepared by N.G. Lund. Able assistance in the field,

office and laboratory was provided by Tim Maunula. This paper was critically read by R.W. Boyle, E.H.W. Hornbrook, I.R. Jonasson, and W.W. Shilts.

References

- Armands, G.
1967: Geochemical prospecting of a uraniferous bog deposit at Masugusbyn, northern Sweden; in *Geochemical Prospecting in Fennoscandia*, A. Kvalheim, ed., Interscience, New York, p. 127-154.
- Boulanger, A., Evans, D.J.R., and Raby, B.F.
1975: Uranium analysis by neutron activation delayed neutron counting; *Proceedings 7th Annual Symposium of the Canadian Mineral Analysts*, Thunder Bay, Ontario, Sept. 22-23, 1975.
- Bowes, W.A., Bales, W.E., and Haselton, G.M.
1957: Geology of the uraniferous bog deposit at Petit Ranch, Kern County, California; *United States Atomic Energy Commission, RME-2063, Pt. 1*, p. 1-29.
- Boyle, R.W.
1977: Cupriferous bogs in the Sackville area, New Brunswick, Canada; *Journal of Geochemical Exploration*, v. 8, p. 495-527.
- Brown, R.J.E.
1967: Permafrost in Canada; *Geological Survey of Canada, Map 1246A*.
- Coker, W.B.
1976: Geochemical follow-up studies, northwestern Manitoba; in *Report of Activities, Part C, Geological Survey of Canada, Paper 76-1C*, p. 263-267.
- Dyck, W.
1969: Field and laboratory methods used by the Geological Survey of Canada in geochemical surveys, No. 10 Radon determination apparatus for geochemical prospecting for uranium; *Geological Survey of Canada, Paper 68-21*, 30 p.
- Fraser, J.A.
1962: Kasmere Lake, Manitoba; *Geological Survey of Canada, Map 31-1962*.
- Geological Survey of Canada
1976: Airborne gamma-ray spectrometry data, Kasmere Lake, Manitoba, NTS 64N; *Geological Survey of Canada, Open File 318*.
- 1977: Airborne radioactivity maps and profiles, Manitoba, 64 N/6; *Geological Survey of Canada, Open File 450*.
- 1978: Canada-Manitoba, Uranium Reconnaissance Program, Aeromagnetic gradiometer survey, Kasmere Lake area (64N), Manitoba; *Geological Survey of Canada, Open File 528*.
- Hornbrook, E.H.W., Garrett, R.G., and Lynch, J.J.
1976: Regional lake sediment geochemical reconnaissance data, north-central Manitoba, NTS 64N; *Geological Survey of Canada, Open File 322*.
- Korpijaakko, E.O. and Woolnough, D.F.
1977: Peatland survey and inventory; in *Muskeg and the Northern Environment in Canada*, N.W. Radforth and C.O. Brawner, ed., University of Toronto Press, Toronto, p. 63-81.

- Money, P.L.
1968: The Wollaston Lake fold-belt system, Saskatchewan-Manitoba; *Canadian Journal of Earth Sciences*, v. 5, p. 1489-1504.
- Nichols, H.
1974: Arctic North American palaeoecology: the recent history of vegetation and climate deduced from pollen analysis; *in* *Arctic and Alpine Environments*, J.D. Ives and R.G. Barry, ed., Methuen, London, p. 637-667.
- Salmi, M.
1967: Peat in prospecting: applications in Finland; *in* *Geochemical Prospecting in Fennoscandia*, A. Kvalheim, ed., Interscience, New York, p. 113-126.
- Smee, B.W., Hall, G.E.M., and Koop, D.J.
1978: Analysis of fluoride, chloride, nitrate and sulphate in natural waters using ion chromatography; *Journal of Geochemical Exploration*, v. 10, no. 3, p. 245-258.
- Smith, A.Y. and Lynch, J.J.
1969: Field and laboratory methods used by the Geological Survey of Canada in geochemical surveys, No. 11 Uranium in soil, stream sediment and water; *Geological Survey of Canada*, Paper 69-40, 9 p.
- Smith, R.T. and Gallagher, M.J.
1975: Geochemical dispersion through till and peat from metalliferous mineralization in Sutherland, Scotland; *in* *Prospecting in Areas of Glaciated Terrain - 1975*, M.J. Jones, ed., Institute of Mining and Metallurgy, London, p. 134-148.
- Szalay, A.
1964: The cation-exchange properties of humic acids and their importance in the geochemical enrichment of UO_2^{2+} and other cations; *Geochimica et Cosmochimica Acta*, v. 28, p. 1605-1614.
- Thomas, J.F.J. and Lynch, J.J.
1960: Determination of carbonate alkalinity in natural waters; *Journal American Water Works Association*, v. 52, no. 2, p. 259-268.
- Toverud, Ö.
1977: Chemical and mineralogical aspects of some geochemical anomalies in glacial drift and peat in northern Sweden; *Sveriges Geologiska Undersökning*, C729, 37 p.
- Veillette, J.
1975: Modified CRREL ice coring augers; *in* *Report of Activities, Part A*, Geological Survey of Canada, Paper 75-1A, p. 425.
- Veillette, J. and Nixon, F.M.
1976: Permafrost coring equipment; *in* *Report of Activities, Part A*, Geological Survey of Canada, Paper 76-1A, p. 269.
- Walmsley, M.E.
1977: Physical and chemical properties of peats; *in* *Muskeg and the Northern Environment in Canada* (N.W. Radforth and C.O. Brawner, Editors); University of Toronto Press, Toronto, p. 82-129.
- Weber, W., Schedewitz, D.C.P., Lamb, C.F., and Thomas, K.A.
1975: Geology of the Kasmere Lake - Whiskey Jack Lake (North Half) Area; *Manitoba Mineral Resources Division*; Publication 74-2.

**INVESTIGATION AND REGIONAL SIGNIFICANCE OF AIRBORNE GAMMA RAY
SPECTROMETRY PATTERNS IN THE SHARBOT LAKE AREA, EASTERN ONTARIO**

Project 760045

K.L. Ford and B.W. Charbonneau
Resource Geophysics and Geochemistry Division

Ford, K.L. and Charbonneau, B.W., Investigation and regional significance of airborne gamma ray spectrometry patterns in the Sharbot Lake area, eastern Ontario; in Current Research, Part B, Geological Survey of Canada, Paper 79-1B, p. 207-222, 1979.

Abstract

Airborne gamma ray spectrometry surveys carried out in the Sharbot Lake area of eastern Ontario in 1977 indicate three well defined belts of radioactive pegmatites. Results of field investigations in 1978 confirm the significantly elevated levels of uranium concentration in the pegmatites. The high eU/eTh ratio level compared with other Grenvillian pegmatite districts is distinctive. The airborne gamma ray spectrometry contour maps help to present a comprehensive overview of the radioelement distribution patterns for an area which has received only sporadic interest in the past.

Introduction and General Discussion

Airborne gamma ray spectrometric surveys covering some 110 000 km² of south-central and southeastern Ontario and portions of western Quebec were flown between 1974 and 1977. These data have been released as Geological Survey of Canada Open Files 262, (41 J); 331, (31 F); 428, (31 C) and Geophysical Series Maps 35431G, (31 D); 35531G, (31 E); 36231, (31 L); 35841, (41 H); and 35941G, (41 I). The extent of coverage is shown by the solid line on a portion of the Geological Map of Canada (Douglas, 1969) (Fig. 24.1) along with additional surveys covering some 90 000 km² of east-central Ontario and western Quebec (dashed line) to be released in 1979. In addition to these surveys flown at 5 km line spacing, surveys with line spacings ranging from 1/4 mile to 1 km were flown covering the following areas, also indicated on Figure 24.1, EL (Elliot Lake, Geol. Surv. Can., Open File 75); B (Bancroft, Geol. Surv. Can., Open File 45); ML (Mont Laurier, Geol. Surv. Can., Open File 110); OA (Ottawa-Arnprior, Geol. Surv. Can., Open File 264) and SL (Sharbot Lake, Geol. Surv. Can., Open File 582).

The Geological Survey of Canada has been conducting systematic airborne gamma ray spectrometer surveys since 1969 using a survey system consisting of 50 litres of NaI(Tl) detectors mounted in a Short Skyvan aircraft (Richardson et al., 1975; Bristow, in press). These surveys have been useful in mapping the regional radioelement distribution patterns, showing geological relationships and in outlining uraniferous geochemical provinces. Charbonneau et al., 1976 investigated the relationships between airborne radioelement patterns and ground level concentrations. They stated that measurement of ground level radioelement contents from the air represents an average surface concentration for an area comprised of variable amounts of overburden, vegetation, water and outcrop. For this reason the average surface concentration is generally somewhat lower than the radioelement concentration in overburden. Since the amount of outcrop in any area is generally only a small percentage of the total area, the relationship between average surface concentration and outcrop concentration is more variable. Charbonneau et al., 1976 concluded that airborne radioelement contour maps give a relative indication of bedrock concentration. For example, average surface concentrations of 2-3 ppm eU correspond to overburden concentrations of 3 to 4 ppm and to bedrock concentrations of 7 to 8 ppm.

The purpose of this present investigation is to relate radioelement distribution patterns determined by airborne

gamma ray spectrometry in the Sharbot Lake area of eastern Ontario to the known geology and to illustrate the significance of these patterns with respect to the area from east-central Ontario to western Quebec.

Regional Radioelement Patterns

Figures 24.2, 24.3 and 24.4 show the regional distribution patterns for equivalent uranium, equivalent thorium and the eU/eTh ratio respectively for a varied terrane of Precambrian rocks of the Grenville, Superior and Southern provinces and bordering areas of Paleozoic rocks. Figure 24.2, the equivalent uranium map, presents a good example of the regional correlation between areas of known uranium mineralization with zones of regional enrichment (Darnley et al., 1977). On Figure 24.2, six areas have been indicated. These are: (1) Elliot Lake, (2) Sudbury-Georgian Bay, (3) Parry Sound, (4) Bancroft-Anstruther, (5) Renfrew-Huddersfield and (6) Sharbot Lake.

Prominent anomalies in the Elliot Lake region (1) correlate mainly with radioactive quartz monzonites north and northwest of the uranium deposits in the Quirke Lake syncline. In situ gamma ray spectrometry analyses of granitic bedrock in areas where airborne values exceeded 3 ppm eU and 15 ppm eTh gave concentrations greater than 10 ppm eU and 50 ppm eTh over extensive areas (Charbonneau et al., 1976).

Increases in radioelement concentrations along the Grenville Front (2) apparently relate to felsic igneous rocks as shown on Ontario Division of Mines Geological Compilation Series Map 2188. Pegmatitic uranium occurrences have been known in the Parry Sound district (3) for some time (Lang, 1952; Ruzicka, 1979). Figure 24.2 indicates a band of elevated equivalent uranium values trending northeast in the Parry Sound area.

Increases in equivalent uranium and eU/eTh ratio are particularly evident in the southeast portion of Figures 24.2 and 24.4 respectively. This area corresponds to the distribution of late Precambrian metavolcanic rocks, marble and other metasedimentary rocks and a variety of intrusive rocks and pegmatites of the Grenville Supergroup.

The Bancroft-Anstruther (4) and Renfrew-Huddersfield (5) areas are both near the base of the Grenville Supergroup. The Mont Laurier area farther to the northeast is similarly located (ML, Fig. 24.1). Several authors (Allen, 1971; Bright, 1975 and Lumbers, 1975) have considered the correlation of uranium occurrences to the basal zone of the

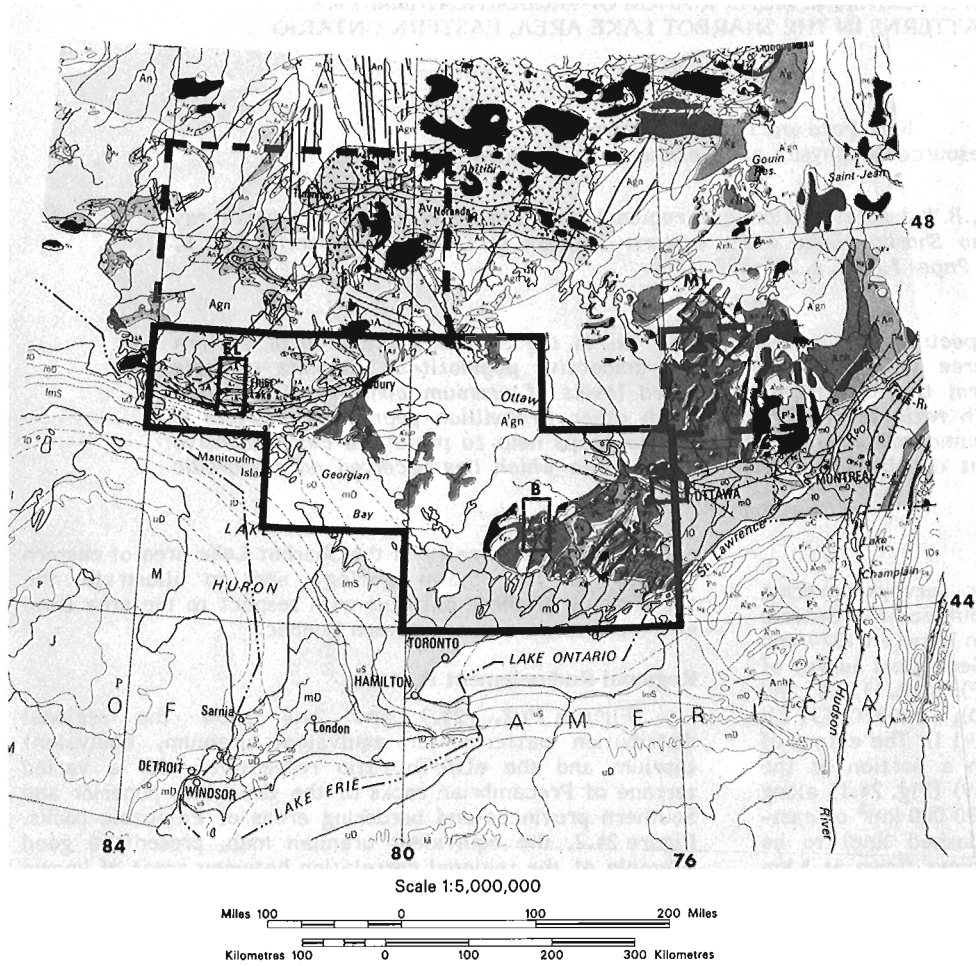
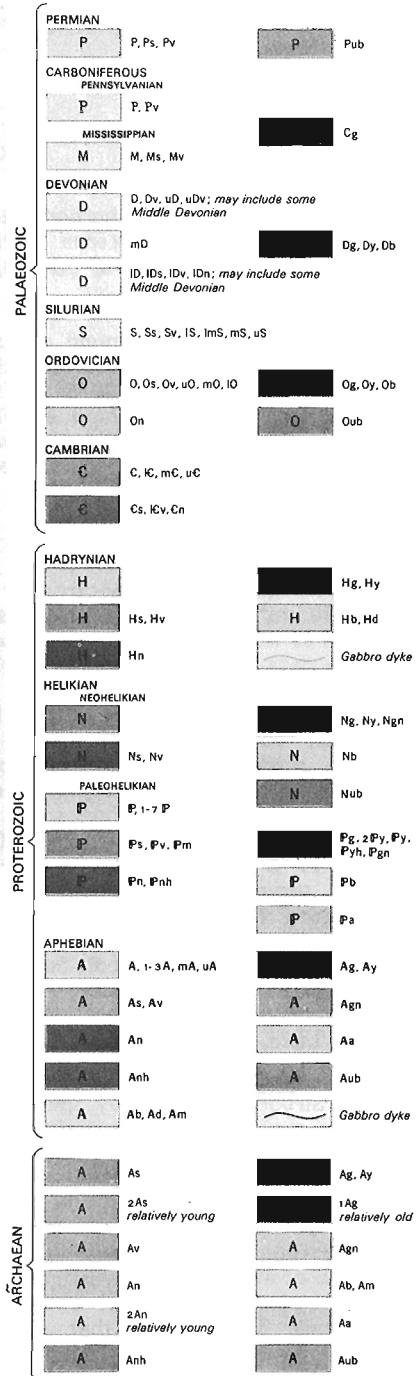


Figure 24.1. Regional geology and airborne gamma ray spectrometry coverage.



Grenville Supergroup to be significant, postulating that uraniumiferous pegmatites were derived anatectically from pre-existing basal sediments that were enriched in uranium and thorium.

The Sharbot Lake area (6) is significantly different from the Bancroft-Anstruther, Renfrew-Huddersfield (Charbonneau and Jonasson, 1975) and the Mont Laurier areas by virtue of its regionally high eU/eTh ratio (Fig. 24.4) (Charbonneau, 1977). The Mont Laurier area has a moderately high eU/eTh ratio but it is not as prominent as that for the Sharbot Lake area. The Bancroft area has only a slight eU/eTh ratio increase (Darnley and Grasty, 1971). Charbonneau et al. (1976) have published values which indicate average eU/eTh ratios of about 0.7 in pegmatites of the Mont Laurier area. The current authors made a brief examination of pegmatites in the zone running northeast through Bancroft and found that eU/eTh ratios average about 0.3-0.4. Data presented later in this paper illustrates that the Sharbot Lake eU/eTh ratios run close to 1. The low thorium levels within the Sharbot Lake area are in sharp contrast to the higher thorium levels in the Bancroft-Anstruther, Renfrew-Huddersfield and Mont Laurier areas (Fig. 24.3).

In addition to the above six areas three isolated features are indicated by numbers 7, 8 and 9 on Figure 24.2. One of these features along the southern edge of N.T.S. map sheet 41 I (7) corresponds to a known uranium occurrence in

Bigwood Township (Ont. Dept. Mines, 1971; Lang et al., 1962), with airborne equivalent uranium values > 1.6 ppm and eU/eTh ratio > 0.5. A second isolated feature occurs in the northeast corner of N.T.S. 41 I (8) and is associated with a felsic igneous intrusion at the southern end of Lake Temagami in Vogt Township. Airborne equivalent uranium values exceed 2 ppm with attendant equivalent thorium values > 10 ppm. The third and most interesting isolated feature occurs 100 km east of North Bay just inside the Algonquin Provincial Park boundaries (9). Airborne equivalent thorium values exceed 20 ppm with no attendant uranium or potassium increase. It is interesting to note that this anomaly is on trend with the alkalic complexes of the Lake Nipissing area and that fenitized boulders have been recognized in the area (pers. comm.; R. Barlow; Ont. Geol. Surv.).

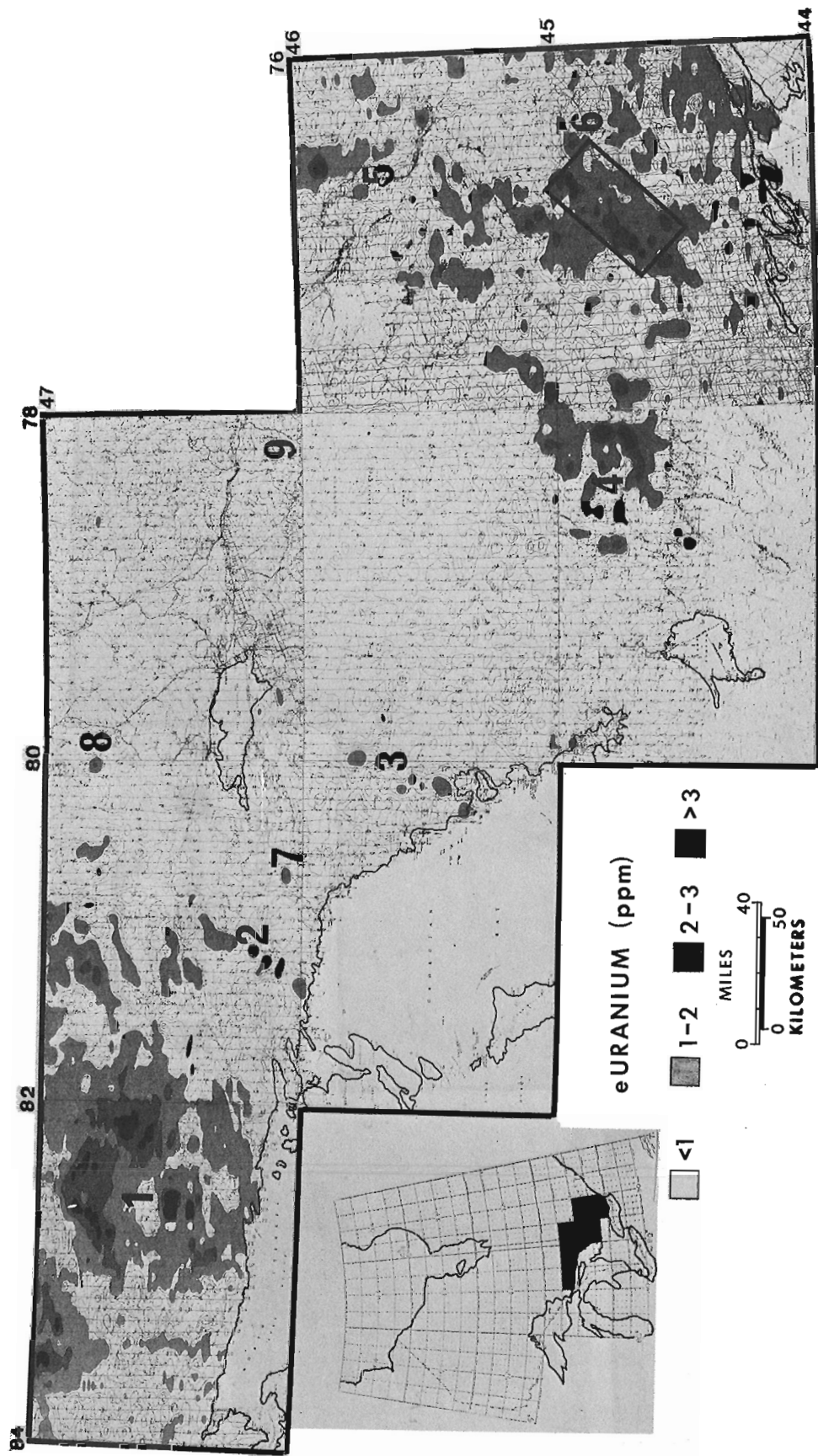


Figure 24.2. Regional equivalent uranium map showing the six regional radioactive features including the Sharbot Lake area.

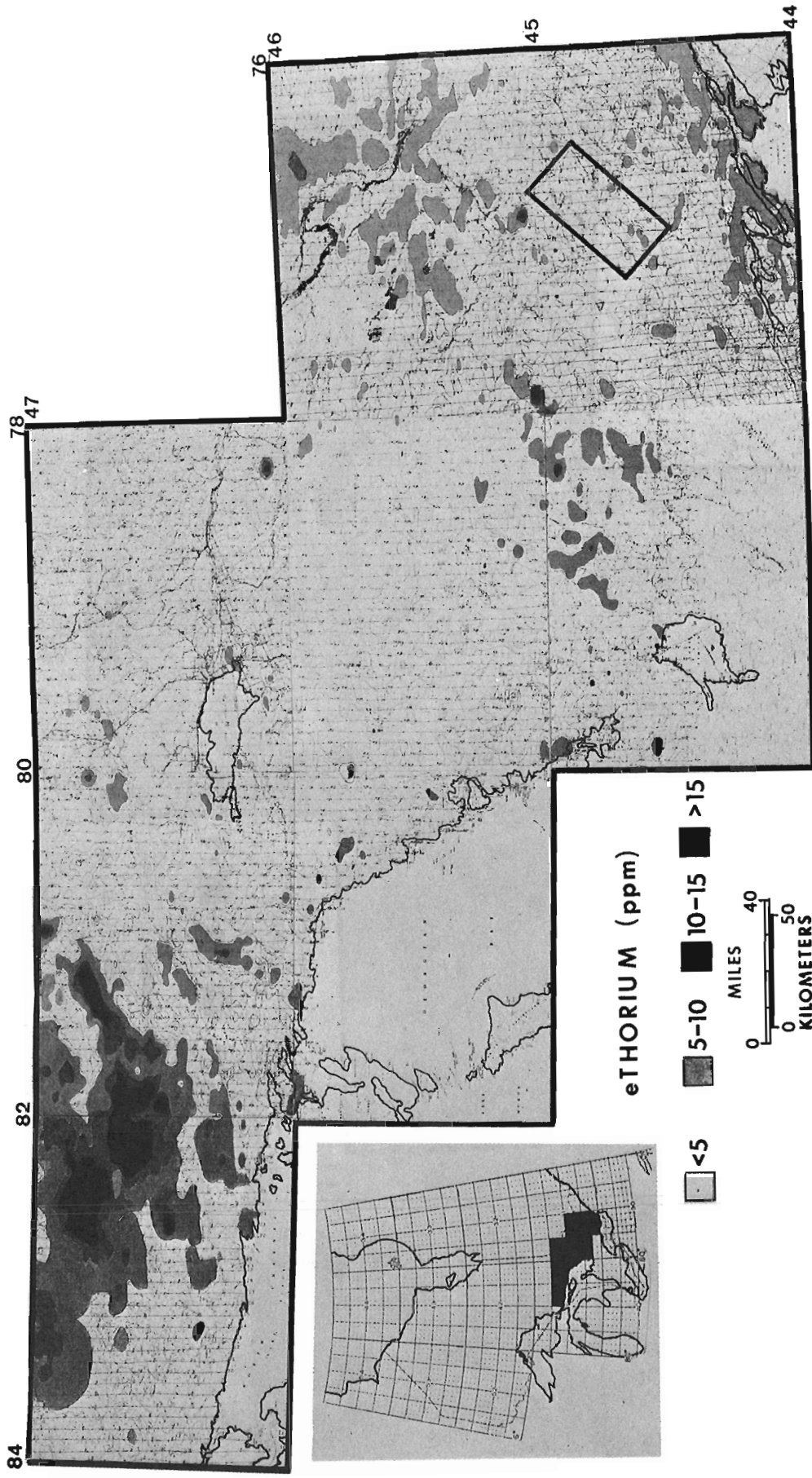


Figure 24.3. Regional equivalent thorium map.

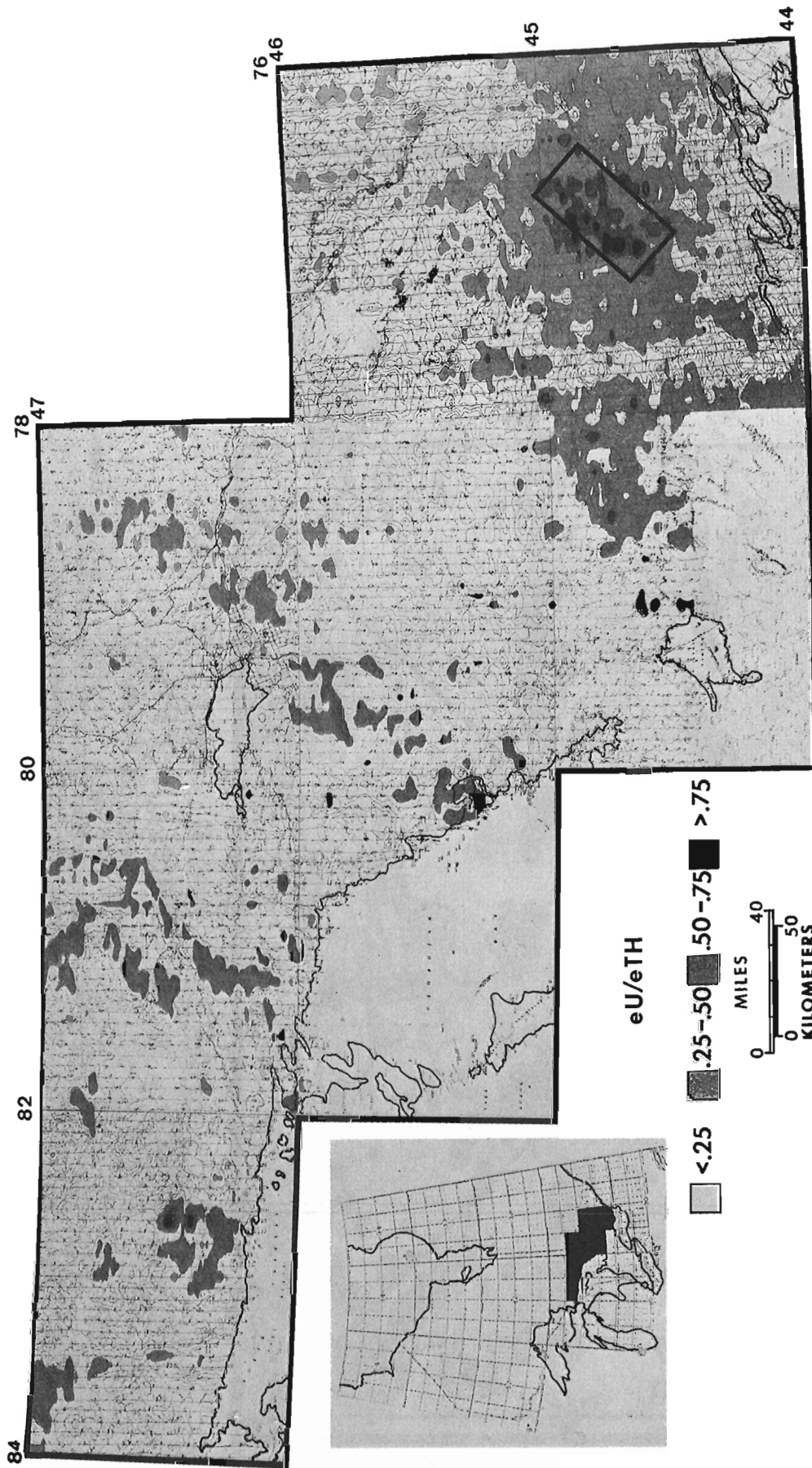


Figure 24.4. Regional equivalent uranium/thorium map.

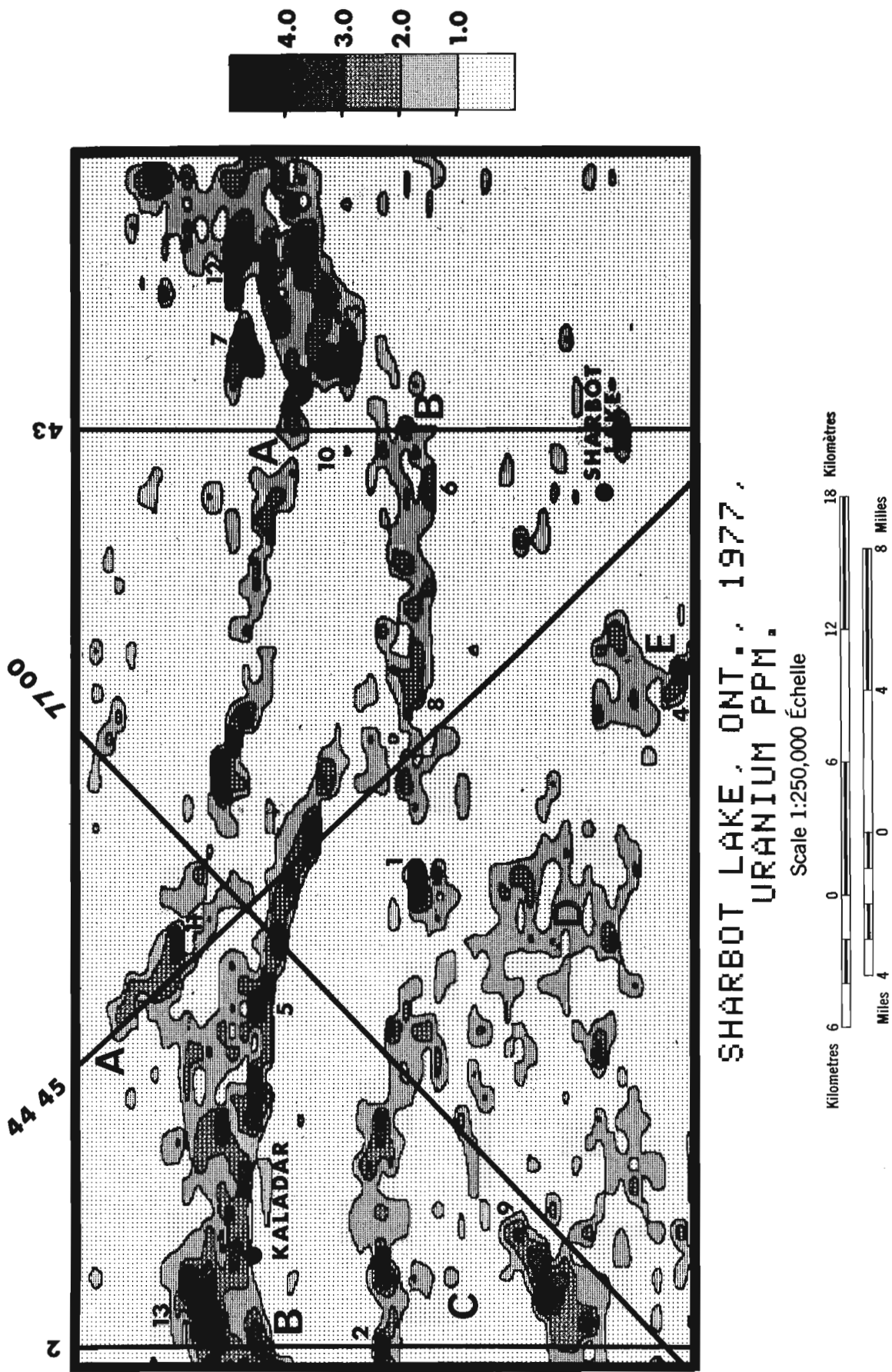


Figure 24.5. Sharbot Lake equivalent uranium map showing the location of the prominent radioactive belts, various pegmatite localities where in situ measurements were conducted and position of selected airborne profiles.

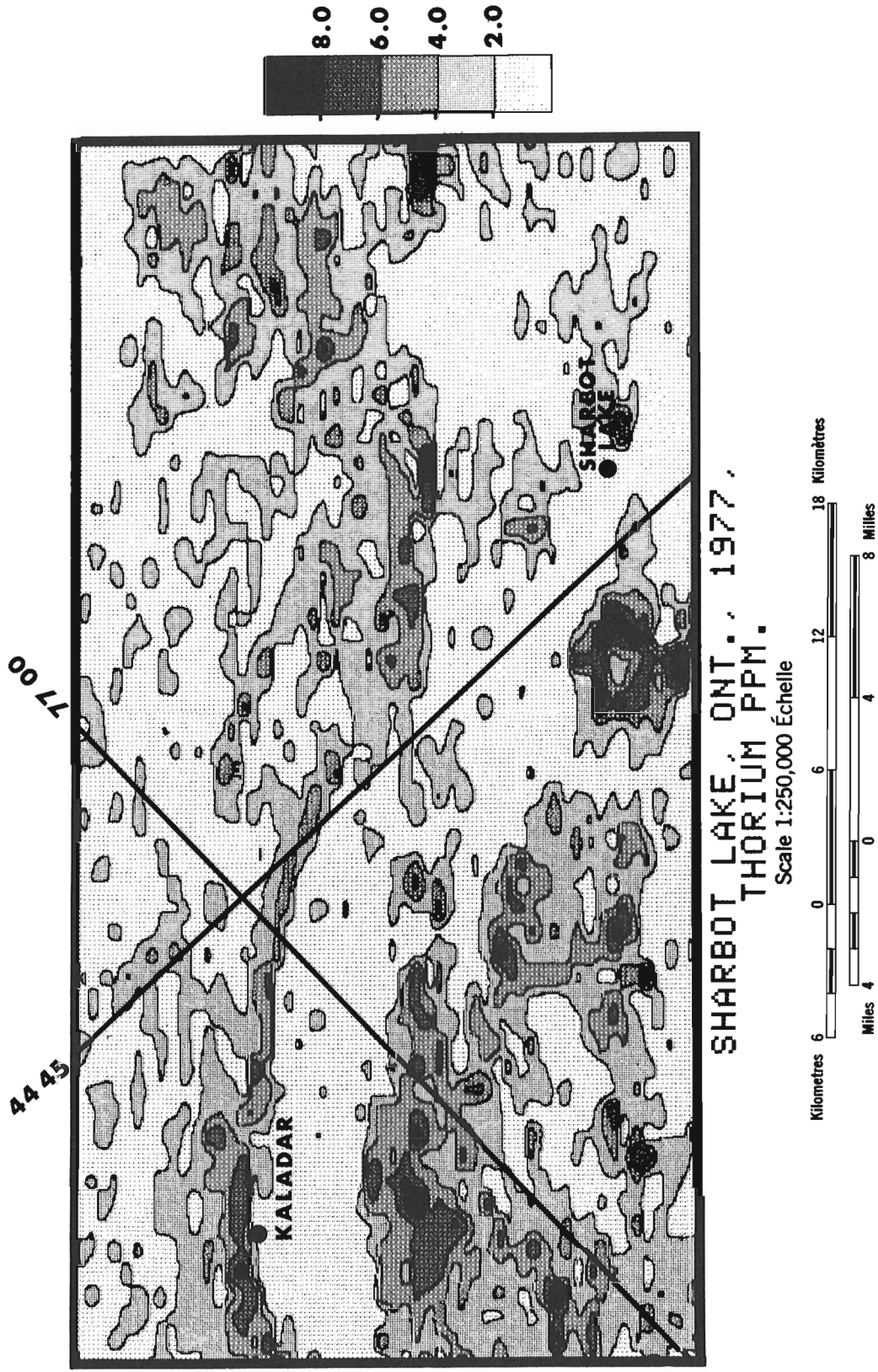


Figure 24.6. Sharbot Lake equivalent thorium map.

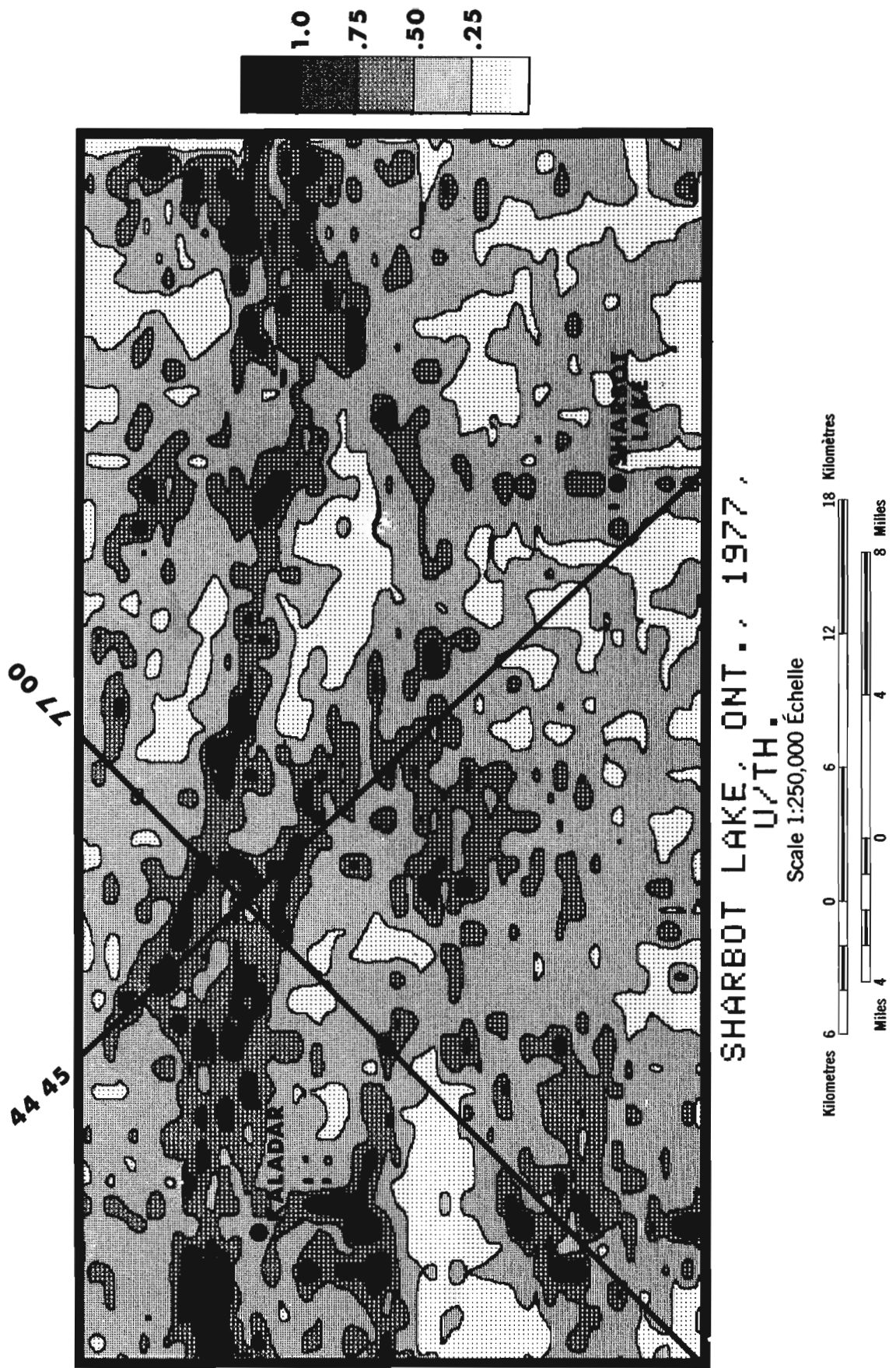


Figure 24.7. Sharbot Lake equivalent uranium/equivalent thorium map.

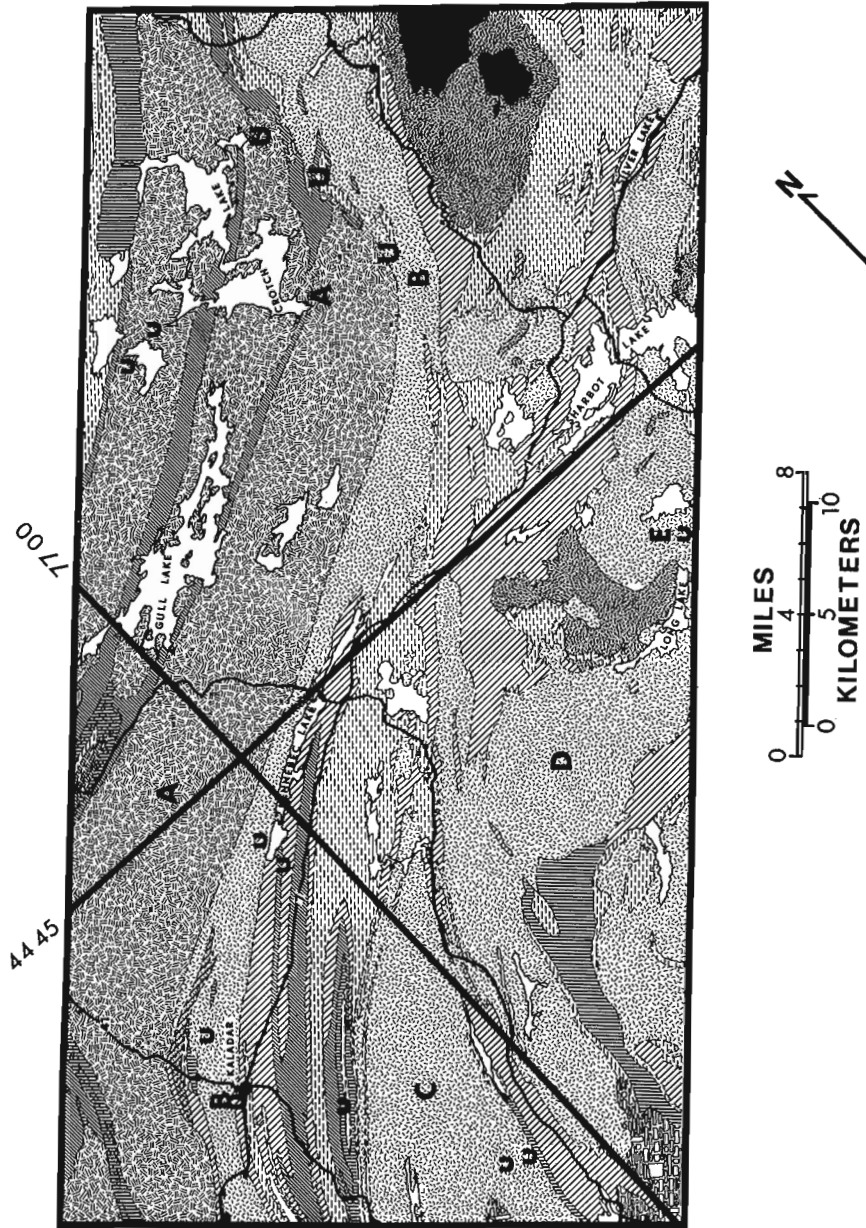
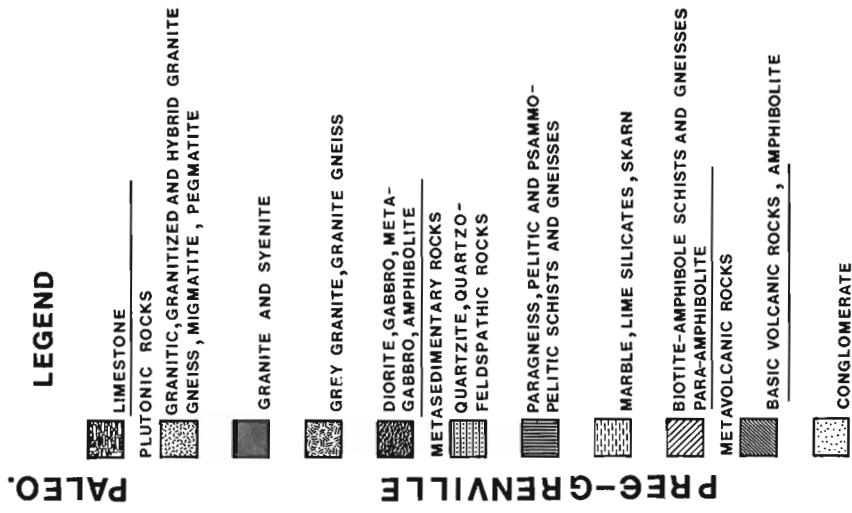
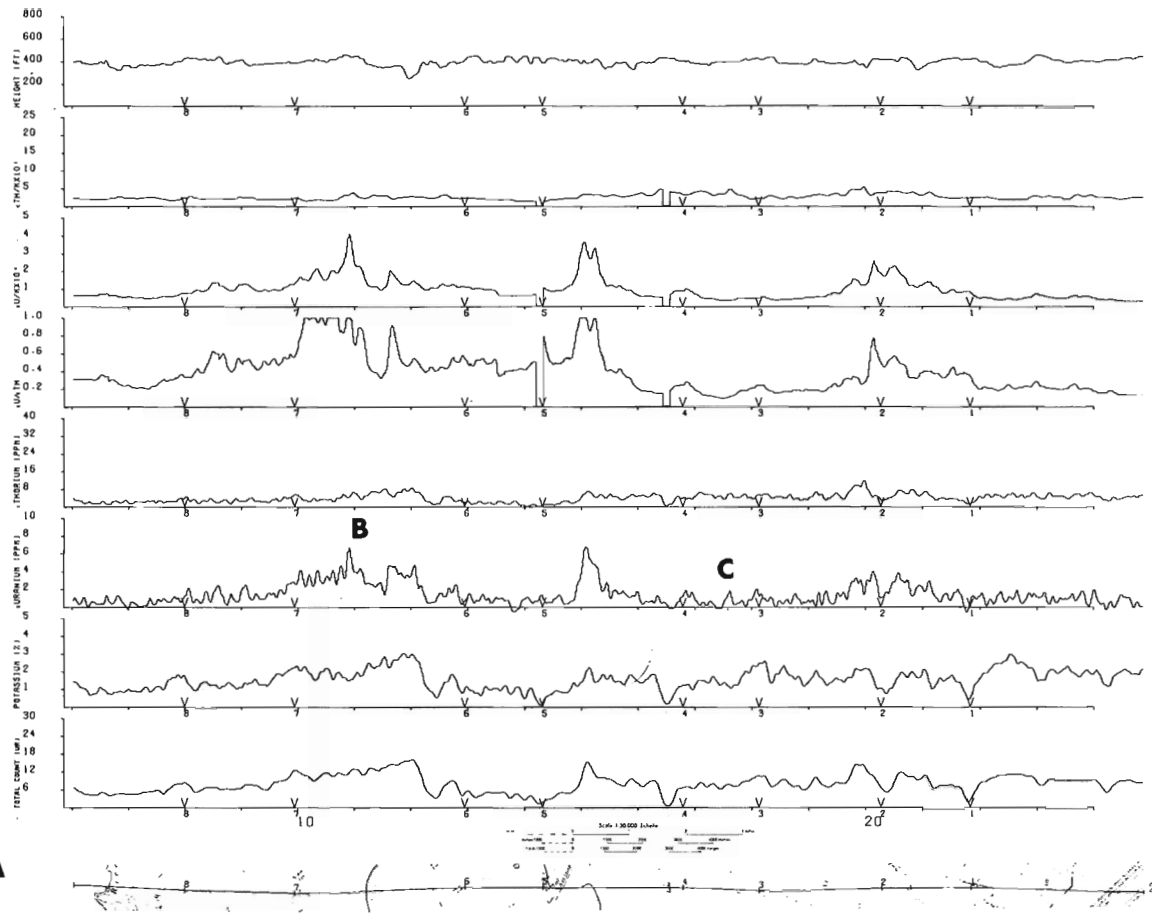


Figure 24.8. Sharbot Lake geology (after Hewitt, 1964).

SHARBOT LAKE AREA ONTARIO 1977.
LINE 2

A



SHARBOT LAKE AREA ONTARIO 1977.
LINE 43

B

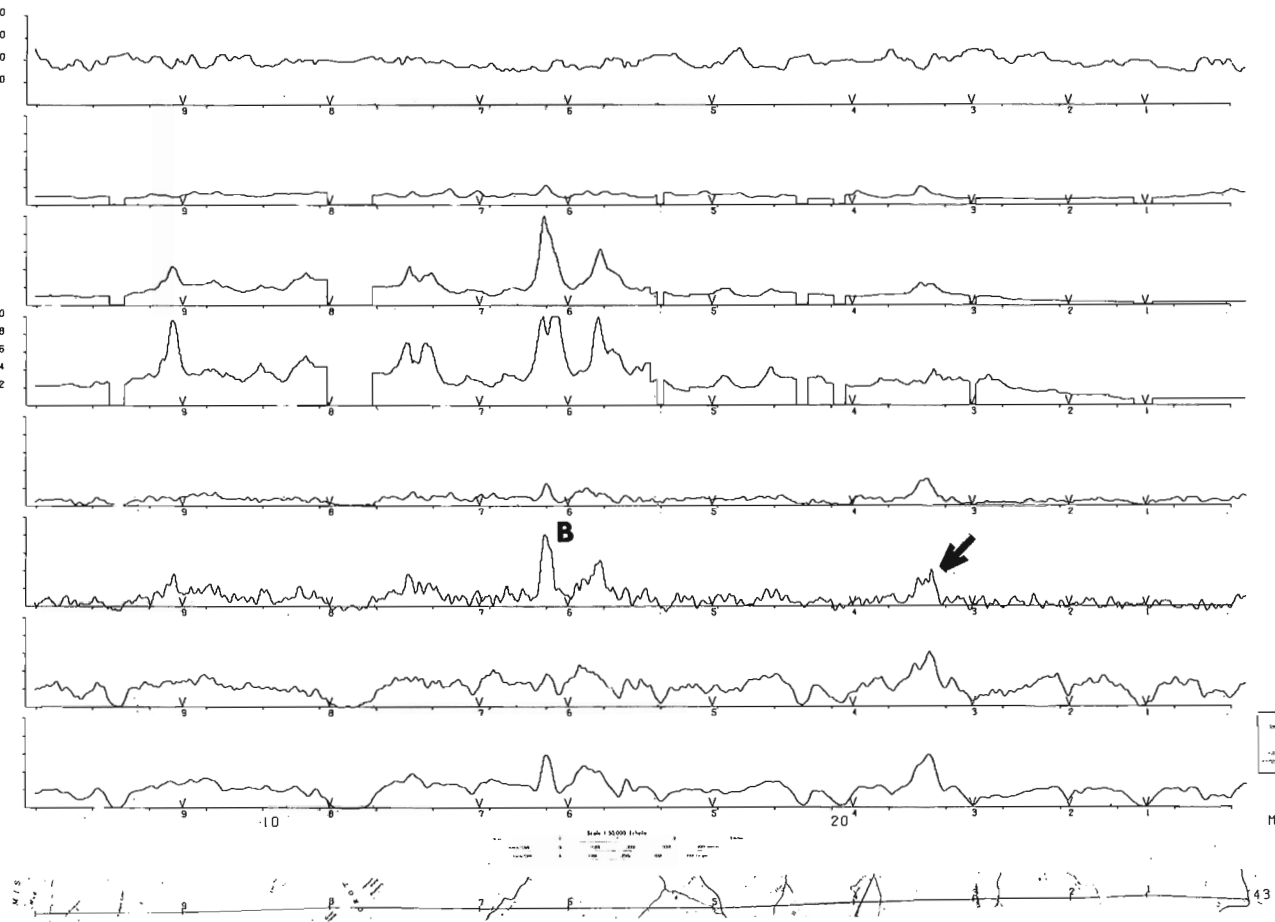


Figure 24.9. Two selected airborne profiles from the Sharbot Lake survey.

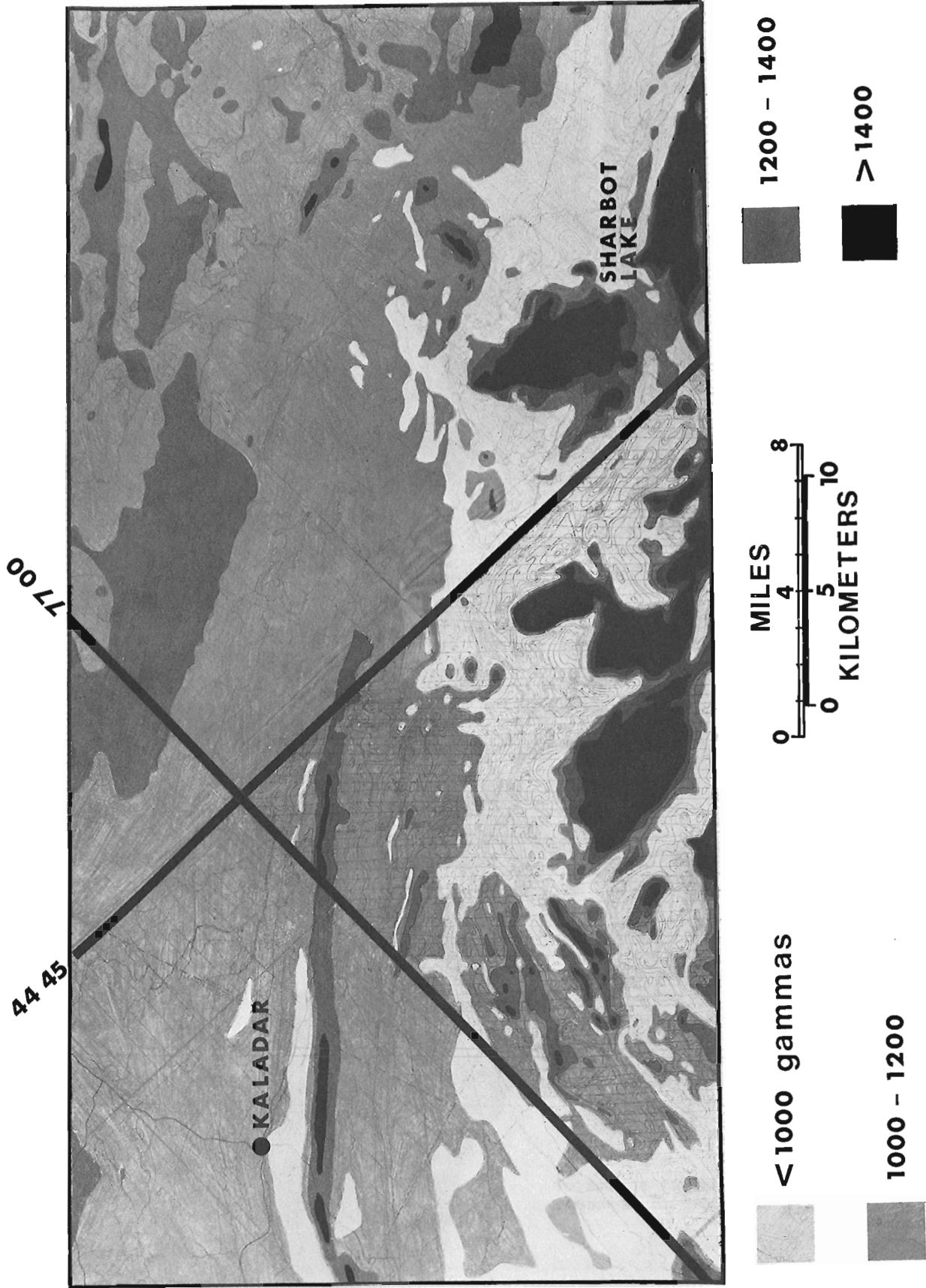


Figure 24.10. Sharbot Lake total field aeromagnetic map.

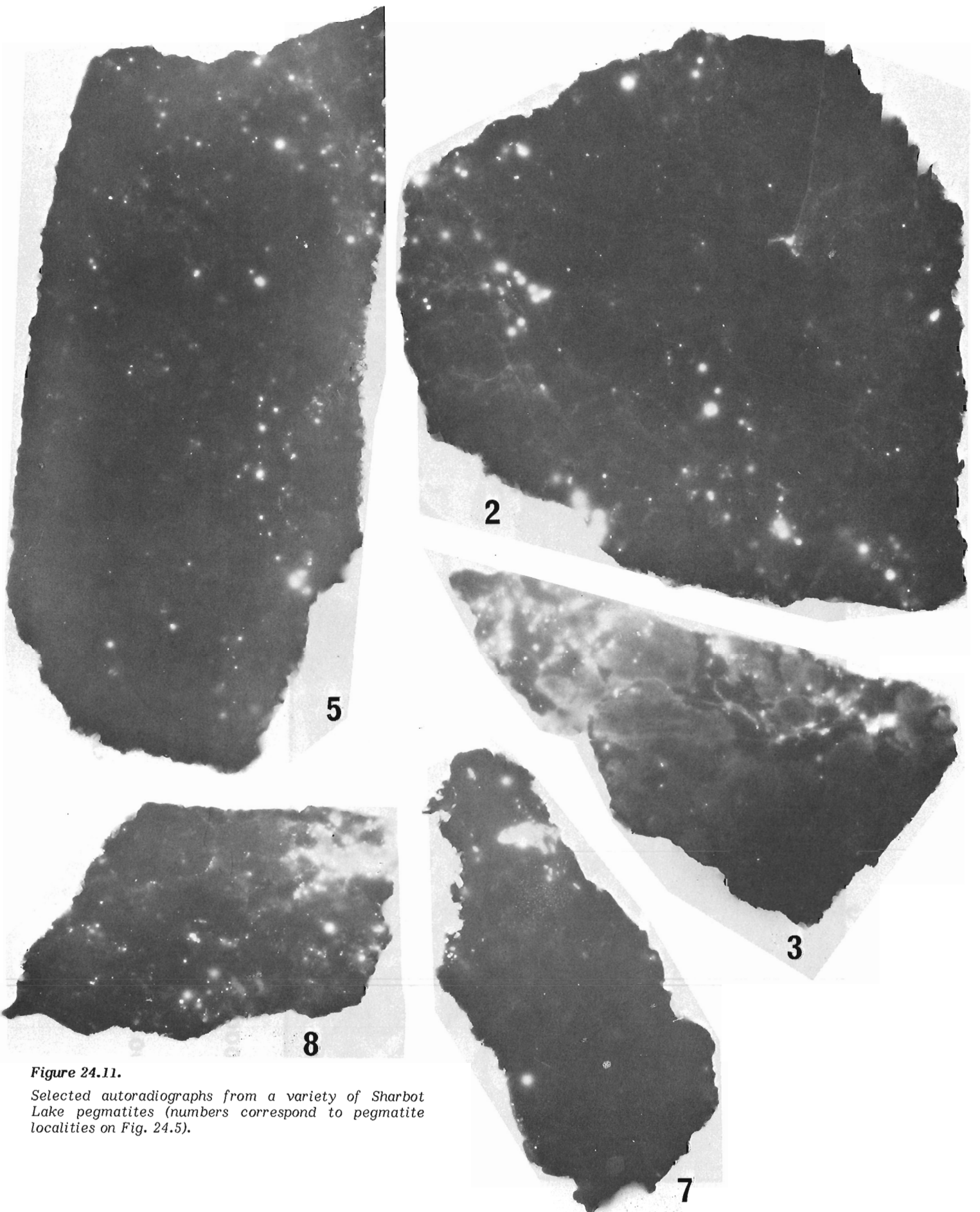


Figure 24.11.
Selected autoradiographs from a variety of Sharbot Lake pegmatites (numbers correspond to pegmatite localities on Fig. 24.5).

Sharbot Lake Area

Figures 24.5, 24.6 and 24.7 represent equivalent uranium, equivalent thorium and eU/eTh ratio maps for the 1500 km² Sharbot Lake survey. This survey was flown with 1 km line spacing in the fall of 1977 (Geol. Surv. Can., Open File 582). Figure 24.8 represents the known geology as compiled by Hewitt, 1964. Of the three airborne gamma ray spectrometry maps, the equivalent uranium map (Fig. 24.5) shows the strongest definition of pattern. Comparison between these gamma ray spectrometry patterns and geology shows a number of interesting features, some of which have been indicated alphabetically on Figures 24.5 and 24.8.

One of the most prominent of the features is the band (B) of anomalous equivalent uranium values trending northeast from Kaladar to the eastern edge of Crotch Lake. This band corresponds to a belt of granitized and hybrid granite gneiss (Lavant-Addington gneiss) containing numerous metasedimentary inclusions along with abundant pegmatitic units. These pegmatites in places intrude the Northbrook granodiorite as well. Another prominent band (A) of elevated equivalent uranium values corresponds to a zone of pegmatitic occurrences within the Northbrook-Crotch Lake granodiorite, a member of the biotite-diorite series (Lumbers, 1967). Belt-like features A and B appear to merge in

Palmerston Township east of Crotch Lake. A third belt-like feature is evident in the southern corner of the survey bordering the Mellon Lake gneiss (C). The equivalent uranium anomalies along the western edge of the Mellon Lake gneiss correspond to pegmatitic bodies intruding the supracrustal rocks of the Clare River structure and a thin lens of pink-weathering quartz monzonite separating the supracrustal sequence from the Mellon Lake gneiss. Chappell (1978) considers this lens of quartz monzonite to be equivalent to the Addington gneiss north of Kaladar and the Mellon Lake gneiss to be equivalent to the Northbrook-Crotch Lake granodiorite. The elevated equivalent uranium levels along the eastern edge of the Mellon Lake gneiss correspond to pegmatites intruding the Mellon Lake gneiss and the supracrustal metasediments. Anomalies D and E are not belt-like but are more ovoid in shape than the previously described belt-like features and unlike these other features contain more extensive areas of elevated equivalent thorium values (Fig. 24.6). These features correspond to granitic bodies.

Figure 24.6, the equivalent thorium map shows the low levels of thorium noted previously on Figure 24.3. Although the levels on a regional basis may be considered low some of the features described from the equivalent uranium map have attendant increases in equivalent thorium. In particular features D and E along with portions of B (loc. 6, Fig. 24.5)

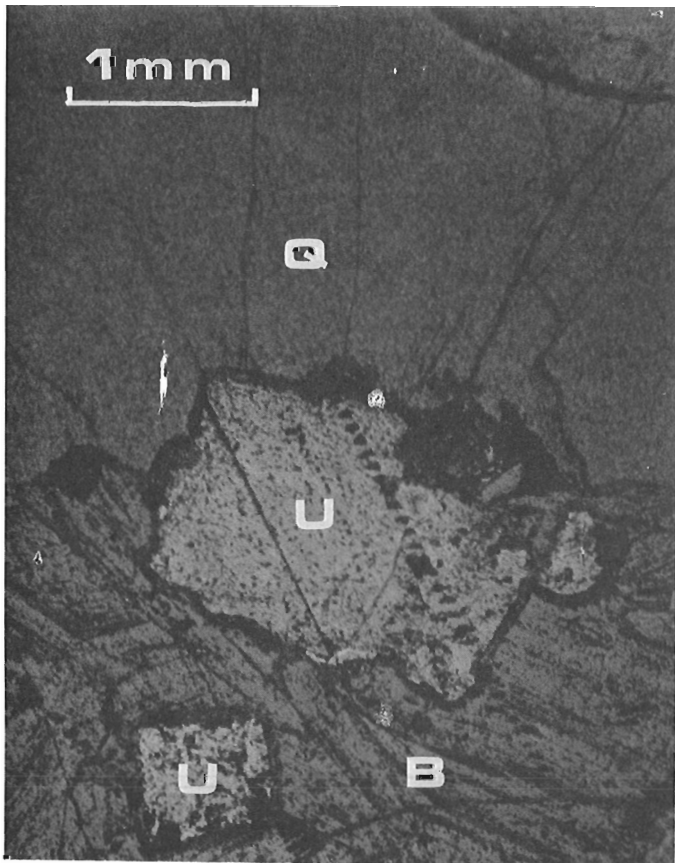


Figure 24.12A. Uraninite (U) associated with quartz (Q) and biotite (B) from locality 3 (Fig. 24.5), reflected light.

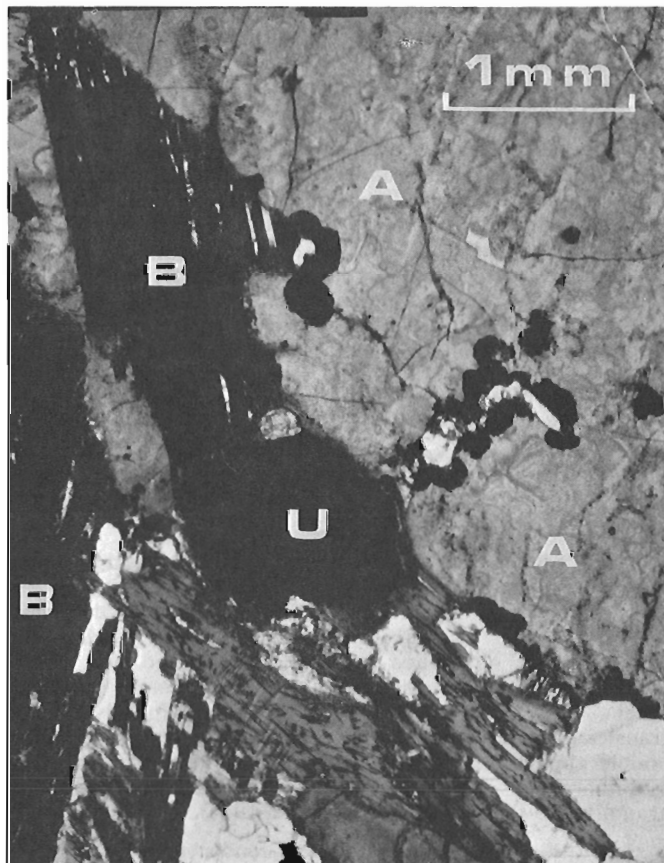


Figure 24.12B. Uraninite (U) and allanite (A) associated with biotite (B) and quartz from locality 7 (Fig. 24.5), transmitted light.

have elevated levels of equivalent thorium. This results in these features having lower eU/eTh ratios than the majority of belts A, B and C as shown on Figure 24.7. As well as showing elevated eU/eTh ratios over most of belts A, B and C, Figure 24.7 also indicates that the majority of the survey area has elevated eU/eTh ratio levels when compared to the general crustal average of 0.25 (Clark et al., 1966). These elevated levels are even more evident on the regional eU/eTh ratio map (Fig. 24.4).

Figure 24.9 shows two airborne profiles from the survey area. The location of these profiles can be seen on Figure 24.5. The profiles show many of the already discussed features, in particular the low thorium and high eU/eTh levels. Pegmatitic zones corresponding to belt B and those bordering the Mellon Lake gneiss (C) are quite evident on line 2 (Fig. 24.9A). Line 43 (Fig. 24.9B) shows the strong response to the pegmatitic mineralization at Mideast Developments Property in Olden Township on belt (B) which in contoured form (Fig. 24.5) has only a weak response (Barlow and Ware, 1977). This weaker contoured response is the result of smoothing by the computer programs used to produce the contour maps which tends to reduce some sharp anomalous features present in profile form (Cameron et al., 1976). Line 43 (arrow) also shows the type of response from the granite masses along the eastern edge of the survey area with their decreased concentrations of equivalent uranium and increased levels of thorium and potassium. The total count profile of line 43 indicates the importance of using a differential spectrometry system as opposed to a total count system. The total count response from a mineralized pegmatite is less than the response from a granitic mass for this particular example.

The aeromagnetic map (Fig. 24.10) provides data which help define and differentiate the granitic and dioritic rocks along the southeastern boundary of the survey area. In particular the intrusive mass just west of Long Lake is well defined magnetically. This unit corresponds to unit D on Figures 24.5 and 24.8. A prominent magnetic anomaly just north of Long Lake relates to a gabbroic-dioritic mass. East of this body, a granitic unit has some portions with a high magnetic expression. This unit corresponds to anomaly E on Figures 24.5 and 24.8. Magnetic anomalies also relate to granitic intrusive rocks northwest and northeast of Sharbot Lake. These bodies have weak radiometric expressions. A large gabbroic mass near the northeastern margin of the survey shows only a low magnetic response in contrast to the prominent magnetic signature of the gabbroic body near Long Lake.

In addition to the correlations described above a prominent change in magnetic character dividing the southeastern half from the northwestern half of the survey area is evident. West of this north-northeast trending zone the magnetic anomalies are generally broad and of low amplitude. This subdivision may indicate a major geological break. This zone also correlates approximately with a transition from intermediate grade metamorphism (lower and middle almandine amphibolite) to the northwest to high grade metamorphism (upper almandine amphibolite and locally granulite) to the southeast (Lumbers, 1964).

Detailed geochemical studies, conducted as follow-up to the reconnaissance lake sediment geochemistry and reconnaissance airborne radiometric surveys of 1976 were carried out over certain portions of the detailed Sharbot Lake airborne survey (Coker and Closs, 1979). Uranium anomalies in the geochemical data correlate well in the position of airborne uranium anomalies, particularly in the Crotch Lake area and north of Kaladar.

Known uranium occurrences (indicated by "U" symbols on Fig. 24.8) are coincident with high equivalent uranium on

Figure 24.5. These locations are taken from Gordon et al. (1979). Individual occurrences are marked by a small "u", areas of several individual occurrences are indicated by a large "U".

In situ gamma ray spectrometry measurements were taken on pegmatites within many of the anomalous features of the Sharbot Lake survey. The locations of these sites are shown on Figure 24.5. The average radioelement concentrations at each location (Table 24.1) were determined by first surveying the pegmatitic outcrops with a total count scintillometer followed by in situ spectrometry measurements at those spots considered to be representative of the average radioelement concentrations. The maximum values reported represent single measurements for an area less than a square metre in size. Radioelement concentrations less than the minimum range value (Table 24.1) were encountered but these were not considered to be representative of the average radioelement concentration.

The average radioelement contents of all the pegmatites on Table 24.1 (excluding the three low values from locality 10) indicate approximately equal equivalent uranium and equivalent thorium values (29 ppm eU and 30 ppm eTh). An analysis of the data in Table 24.1 indicates that there is no substantial difference in average pegmatite radioelement contents between belt-like features A, B and C (Fig. 24.8). Radioelement variation within the belt-like features is however significant. For example, localities 3 and 8 are within the same belt-like feature (B) however the radioelement values are quite different (45 ppm eU and 19 ppm eTh for locality 3 as opposed to 27 ppm eU and 45 ppm eTh for locality 8). This radioelement variation along belts is probably related in part to the influence of host rocks.

The maximum measured levels of radioelements shown in Table 24.1 generally correspond to biotite rich portions of pegmatites, for example, locality 3. However, many very radioactive patches show no correlation with mafic rich portions, for example, localities 2 and 8. Magnetite was recognized in a few localities and hematization was usually noted in zones of increased radioactivity. Garnet and tourmaline are abundant accessories at localities 2, 3 and 8. Molybdenite was recognized at locality 3.

Autoradiographs of pegmatite samples from localities 2, 3, 5, 7 and 8 (Fig. 24.5) comprise Figure 24.11. These samples were collected at spots having the highest radioelement concentrations (maximum measured concentration, Table 24.1). The radioactive minerals, which are generally dispersed within the pegmatite specimens (i.e. Fig. 24.11.2) are mainly uraninite. Some redistribution of uranium is evident along fractures. Allanite is also common as an accessory mineral and is weakly radioactive. Zircon and sphene are also present but are only very weakly radioactive.

Examples of some of the radioactive mineral species comprise Figure 24.12. Figure 24.12A (reflected light) shows a cube of uraninite (U) associated with biotite (B) and quartz (Q). Figure 24.12B (transmitted light) shows uraninite (U) associated with biotite (B) and a large allanite (A) grain.

Summary

Uraniferous pegmatites in the Sharbot Lake area have been known for some years (Lang, 1952). However, it was not until publication of the airborne gamma ray spectrometer survey covering the Sharbot Lake area that a comprehensive overview of the radioelement distribution patterns in the area was made possible. In particular the publication of this survey has enabled a comparison with detailed airborne surveys published covering other major pegmatite areas in the Grenville, namely Bancroft and Mont Laurier.

Table 24.1

Compilation of in situ gamma ray spectrometry measurements, Sharbot Lake, Ontario

Locality	Rock Type(*)	eU ppm		eTh ppm		Maximum Measured Concentration	
		Average(**)	Range(**)	Average(**)	Range(**)	eU ppm	eTh ppm
1-Arden	Pegmatite (4)	22	(17-26)	38	(26-49)	39	107
2-Mitten Lake	Pegmatite (3)	31	(16-36)	19	(15-24)	505	199
	Pink Granite Gneiss (1)	3		16			
3-Black Creek	Pegmatite (5)	45	(29-67)	19	(10-27)	6953	2594
4-Legatt Lake	Granite (5)	5	(3-8)	21	(12-31)		
5-Kennebec Lake	Pegmatite (5)	37	(14-54)	29	(15-39)	391	212
	Granodiorite (3)	3	(2-3)	9	(6-10)		
6-Smith Lake	Pegmatite (3)	15	(10-23)	37	(28-49)	84	169
	Pink Granite Gneiss (5)	10	(6-13)	36	(33-41)		
7-Big Black Bay	Pegmatite (1)	33		40		144	149
8-Sharbot Creek	Pegmatite (5)	27	(21-34)	45	(34-62)	810	632
	Marble (2)	3		4			
9-Sheffield Long Lake	Pegmatite (3)	21	(17-27)	39	(31-52)	152	287
10-Clarendon Road	Pegmatite (1)						
	(amphibolite host-rock)	35		12		87	39
	Pegmatite (3)						
	(granodiorite host-rock)	2	(1-3)	4	(2-6)		
11-Dead Creek	Granodiorite (4)	2	(1-3)	5	(2-8)		
	Pegmatite (4)	25	(9-40)	21	(13-39)		
	Granodiorite (2)	1		4	(4-5)		
12-Crotch Lake	Pegmatite (3)	27	(17-44)	27	(20-32)	251	105
13-Kaladar	Pegmatite (1)	32		17		77	21
	Granodiorite (4)	4	(2-5)	6	(5-7)		
	Hematized Patch on Granodiorite (1)					532	161

*Number of measurements considered for average values.

**Excluding maximum measured concentrations.

The ground investigations conducted to date reaffirms the significant features shown on the detailed survey as well as those shown on the regional compilations. In particular the high eU/eTh ratio for the Sharbot Lake area relative to other Grenville pegmatite areas has been confirmed.

Three major pegmatite belts in the Sharbot Lake area are well defined in their distribution. One of these belts, is located within the Northbrook granodiorite south of Big Gull Lake (A). A second pegmatite belt (B) follows the Lavant-Addington gneiss south of the Northbrook granodiorite and merges with the first belt-like feature (A) in Palmerston Township. A third pegmatite belt occurs peripheral to the Mellon Lake gneiss (C).

Two main theories have been offered in the literature for derivation of the radioactive Grenville pegmatites. The most popular at present is that they were derived anatectically from a radioelement rich sediment near the base of the Grenville Supergroup (Allen, 1971; Bright, 1975; Lumbers, 1975). Another viewpoint is that the pegmatites in these Grenville areas have been derived from young "granites" (pers. comm.; A.D. Fowler; McGill Univ., Montreal). Another possibility is that the pegmatite belts A, B, C may be controlled by major shear zones.

Further investigations should involve a more detailed investigation of selected pegmatites and their host rocks within belts A, B, C in the area supported by a regional investigation of the radioelement contents of various rock units in an effort to obtain more precise data concerning the origin of the pegmatites and their possible economic significance.

Acknowledgments

The authors would like to acknowledge the efforts of several people within the Geological Survey of Canada. P.B. Holman carried out the airborne survey operations and map compilation. The paper was critically read by K.A. Richardson and G.R. Bernius.

References

- Allen, J.M.
1971: The genesis of Precambrian uranium deposits in eastern Canada and the uraniumiferous pegmatites of the Mont Laurier area, Quebec; Unpublished M.Sc. Thesis, Queen's University, Kingston, Ont.
- Barlow, R.D. and Ware, C.
1977: Geophysical, geochemical, and geological investigations of some uranium occurrences, Sharbot Lake area, Southeastern Ontario; in Summary of Field Work, 1977, Ontario Geological Survey Miscellaneous Paper 75, p. 174-177.
- Bright, E.G.
1975: Cavendish and Anstruther Townships, Peterborough County; in Summary of Fieldwork, 1975, Ontario Division of Mines Miscellaneous Paper 63, p. 94-97.
- Bristow, Q.
Airborne instrumentation in uranium exploration; in Geophysics and Geochemistry in the Search for Metallic Ores; Peter J. Hood, editor, Geological Survey of Canada Economic Geology Report 31. (in press)
- Cameron, G.W., Elliott, B.E., and Richardson, K.A.
1976: Effect of line spacing on contoured airborne gamma-ray spectrometry data; IAEA Symposium on Exploration for Uranium Ore Deposits; Vienna, Austria, IAEA SM 208/2.
- Chappell, J.F.
1978: The Clare River structure and its tectonic setting; Unpublished Ph.D. Thesis, Carleton University, Ottawa, Ont.

- Charbonneau, B.W.
1977: Radioelement distribution patterns in the Frontenac Axis, Ontario; in *Current Research, Part A, Geological Survey of Canada, Paper 77-1B*, p. 337-340.
- Charbonneau, B.W. and Jonasson, I.R.
1975: Radioactive pegmatites in the Renfrew area, Ontario; in *Report of Activities, Part C, Geological Survey of Canada, Paper 75-1*, p. 285-290.
- Charbonneau, B.W., Killeen, P.G., Carson, J.M., Cameron, G.W., and Richardson, K.A.
1976: Significance of radioelement concentration measurements made by airborne gamma-ray spectrometry over the Canadian Shield; IAEA Symposium on Exploration for Uranium Ore Deposits, Vienna, Austria, 1976, STI/PUB/434, p. 35-53, IAEA-SM-208/3.
- Clark, S.P. Jr., Peterman, Z.E., and Heier, K.S.
1966: Abundances of uranium, thorium and potassium; in *Handbook of Physical Constants, Geological Society of America, Memoir 97*, p. 521-541.
- Coker, W.B. and Closs, L.G.
1979: Detailed geochemical studies, southeastern Ontario; in *Current Research, Part A, Geological Survey of Canada, Paper 79-1A*, p. 247-252.
- Darnley, A.G., Charbonneau, B.W., and Richardson, K.A.
1977: The distribution of uranium in rocks as a guide to the recognition of uraniferous regions; Symposium on Recognition and Evaluation of Uraniferous Regions, IAEA, Vienna, Austria, 1975, IAEA, TC 25/9, p. 55-56.
- Darnley, A.G. and Grasty, R.L.
1971: Mapping from the air by gamma-ray spectrometry; Canadian Institute of Mining Metallurgical Bulletin, Special Volume, No. 11, Geochemical Exploration, 1971.
- Douglas, R.J.W.
1969: Geological Map of Canada; Geological Survey of Canada, Map 1250A.
- Gordon, J.B., Springer, J.S., and MacDonald, C.A.
1979: Uranium mineral potential chart of Lennox and Addington and Frontenac Counties, Southern Ontario; Ontario Geological Survey Open File Report 5260, Chart G, Compilation 1978.
- Hewitt, D.F.
1964: Geological notes for maps nos. 2053 and 2054, Madoc-Gananoque area; Ontario Department of Mines, Geological Circular No. 12.
- Lang, A.H.
1952: Canadian deposits of uranium and thorium; Geological Survey of Canada, Economic Geology Report No. 16.
- Lang, A.H., Griffith, J.W., and Steacy, H.R.
1962: Canadian deposits of uranium and thorium; Geological Survey of Canada, Economic Geology Report No. 16 2nd ed.
- Lumbers, S.B.
1964: Relationship of mineral deposits in intrusive rocks and metamorphism in part of the Grenville province of southeastern Ontario; Ontario Department of Mines, Preliminary Report 1964-4.
1967: Geology and mineral deposits of the Bancroft-Madoc area; in *Guidebook to Geology in Parts of Eastern Ontario and Western Quebec, Geological Association of Canada Annual Meeting, Kingston*, p. 13-30.
1975: Pembroke area, District of Nipissing and County of Renfrew; in *Summary of Fieldwork, 1975, Ontario Division of Mines, Miscellaneous Paper 63*, p. 91-93.
- Ontario Department of Mines and Northern Affairs
1971: Sudbury-Cobalt Sheet, Geological Compilation Series, Map 2188.
- Richardson, K.A., Darnley, A.G., and Charbonneau, B.W.
1975: The airborne gamma-ray spectrometric measurements over the Canadian Shield; Natural Radiation Environment II, United States Energy Research and Development Administration, Conf. 720805-P2, p. 681-704.
- Ruzicka, V.
1979: Uranium and thorium in Canada, 1978; in *Current Research, Part A, Geological Survey of Canada, Paper 79-1A*, p. 139-155.

25. GENETIC CONTROLS OF SELWYN BASIN STRATIFORM BARITE/SPHALERITE/GALENA DEPOSITS: AN INVESTIGATION OF THE DOMINANT BARIUM MINERALOGY OF THE TEA DEPOSIT, YUKON

Project 770063

J.W. Lydon, R.D. Lancaster, and P. Karkkainen
Regional and Economic Geology Division

Lydon, J.W., Lancaster, R.D., and Karkkainen, P., Genetic controls of Selwyn Basin stratiform barite/sphalerite/galena deposits: An investigation of the dominant barium mineralogy of the Tea deposit, Yukon; in *Current Research, Part B, Geological Survey of Canada, Paper 79-1B*, p. 223-229, 1979.

Abstract

A brief review of the pertinent geological and chemical evidence leads to the conclusion that the bedded sulphide and barite deposits of the Macmillan Pass area are both the result of direct precipitation from hydrothermal discharges and that the differences in chemistry between the two types are probably the result of different depositional environments. A preliminary investigation of the Tea barite deposit, designed to evaluate the genetic relationship of the reported barite-witherite-calcite assemblage and the constraints that this would impose on a genetic model for the deposits, is described. The present investigation failed to confirm the presence of witherite, but points out several features which confirms the sedimentary nature of the barite.

Introduction

During the 1978 field season, a preliminary field study and sampling program was carried out on selected stratiform sulphide/sulphate occurrences in the Macmillan Pass area of the Yukon (Fig. 25.1). The work forms part of the initial phase of a continuing program to determine the ore forming processes responsible for stratiform lead-zinc deposits of Selwyn Basin. Investigations during the first year were designed to acquire a basic knowledge of the deposits and to determine methodologies best suited to the geological problems involved.

The field work (by J.W.L. and R.D.L.) included the collection of samples which were representative of the mineralogical, textural and structural variations shown by each deposit. Laboratory investigations in progress include chemical, mineralogical, and sulphur isotope analyses of these samples. This report deals only with results obtained to date on qualitative determinations of the dominant mineralogy of the Tea property (by J.W.L. and P.K.) and the implications they have on some genetic models of the Macmillan Pass area barite deposits.

Genetic Models Applicable to the Macmillan Pass Area Barite Deposits

The general geological setting of the Macmillan Pass area stratiform barite and sphalerite/galena deposits has been summarized by Dawson (1977). All are essentially laminated to massive bedded deposits and occur within a dominantly shale/siltstone succession, which forms the Canol Formation of Devonian-Mississippian age (Fig. 25.2). Geological investigations by Ogilvie Joint Venture (Smith, 1978) and the Hudson Bay Exploration and Development Company (Ken Taylor, pers. comm.) indicates that the Tom, Jason, Gary, and Pete deposits occur within a northwest trending graben-like structure, which formed as the result of subsidence along growth faults during early Canol time. The approximate eastern and western limits of this trough are indicated on Figure 25.1 and stratigraphical relationships within it are illustrated in Figure 25.2. Smith (op. cit.) recognized three main episodes of fault movement, each of which were accompanied by hydrothermal and volcanic activity. The intervening periods were characterized by deposition of turbidites with flow directions from the northwest to southeast. By Imperial Formation time, growth fault movement had apparently ceased, the trough had been completely filled, and current directions were from the northeast to southwest.

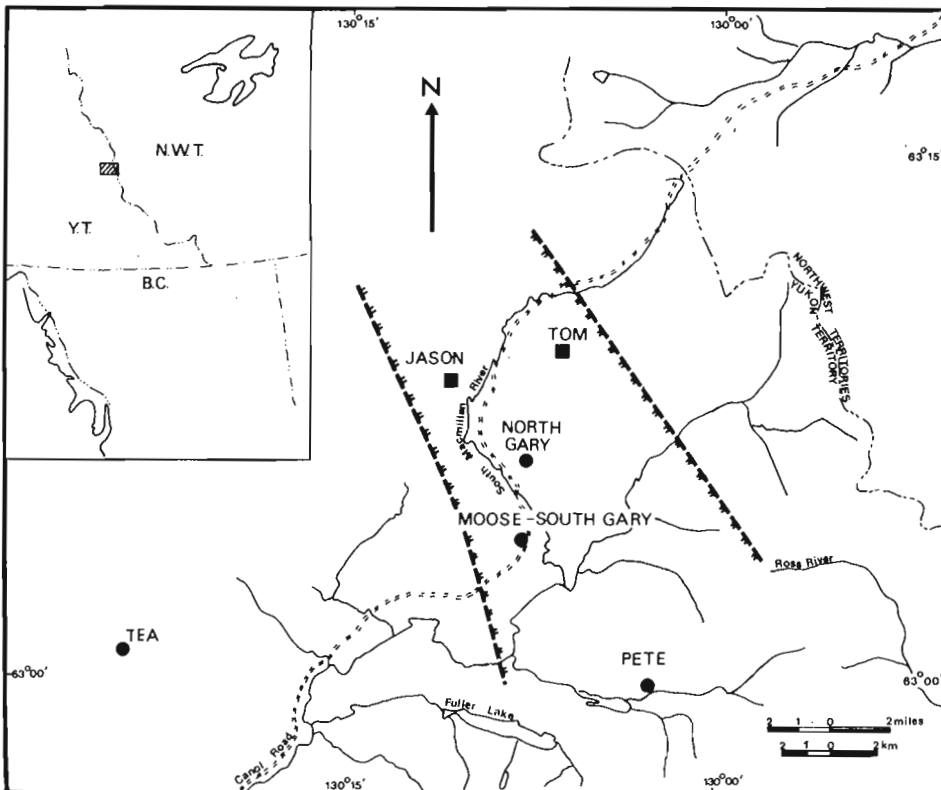


Figure 25.1. Location of the bedded sulphide/barite (squares) and barite (circles) deposits of the Macmillan Pass area. The hatched lines indicate the approximate extent of the synsedimentary graben structure.

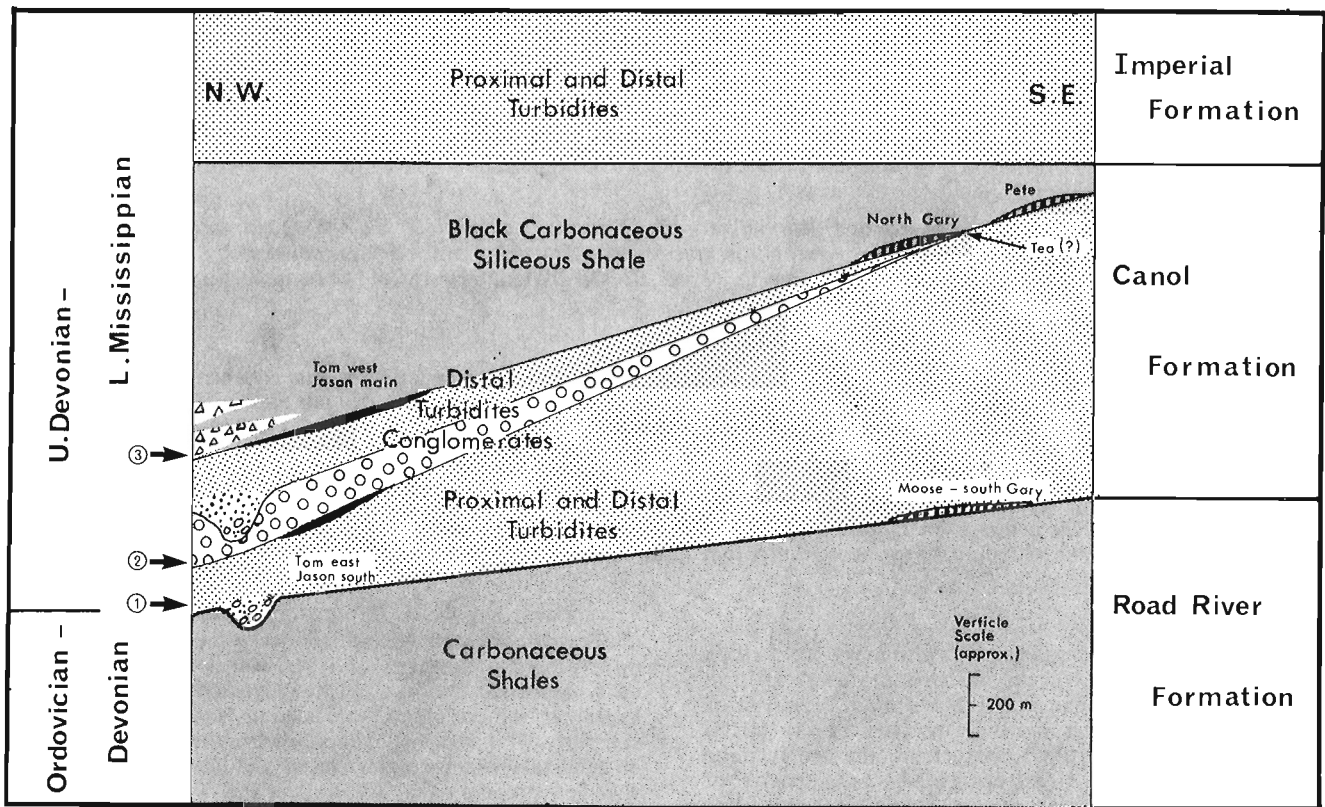


Figure 25.2. Schematic stratigraphic relationships within the graben structure after the data and interpretation of Smith (1978). Arbitrary horizontal datum is the base of the Imperial Formation. Numbered arrows refer to the tectonic episodes mentioned in text.

Smith (op. cit.) considered that the Moose – South Gary barite-chert-limestone deposit formed as the result of hydrothermal activity accompanying the first tectonic episode at the base of the Canol Formation. The high grade Tom-east and Jason-south zones are considered by him to be temporally associated with the second tectonic episode, whereas the lower grade, barite rich deposits of the Tom-west and Jason-main zones and the barite-chert-limestone deposits of North Gary (Gargantua) and Pete, accompanied the third and final tectonic episode. If the chert pebble conglomerate underlying the Tea deposit (Carne, 1976) is correlative with the chert pebble conglomerate horizon of the Tom-Jason area, then the Tea deposit is also approximately temporally associated with the third tectonic episode.

If, as this interpretation suggests, all the deposits are genetically associated with the same endogenic processes operating in the same area over a time interval probably short enough to consider the geothermal regime essentially constant, then the question remains as to why important lead-zinc sulphide concentrations accompany the barite mineralization in two localities (Tom, Jason) but not the others. It is a reasonable assumption that the reservoir temperatures of hydrothermal systems of the same area and same geothermal regime were essentially the same. Furthermore, if the evidence from volcanogenic massive sulphides is any indication, ore forming hydrothermal systems of the same area and essentially the same geological age, tend to originate from mineralogically similar (presumably the same) aquifer units (J.W. Lydon and C. Jay Hodgson, work in progress). Consequently, the physicochemical properties of hydrothermal solutions associated with the same endogenic processes in the same area during the same time interval should be correspondingly similar (Lydon, 1978a). The

chemical nature of solutions capable of transporting significant quantities of base metal and depositing them as sulphides (Lydon, 1977) is very similar to that required for the transportation of significant quantities of barium and its deposition as barite (Blount, 1977) in that both require that the dominant aqueous sulphur species be in a reduced form (H_2S , HS^- or S^{2-}) in order to achieve the very low activities of SO_4^{2-} that are permissible. Although differences in the reduced sulphur content could explain some variation in the barium:base metal content of hydrothermal solutions in the reservoir zone, there does not seem to be an adequate model to explain why the hydrothermal solutions simply did not leach any base metals during their generation if they were capable of leaching barium, and therefore alternate explanations for the differences in chemistry between the barite deposits and the zinc/lead-rich deposits must be sought. Several alternative models are suggested:

1. Differences in the Cooling Versus Oxidation Rates of the Discharged Hydrothermal Solutions.

The solubilities of sphalerite and galena increase with a) increasing temperature, b) the activity of the complexing ligand and c) increasing aSO_4^{2-}/aS^{2-} ratios at constant total sulphur contents of solution. According to Blount (1977) a) the solubility of barite decreases with increasing temperature in aqueous solutions of less than 1 molal NaCl but increases slightly in solutions with higher NaCl contents; b) the enhancement of the solubility of barite by increasing Cl^- concentrations is much less than that of sphalerite and galena, whereas c) an increase in aSO_4^{2-}/aS^{2-} ratio at constant total sulphur control of solution greatly decreases barite solubilities. Thus the three different processes of cooling, dilution and oxidation will tend to produce precipitates of

different sphalerite and galena:barite ratios from reduced solutions of initially similar temperature and chemical composition. Generally the sulphide/(sulphide + barite) ratio of the precipitate will progressively change from 1 to 0 as a reduced sulphur-containing aqueous solution is separately cooled, diluted or oxidized, the actual ratio and paragenesis depending upon the relative rates of these three distinct processes. In order to produce a barite precipitate free of lead and zinc sulphides, the rate at which reduced sulphur species are oxidized to the sulphate ion, which may then associate with the barium ion to precipitate barite, must greatly exceed the rate at which the reduced sulphur species associate with the metal ions to precipitate sulphides. That the cause of fractionation between metal sulphides and barite in a hydrothermal precipitate is largely a process of oxidation of the hydrothermal solutions is suggested by sulphur isotope studies on the Mogul 'G' Ireland (Grieg et al., 1971) and Rammelsberg, Germany (Anger et al., 1966) deposits, two well known examples of stratiform lead zinc deposits that show a lateral and vertical zonation from sulphide ore to barite ore. The studies indicate that the ore solutions undergo a progressive oxidation from the sulphide to the barite zones, and the fact that the majority of the barite samples have a sulphur isotope composition similar to that of contemporaneous ocean water further suggest that it is the mixing of oxygenated ocean water with the ore solutions that is the major cause of the oxidation process. This dual source of the sulphate ion (from contemporaneous ocean water and from the oxidation of hydrothermal reduced sulphur species) in the formation of stratiform barite deposits is consistent with the sulphur isotope distribution patterns both in sulphide/barite deposits (Anger et al., op. cit.) and laterally extensive barren barite (perhaps aptly called baritite) formations devoid of any known sulphide mineralization, such as in the Upper Devonian of Nevada (Rye et al., 1978).

If this argument is correct, then the rate of oxidation of hydrothermal solutions discharged into a marine environment, and therefore the barite:sulphide ratio of the deposit, is largely determined by the rate and extent of mixing of the hydrothermal solutions with marine water. Apart from density considerations (Sato, 1972), the rate of discharge and local submarine topography are perhaps the most important factors which determine the rate and extent of this mixing process. High rates of discharge into a topographic basin provide the optimum conditions for the displacement of marine water from the vent area, and the brine barrier or pool thus formed would tend to insulate succeeding hydrothermal flow from immediate interaction with normal marine water. Low rates of discharge, especially from topographic highs, are less likely to effect any significant displacement of or modification to the chemistry of the ambient marine waters, and hence the immediate reaction between any dissolved barium and marine sulphate to form barite would be inevitable. It is thought that such a process involving low discharge rates, or seepage, of hydrothermal solutions is responsible for the high barite concentrations found in sediment of the East Pacific Rise (Boström, et al., 1973).

2. Concentrations of Barite by Mechanical Processes

Although, as can be surmised from the above discussion and a review of the literature, there is strong evidence that most stratiform barite deposits are chemical precipitates, the possibility exists that mechanical processes may have been important in the formation of the Macmillan Pass area deposits. There is evidence (graded bedding, crossbedding, slump structures, etc.) in some stratiform barite deposits that there has been mechanical movement of the barite, and some barite deposits have been ascribed a dominantly detrital origin (Heinrichs and Reimer, 1977; Reimer, 1978). The fact

that the Gary, Moose and Pete deposits occur in lower fan turbidite sequences down current from a potential barite source (the Tom-Jason area) may provide the basis for an argument that the laminated barite deposits are themselves turbidites that were transported and deposited under conditions too oxidizing for the preservation of sulphides. However, the mineralogical assemblages of barite, quartz (chert) and calcite (limestone) that comprise these deposits suggests that the association is the result of a chemical, and not a mechanical, induction.

3. Biochemical Concentration of Barium

The possibility that barite concentration may result from the biochemical cycles of the oceans has been entertained by some authors e.g. Revelle et al. (1955). However, such deposits would be of great lateral extent and could only reach significant levels of barite concentration in sedimentary basins starved of detrital material for considerable time periods. Since this is not compatible with the geological setting of the Macmillan Pass deposits, such an origin for them is not considered probable.

The Significance of the Tea Barite Deposit

The geology of the Tea barite deposit has been described by Carne (1976). The feature of this deposit with the most fundamental implications in the formulation of a genetic model applicable to the Macmillan Pass area deposits was the reported occurrence of witherite as a significant mineralogical constituent. From the description and measured section published by Carne (op. cit.), it appeared that the witherite was interbedded with the barite, chert and limestone that formed the remainder of the mineralized succession, and thus may have been a primary chemical sediment. The chemical significance of a witherite-barite-calcite assemblage can be conveniently explained in terms of Figure 25.3.

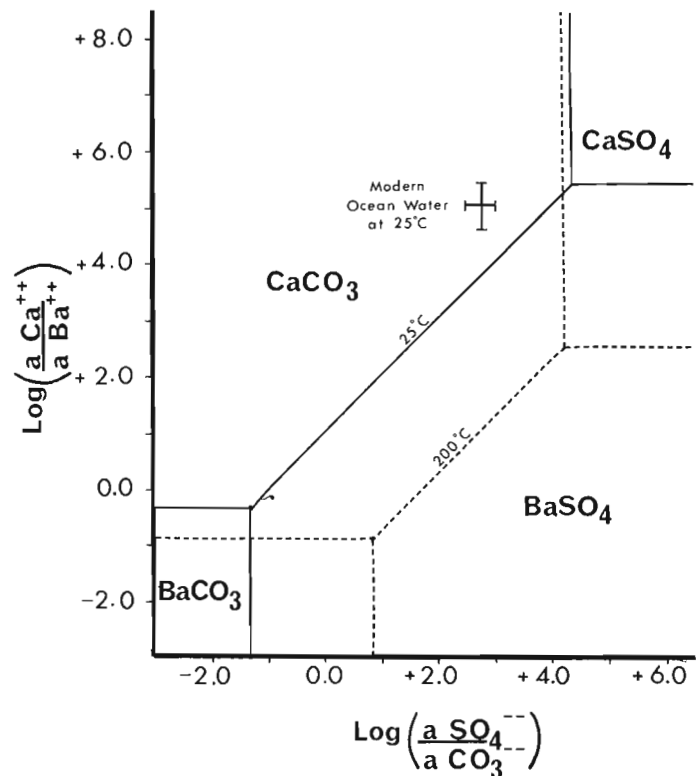
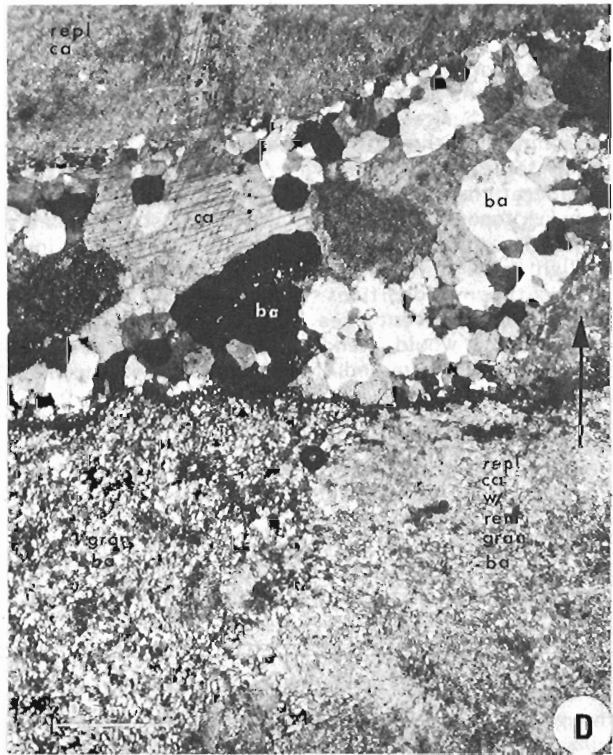
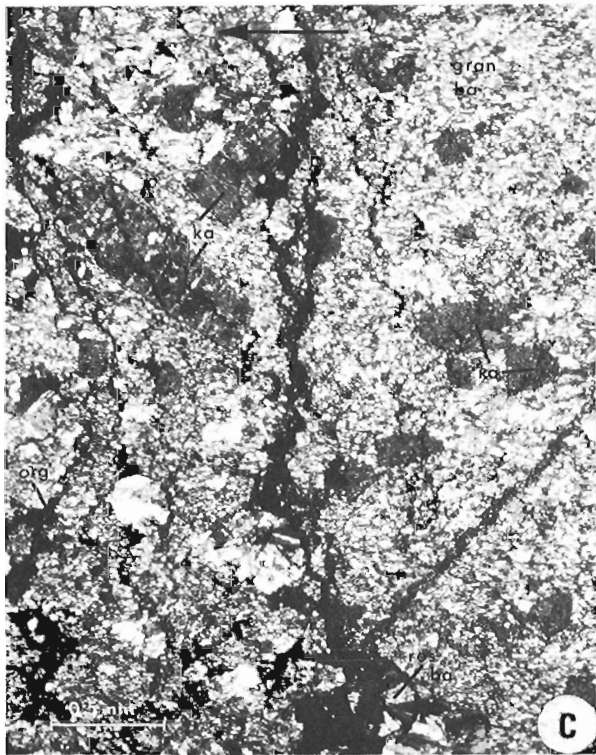
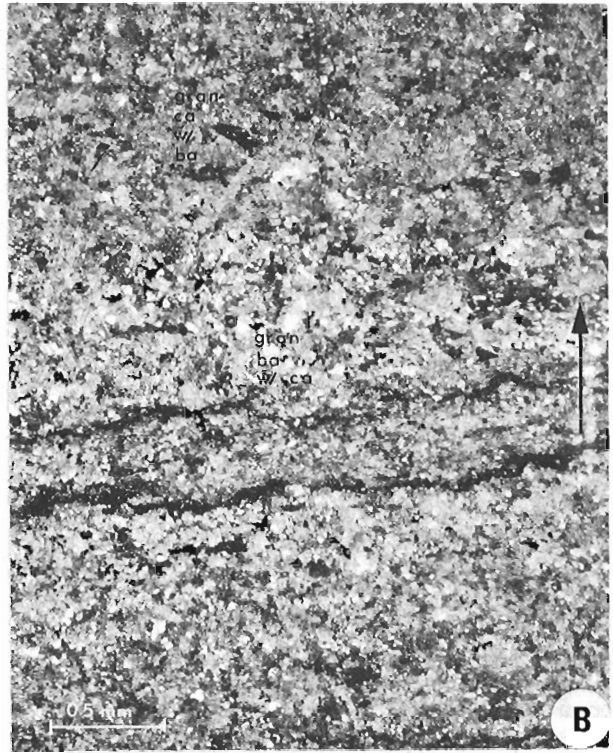
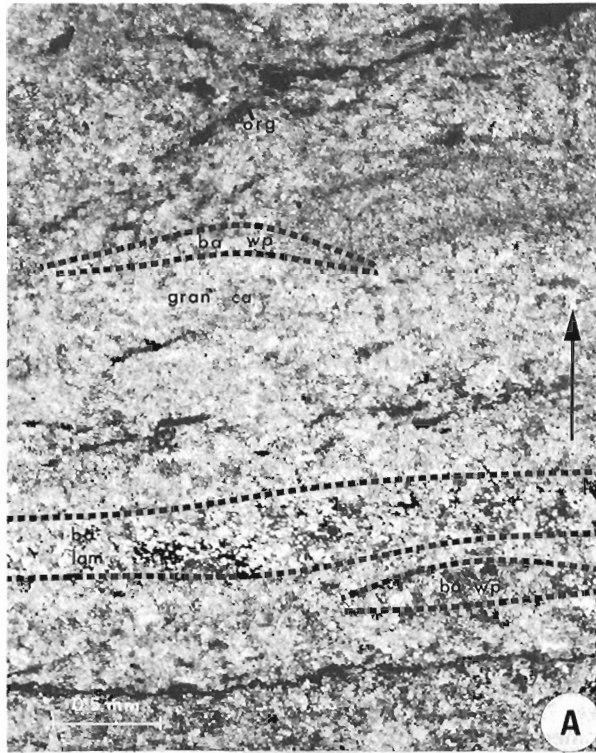


Figure 25.3. Activity diagram of part of the system CaO-H₂O-CO₂-H₂SO₄ at 1 atmosphere pressure.



ba = barite	org = organic material	wp = wisp
ca = calcite	gran = granular	ros = rosette/concretion
ka = kaolinite	lam = lamination	repl = replacement

Figure 25.4. Photomicrographs showing some textural and structural relationships in baritic rocks of the Tea deposit. Crossed polarizers. Arrows indicate stratigraphic tops.

The thermodynamic data used in the construction of this diagram was obtained from a variety of sources. The dissociation constants of calcite, anhydrite, barite and witherite at 25°C and 1 atmosphere were calculated from ΔH_f° and S° values for the ions reported in Helgeson (1969) and for the crystalline phases reported in Helgeson et al. (1978). Significant discrepancies exist for the reported value of ΔH_f° for witherite, and the value used to give a Log K association of 8.3 represents an average of the values obtained from the data listed by Garrels et al. (1960), Garrels and Christ (1965), Krauskopf (1967) and the Handbook of Chemistry and Physics (59th edition). The range of values listed by these authors would give an uncertainty of about ± 0.5 log units to the field of witherite at 25°C on Figure 25.3. The phase boundaries at 200°C were calculated directly from the dissociation constants for calcite, anhydrite and barite calculated by Helgeson (1969) and from the dissociation constant for witherite determined experimentally by Malinin (1963). The molalities of chemical species in modern ocean water at 25°C and 1 atmosphere were taken from Garrels and Thomson (1962), Woolery and Walters (1975), Table 12-6 in Smith (1974), and Krauskopf (1967). Activity coefficients used for Ca^{++} , Ba^{++} , SO_4^- and CO_3^- were 0.28, 0.23, 0.21 and 0.20 respectively. The bars in Figure 25.3 represent the range of the activity ratios in modern ocean water obtained from the variation in the data set used. The composition of ocean water has probably changed with time, as, for example, suggested by sulphur isotope data (Thode and Monster, 1965), but its position on Figure 25.3 for the Devonian-Mississippian is unlikely to be far removed from that of modern oceans, as indicated by the occurrence of limestones and evaporites of that age period.

As can be seen from Figure 25.3, a coevally precipitated calcite-barite-witherite assemblage would indicate that the chemical characteristics of the coexisting aqueous solution at 25°C must be far removed from that of normal ocean water. Since the topology of the diagram changes only slightly with temperature (phase boundaries at 200°C are indicated for comparison), the same observation would apply for all likely temperatures of deposition. Considering the low activity product for barite and assuming calcium concentrations within an order of magnitude of modern ocean water, it may be deduced that the major difference would be that the solutions from which the witherite precipitated must have been virtually depleted in the sulphate ion. Various circumstances can be envisaged to explain this condition:

1. The sulphur of the coexisting solutions was in a reduced state, and hence precipitation possibly took place in a hydrothermal brine pool. In this case, according to the above model, the absence of sulphides would be anomalous and therefore either the model is in need of revision or the presence of sulphides should be sought.
2. The coexisting solutions actually were sulphur deficient, in which case they may have been fresh water and not marine. This would imply misinterpretation of the geology of the area and that the setting was, say, estuarine and not marine. The presence of large quantities of barite in the deposit, however, dictates that sulphur was an abundant constituent of the aqueous system.
3. The sulphate deficiency during witherite precipitation could be explained by the fixation of aqueous sulphate present in barite. This would imply that barium concentrations and discharge rates of the mineralizing solution were very high, in order to maintain a displacement of normal ocean water. Again, following the predictions of the model, a sulphide deposit would be expected under such conditions.

In order to investigate these and other implications, an examination of the Tea barite deposit was undertaken, to determine, as the first step, the relation of the reported witherite to the barite and calcite, and in particular whether the witherite actually was a primary sediment, or whether it was a secondary alteration product. Witherite is a rare mineral in stratiform base metal or barium deposits, having been reported in significant quantities only in the Rosh Pinah deposit, where it is one of several secondary barium minerals (Page and Watson, 1976). Its presence as a possible primary mineral at the Tea deposit was therefore of great scientific interest.

Sampling and Analytical Procedures and Results

Not knowing the exact location of Carne's (1976) measured section through the barite horizon (2b), carbonate horizons were identified by their effervescence when sprayed with dilute hydrochloric acid. The identification of two main carbonate-rich sections, one about 10 m thick in the lower part of the main natural exposure on the property and the other about two thirds up the exposure, seemed to correspond to the main witherite bearing sections mapped by Carne. A total of 18 samples were taken of the effervescent rock and its contacts with adjacent barite.

In the laboratory all the samples were tested for acid soluble barium by digesting about 1 g of pulverized rock in dilute hydrochloric acid for about 5 minutes, filtering, and then adding the filtrate to test tubes containing dilute sulphuric acid. The presence of barium would be indicated by the immediate precipitation of barium sulphate, which would impart an homogeneous milky appearance to the solution. The sensitivity of the method was verified by spiking a nonreactive sample (of barite) with about 5 per cent by weight of witherite, which produced the typical milky turbidity. All the samples collected from the Tea property gave a negative reaction to this test. Those samples rich in calcite, however, did produce a precipitate of calcium sulphate (verified by XRD). However, the calcium reaction is distinct from the barium reaction, in that there is a 2-5 second delay in precipitation of the calcium sulphate, which forms clots of fine needle-like crystals rather like shreds of cottonwool, as compared to the immediate crystallization of granular barium sulphate which forms the typical "barium milk". With high concentrations of calcium, the interlocking needles of calcium sulphate temporarily so effectively "bound" the solution that the test tube could be inverted without any loss of liquid, a phenomenon which did not happen with a barium sulphate precipitate.

The dominant mineralogy of 16 Tea samples was determined by X-ray diffractometry to be barite mixed in various proportions with calcite and/or quartz. Witherite, anhydrite and gypsum were not detected.

Examination of thin sections shows that most of the primary mineralogy is fine grained (<50 microns) and granular. There is a gradation from wisps and laminae of barite granules in a granular calcite matrix (Fig. 25.4A), through barite granules scattered in a granular calcite matrix (Fig. 25.4B) to barite composed entirely of barite granules (bottom left hand of Fig. 25.4D). Organic material is common as small patches elongated parallel to the bedding and as concentrations along stylolites (Fig. 25.4A, 4B, 4C). In places and perhaps more prominently near the upper and lower contacts of the barite section, calcite appears to be replacing the granular barite. In these cases, the matrix calcite is in optical continuity over several millimetres, and may (bottom right hand part of Fig. 25.4D) or may not (top of Fig. 25.4D) contain remnant granular barite. Replacement of barite by calcite has been described from other barite deposits (Bogoch and Shirav, 1978). A small proportion of the

total barite and calcite occurs as much coarser crystals in veins (4D). Bladed or prismatic barite common in some deposits (e.g. Heinrichs and Reimer, 1977; Bogoch and Shirav, 1978; Lydon, 1978b) was not observed in the thin sections. However some horizons contain rosettes or concretions of barite (4C), another commonly described form (e.g. Shawe et al., 1969) and which are interpreted as diagenetic features. The dark pseudomorphs in Figure 25.4C were determined by X-ray powder diffraction (Debye-Scheerer camera method) to consist of kaolinite and minor barite, and also were probably an original diagenetic feature, although their original mineralogy has not yet been determined.

Conclusions

The fine grained granular nature of the barite and calcite, their megascopic and microscopic structural relationships, and the diagenetic features suggest that both were constituents of a primary sediment. However, the investigations to date have failed to confirm the presence of witherite. In view of the fact that Carne's original identification did not include an X-ray confirmation (R.C. Carne, pers. comm.) the presence of significant witherite at the Tea deposit should perhaps be regarded as only a tentative identification pending further investigations.

With reference to Figure 25.3, it can be seen that a calcite-barite assemblage may coexist with solutions that are only slightly modified ocean water. The main difference is that the barium content would have to be increased by one or two orders of magnitude, which could theoretically be accomplished by the addition of a few ppm Ba to ocean water. As noted above, this would imply the involvement of hydrothermal solutions in the process of mineralization. The close association of primary calcite with the barite, suggests that the precipitation of the former may depend on the precipitation of the latter, if both calcium and barium were transported by brines of the Na-Ca-Cl type, but the great affinity of the sulphate ion for barium allowed calcium saturation only with respect to the carbonate.

The present investigation of the Tea deposit based only on qualitative mineralogy does not lead to an unequivocal interpretation of the nature and origins of the solutions responsible for the stratiform barite or barite/sulphide deposits of the Macmillan Pass area. Further investigations are planned, based not only on more detailed field examinations but on other laboratory methods and interpretative models such as quantitative mineralogy and sulphur isotope fractionation patterns.

Acknowledgments

The field work benefitted greatly from the guidance, co-operation and hospitality of the mining exploration companies working in the area, and in this regard the authors would like to thank Drs. Clyde Smith and K. Lu (Ogilvie Joint Venture), Mr. O.S. Hairsine (Cordilleran Engineering Ltd.) and Mr. Ken Taylor (Hudson Bay Exploration and Development). Mr. J.S. Brock (Welcome North Mines) is thanked for his permission to examine and sample the Tea deposit. Mr. A.C. Roberts carried out the XRD determinations by the Debye-Scheerer camera method. Dr. D.F. Sangster acted as critical reader, and he is thanked for his suggestions that improved the quality of the manuscript.

References

- Anger, G., Nielsen, H., Puchelt, H., and Ricke, W.
1966: Sulfur isotopes in the Rammelsberg ore deposit (Germany); *Economic Geology*, v. 61, p. 511-536.
- Blount, C.W.
1977: Barite solubilities and thermodynamic quantities up to 300°C and 1400 bars; *American Mineralogist*, v. 62, p. 942-957.
- Bogoch, R. and Shirav, M.
1978: Petrogenesis of a Senonian barite deposit, Judean Desert, Israel; *Mineralium Deposita*, v. 13, p. 383-390.
- Bostrom, K., Joensum, O., Moore, C., Bostrom, B., Dalziel, M., and Horowitz, A.
1973: Geochemistry of barium in pelagic sediments; *Lithos*, v. 6, p. 159-174.
- Carne, R.C.
1976: The Tea barite deposit; Canada Department of Indian and Northern Affairs, Open File Report EGS 1976-16, p. 20-31.
- Dawson, K.M.
1977: Regional metallogeny of the Northern Cordillera; in Report of Activities, Part A, Geological Survey of Canada, Paper 77-1A, p. 1-4.
- Garrels, R.M. and Christ, C.L.
1965: Solutions, minerals, and equilibria; Harper and Row Publishers, New York, 450 p.
- Garrels, R.M. and Thomson, M.E.
1962: A chemical model for sea water at 25°C and one atmosphere total pressure; *American Journal of Science*, v. 260, p. 57-66.
- Garrels, R.M., Thomson, M.E., and Siever, R.
1960: Stability of some carbonates at 25°C and one atmosphere total pressure; *American Journal of Science*, v. 258, p. 402-418.
- Greig, J.A., Baadsgaard, H., Cumming, G.L., Folinsbee, R.E., Krouse, H.R., Ohmoto, H., Sasaki, A., and Smejkal, V.
1971: Lead and sulphur isotopes of the Irish base metal mines in Carboniferous host rocks; *Society of Mining Geology Japan, Special Issue 2*, p. 84-92.
- Heinrichs, T.K. and Reimer, T.O.
1977: A sedimentary barite deposit from the Archean Fig Tree Group of the Barberton Mountain Land (South Africa); *Economic Geology*, v. 72, p. 1426-1441.
- Helgeson, H.C.
1969: Thermodynamics of hydrothermal systems at elevated temperatures and pressures; *American Journal of Science*, v. 267, p. 729-804.
- Helgeson, H.C., Delany, J.M., Nesbitt, H.W., and Bird, D.K.
1978: Summary and critique of the thermodynamic properties of rock forming minerals; *American Journal of Science*, v. 278-A, 229 p.
- Krauskopf, K.B.
1967: Introduction to geochemistry; McGraw-Hill Inc., 721 p.

- Lydon, J.W.
 1977: The significance of metal ratios of hydrothermal ore deposits; Unpublished Ph.D. thesis, Queen's University, Kingston.
 1978a: Some criteria for the categorization of hydrothermal base metal deposits; in *Current Research, Part A*, Geological Survey of Canada, Paper 78-1A, p. 299-302.
 1978b: Observations on some lead-zinc deposits of Nova Scotia; in *Current Research, Part A*, Geological Survey of Canada, Paper 78-1A, p. 293-298.
- Malinin, S.D.
 1963: An experimental investigation of the solubility of calcite and witherite under hydrothermal conditions; *Geochemistry*, No. 7, p. 650-667 (transl.).
- Page, D.C. and Watson, M.D.
 1976: The Pb-Zn Deposit of Rosh Pinah Mine, South West Africa; *Economic Geology*, v. 71, p. 306-327.
- Reimer, T.D.
 1978: Detrital barytes in the Karoo supergroup of southern Africa; *Mineralium Deposita*, v. 13, p. 235-244.
- Revelle, R.R., Bramlette, M., Arrhenius, G., and Goldberg, E.D.
 1955: Pelagic sediments in the Pacific; *Geological Society of America*, Special Paper 62, p. 221-236.
- Rye, R.O., Shawe, D.R., and Poole, F.G.
 1978: Stable isotope studies of bedded barite at East Northumberland Canyon in Toquima Range, Central Nevada; U.S. Geological Survey, *Journal of Research*, v. 6, p. 221-229.
- Sato, T.
 1972: Behaviours of ore-forming solutions in sea water; *Mining Geology (Tokyo)*, v. 22, p. 31-42.
- Shawe, D.R., Poole, F.G., and Brobst, D.A.
 1969: Newly discovered bedded barite deposits in East Northumberland Canyon, Nye County, Nevada; *Economic Geology*, v. 64, p. 245-254.
- Smith, C.L.
 1978: Geological setting of Jason and Tom deposits, Macmillan Pass area, Eastern Yukon; Summary of presentation, Whitehorse Geoscience Forum 1978, 6 p.
- Smith, F.G. (editor)
 1974: *Handbook of marine science*; Volume 1, CRC Press, Inc., 627 p.
- Thode, H.G. and Monster, J.
 1965: Sulfur-isotope geochemistry of petroleum, evaporites, and ancient seas; in *Fluids in subsurface environments*, American Association of Petroleum Geologists, *Memoir* 4, p. 367-377.
- Woolery, T.J. and Walters, L.J.
 1975: Calculation of equilibrium distributions of chemical species in aqueous solutions by means of monotone sequences; *Mathematical Geology*, v. 7, p. 99-115.

26. **GEOLOGICAL/GEOPHYSICAL STUDIES IN BAFFIN BAY AND SCOTT INLET-BUCHAN GULF AND CAPE DYER-CUMBERLAND SOUND AREAS OF THE BAFFIN ISLAND SHELF**

Projects 760015 and 760039

B. MacLean and R.K.H. Falconer
Atlantic Geoscience Centre, Dartmouth

MacLean, B. and Falconer, R.K.H., Geological/geophysical studies in Baffin Bay and Scott Inlet-Buchan Gulf and Cape Dyer-Cumberland Sound areas of the Baffin Island Shelf; in Current Research, Part B, Geological Survey of Canada, Paper 79-1B, p. 231-244, 1979.

Abstract

Marine geological and geophysical studies on the Baffin Island shelf in 1978 by the Atlantic Geoscience Centre were concentrated in the Scott Inlet oil seep area and in the Buchan Gulf area on the northeastern part of the shelf, and between Cape Dyer and Cumberland Sound on the southeastern part of the shelf.

Upper Cretaceous (Senonian) marine calcareous siltstones underlie central and inner Buchan Gulf Trough. These, and possibly older strata, probably underlie Tertiary rocks offshore from Scott Inlet and may locally outcrop. Pre-Tertiary strata flanking a structural high at the outer part of the south wall of Scott Trough are a probable source of hydrocarbon seepage. Gravity and magnetic data at Scott Inlet indicate a thick sedimentary section, whereas the Buchan Gulf section probably is thinner.

Earthquake activity in northern Baffin Island and Baffin Bay was monitored with three ocean bottom seismometers in the Bay and three temporary seismographs onshore. At least forty events were detected in ten days.

Studies of the shelf south of Cape Dyer further delineated the extent of various rock units and outlined a diapiric ridge structure that extends over a distance in excess of 80 km.

Introduction

Geological and geophysical programs to extend on-going studies of the geology of the Baffin Island continental shelf and to measure seismicity in Baffin Bay were carried out from Bedford Institute of Oceanography's **C.S.S. Hudson** during September 18 – October 23, 1978 (cruise 78-029). The shelf studies were concentrated in two main areas: 1) in the vicinity of the oil seep offshore from Scott Inlet and in the adjoining Buchan Gulf area on the northeastern part of the shelf, and 2) between Cape Dyer and Cumberland Sound on the southeastern part of the shelf. Geophysical studies and a few sample stations were carried out enroute between the two main study areas on the shelf. Cruise track and stations occupied are indicated in Figures 26.1, 26.2. The seismicity studies were carried out with ocean bottom seismometers placed off the shelf east of Pond Inlet in conjunction with Earth Physics Branch shore stations.

The continental shelf studies were directed toward 1) delineating the areal extent and structural relationships of the main bedrock units, 2) obtaining information as to the age, lithology and physical properties of these rocks, and 3) attempting to identify the geological origin of the oil seep in Scott Inlet area more closely. These studies were carried out by means of conventional shallow seismic and Huntex high resolution reflection profiling, bathymetric, magnetic, gravity and sidescan sonar profiling, and seismic refraction measurements, all in conjunction with geologic sampling using the BIO underwater electric drill and by dredging. The techniques employed have been outlined previously by MacLean et al. (1977, 1978). Bedrock sampling in the Cape Dyer – Cumberland Sound area was considerably hampered by bad weather.

Vibracoring, piston coring, grab sampling and bottom photography were carried out along with the acoustic profiling to obtain additional reconnaissance data on the unconsolidated sediments.

Scott Inlet – Buchan Gulf Area

A submarine trough which is cut some 700 m into the predominantly sedimentary rocks of the shelf extends seaward from the mouth of Scott Inlet fiord. A similar trough extends across the shelf from the mouths of Royal Society, Cambridge, and adjacent fiords collectively referred to as the Buchan Gulf area, 90 km north of Scott Inlet. In 1976 an oil seep was discovered at Scott Inlet (Loncarevic and Falconer, 1977). During further studies in 1977 oil slicks were observed north of Scott Inlet (Levy, 1978). This, plus the structural similarity of Buchan Trough to Scott Trough suggested that oil might also be seeping at Buchan Trough.

Regional interpretations of the geology and the free air gravity in the Scott Inlet – Buchan Gulf area are shown in Figures 26.3, 26.4. The coastal landmass is composed of Precambrian metamorphic complexes, locally mantled by Quaternary glacial and marine foreland deposits (Jackson et al., 1979). Offshore the general bedrock pattern, which is the subject of this paper, is one of sedimentary rocks underlying most of the shelf and the occurrence of basement highs near the shelf edge. The stratigraphic succession offshore is known to include Upper Cretaceous (Senonian) rocks in the floor of Buchan Trough and Tertiary (late Eocene) strata in the walls of Scott Trough. These age assignments are from palynological studies of drill cores and dredge samples by G.L. Williams (pers. comm., 1978, 1979).

Studies in the Scott Inlet area in 1978 confirmed the presence of a structural high outcropping at the south wall of the submarine trough and supported its association with hydrocarbon seepage as reported by MacLean (1978) from reconnaissance of the area in 1977. In detail, the high consists of two basement ridges separated at the surface by strata that occupy a small half-graben (Fig. 26.5). Two short drill cores of metamorphic rocks were recovered from the westernmost of the ridges (Fig. 26.3, 26.5, Table 26.1). Positive magnetic and gravity anomalies are associated with

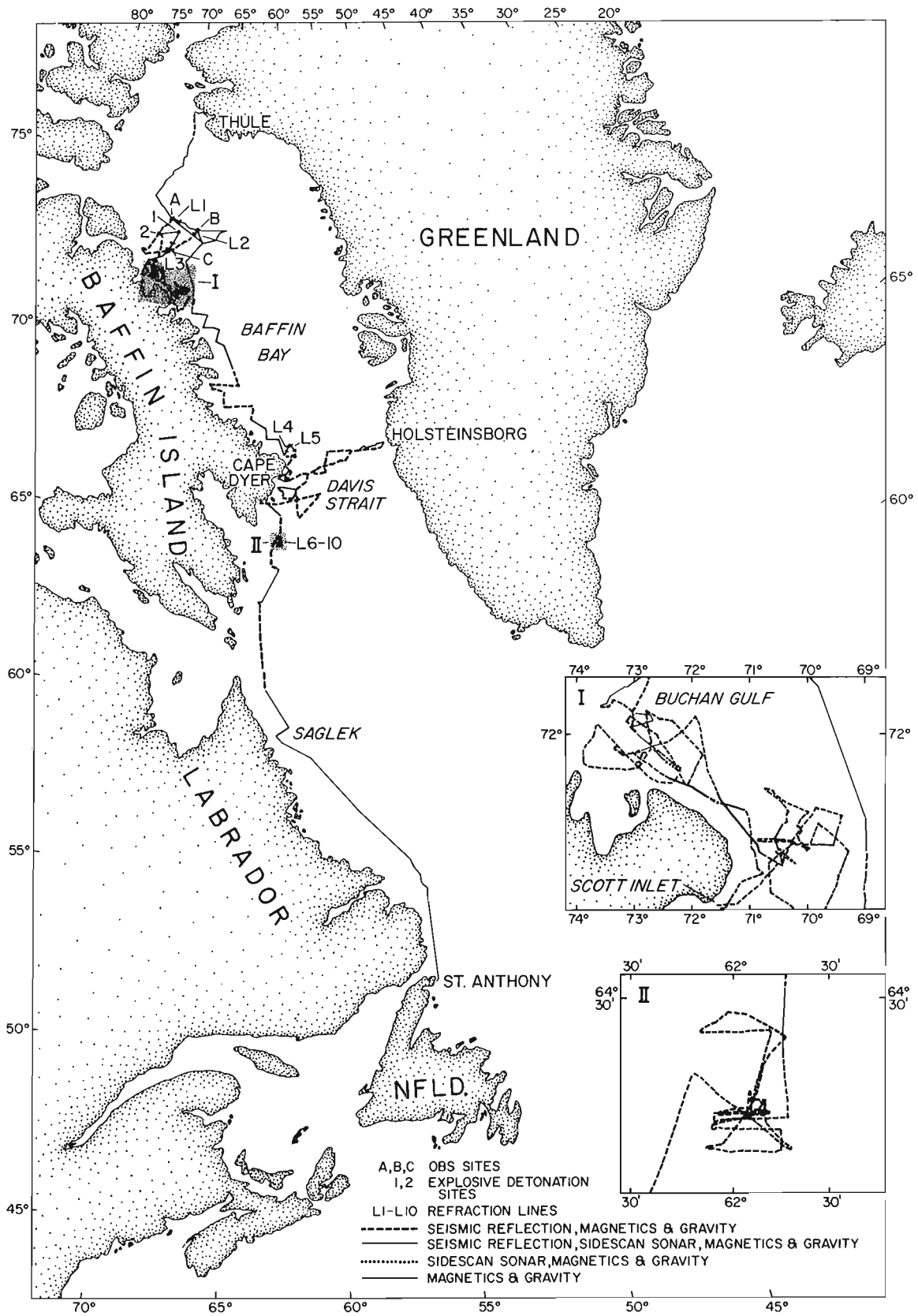


Figure 26.1. Tracks showing types of underway data collected and ocean bottom seismometer sites. Cruise 78-029.

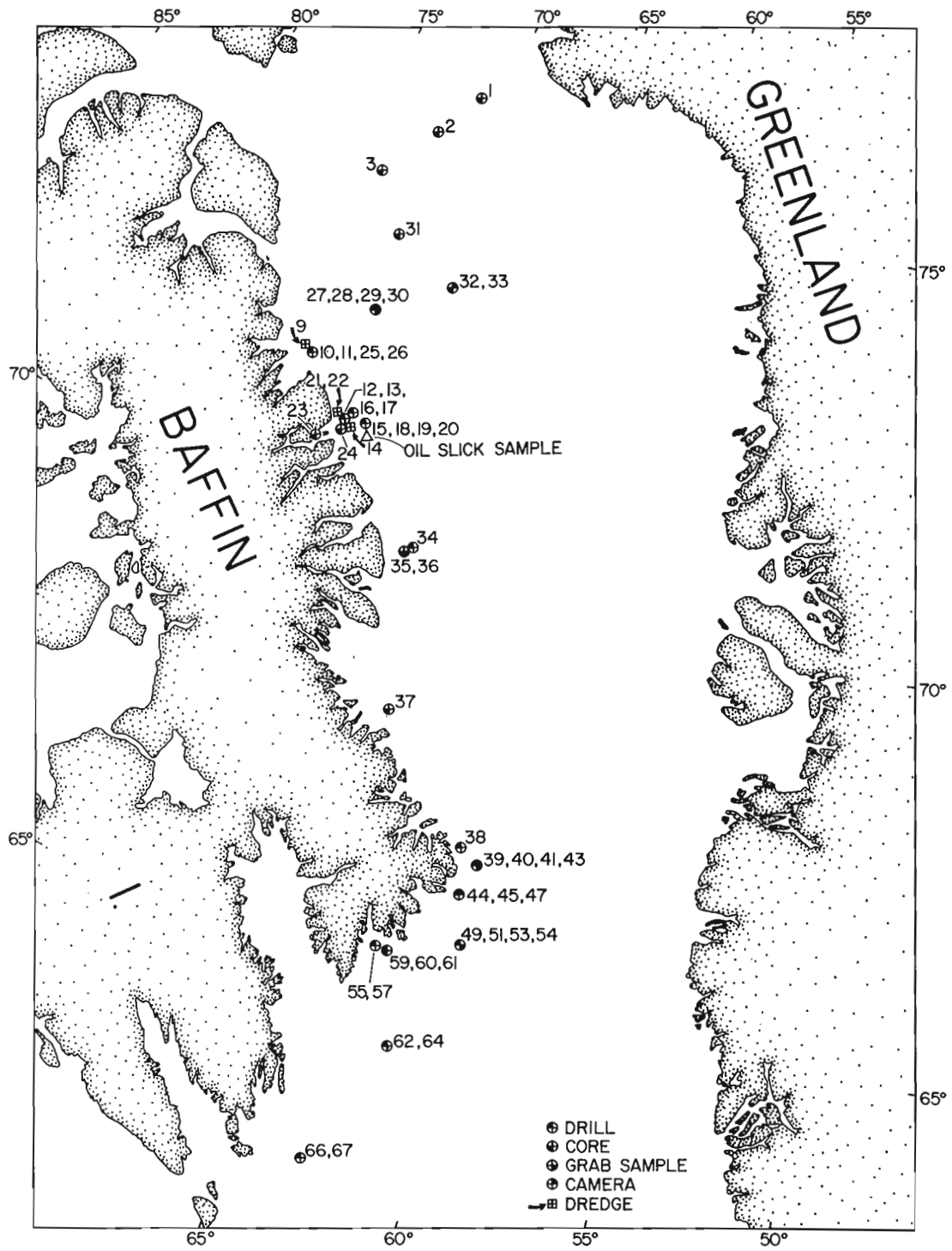


Figure 26.2. Geological stations occupied during cruise 78-029.

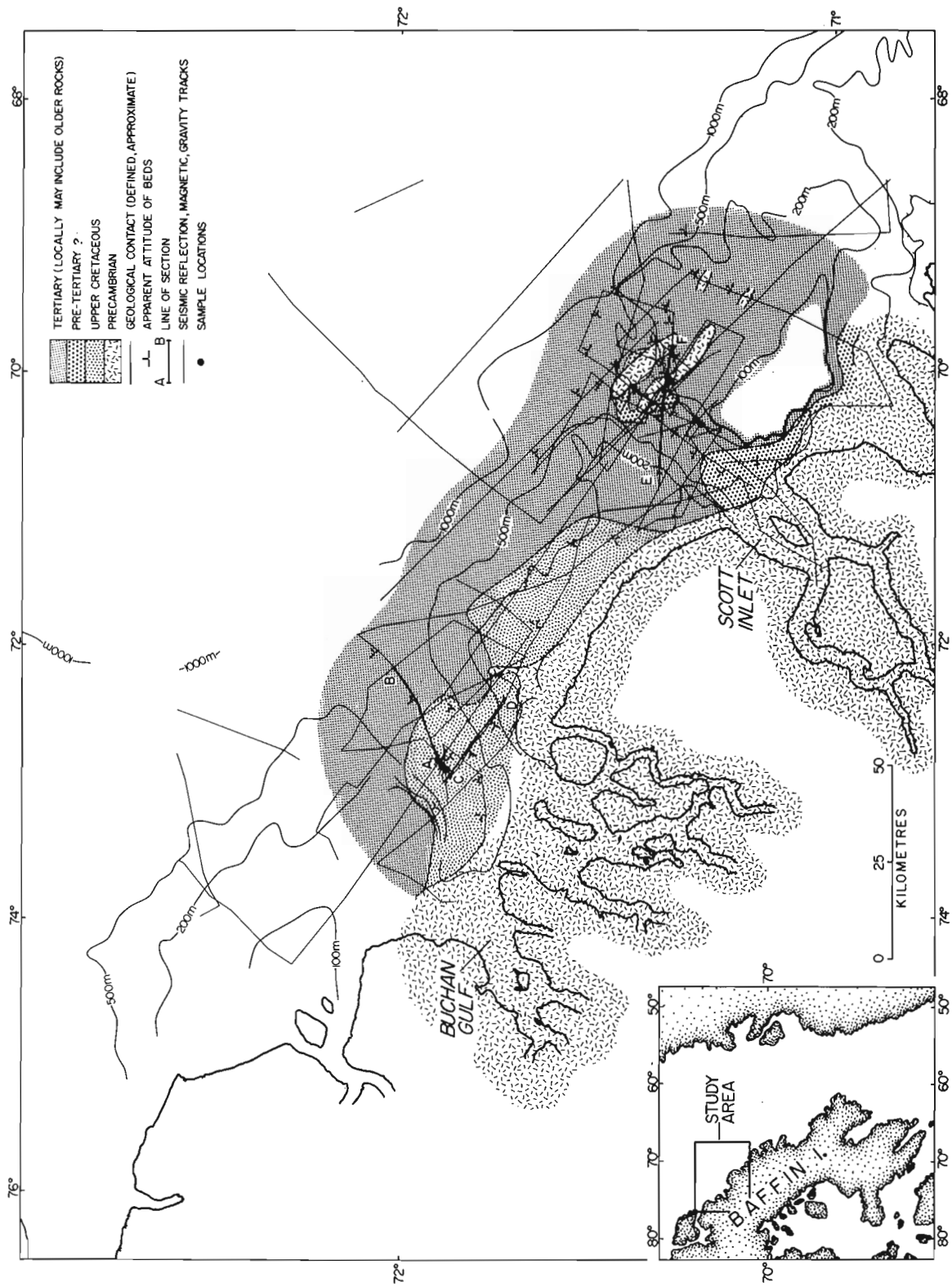


Figure 26.3. Geological map of Scott Inlet — Buchan Gulf offshore area. Control tracks (seismic reflection, together with gravity and magnetic profiles) and sample stations are indicated. The unstippled area within the 100 m bathymetric contour east of the entrance to Scott Inlet fiord contains shallow water (Hecla and Griper Banks) and so far has not been geophysically surveyed.

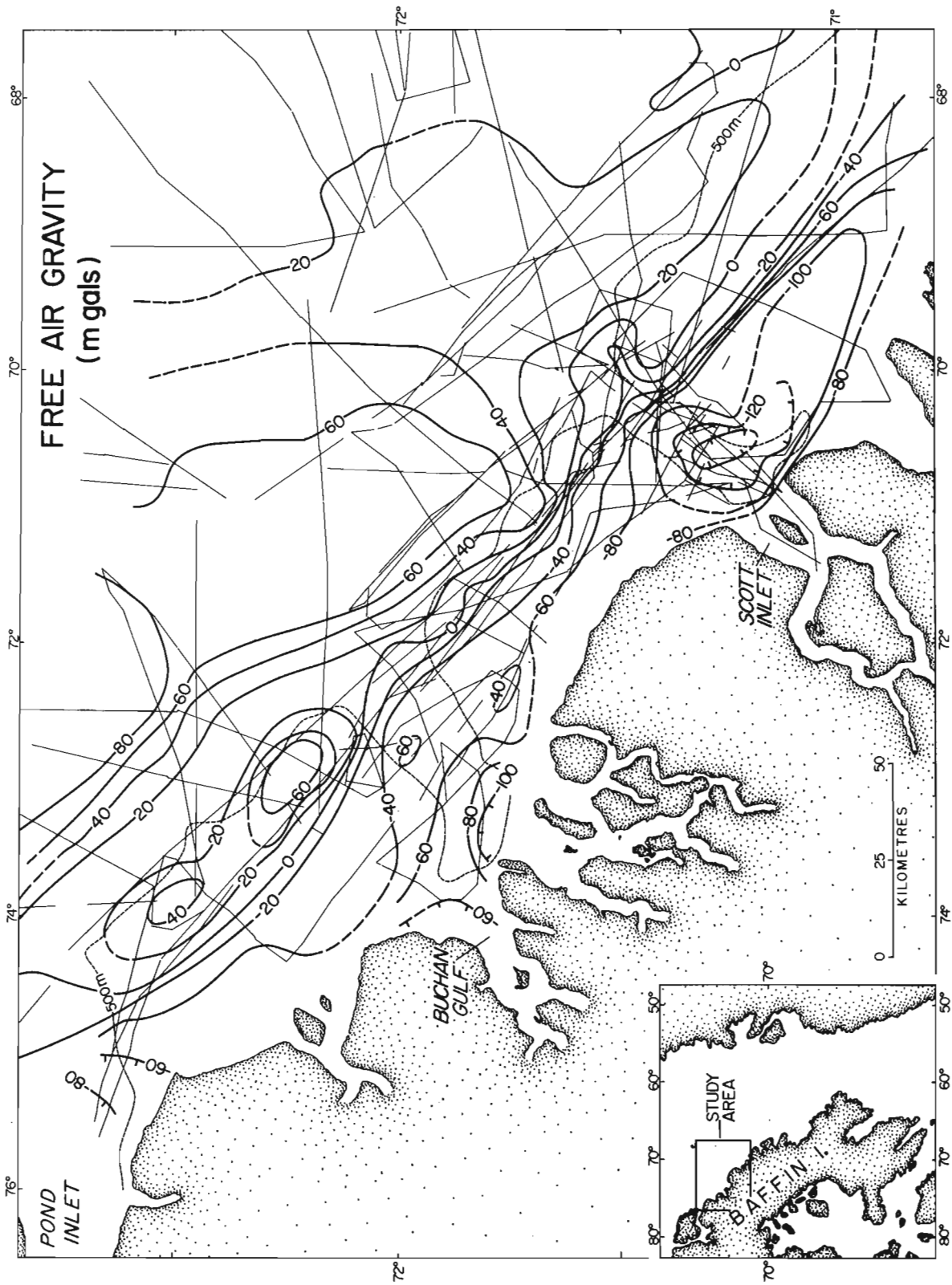


Figure 26.4. Free air gravity map of Scott Inlet – Buchan Gulf offshore area. Solid lines indicate gravity tracks. The dashed line marks the 500 m bathymetric contour.

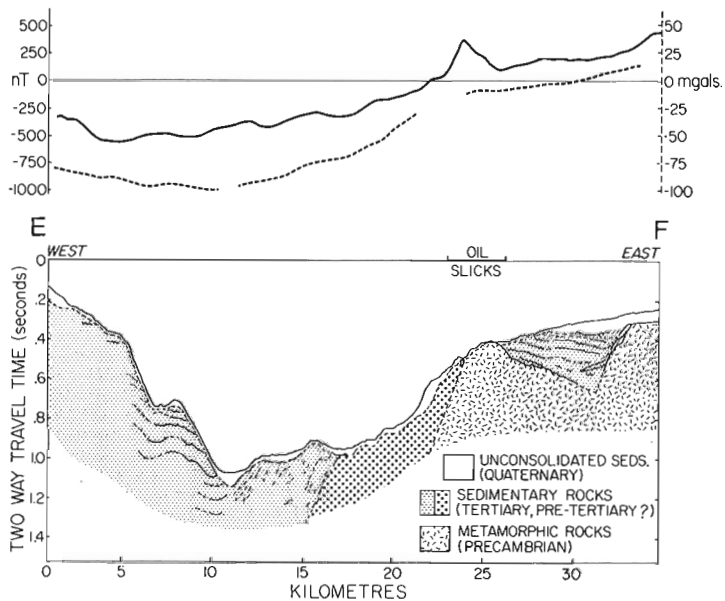


Figure 26.5. Cross-section E-F (see Fig. 26.3 for location) across the outer part of Scott Inlet trough showing Precambrian rocks of the structural high and adjoining sedimentary sequences. The extent of an oil slick along track over the westernmost basement ridge on September 24, 1978 is also indicated. Magnetic (solid) and gravity (dashed) profiles accompany the section.

the ridges. The basement high extends south as a subsurface feature to at least 69°W. Magnetic anomalies suggest that the high extends right across the mouth of the trough. However, it must plunge northward as it is not seen on seismic reflection profiles beyond the mid-line of the trough. Elsewhere the walls of the Scott trough consist mainly of flat-lying Tertiary strata as seen at the western side of the trough in Figure 26.5. However, towards the basement high these rocks assume a westerly dip. Strata flanking the western side of the high (Fig. 26.3, 26.5) are acoustically harder than the overlying Tertiary sediments. Rocks of similar seismic and magnetic character underlie the inner part of the Scott Trough. These rocks (designated pre-Tertiary on Fig. 26.3, 26.5) apparently are acoustically harder than the Upper Cretaceous rocks in Buchan Trough and may be older. Strata in the floor midway along Scott Trough have been disturbed by folding and faulting, but seem to be part of the Tertiary sequence sampled by MacLean (1978) that forms the walls, so have been mapped with that unit. They may, however, locally include some Upper Cretaceous strata, which are presumed to be present beneath the Tertiary sequence here as at Buchan.

Scott Inlet is marked by a very conspicuous gravity negative of -145 mgals (Fig. 26.4). This anomaly is a local feature superimposed on a regional coast parallel negative trend which is coincident with a continuous U-shaped magnetic anomaly landward of the offshore basement high. The regional gravity and magnetic negatives extend north of where, on the basis of magnetics, the basement high ends just north of Scott Inlet. A refraction line of Jackson et al. (1977) between Scott and Buchan inlets along the zero milligal contour revealed 4 km of sediment. The regional magnetic and gravity negatives suggest that even more sediment may be present in the structural depression extending from south of Scott Inlet northward across the trough. The sedimentary

Table 26.1
1978 bedrock sample station* data

Station	Location		Water Depth (m)	Seafloor Penetration (cm)	Results
	Lat.	Long.			
10	71°53.6'N	72°55.3'W	567	243	19 cm core dark grey siltstone
19	71°23.7'N	70°03.3'W	269	392	61 cm core metamorphic rock
20	71°23.1'N	70°03.9'W	274	177	73 cm core metamorphic rock
22	71°19.0'N	70°23.9'W	dredged interval 640 – 550 m		sandstone sample recovered
25	71°54.3'N	72°53.8'W	545	341	18 cm core dark grey siltstone
26	71°54.2'N	72°53.6'W	539	222	71 cm core dark grey siltstone
34	70°12.7'N	66°42.5'W	118	520	95 cm core metamorphic rock
44	66°23.7'N	61°06.9'W	164	125	76 cm core metamorphic rock
47	66°23.7'N	61°06.7'W	166	292	72 cm core metamorphic rock
57	65°26.9'N	63°07.5'W	196	535	232 cm core metamorphic rock
60	65°25.8'N	62°43.5'W	124	157	144 cm core metamorphic rock

*Drill stations, except No. 22 which was a dredge station.

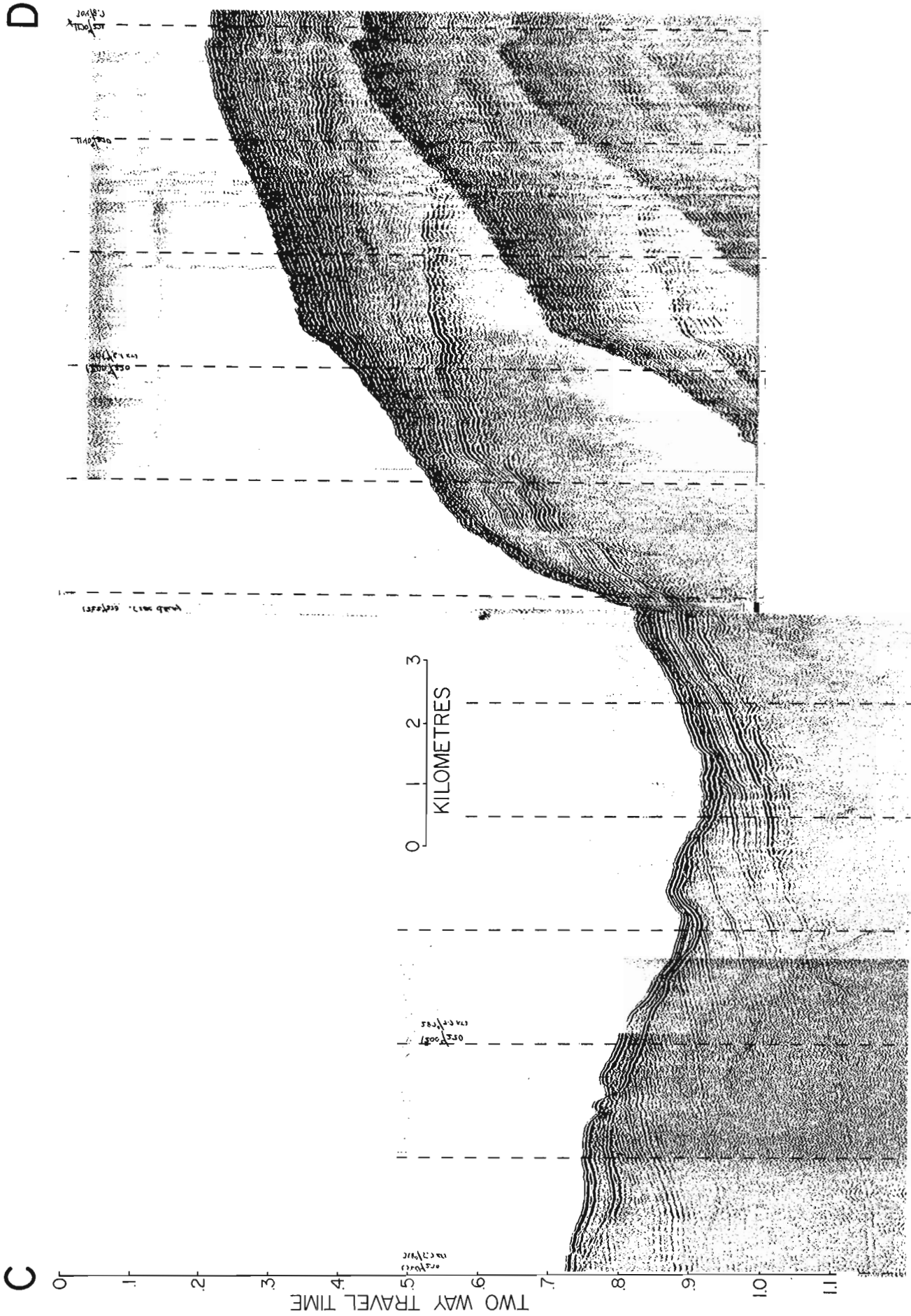


Figure 26.6. Profile C-D (see Fig. 26.3 for location). Seismic reflection record across inner central section of Buchanan Trough showing Cretaceous strata thickening to the northwest beneath the floor of the trough. Drill core samples from these strata were obtained just to the northeast of C.

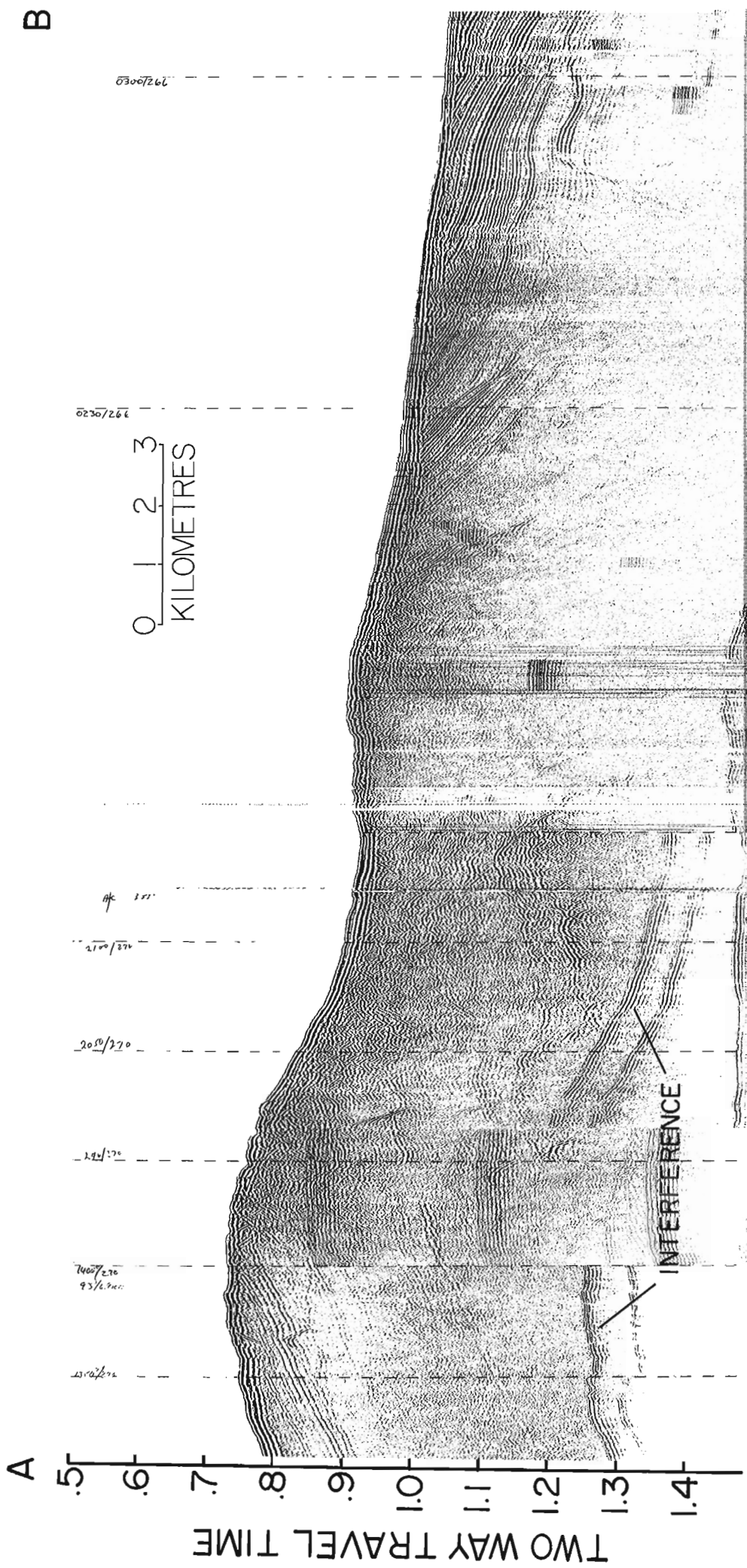


Figure 26.7. Profile A-B (see Fig. 26.3 for location). Seismic reflection record along the axis of Buchan Trough showing Cretaceous strata dipping northwesterly at A, thinning over a basement ridge a little west of the profile mid-point, and overlain toward B by seaward dipping strata presumed to be of Tertiary age.

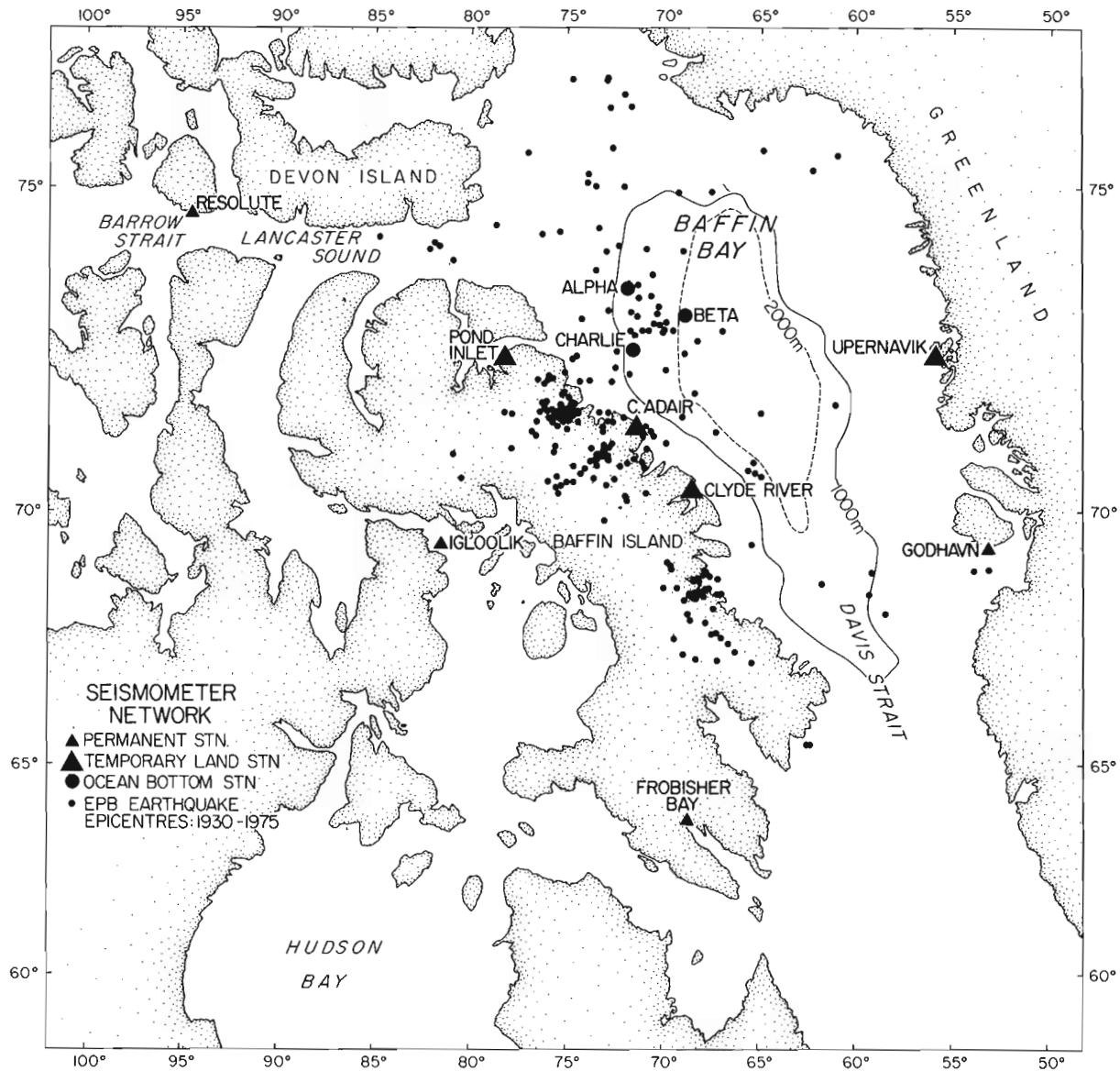


Figure 26.8. Earthquake activity in the Baffin Bay region and locations of seismometers. Only epicentres north of 65°N and east of 90°W are plotted.

section probably thins south of Buchan Trough as gravity anomalies become less negative and magnetic anomalies in the Buchan area are positive and indicative of shallow basement.

Cores of Upper Cretaceous (Senonian) (G.L. Williams, pers. comm., 1979) dark grey calcareous siltstone of probable neritic origin were recovered on three drilling attempts at two localities in the floor of Buchan Trough (Table 26.1, Fig. 26.3). The nearest previously established occurrence of Cretaceous rocks is in the Pond Inlet – Bylot Island area 200 km to the northwest where they have been described by Jackson and Davidson (1975) and Jackson et al. (1975). Assemblages in the samples from Buchan Trough resemble Senonian dinoflagellate assemblages from Bylot Island (G.L. Williams and N.S. Ioannides, pers. comm., 1979). Layered sediments observed from the air in stream channels cut into the Quaternary forelands adjacent to the entrance to Scott Inlet may include rocks of Cretaceous-Paleogene age (Jackson et al., 1979; G.D. Jackson, pers. comm., 1979). The Cretaceous strata sampled at Buchan Gulf thicken northward

and westward over basement rocks in the central and inner part of the trough (Fig. 26.6, 26.7), underlie inferred Tertiary strata farther seaward (Fig. 26.7), and are thought to form the bedrock across part of the area between Buchan Gulf and Scott Inlet (Fig. 26.3).

North of Buchan Trough a belt of positive gravity anomalies extends parallel to the shelf edge for 80 km. Large positive magnetic anomalies, up to 1500 nT, coincide with the belt, but two separate features are indicated. Keen et al. (1972), from a magnetic, gravity, and seismic profile across part of the feature, and model studies, conclude that basic intrusives are the probable source of the feature.

Probable Sources of Seepage

Thin oil slicks were observed at several localities in the Scott Inlet area where they had been observed in 1977 (Levy, 1978). A more noticeable oil slick and bubbles were present in the vicinity of the westernmost basement high at the outer part of the Scott Trough (Fig. 26.5) where they previously had

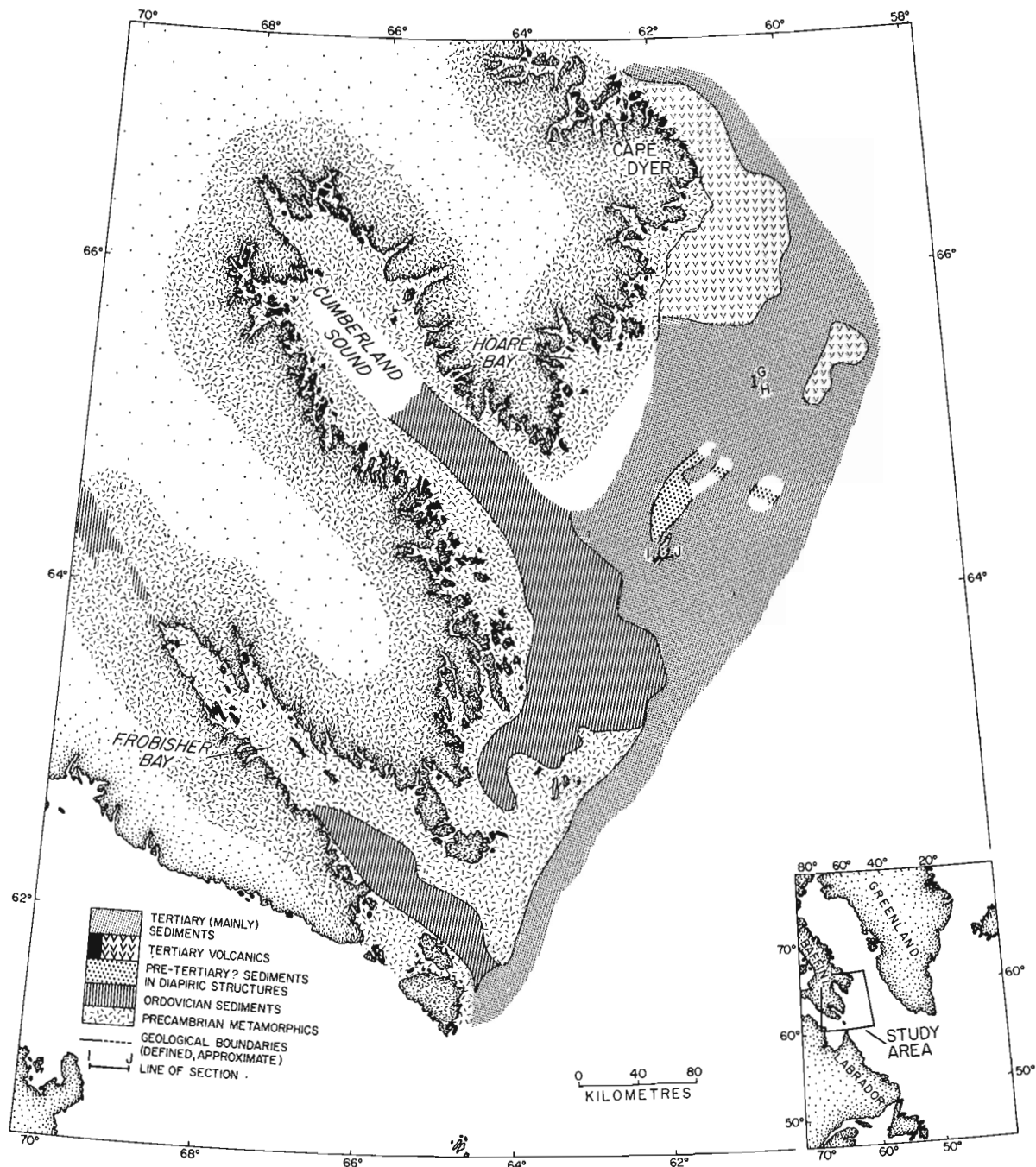


Figure 26.9. Generalized geological map of the Baffin Island shelf from Cape Searle to Resolution Island. (Land geology from Blackadar, 1967; Clarke and Upton, 1971; Jackson and Taylor, 1972.)

been observed in 1976 and 1977 (Loncarevic and Falconer, 1977; Levy, 1978). An oil slick at this locality was also observed during aerial surveys of the area in 1978 by Canada Centre for Remote Sensing. Persistence in time and space of the slick and bubbling point to this as an area of seepage and the underlying geological structure is compatible with such a conclusion. Seepage is thought to occur through migration of hydrocarbons updip in the strata flanking the basement high or along the contact with the basement rocks. A slick also was observed east of F (Fig. 26.3, 26.5) where strata flank the east side of the basement high. Seepage may occur elsewhere along the Scott Trough and farther northward along the shelf, e.g. Buchan Trough. No slicks were observed at Buchan

Trough, but methane anomalies were encountered (E.M. Levy, pers. comm., 1979). Acoustic masking possibly caused by gas has been observed on some of the seismic profiles between Buchan Gulf and Scott Inlet.

The samples of Upper Cretaceous rock obtained indicate that marine conditions existed in this region at that time. Plate tectonic predictions (e.g. Srivastava, 1978) imply that Baffin Bay began opening about that time, but significant spreading did not occur until 20 million years later. The sediment filled depression on the shelf bounded by offshore basement highs could be a tensional marginal trough related to the opening. It probably predates significant spreading.

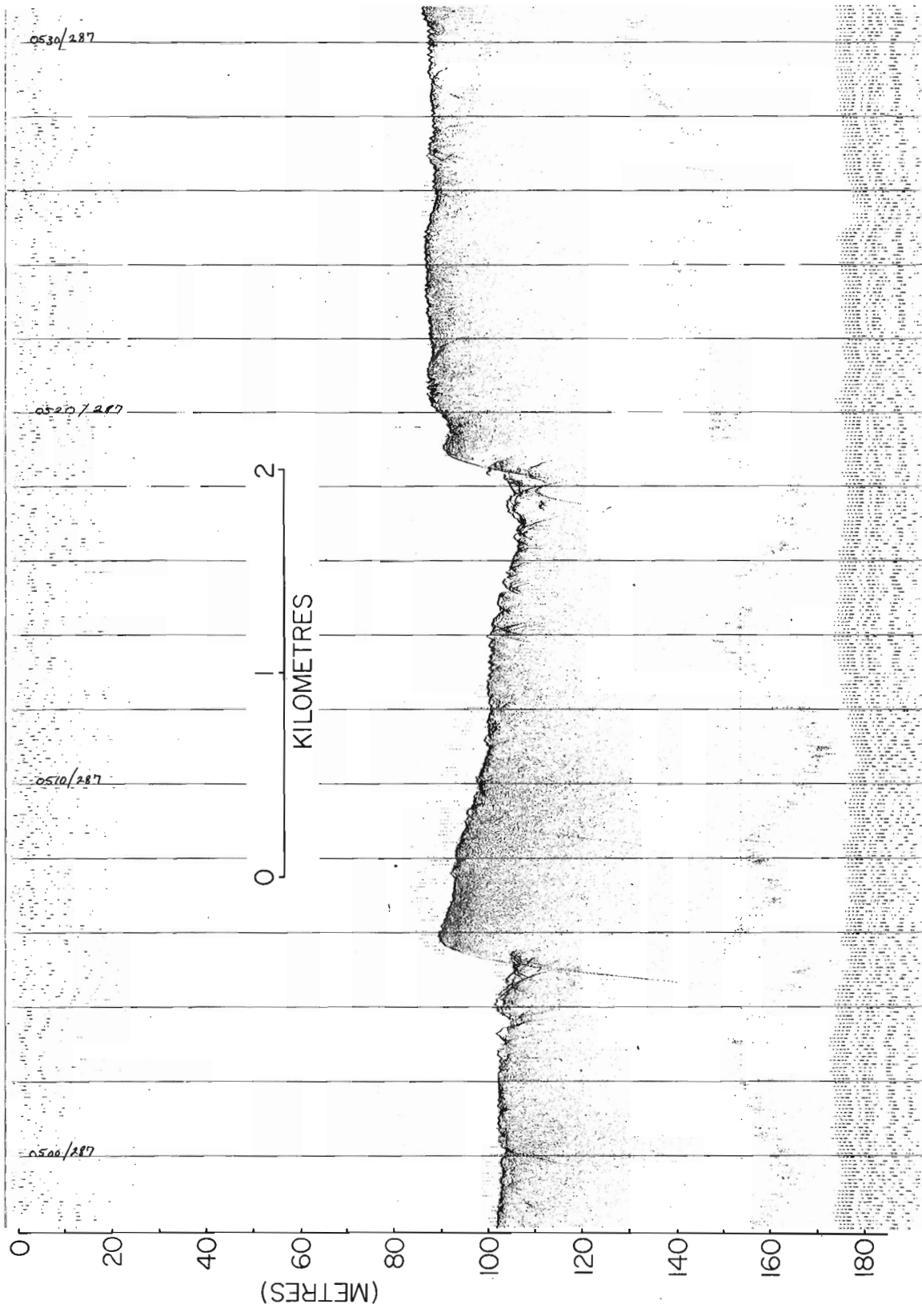


Figure 26.10. Profile G-H (see Fig. 26.9 for location). Hunttec high resolution record showing scarps apparently of relatively recent fault origin on the central part of the shelf east of Hoare Bay. Vertical scale is equivalent to the velocity of sound in water.

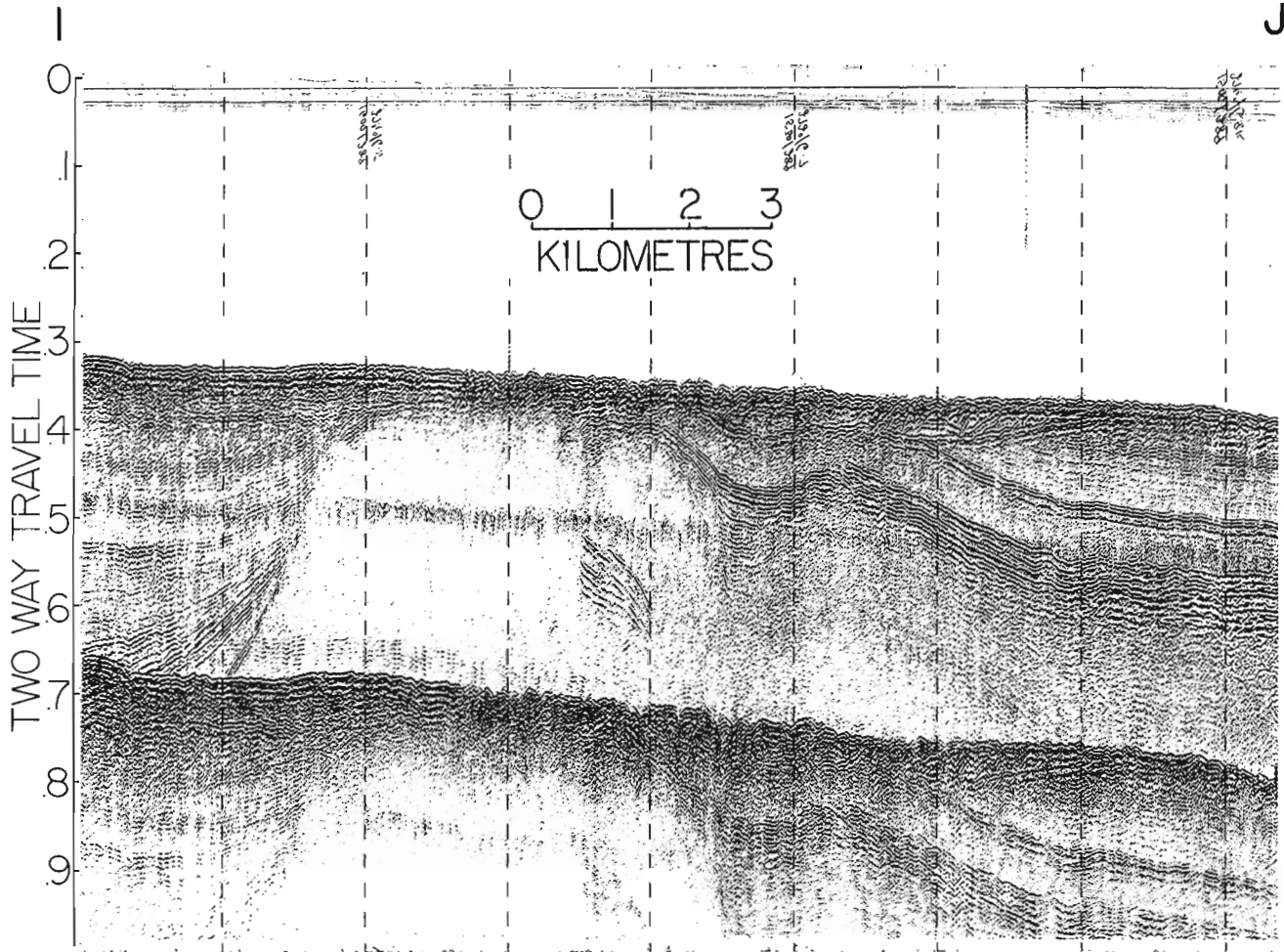


Figure 26.11. Profile I-J (see Fig. 26.9 for location). Seismic reflection record across a diapiric ridge structure east of Cumberland Sound.

The presence of marine Upper Cretaceous strata at Buchan Trough must be regarded as encouraging to the search for petroleum resources in the Baffin Bay region. The percentage of organic carbon in the samples (1%, M.A. Rashid, pers. comm., 1979) is at a level generally considered adequate for a source rock, if other factors such as maturity and carbon origin are favourable (Welte, 1965). Further analyses to determine the source potential of these rocks are in progress. While not indicative of the presence of hydrocarbons in exploitable quantities the occurrence of the seeps does indicate that conditions favourable for the generation of hydrocarbons have existed in the region.

Seismicity

The existence of seismic activity in northern Baffin Bay and on Baffin Island (Fig. 26.8) has been clearly established by the Canadian and worldwide seismograph networks. The networks generally detect only events of magnitude 3.5 and above with epicentre uncertainties of 50 km. The activity appears to occur in an offshore group and in a separate onshore group concentrated near the coast between Pond Inlet and Clyde Inlet. In order to better understand the reason for the seismic activity, to detect lower magnitude events, and to accurately locate them, a local seismicity study was done jointly by three groups. The Atlantic Geoscience Centre laid three ocean bottom seismometers

(OBS's) in Baffin Bay from CSS **Hudson**. The Seismology Division of Earth Physics Branch, Ottawa, established temporary shore seismographs at Pond Inlet, Clyde River, and Cape Adair and the Danish Geodetic Survey established a temporary station at Upernavik.

The three OBS's were laid in a 100 km sided triangle (Fig. 26.8). They were down for 10 days during which time at least 40 events were recorded. About half were detected on only one instrument and appear to be close to the respective instrument. The Baffin Island temporary network detected at least 20 events during the same time, apparently all in Baffin Island or nearshore. The largest was a magnitude 3 event in the Buchan Gulf area. That event and several others of the "land group" were clearly recorded by the OBS's. Two 450 kg shots fired offshore close to the OBS triangle were well recorded by the OBS's and Baffin Island stations and should provide good "artificial earthquakes" for network calibration.

Southeastern Baffin Island Shelf

Figure 26.9 shows the surface bedrock geology of the southeastern Baffin Island shelf. Studies in this area in 1978 were principally between Cape Dyer and Cumberland Sound. They were designed to further establish the shoreward extent and stratigraphic relationships of the volcanic and sedimentary units previously reported by Grant (1975) and further defined by MacLean et al. (1977, 1978), and to obtain additional data on diapiric structures off Cumberland Sound.

The two offshore areas of Tertiary (Paleocene) volcanic rocks shown in Figure 26.9 are as presented by MacLean et al. (1978). A third area of volcanics previously was inferred south of the main offshore volcanic area on the basis of magnetic data. Seismic reflection data obtained in 1978 indicate that this is a subsurface feature covered by Cenozoic sediments. Four scarps, with south side down, were observed on a north to south seismic reflection profile across this feature. Two of these are illustrated in Figure 26.10. Apparently they are of relatively recent fault origin. Weather and time did not permit additional profiles to establish strike of the scarps, but the data obtained suggests a series of small en echelon blocks tilted slightly downward to the north.

Drill samples of metamorphic rocks recovered off Exeter Bay just south of Cape Dyer (Fig. 26.2, stn. 44 and 47, Table 26.1) established that the area is underlain by Precambrian rocks and a change noted in the magnetic anomaly pattern (MacLean et al., 1978) therefore reflects the volcanic-Precambrian boundary rather than the presence of less magnetic subaqueous volcanics.

At the southern boundary of the main area of volcanics offshore, the volcanic rocks appear to be overlapped by younger strata, which consequently have been included in the Tertiary map unit, although the seismic data suggest the possibility of some minor faulting. The precise shoreward extent of these sediments off Hoare Bay is uncertain. Precambrian basement rocks which in the Hoare Bay area have an unusually smooth magnetic anomaly signature were sampled at two localities (Fig. 26.2, stn. 57, 60, Table 26.1) and were found to extend seaward to the edge of the area stippled in Figure 26.9. Strata older than Tertiary may be present at the bedrock surface seaward of this boundary. If so, they may correlate with Ordovician rocks delineated and sampled at several localities south of Cumberland Sound (MacLean et al., 1977; MacLean, 1978). Ordovician rocks also underlie the southern side of Frobisher Bay and probably much of Cumberland Sound.

Diapiric Structure

Seismic reflection, magnetic and gravity profiles and seismic refraction measurements were obtained over diapiric structures that underlie the shelf 75 km east of the entrance to Cumberland Sound (Fig. 26.9). The seismic character and shape of these structures is illustrated in Figure 26.11. Typically the west side is steep and the east side apparently more gentle. Similar shaped structures were encountered by Grant (1975) at two localities farther east (Fig. 26.9), but their relationship to the delineated structure is as yet uncertain. The magnetic signature across the features is mainly quite flat except for a few small associated anomalies in the northern part. The northward extent of these structures has not been established, but the fact that they are approximately on trend with the structurally high area of volcanic rocks to the northeast suggests the possibility of some common underlying structural control. S.P. Srivastava in 1974 obtained a short drill core of Albian-Cenomanian sandstone (MacLean et al., 1977) in the vicinity of the small separate structure illustrated in Figure 26.11. In view of the age of this sample and the uplift of strata flanking the structure, Mesozoic and/or older rocks probably are represented here. Although depth to the base of the structure is not known, its size (80 km delineated length), possibilities for entrapping structures against its flanks, and important petroleum reservoirs associated with diapirs elsewhere, suggest structures of this type may be of potential resource significance in this area.

Discussion

Baffin Island is topographically high in the east and slopes downward to the southwest. The Precambrian terrain that forms almost the entire east coast of Baffin Island stands structurally high relative to the rocks of the shelf. Lower Paleozoic strata (Ordovician, Silurian, and some Cambrian rocks in the northwest) occur along western Baffin Island. Ordovician strata also occur at outliers at the head of Frobisher Bay, and underlie much of the inner and central parts of the shelf between Frobisher Bay and Cumberland Sound, and appear to underlie the Frobisher Bay and Cumberland Sound grabens. The Ordovician strata on the shelf were deposited in marine nearshore to outer shelf-upper bathyal environments. Subsequently they were subjected to folding and faulting, and have been extensively bevelled by erosion (MacLean et al., 1977). Where they occur close to shore near Brevoort Island, between Cumberland Sound and Frobisher Bay, the strata dip shoreward and the contact with the basement rocks though not visible on the seismic data must be a fault. The wide occurrence of remnants of Ordovician rocks through the region suggests that the original distribution of these rocks was more widespread. The formation of the Frobisher Bay half graben and the Cumberland Sound graben and uplift of the landmass relative to the shelf must have occurred before the Ordovician strata were completely stripped from the adjacent landmass. It is not possible, however, to say when this movement took place. At Cape Dyer Paleocene rocks lie directly on Precambrian basement (Clarke and Upton, 1971). If Ordovician strata had been present at Cape Dyer, their complete removal by Paleocene time would imply pre-Paleocene formation of the Cumberland Sound and Frobisher Bay grabens (which we previously argued must have taken place before complete removal of Ordovician rocks from adjacent areas). Subaqueous Paleocene volcanics onshore at Cape Dyer now stand 600 m higher than their counterparts on the shelf. As the land must have been near to slightly below sea level during the Paleocene, uplift must have taken place since then. It is possible that the tectonic history of the Cape Dyer area may have been quite different from the Frobisher Bay – Cumberland Sound area, and there may have been more than one period of uplift.

In northern Baffin Island Lower Cretaceous to possibly mid-Tertiary (Eocene) marine and paralic rocks preserved in structural depressions at Pond Inlet and Bylot Island now stand up to 600 m above sea level (Jackson et al., 1975). In the Buchan Gulf – Scott Inlet area, marine rocks of Upper Cretaceous to Eocene ages are present on the continental shelf. This indicates a 600 m vertical movement of the land relative to the shelf since Eocene time, much the same as at Cape Dyer. Thus, the tectonic movements seem to have been relatively similar from Cape Dyer to Lancaster Sound, at least since the Eocene. The fact that older rocks form most of the shelf south of Cumberland Sound indicates that this area has stood structurally higher than the region to the north where younger sediments predominate.

A Cretaceous, or older, age for the Frobisher and Cumberland grabens and the coast parallel sedimentary trough off Scott Inlet would agree with plate tectonic models (e.g. Srivastava, 1978) which predict initiation of rifting by at the latest, Late Cretaceous. The post-Eocene land uplift from Cape Dyer to Lancaster Sound occurs after spreading is assumed to have stopped.

Acknowledgments

We are grateful to Captains D. Deer and L. Strum, Officers, Crew and Scientific Staff aboard *CSS Hudson* for their co-operation and assistance in carrying out these investigations; to G.L. Williams and M.A. Rashid for Palynological and Organic Chemistry studies, respectively, and to C.E. Keen and A.C. Grant for review of the manuscript.

References

- Blackadar, R.G.
1967: Geological reconnaissance, southern Baffin Island, District of Franklin; Geological Survey of Canada, Paper 66-47, 32 p.
- Clarke, D.B. and Upton, B.G.J.
1971: Tertiary basalts of Baffin Island: field relations and tectonic setting; Canadian Journal of Earth Sciences, v. 8, p. 248-258.
- Grant, A.C.
1975: Geophysical results from the continental margin off southern Baffin Island; in Canada's Continental Margins and Offshore Petroleum Exploration, C.J. Yorath, E.R. Parker and D.J. Glass, ed., Canadian Society Petroleum Geologists, Memoir 4, p. 411-431.
- Jackson, G.D. and Davidson, A.
1975: Bylot Island map-area, District of Franklin; Geological Survey of Canada, Paper 74-29, 12 p.
- Jackson, G.D. and Taylor, F.C.
1972: Correlation of major Aphebian rock units in the northeastern Canadian Shield; Canadian Journal of Earth Sciences, v. 9, p. 1650-1669.
- Jackson, G.D., Davidson, A., and Morgan, W.C.
1975: Geology of the Pond Inlet map-area, Baffin Island, District of Franklin; Geological Survey of Canada, Paper 74-25, 33 p.
- Jackson, G.D., Morgan, W.C., and Davidson, A.
1979: Geology, Buchan Gulf-Scott Inlet, District of Franklin; Geological Survey of Canada, Map 1449A.
- Jackson, H.R., Keen, C.E., and Barrett, D.L.
1977: Geophysical studies of the eastern continental margin of Baffin Bay and in Lancaster Sound; Canadian Journal of Earth Sciences, v. 14, p. 1991-2001.
- Keen, C.E., Barrett, D.L., and Manchester, K.S.
1972: Geophysical studies in Baffin Bay and some tectonic implications; Canadian Journal of Earth Sciences, v. 9, p. 239-256.
- Levy, E.M.
1978: Visual and chemical evidence for a natural seep at Scott Inlet, Baffin Island; in Current Research, Part B, Geological Survey of Canada, Paper 78-1B, p. 21-26.
- Loncarevic, B.D. and Falconer, R.K.H.
1977: An oil slick occurrence off Baffin Island; in Report of Activities, Part A, Geological Survey of Canada, Paper 77-1A, p. 523-524.
- MacLean, B.
1978: Marine geological-geophysical investigations in 1977 of the Scott Inlet and Cape Dyer-Frobisher Bay areas of the Baffin Island Continental Shelf; in Current Research, Part B, Geological Survey of Canada, Paper 78-1B, p. 13-20.
- MacLean, B., Jansa, L.F., Falconer, R.K.H., and Srivastava, S.P.
1977: Ordovician strata on the southeastern Baffin Island shelf revealed by shallow drilling; Canadian Journal of Earth Sciences, v. 14, p. 1925-1939.
- MacLean, B., Falconer, R.K.H., and Clarke, D.B.
1978: Tertiary basalts of western Davis Strait; bedrock core samples and geophysical data; Canadian Journal of Earth Sciences, v. 15, p. 773-780.
- Srivastava, S.P.
1978: Evolution of the Labrador Sea and its bearing on the early evolution of the North Atlantic; Geophysical Journal, Royal Astronomical Society, v. 52, p. 313-357.
- Welte, D.H.
1965: Relation between petroleum and source rock; American Association Petroleum Geologists, Bull., v. 49, p. 2246-2268.

**GEOPHYSICAL AND SEDIMENTARY STUDIES IN THE CHIGNECTO BAY SYSTEM,
BAY OF FUNDY – A PROGRESS REPORT**

Project 780022

Carl Leonetto Amos and Ken W. Asprey
Atlantic Geoscience Centre, Dartmouth

Amos, Leonetto Carl and Asprey, W. Ken, Geophysical and sedimentary studies in the Chignecto Bay system, Bay of Fundy – a progress report; in Current Research, Part B, Geological Survey of Canada, Paper 79-1B, p. 245-252, 1979.

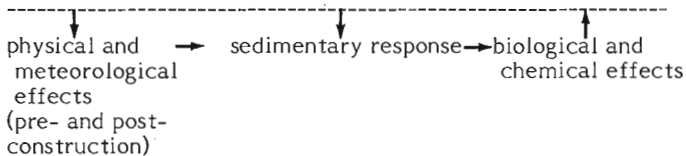
Abstract

A multidisciplinary survey of Chignecto Bay has been underway since May 1978. Information on the surficial geology, sediment transport and physical oceanography has been collected with a view to characterizing the sedimentary environment of the bay. These data will provide the necessary boundary conditions to a predictive model which will assess siltation resulting from potential tidal power development in the region. This work is only one of many aspects of the environment being researched in Chignecto Bay at present.

INTRODUCTION

Sedimentation studies and regional geological research have been designed and implemented to quantitatively determine the changes in the sedimentary character of a tidal region affected by a potential tidal power project in the Bay of Fundy (Tidal Power Review Board, 1977). These studies of the bay head waters were initiated by Atlantic Geoscience Centre in February, 1975 and were conducted exclusively in the Minas Basin area (Amos and Joice, 1977; see Fig. 27.1). During the subsequent three years, methodologies, concepts, technologies, sampling techniques, sampling intervals and data reduction routines were evolved to efficiently answer some of our questions. The experience gained during that time is now being applied to the Chignecto Bay system (see Fig. 27.1), presently considered the most likely site for tidal power development.

From an environmental point of view an assessment of the effects of marine constructions, such as a tidal power plant, requires a *a priori* knowledge of the pre- and post-constructional physical oceanographic conditions. Furthermore, a knowledge of the ensuing sedimentary character is essential to make valid judgments on the biological and chemical effects of such constructions. Schematically, the critical path of data acquisition for such environmental impact statements is as follows:



Data were originally collected within the Minas Basin system. Recently similar data from the Chignecto Bay system were collected and analyzed. The data collected fall within three distinct conceptual categories of research. Each component must be defined and quantified in order to make reasonable predictions of the post-constructional sedimentary character of the region affected by the proposed marine construction.

Category One – The present day sedimentary character

- the documentation of the present day distribution of sediment both in suspension and at the seabed.
- the sampling interpretation and mapping of the surficial sedimentary cover on a regional basis.
- the determination of the sediment budget, either being supplied to, or removed from that system.

Category Two – The dynamics of the sediment distribution

- the determination of the rates of transport and instantaneous fluxes of material moving both in suspension and along the bed.
- the measurement of the dominant physical and meteorological conditions, considered to be governing the sedimentary character.
- temporal variations (seasonal, lunar and tidal) of the above.

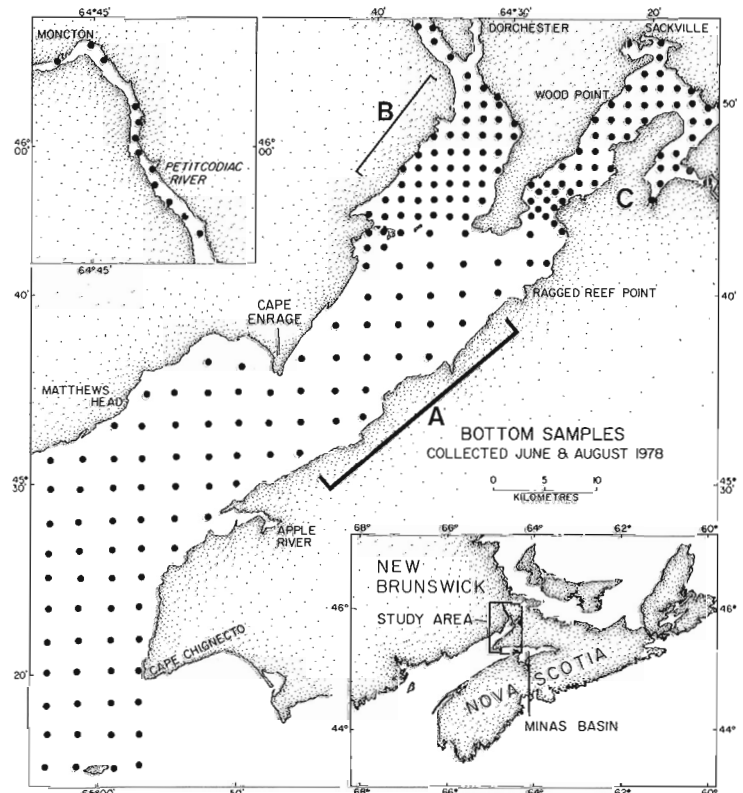


Figure 27.1. Chignecto Bay system A) Chignecto Bay, B) Shepody Bay, and C) Cumberland Basin. The dots show sites where seabed samples were taken and analyzed for grain size and macrofaunal composition.

Category Three – Numerical simulation and prediction of sedimentation

– the adaptation or design of a numerically predictive model, having as input and boundary conditions, data derived from categories one and two. Quantitative sedimentation predictions can only be made with confidence using such models with an adequate empirically derived data base (Basco et al., 1974).

THE CHIGNECTO BAY SYSTEM

The Chignecto Bay system, unlike the Minas Basin system, has very little published information describing it. The published data which exists is reviewed by the Atlantic Tidal Power Programming Board (1969) and the Tidal Power

Review Board (1977). References to this information and to data dealing with the Bay of Fundy as a whole are listed in a recently published bibliography (Moyses, 1978).

The system, situated at the head of the Bay of Fundy, may be subdivided into three distinct geomorphic zones which are part of the Carboniferous-Triassic physiographic province of the maritime region. These zones are:

1. Shepody Bay (area = 175.9 km²; perimeter = 94.0 km; spring tidal prism = 1.43 km³).
2. Cumberland Basin (area = 121.1 km²; perimeter = 68.6 km; spring tidal prism = 0.90 km³).
3. Chignecto Bay sensu stricto (inner and outer) (area = 504.8 km²; perimeter = 106.7 km; spring tidal prism = 5.56 km³).

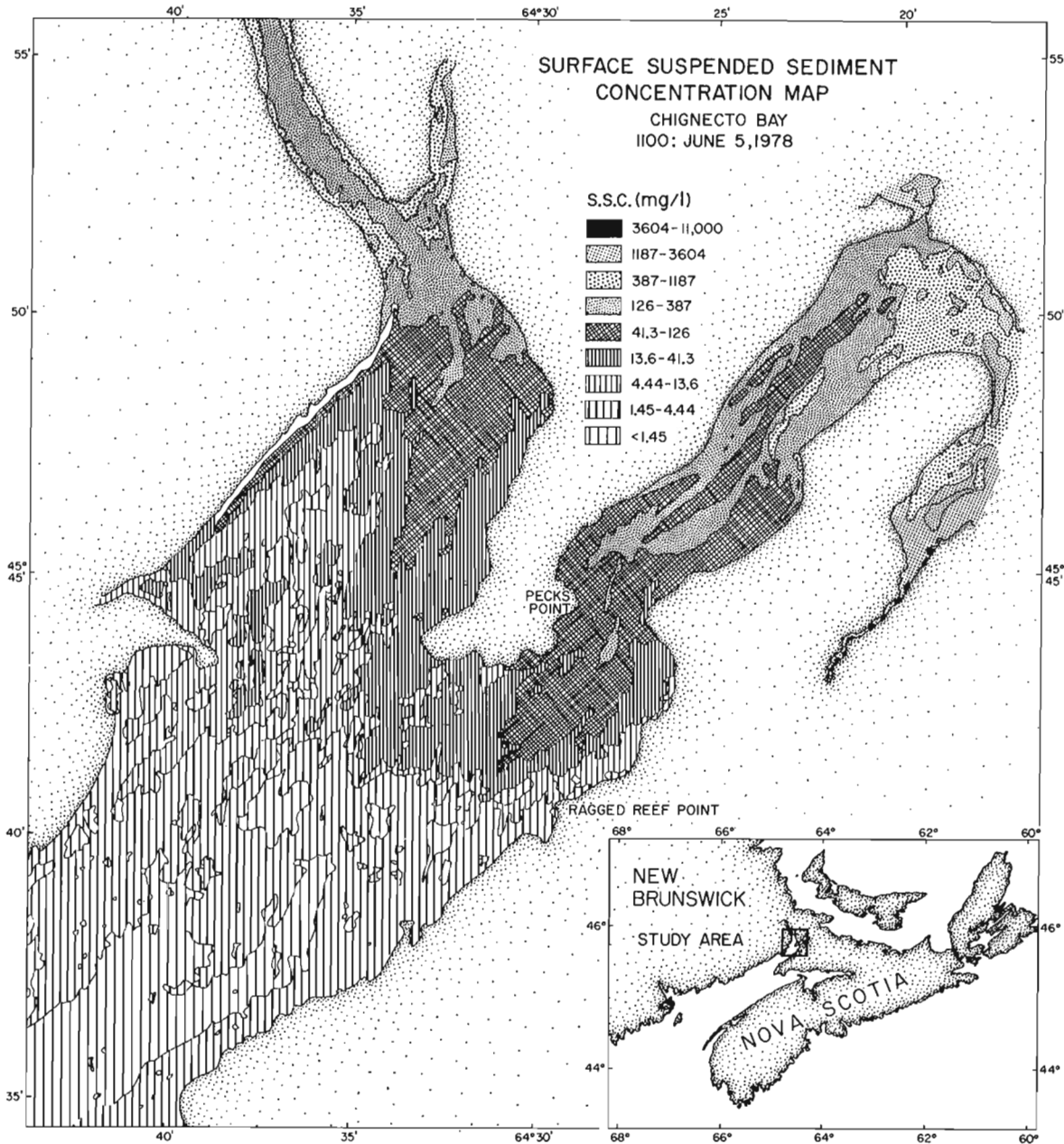


Figure 27.2. The distribution of 9 levels of suspended sediment concentrations within the surface waters of the Chignecto Bay system. The concentration levels were discriminated from Landsat data applying a calibration recently derived for the region (Amos and Alföldi, 1979). The complexity of the sediment distribution is immediately apparent.

The region is subject to large semidiurnal tides (Cape Enragé Predictions, MEDS, 1978: mean spring tidal range = 11.3 m; mean neap tidal range = 7.2 m). These tides inundate in a six hour period the expansive intertidal region (210.6 km²) and subtidal zone (591.2 km²) with up to 7.89 km³ of seawater. Consequently, strong tidal currents of 2-3 ms⁻¹ result, peaking at mid-flood and -ebb stages of the tide.

The system is parallel to the dominant southwest winds and is exposed to the open Bay of Fundy. As a result, Chignecto Bay is often disturbed by a combination of north Atlantic swell and locally generated waves. The generally dynamic nature of the marine environments in this area caused frequent delays in data collection, and warranted considerable caution at all times. The rate of shipboard equipment failure was high because of the rigorous conditions. Furthermore, docking facilities could only be reached during high tide. Appreciating these limitations, it is not surprising that very few data had previously been collected in the area.

Data collection began during May, 1978 and comprised a geophysical and hydrographic survey (24 May-8 June, 1978), a land based survey of the marginal regions (24 May-24 June, 1978), and an oceanographic cruise aboard *CSS Dawson* (4-22 August, 1978). The data gathered throughout the surveys and the initial findings and interpretations of the results are described below.

Category One – the present day sedimentary character

The distribution of bottom sediments

Bottom samples were initially collected within Shepody Bay (69 samples) and Cumberland Basin (61 samples). These samples were collected on a 1.5 km grid. Later in Chignecto Bay the spacing was expanded to 3.0 km with 95 samples collected. The subtidal samples were collected using a 0.2 m³ Van Veen sampler and intertidal samples were collected manually. They were subsequently analyzed for grain size distribution, carbon/nitrogen ratios and macrofaunal assemblages (see Fig. 27.1 for the sample locations).

The material is generally multimodal. It comprises a surface lag layer which armours underlying finer material. These sediments are, in places, subject to considerable biogenic activity.

Most of the subtidal region is covered by a gravel, pebble and sand veneer similar to the surficial sediment distribution of Minas Basin. The higher regions of Shepody Bay and Cumberland Basin, however, have mud accumulating at the seabed.

The distribution of suspended sediments

The distribution of suspended particulate matter (SPM) was measured areally by use of the Landsat multispectral scanner (NASA, 1976) and vertically and temporally by direct sampling.

Radiant energy reflected from the sea surface is recorded within the visible part of the electromagnetic spectrum by Landsats 2 and 3. Applying various transforms to this data (Alföldi and Munday, 1978) one can produce an accurate ($\pm 12\%$) relationship to the suspended sediment concentration (SSC) within the Bay of Fundy waters (Amos and Alföldi, in press). Figure 27.2 shows the SSC of Chignecto Bay system at 1100 hours (local time) on the 6 June, 1978. It demonstrates the complexity in the distribution of SSC and the potential problems of representative sampling, but highlights a general increase in SSC headwards into the bay from 1.4 mg/l to a maximum concentration of approximately 3000 mg/l.

The vertical distribution of SPM was measured at 13 locations over a total of 15 individual tidal cycles. Samples were collected from five equally spaced depth intervals at each hour for a duration of 16 hours. Measurements began 2 hours before low water and continued for 2 hours after the successive low water.

There is a consistent increase in SPM from surface to bottom. Often sharp gradations were measured (from light attenuation profiles) separating the clearer water from more turbid layers below. This contrasts with results from the Minas Basin, which is vertically mixed at all times.



Figure 27.3.

The *MFV Oran II* used during these studies.

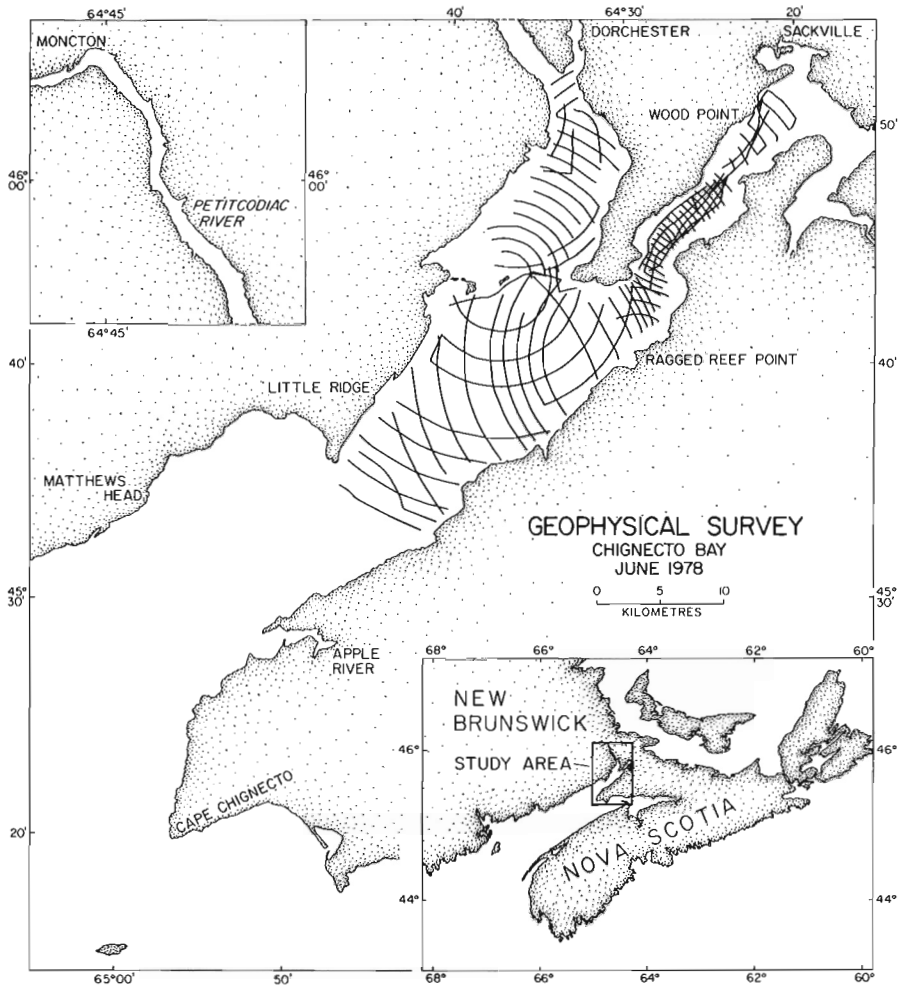


Figure 27.4.

Survey lines completed during May/June, 1978; aboard *MFV Oran II*. Bathymetric, high resolution seismic reflection, side scan sonar and subbottom profile data were collected along the lines.

Figure 27.5.

The location of gravity core sites and survey lines travelled during an air gun, low resolution, seismic reflection survey of Chignecto Bay. The work was carried out aboard *CSS Dawson* during August, 1978.

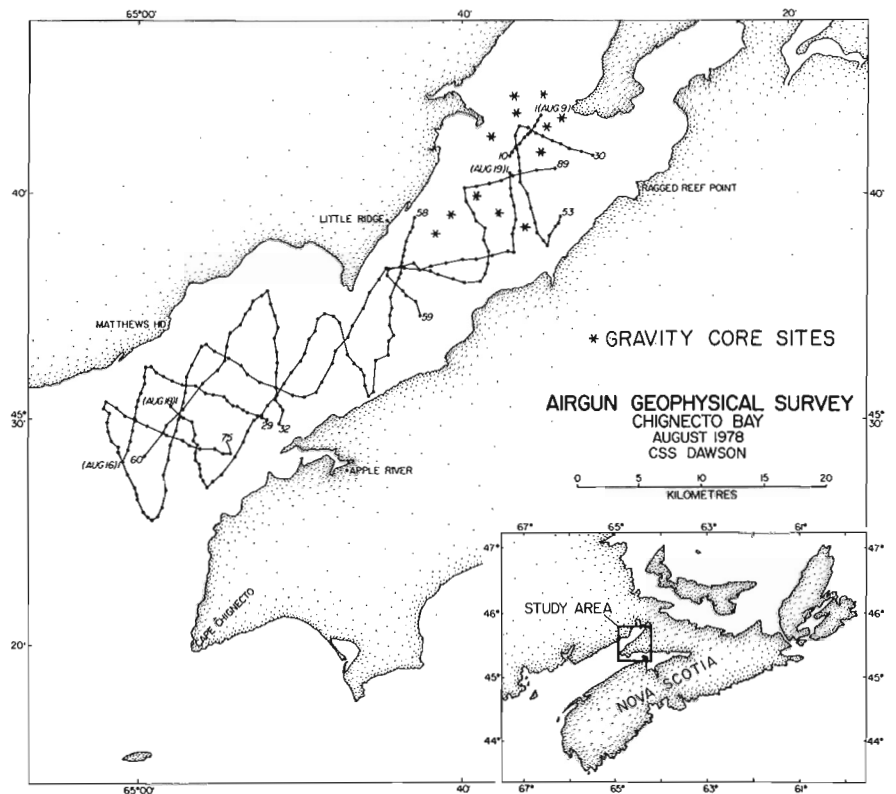


Figure 27.6.

The location of the four sites from which surface water samples were gathered on a regular basis throughout the survey period. The catchment areas, of which these samples are representative, are also shown.

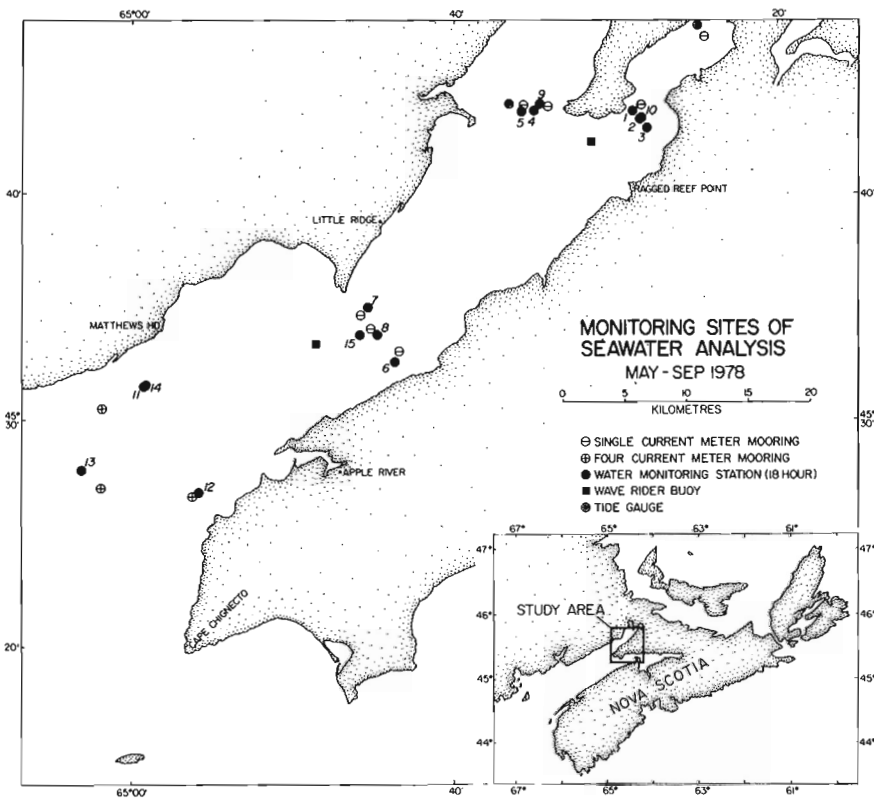
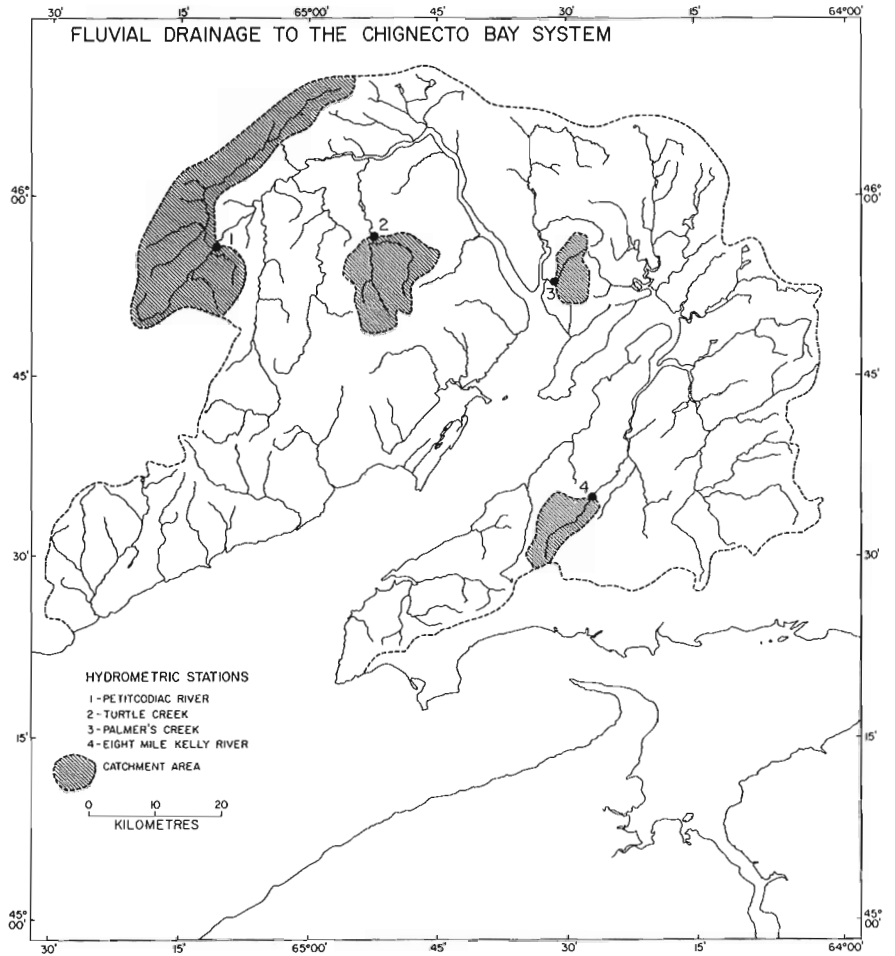


Figure 27.7.

The location of sites from which physical oceanographic data were collected.

The geophysical and hydrographic survey

Seismic reflection, bathymetric and side scan sonar data were collected in association with Canadian Hydrographic Service during a recent survey aboard **MFV Oran II** (Fig. 27.3). High resolution seismic profiling was obtained using the Nova Scotia Research Foundation Shallow Towed System, which consisted of a towed "boomer" (that supplied a multifrequency acoustic pulse) and an external, directional hydrophone to record the reflected pulse. Bathymetric and subbottom information were also collected using a Dual Frequency Raytheon Souder DE-719 (200 kHz and 3.5 kHz respectively). A 200 kHz Klein Side Scan Sonar model 401 was used to record seabed reflectivity. Navigation was accurate to within a boat length. This was achieved using a range/range Mini Ranger, Mark II system, with three slave transmitters located on hydrographic bench marks. The calibration of the transmitters and production of the boat board charts was done by Canadian Hydrographic Service.

In all, 587 km of survey lines were completed. Of this total distance, 106 km were collected in Shepody Bay, 125 km were collected in Cumberland Basin, and the remaining 256 km were from Chignecto Bay (Fig. 27.4).

Penetration of the surficial sedimentary column was inhibited in parts of Shepody Bay and Cumberland Basin by "acoustic masking", the effect of gas charged sediments on the attenuation of the acoustic signal. However, up to 100 m of unconsolidated sediment was identified, and comprising two compacted laminated units, overlain by younger deposits of gravel, pebbles, sand and mud. The older units, which outcrop over a large part of the system's subtidal area, are thought to be proglacial marine silts. Cores taken of these sediments are presently being analyzed to determine their ages and composition.

A lower resolution seismic reflection system was used aboard **CSS Dawson** during the summer, 1978, to determine the nature of the bedrock surface. A 10 cubic inch air gun source (surface towed) was used to survey 230 km of Chignecto Bay. The profiles indicate that the thickest surficial cover occurs along the centre of the Bay and infills an incised drainage system, cut into the bedrock and graded to 120 m below present mean sea level. The location of these seismic lines is shown in Figure 27.5.

The budget of sediments

River supply. Surface one litre water samples were collected every second day from four rivers draining into the Chignecto Bay system. These samples were analyzed for SSC and percentage organic detritus. Sampling began 1 April, 1978 and continued through until 31 December, 1978. The sampling sites are fed by water and sediment derived from a catchment area of 635 km² (see Fig. 27.6). This information and documented information (Inland Waters reports) will be used to compute the total fluvial input of inorganic detritus extrapolated over the entire catchment area of the Chignecto Bay system (6005 km²). Due to the paucity of sampling the results will provide "order of magnitude" information only.

Sea water analysis. Four reference profiles, along which seawater monitoring took place, were established to define the mass transport of suspended particulate matter (SPM) and dissolved and particulate organic carbon between each of the Chignecto Bay geomorphic zones. These profiles were situated at the mouth of Shepody Bay, at the mouth of Cumberland Basin, from Cape Enragé to Sandy Point (separating upper and lower Chignecto Bay) and from Point Wolfe to Squally Point (the mouth of Chignecto Bay; see Fig. 27.7). Biological, chemical and physical data were collected synoptically in conjunction with Marine Ecology

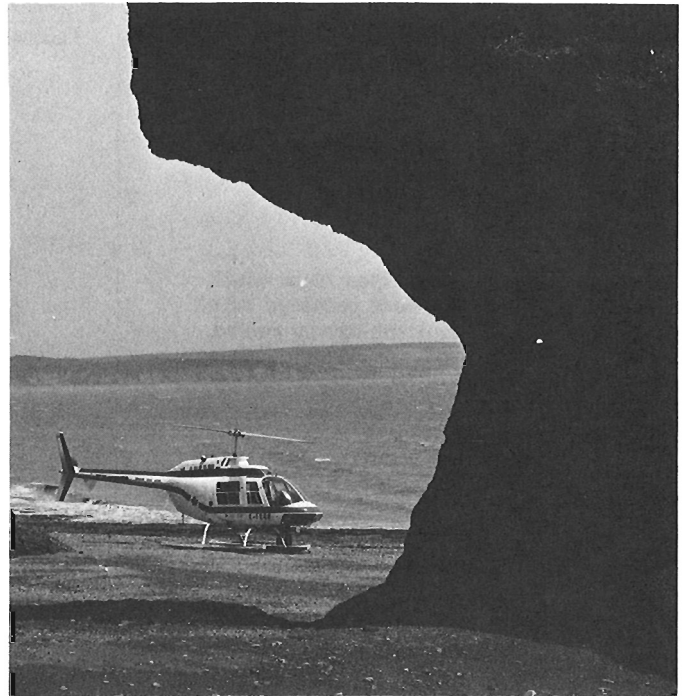


Figure 27.8. A profile of an erosive cliff in Chignecto Bay and the MOT helicopter used to measure cliff heights.

Laboratory (MEL), Department of Fisheries and the Environment, Dartmouth, N.S. and Acadia University, Wolfville, N.S., in order to adequately define the water masses and the material associated with them. The parameters measured were:

- suspended sediment concentration
- current speed and direction
- temperature (reversing thermometers and CTD)
- salinity (laboratory analysis and CTD)
- attenuation (480 nm; 520 nm; 620 nm; 680 nm; and 450-710 nm; after Larsen, 1973)
- chlorophyll a
- phaeophytin
- particulate organic carbon
- particulate organic nitrogen
- dissolved organic carbon
- inorganic nutrients (silicate, phosphate, ammonia, nitrate, and nitrite)
- zooplankton

The net flux and residual transfer of these parameters between each area of the Chignecto Bay system will be calculated. The mass transfer of SPM is an essential part of the budget of sediment analysis.

Cliff input. The eroding, high cliffs surrounding the bay have been surveyed for the constituent rock type and height. The recession rates are being determined by stereoscopic analysis of sequential aerial photographic surveys which were carried out periodically during the last 30 years. Volumes of cliff derived material will be calculated for specific sections of the bordering cliff line. Much of the cliff is composed of shales and mudstones which will breakdown, on erosion, into

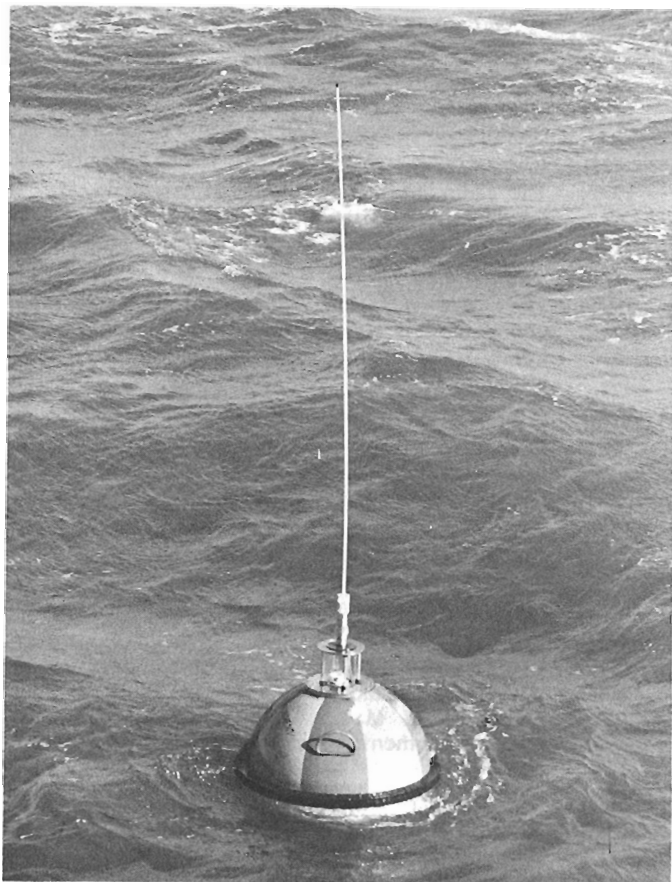


Figure 27.9. A datowell 6000 Wave Rider Buoy.

silt sized particles. This may account for the relatively small amount of flocculated material in suspension (visual observation) compared to suspended material found in Minas Basin which shows a high degree of flocculation.

The height (84 measurements) and the composition of the cliffs were determined by field measurements made around the perimeter of Chignecto Bay (Fig. 27.8).

Category Two – the dynamics of the sediment distribution

Suspended sediment transport

The residual mass transport of suspended sediment is determined by calculating the instantaneous sediment fluxes for each of the 16 hourly sampling profiles (see earlier section) made at each station and then integrating these flux profiles with respect to depth and time (over the flood and ebb phases of the tide respectively). The difference between flood and ebb mass sediment transport is then computed. The reliability of the final calculation is assessed by repeated surveys throughout the year, by duplicate analyses and by reference to long term physical oceanographic data. The lateral, seasonal and lunar variations in the residual transport of sediment will be assessed by reoccupying reference stations shown in Figure 27.7 during cruises planned for April, August and October, 1979.

Bedload transport

No quantitative measurements of the mass transport of bed material have been made. Qualitative information, however, is derived from the distribution of bedforms such as sand waves, megaripples, sand ribbons and scour marks

identified on the side scan sonar records. Almost without exception, there appears to be a net movement of material headwards towards Shepody Bay and Cumberland Basin.

Physical oceanography

Currents. Eleven sites were monitored for periods of 14-59 days to measure lunar variations in current speed and direction, temperature and salinity. The three outer sites (see Fig. 27.7) were equipped with four meters (Aanderaas) spaced at 10 m depth intervals to determine the vertical current velocity distribution over a lunar cycle and to assess the effects of bottom friction on tidal flow. These analyses will be conducted by Atlantic Oceanographic Laboratory (AOL), Department of Fisheries and the Environment, Dartmouth, N.S.

Waves. Two datowell 6000 wave rider buoys (Fig. 27.9) were moored at the head and mouth of Chignecto Bay respectively (see Fig. 27.7) from 13 June – 13 December, 1978. These buoys recorded the wave height and wave period for 20 minute intervals every three hours and the data were telemetered to a shore receiver station at Cape Enragé where it was recorded on tape. Digitization and spectral analyses of this information will be performed by Marine Environmental Data Service (MEDS), Ottawa and monthly reports on wave conditions will be compiled. The latter buoy is still operating.

Meteorological conditions. An MSI weather station was installed at Cape Enragé to measure wind speed and direction in conjunction with the wave data (Fig. 27.10). The station was operational from 24 May – 1 December, 1978. The analog output is being abstracted by Atmospheric Environment Service, Bedford, N.S. These data will be compared to the wave data and relationships of the two sets assessed. No other meteorological information was collected.



Figure 27.10. An MRI weather station at Cape Enragé.

Category Three – numerical simulation

Information within categories one and two, gathered in the Minas Basin system, has been digitized and adapted to interface with a numerical model designed to predict post-tidal barrage tidal amplitude changes in the Bay of Fundy (Greenberg, 1977; Tidal Power Review Board, 1977). Data on bathymetry, sources of material and volumes of sediments input or removed from the system, SSC, critical erosion velocities, critical deposition velocities, rates of erosion, rates of deposition, flocculation rates of suspended material, settling rates and the appropriate sediment entrainment equations are being used as input and boundary conditions to the model. The bottom distribution of sediments is used to calibrate the model. After calibration, the model will assess the post barrage transport and deposition of material within the Minas Basin system. The model resolves only to 1.5 km (the grid size) and therefore the results of the model will be indicative of general trends only.

A more detailed model with a grid size of 0.5 km is presently being designed to simulate the Chignecto Bay system. The experiences gained from the Minas Basin model will be used to select, implement and calibrate the appropriate sediment transport parameters.

ACKNOWLEDGMENTS

This work was carried out in association with a number of individuals from a variety of institutes, universities and government departments. This spirit of co-operation has proved both an excellent learning experience and a rewarding means of data collection. We are indebted to the following for their assistance and input: M. Gorveatt, R. Murphy, F. Jodrey and F. Ewing for their "in field" support, equipment supply and program co-ordination. Cyril Garrison and crew of **MFV Oran II**, Ministry of Transport helicopter division for the air support, A. Swyers for assistance in deploying current meter moorings. H. Leslie and G. McRae for laboratory analyses, D. Gordon and P. Keiser for biological analyses, H. Josenhans for assistance during the geophysical program, D. Blaney and Canadian Hydrographic Service for bathymetric data and navigational control, the scientific staff and crew of **CSS Dawson** during cruise 78-025 and to other contributors who helped support this program.

REFERENCES

- Alföldi, T.T. and Munday, J.C.
1978: Water quality analysis by digital chromaticity mapping of Landsat data; Canadian Journal of Remote Sensing, v. 4 (2), p. 108-125.
- Amos, C.L. and Joice, G.H.E.
1977: The sediment budget of the Minas Basin, Bay of Fundy, N.S.; Bedford Institute of Oceanography Data Series, B1-D-77-3, p. 411.
- Amos, C.L. and Alföldi, T.T.
1979: The determination of suspended sediment concentration in a microtidal system using Landsat data; Journal of Sedimentary Petrology, 49 (1), p. 159-174.
- Atlantic Tidal Power Programming Board
1969: Feasibility of tidal power development in the Bay of Fundy; Halifax, N.S., p. 181.
- Basco, D.R., Bouma, A.H., and Dunlap, W.A.
1974: Assessment of the factors controlling the long term fate of dredged material deposited in unconfined subaqueous disposal areas; Dredged Material Research Program W.E.S., Miss., p. 238.
- Greenberg, D.
1977: Effects of tidal power development on the physical oceanography of the Bay of Fundy and Gulf of Maine; in Fundy tidal power and the environment; Acadia University Institute, p. 200-232.
- Larsen, E.
1973: An in situ optical beam attenuation meter; Bedford Institute of Oceanography Report Series, B1-R-73-3, p. 74.
- Moyse, C.M.
1978: Bay of Fundy environmental and tidal power bibliography; Fisheries and Marine Service Technical Report No. 822, p. 36.
- National Aeronautics and Space Administration
1976: Landsat data users Handbook; Goddard Space Flight Center, Document 76SDS4258.
- Tidal Power Review Board and Management Committee
1977: Reassessment of Fundy Tidal Power; Thorn Press Ltd., p. 516.

Project 760062

R.L. Christie
Institute of Sedimentary and Petroleum Geology, Calgary

Christie, R.L., Phosphorite in sedimentary basins of Western Canada; in Current Research, Part B, Geological Survey of Canada, Paper 79-1B, p. 253-258, 1979.

Abstract

Occurrences of sedimentary phosphate were recognized in Western Canada over 60 years ago, and phosphorite is now known in beds of Precambrian, Cambrian, Ordovician, Mississippian, Permian, Triassic, Jurassic, and Cretaceous ages. From a study of the sedimentological and paleogeographical aspects of the occurrences it can be suggested that phosphate concentrations tend to lie along or near the miogeosyncline-platform 'hinge line' and the miogeosynclinal carbonate-shale facies boundary of the Cordilleran Geosyncline. Phosphorite is more widespread in Mesozoic than in Paleozoic rocks and evidently relates to a broad spectrum of sedimentary conditions.

Introduction

Occurrences of sedimentary phosphate rock, or phosphorite, in western Canada have been known for many decades and certain of them were, at one time or another, explored for possible commercial production. Some recently reported occurrences in western Canadian sedimentary basins invite a review of bedded phosphates in these regions.

The Geological Survey of Canada recently began a study of Canadian bedded phosphates; the objectives of the project are to assemble information on identified Canadian occurrences and to evaluate the potential for further discoveries. This is one of a series of interim reports on this continuing study.

Definitions

Phosphate is an informal term generally employed to describe a rock, mineral, or salt containing one or more phosphorous compounds. Phosphate rock (a geological term) contains one or more phosphate minerals, usually calcium phosphate (apatite), in sufficient quantity for use, either directly or after beneficiation, in the manufacture of phosphate products. The most widely used ore is sedimentary phosphate rock or phosphorite. Other phosphate rocks include: phosphatized limestones, sandstones, shales, and igneous rocks; guano; and igneous and metamorphic apatite. Phosphate rock is generally graded by stating the P_2O_5 equivalent in per cent.

Phosphorites are variable in colour and texture: white to dark brownish grey, shaly to sandy rocks. Rounded to ovoid structureless pellets are characteristically present, but massive phosphate 'matrix' is also common. They are not very distinctive rocks and can be overlooked or misidentified. A bluish-grey 'phosphate bloom' is often present on weathered surfaces.

The Phosphate Industry in Canada

The Canadian industry depends entirely on imported phosphate rock, which is mined mainly in the United States. Occurrences of sedimentary and igneous apatite are widespread in Canada, but grades and mining conditions of the deposits discovered to date are not economical.

Canada imported about 3 million metric tons of phosphate rock in 1978 (over 115 million tons are mined annually in about 30 countries in the world) (G.S. Barry, Industrial Minerals Section, Department of Energy, Mines and Resources, pers. comm.). About 90 per cent of the Canadian

import was used in the manufacture of fertilizers and of stock and poultry feed, and about 10 per cent in the manufacture of chemicals, refractories, medicines and drugs, and in food processing. Phosphate fertilizers are normally produced by decomposing phosphate rock with sulphuric acid; elemental phosphorus, mainly used in the manufacture of industrial compounds, is produced by thermal reduction using coke and siliceous flux in electric furnaces (Boyd, 1976).

Phosphate fertilizers are needed to replace phosphorus removed from agricultural land by cropping. It is clear that the world demand for mineral phosphate must rise in order to aid food production for an increased population.

History of Mining¹

The earliest recorded mining of phosphate rock is 1847, when a few tons of nodules (coprolites) were produced from Pliocene beds near Suffolk in England. Igneous apatite was mined as early as 1851 in Norway. The search for phosphate rock intensified after the discovery that agricultural crops could be increased by the application of bones or phosphate rock that had been treated with sulphuric acid.

The mining of phosphate rock in North America began in the period 1863-70 with the recovery of pegmatitic apatite in the township of North Burgess, Lanark County, Ontario. The ore was shipped to Great Britain for conversion to superphosphate fertilizer. Other deposits in Ontario and Quebec had been noted by the Geological Survey and were soon brought into production.

The first production in the U.S.A. began in 1867, when a few tons of South Carolina sedimentary phosphate were mined. Annual production in the U.S.A. had reached 65 000 tons (59 000 metric tons) by 1870. By 1875, mining of the Precambrian apatite deposits in Canada had virtually ceased because of high land prices and shipping costs. However, a short-lived 'phosphate boom' took place between 1875 and 1880 when shipping costs declined and easily mined, high-grade apatite deposits were found in the townships of Wakefield, Templeton, and Hull, Quebec. Production began from the vastly more easily mined Florida deposits in 1888, and by 1890 the price of phosphate rock dropped drastically, ending Canadian phosphate mining. The last activity in Ontario and Quebec took place in 1894; thereafter, phosphate rock was imported from the U.S.A., except for small amounts of apatite that continued to be derived from mica mines.

Mining began in the 'Western States' (Idaho, Montana, Utah and Wyoming) — the last major deposits to be developed in the U.S.A. — in 1906.

¹ Material for this section was obtained from: Spence, 1920; Cathcart and Gulbrandsen, 1973; McKelvey, 1967.

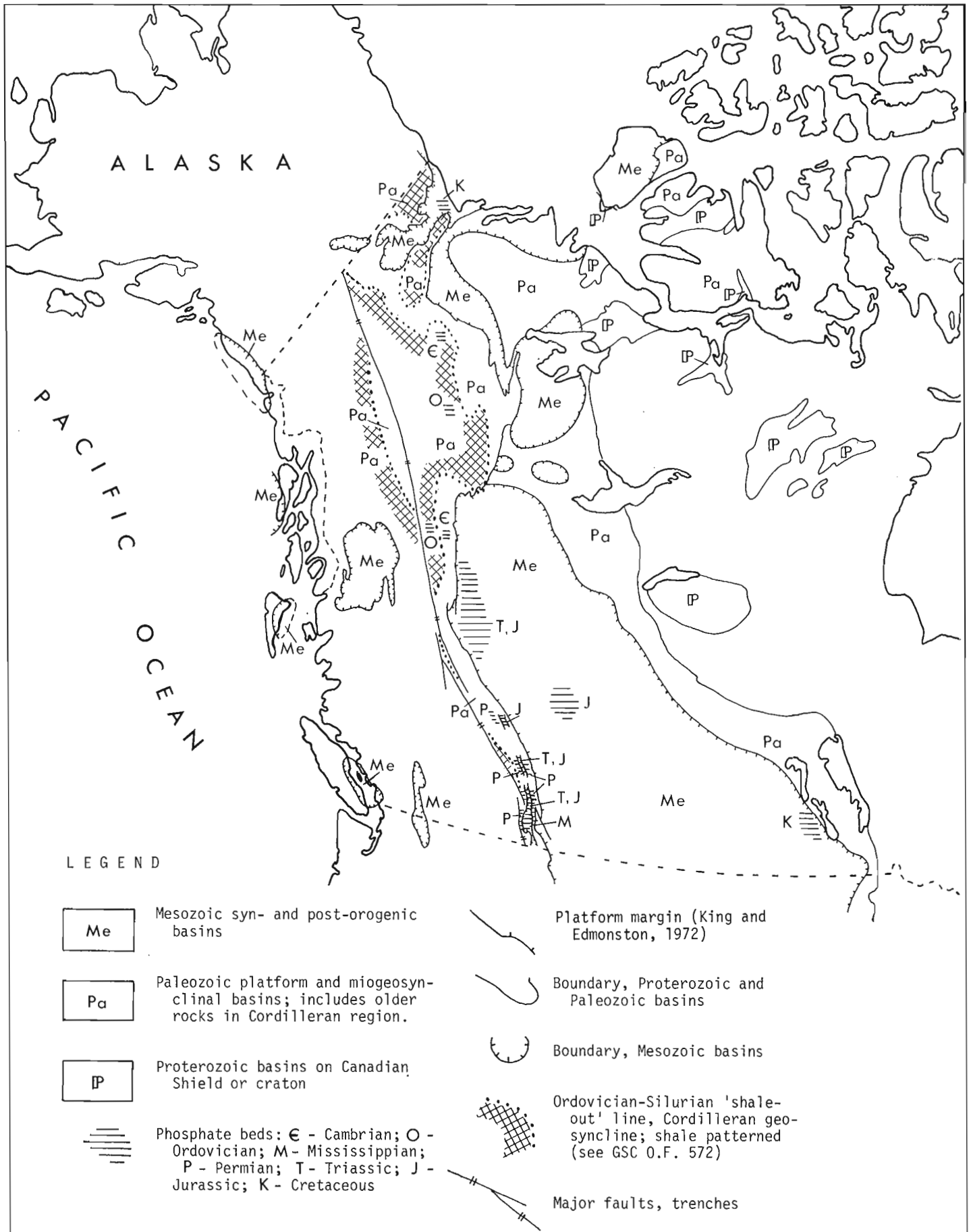


Figure 28.1. Phosphorite occurrences in western Canada basins.

World Phosphate Deposits

Phosphate ore is mined from three main sources (in decreasing importance): sedimentary phosphate (more than 80 per cent of world production); igneous apatite (about 17 per cent of world production); and guano-derived deposits.

The sedimentary phosphate deposits have been found on every continent except Antarctica, and range in age from Precambrian to Holocene. Most of the phosphorites are of marine origin, or result from weathering of marine deposits. The principal sedimentary deposits are those of Morocco, Florida, and the Western States region of the United States.

Classification of Sedimentary Phosphate Deposits

Sedimentary phosphate deposits have been classified by several descriptive and genetic schemes. Classification is difficult due to the variety of processes that have operated. A scheme that has proved useful in discussing the origin of phosphorites is as follows:

- A. Marine
 - 1. Geosynclinal
 - 2. Platform
 - 3. Shelf
- B. Derived
 - 1. Residual
 - 2. Phosphatized Rock
 - 3. Reworked

This classification was described and illustrated by Christie (1978), who followed a genetic scheme published by Cook (1976). Phosphate deposits in the western Canadian basins will probably be one or more of the first three types: geosynclinal, platform, or shelf. Residual and phosphatized rock deposits on young (e.g. Tertiary) surfaces would have been removed, except under unusual circumstances, by the widespread glacial erosion that characterizes most Canadian terrain; these types, however, could occur as subcrop, buried deposits. Reworked deposits, represented by the 'River Pebble' phosphates of the Bone Valley Formation of Florida, are evidently a rarity.

Phosphorite in Western Canada

Sedimentary phosphate deposits were discovered in the southern Canadian Rockies shortly after 1906, when the Western States phosphate field was developed (see Telfer, 1933, p. 566).

A thorough study of the region between the 49th Parallel and Jasper was carried out in 1925 and later by L. Telfer, who eventually published descriptions and maps (Telfer, 1933). The principal deposits, those of basal Jurassic beds on the east flank of the Fernie Synclinorium, have been studied intermittently by several exploration companies, but none has proven suitable for economic development.

Phosphatic horizons of a wide range in ages have been discovered over the years, in part as a result of the continuing search for mineable phosphorite and in part following the recognition of phosphorite as a sedimentological 'marker'. Phosphorite is now known in beds of Precambrian, Cambrian, Ordovician, Mississippian, Permian, Triassic, Jurassic, and Cretaceous ages in western Canada. Some of these occurrences are reviewed below.

The occurrences of phosphorite in beds of various ages in Western Canada, as discussed below, were noted in published literature, in unpublished information contributed by officers of the Geological Survey of Canada, and in communications from private exploration geologists. Many of the recently discovered phosphate localities were identified in the course of uranium exploration, a not surprising

development considering the association between marine apatite and uranium and the availability of sensitive scintillometers and gamma-ray spectrometers (see Cathcart, 1978; Christie, 1978, p. 6-7; Hale, 1967).

The grade, thickness, extent, and mining conditions necessary for a phosphate deposit to be considered economic form a complex equation, as with any mineral commodity. No attempt is made in this paper, therefore, to distinguish economic from other occurrences. Indeed, the mere presence of recognizable phosphorite, at the present state of knowledge, is considered significant. Compilation of reliable figures for thickness and grade will presumably be practicable in the near future.

Proterozoic

Certain beds in the upper part of the Athabasca Formation contain phosphate that may be marine in origin (information from a confidential source, with permission). The apatite occurs mainly as a matrix in fine grained sandstone; grades of between 15 and 20 per cent P_2O_5 are reported. These Proterozoic occurrences are not marked in Figure 28.1, but Aphebian and Hadrynian unmetamorphosed sedimentary basins of western Canada are shown.

The Athabasca Formation consists mainly of cross-bedded orthoquartzite, with rare interbeds of shale and quartz-pebble conglomerate. The formation is considered to be a product of slow erosion of a tectonically stable source area, the sediments deposited in a fluvial, partly marine environment. The source areas lay to the east and southeast of the present outcrops (Fahrig, 1961).

Cambrian

Phosphate occurs in slightly anomalous amounts in a Cambrian, basal shale unit of the Cambro-Ordovician Road River Formation in the Bonnet Plume map-area of Yukon Territory (see Fig. 28.1). The phosphate content averages 0.97 per cent P_2O_5 over 97 m of section, and a hand specimen contains 8.2 per cent P_2O_5 . The phosphatic section overlies a 2.5 m interval containing bedded barite and is overlain by thin bedded argillaceous limestone. The phosphatic section lies in the Misty Creek Embayment, a northeastern lower Paleozoic depositional embayment in the generally northwest-trending carbonate belt that flanks the Mackenzie Arch (Cecile, pers. comm., 1978).

A second Cordilleran phosphate occurrence of Cambrian age lies near the head of Muskwa River, northeastern British Columbia (see Fig. 28.1). There, black phosphate nodules 0.5 to 1 cm in diameter occur in Upper Cambrian basal shales that underlie the Ordovician Kechika Formation. The nodules are scattered throughout 100 m of section, the uppermost beds 120 m below the base of the Kechika carbonate-rocks. The grades are estimated to be low (analyses are not available); the occurrence is important for sedimentological reasons (Cecile and Norford, 1979, p. 225).

Ordovician

Black phosphatic 'pavements' lie at widely (several metres) spaced horizons in the Kechika and Road River formations in northeastern British Columbia, west of the Cambrian locality described above (see Fig. 28.1). The 'pavements' are about 1 to 5 cm thick. In the Kechika Formation, the phosphatic beds occur in two sedimentary units, one consisting of alternating lime-rich and more shaly calcilutite and calcisiltite and the other, at the top of the formation, of argillaceous calcilutite with minor calcareous shale. In the overlying Road River Formation, in the same measured section, phosphorite occurs 33 and 41 m above the

base of the unit. The uppermost Kechika phosphorite is associated with 'nodule' conglomerate that is interpreted to be a lag deposit resulting from winnowing of partly lithified sediments in deep water not far from the shelf edge (Cecile and Norford, 1979, p. 225-226). X-ray diffraction analysis of the phosphorites gave values between 1 and 25 per cent P_2O_5 . A sample in the Kechika Formation also assayed 196 to 220 ppm uranium (Cecile and Norford, 1979, p. 226).

High phosphate values have been obtained from black shales, black siltstones, and dark, impure limestones equivalent to the Ordovician Road River Formation in the southern Selwyn Mountains, District of Mackenzie (see Fig. 28.1). The shales are considered to be basinal and to lie within a transitional carbonate zone of an outer shelf facies. Phosphate values of 15.3 and 20.0 per cent P_2O_5 were discovered in the course of exploration for massive sulphides; high uranium, zinc, and vanadium values are reported with the phosphate assays (Dawson, 1979, p. 376, and pers. comm.).

Mississippian

Thin beds of phosphorite with grades up to 22 per cent P_2O_5 lie within the Exshaw Formation in the southern Rocky Mountains. The Exshaw Formation is a thin (11 m) black shale unit that disconformably overlies Devonian carbonate rocks. Two phosphatic, pelletal to nodular shale beds separated by about 3 m of black silty to cherty shale extend northward from the International Boundary. About 90 km north the phosphate appears to become dispersed into four lenticular zones of pelletal phosphate rock in about 4.5 m of black, silty shale; near latitude 50°N, only a 2 to 5 cm bed of black, oolitic phosphorite is present, and in places this is discontinuous. Grades of 4 to 22 per cent P_2O_5 are reported (Western Warner Oils, pers. comm.; F.A. Peel, consulting geologist at these localities).

Permian

Phosphorite beds in formations of Permian age in the southern Rocky Mountains form a northern extension of the well-known 'Phosphoria' of the Western States phosphate field of Wyoming, Idaho, Montana, and Utah. The Canadian part of the basin, however, is much dissected by thrust faults and only in recent years have the stratigraphy and nomenclature been clarified (see MacRae and McGugan, 1977; Norris, 1965). The earliest phosphate discoveries in the Canadian Rockies were those, found in 1915, in the then-named "Rocky Mountain Quartzites" (see de Schmid, 1916); the phosphate beds are now included in the Ishbel Group and known to be Permian in age.

The Ishbel Group in the southern Rockies has been divided into four formations, from the base: Johnson Canyon, silicified limestone; Telford, sandy carbonate rocks; Ross Creek, siltstone, chert and carbonate rock; and Ranger Canyon, chert and sandstone. The Telford and Ross Creek formations are of limited extent. Phosphate beds occur in the Johnson Canyon, Ross Creek, and Ranger Canyon units. The Ross Creek Formation, in particular, has been regarded as a potential source of mineable phosphates (MacRae and McGugan, 1977).

The phosphates of the Ishbel Group occur as: irregular laminae; angular to rounded clasts; pellets; (rare) ooliths; phosphatic conglomerate, sandstone, and siltstone; and phosphatic bone fragments. The aggregate thickness of phosphatic beds is variable, but commonly about 1 m, and is 3.9 m west of Fernie, British Columbia. Grades from 3 to 27 per cent are recorded (MacRae and McGugan, 1977; Telfer, 1933).

The Permian phosphoritic basin extends northward to Jasper, where 0.24 m of phosphorite has been noted, but perhaps not far beyond (see Fig. 28.1). The northerly and northwesterly sedimentary trends and the eastern limit of the Permian phosphorite basin were effectively shown by Telfer (1933, p. 575, Fig. 2).

Ishbel lithologies are taken to indicate a shallow-shelf environment, with a northerly trending hinge line in the eastern sequences. The proximity of the hinge line would account for the numerous disconformities, paraconformities, and condensation of sections ('condensed conglomeratic sequences'). A low-lying hinterland, low-energy shoreline environment, and an arid, tropical to subtropical climate are envisioned (MacRae and McGugan, 1977, p. 764).

Triassic

Marine apatite is present in dispersed form in the Triassic Spray River Group of the southern Rockies (between the International Boundary and Smoky River) and in the equivalent Sulphur Mountain, Toad, Liard, Charlie Lake, Baldonnel, and Doig formations to the north. The Spray River is about 140 m thick at Crownsnest Pass, but the group increases to 850 m near Smoky River. The phosphate mineral generally occurs in low concentrations — 1 or 2 per cent of the mineral components — but within certain stratigraphic intervals may be higher: up to 30 per cent P_2O_5 (Gibson, 1975, p. 20; Telfer, 1933).

The black shale of the Spray River Group, infolded with the Jurassic and Cretaceous beds of the southern foothills, is mentioned by Telfer (1933, p. 599) as generally assaying "from 2 to 4 per cent tricalcium phosphate with, occasionally, samples assaying as high as 14 per cent". No specific localities, however, were noted. In the Smoky River-Pine Pass region, phosphorite concentrations occur as phosphatic conglomerate and sandstone beds up to 15 cm thick in the Vega-Phroso and Whistler Members of the Sulphur Mountain shaly and dolomitic siltstone formation, and as thin lenses and random nodules in the lower part of the Toad Formation of calcareous siltstone and shale. The cryptocrystalline apatite commonly forms well-rounded grains, pellets, and ooliths; these three types, in addition, combine to form subangular to well-rounded phosphate clasts of conglomerate beds at the base of the Whistler Formation. Phosphate mineral also replaces some limestone, dolostone, and siltstone (Gibson, 1975).

The Triassic phosphorites were evidently deposited near the western margin of an open marine shelf with a relatively deep basin to the west. Source areas lay mainly to the east and northeast. The periods during which grains, ooliths, and clasts of phosphate were deposited are presumed to be characterized by shallow water and high energy conditions. Evaporites, red beds, intraformational conglomerate, and solution breccia in certain areas suggest shallow water, evaporite conditions in broad intertidal to tidal flat environment (Gibson, 1975, p. 30-33).

Jurassic

Black pelletal and nodular phosphorite beds form the basal 1 or 2 m of the Jurassic Fernie Formation in the southern Rockies, and this phosphate rock has been an important goal for exploration in the Fernie Synclinorium of southeastern British Columbia. Phosphatic, fossiliferous sandstone, the 'Phosphatic Belemnite Bed' of Telfer (1933), lies some 45 to 75 m above the base of the Fernie, and varies in thickness from 1.5 to 6 m. In addition, the Jurassic shales generally contain a higher than average amount of apatite throughout the sections (Telfer, 1933).

The Fernie black shale formation is about 180 to 300 m thick in the southern foothills and Rocky Mountains, where it lies on eroded Triassic and Paleozoic rocks. The lower shale beds pass upward into dark shale with siltstone and sandstone characterized by belemnite conglomerates (the 'Belemnite Bed'). Basal Fernie beds are thinner but still phosphatic northward, between Bow and Athabasca rivers, where they are included in the Nordegg Member, 9 to 30 m of black, cherty and phosphatic dolomite or limestone with siltstone and shale. The basal beds are phosphatic in part at least as far north as the Peace River Foothills (see Fig. 28.1).

The Jurassic in the subsurface of the adjacent Interior Platform, lithologically similar to that of the Rockies and foothills, is bounded by an irregular erosional edge. The Jurassic reappears in the Williston Basin of southern Saskatchewan and Manitoba, where it is up to 430 m thick (Stott, 1970).

A phosphatic facies of the Nordegg Member has been encountered at depths of 1200 to 1800 m in wells in the Paddle River region northwest of Edmonton (see Fig. 28.1). Conglomeratic or pebble phosphorite occurs with pelletal phosphorite, sandstone and chert beds over an interval from 1.5 to 15 m thick. The highest assay obtained, from a phosphate pebble in a pebble bed, was 31 per cent P_2O_5 . The Nordegg here appears to be 'subcrop' beneath Lower Cretaceous beds; the phosphate may have been leached and redeposited or concentrated as a lag deposit in Late Jurassic and Early Cretaceous time (J.R. Century, pers. comm.).

Cretaceous

Phosphate is present in two widely separated and disparate types of Cretaceous beds in western Canada: in the Ashville Group west of Lake Dauphin in Manitoba, and in unnamed, shaly flyschoid beds west of the Mackenzie Delta.

The Manitoba occurrence is a 5 cm thick, black layer of phosphatic fish remains, presumably one of the 'Fish Scales beds' of the marine shale, Ashville Group. The base of the Fish Scale Sand is taken as the boundary between Lower and Upper Cretaceous in this region. The phosphatic beds evidently resulted from a mid-Cretaceous marine transgression of the broad, generally alluvial plain of the eastern part of the Western Canada Sedimentary Basin (Stott, 1970; de Schmid, 1916, p. 1; British Sulphur Corporation, 1971, pt. 1, p. 3).

Phosphatic ironstones associated with a thick, mid-Cretaceous flyschoid sequence were discovered recently in northern Richardson Mountains, Yukon Territory. The ironstones and shale are an eastern facies equivalent of the flysch, much reduced in thickness. The ironstone occurs mainly as thin beds, each separated from adjacent beds by thin layers of ferruginous shale. Phosphate minerals occur as a 'mud matrix', as sparry replacement cement, and as veinlets in the ironstones; ironstone includes compact microcrystalline siderite, medium grained to pebbly ironstone-intraclast wackestones and packstones, and pyrite-phosphate rock. The phosphate content is highly variable, ranging up to 33 per cent P_2O_5 . The bedded deposits are also of interest for high iron and manganese contents (33% Fe_2O_3 ; 5% MnO), and for many rare and new phosphate and other minerals (Young, 1977).

The ironstone-phosphate beds of northern Yukon are somewhat distinctive among phosphate deposits of the world, and are not easily fitted in to the usual schemes for classifying phosphorites (see Christie, 1978, p. 45). The association of marine apatite with both iron and flyschoid sediments is not accounted for by the conventional models for formation of phosphorite. On the other hand brecciation,

possibly due to working by bottom currents, and proximity to a contemporary arch (the beds thinning towards it) are features found in many sites of phosphate deposition.

Western Canadian Phosphoritic Basins

The sedimentary phosphatic rocks of western Canada were reviewed, above, for two purposes: a) the identification of phosphatic basins or provinces; and b) the development of sedimentological 'models', for specific regions, that may aid further search for phosphorite (see Christie, 1978, p. 7-8).

What is the potential for useful phosphorite-bearing basins in western Canada? It is perhaps too early for a clear answer to this question; nevertheless, it may be helpful to examine certain basins in sedimentological and paleo-geographic contexts.

Precambrian Cratonic Basins

Relatively undisturbed remnants of these basins, of several ages, lie scattered on the Canadian Shield. As noted earlier, marine phosphorite may be present in the Athabasca Formation, and explorationists should be alert for other occurrences. Relatively little literature is available for Precambrian phosphorites; such deposits, however, are now being studied in, for example, India and northern Michigan (Chauhan, in press; Cannon and Klasner, 1976).

Phosphorite associations with limestone-chert, stromatolites, evaporites, and unconformities or disconformities may be expected.

Cordilleran Miogeosyncline

The Cordilleran Geosyncline is large and complex (see Fig. 28.1). From present data it appears clear that conditions favoured deposition of phosphorite at different places and at various times. The presence of arches (e.g. the Mackenzie Arch) and shelf-edge or hinge-line sites of deposition, perhaps in a suitable paleolatitude position, may account for the Cambrian and Ordovician phosphorites of east-central Yukon and northeastern British Columbia. Phosphorite deposited in Mississippian to Permian times in the southern part of the (Canadian) geosyncline appears to be related to repeated transgressions and regressions of marine deposition, under quiet tectonic conditions, with accompanying 'condensation' of sections.

As with the Cambro-Ordovician occurrences, the upper Paleozoic phosphorites appear to occur in a narrow belt near a former sedimentary hinge line. Favourable paleolatitudes for Siluro-Devonian phosphorite presumably will lie north of the Mississippian-Permian phosphate basin; that is north of present latitude 53°N.

Platform, Western Canada Sedimentary Basin

Beds enclosing Triassic and Jurassic phosphorites here are included with the platform deposits of the Western Canada Sedimentary Basin, or those units now underlying the foothills and the Interior Plains. The Triassic strata of the southern Rockies, however, are perhaps transitional in nature: a strong carbonate component is present and the Triassic units are truncated by an unconformity at the base of Jurassic beds.

Phosphorite is present in Triassic and Jurassic marine shales and siltstones between the International Boundary and the Peace River region, and is present in basal Jurassic units eastward to their eroded (subcrop) edge. This region is clearly platformal, but is marginal to the latest phases of the eastern miogeosynclinal troughs of the Cordilleran

Geosyncline. A 'model' combining some features of cratonic basin with the miogeosynclinal type of phosphate deposition appears to be needed. Exploration in this region can best be carried out by testing drill core using reagents and gamma logs.

Cordilleran Successor Basins

Some syn- and post-orogenic basins in the Cordillera are shown in Figure 28.1; phosphate has been found in Cretaceous beds in one of them – in northern Yukon. The flysch-ironstone-phosphate association is unusual and intriguing. Further study of this and similar deposits may provide clues for exploration of the successor basins. Such basins in the Canadian Cordillera, however, vary in tectonic and sedimentary style and do not lend themselves to easy generalizations.

References

- Boyd, B.W.
1976: Phosphate; no. 35 in Canadian Minerals Yearbook, 1975; Canada, Department of Energy, Mines and Resources, cat. no. M38-5125.
- British Sulphur Corporation
1971: World Survey of Phosphate Deposits, 3rd edition; British Sulphur Corporation, London.
- Cannon, W.F. and Klasner, J.S.
1976: Phosphorite and other apatite-bearing sedimentary rocks in the Precambrian of northern Michigan; United States Geological Survey, Circular 746.
- Cathcart, J.B.
1978: Uranium in phosphate rock; United States Geological Survey, Professional Paper 988A.
- Cathcart, J.B. and Gulbrandsen, R.A.
1973: Phosphate deposits; in United States Mineral Resources; United States Geological Survey, Professional Paper 820, p. 515-525.
- Cecile, M.P.
1978: Report on Road River stratigraphy and the Misty Creek Embayment, Bonnet Plume and surrounding map-areas, Northwest Territories; in Current Research, Part A, Geological Survey of Canada, Paper 78-1A, p. 371-377.
- Cecile, M.P. and Norford, B.S.
1979: Basin to platform transition, lower Paleozoic strata of Ware and Trutch map-areas, northeastern British Columbia; in Current Research, Part A, Geological Survey of Canada, Paper 79-1A, p. 219-226.
- Chauhan, D.S.
Phosphate bearing stromatolites of the Precambrian Aravalli phosphorite deposits of the Udaipur region, their environmental significance and genesis of phosphorite; Precambrian Research. (in press)
- Christie, R.L.
1978: Sedimentary phosphate deposits – an interim review; Geological Survey of Canada, Paper 78-20.
- Cook, P.J.
1976: Sedimentary phosphate deposits; in Handbook of Strata-bound and Strataform Ore Deposits, K.H. Wolf, ed.; Elsevier, Amsterdam, v. 7, p. 505-535.
- Dawson, K.M.
1979: Regional metallogeny of the northern Cordillera: recent stratiform base metal discoveries in Yukon Territory and District of Mackenzie; in Current Research, Part A, Geological Survey of Canada, Paper 79-1A, p. 375-376.
- de Schmid, H.S.
1916: Investigation of a reported discovery of phosphate in Alberta; Mines Branch, Department of Mines, Canada, Bulletin 12.
- Fahrig, W.F.
1961: The geology of the Athabasca Formation; Geological Survey of Canada, Bulletin 68.
- Gibson, D.W.
1975: Triassic rocks of the Rocky Mountain Foothills and Front Ranges of northeastern British Columbia and west-central Alberta; Geological Survey of Canada, Bulletin 247.
- Hale, L.A.
1967: Phosphate exploration using gamma-radiation logs, Dry Valley, Idaho; in Anatomy of the western phosphate field, L.A. Hale, ed.; Intermountain Association of Geologists, 15th Field Conference, Salt Lake City, p. 147-159.
- King, P.B. and Edmonston, G.J.
1972: Generalized tectonic map of North America; United States Geological Survey, Miscellaneous Geologic Investigations, Map I-688.
- MacRae, J. and McGugan, A.
1977: Permian stratigraphy and sedimentology – southwestern Alberta and southeastern British Columbia; Canadian Society of Petroleum Geologists, Bulletin, v. 25, p. 752-766.
- McKelvey, V.E.
1967: Phosphate deposits; United States Geological Survey, Bulletin 1252-D,
- Norris, D.K.
1965: Stratigraphy of the Rocky Mountain Group in the southeastern Cordillera of Canada; Geological Survey of Canada, Bulletin 125.
- Spence, H.S.
1920: Phosphate in Canada; Mines Branch, Department of Mines, Publication 396.
- Stott, D.F.
1970: Mesozoic; in Geology of Western Canada, by R.J.W. Douglas, H. Gabrielse, J.O. Wheeler, D.F. Stott, and H.R. Belyea; in Geology and Economic Minerals of Canada; Geological Survey of Canada, Economic Geology Report No. 1, 5th ed., Chap. VIII, p. 367-488.
- Telfer, L.
1933: Phosphate in the Canadian Rockies; Canadian Institute of Mining and Metallurgy, Bulletin 260, p. 566-605.
- Tipper, H.W. (compiler)
1978: Tectonic assemblage map of the Canadian Cordillera with adjacent parts of the United States of America, scale 1:2 000 000; Geological Survey of Canada, Open File 572.
- Young, F.G.
1977: The mid-Cretaceous flysch and phosphatic ironstone sequence, northern Richardson Mountains, Yukon Territory; in Report of Activities, Part C, Geological Survey of Canada, Paper 77-1C, p. 67-74.

AN OCCURRENCE OF THE APPARATUS OF "PROONEOTODUS" (CONODONTOPHORIDA)
FROM THE ROAD RIVER FORMATION, NORTHWEST TERRITORIES

Project 500029

R.S. Tipnis and B.D.E. Chatterton¹
Institute of Sedimentary and Petroleum Geology, Calgary

Tipnis, R.S. and Chatterton, B.D.E., An occurrence of the apparatus of "Prooneotodus" (Conodontophorida) from the Road River Formation, Northwest Territories; in Current Research, Part B, Geological Survey of Canada, Paper 79-1B, p. 259-262, 1979.

Abstract

Discovery of an almost complete apparatus of "Prooneotodus" tenuis consisting of two parallel, opposed half-apparatuses with at least 22 (? as many as 24) elements is detailed. The half-apparatuses are crescent shaped in cross-section with distinctly larger elements occurring medially and elements progressively smaller toward the tips of the crescents. The elements appear to be composed of two layers of calcium phosphate separated by a gap of similar thickness to the layers. Whereas the inner layer forms a discrete cone, the outer layers of adjacent elements are fused to one another. The elements of the two half-apparatuses were joined to one another to form a structure which almost certainly did not function as a lophophore-supporting device, but possibly as a grasping structure.

Introduction

Landing (1977) reported natural assemblages of "Prooneotodus" tenuis (Müller) from the Germantown Formation, Taconic allochthon, eastern New York. The "P." tenuis apparatus had been determined previously only from impressions found on shale surfaces (Miller and Rushton, 1973; Müller and Andres, 1976). In discussing his findings, Landing (op. cit.) provided new data regarding the nature of the clusters; considered the possibility of these clusters belonging to protoconodonts in the sense of Bengston (1976) as opposed to paraconodonts (as was previously assumed by Müller and Nogami, 1971); supported the 'external sclerite' model of Bengston (1976); and rejected Conway Morris's (1976) hypothesis that the "conodont animal" *Odontogriphus omalus* Conway Morris was lophophorate.

This report documents similar clusters from northern Canada. All except one of the clusters reported here are similar to those described by Landing (1977). The exception in the present collection provides additional data, notably with respect to the number of elements that make up the cluster (at least 22 (24?)), the general shape and arrangement of the cluster, and the double lamellar structure of many of its constituent elements.

Locality

Three samples of Late Cambrian (Trempealeuan) age from the lower and middle parts of the RRal map-unit, Road River Formation (Cecile, 1978; Fig. 68.1, Secs. 31 and 44), in the Bonnet Plume map area, Northwest Territories, yielded the "Prooneotodus" clusters. The best clusters were from GSC locality C-69429, collected 170 m above the base of RRal map unit at Section 31. This locality yielded six clusters. Excepting a few phosphatic microfossils and indeterminate inarticulate brachiopods, the sample was devoid of any identifiable fossils. The RRal map unit comprises thin bedded rhythmic argillaceous limestone, limestone and minor calcareous shale with slumped bedding and small scale ripple crosslamination. Cecile (written comm., January 31, 1978) interpreted the unit as a basin/slope facies at this level. Other clusters occur at a level near the lower middle part of the RRal map unit at Section 44 (Cecile, 1978, Fig. 61.2). Altogether, six poorly preserved and incomplete clusters were recovered from this section. Here also the map unit is interpreted as a basin/slope facies. Landing (1977) noted that clusters of "Prooneotodus" were rare. His own interpretation of the

depositional environment for the Germantown Formation suggests a basin/slope facies. The preservation of such delicate structures was possibly due to accumulation of un lithified carbonate sediments "as a turbidite flow and the deposition of sediment as a single event" (Landing, 1977, p. 1079-1080). Landing further noted that such a preservation may have been aided by slow decomposition in cold deep water that contained little bottom fauna.

Description of an Almost Complete Cluster

The most important cluster (GSC 58271), also the most complete discovered to date, is illustrated in four views (Pl. 29.1, figs. 6-9) and described below. Additional clusters (Pl. 29.1, figs. 1-5) emphasize the close similarity with Landing's (1977) clusters and his terminology is used in the plate descriptions.

Lateral view (fig. 6). This shows the basic arrangement of the two parallel-opposed half-apparatuses. The stacking of the individual elements can be seen. Important aspects of this apparatus are the proximity of the basal parts of the half-apparatuses, the wider space between the 'distal' parts of the two half-apparatuses, and the almost parallel arrangement of the elements within each half-apparatus. Although this could be a result of taphonomic processes, it may also be the result of the apparatus being 'frozen' in an 'open' position. Most of the elements are broken near the tips, and this makes it difficult to determine their relative lengths. However, the medial elements of the two half-apparatuses appear to be somewhat larger than those toward the sides (they are larger distally than the more lateral elements).

Oral view (fig. 7). The 'upper' (in the sense of its position on the plate) half-apparatus includes 10 (as many as 12?) individual elements that are arranged in a rough crescent. In cross-section the arrangement of the elements in two closely opposed crescentic clusters (half-apparatuses) is quite distinct from the almost "figure 8" arrangement of the elements in *Odontogriphus omalus* Conway Morris (Conway Morris, 1976, Text-fig. 5). The 'lower' half-apparatus consists of 12 elements also arranged in a rough crescent, with a possible fold at the left side. In both 'upper' and 'lower' half-apparatuses the larger elements are situated nearer the medial parts of the crescent. Between the 'upper' and 'lower' half-apparatuses, more or less central to the open space is a

¹University of Alberta, Edmonton, Alberta.

branch-like structure. Its relationship, if any, with the conical elements is difficult to determine; and it may just be an artifact of preservation.

In most of these half-apparatuses, each conical element consists of an inner and an outer cone. The inner cone appears to be well separated from the outer cone; its 'wall' consists of a single lamella which is of the same thickness as that of the outer cone (fig. 9). A 'basal' cavity extends close to the tip of the cone. The surface textures of the inner and outer cones are similar (fig. 8). The structure of the lamellae of both the inner and outer walls is identical, and consists of fine crystallites arranged perpendicular to the surface of the lamellae. The outer cones give the impression of enveloping the inner cones in a continuous fashion with a gap between the two lamellae. The outer lamellae of adjacent elements frequently merge or become fused so that the elements are rigidly held together, at least along parts of their basal and medial portions. This is certainly true of most of the elements and may be true of all of the elements of each half-apparatus. Thus, all of the elements in each half-apparatus may have acted in unison. Not all of the clusters recovered show this lateral fusion of the elements. This could be the result of preservation, ontogenetic change, or variation within a population. The fusion of the outer lamellae in the two half-apparatuses of the apparatus figured in Plate 29.1, figures 6 to 9 suggests that the crescentic shape of these structures is not due to their being partly enrolled after death.

Discussion of Growth and Function of the Apparatuses

The structure of the cones in these apparatuses, consisting of two similar layers with a distinct gap separating them, is different from that previously described for proto-, para-, and euconodonts. We suggest below two possible mechanisms for the origin of this structure. The first assumes that growth of the "**Prooneotodus**" *tenuis* apparatuses described above may have been, in part, analogous to the growth of euconodonts as proposed by Bengston (1976).

Bengston (op. cit.) suggested that protoconodonts were external sclerites that grew by basal accretion, whereas paraconodonts were surrounded by an epithelium only in the initial stages. He considered euconodonts to be usually covered by an epithelium. They could however extrude when in use. If conodontophorids were indeed able to extrude their elements, then even proto- and paraconodonts may have possessed this property of retraction and extrusion. It is possible, therefore, that the elements described here may have had two stages of secretory history. The inner cones grew like protoconodonts in the manner suggested by Bengston (1976). At a later stage, these elements may have been retracted into the epithelium where the outer layer was formed in a manner analogous to euconodonts. This may explain the common sheath that forms a boundary between the two adjacent elements, but does not satisfactorily explain the existence of a gap between the inner and outer lamellae of each element. This gap probably was occupied by a layer of soft tissue that surrounded and coated the inner cones. This layer of tissue could have secreted phosphatic material along its external surface (an untested assumption). Where two of these layers were closely pressed between adjacent elements, they could have formed a common lamella and caused adjacent elements to fuse together. Following the addition of the second layer of calcium phosphate, the elements could have been extruded, and could have functioned normally.

A more favoured mechanism envisaged for producing the distinctive structure of these elements is the almost simultaneous basal secretion of these elements. The outer

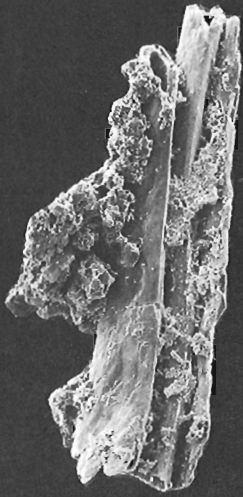
lamellae would be secreted first and the inner lamellae would be secreted soon after by segregation of tissue within the region of the basal cavities of the outer lamellae. The cavities and lamellae would continue to be produced at the bases of the elements by multiplication of cells of the soft tissue and secretion of crystallites of the lamellae. This hypothesis requires fusion of the outer elements early in the life history of the conodont animal. The variation in the presence or absence of the fusion between the outer lamellae would have resulted from a variation in the proximity of elements. Elements secreted close to one another might cause merging of the zones of secretion of the outer lamellae, with the resultant production of lamellae common to more than one element. It is important to note that only a few of the discussed elements and apparatuses of **Prooneotodus** show a bi-lamellar structure with a tendency for the outer lamellae of adjacent elements to be joined to one another. Some of the specimens illustrated by Landing (1977, Pl. 1, fig. 7; Pl. 2, figs. 3, 5, 9) and Bengston (1976, Fig. 7) may show this arrangement. The absence of two lamellae in solitary elements (or even in clusters) of "**Prooneotodus**" could be the result of either the original secretion of only one layer or the separation of the inner and outer layers after death.

It is interesting to speculate briefly on the functional reasons for (1) the bilamellar structure of the elements and (2) the fusion of outer lamellae, or the formation of common outer lamellae, between adjacent elements. The simplest explanation for the formation of more than one lamella appears to be the need for greater structural strength for each individual element. Landing (1977) suggested that the elements of each half-apparatus acted together as a single functioning unit, whose function was probably to physically grasp various objects (food, enemies or sexual partners?).

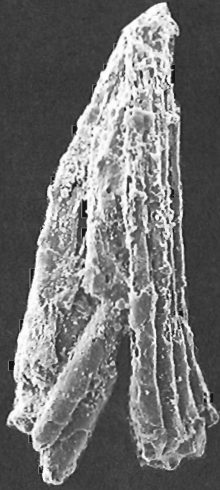
Plate 29.1 (right)

"Prooneotodus" *tenuis* (Müller)

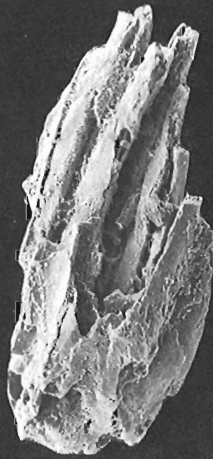
- Figure 1. Three-element incomplete half-apparatus probably from the sagittal (medial) region, x190, figured specimen GSC 58272; GSC locality C-69429.
- Figure 2. Incomplete half-apparatus. Left portion with 3 elements (two broken); right portion with 5 elements, x190, figured specimen GSC 58273, GSC locality C-69429.
- Figure 3. Eight-element incomplete half-apparatus, x190, figured specimen GSC 58274, GSC locality C-69429.
- Figure 4. Nine-element incomplete half-apparatus, x75, figured specimen GSC 58275, GSC locality C-69361-250'.
- Figure 5. A lateral view of the tip of the cluster illustrated in Figure 4, x150.
- Figures 6-9. Figure 6 - Lateral view of two almost complete parallel-opposed half-apparatuses, x275 (apparatus probably 'frozen' in an 'open' position). Figure 7 - Upper view of the nearly complete apparatus showing tips of 12(?) elements on the lower side, x220. Figure 8 - Oblique upper view showing the characteristic inner cones and the enveloping outer cones, x475. Figure 9 - Upper view of two adjacent elements showing fusion of the common sheath, x3000, figured specimen GSC 58271, GSC locality C-69429.



1



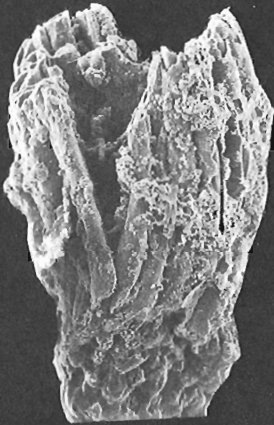
2



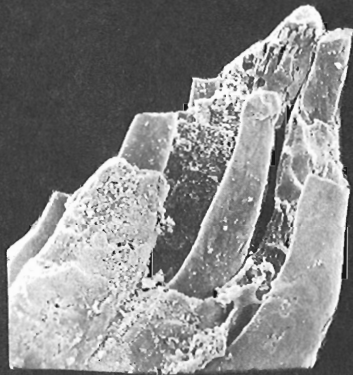
3



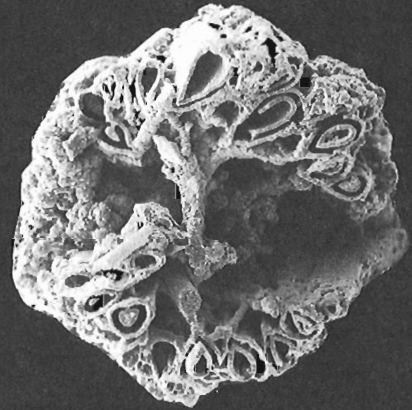
4



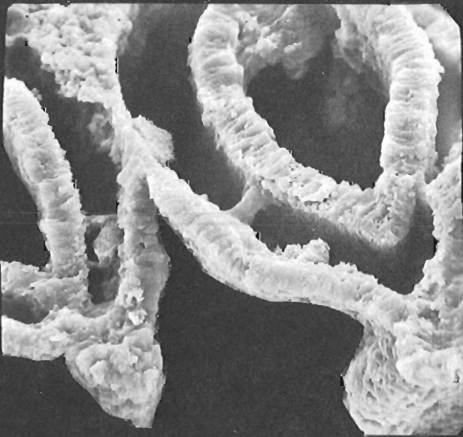
6



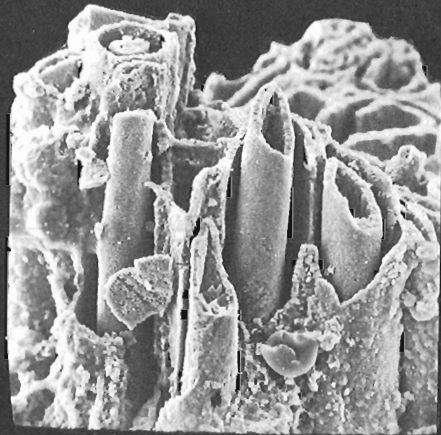
5



7



9



8

The elements of one of these half-apparatuses would have provided each other with support so that the strength of the whole unit was greater than that of any of its individual constituents (the elements). The main problem with such a unit, consisting of smooth, slightly curved conical elements arranged in a subparallel fashion, would have been the danger of the component elements slipping relative to one another (with the greater danger of breakage). The fusion of adjacent elements by the formation of common outer lamellae would appear to be an efficient method of preventing neighbouring elements slipping relative to one another, enabling the half-apparatus to act as a single unit. Both of these explanations would be consistent with an increase in efficiency for a physical grasping or biting function for the apparatus; and would not be compatible with the hypothesis that individual elements acted as the internal support for lophophore filaments (Lindström, 1973, 1974; Conway Morris, 1976). Indeed, with the fusion of adjacent elements to one another, it is difficult to see how these elements could have acted as internal supports for more than two lophophore filaments (one for each half-apparatus). The three dimensional morphology of the two half-apparatuses 'frozen' together in the apparatus figures in Plate 29.1, figures 6 to 9, with the half-apparatuses arranged opposed to one another with the tips of the elements curving toward one another also resembles a grasping structure rather than a lophophore support.

Both of these alternative hypotheses would suggest that the conodont elements were exposed (not covered by soft tissues) while they functioned as grasping(?) structures. Several workers, besides Bengston (1976) and Landing (1977), have suggested that conodonts may have functioned in a partly or completely exposed position. Barnes et al. (1973) considered that the secretion of white matter in euconodonts could have resulted from the eruption of tips of denticles from the soft tissue, and the disruption of a regular vascular supply, with resultant replacement of "central growth canals" by more disordered white matter. Carls (1977) suggested that euconodonts may have been embedded in soft tissues while the conodont structure was at rest, but extruded by the retraction of the soft tissues around the elements when the apparatus was functioning.

Fused groups of conical euconodonts have been described by several workers, Barnes (1967), Pollock (1969), Nicoll (1977) and Nowlan (1979). Nicoll (1977) stated that the two acodinan elements that he found fused to one another may have functioned as a fused unit during the life of the conodont animal, in a manner analogous to that of a compound element, with the denticles discrete and not pressed against one another. The elements of *Belodina* described by Barnes (1967), and the elements of *Panderodus* described by Pollock (1969) could have functioned together in units analogous to the half apparatuses described here. The clusters of elements of *Belodina* described by Nowlan (1979) were considered by him to be the result of a post-mortem association; and were not considered to represent truly the number and arrangement of elements in the *Belodina* apparatus. Should these euconodonts have acted together as functioning units, such morphological features as a ridge and groove microornament (*Panderodus* and *Neopanderodus*) or grooves, ridges and striations running along the cusps (*Belodina*, *Belodella*, *Walliserodus*) could have functioned to provide friction or interlocking between adjacent elements.

Acknowledgments

We gratefully acknowledge C.R. Barnes and E. Landing, University of Waterloo for reading an earlier draft of this manuscript and making several useful comments. R.S. Tipnis thanks T.T. Uyeno for his general support.

References

- Barnes, C.R.
1967: A questionable natural conodont assemblage from Middle Ordovician limestone, Ottawa, Canada; *Journal of Paleontology*, v. 6, p. 1557-1560.
- Barnes, C.R., Sass, D.B., and Monroe, E.A.
1973: Ultrastructure of some Ordovician conodonts; *Geological Society of America, Special Paper 141*, p. 1-30.
- Bengston, S.
1976: The structure of some Middle Cambrian conodonts, and the early evolution of conodont structure and function; *Lethaia*, v. 9, p. 185-206.
- Carls, P.
1977: Could conodonts be lost and replaced?; *Neues Jahrbuch für Geologie und Paläontologie, Abhandlungen*, v. 155, p. 18-64.
- Cecile, M.P.
1978: Report on Road River stratigraphy and the Misty Creek Embayment, Bonnet Plume and surrounding map-areas, Northwest Territories; *Geological Survey of Canada, Paper 78-1A*, p. 371-377.
- Conway Morris, S.
1976: A new Cambrian lophophorate from the Burgess Shale of British Columbia; *Palaeontology*, v. 19, p. 199-222.
- Landing, E.
1977: "*Prooneotodus*" *tenuis* (Müller, 1959) apparatuses from the Taconic allochthon, eastern New York: construction, taphonomy and the protoconodont "supertooth" model; *Journal of Paleontology*, v. 51, p. 1072-1084.
- Lindström, M.
1973: On the affinities of conodonts; *Geological Society of America, Special Paper 141*, p. 85-102.
1974: The conodont apparatus as a food-gathering mechanism; *Paleontology*, v. 17, p. 729-744.
- Miller, J.F. and Rushton, A.W.A.
1973: Natural conodont assemblages from the Upper Cambrian of Warwickshire, Great Britain; *Geological Society of America, Abstracts with Programs*, v. 5, p. 338-339.
- Müller, K.J. and Andres, D.
1976: Eine Conodontengruppe von *Prooneotodus tenuis* (Müller, 1959) in natürlichem Zusammenhang aus dem oberen Kambrium vom Schweden; *Paläontologische Zeitschrift*, v. 50, p. 193-200.
- Müller, K.J. and Nogami, Y.
1971: Über den Feinbau der Conodonten; *Kyoto University, Memoirs of the Faculty of Science, Geology and Mineralogy Series*, v. 38, p. 1-87.
- Nicoll, R.S.
1977: Conodont apparatuses in an Upper Devonian palaeoniscoid fish from the Canning Basin, Western Australia; *Bureau of Mineral Resources, Journal of Australian Geology and Geophysics*, v. 2, p. 217-228.
- Nowlan, G.S.
1979: Fused clusters of the conodont genus *Belodina* Ethington from the Thumb Mountain Formation (Ordovician), Ellesmere Island, District of Franklin; *Geological Survey of Canada, Paper 79-1A*, p. 213-218.
- Pollock, C.A.
1969: Fused Silurian conodont clusters from Indiana; *Journal of Paleontology*, v. 43, p. 929-935.

COMMENTS ON THE PROTEROZOIC STRATIGRAPHY OF VICTORIA ISLAND
AND THE COPPERMINE AREA, NORTHWEST TERRITORIES

J. Dixon

Institute of Sedimentary and Petroleum Geology, Calgary

Dixon, J., *Comments on the Proterozoic stratigraphy of Victoria Island and the Coppermine area, Northwest Territories; in Current Research, Part B, Geological Survey of Canada, Paper 79-1B, p. 263-267, 1979.*

Abstract

The age and correlation of the Precambrian sedimentary rocks in the Wellington and Duke of York inliers is not clear; ages ranging from Archean to Hadrynian have been suggested. A review of the literature and new field data help to clarify the problem. Differing structural trends and lithotypes clearly indicate that the rocks of the two inliers belong to separate successions. The rocks of the Wellington inlier are correlated with member Bp of the Apebian Burnside River Formation and those of the Duke of York inlier with the upper parts of the Hadrynian Rae Group and the Glenelg Formation. In the Coppermine area, rocks identified as units 24 and 25, originally classified as part of the Rae Group, are Cambrian and are probably equivalents of the Saline River Formation.

Introduction

Victoria Island and the Coppermine area are underlain by extensive Proterozoic sedimentary rocks (Fig. 30.1). On Victoria Island, Proterozoic rocks are exposed in three inliers, the Minto Arch and the Wellington and Duke of York inliers. The regional geology of Victoria Island was described by Thorsteinsson and Tozer (1962) and that of the Coppermine area by Baragar and Donaldson (1973). Christie et al. (1972, p. 77-82) discussed the tectonic and stratigraphic significance of Proterozoic rocks in the two areas and also offered some alternative correlations. A more recent correlation scheme and discussion of the stratigraphy of the two areas were proposed by Young (1977).

This report reviews some aspects of the regional correlations of previous workers and presents data obtained in the summer of 1973.

Acknowledgments

I would like to thank Union Oil and Amoco Canada for permission to publish data collected during the 1973 field season. Also, I extend my thanks to the geologists and assistants from the two companies who helped collect much of the field data. D.G.F. Long and M.P. Cecile offered many valuable suggestions to improve the paper.

Stratigraphy

Wellington Inlier

Thorsteinsson and Tozer (1962) identified three units within the Wellington inlier. Map unit 1, identified only at the head of Hadley Bay, consists of grey and pink quartzites with minor amounts of micaceous quartzite, micaceous hematitic quartzite and greywacke. The beds dip steeply to the northwest, are partly schistose, and are intruded by diabase dykes and quartz veinlets. These observations were verified by the author and others in 1973, although the presence of schistosity was queried. In the same area of Hadley Bay, a granodiorite body (map unit 2) was recognized and tentatively interpreted by Thorsteinsson and Tozer (op. cit.) to intrude map unit 1 strata. The third unit identified by Thorsteinsson and Tozer (op. cit.), occupying the southern part of the Wellington inlier, between Washburn Lake and Wellington Bay (Fig. 30.2), was correlated with the basal clastic rocks of the Glenelg Formation in the Minto Arch.

The discovery of a granite and some suspicions of the correlations in the southern part of the Wellington inlier confirmed the need to re-evaluate some aspects of the work by Thorsteinsson and Tozer (op. cit.).

The rocks at the southern end of the Wellington inlier are mostly bright red to pink quartzitic sandstone and conglomerate. Siltstone and cherty ironstone occur about 10 km south of Washburn Lake, the latter as a 15 m thick bed in association with quartzitic sandstone. The coarse clastic units tend to be thickly bedded and crossbedding is very common. Young (1974, p. 20) interpreted these units as fluvial deposits with an easterly source area. Young (op. cit.) used Thorsteinsson and Tozer's (1962) correlation with the Glenelg Formation but he later revised it (Young and Jefferson, 1975). Silica cement is ubiquitous and most of the rocks are well indurated. The lack of vertically persistent sections prevented reliable thickness measurements but a composite section indicated at least 120 m of exposed strata.

The rocks in the southern part of the inlier contrast markedly with the basal sandstones of the Glenelg Formation of the Minto Arch, which are predominantly grey, with only a slightly pinkish colour, fine grained, quartzitic, and very

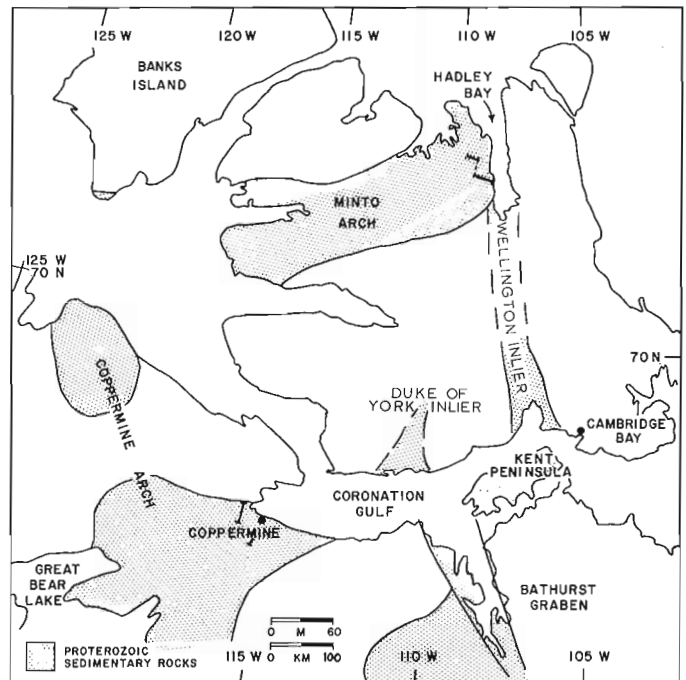


Figure 30.1. Distribution of Proterozoic sedimentary rocks, Victoria Island and adjacent mainland. Also shown are the approximate positions of the composite sections illustrated in Figure 30.5 (Hadley Bay and Coppermine).

commonly interbedded with greenish black silty shales. Conglomerates are rare, and the basal part grades upward into a predominantly shale succession (Fig. 30.5). A marine origin is assigned to the basal Glenelg Formation, in contrast to the fluvial origin of sediments from the southern part of the Wellington inlier.

Rocks more similar to those of the Wellington inlier occur to the south, on the Kent Peninsula and in Bathurst Inlet area (Fig. 30.1). On the Kent Peninsula, Fraser (1964) reported the presence of a pink quartzite unit (unit 11 of the Goulburn Group), later named the Burnside River Formation (Tremblay, 1968), which is comparable in lithotypes and structural attitude to rocks from the adjacent Wellington inlier. Young and Jefferson (1975, p. 1735) also noted the similarity. Detailed descriptions of the Burnside River Formation by Campbell and Cecile (1975, 1976, 1979) indicate that rocks of member Bp are correlative with those at the southern end of the Wellington inlier on the basis of lithological descriptions and paleocurrent trends; e.g. both areas contain red or pink quartzitic sandstones and conglomerates derived from an easterly source.

Correlation of the Wellington inlier rocks with those of the Bathurst Inlet and Coppermine areas has been suggested by previous workers (Stockwell et al., in Douglas, 1970, p. 84) but only Young and Jefferson (1975), Long (1978, p. 330), Campbell and Cecile (1979) and I have made specific correlations with the Burnside River Formation. The age of the Burnside River Formation is generally accepted as Aphebian (Tremblay, 1968; Stockwell and Williams, 1964, p. 12; Wright, 1967, p. 46; Stockwell et al., in Douglas, 1970, p. 76; Campbell and Cecile, 1976; Campbell, 1978).

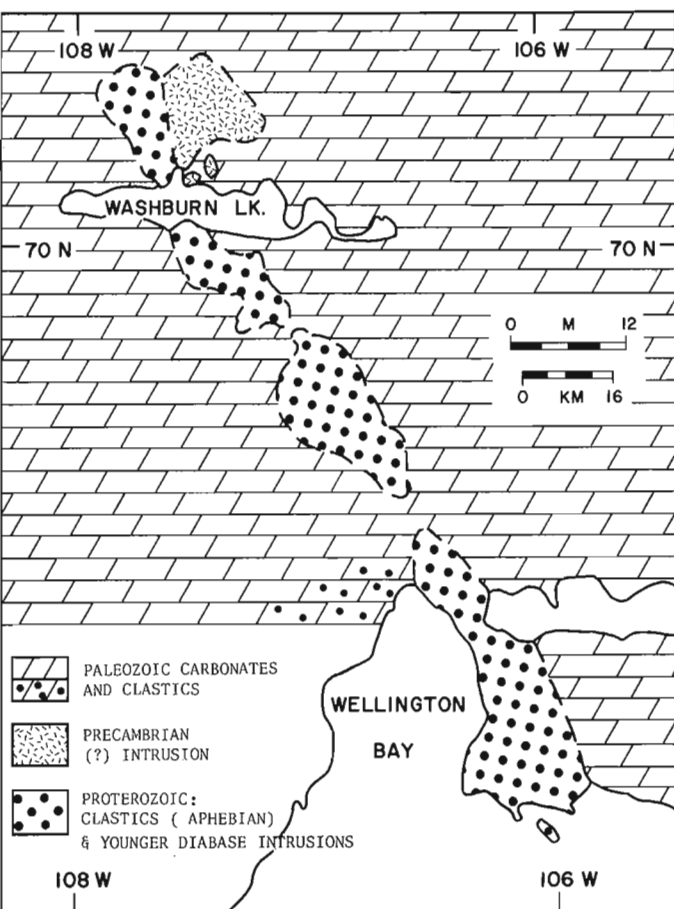


Figure 30.2. Geological sketch map of the southern part of the Wellington inlier, Victoria Island.

In the vicinity of Wellington Bay, Victoria Island (Fig. 30.2), Christie (in Christie et al., 1972, p. 78) recognized gently and steeply dipping strata which led him to suggest that two successions could be present. The steeply dipping strata were interpreted as part of the Hudsonian basement (i.e. Aphebian) and the more gently dipping strata as part of a young succession. Young (1974) noted there was a gradual change in dip between the steeply- and gently-dipping strata and that the two successions were similar. This was confirmed by our 1973 observations and it was also noted that the steeply-dipping strata are adjacent to a large, westward dipping diabase dyke. It is therefore unlikely that two successions are present, as suggested by Christie (op. cit.).

The granitic body exposed north of Washburn Lake (Fig. 30.2) may be intrusive, although contacts were not located. Topographically the granitic body is more prominent than the adjacent Proterozoic clastic rocks and in the approximate position of the contact there is a shallow, north-south linear depression. Paleozoic carbonate rocks were seen to surround knolls and fill in depressions and joints on the igneous rock, confirming previous conclusions that the Wellington inlier is part of an exhumed topographic surface (Thorsteinsson and Tozer, 1962; Christie et al., 1972).

The Washburn Lake igneous body is granodiorite and may belong to the same suite of igneous intrusions as the granodiorite at Hadley Bay and the latter has a K-Ar age of 2405 Ma (Thorsteinsson and Tozer, 1962, p. 25). However, a K-Ar age of 1673 Ma, ± 42 Ma (Aphebian) was obtained from muscovite in the Washburn Lake igneous rock (W.A. Gibbons, in Campbell and Cecile, 1979). The Washburn granodiorite may be contemporaneous with the Dismal Lakes granitic intrusions mapped east of Great Bear Lake and dated as Aphebian by Baragar and Donaldson (1973, p. 12, Map 1338A). Due to the uncertain field relationships between the igneous and Proterozoic sedimentary rocks, and the lack of reliability of K-Ar dating, the age of the granodiorites remains debatable.

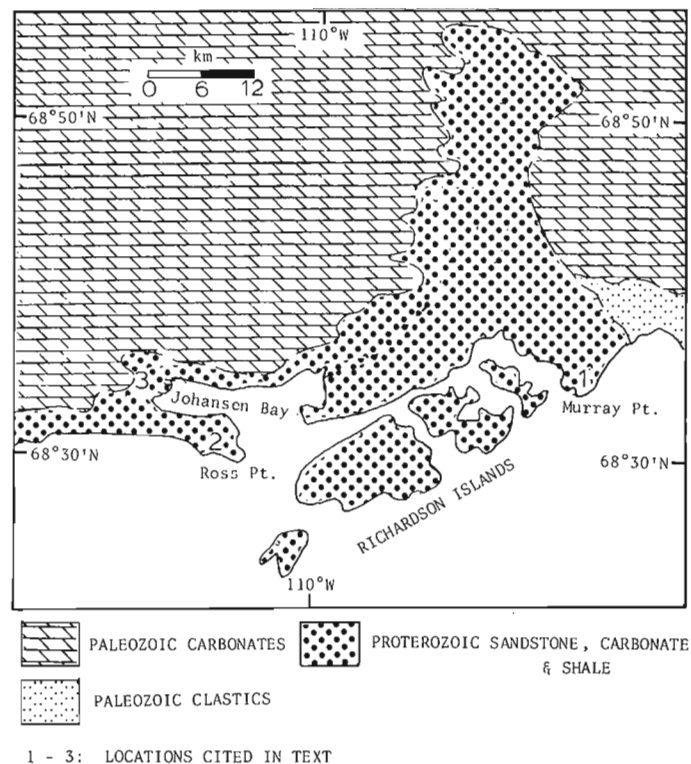
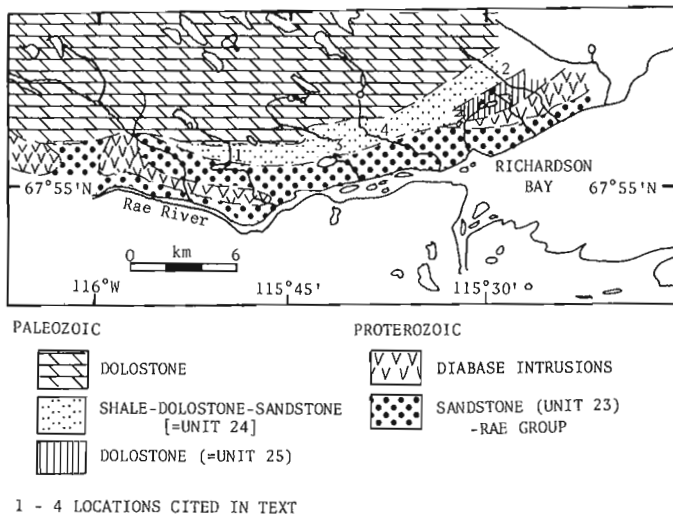


Figure 30.3. Geological sketch map of the Duke of York inlier, Victoria Island.



1 - 4 LOCATIONS CITED IN TEXT
Figure 30.4. Geological sketch map of the Rae River area, Coppermine.

The relationship between the sedimentary rocks at Hadley Bay (map unit 1) and those at the southern end of the Wellington inlier is still not clear. The contrast in lithotypes, structural attitudes and apparently higher degree of metamorphism at Hadley Bay could be interpreted to indicate two separate sequences. Christie (in Christie et al., 1972) implied that they were two separate sequences and that the Hadley Bay one was older, an interpretation which fits the available data.

Duke of York Inlier

Thorsteinsson and Tozer (1962) originally correlated the rocks in the Duke of York inlier with the Glenelg Formation. Christie (in Christie et al., 1972, p. 79) considered these rocks to be a landward continuation of the arcuate outcrops of the Duke of York archipelago in the Coronation Gulf. The rocks of the archipelago and Duke of York inlier are predominantly diabase sills but Proterozoic sedimentary rocks are present locally. Baragar and Donaldson (1973) included the island outcrops in the Hadrynian Rae Group.

Scattered outcrop and topographic dominance of the diabase intrusions in the Duke of York inlier made it difficult to compile a continuous section but, from exposures at Murray Point, Ross Point and the western end of Johansen Bay (loc. 1 to 3, respectively, Fig. 30.3), a general succession was compiled. At Murray Point there are about 187 m of interbedded shale, argillaceous limestone, limestone and dolostone with stromatolite horizons. These are overlain by about 119 m of light pink to grey weathering, thickly bedded to massive, fine- and medium-grained quartzose sandstones interbedded with shale. At Ross Point, 110 m of grey weathering, fine- and medium-grained quartzose sandstone containing local occurrences of low angle crossbedding were measured. The Ross Point section probably overlies the Murray Point section. A stromatolitic dolostone of unknown thickness was located at the western end of Johansen Bay and is stratigraphically higher than the Ross Point section. A minimum thickness of 416 m of Proterozoic sedimentary rock is present within the Duke of York inlier but, because the above locations are widely separated, the intervening areas could contain a significant thickness of strata.

The differences in lithotypes and structural trends preclude any correlation between the Duke of York and Wellington inliers. Rocks within the Duke of York inlier dip gently northwestward, whereas those in the southern part of

the Wellington inlier dip to the west and southwest. Gravity data across southern Victoria Island (Hornal and Boyd, 1972) show a gravity maximum along the Wellington inlier and an adjacent low to the west. The steep gradient between the two gravity features could indicate a major fault zone, possibly a northerly extension of the eastern fault zone of the Bathurst graben.

The structural continuity between the Duke of York inlier, the outcrops in the Duke of York archipelago and the Hadrynian Rae Group of the Coppermine area suggest a direct correlation. Furthermore, the sandstones of unit 23 in the Rae Group (Baragar and Donaldson, 1973, p. 11, Map 1337A) are comparable to those at Ross Point and Murray Point; both are quartzose, predominantly grey in colour, locally crossbedded and both have thick successions with virtually no shale interbeds. However, there are some differences, notably in thicknesses – approximately 91 m in the Coppermine area as opposed to at least 229 m in the Duke of York inlier. Also the interbedded carbonate and shale sequence at Murray Point is not directly comparable to unit 22, a stromatolitic dolostone, in the Rae Group. Some of these differences could be accounted for by the lack of exposure in the upper and lower contacts of unit 23.

There are also many similarities between the Duke of York inlier rocks and the upper part of the Glenelg Formation in the Minto Arch. The carbonate-shale sequence could be equivalent to the upper part of the Glenelg dolostone unit, the sandstone at Ross and Murray points equivalent to the upper clastics of the Glenelg Formation and the stromatolite bed at Johansen Bay equivalent to a stromatolite bed at the top of the Glenelg Formation (Fig. 30.5). The stromatolite beds at Johansen Bay and in the upper Glenelg Formation show a similar external form, large low amplitude mounds made up of columnar stromatolites (see Young and Long, 1976, Fig. 2 for an illustration of the Glenelg stromatolites).

Coppermine Area

The work of Baragar and Donaldson (1973) is the most comprehensive available geological report for the Coppermine area and was used as a guide during our 1973 field work. Strata of Helikian to Paleozoic age were examined and, for the most part, there was close agreement with Baragar and Donaldson's work. However, units 24 and 25 of the Rae Group, exposed north of Rae River, were found to be incorrectly dated and consequently mismapped. Very small, chitinous, inarticulate brachiopods were found in thin bedded, fine grained sandstones and dolostones in what Baragar and Donaldson had mapped as unit 24 of the Proterozoic Rae Group (loc. 1, Fig. 30.4). The stratigraphic position of unit 24, underlying Paleozoic carbonates and a regional comparison with nearby basal Paleozoic sequences indicated a Cambrian age for unit 24 (Fig. 30.4).

North of Richardson Bay, at locality 2 (Fig. 30.4), a 45.6 m dolostone and dolomitic shale succession, presumably equivalent to Baragar and Donaldson's unit 25, occurs beneath a 62.5 m sequence of red and green gypsiferous shales interbedded with thin beds of sandstone and dolostone. As mapped in the field, the gypsiferous shale sequence appeared to be contiguous with the strata at locality 1 and presumably also equivalent to Baragar and Donaldson's unit 24. However, at locality 2 (Fig. 30.4), unit 25 may be the Cambrian. There is no apparent structural or major sedimentological break between the dolostone and gypsiferous shale successions; both appear to be part of the same overall sedimentary sequence. The dolostone (unit 25) appears to be replaced westward by a shalier and sandier facies when traced to localities 1 and 3 (Fig. 30.4). A prominent orange or brown weathering dolostone bed, up to 6 m thick and containing columnar and laterally linked domal stromatolites, is present at localities 3 and 4 and forms a topographic bench which, when traced to

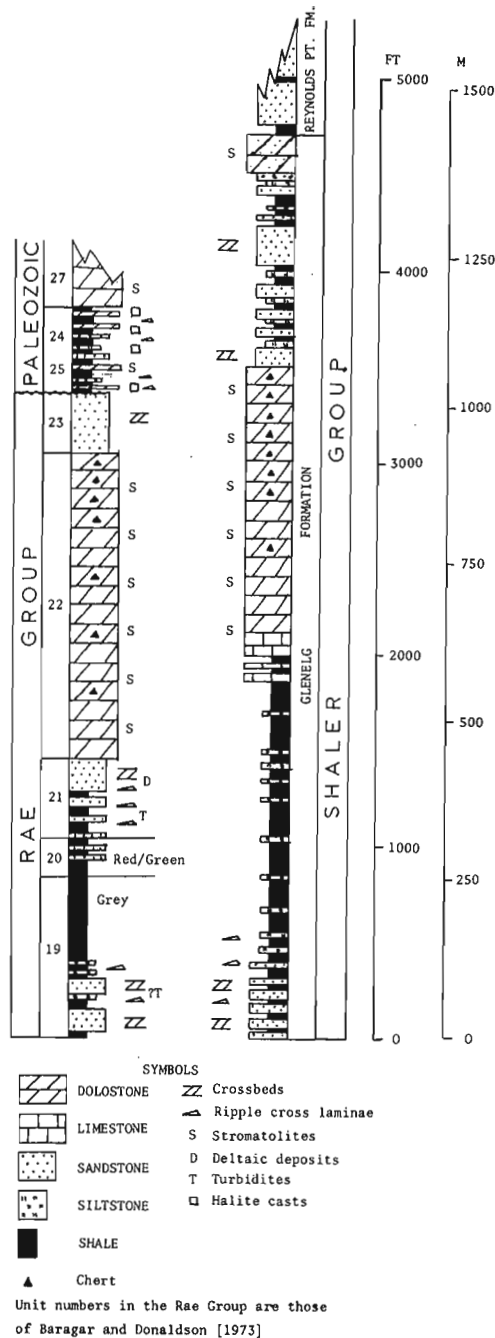


Figure 30.5. Comparison of the Rae Group and Glenelg Formation successions from the Coppermine and Hadley Bay areas respectively (see Fig. 30.1 for approximate geographic locations).

locality 2, appears to coincide with the top of the dolostone succession (unit 25). The orange weathering dolostone appears to occur within the Cambrian sequence at locality 3, forms the only exposure at locality 4 and apparently is absent at locality 1.

Baragar and Donaldson (1973) mapped units 24 and 25 as far as 116°40'W, whereas during the 1973 work these units could not be identified west of Longitude 116°W. Paleozoic dolostone of unit 27 was seen to lie close to Proterozoic intrusions at about 116°W, such that units 24 and 25 must thin westward to a zero edge at about 116°W.

The presence of sedimentary features indicative of high evaporation and a shallow water marine environment in units 24 and 25 and their probable Cambrian age indicate a correlation with the evaporite sequence of the Saline River Formation present in the Anderson-Horton Plains area west of the Coppermine Arch. Locality 2 contained the thickest section (107 m) but tentative correlations between the section at localities 1, 2 and 3 suggest that at least 134 m of section are present. However, in no places were the basal and upper parts of the sequence exposed.

Discussion

The correlation of some of the Wellington inlier rocks with the Apehian Burnside River Formation of the Bathurst Inlet area demonstrates stratigraphic separation between the Wellington inlier rocks and the Hadrynian strata of the Duke of York inlier and Minto Arch. However, the relationship between the strata in the Duke of York inlier and Minto Arch has not been made very clear by previous workers.

Young and Jefferson (1975, Fig. 1), Young and Long (1976, Fig. 1) and Young (1977, Fig. 1) included the Duke of York inlier in the Hadrynian Amundsen Basin and, presumably, intended a correlation with the Rae and Shaler groups. Young and Jefferson (1975, p. 1735) stated that the Duke of York inlier rocks were part of the Shaler Group and also noted the physical continuity of the diabase sills between the Richardson Islands and those in the Rae Group of the Coppermine area. However, very little data were presented to support these conclusions. In the preceding sections it was stated that the Duke of York inlier rocks show many lithological similarities to both the upper part of the Rae Group and the upper Glenelg Formation and this would help further substantiate the correlation of the Rae Group with the Glenelg Formation suggested by Young (1977).

While accepting most of Young's (1977) correlations between the Coppermine area and Minto Arch, I would like to point out some problems. If my proposal is accepted of a Cambrian age for units 24 and 25, previously assigned to the Hadrynian Rae Group (Baragar and Donaldson, 1973), then it precludes their use as distinct Hadrynian marker beds in regional correlations as proposed by Young (1977, Fig. 1, p. 1779) who correlated units 24 and 25 with the basal part of the Reynolds Point Formation of the Shaler Group.

Although the general successions of the Rae Group and Glenelg Formation are generally similar (Fig. 30.5), there are differences in detail. Units 19, 20 and 21 of the Rae Group have no direct equivalents in the basal part of the Glenelg Formation. Each of these Rae Group units is a distinct lithostratigraphic division with sharp, possibly disconformable, boundaries; whereas the basal Glenelg Formation appears to be a continuous succession with gradational lithological changes. However, these differences could be due to local paleogeographic conditions and need not detract from Young's (1977) correlation of the Glenelg Formation with the Rae Group.

References

Baragar, W.R.A. and Donaldson, J.A.
1973: Coppermine and Dismal Lakes map area; Geological Survey of Canada, Paper 71-39.

Campbell, F.H.A.
1978: Geology of the Helikian rocks of the Bathurst Inlet area, Coronation Gulf, Northwest Territories; in Current Research, Part A, Geological Survey of Canada, Paper 78-1A, p. 97-106.

- Campbell, F.H.A. and Cecile, M.P.
 1975: Report on the geology of the Kilohigok Basin, Goulburn Group, Bathurst Inlet, N.W.T.; in Report of Activities, Part A, Geological Survey of Canada, Paper 75-1A, p. 297-306.
 1976: Geology of the Kilohigok Basin, Goulburn Group, Bathurst Inlet, District of Mackenzie; in Report of Activities, Part A, Geological Survey of Canada, Paper 76-1A, p. 369-377.
 1979: The northeastern margin of the Aphebian Kilohigok Basin, Melville Sound, Victoria Island, N.W.T.; in Current Research, Part A, Geological Survey of Canada, Paper 79-1A, p. 91-94.
- Christie, R.L., Cook, D.G., Nassichuk, W.W., Trettin, H.P., and Yorath, C.J.
 1972: Field excursion A66 — The Canadian Arctic Islands and the Mackenzie region; 24th International Geological Congress, Montreal, Guidebook.
- Douglas, R.J.W., Editor
 1970: Geology and economic minerals of Canada; Geological Survey of Canada, Economic Geology Report No. 1, 5 ed.
- Fraser, J.A.
 1964: Geological notes on the northeastern District of Mackenzie, Northwest Territories; Geological Survey of Canada, Paper 63-40.
- Hornal, R.W. and Boyd, J.B.
 1972: Gravity measurements in the Slave and Bear structural provinces, Northwest Territories; Energy, Mines and Resources, Earth Physics Branch, Ottawa, Canada, Maps 94 and 95.
- Long, D.G.F.
 1978: Proterozoic stream deposits: some problems of recognition and interpretation of ancient sandy fluvial systems; in Fluvial Sedimentology, A.D. Miall, Editor; Canadian Society of Petroleum Geologists, Memoir 5, p. 313-341.
- Stockwell, C.H. and Williams, H.
 1964: Age determinations and geological studies. Part II: Geological studies; Geological Survey of Canada, Paper 64-17 (Part II).
- Thorsteinsson, R. and Tozer, E.T.
 1962: Banks, Victoria and Stefansson Islands, Arctic Archipelago; Geological Survey of Canada, Memoir 330.
- Tremblay, L.P.
 1968: Preliminary account of the Goulburn Group, Northwest Territories, Canada; Geological Survey of Canada, Paper 67-8.
- Wright, G.M.M.
 1967: Geology of the southeastern Barren Grounds, parts of the Districts of Mackenzie and Keewatin (Operation Keewatin, Baker, Thelon); Geological Survey of Canada, Memoir 350.
- Young, G.M.
 1974: Stratigraphy, paleocurrents and stromatolites of the Hadrynian (Upper Precambrian) rocks of Victoria Island, Arctic Archipelago, Canada; Precambrian Research, v. 1, p. 13-41.
 1977: Stratigraphic correlation of upper Proterozoic rocks of northwestern Canada; Canadian Journal of Earth Sciences, v. 14, p. 1771-1787.
- Young, G.M. and Jefferson, C.W.
 1975: Late Precambrian shallow water deposits, Banks and Victoria Islands, Arctic Archipelago; Canadian Journal of Earth Sciences, v. 12, p. 1734-1748.
- Young, G.M. and Long, D.G.
 1976: Stromatolites and basin analysis: an example from the upper Proterozoic of northwestern Canada; Paleogeography, Paleoclimatology and Paleogeology, v. 19, p. 303-318.

Project 730051

H.P. Trettin¹, C.R. Barnes², J.Wm. Kerr¹, B.S. Norford¹,
A.E.H. Pedder¹, J. Riva³, R.S. Tipnis⁴, and T.T. Uyeno¹

Trettin, H.P., Barnes, C.R., Kerr, J.Wm., Norford, B.S., Pedder, A.E.H., Riva, J., Tipnis, R.S., and Uyeno, T.T., *Progress in lower Paleozoic stratigraphy, northern Ellesmere Island, District of Franklin; in Current Research, Part B, Geological Survey of Canada, Paper 79-1B, p. 269-279, 1979.*

Abstract

Three major depositional phases have previously been distinguished in the Hazen Plateau and southern Grantland Mountains region of northern Ellesmere Island: a phase of nonmarine to shallow marine clastic deposition (Grant Land Formation) and the starved basin and flysch phases of the deep but ensialic Hazen Trough. New fossil identifications indicate that the Grant Land-Hazen contact is middle to late Early Cambrian at Ella Bay, Archer Fiord, but no older than Late Cambrian east of the head of Tanquary Fiord. Most of the Grant Land Formation now appears to be Early Cambrian in age and correlative with the clastic Ellesmere Group of central Ellesmere Island. The Grant Land Formation probably was derived from the ancient Pearya Mountains to the north, and the Ellesmere Group both from the Pearya Mountains and the Canadian Shield. The Hazen-Imina contact is close to the Ordovician-Silurian boundary at some localities and of different Llandoveryan ages at others. A thick volcanic unit at Yelverton Inlet, separated from the underlying Grant Land Formation by a tongue of the lower Hazen Formation, extends in age upward to the early or middle Llandoveryan. It is overlain by three shallow marine, predominantly sedimentary units the middle of which contains conodonts and corals of middle to late Llandoveryan age. The sediments are overlain by the Imina Formation, here divided into three members with a combined age range from late Llandoveryan(?) to early Ludlovian. A comparable volcanic-sedimentary succession had earlier been reported from the M'Clintock Inlet region, but the top of the volcanic unit there is early Ashgillian in age and that of the shallow marine sedimentary unit middle or late Ashgillian. The stratigraphic framework of that area has been extended downward into the early(?) Ordovician, but fossils of pre-late middle Ordovician age are lacking. New fossil finds indicate that on Judge Daly Promontory the Imina Formation overlies not the Cornwallis Group but a limestone of Ashgillian age correlative with the lower Allen Bay Formation.

Introduction

This paper reports significant modifications in the lower Paleozoic stratigraphic framework of northern Ellesmere Island. It is based on: (1) field observations in 1977; (2) identifications of fossils collected in 1977 and 1975 (both by Trettin); and (3) re-identifications of fossils collected in earlier years by J.Wm. Kerr, W.W. Nassichuk, and H.P. Trettin. The field work in 1975 and 1977 formed part of GSC Project 730057, designed to complete the reconnaissance geology of northern Ellesmere Island.

The fossil identifications are the most important part of this report. They were made by C.R. Barnes, W.H. Fritz, B.S. Norford, A.E.H. Pedder, J. Riva, R. Thorsteinsson, R.S. Tipnis, and T.T. Uyeno, and their contributions are apparent from the Appendix. J.Wm. Kerr provided an unpublished manuscript on a section south of Greely Fiord, measured in 1962 (Fig. 31.1, area VI). Trettin is responsible for the compilation of the data.

The Director and officers of the Continental Polar Shelf Project are thanked for help during the 1975 and 1977 field seasons. The manuscript has benefitted from critical reading by U. Mayr and A.D. Miall.

Depositional Framework

The oldest known deposits in northern Ellesmere Island, assigned to the Grant Land Formation, are nonmarine and shallow marine in origin. Subsequently three major depositional belts developed, the central Hazen Trough, and unstable shelves bordering it on the southeast and northwest. The Hazen Trough had two main phases of sedimentation, a

starved basin phase, represented by the Hazen Formation, and a flysch phase represented by the Imina Formation. The southeastern shelf received mainly carbonate sediments with lesser amounts of craton-derived clastic sediments and some evaporites; its stratigraphic units are extensive laterally. The northwestern belt received volcanic rocks, generally siliceous to intermediate in composition and pyroclastic in origin, carbonate shelf sediments, and shallow marine to nonmarine clastic sediments, all characterized by marked facies changes over short distances. Recent information from the northeasternmost part of this belt (east of M'Clintock Inlet) is not included here because studies there, by U. Mayr and H.P. Trettin, have not yet been completed.

The stratigraphy of the southeastern shelf has been described by Norford (1966) and Kerr (1967, 1968) and that of Hazen Trough and northwestern belt by Trettin (1969a,b, 1971, 1976, 1978, and in press). Interpretative aspects are discussed by Trettin and Balkwill (1979).

Rock Units

Grant Land Formation

Distribution, Thickness, and Lithology This formation was established for clastic sediments in northern Ellesmere Island that underlie the Hazen Formation; its base is not exposed. The type section at Hare Fiord contains about 1100 m of strata, but the actual thickness is probably much greater. Thick successions are exposed in the Grantland Mountains* and northern Axel Heiberg Island, and relatively thin uppermost parts at St. Patrick Bay and Ella Bay, and on northwestern Judge Daly Promontory.

¹ Institute of Sedimentary and Petroleum Geology, Calgary

² University of Waterloo, Waterloo, Ontario

³ Université Laval, Québec, Québec

⁴ Visiting Post-Doctoral Fellow, ISPG, Calgary

* Previous spelling Grant Land Mountains; present spelling Grantland Mountains. The Grant Land Formation was named when the earlier spelling still was valid.

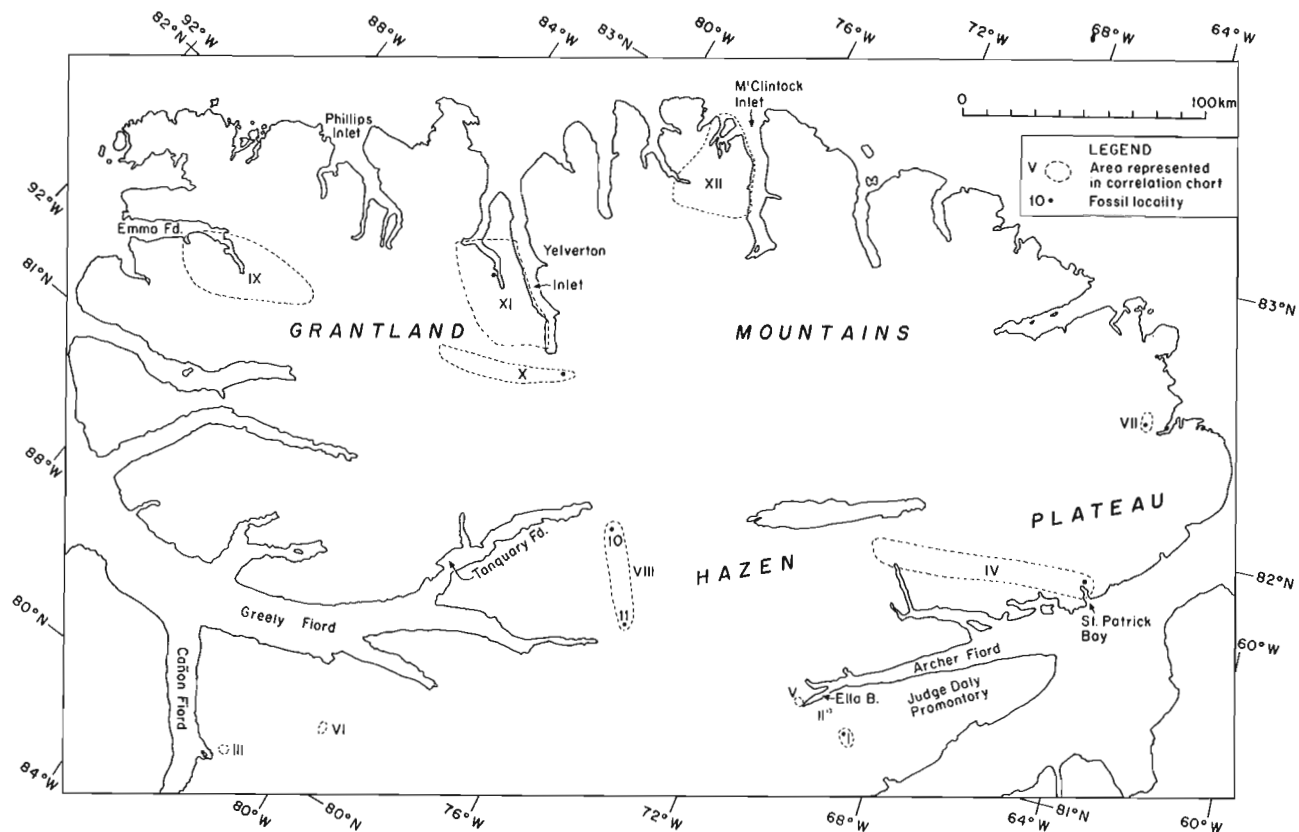


Figure 31.1. Index.

The succession in the Grantland Mountains consists mainly of alternating units of quartzose, variably feldspathic sandstone, and green, red and grey phyllite or slate with minor amounts of pebble conglomerate. The sandstones are medium to coarse grained in the lower part of the succession; they decrease both in grain size and abundance stratigraphically upward. The lower and middle parts of the succession probably were deposited by braided rivers; the uppermost part, which underlies deeper water sediments of the Hazen Formation, must be marine.

The strata at St. Patrick Bay, consisting of green and red slate and phyllite, are similar, both macroscopically by and microscopically, to the uppermost part of the formation in the Grantland Mountains.

A key section northwest of the head of Ella Bay was studied in detail in 1977 (Fig. 31.1-31.3). It is about 207 m thick and consists mainly of clayey to sandy, slaty siltstone with small amounts of very fine grained silty sandstone. The rocks are medium light grey to greenish grey and show flat lamination and small-scale cross-lamination, including flaser bedding. Petrographically, they are comparable to the strata at St. Patrick Bay but differ from them macroscopically by the absence of red beds.

Age and Correlation Macrofossils had previously not been found in the Grant Land Formation, and analyses for chitinozoans also were unsuccessful. The formation was tentatively considered as Middle to Late Cambrian in age because graptolites from the lower part of the Hazen Formation suggested that the Grant Land-Hazen contact probably is no older than latest Cambrian. The present collections indicate that this contact is markedly diachronous. At Ella Bay, it clearly is middle to late Early Cambrian (Appendix, identifications 4, 5) and tentatively

correlated with a level in the upper part of the Kane Basin Formation (see below, Hazen Formation). East of the head of Tanquary Fiord, on the other hand, it can be no older than Late Cambrian (identification 10). The age of the base of the formation, and the correlation of its lower and middle parts still are a matter of conjecture. At present it is presumed that all of the Grant Land Formation in the south (St. Patrick Bay, Ella Bay, northwestern Judge Daly Promontory), and lower and middle parts of the formation in the Grantland Mountains are correlative with the bulk of the Ellesmere Group (except for the upper part of the Kane Basin Formation).

Provenance of Grant Land Formation and Parts of Ellesmere Group It was previously thought that the Grant Land Formation was derived from northerly sources (the ancient Pearya Mountains) because its clastic sediments are markedly coarser than those of the presumably correlative Parrish Glacier and Copes Bay formations. In spite of the revised correlation, this view still seems to be valid, for three reasons. (1) The lower and middle parts of the Grant Land Formation in the Grantland Mountains are coarser grained than any of the Cambrian clastic units in central Ellesmere Island (including the Ellesmere Group). (2) Paleocurrent determinations are difficult to make in the Grant Land Formation, but a few measurements from north of the head of Tanquary Fiord indicate transport in southerly directions. (3) Plagioclase is more abundant than K-feldspar in most specimens from the Grant Land Formation (Fig. 31.2). Numerous X-ray analyses on various lower Paleozoic and Devonian samples from northern and central Ellesmere Island have shown that this usually is the case with sediments derived from the Pearya orogenic welt; sediments derived from the Canadian Shield, on the other hand, are much richer

in K-feldspar. Probable reasons for this rule of thumb, and limitations to it, are discussed by Trettin (1978, p. 73-74). Briefly, Pearya seems to have included a large proportion of relatively young low grade metamorphic terrains that contained much albite, a feldspar relatively stable under surface conditions and hence preserved in derived sediments. The Arctic part of the Churchill Province, on the other hand, is older (probably Archean) and probably included a higher proportion of terrains of amphibolite or granulite grade. (Present outcrops in southeastern Ellesmere Island are of granulite grade (Frisch et al., 1978).) Such regions usually have a higher K-feldspar content than the low grade terrains and, furthermore, the plagioclase in them is relatively unstable and selectively destroyed during weathering. However, the proportion of plagioclase to K-feldspar in sediments can be changed by postdepositional processes such as metamorphism, metasomatism or selective replacement by clay minerals.

Feldspar composition and facies relationships suggest that the Rawlings Bay Formation of the Ellesmere Group was derived from the Shield whereas the Ritter Bay Formation was derived from the Pearya Mountains. Specimens from the Ritter Bay Formation in area I resemble specimens from the upper part of the Grant Land Formation in areas IV, V, and VIII, not only by the predominance of plagioclase over K-feldspar, but also in various petrographic aspects; for example, a relatively high content of chlorite that is pseudomorphous after mica and occurs in flakes considerably larger than associated other mineral clasts.

Hazen Formation

The Hazen Formation comprises a condensed succession of resedimented carbonate deposits, fine grained clastic sediments, and primary and replacement chert in the Hazen Plateau region, that lies stratigraphically between Grant Land and Imina formations. In most areas the formation is divisible into a lower member rich in carbonate rocks and an upper member rich in chert. The carbonate sediments include submarine slides, boulder to pebble conglomerate, and lime packstone, wackestone and mudstone. They were derived from both adjacent shelves, as were the associated clastic sediments. Those parts of the Hazen Formation close to the southeastern shelf are characterized by submarine slides and coarse conglomerates (Fig. 31.8) and by the predominance of K-feldspar over plagioclase in the clastic sediments (Fig. 31.2). Both sediments and fauna indicate deposition in progressively deeper waters (Fig. 31.2).

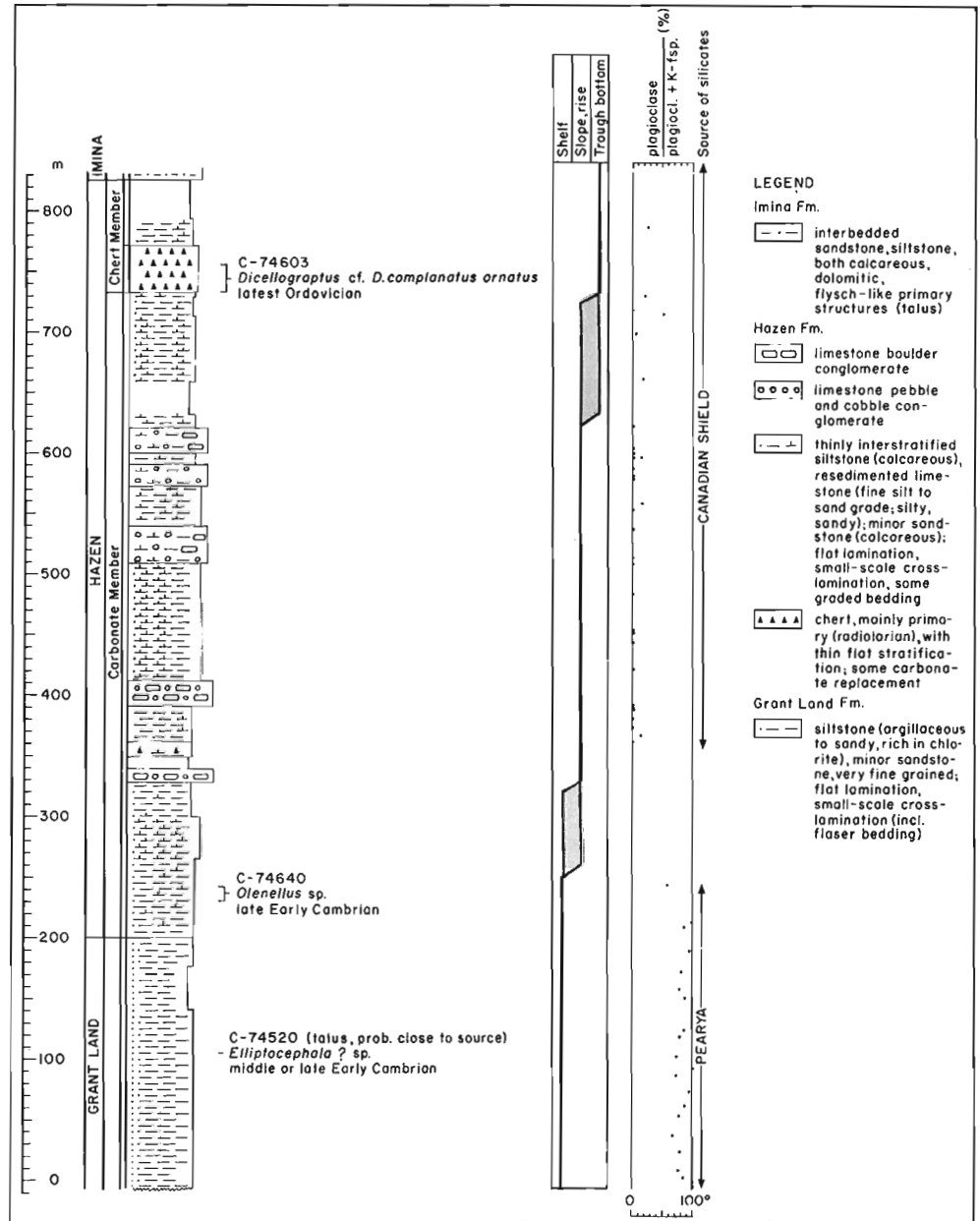
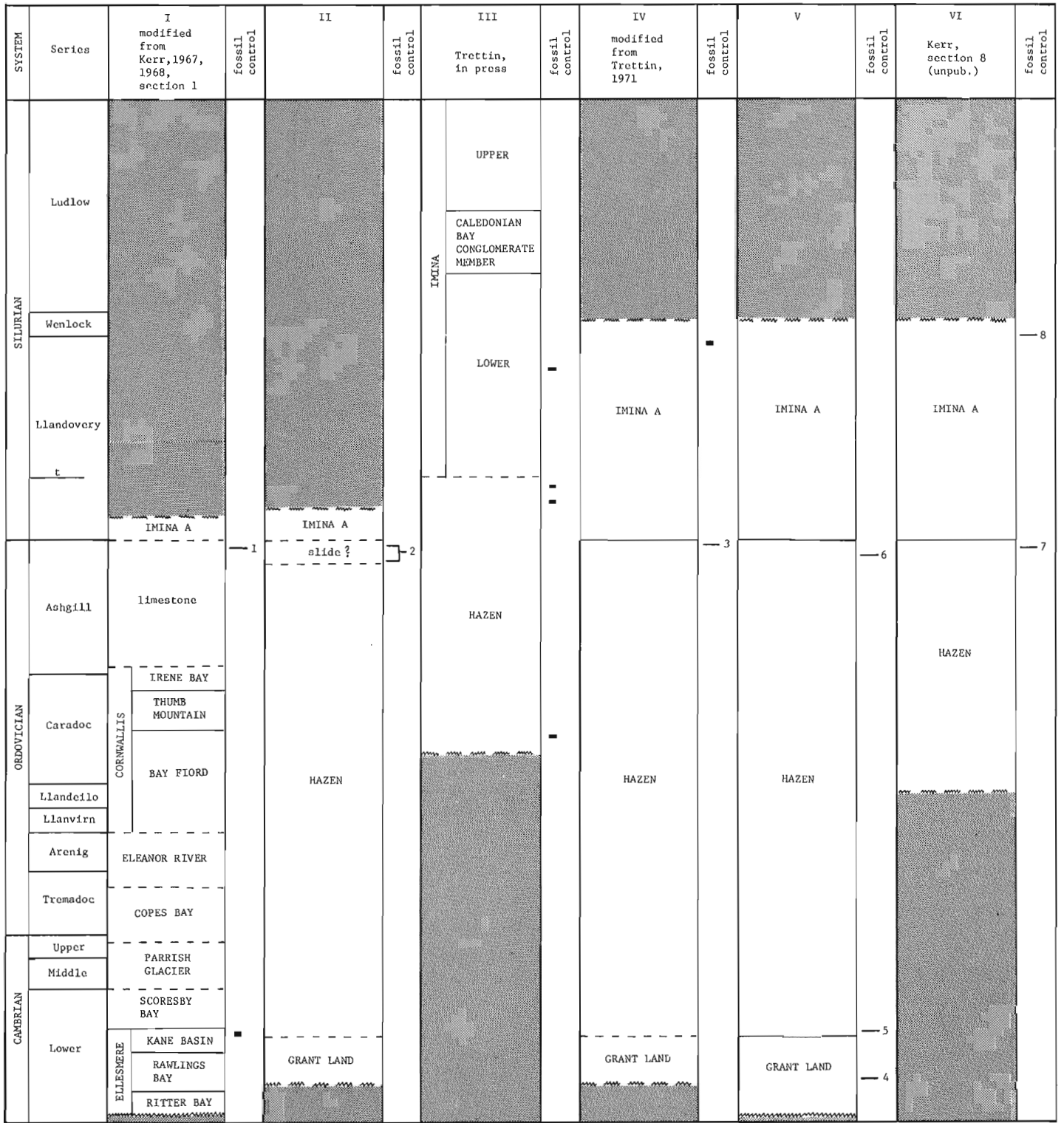


Figure 31.2. Columnar presentation of section north of head of Ella Bay (Fig. 31.1, area V). Plagioclase/K-feldspar ratios based on peak heights in X-ray diffractograms.

In 1977, the known outcrop area of the Hazen Formation was extended significantly, especially at Ella Bay and on northwestern Judge Daly Promontory. The original member C of the Zebra Cliffs Formation at M'Clintock Inlet and the former map unit 7 at Yelverton Inlet (Trettin, 1976, Fig. 11) now both are assigned to the Hazen Formation (area X).

Previous fossil identifications suggested that the formation is restricted to the early and middle Ordovician, but the present identifications demonstrate a much wider range - late Early Cambrian to Llandoveryan.

At Ella Bay (Fig. 31.1, area V), the base of the Hazen Formation is placed at the base of the lowest (resedimented) limestone. The lower part of the Hazen Formation also differs from the Grant Land Formation by its darker tone (Fig. 31.4). *Olenellus* sp. (Fig. 31.6) was found in slate 32 to



- conformable contact, age established
- - - age approximate
- age assumed
- ∩ angular unconformity, age established
- age assumed
- ~~~~~ limit of exposure age established
- ~ ~ ~ ~ ~ age approximate or assumed
- covered or removed by post-Ludlovian erosion
- ▨ removed by Middle Ordovician or earlier erosion
- 3 fossil identification in this report
- fossil identification in published report cited
- t= base of Telychian Stage (upper of four Llandoverian stages in Britain)

Figure 31.3. Correlation chart. Age assignments for area I are partly based on studies by Barnes (1974) and Nowlan (1976) in other parts of the Arctic Islands.

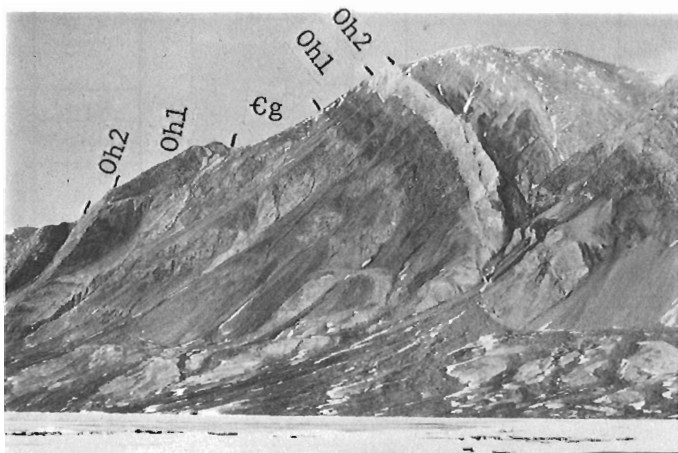
40 m above the base of the formation, and associated trace fossils (Fig. 31.7) show that trilobites lived in this environment so that these fossils are not re-sedimented. *Olenellus* also occurs in the upper part of the Kane Basin Formation (Kerr, 1967), and the base of the Hazen Formation therefore is tentatively correlated with the base of the *Olenellus*-bearing limestone in the former. The conodonts from the base of the Hazen Formation east of Tanquary Fiord (area VIII, identification 10), on the other hand, indicate an age no older than Late Cambrian and possibly as young as Early Ordovician.

Graptolites of the late Ashgillian *Dicellograptus complanatus ornatus* Zone have been collected from near the top of the formation in four areas (IV, V, VI, XII), suggesting that it is close to the Ordovician-Silurian boundary there. Llandoveryan ages for that boundary are inferred at localities III and VII from graptolites (of different ages) and at locality X from conodonts and corals.

Imina Formation

The Imina Formation is a thick succession of sandstone and siltstone with less abundant conglomerate that shows flysch-like primary structures. A suitable type section is not exposed in the type area in northwesternmost Ellesmere Island, but excellent reference sections east of Cañon Fiord have been studied in some detail (Trettin, in press). Detailed studies of very short sections, made on the Hazen Plateau in 1977, confirm that the sediments were transported by concentrated and dilute sediment gravity flows, and probably also by bottom currents.

In northern Ellesmere Island, three informal members, A, B, and C, are presently distinguished. The widely distributed member A consists largely of calcareous and dolomitic sandstone and siltstone. At Emma Fiord, where it is overlain by pelite of the Lands Lökk Formation, it probably is limited to the Llandoveryan; elsewhere it probably is late Llandoveryan and Wenlockian in age. The most common graptolite in this unit is *Monograptus* aff. *M. priodon* (Bronn) (e.g. identification 11 and references cited).



eg = Grant Land Formation
Oh1 = lower recessive unit of Hazen Formation
Oh2 = lowermost limestone conglomerate

Figure 31.4 Core of Archer Fiord Anticlinorium on south-east side of Ella Bay (Fig. 31.1, area V), looking northeast. GSC 199480



Figure 31.5. *Elliptocephala?* sp. from Grant Land Formation at Ella Bay section. GSC 58513

Member B, characterized by a large proportion of pelitic sediments and a low carbonate content of the clastic rocks, is extensively exposed on the north coast of Ellesmere Island where it has been traced from south of Phillips Inlet to south of M'Clintock Inlet. Member C, characterized by the presence of pebble conglomerate and also a low carbonate content, is recognized only southeast of Phillips Inlet. Lithological correlation with parts of the Lands Lökk Formation at Emma Fiord suggests that both units are early Ludlovian in age.

Previous paleocurrent and provenance studies have shown that member A was derived mainly from low grade metamorphic terrains of the Pearya orogenic belt to the north whereas member C, as well as the Caledonian Bay Conglomerate Member of the Imina Formation (area III), and member C of the Lands Lökk Formation, came mainly from lower Paleozoic sources to the west that included the Rens Fiord Uplift of northern Axel Heiberg Island. The westerly provenance probably explains the limited eastward extent of the conglomerates of member C of the Imina Formation.

Ordovician-Lower Silurian Units of Yelverton Inlet Area

A thick succession of variably metamorphosed beds, lying stratigraphically between Hazen and Imina formations, was investigated in the Yelverton Inlet region (XI) mainly in 1975, with some follow-up work in 1977. It is divisible into a lower unit, composed mainly of volcanic rocks, with local shelf carbonates and fine grained clastic sediments, and an upper unit, composed mainly of shelf carbonate and clastic sediments with small amounts of volcanic rocks. The volcanic rocks are separated from the underlying Grant Land Formation by a tongue, about 100 to 200 m thick, of the lower Hazen Formation. Conodonts from limestone, presumably in the uppermost part of the volcanic unit, are of Llandoveryan, probably early or middle Llandoveryan, age (identification 13). The volcanic rocks are separated from correlative, almost completely chertified strata of the Hazen Formation to the southeast (in area X of Fig. 31.1) by a belt, about 20 km wide, covered with younger and older rocks.

The overlying predominantly sedimentary unit is divisible into three subunits. The lower subunit consists of: phyllitic pelite and sandstone, in part conglomeratic; dolomite; minor amounts of limestone; and local conglomerate of cobble to boulder grade. The last occurs immediately adjacent to a serpentinized diatreme and probably was

Figure 31.6.

Olenellus sp. from Hazen Formation, Ella Bay section; X1.65. (GSC 56649; photo 202029-F by W.H. Fritz).

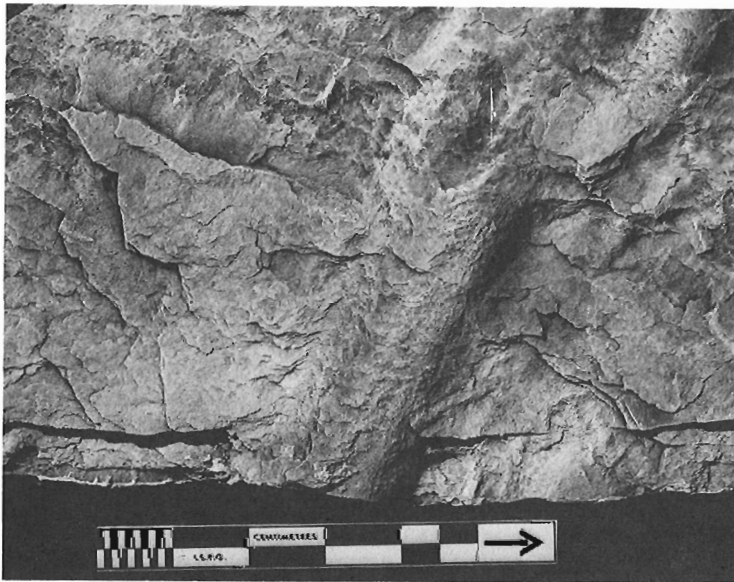
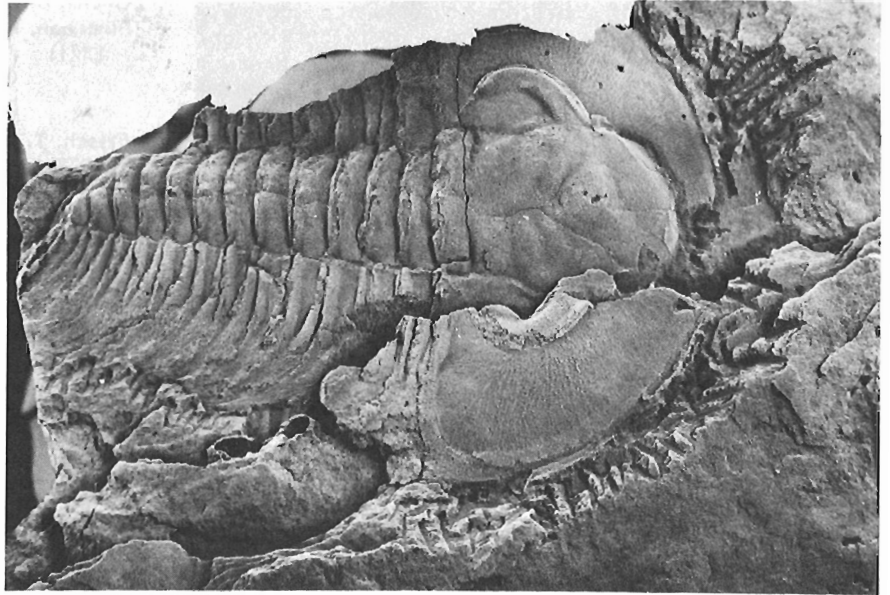


Figure 31.7.

Crawling track of trilobite from *Olenellus*-bearing beds of Hazen Formation at Ella Bay section.

formed by an explosion. The conglomeratic pelite and sandstone beds contain phenoclasts of dolostone, siltstone, etc. that are ellipsoidal in cross-section. They differ from typical shallow marine intraformational conglomerate by the poor sorting and random distribution of the phenoclasts. They have been seen in several other areas on the north coast of Ellesmere Island and probably constitute a time marker caused by unusual events possibly volcanic explosions or earthquakes that set off tsunamis with extensive debris flows in their wake. In some parts of area XI, the lower subunit seems to be absent.

The second subunit consists of marble, tentatively correlated with a shelf limestone that overlies the Hazen Formation south of Yelverton Inlet in area X. Conodonts and corals from the latter area (identification 12) have a middle or late Llandoveryan age.

The third subunit is composed of metamorphosed arenaceous and pelitic sediments with lesser amounts of carbonate and volcanic rocks. It probably is overlain by the Imina Formation, but the contact is not exposed.

Lower(?) and Middle(?) Ordovician Units of M'Clintock Inlet Area

The oldest lower Paleozoic beds observed west of M'Clintock Inlet are thinly stratified, greenish, greyish, and purplish pelitic carbonate rocks and related calcareous and dolomitic phyllites with some volcanic rocks that are overlain by dark grey slate and chert beds. The dark grey strata are interpreted as a tongue of the lower Hazen Formation, and the multicoloured beds as shelf equivalents of that unit. These predominantly sedimentary rocks are succeeded by a volcanic unit, in turn unconformably overlain by the upper

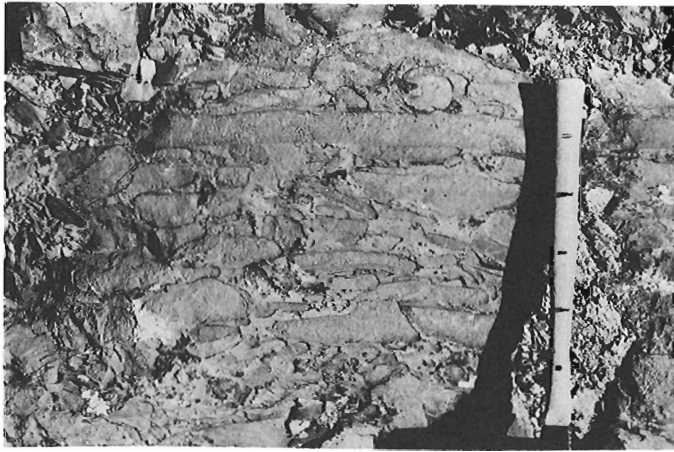


Figure 31.8. Elongate limestone boulders in Hazen Formation, Ella Bay section, 321-327 m; hammer handle is 30 cm long. GSC 199481

middle Ordovician Cape Discovery Formation. The upper middle Ordovician to upper Silurian succession in the M'Clintock Inlet area is described by Trettin (1969b).

Ordovician Units of Judge Daly Promontory

On Judge Daly Promontory, the Imina Formation overlies an upper Ordovician shelf limestone unit correlative with the lower Allen Bay formation and not the Cornwallis Group as previously presumed (area I, identification 1). Elsewhere in central Ellesmere Island, the flysch deposits are separated from underlying shelf carbonates by intervening starved-basin, slope, or back-reef basin sediments assigned to Hazen or Cape Phillips Formation; the absence of these deposits in area I remains to be explained. One possible explanation would be that the southeastern slope of the Hazen Trough was so steep in this area that sediments of slope facies could not accumulate on it, but that trough bottom sediments of flysch facies abutted against it laterally. When the shelf margin subsided deeply (as demonstrated, for example, at Cañon Fiord), the trough bottom facies overstepped the shelf facies. Another stratigraphic anomaly on Judge Daly Promontory is the occurrence of shelf carbonates with early middle Ordovician conodonts between Hazen and Imina formations in area II (identification 2). These strata were tentatively interpreted as part of a submarine slide (Trettin in Tipnis, 1978), but more field work is required to verify this.

References

Aldridge, R.J.

1972: Llandovery conodonts from the Welsh Borderland; British Museum (Natural History), Bulletin, Geology, v. 22, p. 127-231.

1975: The stratigraphic distribution of conodonts in the British Silurian; Geological Society of London, Journal, v. 131, p. 607-618.

Barnes, C.R.

1974: Ordovician conodont biostratigraphy of the Canadian Arctic; in Proceedings of the symposium on the geology of the Canadian Arctic, J.D. Aitken and D.F. Glass, Eds.; Geological Association of Canada and Canadian Society of Petroleum Geologists, p. 221-240.

Cocks, L.R.M., Holland, C.H., Richards, R.B., and Strachan, I.

1971: A correlation of Silurian rocks in the British Isles; Geological Society of London, Journal, v. 127, p. 103-136.

Frisch, T., Morgan, W.C., and Dunning, G.R.

1978: Reconnaissance geology of the Precambrian Shield on Ellesmere and Coburg Islands, Canadian Arctic Archipelago; in Current Research, Part A, Geological Survey of Canada, Paper 78-1A, p. 135-138.

Kerr, J.Wm.

1967: Stratigraphy of central and eastern Ellesmere Island, Arctic Canada. Part I. Proterozoic and Cambrian; Geological Survey of Canada, Paper 67-27, Part I.

1968: Stratigraphy of central and eastern Ellesmere Island, Arctic Canada. Part II. Ordovician; Geological Survey of Canada, Paper 67-27, Part II.

Klaamann, E.R.

1964: Pozdneordovikskie i rannesilurijskie Favositida Estonii; Institut Geologii Akademii Nauk Estonskoy SSSR, Tallin.

McLean, R.A.

1977: Early Silurian (Late Llandovery) rugose corals from western North Greenland; Grønlands Geologiske Undersøgelse, Bulletin 121.

Mirza, K.

1976: Late Ordovician to Late Silurian stratigraphy and conodont biostratigraphy of the eastern Arctic Islands; unpublished M.Sc. thesis, University of Waterloo, Waterloo, Ontario.

Nassichuk, W.W. and Christie, R.L.

1969: Upper Paleozoic and Mesozoic stratigraphy in the Yelverton Pass region, Ellesmere Island, District of Franklin; Geological Survey of Canada, Paper 68-31.

Norford, B.S.

1966: Ordovician stratigraphic section at Daly River, northeast Ellesmere Island, District of Franklin; Geological Survey of Canada, Paper 66-55.

Nowlan, G.S.

1976: Late Cambrian to late Ordovician conodont evolution and biostratigraphy of the Franklinian miogeosyncline, eastern Canadian Arctic islands; unpublished Ph.D. thesis, University of Waterloo, Waterloo, Ontario.

Pedder, A.E.H.

Lower Silurian stromatoporoid and corals from Yelverton Inlet region, northern Ellesmere Island; in Contributions to Canadian Paleontology, Geological Survey of Canada, Bulletin. (in prep.).

Poulsen, C.

1941: The Silurian faunas of North Greenland. II. The fauna of the Offley Island Formation, Part I. Coelenterata; Meddelelser om Grønland, Band 72, Nr. 2.

Schönlaub, H.P.

1971: Zur Problematic der Conodonten-Chronologie an der Wende Ordoviz/Silur mit besonderer Berücksichtigung der Verhältnisse im Llandovery; Geologica et Palaeontologica, v. 5, p. 35-57.

Stel, J.H.

1978: Studies on the paleobiology of favositids; Ph.D. thesis (published), University of Groningen, The Netherlands.

Tipnis, R.S.

- 1978: Early Middle Ordovician conodonts of North Atlantic Province from northeastern Ellesmere Island, Arctic Canada; in *Current Research, Part C*, Geological Survey of Canada, Paper 78-1C, p. 75-79.

Trettin, H.P.

- 1969a: Pre-Mississippian geology of northern Axel Heiberg and northwestern Ellesmere Islands, Arctic Archipelago; Geological Survey of Canada, Bulletin 171.
- 1969b: Geology of Ordovician to Pennsylvanian rocks, McClinton Inlet, north coast of Ellesmere Island, Canadian Arctic Archipelago; Geological Survey of Canada, Bulletin 183.
- 1971: Geology of lower Paleozoic formations, Hazen Plateau and southern Grant Land Mountains, Ellesmere Island, Arctic Archipelago; Geological Survey of Canada, Bulletin 203.
- 1976: Reconnaissance of lower Paleozoic geology, Agassiz Ice Cap to Yelverton Bay, northern Ellesmere Island; in *Report of Activities, Part A*, Geological Survey of Canada, Paper 76-1A, p. 431-444.

Trettin, H.P. (cont.)

- 1978: Devonian stratigraphy, west-central Ellesmere Island, Arctic Archipelago; Geological Survey of Canada, Bulletin 302.

Middle Ordovician to Lower Devonian deep-water succession at southeastern margin of Hazen Trough, Cañon Fiord, Ellesmere Island; Geological Survey of Canada, Bulletin 272. (in press)

Trettin, H.P. and Balkwill, H.R.

- 1979: Contributions to the tectonic history of the Inuitian Province, Arctic Canada; *Canadian Journal of Earth Sciences*, v. 16, p. 748-769.

Viyra, V. Ya.

- 1977: Sostav i rasprostranenie konodontov v silure Pribaltiki (skv. Okhesaare, Kunkoyay, Ukmerge i dr.); *Fatsii i fauna silura Pribaltiki*, D.L. Kal'o, Ed.; Institut Geologii Akademii Nauk Estonskoy SSR, Tallin, p. 179-192.

Walliser, O.H.

- 1964: Conodonten des Silurs; *Hessisches Landesamt für Bodenforschung, Abhandlungen*, v. 41.
- 1971: Conodont biostratigraphy of the Silurian of Europe; *Geological Society of America, Memoir* 127, p. 195-206.

Appendix: Summary of Fossil Identifications

The collections were made by Trettin in 1975 or 1977, except where otherwise indicated. Comments accompanying the various paleontological reports have in some cases been abbreviated or left out, but will be reproduced fully in the final reports. For stratigraphic position of the collections, see Figures 31.2 and 31.3.

- 1 Uppermost part of limestone unit underlying Imina Formation (equivalent to the lower Allen Bay Formation).
GSC locality C-75273: **Bighornia** sp., **Catenipora** sp.; late Ordovician, Ashgillian. (Identified by B.S. Norford)
- 2 Limestone unit, intercalated between Hazen and Imina formations, upper 20 m of 36 m thick section; possibly submarine slide (cf. Trettin in Tipnis, 1978).
GSC locality C-74617: **Panderodus gracilis** (Branson and Mehl), **Belodina leithi** Ethington and Furnish sensu fructo, **Belodina compressa** (Branson and Mehl), **Belodina monitorenensis** Ethington and Schumacher, **Protopanderodus insculptus** (Branson and Mehl).
GSC locality C-74618: **Panderodus gracilis** (Branson and Mehl), aff. **Drepanoistodus forceps** (Lindström), **Oistodus venustus** Stauffer, "**Oistodus**" sp. aff. "**O.**" **nevadensis** Ethington and Schumacher, **Pygodus** sp., "**Roundya**" **pyramidalis** Sweet and Bergström, **Tetraprioniodus** cf. **T. lindstroemi** Sweet and Bergström, **Periodon aculeatus** Hadding, **Phragmodus** sp.; probably post-middle Llanvirnian, pre-Caradocian because of the presence of **Pygodus**. (Identified by R.S. Tipnis)
- 3 Hazen Formation, chert member, about 7 m below top of formation.
GSC locality C-64: **Climacograptus hastatus** T.S. Hall, **Climacograptus longispinus** hvalross Ross and Berry, **Orthograptus** cf. **O. amplexicaulis abbreviatus** Elles and Wood, **Glyptograptus** cf. **G. occidentalis** Ruedemann; late Ordovician, late Ashgillian, Zone of **Dicellograptus complanatus ornatus**. (Collected by H.P. Trettin, 1967; reidentified by J. Riva)
4. Grant Land Formation, 94.5 m below top of incomplete section; talus, probably close to source.
GSC locality C-74520: **Elliptocephala**? sp. **Elliptocephala** is known from the Taconic sequence in New York and from boulders in the Levis Formation of the St. Lawrence Lowland, Quebec. At both localities strata containing the genus belong to the **Bonnia-Olenellus** Zone. The assignment of the present specimen is questioned because of the exceptionally wide border furrow on the cephalon, and therefore the age must also be questioned, but it can be stated as probably belonging to either the **Bonnia-Olenellus** or the **Nevadella** Zone; middle or late Early Cambrian (GSC type number 58513; see Fig. 31.5). (Identified by W.H. Fritz)
- 5 Hazen Formation, carbonate member, 32-40 m above base of formation.
GSC locality C-74640: **Olenellus** sp. (GSC type number 56649; see Fig. 31.6); late Early Cambrian, **Bonnia-Olenellus** Zone. (Identified by W.H. Fritz)
- 6 Hazen Formation, chert member, 553.5-555.5 m above base of formation.
GSC locality C-74603: ?**Climacograptus** sp., **Dicellograptus** cf. **D. complanatus ornatus** Elles and Wood, **Orthograptus** sp.; late Ordovician, probably late Ashgillian, probably Zone of **Dicellograptus complanatus ornatus**. (Identified by B.S. Norford)
- 7 Hazen Formation, chert member 0-30 m below top of formation.
GSC locality 51962: **Climacograptus hastatus** T.S. Hall, **Climacograptus** of the **longispinus** type, **Climacograptus pacificus** (Ruedemann), **Orthograptus** sp. or some other biserial form; late Ordovician, late Ashgillian, Zone of **Dicellograptus complanatus ornatus**. (Collected by J.Wm. Kerr, 1962; identified by J. Riva)
- 8 Imina Formation, member A, about 600 m above base.
GSC locality 51963: **Stomatograptus** sp., **Monograptus** cf. **M. priodon** (Bronn); Silurian, latest Llandoveryan or earliest Wenlockian. (Collected by J.Wm. Kerr, 1962; identified by R. Thorsteinsson)
- 9 Hazen Formation, chert member, upper few metres.
GSC locality C-74700: **Monograptus** spp., diplograptid; early Silurian, Llandoveryan, older than latest Llandoveryan. (Identified by B.S. Norford)
- 10 Hazen Formation, carbonate member, basal 10 m or so.
GSC locality C-54784: acodiform, oistodiform, drepanodiform specimens; Late Cambrian to Late Ordovician, possibly Early Ordovician. (Identified by C.R. Barnes)

- 11 Imina Formation, member A; position unknown.

GSC locality C-54052: **Monograptus** aff. **M. priodon** (Bronn); Silurian, late Llandoveryan or Wenlockian. (Identified by B.S. Norford)

- 12 Unnamed limestone overlying Hazen Formation (map unit 8 of Trettin, 1976, but not Marvin Formation, as previously assumed).

GSC locality C-54790: **Aulacognathus** sp., **Belodella?** sp., **Belodina?** sp., "**Carniodus?**" sp., **Panderodus simplex** (Branson and Mehl), **P.** sp.; early Silurian, late Llandoveryan (Telychian) or slightly older, **celloni** Zone or slightly older. **Aulacognathus** sp. differs in some important features from **Aulacognathus bullatus** Nicoll and Rexroad and may be slightly older. **Aulacognathus bullatus** has been reported from the **Icriodella inconstans** Zone of Aldridge (1972), of C₅ subdivision of the upper Llandovery Series (Telychian Stage). The **inconstans** Zone is identical with the **celloni** Zone. The specimens identified as **Belodina?** sp. and **Belodella?** sp. are new and morphologically transitional between "typical" **Belodina** (restricted to the Ordovician) and **Belodella**. "**Carniodus?**" sp. is fragmentary, so a definite assignment cannot be made. "**Carniodus**" has been reported from the **celloni** Zone and the underlying Bereich I of Walliser (1964, 1971). (Identified by T.T. Uyeno)

GSC locality C-54807 (same locality as C-54790): **Ecclimadictyon pandum** Nestor, **Favosites gothlandicus** Lamarck, **Angopora hisingeri** (Edwards and Haime) (sensu lato of Stel, 1978, p. 5b), **Paleofavosites multiporus** (Sokolov), **Halysites** sp. cf. **H. suessmilchi** Etheridge; early Silurian, Llandoveryan, probably equivalent to Raikküla "Stage" of Estonia (see below).

GSC locality 74814 (approximately same location and stratigraphic level as C-54790): **Favosites gothlandicus** Lamarck, **Favosites subfavosus** Klaamann, **Halysites** sp. cf. **H. suessmilchi** Etheridge, **Propora** (sensu lato) sp. nov., **Pseudophaulactis** sp. indet., **Pseudopilophyllum** sp. nov., **Craterophyllum vatium** McLean; early Silurian, Llandoveryan, upper Raikküla or Adavere "Stage" of Estonia (=middle or upper Llandovery). This fauna is related to that of the Offley Island Formation of western north Greenland (Poulsen, 1941; McLean, 1977). The specimens of **Favosites gothlandicus** are small and have extremely fine septal apparatus. Such forms, as well as **Paleofavosites multiporus** and **Favosites subfavosus**, are known from the Raikküla "Stage" in Estonia (Klaamann, 1964). Cocks et al. (1971, Fig. 9) correlate the Raikküla "Stage" with an interval in the middle Llandovery, encompassing the **cyphus** to **convolutus** graptolite zones of Britain, and Vavra (1977) has established a correlation between the "bottom part" of the overlying Adavere "Stage" and the European **celloni** conodont Zone, which is approximately equivalent to the British upper Llandoveryan **inconstans** Zone (Aldridge, 1975). [Collected by W.W. Nassichuk, 1966 (see Nassichuk and Christie, 1969) and re-identified by A.E.H. Pedder; full report in Pedder, in prep.]

- 13 Limestone in fault slice of unnamed volcanic unit in Yelverton Inlet region; probably from upper part of unit.

GSC localities C-54800, C-54801: **Astropentagnathus** n. sp., cf. **Falcodus?** n. sp. sensu fructo (of Schönlaub, 1971), **Ozarkodina** cf. **O. gaertneri** sensu fructo Walliser (a form element of **Pterospathodus** cf. **P. amorphognathoides**), **Panderodus** sp., **Belodina?** sp.; early Silurian, early to middle Llandoveryan. The **Belodina?** sp. specimens are grey and poorly preserved; this genus is not known to occur in strata younger than Ordovician. The platform elements of **Astropentagnathus** n. sp. suggest that it is ancestral to **A. irregularis** Mostler reported by Schönlaub (1971) from the lower part of the **celloni** Zone in the Carnic Alps and from the lower part of the Cape Storm Formation (transitional facies) by Mirza (1976). **Falcodus** n. sp. also was reported by Schönlaub (op. cit.) from the **celloni** Zone. The specimen identified as **Ozarkodina** cf. **O. gaertneri** sensu fructo Walliser consists of a single fragmentary element only; it belongs within **Pterospathodus amorphognathoides**. The **P. amorphognathoides** Zone is of late Llandoveryan-early Wenlockian age. The tentative age assignment for this limited material is based on the **Astropentagnathus** n. sp. (Identified by C.R. Barnes)

**PETROLOGY OF BASEMENT ROCKS AT THE RABBIT LAKE DEPOSIT AND
PROGRESSIVE ALTERATION OF PITCHBLLENDE IN AN OXIDATION ZONE OF URANIUM DEPOSITS
IN SASKATCHEWAN**

Project 750059

J. Rimsaite
Regional and Economic Geology Division

Rimsaite, J., *Petrology of basement rocks at the Rabbit Lake deposit and progressive alteration of pitchblende in an oxidation zone of uranium deposits in Saskatchewan*; in *Current Research, Part B, Geological Survey of Canada, Paper 79-1B, p. 281-299, 1979.*

Abstract

Transition of pitchblende to brightly coloured uranyl-bearing mineral aggregates and alteration of their host rocks were studied using optical, X-ray diffraction, thermogravimetric, differential thermal, chemical, and electron microprobe methods on samples collected from uranium deposits in northern Saskatchewan. Specimens from the Rabbit Lake deposit, which were studied in detail, were compared to specimens from the Cluff Lake deposit and from the Beaverlodge area. This study determined the quantities of uranium, radiogenic lead and associated elements removed from pitchblende and coexisting minerals during their alteration, and mode of redeposition of mobilized elements as secondary minerals in the oxidation zone. Alteration of host rocks preceding uranium mineralization and the other forms of alteration of pitchblende, such as silicification and replacement by sulphides and arsenides, are briefly discussed and illustrated by selected chemical and electron microprobe analyses. Chemical trends during progressive alteration are illustrated diagrammatically. Data on natural chemical and mineralogical readjustments of uranium and radiogenic lead compounds in changing environmental conditions are described.

Introduction

This study is an extension of previous studies of rock and mineral alteration in the Rabbit Lake deposit (Rimsaite, 1978a), and is partly based on papers presented at the 25th International Geological Congress and at the Poster Session during the "Short Course in Uranium Deposits" (Rimsaite, 1976, 1978b).

The Rabbit Lake deposit (58°11'00"N, 103°42'36"W) is 5 km west of Wollaston Lake (NTS 64) in a breccia zone of Apehian metasediments near the southeastern edge of the Athabasca Basin (Fig. 32.1).

The Cluff Lake deposit 58°30'N, 109°30'W is associated with the circular Carswell Structure within the Athabasca

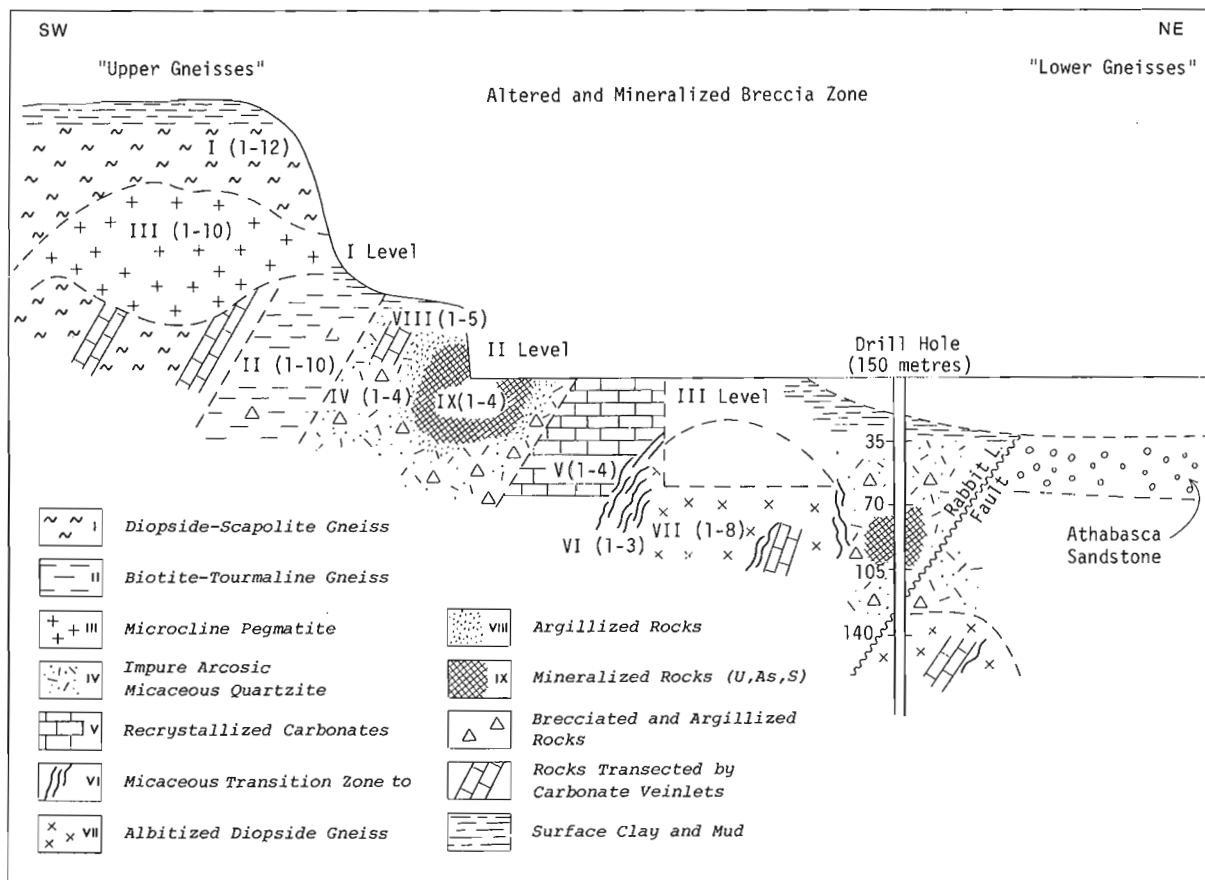


Figure 32.1. Schematic representation of the principal rock types and sampling localities at the Rabbit Lake deposit, in northern Saskatchewan.

Basin. The pitchblende occurs in faults and fractures mainly within, and around, upthrust blocks of the Athabasca Sandstone on the basement rocks (Harper, 1978).

The author visited these deposits in 1975, and the Rabbit Lake deposit again in 1977, and collected ore and rock specimens, including uranyl-bearing mineral aggregates from the oxidation zones in the open pit and in drill cores. In the open pit, the brightly coloured oxidation zones coincide with the ground water level. In the drill cores, uranyl-bearing compounds occur in late fractures and shear zones that transect pitchblende-bearing rocks and are associated with hydrated clays, calcite and, hydrous iron oxides.

The Fay-Ace-Verna mine (59°35'N, 108°28'W), owned by Eldorado Nuclear Ltd., is north of Lake Athabasca in the Beaverlodge area. The oxidized samples were collected at the surface near the ventilation pipe. Uranium mines in the Beaverlodge Lake area have been studied and described by Robinson (1955), Bowie (1955), Koeppel (1968), Tremblay (1978), and many others. Pitchblende occurs mainly in fractures of the altered Fay Complex of the Archean Tazin Group rocks along St. Louis fault.

Specimens representing main types of rocks and ores, and their altered equivalents, have been examined in thin sections and in oil immersion mounts under a petrographic

NINE PRINCIPAL ROCK TYPES AND THEIR MINERALOGY IN RABBIT LAKE URANIUM DEPOSIT, SASKATCHEWAN

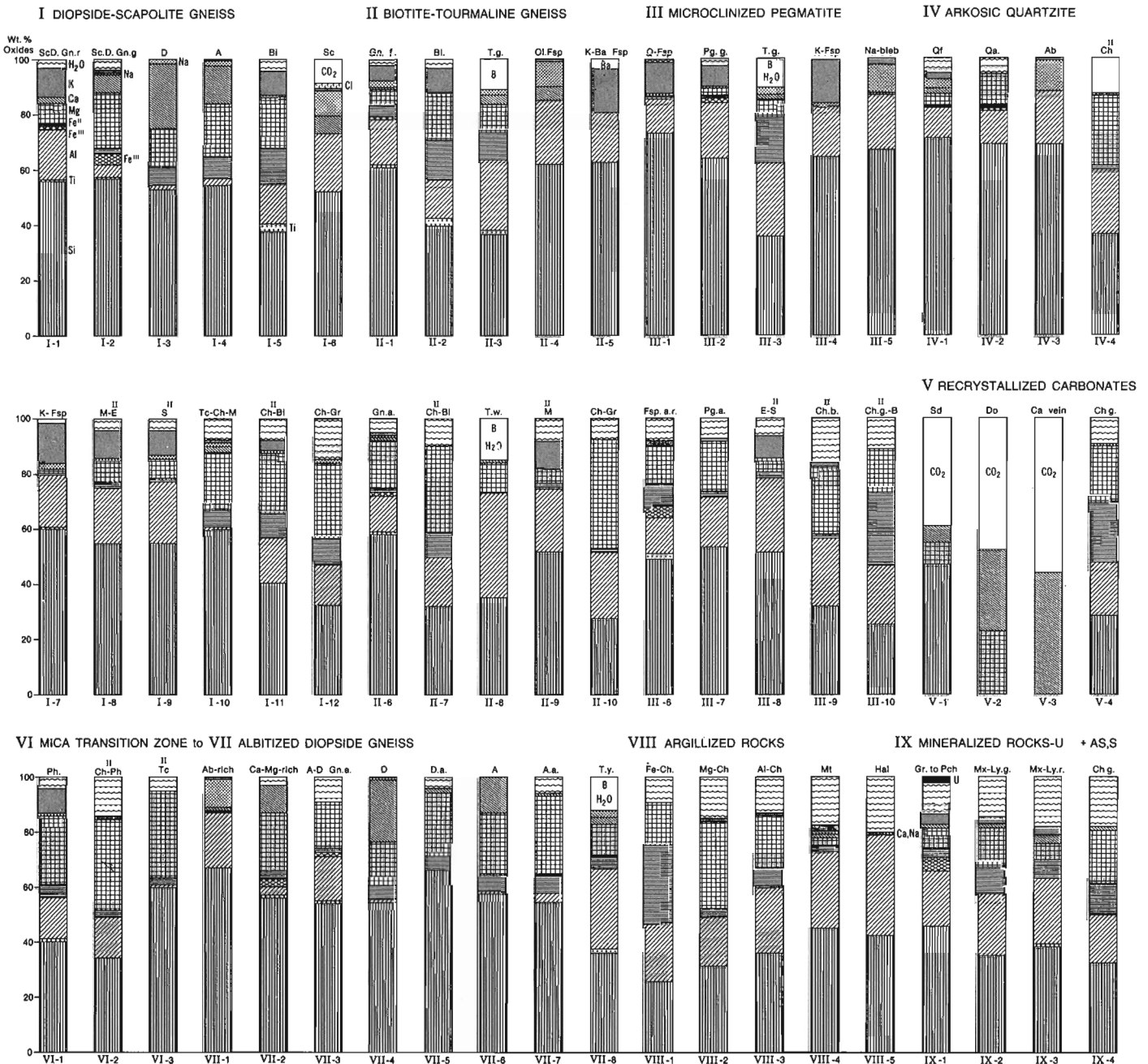


Figure 32.2. Diagrammatic illustration of chemical compositions of fresh and altered rocks and minerals at the Rabbit Lake deposit. Analyses of these samples are given in Table 32.1.

microscope. Selected specimens were studied by chemical, electron microprobe, X-ray diffraction (XRD), thermogravimetric (TG), and differential thermal analysis (DTA) in an attempt to learn more about chemical and mineralogical trends during alteration of pitchblende in various environments, as well as to establish natural environmental conditions of recrystallization of liberated uranium and lead in secondary minerals. Chemical analyses are presented graphically in Figures 32.2, 32.3, and 32.7, and in Tables 32.1, 32.3. Abbreviations used in figures and tables are listed in the Appendix.

Isotope analyses of uranium and lead were made on selected concentrates of pitchblende, secondary Pb-rich and Pb-poor uraniferous mineral aggregates, and associated sulphides (galena and pyrite) at the University of Alberta to determine temporal relationship between the alteration and decomposition of pitchblende and redeposition of the mobilized uranium and radiogenic lead in secondary minerals (Cumming and Rimsaite, 1979).

This report consists of three parts:

1. petrographic and mineralogical characteristics of fresh and altered basement rocks in the Rabbit Lake deposit based on the author's optical studies and on chemical analyses made by Central Laboratories and Administrative Services Division of the Geological Survey of Canada;
2. alteration of pitchblende preceding oxidation; and
3. alteration of pitchblende and recrystallization of liberated uranium in oxidation zones of uranium deposits at the Rabbit Lake, Cluff Lake, and in the Beaverlodge area.

Acknowledgments

Mineralogical and petrological studies by the author were supported by X-ray identification of minerals by A.C. Roberts; chemical, electron microprobe and spectrographic analyses by P.G. Bélanger, M. Bonardi, J.-L. Bouvier, G.R. Lachance, A.G. Plant and G.J. Pringle, all of the Central Laboratories and Administrative Service Division. Drawings were prepared by the Staff of the Cartography Section at the Geological Survey of Canada. Their assistance is gratefully acknowledged.

Gulf Minerals Limited, Uranerz Canada Limited, AMOK Limited and Eldorado Nuclear Limited are thanked for the permission to visit their properties and for the guidance in the field.

Petrographic and Mineralogical Characteristics of the Principal Types of Basement Rocks at the Rabbit Lake Deposit

At the Rabbit Lake deposit, pitchblende occurs in broken fragments and bands in breccia and in fracture zones of altered metasediments of Aphebian age (Fig. 32.1). From the time of Hudsonian Orogeny to present, metasediments have been affected by several periods of recurring fracturing and brecciation, followed by diverse chemical and mineralogical alterations (Rimsaite, 1978a). Three geological events caused marked alterations of the basement metasediments:

1. emplacement of pegmatites and granitic rocks accompanied by feldspathization and tourmalinization of metasediments and formation of skarn minerals;
2. fracturing and alteration of metasediments to phyllosilicate-bearing rocks that are suitable for precipitation of pitchblende; and
3. repeated fracturing of pitchblende-bearing rocks followed by complex progressive alteration and redistribution of chemical constituents, including uranium and radiogenic lead.

In addition to marked hydration, some elements, such as sulphur, arsenic, selenium, cobalt and nickel, were added through fractures after deposition of uranium and partly replaced pitchblende (Rimsaite, 1977a, Fig. 44.4a).

Simplified field relationships between principal rock types collected for this study from the open pit are shown schematically in Figure 32.1. Contacts between different rock types are masked by running water and slumping surface clay and mud that smear the walls of the pit. Soft micaceous rocks have been more deformed by shearing and brecciation than compact microcline pegmatite and albitized diopside gneisses. Nine principal rock types located above the main fault (Fig. 32.1) have been referred to as "upper gneiss" by Knipping (1974). Because metasediments consist of interbedded silicate and dolomite bands transected by calcite veins, the field term "calc-silicate rocks" is also used. On the basis of thin section studies and abundance of secondary phyllosilicates, the following nine types of rocks have been distinguished among the "upper gneisses": I: diopside-scapolite gneiss; II: biotite-tourmaline gneiss; III: microcline pegmatite; IV: arkosic quartzite; V: recrystallized carbonates; VI: phlogopite-rich transition zone, grading to VII: albitized diopside gneiss; VIII: argillized rocks and IX: mineralized phyllosilicate-bearing rocks that contain U, with or without Co, Ni, As, and S. Chemical analyses of these rocks and of their minerals are given in Table 32.1, and chemical trends during alteration are illustrated in Figure 32.2. Chemical, mineralogical, and petrographic variations, which were found in drill core that intersects high grade ore and a zone replaced by sulphides and arsenides, are presented in Table 32.1a and illustrated in Figure 32.3. Table 32.3 presents results of emission spectrographic analyses of accessory minerals and heavy fractions (specific gravity > 3.3), separated from gneisses and pegmatite. The following descriptions of rocks and their altered equivalents illustrate chemical and mineralogical changes during alteration, and provide data on the diversity of liberated ions and of depleted phyllosilicates that are available for reactions with mobilized uranium.

I. Scapolite-Diopside Gneiss

Specimens of the scapolite-diopside gneiss have been collected from the first level of the southwestern wall in the open pit. Scapolite-diopside gneiss is banded and consists of green diopside-amphibole-chlorite bands interlayered with red feldspar-scapolite-quartz bands, all transected by fractures filled with calcite and minor barite. Diopside and tremolite are partly to completely altered to fibrous aggregates of chlorite and talc. Scapolite and plagioclase are partly replaced by phengitic sericite, eastonite and sericite-chlorite aggregates. Biotite is altered to chlorite along basal cleavage planes and coated by thin rims of potassic feldspar (Rimsaite, 1978a, Figs. 58.1a, 1b). Microcline is porphyroblastic and probably genetically related to coarse grained microcline in pegmatites. Microcline is partly argillized and contains red and pink altered patches. Red scapolite-feldspar-rich layers contain abundant alumina and alkalis (mainly potassium), and differ from the green ferromagnesian calc-silicate layers (Fig. 32.2, analyses I-1, I-2). For these Mg-rich rocks, the term "ferromagnesian calc-silicates" is more appropriate than "calc-silicates", because magnesium concentrations are three times as high as those of calcium (Table 32.1, analyses I-1, I-2). Alteration of green diopside-amphibole layers to chlorite and talc involves loss of silica (to 40 weight per cent) and almost total loss of calcium, compensated by the apparent increase in magnesium and water (Fig. 32.2, analyses I-9 to I-12). Silica contents in secondary talc-like phyllosilicates are slightly higher than in the parent diopside and amphibole. Sericitization of feldspar involves loss of silica and potassium, and gains of magnesium and water.

Table 32.1

Partial chemical and electron microprobe analyses of selected minerals and rocks showing chemical trends related to alterations of principal rock types above Rabbit Lake fault

Sample no. as in Fig. 32.2	Description of sample	Type of Analysis*	SiO ₂	TiO ₂	Al ₂ O ₃	Fe ₂ O ₃	Weight % FeO (FeO)**	MgO	CaO	Na ₂ O	K ₂ O	H ₂ O
<u>I. Diopside-scapolite gneiss</u>												
I-1	Red areas of gneiss	C.A.	55.0	0.5	17.1	1.0	1.0	7.0	2.0	0.0	10.0	2.8
I-2	Green areas in gneiss	C.A.	55.7	0.3	5.1	4.0	1.7	20.4	7.0	0.3	1.3	4.1
I-3	Diopside in I-2	E.P.	52.8	0.0	1.3		(5.8)	14.5	23.9	1.4	0.0	
I-4	Amphibole in I-2	E.P.	54.3	0.1	2.0		(8.0)	19.1	12.9	1.2	0.2	
I-5***	Biotite	E.P.	38.0	2.2	13.7		(13.0)	19.0	0.2	0.3	8.8	
I-6***	Scapolite	E.P.	51.8	0.0	20.9		0.0	0.1	6.5	9.2	0.3	
I-7	K-feldspar	E.P.	59.9	0.1	19.0		(0.6)	1.1	0.2	1.7	14.3	
I-8	Muscovite-eastonite	E.P.	54.7	0.0	20.0		(1.9)	8.1	0.3	0.6	10.0	
I-9	Phengitic sericite	E.P.	54.3	0.0	22.2		(1.2)	6.3	0.1	0.7	9.6	
I-10	Talc-chlorite after I-3	E.P.	59.0	0.0	1.1		(5.6)	22.6	2.4	1.1	1.0	
I-11	Chloritized biotite	E.P.	40.2	0.0	16.2		(8.9)	22.1	0.1	0.8	3.3	
I-12	Chlorite in groundmass	E.P.	32.3	0.0	14.2		(10.2)	26.9	0.2	1.4	0.0	
<u>II. Biotite-tourmaline gneiss</u>												
II-1	Fresh gneiss	C.A.	61.1	0.6	16.5	0.6	4.1	4.9	0.6	2.4	5.8	1.7
II-2	Biotite	C.A.	38.2	2.6	14.4	2.0	12.2	16.8	0.0	0.2	9.3	4.8
II-3	Tourmaline green	E.P.	36.4	1.3	26.0		(8.8)	10.2	2.8	1.9	0.0	
II-4	Oligoclase	E.P.	62.2	0.0	22.9		0.0	0.0	4.5	8.7	0.2	
II-5***	K, Ba-feldspar	E.P.	62.5	0.0	18.4		0.0	0.0	0.0	1.2	14.6	
II-6	Altered rock	C.A.	57.9	0.7	12.9	1.2	0.7	17.4	0.8	0.1	0.6	8.3
II-7	Chlorite after biotite	E.P.	31.8	0.9	18.4		(8.8)	30.6	0.0	0.0	0.0	
II-8	Tourmaline white	E.P.	34.9	0.2	37.5		(0.2)	9.6	0.1	0.8	0.0	
II-9	Phengitic sericite	E.P.	51.4	0.0	24.1		(1.5)	5.3	0.1	0.3	9.4	
II-10	Chloritic aggregates	E.P.	27.3	0.0	23.5		(1.0)	29.2	0.0	0.0	0.0	
II-11	Chlorite in fractures	E.P.	31.4	0.0	14.9		(13.0)	25.7	0.0	0.0	0.0	
<u>III. Microcline pegmatite</u>												
III-1	Feldspar-rich areas	C.A.	72.7	0.0	15.0	0.0	0.4	0.6	0.1	1.0	10.5	0.
III-2	Green areas	C.A.	63.9	0.1	18.5	1.7	0.5	2.5	0.1	1.3	10.0	2.
III-3	Tourmaline green	E.P.	35.4	0.4	27.2		(15.9)	6.1	1.3	2.4	0.1	
III-4	Pethite, K-feldspar	E.P.	64.3	0.0	18.2		0.0	0.0	0.0	1.4	15.1	
III-5	Na-blebs in III-4	E.P.	66.8	0.0	19.8		0.0	0.0	0.6	10.8	1.8	
III-6	Red-stained pegmatite	C.A.	49.0	2.0	13.0	4.1	8.1	11.0	0.2	0.0	2.0	6.
III-7	Green Fe-Mg minerals	C.A.	53.5	0.0	17.6	0.5	0.6	18.6	0.1	0.0	0.6	8.
III-8	Eastonite – sericite	E.P.	51.6	0.0	27.1		(1.9)	5.6	0.3	0.0	8.7	
III-9	Chlorite brown	E.P.	31.7	0.0	24.4		(1.1)	25.8	0.1	0.1	0.9	
III-10	Chlorite green	E.P.	25.4	0.1	21.3		(26.3)	15.3	0.0	0.0	0.0	
<u>IV. Arkosic quartzite</u>												
IV-1	Arkosic quartzite	C.A.	71.0	0.3	11.0		0.7	4.0	2.0	4.0	2.0	5.0
IV-2	Quartzite altered	C.A.	68.7	0.3	12.0	0.3	0.8	11.3	0.2	0.0	0.2	6.2
IV-3	Albite	E.P.	68.8	0.0	19.4	–	–	–	–	11.2	0.0	–
IV-4	Secondary phyllosilicates	E.P.	36.1	0.0	25.1		(1.3)	24.7	0.1	0.0	0.3	12.4

Table 32.1 (cont.)

Sample no. as in Fig. 32.2	Description of sample	Type of Analysis*	SiO ₂	TiO ₂	Al ₂ O ₃	Fe ₂ O ₃	Weight % FeO (FeO)**	MgO	CaO	Na ₂ O	K ₂ O	H ₂ O
<u>V. Recrystallized carbonates</u>												
V-1	Siderite	E.P.					(46.8)	7.9	5.6			
V-2	Dolomite	E.P.						23.0	29.4			
V-3	Calcite	E.P.							44.0			
V-4	Ferromagnesian minerals	C.A.	29.0	3.7	16.3	4.1	20.6	13.3	1.3	0.1	0.2	9.7
<u>VI. Micaceous transition zone</u>												
VI-1	Phlogopite	C.A.	38.9	0.5	13.7	1.0	2.3	27.3	0.1	0.6	8.9	6.8
VI-2	Chloritized phlogopite	E.P.	34.1	0.0	15.3		(2.5)	34.4	0.0	0.0	0.3	
VI-3	Talc-like aggregates	E.P.	59.8	0.0	0.7		(2.2)	31.0	0.0	0.0	0.0	
<u>VII. Albitized diopside gneiss</u>												
VII-1	Feldspar-rich areas	C.A.	67.0	0.0	20.0		0.3	0.4	1.0	11.0	0.5	0.0
VII-2	Diopside-rich, green	C.A.	56.0	1.0	3.0	3.0	2.4	20.0	10.0	0.2	0.2	2.7
VII-3	Altered gneiss, red	C.A.	53.9	0.7	15.6	1.6	0.6	17.8	0.4	0.2	0.2	8.9
VII-4	Pyroxene fresh	E.P.	54.4	0.0	0.5		(4.8)	15.4	23.9	0.7	0.0	
VII-5	Pyroxene altered	E.P.	66.2	0.0	0.4		(4.8)	23.5	1.3	0.0	0.0	
VII-6	Amphibole fresh	E.P.	57.4	0.0	0.4		(6.3)	21.3	12.9	0.0	0.0	
VII-7	Amphibole altered	E.P.	54.4	0.0	3.4		(6.3)	28.8	0.3	0.0	0.0	
VII-8	Tourmaline yellow	E.P.	35.8	1.3	29.1		(4.1)	11.4	2.2	2.0	0.0	
<u>VIII. Argillized rocks</u>												
VIII-1	Fe-rich chlorite	E.P.	28.3	0.1	18.8		(20.3)	20.0	0.0	0.2	0.1	
VIII-2	Mg-rich chlorite	E.P.	32.0	0.0	17.9		(3.0)	31.6	0.0	0.0	0.6	
VIII-3	Al-rich chlorite	E.P.	34.6	0.1	23.1		(8.0)	19.9	0.2	0.0	0.5	
VIII-4	Montmorillonitic clay	E.P.	44.6	0.1	28.0		(1.8)	2.7	1.0	0.9	2.1	
VIII-5	Halloysitic clay	E.P.	42.7	0.0	36.2		0.0	0.5	0.0	0.4	0.2	
<u>IX. Mineralized rocks containing U, Co, Cu, Ni, S, Se</u>												
IX-1***	U-mixed layer silicate	C.A.	44.8	0.2	19.7	4.6	2.7	10.6	0.7	0.1	2.6	11.8
IX-2	Green groundmass, U-ore	E.P.	34.4	0.0	22.5		(9.6)	13.1	0.2	0.6	2.5	
IX-3	Orange groundmass, U-ore	E.P.	38.1	0.5	24.1		(6.7)	5.8	2.4	0.4	2.3	
IX-4	Groundmass, S, As, U-ore	E.P.	32.6	0.0	17.0		(11.4)	18.8	0.4	0.1	0.1	

*Type of analysis: C.A. = chemical analyses by J.-L. Bouvier, G.R. Lachance and Staff of Analytical Chemistry Section, Geological Survey of Canada;

E.P. = electron microprobe analyses by G.R. Lachance, M. Bonardi, A.G. Plant and G.J. Pringle of the Mineralogy Section, Geological Survey of Canada.

** (FeO) in brackets = total iron determined by electron microprobe and reported as FeO.

*** Other constituents (wt. %) in following samples: I-6, Cl = 1.65%; II-5, BaO = 1.7%; I-5, F = 1%; IX-1, U = 0.7%, Pb = 0.1%

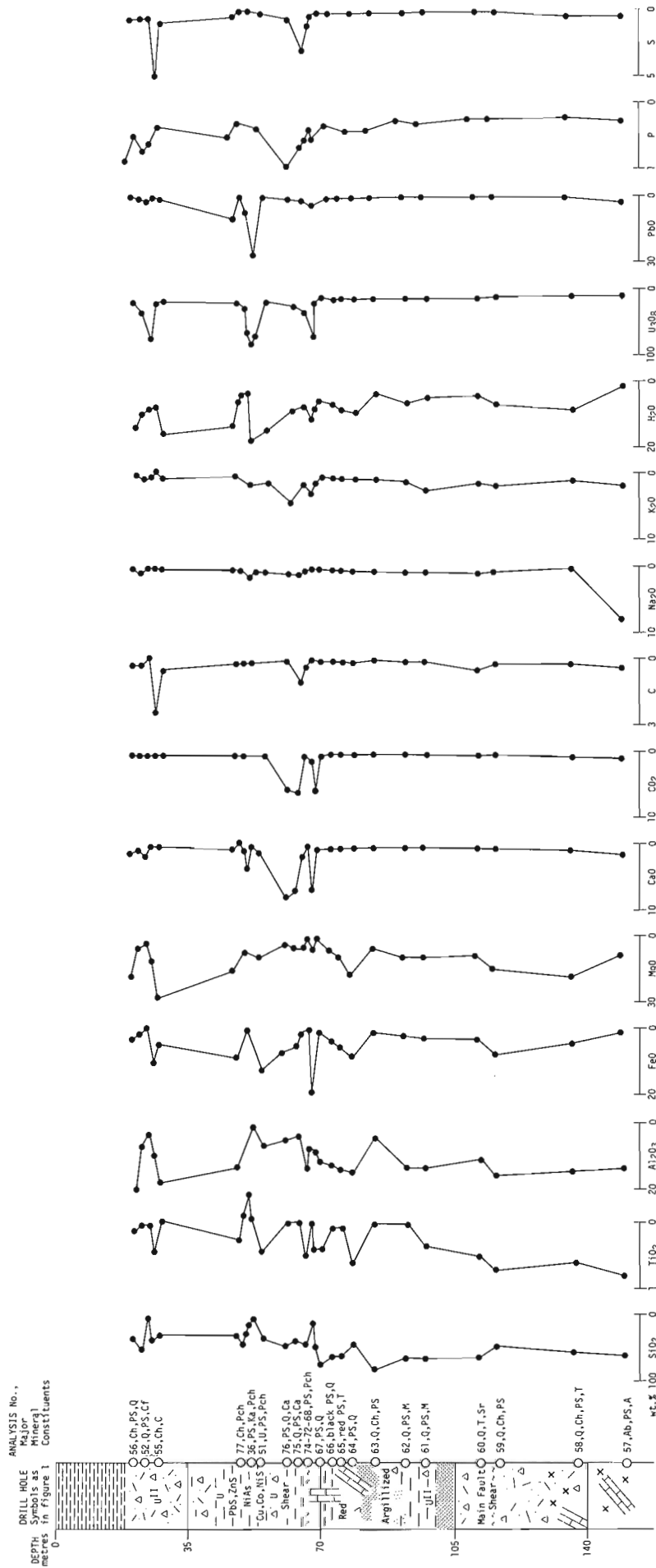
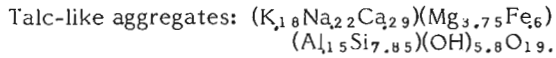
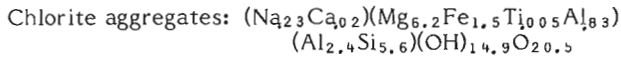
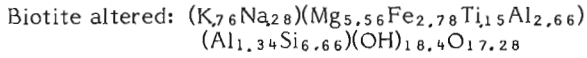
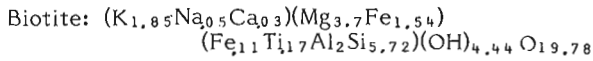
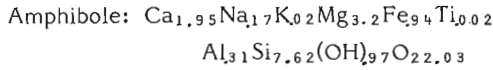
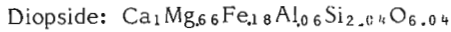


Figure 32.3. Diagrammatic representation of drill core samples collected for chemical and petrographic studies and variation of chemical constituents with depth. Analyses of these samples are given in Table 32.1a.

Structural formulae of ferromagnesian minerals in diopside-scapolite gneiss are:



Structural formulae of the ferromagnesian minerals differ from their ideal structures.

II. Biotite-Tourmaline Gneiss

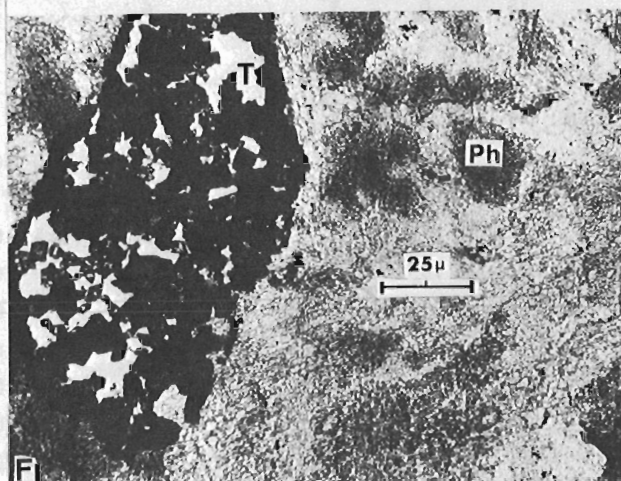
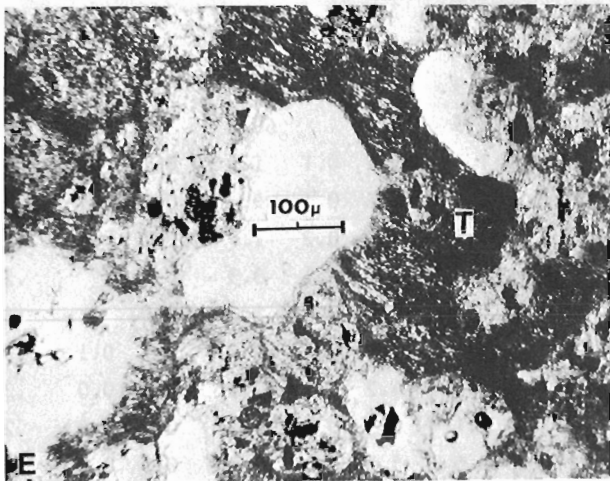
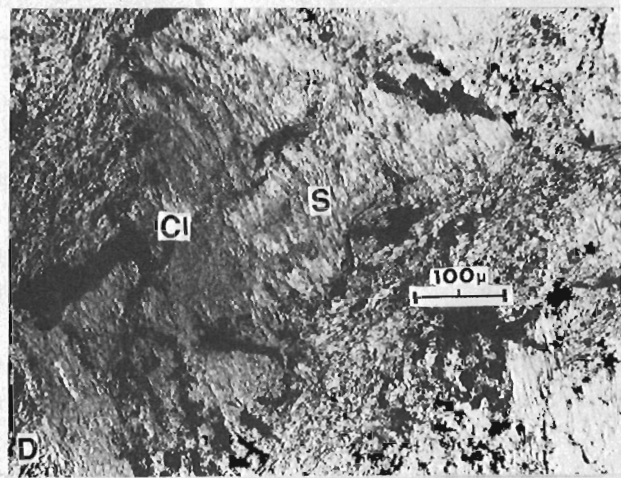
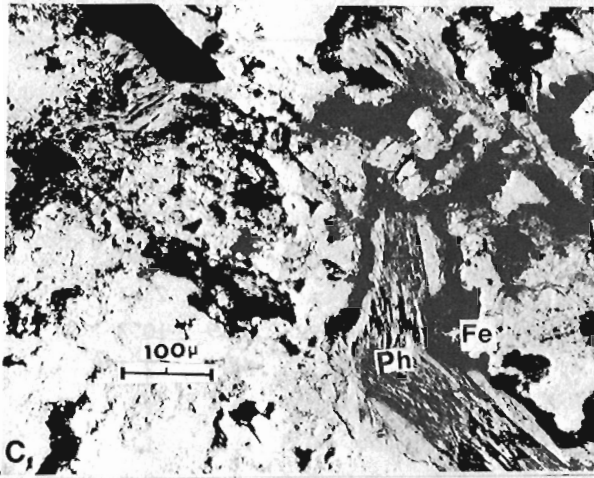
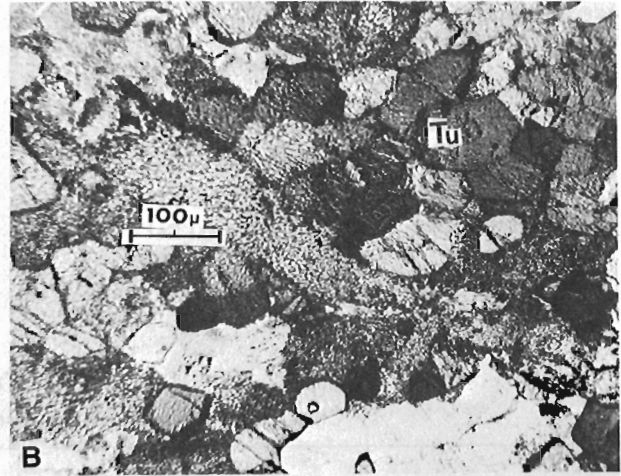
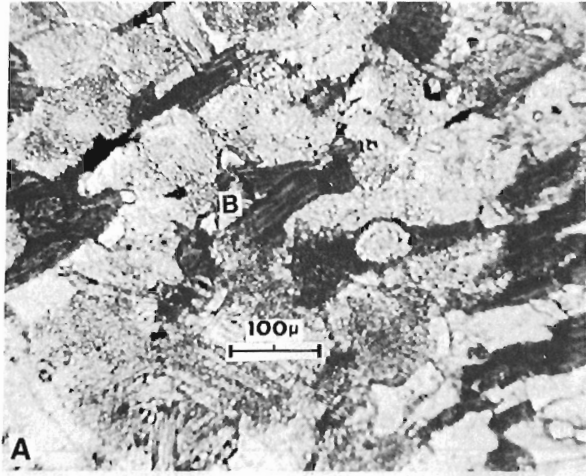
Biotite-tourmaline gneiss is interbedded with arkosic quartzite and transected by microcline pegmatites. The gneiss consists of banded biotite-quartz-feldspar layers transected by tourmaline-rich bands that in turn are cut by chlorite-filled fractures. The lamellar oligoclase is stained red with iron oxides that are removed locally leaving bleached argillized patches (Fig. 32.5C, E). Potassium feldspar contains barium and thereby differs from perthitic microcline in pegmatite. Tourmaline may be genetically related to pegmatitic activity. Biotite and tourmaline are iron-rich and green, and, in altered portions of the gneiss, are replaced by vermiculite, chlorite, and secondary white radiating tourmaline aggregates (Fig. 32.4E; Rimsaite, 1977a, Fig. 44.1h, i). Brecciated and altered biotite-tourmaline gneiss that contains secondary tourmaline and K-depleted biotite is an important host for the interstitial pitchblende of

Table 32.1a
Chemical analyses* of drill core samples showing variations with depth

Sample no. as in Fig. 32.3	Weight%																
	SiO ₂	TiO ₂	Al ₂ O ₃	Fe ₂ O ₃	FeO	MgO	CaO	Na ₂ O	K ₂ O	H ₂ O	S	U ₃ O ₈	PbO	C	P ₂ O ₅	CO ₂	
JR-56	39.	.15	21.		3.	19.	1.2	0.0	0.2	14.6	0.6	3.5	0.0	.2	.6	0.	
JR-52	54.	.04	7.		2.	5.	1.1	0.3	0.4	9.5	0.3	17.	0.2	.2	.2	0.	
JR-53	10.	.01	3.		0.1	2.	1.6	0.0	1.1	8.4	0.4	60.	0.5	.0	.5	0.	
JR-54	38.	.45	10.		10.	15.	0.5	0.0	0.1	8.2	5.	4.5	0.1	2.7	.4	0.	
JR-55	34.	.00	18.		5.	28.	0.4	0.0	0.3	15.1	0.8	0.8	0.0	.6	.1	0.	
36PS**	41.	.02	23.5		0.4	10.4	0.4	0.2	1.7	20.							
36Ka**	15.6						0.8			3.		52.2	28.3				
36Pch**	0.4											81.9	10.7				
36Uph**	18.7						4.2			4.		70.5	2.3				
JR-77	32.	.4	14.		9.	15.	0.8	0.1	0.1	13.5	.5	9.	1.	0.1	.3	.1	
JR-51	34.	.45	7.		12.	12.	1.4	0.0	1.2	15.	0.3	18.	1.		.2	.3	
JR-76	42.	.1	5.		7.	6.	8.	0.1	4.5	8.6	0.6	8.	0.4	0.1	.8	5.3	
JR-75	38.	.0	3.		6.	7.	7.	0.6	2.0	7.1	3.	12.	0.6	1.	.5	5.6	
JR-74PS**	35.	.5	14.		3.	7.	2.	0.8	2.5	11.7	.9	22.	0.1		.4	.2	
JR-71Gn**	46.	.4	10.		8.	7.	5.	0.0	0.9	9.2	.1	10.	0.3		.4	3.7	
JR-72Pch**	9.		5.		1.	5.	.5	0.2	1.5			60.		0.3		.1	
JR-70Ca**	47.	.5	10.		8.	7.	10.	0.0	1.	9.2	0.1	1.5	0.1		.5	7.8	
JR-68PS**	36.	.4	7.		20.	7.	8.	0.1	1.	8.6	0.1	5.	0.5	0.1	.3	6.1	
JR-67	77.	.4	9.		1.	4.5	0.6	0.1	0.2	6.5	0.2	1.4	0.2		.4	0.	
JR-66	67.	.05	11.		4.	8.	0.5	0.1	0.3	7.1	0.1	3.3	0.0		.2	0.	
JR-65	62.	.07	14.	6.0		10.	0.5	0.	0.3	8.4	0.1	1.2	0.0		.3	0.	
JR-64	49.	.64	15.	8.2	0.8	16.	0.4	0.	0.4	10.0	0.1	0.8		0.1	.3	0.	
JR-63	83.	.1	5.		1.0	5.	0.5	0.	0.1	4.2	0.1	2.3	0.0	0.0	.3	0.	
JR-62	67.	.1	14.		2.0	10.	0.3	0.	1.1	6.3	0.0	0.3	0.0	0.0	.2	0.	
JR-61	65.	.4	13.		3.0	10.	0.4	0.	2.5	5.5	0.1	0.9	0.0	0.0	.2	0.	
JR-60	69.	.5	11.		4.0	9.	0.2	0.4	1.1	5.2	0.1	0.4	0.0	0.5	.2	0.	
JR-59	51.	.7	18.	1.5	6.5	14.	0.2	0.0	1.7	7.4	0.1	0.8	0.0	0.1	.2	0.	
JR-58	57.	.6	15.	0.5	2.5	17.	0.3	0.0	0.2	8.5	0.1	0.6	0.0		.2	0.	
JR-57	62.	.8	16.	0.0	1.	9.	1.7	7.6	0.7	3.5	0.1	0.4	0.0	0.3	.2	.7	

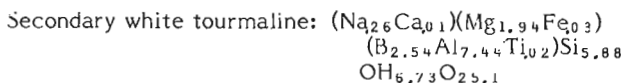
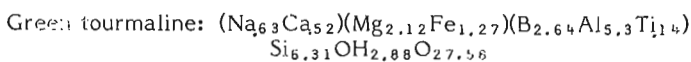
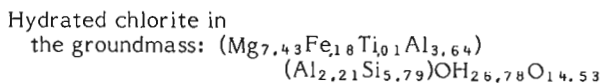
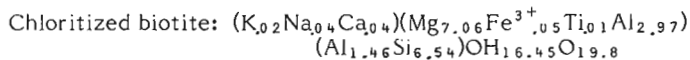
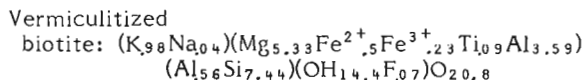
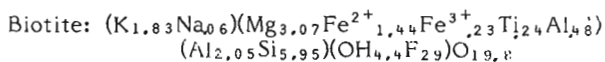
* Chemical and XFD-S30 analyses by J.-L. Bouvier, G.R. Lachance and Staff of CLAS Division.

** Series of related fractions from the same sample; abbreviations of major constituents are listed in Appendix.



types P-2 and P-5 and secondary uranyl-bearing mineral aggregates. Uranophane and boltwoodite crystallize in fractures and vugs, whereas galena and pitchblende of type P-5 precipitate in fractures of vermiculitized biotite (Fig. 32.4E). Chemical differences between fresh and altered biotite-tourmaline gneisses, and between biotite, tourmaline, and oligoclase and their alteration products are shown in Figure 32.2 (columns II-1 to II-5 (for fresh) and II-6 to II-10 (for alteration products)). Chemical changes involve apparent losses of alkalis, calcium, iron, titanium and silica, redistribution of alumina, and gains of magnesium and water.

Structural formulae of minerals in this unit are:



III. Microcline Pegmatite

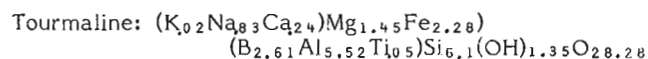
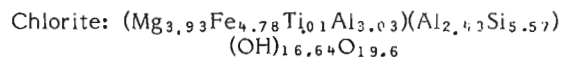
Granite and pegmatites are abundant southeast of the mineralized area where some drill cores intersected as many as 20 pegmatite dykes. In the pegmatite studied, the predominant mineral is porphyroblastic microcline and microcline perthite (Fig. 32.5A). Microcline has crystallized at the spatial expense of pre-existing minerals, pushing aside chloritized biotite. Perthite in turn is replaced by blebs of albite, which suggest that the pegmatite has formed by feldspathization and recrystallization of pre-existing

Figure 32.4.

Illustrations of minerals in green areas of gneisses. GSC 20414-E

- A. Quartz-oligoclase-biotite (B) bands in biotite-tourmaline gneiss.
- B. Tourmaline-rich bands in biotite-tourmaline gneiss. Tourmaline (Tu) is euhedral and green, giving the rock green colour.
- C. Micaceous bands consist of bent phlogopite (Ph) that is partly altered to green chlorite. Iron oxides (Fe) precipitate along chloritized edges of mica.
- D. Chlorite vein (Cl) transects sericite aggregates (S) that pseudomorphously replace feldspar.
- E. Altered gneiss consists of speckled vermiculitized mica and contains large holes left after quartz grains have been washed out in a stream of water producing a porous rock. Opaque specks in altered mica are iron and titanium oxides (T).
- F. Fine grained phyllosilicates in altered albitized diopside gneiss. Green patches of hydrated ferromagnesian minerals consist of talc, chlorite, and remnants of phlogopite (Ph) and contain large aggregates of anatase (T) in calcite matrix that pseudomorphously replace titanite.

gneisses. The albite blebs in microcline perthite from the pegmatite are similar in chemical composition to albite feldspar in arkosic quartzite and in albitized diopside gneiss (Fig. 32.2, columns III-5, IV-3, and VII-1). Feldspar is coloured red by initial argillization and apparently amorphous iron oxides. The only ferromagnesian silicate biotite is almost entirely replaced by iron-rich bright green chlorite. Chlorite is associated with abundant anatase aggregates that have crystallized from the titania originally present in the parent biotite. Green tourmaline is an accessory mineral. Chlorite and tourmaline from the pegmatite contain relatively high proportions of iron, as can be seen from their structural formulae below:



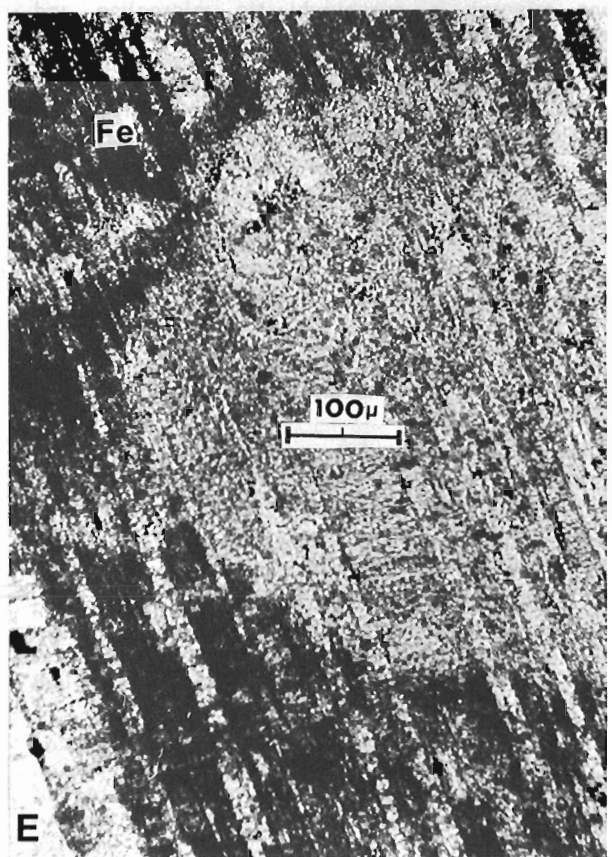
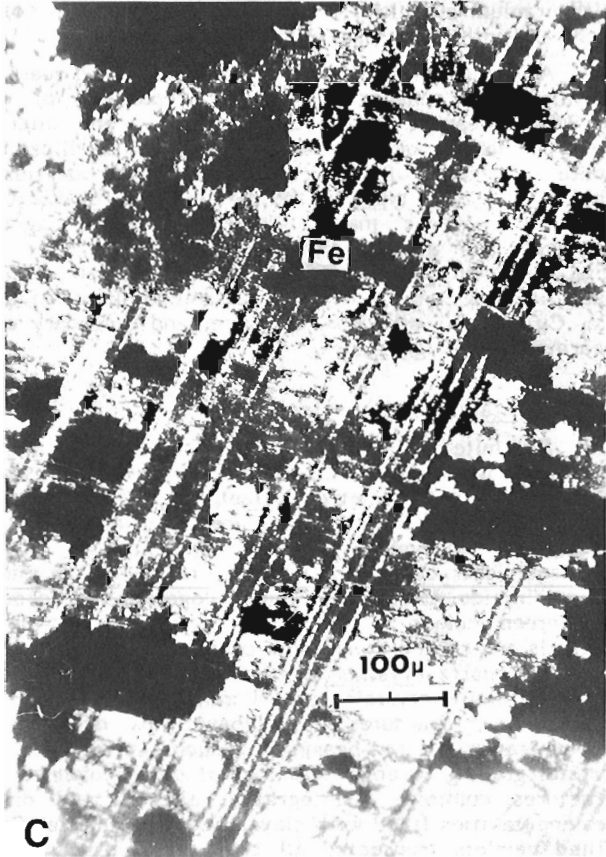
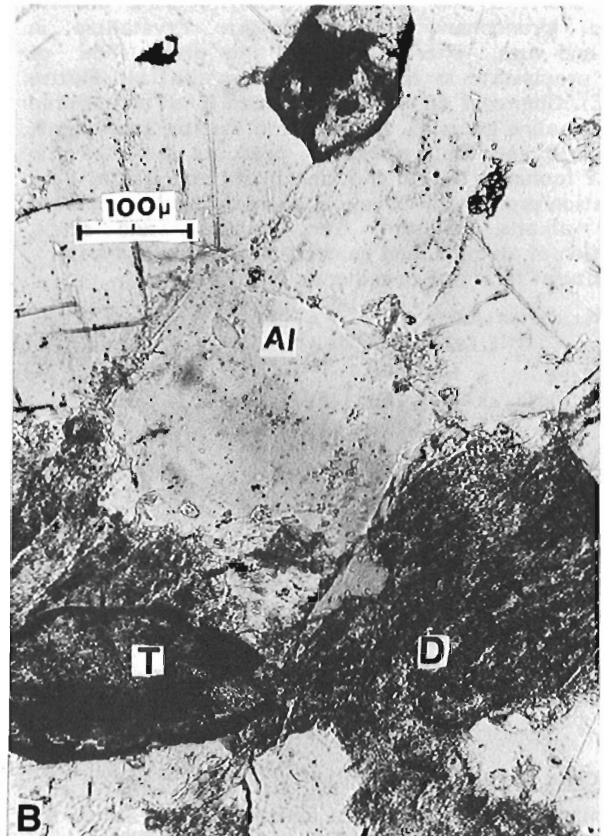
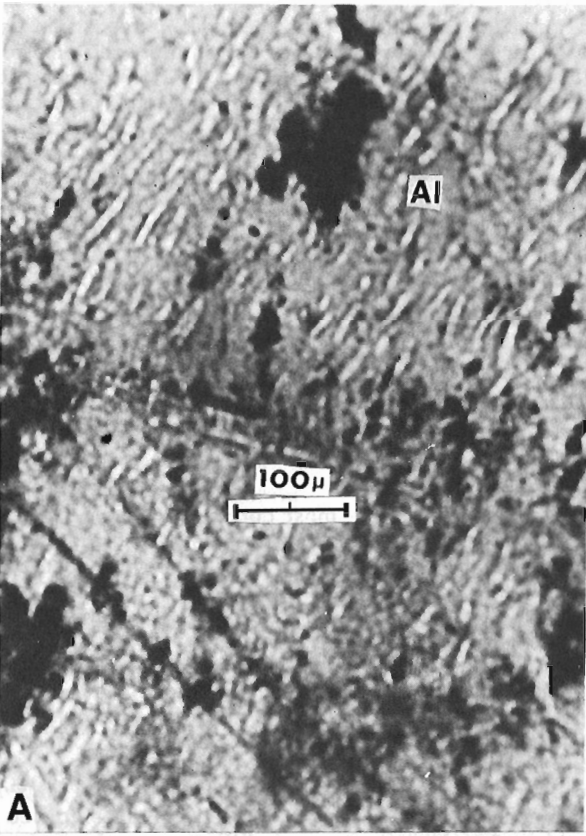
IV. Arkosic Quartzite

Quartzite is the most common rock type in the Rabbit Lake deposit. This unit consists mainly of quartz and variable quantities of albite and interstitial biotite. Quartzose veins, which are composed of euhedral zoned quartz grains, transect all types of gneisses (Rimsaite, 1977a, Fig. 44.1a). In fault and shear zones, quartzite is fractured, mylonitized, locally altered to clay, and impregnated with black carbon dust. At initial stages of alteration, feldspar and biotite were pseudomorphously replaced by fine grained quartz, sericite, and chlorite aggregates (Fig. 32.4C, D). This type of alteration involved losses of alkalis, calcium, and silica; redistribution of alumina; and apparent increases of magnesium and water. Liberated silica silicified altered rocks, forming crusts and filling several generations of transecting fractures. Some of the liberated silica reacted with uranium mobilized from pitchblende to form coffinite along and within fractures of calcite and quartz.

At the advanced stage of alteration, altered quartzite is argillitic and consists of various proportions of quartz (to 90%), bleached and hydrated biotite, and interstitial montmorillonitic or halloysitic clays. All argillized rocks contain remnants of quartz and altered accessory minerals that may indicate types of the parent rock. Argillization of quartzite involves marked losses of iron, magnesium, titanium, and alkalis, and gains of alumina and water (Fig. 32.2, columns VIII-4 and VIII-5). In the open pit, altered quartzite is a common host for disseminated carbon, pyrite, Co, Cu, and Ni sulphides, coffinite, and secondary uranyl-bearing mineral aggregates.

V. Recrystallized Carbonates

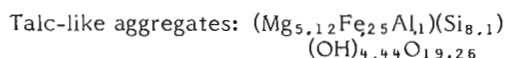
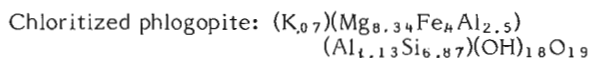
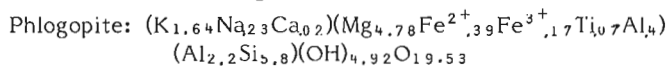
Dolomite marbles are the most abundant carbonates exposed in the southwestern wall of the pit. Large crystals of dolomite (a few centimetres in size), associated with euhedral quartz and white radiating tourmaline, are common in quartzite. Dolomite layers adjacent to albitized metasediments contain skarn-like ferromagnesian minerals, green diopside, chlorite, talc, and phlogopite that account for the green colour of carbonate rocks. Locally dolomite crystals are coated by red iron oxides and contain groups of euhedral quartz crystals overgrown on fractures and vugs. Some dolomite crystals contain minute specks of red iron oxides along fractures and appear pink due to higher concentration of iron-bearing inclusions at the base of the crystal grading to colourless tops of clean dolomite. Along fractures dolomite disintegrated, altered, and dissolved leaving cavities filled with clays, mud, and calcite. Calcite-filled veinlets transected all types of gneisses, fractured pitchblende, and cemented brecciated fragments. Pure calcite, magnesian calcite, dolomite and small quantities of



siderite occur together as fracture fillings and in vugs of altered rocks. Veinlets filled with pure calcite appear to be the youngest. Alteration and dissolution of dolomite marbles results in liberation of magnesium that may react with silica, alumina, and K-depleted micas to form Mg-rich chlorite, whereas liberated calcium recrystallizes as secondary calcite in veinlets and patches replacing silicate rocks. Both calcium and magnesium react with liberated uranium forming uranophane needles that grade to sklodowskite towards the tip of a needle, and hydrous carbonates, bayleyite and liebigite (Fig. 32.6).

VI. Micaceous transition zone

The micaceous transition zone is very irregular, forming pockets, patches, and bands between dolomite marble and albitized diopside gneiss. This zone is very rich in magnesium and calcium, and relatively poor in silica, alumina, and iron. The predominant mineral is phlogopite, partly altered to bright green chlorite along the basal cleavage planes and minor diopside altered to talc in dolomite groundmass. Chemical changes associated with chloritization of phlogopite involved losses of alkalis, iron and silica, and gains of water and magnesium. The major structural change during biotite alteration to chlorite took place in the interlayer of the mica where potassium was replaced by a brucite layer as can be seen from the following structural formulae:



Additional magnesium to form brucite interlayer in chlorite is probably derived from altered dolomite.

VII. Albitized Diopside Gneiss

The micaceous transition zone grades from dolomite marbles to albitized diopside gneiss. Specimens of albitized gneiss were collected in the pit and below the main fault from drill cores (Fig. 32.3). Metasediments below the main fault have been referred to as "footwall quartzite" by Knipping (1974).

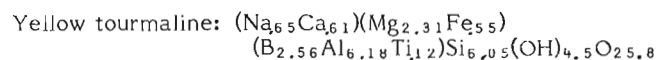
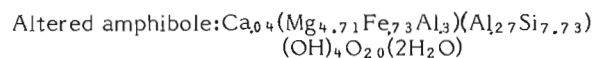
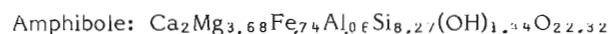
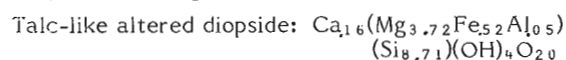
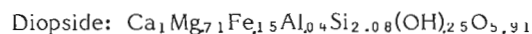
Major constituents of the gneiss are relatively fresh, medium grained albite intergrowths that enclose partly altered remnants of diopside and amphibole-rich fragments, local segregations of phlogopite had patches of carbonate.

Figure 32.5.

Illustrations of red feldspathic areas in microcline pegmatite and in gneisses. GSC 20414-D

- A *Microcline perthite with albite blebs (Al) and red iron oxides (black aggregates) that give red colour to the feldspar.*
- B *Albitized diopside gneiss contains patches of altered diopside (D) and titanite (T) in a mosaic of relatively fresh albite (Al). Titanite is red-brown and slightly radioactive.*
- C *Lamellar oligoclase replaced by an aggregate of sericite and quartz with patches of red iron oxides (Fe) in biotite gneiss.*
- E *Lamellar feldspar stained red by iron oxides (Fe) with a round bleached patch in the centre due to the removal of iron from this area.*

Albitized gneisses and their contact zones with dolomite marbles contain abundant sphene, yellow Mg-rich tourmaline, apatite and minor epidote and allanite (Fig. 32.5B). Some grains of sphene and apatite are radioactive and contain minute specks and thin rims of pitchblende. The altered phlogopite has double pleochroic halos surrounding radioactive thorium-bearing accessory minerals (Rimsaite, 1977a, Fig. 44.2). Albite-rich areas contain high concentrations of silica, sodium, and alumina, compared to green, partly altered patches of calcium-magnesium silicates that contain abundant calcium, magnesium, ferrous and ferric iron, and relatively low concentrations of alumina. Altered gneiss has more water and an intermediate chemical composition between that of albite-rich and diopside-rich portions of the rock (Fig. 32.2, columns VII-1, VII-2, VII-3). Diopside and amphibole alter to pale green Al-poor, Mg-rich aggregates of chlorite, serpentine and talc. This type of alteration involves apparent increases in magnesium and water, and almost complete removal of calcium. The additional magnesium to form the secondary minerals is probably derived from adjacent dolomite. Yellow tourmaline contains the highest magnesium content of the tourmalines in the Rabbit Lake area. Small remnants of phlogopite and coarse aggregates of anatase that pseudomorphously replace titanite, are present in a serpentine-chlorite-talc groundmass (Fig. 32.4F). Chemical formulae of Ca-Mg minerals are given for comparison with those of the same mineral species in diopside-scapolite gneiss.



VIII. Argillized Rocks

Argillized rocks are abundant in breccia zones in the pit, in drill core samples, and as white cappings around uranyl-bearing aggregates that surround black pitchblende-bearing fragments. Because of marked chemical and mineralogical changes, it is not always possible to identify types of a parent gneiss, and thus argillized rocks are described as a separate group. In the field, argillized rocks resemble sedimentary clays and soils, but their "in situ" origin is evident from the pseudomorphous replacement textures, abundant residual quartz, and remnant accessory minerals. Most of the medium grained phyllosilicates and clay minerals (grain size less than 2 mm) have been derived by alteration and decomposition of metamorphic minerals. Depending on local environmental conditions, a single biotite flake alters to Fe-rich, Mg-rich and Al-rich chlorite and muscovite (Fig. 32.2, columns VIII-1 to VIII-3).

The walls of the pit are wet and covered with surface clays and mud. Wet and muddy walls have been observed in areas under swamps and under the pumped-out lake. In such wet areas, chloritic and sericitic rocks are soaked wet, bleached, hydrated and altered to expanding phyllosilicates. Montmorillonitic clays pick up as much as 20 weight per cent water. Alkalis, iron, and magnesium are removed and the hydrated rocks consist mainly of silica, alumina and water. Locally, uranium is present as hydrous uranyl-bearing compounds, such as zippeite, bayleyite, liebigite, uranophane and amorphous phyllosilicates. Uranyl-bearing carbonates crystallize as minute globular aggregates on the wet walls of the pit (Fig. 32.6). Radioactive amorphous crusts form in

Table 32.2

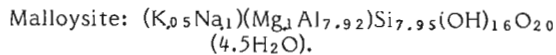
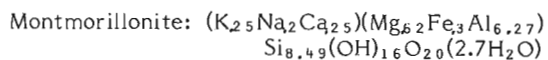
Chemical compositions of selected pitchblende and associated secondary radioactive minerals in uranium deposits, Saskatchewan

Sample no. as in Fig. 32.1	Identification of samples	Electron microprobe analyses* (weight %)									
		Si	Al	Mg	Ca	K	Th	Y	Pb	U	Pb/U
<u>Rabbit Lake deposit</u>											
I-1	Thorium and REE accessory minerals in altered mica	5.5			2.0		40.0	5.4	0.6		
I-2	JR-36 Pitchblende type P-1	2.2							21.5	56.5	1/2.6
I-3	JR-36 Pitchblende type P-2	0.1			0.9				10.3	73.0	1/7.1
I-4	RL-2 Pitchblende type P-3	0.5			1.8				5.6	73.0	1/13
I-5	JR-31 Pitchblende type P-4	3.1							1.2	72.6	1/60
I-6	JR-31 Pitchblende type P-5	5.8			2.0				0.0	55.6	< 1/556
I-7	JR-36-O (Pb)U ₃ O ₇ (nH ₂ O)	4.7			0.8				23.0	46.2	1/2
I-8	JR-36-O Kasolite	7.3			0.6				26.0	46.0	1/1.7
I-9	JR-8 Masuyite	1.5			0.5				19.4	58.2	1/3
I-10	JR-8 Uranophane	5.9			4.4				0.0	61.1	< 1/611
I-11	JR-27 Sklodowskite-like	6.4	0.7	1.6		0.2			0.1	66.8	1/668
I-12	JR-27 Boltwoodite-like	6.5	0.7		0.5	3.5			1.3	60.7	1/46
I-13	RKp-10 Coffinite	7.7	0.8		0.8	0.1			0.0	77.3	< 1/773
I-14	JR-38 U-halloysite veins	19.9	19.	0.3	1.2	0.1			0.0	6.1	< 1/61
I-15	RKp-10 U-mixed-layer clay	14.7	6.7	3.1	0.4	3.1			0.0	40.0	F1/40
<u>Cluff Lake despoit</u>											
II-1	Pitchblende granules	0.7			0.7				9.6	72.5	1/7.5
II-2	Kasolite in hydrocarbon	4.3							31.7	44.5	1/1.4
II-3	Unidentified mineral X-1	1.1			1.7				0.0	66.7	< 1/667
II-4	Amorphous aggregates X-2	0.6			2.4				0.1	70.1	1/700
II-5	Heterogeneous hydrocarbons	0.3	0.3	0.3	2.0			0.8	< 1.	7.	< 1/7

* Analysts: M. Bonardi, A.G. Plant and G.J. Pringle all of the Mineralogy Section, GSC.

fractures of argillized rocks indicating that some of the liberated, and dissolved, uranium precipitated after argillization.

Structural formulae of montmorillonitic and halloysitic aggregates is given for comparison with those of micaceous and chloritic minerals:



IX. Mineralized Rocks Containing U, Cu, Co, Ni, As, S, Se

In the field, mineralized rocks that contain pitchblende appear dark green, grey, or black as a result of disseminated opaque minerals and/or amorphous carbon. They are located in a breccia zone as irregular fragments or blocks reaching several metres in length. These black-grey radioactive blocks constitute the high grade ore (> 0.5 weight per cent U₃O₈).

They are surrounded by an oxidized bright yellow halo which in turn grades into a band of bleached clay. The radioactive blocks are commonly fractured and transected by red and white veinlets filled with hydrated iron oxides, uranophane, and carbonates. Blocks of high grade ore were studied in the

Figure 32.6.

Illustrations of hydrous uranyl-bearing carbonates GSC 203414-L

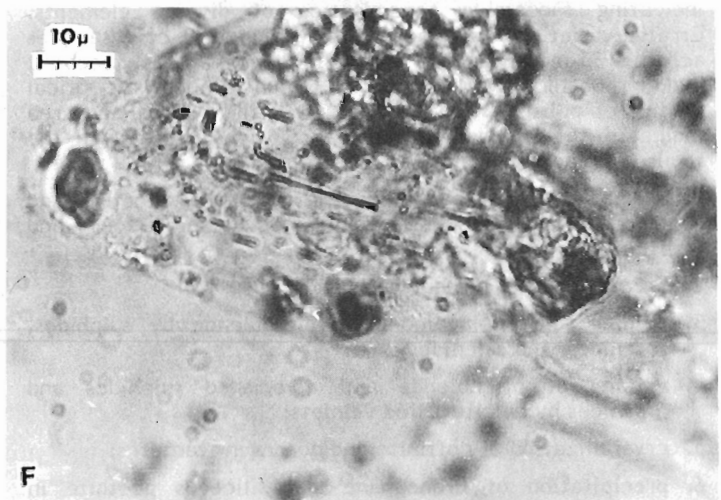
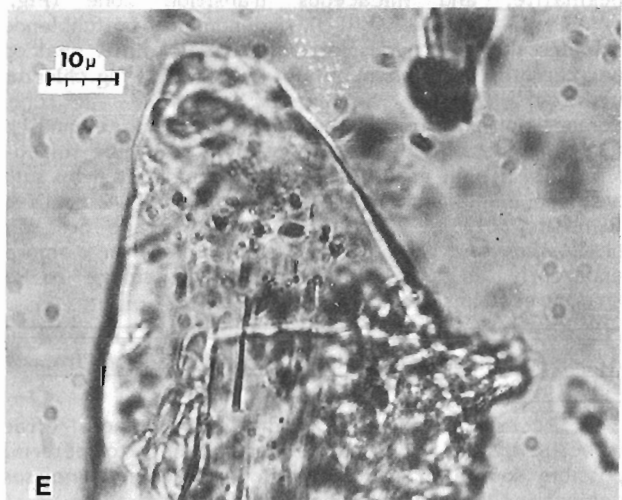
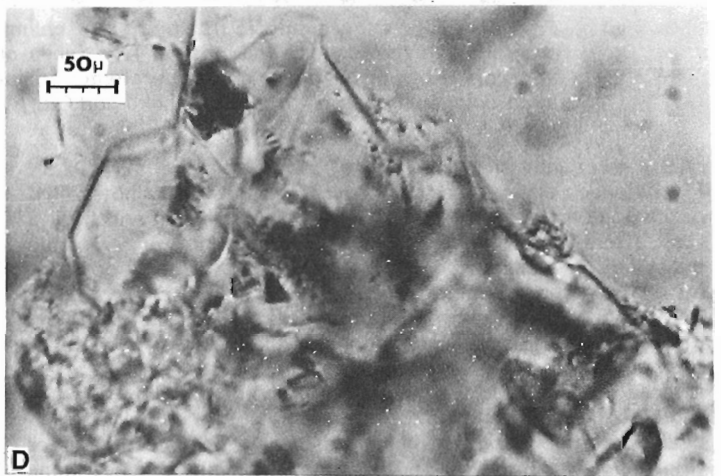
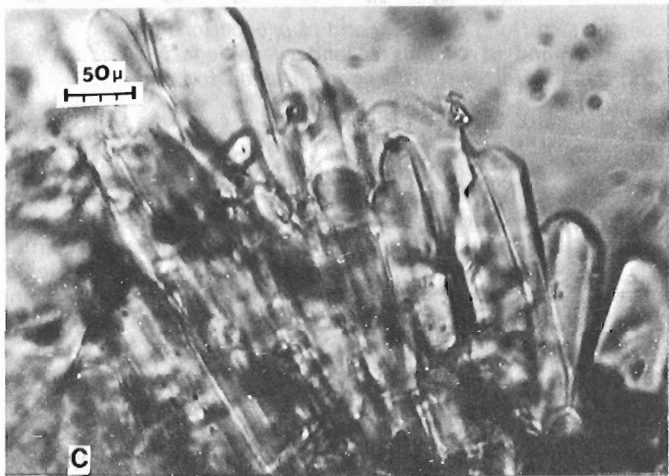
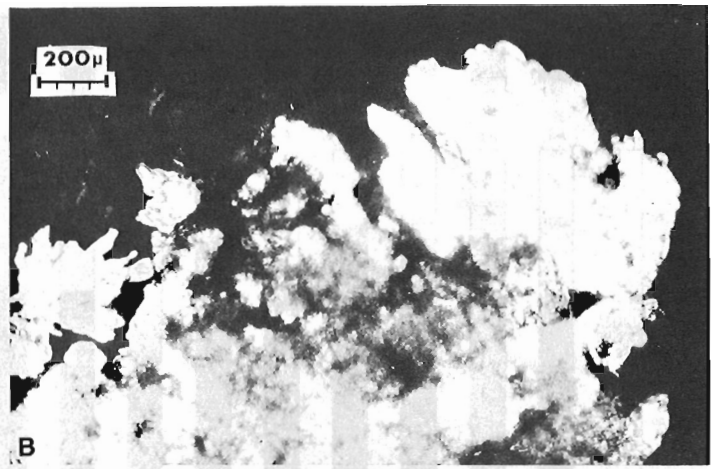
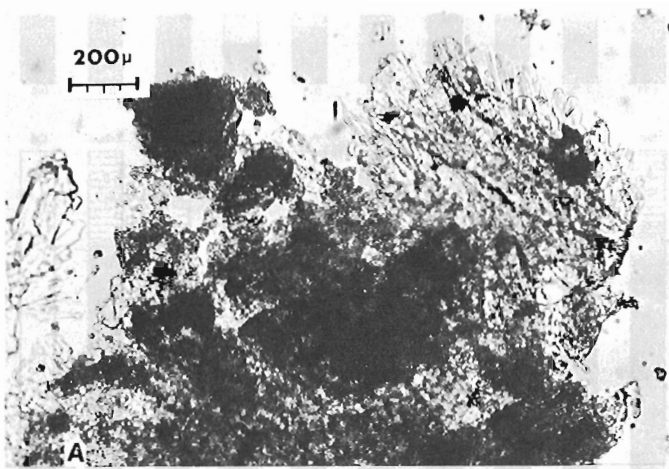
A Greenish yellow crusts consist of liebigite plates, bayleyite prisms, and fine grained speckled aggregates. Oil immersion mount in transmitted light.

B Same as in Figure 32.6A but crossed nicols. Hydrous uranyl-bearing carbonates are strongly birefringent and exhibit bright interference colours.

C Enlarged view of a group of prismatic bayleyite crystals from a crust in Figure 32.6A.

D Enlarged platy liebigite crystals from a crust in Figure 32.6A.

E and D Enlarged prism of bayleyite in an oil immersion mount (refractive index of the oil, RI = 1.46). Bayleyite has a higher RI in the direction of elongation and exhibits high relief in Figure 32.6E. It has the lower index in the direction perpendicular to elongation and is hardly visible in Figure 32.6F where RI of the mineral is very similar to that of the oil. Bayleyite crystals are heterogeneous and contain numerous platy and rod-like inclusions.



FIVE TYPES OF PITCHBLLENDE (P-1 TO P-5) AND OTHER RADIOACTIVE MINERALS IN SASKATCHEWAN.

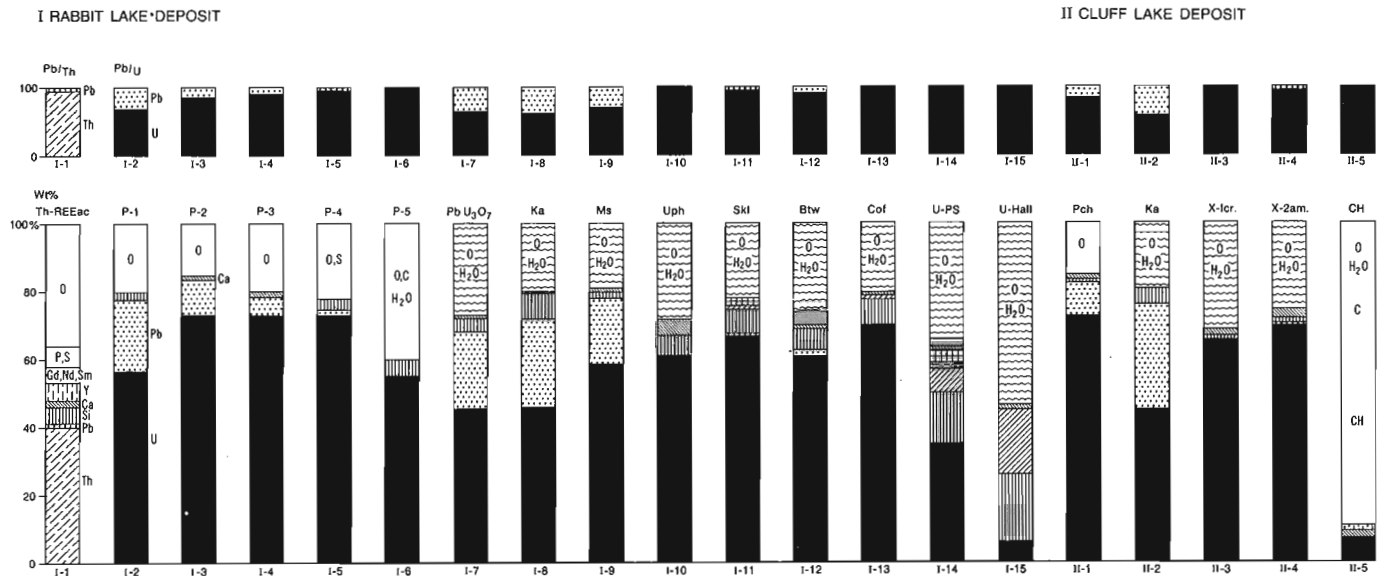
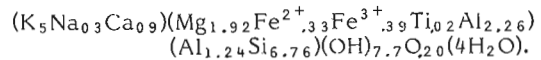


Figure 32.7. Diagrammatic illustration of chemical composition (long columns) and of proportions of uranium and lead (short columns) in five types of pitchblende and in various secondary radioactive minerals showing chemical and mineralogical trends of pitchblende alteration preceding oxidation and in an oxidation zone of the Rabbit Lake and Cluff Lake deposits.

open pit and in drill core samples (Fig. 32.1, 32.3). Pitchblende crystallized in narrow bands and botryoidal patches, commonly less than a few millimetres in width, in a rock altered to secondary phyllosilicates containing variable quantities of remnant quartz, altered biotite and accessory minerals, tourmaline, apatite, and titanium oxides. Pitchblende bands and the host rocks are fractured and altered. Only small remnants of the primary unaltered pitchblende (a few micrometres in size) are present in altered, Pb-depleted and silicified pitchblende. Alteration of pitchblende and its replacements by bright yellow uranyl-bearing compounds were observed also in drill core samples (Fig. 32.3, specimen 36, depth 50 m). Mineralized zones along the rock fractures display erratic chemical variations, indicating successive precipitation of diverse elements. Erratic variations have been observed in drill core samples across a 30-m wide zone containing uranium, copper, cobalt, nickel, arsenic, sulphur, and selenium minerals. Optical studies of polished thin sections from the mineralized area indicated the following temporal relationship between the recurring fracturing and fracture-fillings:

1. formation of green mixed-layer phyllosilicates and chlorite along slickensided surfaces of shear zones and fractures;
2. precipitation of pitchblende bands;
3. veining and replacement of pitchblende by sulphides, arsenides, and selenides;
4. veining of pitchblende and associated sulphides and arsenides by calcite-filled veinlets;
5. crystallization of coffinite and quartz in fractures;
6. precipitation of uranophane and siliceous goethite in fractures;
7. precipitation of serpentine and galena in fractures; and
8. repeated fracturing and precipitation of secondary calcite that cements broken crusts of pitchblende and goethite.

Groundmass silicates in high grade pitchblende ore consist of kaolinite and of green and red varieties of mixed-layer phyllosilicates that are composed of chlorite, mica and montmorillonite-like layers. The phyllosilicates contain relatively low concentrations of silica, moderate quantities of alumina and magnesia, variable quantities of iron and potassium, and relatively high quantities of water, evident from the structural formula:



Mixed-layer phyllosilicates resemble in chemical composition altered and hydrated micas from gneisses, quartzite, pegmatite, and micaceous transition zone (Fig. 32.2, columns IX-1 to IX-3, VIII-3). Groundmass of pitchblende-rich samples that are partly replaced by nickeline, chalcopryrite and carrollite consists mainly of hydrated Al-Mg chlorite. The hydrated chlorite aggregates resemble in chemical composition chlorites from slickensided surfaces and contain more magnesium and less potassium than the mixed-layer silicates in high grade uranium ore unaffected by sulphide-arsenide emplacement (Fig. 32.2, columns IX-2 to IX-4, and Rimsaite, 1978a, Table 58.2). In high grade ore samples, phyllosilicates are poorly crystallized or amorphous, apparently as a result of radiation damage to crystal structures (Rimsaite, 1978a, Fig. 58.6).

Accessory Minerals and Heavy Mineral Fractions from Selected Basement Rocks

Accessory minerals and heavy mineral fractions (specific gravity > 3.3) have been studied to determine a possible source of radioactivity in basement gneisses and pegmatites. The most probable source of uranium is altered thorium and rare earths element-bearing grains that produce double pleochroic halos in altered mica and are associated with recrystallized anatase (Rimsaite, 1977a, Fig. 44.2). Electron microprobe analyses of Th-bearing grains that occur in quartz veins as intergrowths with anatase and marcasite are given in Figure 32.7 (column I-1) and Table 32.2. Thorium-bearing accessory minerals contain variable quantities of uranium.

Titanite and chlor-apatite mixtures from altered rocks in the open pit contain small quantities of uranium that is present in minute radioactive inclusions in apatite and as thin crusts of pitchblende of type P-5 on titanite grains. Radioactive crusts are probably secondary, formed by precipitation of uranium released from fractured pitchblende bands of type 1 and 2. Titanite-rich concentrates from fresh albitized diopside gneiss contain small quantities of antimony, cadmium, cerium, chromium, lanthanum, neodymium, niobium, vanadium, ytterbium, yttrium, and zirconium. Titanite-bearing concentrates from altered rocks contain traces of niobium but lesser quantities of the rare earth elements than concentrates from fresh rocks (Table 32.3, specimens 2, 3 and 4).

Tourmaline-rich concentrate from microcline pegmatite contains traces of tungsten (Table 32.3, analysis 6). Tungsten-bearing minerals may be present as discrete grains within tourmaline, but their presence was not confirmed.

Pyrite-rich concentrate from a carbon-bearing quartzite in the open pit contains small quantities of cobalt, copper, lead, molybdenum, nickel, silver, and uranium (Table 32.3, analyses 7 and 8). The uranium in pyrite is present in secondary minerals; cobalt concentrates mainly in the core of pyrite and in thin veinlets of carrollite; and lead is radiogenic (Cumming and Rimsaite, 1979). Teledyne Isotopes laboratory reported $\delta S^{34} = 4.1$ and 4.3% for the sulphur of pyrite.

Fine grained black heavy minerals associated with pyrite and carbon in quartzite contain small quantities of cerium, cobalt, copper, nickel, lanthanum, lead, thorium, and uranium (Table 32.3, specimen 9).

The last four columns in Table 32.3 provide data on the quantities of minor elements in secondary uranium-bearing minerals. Pitchblende of type P-4 that is intergrown with minute specks of sulphides, selenides and arsenides contains arsenic, cobalt, copper, nickel, lead, scandium, strontium, vanadium, yttrium, and zinc.

Uranyl-bearing secondary mineral aggregates contain cerium, neodymium, strontium, ytterbium, and yttrium. The rare earth elements in secondary uranyl-bearing mineral aggregates might have been derived from the thorium and rare earth element-bearing minerals from basement rocks.

Alterations of Pitchblende Preceding Extensive Oxidation

From the above description of uranium-mineralized rocks it is evident that the pitchblende in the Rabbit Lake deposit was affected by several types of alteration before oxidation and replacement by uranyl-bearing mineral aggregates. The most important alterations of pitchblende preceding oxidation are: Depletion of lead from the original pitchblende; replacement of pitchblende by sulphides and arsenides that resulted in mobilization of uranium and lead, followed by recrystallization of the mobilized uranium in different types of secondary pitchblende; silicification and reactions between silica and uranium to form coffinite; and replacement of pitchblende by secondary minerals of the groundmass and reactions that resulted in formation of uraniferous mixed-layer phyllosilicates.

Depletion of Lead from the Original Pitchblende

Fresh pitchblende of the Precambrian age contains measurable quantities of radiogenic lead that accumulates with time as a result of radioactive decay of uranium and its daughter elements. Because of natural diffusion of lead and possible escape of radon gas from fractured pitchblende, the lead content, and its isotopic composition in the pitchblende vary. The lead concentration usually decreases along

fractures and edges of pitchblende bands. The original fresh pitchblende of type P-1 that contains normal proportions of uranium and radiogenic lead, grades to lead-depleted pitchblende of type P-2. The magnitude of depletion of lead varies and can be measured as a Pb/U ratio in different portions of pitchblende using electron microprobe analyses. At the Rabbit Lake deposit, the Pb/U ratio in pitchblende of type P-1 decreases from 1/2.6 to 1/7 with increasing depletion of lead and pitchblende grades to Pb-depleted type P-2. Ratios of Pb/U in pitchblende of type P-1 and type P-2 are given in Table 32.2 and illustrated in Figure 32.7. Further depletion of lead takes place during resorption and replacement of pitchblende of type P-2 by sulphides and silicates. The mobilized radiogenic lead reacts with sulphur to form radiogenic galena, and the Pb/U ratio in partly replaced remnants of pitchblende decreases from 1/7 in unresorbed Pb-depleted pitchblende of type P-2 to 1/613 in small fragments of replaced pitchblende of type P-2 (Fig. 32.7; Cumming and Rimsaite, 1979). Locally, small fragments of partly-replaced pitchblende recrystallized to euhedral rectangular pitchblende of type P-3 (Table 32.2, Fig. 32.7; Rimsaite, 1978b).

Replacement of Pitchblende by Sulphides and Arsenides and Recrystallization of Mobilized Uranium as Secondary Pitchblende of Types P-4 and P-5

Replacement of pitchblende of type P-2 by nickeline and sulphides has been illustrated by Rimsaite (1977a, b, 1978b). Emplacement of sulphides and arsenides followed brecciation and fracturing of pitchblende of type P-1. The partly replaced pitchblende lost much of the radiogenic lead and liberated uranium recrystallized with minute specks of sulphides and arsenides as pitchblende of type P-4, and as narrow rims of pure pitchblende of type P-5. Pitchblende of type P-5 precipitated on surfaces and in fractures of quartz, calcite, pyrite, chalcocite, hydrocarbons and altered biotite. The mobilized radiogenic lead recrystallized as galena. Koepfel (1968) suggested three periods of episodic losses of lead from pitchblende, 1100 Ma, 270 Ma, and 0-100 Ma ago in the Beaverlodge area. Cumming and Rimsaite (1979) dated radiogenic galena and associated pitchblende of types P-4 and P-5 from a specimen replaced by nickeline, sphalerite, chalcocite, and carrollite, and obtained an age of 850 Ma for crystallization of sulphides and arsenides.

Precipitation of sulphides, selenides, and arsenides is spatially and lithologically restricted, and was probably a short-lasting event. However, optical studies of textures and the relationship between different types of pitchblende and associated galenas indicate several periods of mobilization and recrystallization of the radiogenic lead that diffused out from pitchblende into fractures and recrystallized firstly as galena cubes of various sizes and later as galena veinlets in a phyllosilicate groundmass adjacent to calcite-filled fractures.

Silicification of Pitchblende and Reactions between Silica and Uranium to Form Coffinite

Large quantities of silica are set free during replacement of feldspars by phyllosilicates. Mobilized silica precipitates as secondary quartz in fractures of minerals and rocks. Some silica also precipitates in fractures and on surfaces of pitchblende bands, and reacts with mobilized uranium to form coffinite. Coffinite precipitates as bands in zoned quartz; as coatings on pitchblende and quartz; along quartz veins and within fractures filled with quartz and calcite (Rimsaite, 1978b, Fig. 6, 7). Coffinite-coated fractures in quartz also contain calcite and thin bands of pitchblende of type P-5, indicating that silicification is associated with carbonatization (Fig. 7, columns I-6 and I-13). Coffinite overgrowths on euhedral smoky quartz from the

Table 32.3
Emission spectrochemical analyses* of selected elements in accessory and ore minerals

Weight % elements	Specimens***													
	1	2	3	4	5	6	7	8	9	10	11	12	13	
B		.01	.005		1.	1.				.05	.03	.03	.02	
Ba	.001	.007		.015	.005	.005	.005	.001		.07	.07	.05	.3	
Be					.002	.02							.005	
Co		.002	.003	.002	.01	.07	.07	.5	1.	.07	.15	.07	.15	
Cr	.001	.03	.005	.15	.007	.05		.003	.003	.002	.003	.003	.02	
Cu	.001	.002	.003	.01	.05	.1	.01	1.	3.	.15	10.	.7	.02	
La		.05	.07	.3		.07			.15					
Mo	.03					.02	.3		.02					
Mn	.01	.03	.03	.015	.03	.01	.002		.003	.3	.05	.07	.05	
Nd		.1	.1	.5		.05			.07				.1	
Ni	.07	.01	.003	.015	.015	.05	.1	.15	.3	.5	.1	.1		
Pb							.15	.07	.1	3.	3.	.7	7.	
Sc		.005	.002	.005	.003	.01			.001		.03		.015	
Sr		.002	.01	.002	.007	.007			.002	.05	.05	.03	.03	
U**	.5		.15	.15	.5		.5	.2	.3	30.	30.	30.	25.	
V		.02	.007	.07	.05	.05			.07	.3	.2	.07	.1	
Y		.02	.07	.3	.007	.01				.2	.3		.3	
Yb		.002	.003	.015		.002	.002	.002					.05	
Zr	.015	.01	.02	.07	.015	.02			.015				.01	
Other	.007	Nb .03	Nb .07	Nb Ce .5 Cd .5 Sb .3	.2	W .003	Ag .001	Ag .15 Th .05	Ce 1.5 Th .07	As 7.		.15		Ce

* Analyst P.G. Bélanger of the Analytical Chemistry Section, Geological Survey of Canada;

** Uranium in apatite and titanite is in discrete inclusions and/or crusts of pitchblende of type P-5;

*** Specimens are as follows:

1. Mainly apatite from altered rock in open pit, II-level.
2. Chlor-apatite and titanite from argillized diopside gneiss in open pit, III-level.
3. Apatite and anatase from sericitized and argillized microcline pegmatite in shear zone 20 metres above main fault (drill core sample).
4. Mainly titanite from albitized diopside gneiss in open pit III-level.
5. Mainly tourmaline from altered rock, open pit, II-level.
6. Mainly tourmaline from microcline-biotite pegmatite in open pit III-level.
7. Pyrite from black impure quartzite in open pit III-level. For isotopic analysis of lead from this pyrite see Cumming and Rimsaite, 1979.
8. Pyrite from black C-bearing quartzite in open pit, II-level. In this pyrite $\delta S^{34} = 4.1\%$.
9. Black heavy fraction (specific gravity > 3.3) associated with pyrite No. 8.
10. Pitchblende of types P-4 and P-5 intergrown with galena, sphalerite, carrollite and nickeline from a drill core sample at 50-metre depth.
11. Pitchblende of types P-4 and P-5, coffinite and Cu-sulphides from 60-metre depth.
12. Pitchblende of types P-4 and P-5, coffinite and U-phyllsilicates from a drill core at 63-metre depth.
13. Uranyl-bearing mineral aggregates from the open pit, II-level.

Rabbit Lake deposit yielded an isotopic Pb/U age of about 200 Ma (Cumming and Rimsaite, 1979) and coffinite in the Beaverlodge area crystallized apparently 100 Ma ago (Koeppel, 1968).

Replacement of Pitchblende by Secondary Minerals and Reactions Between Hydrated Mica and Mobilized Uranium to Form Uraniferous Mixed-Layer Phyllosilicates

Fragments of fractured pitchblende in breccias disintegrated in the groundmass and were partly replaced by phyllosilicates and carbonates. Some of the mobilized uranium precipitated along basal fractures of K-depleted micas. Uranium also precipitated in fractures of the host rock and spreaded from the U-filled fracture into the groundmass where it was apparently captured by the interlayer of the montmorillonitic component of mixed-layer phyllosilicates (Fig. 32.7, column I-14). The uraniferous phyllosilicates contain about 2-3 weight per cent potassium and are poorly-crystallized or amorphous (Rimsaite, 1978a). Reactions between the liberated uranium and mixed-layer phyllosilicates took place about 440 Ma ago (Cumming and Rimsaite, 1979).

Reactions in the Oxidation Zone and Replacement of Pitchblende by Uranyl-Bearing Mineral Aggregates

Complex mineralogy and geochemistry of the Rabbit Lake deposit is evident from the description of ore and rock minerals. Diverse silicates, carbonates, sulphides, and arsenides are present in addition to uranium minerals being the potential suppliers of various elements for the reactions and mineralogical readjustments in the oxidizing environment. In the oxidation zone that coincides with the ground water level, and in several zones below the present ground water level, rocks are altered, partly disintegrated to soil-like material and stained red or yellow by hydrous iron oxides and/or uranyl-bearing mineral aggregates. Selected examples of simple reactions in the supergene zone observed in uranium deposits in Saskatchewan are as follows:

- a. reactions producing the driving force for weathering:

$$\text{atmospheric oxygen} \longrightarrow \text{oxygen dissolved in ground water};$$
- b. cathodic reduction of dissolved oxygen radicals:

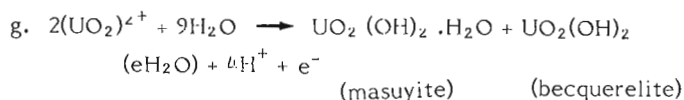
$$\text{O}_2 + 2\text{H}_2\text{O} + 4\text{e}^- \longrightarrow 4(\text{OH})^-;$$
- c. disconnected sulphide reactions (anodic):

$$\text{FeS}_2 + 8\text{H}_2\text{O} \longrightarrow 16\text{H}^+ + \text{Fe}^{2+} + 2\text{SO}_4^{2-} + 14\text{e}^-;$$
 (alteration of pyrite)
- d. $\text{CuFeS}_2 + 4\text{H}_2\text{O} \longrightarrow \text{CuS} + \text{SO}_4^{2-} + 8\text{H}^+ + 8\text{e}^-;$
 (oxidation of chalcopyrite) Covellite; SO_4^{2-} formed during reactions (c) and (d) is available for reactions with liberated uranium to form zippeite;
- e. carbonate exchange and acid buffering reactions:

$$(\text{Mg}, \text{Ca})\text{CO}_3 + \text{H}^+ \rightleftharpoons (\text{Mg}, \text{Ca})^{2+} + \text{HCO}_3^-$$
 (decomposition of dolomite); HCO_3^- is available for reactions with uranyl and other ions form secondary carbonates, including bayleyite and liebigite.
 Reactions continue as follows:

$$(\text{UO}_2, \text{Mg}, \text{Ca}, \text{Fe}, \text{Cu})^{2+} + (\text{OH})^- + \text{HCO}_3^- \longrightarrow (\text{UO}_2, \text{Mg}, \text{Ca}, \text{Fe}, \text{Cu})\text{CO}_3 + \text{H}_2\text{O};$$
 The newly-formed carbonates include bayleyite, liebigite, calcite, siderite, and malachite, all identified in the Rabbit Lake deposit, and some in the Beaverlodge area;
- f. shallow weathering reactions:

$$\text{Fe}^{2+} + 2\text{H}_2\text{O} \longrightarrow \text{FeOOH} + 3\text{H}^+ + \text{e}^-;$$
 (goethite)



Oxidized Minerals in the Rabbit Lake Deposit

Pseudomorphous replacements of pitchblende bands by uranyl-bearing mineral aggregates have been observed in the drill core samples from a depth of 50 m (specimen 36) and in open pit (Fig. 32.3, 32.7, columns I-7 to I-12). In drill core sample 36, at the initial stage of alteration, pitchblende alters to Pb-rich orange-red aggregates of Pb-bearing triuranium heptaoxide and kasolite that contain relatively high Pb/U ratio of 1/1.7. In an oxidation zone exposed in the pit, pitchblende is replaced by Pb-rich masuyite that has U/Pb ratio of 1/2. This stage of alteration involves an apparent decrease of uranium content and increases of radiogenic lead, silica and water in the alteration products. Assuming that proportions of uranium and lead have not changed by the removal of the parent uranium and addition of the daughter element lead, the age of these Pb-rich compounds should be about 4 Ga which is improbable. The Pb-rich uranyl-bearing aggregates contain less than 0.2 per cent common lead and yield unusual isotope ratios of $^{206}\text{Pb}/^{238}\text{U}$ and $^{207}\text{Pb}/^{235}\text{U}$ that fall above the concordia curve (Rimsaite, 1978b; Cumming and Rimsaite, 1979). With progressive alteration and losses of lead, the bright orange-red colour changes to pale yellow, and the Pb-rich uranyl-bearing mineral aggregates recrystallize to the Pb-poor uranyl-bearing hydrous oxides woelsendorfite, becquerelite, soddyite, and complex silicates. Reactions with additional ions of Ca, Mg, and K result in crystallization of uranophane, sklodowskite and boltwoodite. The uranyl-bearing radioactive mineral aggregates are ultimately replaced by white montmorillonitic and halloysitic clays that at the initial stage of replacement contain small portions of uranium (Fig. 32.7, column I-15). Argillization of uranyl-bearing minerals involves replacement of all chemical constituents by silica, alumina, and water. Uranyl-bearing mineral aggregates that form in humid oxidizing environments after argillization include liebigite, bayleyite, zippeite and amorphous radioactive crusts in kaolinitized rocks.

Some of the physicochemical properties of uranyl-bearing minerals, such as their thermal stability and water content in the structure can be used as indicators of environmental conditions. Bayleyite contains eighteen molecules of water in the structure and apparently disintegrates to yellow powder in dry atmosphere (Fig. 32.6; Axelrod et al., 1951). Hydrous uranyl-bearing mineral aggregates lose most of the water at a low temperature between 100°C and 200°C and thus resemble montmorillonite (Rimsaite, 1978b). Presence of crystalline hydrous uranyl-bearing minerals in a deposit is an indication that the temperature has not exceeded 100°C after their formation.

Oxidation of Pitchblende in the Cluff Lake Deposit

In the oxidation zone at the ground water level, chemical trends accompanying alteration of pitchblende to uranyl-bearing mineral aggregates are similar to those observed in the Rabbit Lake deposit (Fig. 32.7, columns II-1 to II-4). At the initial stage of alteration, the Pb-rich mineral is kasolite, preserved in fractures of hydrocarbon. At the later stages of alteration, two unidentified Pb-poor mineral aggregates replace earlier-formed minerals; one is crystalline (X-1), the other is amorphous (X-2). The unidentified mineral aggregates are hydrated and precipitate around relatively coarse grains of hydrocarbon ("thucholite"), (Fig. 32.7, last column). In the Cluff Lake deposit some of the liberated lead crystallizes as wulfenite aggregates, thus involving reactions between lead and molybdenum oxides. Wulfenite crystallizes in fractures filled with hematite, quartz and sericite-like aggregates (Rimsaite, 1977b, Fig. 20.2).

Secondary Lead and Uranyl-bearing Minerals from the Oxidation Zone in the Beaverlodge Area

In addition to uranyl-bearing oxide, silicate, sulphate, and carbonate minerals observed in the Rabbit Lake deposit, Robinson (1955) reported uranium-lead oxides and chemically complex compounds containing Cu, As, and V. These included fourmarierite, $PbU_4O_{13}(7H_2O)$; cuprosklodowskite, $Cu(UO)_2Si_2O_7(6H_2O)$; metazeunerite, $Cu(UO)_2(AsO_4)_2(8H_2O)$; and tyuyamunite, $Ca(UO_2)_2(VO_4)_2(nH_2O)$ that was associated with nolanite. An oxidized sample collected by the author contained uranophane, soddyite $(UO_2)_2SiO_4(2H_2O)$, and amorphous uranium-bearing aggregates.

Summary and Conclusions

Petrological, mineralogical, and geochemical studies of the principal rock types in the Rabbit Lake deposit have been conducted to determine the evolution of phyllosilicate-rich host rocks suitable for precipitation of pitchblende, sulphides, selenides, and arsenides. Basement rocks of Aphebian age are metasediments that have been affected by the following geological processes: recurring deformations; brecciation, shearing, fracturing and mylonitization; feldspathization of gneisses and crystallization of pegmatitic rocks; hydration of metasediments and replacement of metamorphic feldspars and ferromagnesian calc-silicates by phyllosilicates. This stage of alteration involved redistribution of chemical constituents; precipitation of pitchblende and subsequent crystallization of sulphides and arsenides; and fracturing and alterations of pitchblende, sulphides, arsenides and host rocks.

Alteration of pitchblende preceding oxidation included depletion of lead, recrystallization of mobilized uranium as secondary pitchblende of several types and generations, replacement of pitchblende by sulphides and arsenides, silicification of pitchblende, reactions between mobilized uranium and silica to form coffinite and reactions between uranium and hydrated silicates to form uraniferous mixed-layer phyllosilicates, followed by repeated fracturing and cementation by silica and calcite.

In the oxidation zone of the Rabbit Lake, Cluff Lake, and Beaverlodge uranium deposits, chemical reactions involved hydration and decomposition of diverse minerals that resulted in releases of various elements, followed by reactions between mobilized uranium and other ions and partly-decomposed minerals. The initial stage of oxidation of pitchblende involved crystallization of Pb-rich uranyl-bearing mineral aggregates, including hydrous oxides and silicates. With advancing alteration accompanied by losses of lead, Pb-rich uranyl-bearing mineral aggregates have been gradationally replaced by Pb-poor uranyl-bearing aggregates and ultimately replaced by montmorillonitic and halloysitic clays. Crystallization of uranyl-bearing hydrous sulphides, carbonates, arsenates, and vanadates apparently followed argillization. The existence of diverse uranium-bearing compounds indicates potential ability of uranium minerals to change atomic structures and adjust to the changing physicochemical environment. By changing chemical-mineralogical compositions and adapting suitable crystal structures, uranium can survive under diverse environmental conditions. In the uranium deposits of northern Saskatchewan studied, the transition of uranium minerals starts with various pitchblende types in an anhydrous reducing and neutral environment, passes through uranium-lead-silica compounds, and grades to a series of chemically complex hydrated uranyl-bearing mineral aggregates in the oxidation zone.

References

- Aexlrod, J.M., Grimaldi, F.S., Milton, C., and Murata, K.J.
1951: The uranium minerals from Hillside Mine, Yevapai County, Arizona; *American Mineralogist*, v. 36, no. 1-2, p. 1-22.
- Bowie, S.H.U.
1955: Thucholite and hisingerite-pitchblende complexes from Nicholson Mine, Saskatchewan, Canada; *Geological Survey of Great Britain, Bulletin 10*, p. 45-55.
- Cumming, G.L. and Rimsaite, J.
1979: Isotopic studies of lead-depleted pitchblende, secondary radioactive minerals and sulphides from the Rabbit Lake uranium deposit, Saskatchewan; in *Abstracts with Programs, Geological Association of Canada*, v. 4., p. 45.
- Harper, C.T.
1978: Geology of the Cluff Lake uranium deposits; Canadian Institute of Mining and Metallurgy, 80th Annual Geological Meeting, Vancouver, Abstracts, p. 76.
- Knipping, H.D.
1974: The concepts of supergene versus hypogene emplacement of uranium in Rabbit Lake, Saskatchewan, Canada; Symposium: Formation of Uranium Deposits; International Atomic Energy Agency - SM - 183/38, p. 531-549.
- Koepfel, V.
1968: Age and history of the uranium mineralization of the Beaverlodge area, Saskatchewan, Canada; *Geological Survey of Canada, Paper 67-31*, p. 1-111.
- Rimsaite, J.Y.H.
1976: Progressive alteration of pitchblende in an oxidation zone of uranium deposits; 25th International Geological Congress, Sydney, Australia; Abstracts, v. 2, p. 594-595.
- 1977a: Mineral Assemblages at the Rabbit Lake uranium deposits, Saskatchewan; in Report of Activities Part B, *Geological Survey of Canada, Paper 77-1B*, p. 235-246.
- 1977b: Occurrences of rare secondary U- and Pb-bearing mineral aggregates in uranium deposits, northern Saskatchewan; in Report of Activities, Part C; *Geological Survey of Canada, Paper 77-1C*, p. 95-97.
- 1978a: Layer silicates and clays in the Rabbit Lake uranium deposit, Saskatchewan; in *Current Research, Part A, Geological Survey of Canada, Paper 78-1A*, p. 303-315.
- 1978b: Application of mineralogy to the study of multi-stage uranium mineralization in remobilized uranium deposits, Saskatchewan; *Mineralogical Association of Canada, Short Course in Uranium Deposits*, Toronto, M.M. Kimberley (ed.), p. 403-430.
- Robinson, S.C.
1955: Mineralogy of uranium deposits, Goldfields, Saskatchewan; *Geological Survey of Canada, Bulletin 31*, p. 1-128.
- Tremblay, L.P.
1978: Geologic setting of the Beaverlodge-type of vein-uranium deposit and its comparison to that of the unconformity-type; *Mineralogical Association of Canada, Short Course in Uranium Deposits*, Toronto, M.M. Kimberley (ed.), p. 431-456.

APPENDIX

Abbreviations in figures and tables

A = Amphibole;
a = altered;
Ab = albite;
ac = accessories;
Al = aluminum (Al-rich);
As = arsenic (arsenides).

B = boron;
b = brown;
Ba = barium;
Br = brannerite;
Btw = Boltwoodite

C = carbon;
Ca = calcium (calcite);
CH = hydrocarbons;
Ch = Chlorite;
Cf = Coffinite;
cr = crystalline

D = Diopside;
Do = Dolomite

E = Eastonite;
e = euhedral

f = fresh;
Fe = iron (Fe-rich);
Fsp = feldspar

g = green;
Ga = galena;
Gn = Gneiss;
Gr = groundmass

Hall = Halloysite;
He = Hematite;
H₂O = water (hydrous)

i = isotopic

K = potassium;
Ka = kasolite

Ly = layer (silicate)

M = Mica;
Mg = magnesium (Mg-rich);
Ms = Masuyite;
Mt = Montmorillonite;
Mx-Ly = mixed-layer silicates

Na = sodium

O = Oligoclase

P = phosphorus;
P-1 to P-5 = types of pitchblende;
Pch = pitchblende;
Pg = pegmatite;
Ph = Phlogopite;
PS = Phyllosilicate (layer silicate, e.g. chlorite, mica);
Py = Pyrite

Q = Quartz (quartzite, quartzitic)

r = red;
REE = rare earths elements

S = sulphur (sulphides);
Sc = Scapolite;
Sd = Siderite;
Se = selenide;
SkI = Skłodowskite;
Sr = sericite

T = Tourmaline;
Tc = Talc;
Th = Thorium

U_I = uranium (uraniferous);
U_{II} = secondary uranium-bearing minerals;
Uph = Uranophane

w = white

X = unidentified minerals (mineral aggregates)

y = yellow

II = secondary alteration product (M^{II} = secondary mica)

**MAGNETOSTRATIGRAPHY OF PLEISTOCENE SEDIMENTS OF BANKS ISLAND,
NORTHWEST TERRITORIES: A FEASIBILITY STUDY**

Project 740065

W.A. Morris¹ and J-S. Vincent
Terrain Sciences Division

Morris, W.A. and Vincent, J-S., Magnetostatigraphy of Pleistocene sediments of Banks Island, Northwest Territories: A feasibility study; in Current Research, Part B, Geological Survey of Canada, Paper 79-1B, p. 301-306, 1979.

Abstract

Stratigraphic sections on Banks Island in the Canadian Arctic record successive Quaternary glacial and nonglacial episodes. A feasibility study was undertaken in order to establish if paleomagnetism could be used to improve a chronostratigraphic framework for these episodes. It is demonstrated that the sediments collected fulfil the necessary criteria for the application of paleomagnetism. Even though the study was not aimed at defining magnetostatigraphic time zones, one of the suite of samples has revealed upon alternating field cleaning a shallowly, negatively inclined magnetic vector which could relate to a geomagnetic excursion. The samples indicating this possible excursion are from marine sediments belonging to an interglaciation that precedes the Sangamonian interglaciation and therefore is at least older than ca. 225 Ka. If this excursion can be validated during intensive paleomagnetic investigation, it means that a chronostratigraphic marker horizon has been found which possibly could be used for correlation purposes in the Arctic.

Introduction

A long stratigraphic record of Quaternary glacial and nonglacial events is present on Banks Island in the Canadian Arctic (Fig. 33.1). Mapping of surficial deposits (Vincent, 1978a) and stratigraphic investigations (Vincent, 1978b) have led to the recognition of at least three full glaciations with associated marine and glaciolacustrine phases (Vincent, 1978c).

One of the problems in the investigation of the Quaternary history of Banks Island is that of obtaining absolute ages for the recognized events. Radiocarbon dating is useful only for dating the most recent Quaternary units present on the island. Amino acid dating was attempted but up to now has been useful mainly as a correlating tool. As they are developed further, the uranium-series method for dating shells and the thermoluminescence method for dating glacial sediments may be more useful in the future. It was felt that paleomagnetism studies could help, at this time, in providing at least a rough chronostratigraphic framework.

Numerous paleomagnetic investigations have been conducted in the Arctic. Among others, Steuerwald et al. (1968) studied Late Tertiary and Quaternary sediments of the Arctic Ocean. Vilks et al. (1977) and Noltimier and Colinvaux (1976) respectively studied Late Quaternary Beaufort Sea sediments and Late Quaternary sediments from Lake Imuruk, Seward Peninsula, Alaska; in both these studies a geomagnetic excursion is thought to be recorded. Recently Richardson (1978) investigated lacustrine and raised marine sediments on Ellesmere and Devon islands while Locke (1978) studied raised marine sediments on Baffin Island.

This feasibility study was undertaken: (1) to establish if sediments adequate for paleomagnetic work could be sampled in a frozen state, thawed, and then reliably measured; (2) to establish if the sediments carried enough magnetic grains to make them paleomagnetically measurable, and (3) to establish whether the magnetic grains were of a grain size and composition that would faithfully record geomagnetic fields.

Acknowledgments

We are indebted to the Polar Continental Shelf Project which provided logistical support during the 1977 field season. Assistance in collecting the samples was provided by students A. Doiron and F. Auger, Université du Québec à Montréal and

University of Ottawa, respectively. Thanks are extended to R.J. Fulton and R.J. Richardson for their helpful comments on the manuscript.

Location and Description of Sampling Site

Samples for paleomagnetic studies were collected from a section, on the Amundsen Gulf coast, situated 4 km east of the mouth of Nelson River at 71°14'20"N, 122°20'20"W (Fig. 33.1). The precise stratigraphic locations of the sampled units are indicated in the geological section showing the lithostratigraphy of the Quaternary sediments (Fig. 33.2).

Samples 1 to 6 (location 1) were taken in a frozen clayey silt till which lies below seven different till sheets and two suites of sediments interpreted as being interglacial on the basis of preliminary paleoecological and geological evidence. Samples 7 to 12 (location 2) were collected in frozen marine silty clay at the base of the lower interglacial sequence. The upper interglacial suite is possibly Sangamonian in age, and the age of the lower suite is that of an older interglacial of undetermined age.

Field Sampling

Six samples were collected from each of the two stratigraphic horizons. Each of the six samples yielded two, and sometimes three, specimens for paleomagnetic analysis. Because the sediments sampled were located in permafrost, some difficulties in sampling were encountered and hence small errors probably were introduced during the sampling procedure. The samples were collected using a U-channel driven into the permafrost. The direction of the channel was oriented by sun compass; however, because the bottom of the U channel could not be kept perfectly horizontal during sampling, some small errors were introduced. This could cause errors in declination for magnetizations with steep inclinations and in inclination for sediments with shallowly inclined remanences. After extrusion in the field the samples were wrapped tightly while in a frozen state in clear plastic and aluminum foil and permitted to thaw.

Laboratory Treatment

Prior to laboratory treatment the specimens had dried into firm cubes. They were sliced dry with a diamond wheel to produce uniform specimens; each was coated with a plastic film to prevent further crumbling during paleomagnetic

¹Morris Magnetics, 109-1400 Appleton Drive, Ottawa, Ontario K1B 4R9.

processing. Because of the friable nature of the specimens, only alternating field demagnetization was permitted; each specimen was demagnetized in 10 or 50 Oe steps to a maximum of 200 Oe. All demagnetizations which exhibited significant directional shifts were analyzed for multi-component magnetizations by vector subtraction. Individual vectors were recognized from vector diagrams of directional changes during demagnetization (Roy and Park, 1974).

General Considerations on Paleomagnetic Studies

The variation with time of the local magnetic field direction at any spot on the Earth's surface arises from three variables. In order of increasing time duration these variables are secular variation, field reversal, and polar wander. Relative to the time frame involved in the paleomagnetic study of Pleistocene sediments, only the first two variables need be considered. Of these, by far the most important is field reversal which provides a globally applicable chronostratigraphic marker horizon.

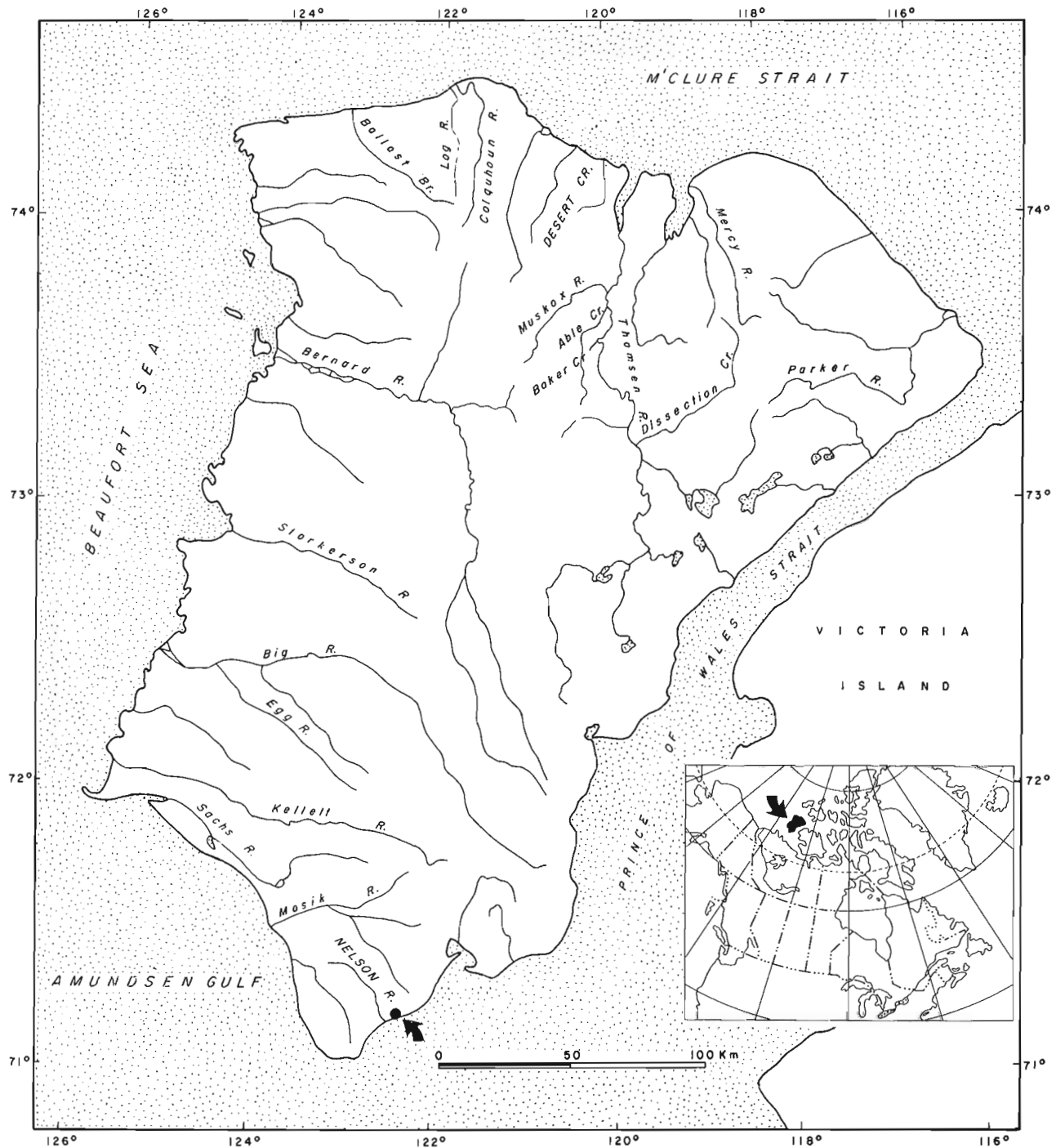


Figure 33.1. Map of Banks Island showing the location of the section studied.

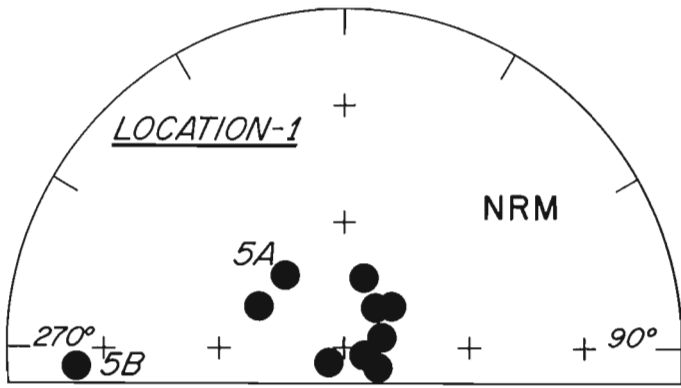


Figure 33.3. Stereonet plot of the NRM directions of specimens 1 to 6 collected at the lower locality (1). Black circles indicate downward (positively) inclined magnetic vectors.

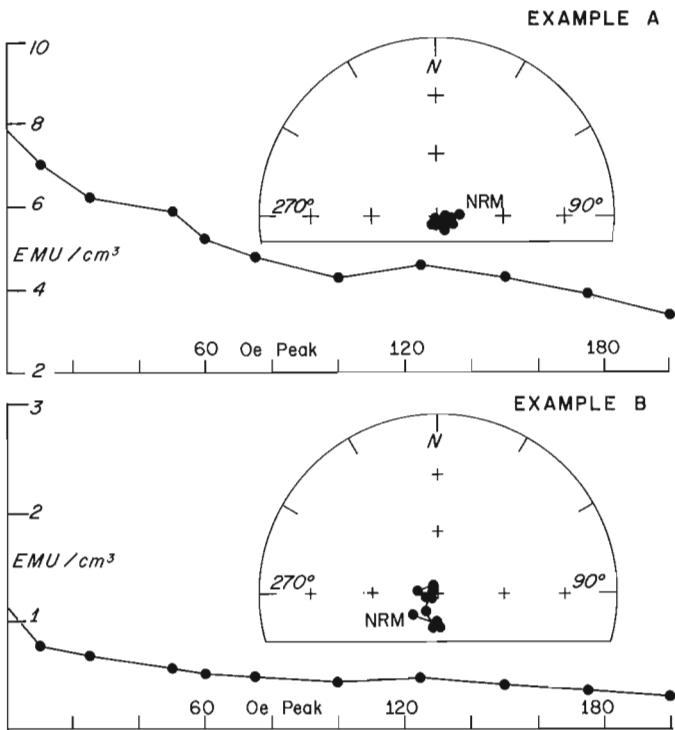


Figure 33.4. Stereonet plot of the sequential changes of remanence direction upon AF demagnetization together with a graphical representation of the change of remanence intensity with increasing demagnetization. The NRM direction is shown by the symbol N. Example A shows no change of remanence direction upon demagnetization; example B shows a small, steep northerly migration of remanence direction.

during the initial demagnetization steps) remanences were observed in some of the specimens. Remanence directions are well grouped for samples of the same site. The lower samples (1-6, location 1) have retained a remanence direction that is similar to the present field direction of the Earth, while samples (7-12) from the upper locality (location 2) have a shallowly inclined magnetic vector. The most notable feature of these shallowly directed remanences is that after AF (alternating field) cleaning they are negatively inclined. Whether this was part of a real geomagnetic excursion cannot be definitely established from the present limited data base.

Magnetic Observations

The average NRM (natural remanent magnetization) intensity of specimens (1-6, location 1) from the lower locality is $6.24 \pm 2.82 \text{ emu/cm}^3$. NRM of most specimens is loosely grouped around $D = 030^\circ$ (declination), $I = +75^\circ$ (inclination) (see Fig. 33.3). Only one specimen 5B appears to carry a divergent remanent direction. Upon AF demagnetization most specimens exhibit only small changes of remanence direction. In all cases the direction changes, which do not seem to have systematic pattern, are towards steeper inclinations (Fig. 33.4). The average median destructive field of the specimens is $80.0 \pm 10.0 \text{ Oe}$. After demagnetization above 200 Oe less than 20 per cent of the NRM intensity of most samples remained. This level of loss of NRM intensity is consistent with the main remanence carrier residing in a fairly coarse grained titanomagnetite. The mean direction of the samples after cleaning was $D = 070^\circ$, $I = +85^\circ$, a direction closely approximating the present field direction of the Earth at the sampling locality.

Throughout the AF treatment specimen 5B continued to give anomalous remanence directions. Moreover, its NRM intensity (9.42 emu/cm^3) was noticeably greater than the average; its median destructive field was 125 Oe, again quite distinct from the other specimens. In contrast, specimen 5A, the other part of this sample, behaved similarly to all other specimens from this locality. Whatever explanation is invoked to explain the anomalous direction of specimen 5B, the fact is that only a single specimen is affected. One explanation is that the remanence of specimen 5B is dominated by the inherited remanence of some rock fragment contained within the till matrix whose magnetic vector was not aligned along the Earth's field direction at the time of till deposition. Other paleomagnetic problems in measuring till samples have been discussed by Stupavsky and Gravenor (1975).

Except for specimen 8A, all specimens (7-12, location 2) from the upper locality have NRM directions with much shallower inclinations of approximately $+30^\circ$ (Fig. 33.5). There appears to be some variation in declination with a mean around $D = 075^\circ$. A similar variation is not observed in inclination. It therefore appears that some errors were introduced during the sampling and measuring procedure. Except for specimen 7A, which is more strongly magnetized than the other specimens, the mean NRM intensity of $0.706 \pm 0.15 \text{ emu/cm}^3$ is noticeably lower than that recorded by specimens from locality 1. Upon demagnetization all specimens, including specimen 8A, exhibit a systematic trend towards a shallower and negatively inclined direction. Most of these changes are shown during the first 50 Oe AF treatment (Fig. 33.6). The direction change is associated with only relatively small changes of remanent intensity. Vector subtraction of the $\text{NRM} - (D, I)_{50}$ suggests that the vector removed during this direction change is aligned very closely with the present magnetic field direction of the Earth. Because of this directional similarity, it is difficult to decide whether this steeply inclined vector arises from viscous remanent buildup or postdepositional formation of goethite which has retained a chemical magnetization associated with hydration.

The median destructive field of $130 \pm 20 \text{ Oe}$ is significantly higher than that for specimens of the lower locality, probably reflecting the lower mean average grain size of this locality. Upon demagnetization all specimens exhibit slightly negative remanence inclinations with a declination of approximately $D = 065^\circ$ (Fig. 33.6). AF treatment produces an improved grouping between the remanence vectors of these specimens suggesting that the error introduced by the sampling and measuring difficulties is probably of the order of 10° in declination.

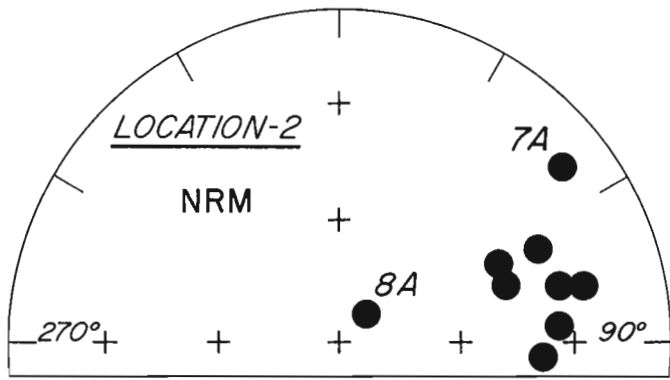


Figure 33.5. Stereonet plot of the NRM directions of specimens 7 to 12 collected at the upper locality (2). Black circles indicate downward (positively) inclined magnetic vectors.

The mean remanence vector of the upper specimens, after AF cleaning at $D = 065^\circ$ $I = -05^\circ$ is highly divergent from that expected from sediments of Quaternary age (Fig. 33.6). The direction cannot be explained by postdepositional compaction, as the required compaction would be at least 25:1 (Blow and Hamilton, 1978) which would only produce extremely shallow positive inclinations. One possible mechanism that could produce such shallow negative inclinations is a postdepositional bedding slump. Other mechanisms have been discussed by Verosub and Banerjee (1977); most of these however appear inapplicable to this study, and the most logical explanation is that the specimens have recorded a portion of some geomagnetic excursion. To confirm this, a full paleomagnetic study must be completed. During a field reversal the strength of the Earth's field decays and then rebuilds again in the opposite polarity (Creer and Ispir, 1970). In keeping with this model, it is noted that the NRM intensity of the upper specimens (location 2) is much lower than that of the lower specimens (location 1). Remanence saturation tests indicate that at least some of this difference is caused by the presence of phases carrying differing amounts of remanence. These tests also indicate, however, that the differences in magnetic mineral content cannot fully explain the differences in remanent intensity at the two localities. It is suggested therefore that part of this difference originates from sediment deposition during a period of weaker magnetic field – a geomagnetic excursion.

Age of Samples

The gravels immediately underlying the upper organic bed (Fig. 33.2) are believed to have been laid down in the Big Sea, a marine transgression that followed the retreating ice of the Thomsen Glaciation (Vincent, 1978c). Amino acid ratios on shells from Big Sea deltaic gravels that were lithostratigraphically correlated with the gravels in the section discussed here provided an estimated age that predates the last (Sangamonian) interglaciation (G.H. Miller, pers. comm., 1978). Based on various paleoecological studies¹, the organic bed is believed to have formed during a climate somewhat warmer than that at present and therefore may be interglacial in character. The lower suite of organic deposits (Fig. 33.2) also is believed, based on the paleoecology² of the flora and fauna, to represent an interglacial episode. Because the marine sediments from which samples 7-12 were collected underlie the lower suite of organic sediments, it can be said that the marine sediments possibly record an excursion that is at least older than the glaciation and part of

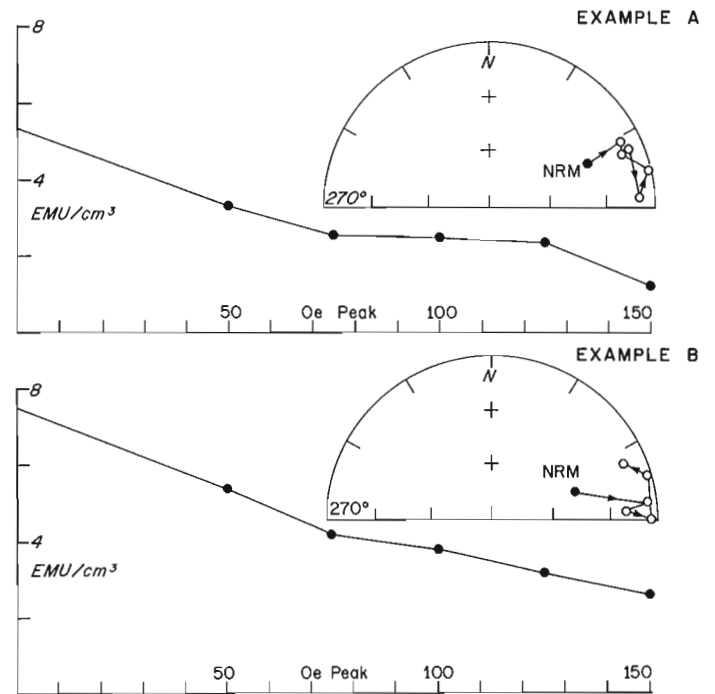


Figure 33.6. Stereonet plot of the sequential changes of remanence direction upon AF demagnetization together with a graphical representation of the change of remanence intensity with decreasing demagnetization. Black circles denote positive remanence directions, and open circles denote negative remanence directions. Both examples show the migration away from the present field direction of the Earth towards a shallowly negatively inclined vector directed towards the east.

the interglaciation which precede at least the last interglaciation (Sangamonian). Oxygen isotope stratigraphy shows that the interglaciation (stage 7) preceding the Sangamonian occurred ca. 225 Ka (Shackleton and Opdyke, 1973). The youngest possible known excursion that could be recorded in the upper specimens would then be older than Biwa I "event" (ca. 180 ± 0.02 Ka, McDougall, in press). Since the lower samples (location 1), which have normal polarity, cannot give any indication of the age of the till sheet from which they were collected, no limiting age for this till can be put forward.

Conclusions

The paleomagnetic specimens examined in this feasibility study fulfil all the necessary criteria for the application of paleomagnetism as a tool for magnetostratigraphy on Banks Island. Most significant is the fact that the specimens from the upper locality appear to have recorded a segment of a geomagnetic excursion. Although it seems unlikely that these shallowly negatively inclined vectors could have arisen from any mechanical depositional mechanism, two simple tests could confirm that this is definitely a geomagnetic excursion. First, one could establish the sequential change of remanence vector with time by sampling a number of closely spaced horizons above and below those sampled at this locality. Secondly, by taking paleomagnetic samples from the same stratigraphic unit in another section, a different sequence of remanence directions should be exhibited if the deposit could be shown to be diachronous. The information then available would conform

¹ Unpublished GSC Fossil Arthropod Report 76-16 and Plant Macrofossil Report 78-6, J.V. Matthews, Jr.; unpublished GSC Palynological Report 79-6, R.J. Mott.

² Unpublished GSC Fossil Arthropod Report 78-6 and Plant Macrofossil Report 78-6, J.V. Matthews, Jr.

to the format suggested by Verosub and Banerjee (1977) for the definition of a geomagnetic excursion. If similar geomagnetic excursions can be substantiated for deposits of similar ages by these types of tests, then natural processes (slumping, burrowing organisms, etc.) can be eliminated as causes of anomalous remanence directions.

Although these data do not permit any firm conclusions to be drawn, they show that the section studied has excellent potential for defining magnetostratigraphic time zones. Because the upper samples possibly may have recorded a geomagnetic excursion, which is commonly of geologically short duration, this provides the possibility of a chronostratigraphic marker horizon for precise correlations in the Arctic.

References

- Blow, R.A. and Hamilton, N.
1978: Effect of compaction on the acquisition of a detrital remanent magnetization in fine-grained sediments; Royal Astronomical Society, Geophysical Journal, v. 52, no. 1, p. 13-23.
- Clark, H.C. and Kennett, J.P.
1973: Paleomagnetic excursion recorded in latest Pleistocene deep sea sediments, Gulf of Mexico; Earth and Planetary Science Letters, v. 19, p. 267-274.
- Creer, K.M. and Ispir, Y.
1970: An interpretation of the behaviour of the geomagnetic field during polarity transitions; Physics of Earth and Planetary Interiors, v. 2, p. 283-293.
- Denham, C.R. and Cox, A.
1971: Evidence that the Laschamp polarity event did not occur 13 300-30 400 years ago; Earth and Planetary Science Letters, v. 13, p. 181-190.
- Locke, W.W. III
1978: Paleomagnetism of a raised marine section, Cape Dyer, N.W.T., Canada; in Abstract of the Fifth Biennial Meeting of the American Quaternary Association, Edmonton, p. 220.
- McDougall, I.
The present status of the geomagnetic polarity time scale; in The Earth: Its Origin, Structure and Evolution, ed. M.W. McElhinny; Academic Press, London. (in press)
- Noel, M. and Tarling, D.H.
1975: The Laschamp geomagnetic 'event'; Nature, v. 253, p. 705-711.
- Noltimier, H.C. and Colinvaux, P.A.
1976: Geomagnetic excursion from Imuruk Lake, Alaska; Nature, v. 259, no. 5540, p. 197-200.
- Richardson, R.J.
1978: Observations on the paleomagnetism of some sediments from Ellesmere and Devon islands, District of Franklin; in Current Research, Part C, Geological Survey of Canada, Paper 78-1C, p. 105-107.
- Roy, J.L. and Park, J.K.
1974: The magnetization process of certain red beds: vector analysis of chemical and thermal results; Canadian Journal of Earth Sciences, v. 11, p. 437-471.
- Shackleton, N.J. and Opdyke, N.D.
1973: Oxygen isotope and paleomagnetic stratigraphy of equatorial Pacific core v28-238: Oxygen isotope paleotemperatures and ice volumes on a 10^5 -year and 10^6 -year scale; Quaternary Research, v. 3, p. 39-55.
- Steuerwald, B.A., Clark, D.L., and Andrew, J.A.
1968: Magnetic stratigraphy and faunal patterns in Arctic Ocean sediments; Earth and Planetary Science Letters, v. 5, no. 2, p. 79-85.
- Stupavsky, M. and Gravenor, C.P.
1975: Magnetic fabric around boulders in till; Geological Society of America Bulletin, v. 86, p. 1534-1536.
- Verosub, K.L. and Banerjee, S.K.
1977: Geomagnetic excursions and their paleomagnetic record; Reviews of Geophysics and Space Physics, v. 15, no. 2, p. 145-155.
- Vilks, G., Hall, J.M., and Piper, D.J.W.
1977: The natural remanent magnetization of sediment cores from the Beaufort Sea; Canadian Journal of Earth Sciences, v. 14, p. 2007-2012.
- Vincent, J-S.
1978a: Lithostratigraphy of the Quaternary sediments east of Jesse Bay, Banks Island, N.W.T.; in Current Research, Part A, Geological Survey of Canada, Paper 78-1A, p. 189-193.
1978b: Surficial geology of Banks Island, District of Franklin, N.W.T.; Geological Survey of Canada, Open File 577.
1978c: Limits of ice advance, glacial lakes, and marine transgressions on Banks Island, District of Franklin: a preliminary interpretation; in Current Research, Part C, Geological Survey of Canada, Paper 78-1C, p. 53-62.

**RADIOCARBON-DATED HOLOCENE EMERGENCE OF SOMERSET ISLAND,
CENTRAL CANADIAN ARCTIC**

Project 750071

Arthur S. Dyke
Terrain Sciences Division

Dyke, Arthur S., Radiocarbon-dated Holocene emergence of Somerset Island, central Canadian Arctic; in Current Research, Part B, Geological Survey of Canada, Paper 79-1B, p. 307-318, 1979.

Abstract

Thirty-six radiocarbon dates on marine shells, whale and walrus bones, and driftwood are used to reconstruct the Holocene emergence of Somerset Island. Nine dates, all around 9200 ± 100 years, pertain to the marine limit. The 9200 ± 100 year old shoreline has a parabolic profile that rises and steepens west-southwestward; its maximum gradient is in the area of the late Wisconsin Laurentide Ice Sheet limit. The shoreline lies at 76 m a.s.l. in the northeast and 157 m a.s.l. in the southwest part of the island. Emergence curves are drawn for Cape Anne, Cunningham Inlet, Rodd Bay, and the Creswell River lowland. Early emergence rates were 8 to 11 m/100 years, and 56 per cent of total emergence was accomplished in the first 1000 years. Emergence has proceeded at a constant rate at each site during the last 5000 to 6000 years but has varied spatially from 46 cm/100 years in the west to 28 cm/100 years in the east. The 5000 year old shoreline declines from 22 m a.s.l. in the west to 14 m a.s.l. in the east with an average gradient of $6.2 \text{ cm} \cdot \text{km}^{-1}$.

Introduction

Emergence of coastal areas of Canada during the Holocene resulted from removal of large ice sheets which covered most of the country during late Wisconsin time. Postglacial emergence of both glaciated areas and areas peripheral to ice sheets is believed to be a combination of three responses: reduction (initially) and removal (eventually) of the gravitational attraction of the ocean by the ice sheet; elastic recovery of the crust from isostatic depression; and delayed recovery as viscous mantle material returns to its former position beneath the glaciated area (Farrell and Clark, 1976). The gravitational and elastic responses are instantaneous, and their contributions to determining the emergence rate depend on the rate of glacier recession. The recovery rate after the ice sheet has melted is a function mainly of mantle viscosity. The amount and rate of emergence that can be explained by each of these three factors vary with location with respect to the centre of the ice sheet, with configuration of the ice margin, and with rate of unloading. By way of example, Clark (1976) calculated that 54 m out of a total 135 m (40 per cent) of measured Holocene emergence at the margin of the Greenland Ice Sheet resulted from instantaneous effects.

Quaternary geologists have studied the rate and spatial pattern of emergence of glaciated areas since the advent of radiocarbon dating, both in its own right as the last major global movement of the earth's crust, and as an indicator of the configuration and history of former ice sheets. Geophysicists use emergence data and ice sheet histories as inputs in modelling properties of the earth's crust, mantle, and even core (e.g. Walcott, 1970a, b; Cathles, 1975; Farrell and Clark, 1976). More recently, using an approximate earth physics model, sea level data alone have been used to calculate the glacial history of Glacier Bay, Alaska (Clark, 1977). The purpose of this paper is to analyze a substantial body of data on the Holocene emergence of Somerset Island, located in the central Canadian Arctic Archipelago (Fig. 34.1, inset) and near the periphery of the late Wisconsin Laurentide Ice Sheet (Prest, 1969; Dyke, 1978a, b, 1979).

Acknowledgments

Field work during 1975 and 1977 was supported by the Polar Continental Shelf Project through its base at Resolute Bay managed by Mr. Fred Alt. Capable field assistance was rendered by Mr. Robert Hélie and Mr. Steven Black. Many

species identifications and notes on sample preservation were provided by Dr. W. Blake, Jr., Director of GSC's Radiocarbon Laboratory. Dr. Blake also arranged for the age determinations at the Saskatoon Radiocarbon Laboratory of the National Museums of Canada. R.B. Taylor, Atlantic Geoscience Centre, kindly allowed me to use one of his unpublished radiocarbon dates. Critical comments by Dr. R.J. Fulton and Mr. D.A. Hodgson of the Geological Survey of Canada helped in clarifying parts of the text.

Growth of the Data Base

The first radiocarbon date relating to high Holocene sea levels on Somerset Island was on a shell sample collected in 1959 by J.B. Bird from Four Rivers Bay on the west coast adjacent to Stanwell-Fletcher Lake (Fig. 34.1 — L-517-A; Olson and Broecker, 1961). B.G. Craig collected several samples of marine shells and one sample of whale bone from raised marine sediments on the island in 1962, and two dates, GSC-150 from Cunningham Inlet and GSC-136 from the southern end of the island, are reported by Craig (1964). A shell sample collected by J.P. Coakley near the eastern shore of Stanwell-Fletcher Lake (GSC-617) was reported by Rust and Coakley (1970) along with two additional datings on Craig's shell samples (GSC-616; GSC-652) and a date on a shell sample (GSC-319) collected near Aston Bay by Smith (1972). Six dates were used to construct an uplift curve which was "corrected" for eustatic sea level rise according to Shepard (1960) (Rust and Coakley, 1970, p. 906). The curve was based on the assumption, not explicitly stated in their text, that the elevations at which the samples were collected represent relative sea level positions at the times of death of the organisms, that is, none of the shells died in offshore, deep water environments.

The next dated samples (GSC-2080; GSC-2081) were driftwood logs from Cunningham Inlet (Taylor, 1975). Blake (1975) used one of these dates to help define the trend of isobases on the 5000 year old shoreline in southeastern Queen Elizabeth Islands. An additional log collected from Cunningham Inlet by R.B. Taylor in 1975 has since been dated (GSC-2233).

A large number of shell and whale bone samples and two driftwood samples were collected in 1975 and 1977 during the course of field work for the interpretation of the Quaternary geology of Somerset Island and adjacent areas. Twenty-five samples have now been dated, which brings the total number

of dates on Holocene sea level features on Somerset Island to 36. Of these dates, 17 are on shells, 13 are on whale bone, 5 are on driftwood, and 1 is on a walrus tusk. The locations and ages of all samples are shown in Figure 34.1, and information on laboratory number, age, material dated, location, sample elevation, elevation of relative sea level at time of death of the organisms, sedimentological context of the samples, and dating procedures is provided in Tables 34.1 and 34.2.

Character of Raised Marine Sediments and Marine Limit

At any location, the most important former sea level to map and date is the highest, i.e. the marine limit. In the Creswell Bay area (Dyke, 1978a, b, 1979), in a valley just south of Batty Bay (Netterville et al., 1976b), and possibly in

other areas, the highest marine sediments apparently were deposited during a high sea level episode associated with glacial recession prior to the late Wisconsin glacial maximum (Fig. 34.1). Similar, possibly correlative, old sediments have been dated on northeastern Boothia Peninsula, just south of the study area (Dyke, 1979). All other fossils from the locally highest marine sediments, however, are early Holocene.

Figure 34.1 shows the approximate limit of the early Holocene sea, derived mainly from surficial geology maps of Netterville et al. (1976a). Along the east coast between Rodd Bay and Fury Beach the limit lies along a nearly vertical, 300 to 400 m high cliff, and significant areas of overlap occur only in the lower courses of two valleys. On the north coast, in Creswell Bay, and on the east coast of the southern peninsula, the area of marine overlap is dominated by parallel raised gravel beach ridges mostly composed of subangular carbonate rock fragments (Fig. 34.2). Along the entire west coast and in the Stanwell-Fletcher Lake basin, the dominant material below marine limit is wave-modified till derived from the crystalline shield. Along all coasts, a few perched deltas occur at and below marine limit (Fig. 34.3).

The Holocene marine limit features, mostly beaches and deltas, are analogous to those forming at the present coastline, and it has not been possible to unequivocally correlate them with glacial features. Hence, inference of a glacial history from the emergence history may be tenuous. Of features examined so far, the delta shown in Figure 34.3 is the one most likely to have been deposited near an ice front. It occupies the mouth of a deep V-shaped canyon that probably was cut or modified by glacial meltwater, and numerous ice marginal meltwater channels occur on adjacent hillsides. It seems likely then that the delta was deposited by meltwater. If so, in the Stanwell-Fletcher Lake area and areas upglacier (west), the Holocene marine limit was formed at the time of deglaciation. Better evidence of regional ice recession associated with marine submergence during the early Holocene has been found on northern Boothia Peninsula, and it is likely that the two adjacent areas have a similar deglacial history (Dyke, 1979).

Holocene Marine Limit Dates

All 36 dates on Holocene raised marine features are plotted in histogram form in Figure 34.4. The striking feature of this distribution is the large number of samples (9) which have yielded ages of about 9200 ± 100 years B.P. This has resulted from the emphasis placed on dating the marine limit. In most of Canada, however, the marine limit is a strongly time-transgressive feature because it was formed as the sea transgressed sequentially deglaciated land (Andrews, 1970). The tight clustering of the oldest dates from Somerset Island around 9200 ± 100 years means that the marine limit deposits were laid down

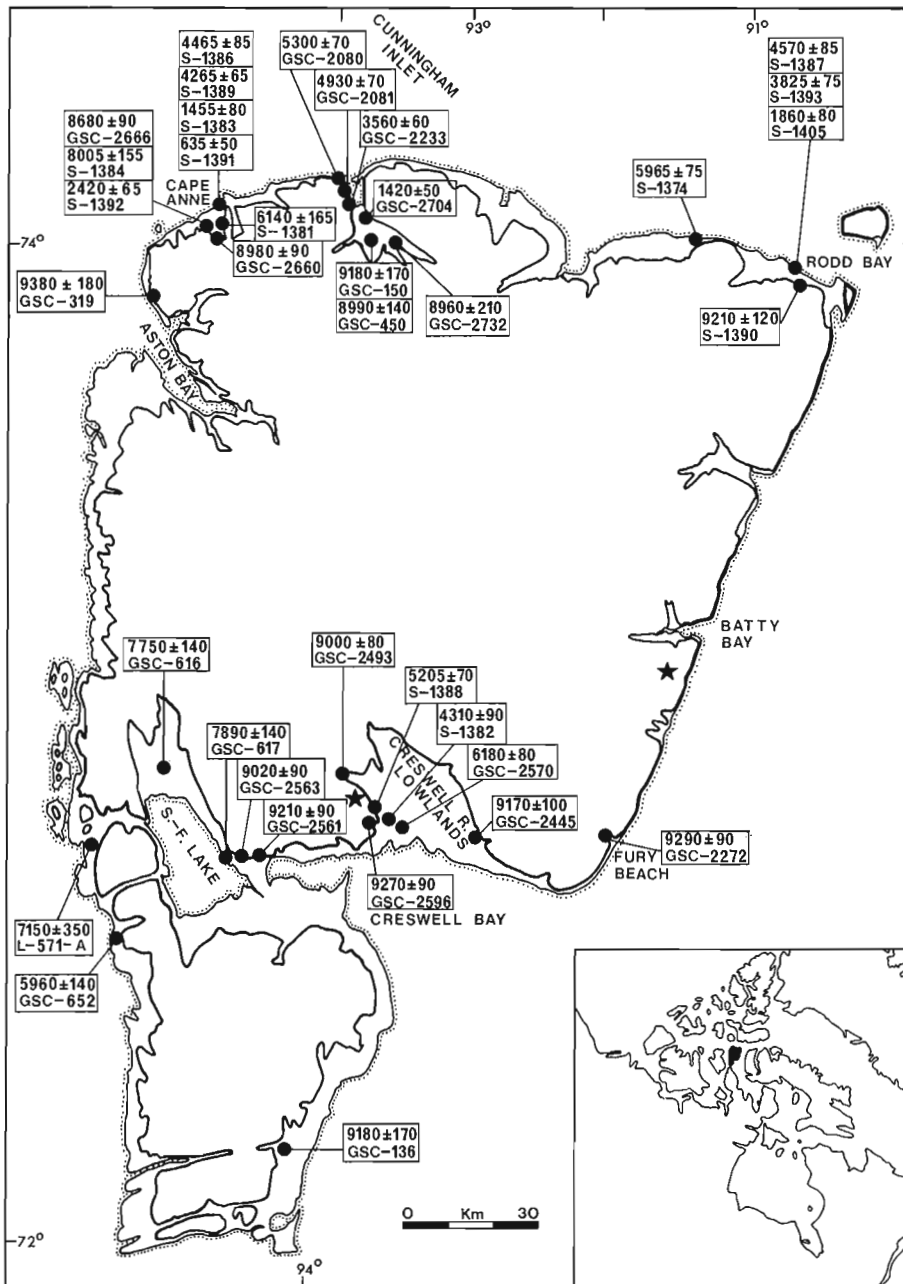


Figure 34.1. Holocene marine limit (heavy black line) and radiocarbon dates on Somerset Island. Stars show locations of dated and probable pre-late Wisconsin marine sediments.



Figure 34.2. Raised gravel beach ridges extending to or near marine limit about 40 km east of Cunningham Inlet; bone and driftwood samples came from this type of sediment. (GSC 203478-H)



Figure 34.3. Remnant of a raised marine delta terrace at 157 m a.s.l. between the southeast shore of Stanwell-Fletcher Lake and the head of Creswell Bay. Shells from clayey silt in the exposure in the foreground (arrow) dated 9210 ± 90 years old (GSC-2561). (GSC 203489-F)

Table 34.1
Radiocarbon dates on raised marine features, northern Somerset Island

Laboratory No. (Field No.) ¹	Uncorrected (Corrected) Radiocarbon Ages ²	Material dated ³	Latitude Longitude	Sample elevation (m) ⁴	Relative sea level (m) ⁵	Comments ⁶
<u>ASTON BAY</u>						
GSC-319	9380 ± 180	Mya truncata	73°53'30" 95°19'	119-122	122	Shells fragments from surface of highest beach ridge, considered to mark marine limit. Collected 1964 by D.I. Smith, University of Bristol. (Craig, 1964; Smith, 1972.)
<u>CAPE ANNE</u>						
GSC-2660 (DCA-77-S19)	8980 ± 90 (9000 ± 90)	Mya truncata	74°01'19" 93°45'	95-99	99	Shells from slightly fossiliferous topset gravels and upper 3 m of foreset sand of highest delta in vicinity forming a terrace at 99 m a.s.l. Sample included both whole valves and fragments, some with pitting, iron staining, and encrustations; pieces of periostracum on some shells. Twelve whole valves (47.0 g) dated after scraping and cleaning with distilled water; 20% leach; one 3-day count in 5 L counter.
GSC-2666 (DCA-77-S18)	8680 ± 90	Mya truncata	74°01'25" 94°53'	60-65	67	Shells from highly fossiliferous foreset sands immediately below topset gravels forming the highest deltaic terrace in vicinity at 67 m a.s.l. Shells were thin and mostly whole valves; some had periostracum, and most had iron staining. Date based on 20.1 g of material; 20% leach; one 3-day count in 5 L counter.
S-1384 (DCA-77-B21)	8005 ± 155	Whale bone	74°01'20" 94°53'	50	50	One of many pieces of bone, all nearly completely embedded in gravel; lichen and moss on exposed upper part.
S-1381 (DCA-77-B24)	6140 ± 165	Whale bone	74°01'50" 94°48'	69	69	One of many vertebrae embedded in surface of marine sand; lichen and moss on exposed upper part.
S-1386 (DCA-77-B12)	4465 ± 85	Whale bone	74°03'30" 94°48'	28	28	Large rib 80% embedded in raised gravel beach ridge.
S-1389 (DCA-77-B10)	4265 ± 65	Whale bone	74°03'20" 94°48'30"	18	18	Bone around blowhole of whale skull; nearly whole skeleton scattered along about 100 m length of single raised gravel beach ridge; most bones more than 50% embedded in beach gravel; lichens and rootlets on surface.
S-1392 (DCA-77-B9)	2420 ± 65	Walrus tusk	74°02' 94°51'	103	?	Tusk from walrus skull; both tusks in skull at time of collection. Apparently entire animal present at site; skull about 50% embedded in gravelly sand on gentle hillside.
S-1383 (DCA-77-B13)	1455 ± 80	Whale bone	74°04' 94°48'30"	7.5	7.5	One of several vertebrae, partly embedded in raised gravel beach ridge; minor lichen cover on exposed upper part.
S-1391 (DCA-77-B22)	635 ± 50	Whale bone	74°04'50" 94°47'	4	4	Vertebra partly embedded in crest of raised gravel beach ridge; minor lichen cover on surface.

CUNNINGHAM INLET

GSC-150 (CD 97b/62)	9180 ± 170	Hiatella arctica	73°59' 93°40'	62	>62	Shells, nearly all articulated and in living position, from surface of eroded marine silt. Relates to sea level much higher than site (Craig, 1964).
GSC-450 (CD 97c/62)	8990 ± 140	Whale bone	73°59' 93°40'	66	66	Vertebra from surface of silts near site of GSC-150. Whole skeleton present (Craig, 1964). Date on organic fraction; inorganic fraction dated 4990 ± 130 years.
GSC-2732 (NJ-75-55)	8960 ± 210 (8990 ± 210)	Mya truncata	73°59' 93°20'	102	102	Shell fragments with little periostracum and some encrustation from mudboils on surface of uppermost gravels of a delta. Clean fragments (7.15 g) used for dating after 10% leach; two 2-day counts in 2 L counter; sample mixed with dead gas for counting.
GSC-2080	5300 ± 70	Wood (Picea)	74°08'55" 93°55'	21	21	Wood buried in frozen raised beach gravel (Taylor, 1975); 9 g burnt; one 2-day count in 5 L counter.
GSC-2081	4930 ± 70	Wood (Picea)	74°07'55" 93°53'50"	17	>17	Driftwood log partly exposed in stream bank composed of solifluction debris (Taylor, 1975); 9.1 g burnt; one 2-day count in 5 L counter.
GSC-2233 (Tu-75-5)	3560 ± 60	Wood (Picea)	74°06'40" 94°15'30"	13	13	Driftwood log, all but end embedded in sandy gravel raised beach (R.B. Taylor). 11.4 g dated; one 2-day count in 5 L counter.
GSC-2704 (NJ-75-60)	1420 ± 50	Wood (Picea)	74°04' 93°34'	5	5	Driftwood log, 70% embedded in crest of shingle beach ridge. Ten rings (11.7 g) used for date; two 1-day counts in 5 L counter.

RODD BAY

S-1390 (DCA-77-B15)	9210 ± 120	Whale bone	73°55'40" 90°37'30"	76	76	Large whale bone, almost completely embedded in beach gravel, lower part within permafrost. No rootlet penetration.
S-1374 (DCA-77-WD2)	5965 ± 75	Wood (Picea)	74°00'30" 91°19'30"	18	18	Sample from 3 m-long log found in ice-wedge trough on gravel beach ridge.
S-1387 (DCA-77-B16)	4570 ± 85	Whale bone	73°57'15" 90°38'	14	14	Bone embedded in surface of gravel beach ridge; lichens and moss on exposed upper part.
S-1393 (DCA-77-B17)	3825 ± 75	Whale bone	73°57'30" 90°38'	10	10	Bone embedded in surface of gravel beach ridge; lichens and moss on exposed upper part.
S-1405 (DCA-77-B19)	1860 ± 80	Whale bone	73°57'45" 90°38'	4.5	4.5	Bone embedded in surface of gravel beach ridge; lichens and moss on exposed upper part.

¹ GSC: Geological Survey of Canada Radiocarbon Laboratory.

S: Radiocarbon Laboratory of the National Museums of Canada and the Saskatchewan Research Council, Saskatoon.

² Corrected ages not used in this paper as they are not available for all dates.

Standard error on GSC dates based on 2 sigma criterion; i.e. probability is 95.5% that true age lies within stated limits.

Standard error on S dates based on 1 sigma criterion; i.e. probability is 68% that true age lies within stated limits.

Error terms on S dates were doubled in constructing emergence curves.

³ All shells composed of aragonite as determined by X-Ray Diffraction Laboratory, GSC.

Dated shells identified by W. Blake, Jr., Radiocarbon Laboratory, GSC.

Driftwood identified by R. J. Mott and L. D. Farley-Gill, Quaternary Paleocology Laboratory, GSC.

Whale bones not identified as to species but likely are *Balaena mysticetus*.

⁴ High tide line used as datum.

⁵ Position of sea level in metres above present high tide at time of death of organism.

⁶ All samples collected by the author unless otherwise noted.

Table 34.2
Radiocarbon dates on raised marine features, southern Somerset Island¹

Laboratory No. (Field No.)	Uncorrected (Corrected) Radiocarbon Ages (years B.P.)	Material dated	Latitude Longitude	Sample elevation (m)	Relative sea level (m)	Comments
CRESWELL RIVER LOWLAND (WEST)						
GSC-2596 (DCA-77-S13)	9270 ± 90	Hiatella arctica	72°50'45" 93°36'	120	125	Whole valves collected from fossiliferous upper foreset sands of a delta forming a terrace at 125 m a.s.l. Terrace accordant with wave-cut platform in bedrock. Date on 14 valves (28.6 g) scraped clean prior to burning; one 3-day count in 2 L counter.
GSC-2493 (NJ-75-76)	9000 ± 80 (9030 ± 80)	Hiatella arctica	72°56' 93°46'	80-85	90	Whole and few paired valves of Hiatella arctica and Mya truncata from fresh cut in bottomset deltaic silts overlain by foreset sands and topset gravels forming a large terrace at 90 m a.s.l. Much smaller terrace remnant at 108 m a.s.l. behind main terrace. Date based on 33 cleanest valves (25.2 g); one 4-day count in 2 L counter.
GSC-2570 (DCA-77-S16)	6180 ± 80 (6180 ± 80)	Serripes groenlandicus	72°52'30" 93°30'	10	>14	Whole valves, some with periostracum, from horizontally bedded sands exposed in fresh stream cut. Sands extend up to an extensive flat surface at 14 m a.s.l.; 28.5 g dated; two 1-day counts in 2 L counter.
S-1388 (DCA-77-B1)	5205 ± 70	Whale bone	72°51'40" 93°34'	73	73	Long fin-shaped bone embedded 80% of its length in raised gravel beach ridge. Possible rootlet and lichen contamination.
S-1382 (DCA-77-B8)	4310 ± 90	Whale bone	72°52'20" 93°32'	22	22	Part of a skull embedded 80% in beach gravel. Possible rootlet and lichen contamination.
CRESWELL RIVER LOWLAND (EAST)						
GSC-2445 (NJ-75-74)	9170 ± 100 (9200 ± 100)	Mya truncata	72°48'50" 92°56'	84-88	>90	Shells from silty sand overlain by 2 m of beach gravel. Ten valves (20.0 g) used for dating. These had little or no encrustation, but some discoloration and pitting. Four valves had periostracum. One 3-day count in 2 L counter; sample mixed with dead gas for counting.
STANWELL-FLETCHER LAKE AREA						
GSC-2561 (DCA-77-S8)	9210 ± 90 (9240 ± 90)	Mya truncata	72°46'30" 94°21'	107	157	Fragments, whole valves, and a few paired valves of Hiatella arctica and Mya truncata from clayey silt overlain by gravel scree in a shallow stream cut on a steep slope below a deltaic terrace remnant at 157 m a.s.l. Many valves had periostracum and some had iron stains. Twenty-three valves of Mya (27.9 g) used for dating; one 3-day count in 2 L counter.
GSC-2563 (DCA-77-S6)	9020 ± 90 (9060 ± 90)	Mya truncata	72°46'15" 94°31'	71	>75	Mostly whole valves, some paired and most with periostracum, of Hiatella arctica and Mya truncata from a single couplet of horizontally bedded sand and silt from a fresh section below a deltaic terrace at 75 m a.s.l. Nine valves of Mya (27.8 g) used for dating; one 3-day count in 2 L counter.

GSC-617 (SF1)	7890 ± 140	Clinocardium ciliatum Serripes groenlandicus Mya truncata	72°46' 94°30'	26	>26	Shells from surface of riverbank exposure in sands thought to be shoreline deposits. Collected July 1965 by J. Coakley, then with University of Ottawa (Rust and Coakley, 1970).
GSC-616 (CD/TA/12/62)	7750 ± 140	Serripes groenlandicus	72°58' 95°03'	46	>46	Shells from surface of deltaic or beach sand. Collected by F.C. Taylor, 1962, for B.G. Craig (Craig, 1964; Rust and Coakley, 1970).
L-571-A	7150 ± 350	Macoma Cardium Hiatella arctica	72°47' 95°37'	30	>30	Shells from terrace 30 m a.s.l.; 10% leach prior to dating. Collected 1959 by J.B. Bird, McGill University (Olson and Broecker, 1961; Craig, 1964).
GSC-652 (CD 131C/62)	5960 ± 140	Astarte borealis Serripes groenlandicus Macoma calcareo Mya truncata Hiatella arctica	72°36' 95°20'	13	>21	Shells from bedded sand in delta with terrace at 21 m a.s.l. One <i>Mya</i> had syphon and many other shells had periostracum attached, so the shell was not transported very far. Collected 1962 by B.G. Craig; reported by Rust and Coakley (1970).
<u>FURY BEACH</u>						
GSC-2272 (NJ-75-142)	9290 ± 90 (9310 ± 90)	<i>Mya truncata</i>	72°49'10" 92°01'	90	90	<i>Hiatella arctica</i> and <i>Mya truncata</i> (former dominant) valves and fragments, all with periostracum, and few fragments of <i>Balanus</i> sp. from a single sand horizon 5 m below top of a delta terrace and from sandy scree immediately below the shell-bearing sand; 26 g dated; one 3-day count in 2 L counter. Collected 1975 by J.A. Netterville (Netterville in Lowdon et al., 1977).
<u>SOUTHEAST CORNER</u>						
GSC-136 (CD 110c/62)	9180 ± 170	<i>Hiatella</i> arctica <i>Mya truncata</i>	72°11'30" 94°05'	127	>127	From surface of sand terrace showing deltaic foreset bedding in gullies. Collected 1962 by B.G. Craig (Craig, 1964).
1 All footnotes to Table 34.1 also apply to Table 34.2.						

everywhere on the north and east coast at essentially the same time. In terms of deglacial history, this means that either the whole length of these coasts became ice free 9200 ± 100 years ago or that they were not covered by ice during the late Wisconsin and the sea transgressed to its maximum Holocene level at this time. This does not necessarily hold true for the west coast as the marine limit has not been dated anywhere along its length.

In any case, the 9200 ± 100 year old strandline is a well dated feature, and its geometry is a measure of the amount and nature of crustal delevelling that has occurred since that time. The northeast corner of the island has emerged less than 80 m in the last 9200 years (Fig. 34.5); the highest distinct beach ridge in that vicinity, at 76 m a.s.l., contained whale bone which has been dated at 9210 ± 120 years (S-1390). The Fury Beach area has experienced about 90 m of emergence, as indicated by a date of 9290 ± 90 years (GSC-2272) on shells from sand directly below a delta terrace at that level. On the western side of the Creswell River lowland, shells from sand immediately below topset deltaic gravels forming a terrace at 125 m were dated at 9270 ± 90 years (GSC-2596). The highest beach ridge in outer Aston Bay, on the northwest coast of the island, lies at 122 m a.s.l., and shells from it were dated at 9380 ± 180 years (GSC-319). The latter two dates, then, define the trend of the 125 m isobase (Fig. 34.5). Eastern Stanwell-Fletcher Lake basin has been raised by at least 107 m in the last 9200 years, as shells collected at that elevation were dated at 9210 ± 90 years B.P. (GSC-2561). These shells, however, come from clayey silts, typical deep water or basal deltaic sediments, directly downslope from the marine limit delta terrace at 157 m a.s.l. (Fig. 34.3). Hence, it is most likely that the area has experienced about 160 m of emergence (Fig. 34.5).

In summary, the data define a shoreline which has been tilted up towards the west-southwest. The extent of delevelling throughout the area is not uniform, however, for in the west the shoreline has an average gradient of 1.4 m·km⁻¹ compared to 0.7 m·km⁻¹ across the central region, and 0.13 m·km⁻¹ in the east. Thus, the shoreline has a parabolic profile which steepens westward. The maximum gradient occurs in the area containing a large number of ice marginal features which Dyke (1978a, Fig. 1) considered to mark the Wisconsin glacial limit. The strandline data suggest that ice stood at that limit during late Wisconsin time.

Emergence Curves

The dated samples comprise two large spatial sets of data, one in the north and one in the south (Fig. 34.1; Tables 34.1 and 34.2). Because an emergence curve ideally represents a single point on the earth's surface, efforts were made to collect samples from a variety of elevations but within as small an area as possible. These efforts were particularly successful in the north where groups of samples were obtained from near Cape Anne, Cunningham Inlet, and Rodd Bay. Sufficient samples were dated from each locality to permit construction of an emergence curve (Fig. 34.6) and each is discussed below. The set of data from the south are less useful but are analyzed to the extent possible (Fig. 34.7). Elevations measured by B.G. Craig were done by surveying altimeter; those by R.B. Taylor by levelling; those by me by surveying altimeter, with measurements often repeated. In plotting samples in Figures 34.6 and 34.7, errors of ± 1 m are assigned to Taylor's levelled samples; on other samples, errors of ± 4 m are assigned subjectively to values of more than 40 m, ± 3 m to values between 10 and 40 m, and ± 1 m to values less than 10 m.

Cape Anne

Nine samples from the Cape Anne area and one from Aston Bay, 15 km southwest, have been dated (Fig. 34.1, 34.6). Seven of these samples define a smooth curve.

The lower 50 m of the curve is controlled by 4 dates on whale bone (S-1391, S-1381, S-1389, S-1384) embedded in raised gravel beach ridges. The basic assumption here is that the bones arrived at the shoreline as a result of stranding of whales in the intertidal zone or slightly below it. Blake (1975) and Barr (1971) made a similar assumption; and the latter (p. 251-252) stated: "...natural strandings of whales on the gently shelving beaches... is a reasonably common phenomenon at present (Ray, 1961; Dudok Van Heel, 1962, 1966)... Mass strandings of whales occur most frequently on gently sloping sandy or muddy beaches..., from which the whales, using their sonar (echo-sounding by means of ultra high-frequency vibrations), are unable to obtain a good echo".

The upper part of the curve is controlled by three shell dates, all on the species *Mya truncata*. The lowest of these samples (GSC-2666) came from the uppermost foreset facies of a delta immediately below the topset (intertidal) gravels. No higher terrace occurs on the adjacent hillslopes so the topset beds are taken to represent relative sea level during deposition of the delta. The middle sample (GSC-2660) came from the topset gravels and upper 3 m of foreset sands of the highest deltaic sediments in the Cape Anne vicinity, and again, the gravels are considered to mark relative sea level. The highest sample (GSC-319) came from a raised beach ridge at 122 m a.s.l. which probably marks the marine limit in outer Aston Bay.

Three samples fall above the curve, that is, they are considerably too young for their elevations. The only explanation that can be offered at present for the lowest two (S-1381 and S-1386), both of which are whale bone samples, is that they contained a high concentration of plant rootlet and soil contaminants which were not removed during preparation of the samples in the laboratory before dating. The sample from 103 m a.s.l. (S-1392) consisted of an ivory walrus tusk. It was still rooted in the skull when discovered, and it appeared that the entire skeleton was present at the site, with most bones partly embedded in gravelly sand. If the animal died at or near sea level it must have done so about 9000 years ago, which would make it the oldest of the few known early Holocene walrus from Arctic Canada (Harrington, 1975). If the date is correct, it must either have been dragged inland by men or animals or have wandered inland of its own accord, perhaps while sick and disoriented, and the enclosing sediment must be colluvium reworked from the adjacent hillslope. The cranium, mandible, scapula, humerus, radius, ulna, femur fragment, and an unidentified bone fragment from this walrus skeleton are now part of the collections of the National Museums of Canada (NMC34510 A-H, C.R. Harrington, pers. comm., 1977).

Cunningham Inlet

Seven samples from the Cunningham Inlet area have been dated and 6 are used to define an emergence curve (Fig. 34.1, 34.6). The other sample consisted of shells from deep water deltaic silts at 62 m a.s.l. They dated 9180 ± 170 years (GSC-150) and probably relate to the marine limit which lies at 102 m or more above sea level. The lower 20 m of the curve is controlled by 4 dates on driftwood. Three of these samples (GSC-2080, GSC-2233, GSC-2704) came from raised beach gravel; the other (GSC-2081) came from solifluction debris, which indicates that it has moved some distance downslope, and the curve is drawn so as to pass directly above it. The upper part of the curve is controlled by 2 dates, one on whale bone and one on shells. The whale skeleton from which the sample (vertebra) was taken is scattered over a small area of the surface of eroded marine silts. It is likely, therefore, that it has moved downslope since emergence, although the close proximity of the various parts of the skeleton indicate that it has not been moved far. Still, the underlying sediment is not littoral, but offshore, and the curve, therefore, is drawn so as to pass just above the sample point. The shell sample consisted of fragments from

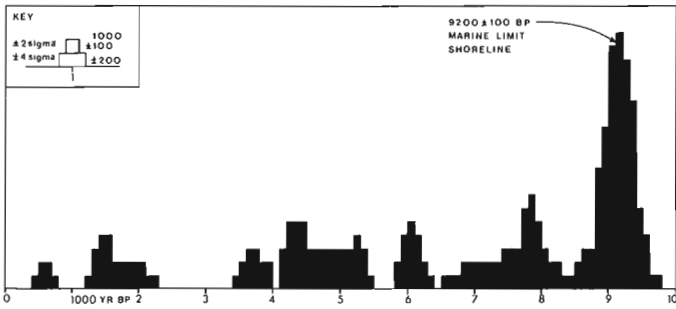


Figure 34.4. Histogram of 36 radiocarbon dates relating to Holocene raised marine features. Note the tight grouping of dates on the Holocene marine limit.

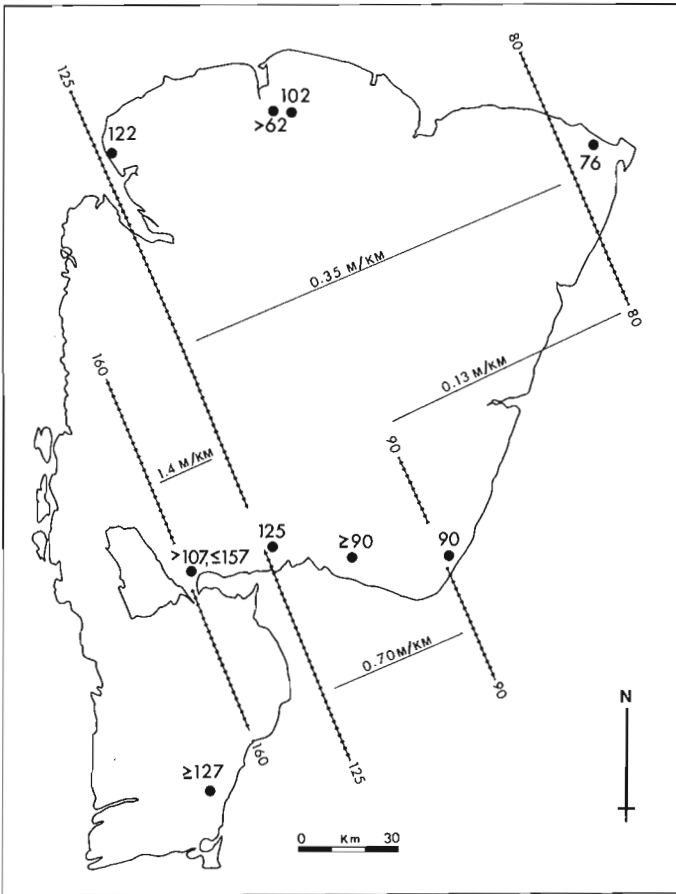


Figure 34.5. Isobases (barbed lines) on the 9200 ± 100 year old shoreline on Somerset Island, with average gradients noted along orthogonal lines; numbers are elevations (m a.s.l.).

the surface of a perched delta terrace composed of gravel, and this is considered to record relative sea level position at the time of deposition. The curve is drawn so as to intersect the older end of the statistical error term on the date as this brings it into parallel alignment with the Cape Anne curve.

Rodd Bay

Five samples from the Rodd Bay area (Fig. 34.1, 34.6), four on whale bone and one on driftwood, have been dated. The bone samples (S-1390, S-1387, S-1393, S-1405) were embedded in raised gravel beaches, and the curve is drawn so

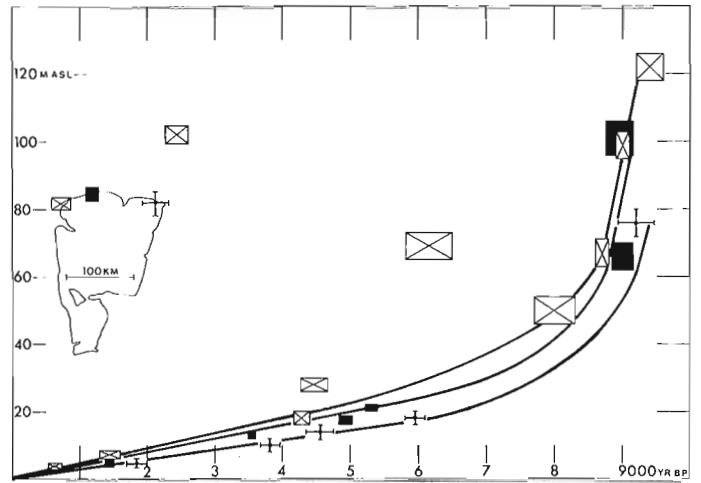


Figure 34.6. Emergence curves for Cape Anne (rectangles with diagonals), Cunningham Inlet (solid black rectangles), and Rodd Bay (crosses). The height of each symbol is the estimated error on elevation measurements, and the width is 2 sigma error on the radiocarbon age determination.

as to pass directly through these points. The driftwood sample was split from a 3 m-long log found lying in an ice-wedge trough that trends along the axis of a raised gravel beach ridge. It may have rolled downslope some distance after its original deposition, but it is unlikely that it moved far before encountering the ice-wedge trough as these features are closely spaced in the raised beach terrains and they occur on even the youngest features. Its position is exactly what would be expected from extrapolation of the curve drawn through the younger whale bone dates, so it probably has not moved significantly since deposition. The shape of the curve in the 6000 to 9000 year range has been drawn to mimic the other two curves, but future dating may make modifications necessary.

Creswell River Lowland

Three shell and two whale bone samples from the western side, and one shell sample from the eastern side, of the Creswell River lowland have been dated (Fig. 34.1, 34.7). These do not obviously define an emergence curve; however, the uppermost 2 shell samples (GSC-2596, GSC-2493) and the whale bone sample at 22 m a.s.l. (S-1382) fall exactly on the Cape Anne curve, traced again in Figure 34.7. It is reasonable that curves for both areas should be the same because both areas lie on the same isobase on the 9200 ± 100 year old shoreline (Fig. 34.5). The fact that the whale bone dated at 4310 ± 90 years (S-1382) falls on this curve indicates that the isobase trends remained constant throughout the early and middle Holocene.

Two dates do not fit on the curve: shells from horizontally bedded sands 4 m below an extensive terrace at 14 m a.s.l. (GSC-2570, 6180 ± 80 years) must relate to a relative sea level position of more than 14 m; and the date on a whale bone from a raised beach at 73 m a.s.l. (S-1388, 5205 ± 70 years) is much too young. The latter sample was nearly completely embedded in beach gravel. The only explanation for its anomalous age that can be offered at present is that it contained plant and soil contaminants that were not removed during laboratory pretreatment.

An additional find of interest in this area is a walrus tusk that was embedded in beach gravel at 83 m a.s.l. Because control was already available on the 90 m level in this area, the specimen was not used for radiocarbon dating but was placed in the National Museums of Canada

collections (NMC 34514, C.R. Harington, pers. comm., 1977). If the animal died at the time of formation of the beach at 83 m a.s.l., which seems most likely, it must be about 8900 ± 100 years old. This extends the known range of walrus habitation of the Arctic Archipelago by about 1500 years (Harington, 1975).

Stanwell-Fletcher Lake and Fury Beach Areas

The six samples from the Stanwell-Fletcher Lake area cannot be used to construct an emergence curve. Four dates (GSC-2563, GSC-617, L-517-A, and GSC-652), all on shells, fall below the Creswell River lowland/Cape Anne curve. This indicates that the shells lived in deep water environments. A curve for Stanwell-Fletcher Lake should sit slightly above the Creswell River lowland curve because the strandlines rise westward. The four samples, dating between 3900 and 8000 years old, were the basis of the uplift curve presented by Rust and Coakley (1970). Hence, the validity of that curve should now be reconsidered.

The easternmost sample from the southern part of the island is from Fury Beach. No lower samples have been dated to define an emergence curve. The curve for this area, however, should lie below that for Creswell River lowland; a partial curve is shown in Figure 34.7 to suggest this likely relationship.

Form of the Curves and Rates of Emergence

All relative sea level curves for various points in Arctic Canada have the same general appearance inasmuch as they show rapid initial emergence succeeded by slower emergence (e.g. Løken, 1965; Andrews and Falconer, 1969; Barr, 1971; Blake, 1975; England, 1976) or by submergence (Dyke, in press).

The data from northern Somerset Island (Fig. 34.6) are best fit, in the case of all three curves, by straight lines indicating a constant rate of emergence during the last 5000 to 6000 years. These rates, which are also the contemporary emergence rates, are: 0.46 m/100 years (0.46 cm/year) for Cape Anne, 0.40 m/100 years for

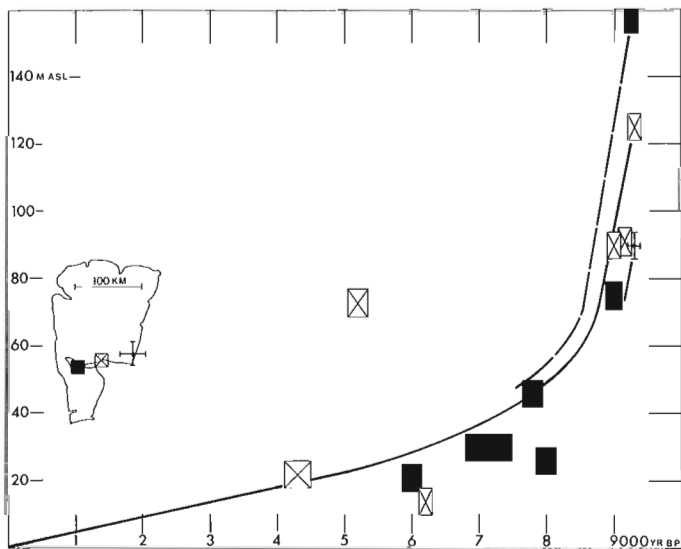


Figure 34.7. Emergence curve for the Creswell River lowland (rectangles with diagonals), traced from the Cape Anne curve, and partial curves for the Stanwell-Fletcher Lake area (solid black rectangles) and Fury Beach (cross). The height of each symbol is the estimated error on elevation measurements, and the width is 2 sigma error on the radiocarbon age determination.

Cunningham Inlet, and 0.28 m/100 years for Rodd Bay. They compare favourably with the average rate of somewhat less than 0.30 m/100 years for emergence over the last 2400 years at Cape Storm, southern Ellesmere Island (Blake, 1975, p. 58).

For the Cape Anne curve, a straight line also provides the best description of the initial emergence. The land emerged 55 m between 9380 ± 180 and 8680 ± 90 years ago at an average rate of 8 to 11 m/100 years, and 50 per cent of total emergence was accomplished within about 750 years. Andrews (1970, p. 33) calculated that 33 per cent of uplift in Arctic Canada occurred in the first 1000 years after deglaciation (or after onset of emergence). In the Cape Anne-Aston Bay area about 56 per cent of emergence was accomplished in the first 1000 years. Had the emergence curve been "corrected" for eustatic sea level rise to produce an uplift curve as Andrews did, it would have been steepened; thus, uplift (by that definition) accomplished in the first 1000 years would exceed 56 per cent. The curves presented here are not corrected for the global change in ocean volume during the Holocene for it has been recognized that "eustatic" sea level response was by no means globally uniform (Walcott, 1972; Clark et al., 1978).

A rapid early Holocene emergence rate is also indicated by the extremely well dated curve for Cape Storm, where more than half of the total emergence occurred in the first 1000 years (Blake, 1975). Hence, it may be that the equations of Andrews (1970) do not adequately describe the emergence of the central and northern Canadian Arctic Archipelago. However, the early emergence rates of Greenland are similar to those reported here: Washburn and Stuiver (1962) derived an emergence rate of 9 m/100 years for the Mesters Vig area

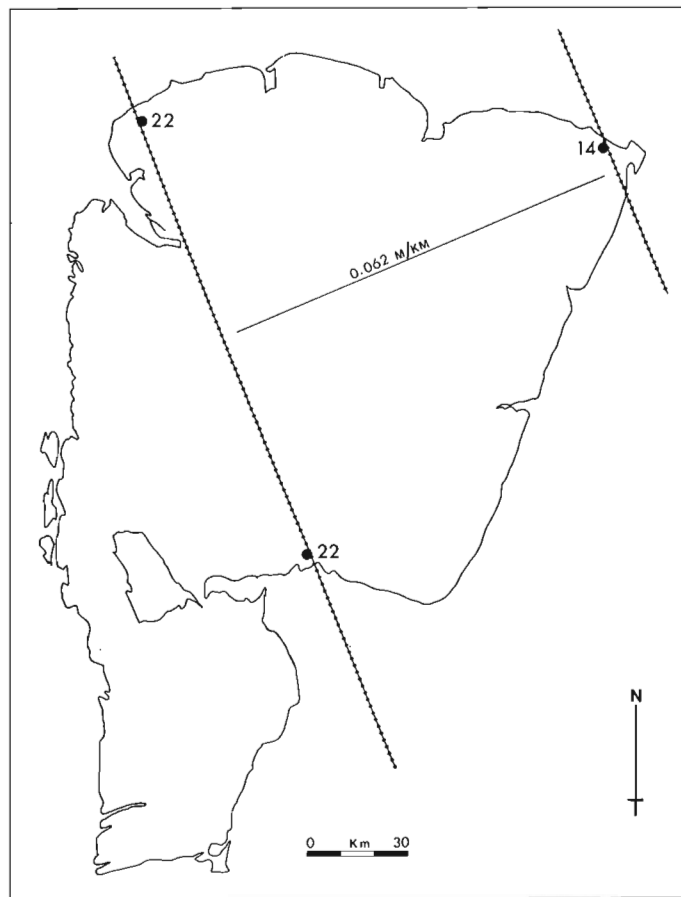


Figure 34.8. Isobases on the 5000 year old shoreline on Somerset Island, with average gradient noted along the orthogonal line.

of Northeast Greenland and Ten Brink (1974) gave a value of 10.5 m/100 years for the Søndre Strømfjord region of West Greenland. Clark (1976) proposed that these rapid emergence rates were the instantaneous gravitational and elastic crustal responses to a rapid recession of the Greenland Ice Sheet during the early Holocene, rather than the result of a weak crust and low viscosity mantle under the area as had been proposed by Ten Brink (1974). The same explanation likely applies to the Canadian area, and Dyke (1979) has invoked it to explain the even more rapid emergence rate of 30 m/100 years within the first two centuries of deglaciation of northern Boothia Peninsula, where the ice sheet was retreating at an average rate of 300 m/year (30 km/100 years).

The 5000 Year Old Shoreline

The 5000 year old shoreline is of special interest in Arctic Canada because it is characterized, at least in the southeastern Queen Elizabeth Islands, by an accumulation of pumice which allows its recognition in the field without recourse to radiocarbon dates. Blake (1970, 1975) has made a special study of this shoreline and, although no pumice was discovered on Somerset Island, the emergence curves provide an opportunity of extending southward our mapping of the feature. The curves also indicate the elevations at which any future search of the island for pumice should be concentrated. In addition, the geometry of the 5000 year old shoreline may be of use in geophysical modelling as recovery of the earth's crust during the last 5000 years should be primarily a response to flow of mantle material, whereas the early Holocene recovery also incorporated instantaneous effects.

Isobases on the 5000 year old shoreline (Fig. 34.8) show that it lies more than 22 m a.s.l. in western Somerset Island and about 14 m a.s.l. in the northeast. Blake (1975, p. 14) showed a 17 m isobase passing through Cunningham Inlet; no value is shown in Figure 34.8, but I would prefer a slightly higher value because the driftwood dated at 4930 ± 70 years (GSC-2081) came from solifluction debris at 17 m a.s.l. which indicates that it had moved some distance downslope (Table 34.1, Fig. 34.6). Isobases on both the 9200 and 5000 year old shorelines on Somerset Island trend north-northwest – south-southeast, whereas Blake's isobases on the 5000 year old shoreline on southern Ellesmere Island trend northeast-southwest. This is not seen as a conflict between the two sets of data, but rather as an indication that the isobases over the larger area are curved and assume a more northerly, followed by easterly, orientation as they progress southward.

The average gradient of the 5000 year old shoreline across central and eastern Somerset Island is $0.062 \text{ m} \cdot \text{km}^{-1}$ ($6.2 \text{ cm} \cdot \text{km}^{-1}$) or approximately one-sixth that of the 9200 year old shoreline in the same area (cf. Fig. 34.5, 34.8). Blake (1975, p. 13) showed that the 5000 year old shoreline in southern Ellesmere Island has an almost identical gradient of "a little over 6 cm/km". In contrast to these areas, the 5000 year old shoreline in western Baffin Island (the Foxe Basin coast) is tilted much more steeply at $25.0 \text{ cm} \cdot \text{km}^{-1}$ (Andrews and Dugdale, 1970), and the 5600 to 5700 year old shoreline in Cumberland Sound, southeastern Baffin Island has a gradient of 70 to $87 \text{ cm} \cdot \text{km}^{-1}$ (Dyke, in press). Too few such calculations are available to establish a geographical pattern and interpret the physical significance of these data.

Summary

The coastal fringe of Somerset Island was overlapped by the early Holocene sea, and an earlier sea apparently extended higher. Holocene marine limit features have not been definitely correlated with glacial features. However, a delta at 157 m a.s.l. near Stanwell-Fletcher Lake probably

was deposited by meltwater; if so, marine limit on the western side of the island was formed at the time of deglaciation, as it was on northern Boothia Peninsula (Dyke, 1979).

Thirty-six radiocarbon dates on marine shells (17), whale bones (13), driftwood (5), and a walrus tusk (1) have been obtained. Nine of these are on the marine limit and are 9200 ± 100 years old. The 9200 year old shoreline rises from 76 m a.s.l. in the northeastern part of the island to more than 157 m a.s.l. in the southwest and has a parabolic gradient that steepens westward. The area of steepest gradient ($1.4 \text{ m} \cdot \text{km}^{-1}$) contains numerous ice marginal features that Dyke (1978a, b) considered to mark the Wisconsin glacial limit. The steep gradient, therefore, may have been caused by sharp crustal deflection near the late Wisconsin ice margin.

Most of the radiocarbon-dated samples are from five locations: Cape Anne, Cunningham Inlet, and Rodd Bay on the north coast; Stanwell-Fletcher Lake and the Creswell River lowland on the south and southwest coasts. Well controlled emergence curves are constructed for each north coast site. The southern data is less useful, but the Creswell River lowland data fit on the Cape Anne curve, indicating that both sites lie on the same isobase. The shell dates from the Stanwell-Fletcher Lake area are of little use in constructing an emergence or uplift curve. Hence the uplift curve published by Rust and Coakley (1970) should no longer be used.

The Cape Anne area (and the Creswell River lowland) emerged 8 to 11 m per century during the first 500 years of emergence, and 56 per cent of total emergence was completed in 1000 years. This is much more than would be predicted by Andrews' (1970) equations but is similar to rapid early emergence of Cape Storm, Ellesmere Island (Blake, 1975), and East and West Greenland (Washburn and Stuiver, 1962; Ten Brink, 1974). The rapid emergence probably comprises the gravitational and elastic crustal responses to rapid deglaciation as proposed by Clark (1976).

The rate of emergence during the last 5000 to 6000 years was constant at each site but varied spatially: Cape Anne and Creswell River lowland emerged 46 cm/100 years; Cunningham Inlet, 40 cm/100 years; and Rodd Bay, 28 cm/100 years. This is similar to emergence at Cape Storm over the last 2400 years (Blake, 1975).

The 5000 year old shoreline, which has been studied extensively in the southeastern Queen Elizabeth Islands (Blake, 1970, 1975), lies at 22 m a.s.l. at Cape Anne and in the Creswell River lowland and declines to 14 m a.s.l. at Rodd Bay. Its average gradient in the intervening area is $6.2 \text{ cm} \cdot \text{km}^{-1}$. This is nearly identical to its gradient in southern Ellesmere Island.

References

- Andrews, J.T.
1970: A geomorphological study of postglacial uplift with particular reference to Arctic Canada; Institute of British Geographers, Special Publication no. 2, 156 p.
- Andrews, J.T. and Dugdale, R.E.
1970: Age prediction of glacioisostatic strandlines based on their gradients; Geological Society of America Bulletin, v. 81, p. 3769-3772.
- Andrews, J.T. and Falconer, G.
1969: Late glacial and post-glacial history and emergence of the Ottawa Islands, Hudson Bay, N.W.T.: evidence on the deglaciation of Hudson Bay; Canadian Journal of Earth Sciences, v. 6, p. 1263-1276.

- Barr, W.
1971: Postglacial isostatic movement in northeastern Devon Island: a re-appraisal; *Arctic*, v. 24, p. 249-268.
- Blake, W., Jr.
1970: Studies of glacial histories in Arctic Canada I: Pumice, radiocarbon dates, and differential postglacial uplift in the eastern Queen Elizabeth Islands; *Canadian Journal of Earth Sciences*, v. 7, p. 634-664.
1975: Radiocarbon age determinations and postglacial emergence at Cape Storm, southern Ellesmere Island, Arctic Canada; *Geografiska Annaler, Series A*, v. 57, p. 1-71.
- Cathles, L.W.
1975: *The Viscosity of the Earth's Mantle*; Princeton University Press, Princeton, N.J., 386 p.
- Clark, J.A.
1976: Greenland's rapid postglacial emergence: a result of ice-water gravitation attraction; *Geology*, v. 4, p. 310-312.
1977: An inverse problem in glacial geology: the reconstruction of glacier thinning in Glacier Bay, Alaska between A.D. 1910 and 1960 from relative sea level data; *Journal of Glaciology*, v. 18, p. 481-503.
- Clark, J.A., Farrell, W.E., and Peltier, W.R.
1978: Global changes in postglacial sea level: a numerical calculation; *Quaternary Research*, v. 9, p. 265-287.
- Craig, B.G.
1964: Surficial geology of Boothia Peninsula and Somerset, King William, and Prince of Wales Islands, District of Franklin; Geological Survey of Canada, Paper 63-44, 10 p.
- Dudok Van Heel, W.H.
1962: Sound and cetacea; *Netherlands Journal of Sea Research*, v. 1, p. 407-507.
1966: Navigations in cetaceans; in *Whales, Dolphins, and Porpoises*, ed. K.S. Norris; University of California Press, p. 597-606.
- Dyke, A.S.
1978a: Glacial history of and marine limits on southern Somerset Island, District of Franklin; in *Current Research, Part B*, Geological Survey of Canada, Paper 78-1B, p. 218-224.
1978b: Glacial and marine limits on Somerset Island, Northwest Territories; *Geological Society of America, Abstracts with Programs*, v. 10, p. 394.
1979: Glacial geology of northern Boothia Peninsula; in *Current Research, Part B*, Geological Survey of Canada, Paper 79-1B, p. 000-000.
Glacial and sea level history of southwestern Cumberland Peninsula, Baffin Island, Canada; *Arctic and Alpine Research*, v. 11. (in press)
- England, J.H.
1976: Postglacial isobases and uplift curves from the Canadian and Greenland High Arctic; *Arctic and Alpine Research*, v. 8, p. 61-78.
- Farrell, W.E. and Clark, J.A.
1976: On postglacial sea level; *Geophysical Journal of the Royal Astronomical Society*, v. 46, p. 647-667.
- Harington, C.R.
1975: A postglacial walrus (*odobenus rosmanus*) from Bathurst Island, Northwest Territories; *Canadian Field-Naturalist*, v. 89, p. 249-261.
- Løken, O.H.
1965: Postglacial emergence at the south end of Inugsuin Fiord, Baffin Island, N.W.T.; *Geographical Bulletin*, v. 7, p. 341-359.
- Lowdon, J.A., Robertson, I.M., and Blake, W., Jr.
1977: Geological Survey of Canada radiocarbon dates XVII; Geological Survey of Canada, Paper 77-7, 25 p.
- Netterville, J.A., Dyke, A.S., and Thomas, R.D.
1976a: Surficial geology and geomorphology of Somerset and northern Prince of Wales islands; Geological Survey of Canada, Open File 357, scale 1:125 000.
Netterville, J.A., Dyke, A.S., Thomas, R.D., and Drabinsky, K.A.
1976b: Terrain inventory and Quaternary geology, Somerset, Prince of Wales, and adjacent islands; in *Report of Activities, Part A*, Geological Survey of Canada, Paper 76-1A, p. 145-154.
- Olson, E.A. and Broecker, W.S.
1961: Lamont natural radiocarbon measurements VII; *Radiocarbon*, v. 3, p. 141-175.
- Prest, V.K.
1969: Retreat of Wisconsin and Recent ice in North America; Geological Survey of Canada, Map 1257A.
- Ray, C.
1961: A question of whale behaviour; *Natural History*, v. 70, no. 46.
- Rust, B.R. and Coakley, J.P.
1970: Physico-chemical characteristics and postglacial desalinization of Stanwell-Fletcher Lake, Arctic Canada; *Canadian Journal of Earth Sciences*, v. 7, p. 900-911.
- Shepard, F.P.
1960: Rise of sea level along northwest Gulf of Mexico; in *Recent Sediments, Northwest Gulf of Mexico*, ed. F.P. Shepard, F.B. Phleger, and T.H. Van Andel; American Association of Petroleum Geologists, Tulsa, Oklahoma, p. 338-344.
- Smith, D.I.
1972: The solution of limestone in an arctic environment; in *Polar Geomorphology*, ed. R.J. Price and D.E. Sugden; Institute of British Geographers, Special Publication no. 4, p. 187-200.
- Taylor, R.B.
1975: Coastal investigation on northern Somerset Island, District of Franklin; in *Report of Activities, Part A*, Geological Survey of Canada, Paper 75-1A, p. 501-504.
- Ten Brink, N.W.
1974: Glacio-isostasy: new data from West Greenland and geophysical implications; *Geological Society of America Bulletin*, v. 85, p. 219-228.
- Walcott, R.I.
1970a: Isostatic response to loading of the crust in Canada; *Canadian Journal of Earth Sciences*, v. 7, p. 716-726.
1970b: Flexural rigidity, thickness, and viscosity of the lithosphere; *Journal of Geophysical Research*, v. 75, p. 3941-3954.
1972: Past sea levels, eustasy and deformation of the earth; *Quaternary Research*, v. 2, p. 1-14.
- Washburn, A.L. and Stuiver, M.
1962: Radiocarbon-dated postglacial delevelling in northeast Greenland and its implications; *Arctic*, v. 15, p. 66-72.

A.N. LeCheminant, R.W. Leatherbarrow¹, and A.R. Miller
Regional and Economic Geology Division

LeCheminant, A.N., Leatherbarrow, R.W., and Miller, A.R., Thirty Mile Lake map area, District of Keewatin; in Current Research, Part B, Geological Survey of Canada, Paper 79-1B, p. 319-327, 1979.

Abstract

The west half of the Thirty Mile Lake map area straddles the central portion of the Baker Lake Basin, a 50 km wide, northeasterly trending structural depression filled with continental sediments and volcanics of the Paleohelikian or Late Apehbian Dubawnt Group. The northern part of the basin is underlain by Archean (?) ortho- and paragneisses of the Armit Lake Block and the southern part by similar gneisses of the Thirty Mile Domain. A third gneiss domain in the south half of the map area comprises mainly orthogneisses that record Apehbian (?) metamorphism and northeast trending deformation.

Dubawnt Group rocks consist of basal sequences of alluvial fan and fluvial deposits which are unconformably overlain by or in fault contact with alkaline lavas and pyroclastics of the Christopher Island Formation. Alluvial fan deposits of the Kunwak Formation record a period of local uplift and faulting during a magmatic hiatus that separates the Christopher Island alkaline volcanism from acid calc-alkaline volcanism of the overlying Pitz Formation. Stocks of hypabyssal fluorite-bearing granite, which intrude the Christopher Island Formation, are probably cogenetic with Pitz Formation lavas. Thelon Formation sandstones and conglomerates are confined to limited exposures in the north part of the map area.

Introduction

The west half of the Thirty Mile Lake map area (65P W1/2) is underlain by rocks of the Churchill Structural Province that can be divided into two main groups: 1) granitoid gneisses of both Archean and Apehbian ages, and 2) unmetamorphosed continental sediments and volcanics of the late Apehbian or Paleohelikian Dubawnt Group. 1:250 000 scale mapping of approximately 70 per cent of the area was completed during the 1978 field season. Previous mapping was limited to reconnaissance traverses during Operation Baker (Wright, 1955, 1967). Adjoining areas have been mapped by Donaldson (1965, 1966), Eade and Chandler (1974), and LeCheminant et al. (1977, 1979).

Archean and Apehbian Granitoid Gneisses

Regional Setting

Granitoid gneisses of diverse composition, texture, and structural style form the basement to sedimentary and volcanic rocks of the Dubawnt Group (Fig. 35.1). Amphibolite facies ortho- and paragneisses of the Armit Lake Block of the Churchill Structural Province (Heywood and Schau, 1978) underlie the northwest corner of the area. These are called here the Princess Mary gneisses.

Gneisses south of the Dubawnt Group rocks have been divided into a northern and southern domain based on lithologic and/or structural criteria. Gneisses of the northern domain, here named the Thirty Mile domain, are well exposed north of Forde Lake and form the southern basement to rocks of the Dubawnt Group (Fig. 35.2). The Thirty Mile domain includes cataclastic felsic ortho- and paragneisses exposed in the east half of the Thirty Mile Lake map area (LeCheminant et al., 1977). The northwest structural trends of the Thirty Mile domain are interrupted by narrow, north-east trending zones of intense shearing. The gneisses are intruded by numerous northeast- to east-trending diabases and younger east to east-southeast trending alkaline lamprophyres and feldspar porphyry dykes.

The boundary between the Thirty Mile domain and the southern domain is marked by a distinct change from north-west to northeast structural trends (Fig. 35.1). Southern

domain rocks, mainly granitic to granodioritic orthogneisses, range from well layered to nebulitic. The gneisses have been intruded by numerous granite, aplite and pegmatite dykes. Syenitic and granitic plutons are the youngest rocks in the southern domain.

Princess Mary Gneisses

Ortho- and paragneisses, basement to the Dubawnt Group, underlie a small area west of Princess Mary Lake in the northwest corner of the map area (Fig. 35.1). The gneisses are well exposed and consist of granodioritic to granitic gneiss interlayered with biotite-hornblende-plagioclase gneiss and garnet-biotite-hornblende-plagioclase-quartz paragneiss. Thin bands of lean iron-formation are associated with the paragneiss. Gneissosity trends are consistently north to east-northeast with moderate to steep easterly dips.

The gneisses are cut by diabase dykes which are deformed and metamorphosed. Chill margins can still be distinguished in spite of the development of a hornblende foliation. Dykes of white granite pegmatite cut both the gneisses and metamorphosed diabase. 1-3 m wide, undeformed biotite lamprophyre dykes trending 100°, which contain numerous gneiss xenoliths, cut all units.

The Princess Mary gneisses are in contact with biotite trachyte lavas of the Christopher Island Formation to the south and conglomerate and pebbly sandstone of the Thelon Formation to the east. Contacts are not exposed and may be faults or unconformities. Gneisses adjacent to the contact commonly are microfractured with epidote-chlorite-quartz-calcite alteration and veining.

Thirty Mile Domain

The Thirty Mile domain is underlain by a variety of cataclastic felsic and mafic gneisses that record at least three phases of deformation. Dominant lithologies include 'black and white' gneiss, gneissic granodiorite, and less commonly, gneissic granite and augen granite gneiss. Cataclasite, protomylonite and mylonite gneiss are locally developed in narrow northeast to east-northeast shear zones.

¹ Carleton University, Ottawa.

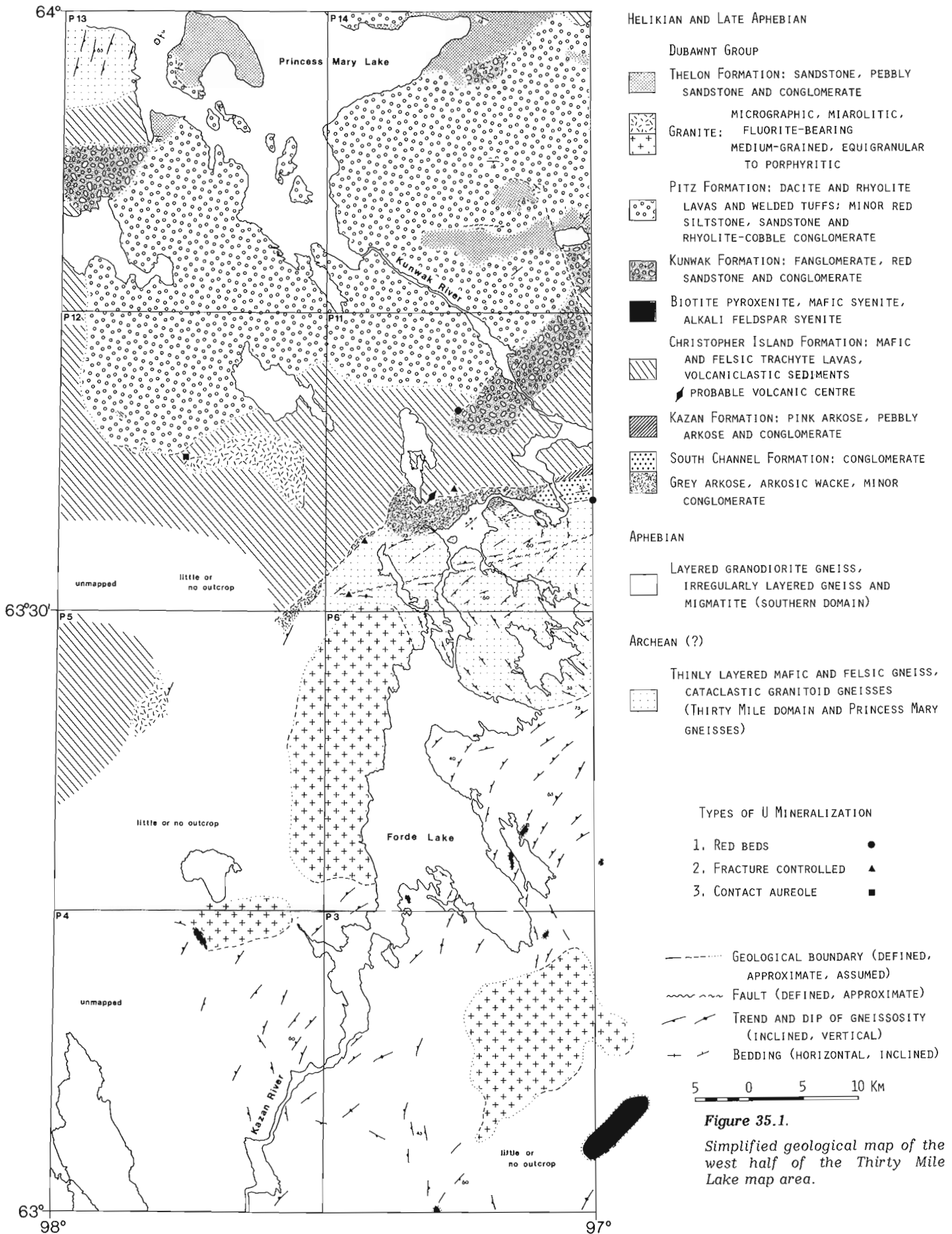


Figure 35.1.

Simplified geological map of the west half of the Thirty Mile Lake map area.

The 'black and white' gneiss comprises thin layers of amphibolite, hornblende-plagioclase gneiss, and garnet-plagioclase-biotite gneiss alternating with white weathering leucocratic gneiss. Although these gneisses typically are thinly interbanded they include zones of agmatite containing rafts of mafic gneiss in leucocratic white gneiss. Garnet-bearing layers contain isolated rounded porphyroblasts of garnet up to 1 cm in diameter. These porphyroblasts are partly or wholly altered to chlorite-mica intergrowths that weather out to form a characteristic pitted surface. Mortar structure and quartz ribbons are developed within leucocratic layers. The 'black' gneisses may be derived from a sequence of intermediate and mafic volcanics, mafic tuffs and volcanogenic sediments whereas 'white' layers may be felsic volcanics and/or younger intrusive rocks.

Irregular bodies of grey gneissic granodiorite and pink granitic augen gneiss occur within the 'black and white' gneiss. The gneisses contain lenses and layers of mafic-rich gneiss and amphibolite and are probably orthogneisses.

At least three phases of deformation have affected gneisses of the Thirty Mile domain. The first developed a hornblende-biotite foliation parallel to compositional layering that was subsequently folded by a second period of penetrative deformation to produce tight to subisoclinal northwest trending folds. Limbs of second phase minor folds are attenuated and commonly sheared off. Quartz ribbons developed in leucocratic layers parallel the axial surfaces of second phase folds. Hornblende and quartz rods locally parallel the hinge lines of minor folds.

Amphibolite grade metamorphism accompanied the early deformation events but details of timing and distribution are obscured by lack of diagnostic metamorphic mineral assemblages and by retrograde metamorphism associated with third phase brittle deformation.

Nonpenetrative features represent the third phase of deformation. Cataclasite, protomylonite and mylonite gneisses form narrow shear zones that separate blocks of gneiss with different structural trends. Textures within these zones are gradational even on the scale of a single thin section. Chlorite, epidote, quartz and carbonate veining and alteration are prominently developed within and adjacent to these shears. Intense microfracturing and microbrecciation occurs in gneisses adjacent to northeast faults separating rocks of the Thirty Mile domain from basal formations of the Dubawnt Group.

Dykes A prominent swarm of east to northeast trending diabase dykes occurs throughout the Thirty Mile domain and forms up to 6 per cent of the exposed bedrock. The dykes range in width from less than 1 m to more than 50 m and individual dykes have been traced for up to 5 km. Although chill margins and original ophitic textures are usually preserved, the dykes are partly to completely altered. Contacts are sheared with development of narrow zones of mafic schist or open sigmoidal fractures within the diabase. Dykes are often boudinaged or offset by minor faults. Cataclastic foliation within immediately adjacent gneisses may swing sharply to parallel diabase contacts. Thin sections reveal that original pyroxenes have been replaced by actinolite and/or hornblende. Thin rims of garnet may separate amphibole and plagioclase. Patches of epidote, chlorite and carbonate are ubiquitous. Detailed study of the distribution, orientation and metamorphism of the diabase dykes could provide precise information on the development of late brittle deformation features and associated low-grade metamorphism within the Thirty Mile domain.

Biotite-lamprophyre, biotite-feldspar porphyry and rare quartz porphyry dykes cut all rock units within the Thirty Mile domain. The dykes, which are fresh and undeformed, have east to east-southeast trends and cut diabase dykes or may intrude along diabase-gneiss contacts. Biotite-lamprophyre has been observed chilled against biotite-feldspar porphyry and vice versa in multiple intrusion dykes.

A K-Ar age of 1832 ± 45 Ma on hornblende and 1767 ± 42 Ma on biotite was obtained from a biotite-lamprophyre dyke cutting the Thirty Mile domain east of the map area (Wanless et al. in prep.). This is accordant with 1786 ± 26 Ma obtained from an Rb-Sr whole rock isochron on alkaline volcanics of the Christopher Island Formation (Wanless and Loveridge, 1972; $1.42 \times 10^{-11} \text{yr}^{-1}$ decay constant). Within the map area similar lamprophyre and feldspar porphyry dykes cut basal sedimentary sequences and alkaline lavas of the Dubawnt Group north of the Thirty Mile domain. A few lamprophyre dykes can be traced across the basal unconformity.

Southern Domain

The Southern domain is underlain by granitoid orthogneisses that are intruded by small alkaline stocks and granite plutons. Orthogneisses consist mainly of well layered grey granodiorite gneiss and migmatitic and/or nebulitic granite gneiss. Mafic minerals are typically biotite and hornblende. Colour indices of these rocks are generally less than 10. Rare, locally garnetiferous, biotite paragneiss bands are interlayered with the granodiorite gneiss. Migmatitic gneisses adjacent to granite plutons contain concordant pegmatite sheets, which have a weak foliation. Both the gneisses and concordant pegmatite are cut by networks of undeformed younger pegmatite, granite and aplite dykes.

The orthogneisses contain hornblende and/or biotite-rich boudins and locally crosscutting amphibolite dyke segments that may represent metamorphosed relicts of the dyke swarms present in the Thirty Mile domain.

Southern domain gneisses have been penetratively deformed twice. The first event resulted in the formation of a biotite-hornblende foliation parallel to compositional layering. Second phase northeast trending structures refold first phase foliation. The event was accompanied by local growth of biotite in axial planes. Continuity of northeast structures in areas of poor exposure can be inferred from the regional aeromagnetic map (GSC Map 7841G).

The northeast trending deformation in the southern domain is probably Archean and is younger than the penetrative deformation events (Archean?) recorded by gneisses in the Thirty Mile domain. The boundary between the two domains is a narrow zone across which diabase dykes show increasing metamorphic grade into the southern domain and dominant structural trends change from northwest to northeast.

Alkaline Intrusive Rocks Small alkaline complexes intrude the southern domain gneisses (Fig. 35.1). Intrusive contacts are generally parallel or subparallel to regional foliation trends and the rocks display a wide range of textural and compositional characteristics. Most intrusive phases are medium- to coarse-grained and porphyritic. Biotite pyroxenite and mafic-rich syenite predominate, but leucocratic alkali feldspar syenites are not uncommon. Quartz-bearing phases are locally present. Small dykes of undeformed pink granite and aplite crosscut the alkaline rocks.

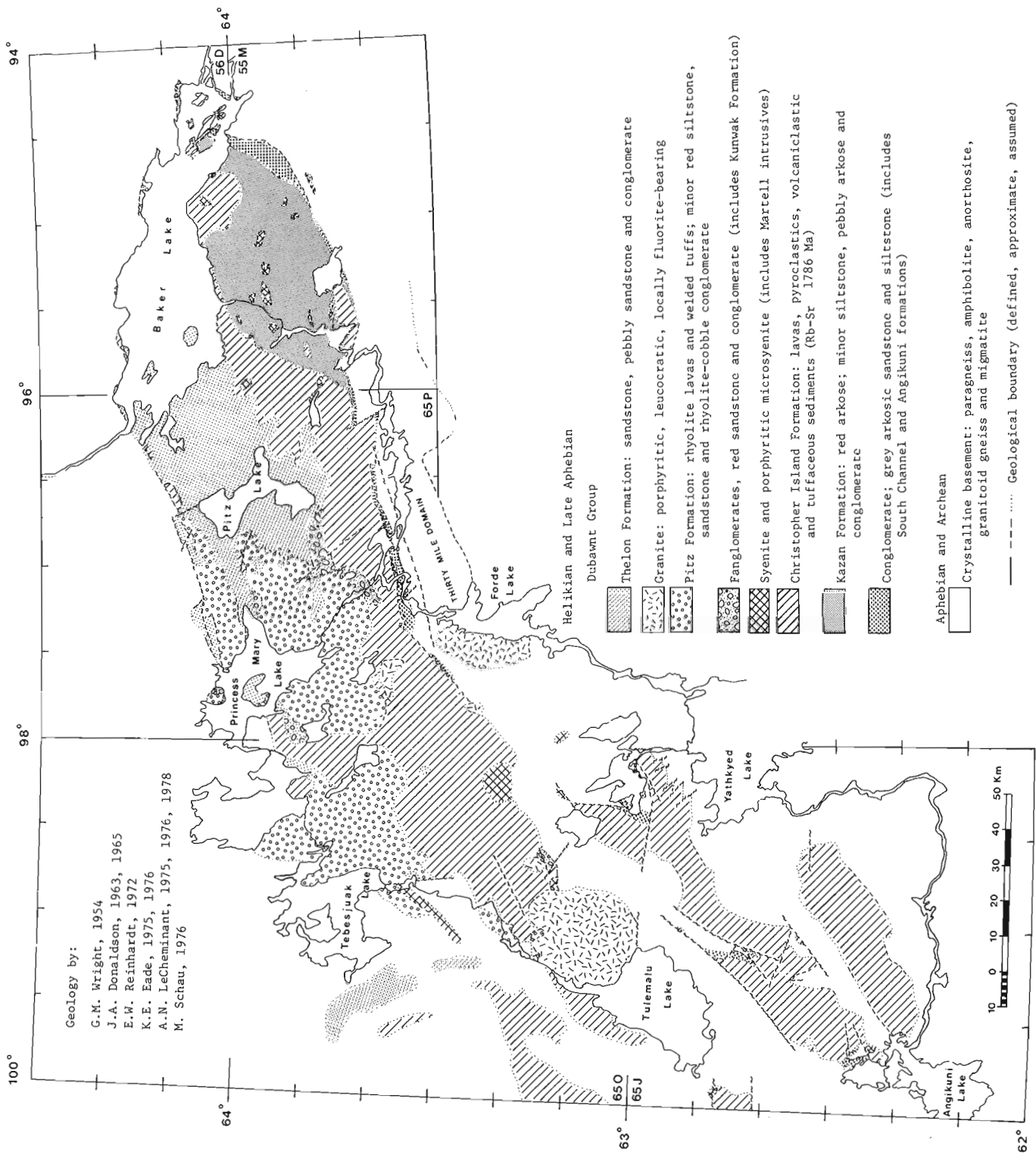


Figure 35.2. Distribution of Dubawnt Group rocks in the Baker Lake Basin and smaller subparallel basins between Tulemalu Lake and Yathkyed Lake.

Similar alkaline complexes intrude basement gneisses in the map area to the east (LeCheminant et al., 1977). Accounts of the petrography, chemistry and intrusive history of two of these bodies have been given by Morrison (1977) and Murdoch (1979). The rocks are chemically and mineralogically similar to the lamprophyre dykes and hypabyssal Martell Syenite that intrude both the Thirty Mile domain and the lower formations of the Dubawnt Group.

On the central peninsula east of Forde Lake a fine grained subporphyritic alkali feldspar syenite dyke 30 m wide has been traced through discontinuous outcrop for 1.5 km. The northeast trending dyke has a well developed biotite foliation and is emplaced parallel to the trend of the surrounding gneisses. The dyke is anomalously radioactive and a representative sample contains 40.5 ppm U and 260 ppm Th. The radioactivity is due to abundant euhedral to subhedral brown sphene and disseminated equant metamict grains which may have been monazite or thorite.

Granite Large plutons of massive equigranular to porphyritic pink granite are the youngest unit within the southern domain (Fig. 35.1). The pluton southeast of Forde Lake underlies an area of extremely sparse outcrop and the few exposures are typically heaved, a consequence of well developed vertical and horizontal joint sets. The granite is leucocratic, fine- to medium-grained, and contains aplitic phases and rafts of granite gneiss near the contacts. Aplite and pegmatite dykes cut surrounding gneisses.

The pluton west of Forde Lake has fine- to medium-grained border phases ranging in composition from quartz syenite to granite. The rocks are generally massive and equigranular but weakly foliated and/or porphyritic variants are present. Border phases contain xenoliths of granodiorite gneiss, mafic gneiss and mafic syenite. Central portions of the pluton consist of homogeneous medium grained porphyritic biotite granite with alkali feldspar phenocrysts to 1.5 cm. Accessory minerals include biotite, magnetite, sphene and fluorite, and the alteration assemblage is epidote, sericite and chlorite. A few quartz-epidote veins and rare pegmatite dykes are the only crosscutting features within the pluton.

Dubawnt Group

Regional Setting

The northern half of the map area straddles the central portion of a major east-northeast to northeast trending structural depression filled with continental sediments and volcanics of the Dubawnt Group. The structural depression, here named the Baker Lake Basin, can be traced over 300 km from the east end of Baker Lake to Tulemalu Lake (Fig. 35.2). Structurally, the basin is a complex graben with an average width of 50 km and a generally asymmetric cross-section. The boundaries are unconformities or either vertical or steeply dipping normal faults (Donaldson, 1965, 1966; LeCheminant et al., 1977, 1979). The southwestern limits of the Baker Lake Basin remain to be defined by mapping in 65Ø and 65K scheduled for 1979 and 1980. Smaller subparallel basins containing Dubawnt Group rocks in 65J and 65Ñ are shown in Figure 35.2 and have been described by Eade (1976), Eade and Blake (1977) and LeCheminant et al. (1979).

Although the Baker Lake Basin is generally parallel to earlier structural trends in the Archean and Aphebian basement, the bounding unconformities and faults in the Thirty Mile Lake map area often sharply truncate basement gneissosity (Fig. 35.1). The Dubawnt Group rocks in the map area consist of basal sedimentary sequences exposed along

the south edge of the basin which are unconformably overlain by or in fault contact with alkaline lavas and pyroclastics of the Christopher Island Formation. Conglomerates and sandstones of the Kunwak Formation overlie the Christopher Island Formation and record a period of alluvial fan sedimentation prior to extrusion of acid lavas and pyroclastics of the Pitz Formation. Stocks of fluorite-bearing granite, which intrude the alkaline volcanic rocks, are probably cogenetic with Pitz Formation lavas. Sandstones and conglomerates of the Thelon Formation are confined to limited exposures in the north part of the map area.

Basal Sedimentary Sequences

Coarse polymictic conglomerates of the South Channel Formation unconformably overlie intensely fractured cataclastic gneisses of the Thirty Mile domain (Fig. 35.1). The regolith zone, which is up to 2 m thick, consists of angular fragments of basement rock replaced and cemented by carbonate, quartz and hematite. The light grey to pink conglomerate typically contains subrounded clasts of gneissic granitoid rocks, foliated mafic rocks (amphibolite and meta-diabase) and quartz in approximate proportions 80:15:5. Mean clast size is 3-10 cm. Maximum sizes commonly range from 20-50 cm although boulders up to 2 m in diameter are present within a few metres of the basal unconformity. Bedding, defined by thin arkose lenses, dips 45°-60° to the north. The South Channel Formation exceeds 1500 m in thickness at the east boundary of the map area in 65P/11 and passes transitionally upward into pale pink arkose of the Kazan Formation. The succession probably represents stream-channel and fluvial deposits. Both formations are intruded by east to east-southeast trending porphyritic syenite and biotite-lamprophyre dykes.

The Kazan and South Channel formations are truncated by a northeast trending fault. Sedimentary sequences exposed to the west of the fault are probably correlative with the South Channel and Kazan formations but are typically grey and contain substantially less coarse clastic detritus. These sequences, which unconformably overlie Thirty Mile domain gneisses, comprise laminated fine grained grey arkose and arkosic wacke. Interbedded conglomerate lenses, usually less than 10 m thick, are similar to conglomerates of the South Channel Formation. Arkosic rocks are crossbedded and contain pebbly or conglomeratic channel scours and rare ripple marks. Carbonate-rich laminae and thin black heavy mineral concentrations are characteristically present. The arkosic wackes consist of 0.1-1.5 mm subrounded quartz, plagioclase and microcline grains set in a sericite, chlorite and carbonate matrix.

Isolated exposures of the arkosic sequence in southwest 65P/11 and southeast 65P/12 are intensely altered and rocks adjacent to the northeast trending fault may be microfractured or sheared. White to greenish white silicified and sericitized arkosic wackes, resembling quartzite, underlie the Christopher Island Formation eruptive centre in 65P/11. A weak fracture cleavage is developed in calcareous beds. The alteration is associated with epidote and quartz veining and may be related to the northeast faulting. It predates the development of the eruptive centre since blocks of both altered and unaltered arkosic wacke occur as accidental fragments in the vent agglomerate.

Christopher Island Formation

Lavas, pyroclastics and volcanoclastic sediments of the Christopher Island Formation unconformably overlie the basal sedimentary sequences or are faulted against cataclastic gneisses of the Thirty Mile domain. The alkaline volcanic rocks are similar to those in adjacent map areas described by LeCheminant et al. (1979) and Blake (in press).

In the west half of 65P the formation comprises mafic and felsic trachyte lavas and thin interflow units of volcanic breccia, immature volcanic wacke, arkosic wacke and siltstone. Maroon to maroon-grey weathering, massive, porphyritic mafic trachytes, the dominant lithology, contain phenocrysts of clinopyroxene, phlogopite, plagioclase and alkali feldspar in variable proportions. Feldspar-rich lavas have well developed trachytic textures. Interflow sediments are, for the most part, immature, poorly sorted wackes that contain angular or subangular crystal and lithic fragments derived from the trachyte succession. Dark grey to maroon, dense volcanic wackes, which contain in excess of 50 per cent clinopyroxene and phlogopite crystals, may be reworked mafic crystal tuffs. Epidote, chlorite, calcite and tremolite/actinolite alteration occurs throughout the Christopher Island successions. A northwesterly trending swarm of porphyritic syenite dykes intrude mafic trachyte successions in the southwest corner of 65P/11.

An eruptive centre in 65P/11 (Fig. 35.1) is distinguished by a northwest dipping succession of agglomerates, lapilli tuffs, and tuffaceous wackes that are exposed over an area approximately 0.5 by 2.5 km. The succession trends northeast and has a well defined central area about 1 km long containing coarse agglomerates with bombs to 1.3 m and accidental fragments up to 2 m in diameter. The succession lies directly on and has been emplaced through intensely sericitized white arkosic wackes of the basal sedimentary sequence. The distribution of pyroclastic deposits suggests eruptions occurred along a northeast trending fissure perhaps related to the major fault mapped to the southwest (Fig. 35.1). Numerous northwesterly trending porphyritic syenite and lamprophyre dykes intrude the vent area.

Coarse agglomerates in the central area contain bombs of mafic trachyte which are aligned and flattened in the plane of a well developed eutaxitic foliation. Accidental fragments are common and include volcanoclastic conglomerate, grey and white arkosic wacke, and cataclastic granitoid gneiss. Bombs and large accidental fragments are suspended in a heterogeneous dark grey-green matrix of much finer debris. The pyroclastic deposits range from unsorted and chaotic coarse agglomerates to well sorted tuff beds.

The matrix of the coarse agglomerates and the lapilli tuffs contain flattened green lenticles (shards?) which partly wrap around small lithic and crystal fragments. Thin sections reveal that the lenticles contain phlogopite phenocrysts set in a matrix of phlogopite, tremolite, potassic feldspar, carbonate and sphene. Crystal fragments include quartz, plagioclase, microcline, phlogopite, apatite, and an unusual colour zoned light brown feldspar. The very fine recrystallized matrix surrounding the fragments contains phlogopite, talc, tremolite, potassic feldspar, apatite and carbonate. All units within the pyroclastic succession have been affected by extensive carbonate veining and replacement.

Preliminary energy dispersive studies show that the light brown feldspar crystals are almost pure potassic feldspar with trace Fe and Ba. Small grains of rare-earth-bearing minerals containing more Ce than La (monazite and probably allanite) are rare constituents in the matrix. The matrix carbonate is calcite which contains up to 4 per cent SrO and trace Mg, Fe, and Mn. Vein and replacement calcite in trachyte fragments contains less Sr and the same trace elements. High Sr contents suggest the carbonate is of primary magmatic origin and was not derived from underlying sediments or basement. Explosive volcanism probably was due to release of volatiles, perhaps rich in CO₂, from the intruding carbonate-bearing alkaline magma.

Northeast of the eruptive centre an area approximately 1 by 5 km is underlain by porphyritic felsic trachyte lava containing potassic feldspar and plagioclase phenocrysts to 5 mm in an orange-red, locally flow-banded, aphanitic matrix. The felsic lava has steep contacts with pyroclastic deposits to the south and mafic trachyte lavas to the north and west. The lava may be a volcanic dome developed on the flank of the older eruptive centre.

Kunwak Formation

The name, Kunwak Formation, is here proposed for a sequence of relatively flat lying volcanoclastic sediments that overlie the Christopher Island Formation and are succeeded by lavas of the Pitz Formation. The formation is named for the river that flows from Tulemalu Lake to join the Kazan River west of Thirty Mile Lake (Fig. 35.2). The best exposures of the formation are between the Kunwak River and Pitz Lake. A complete stratigraphic sequence is nowhere observed.

Outcrops of the formation are typically rubbly weathering and poorly exposed, with the exception of a few 15-20 m high cliffs near the eastern boundary of the map area. The scarps comprise even, parallel bedded, maroon to red-brown conglomerate with thin interbeds of medium- to coarse-grained lithic sandstone. Conglomerate beds range in thickness from 0.2 to 1.6 m and are massive or crudely graded and poorly sorted. The coarse conglomerates are made up of subrounded to subangular clasts of trachyte and rare vein quartz and well indurated red arkose in a calcite cemented matrix of subangular to angular sand-sized fragments. Clasts typically range in size from 1-20 cm, with a few boulders to 50 cm.

Lithic sandstone interbeds range in grain size from fine to very coarse and contain planar and trough crossbeds and rare ripple marks. Lustre mottling is a characteristic feature of the calcite cement. Calcite veins and stockworks are common throughout the formation.

The Kunwak Formation is interpreted as alluvial fan deposits resulting from local uplift and faulting within the Baker Lake Basin during a magmatic hiatus that separates the alkaline volcanism of the Christopher Island Formation from acid calc-alkaline volcanism of the Pitz Formation. The present distribution of the formation within the map area reflects both the recessive weathering character of the sediments and its local development. Similar red clastic successions consisting of debris flow sequences interbedded with stream-channel deposits occur to the southwest in the Tebesjuak Lake map area (LeCheminant et al., 1979).

Pitz Formation

Lavas and sediments of the Pitz Formation unconformably or disconformably overlie volcanics of the Christopher Island Formation and concordantly overlie sediments of the Kunwak Formation. The formation comprises rhyolites and dacites, containing abundant feldspar phenocrysts and subordinate rounded quartz 'eyes', with local interflow lenses of rhyolite-cobble conglomerate, breccia, red lithic sandstone and siltstone. Flow-banded rhyolite and welded crystal tuff are present near the base of the formation southwest of Princess Mary Lake. East of Princess Mary Lake the formation is at least 150 m thick.

Basal flows of the formation are commonly exposed in 5-10 m high cliffs forming low hills. Closely spaced joint sets with a distinct basal parting typically give a columnar appearance to cliff faces. The dominant lithology east of the Kunwak River is a dark red-brown dacite containing up to

35 per cent plagioclase and potassic feldspar phenocrysts to 1 cm and 1-5 per cent small (1-3 mm) quartz eyes. Mafic phenocrysts, completely replaced by iron oxides, form distinct 'clots' within feldspar phenocrysts. The matrix is aphanitic. West of the Kunwak River the dacite flows are interstratified with massive and flow-banded, greyish red rhyolite lavas and welded crystal tuffs. The sparsely porphyritic rhyolite lavas commonly contain purple fluorite, both as an accessory mineral and in veinlets. Topaz is associated with white mica and fluorite in a spherulitic, flow-banded rhyolite adjacent to a small miarolitic granite near the west boundary of the map area. The crystal tuffs are moderately to densely welded and contain euhedral and broken quartz and alkali feldspar crystals set in a matrix of welded and devitrified shards.

Pitz lavas and interflow sedimentary rocks exposed east of Princess Mary Lake record a complicated history of contemporaneous volcanism, autobrecciation, mass-wasting and stream-channel activity. Flat lying to gently dipping mauve and maroon, abundantly porphyritic rhyolites are intercalated with red fanglomerates composed of angular to subangular clasts of rhyolite set in a reddish orange silt and sand-sized matrix. Massive, unsorted beds containing angular lava fragments may be interbedded with waterlaid laminated red siltstones and sandstones. A fanglomerate deposit more than 100 m thick derived entirely from Pitz lavas is exposed in a cliff section on the west side of the large horseshoe island in Princess Mary Lake. The deposit is overlain by pink basal conglomerates and white pebbly sandstones of the Thelon Formation.

Granite

Stocks of hypabyssal, locally miarolitic and/or fluorite-bearing granite intrude volcanic rocks of the Christopher Island Formation in 65P/5 and 65P/12 (Fig. 35.1). The largest of these is a poorly exposed composite intrusion 12 km long and up to 5 km wide that is made up of three phases. The border phase is a fine- to medium-grained, subporphyritic grey biotite granite rich in accessory sphene and magnetite. A similar granite, which contains accessory deep purple fluorite, makes up the central phase of the intrusion. A representative sample contains 18.6 ppm U. Syenitic rocks form a crescent-shaped body entirely enclosed within the eastern half of the stock. This phase comprises fine- to medium-grained, equigranular pink biotite-hornblende syenite and quartz syenite, both with up to 2 per cent magnetite. Rocks of the syenitic phase and the granitic border phase are locally fractured and filled with hematite or specularite.

Trachyte lavas of the Christopher Island Formation adjacent to the intrusion have been metamorphosed to assemblages indicative of albite-epidote facies contact metamorphism. The hornfels zone, up to 75 m wide, is characterized by chlorite-epidote-actinolite replacement of both mafic phenocrysts and groundmass in the trachyte lavas. Mineralized zones within the contact aureole are described in the section on economic geology.

A small stock of pink, miarolitic, micrographic granite outcrops west of the previously described intrusion. Contacts with lavas of the surrounding Christopher Island and Pitz formations are not exposed. The potassic biotite granite contains miarolitic cavities lined with specularite, fluorite, quartz and potassic feldspar. A representative sample contains 13.3 ppm U. An unusual feature is the presence of well

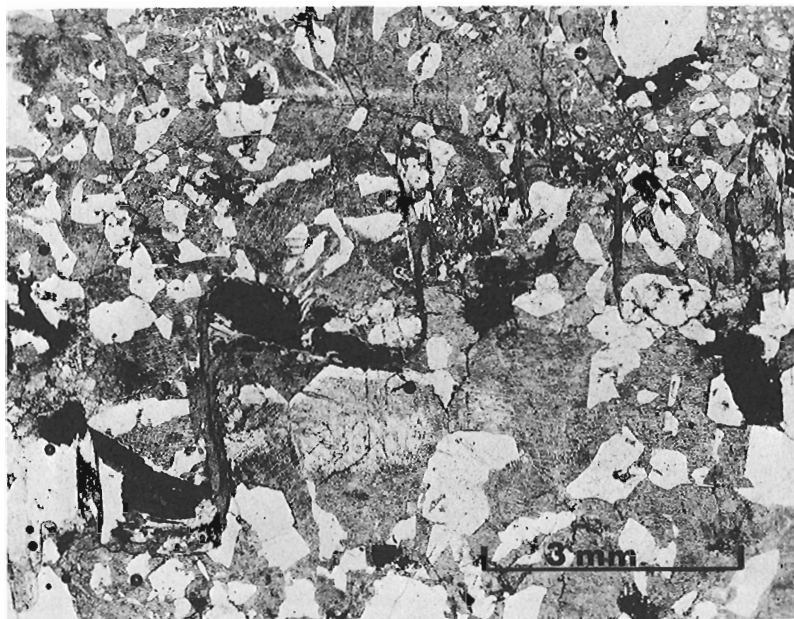


Figure 35.3. Photomicrograph of a small scale macrostylolite cutting grain boundaries in micrographic fluorite granite. (GSC 203496-M)

Table 35.1
Analyses (ppm) of mineralized Christopher Island breccia and fluorite granite

	Fluorite granite	Mineralized brecciated trachyte
U	18.6*	849*
Cu	2	19
Pb	78	186
Mo	3	2
Bi	N.D.	N.D.
As	N.D.	9
Sb	7	N.D.
Sn	N.D.	N.D.
W	2	8
Ag	0.2	0.2
Au (ppb)	N.D.	15**

* Analyses by neutron activation.
** Lower limit of detection 10 ppb with precision of \pm ppb at this level.
N.D. = Not detected.

developed, small scale macrostylolites. In one example the stylolitic seam cuts across all minerals in the rock, postdates the micrographic intergrowth, and separates parallel-sided teeth that interpenetrate up to 3 mm (Fig. 35.3). The seam is composed of chlorite, or less commonly sericite or opaques. There is no optical indication of strain in alkali feldspar or quartz grains adjacent to the suture. Stylolites in igneous rocks are rare, but a few occurrences are known from rhyolite lavas and welded tuffs (Bloss, 1954; Burma and Riley, 1955; Golding and Conolly, 1962). Significantly, this occurrence is in granite of composition and mineralogy similar to the rhyolite flows and demonstrates that conditions for stylolite development can exist in hypabyssal intrusive rocks.

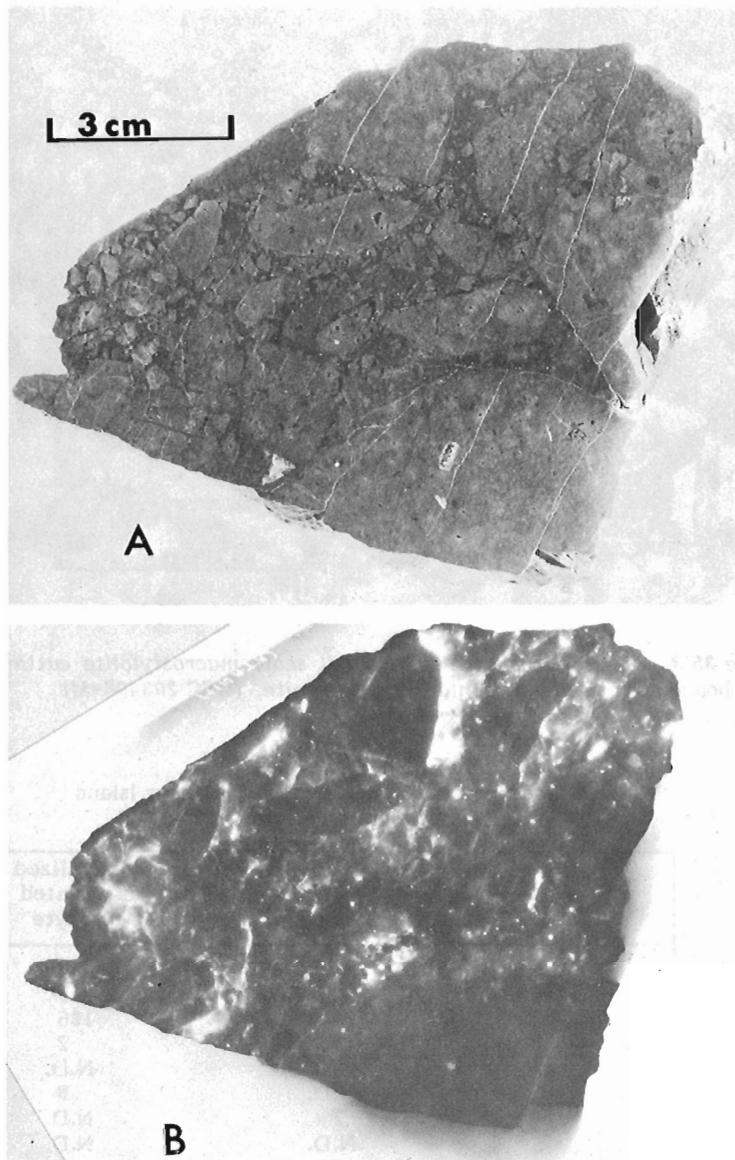


Figure 35.4. Polished slab (A) and autoradiograph (B) showing the distribution of U mineralization in Christopher Island brecciated trachyte. (GSC 203345-N,O)

Thelon Formation

Exposures of the Thelon Formation are restricted to low lying areas in 65P/14 and islands in Princess Mary Lake (Fig. 35.1). The formation comprises flat lying, crossbedded sandstone, pebbly sandstone and conglomerate. Crossbeds indicate transport directions are west and southwest, approximately parallel to the north boundary of the Baker Lake Basin. Within the map area cream to pale pink pebbly sandstones, containing well rounded pebbles and scattered cobbles of white vein quartz and red or grey impure quartzite, are the dominant lithology. The matrix is white clay (kaolinite). Basal conglomerates overlying Pitz Formation porphyritic lavas contain boulders of porphyritic rhyolite lava to 50 cm and can be interbedded with red lithic sandstones closely resembling interflow sediments of the Pitz Formation. The more mature pebbly sandstones underlie valleys up to 100 m below the present level of basal conglomerates and lithic sandstones that rest directly on rocks of the Pitz Formation. Apparently the Thelon Formation was laid down on a surface of significant local relief.

The Baker Lake Basin (Fig. 35.2) records the history of an extensional tectonic regime, closely associated with basement uplift and volcanic activity, that developed at about 1800 Ma. The sedimentary rocks of the basin primarily reflect two environments of deposition: 1) alluvial fans (South Channel, Kunwak and Pitz formations) and 2) rivers and perhaps shallow lakes (Kazan, Christopher Island and Thelon formations). These deposits record abrupt changes in relief both peripheral to and within the basin. However, there is no significant change in depositional environments during the evolution of the basin.

The development of the basin proceeded from an initial uplift stage to alkaline volcanism. Cycles of subaerial alkaline volcanism began with explosive activity followed by effusions of mafic then felsic trachyte lavas (LeCheminant et al., 1979). Thick alkaline volcanic successions developed in the central and southwest parts of the basin. Structural evolution continued with local uplift and faulting during a magmatic hiatus that separated the alkaline volcanism from acid volcanism and plutonism. Resultant rhyolites and granites are evidence of substantial melting of continental crust which may have been triggered by elevation of geoisotherms as basic alkaline magmas rose from the upper mantle (Fyfe, 1973). The acid volcanism and plutonism was the last major event in the structural development of the Baker Lake Basin. Minor faulting may be contemporaneous with infilling of the northwest side of the basin by mature sediments of the Thelon Formation.

Economic Geology

Three types of uranium occurrences have been recognized within the map area: 1) redbed mineralization near unconformities, 2) fracture controlled mineralization, and 3) contact aureole mineralization. The occurrences are shown in Figure 35.1 and have been briefly described by Miller (1979). The map area is within the region covered by a program of reconnaissance and detailed till sampling undertaken by Klassen and Shilts (1977) to study glacial dispersion of uranium. Regional lake sediment geochemical reconnaissance data and airborne radiometrics are available on 1:250 000 maps (GSC Open File 416, 1977; and Geophysical Map Series 36665G, 1977).

Contact aureole mineralization is present within metasomatically altered Christopher Island volcanic rocks adjacent to a composite fluorite-bearing granite (Fig. 35.1). The UTM location was incorrectly reported by Miller (1979) and should be recorded as 7056180N, 561590E (65P/12). Anomalous radioactivity occurs sporadically within a 60 by 140 m zone along the northwestern granite-volcanic contact. Volcanic rocks are porphyritic mafic trachyte lavas and brecciated equivalents. The breccia consists of sub-angular to subrounded trachyte fragments to 10 cm set in a fine grained matrix composed of lithic fragments (Fig. 35.4). The alteration assemblage within the mineralized zone is present as fracture filling in the massive lavas and as replacements of both matrix and trachyte fragments in the breccia. The assemblage is grossularite-quartz-epidote-actinolite-chlorite-purple fluorite-albite-magnetite-calcite. Intense fluorine metasomatism is a characteristic feature of the mineralized volcanic rocks.

Highest radioactivity was encountered within brecciated trachyte. The autoradiograph in Figure 35.4 illustrates intense impregnations of uranium in the breccia matrix between large trachyte fragments. Energy dispersive study shows U and Pb are contained within a very fine grained (<0.04 mm) Ca-Ti-Si phase that is disseminated

throughout the breccia. Multielement analysis (Bonder-Clegg, Ottawa) of the mineralized breccia and the fluorite-bearing granite shows significant U, Pb, and Cu enrichment in the breccia compared to the granite (Table 35.1).

Acknowledgments

The authors wish to thank G.W. Booth, K.J. Bawden, C. Beaudry and B.H. Murdoch for their capable field assistance. We are indebted to M.B. Lambert for his field observations and subsequent interest in volcanic rocks of the Dubawnt Group. A.G. Plant carried out the energy dispersive investigations and M.J. Murray assisted with drafting and petrographic work.

References

- Blake, D.H.
Volcanic rocks of the Paleohelikian Dubawnt Group in the Baker Lake-Angikuni Lake areas, District of Keewatin, N.W.T.; Geological Survey of Canada, Bulletin 309. (in press)
- Bloss, F.D.
1954: Microstylonites in a rhyolite porphyry; *Journal of Sedimentary Petrology*, v. 24, p. 252-254.
- Burma, B.H. and Riley, C.M.
1955: Two unusual occurrences of microstylonites; *Journal of Sedimentary Petrology*, v. 25, p. 38-40.
- Donaldson, J.A.
1965: The Dubawnt Group, Districts of Keewatin and Mackenzie; Geological Survey of Canada, Paper 64-20.
1966: Shultz Lake, District of Keewatin, map with descriptive notes; Geological Survey of Canada, Map 7-1966.
- Eade, K.E.
1976: Geology of the Tulemalu Lake map-area (65J), District of Keewatin; in Report of Activities, Part A, Geological Survey of Canada, Paper 76-1A, p. 379-381.
- Eade, K.E. and Blake, D.H.
1977: Geology of the Tulemalu Lake Map-Area, District of Keewatin; in Report of Activities, Part A, Geological Survey of Canada, Paper 77-1A, p. 209-211.
- Eade, K.E. and Chandler, F.W.
1974: Watterson Lake (65G, West Half) and Ferguson Lake (65I, West Half) Map-Areas, District of Keewatin; in Report of Activities, Part A, Geological Survey of Canada, Paper 74-1A, p. 161-162.
- Fyfe, W.S.
1973: Granites Past and Present; in Special Publication, Geological Society of South Africa, 3, p. 13-16.
- Golding, H.G. and Conolly, J.R.
1962: Stylolites in volcanic rocks; *Journal of Sedimentary Petrology*, v. 32, p. 534-538.
- Heywood, W.W. and Schau, Mikkel
1978: A subdivision of the Northern Churchill Structural Province; in Current Research, Part A, Geological Survey of Canada, Paper 78-1A, p. 139-143.
- Klassen, R.A. and Shilts, W.W.
1977: Glacial dispersal of uranium in the District of Keewatin, Canada; in Prospecting in areas of glaciated terrain, Jones, M.J., editor, The Institution of Mining and Metallurgy, London, p. 80-88.
- LeCheminant, A.N., Blake, D.H., Leatherbarrow, R.W., and deBie, L.
1977: Geological Studies: Thirty Mile Lake and MacQuoid Lake Map-Areas, District of Keewatin; in Report of Activities, Part A, Geological Survey of Canada, Paper 77-1A, p. 205-208.
- LeCheminant, A.N., Lambert, M.B., Miller, A.R., and Booth, G.W.
1979: Geological studies: Tebesjuak Lake map area, District of Keewatin; in Current Research, Part A, Geological Survey of Canada, Paper 79-1A, p. 179-186.
- Miller, A.R.
1979: Uranium Geology in the Central Baker Lake Basin; in Current Research, Part A, Geological Survey of Canada, Paper 79-1A, p. 57-59.
- Morrison, I.R.
1977: Petrology and Petrochemistry of the Cookie Monster Alkaline Intrusion, Keewatin District, Northwest Territories; unpublished B.Sc. thesis, University of Western Ontario, London, Ontario, 54 p.
- Murdoch, B.H.
1979: Geology of the Tattanniq Alkaline Intrusion; unpublished B.Sc. thesis, Carleton University, Ottawa, 62 p.
- Wanless, R.K. and Loveridge, W.D.
1972: Rubidium-Strontium Isochron Age Studies, Report 1; Geological Survey of Canada, Paper 72-23, p. 25-31.
- Wright, G.M.
1955: Geological notes on central District of Keewatin; Geological Survey of Canada, Paper 55-17.
1967: Geology of the southeastern barren grounds, parts of the Districts of Mackenzie and Keewatin (Operation Keewatin, Baker, Thelon); Geological Survey of Canada, Memoir 350.

**THE GRENVILLE OF LABRADOR: A POSSIBLE TARGET FOR URANIUM EXPLORATION
IN LIGHT OF RECENT GEOLOGICAL AND GEOCHEMICAL INVESTIGATIONS**

Project 750010

J.A. Kerswill and J.W. McConnell¹
Regional and Economic Geology Division

Kerswill, J.A. and McConnell, J.W., The Grenville of Labrador: A possible target for uranium exploration in light of recent geological and geochemical investigations; in Current Research, Part B, Geological Survey of Canada, Paper 79-1B, p. 329-339, 1979.

Abstract

Detailed follow-up investigation of an extensive regional reconnaissance lake sediment and lake water uranium anomaly north of Lake Melville, Labrador (NTS 13G/14) has resulted in the discovery of ore grade uranium mineralization in granitic gneisses of the Grenville Province. Airborne radiometric surveying, lake water, and lake sediment sampling and subsequent ground spectrometer surveying were effective in defining the area where the discovery was made.

The mineralization of unknown continuity and extent is conformable with the regional foliation of the host gneisses and is confined within siliceous garnetiferous horizons that are most radioactive around segregations of biotite and chlorite. Uraninite occurs as disseminated, essentially cubic, grains in association with molybdenite, pyrite, and fluorite.

A tentative genetic model can be proposed that involves concentration of uranium in a felsic volatile-rich melt derived during anatexis associated with the Grenville Orogeny.

Introduction

Ore grade uranium mineralization has been discovered both in boulders and in outcrop by a field party of the Newfoundland Department of Mines and Energy in the Lowland Point-Charley Point area north of Lake Melville in the Grenville Province of Labrador. A report on the lake, soil and rock geochemistry and ground and airborne radiometric work has been released (McConnell, 1978). The party was engaged in the follow-up of several Uranium Reconnaissance Program (URP) regional lake sediment and lake water uranium anomalies (Fig. 36.1, GSC Open Files 509, 510, 511, 512, 513). The discovery, in regional anomaly G-1 (Fig. 36.1, 36.2), was made during the course of a detailed lake sediment, lake water, and airborne radiometric survey. The localities where uranium mineralization was subsequently found (Zones A, B, and C, Fig. 36.2) were chosen by John McConnell for ground examination on the basis of results from his preliminary follow-up. John Kerswill joined the Newfoundland field party in early August as their ground investigation was getting underway.

This work was concentrated in Zone A where it included cutting a one kilometre square grid with lines spaced at 150 m, overburden sampling of the grid at 50 m intervals, and spectrometer surveying with readings every 25 m accompanied by limited geological mapping and rock sampling. A number of vegetation samples were also collected.

Petrographic investigations and geochemical work on the rock samples are currently in progress. This report is preliminary in nature and documents the results of some of the field and laboratory work.

Geological Setting of the Regional Geochemical Anomaly

Reconnaissance geological mapping (Stevenson, 1962, 1970) indicated that regional anomaly G-1 is underlain by granitic gneisses of the Grenville Province. They have been described (Stevenson, 1962) as well-foliated gneisses that include heterogeneous banded or veined gneisses and more homogeneous granitoid gneisses that are most commonly granodioritic in composition. They appear to be gradational into paragneiss and often contain pegmatitic material (Stevenson, 1970).

Hadrynian arkosic sandstone of the Double Mer Formation unconformably overlies the granitic gneiss to the north and west of the anomaly (Fig. 36.1, 36.2). Intrusive rocks of the anorthosite suite occur south of Lake Melville and underlie part of regional anomaly G-2. A generalized geological legend that accompanies the recent GSC Open File releases (Open Files 509, 510, 511, 512, and 513) is reproduced as Table 36.1.

Regional Geochemistry

The G-1 regional lake sediment anomaly outlined on the basis of the 1977 URP survey (Fig. 36.2) represents only moderate uranium levels relative to mineralized and anomalous regions elsewhere in Canada including the Central Mineral Belt of Labrador which hosts numerous uranium occurrences notably the Kitts and Michelin deposits (Fig. 36.1). Of the 30 sediment samples from the area only 9 exceed 10 ppm U and the maximum value is only 79 ppm. In other anomalous regions sediments containing up to several hundred ppm U and, locally, even in excess of 1000 ppm have been encountered (Butler and Davenport, 1978). The area received follow-up attention because the level of U in sediments and waters was clearly anomalous with respect to the large sample population collected over Grenville terrane. Of 3441 samples collected from the Grenville portion of the survey area only 3.3 per cent exceeded 10 ppm U. Thus it seemed that either the entire Grenville area surveyed was lacking in uranium or other factors inhibited a more typical dispersion and accumulation of uranium in lake sediments.

Other elements of possible interest in a granitic terrane include Cu, Pb, Zn, Mo, and F. Analyses for Cu, Zn, and F show the sediments from G-1, almost without exception, have concentrations near the mean values of all 832 samples collected in the NTS 13 G map sheet area. Mo is notably lacking in the G-1 sediments; all samples analyzed contained less than the 2 ppm detection limit. Analyses of Pb on the other hand indicated a moderate but pervasive enrichment. All samples had Pb contents in the top 15 per cent of the NTS 13 G lead data and the higher values are partially coincident with the highest U values and may be largely of radiogenic origin.

¹Newfoundland Department of Mines and Energy

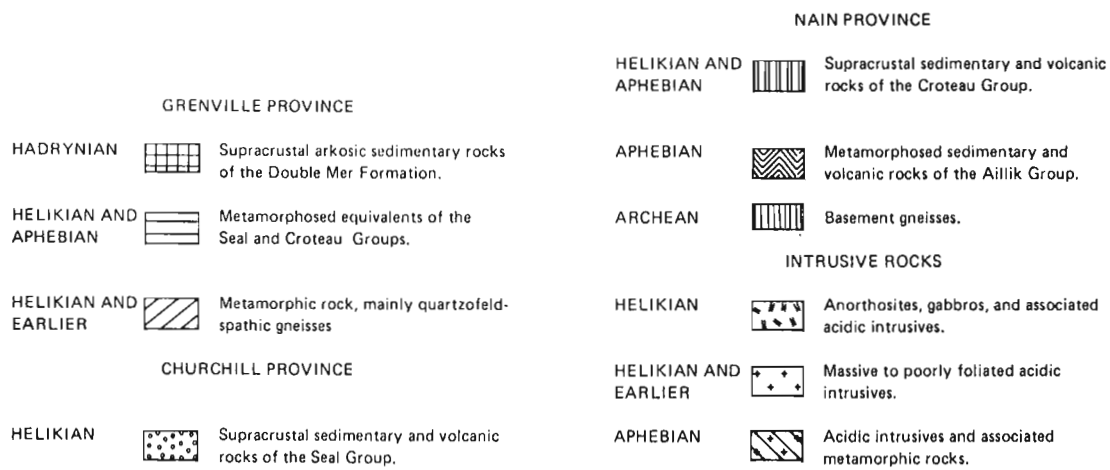
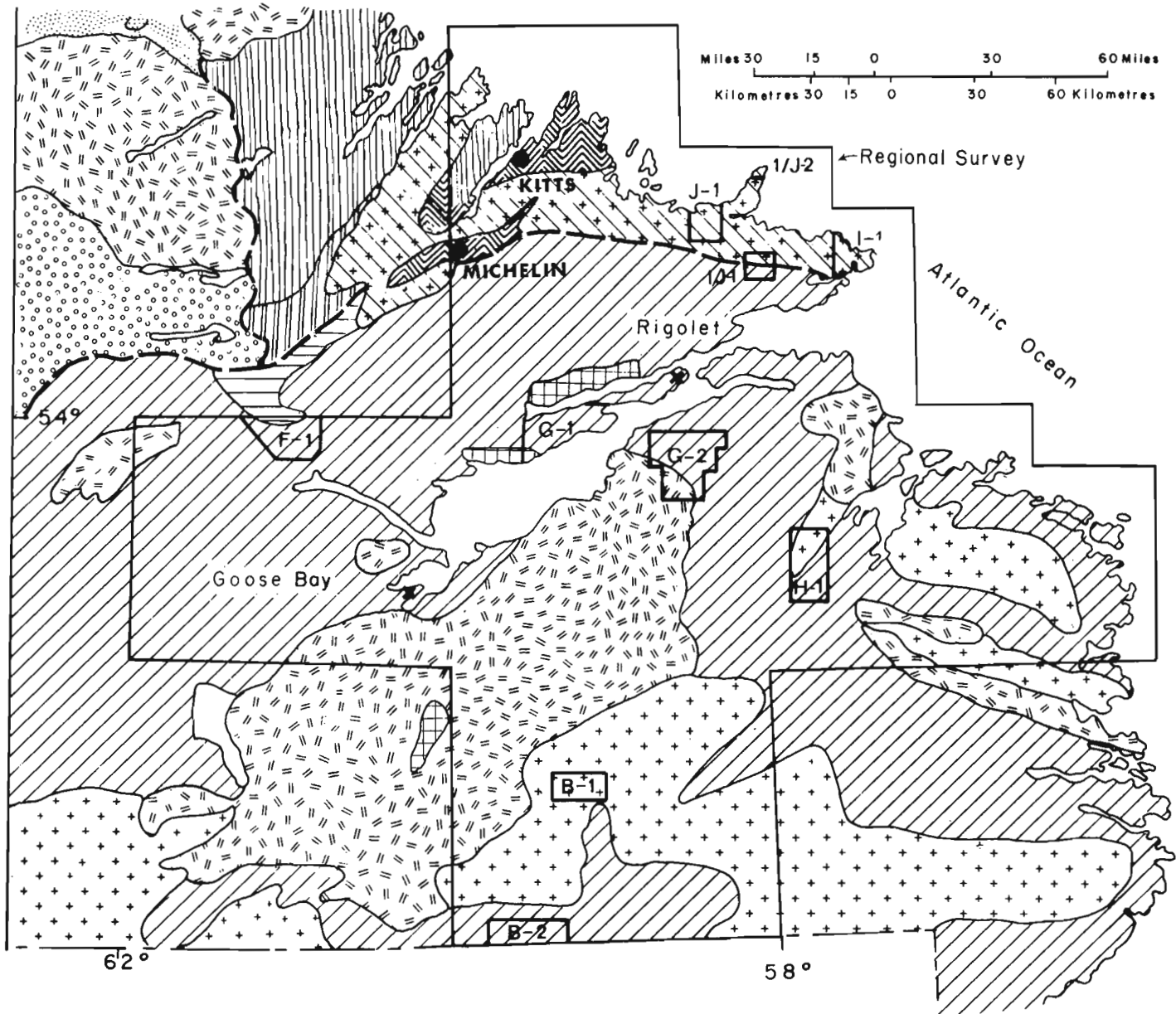


Figure 36.1. Location of the ten areas selected for geochemical follow-up studies in 1978 in relation to the 1977 regional survey area.

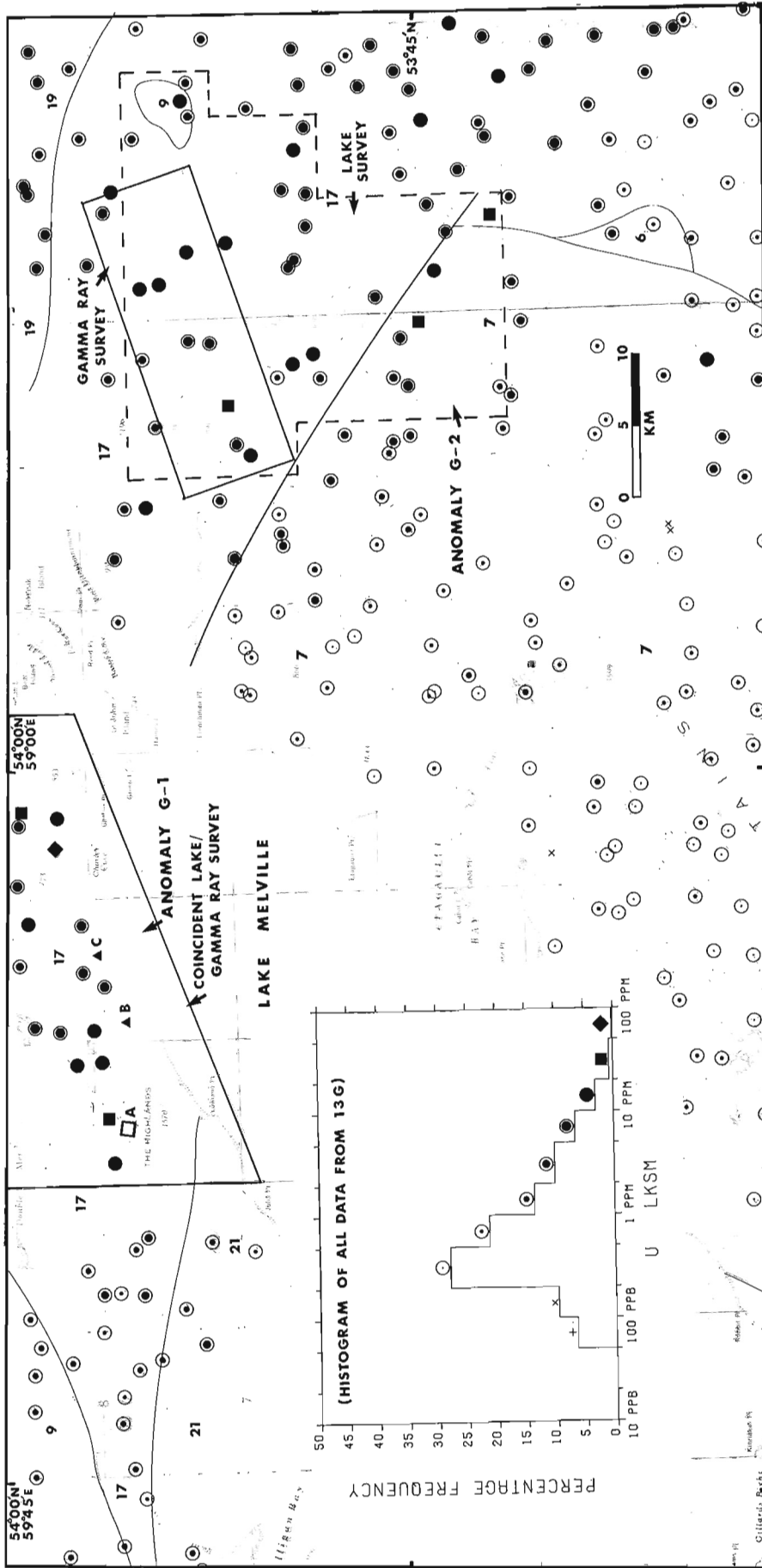


Figure 36.2. Regional anomalies G-1 and G-2 (from McConnell, 1978, modified after GSC Open File 511). The legend for this figure corresponds to Table 36-1.

Table 36.1

Generalized geological legend for area covered by URP Geochemical Survey
(GSC Open Files 509, 510, 511, 512, and 513)

SEDIMENTARY, VOLCANIC AND METAMORPHIC ROCKS	INTRUSIVE ROCKS
HADRYNIAN	CAMBRIAN AND EARLIER
21 Red conglomerate, arkose [ARKS], sandstone and shale	11 Diabase dykes. Radiometric ages range from Cambrian to Archean
GRENVILLE PROVINCE	HELIXIAN
HELIXIAN AND/OR APHEBIAN	NEOHELIXIAN AND EARLIER (?)
20 [MPRK] Metaquartzite, schistose grit and conglomerate, sheared felsic porphyry, greenstone, chlorite-epidote schist, quartz-sericite schist	10 Gabbro, norite [NORT], and diabase sills
19 [GRGS] Mainly garnetiferous biotite - quartz - feldspar paragneisses	9 Granite to granodiorite [GRDR] massive to poorly foliated, porphyritic in part. Includes some granitic gneiss and minor syenite. Generally with gradational contacts
HELIXIAN AND EARLIER (?)	PALEOHELIXIAN
18 Paragneisses [PRGS], granitoid gneisses of probable sedimentary origin, minor quartzite and marble. May locally grade into veined gneisses and migmatites	8 Adamellite suite: adamellite [QZMZ], monzonite, syenite, granodiorite, granite and their hypersthene - bearing equivalent forsunite, mangerite, opdalite and charnockite. Includes minor gabbro, norite, anorthositic gabbro and anorthosite. Closely associated with anorthosite
17 Granitic gneisses [GRNG]: mainly pink quartzo-feldspathic gneisses, commonly banded and migmatitic. Locally porphyroblastic. Minor amphibolite, quartz-rich gneisses, sillimnite gneisses, sillimnite - and garnet - bearing schists, and calc-silicate rock	7 Anorthosite suite: anorthosites [ANRS], anorthositic gabbro, leucotroctolite; minor gabbro, monzonite, granodiorite, ferrosyenite
16 Plagioclase - quartz - pyroxene granulite [GRNL]	6 [UMFC] Gabbro, norite, anorthositic gabbro, troctolite, diorite, derived basic gneiss and amphibolite
15 Intermediate to basic gneisses, amphibolite [AMPB]	APHEBIAN
NAIN PROVINCE	5 Syenite, monzonite, syenodiorite
PALEOHELIXIAN	4 Granite [GRNT], quartz, monzonite, granodiorite, quartz diorite. Generally massive
14 Intermediate to acidic volcanics [AEXV] (mainly porphyritic flows), feldspathic quartzite and minor conglomerate	3 Gabbro [GBBR], metagabbro, glomeroporphyritic gabbro and diorite
APHEBIAN	2 Well foliated feldspar - quartz - hornblende - biotite granitic gneiss [HBDG], chlorite - epidote - quartz - feldspar gneiss, amphibolite, migmatite.
13 Feldspathic quartzite [QRTZ], conglomerate, argillite, basic volcanic rocks [BEXV]	1 Well foliated granodiorite and granodioritic gneiss [GRDG]
ARCHEAN	
12 Granitic and granodiorite gneiss [GNSS], migmatite, granulite, amphibolite; minor paragneisses and meta-sedimentary rocks. Small ultrabasic intrusions included. Diabase dykes locally abundant	

Preliminary Follow-up During 1978 Field SeasonLake Sediment and Water Sampling

A total of 166 sediment/water samples were collected from G-1 giving a sample density of about 1 sample per 3.3 km². Most lakes and large ponds were sampled. Water samples were analyzed for pH and acidified in the field before being shipped out for U analysis by the Fission Track method. These data were available in the field about three weeks later. Lake sediment data were not available until after the field season.

Airborne Radiometric Survey

About 550 line km were flown using a McPhar Spectra-II spectrometer with a 4097 cm³ sodium iodide detector mounted in a Bell 206-B helicopter. A terrain clearance of about 60 m and a ground speed of about 100 km/h were maintained along flight spacings of 1 km. The "stripped" values for the total count, potassium, uranium and thorium channels, were output on paper tape in the field.

The discovery of the uranium mineralization in bedrock can be linked most directly to the airborne radiometric work. By surface prospecting in the areas of the strongest uranium channel responses, one man in one day with the aid of a spectrometer and helicopter was able to locate three

mineralized locations spread over a distance of 13 km. One of these, Zone A, was gridded and more detailed overburden and radiometric studies were made. The U analyses of the lake waters became available a few days after gridding had begun (Fig. 36.3). One of the three mineralized occurrences (B) is immediately adjacent to the lake with the highest U in water of any sample collected during the summer, 2.15 ppb. The grid area (A) is ringed by lakes which have U contents ranging from 0.42 to 0.87 ppb. Such concentrations were only encountered in the top 1 per cent of water analyses from the NTS 13 G map sheet in the regional URP survey.

The uranium analyses for the lake sediments were available about 6 weeks after the close of the field season. The contoured data map shows the grid area to be located quite centrally within the most extensive (seven samples) 50 ppm contour of the G-1 anomaly (Fig. 36.4). Of particular note is the areal extent of the contoured area, approximately 8 km². In the regional survey only 2 of the 832 samples from the NTS 13 G map sheet exceeded 50 ppm.

Thus, although the airborne radiometric data may be credited with contributing most directly to the discoveries, ground prospecting in the areas outlined by the most favourable geochemical responses would likely have produced similar results. Indeed some of the most promising geochemical anomalies still await the prospector's attention.

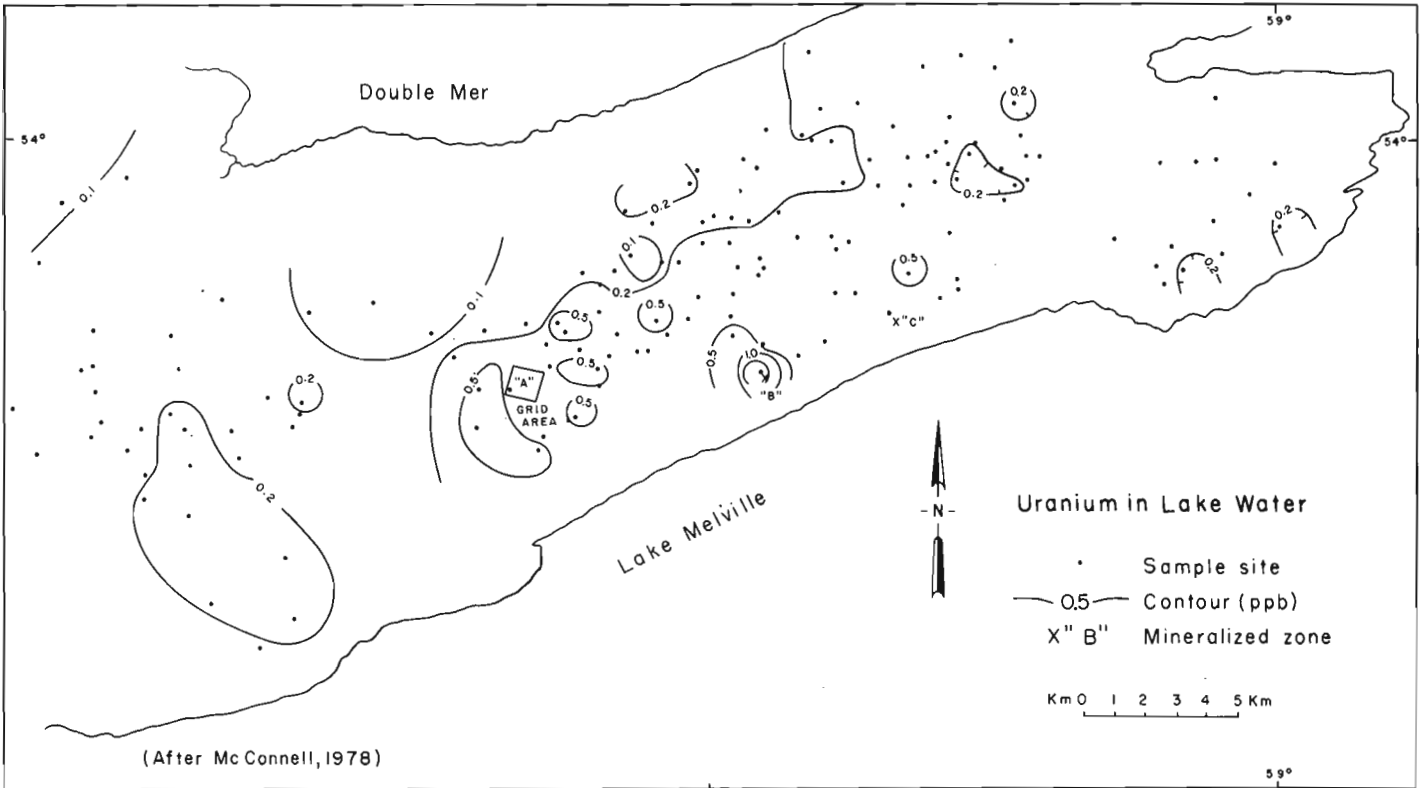


Figure 36.3. Uranium in lake waters, Anomaly G-1.

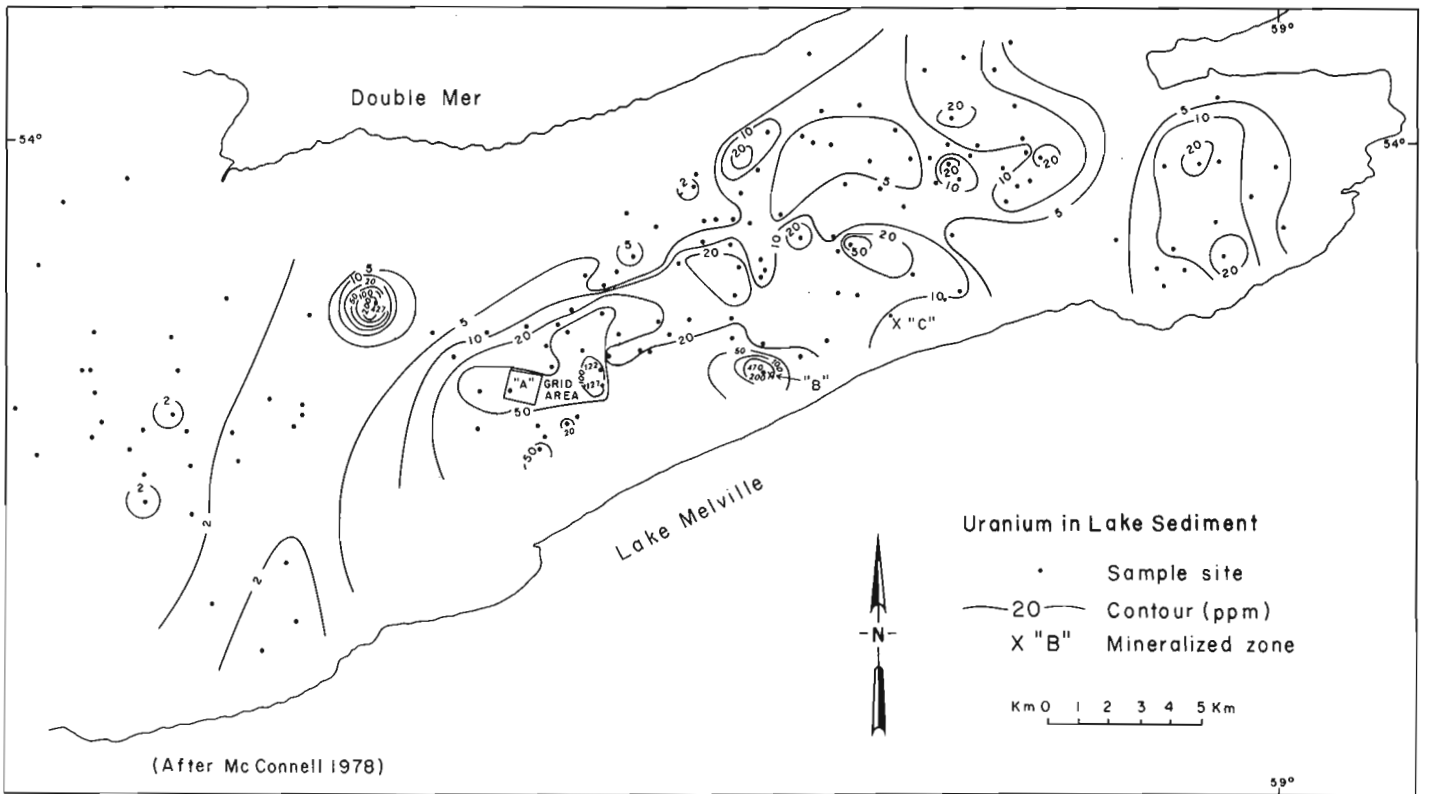


Figure 36.4. Uranium in lake sediments, Anomaly G-1.

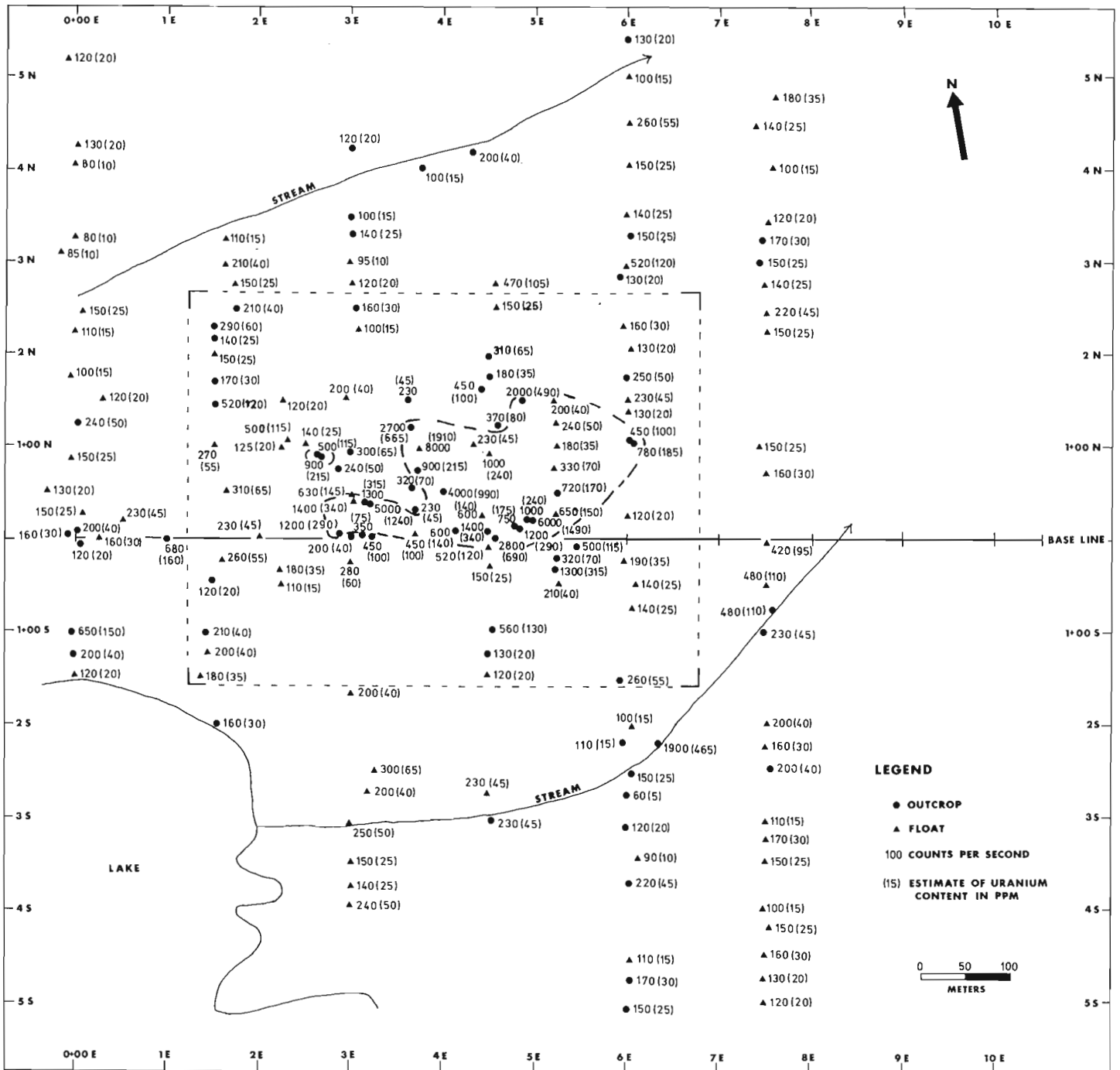


Figure 36.5. Spectrometer survey results over Zone A Grid (modified after McConnell, 1978).

Detailed Follow-up

Introduction

On the basis of encouraging spectrometer readings in the A Zone, a one kilometre square grid was cut and chained with lines at 150 m spacings. The base line parallels the regional foliation (100°). Outcrop is sporadic and represents about 1-2 per cent of the surface area. Overburden varies in thickness from nil to about 5 m. Scrubby black spruce is the predominant tree with some balsam fir in the surveyed areas. Spectrometer surveying, overburden and rock sampling and limited mapping were done over the grid.

Geology and Uranium Mineralization of the Zone A Grid

The outcrops and boulders of the grid area are principally granitoid rocks of quartz monzonitic to granitic composition that were mapped as granitic gneiss. Hand specimens commonly look massive but virtually all outcrops appeared foliated although the intensity of foliation is quite varied. The strike of the foliation as defined by alignment of mafic minerals, principally biotite, is $100-110^\circ$ and essentially parallels the regional foliation. With the present level of mapping it is not possible to determine whether the original nature of the gneissic material was intrusive or sedimentary or both. Some outcrops looked like orthogneiss and others like paragneiss.

Textures of the granitoid rocks are variable ranging from typically granitic to pegmatitic. There appears to be a continuous gradation from the more common medium grained varieties to the more locally distributed pegmatitic phases. Relative percentages of quartz, plagioclase and K-feldspar are also quite variable within the limits expected in the compositional range from quartz-monzonite through granite. Mafic mineral content rarely exceeds 10 per cent and is typically less than 5 per cent.

The uranium mineralization is conformable to the regional foliation and appears confined to particular horizons within the gneiss. These horizons are often garnetiferous and more siliceous than the more common weakly radioactive quartz-feldspar gneisses of the area. Quartz occurs in patches or veins parallel to the foliation and not just interstitially as it does in unmineralized rocks. Within the garnetiferous horizons the greatest radioactivity is intimately associated with biotite and chlorite. Indeed it seems that uranium mineralization is of ore grade only where segregations of ferromagnesian minerals occur. Areas of greatest radioactivity appear to contain small fractures that occur along the mafic bands. Grain size within the radioactive gneisses may be larger than average and the rock locally is pegmatitic but the pegmatitic phases are concordant and appear gradational with the finer grained gneisses. Yellow secondary uranium staining and specks of molybdenite and pyrite were seen in a radioactive boulder at 3 + 74E, 0 + 96N (Fig. 36.5, 36.6).

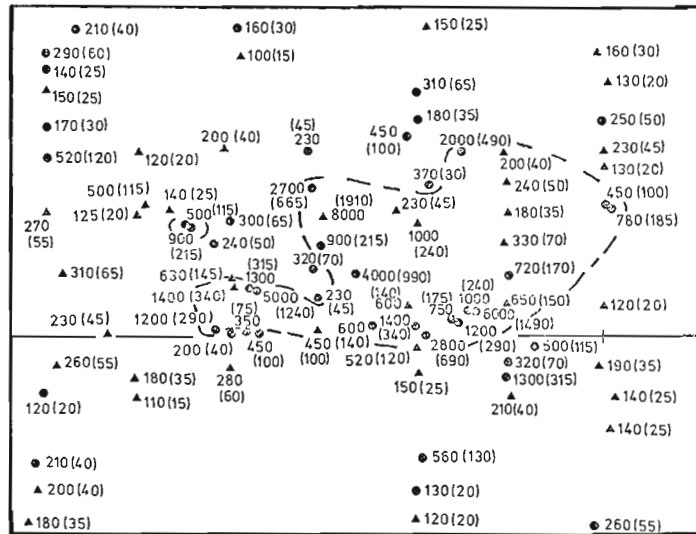


Figure 36.6. Spectrometer survey results over anomalous area.

Autoradiographs were made from polished slabs cut from samples of the radioactive boulder (Plate 36.1). Examination of the autoradiographs indicates the radioactive mineral is finely disseminated although locally concentrated within two of the three samples. Veins containing radioactive minerals are not apparent. The concentration of the radioactive minerals is directly proportional to the percentage of biotite and chlorite in association with garnet.

A thin section was made from a sample of the boulder and the radioactive mineral was identified petrographically and by X-ray analysis. Uraninite is the only primary radioactive mineral that has been found and it occurs as individual, often cubic, grains surrounded by an alteration halo of unknown mineralogy. The uraninite is commonly completely enclosed by biotite, chlorite or garnet and its grains average 0.1 to 0.15 mm but range up to 0.25 mm. Purple fluorite occurs along cleavage planes in numerous biotite grains.

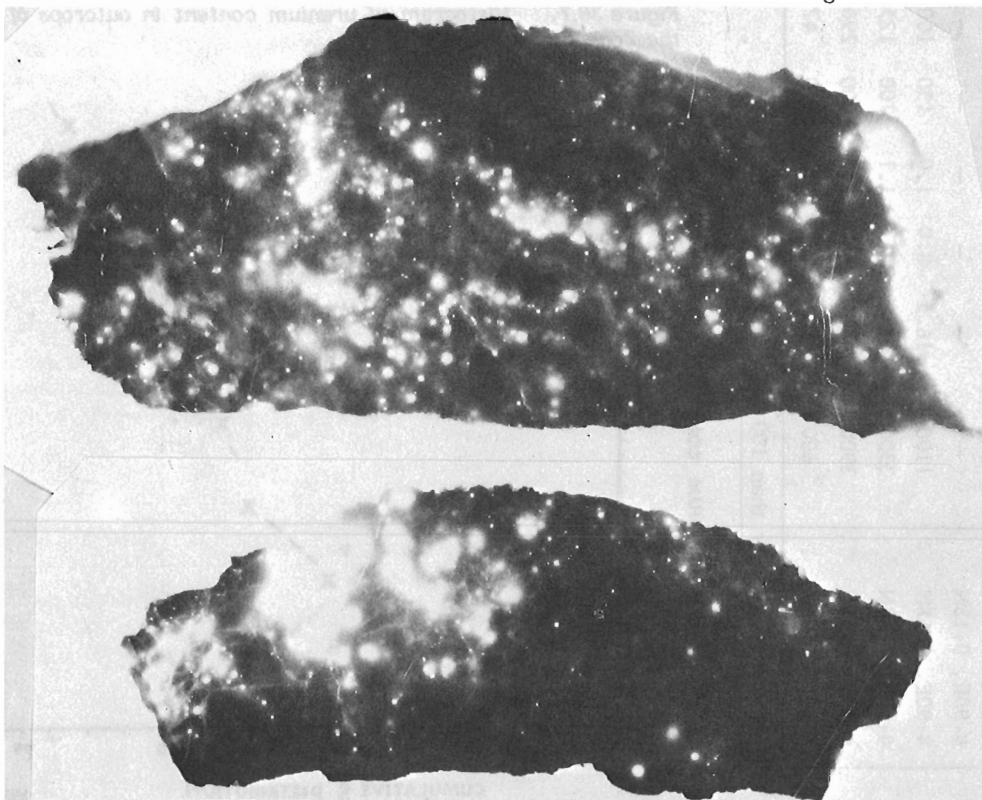


Plate 36.1. Autoradiographs of samples from radioactive boulder at Grid Location 3 + 74E, 0 + 96N.

To summarize, the laboratory work confirmed the close relationship between uranium mineralization and the garnet-ferromagnesian mineral association that was noted in the field. It is also worthwhile to note that U analyses of four samples collected from the boulder are similar to the radiometric estimate of the U content. Uranium analyses of 2932 ppm, 1439 ppm, 1366 ppm and 431 ppm (McConnell, 1978) correspond to a radiometric assay of approximately 2500 ppm in the most radioactive portion of the boulder. Molybdenum was also analyzed and the matching contents are 464 ppm, 178 ppm, 159 ppm and 92 ppm.

A brief visit to the showing at Zone C indicated a similar style of mineralization. Radioactivity is associated with garnetiferous siliceous granitic gneisses that appear to be interbanded with more mafic gneisses. Black tourmaline was noted in the area of greatest radioactivity.

Table 36.2 Spectrometer readings (Scintrex GIS-4 and McPhar TV-1A) at 10 stations in the Zone A Grid

Station	SCINTREX GIS-4 (counts per second)				McPHAR TV-1A (counts per minute)										U ppm Best Estimate
	Total Counts	K+U +Th	U+ Th	Th	Total Counts	U+ Th	U ppm	Th ppm	U ppm	Th ppm	U ppm	Th ppm	ΔU ppm	% Difference	
3+74E, 0+96N	8060	155	76	4.3	++	9250	2700	790	500	2200	320	500	20	2500	
4+50E, 0+10N	1380	23	11	1.0	57000	1300	300	100	120	250	65	50	18	275	
4+50E, 0+10N	2800	49	25	1.4	++	2750	900	190	150	650	85	250	32	775	
4+80E, 0+8N	1000	16	8	.6	40000	800	250	20	80	150	35	100	57	200	
4+90E, 0+18N	6000	110	53	3.0	++	5700	1900	520	350	1300	220	600	38	1600	
4+90E, 0+18N	-	-	-	-	++	4700	-	-	180	1200	100	-	-	-	
4+90E, 0+18N	1100	16.5	8.0	1.0	40000	800	150	100	80	150	35	0	0	150	
4+90E, 0+18N	3300	47.0	20	1.1	++	2400	700	125	70	600	35	100	15	650	
4+00E, 0+50N	3900	58	30	1.9	++	5000	1000	290	325	1100	200	100	10	1050	
4+15E, 0+15N	600	9	4.8	.7	25000	400	50	42	50	50	15	0	0	50	

++indicates greater than 100 000 counts/minute

Results of Spectrometer Survey in Zone A Grid

Spectrometer readings (Scintrex GIS-4) on the total count channel taken over outcrop and float within the grid area are plotted in Fig. 36.5. An anomalous area exists near the centre of the grid when readings above 600 counts per second over outcrop are contoured. The anomaly is more clearly illustrated in Figure 36.6. It extends for approximately 300 m along the strike of the regional foliation and has a width of between 50 and 150 m. The southernmost portion of the anomaly received most of the attention during the field work because of the greater concentration of outcrop and higher readings. This area may contain a number

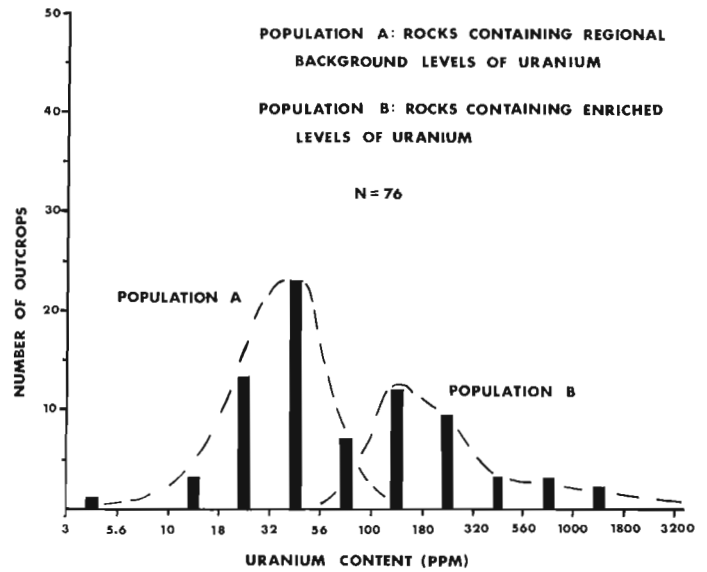


Figure 36.7. Histogram of uranium content in outcrops of the Zone A Grid.

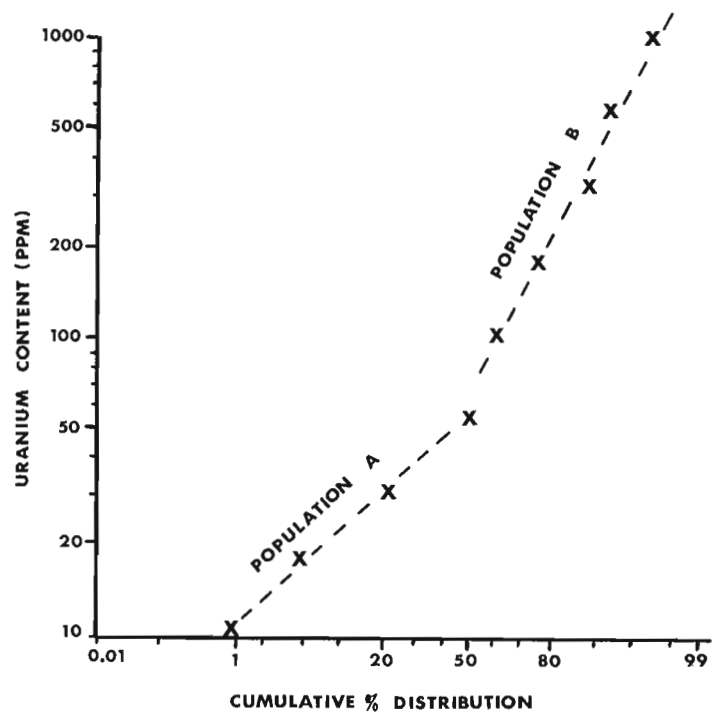
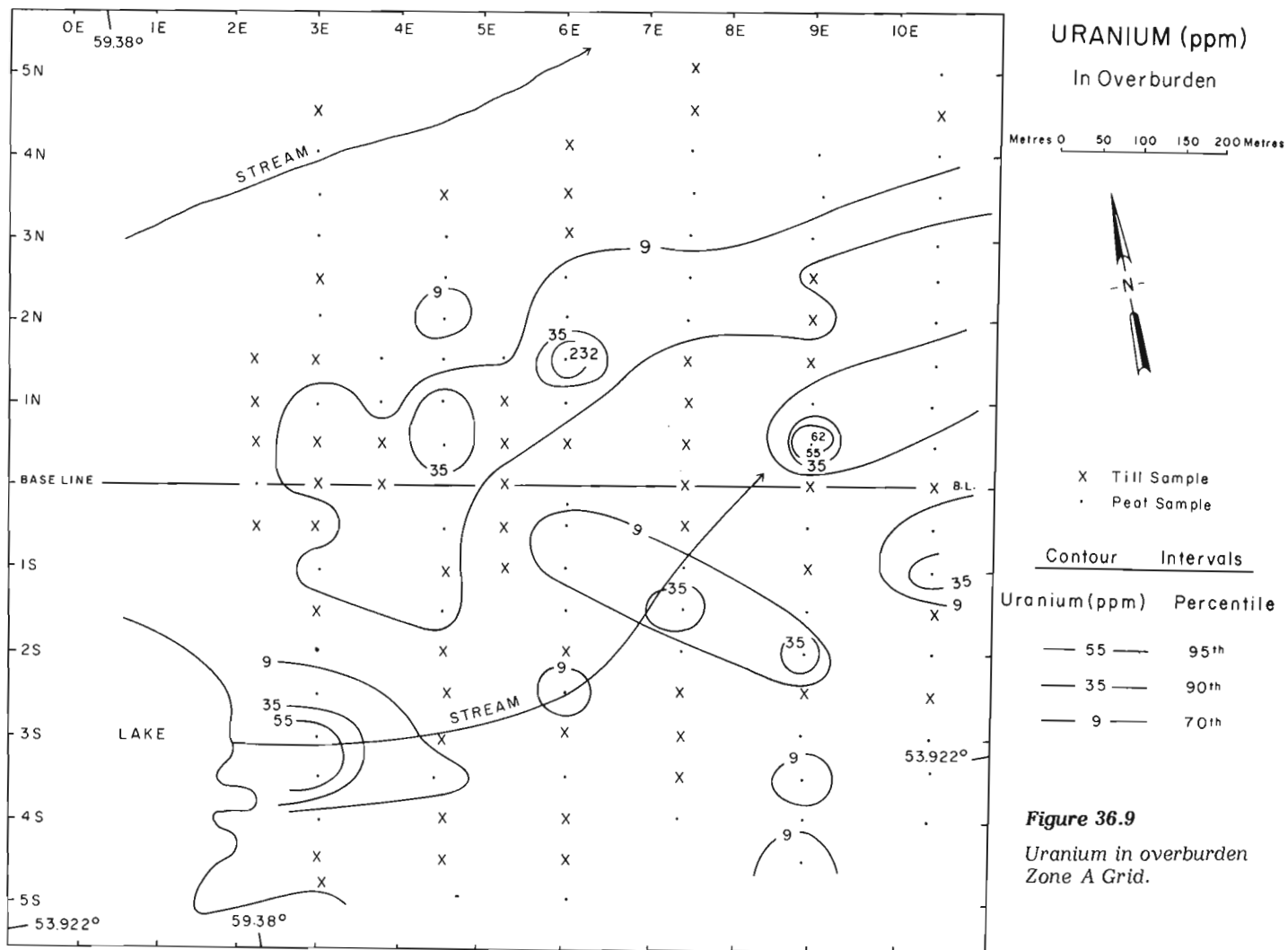


Figure 36.8. Cumulative frequency plot of uranium content in outcrops of the Zone A Grid.



of narrower zones again paralleling the regional trend of the gneisses. Complete spectrometer readings for 10 stations, 9 of which are over outcrop, are presented in Table 36.2.

Grid lines east of 7 + 50E were not surveyed by spectrometer so it is possible that continuations of the anomalous area may exist to the east or that new areas of radioactivity may be found within the boundaries of the present grid.

The total count readings taken over outcrops of the grid area were reduced to approximate uranium contents expressed in ppm (values in brackets in Fig. 36.5, 36.6). This was done using relationships derived from plotting total count channel and U + Th channel readings against calculated U content in ppm for the set of 10 stations in Table 36.2. The calculated U values were determined by using equations for the reduction of GIS-4 spectrometer readings supplied by Scintrex and through use of a known calibration curve for the McPhar TV-1 readings. The plots indicate that a conservative U estimate can be obtained by dividing the total count GIS-4 reading by a factor of four after subtracting 40 counts per second due to regional background. The resultant values for U are semi-quantitative at best but are generally consistent with estimates of U content derived from reduction of the McPhar TV-1 readings (Table 36.2).

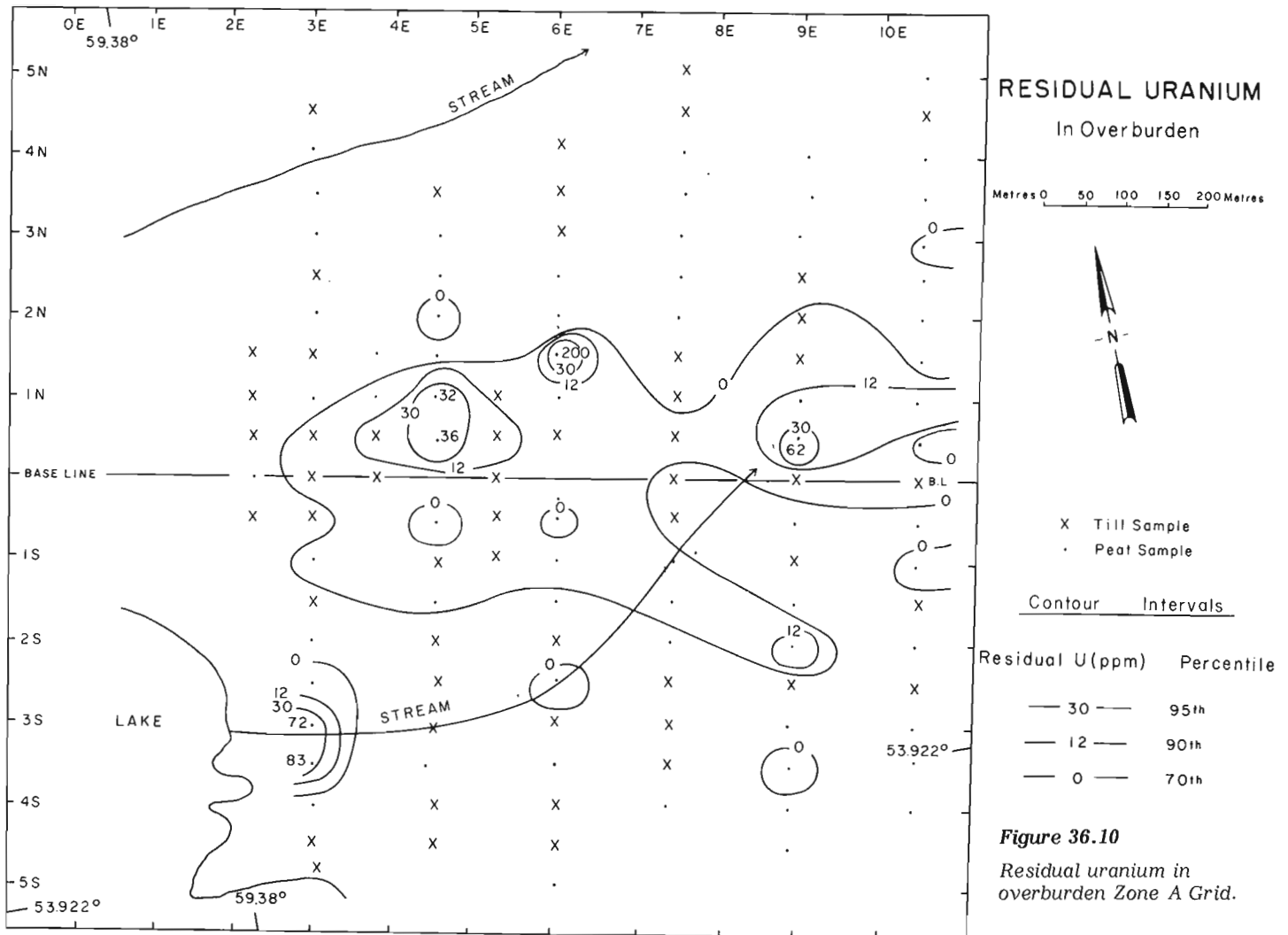
Examination of the data on the concentration of U in outcrops of the study area indicates the presence of two distinct lognormal sample populations. The two populations,

A and B, though discernible from a histogram as an apparently bimodal distribution (Fig. 36.7), are more clearly illustrated on a cumulative frequency plot (Fig. 36.8) where they appear as two straight lines with different slopes. This interpretation of the cumulative frequency plot follows the method of Tennant and White (1959). Histograms of U content in float and of U content in float and outcrop combined are similar to that in Figure 36.7 and thus strengthens the concept of two distinct sample populations.

The two populations can be characterized by their different average contents of U and by their different ranges. Population A has a mode and probable average of 40 ppm with a range from less than 10 ppm to 500 ppm. Population B has a mode and probable average of about 150 ppm with a range from 50 ppm to greater than 1000 ppm.

Results of Overburden Sampling

In an attempt to gain a better understanding of the extent of the mineralization and of the nature of any secondary dispersion haloes, overburden samples (N=126) were collected along most of the grid lines at 50 m spacings. At a given sample site, generally one of two kinds of overburden was found — a black organic-rich, peaty material usually very wet, or, a loosely compacted local till with little or no evidence of a soil profile. The two sample media, as classified by the sampling crew, are distinguished on the maps (Fig. 36.9, 36.10). Sample depths averaged 30 cm.



Only the distribution of U is discussed here. The observed values ranged from 1.5 to 232 ppm with an arithmetic mean of 13.5 ppm. The raw data are plotted in Figure 36.9. Contouring has revealed a major northeastern linear trend of high values across the central part of the grid and parallel to the 2 streams. Other isolated high values occur as a prominent four sample cluster in the southwestern corner. Inspection of these patterns indicates that the higher U values tend to occur in the organic-rich samples. This relationship was quantified by calculating a least squares linear regression for all samples for the variables uranium and loss-on-ignition. The resultant regression equation is: $U(\text{predicted}) = 3.49 + 0.307 (\% \text{ L.O.I.})$. The Pearson correlation coefficient for the 2 variables is 0.39. The good correlation and the moderately steep slope of the equation indicate that the L.O.I. in a sample may significantly affect the U content. The residual uranium values were calculated using the equation $U(\text{residual}) = U(\text{observed}) - U(\text{predicted})$ and plotted on the grid map (Fig. 36.10). Cumulative frequency plots of raw values and of residual values were constructed and used to determine equal percentile contour levels to facilitate comparison of the two distribution patterns.

The pattern formed by the distribution of U residuals is more compatible with the observed geologic and radiometric features. Firstly, the zone of high values (> 70th percentile) is more coherent than the somewhat erratic distribution of the raw U data. Secondly, the zone is highest and broadest in the central portion of the grid which coincides with the area of highest radiometric readings. Thirdly, the major zone trends about 100° rather than northeast as does the raw data

plot. The 100° trend is parallel to the strike of the regional foliation and to the strike of mineralized zones observed in outcrop. The northeastern trend may reflect the orientation of a boggy zone paralleling the local drainage features.

An interesting example of what appears to be a strong hydromorphic anomaly unrelated to any local U mineralization occurs in the southwestern portion of the grid in samples surrounding the stream draining the lake. A moderate amount of frost-heaved and outcropping gneiss in the immediate area has no more than high background radioactivity. The samples concerned are from a boggy area saturated by very slowly moving lake water just as it enters the stream. It appears that U is being fixed in the organic-rich overburden here probably as a result of a change from oxidizing conditions found on the surface of the lake to sharply reducing conditions produced by the oxidizing of organic matter in the bog. That such a phenomenon is occurring is further suggested by the fact that the 2 samples with the highest U content also have high Cu contents (15 and 17 ppm) relative to other grid samples even over mineralized areas. Moreover, Cu does not appear to be otherwise associated with the uranium mineralization as the highest two Cu analyses from mineralized rock are only 24 and 64 ppm.

Genetic Model for Uranium Mineralization

A preliminary and certainly tentative two-stage genetic model can be proposed to account for the observed style of uranium mineralization. In the first stage uranium was concentrated in the sediments and/or granites of the study

area prior to the Grenville orogeny to produce a region with uranium content several times the crustal average. It is these rocks that are represented by Population A of the bimodal frequency distribution. During the Grenville orogeny the crust, already enriched in U, was metamorphosed and uranium was concentrated in the felsic volatile-rich melt phase during anatexis or ultrametamorphism (Population B). Concentrations of uranium approached ore grade only where the relatively great amounts of uranium in the most siliceous melt fraction came in contact with crystallizing ferromagnesian minerals and garnet. Uranyl ions in the melt were reduced in the presence of these minerals and coprecipitated to form uraninite. The ore grade material represents the greatest uranium contents in Population B.

Significance of the Uranium Mineralization

At this stage of investigation it is impossible to quantify the undiscovered uranium resources that may be present in the Grenville gneisses north of Lake Melville. It can be stated, however, that significant indications of ore grade uranium mineralization do exist in two locations (Zone A and Zone C) within a regionally defined geochemical anomaly that covers approximately 240 km². This area which has not previously been explored for uranium can be viewed as a reasonable target for uranium exploration.

Within the more thoroughly studied grid area of Zone A the continuity and extent of mineralization cannot be defined without considerable stripping and trenching coupled with more detailed geochemical and spectrometer surveying and geological mapping. Indications at present are that the uranium mineralization achieves ore grade only locally and that such concentrations are of minimal extent. The existence of two lognormal distributions for uranium, however, suggests that ore grade material is from an enriched population and does not just represent the high valued very small portion of a background population. Such an enriched population can be reasonably expected to contain a significant amount of ore grade material.

Further work in this portion of the Grenville of Labrador could lead to a quantitative assessment of its uranium potential. Such work would also provide the data necessary to construct a sound genetic model that would be a useful guide in uranium exploration.

Acknowledgments

Appreciation is expressed for the valuable criticisms of this paper made by P.H. Davenport and B.A. Greene of the Newfoundland Department of Mines and Energy. We would also like to thank D.M. Watson and A.C. Roberts of the Geological Survey of Canada for their mineralogical identifications and autoradiography. We are grateful to V. Ruzicka for the interest he has shown in this endeavour.

References

- Butler, A.J. and Davenport, P.H.
1978: A lake sediment geochemical survey of the Meelapeg Lake area, central Newfoundland; Newfoundland Department of Mines and Energy, Open File 986.
- Geological Survey of Canada
1977: National Geochemical Reconnaissance release, regional lake sediment and water geochemical reconnaissance data, Labrador, Nfld., NGR 22-1977, NTS 13G; Geological Survey of Canada, Open File 511.
- McConnell, J.W.
1978: Geochemical lake sediment, lake water, radiometric, rock and overburden surveys in Labrador – Follow-up studies of 10 anomalous areas within the 1977 Uranium Reconnaissance Program Lake Survey; Newfoundland Department of Mines and Energy, Open File Lab. 408.
- Stevenson, I.M.
1962: Battle Harbour – Cartwright, Coast of Labrador; Geological Survey of Canada, Map 22-1962.
1970: Rigolet and Groswater Bay map areas, Newfoundland (Labrador); Geological Survey of Canada, Paper 69-48.
- Tennant, C.B. and White, M.L.
1959: Study of the distribution of some geochemical data; *Economic Geology*, v. 54, p. 1281-1290.

Project 780025

Ingo Ermanovics and Mati Raudsepp¹
Regional and Economic Geology Division

Ermanovics, Ingo and Raudsepp, Mati, Geology of the Hopedale Block of eastern Nain Province, Labrador: Report I; in Current Research, Part B, Geological Survey of Canada, Paper 79-1B, p. 341-348, 1979.

Abstract

Florence Lake group volcanic rocks of possibly late Archean age overlie complexly deformed amphibolite and tonalite gneiss metamorphosed to upper amphibolite facies. It is postulated that they are separated by an unconformity. The Florence Lake group comprises equal parts of mafic lavas and sills, and intermediate to felsic pyroclastic rocks and sills. Pyroclastic rocks include tuff, lapilli tuff, lapillistone, and volcanic breccia, all generally calcareous. Sparse copper mineralization, barren pyrite beds and disseminated sulphides occur in tuffaceous rocks. This succession is intruded by granodioritic rocks, and both are folded and metamorphosed to middle and upper greenschist facies. Proterozoic diabase and gabbro dykes, likely of two stages, intrude all rocks of the Hopedale block.

Introduction

This is the first contribution of a four-year program to provide a bedrock data base for use in exploring for, and in evaluating the mineral resources in the Hopedale block of Archean rocks in Labrador. The results to date derive from bedrock mapping in parts of 13K/10, 15, 13N/1, 2, 8, during the 1978 field season. Eventual map publication will be at 1:100 000 scale, complementing work in progress at similar

scales in the Central Mineral Belt and Elsonian intrusive suite by geologists of the Newfoundland Department of Mines and Energy.

Archean rocks of the project area (Hopedale block) are bounded roughly by latitudes 60° to 62° and longitudes 54°30' to 56° (Fig. 37.1). Access is by ship along the Atlantic Coast (dock at Hopedale) and by fixed wing aircraft from Goose Bay to inland lakes and rivers. Areas of low elevation

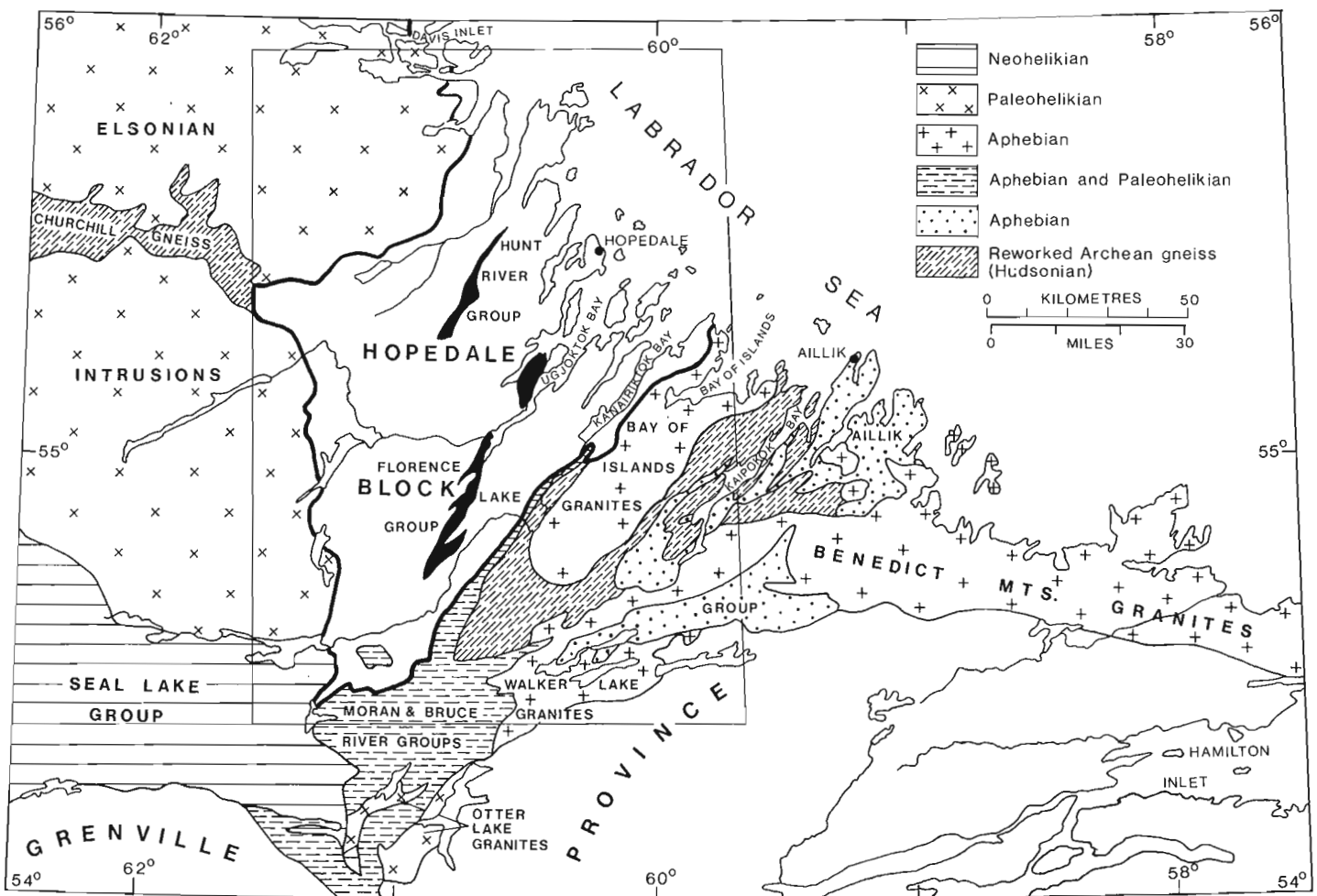


Figure 37.1. Regional geological setting of the Hopedale block (after Greene, 1970 and Smyth et al., 1978). Box shows area of Figure 37.2. The Hopedale block is outlined with thick line.

¹Department of Earth Sciences, University of Manitoba, Winnipeg, Manitoba R3T 2N2

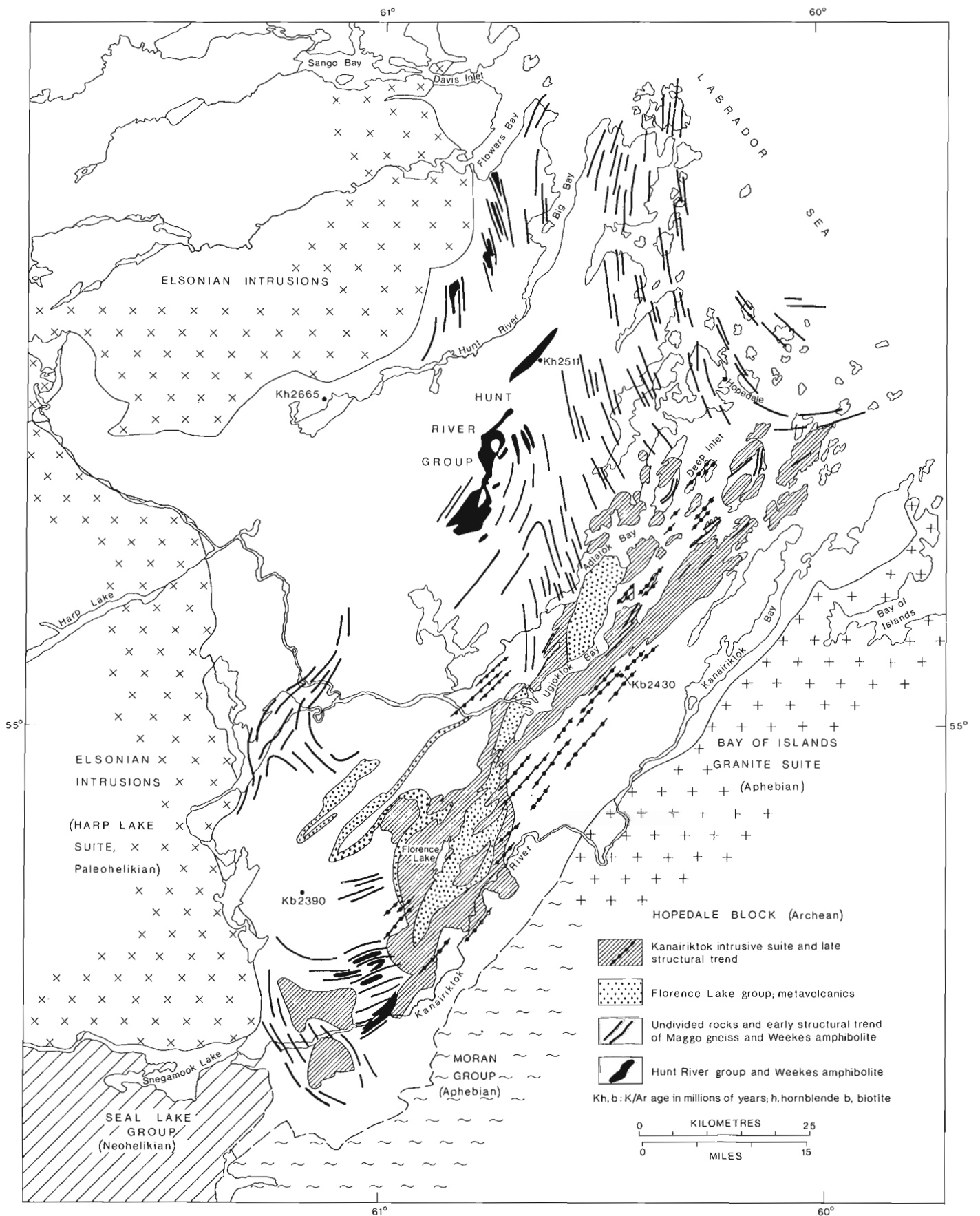


Figure 37.2. Schematic illustration of major lithologic and structural elements of the Hopedale block in Florence Lake-Hopedale areas.

inland are underlain by glacial debris and rock exposure on lakes and rivers is consequently poor. However, outcrop is plentiful along the ocean coast. The terrain is rugged and relief of 200 m or more is common.

The geology of parts of the Hopedale block is known from regional reconnaissance studies by Kranck (1953), Christie et al. (1953), Fahrig (1959), Williams (1970), Taylor (1977), Collerson et al. (1976), Brinex Company (1962a, b, 1964, 1971a, b), and from detailed work in the Hunt River area by Jesseau (1976). The authors wish to acknowledge the technical and logistical assistance provided by Brinex Company and staff of the Department of Mines and Energy, Newfoundland and Labrador. Most of the petrographic detail of diabase dykes was provided by S. Tella (pers. comm., 1979). An interim map entitled Florence Lake-Ugjohtok Bay (13K/15, 13N/1, 2) is in preparation.

General Geology

Rocks of the Hopedale block (Fig. 37.1, 37.2) are assumed to be Archean and comprise ortho- and paragneiss and metavolcanic rocks of various ages. These are intruded by rocks of the Elsonian igneous suite in the north and west where contact metamorphism has reset Archean K-Ar ages in rocks near contacts. Hill (1979, pers. comm.) reported an orthopyroxene-clinopyroxene-spinel hornfels facies. To the south the Archean rocks are unconformably overlain by Neohelikian Seal Lake Group and by Aphebian Moran Lake Group. Cataclasis observed in Archean rocks near the unconformity and near Moran Lake Group outliers is probably related to multiphase Hudsonian deformation which affected the Moran Lake Group (Smyth et al., 1978). In the southeast, rocks of the Hopedale block are intruded by a massive to foliated granite suite (Bay of Islands granite). Fluorite, radioactive sphene, zircon, and allanite in the late granitic phases suggest that part of the complex was derived from the Aphebian Aillik metallogenic province (Gandhi, 1978).

Results from the 1978 field season permit a major two-fold division of the rocks of the Hopedale block separated by a possible unconformity. The older division is here defined as Maggo gneiss (granoblastic, layered orthogneiss), and Weekes amphibolite (layered amphibolite). The latter is thought to be the lithostratigraphic equivalent of the Hunt River group defined by Jesseau (1976). Both subdivisions are in upper amphibolite facies (M_1) and are overprinted by middle greenschist metamorphism (M_2). The younger division is here defined as the Florence Lake group of volcanic rocks and the Kanairiktok intrusive suite of granodioritic intrusions which have been folded and metamorphosed to middle greenschist facies (M_2). The Florence Lake group is characterized by mafic flows (basalt-andesite) and intermediate to felsic pyroclastic rocks.

Airphoto interpretation of gneissic trends and limited mapping (Fig. 37.2) shows an older gneiss trend (north to northwest) discordant to a younger northeast trend. This structural discordance, combined with the metamorphic evidence, is used to postulate an unconformity between the Florence Lake group and older Maggo gneiss and Weekes amphibolite.

The calcareous character of the felsic and intermediate tuffs, as well as disseminated sulphides and Cu-stain in quartz veins, suggests that the Florence Lake succession may be an attractive exploration target for exhalative mineral deposits.

Description of Formations

Maggo gneiss, Weekes amphibolite and Kanairiktok intrusive suite are subdivisions defined here to replace parts of what is commonly called Hopedale gneiss. Kranck (1953) and Christie et al. (1953) used the term Hopedale gneiss to

distinguish between a well banded gneiss of amphibolite-granulite facies southeast of Kaipokok Bay (Domino gneiss) and a schlieric foliated gneiss with abundant amphibolite inclusions northwest of Kaipokok Bay (Hopedale gneiss). In Kaipokok Bay area, Sutton (1972) used the term Hopedale Complex to distinguish reworked Archean gneisses (Hudsonian) from deformed Aphebian English River greenstones and massive to deformed Aphebian granites. Taylor (1977) has used Hopedale Gneiss for all Archean rocks of eastern Nain Subprovince.

Weekes Amphibolite

Mapped as the oldest rocks are ubiquitous rafts of coarse grained, metamorphically layered amphibolite within layered tonalite gneiss (Maggo gneiss). Layers vary from 10 to 100 cm thick and contain hornblende, biotite, plagioclase, garnet, diopside, and rare orthopyroxenes (M_1 -metamorphism). Middle greenschist assemblages include actinolite/tremolite, epidote, biotite, chlorite, carbonate, and feldspar (retrograde or M_2 -metamorphism). Most rafts range from 3 to 6 m thick and 6 to 200 m in length. However, 3 km southeast of Weekes Lake (20 km northeast of Snegamook Lake) and west of Big Bay (Hill, 1978), units have been mapped containing 60 to almost 100 per cent amphibolite in tonalite gneiss. Both amphibolite rafts and mappable units are interpreted here to be lithostratigraphically similar to amphibolite members of the Hunt River group, which records several deformations and metamorphisms (Jesseau, 1976).

Maggo Gneiss

Maggo gneiss is a granoblastic tonalite and is interpreted as intruding the Weekes amphibolite. The contact between a layered tonalite unit (Maggo gneiss?) and amphibolite of the Hunt River group (Weekes amphibolite?) at Hunt River is abrupt and was tentatively interpreted by Jesseau (1976) to be a faulted contact. The gneiss is medium grained, granoblastic, leucocratic (generally 5 to 10% biotite and 2 to 5% hornblende) and various shades of grey. Pegmatite and aplite of several ages are lit-par-lit as well as cross-cutting. Biotite, hornblende, quartz, oligoclase, and sparse garnet in varying proportions are arranged in layers. Overprinting by middle greenschist facies produced poikiloblastic epidote, chlorite, muscovite and quartz + feldspar symplectites, commonly with planar fabrics discordant to layering.

The Maggo gneiss is characterized by the presence of medium grained, granoblastic hornblende-plagioclase layers that are generally concordant with the tonalite gneiss and are isoclinally folded with the tonalite gneiss. They are thought to have originated as basic dykes (Plate 37.1, fig. 1). The near concordance is a result of deformation and locally discordance of 10 to 15° can be observed. Locally the dykes are intruded by the tonalite gneiss (Plate 37.1, fig. 4). Coarsened hornblende rims 4 cm thick on amphibolite inclusions formed after the last deformation and disruption of dykes. Pegmatite with hornblende generally surrounds the mafic layers. Jesseau (1976) observed 'mafic lenses' in a unit of layered gneiss (Maggo gneiss?) adjacent to rocks of the Hunt River group but interpreted these as volcanic rock inclusions. The dykes are a useful criterion for distinguishing Maggo gneiss from younger, gneissic Kanairiktok intrusives where these rocks are highly strained.

Florence Lake Group

The Florence Lake succession consists of mafic flows and intermediate to felsic pyroclastic rocks. Epiclastic rocks are rare and flows more felsic than basalt-andesite were not recognized. The group forms a belt 65 km long extending in a

Table of Formations

Eon	Map Unit	Lithology
Proterozoic	Undivided dykes: diabase and gabbro	Harp Lake dykes: olivine and mauve-coloured augite; 5 to 15% altered; post 1.45 Ga. Kikkertavak dykes; pigeonite (\pm augite) and rims of hornblende on pyroxene; 40 to 70% altered to actinolite, carbonate, chlorite, zoisite, sericite-muscovite and leucoxene.
	Intrusive contact	
?	?	
Archean or Early Proterozoic	Kanairiktok intrusive suite	Foliated, grey to pale pink, coarse and medium grained, biotite/hornblende, granodiorite, tonalite and minor pink granite; mafics altered to actinolite/tremolite, epidote, chlorite, muscovite and calcite (M_2 -metamorphism).
	Intrusive contact	
	Meta-ultramafic suite	Serpentinite, metapyroxenite, minor metagabbro.
	Intrusive contact	
	Florence Lake group	M_2 -metamorphism.
	Lise Lake formation	Felsic (colour index <15-20) tuff, lapilli tuff, lappilistone; poorly sorted, locally banded; generally not reworked; disseminated sulphides and rare cherty pyrite horizons; generally grades to aphanitic members containing blue quartz clasts; includes 20% intermediate rocks.
	Adlatok formation	Intermediate (colour index 15-20 – 35-40) pyroclastic rocks with minor argillaceous sandstone and siltstone; tuff, lapilli tuff, volcanic breccia; poorly sorted but locally finely layered; porphyritic sills; includes 50% mafic and felsic rocks; quartz veins with blue Cu stain.
Schist Lakes formation	Mafic (colour index 35-40 – 70) layered flows and sills intercalated with 20% intermediate and felsic rocks; sills reflect composition of host rocks; minor ferruginous metachert sulphide facies.	
?	?	
Archean	? Unconformity ?	
		$M_1 + M_2$ -metamorphism
	Maggo gneiss	Medium grained, granoblastic, mafic hornblende-andesine dykes; layered, leucocratic, biotite-tonalite gneiss with sparse garnet; abundant felsic lit-par-lit aplite and hornblende-bearing pegmatite.
	Weekes amphibolite	Remnants of presumed Hunt River group amphibolite probably intruded by tonalite; coarse grained, layered hornblende + plagioclase + garnet (\pm pyroxene and M_2 biotite, epidote and actinolite); medium grained, granoblastic hornblende gneiss.

north-northeasterly direction (Fig. 37.2). Between Ugjoktok and Adlatok bays the succession has a map thickness of 5 km and ratio of mafic flows to intermediate and felsic pyroclastic rocks is 3:1. To the southwest the main belt consists of mafic flows and pyroclastics in a ratio of 2:1. The sequences to the northeast and southwest are probably time stratigraphic equivalents.

Volcanic rocks are everywhere intruded by rocks of the Kanairiktok intrusive suite. The top and bottom of the volcanic succession are not known. Three formations based on colour index and texture are as follows:

Schist Lakes formation: colour index 35-40 – 70; includes 20 per cent intermediate and felsic rocks.

Adlatok formation: colour index 15-20 – 35-40; includes 50 per cent mafic and felsic rocks.

Lise Lake formation: colour index <15-20; includes 20 per cent intermediate rocks.

Schist Lakes Formation

This formation comprises mainly fine- to medium-grained, foliated, pale to medium green, flows and sills. Flows locally exhibit saucer-like pillows with long dimensions up to 1 m and maximum widths up to 20 cm. Relict basaltic textures are locally present but the mafic mineralogy is altered to secondary chlorite, carbonate, amphiboles (cummingtonite and tremolite/actinolite), epidote, quartz and veins of quartz + carbonate + epidote. Sills are also present and these locally show medium- to coarse-grained cumulate texture; primary texture and some mineralogy is rarely preserved. Relict euhedral zoned plagioclases and pyroxenes, pseudomorphed by magnetite dust and colourless amphibole or serpentine, are recognized in ultramafites.

Some mafic rocks are locally layered, especially near contacts with intrusive granitic rocks. Gneissic layers range from ultramafic to intermediate with xenoblastic-poikiloblastic garnet. Quartz, leucogranite and pegmatite veins locally represent 5 per cent of the outcrop. Metamorphic banding (contact metamorphism) and mineralogy are best developed where rafts of these supracrustals lie in meta-granodioritic rocks of the Kanairiktok suite (Plate 37.1, fig. 3). Here, contact metamorphism has produced plagioclase, diopside, hornblende, and garnet. However, this assemblage is retrogressed to greenschist facies during M₂ metamorphism, which is a regional prograde facies for the Florence Lake group and granodioritic rocks intruding it.

Flows exhibiting primary alteration (pre-metamorphic) were recognized. These are patchy pale green, fine grained epidote- and carbonate-rich (5-30%) rocks with 5 to 10 per cent veins of epidote and carbonate. The member is generally brecciated and is probably a fumarolically altered flow breccia. Rusty ferruginous schist with felsic and intermediate tuff contains 1 to 2 per cent disseminated pyrite.

Intercalated with mafic rocks are felsic and intermediate tuffs that contain quartz and feldspar porphyry sills similar in composition to those found in Lise Lake and Adlatok formations. Impure limestone (10 to 20% muscovite + quartz + amphibolite + sulphides + tourmaline) locally forms beds 0.5 to 3 m thick.

Adlatok Formation

Pyroclastic rocks comprise intermediate to felsic tuffs, lapilli tuff, lapillistone, tuff breccia and volcanic breccia.

Tuffs are schistose, pale olive-green, with weathered and 'fresh' surfaces commonly pitted. Locally, they have fine layering (1-5 cm) that is probably primary bedding

accentuated by metamorphic mineral growth. Composition and texture vary widely. Sand-sized clastic quartz (10-30%) locally gives way to entirely clastic feldspar and felsic to intermediate volcanic rock fragments. Quartz-rich varieties are probably reworked. Tuffs are poorly sorted, and those fragments not highly strained are angular to subrounded. Locally, felsic to intermediate lapilli-rich layers contain calcareous or argillaceous matrix. Rare poikiloblastic garnet occurs in most mafic layers. Matrices of chlorite, carbonate, epidote, and muscovite contain poikiloblastic-porphyroblastic, rusty calcite, and epidote. Altered feldspar, quartzite, and feldspar-quartz clasts are readily recognized.

Lapilli tuff and lapillistone are pale to medium green schists in which fragments weather paler than 'matrix'. Such 'matrix' is chlorite-rich with cummingtonite and carbonate, and probably represents recrystallized mafic fragments 2 to 64 mm in length. Layering (bedding) is common and varies from 0.5 to 30 m.

Coarser fragmental rocks (25 cm fragments) are recognized as tuff breccia and volcanic breccia. Locally, calcite-rich lenses and quartz veins make up 5 per cent of the outcrop. Flattened fragments attain length to thickness ratios of 20:1.

Sandstones and siltstones are locally developed, but generally the unit is a succession of carbonate-rich argillaceous(?) pyroclastic rocks.

Lise Lake Formation

This unit includes felsic to intermediate tuff, lapilli tuff, lapillistone and spotted tuff, as well as sills and undivided felsic volcanic rocks.

Tuffs are strongly foliated, generally white, pale green to buff weathering or variegated. They contain abundant euhedral and zoned feldspar crystals, crystal fragments, felsic to intermediate volcanic rock fragments, and less than 10 per cent calcite quartz. The rocks are only locally reworked and are generally poorly sorted, with angular fragments. The formation contains 20 per cent interbedded, texturally identical rocks constituting the Adlatok formation. Beds, probably altered during folding and metamorphism, are 0.25 to 5.0 m thick. Fragments in lapillistone attain lengths of 3 cm.

Spotted tuff is a distinctive unit. Rusty crystals (1 x 2 mm in size) of red-brown calcite form tabular porphyroblasts. The rock also contains relict euhedral plagioclase in a uniform matrix of quartz, muscovite, chlorite, carbonate and epidote.

Quartz veins carrying pyrite and chalcopyrite generally intrude unbedded felsic tuffs and sills, which themselves contain 1 to 2 per cent finely disseminated sulphide.

One member, separately mapped in only one locality, but also recognized locally throughout the felsic formations, is an aphanitic pale green to pale pink tuff with glassy appearance and blue quartz eyes. This unit generally contains pyrite-rich beds.

Meta-ultramafic Suite

Ultramafic rocks intrude the Florence Lake group 2 km south of Florence Lake and amphibolite 3 km north of Kanairiktok River at longitude 61°02'. The regionally concordant ultramafites south of Florence Lake have a strike length of 8 km and vary from 0 to 300 m in thickness. The rocks have not been studied in detail, but reddish brown and blue-grey weathering phases seem to predominate.

Red-brown phases (dark green in fresh surface) are fine grained to massive with soft weathering rinds of carbonate and talc and pillow-like joints. Blue-grey phases are layered

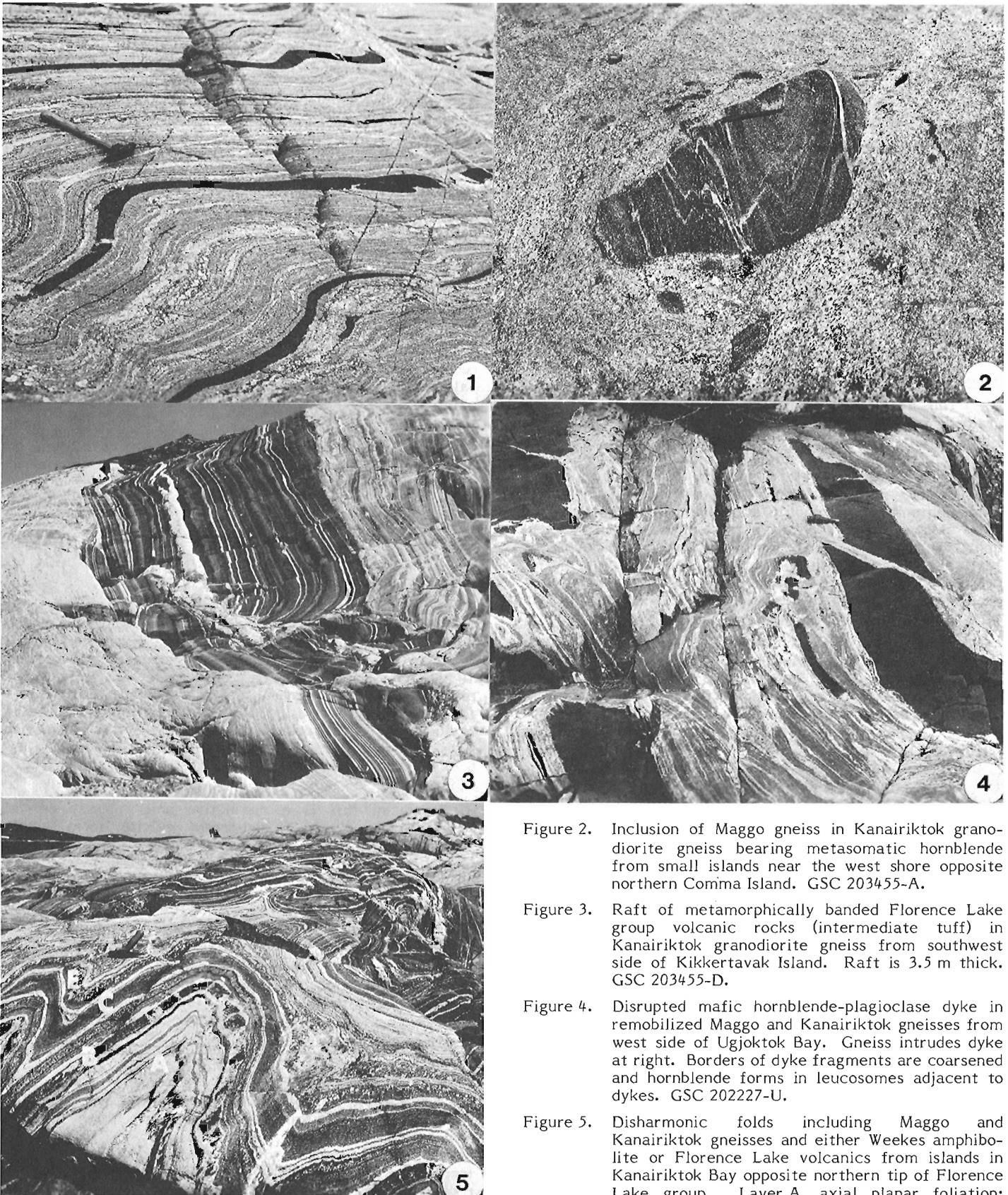


Figure 1. Three limbs of isoclinal folds in granoblastic Maggo gneiss containing a hornblende-plagioclase dyke from west shore of Adlatok Bay. GSC 202227-V.

Figure 2. Inclusion of Maggo gneiss in Kanairiktok granodiorite gneiss bearing metasomatic hornblende from small islands near the west shore opposite northern Comma Island. GSC 203455-A.

Figure 3. Raft of metamorphically banded Florence Lake group volcanic rocks (intermediate tuff) in Kanairiktok granodiorite gneiss from southwest side of Kikkertavak Island. Raft is 3.5 m thick. GSC 203455-D.

Figure 4. Disrupted mafic hornblende-plagioclase dyke in remobilized Maggo and Kanairiktok gneisses from west side of Ugjoktok Bay. Gneiss intrudes dyke at right. Borders of dyke fragments are coarsened and hornblende forms in leucosomes adjacent to dykes. GSC 202227-U.

Figure 5. Disharmonic folds including Maggo and Kanairiktok gneisses and either Weekes amphibolite or Florence Lake volcanics from islands in Kanairiktok Bay opposite northern tip of Florence Lake group. Layer A, axial planar foliation; layer B, mafic layer boudined on left limb, and deformed by axial planar foliation on right limb; layer C, folded gneissosity; layer E, axial planar augen comprising garnet centres surrounded by plagioclase surrounded by hornblende. GSC 202227-W.

to massive. The thickness of discontinuous layers (2 to 3 m long) varies from 1 to 10 cm; tremolite-rich layers are separated by several metres of serpentinitic rock. Gabbroic layers and brittle asbestos fibre 0.5 cm long with calcite have been identified.

Kanairiktok Intrusive Suite

A great variety of foliated and gneissic rocks, predominantly granodioritic to tonalitic in composition, occurs in the map area. No massive granite was recognized within the Hopedale block, although pegmatite related to Proterozoic intrusions occurs near the edge of the block.

Two main phases were mapped. One, a medium- to coarse-grained, pale pink, leuco- to mesocratic granodiorite, intrudes and surrounds the Florence Lake group. Mafic minerals are secondary poikiloblastic epidote and chlorite + carbonate after hornblende. Preliminary information suggests that this phase, mixed with Maggo gneiss, extends eastward to the Proterozoic unconformity (Fig. 37.2) where it is overlain by Moran Lake Group and intruded by Bay of Islands granite. Locally, tonalitic and granitic, as well as older augen tonalite phases, constitute the Kanairiktok suite. Volcanic rock rafts and inclusions are common near the volcanic belt where granodiorite also exhibits cataclasis and kink-folds. The second main phase is a leucocratic, light grey, porphyroblastic augen (plagioclase + quartz) gneiss exhibiting various degrees of strain. This phase intrudes volcanic rocks in Adlatok Bay immediately northeast of the northernmost extent of the belt. Locally, the rock contains hornblende as a result of reaction with mafic gneiss (Plate 37.1, fig. 2, 4).

Both phases are metamorphosed to greenschist facies. Zoned, crushed and partly recrystallized andesine is 80 per cent saussurite. Epidote forms poikiloblastic grains with quartz in areas of quartz + plagioclase symplectite. Relict hornblende occurs with new biotite + chlorite + muscovite bent around elongated pods of quartz and feldspar. In areas of high strain, Maggo gneiss and gneissic Kanairiktok rocks are distinguished by the occurrence of hornblende-plagioclase dykes in older Maggo gneiss.

Undivided Diabase and Gabbro Dykes

Abundant diabase and gabbroic dykes, generally striking 025° to 045° characterize the Hopedale block. Dykes vary from 0.5 to 100 m in thickness and tend to be subparallel to host rock gneissosity. Consequently, a number of dykes strike northwest or north in areas where regional foliation is northerly. Taylor (1977) considered the dykes to be Neohelikian on the basis of three K-Ar whole-rock analyses (ca. 1.1 Ga).

East and west of the Hopedale block, dykes striking 045° to 070° intrude Aphebian(?) Bay of Islands granite, Aillik Group sediments (Fahrig and Larochelle, 1972; Taylor, 1977), and Harp Lake suite (Meyers and Emslie, 1977). Harp dykes are post 1.45 Ga and two whole-rock K-Ar analyses yielded ages of 1.1 and 1.3 Ga.

Some dykes within the Hopedale block also show strike directions between 045° and 070°, and like Harp and Aillik dykes contain mauve-coloured titanite and 10 to 20 per cent fresh to slightly altered olivine in dykes that overall are 5 to 15 per cent altered. A set of dykes considered to be older (Kikkertavak dykes) than the olivine-bearing ones are 40 to 70 per cent altered and some contain epidote, actinolite, chlorite and carbonate. Among the altered dykes, a further two-fold division can be made on the basis of the presence or absence of amphibole rims around pigeonite. A number of gabbroic dykes have dioritic differentiates and some show pervasive cataclasis. Kranck (1953) reported that some dykes have brecciated contacts. Altered dykes generally show no internal tectonite fabric and none contain orthopyroxene.

Evidence for at least two ages of dykes is also provided by paleomagnetic studies which show diffuse grouping of paleopoles from dykes sampled south and north of Hopedale (K.W. Christie, pers. comm., 1978). Some dykes contain sericitized plagioclase crystals 20 cm in length in aphanitic, chilled contact zones. Others show definitive as well as ambiguous crosscutting relationships. An analysis relating swarm directions to mineralogy, to grain size, and to paleomagnetic pole positions, is in progress.

Metamorphism, Structure, and Geochronology

Early layered Weekes amphibolite contains hornblende, plagioclase, clinopyroxene, and garnet. Maggo gneiss associated with this amphibolite and characterized by gneissic, mafic, hornblende-plagioclase sheets (dykes), contains biotite, hornblende, and garnet. Together these assemblages reflect middle to upper amphibolite facies metamorphism (M_1). Isoclinal folds defined by north-striking layering in Maggo gneiss are transposed to a northeasterly direction along Ugjoktok and Adlatok bays, where Kanairiktok rocks predominate. This structural trend, the same trend as axial planes of the Florence Lake volcanic belt, persists eastward to the unconformity and intrusive contact of Aphebian rocks.

The Florence Lake succession and Kanairiktok suite that intrude it contain actinolite/tremolite, cummingtonite, poikiloblastic epidote, chlorite, muscovite, calcite, possibly biotite, and partly recrystallized feldspar and quartz. These assemblages constitute middle greenschist facies (M_2) which is seen as a retrograde metamorphism in Maggo gneiss and Weekes amphibolite and in contact metamorphosed borders and rafts of Florence Lake group rocks. Contact metamorphism has produced garnet + andalusite; B. Ryan (pers. comm., 1979) has noted garnet + cordierite + staurolite in metasedimentary rafts northwest of Florence Lake. Flattening in M_2 assemblages is locally intense and regional F_2 folds are characterized by meso- and microscopic chevron folds. Together, the metamorphism and regional structural discordance are taken as evidence of an unconformable relationship between Maggo gneiss (M_1) and Florence Lake group succession (M_2).

Jesseau (1976) recognized four deformational styles in the Hunt River amphibolites, indicating that the present analysis is far from complete. Hill (1978) also found two groups of gneiss in which the younger member intrudes a more complexly deformed amphibolite-bearing gneiss in Davis Inlet.

Three K-Ar biotite and hornblende ages, GSC 61-196 (Lowdon et al., 1963), GSC 62-178 (Leech et al., 1963) and GSC 63-172 (Wanless et al., 1965) show that some rocks of the Hopedale block cooled past their blocking temperatures 2.4 (biotite) to 2.7 (hornblende) Ga ago. Sample GSC 62-178 (biotite from 'granitic gneiss') was collected 6 km from Florence Lake group east of the head of Ugjoktok Bay, but it is not known whether the sample represents Maggo or Kanairiktok gneiss. If the sample was Maggo gneiss then the age reflects either cooling from amphibolite facies or contact metamorphism during Kanairiktok intrusion, or greenschist facies during M_2 -metamorphism. If the latter two events are reflected in this age of 2.4 Ga, then the unconformity and indeed Florence Lake group are Archean. However, middle greenschist metamorphism may not be represented by this age and consequently the age of the volcanic rocks is not known. Judging from their gross lithology and metallogenesis they are thought to be Archean.

Conclusion

The Florence Lake volcanic succession was deposited on Archean Maggo gneiss and Weekes amphibolite that record polyphase deformation and metamorphism prior to deposition of the Florence Lake group. The Florence Lake group

comprises a bimodal succession of basal(?) mafic flows and sills (Schist Lakes formation) with upward(?) development of intermediate (Adlatok formation) and felsic (Lise Lake formation) pyroclastic rocks and sills. Sills reflect host compositions and those in mafic flows develop layers that may be cumulate textures. Pyroclastic rocks include tuff, lapilli tuff, lapillistone and volcanic breccia, generally rich in calcite. Although rare occurrences of limestone, siltstone and sandstone were noted, the succession lacks epiclastic rocks and flows less mafic than basalt-andesite. A suite of meta-ultramafic rocks intrudes Florence Lake group and Weekes amphibolite.

The volcanic environment is seen as one with calc-alkaline flows with two-thirds to one-half pyroclastic and fumarolic activity. Although pyroclastic rocks have well developed layering (bedding) locally, they are generally poorly sorted and not reworked. In several localities massive pyrite and pyrite-rich beds are developed in intercalated intermediate tuffs and mafic volcanics. Felsic rocks generally carry disseminated sulphides and pyrite-rich beds. Quartz veins with pyrite and copper-stain were noted, particularly in the northern portion of the belt. These rocks represent a favourable target for exploration of exhalative-fumarolic-related sulphide deposits.

Granodioritic rocks (Kanairiktok intrusive suite) intrude all other units and represent the last major igneous activity in the area. The last phase of deformation generally produced northeast-trending disharmonic folds in all rocks east of Adlatok and Ugjoktok bays (Plate 37.1, fig. 5). The transposition of northerly striking Maggo gneiss into the northeast M₂ trend may have occurred at this time. If this trend direction is of Archean age then the uraniferous Aphebian Aillik deposits were developed on northeast-southwest-trending Archean paleosurfaces whose structural trend was mimicked by the Hudsonian orogeny.

Diabase and gabbro dykes in the Hopedale block may be of at least two ages, based on swarm direction and composition. The older swarm (Kikkertavak dykes) predominates and strikes 025° to 045°. They exhibit altered mineralogy (40-70% altered), indicative of subgreenschist facies. The younger suite (5 to 15 per cent altered) contains mauve-beige titaniferous augite and 10 to 20 per cent olivine, characteristics shared by Harp and Aillik dykes. The older suite, typical of Archean terrane in Nain Province, is apparently recognized neither in the Moran Lake group nor in the Aillik Group, and hence these dykes may be early Aphebian (B. Ryan, pers. comm., 1978), altered during Hudsonian orogeny.

References

Brinex

- 1962a: Geological plan, Anomaly 13B; Map G63001-3; scale 1 inch = 200 ft.
- 1962b: Geology of Second Chance Lake; Map G63001-10; scale 1 inch = 2640 ft.
- 1964: Shapiro/Ujutok concession, Labrador geology; Map G64010; scale approx. 1 inch = 3333 ft.
- 1971a: Geological survey northwest of Florence Lake 6-03/1970; Map G71007-1; scale 1 inch = 2000 ft.
- 1971b: Geological survey Ujutok Bay 6-03/1970; Map G71006-1; scale 1 inch = 2000 ft.

Christie, A.M., Roscoe, S.M., and Fahrig, W.F.

- 1953: Preliminary Map, Central Labrador Coast, Newfoundland; Geological Survey of Canada, Paper 53-14, 3 p.

Collerson, K.D., Jesseau, C.W., and Bridgwater, D.

- 1976: Crustal development of the Archean gneiss complex: Eastern Labrador; in *The Early History of the Earth*, Brian F. Windley, ed., John Wiley & Sons, p. 237-253.

Fahrig, W.F.

- 1959: Snegamook Lake (west half), Newfoundland; Geological Survey of Canada, Map 1079A, scale 1 inch = 4 miles.

Fahrig, W.F. and Laroche, A.

- 1972: Paleomagnetism of the Michael Gabbro and possible evidence of the rotation of Makkovik Subprovince; *Canadian Journal of Earth Sciences*, v. 9, p. 1287-1296.

Gandhi, S.S.

- 1978: Geological setting and genetic aspects of uranium occurrences in the Kaipokok Bay - Big River area, Labrador; *Economic Geology*, v. 73, no. 8, p. 1492-1522.

Greene, B.A.

- 1970: Geological Map of Labrador; Department of Mines and Energy, Newfoundland; Map scale 1:1 000 000.

Hill, John

- 1978: Summary of the Geology of the Davis Inlet area; in *Preliminary Project Reports, for 1978*, Department of Mines and Energy, Newfoundland, Report 78-10, p. 91-93.

Jesseau, C.W.

- 1976: A structural-metamorphic and geochemical study of the Hunt River supracrustal belt, Nain Province, Labrador; unpubl. M.Sc. thesis, Memorial University of Newfoundland, 211 p.

Kranck, E.H.

- 1953: Bedrock geology of the Seaboard of Labrador between Domino Run and Hopedale, Newfoundland; Geological Survey of Canada, Bulletin 26, 45 p.

Leech, G.B., Lowdon, J.A., Stockwell, C.H., and Wanless, R.K.

- 1963: Age determinations and geological studies; Geological Survey of Canada, Paper 62-17.

Lowdon, J.A., Stockwell, C.H., Tipper, H.W., and Wanless, R.K.

- 1963: Age determinations and geological studies, Report 3; Geological Survey of Canada, Paper 62-17, 140 p.

Meyers, R.E. and Emslie, R.F.

- 1977: The Harp dikes and their relationship to the Helikian geological record in central Labrador; *Canadian Journal of Earth Sciences*, v. 14, p. 2683-2696.

Smyth, W.R., Marten, B.E., and Ryan, A.B.

- 1978: A major Aphebian-Helikian unconformity within the Central Mineral Belt of Labrador: definition of new group and metallogenic implications; *Canadian Journal of Earth Sciences*, v. 15, p. 1954-1966.

Sutton, J.S.

- 1972: The Precambrian gneisses and supracrustal rocks of the western shore of Kaipokok Bay, Labrador, Newfoundland; *Canadian Journal of Earth Sciences*, v. 9, p. 1677-1692.

Taylor, F.C.

- 1977: Geology - Hopedale, Newfoundland; Geological Survey of Canada, Map 1443A.

Wanless, R.K., Stevens, R.D., Lachance, G.R., and Rimsaite, R.Y.H.

- 1965: Age determinations and geological studies; Geological Survey of Canada, Paper 64-19 (Part 1).

Williams, F.M.G.

- 1970: Snegamook Lake (east half), Newfoundland; Geological Survey of Canada, Open File 42.

Project 770035

P.A. Egginton
Terrain Sciences Division

Egginton, P.A., *Mudboil activity, central District of Keewatin; in Current Research, Part B, Geological Survey of Canada, Paper 79-1B, p. 349-356, 1979.*

Abstract

A variety of processes cause horizontal and vertical movements in mudboils in central District of Keewatin. Differential heaving was found to cause horizontal displacements by inducing creep and by locally concentrating moisture such that gelifluction occurred when the muds thawed. Mudboils immediately upslope and downslope of snow patches, because of excessive moisture, experienced the most rapid surface displacements (0.6 m/year). Caribou migration may be another process responsible for inducing activity from time to time in mudboils over a large portion of central Keewatin.

Introduction

Mudboils are ubiquitous on the till and marine silts of central District of Keewatin (Egginton and Shilts, 1978; Shilts, 1978). The mudboils vary greatly in size, ranging from a few tens of centimetres to several metres in diameter. The form is typically round on low angle slopes but becomes elongate and/or step-like on slopes greater than a few degrees (Fig. 38.1). A vegetated border commonly gives the feature its patterned form. The mudboils can be mobile as vegetation commonly is found included at the downslope edge of the features, a result of overriding and of burial of vegetation by extruded or flowing muds. This paper reports on movements associated with this mobile patterned form.

Acknowledgments

I would like to thank W.W. Shilts for providing the 1973 and 1975 data presented in this report. Thanks also are extended to the personnel and to the owner of Henik Lake Lodge (Grand Domain Retreats) for the support they provided during the 1977 and 1978 field seasons.

Instrumentation

A number of slopes in central District of Keewatin, in the vicinity of Victory, North Henik, Kaminak, and Ferguson lakes (Fig. 38.2) are being monitored using a variety of techniques to provide information on the type and magnitude of movement associated with mudboils (Egginton and Shilts, 1978).

Numbered aluminum tags held by nails were placed at predetermined spacings on the surface of individual mudboils (30 to a mudboil). The spacings between the tags were remeasured over time and give data on movement relative to other tags.

At nine sites clear plastic tubes 10 cm diameter and 183 cm long were buried at or near the bottom of the active layer. The plastic tubes were slotted to permit mud intrusion. Large boulders weighing up to 20 kg were placed on the tubes when they were installed in 1973.

Bench marks, consisting of 2 cm diameter copper clad rods, the type commonly used by the Geodetic Survey, Energy, Mines and Resources, were installed on 12 slopes and



Figure 38.1. Mudboils displaying a step-like form, Kaminak Lake. The notebook in the foreground gives scale. (GSC 203165-1)

were used in conjunction with a theodolite to provide measurements of the vertical and horizontal position of 20 or more wooden targets placed along each slope. The targets consisted of 2 cm squares, 0.5 cm thick, with a central notched sighting screw.

In addition, two types of heave recorders were installed on various slopes at North Henik and Kaminak lakes. The simplest type consisted of a scribe of hardened steel mounted on an inverted 'T' plate. A copper-clad rod anchored to permafrost passed through the stem of the plate. Any vertical movement of the plate and the ground caused the scribe to move up or down the rod, recording the event (Fig. 38.3). Several modified hygrothermographs were mounted on copper-clad rods anchored in the permafrost. The instrument was modified such that any vertical movement of the ground surface (transmitted through an aluminum rod) caused one of the pen arms to move against the drum (Fig. 38.4). In this manner a continuous record of heave or subsidence was maintained at a number of sites located in the central portions of mudboils or in the vegetated borders.

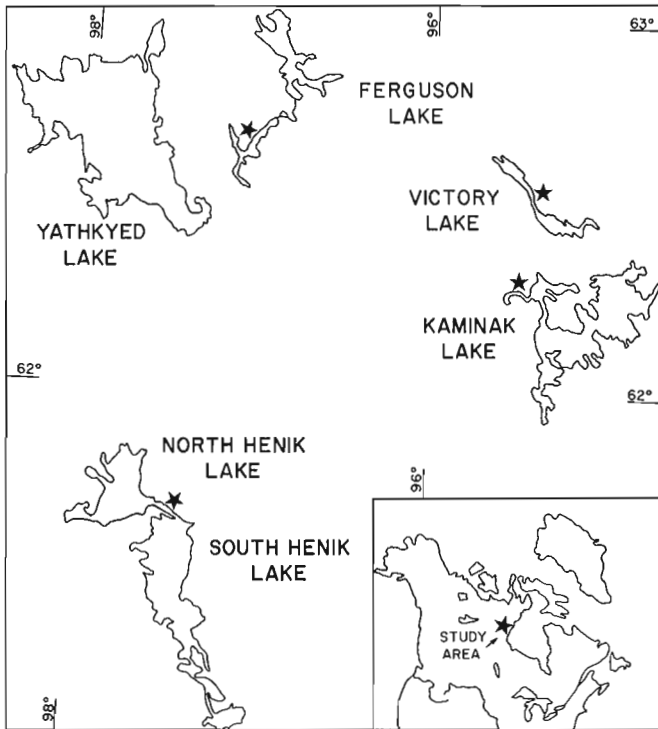


Figure 38.2. The location of study sites (stars), central District of Keewatin.

Observations

Horizontal Movements

Aluminum tags were first installed in 1973 at two mudboils (no. 5 and no. 6) in the vicinity of Kaminak Lake; the sites were revisited in 1976, 1977, (Egginton and Shilts, 1978) and 1978. A plan view of these mudboils showing central areas of expansion over various times is presented in Figure 38.5. Areas of high activity in one year usually continued to be highly active in subsequent years; however, during some years new areas of activity developed and older ones stabilized. Active areas were readily identified in the field as they contained a greater proportion of fines and had higher moisture contents than the surrounding muds.

Within mudboils no. 5 and no. 6 maximum horizontal movements over the period 1973 to 1978 were 8.0 and 16.0 cm; the maximum recorded values for 1976-77 were 2.0 and 8.0 cm and for 1977-78 were 2.5 and 8.0 cm, for mudboils no. 5 and no. 6, respectively. Over the 5 year period of observation 54 to 89% (for mudboils no. 5 and no. 6, respectively) of all tagged markers moved more than 1 cm while 15 to 22% (for mudboils no. 5 and no. 6, respectively) moved more than 4.0 cm.

Wooden targets surveyed to fixed bench marks provided accurate measurements of surface movement on mudboils over time. Nine slopes were surveyed over the period 1977-1978. Target movements are given for two representative slopes at North Henik Lake (Table 38.1). Movements in the x direction are across the general slope, and movements in the y direction are in the downslope direction. The total horizontal distance moved is given as ΔT ; typical values of ΔT ranged from 1 to 3 cm. Movements were not solely in the general downslope direction; a considerable cross-slope component was typical (cf. Δy and Δx , Table 38.1). The movement was generally away from areas of high microrelief and away from centres of heaving.

At one mudboil the target was displaced by localized gelifluction. The mud, which has a low liquid limit (typically less than 15%), became fluid and moved some 21.7 cm before stabilizing (target 19, site A, Table 38.1). This type of movement was particularly prevalent at study sites in the Kaminak Lake area immediately above or below snow patches which persisted through the early summer months.

Vertical Movements

Annual Movement Plastic tubing installed in 1973 in mudboils in the vicinity of Kaminak and Victory lakes were revisited in 1975, 1977, and 1978. The depth below the ground surface to both the tube bottom and the mud surface within the tube was determined. Boulders originally placed on top of the tubes to keep them positioned near the bottom of the active layer apparently fell off some sites soon after installation. The tubes subsequently were extruded from the ground at rates of up to 35.5 cm/year, although lower rates were more typical (Table 38.2). Over the same period, and possibly synchronously with tube extrusion, mud was intruded to various levels within the tubes.

Yearly subsidence data (subsidence being defined here as the settlement resulting from the thawing of yearly heaved ground) are presented for three recorder sites at North Henik Lake (Fig. 38.6). Sites no. 1 and no. 4 were located in the central portions of mudboils, and site no. 5 was located within the vegetated border of a mudboil. The shape of the subsidence curve at the vegetated border site (site no. 5) is quite different from that for sites no. 1 and no. 4 as subsidence in the former occurred at a more constant rate

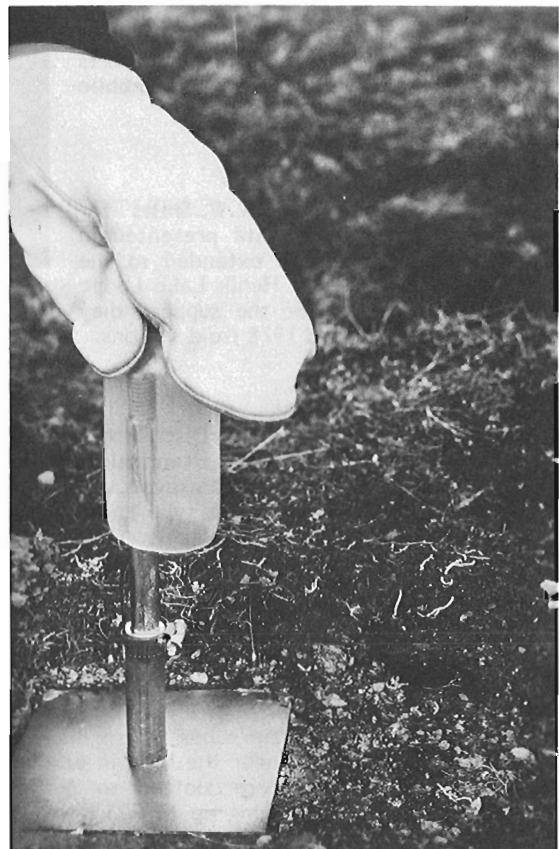


Figure 38.3. A scribe recorder used to monitor surface heave. Vertical ground movements cause the hardened steel scribe (held in place by the pipe clamp) to scratch the permafrost-anchored, copper-clad rod. (GSC 203502-A)

over a longer time period. Between 87 and 91% of the total subsidence recorded at sites no. 1 and no. 4 had occurred by July 1 compared with 71% at the vegetated site (no. 5). The ground had begun to thaw somewhat by the time measurements commenced in 1978; thus, values of yearly subsidence of 8.7 and 7.1 cm for sites no. 1 and no. 4 and 3.8 cm for the vegetated site (no. 5) are likely minimal.

Thaw Depths, 1978 The depths of thaw through time (1978) are shown for mudboil centres and vegetated borders in the Henik lakes area (Fig. 38.7). The data points represent the average of several measurements. The thaw depths varied considerably at a point in time as an indeterminate function of mudboil size and the insulative quality of the vegetation border. The values for September are probably very close to yearly maxima. Thaw depths increased from July 1 to September 2 by a factor of 2.5 for the central mudboils and a factor of 2 for the vegetated borders. In spite of this, limited subsidence accompanied ground thaw after July 1 (cf. Fig. 38.6, 38.7).

Short Term Vertical Movements The modified hygrothermographs provided a continual trace of heave and/or subsidence over time. Two major freezebacks and several minor ones were recorded during the spring of 1978. Figure 38.8 shows a portion of the heave and air temperature record at site no. 3, North Henik Lake for the period June 6 to 14, 1978. Due to the recorder mechanism an upward movement on the graph indicates subsidence, a downward movement heave. The response of the ground (i.e., heave or subsidence) to temperature fluctuations above or below the

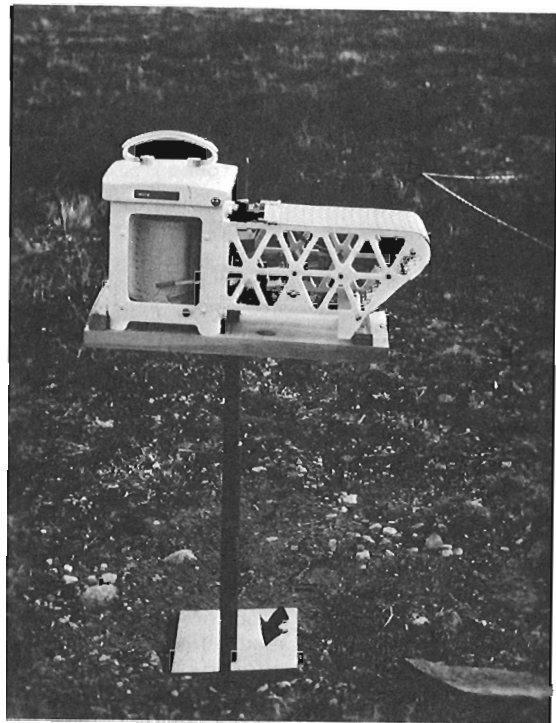


Figure 38.4. A modified hygrothermograph used to monitor surface heave. Vertical movements of the bottom ground plate (see arrow) are transmitted through an aluminum rod to the pen mechanism, and the event is recorded. (GSC 203502-B)

Table 38.1

Horizontal movement occurring on two slopes, North Henik Lake, 1977-78.
 Δx , downslope movement Δy , and total movement ΔT are given (cm)

Target	Downslope movement Δy	SITE A		Downslope movement Δy	SITE B	
		Cross-slope movement Δx	Total movement ΔT		Cross-slope movement Δx	Total movement ΔT
a	-	-	-	-	-	-
b	-	-	-	1.6	4.0	4.3
c	-	-	-	-	-	-
1	2.8	0.6	2.9	1.8	1.6	2.4
2	0.1	0.1	0.1	1.6	1.1	2.0
3	1.5	5.7	5.9	1.7	1.3	2.2
4	2.2	0.1	2.2	0.9	2.6	2.8
5	1.1	0.5	1.2	1.9	2.4	3.1
6	2.9	0.4	2.9	2.2	1.0	2.4
7	1.8	0.5	1.9	1.9	1.3	2.3
8	1.1	1.1	1.6	-	-	-
9	-	-	-	1.0	1.3	1.6
10	-	-	-	0.0	0.0	0.0
11	-	-	-	2.1	2.0	2.9
12	-	-	-	0.7	0.8	1.1
13	2.8	0.3	2.8	1.3	2.5	2.8
14	0.7	0.4	0.8	2.6	0.7	2.7
15	-	-	-	-	-	-
16	-	-	-	1.2	3.0	3.2
17	1.7	2.9	3.4	-	-	-
18	1.1	0.6	1.3	2.8	3.0	4.1
19	4.3	21.0	21.7	0.2	0.8	0.8
20	0.5	0.5	0.7	0.2	0.2	0.2

freezing point was highly variable but was most pronounced when the temperature fluctuation was of extended duration. At site no. 3 and at other sites, a lag time of 2 to 8 hours between air temperature fluctuation and ground movement was typical.

Air temperatures as low as -9°C over the period June 6 to 8 were sufficient to cause a partial freezeback and a heave of 1.4 cm at site no. 3 (Fig. 38.7); however, temperatures of 4°C maintained for a short duration caused a subsidence on June 8, 1978. Ground movement then remained fairly stable, and mean daily air temperatures were consistently below 0°C until June 12, 1978.

Short Term Thaw Depth Progression

The response of thaw depth to temperature fluctuations over the period June 5 to 14, 1978 was also monitored using a thin metal probe at a mudboil of similar size and adjacent to site no. 3, North Henik Lake. On June 5, at the start of the freezeback described above, the depth of thaw in the mudboil centre was 19 cm and in the vegetated border was 4 cm. By June 6 a perched frozen zone extended to a depth of 0 to 7 cm in the mudboil centre and was underlain by an unfrozen zone extending to 20 cm; the same configuration was found at depths of 0 to 4 cm and 4 to 5 cm in the vegetated border. By 1800h on June 8 the depth of thaw reduced to 12 cm but the perched frozen zone had disappeared; its demise resulted in a subsidence of 0.5 cm and was caused by increased air temperatures on June 8 (Fig. 38.8). Continued low temperatures after June 8 caused further freezeback and the development of another perched frozen zone by June 10. Some minor heaving had occurred by June 12 (Fig. 38.8, 38.9). On June 10 moisture content at the bottom of the perched frozen zone was 13% while the underlying unfrozen zone was somewhat desiccated at 8.5%. This suggests that moisture migrated upward towards the freezing front. The freezeback ended as the temperature rose to 20°C over the period June 12 to 14, producing a subsidence of 1.1 cm.

Discussion

Vertical-Movement Processes

The maximum subsidence value recorded in the Henik lakes area during summer 1978 was 8.7 cm. This value in all probability is fairly representative of the total heave experienced during freeze-up in 1977-78.

Over the period 1977-78 tubes buried at depth within the central portions of mudboils within the Kaminak and Victory Lake areas were extruded at maximum rates of 16.0 to 35.5 cm/year (Table 38.2). Similar vertical surface movements, attributed to heave, have been reported by

Table 38.2

Vertical movements associated with plastic tubes inserted in mudboils, Victory and Kaminak Lakes (all measurements are taken from the ground surface)

		Victory Lake Sites				Kaminak Lake Sites			
		#104	#105	#106	#107	#4	#2A	#2B	#5
A	1973	125.0	150.0	120.0	137.0	85.0	-	-	-
	1975	-	-	-	-	-	-	-	61.0
	1977	112.5	96.0	89.0	85.0	60.0	70.0	76.0	45.0
	1978	77.0	-	-	-	44.0	70.0	66.0	47.0
B	1973-1977	4.2	13.5	7.8	13.0	-	-	-	-
	1975-1977	-	-	-	-	8.3	-	-	8.0
	1977-1978	35.5	-	-	-	16.0	0.0	10.0	-2.0
	1973-1978	12.0	-	-	-	10.3	-	-	-
C	1977	115.0	96.0	83.0	-	36.0	38.0	67.0	27.0
	1978	64.0	51.0	15.0	-	47.0	53.0	35.0	32.0

A - Depth of tube bottom below ground surface (cm)
 B - Rate of extrusion of the tube from the mudboil (cm/year)
 C - Depth to intruded mud within the tube (cm)

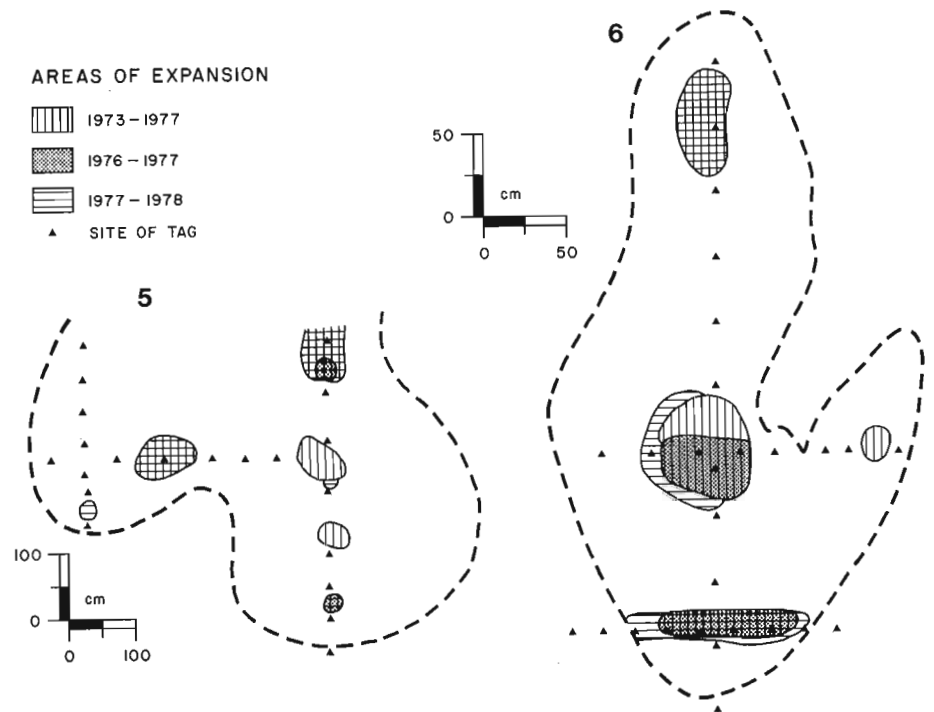


Figure 38.5. A plan view of mudboils 5 and 6 near Kaminak Lake showing areas of rapid expansion over various periods.

Mackay et al. (1979) on earth hummocks (approximately 16 cm) in Inuvik, Northwest Territories and by Fahey (1973) on mudboil-like features (30 cm) in Colorado. It is not entirely clear at the Keewatin sites, however, whether tube extrusion from depth is attributable solely to heave. The presence of diapiric injection structures, first described by Shilts (1978), and the presence of muds intruded into the plastic tubes (cf. 1977 and 1978 values, site no. 104, C, Table 38.2) suggest that differential pressures exist within the mudboils for at least limited periods of time. Tube extrusion may result, in part, from these differential (hydrostatic or artesian) pressures.

Substantial water migration is associated with heave at some field sites. If it is assumed that the measured expansion (heave) results solely from pore water within the mudboils, then a column of water about 87 cm high would be required to produce the measured heave of 8.7 cm at the Henik Lake site. If tube expulsion at Victory Lake is related solely to heave then a column of water 355 cm high would be

required to produce the required heave of 35.5 cm. Because moisture contents in these muds, even at saturation, are less than 20% by weight, and because active layers reach maximum thicknesses of 120 to 180 cm, a substantial influx of water must occur at freeze-up to generate such heave.

Horizontal-Movement Processes

Ground heaving may lead to horizontal displacement of the soil by creep (Washburn, 1967). Potential creep can be calculated if the slope angle and total heave are known. For example heave of 35.5 cm on an assumed uniform slope of 2° (Victory Lake) or 8.7 cm on an assumed uniform slope of 6° (North Henik Lake) produces a potential creep of 1.2 and 0.9 cm, respectively. The term 'potential' is used as capillary pressures tend to make the soil settle back somewhat towards its original position (Washburn, 1967). On the other hand, slopes are rarely uniform, and in central District of Keewatin microrelief is such that local gradients may exceed the general slope by a factor of 2. In such areas actual creep may exceed the potential creep described above.

At the Henik lakes sites horizontal movements were typically of the order of 1 to 3 cm (Table 38.1, ΔT) or somewhat greater than the potential creep described above. The additional movement may, in part, be associated with locally steeper slopes which induce additional creep, or these movements may result from gelifluction. In practice, creep and gelifluction often overlap to such a degree that it is impossible to separate and measure absolutely these various components of horizontal movement. No attempt is made to do so here.

During the heaving process, moisture presumably is drawn to and concentrated in the upper portion of the active layer; samples taken at depths of 50 cm and greater were found to be desiccated in comparison to near-surface samples. The concentration of ice in the upper portion of the active layer may explain why most of the subsidence and horizontal movement recorded in 1978 at the Henik lakes sites occurred in the early summer when the active layer was thawed to less than 50 cm depth (that is little or no ice existed below 50 cm).

Plasticity indices and liquid limits for the muds are low, 0-6% and 12-15%, respectively. These values may be reached when the relatively ice-rich portion of the upper active layer thaws, producing flow-like movement such as that recorded at North Henik Lake (site A, target 19, Table 38.1). As soon as the muds thaw, they dry out and harden rapidly. Spring freezebacks may produce additional heave and horizontal movement by drawing moisture to the surface.

Highly active portions of mudboils (Fig. 38.5) may represent areas of differential heaving where moisture becomes locally concentrated during freeze-up. Because of differential heaving, these active areas experience greater creep and, because of the higher moisture concentration, on thawing, also may experience greater gelifluction than the surrounding muds. At Victory Lake areas of high activity within mudboils are also centres of diapiric injection (Shilts, 1978; Egginton and Shilts, 1978). The relative importance of each process in maintaining areas of expansion in mudboils is not known.

The presence of snow patches through the early summer also may contribute significantly to mud movement. Water moving downslope as interflow within the active layer was observed to come to the surface as the thawed portion of the active layer thinned upslope of a snow patch. This water and snowmelt caused the muds to become saturated. At Kaminak Lake in 1978 mudflows, 0.6 m long, originating from mudboil centres were common both upslope and downslope of snow patches.

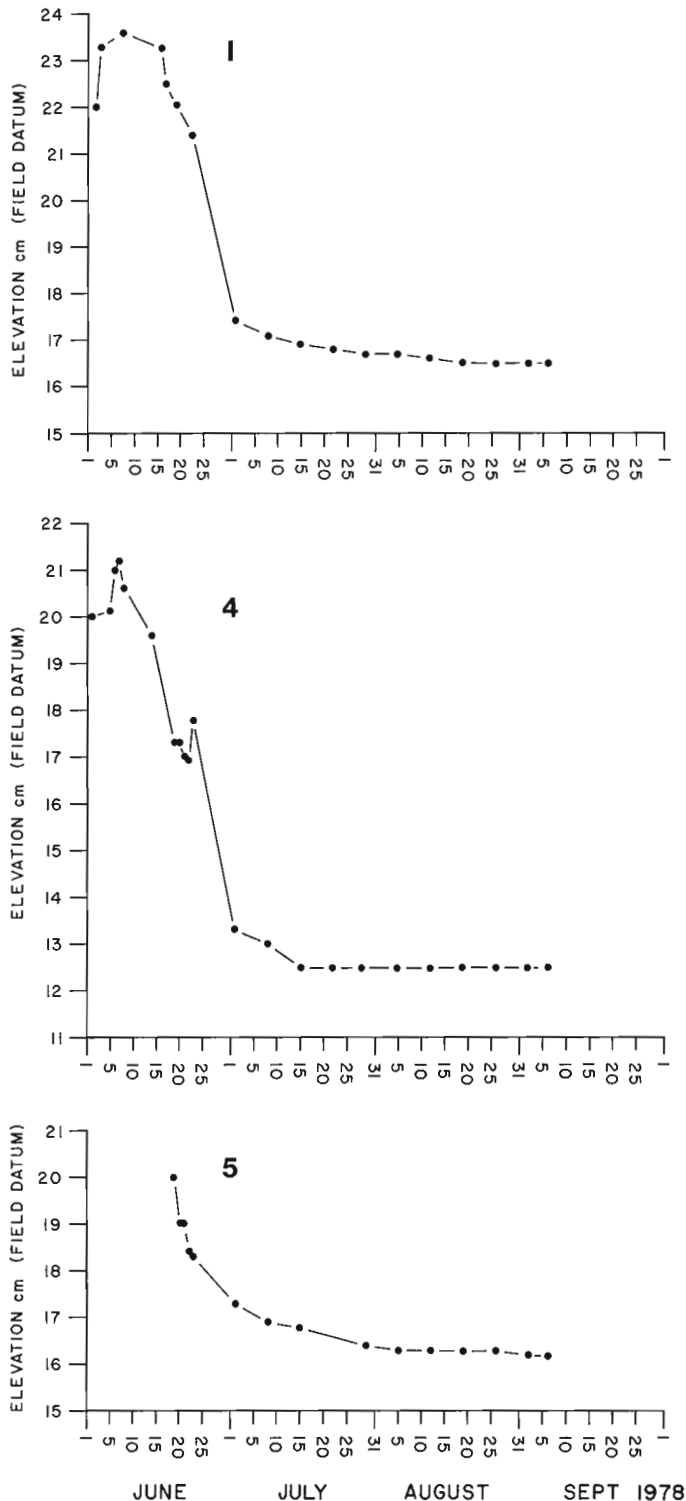


Figure 38.6. Subsidence over time at two mudboil centres (sites 1 and 4) and a vegetated border (site 5) of a mudboil at North Henik Lake.

Figure 38.7

Thaw depth for the central portion of a mudboil and a vegetated border, 1978, Henik lakes area.

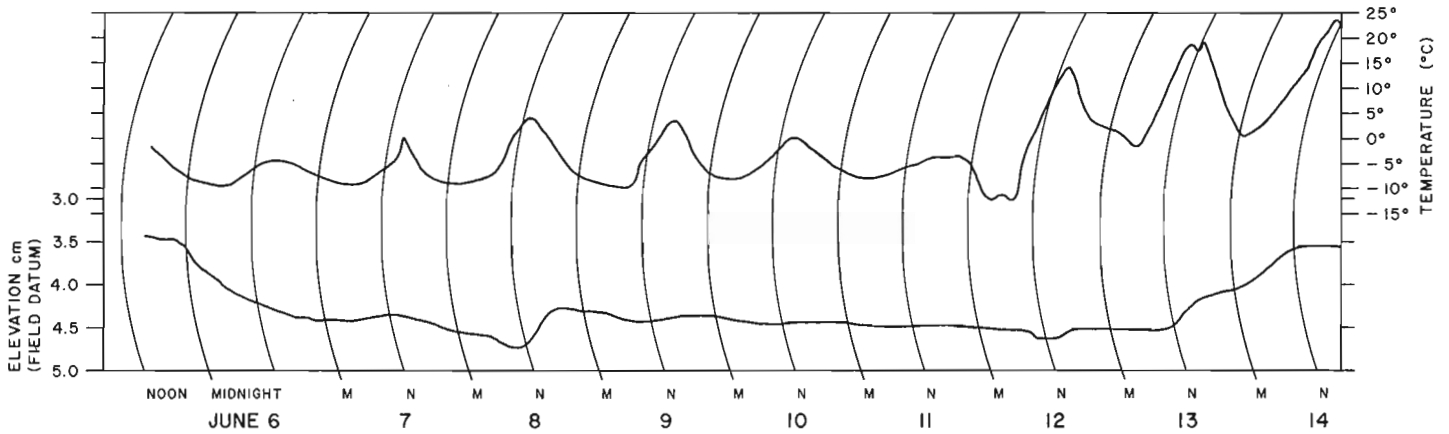
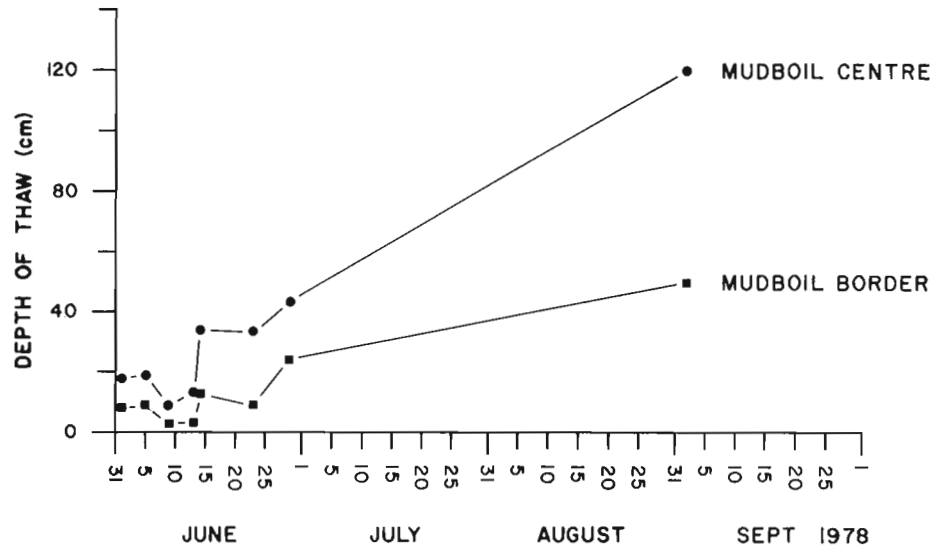


Figure 38.8. Continual trace of air temperature (upper line) and ground movement (lower line) during the period June 6 to 14, 1978 at site 3, North Henik Lake. Note that an upward fluctuation of the ground movement line indicates subsidence, and a downward one indicates heave.

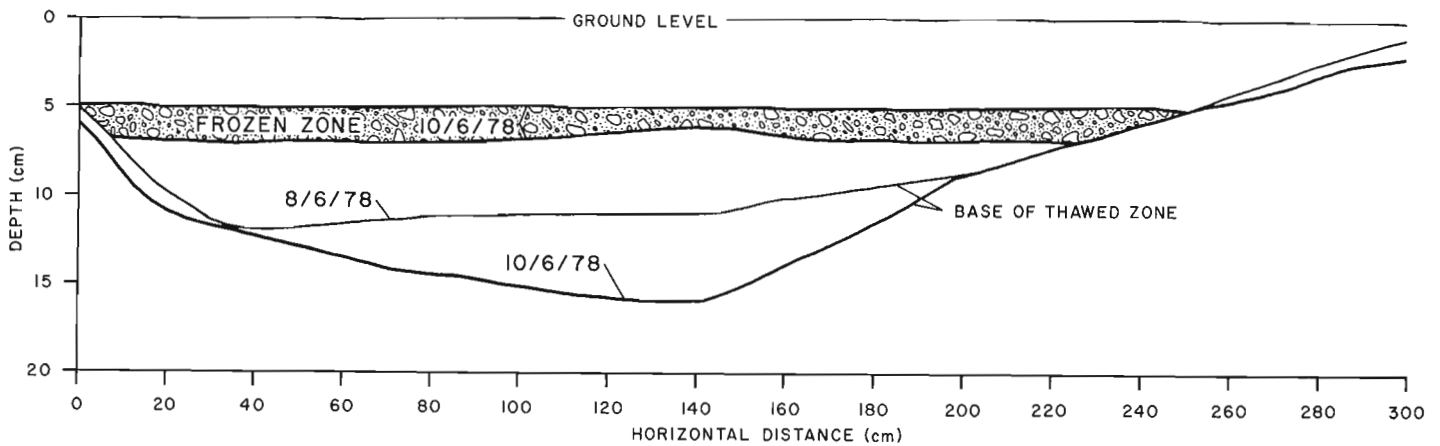


Figure 38.9. Thawed portion of active layer and perched frozen zone for a mudboil at Henik lakes.

Figure 38.10.

Caribou trails, Victory Lake. The raised vegetation on either side of the trails is relatively thick and lush and encourages the use of the trails as they offer the least resistance to travel. (GSC 203502-C)



It seems highly likely, given the low liquid and plastic limits of these muds, that heavy summer rainfalls will induce rapid movements as suggested by Shilts (1978). To date, however, data are not available on this particular aspect.

Caribou Migration

'Natural disturbances' may contribute significantly to mudboil development and activity (Shilts and Dean, 1975). All the sites studied are within the general migratory route used by the Kaminuriac caribou herd. Caribou trails through the tundra are especially visible at Victory Lake because of their high density (Fig. 38.10). Mudboil development is particularly active, and mudboils in the trails tend to be elongate and to coalesce. Where vegetation is not thick, individual trails disappear and the animals range over the entire area rather than along specific routes.

Over the period June 21 to 30, 1978 some 11 000 caribou moved through the Victory Lake area. All instrumented sites were disturbed or destroyed. More than 50 hoof prints were common on mudboils less than 2 m² in area. The effect of the caribou can be appreciated better when it is realized that even small loads (50 to 100 kg) applied repetitively to a mudboil surface can cause the mudboil to become fluid or plastic (Shilts, 1978). It was not possible to document in absolute terms the effect that the caribou had on mudboil activity at Victory Lake; this type of disturbance, however, is common in the area. An island in a small lake in the vicinity of Edehon Lake, about 100 km south of the Henik lakes area, was observed to have a strip of highly active mudboils across its centre with stable mudboils on either side. The strip was associated with a caribou wading route through the lake in 1978. Hoof prints were visible on both sides of the lake and on the island. Rib and trough features (see Shilts and Dean, 1975) within the shallow portions of the lake crossed by the caribou also were disturbed (W.W. Shilts, pers. comm., 1979). Yearly caribou migration routes through central District of Keewatin are highly variable areally; as such, caribou movement may be responsible for inducing activity from time to time in mudboils over a large region of central Keewatin.

Summary

A variety of processes may be responsible for mudboil formation and for the horizontal and vertical movements within the features over time (Shilts, 1978). In any one year, however, a specific process may or may not be significant.

In 1978 maximum surface horizontal movements of up to 60 cm were recorded on mudboils in central District of Keewatin, although values of 1 to 3 cm were more typical. Yearly vertical displacements, typically 8.7 cm with a maximum of 35.5 cm, were measured in several mudboils.

Based upon field observation of soil structure, Shilts (1978) suggested that diapirism caused by hydrostatic or other differential pressures may be significant in mudboil formation and activity. The intrusion of mud (up to 51 cm/year, Table 38.2) into tubes placed within mudboil centres supports the contention that differential pressures are generated within these features; however, the mechanism is poorly understood.

Heaving is a major cause of horizontal movement in mudboils as 1) the muds are displaced downslope (creep) upon thawing and 2) heaving tends to concentrate moisture at or near the surface. The moisture concentration may be sufficient to induce gelifluction on thawing. By similarly concentrating moisture at the surface, major spring freezebacks also may be important in inducing horizontal movement in mudboils.

The highly active areas of expansion within mudboils experience differential heaving during spring freezebacks and presumably during annual freeze-up. At Victory Lake these areas were also observed to be centres of diapirism. The relative importance of each process is not known.

Snow patches which persist through the early summer promote mudboil activity by providing moisture through snowmelt and by concentrating moisture, moving downslope as interflow, at or near the surface.

It is speculated that low frequency, high energy, summer precipitation will generate rapid mudboil movements.

Caribou migration may contribute significantly to mudboil development and activity over a large portion of central Keewatin.

References

- Egginton, P.A. and Shilts, W.W.
1978: Rates of movement associated with mudboils, Central District of Keewatin; in Current Research, Part B, Geological Survey of Canada, Paper 78-1B, p. 203-206.
- Fahey, B.D.
1973: Seasonal frost heave and frost penetration measurements in the Indian Peaks region of the Colorado Front Range; Arctic and Alpine Research, v. 6, p. 63.
- Mackay, J.R., Ostrick, J., Lewis, C.P., and Mackay, D.K.
1979: Frost heave at ground temperatures below 0°C at Inuvik, Northwest Territories; in Current Research, Part A, Geological Survey of Canada, Paper 79-1A, p. 403-405.
- Shilts, W.W.
1978: Nature and genesis of mudboils, central Keewatin, Canada; Canadian Journal of Earth Sciences, v. 15, p. 1053-1068.
- Shilts, W.W. and Dean, W.E.
1975: Permafrost features under Arctic lakes, District of Keewatin; Canadian Journal of Earth Sciences, v. 12, p. 649-662.
- Washburn, A.L.
1967: Instrumental observations of mass wasting in the Mestrs. Vig. District, north-east Greenland; Meddeleser om Grønland, v. 166, no. 4, 313 p.

HIGH RESOLUTION REFLECTION SEISMOLOGY STUDIES ON LATE QUATERNARY SEDIMENTS OF THE NORTHEAST NEWFOUNDLAND CONTINENTAL SHELF

C.T. Dale¹ and R.T. Haworth
Atlantic Geoscience Centre, Dartmouth

Dale, C.T. and Haworth, R.T., *High resolution reflection seismology studies on Late Quaternary sediments of the northeast Newfoundland continental shelf*; in *Current Research, Part B, Geological Survey of Canada, Paper 79-1B*, p. 357-364, 1979.

Abstract

A surficial seismic facies analysis for the northeast Newfoundland continental shelf has resulted in 5 mappable units. Variations in lithologic and geotechnical parameters in 6 cores within the area of seismic coverage provided the basis for correlations between the seismic and sedimentary facies. This suggests that lithological mapping on the basis of seismic character and limited core control may be well founded. However, an explanation of the fine detail and variability in the seismic record will have to wait for the results of synthetic seismogram analysis based on sound speed and density measurements made on the cores.

Introduction

A preliminary analysis of bathymetry, airgun seismics, Hunttec deep tow system (DTS) (Hutchins et al., 1976), high resolution seismics, and sidescan sonar data has enabled us to identify and map 5 surficial seismostratigraphic units on the northeast Newfoundland continental shelf area. A multiparameter geoscience cruise to the northeast Newfoundland continental shelf in August 1975 (Haworth et al., 1976b) was followed by a further cruise to the study area (Fig. 39.1) to examine these seismic units in more detail; the total data coverage to date is shown in Figure 39.2. In addition to extended geophysical surveying, sediment piston cores were collected at 11 locations identified from DTS records where a maximum number of seismostratigraphic horizons could be penetrated beneath the seabed in approximately 10 m. Measurements of p-wave velocities were made on the cores as soon as they were brought onboard ship and later six cores, with maximum sedimentary variability and adequate DTS data coverage, were chosen for detailed geotechnical analysis. An initial example of the results of that analysis, including interparameter correlations and correlations with seismic events are presented here. Further analysis is proceeding as part of the senior author's graduate work at Dalhousie University.

Navigation

Obtaining accurate real time navigation in this area is difficult due to the close proximity of the Loran-C baseline and the necessary correction for the overland phase lag received from the Cape Race transmitter (southeastern Newfoundland) (Haworth et al., 1976b). Using the Austron Loran-C navigation system in range-range mode in this area expected positioning accuracy is between 150 m to 300 m. The lower accuracy is to be expected close to the Angissoq (southern tip of Greenland)-Cape Race baseline. However, experience gained in 1975 resulted in good real time navigation when returning to proposed sampling sites. We expect that the 150 m accuracy is appropriate and postcruise processing of the navigation data has also indicated that only minor errors in location exist.

Collection of Seismic and Bathymetry Data

The bathymetric map (Fig. 39.3) is an updated version of that produced in 1975. These data were collected using a conventional 12 kHz widebeam echo sounder and digitized onboard ship every 5 minutes and at peaks and troughs. Manual picking of the bathymetry records after the cruise and additional data from the northeasterly corner of the study area (Karlsen 75-018 cruise, see Haworth et al., 1976a) were used in preparation of Figure 39.3.

During the cruise simultaneous seismic reflection profiles from both the Hunttec DTS, a broadband deep towed boomer, and airgun systems were used to produce our surficial seismic facies map (Fig. 39.4). A $624 \times 10^{-5} \text{ m}^3$ (40 in^3) airgun operating at 10 MPa (1500 psi) was normally used with a 2 second repetition rate. These seismic data were recorded in analogue form on a Hewlett-Packard F.M. tape recorder and filtered and displayed in the normal manner on an E.P.C. seismic recorder. Hunttec DTS data were collected at a firing rate of $3/4$ sec using an excitation voltage of approximately 5 kV, and recorded in a similar fashion to the airgun data. Postcruise digital analysis of the Hunttec DTS data formed a significant part of the study reported here.

Sidescan sonar data were also collected on slow speed lines using the BIO system (Jollimore, 1975). However, the deeper troughs and basin regions were out of the range of the system even at towing speeds as low as 3 to 4 knots.

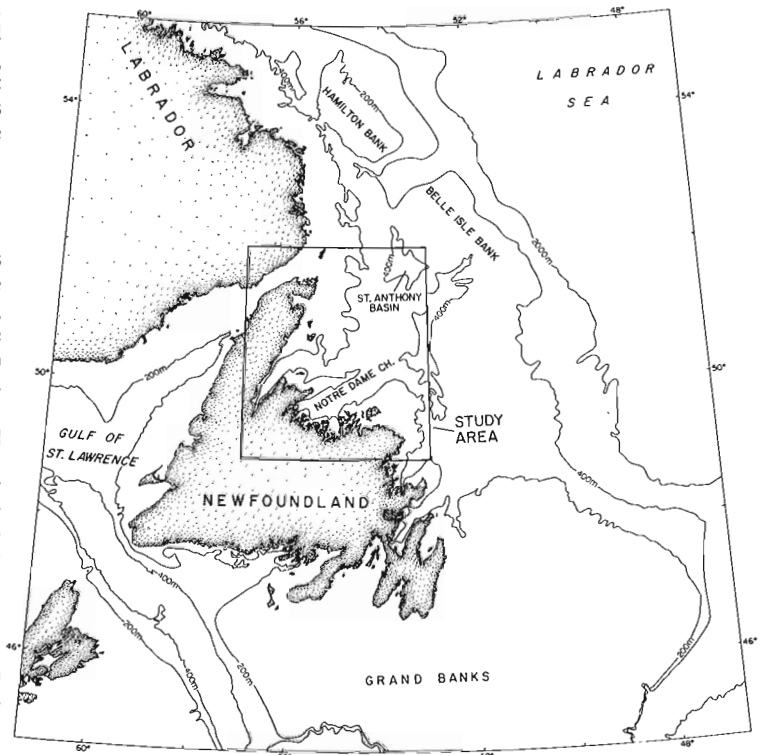


Figure 39.1. Location of the study area and its relation to the adjacent continental shelf.

¹Department of Geology, Dalhousie University, Halifax, Nova Scotia

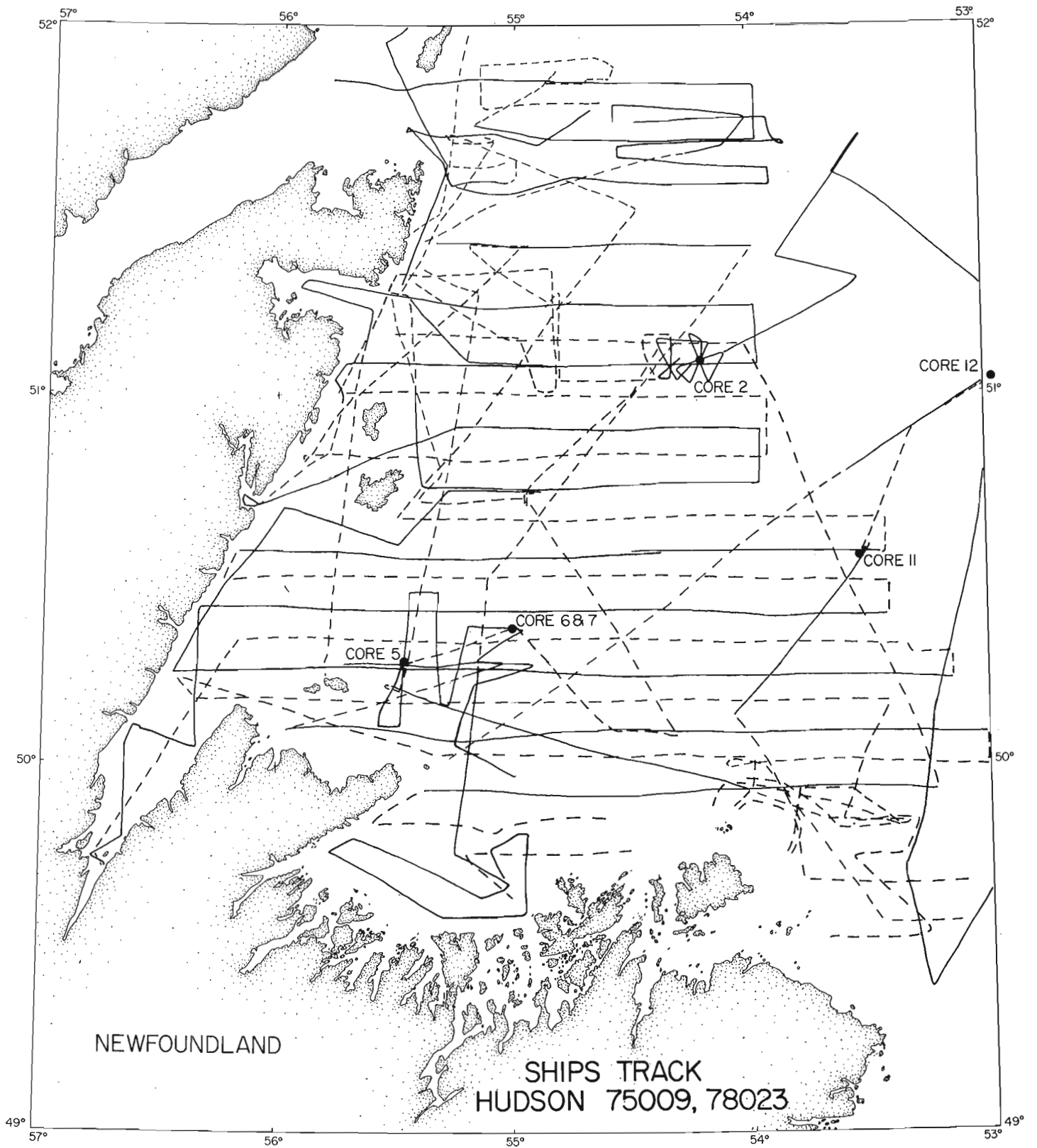


Figure 39.2. Data coverage within the study area. Solid lines are those with Hunttec DTS and small airgun coverage, dashed lines have bathymetry data coverage. Core sites shown as solid dots.

Playback of Hunttec Data

In order to investigate the reflection process within surficial sediments, the raw Hunttec data (Fig. 39.5a, b) have to be further expanded and played back as individual shots (Fig. 39.5c). To do this digital playback system, built around a PDP-11 minicomputer, and developed by Parrott (1978), was utilized. The analogue tape recordings made at sea were transcribed at calibrated levels, filtered using a Kronhite filter as required, digitized shot by shot and sorted on

conventional 9-track magnetic computer tapes. We chose a digitizing interval of $10 \mu\text{s}$. This gives a Nyquist frequency of 50 kHz (outside the frequency range of the Hunttec boomer source) which, although unnecessary for fidelity alone, results in the required smooth display of the individual shots when output as "wiggly traces" on the Anac graphics system (Fig. 39.5c). Unfortunately due to an operator error, onboard recording calibration levels were set too high resulting in low recorded signal levels and correspondingly poor signal-to-noise ratios.

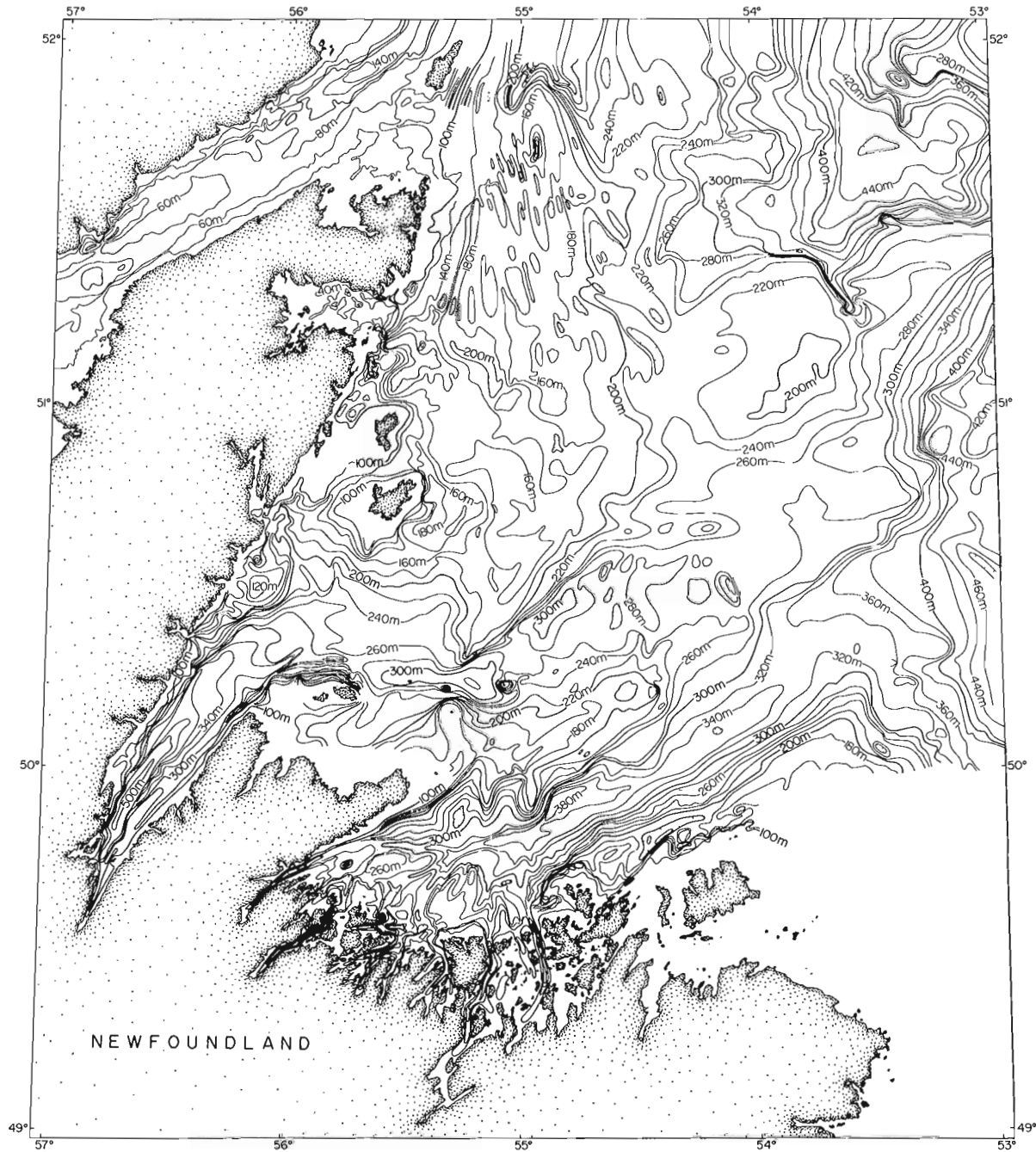


Figure 39.3. Bathymetry map, northeast of Newfoundland. Scale 1:2 000 000.

The 3/4 sec repetition rate means that there are 160 separate "shots" between each 2-minute mark on the analogue graphic record; this corresponds to a shot for approximately every 2 m moved over the ground at 5 knots. The Fresnel zone of acoustic illumination is dependent upon the towing distance from the seabed; nonetheless the density of data is extremely high and this in itself presents analysis problems.

Seismic Data Interpretation

The seismic facies map (Fig. 39.4) was initially prepared at 1:250 000 from all the DTS and airgun data and later reduced to 1:2 000 000. While core analysis and comparison to the seismic data indicate the units shown in Figure 39.4 may resemble the gross nature of the surficial geology, we are constrained by the resolution of the Huntex system and our ability to accurately and objectively distinguish between the units. Their distribution was mapped by locating the contacts between the seismic units (identified by circles in Fig. 39.4) and extrapolating between these points on the basis of bathymetry.

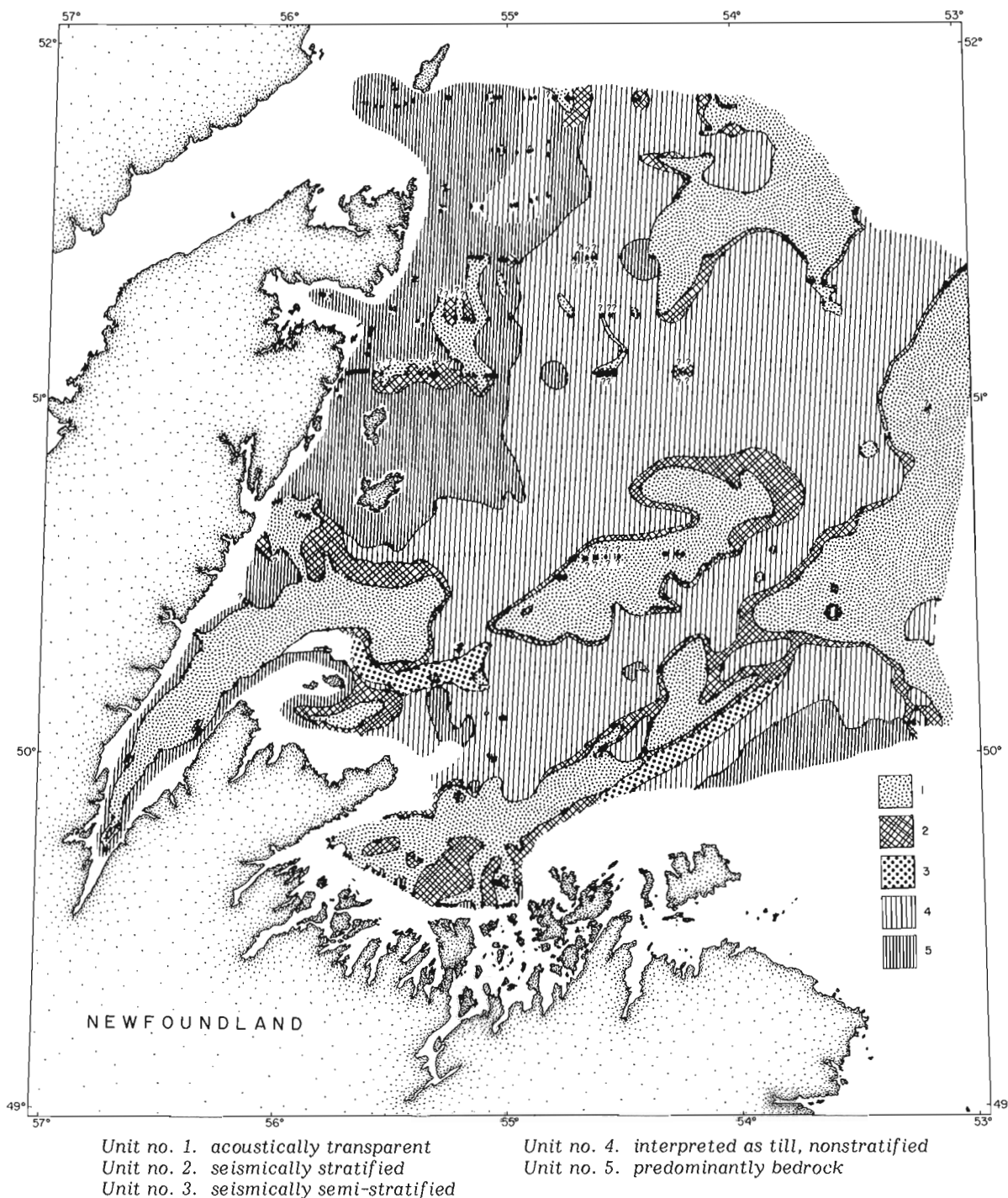


Figure 39.4. Surficial seismic facies map. More details given in the text.

Five seismic facies have been mapped; the seismic section in Figures 39.5a and b exhibits four of these different units: Unit 1, an acoustically transparent layer, is generally found ponded in the basins and troughs of the study area (compare Fig. 39.3 and 39.4). Underlying this, and often appearing to outcrop around Unit 1 is a seismically stratified unit (Unit 2). No samples have been collected from this unit where it outcrops but it was sampled where it occurs beneath Unit 1. On the seismic record it is intermediate in character between units 1 and 4. Unit 4 exhibits the character of a nonstratified, highly scattering medium; this is interpreted as till. It is widespread and of varying thickness throughout the shelf. Unit 3 has only been identified in two regions. It appears to be semi-stratified and allows only limited seismic penetration. In close proximity to Unit 3 we see till type material which may be genetically related to this stratified unit. Unit 5 is interpreted as bedrock. This unit as mapped in Figure 39.4 is predominantly bedrock outcrop but may be covered by 10-20 cm of sediment. Our seismic facies map is a simplification, pockets and gradations of sediments will exist but on a regional scale the facies map provides us with a good basis for geological interpretation using the core control obtained.

Core Collection and Analysis

In order to sample as many different seismostratigraphic units as possible, core sites were identified from Huntect survey data. An example of such data over a typical core site is shown in Figure 39.5. Samples were generally obtained where 3 units could be sampled in a 10-m section; such locations were found at the edges of basins containing ponded sediments.

Of the 11 locations at which piston cores were collected using a Benthos piston corer, six have acceptable Huntect data coverage once digital playback and the signal-to-noise problem are considered. The cores vary between 5 m and 11 m in length and penetrate at least 3 distinct sedimentological units. As soon as possible after recovery, the cores were scanned for sound speed, transversely through the core, using a pulsed sound method (Winokur and Chanesman, 1966). No attempt has been made to measure the sound speed vertically in the cores due to the experimental difficulties and the doubtful increase in information such measurements would yield. Measurements of time delay for transmission were recorded and, after calibration, used to compute velocities. The velocities recorded are believed accurate to approximately $\pm 5 \text{ ms}^{-1}$ and in these sediments no evidence for transverse anisotropy was found within the experimental error. Measurements were taken at 5 cm intervals with intermediate measurements wherever obvious increases or decreases in the time delay occurred; this methodology should limit unwanted biasing of the velocity profiles. These data have been digitized for ease of access and modelling purposes. In addition to sound speed the following parameters were also determined: lithological and X-ray analysis, grain size (percentage, weight, sand, silt and clay), bulk density, porosity, moisture content and undisturbed and remoulded shear strength. Figure 39.6 illustrates these data for core no. 6, collected at the location indicated on the seismic section (Fig. 39.5a). The following sampling procedure was adopted to minimize disturbance while measuring the physical properties of the sediments. Sampling locations down core were chosen using X-radiographs of the unsplit cores and the lithological variations observed once the cores had been carefully split. No significant disturbance has been found in any of the cores. After splitting the core, shear strengths were measured by direct insertion of a Wykham Farrance vane shear apparatus. Next, a small (approximately 50 gram) sample was cut out of the core adjacent to the location of the shear vane

measurement. This sample was carefully trimmed to remove sediment close to the core barrel where disturbance occurs during the coring process, and kept in a cold box to minimize desiccation prior to weighing. A straightforward buoyancy technique, using Varsol as the displaced fluid, was employed to measure the bulk density. The samples were then dried in an oven for 24 hours, cooled and weighed again to determine porosity (after salinity correction) and water content. In these calculations we assumed a saturated, gas-free sediment; this was felt justifiable because the cores showed little or no tendency to crack as do gassy cores.

The correlations between porosity, density, and moisture content are striking and similar to those found by others (e.g. Tucholke and Shirley, 1979). The shear strength profiles show a general increase in strength with depth, probably a function of compaction. The results from deeper layers of sand and gravel in the core must be viewed with caution because the validity of the vane shear method is dependent upon measurements being made in cohesive undrained sediments. It should also be noted that the number of sound speed data is much higher than the bulk property information due to the relative ease of sampling for the former data. In Figure 39.6, we report only the actual measurements made. Individually all the different sedimentary units were sampled but the physical variations will be more frequent than shown; for example, small repetitive layers were only sampled once, rather than every time a lithological change occurred. In the future, modelling may require that inferences of geotechnical variations be made where lithological differences are clearly visible.

Lithological units have been identified on the basis of texture and colour. Unit A, occurring in the uppermost metre, is dark brown (7.5 YR 4/2, Munsell, soil colour charts, 1954) with a darker and ore sandy surface layer of approximately 3 cm. This is underlain by unit B, dark grey (2.5Y 4/1) in colour and with a higher gravel fraction probably due to increased ice rafting. Unit C is rich in detrital carbonate and also has a significant gravel component. It is greyish brown (2.5Y 5/1) and this colour distinguishes the unit from the other grey sediments. Unit D is a dark grey colour (2.5Y 4/1) and grades, increasing in gravel fraction, down core. The boundary between units D and E is rather vague due to a gradational colour change, over approximately a metre, to weak red (10R 4/2). A possible marker of this boundary is the thin laminations of siliceous material found in the upper part of the unit. A shell from this level has been analyzed by amino acid racimization techniques and indicates an age no greater than 15 000 years BP (R.A. Nelson, pers. comm., 1979). The unit increases appreciably in gravel content and terminates above unit F which has alternating layers of clay, dusky red (10R 3/2) in colour and weak red gravelly sediments. Unit G, again weak red (10R 4/2), is composed of interlaminated silts and sands. Unit G grades into a sandy layer overlying unit H which appears to be a till due to its very poor sorting and lack of stratification. We interpret this sequence as having been deposited continuously from a time prior to the last glacial retreat to the present day. More detailed stratigraphic studies on these cores are in progress at Dalhousie University.

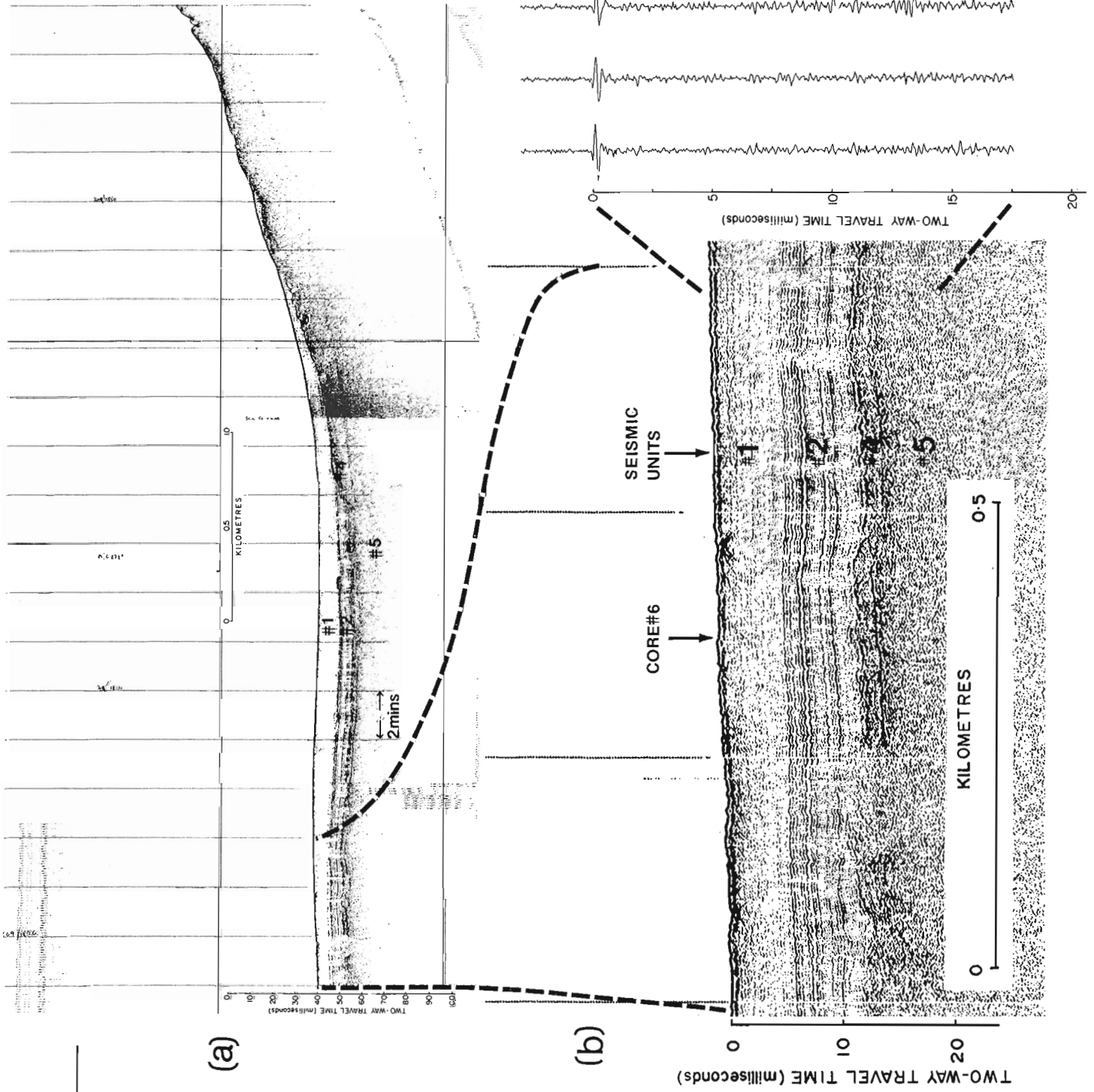
Correlation of Seismic and Sedimentary Lithologies

A qualitative correlation is immediately apparent: the acoustically transparent facies (unit 1) corresponds to the uppermost grey sediments in the core (units A, B and C, Fig. 39.6). Minor seismic events are probably due to coherent layers with a high gravel concentration or small changes in bulk properties. Pebbles are the major cause of the acoustic scanning anomalies, but in order for a coherent reflection to be observed for a continuous pebbly layer it must be approximately as thick as the seismic pulse is long (ignoring the second order effects of scattering and spherical seismic waves).

Figure 39.5.

Huntec DTS data over core site no. 6. Scale expansion increases as shown. Units 1 to 4 are discussed in the text.

- a. Shows the general setting of the core site.
- b. An expansion of the graphic record of the site itself.
- c. Digital playback and display of individual "shots" as "wiggly traces".



(c)

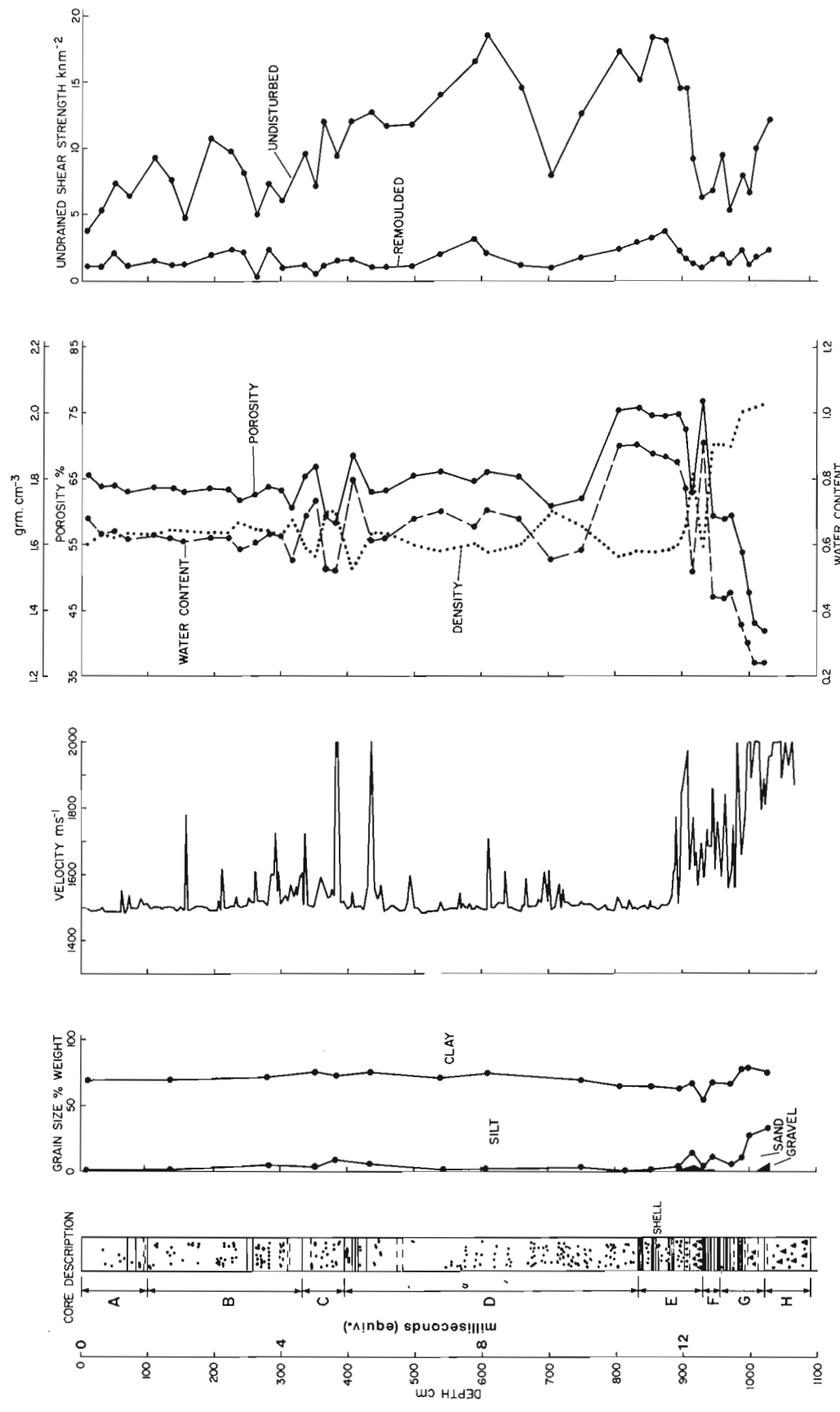


Figure 39.6. Lithological and geotechnical analysis results for core no. 6. Units A to H explained in the text. Dots are pebbles identified from X-radiographs of the cores. Equivalent two-way travel time in milliseconds is indicated next to the depth scale.

The seismo-stratified facies (unit 2) is related to units D, E and F, which exhibit noticeable velocity and density variations in the lower part of the core. The details of this relationship are unclear but the seismic record indicates that these physical variations within the core lithologies are continuous over large areas. It is hoped that converting the geotechnical data from distance down core to equivalent 2-way travel time and synthetic seismogram analysis will aid our discrimination of seismic events and also point to the size effect that "peg-leg" multiples play.

The measured values of velocity and density will be used to produce an impulse response for a model of 1000 layers excluding multiples. This will be convolved with the Hunttec source pulse to produce a synthetic seismogram. A similar computation, but including multiples, will also be done to determine quantitatively the multiple effect (e.g. Anstey, 1960; Trorey, 1962).

Finally, the till arrival Unit G corresponds to the velocity and density increases shown for unit 4. The sediment is very poorly sorted and rough surfaced and would give rise to the typically incoherent reflections observed.

Although this qualitative comparison seems good and suggests that lithological mapping on the basis of seismic character and limited core control data may be well founded, the controlling parameters are the physical variability of the sediments, seismic resolution and the sound transmission characteristics. In order to correlate seismic to sedimentary lithologies, corresponding physical variations must accompany lithological variations. In our case this preliminary investigation shows that this is apparently the situation, though the explanation of very fine detail and variability in our seismic units across the shelf will have to wait for the results of synthetic seismogram analysis.

References

- Anstey, N.A.
1960: Attacking the problems of the synthetic seismogram; *Geophysical Prospecting*, v. 8, p. 242-259.
- Haworth, R.T., Grant, A.C., and Folinsbee, R.A.
1976a: Geology of the continental shelf off southeastern Labrador; in *Report of Activities, Part C, Geological Survey of Canada*, Paper 76-1C, p. 61-70.
- Haworth, R.T., Poole, W.H., Grant, A.C., and Stanford, B.V.
1976b: Marine geoscience survey northeast of Newfoundland; in *Report of Activities, Part A, Geological Survey of Canada*, Paper 76-1A, p. 7-15.
- Hutchins, R.W., McKeown, D.L., and King, L.H.
1976: A deep tow high resolution seismic system for continental shelf mapping; *Geoscience Canada*, v. 3, p. 95-100.
- Jollimore, P.G.
1975: A medium range sidescan sonar for use in coastal waters. Design criteria and operational experiences; in *Proceedings of the IEEE Conference on Engineering in the Ocean Environment*, Halifax, N.S., Institute of Electrical and Electronic Engineers Inc. N.Y., v. 2, p. 108-114.
- Parrott, D.R.
1978: An interactive program for analyzing high resolution seismic data on the PDP-11/20 minicomputer; *Hunttec Internal Report H7803-01/SB/DRP*.
- Trorey, A.W.
1962: Theoretical seismograms with frequency and depth dependent absorption; *Geophysics*, v. XXVII, no. 6, pt. 1, p. 766-785.
- Tucholke, B.E. and Shirley, D.J.
1979: Comparison of laboratory and in situ compressional-wave velocity measurements on sediment cores from the Western North Atlantic; *Journal of Geophysical Research*, v. 84, no. 132, p. 687-695.
- Winokur, R.S. and Chanesman, S.
1966: A pulse method for sound speed measurements in cored ocean bottom sediments. Informal manuscript, I.M. No. 66-5, Acoustical Oceanography Branch, N.S. Navy Oceanographic Office.

Project 730063

H.J. Greenwood¹

Regional and Economic Geology Division

Greenwood, H.J., *Thermodynamic properties of edenite; in Current Research, Part B, Geological Survey of Canada, Paper 79-1B, p. 365-370, 1979.*

Abstract

The amphibole end member edenite is significant in many metamorphic equilibria, but its thermodynamic properties are largely unknown. This study was initiated to determine those thermodynamic properties that would be useful in estimating the pressure-temperature conditions of formation of amphibole-bearing metamorphic assemblages. Hydrothermal phase equilibrium experiments were conducted and products analyzed optically and by X-ray diffraction. The results to date are inconclusive because pure edenite could not be synthesized. It appears that a previously published equilibrium is incorrect. Pure edenite has a more restricted stability field than previously predicted. Work on edenite is continuing.

Introduction

The amphibole end-member edenite ($\text{NaCa}_2\text{Mg}_5\text{Si}_7\text{O}_{22}(\text{OH})_2$) is involved in many geologically significant equilibria. An investigation has been initiated to determine the thermodynamic properties of the pure phase, and was funded by the Department of Energy, Mines and Resources (Geological Survey of Canada). This study is incomplete at present, and work to date has taken the following path. The experimental work reported by Widmark (1974) was combined with the data collected by Helgeson et al. (1978). The thermodynamic data and the experimental results were combined to estimate thermodynamic parameters for the amphibole edenite and these new parameters were then combined with the data presented by Helgeson et al. to calculate a number of other equilibria prior to investigating them experimentally.

Hydrothermal phase equilibrium experiments and syntheses were then conducted in an attempt to verify the computed location of the equilibria. These attempts were supplemented by an investigation of the solid solution range of the amphibole produced, and finally an assessment was made of the quality of the data due to Widmark and the probable positions of the equilibria.

It has not been possible to synthesize 100 per cent edenite. Synthesis runs using different starting materials produced a variety of phases as well as amphibole. Extended runs on the bulk composition edenite + 4 quartz showed that the initially edenitic amphibole changed with time toward more tremolitic compositions. This result suggests that the experiments of Widmark do not in fact represent equilibrium and that edenite has a more restricted stability field than the computations indicate. Work is continuing on the problem of synthesis.

Rationale

A large number of equilibria can be written involving the amphibole edenite and in order to estimate the pressure-temperature conditions of these equilibria it is necessary to have thermodynamic data for the mineral edenite. Such data are presently unavailable and therefore have been estimated on the basis of the experimental data reported by Widmark (1974). Widmark used a mixture of natural labradorite, dolomite, quartz, water, and "seeds" of edenite and calcite. He reported that reversible equilibrium was established between edenite, calcite, labradorite, quartz, water, carbon dioxide at 540°C, 6 kbars, and $x\text{CO}_2 = 0.5$. This report, taken at face value, permits the computation of the heat of formation of edenite. The method adopted was to make successive assumptions about the enthalpy of formation of

edenite and to use this together with data on the other phases to compute the curve reported by Widmark. When the curve was adequately reproduced the enthalpy of edenite that produced this fit was then retained and used for further calculations. The thermodynamic parameters used are reported in Table 40.1.

Results

The results of the calculations are summarized in a number of figures. Figure 40.1 presents the position of the equilibrium albite + 5 dolomite + 4 quartz + $\text{H}_2\text{O} \rightleftharpoons$ edenite + 3 calcite + 7 CO_2 plotted in terms of temperature and mole fraction of $\text{H}_2\text{O}-\text{CO}_2$ mixtures at a variety of pressures. Also shown on the diagram is the equilibrium dolomite + quartz + $\text{H}_2\text{O} \rightleftharpoons$ tremolite + calcite + CO_2 as determined by Skippen (1971). It should be noted that the curve involving edenite at 2 kbars occurs at a lower temperature than the curve involving tremolite at 2 kbars. Because of the additional phase albite in the equilibrium involving edenite these two curves therefore appear to be in their correct relative positions. Another view of the same calculated equilibria is presented in Figure 40.2 showing the same data plotted in terms of pressure and temperature at constant fluid composition. Figure 40.2 shows that at pressures approaching 10 kbars albite will melt in the presence of pure H_2O . It will not however melt in the presence of the gases calculated to be at equilibrium with albite, dolomite, quartz, calcite, and edenite.

In Figure 40.3 is presented the computed position of the equilibrium dolomite + albite + talc \rightleftharpoons edenite + CO_2 . This equilibrium has not been investigated either previously nor in this report. Figure 40.4 presents the computed equilibrium between low albite, tremolite, alpha quartz, and edenite. This is an interesting equilibrium because it involves only solid phases and has a very steep P-T slope. The components tremolite and edenite are involved in mutual solid solution while albite and quartz remain pure. Therefore, the position of the equilibrium for $K = 1$ will correspond to the condition where the mole fraction (activity) of tremolite is equal to the mole fraction of edenite in the amphibole. At higher temperatures the amphibole becomes more edenite-rich and at lower temperatures it becomes more tremolite-rich. That appears to be the most important equilibrium to be studied in the system because the only solid solution variation is in the amphibole. In other words, coexistence of the tremolite-edenite-amphibole in the presence of albite and quartz will be invariant at a particular pressure and temperature. The main thrust of the experimental work described later was intended to determine the value of this equilibrium constant as a function of pressure and temperature and thereby to

¹Department of Geological Sciences, University of British Columbia, Vancouver, British Columbia. V6T 1W5

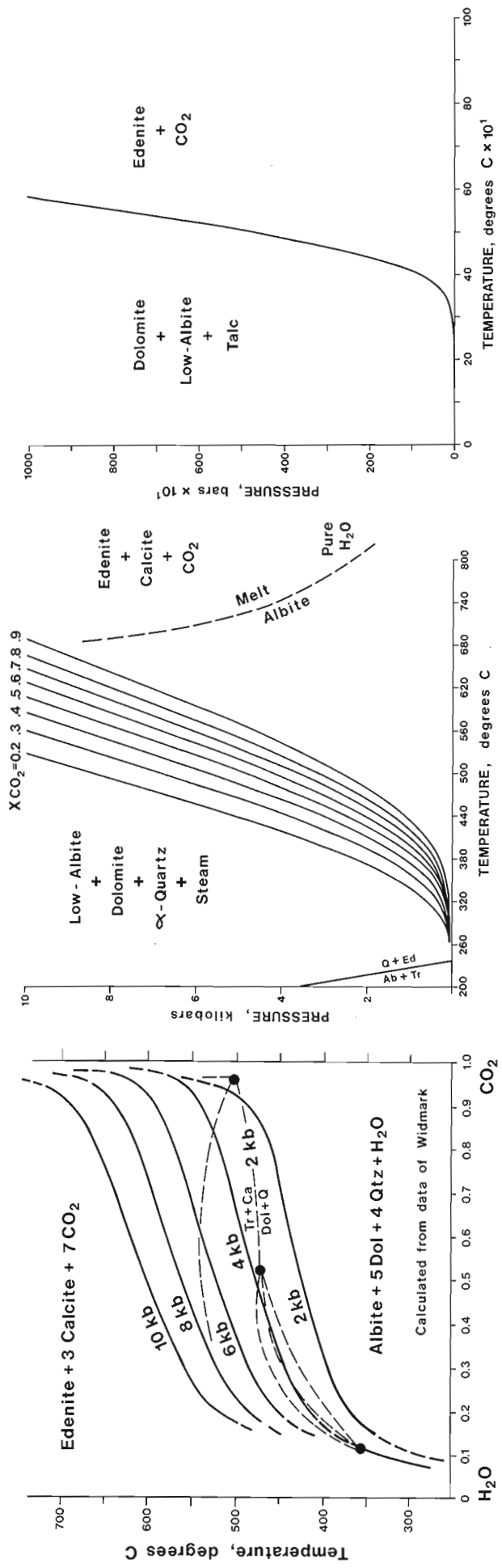


Figure 40.1. The computed equilibrium albite + 5 dolomite + 4 quartz + H₂O \rightleftharpoons edenite + 3 calcite + 7CO₂ in H₂O-CO₂ mixtures at various pressures.

Figure 40.2. The computed equilibrium albite + dolomite + quartz \rightleftharpoons edenite + 3 calcite + 7CO₂ at constant fluid composition.

Figure 40.3. The computed equilibrium dolomite + albite + talc \rightleftharpoons edenite + CO₂.

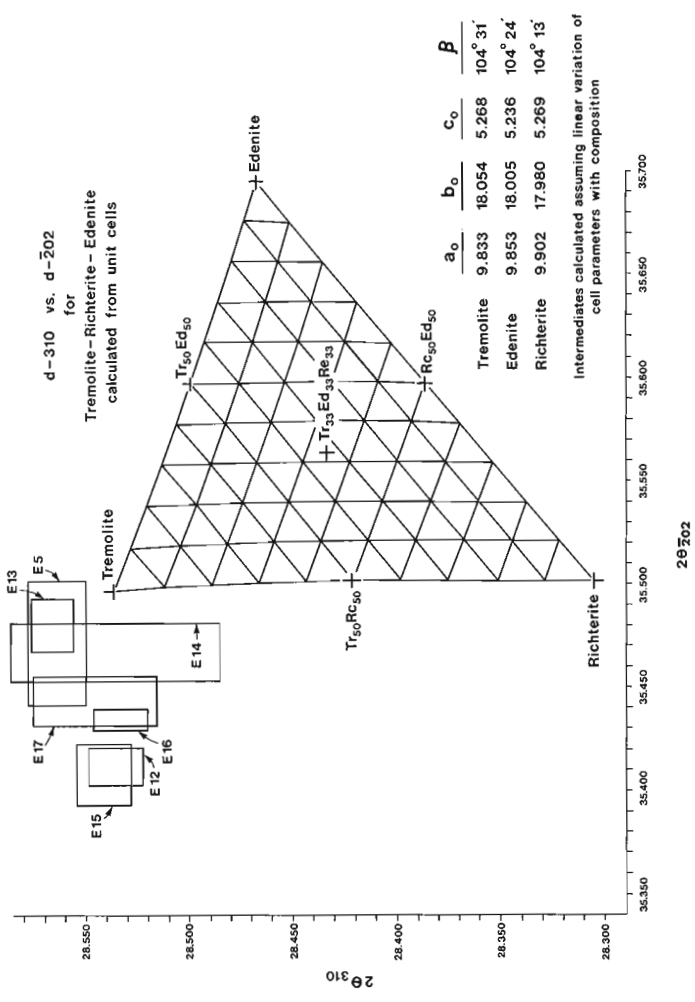


Figure 40.4. The computed equilibrium albite + tremolite \rightleftharpoons quartz + edenite.

Figure 40.5. Computed 2θ₃₁₀ vs 2θ₂₀₂ for amphiboles in the compositional range edenite-tremolite-richterite.

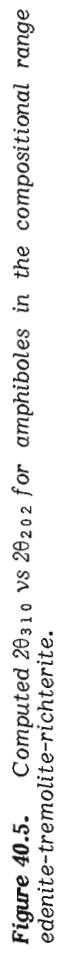
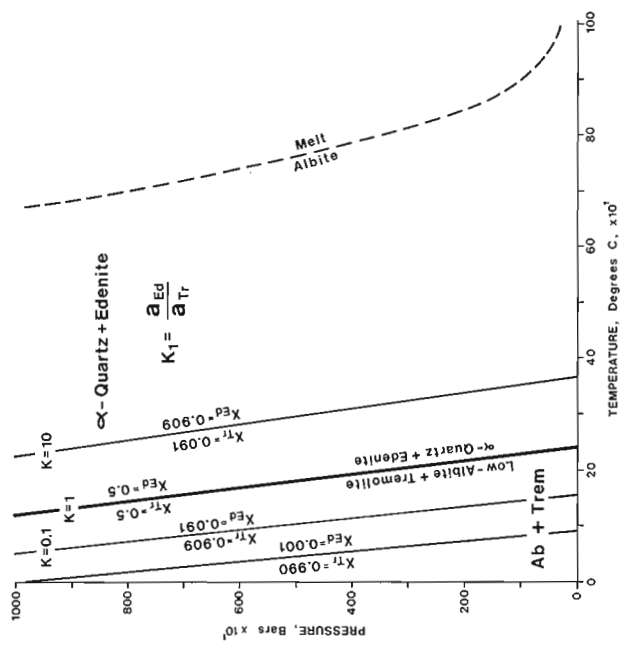


Table 40.1

Tentative thermodynamic properties of Edenite and related phases

Phase	ΔH_f°	ΔS (3rd law)	a	b(10 ³)	c(10 ⁻⁵)	Vol. (cal bar ⁻¹)
Edenite	-3003000.	161.0	205.706	41.1845	-49.3852	6.47706
low albite	-939680.	49.51	61.70	13.90	-15.01	2.39167
alpha-quartz	-217650.	9.88	16.716	0.6045	-4.6066	0.54224
Calcite	-288772	22.1499	24.980	5.240	-6.20	0.88274
Dolomite	-556851	37.090	41.557	23.952	-9.884	1.53776
Diopside	-765598	34.200	52.87	7.840	-15.739	1.57959
Talc	-1410920.	62.34	82.482	41.614	-13.342	3.25646
Wollastonite	-389810.	19.60	26.640	3.600	-6.520	0.95435
Carbon dioxide	-94054.	51.072	10.570	2.100	-2.060	0.0
Steam	-57796.	45.104	7.30	2.460	0.0	0.0

$\Delta C_p = a + bT + cT^{-2}$

Note: A-I values from Helgeson et al. (1978) except the ΔH_f° of Edenite. ΔH_f° Edenite derived by trial and error fit to data of Widmark (1974).

Table 40.2

Descriptions of starting materials for experiments

- A. Bulk composition Edenite-100. Albite + Diopside symplectite crystallized from glass on slow cooling.
- B. Bulk composition Edenite + 4 Quartz Glass fused to glass at 1400°C, rapid quench.
- C. Bulk composition Edenite-100 glass + 5% Diopside crystals quenched from 1300°C.
- D. Albite (synth, high) + Dolomite (synth, ordered) + Quartz in proportions $1Ab + 5Dol + 4Q \rightleftharpoons 1Ed + 3Ca$ Loaded in sealed platinum with oxalic acid.
 $X_{CO_2} = X_{H_2O} = 0.5$

determine the free energy of the reaction and the correct value for the free energy of edenite. As it will be seen this goal was not achieved, although some progress has resulted.

Comments

A few comments on these calculated equilibria may be of interest. The first is that according to the calculations at temperatures about 400° or 500°C in the presence of albite and quartz, amphibole should be strongly edenitic. This does not appear to be borne out by natural assemblages. Second, in Figure 40.1 may be seen a hint of the difficulty that can be expected on experimental work in this system. The proximity of the equilibrium dolomite + quartz \rightleftharpoons tremolite + calcite and the equilibrium albite + dolomite + quartz \rightleftharpoons edenite + calcite suggests that these reactions may compete in rate and in solid solution and that it may be difficult to resolve their locations in the presence of albite. Further, these equilibria are both close to the reaction dolomite + quartz \rightleftharpoons talc + calcite. Thus a certain amount of difficulty may be anticipated.

Experimental Studies

Synthesis

It has not been possible to synthesize 100 per cent edenite. Although the same procedure was followed as reported by Colville et al. (1966), it has not yet proven possible to synthesize edenite without the presence of other phases, in particular diopside and a soda montmorillonite. Ernst (1968) remarked on the difficulty of producing alkali amphiboles without the production of a Na-montmorillonite. This difficulty has been evident in the present study as well.

Table 40.2 provides a description of the materials used for the experiments and these ranged from oxide mixes as used by Colville et al. (1966) to glasses and synthetic minerals crystallized from glasses. Table 40.3 presents the results of the experiments on these materials.

Summarizing the results of Table 40.3, it may be seen that with crystalline starting materials no change is produced after one week between 700° and 800°C and 1 kbar, while with glass starting materials amphibole is ordinarily produced at the highest temperatures. Attempts to produce 100 per cent edenite from glass invariably resulted in the production of a soda montmorillonite and minor amounts of amphibole with variable amounts of diopside, forsterite, and quartz. Attempts to crystallize the bulk composition edenite + 4 quartz (equivalent to albite + tremolite) from glass invariably produced a large amount of amphibole and minor amounts of diopside, albite, and quartz. Recrystallization of these edenite + 4 quartz bulk compositions invariably produced larger amounts of amphibole with a much improved degree of crystallinity. Recrystallization of the edenite 100 compositions resulted in a slow decrease in the amount of montmorillonite and a corresponding slow growth in the amount of amphibole. The only experiments that produced essentially pure amphibole + quartz + albite were those on the bulk composition edenite + 4 quartz and these were run at successively longer times to determine the direction of variation of cell parameters. The objective of these experiments was to verify the position of the equilibrium illustrated in Figure 40.4 and to a certain extent these experiments have been successful.

Table 40.3
Results of experiments on Edenite stability

Run	T°C	Pkb	Duration (days)	Comp.	Starting Material	Product
E-1	820	1.0	7	Ed100	A(Ab + Di)	A no change
E-2	773	1.0	7	Ed100	A(Ab + Di)	A no change
E-3	728	1.0	7	Ed100	A(Ab + Di)	A + minor Fo, little change
E-4	652	1.0	7	Ed100	A(Ab + Di)	minor Fo + Amph.
E-5	823	1.0	7	Ed + 4Q	B(glass)	Amph. + Diop. + Ab
E-6	802	1.0	7	Ed + 4Q	B(glass)	Amph. + Di + Ab
E-7	748	1.0	7	Ed + 4Q	B(glass)	Amph. + Di + Q
E-8	823	1.0	16	Ed100	C(glass)	Di, Q, Ab, <u>Mont.</u>
E-9	798	1.0	16	Ed100	C(glass)	Di, Fo, Amph., <u>Mont.</u>
E-10	777	1.0	16	Ed100	C(glass)	Di, Fo, Amph., <u>Mont.</u>
E-11	752	1.0	16	Ed100	C(glass)	Di, Q, Amph., <u>Mont.</u>
E-12	815 ± 10	1.0(P-loss)	22		Product of E-5	<u>Amph.</u> Trace Ab + Di
E-13	800	1.0	16		Product of E-6	<u>Amph.</u> Minor Ab + Q + Di
E-14	750	1.0	16		Product of E-7	<u>Amph.</u> Minor Ab + Q Better crystallinity
E-15	749	1.0	22		Product of E-12	<u>Amph.</u> , Ab + Q (Di gone)
E-16	802	1.0	22		Product of E-13	<u>Amph.</u> , Ab + Q (No Di)
E-17	824	1.0	21		Product of E-14	<u>Amph.</u> , Ab (minor Di) no Q
E-18	826	1.0	34		Product of E-8	<u>Amph.</u> + Di + Q (reduced <u>Mont.</u>)
E-19	801	1.0	34		Product of E-9	<u>Diop.</u> + Amph. + Q + <u>Mont.</u> Amph. increased
E-20	774	1.0	33		Product of E-10	<u>Mont.</u> + Ab + Di minor Amph.
E-21	750	1.0	22		Product of E-11	<u>Mont.</u> major + Ab + Fo + Di, no amph.
E-22	654	4.0	14	Ed100	C(glass)	<u>Mont.</u> major, Ab, Fo, Di
E-23	698	4.0	31	Ed100	C(glass)	<u>Mont.</u> major, Ab, Di, Amph.
E-24	750	4.0	30	Ed100	C(glass)	<u>Mont.</u> major, Ab, Di, Amph.
E-26	502	4.0	28	D (Ab + Do + Q)		Ab + Dol + Q no change
E-27	597	4.0	28	D (Ab + Do + Q)		<u>Mont.</u> major + Talc Dol. gone, Q gone, Ab reduced, no Amph.
E-28	453	2.0	28	D (Ab + Do + Q)		Ab + Do + Q still major minor <u>Mont.</u> + Talc no Amph.
E-29	501	2.0	27	D (Ab + Do + Q)		Ta + Calcite major Q gone, Dol. nearly gone, Ab reduced, no Amph.
E-30	825	2.0	5	Ed100	oxide mix	<u>Mont.</u> major Ab minor Amph. minor needles
E-31	800	2.0	6	Ed100	oxide mix	<u>Mont.</u> major + Diop Amph. minor
E-32	756	2.0	6	Ed100	oxide mix	<u>Mont.</u> major Di + Amph. minor

Table 40.4
Calculated interplanar spacings for
Tremolite-Edenite-Richterite

Composition	$2\theta_{310}\text{CuK}\alpha$	$2\theta_{202}\text{CuK}\alpha$
Richterite 100	28.3064	35.5012
Rc50-Ed50	28.3872	35.5967
Rc50-Tr50	28.4228	35.5024
Edenite 100	28.4676	35.6957
Tremolite 100	28.5374	35.4973
Tr50-Ed50	28.5014	35.5975
Ed33-Tr33-Rc33	28.4344	35.5640

Based on assuming linear variation of cell parameters with composition, and the following end-member unit cell parameters.

End-member	a_0	b_0	c_0	β
Tremolite	9.833	18.054	5.268	$10^\circ 31'$
Edenite	9.853	18.005	5.236	$104^\circ 24'$
Richterite	9.902	17.980	5.269	$104^\circ 13'$

Table 40.5

Summary of X-ray oscillation of selected runs

Run	$2\theta(310) \pm 1\sigma$	$2\theta(\bar{2}02) \pm 1\sigma$
E-5	$28.564 \pm .014$	$35.472 \pm .035$
E-12	$28.535 \pm .013$	$35.412 \pm .009$
E-13	$28.567 \pm .010$	$35.480 \pm .012$
E-14	$28.536 \pm .057$	$35.468 \pm .014$
E-15	$28.541 \pm .013$	$35.408 \pm .015$
E-16	$28.532 \pm .013$	$35.435 \pm .005$
E-17	$28.545 \pm .036$	$35.444 \pm .012$
Mean $\pm 1\sigma$	$28.5457 \pm .0142$	$35.4456 \pm .029$
Range 1σ	28.5599 28.5315	35.4746 35.4166
	No significant variations	Variation barely significant

Solid Solution

In the expectation that the amphiboles produced would lie in the compositional range somewhere between edenite, tremolite, and richterite, the unit cells of edenite, tremolite, and richterite were used (Table 40.4) to compute the 2θ values for all of the reflections allowed by the space group. These are reported in Table 40.4 and are based on the assumption that the cell parameters vary linearly with composition. The peaks due to (310) and $(\bar{2}02)$ proved to show the most variation of composition and these have been plotted in Figure 40.5. In Figure 40.5 it may be seen that it should be possible to distinguish on the basis of (310) and $(\bar{2}02)$

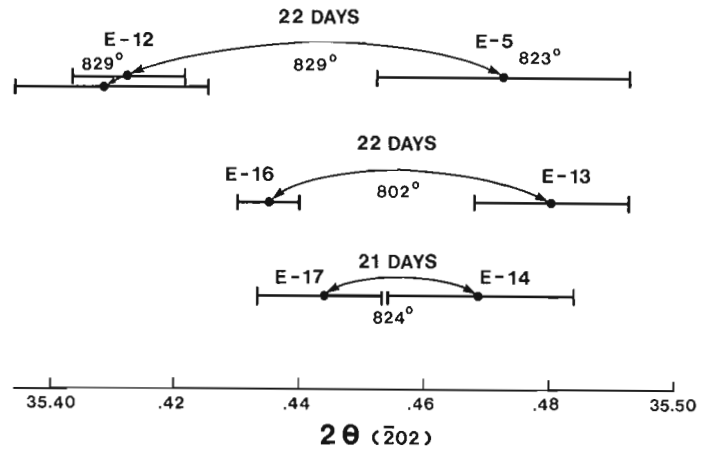


Figure 40.6. Effect on $2\theta_{202}$ of prolonged treatment of run products at high pressures and temperatures.

DIAGRAMMATIC ONLY

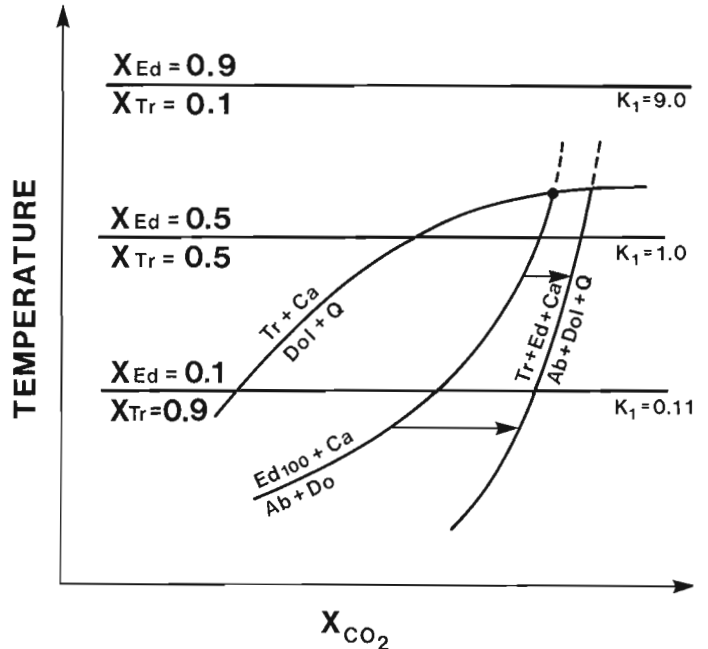


Figure 40.7. Qualitative effect of amphibole solid solution on various equilibria involving edenite.

the variation in composition of the synthetic amphiboles. These X-ray spacings were determined experimentally by means of oscillations between sodium chloride peaks and the amphibole peaks after calibration of the NaCl peaks against the unit cell of silicon metal. The most striking feature of Figure 40.5 is that the synthesized amphiboles plot near the tremolite corner of the triangle and in fact just outside of the permissible composition range. With reference to Table 40.5 it will be seen that the 1σ range in $2\theta(310)$ is nonsignificant within the uncertainty of measurement, while the variation in $2\theta(\bar{2}02)$ is just within the range of being significant.

Reference to Figure 40.6 will show the results of prolonged treatment of run products at high pressures and temperature. Plotted are the values of $2\theta(\bar{2}02)$ and represented in the diagram is the progressive change in several different experiments. After 22 days at 829°C the spacing determined from run E-5 was reduced in size to the spacing measured on run E-12. Similarly, E-13 changed towards E-16, and E-14 changed towards E-17. Without exception, prolonged runs resulted in a reduction in $2\theta(\bar{2}02)$.

The interesting point is that this change in unit cell parameter reflects a move away from the composition of edenite so that we must conclude that the amphiboles are becoming less edenitic with time. The first amphibole synthesized appears to have some edenite component and with time the amphibole becomes more tremolitic and the amount of albite in association with it increases.

This behaviour is contrary to what one might expect from the calculations presented in Figure 40.4. According to those calculations, at temperatures in the neighbourhood of 700° to 800°C the amphibole at equilibrium with albite and quartz should be very rich in edenite and poor in tremolite, while quite the reverse has been observed. Although no microprobe analyses have yet been made of the synthetic amphiboles, it seems quite clear on the present evidence that the free energy used for edenite from the data of Widmark is incorrect, which implies edenite to be far more stable than it actually is.

Effect of Solid-Solid Equilibrium on T-x Diagram

In Figure 40.7 is shown in a purely diagrammatic fashion the effect of the solid-solid equilibrium albite + tremolite \rightleftharpoons edenite + quartz on the solid-vapour equilibria illustrated in Figures 40.1 and 40.2. With increasing temperature the amphibole should become more edenitic with the result that the reaction involving edenitic amphibole should be displaced to higher values of $x\text{CO}_2$ at lower temperatures and that it will be truncated at higher temperatures by the equilibrium dolomite + quartz \rightleftharpoons tremolite + calcite. It is thus necessary to recognize that the edenite-producing equilibrium will produce a different composition of amphibole at every point along its length and thus it must be necessary to conclude that the work of Widmark, which did not demonstrate the composition of the solid solution, must be accepted with a certain amount of caution.

Conclusions and Remarks

The data presented by Widmark (1974) imply that edenite is a very stable amphibole while the experiments conducted so far in this study indicate that the assemblage albite + tremolite is more stable. It seems very likely that the reactions presented by Widmark are not equilibrium reactions in that no account was taken of solid solution in the amphiboles and a natural labradorite was used for the plagioclase. It seems probable that Widmark produced overgrowths of tremolite on the seeds of edenite with which he started and thus was demonstrating not the equilibrium albite + dolomite + quartz \rightleftharpoons edenite + calcite but an overgrowth on edenite seeds of the equilibrium dolomite + quartz \rightleftharpoons tremolite + calcite. It will therefore not be possible to make practical use of the work of Widmark and probably the solid-solid equilibrium shown in Figure 40.4 will be the most important to determine. This work is now going forward. If solid solution shifts in the amphibole compositions can be satisfactorily demonstrated with the microprobe and with X-rays it will be possible to determine the free energy of the reaction albite + tremolite \rightleftharpoons edenite + quartz and therefore to determine the free energy of edenite.

Selected Bibliography

- Charles, R.W.
1975: The phase equilibria of richterite and ferrichterite; *American Mineralogist*, v. 60, p. 367-374.
- Colville, T., Ernst, W.G., and Gilbert, M.C.
1966: Relationships between cell parameters and chemical compositions of monoclinic amphiboles; *American Mineralogist*, v. 51, p. 1727-1754.
- Ernst, W.G.
1968: *Amphiboles; Minerals, Rocks, and Inorganic Materials Series*; Springer-Verlag, New York, 125 p.
- Gordon, T.M. and Greenwood, H.J.
1970: The reaction: dolomite + quartz + water \rightleftharpoons talc + calcite + carbon dioxide; *American Journal of Science*, v. 268, p. 225-242.
- Helgeson, H.C., Delany, J.M., Nesbitt, H.W., and Bird, D.K.
1978: Summary and critique of the thermodynamic properties of rock-forming minerals; *American Journal of Science*, v. 278A, 229 p.
- Pëto, P.
1976: Synthesis and stability of edenitic hornblende, *Progress in Experimental Petrology: Third Progress Report of Research Supported by N.E.R.C. at Edinburgh and Manchester Universities, 1972-75; The Natural Environment Research Council Publications Series D, No. 6, 1976, p. 27-28.*
- Skippen, G.B.
1971: Experimental data for reactions in siliceous marbles; *Journal of Geology*, v. 79, p. 457-481.
1974: An experimental model for low pressure metamorphism of siliceous dolomitic marble; *American Journal of Science*, v. 274, p. 487-509.
- Widmark, E.T.
1974: An edenite-forming reaction: hydrothermal experiments; *Neues Jahrbuch für Mineralogie, Monatshefte*, 1974, Heft 7, p. 323-329, Stuttgart.

Project 760008

R. Claude Gauthier¹
Terrain Sciences Division

Gauthier, R. Claude, Aspects of the glacial history of the north-central Highlands of New Brunswick; in Current Research, Part B, Geological Survey of Canada, Paper 79-1B, p. 371-377, 1979.

Abstract

The deglaciation of the northern New Brunswick Highlands was accomplished mainly by downwasting. Striated bedrock and the dispersion of erratics indicate an eastward glacial flow in the eastern part of the study area. Upper Nepisiguit Valley was occupied by an outlet tongue at one stage during ice retreat. In the central Highlands, many areas are devoid of distinctive glacial morphology; instead, they contain weathered granite, felsenmeers, and tors and lack abraded bedrock surfaces. These aspects are considered as evidence for the presence of a cover of cold-based (non-erosive) ice. During retreat, ice lobes in the surrounding lowlands dammed glacial lakes in the highland parts of Nepisiguit, Little Tobique, and Upsalquitch valleys.

Introduction

The area under study (National Topographic System map areas 21 O/1, 2, 7, 8, 9, and 10) is located in the New Brunswick Highlands (Bostock, 1969) south of Campbellton in north-central New Brunswick (Fig. 41.1). The region includes the highest point of the province, Mount Carleton, at 820 m a.s.l. The general elevation of the area varies from 300 m a.s.l. in the northeast to 450 m in the southwest, with local relief around 250 m. Mountain summits are generally higher than 600 m a.s.l. Regionally, the land is characterized as an undulating upland plateau, with deeply incised rivers flowing from the central area. Nepisiguit Valley locally cuts through the surrounding topography to a maximum depth of 360 m; Jacquet Valley is 225 m deep and has an average width of 600 m.

A more or less radial drainage pattern has developed in the area, reflecting its dome-shaped morphologic character. Deranged drainage, associated with hummocky topography, is apparent in the southwest where numerous small lake basins have been formed.

The New Brunswick Highlands are included entirely in the Miramichi Anticlinorium. Ordovician mafic and acid volcanic rocks and various clastic sedimentary units (mostly included in the Tetagouche Group) are the most common lithologies. Large nonmetamorphosed batholiths of granite, quartz monzonite, and granodiorite are concentrated in the west-central part of the area; these intrusive rocks are of Devonian age.

Fieldwork in the study area was started during summer 1978 and has continued; areas selected on the basis of specific problems remain to be visited and studied in more detail. The density of field observations varies greatly depending on accessibility to areas and on the quality and quantity of exposures. Most of the length of Upsalquitch and Nepisiguit rivers was covered by canoe. A system of forest roads is the primary means of access into the study area; however, these roads require long distances of travelling and give limited information concerning the types of glacial material present, because the forest bordering the roads obscures the landscape. Where available, recent forest-cuts and roadcuts provide information on the morphology, and the roads provide access.

Acknowledgments

Dr. R.J. Fulton kindly provided critical comments which greatly improved this report. I am grateful to B. Needham, my field assistant, for his generous contribution.

Regional Glacial Flow

Evidences of regional glacial flow are widespread in the eastern part of the study area (Fig. 41.1); polished and abraded bedrock, as well as accumulations of lodgment till, is common. A continuation of the same ice flow has been recognized in the adjoining map area to the east and is believed to have reached at least the eastern coast of New Brunswick. But over the rest of the area, however, these evidences are lacking; a discontinuous accumulation of oxidized diamicton gradually replaces the basal till, and the bedrock loses all signs of fresh glacial erosion, exposing a chemically weathered profile. Evidences of glacial transport are present, but no distinctive pattern has yet been recognized.

Where evidence of the regional ice flow is present, numerous (nearly 150) striation sites have been observed. Except for the southeast part of the study area where there is evidence of north-northeast flow, they indicate a consistent and uniform direction of ice flow towards the east, with limited variability. Sites that have preserved a relative chronology are widely scattered and show limited differences in trend (less than 50°) between the two sets of striae. Because this variation is so small, it has not been possible to assign individual striae to specific patterns of movement. As a consequence, it is postulated that the different directions of movement reflect local flow readjustment rather than a gradual reorientation of ice flow with time.

The dispersion of striated bedrock sites as shown in Figure 41.1 may, in part, be a reflection of accessibility, but the lack of glacial flow features over much of the area probably is a reflection of the non-erosive action of the ice in these areas. It has been suggested that this is due to the presence of cold-based ice over the Highlands (Gauthier, 1978b).

Lodgment till in the eastern part of the area contains a variable proportion of fresh, resistant granite erratics from a source area lying to the west. This dispersion pattern is in agreement with striae evidence.

North-northeast Ice Flow

The southeast corner of Figure 41.1 is characterized by a set of distinctive glacial linear features oriented towards the north-northeast. A fluted surface and striated bedrock are the result of a late-glacial flow which succeeded the regional eastward glacial flow. A dashed line has been placed on Figure 41.1 to delineate the approximate western limit of the northward flowing ice. This northward ice flow extends into the adjacent map area (Gauthier, 1978a) and has been

¹Department of Geology, University of Western Ontario, London, Ontario. N6A 5B8

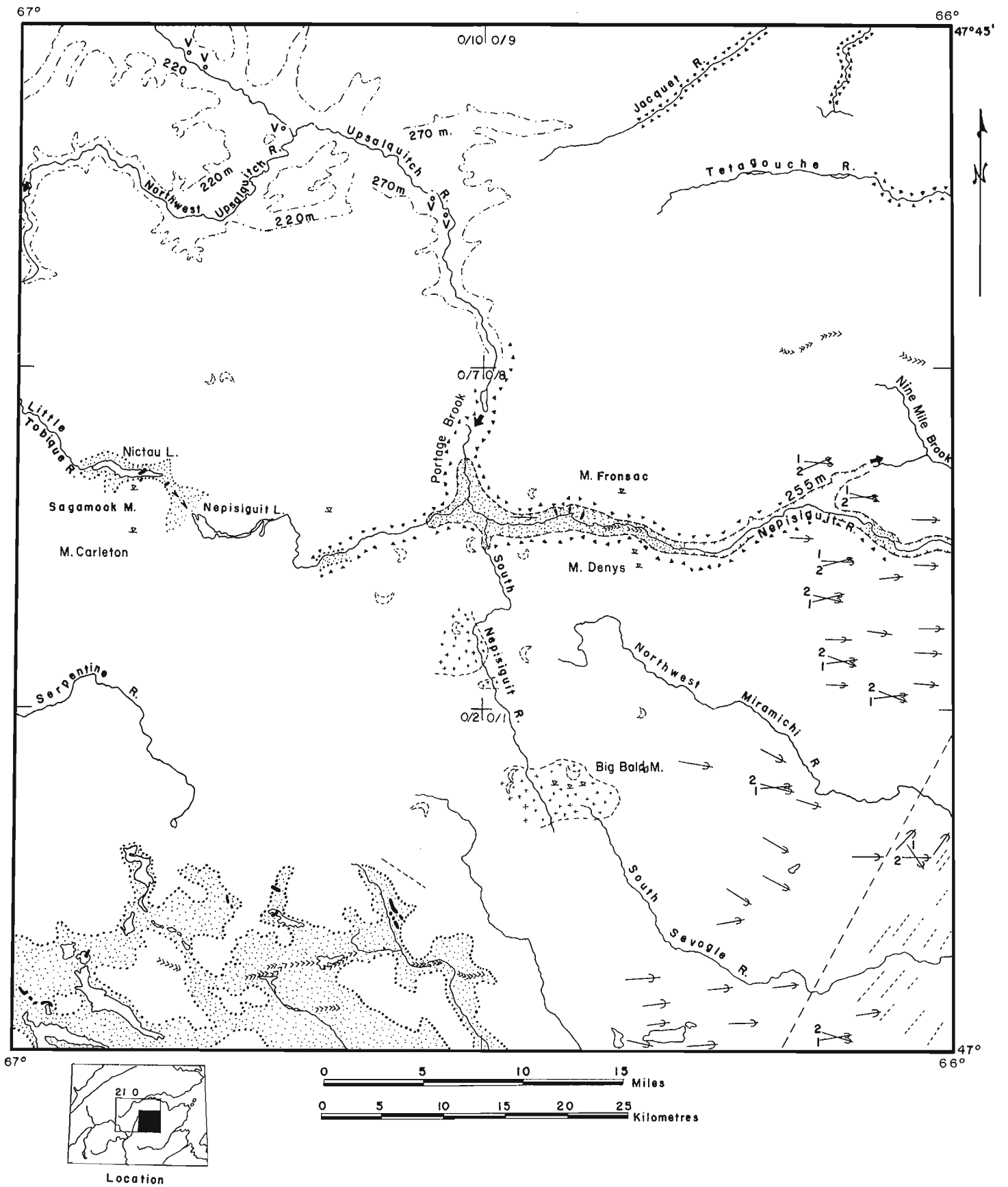


Figure 41.1. Map showing some aspects of the Quaternary geology of the north-central Highlands of New Brunswick.

traced 65 km north to the Bathurst region. No information has been gathered on the southern extension of and the source area for the north-northeast flowing ice. Further information on this ice movement is found in Gauthier (1978a) and Gauthier and Cormier (1977).

Attempts to associate a distinctive lodgment till with the northward flowing ice have not been successful. Nor have definitive ice marginal features been located. Crosscutting striae and the superposition of tills in the area to the east (Gauthier, 1978b) indicate clearly that the north-northeast flow is the last event to affect the area.

Evidence of Glacial Activity

Glacial Disintegration

A large area of hummocky disintegration moraine occupies the southeast part of the study area. The material fills depressions, blanketing the bottom and lower walls of large valleys to a depth of about 40 m. Numerous isolated ice contact ridges and eskers are associated with the ablation material. The present drainage is strongly affected by the hummocky topography; lakes and peat bogs are numerous. A discontinuous esker oriented east-west extends for 30 km. The flow direction is assumed to be eastward but has not been confirmed by field observations. Segments of ice contact morainic ridges, showing no apparent orientation, are spread over the area.

Nepisiguit River System

Nepisiguit Valley distinguishes itself from other valleys in the Highlands by an abundance of glaciofluvial and ice contact sediments. This belt of materials extends 70 km downstream from the river source, Nepisiguit Lakes, and upstream into the drainage system of Little Tobique River at Nictau Lake. The valley system is associated with the

retreat of a tongue of ice that partly filled the valley. Characteristic features associated with this retreat include transverse morainic ridges, kame terraces, pitted outwash, glaciofluvial outwash, lateral moraines, sediment-choked tributaries, and dammed lakes.


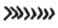


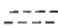



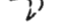

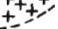

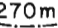


The ice tongue is believed to have been a protuberance extending eastward from the main ice mass that sat on the Highlands. Because of the irregular topography of the Highlands, ice flow was restricted mainly to the valley tongue. The actual length of the lobe remains unknown, and its thickness probably was minimal (less than 40 m).

The character of Nepisiguit Valley differs from the V-shaped valleys of Jacquet and Teta gouche rivers which are deeply incised (up to 225 m) into bedrock and which show no evidence of glacial erosion and sedimentation. Because only this one valley shows evidence of occupation by an active ice tongue, it appears that such lobations were not common during deglaciation.

The Nepisiguit lobe retreated westward over the divide with Little Tobique River. When this occurred, a small glacial lake, draining into Nepisiguit Valley, formed between the retreating ice tongue and the divide. The present drainage divide is at an elevation of 305 m a.s.l.; this means that the level of the glacial lake was 50 m higher than the present level of Nictau Lake. Ice contact ridges related to the retreat of the valley glacier are found in the vicinity of Nictau Lake. Figure 41.2 illustrates the best developed ridge that divides the lake into two segments — Nictau and Little Nictau lakes.

Nepisiguit Valley also was blocked during deglaciation, forming a lake draining via Nine Mile Brook (Fig. 41.1) into meltwater channels that were in contact with the western limit of north-northeast flowing ice. This system drained into Baie des Chaleurs in the Bathurst map area. As the ice retreated, lower phases of this lake drained directly through ice marginal meltwater channels.

LEGEND

	Ice contact morainic ridges
	Esker
	Disintegration moraine
	Flow direction of outwash
	Fluted till
	Approximate western limit of the north-northeastward ice flow
	Deeply incised valley in bedrock
	Cirque-like feature
	Striae; 1 oldest, 2 youngest
	Weathered granite
	Tors and felsenmeer
	270m Maximum extent of glacial lake Upsalquitch and phase level (m)
	Glacial lake outlet
	Limit of 255 m level of glacial lake Nepisiguit
	Varved sediments

Glacial Lake Upsalquitch

During retreat of the ice mass, the northward drainage of Upsalquitch Valley into Baie des Chaleurs was blocked, and glacial lake Upsalquitch formed. As the ice mass retreated to the north, new outlets were opened, and two major lake phases affected the study area (Fig. 41.1).

The first phase of the glacial lake drained towards the south, across the divide into Portage Brook, a tributary of Nepisiguit River (Fig. 41.1). This outlet, at 270 m elevation, was used while Northwest Upsalquitch Valley remained occupied by the ice. Ice retreat from Northwest Upsalquitch Valley would have initiated the second lake phase (Fig. 41.1) by opening a lower outlet (220 m) into Little Tobique River outside the map area. The prior opening of Saint John Valley was essential to the development of this phase. Subsequent and lower phases developed later in the region to the north of the study area.

Varved sediments (see Fig. 41.1) occur along Upsalquitch Valley (Northwest Upsalquitch has not yet been visited). No complete sequence has been found as the base has always been below present river level and the top truncated by postglacial erosion. In one section 500 couplets were counted; this provides a minimum period for the glacial lake. No facies changes were recognized in the varved sequences that could be linked with the different phases of the lake.

Deltas also are present, related to lower levels of the lake. The best developed one is at 220 m in Upsalquitch Valley. A widening of the valley and the development of terraces indicate water level stabilization at this point and the accumulation of deltaic sediments.

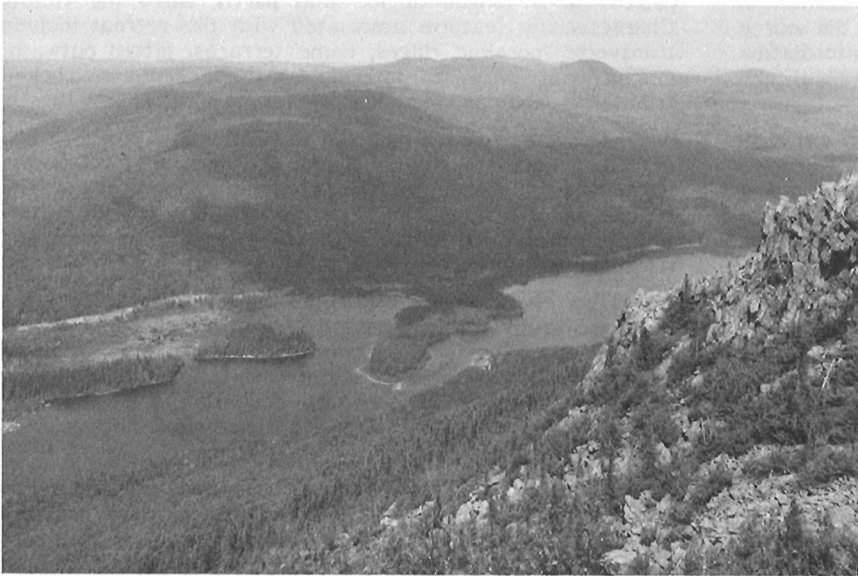


Figure 41.2.

View from the north slope of Sagamook Mountain which is characterized by the development of steps, tors (not visible in this picture), and talus slopes. The ridge crossing Nictau Lake is a morainic feature developed during retreat of the Nepisiguit glacial tongue.

Figure 41.3.

Fractured granite at an early stage of disintegration. The jointed fragments remain solid and coherent. In the lower right of the section, the material is finely fractured and disintegrated; this is contrary to the expected sequence of weathering in which the most highly weathered material would be at the top.



Figure 41.4.

Exposure of grus; the granite is entirely unconsolidated and homogeneous but remains in situ. The original texture is not preserved, and no secondary structures have developed. The thickness of grus is not known (exposed thickness is 2.5 m).

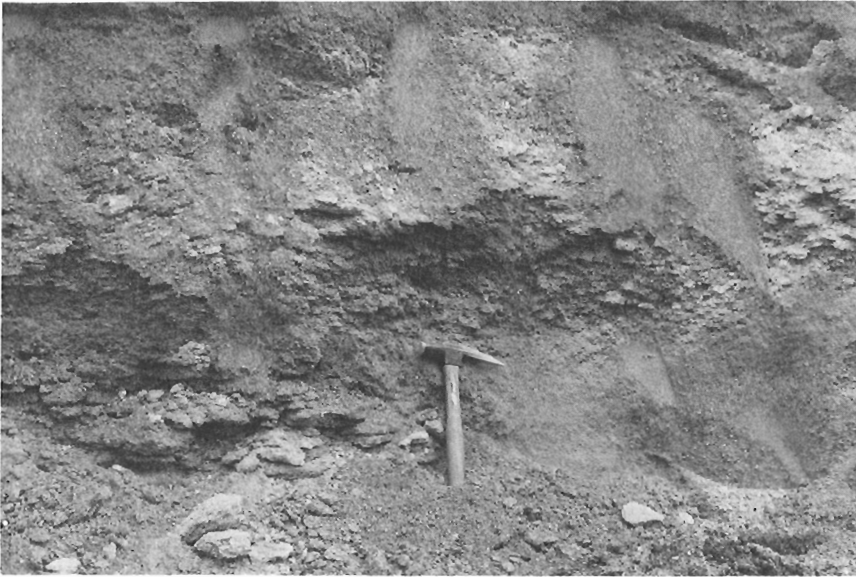


Figure 41.5.

A transition phase between disintegrated and sound granite. The granite at the bottom of the sequence is granular and tends to disintegrate into platy fragments. The original granitic structure is preserved in the lower part of the photograph, but at the top the grus is structureless.

Figure 41.6.

Hillslope tors on the north side of Sagamook Mountain. These prominent features have developed mainly from gelifraction along a dense pattern of joints. The pole on top of the tors is 2.6 m long.

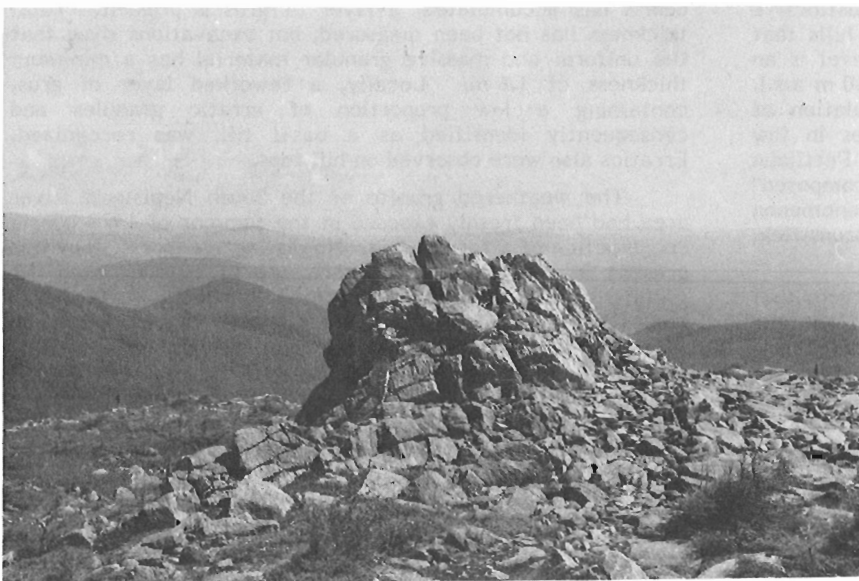
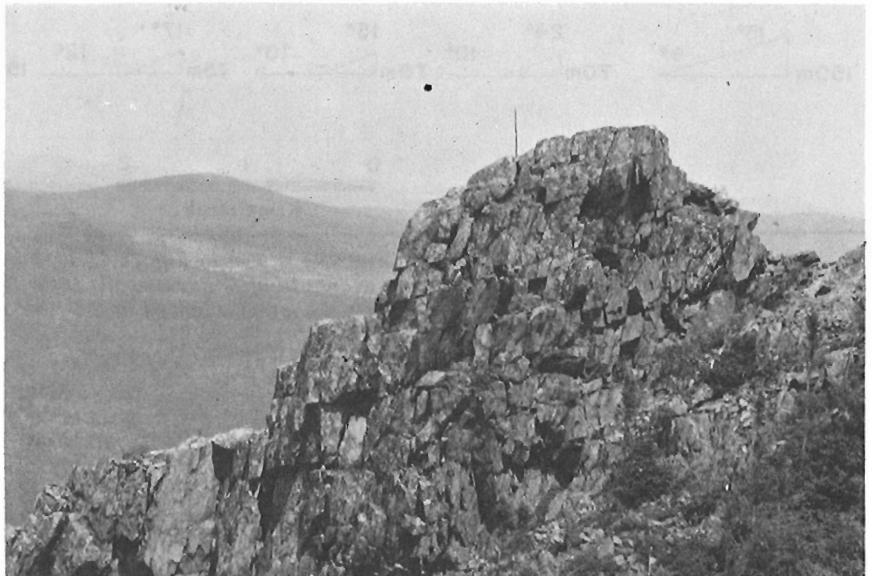


Figure 41.7.

Tor on top of Mount Carleton (highest point in New Brunswick). The tor is 2.8 m high. Note the regular surface of the Highlands.

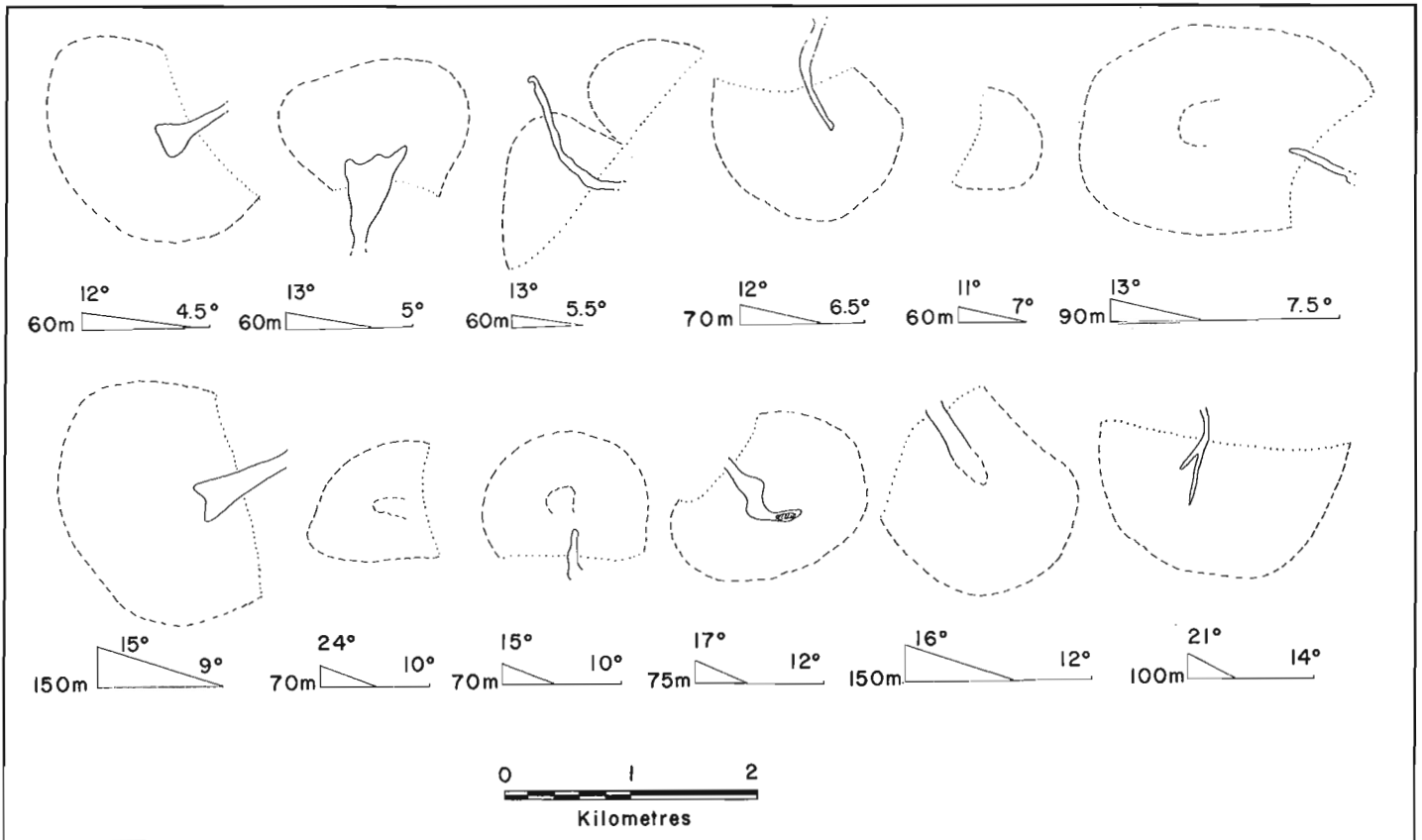


Figure 41.8. Cirque-like features that are shown in Figure 41.1. Parameters given at the base of each feature are: height of the headwall, horizontal length of the headwall, total length of basin, and maximum and average angles of the headwall. The features are shown as oriented in the field (north is at the top of the diagram).

Evidence of Minimal Glacial Erosion

Weathering of Granites

Granitic terrain dominates the central and southwestern parts of the Highlands. In general this area lacks exposures and is inaccessible. In the Big Bald Mountain and South Nepisiguit River areas, the granite is highly disintegrated (Fig. 41.1).

The Big Bald Mountain area has a distinctive morphology, with the presence of several rounded hills that have a local relief of about 150 m. The base level is an undulating plain lying at an average altitude of 460 m a.s.l. Erosion of the hills has resulted in the accumulation of weathered material (grus) of variable thicknesses in low areas. Anderson (1968), following a suggestion by Pettijohn (1975, p. 217), called a similar material a "recomposed" granite in northwestern New Brunswick. The phenomenon seems to be widespread throughout western New Brunswick, where granitic batholiths are present.

Areas with positive relief contain granite outcrops that show various characteristic features resulting from the preferential weathering of the rock. Ball-shaped forms (average diameter from 0.5 to 2 m), gnamma holes (or weathering pits, average diameter from 20 to 50 cm), vertically elongated columns (up to 2 m high), and tors (up to 2 m high) are abundant on the summits of hills. No accumulation of grus is generally present in the high areas. The granite surface is rough, reflecting the microrelief developed by the preferential weathering of coarse grained rock. The structural system of fractures is emphasized by differential weathering along joints; this is especially noticeable where tors remain.

Along hillslopes (commonly less than 30°), exfoliation of granite is the dominant process of alteration. Thin sheets of granite are partially detached from the slopes and are being actively disintegrated. No talus debris has accumulated at the foot of the slopes, suggesting that mechanical disintegration is the dominant mechanism of slope erosion. Exfoliation increases the surface area exposed to disaggregation.

On the undulating plain, where the recomposed granitic debris has accumulated, a layer of grus is present. Total thickness has not been measured, but excavations show that the uniform and massive granular material has a minimum thickness of 1.6 m. Locally, a reworked layer of grus, containing a low proportion of erratic granules and consequently identified as a basal till, was recognized. Erratics also were observed on hill tops.

The weathered granite of the South Nepisiguit River area had been freshly exposed in the summer of 1978 during construction of a forest road. No distinctive morphology was present in this area, but a sequence of cuts exposed the granite at different stages of deterioration. Figures 41.3 and 41.4 illustrate two different types of disintegration affecting the granite. Thin dykes of quartz, preferentially preserved and undeformed, indicate that the grus is in situ. A transition zone between partially disintegrated rock and grus also was exposed (Fig. 41.5). Locally, stringers of white, yellow, and green clay occur in the disintegrated granite.

The exposed sections occur in a low area on the west side of the river. Locally, a thin sequence of till with erratics was observed on top of the altered granite.

Tors and Felsenmeers

The summits of high mountains in the central part of the study area exhibit surfaces where felsenmeers and tors are present (Fig. 41.1). The most prominent features are located on the north slope of Sagamook Mountain where several hillslope tors are concentrated (Fig. 41.6). Tors vary from a few metres up to 10 m high. A layer of in situ fractured material is locally present on the summit and upper slopes of Sagamook Mountain. Where the slope is steep, the fractured rock fragments accumulate as talus on the slopes.

Mounts Carleton (Fig. 41.7) (820 m), Denys (560 m), and Fronsac (620 m) also show well developed felsenmeers and tors. Erratics among the block fields are rare, although they have been observed on top of Mount Denys (granitic cobbles and blocks) and Mount Fronsac. The closest source of granitic material to Mount Denys is located 2 km towards the west.

Cirque-like Features

From airphoto interpretation, 26 cirque-like features have been recognized in the study area. Plan and cross-section views of the 12 best examples (see Fig. 41.1) are shown in Figure 41.8. Because of limited steepness of the headwalls (from 11° to 24°), the low relief of the area (300 m), the low altitude of the basins (averaging 550 m a.s.l.), and the lack of preferential orientation, these features are not defined as cirques. Because of their well defined shapes and their opening onto large valleys, however, they are thought to be relict nivation features, whose formation possibly preceded a general glaciation. No field work has yet been done concerning the cirque-like forms, and it is unlikely that they will be useful for interpretation of the glacial history.

Conclusions

Intensity of Glaciation

Parts of the study area exhibit well defined features of glacial erosion and deposition; other parts lack these features. The hypothesis of cold-based ice centred on the Highlands of New Brunswick (Gauthier, 1978b) can be used to explain this dichotomy. The cold-based ice is explained as resulting from the presence of limited and non-eroding ice behind the protective barrier of the Chic-Choc Mountains in Gaspésie. From this semi-independent ice mass, a radial ice flow pattern developed in the marginal areas of northern New Brunswick. It is not known whether this ice mass was an ice cap that locally accumulated in New Brunswick (Chalmers, 1895, his Northumberland Glacier) or a glacier related to the Laurentide Ice Sheet (McGerrigle, 1952; Lebus and David, 1977). The eastward ice flow system described for the study area represents the main glacial period in northern New Brunswick. It has been traced in the adjacent map area to the east and probably reached the Gulf of St. Lawrence. The entire northern peninsula was affected by this flow.

Relative Chronology of Glacial Events

The north-northeast ice flow that occurred in the southeastern part of the study area and in the adjacent map area succeeded the regional eastward ice flow. The ice likely originated in the large Miramichi drainage basin and was seen by Chalmers (1895) as coalescent with a late ice cap centred in the Gulf of St. Lawrence. The late-glacial ice cap in the Gulf of St. Lawrence was flowing westwardly and southwardly on Prince Edward Island (Prest, 1973) and possibly westwardly in the Kouchibouguac area of New Brunswick (Prest, 1972). The implications of this system are discussed by Gauthier (1978a) in light of evidence gathered in the lowlands around Bathurst. Brinsmead (1979) identified a zone of interlobate moraine along Northwest Miramichi River (National Topographic System map area 21 P/4). This moraine can be visualized as occupying the poorly defined contact zone between the two glaciers.

At the time when the upper part of Nepisiguit Valley was occupied by a receding tongue of ice, its lower course was closed by the north-northeast flowing lobe of ice originating from the Miramichi drainage basin. Consequently, the drainage of the Upper Nepisiguit was obstructed, and the glacial lake that formed drained along the margin of the north-northeast flowing ice into Baie des Chaleurs (Gauthier and Cormier, 1977). Probably at the same time, the first phase of glacial lake Upsalquitch was draining south into Nepisiguit Valley via the Portage Brook outlet.

This gives a picture of deglaciation in which the Highlands emerge from a downwasting ice cap at the same time as the lowlands to the north and east were occupied by active ice.

References

- Anderson, F.P.
1968: Woodstock, Millville, and Coldstream map-areas, Carleton and York counties, New Brunswick; Geological Survey of Canada, Memoir 353, 69 p.
- Bostock, H.S.
1969: Physiographic regions of Canada; Geological Survey of Canada, Map 1254A, scale 1:5 000 000.
- Brinsmead, R.A.
1979: Granular resources of the Sevogle area, NTS 21 P/4; unpublished manuscript, New Brunswick Department of Natural Resources.
- Chalmers, R.
1895: Surface Geology of Eastern New Brunswick, Northwestern Nova Scotia, and a Portion of Prince Edward Island; Geological Survey of Canada, Annual Report, v. VII, pt. M.
- Gauthier, R.C.
1978a: Quelques interprétations de l'inventaire des dépôts de surface, péninsule nord-est du Nouveau-Brunswick; in Current Research, Part A, Commission géologique du Canada, Etude 78-1A, p. 409-412.
1978b: Last glaciation intensity and extent, northeastern New Brunswick; Program with Abstracts, Geological Association of Canada, Mineralogical Association of Canada, and Geological Society of America, Joint Meeting, Toronto, p. 406.
- Gauthier, R.C. et Cormier, V.
1977: Cartographie des dépôts superficiels, péninsule nord-est du Nouveau-Brunswick; in Report of Activities, Part A, Commission géologique du Canada, Etude 77-1A, p. 371-378.
- Lebus, J. et David, P.P.
1977: La stratigraphie et les événements du quaternaire de la partie occidentale de la Gaspésie, Québec; Géographie physique et quaternaire, vol. 31, p. 275-296.
- McGerrigle, H.W.
1952: Pleistocene glaciation of Gaspé Peninsula; Royal Society of Canada Transactions, v. 46, Series III, p. 37-51.
- Pettijohn, F.J.
1975: Sedimentary Rocks; Harper and Row, New York, 3rd edition, 628 p.
- Prest, V.K.
1972: Kouchibouguac National Park, eastern New Brunswick, Geology; unpublished report, Canada, Department of Indian Affairs and Northern Development, 15 p.
1973: Surficial deposits, Prince Edward Island; Geological Survey of Canada, Map 1366A, scale 1 inch to 2 miles.

E.M. Levy¹
Atlantic Geoscience Centre, Dartmouth

Levy, E.M., *Further chemical evidence for natural seepage on the Baffin Island Shelf; in Current Research, Part B, Geological Survey of Canada, Paper 79-1B, p. 379-383, 1979.*

Abstract

A preliminary analysis of the 1978 data concerning dissolved and dispersed petroleum residues in the water column and surface microlayer of the Baffin Island shelf provided further evidence for natural seepage of petroleum from the seabed at Scott Inlet, Buchan Gulf, and possibly northeast of Bylot Island. A model was proposed to account for the observed distributions.

Introduction

In a previous publication, visual and chemical evidence, which suggested natural seepage of petroleum from the seabed off Scott Inlet, Baffin Island, was reported (Levy, 1978). Visible slicks and gas bubbles erupting at the sea surface as well as anomalously high concentrations of petroleum residues in the surface microlayer and in the water column seemed to be associated with the submarine trough which extends seaward across the continental shelf from the fjord at Scott Inlet. Geological and geophysical data for this area demonstrated that a structural high containing two basement ridges underlies the south wall and trends northwesterly across the floor of the trough and that a sedimentary basin is present between the structural high and the coast (MacLean and Falconer, 1979). Seismic records showed that the strata forming the walls of the Scott Inlet trough are flat-lying for the most part and that strata which have been folded and faulted occur in the floor of the trough and in places form the lower part of the walls where they are separated from the overlying strata by an angular unconformity (MacLean, 1978). The geological environment, therefore, provides conditions which are favourable for the migration of hydrocarbons present in the rock formation and their subsequent escape to the water column and appearance at the sea surface.

In view of the southward surface currents in this area, the presence of slicks to the north of Scott Inlet in 1977 led to the postulation that there might also be seepage at Buchan Gulf, where there is a similar bathymetric feature, and at other locations on the Baffin Island continental shelf (Levy, 1978). To investigate these possibilities and to learn more about the seep at Scott Inlet, a multidisciplinary chemical-biological-geological study was carried out by the Bedford Institute of Oceanography during the summer of 1978. This report summarizes some of the preliminary results pertaining to the chemical portion of this study.

Sampling and Analytical Procedures

During the 1978 cruise (78-026) samples of seawater were collected at standard oceanographic depths throughout the water column at Scott Inlet, Buchan Gulf, the entrance to Lancaster Sound and in the northern portion of Baffin Bay (Fig. 42.1). At Scott Inlet and Buchan Gulf, sampling was carried out on grids

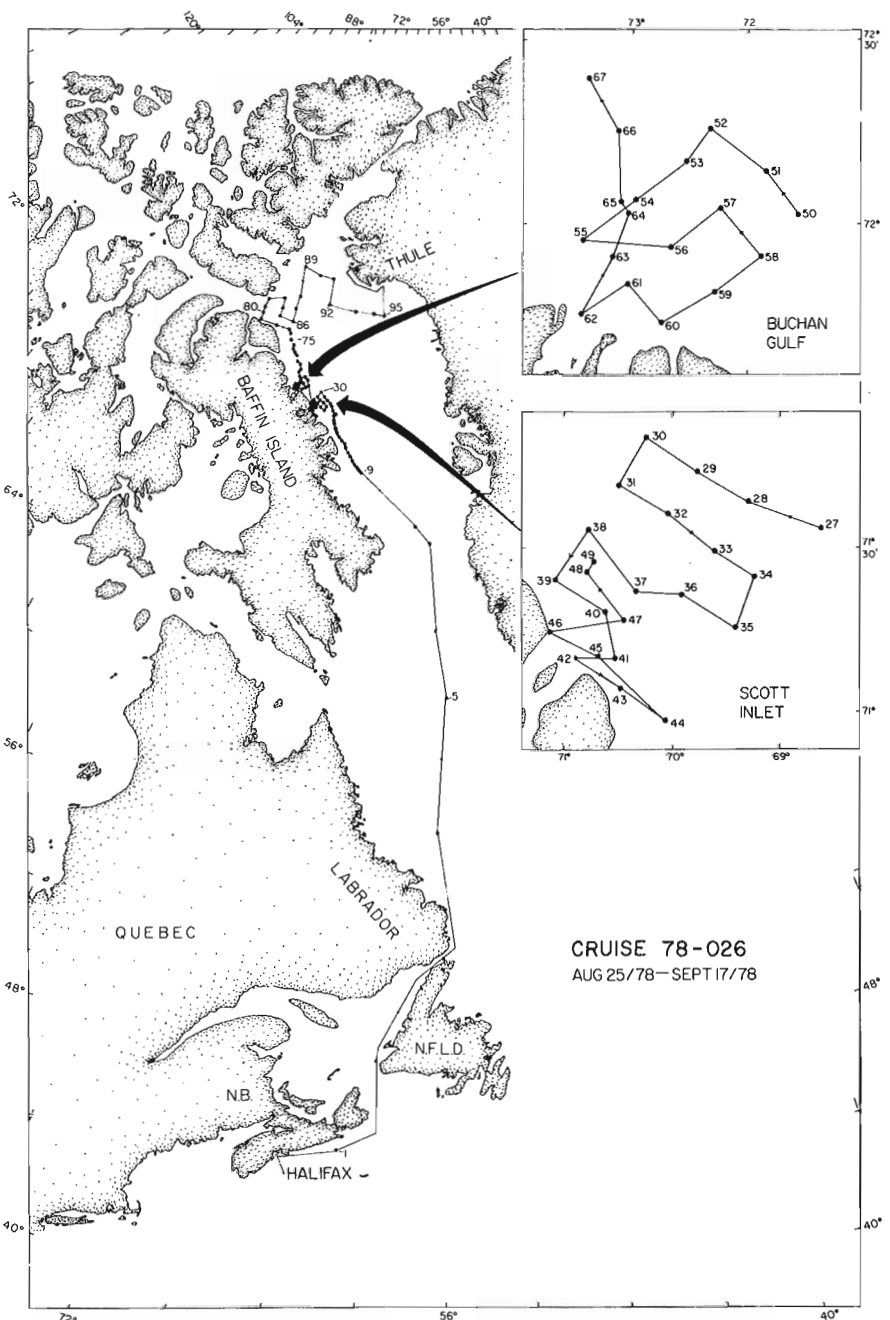


Figure 42.1. 1978 cruise track and location of stations.

¹Department of Fisheries and Oceans, Ocean and Aquatic Sciences, Atlantic Oceanographic Laboratory, Bedford Institute of Oceanography, Dartmouth, N.S. B2Y 4A2

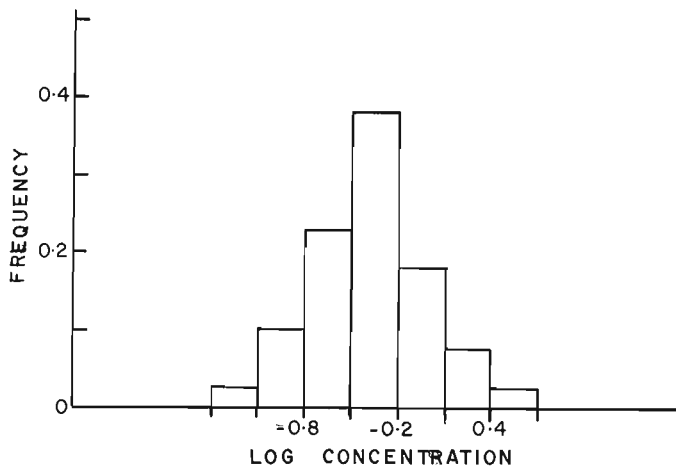


Figure 42.2. Lognormal distribution of 1977 data for dissolved and dispersed petroleum residues in the water column of Baffin Bay.

centred over the submarine troughs that extend seawards across the Baffin Island continental shelf in these areas. Separation between stations was about 19 km. Twenty-three stations were occupied at Scott Inlet (259 samples) and 18 at Buchan Gulf (140 samples). An expanded grid of 17 stations (166 samples) was sampled at the entrance to Lancaster Sound and extended into northern Baffin Bay (75 samples). In addition, stations were occupied en route from Halifax to Baffin Island.

Water samples were collected in 5 L Niskin samplers in a Rosette assembly which was lowered to within a few metres of the bottom and the samples were collected during retrieval. Immediately on recovery, 1 L subsamples were drawn for extraction and subsequent analyses for dissolved and dispersed petroleum residues (Levy, 1977). In addition, duplicate samples were drawn into 250 mL amber glass bottles and capped for the determination of volatile low molecular weight hydrocarbons. One of these was immediately extracted by equilibration with helium (McAuliffe, 1974) and analyzed by gas chromatography while the other was returned to the Institute for more detailed analyses. Processing of these data has not yet been completed. Samples from the surface microlayer were collected with a stainless steel screen (Garrett, 1965).

Results and Discussion

Water Column

It has been demonstrated (Levy, 1978, 1979) that the background level of dissolved and dispersed petroleum residues in the waters of Baffin Bay and adjoining Sounds during 1977 was $0.46 \mu\text{gL}^{-1}$ with subsequently higher concentrations in a few regions, notably the area off Scott Inlet. Although the concentration data for Baffin Bay were lognormally distributed (Fig. 42.2), those for the Scott Inlet area were not. This led to postulation that there were two distinct populations; namely, those samples in which only the general background level was observed and those which contained an additional input of oil from the seepage. However, sufficient data were not available from the 1977 cruise to establish the distributions.

Whereas the 1977 data pertaining to the background levels in Baffin Bay were lognormally distributed, those collected during 1978 at Scott Inlet, Buchan Gulf and Bylot Island failed to meet the stringent criteria imposed on

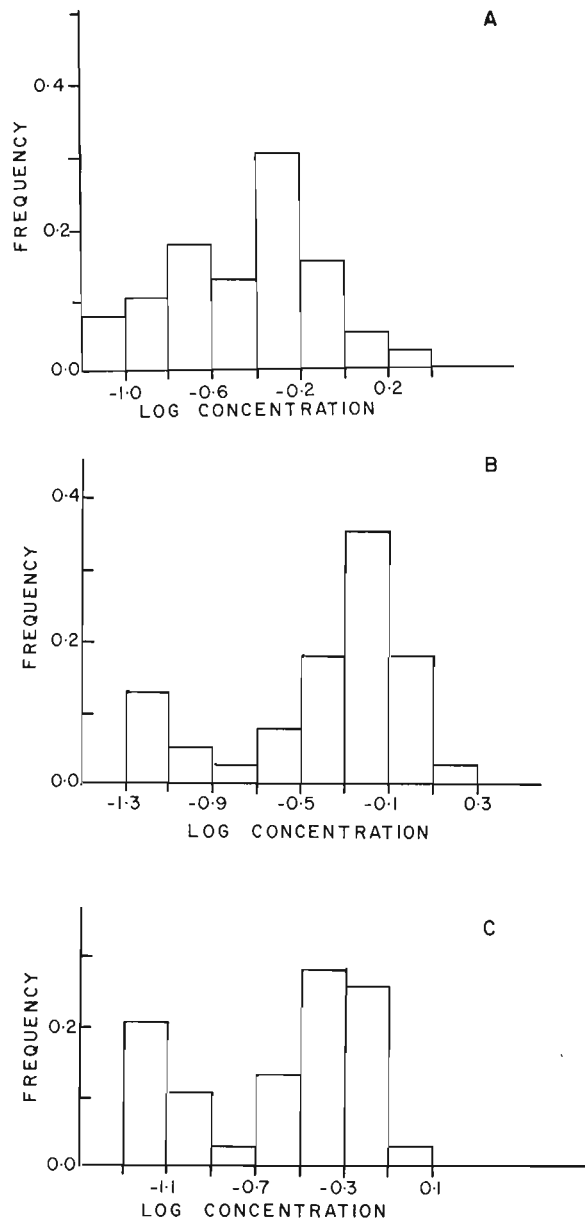


Figure 42.3. Frequency distribution plots of 1978 data for dissolved and dispersed petroleum residues in the water column at Scott Inlet (A), Buchan Gulf (B), and Bylot Island (C).

the χ^2 test by the large number of observations. The frequency distribution plots for these areas (Fig. 42.3) exhibit an almost bimodal character which indicates that two different populations are, indeed, present in the water column.

On the basis of this hypothesis, the observed distribution of dissolved and dispersed petroleum residues in Baffin Bay can be described in terms of a simple box model (Fig. 42.4) throughout which there is a general concentration level of $0.46 \mu\text{gL}^{-1}$ but which receives additional inputs from natural seepage from the seabed in several localities. Potential inputs such as leakage from a sunken wreck or spills occurring at the surface are not consistent with the chemical nature of the material or its distribution in the water column and are not included in the model. Since the seepage at Scott Inlet is believed to consist of small discrete releases from the

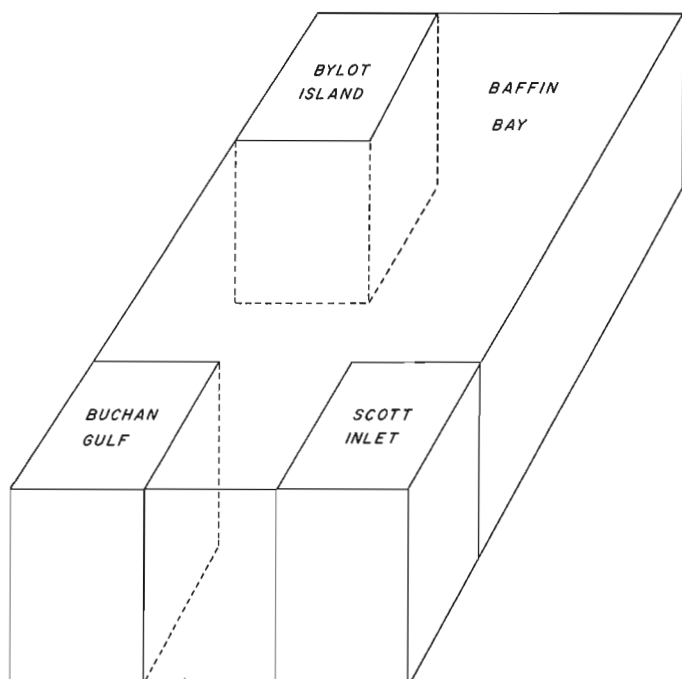


Figure 42.4. Box model describing concentrations of dissolved and dispersed petroleum residues in Baffin Bay.

walls and bottom of the submarine trough, the seep "site" is not localized but consists of many sites which are spread over a considerable area of the seafloor and which are probably not continuously active. Immediately upon escaping from the seabed, the oil droplets begin to rise under the force of their own buoyancy and are swept along by water currents. The result of this is the presence of "swarms" of oil droplets which are non-homogeneously distributed with respect to both space and time in the water body. Within a swarm, there are particles of various sizes that are separated by various distances which are large in relation to the size of sampler. As a result, the probability of catching one or more of them in a sampler at a given time and place in the water column accounts for the variability in the concentration data and the fact that not all samples from a given station, even in the seep areas, have higher than background concentrations. Qualitatively, then, this model can account for the lognormal distribution of the data and the general background level in Baffin Bay as a whole, as well as the elevated and highly variable concentrations observed in those areas where there is a second population of concentration levels arising from dispersed clouds of seep particles superimposed on the general background level.

From the properties of the Gaussian distribution of the log transformed concentration data for Baffin Bay, it can be shown that 99.9 per cent of the samples can be expected to have concentrations of dissolved and dispersed petroleum residues within the range of $0.41\text{--}0.52\ \mu\text{gL}^{-1}$. Accordingly, there should be less than one chance in a thousand of encountering a concentration in excess of $0.52\ \mu\text{gL}^{-1}$ in this population. Concentrations greater than this can therefore be considered as belonging to a different population. (This includes artifacts arising from analytical and sampling errors as well as true concentration anomalies.)

Since a total of 628 samples were collected from Baffin Bay waters during the 1977 cruise it would be predicted that only one observation would fall outside the 99.9 per cent range. In fact, however, 218 samples contained more than $0.52\ \mu\text{gL}^{-1}$ while 94 had concentrations greater than $1\ \mu\text{gL}^{-1}$

Table 42.1
Dissolved/dispersed petroleum residue concentration anomalies – Baffin Island Shelf, 1978

Area	No. Samples	No. Anomalies		Greater than	
		No.	%	$1\ \mu\text{gL}^{-1}$	%
Scott Inlet	259	65	25.1	17	6.6
Buchan Gulf	140	43	30.7	15	10.7
Bylot Island	166	16	9.6	1	0.6

and 6 greater than $5\ \mu\text{gL}^{-1}$. During the 1978 cruise, 565 samples were collected from the waters over the Baffin Island shelf at Scott Inlet, Buchan Gulf and northeast of Bylot Island and 124 anomalies were observed (Table 42.1). In all cases, the statistics support the presence of two (or more) populations of concentration levels.

In the Scott Inlet area, concentration anomalies in 1978 were clustered along the south wall of the trough (Fig. 42.5A) and the trough extension which lies between Hecla and Griper Bank and Baffin Island. In addition, there were high percentages of anomalies at the seaward portion of the Scott Inlet grid. It is pertinent to note also that the anomalies observed during the 1977 cruise are compatible with this contour map. At Buchan Gulf (Fig. 42.5B) although the anomalies tended to congregate over the trough, there was a pronounced offshore component and at the entrance to Lancaster Sound (Fig. 42.5C) anomalies trended in a northeasterly direction from Bylot Island. Notable in this area was the absence of anomalies in the northern portion of Lancaster Sound and the region southeast of Devon Island.

Surface Microlayer

Under suitable meteorological and oceanographic conditions, petroleum-derived components in seawater tend to accumulate at the surface of the sea. As a result, capillary waves are damped and the light reflecting properties of the sea surface are thereby modified. This results in the formation of a surface slick which, under favourable light conditions, is readily discernible. If this surface film is compressed; for example, by encountering a physical barrier or by the convergence of surface circulation cells, iridescence may be observed and in more extreme cases a mousse-like material may be formed. This phenomenon results in a marked enrichment of the surface-active substances in the sea surface microlayer relative to the water immediately below.

During the 1977 cruise weather and sea conditions in the Scott Inlet region were ideal for the formation and observation of surface slicks and extensive areas of the sea surface were covered with slicks (Levy, 1978). Unfortunately, during the chemical phase of the 1978 cruise conditions varied from unsuitable to barely marginal for the formation and observation of surface slicks. As a result, visual observations could not be made and interpreted with a high degree of reliability in 1978.

Surface microlayer concentrations at Scott Inlet were highest over the south wall of the trough (Fig. 42.6A) and over its southern extension. Since this was also the case for the concentration anomalies in the water column, it would seem that two of the most active seep sites during 1978 were in the vicinity of stations 40, 47, 43, and 45. During the 1977 cruise, extensive surface slicks were observed in the former area (Station 21) and extremely high concentrations of petroleum residues in the water column were encountered at the latter (Levy, 1978). Accordingly, these sites have been active for some time and might very well be the major seep

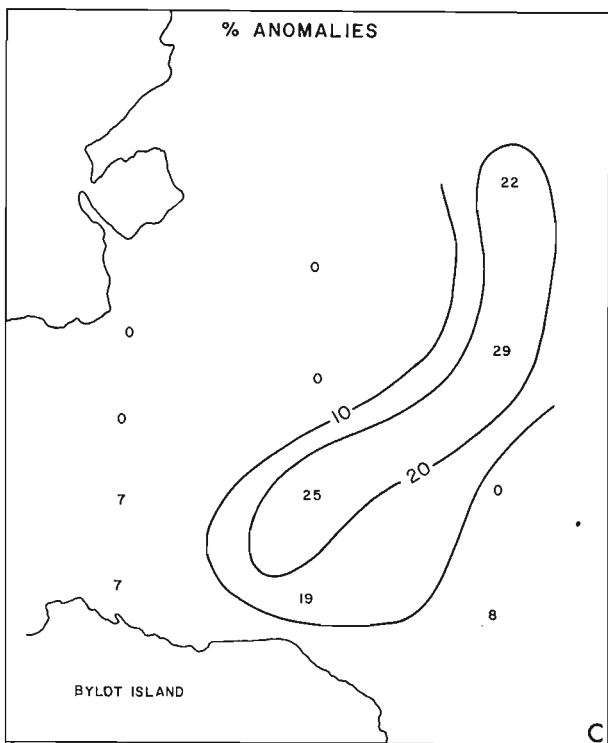
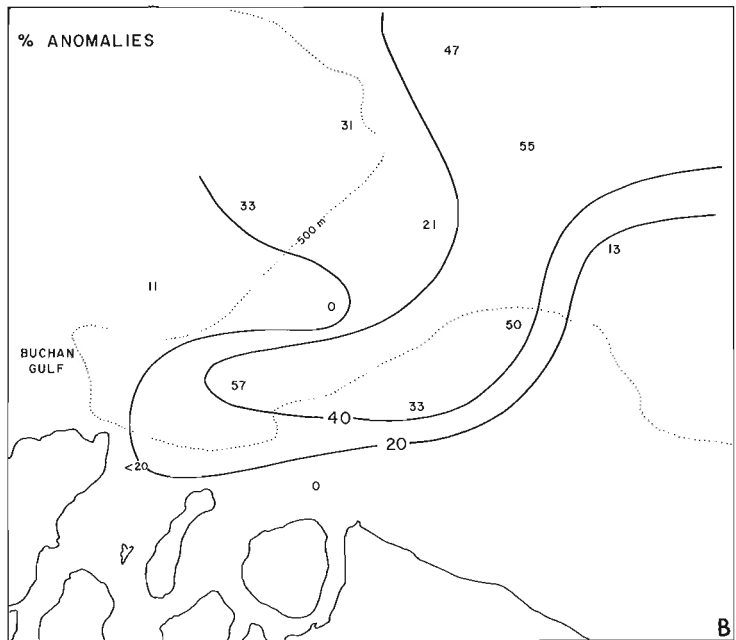
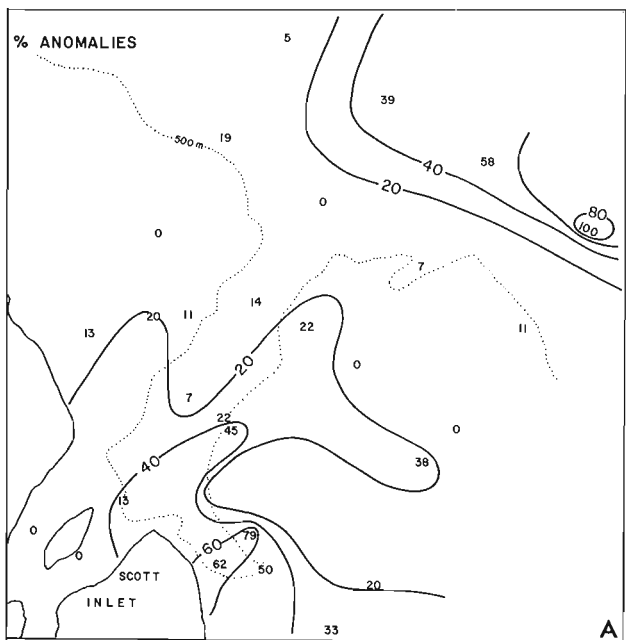


Figure 42.5. Concentration anomalies during 1978 at Scott Inlet (A), Buchan Gulf (B), and Bylot Island (C).

area at Scott Inlet. Regrettably, the 1978 sampling grid did not resample the exact site (Station 20) where the highest surface microlayer concentrations were measured in 1977 and where extensive slicks were present and gas bubbles observed. Slicks in this area were again observed during the geology cruise (MacLean, pers. comm.). Although the 1978 grid failed to locate a more active region, it is possible that they exist and, therefore, the area should be resampled on a more closely spaced grid and over a sufficient period of time to ensure favourable weather and sea conditions so that the sampling program can be complemented and guided by visual observations as was done in 1977.

At Buchan Gulf (Fig. 42.6B) an exceedingly high concentration of petroleum residues ($1200 \mu\text{gL}^{-1}$) in the surface microlayer was observed (Station 61). While this might have been the result of contamination from the ship or other source, a high surface concentration was also observed at Station 60. As it is unlikely that there would be contamination at both stations, it would seem reasonable to conclude that there was active seepage somewhere in this region. In the Bylot Island area (Fig. 42.6C), the surface microlayer concentrations were lowest at those stations which had the highest percentages of concentration anomalies. This is contrary to the trend at Scott Inlet and Buchan Gulf and is probably a consequence of surface currents in this area.

Concluding Remarks

A preliminary analysis of the data collected during 1978 concerning the concentration of dissolved and dispersed petroleum residues in the water column and surface microlayer in several regions of the Baffin Island shelf provided additional evidence for the natural seepage of petroleum from the seabed. The seepage at Scott Inlet was again detected and two of the seep sites were more closely located. In addition, some evidence was gained for seepage at Buchan Gulf and northeast of Bylot Island. Since conditions were not favourable for the formation of well-defined surface slicks at the time the sampling program was carried out, the surface data and observations were not as informative as they might otherwise have been — such are the realities of oceanographic research in the Arctic.

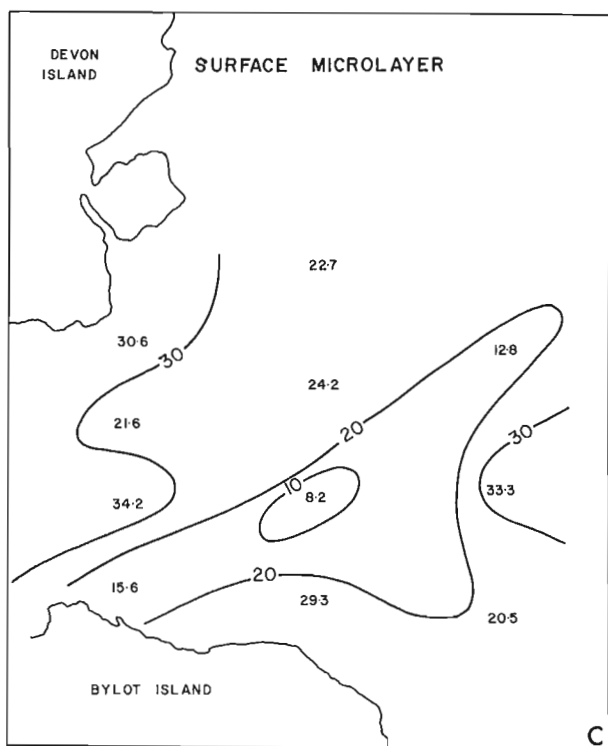
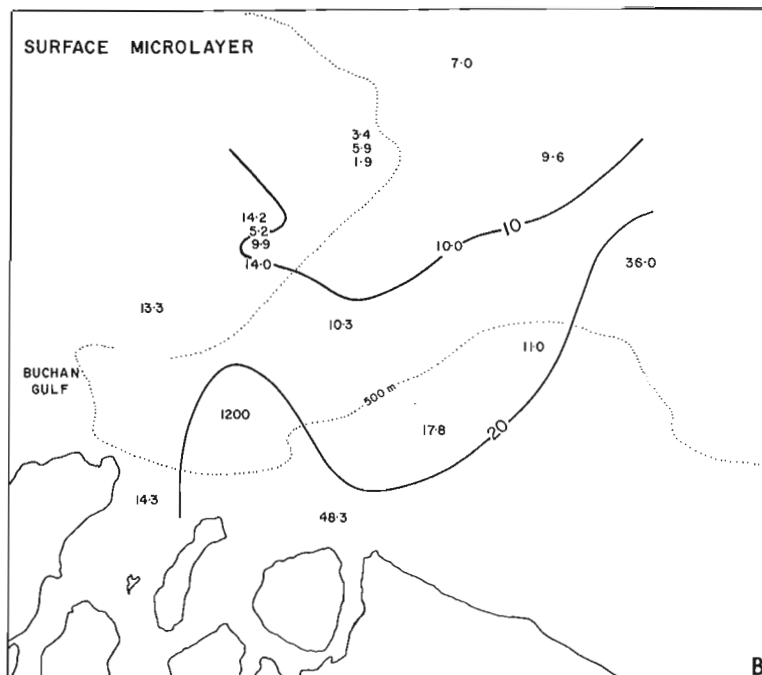
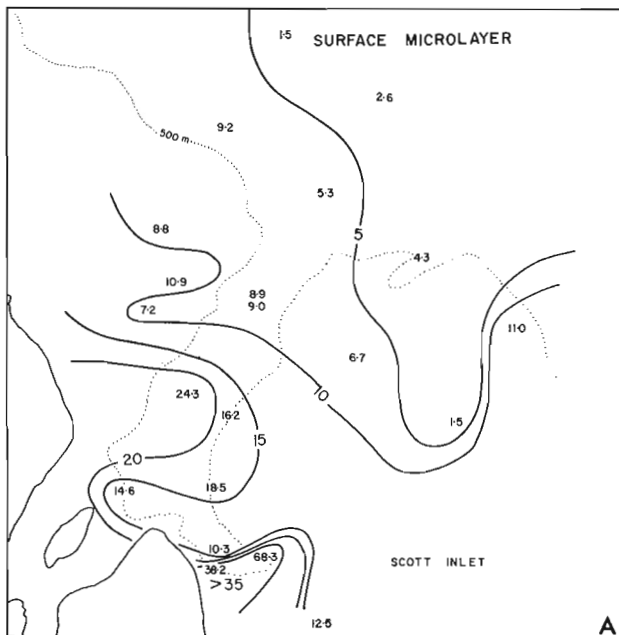


Figure 42.6. Surface microlayer concentrations during 1978 at Scott Inlet (A), Buchan Gulf (B), and Bylot Island (C).

Acknowledgments

Grateful acknowledgment is made to Captain D. Deer, officers and crew of **CSS Hudson** and members of the scientific complement for their co-operation in carrying out a successful field program, to J. Moffatt and D. Conrad for performing the laboratory analysis and to R. Falconer, B. MacLean and R. Pocklington for critically reviewing the manuscript.

References

Garrett, W.D.
 1965: Collection of slick-forming materials from the sea surface; *Limnology and Oceanography*, v. 10, p. 602-605.

Levy, E.M.
 1977: Fluorescence spectrophotometry: principles and practice as related to the determination of dissolved/dispersed petroleum residues in seawater; Bedford Institute of Oceanography Report Series/BI-R-77-7, July, 1979.

1978: Visual and chemical evidence for a natural seep at Scott Inlet, Baffin Island, District of Franklin; in *Current Research, Part B, Geological Survey of Canada*, Paper 78-1B, p. 21-26.

1979: Concentration of petroleum residues in the waters and sediments of Baffin Bay and the Eastern Canadian Arctic, 1977; Bedford Institute of Oceanography Report Series/BI-R-79-3, January, 1979.

MacLean, B.
 1978: Marine geological-geophysical investigations of the Scott Inlet and Cape Dyer-Frobisher Bay areas of the Baffin Island Continental Shelf in 1977; in *Current Research, Part B, Geological Survey of Canada*, Paper 78-1B, p. 13-20.

MacLean, B. and Falconer, R.
 1979: Geological and geophysical studies of Scott Inlet oil seep area; *Northern Miner.* (in press)

McAuliffe, C.D.
 1974: Determination of C₁-C₁₀ hydrocarbons in water; U.S. National Bureau of Standards, Special Publication 409. *Marine Pollution Monitoring (Petroleum)*, p. 121-125.

Project 750071

Arthur S. Dyke
Terrain Sciences Division

Dyke, Arthur S., *Glacial geology of northern Boothia Peninsula, District of Franklin; in Current Research, Part B, Geological Survey of Canada, Paper 79-1B, p. 385-394, 1979.*

Abstract

Mapping of glacial and marine features and radiocarbon dating of fossil marine molluscs have provided much new information on the glacial geology of northern Boothia Peninsula. At the late Wisconsin maximum ice flowed eastward to northeastward over the area. This flow is recorded by large fields of rock drumlins and other ice moulded bedrock forms. During recession, lateral meltwater channels, ice dammed lakes, and moraines were formed. These features document westward recession of the ice mass, whose margins and last flow pattern were topographically controlled. The marine limit near the east coast lies at 215 m a.s.l. and was formed 9230 ± 130 years B.P. The marine limit declines westward in the direction of ice recession to 155 m a.s.l. and less in Wrottesley Valley, where it was formed about 9040 ± 100 years ago. The ice margin retreated about 300 m/year, and the ice surface lowered about 5.5 m/year between 9230 and 9040 years B.P. The initial coastal emergence rate was more than 30 m/100 years. Shells dated at $>23\ 300$ years, from deltaic sediment at 195 m a.s.l. on the northeast coast, probably represent a pre-late Wisconsin marine incursion caused by ice recession. Organics, dated at $>30\ 000$ years, from sands below the Holocene marine limit in Wrottesley Valley, are probably detritus in Holocene marine sediments.

Introduction

The glacial geology of the northern half of Boothia Peninsula (Fig. 43.1, inset) was investigated during field work and airphoto interpretation in 1978. Craig (1964) dealt briefly with the area, and Boydell et al. (1975a, b) mapped the general distribution of surficial materials. This study is part of a more detailed study of the south-central Canadian Arctic Archipelago and adjacent Arctic mainland.

Northern Boothia Peninsula contains an abundance of ice flow and ice marginal features that were previously unmapped. In addition, the marine limit has been mapped and dated at two critical points. This allows establishment of an early Holocene deglacial chronology. Previously dated pre-late Wisconsin materials and the possible correlation of these with "old" materials on Somerset Island are discussed in light of these findings.

Acknowledgments

This study was made possible largely by the logistical support provided by the Polar Continental Shelf Project of Energy, Mines and Resources through their field operations base at Resolute Bay, managed by Mr. Fred Alt. I am thankful to Mr. Robert Hélie and Mr. Steven Black for assistance in the field, and to Dr. R.J. Fulton for his critical reading which helped to clarify several points.

Late Wisconsin Glaciation and Deglaciation

Ice Flow Features

Features, other than striae, shown in Figure 43.1 are easily recognized on 1:60 000 scale airphotos, an indication of their size. Forty striae measured throughout the area are parallel to these features, which confirms that the features were formed by glacial erosion. The most widespread ice flow features are ice moulded bedrock forms which are concentrated in the north and southeast part of the study area. The features include large roches moutonnées, rock drumlins, and crag-and-tail forms, with the latter two being more common.

The bedrock is most strongly ice moulded in the extreme northern part of the peninsula. Ice flowed eastward, normal to the compositional banding in the granitic gneiss

(Fig. 43.2) and normal to one of the major bedrock fracture systems. Hence, the moulded features do not appear to be structurally controlled. Also in this area are deep, east-west oriented, U-shaped troughs, occupied by long lakes or arms of the sea. Their forms are partly due to glacial erosion, although they may have originated as grabens in Tertiary time (Kerr and de Vries, 1977). However, the southernmost of these, occupied by Amituryouak Lake, is crossed obliquely by a strongly developed set of ice moulded bedrock features. This crosscutting indicates that formation of the trough preceded the last major ice advance.

Strongly ice moulded bedrock is also seen southwest of Wrottesley Inlet and west of Abernethy Bay; in both areas the ice flowed northeastward. The rest of the study area is devoid of large ice flow features. In most places, however, the bedrock is moulded into smaller forms, mostly roches moutonnées, on many of which striae and grooves are preserved.

The preferential development of large ice flow features in the north and southeast parts of the area probably reflects the locations of vigorously flowing streams of ice within the ice sheet. These streams did not arise from topographic channelling of the ice, because most of the intervening area is no higher than much of the streamlined terrain. Furthermore, the ice defied topographic channelling in areas of considerable (200 to 400 m) local relief, as around Amituryouak Lake and Wrottesley Valley, a wide and deep graben oriented nearly perpendicular to ice flow (Fig. 43.1).

The uniform nature of the ice flow pattern and the lack of topographic control suggest that the features were imprinted on the terrain by thick ice during glacial maximal conditions. The direction of flow indicates that the dispersal centre of the ice mass lay west of Boothia Peninsula. It is undoubtedly the same centre as that which produced the eastward flow over southern and western Somerset Island immediately north of the present study area (Dyke, 1978a).

Ice Marginal Features

Both erosional and depositional ice marginal features are common, particularly in areas devoid of the large glacier bedforms discussed above (cf. Fig. 43.1, 43.3). Figure 43.3 shows the distribution of ice marginal (lateral) meltwater channels, moraines, and former ice dammed lakes. These are discussed below.

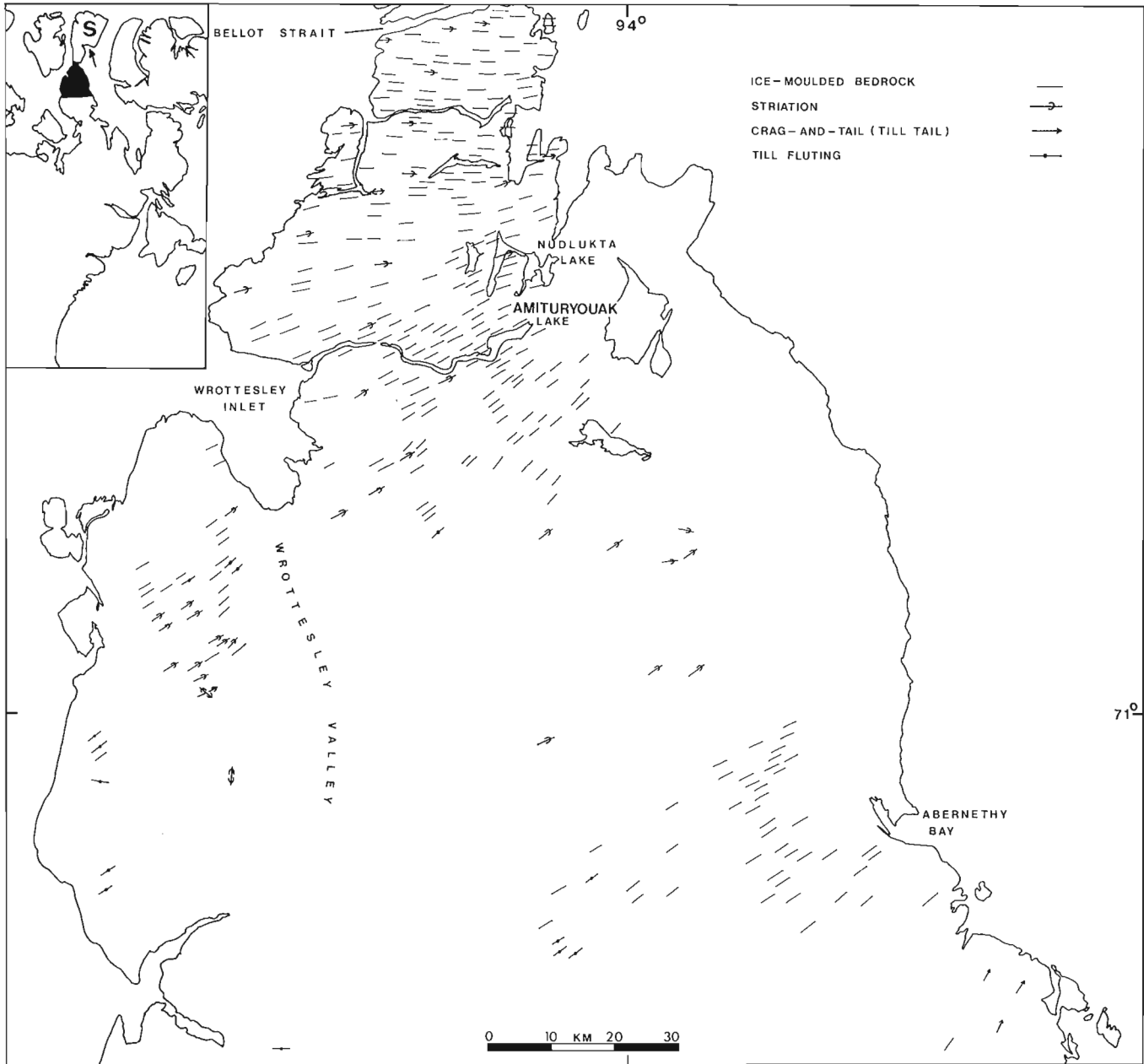


Figure 43.1. Ice flow lineaments on northern Boothia Peninsula. Somerset Island (S) is immediately north of the study area; arrow points to Creswell Bay.

The most common ice marginal features are lateral meltwater channels, but they are confined to areas above the marine limit. These channels run obliquely along hillsides in such a manner that the streams that cut them must have been confined on the downslope side by ice. They are generally incised 1 to 5 m into bedrock and form nested sets of features along many valleysides. Subglacial and proglacial meltwater channels and deposits are also common but are not shown in Figure 43.3 because they are of little use in deciphering ice marginal configurations.

Moraines are the next common ice marginal features, and three general types occur (Fig. 43.3): ridges of till that accumulated at ice fronts on dry land, generally in topographically unconfined areas; ridges of sand and gravel, commonly with distinct ice contact escarpments (kame moraines), that accumulated where ice fronts impinged on

steep slopes above marine limit; and till and boulder ridges of various heights that accumulated at the ice front as it retreated across the former seabed in areas below marine limit on the east coast.

The submarine moraines form three morphologic groups, each occupying a separate area. The northern group occurs between Brentford Bay to just north of Abernethy Bay. They consist of closely spaced parallel lines, 1 to 2 m wide, of boulders which overlie till on a broad lowland plain (Fig. 43.4). These are typical of features commonly referred to as De Geer moraines, which are thought to be annual ice marginal accumulations (Hoppe, 1959; Prest, 1968). The central group, which occurs inland from the head of Abernethy Bay, consists of larger parallel ridges of till, about 5 m high (Fig. 43.5). They probably represent longer stands of the ice front than do the De Geer moraines. The southern



Figure 43.2A. Oblique aerial view of rock drumlins immediately south of Bellot Strait. Ice flowed from right to left, across the compositional banding in the gneiss, clearly visible in the middle foreground. The light-coloured sediment in the foreground is a carbonate-rich till. (GSC 203359-X)



Figure 43.2B. Oblique aerial view of ice moulded bedrock forms near Nudlukta Lake. Ice flowed from left to right. Forms vary from symmetrical rock drumlins to crag-and-tail features. The crags are formed by a resistant vertical band in the gneiss which trends across the ice flow features and extends from the lake shore in the middle foreground to the right skyline. (GSC 203359-Y)

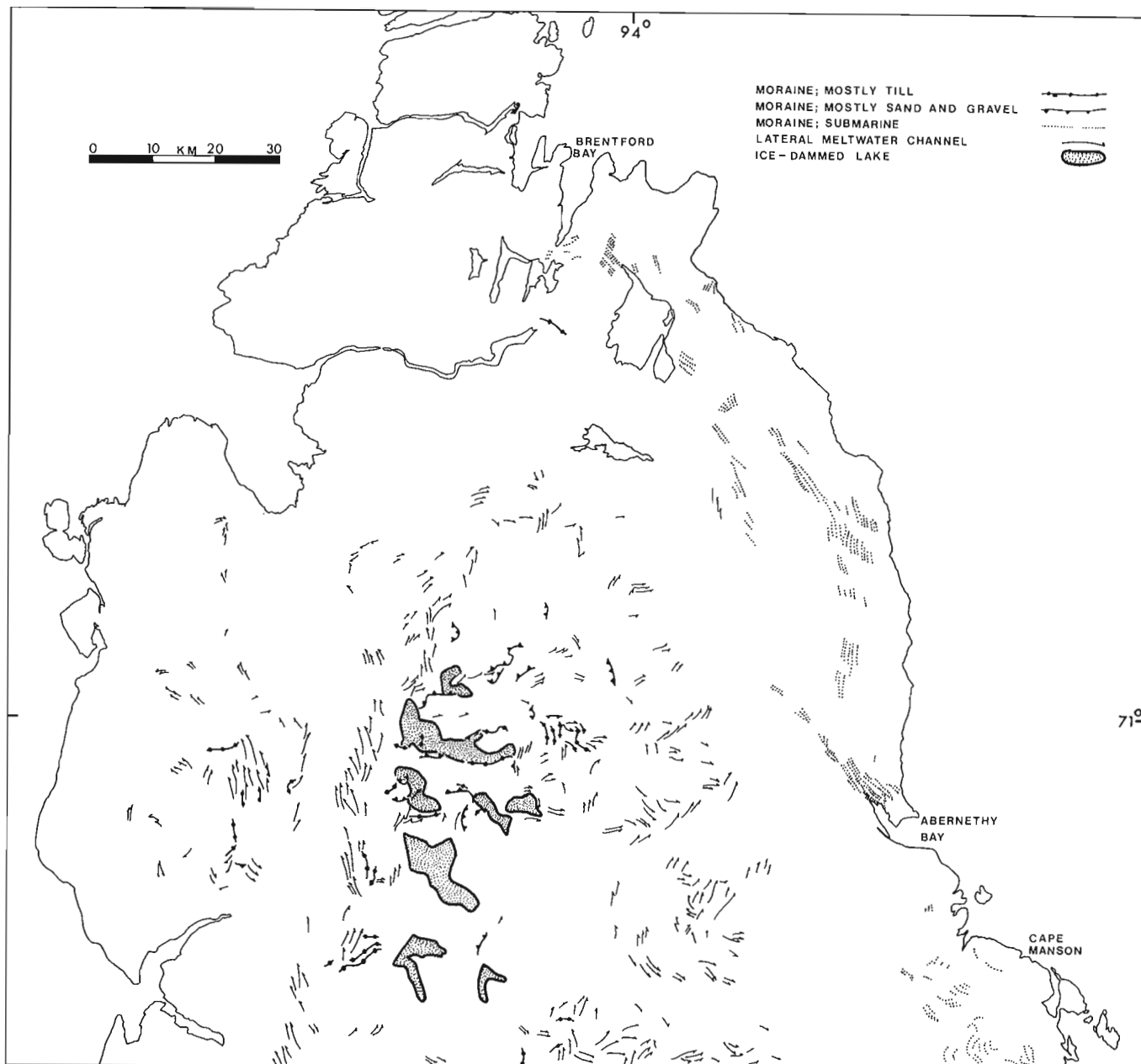


Figure 43.3. Ice marginal features on northern Boothia Peninsula.

group, which occurs inland from Cape Manson, is made up of 1 to 2 m high, subparallel, closely spaced, sinuous ridges, best developed in U-shaped valleys. They closely resemble in morphology the "cross-valley" moraines of Baffin Island (Andrews, 1963).

The third important set of ice marginal features are former glacier dammed lakes (Fig. 43.3). These left weakly developed strandlines and thin veneers of sediment, which indicates that they were short lived. They occupied the headwaters of eight westward draining valleys, indicating a westward recession of the ice margin.

Ice Recession

The ice marginal features (Fig. 43.3) were correlated throughout the region to produce a map of ice recession

(Fig. 43.6). Correlations were based on orientations and relative positions of features, extrapolation of ice-surface gradients defined by the features, and topography. The oldest ice margins, below marine limit on the east coast, were simple broad arcs, subparallel to the modern coastline. Here the ice retreated in the sea, probably quite rapidly, as ablation probably was aided by calving. Above the marine limit, the configurations of the ice margins, and hence the patterns of ice flow, during retreat were controlled largely by topography. Generally, the ice mass retreated westward; interfluves appeared first through the ice and large tongues and lobes remained in the valleys. The largest lobe, that in Wrottesley Valley, however, retreated in the sea. Generally, the ice remained a coherent unit during retreat, and remnant ice caps were left at only two places: on plateaus northeast and southwest of Wrottesley Valley.



Figure 43.4. Oblique aerial view of De Geer moraines about 30 km north of Abernethy Bay. The features are composed entirely of limestone boulders and stones forming 2 m-wide stripes on the surface of a fine grained till. The till supports a nearly complete vegetation cover, whereas the moraines are bare. Seven distinct moraines appear in the foreground and several others in the background. (GSC 203359-T)



Figure 43.5. Oblique aerial view of moraine ridges, about 5 m high, composed of till on a bedrock lowland near the head of Abernethy Bay. Three distinct ridges trend from lower left to upper right. The moraines were modified during the Holocene marine regression when the upper part of the till was winnowed and sorted by wave action to form gravel beach ridges, particularly obvious just left of the middle foreground. (GSC 203359-U)

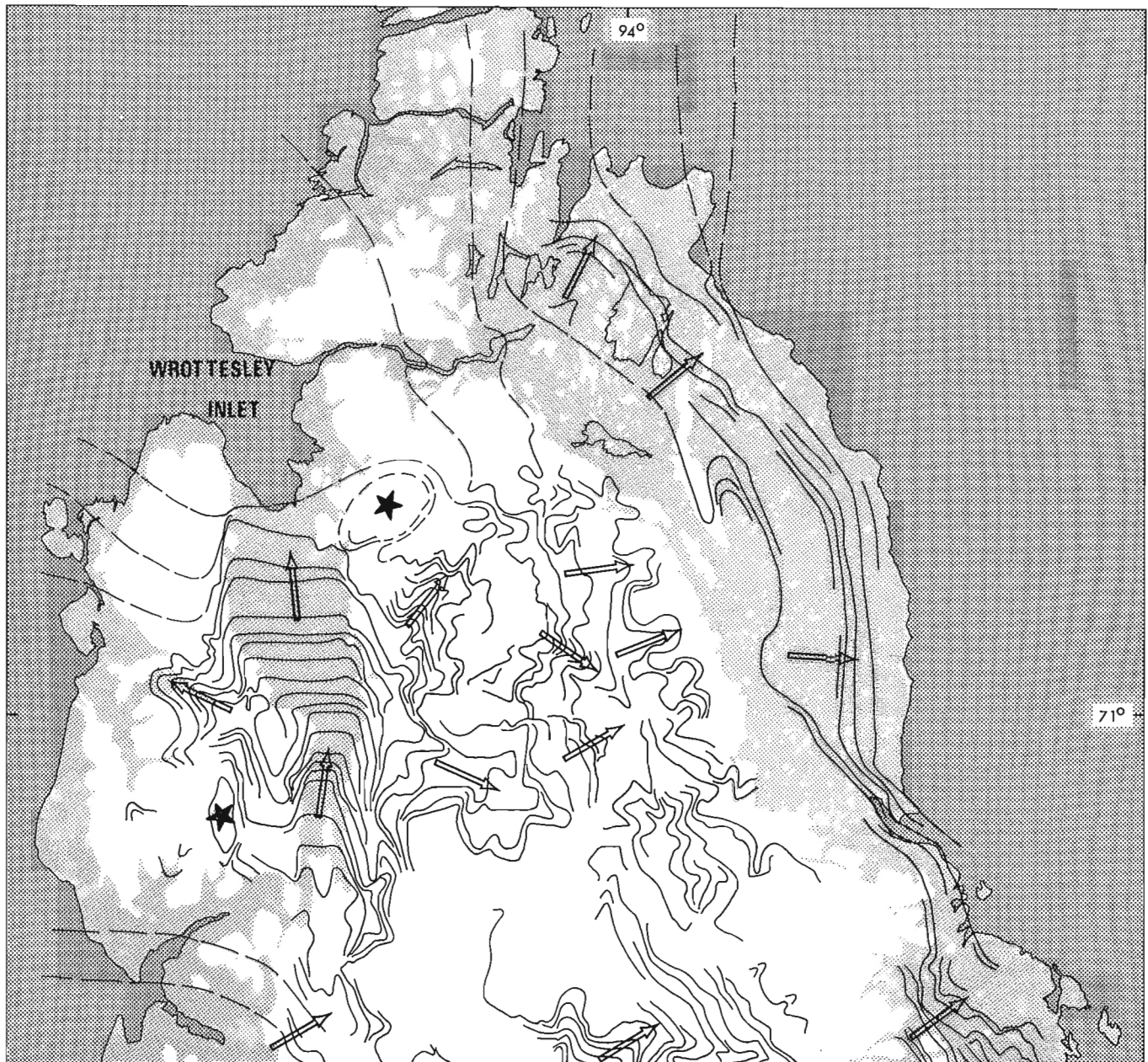


Figure 43.6. Ice margins (shown by black lines) and flow patterns (arrows) during recession of the late Wisconsin ice sheet on northern Boothia Peninsula. Lightly shaded areas were covered by the early Holocene sea, where it is likely that the ice retreated largely by calving. Two remnant ice caps are marked by stars.

Marine Limit and Emergence

Marine Limit and Date of Ice Recession

In areas behind the glacial limit, such as northern Boothia Peninsula, the marine limit is formed at the instant of deglaciation of any land which rises high enough to intersect the former water plane. The marine limit on the northeast coast and in Wrottesley Valley is best marked by the uppermost perched deltas, and in a few places by high beaches, pockets of marine sediment, and washing limits on till. On the west coast, adjacent to Wrottesley Valley, the limit is clearly marked by the uppermost raised beaches, above which are till-covered slopes showing no signs of modification by wave action.

Marine deltas deposited by glacial meltwaters are now perched 215 m above sea level on the northeast coast (Fig. 43.7). Fossils of the marine bivalves, *Mya truncata* and *Hiatella arctica*, the common assemblage in early Holocene marine sediments in the Canadian Arctic, were collected from the foreset sands of one of these marine limit deltas, and a single valve of *Mya truncata* yielded a radiocarbon age of 9230 ± 130 years (GSC-2720). The ice margin stood no more than a few kilometres west of the delta at the time of its deposition.

Ice thickness, and therefore crustal depression, increases in the up-ice direction. However, the marine limit may decline in that direction because much rebound can occur as the ice thins before the margin retreats. This is the

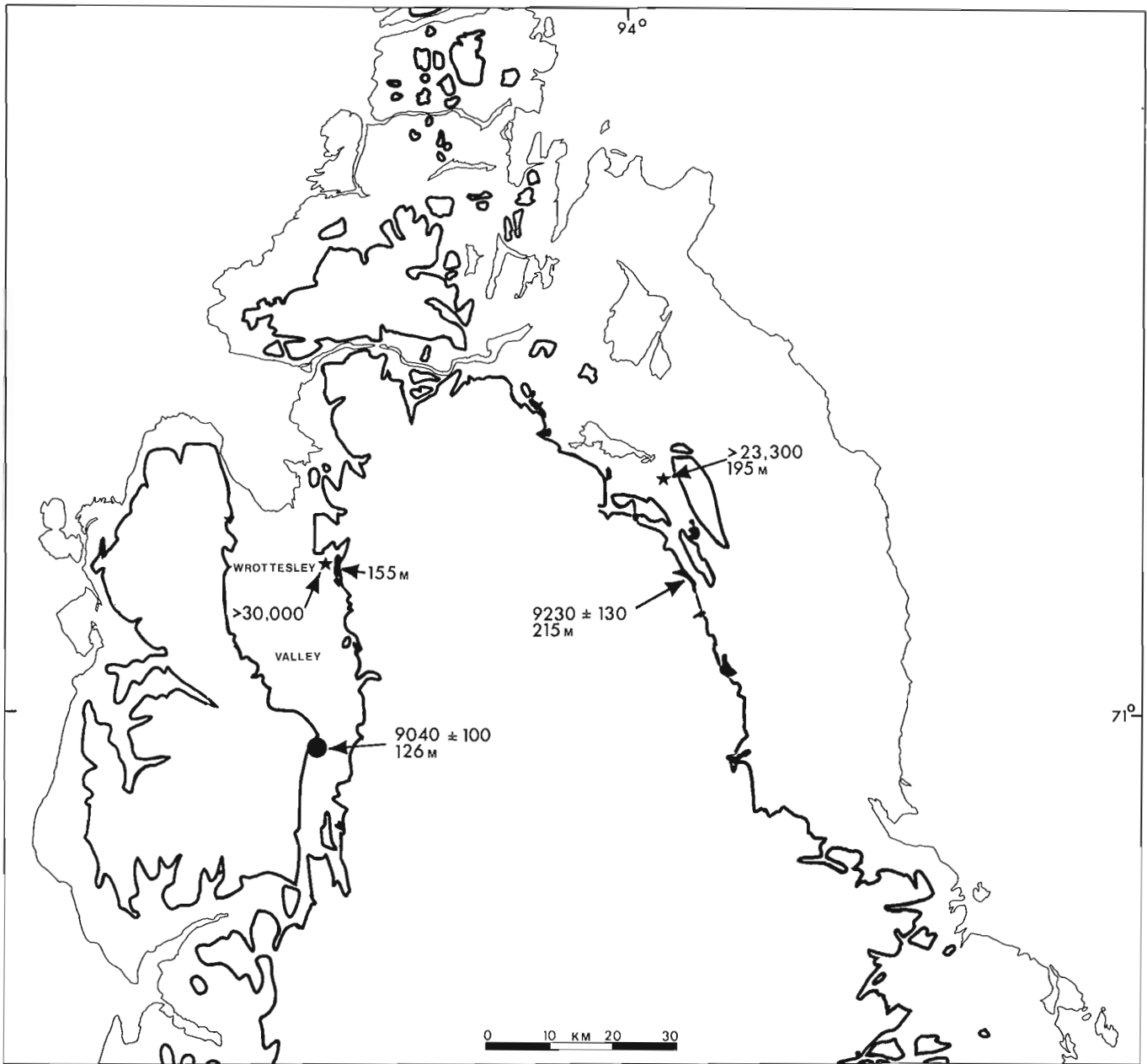


Figure 43.7. Holocene marine limit (heavy line) and marine limit deltas (black areas) and dates on northern Boothia Peninsula, along with locations of samples (shown by stars) of pre-late Wisconsin age.

case on northern Boothia Peninsula, for the marine limit at the mouth of Wrottesley Valley is marked by glaciomarine deltas at only 155 m a.s.l. No marine fossils were found in these deltaic sediments. However, 35 km farther up-valley (southward), where marine limit appears to be at the same elevation or slightly lower, paired valves of *Mya truncata*, *Hiatella arctica*, and *Macoma calcarea* were collected from a small deposit of silt and sand. The silt and sand fill a depression in till at 126 m a.s.l. Sea level was higher than that during deposition of the sediment, which was probably produced by the melting of the glacier, and may have stood at the marine limit. Therefore, a radiocarbon age of 9040 ± 100 years (GSC-2722), which was obtained on the *Mya truncata* valves, is a reasonable approximation of the date of deglaciation of the site.

These two radiocarbon dates, from opposite sides of the peninsula, show that much of the area was deglaciated in a period of about 200 years, or at most, using maximum quoted error terms (± 2 sigma) on both dates, 400 years. Ignoring the error terms on the dates, the average rate of recession of the ice margin between the two fossil sites was 300 m/year (a recession of 60 km in 200 years). If the ice retreated at the same rate across the area east of the eastern fossil site, then the present coastline was deglaciated about 9350 years ago.

Another perspective on the early Holocene ablation rate can be provided by considering the rate of thinning of the ice sheet, in other words, the rate of lowering of the ice surface. Figure 43.8 shows profiles of the ice sheet along a line that passes through the two fossil sites discussed above, and that fortuitously is parallel to the flow lines in the ice sheet

(Fig. 43.1). These profiles are based on the formula given by Nye (1952) and are reasonable reconstructions as they closely approximate the measured profile of the northern Greenland Ice Sheet. Between 9230 ± 130 and 9040 ± 100 years B.P. the ice surface over the Wrottesley Valley fossil site lowered by 1100 m, at an average rate of 5.5 m/year. Between about 9350 and 9040 years ago, 1450 m of ice melted above the site, at an average rate of 4.8 m/year. The total lowering from the time of the stadial maximum, however, cannot be calculated because the glacial limit off eastern Boothia Peninsula has not been mapped.

Early Holocene Emergence

It is also possible to calculate the rate of coastal emergence, a result of the unloading of ice from the crust, immediately following deglaciation. The Wrottesley Valley date of 9040 ± 100 years B.P. relates to a former sea level more than 126 m a.s.l., but no more than 155 m a.s.l., the height of the local marine limit. The 9040 year old shoreline on the east coast is, therefore, 60 m or more below the 215 m marine limit dated at 9230 ± 130 years. Because the ice thickened westward, it is likely that the 9040 year old shoreline dips eastward (Fig. 43.9) as do the early Holocene shorelines on Somerset Island (Dyke, 1978b). This gives an emergence rate of more than 30 m/100 years.

This rate is much higher than early Holocene emergence rates previously reported for Arctic Canada. For example, Andrews (1970, p. 114) derived a rate of about 3.5 m/100 years for uplift occurring 1000 years after deglaciation for sites in Arctic Canada (emergence rates would be less than uplift rates as Andrews used a eustatic sea level correction), and Blake (1975) gave an average rate of 7 m/100 years for emergence between 9000 and 8000 years ago at Cape Storm, southern Ellesmere Island. The latter area was deglaciated about the same time as northern Boothia Peninsula. Perhaps the explanation of the apparent discrepancy is that the higher rate of emergence reported here for northern Boothia Peninsula applies to only the 200 years immediately following deglaciation, that is, the interval when sea level lowering due to reduced gravitational attraction of the sea by the ice sheet and elastic rebound of the crust are significant factors in determining the emergence rate (Clark, 1976; Farrell and Clark, 1976), especially in areas of rapid ice recession. I am not aware of any other calculation of emergence rates for the first few centuries after deglaciation for any other area.

Evidence of Pre-Late Wisconsin Events

Pre-Late Wisconsin Dates

Because dates on the marine limit in areas behind the glacial limit are also dates on deglaciation, the last ice sheet to cover northern Boothia Peninsula was of late Wisconsin age, and it is likely that the strong eastward to northeastward flow pattern was imprinted during the late Wisconsin stadial maximum. Two samples of pre-late Wisconsin age from northern Boothia Peninsula were dated prior to this study; these require explanation in light of the results presented above.

On the northeast coast (Fig. 43.7), B.G. Craig collected shells, mostly fragments, but some with periostracum still attached, from crossbedded deltaic sands forming terraces up to 195 m a.s.l. The sample, which was dated $>23\ 300$ years old (GSC-135; Craig, 1964), contained *Yoldia arctica*, *Clinocardium ciliatum*, *Astarte* sp., and *Hiatella arctica*. The first three species are uncommon at such elevations; in Craig's extensive fossil collection from the central Canadian Arctic, *Yoldia* occurs no higher than 52 m a.s.l., *Clinocardium* no higher than 113 m a.s.l., and *Astarte* no higher than 91 m a.s.l. (see appendix and table by F.J.E. Wagner in Craig, 1964).

The site was revisited in 1974 by mappers from Terrain Sciences Division, and they noted a veneer of till over the crossbedded sands near the contact of the deposit with the adjacent till-covered hillside (A.N. Boydell et al., 1974, unpublished field notes). Because of its position, the till could either have been deposited directly over the sands by glacier ice or have been redeposited by solifluction from the adjacent hillslope. Likewise, the shells could have been redeposited after transportation by glacier ice, but the presence of periostracum on them argues against this. It is most likely therefore that the shells died during deposition of the deltaic sands and that the overlying till represents the late Wisconsin ice advance. If so, the older marine incursion attained heights similar to those reached by the early Holocene sea. This implies that the pre-late Wisconsin and the late Wisconsin ice loads were of similar size. The original fossil collection was small and entirely consumed to make the age determination, so a re-collection is needed to determine their age more precisely.

On the northwest coast in lower Wrottesley Valley, K.A. Drabinsky in 1974 collected plant remains from bedded sands, which he considered glaciofluvial or marine in origin (Fig. 43.7). A single fragment of *Salix* sp. was dated at $>30\ 000$ years old (GSC-2180; Drabinsky in Lowdon and Blake, 1979). M. Kuc (GSC unpublished Bryological Report No. 315) identified the sample as an in situ meso-xeric sod, despite the fact that the material came from bedded sands which had been interpreted as water-laid deposits. The area was re-examined during the course of this study, and it is concluded that the sands from

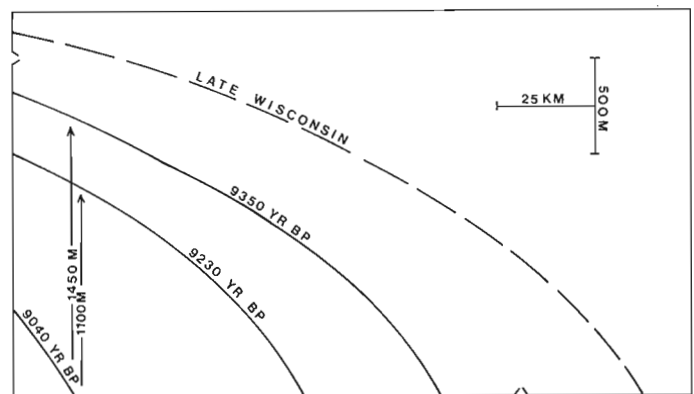


Figure 43.8. Profiles of the retreating ice sheet along a line passing through the two Holocene fossil sites (cf. Fig. 43.7), showing the amount of ice-surface lowering between 9350 and 9040 years B.P.

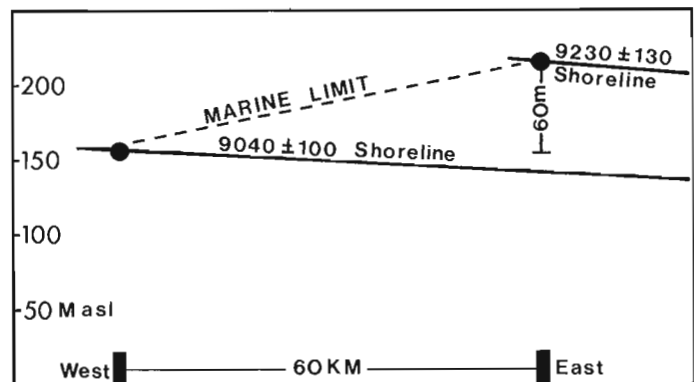


Figure 43.9. Approximate profiles (cf. Fig. 43.7) of the early Holocene shorelines and marine limit; these allow calculation of the rate of initial coastal emergence.

which the plant remains were collected are prodeltaic sediments because they occur immediately downslope from a glaciomarine delta terrace marking the marine limit at 155 m a.s.l. (Fig. 43.7). The marine limit was formed during the early Holocene (see above), so the plant material incorporated in the prodeltaic sands must be detrital.

Similar detrital plant remains were collected by the 1974 mapping party from a conical kame composed of sand in the central part of the peninsula (A.N. Boydell et al., 1974, unpublished field notes). Because the organic material occurs in ice-contact sediments, it is likely that it was brought to the site by glacier ice. Therefore, if the absolute age of the material were measured, it probably would give the date of advance of the last ice sheet across the peninsula.

Correlations

Dyke (1978a, b) presented evidence that the eastward flowing ice on northwestern Somerset Island terminated about 20 km inland from the west coast and that the rest of the island, with the exception of two nunataks, was covered by a radially flowing local ice cap. An ice marginal delta formed during recession of the local ice cap in the Creswell Bay area contained driftwood which dated >38 000 years old, and beaches just below the delta contained well preserved shells estimated to be >40 000 years old, but probably younger than Sangamon, on the basis of the extent of amino acid racemization. Hence, it seems that the local ice cap retreated from at least part of the coastal area during middle or early Wisconsin time. It is possible that the deltaic sediments dated at >23 300 years on northeastern Boothia Peninsula are correlatives of the pre-late Wisconsin sediments in Creswell Bay and, therefore, that the main ice sheet also retreated somewhat at that time. On the other hand, it is also possible that the Somerset Island sediments were deposited during a response to a relatively small, short-lived warming, while the main ice sheet remained stationary because of its greater bulk and, hence, longer response time. If this was the case, there need be no correlation between the two deposits.

Conclusions

During the height of the late Wisconsin Stage, an ice mass flowed eastward and northeastward across northern Boothia Peninsula. The ice was coeval with previously recognized eastward flowing ice on southern and western Somerset Island (Dyke, 1978a, b). The main products of this ice flow were hundreds of square kilometres of severely ice moulded bedrock, mainly rock drumlins and crag-and-tail features, concentrated in two areas which were probably overlain by vigorously flowing streams of ice. Striae measurements confirm the interpretation of the lineaments as glacial features. During recession an abundance of ice marginal features formed, including lateral meltwater channels, former ice dammed lakes, and a variety of morainic forms ranging from De Geer moraines, composed only of lines of boulders deposited on the former seabed, to kame moraines, bulky ridges of sand and gravel with ice contact escarpments. These features form the basis for a map of ice retreat. The ice sheet margin retreated westward and its configuration was topographically controlled. Across most of the area, it retreated as a coherent mass, leaving behind only two small remnant ice caps. As the ice retreated, the sea flooded the isostatically depressed land and reached 215 m above its present level on the east coast. Shells from a marine limit delta deposited by glacial meltwater on the east coast have been dated at 9230 ± 130 years. As the ice retreated the land rebounded, and by the time the sea

reached Wrottesley Valley, about 9040 ± 100 years ago, it stood only 155 m above its present level. The two dates bracket deglaciation of most of the study area, and allow calculation of average rates of retreat (300 m/year), ice surface lowering (5.5 m/year), and initial coastal emergence (more than 30 m/100 years).

Shells dated >23 300 years old had been collected previously from deltaic sediments at 195 m a.s.l. near the northeast coast (Craig, 1964). These sediments may represent a pre-late Wisconsin ice recession and marine incursion and may correlate with pre-late Wisconsin marine sediments in the Creswell Bay area on Somerset Island. Old plant remains in sand near the northwest coast are interpreted as detritus, redeposited in an early Holocene prodeltaic environment.

References

- Andrews, J.T.
1963: Cross-valley moraines of the Rimrock and Isortoq River valleys, Baffin Island, N.W.T.: a descriptive analysis; *Geographical Bulletin*, no. 19, p. 49-77.
1970: A geomorphological study of postglacial uplift with particular reference to Arctic Canada; *Institute of British Geographers, Special Publication No. 2*, 156 p.
- Blake, W., Jr.
1975: Radiocarbon age determinations and postglacial emergence at Cape Storm, southern Ellesmere Island, Arctic Canada; *Geografiska Annaler, Ser. A*, v. 57, p. 1-71.
- Boydell, A.N., Drabinsky, K.A., and Netterville, J.A.
1975a: Terrain inventory and land classification, Boothia Peninsula and northern Keewatin; *In Report of Activities, Part A, Geological Survey of Canada, Paper 75-1A*, p. 393-396.
1975b: Surficial geology and geomorphology, Boothia Peninsula, N.W.T.; *Geological Survey of Canada, Open File 285*, scale 1:125 000.
- Clark, J.A.
1976: Greenland's rapid postglacial emergence: a result of ice-water gravitational attraction; *Geology*, v. 4, p. 310-312.
- Craig, B.G.
1964: Surficial geology of Boothia Peninsula and Somerset, King William, and Prince of Wales Islands, District of Franklin; *Geological Survey of Canada, Paper 63-44*, 10 p.
- Dyke, A.S.
1978a: Glacial history of and marine limits on southern Somerset Island, District of Franklin; *In Current Research, Part B, Geological Survey of Canada, Paper 78-1B*, p. 218-224.
1978b: Glacial and marine limits on Somerset Island, Northwest Territories; *Geological Society of America, Abstracts with Programs*, v. 10, p. 394.
- Farrell, W.E. and Clark, J.A.
1976: On postglacial sea level; *Geophysical Journal of the Royal Astronomical Society*, v. 46, p. 647-667.
- Hoppe, G.
1959: Glacial morphology and inland ice recession in northern Sweden; *Geografiska Annaler*, v. XLI, p. 193-212.

Kerr, J. Wm. and de Vries, C.D.S.

1977: Structural geology of Somerset Island and Boothia Peninsula, District of Franklin; in Report of Activities, Part A, Geological Survey of Canada, Paper 77-1A, p. 107-111.

Lowdon, J.A. and Blake, W., Jr.

1979: Geological Survey of Canada radiocarbon dates XVIII; Geological Survey of Canada, Paper 78-7.

Nye, F.J.

1952: The mechanics of glacier flow; Journal of Glaciology, v. 2, no. 12, p. 81-93.

Prest, V.K.

1968: Nomenclature of moraines and ice flow features as applied to the Glacial Map of Canada; Geological Survey of Canada, Paper 67-57, 32 p.

SCIENTIFIC AND TECHNICAL NOTES – NOTES SCIENTIFIQUES ET TECHNIQUES

AVERAGE DEPTH OF GLACIAL EROSION, CANADIAN SHIELD

C.A. Kaszycki
Atomic Energy of Canada Limited, c/o Geological Survey
of Canada, Ottawa, Ontario. K1A 0E8

W.W. Shilts
Terrain Sciences Division

The extent of glaciation in Canada is such that considerable effort has been devoted to the study of the distribution and character of glacial and related sediments.

However, relatively little research based on field observation and analysis of glacial sediments has been directed towards evaluating the extent of continental erosion attributable to glaciation. This latter question has particular relevance to consideration of the use of the subsurface for disposal of toxic wastes including those arising from the generation of nuclear power.

A review of the literature presented many conflicting viewpoints concerning the amount of glacial erosion that has occurred on the Canadian Shield. Estimates vary from thousands of feet (White, 1972) to a few tens of feet (Flint, 1971). In an attempt to resolve this disparity, samples

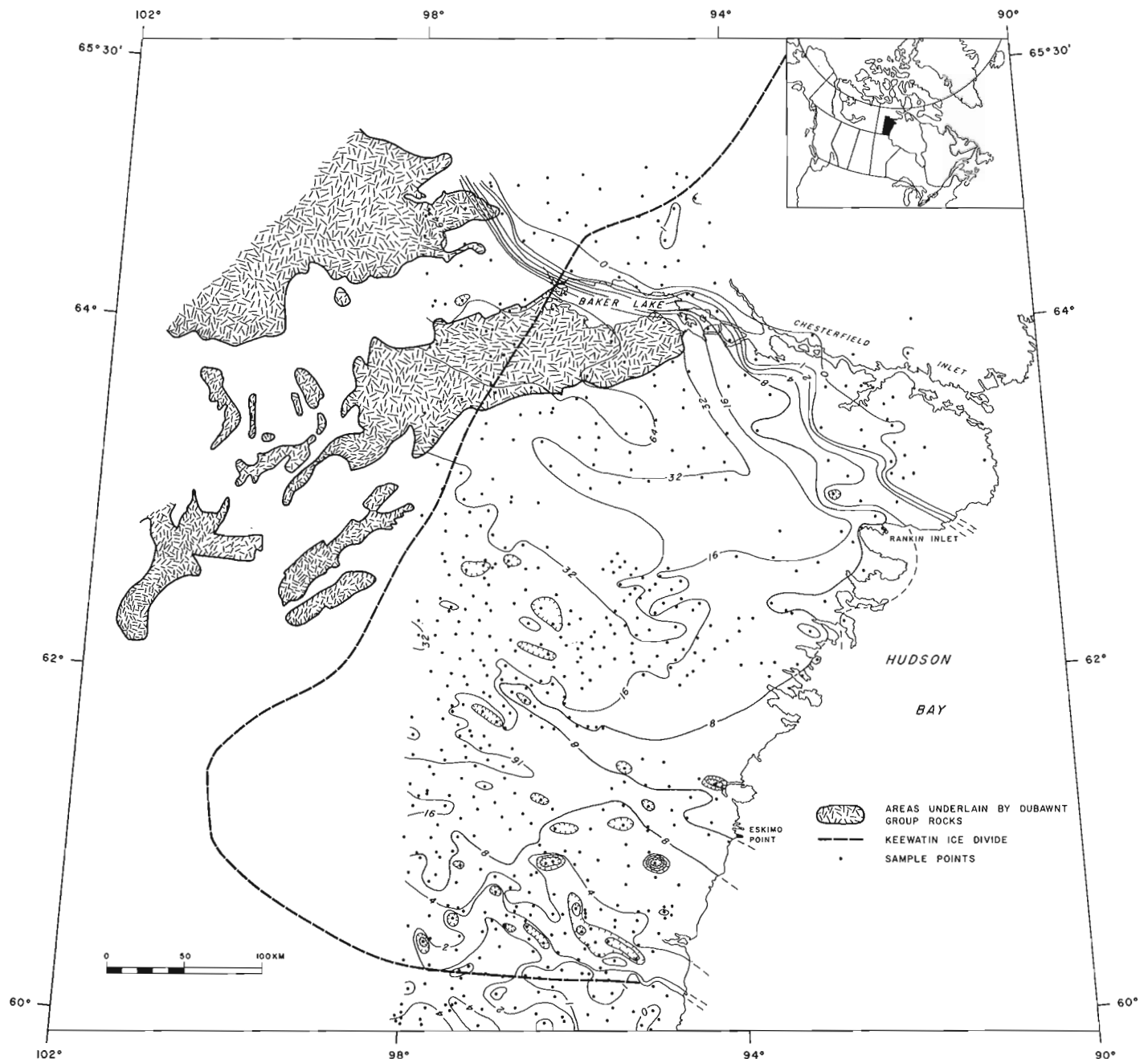


Figure 1. Dispersal of Dubawnt Group erratics. Isopleths represent weight per cent Dubawnt clasts in the 2 to 6 mm fraction of till (Dubawnt outcrops modified from Wright, 1967; LeCheminant et al., 1977; and Donaldson, 1966, 1969). Inset map shows location of study area.

already collected by the Geological Survey of Canada have been used to estimate average amounts of glacial erosion through a study of glacial dispersal of distinctive rock types, specifically the lithologically distinctive rocks of the Dubawnt Group (Donaldson, 1965) in the District of Keewatin (Fig. 1). It was hypothesized that by evaluating the volume of Dubawnt detritus in till located down-ice from Dubawnt outcrops, and by calculating the area of outcrop traversed by ice flow, it would be possible to estimate the average depth of glacial erosion that has occurred in the region. This exercise was designed to develop the techniques of performing such calculations as well as to derive some figures for erosion of a specific rock type.

The Dubawnt Group is composed of relatively flat lying Proterozoic sedimentary and felsic volcanic rocks with characteristic red to purple hues. Their distinctive colour and lithology permit reliable identification in the coarse till fractions. The area of outcrop extends from the eastern end of Baker Lake southwestward for approximately 320 km and is traversed by the central portion of the Keewatin Ice Divide.

The existence of the dispersal train was first noted as a strip of red coloured till extending from the area of Dubawnt outcrop southeastward to the coast of Hudson Bay (Shilts and Boydell, 1974). The distinctive colour of the till is imparted by glacially ground specular hematite, a derivative of the Dubawnt Group rocks. In order to quantify the Dubawnt component, the granule-fine gravel fraction of approximately 800 till samples was examined. Each sample was sieved to obtain particles in the 2 to 6 mm size range, and the percentages of Dubawnt Group rocks were determined on a weight per cent basis. The fine sand and clay fractions of some samples also were examined in order to estimate the Dubawnt component of the till throughout various size fractions.

In the vicinity of the outcrop the Dubawnt component is found to compose approximately 70 to 80 per cent of the granule-fine gravel fraction of the till. This value decreases exponentially with distance in the direction of ice flow (southeastward) until the dispersal train is artificially truncated at the coast of Hudson Bay. At this point Dubawnt erratics comprise 5 to 10 per cent of the 2 to 6 mm size fraction. Mathematical extrapolation of the dispersal curve into Hudson Bay indicates that dispersal could continue for at least 200 km past the coast.

Preliminary calculations of depth of erosion have been based upon the assumption that the Dubawnt component of the granule-fine gravel size fraction is a reasonable approximation of the Dubawnt component of the till as a whole. Knowing the area of dispersal, plus the average depth of till throughout the region (~3 m), the amount or depth of glacial erosion of Dubawnt Group rocks has been estimated to be 5.5 to 8.0 m (a figure in agreement with Flint, 1971). Further, more refined calculations of erosion, taking into account the variation of Dubawnt components throughout various size fractions, and more precise estimations of variation in the depth of till throughout the dispersal area, are not expected to alter this preliminary estimate significantly.

A knowledge of the rate of erosion is useful when attempting to estimate the magnitude of erosion to be expected at one place from that calculated at another. If, for example, the amount of erosion calculated for the Dubawnt dispersal train resulted from only 4000 years of active erosion, it is not necessarily valid to assume that the magnitude of erosion elsewhere on the Canadian Shield, where active erosion may have spanned tens of thousands of years, will be similar to that of the Dubawnt Group rocks.

In order to determine erosion rates for the Dubawnt Group it is necessary to define the period of time during which ice was flowing towards Hudson Bay. The popular view that ice flow features in Keewatin, indicating ice flow

towards Hudson Bay, are of late-glacial origin can be seriously challenged by a study of the Dubawnt dispersal train. The fact that Dubawnt erratics have been transported at least 300 km towards Hudson Bay is inconsistent with the time constraints for debris transport (2000 to 4000 years) imposed by defining the Keewatin Ice Divide as a late-glacial feature formed when rising seawater in Hudson Strait split an ice dome centred on Hudson Bay. The minimum rate of debris transport in the basal ice imposed by these constraints (100 to 300 m/year) is too high to be considered applicable to a largely stagnant wasting ice mass.

If the Keewatin Ice Divide is considered to have been active throughout most of the period of Wisconsin Glaciation, the dispersal of Dubawnt erratics can be assumed to have taken place over a much longer period of time, at a more realistic rate of flow. An average flow rate of 10 m/year would allow 30 000 years for the transportation of Dubawnt erratics over a distance of 300 km. It has been assumed, therefore, that the Keewatin Ice Divide and/or other land-based centres of outflow were active throughout most of the Wisconsin Glaciation and that rates of glacial erosion with respect to the Dubawnt dispersal train may be calculated on this basis. It is evident that the definition of the Dubawnt dispersal train has not only afforded an opportunity to study glacial erosion of the Canadian Shield but has also effected a rethinking of the traditional concept of the configuration of the Laurentide Ice Sheet (Shilts et al., in press).

References

- Donaldson, J.A.
1965: The Dubawnt Group, Districts of Keewatin and Mackenzie; Geological Survey of Canada, Paper 64-20, 11 p.
1966: Geology, Schultz Lake, District of Keewatin; Geological Survey of Canada, Map 7-1966, scale 1 inch to 4 mile.
1969: Descriptive notes (with particular reference to the Late Proterozoic Dubawnt Group) to accompany a geological map of central Thelon Plain, Districts of Keewatin and Mackenzie; Geological Survey of Canada, Paper 68-49, 4 p., Map 16-1968.
- Flint, R.F.
1971: Glacial and Quaternary Geology; John Wiley and Sons Inc., New York, 892 p.
- LeCheminant, A.N., Blake, D.H., Leatherbarrow, R.W., and de Bie, L.
1977: Geological studies: Thirty Mile Lake and MacQuoid Lake map areas, District of Keewatin; in Report of Activities, Part A, Geological Survey of Canada, Paper 77-1A, p. 205-208.
- Shilts, W.W. and Boydell, A.N.
1974: Terrain Mapping in the Churchill - Chesterfield Inlet Corridor, District of Keewatin; in Report of Activities, Part A, Geological Survey of Canada, Paper 74-1A, p. 253-256.
- Shilts, W.W., Cunningham, C.M., and Kaszycki, C.A.
The Keewatin Ice Sheet - reevaluation of the traditional concept of the Laurentide Ice Sheet; Geology. (in press)
- White, W.A.
1972: Deep erosion by continental ice sheets; Geological Society of America Bulletin, v. 83, p. 1037-1056.
- Wright, G.M.
1967: Geology of the southeastern barren grounds, parts of the Districts of Mackenzie and Keewatin (Operations Keewatin, Baker, Thelon); Geological Survey of Canada, Memoir 350, 91 p.

SEISMIC RECONNAISSANCE SURVEY OF THE DUBAWNT GROUP, DISTRICTS OF KEEWATIN AND MACKENZIE

Project 700061

A. Overton
Resource Geophysics and Geochemistry Division

Introduction

A seismic reflection experiment and reconnaissance seismic refraction profiling were conducted at selected locations within areas covered by sedimentary rocks of the Dubawnt Group to determine the effectiveness of the seismic method in defining the sedimentary sequence and thicknesses down to the basement complex (Overton, 1971).

Early economic interest in the area was directed mainly toward the investigation of adjacent greenstone – sedimentary belts and gneissic terranes, since favourable signs of mineralization had not been found within the Dubawnt Group. More recently interest in possible concentrations of secondary uranium minerals, such as the mineralization found in the Proterozoic Athabasca sandstone in northern Saskatchewan, has been directed toward the Dubawnt Group (Roscoe, 1966). Some exploration drilling programs have been conducted in the area (Ruzicka, 1978). As a possible aid to planning and complementing such drilling programs the seismic method was tested as a feasibility study in a reconnaissance program.

The seismic program was confined to lakes within the area to facilitate fixed-wing aircraft landings, seismometer cable layouts and the shooting of small dynamite charges in the water under the ice. The operation was conducted first from the village of Baker Lake, and then from a tent camp at location 22 (Fig. 1). A single-engined Otter aircraft was used to transport instruments and personnel to the work sites on the lakes. Small charges of Geogel 60% explosive were used as the energy sources. A Texas Instruments model 8000 amplifier system with an RS-12P recording oscillograph recorded from a 12 station seismometer array using 7 hz seismometers spaced at 73.2 m on two (high and low) sensitivity levels. The seismometer array was laid out on the ice using a skidoo. The skidoo was also used to move drilling and shooting equipment to the shotpoints. The shotholes were drilled with gasoline powered ice augers at the ends of the seismometer array and at offset distances large enough to get seismic penetration to basement. Penetration to basement was revealed by recorded velocities near 6.1 km/s. Figure 1 shows the locations of the 35 seismic profiles obtained.

Brief Description of Geology

The Dubawnt Group covers an area of approximately 91 000 km² on the Thelon Plain and near Baker Lake in the districts of Keewatin and Mackenzie, Northwest Territories (Fig. 1). Detailed accounts of the geology are given by Donaldson (1965, 1966, 1967a, b, 1969) and Fraser et al. (1970). Accounts of the lithology and regional distribution of basement rocks are given by Wright (1955, 1957, 1967). For

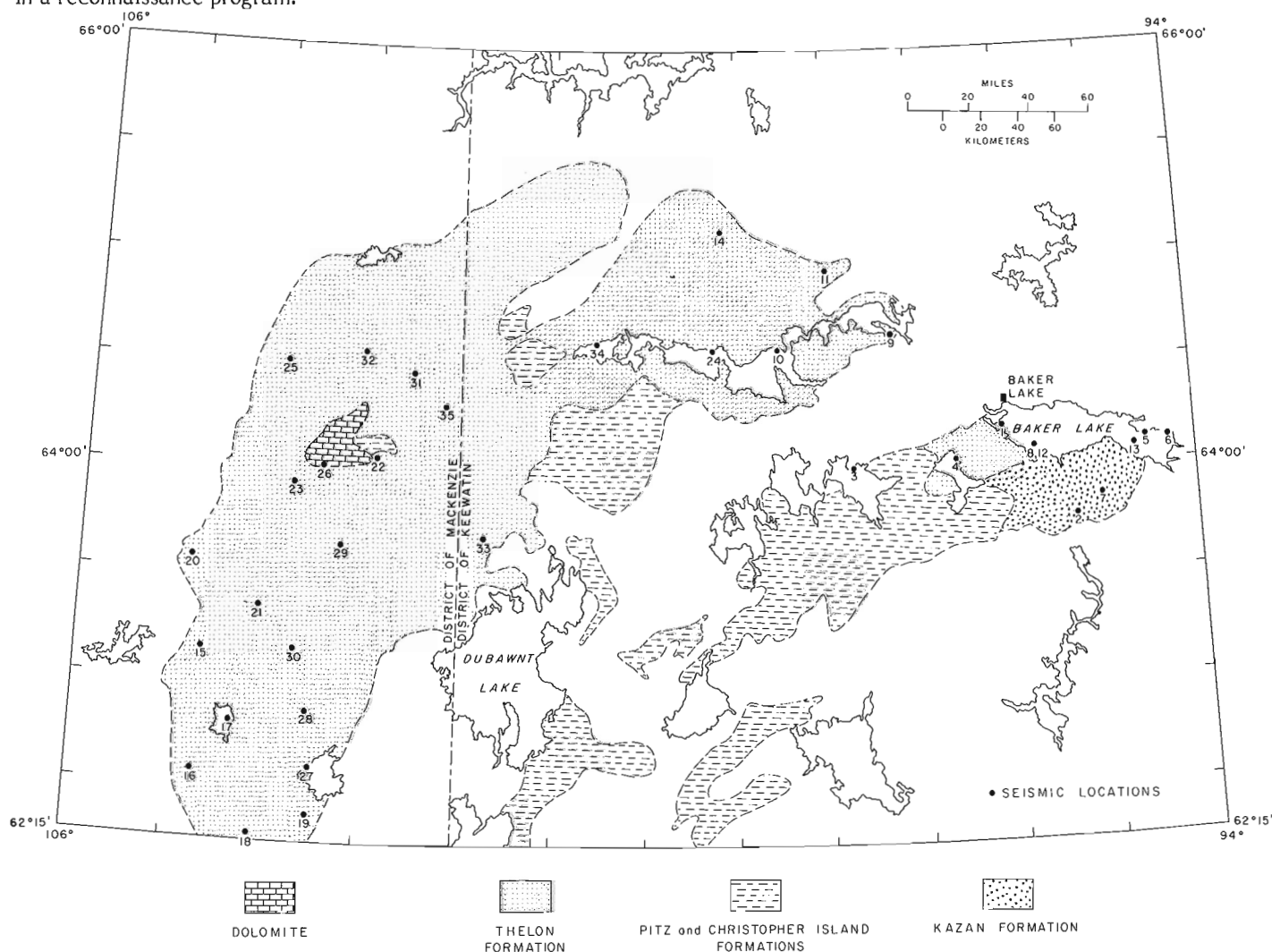


Figure 1. Location map and regional geology.

From: *Scientific and Technical Notes in Current Research, Part B; Geol. Surv. Can., Paper 79-1B.*

the purpose of this note a brief summary of the geology of the Dubawnt Group as it comprises the seismic model is taken from Donaldson (1965, 1967): The Dubawnt Group comprises a lowermost redbed sequence, a middle volcanic sequence, and an uppermost sequence of sandstone, conglomerate, dolostone and minor volcanic rock. These rocks rest unconformably upon metamorphic rocks of the Hudsonian orogen. They are faulted, but not strongly folded, and show no evidence of regional metamorphism. The redbed sequence is up to 5000 m thick and consists of the basal South Channel Formation (mainly coarse conglomerates) and the Kazan Formation (crossbedded arkose, siltstone, and mudstone). These sedimentary rocks are separated by a minor unconformity from the overlying Christopher Island Formation (trachyte, andesite and tuffaceous interflow rocks) and the Pitz Formation (largely porphyritic acid flows). The volcanic sequence is at least 100 m thick. The redbeds and some of the volcanic rocks are intruded by the Martell Syenite which is the intrusive equivalent of the Christopher Island Formation. Resting unconformably on the volcanic sequence and overlapping onto the basement rocks are quartzose sandstone and conglomerate of the Thelon Formation which may exceed 1000 m in thickness.

The layered velocity model largely represented by this geological sequence should lend itself well to studies by standard seismic techniques.

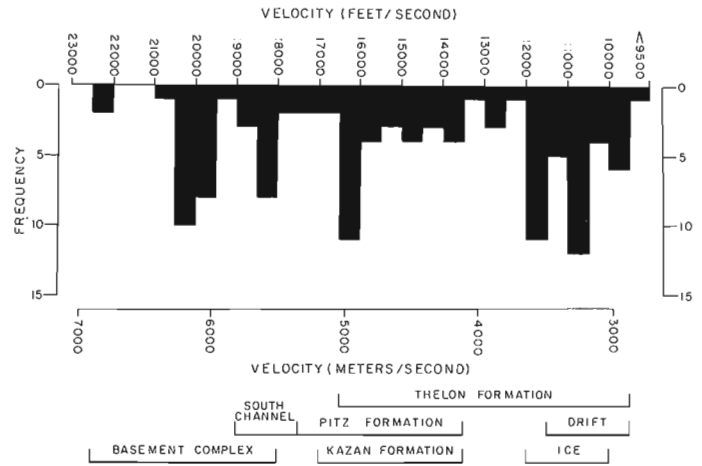


Figure 2. Distribution of observed seismic velocities with tentative correlations with lithology.

Table 1

Velocity-thickness summary for the seismic profiles

Profile	Region	Velocity, km/s	Thickness, metres	Total thickness metres	
1	Baker Lake Basin	(3.14), 4.39, 4.89, 6.1	150, 30, 572	752	
2		4.37, 5.34, 5.70	65, 46	111	
3		2.97, 3.59, 5.58	111, 440	551	
4		3.05, 3.96, 4.88, 6.1	72, 269, 951	1292	
5		(4.21), 5.50, 6.04	140, 75	215	
6		(2.44), 5.03, 5.49	38, 134	172	
7		(4.97), 5.52, (6.1)	142, 436	578	
8		4.75, 5.48, (6.1)	1988, 1290	3278	
13		4.97, 5.58, (6.1)	153, 120	273	
9		Thelon Plain	(4.42), 5.91	276	276
10			4.66, 6.19	284	284
11			4.53, 5.65	434	434
14			3.29, 3.81, 5.56	294, 460	754
15	3.86, 5.64		372	372	
16	3.32, 5.73		387	387	
17	3.52, 4.22, 6.25		539, 309	848	
18	3.14, 4.33, 5.27, 6.1		121, 152, 244	517	
19	3.41, 6.1		175	175	
20	3.29, 5.94		215	215	
21	3.32, 6.1		693	693	
22	3.32, 5.0, (6.1)		462, 1269	1731	
23	3.35, 4.63, (6.1)		381, 1562	1943	
24	3.32, 4.63, (6.1)		298, 633	931	
25	3.14, 4.88, 6.0		177, 757	934	
26	3.44, 3.87, 4.8, (6.1)		132, 375, 958	1465	
27	3.54, 5.09, (6.1)		211, 188	399	
28	4.21, 6.1		1052	1052	
29	3.51, 4.72, 6.1		272, 923	1195	
30	4.51, 5.94		755	755	
31	3.57, 3.72, 4.48, (6.1)		283, 126, 620	1029	
32	4.91, 6.04		1429	1429	
33	3.29, 4.88, 6.1	71, 714	785		
34	2.99, 6.1	771	771		
35	3.6, 4.75, 6.1	280, 1118	1398		

Values in parentheses are assumed.

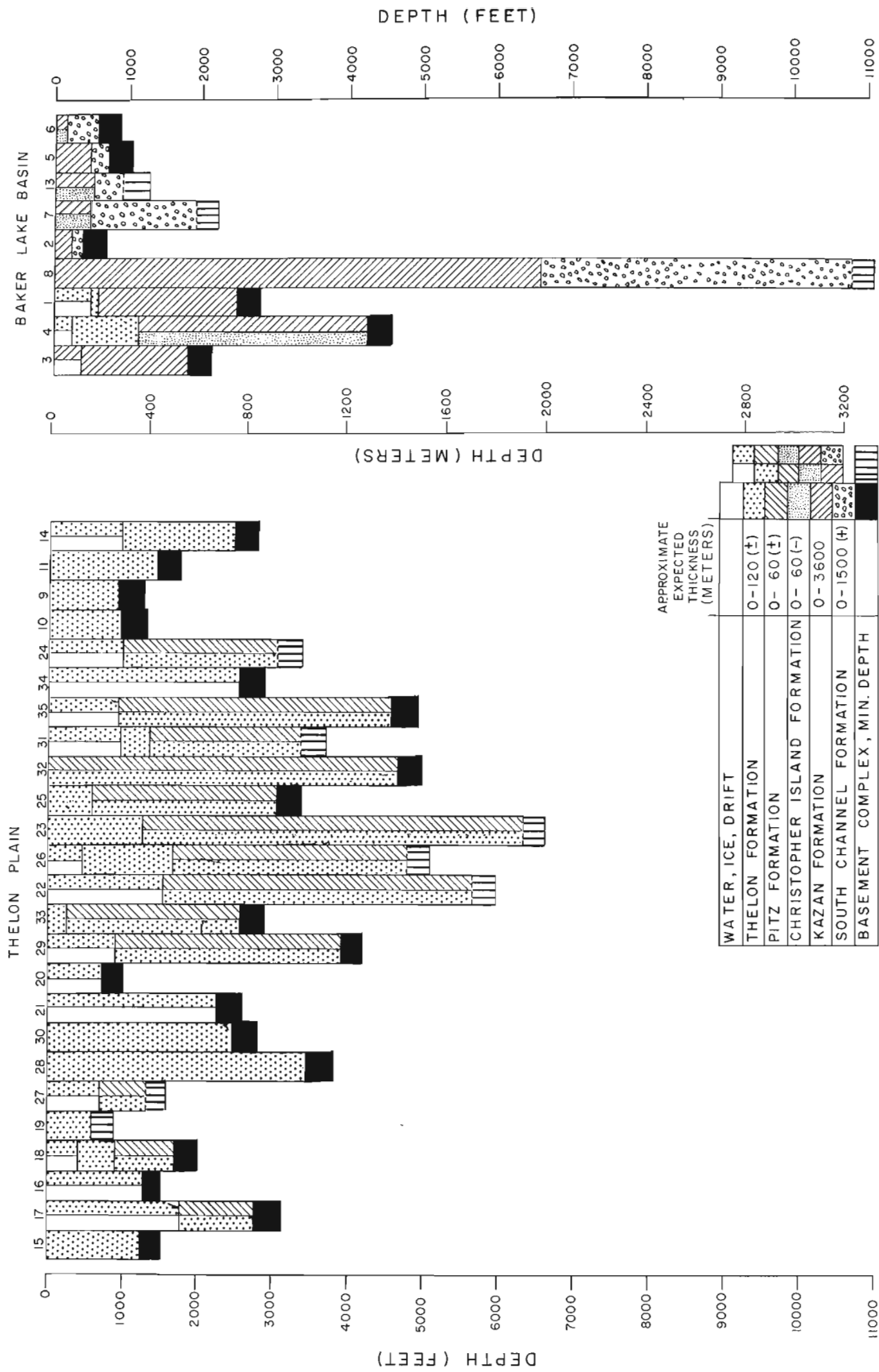


Figure 3. Cross-sectional representation of the seismic results.

Results

Distribution of observed seismic velocities are shown on Figure 2 with tentative lithological correlations. Considerable overlap in correlations are evident revealing the coarseness of correlations in this type of reconnaissance seismic refraction survey. Conducting these surveys on frozen lakes always creates the additional difficulty of recognizing near surface sedimentary velocities in the presence of ice transmitted events having similar velocity. Another factor complicating velocity-lithology correlations is unaccountable dips on lithologic interfaces. The coarse and tentative nature of these lithology-velocity correlations cannot be overstressed.

Table 1 itemizes the seismic velocities and their computed thicknesses for representative layers. Where penetration to the basement complex was not achieved, the basement velocity of 6.1 km/s was assumed (see values in parentheses, Table 1) to be present where measured data terminated, thus giving minimum estimates for basement depths. These results are shown in cross-sectional form on Figure 3 where the velocity layers are interpreted in terms of lithology according to the tentative correlations of Figure 2. The minimum depth estimates to basement are represented by vertical hachures.

The total depth value of nearly 3300 m for profile 8 in the Baker Lake basin has been questioned and rechecked; although the computation is based on the minimum depth hypothesis, and there are other interpretational problems involved, these problems are not unique to profile 8. The indicated depth for profile 8 cannot be appreciably reduced. An alternative would be to accept the depth at 2000 m, which represents a velocity of 5.48 km/s rather than 6.1 km/s. Profile 8 cannot, on the basis of these seismic results, be singled out for this treatment. Other profiles would have to be treated accordingly. If the 3300 m depth for profile 8 is in conflict with geological information, the conflict will have to be resolved on the basis of data quality or interpretation considerations.

A seismic reflection experiment was also conducted near location 8. Although no discernible reflections were observed, the methods used were necessarily crude. The feasibility of the reflection method should still be regarded as favourable in the Dubawnt Group.

Conclusion

The restriction imposed by the use of lakes for conducting seismic surveys results in a coarse grid for mapping a basement which may be structurally complex. Closely spaced continuous seismic profiles on land as well as the lakes would yield greater detail on these complex structures and also on the overlying sedimentary section. The seismic reflection method should be thoroughly tested in the Dubawnt Group for its capability to provide greater structural detail and definition. Seismic profiling across land surfaces would require the drilling of shotholes for small dynamite charges used as the seismic energy source. Mechanical vibrator sources may also be effective and should be tested.

Acknowledgments

This note is based on field data and the writer thanks H.A. MacAulay, R.A. Burns, and the late W. Tyrlik for the organization and conduct of the field program and R.M. Gagne for drafting the figures.

References

- Donaldson, J.A.
1965: The Dubawnt Group, Districts of Keewatin and Mackenzie; Geological Survey of Canada, Paper 64-20.
1966: Study of the Dubawnt Group; in Report of Activities, Part A, Geological Survey of Canada, Paper 66-1A, p. 22.
1967a: Study of the Dubawnt Group; in Report of Activities, Part A, Geological Survey of Canada, Paper 67-1A, p. 23-25.
1967b: Two Proterozoic elastic sequences: a sedimentological comparison; Proceedings of the Geological Association of Canada, v. 18, p. 33-54.
1969: Descriptive note (with particular reference to the late Proterozoic Dubawnt Group) to accompany a geological map of central Thelon Plain, Districts of Keewatin and Mackenzie; Geological Survey of Canada, Paper 68-49.
- Fraser, J.A., Donaldson, J.A., Fahrig, W.F., and Tremblay, L.P.
1970: Helikian basins and geosynclines of the northwestern Canadian Shield; in A.J. Baer (editor), Symposium on basins and geosynclines of the Canadian Shield; Geological Survey of Canada, Paper 70-40, p. 222-225.
- Overton, A.
1971: Seismic survey of the Dubawnt Group; in Report of Activities, Part A, Geological Survey of Canada, Paper 71-1A, p. 58.
- Roscoe, S.M.
1966: Unexplored uranium and thorium resources of Canada; Geological Survey of Canada, Paper 66-12.
- Ruzicka, V.
1978: Evaluation of selected uranium bearing areas in Canada; in Current Research, Part A, Geological Survey of Canada, Paper 78-1A, p. 269.
- Wright, G.M.
1955: Geological notes on central District of Keewatin, Northwest Territories; Geological Survey of Canada, Paper 55-17.
1957: Geological notes on eastern District of Mackenzie, Northwest Territories; Geological Survey of Canada, Paper 56-10.
1967: Geology of the southeastern barren grounds, parts of the Districts of Mackenzie and Keewatin; Geological Survey of Canada, Memoir 350.

DATA ENTRY AND VALIDATION FOR THE CANMINDEX PROJECT

D.D. Picklyk
Director General's Office

Introduction

The advances in recent years in the development of specialized equipment peripheral to large computers as well as accompanying user-oriented software packages has prompted an increasing reliance on various data bases by many scientists to assist them with their research. These advances are manifest by the proliferation of firms offering a variety of specialized services and functions ranging from data entry through data management to special output such as colour graphics. Such products and systems are implemented on a range of computers varying from micros to the largest available mainframes, depending on the specific application.

At the Geological Survey of Canada (GSC) computers have been used in various applications since the mid 1960s. Many specific applications have been described in Gordon and Hutchison (1974) and more general applications to geological field data in Hutchison (1974).

Most literature on the subject of computer files addresses itself to the description of the files and their intended usage (see for example Picklyk et al., 1978; and Cargill and Clark, 1977). Some attention has also been given to data specifications and standards (Burk, 1977; Picklyk, 1975, 1977). However, little has been done in dealing with the most important aspect of any computer file, namely the data which it contains.

Crain (1974), examined the characteristics of computer files intended for processing of scientific data and how they differ from files intended for business applications. He followed this by a paper (Crain, 1975) dealing specifically with the entry and validation of scientific data. In his paper, Crain identified the six types of error that can occur and various methods to minimize the occurrence of errors within each type. The six types that are recognized are: 1) sampling errors; 2) observation error; 3) instrumental errors; 4) reading error; 5) recording errors and 6) coding errors.

The object of this note is to examine in detail the steps that have been taken to minimize the last three types of error as they apply to a specific project within the Geological Survey of Canada and examine the utility of performing data entry in-house using an intelligent terminal. These three types of error are those associated with the manual reading and recording of individual data items. The reading and recording errors are perhaps the most common and their meaning obvious. Coding errors on the other hand result from the assignment of incorrect codes to correctly read and recorded data.

CANMINDEX Project

Since 1974, there has been an on-going project within the GSC to implement a computer processable index to Canadian mineral occurrences. The resultant file and project are both known as CANMINDEX (Canadian Mineral Occurrence Index) and have been described elsewhere (Picklyk, 1975; Picklyk et al., 1978).

The CANMINDEX file is intended to serve as an index in two ways. The first and perhaps most important function of the file is to provide an easily usable index to the spatial distribution of mineral commodities throughout Canada. Secondly, the file provides an index to a limited bibliography

for Canadian mineral occurrences. It is important to note, that for purposes of the file "mineral occurrences" include naturally occurring mineral concentration ranging from classic "occurrences" to the largest producing mines. The file will also be used as the starting point or "front end" for other more comprehensive special purpose files.

CANMINDEX Data, General

By the nature of the objectives of the file, the data within CANMINDEX are relatively simple. Essentially they consist of a unique identifier, name, geographic location, deposit type, commodities present and their status, remarks and map and bibliographic references. The exact data items collected may be ascertained from the appended CANMINDEX coding form. Definitions of each of the items are contained in the coding guide appended to the description of the CANMINDEX file in Picklyk et al. (1978).

As is characteristic of a scientific data file, most of the data are not exact. Although a number of the items are unique and exact (e.g., a mineral occurrence can only have one location), their entry into the file is based on an interpretation of the available data. That is, the geographic position must be plotted onto a map on the basis of a description of the location and then the co-ordinates are scaled off and entered into the file. The activity is rarely performed by our coding staff. Instead, they usually record the "best" available published co-ordinates. For similar reasons, the only possible types of error for data in the file are reading, recording and coding.

CANMINDEX Editing and Validation Procedures

The generalized data flow from source to computer file for the CANMINDEX project are summarized in Figure 1. The points of particular interest are that editing and validation are performed both automatically (using an intelligent terminal) and visually by the coders and chief coder. In general, any fields containing ranges of values or lists of permissible values are automatically checked by the programs coded into the intelligent terminal. All fields of a "comment" nature are visually verified. The kind of information that is coded into these fields is of an interpretive summary nature. That is, summaries of text must be coded according to guidelines established for the file. Verification of these fields consists of ensuring that the guidelines are being adhered to in a uniform, consistent, manner and that the available data is interpreted accurately. This is the main duty of the chief coder and is necessary as it has been found that the individual coders will diverge from established guidelines over time and the only practical way to detect the divergence is to have one individual review all coded input documents.

Referring to the appended coding form, the main characteristics of each of the data items and the editing and validation checks will be discussed.

One of the most fundamental checks that can be made is for presence or absence. In CANMINDEX there are several data items that must be present for each record or else the record is considered invalid. These are Link Number, Component, Entity Coded, How Located, Entity Comment, Province, Geological Province, NTS, Latitude and Longitude or UTM zone, Northing, Easting, Deposit Type, at least one Commodity and Status. The check for presence is made automatically by the intelligent terminal and an attempt by the operator to skip one of these fields results in an audible tone and locked keyboard which forces the operator to make an entry before proceeding. With the exception of the Entity Comment field all of the above items have other editing and validation criteria associated with them. The Link Number

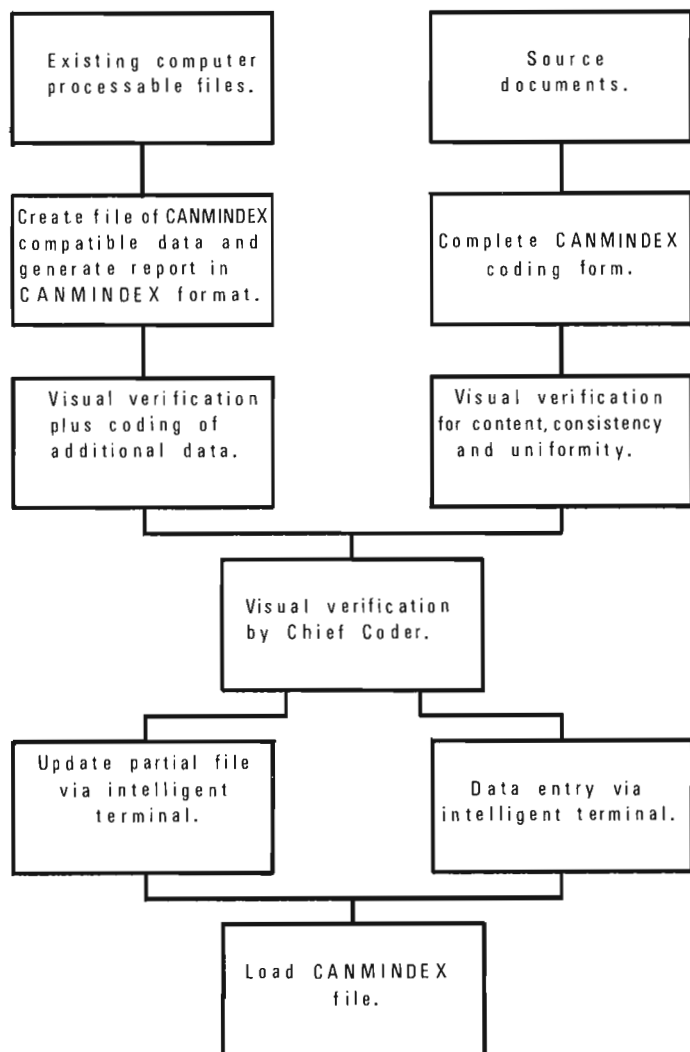


Figure 1. Generalized data flow and edit points for the CANMINDEX project.

and Component must both be numeric. They must also be right justified and this will automatically be performed by the terminal if the operator fails to do so. In all instances, failure to comply with editing or validation criteria results in an audible tone and locked keyboard. The Entity Coded field must contain one of three possible codes. Mnemonics rather than numerics were used as the codes because the valid entries do not form a logical sequence with an implied order. Therefore, it is easier for the coders to remember the descriptive mnemonics rather than arbitrary numbers. The How Located field must also contain an entry from a closed list of valid mnemonics. Mnemonics were used for the same reason as above.

The Province and Geological Province are both tested to ensure they contain a value from lists of valid mnemonics. The NTS (National Topographic System) field is composed of numeric, alphabetic and numeric parts respectively. Each of the components is tested to ensure that the entry complies with the possibilities allowed by the National Topographic System. In addition the entire field is compared with the first three components of the NMI Accession Number as the NTS is imbedded in the accession number. In most instances these numbers are the same. If they are not a warning message is output by the terminal informing the operator that

they are different and corrective action may immediately be taken if necessary. In the Latitude, Longitude, UTM zone, Northing and Easting fields, all values are checked to ensure they are numeric and within possible ranges. For example it is impossible to enter a value of more than 59 minutes or seconds in the Latitude and Longitude fields.

The Deposit Type field must contain an entry from a range of possible numeric values. Numerics rather than mnemonics were used as the list is relatively long (17 possible values) and the definitions for each of the types are rather lengthy so that meaningful mnemonics would be virtually impossible to define. Also, each of the type definitions includes explicit examples so by using numeric codes the coders are forced to consult the list and examples and thereby usually arrive at a better classification. As is obvious from the coding form, each mineral commodity has a status associated with it. This status can range from the commodity merely being reported as present to the commodity being produced. In this case there is an implied order and hierarchy. As a retrieval convenience numeric codes are used for the eight possible valid entries. By using numerics rather than mnemonics it is very easy to access all records above or below a certain status or to extract all records within a specific range of status. Mnemonics could have been used but would have been more cumbersome to use during retrieval.

As noted above, all the previously noted validation checks are performed automatically by the terminal at the time the data are entered. The necessity of employing operators that are familiar with the data should also be apparent when one considers that any corrections that must be made are not simply a matter of choosing a valid value but require that the context of the record as a whole must be taken into account and the available data be interpreted in order to select the correct value. It might also be considered that the automatic validation is the last line of defence as it will be noted in Figure 1 that all input documents have been visually verified twice: once by the coders themselves and again by the chief coder. All further editing and validation, especially of free format fields, results from feed-back from our users.

With regard to the visual verification, two general areas are considered. The first is the "truth" of the data. This verification is performed by the coders by the simple expedient of exchanging completed coding forms and validating each others work. This kind of validation works as all coders are usually compiling data for the same geographic area and therefore all become familiar with the general geology and deposit types. What the process really does is have a fresh mind review the compiled data as experience has shown that coders reviewing their own completed forms will see what they want to see which is not necessarily what has been entered on the coding form.

The second aspect of visual verification addresses the problems of uniformity and consistency of the data. When dealing with a natural phenomenon with a range of diversity such as encountered when considering mineral occurrences, the differences in detail of available information soon become apparent. In order to ensure that a data file will be usable for its intended purpose the same level of detail must be maintained throughout. That is, the level of detail must be uniform as there is nothing to be gained by collecting vast amounts of detailed information, for a small number of records if the objective of the file is to be an index. In reality the level of uniformity that must be maintained is a function of the intended purpose. In our case the CANMINDEX file is intended as an index to mineral occurrences and the commodities which they contain. To comply with the intent of the file, we do not collect detailed

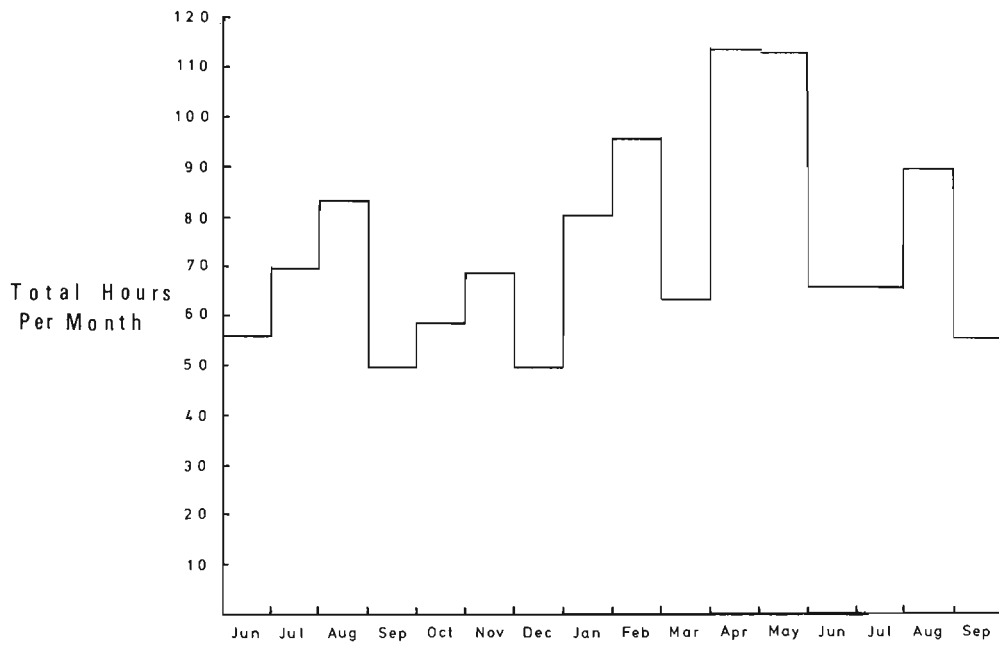


Figure 2
Total monthly terminal usage for all activities, June 1977 to September 1978.

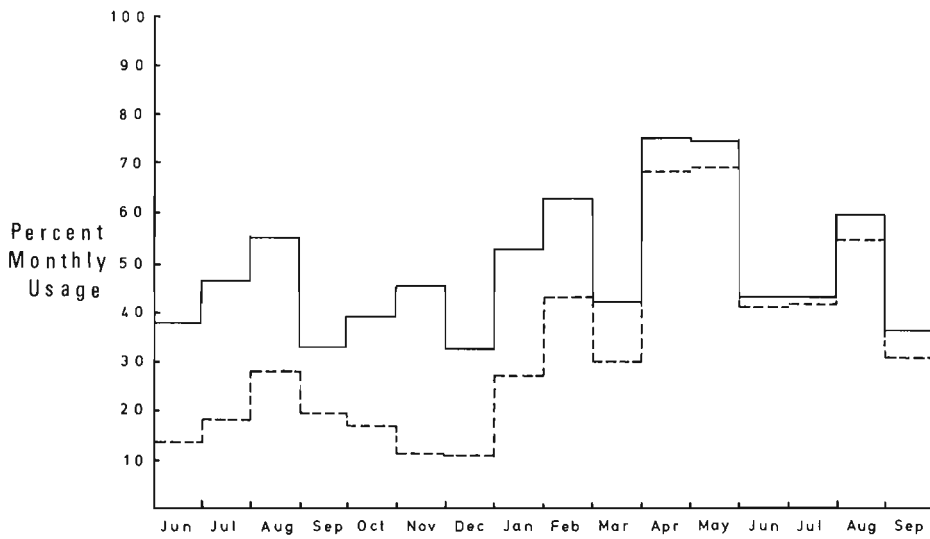


Figure 3
Per cent monthly terminal usage based on 150 hours per month.
— usage for all activities
- - - usage for data entry

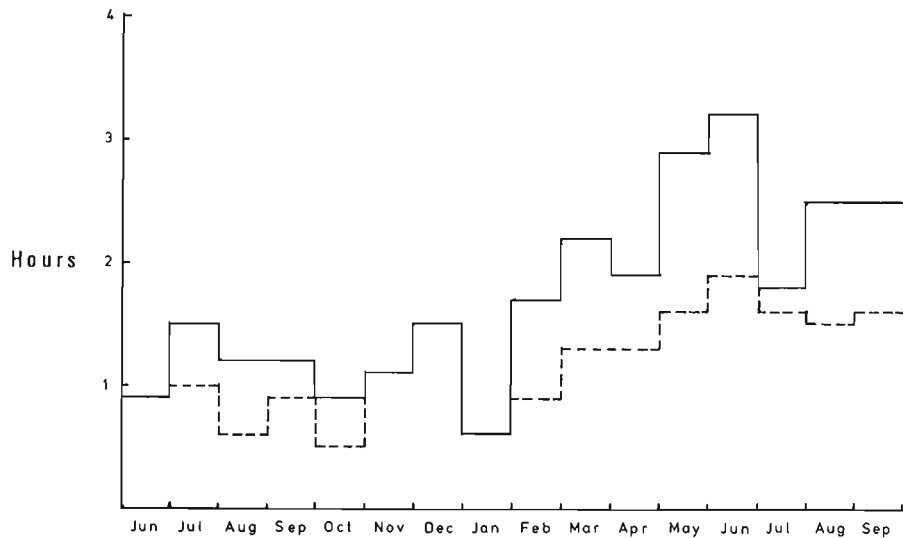


Figure 4
Average daily terminal usage for editing, transmitting and loading.
— per day used
- - - per session

Table 1

Monthly hourly usage and average daily usage for the three main activities performed on the intelligent terminal during the period June 1977 to September 1978

	Dev/Demo Total-Av/Usage		Entry/Update Total-Av/Usage		Retrieval Total-Av/Usage		Month Total Total-Av/Usage	
June /77	29.7	2.1	21.6	1.4	5.3	.3	56.6	2.6
July	34.9	2.1	27.8	1.5	6.8	.5	69.5	3.3
Aug.	39.7	2.3	41.2	2.9	2.1	.3	83.0	3.1
Sept.	9.1	1.0	37.3	2.5	3.1	.4	49.5	2.5
Oct.	30.6	3.1	25.5	2.3	2.3	.4	58.4	3.1
Nov.	47.8	2.4	17.3	1.4	3.5	.3	68.6	3.3
Dec.	29.9	1.9	16.9	1.5	3.0	.4	49.8	2.4
Jan. /78	36.1	2.4	40.8	2.9	3.6	.7	80.5	3.8
Feb.	27.5	1.6	65.8	3.5	2.4	.5	95.7	4.6
Mar.	15.7	2.0	44.9	3.7	2.4	.8	63.0	3.7
Apr.	10.0	2.0	103.2	5.2	0.0	0.0	13.2	5.7
May	5.3	1.3	103.5	4.7	3.4	3.4	112.2	5.1
June	1.5	.5	61.9	3.6	1.9	1.9	65.3	3.8
July	1.5	.7	63.6	3.7	0.0	0.0	65.1	3.8
Aug.	8.2	2.0	82.1	3.5	0.0	0.0	89.4	3.9
Sept.	9.0	1.1	45.7	2.8	.3	.3	55.0	3.2
	336.5		799.1		40.1		1174.8	

mineralogical or other geological information. Consistency applies more specifically to ensuring that the data comply with established definitions and guidelines. In the case of non-numeric geological data, interpretations of the available data are often required. These must comply with definitions to render the file usable. In the case of numeric data the precision and accuracy must be taken into account. Also the analytical technique must often be taken into account as special techniques are used for special purposes which may render the data unsuitable for another application. This often occurs in geochemical programs for example. Although numerical codes are used in the CANMINDEX file, they may be considered in the same way as non-numeric data.

The responsibility for maintaining uniformity and consistency of the file rests with the chief coder. As in the case of the coders it should be apparent why the chief coder must be familiar with the data in order to perform the necessary validation effectively. Although in a sense unverifiable, comment fields are also checked for uniformity and consistency.

"Intelligent Terminal Usage"

Data entry for the project is performed in-house on a leased "intelligent" terminal. The decision to perform the data entry in-house rather than by contract with a service bureau was based on the desire to allow the operators to make any necessary corrections at data entry time rather than during a later editing run. Such corrections cannot be made by service bureau personnel because of the specialized nature of the data. That is, corrections must often be made on the basis of context and interpretation of the available data and are not necessarily a matter of illegibility of the coding form. Another contributing factor was the knowledge that data acquisition for the project would continue for a long period of time and would be continuously updated. Thus the creation and editing of the file is not a one-time effort. As a result it is often better to perform data entry and validation in-house rather than periodically load and edit large quantities of data.

It was accepted that because the personnel were not trained key-stroke operators, their rates of data entry would be lower. It was felt however that the entry rates would increase as the personnel became familiar with the equipment

and procedures. Furthermore, the terminal was to be regarded as a piece of production equipment and operated as continuously as possible. This was to be achieved by having all coders perform data entry in shifts.

Data have been compiled for intelligent terminal usage for the sixteen months beginning in June of 1977 and end in September of 1978. In Table 1, the data are presented in tabular form for four activities of the terminal. These are:

- 1) Development/demonstration; which includes the time spent on system development and demonstration of the equipment/systems to interested potential users. It should be noted that all systems to be used on the terminal must also be developed and tested on the terminal;
- 2) Entry/update; includes all activities related to data entry, visual verification and transmission to the mainframe;
- 3) Retrieval; represents the time spent accessing the data file and is an activity that could be performed on any terminal capable of communicating with the central computer;
- 4) Monthly total; is the simple sum of usage for all activities.

Figures for the total and average usage are presented for each activity. The average usage includes only those days in which a particular activity was performed and is not an average per session of activity nor does it include days in which an activity could have been but was not performed.

The above figures have also been summarized graphically. Figure 2 is a simple summary of the total monthly usage. The most striking aspect of the figure is the high variability. One might have expected a gradual increase in usage leveling off at some near constant rate. In Figure 3 the total usage (solid line) has been plotted as a percentage of the total possible time for usage, based on an average of 150 available hours per month. Also included is a plot of the data entry activity as a percentage of the total possible. The striking feature of the total usage plot is that total utilization exceeding 50% was achieved in only six of the sixteen months. If the terminal is to be considered a piece of production equipment, these figures are probably too low. The plot for data entry does show the expected rising usage with time for this activity. The daily usage pattern for the terminal is reflected in Figure 4. In general we note gradual,

but variable, increase in daily usage with a maximum of just over three hours per day. As expected there is also a gradual increase in session time as the coders become more familiar with the equipment and procedures. For the four months when the average session time is identical to the average daily usage, the terminal was being used exclusively for the purpose for which it was intended, namely: data entry.

Two factors must be taken into consideration when assessing the high degree of variability present in the results. The first is that personnel engaged in data acquisition for the CANMINDEX project are periodically required to participate in other high priority short term projects. Thus most of the periods for which there was relatively low terminal usage can be correlated with times when the coding staff were otherwise engaged. Secondly, most of the coding staff are temporary employees of the agency. As such there is a relatively high turn-over of coders, each of whom must be trained for data acquisition as well as terminal operation. For this reason, coders are unavailable for data entry and for some unknown reason, sessions on the terminal during the familiarization period tend to be short. This is due perhaps to their unfamiliarity with the system and procedures resulting in their interrupting data entry to seek assistance for minor problems.

Although the variations in the rates of usage can be explained, the reason for the generally low rate is not obvious. This is especially true as there is always a backlog of data awaiting entry. The possible explanation is the general reluctance on the part of the coders to perform data entry because their primary activity is assembling and encoding the data from other source documents. Their lack of typing ability and resultant slow entry speed would contribute to such a reluctance. Support for this possibility is provided by the observation that the use of a trained typist (whose only activity with the project is to enter data) results in a much higher entry rate and longer session times. The only drawback is the operators lack of geological knowledge which necessitates consulting with the coders should any problems arise.

Summary and Conclusions

As noted above there are two basic ways in which data can be assembled and validated for computer processing. These are specifically a) by contracting the work to one of the many service bureaus specializing in this activity or b) implementing in-house systems to complete the task. There are advantages and disadvantages to both approaches and the method chosen will usually be dictated by the specific application. In applications which require a once-only assembly of a large amount of data it is usually better to contract the work to a service bureau. This of course implies an extensive post entry editing and validation effort. On the other hand if the application is such that there will be an ongoing influx of data it is worth considering implementing an in-house system. This would require the purchasing of equipment and the hiring and training of staff. Service bureaus may also be used in situations involving an on-going influx of data. However, this can be very expensive and a careful analysis would be required to determine whether or not it would be more cost effective than implementing an in-house system. In the light of terminal usage data now available it appears that our internal procedures for data entry should be re-assessed with consideration being given to contracting the keying. Alternatively, the data entry procedures could be altered so that all keying is performed by a trained operator possessing the necessary typing skills thus freeing the coders to assemble the data for keying. This method is being tried and preliminary results show a higher data entry rate.

With regard to the data, the factors that must be considered are ease of coding versus ease of usage. There are times when mnemonic codes can be used to advantage as well as times when it would be better to use numeric codes. Situations also arise in which both mnemonic and numeric codes are unsuitable and free text must be used even though it may be difficult to edit and validate.

Finally, it should be noted that there is no one system or procedure that will work in all cases. Nevertheless, with the wide variety of manufacturers offering specialized data entry equipment and software as well as service bureaus offering various levels of data entry/validation, of ones own requirements should readily be accommodated following careful analysis.

References

- Burk, C.F. (Editor)
1977: Computer-based files on Mineral Deposits: Guidelines and Recommended Standards for data Content.
- Cargill, S.M. and Clark, A.L. (Editors)
1977: Standards for Computer Applications in Resource Studies; Special Issue, *Mathematical Geology*, v. 9, no. 3.
- Crain, I.K.
1974: The Analysis of Scientific Computer Systems; *INFOR*, v. 12, no. 3, p. 299-311.
1976: Entry and Validation of Scientific Data – How to Prevent "Garbage In"; *Canadian Information Processing Society, 1975 Conference, Regina*, p. 160-170.
- Gordon, T.M. and Hutchison, W.W.
1974: Computer Use in Projects of the Geological Survey of Canada; *Geological Survey of Canada, Paper 74-60*.
- Hutchison, W.W.
1974: Computer-based systems for Geological Field Data; *Geological Survey of Canada, Paper 74-63*.
- Montgomery, J.H., Sinclair, A.J., Wynne-Edwards, H.R., Fox, A.C.L., and Giroux, G.H.
1975: Data Capture in the Construction of MINDEP's Computer-based, Mineral Deposits Files, *Canadian Journal of Earth Sciences*, v. 12, no. 4, p. 698-703.
- Picklyk, D.D.
1975: An Index to Canadian Mineral Occurrences – Preliminary Considerations; *Computers and Geosciences*, v. 2, p. 317-319.
1977: Requirements of the Data to be Used for Resource Appraisal; *Mathematical Geology*, v. 9, no. 3, p. 301-308.
- Picklyk, D.D., Rose, D.G., and Laramee, R.M.
1978: Canadian Mineral Occurrence Index (CANMINDEX) of the Geological Survey of Canada; *Geological Survey of Canada, Paper 78-8*.

STRUCTURE AND PETROLOGY OF THE SOUTHERN PORTION OF THE MALTON GNEISS, BRITISH COLUMBIA

EMR Research Agreement 2239-4-222/77

M.L. Morrison¹
Regional and Economic Geology Division

Introduction

Field work carried out on the southern portion of the Malton gneiss, northern Monashee Mountains, British Columbia, during the summer of 1978 is presented in this report. The field work is a major part of a project designed to determine the lithologic and structural nature of the Malton gneiss and to establish its stratigraphic setting as well as its tectonic and petrologic evolution in relation to the Hadrynian metasedimentary rocks which flank it. Though a large portion of the area remains to be studied, some tentative conclusions can be made at this stage.

Previous reconnaissance mapping on the Malton gneiss was carried out by Campbell (1968). A more detailed program of study on the southeast portion of the Malton gneiss was begun by Giovanella (1966 and 1967).

I wish to acknowledge the assistance and support of P.S. Simony. Financial support is from the Department of Energy, Mines and Resources and is gratefully acknowledged.

Petrology and Stratigraphy

The southern Malton gneiss can be subdivided into four lithologic units. The oldest is a layered paragneiss consisting of fine grained biotite-rich and biotite-poor gneisses, some containing sparse feldspar augen. Other lithologies in the paragneiss are quartzites, para-amphibolites, and muscovite-feldspar-quartz gneisses. The paragneiss sequence exhibits two episodes of leucosome development with the leucosomes largely being confined to the augen biotite gneisses. The virtual absence of pelitic units within the paragneiss sequence makes it difficult to determine the metamorphic grade, but the gneissic character and the presence of leucosomes suggests amphibolite facies. Sparse kyanite found in one layer southwest of Dominion Mountain indicates kyanite grade.

Leucocratic orthogneiss appears to have intruded the paragneisses. This unit is generally massive and is only locally foliated. In most areas it exhibits a well developed lineation of biotite aggregates and elongate feldspar and quartz grains. The foliated regions are usually adjacent to the paragneisses where the biotite concentration increases. This phenomenon possibly represents an early crystallization phase in a now deformed pluton.

A second orthogneiss unit is present in the southern portion of the Malton gneiss. It consists of abundant augen of feldspar, one to two centimetres across, with subordinate biotite and quartz. This augen gneiss has a well developed lineation formed from elongate augen of feldspar and a foliation formed from the planar orientation of biotite flakes.

The relative age of the augen gneiss with respect to the paragneiss and the leucocratic orthogneiss is uncertain. The primary contact relationship between the augen gneiss and the paragneiss is obscured by later zones of shear present at most observed contacts. The relationship between the augen gneiss and leucocratic orthogneiss can possibly be ascertained by the presence of fine grained, grey dykes in both lithologies. These appear to be related to the emplacement of the leucocratic orthogneiss and in places contain inclusions of the augen gneiss. The augen gneiss has thus predated the leucocratic orthogneiss.

A metasedimentary sequence consisting of pelites, semipelites, quartzites, psammites, and grits occurs as a fairly extensive sheet within the Malton gneiss (see Fig. 1, 2). A foliation formed by the planar orientation of micas is ubiquitous, and often two or more crenulation lineations are observed. Randomly oriented porphyroblasts of staurolite and kyanite are commonly found coexisting in the pelitic rocks. This suggests that the maximum metamorphism effecting the metasedimentary sequence reached staurolite-kyanite grade and took place during a period of minimal deformation. Small patches of leucosome are occasionally observed in the metasedimentary rocks, but are confined to the psammites and semipelites. These leucosomes appear to be the same generation as the younger leucosomes found in the paragneiss unit. This conclusion is based on the structural similarity of the leucosomes in the two units placing them chronologically between the same episodes of deformation.

The relative age of the metasedimentary unit is reasonably well determined. One large outcrop, showing a lithologic discordancy between the metasedimentary unit and the augen gneiss with otherwise concordant foliation, suggests an unconformable relationship between the two lithologies. This relationship, along with the presence of only the younger generation of leucosomes in the metasedimentary unit, leads to the conclusion that the paragneiss and the augen gneiss were gneisses before deposition of the metasedimentary parent rock. The paragneiss and the augen gneiss probably represent a basement complex as is postulated by Campbell (1973) and Ghent et al. (1977). The similarity between the metasedimentary unit and the Horsethief Creek Group rocks of Hadrynian age (Ghent et al., 1977) to the south in terms of metamorphic grade, structural history, and lithology strongly suggests that the two units are correlative. The chronological positioning of the leucocratic orthogneiss is less clear. Its only observable relationship to the metasedimentary unit is through a major thrust fault. The leucocratic orthogneiss is, however, commonly found infolded with or in an intrusive contact with the basement lithologies suggesting that the leucocratic orthogneiss should be considered as a part of the basement complex predating the metasedimentary unit.

Structure

At least three phases of folding and perhaps as many as five (Giovanella, 1966) are observed in the southern portion of the Malton gneiss. Two episodes of thrust faulting appear to be associated with specific phases of folding; a final episode of normal faulting cuts across all structures in the area.

The earliest folds are only found on a mesoscopic scale. They are isoclinal with a well developed axial plane foliation. These isoclinal folds themselves fold an earlier foliation and are thus referred to as F_2 with the combined foliation referred to as S_{1-2} . The S_{1-2} foliation represents the predominant planar structure in the study area. The F_2 folds vary in size up to wave lengths of tens of metres. The largest F_2 fold observed infolds the metasedimentary unit into the basement gneisses.

The predominant folding in the southern portion of the Malton gneiss has two styles as can be observed in Figure 2. In the southwest there is a series of large, tight folds overturned to the northeast. These fold the S_{1-2} foliation and the F_2 folds and are thus referred to as F_3 . In the northeastern part of the study area a large upright fold dominates the structure and is part of a regional fold pair shown by Campbell (1968). The F_3 folds are observed to extend over the hinge of the large upright fold without a change in vergence (Fig. 2) suggesting an earlier age for the F_3 folds. The large upright fold is thus tentatively referred to as F_4 .

¹Department of Geology, University of Calgary

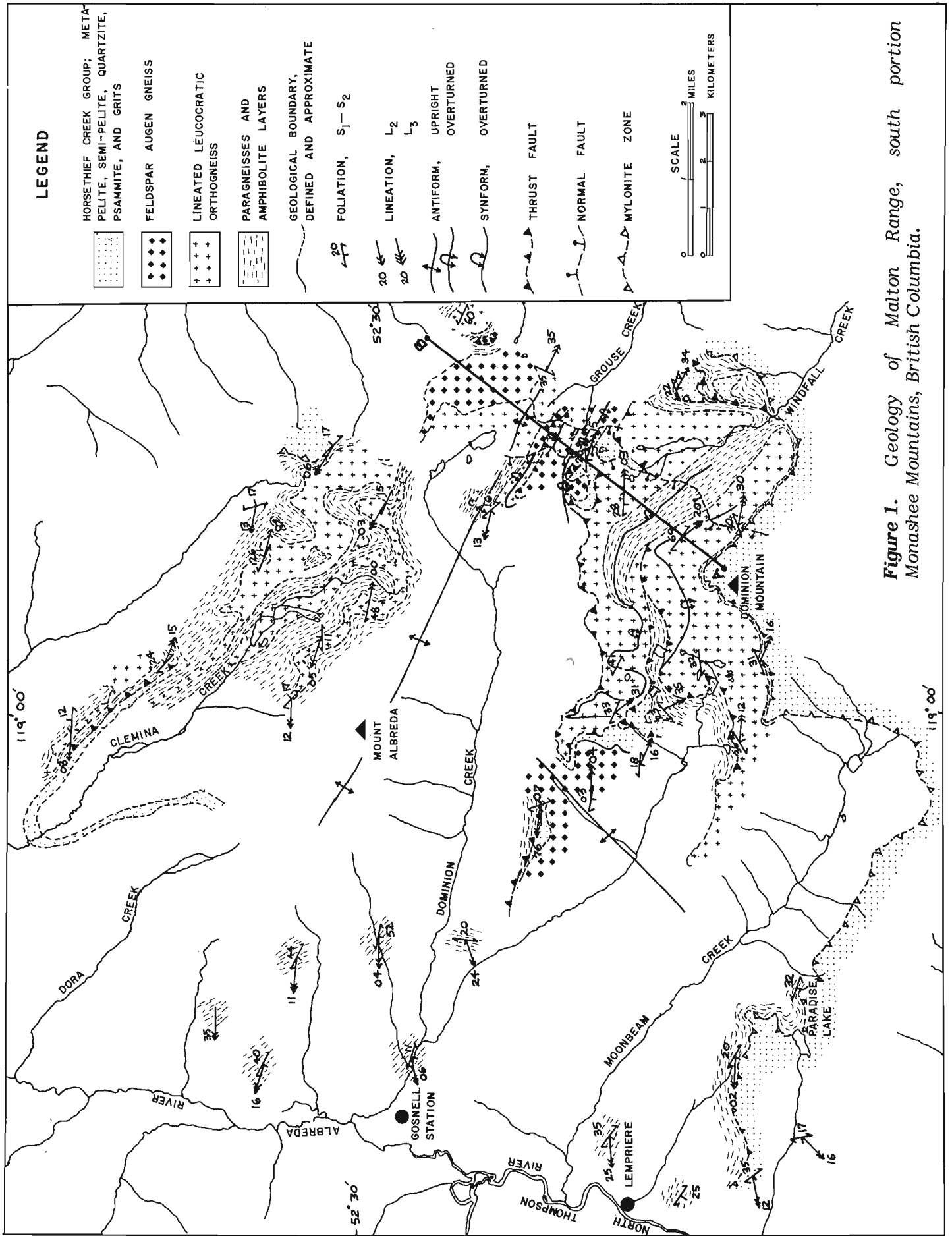


Figure 1. Geology of Malton Range, south portion Monashee Mountains, British Columbia.

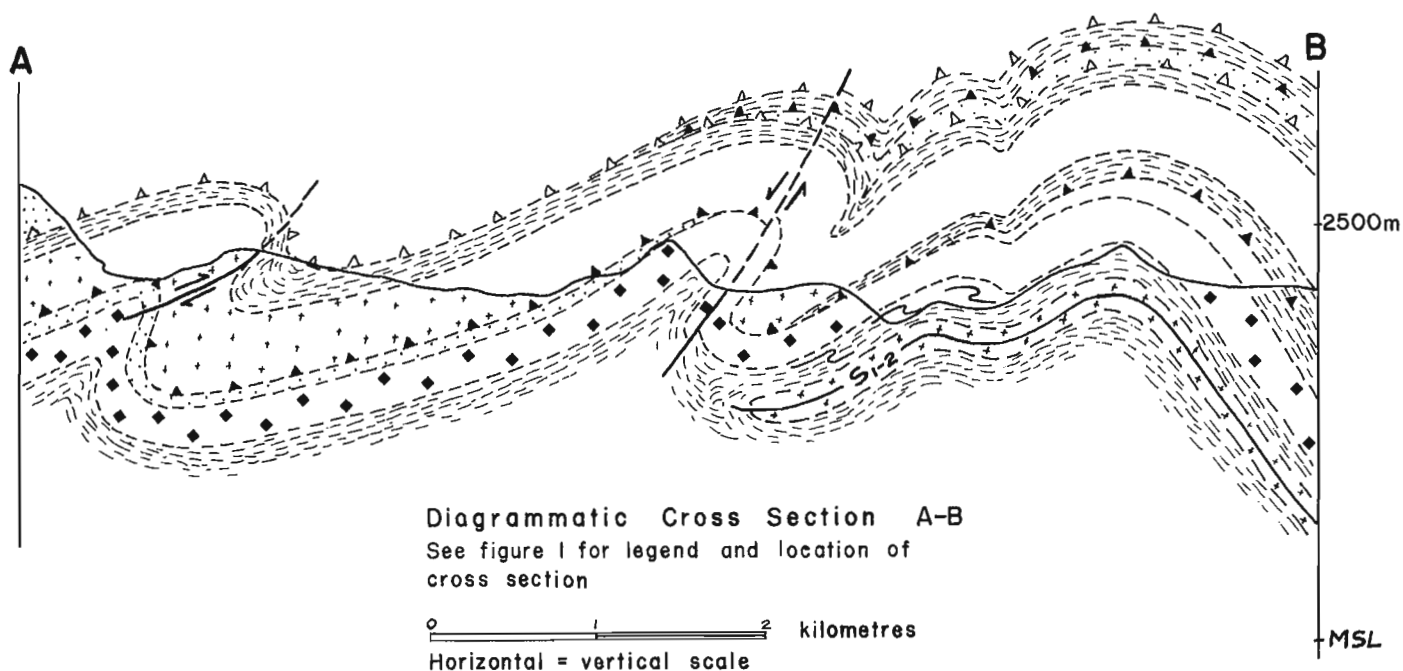


Figure 2. Diagrammatic cross I-I section A-B. See Figure 1 for legend and location of cross I-I section.

In the southwest part of the study area a broad fold, plunging to the southwest, is superimposed on F_3 folds (Fig. 1). The relationship between this fold and the F_4 fold is not known, but in conjunction with the F_4 fold it forms the southern half of a large dome cored with Malton gneiss.

Associated with the folding in the southern portion of the Malton gneiss are two dominant lineations. The earliest is a ubiquitous mineral lineation that parallels the F_2 fold axes and is thus referred to as L_2 . The F_3 fold axes and a commonly found crenulation lineation, which parallels the F_3 fold axes, are called L_3 . The L_2 and L_3 lineations are nearly parallel, and where both are obviously present in the same outcrop they deviate from one another by only 10° to 15° . In the southwest part of the study area, another crenulation lineation is found. This appears to be parallel to the southwest plunging fold found in the same region and therefore postdates the L_2 mineral lineation and a crenulation lineation that is presumably L_3 .

Two major thrust faults of differing ages are found in the study area. The earlier juxtaposes a sequence of orthogneiss and paragneiss of the basement complex over metasedimentary rocks of the Horsethief Creek Group. This thrust fault crosscuts the S_{1-2} foliation and is folded by the F_3 folds. This places the earliest thrusting event somewhere between the deformations associated with F_2 and F_3 . The other major thrust fault in the study area is located about three kilometres northwest of Dominion Mountain (Fig. 1). It is rooted in the axial plane of an F_3 antiform and thus appears to be associated with the same episode of deformation that formed the F_3 folds.

Normal faults, dipping steeply to the northwest, manifest the final phase of deformation affecting the study area. Though only two of the observed normal faults have sufficient displacement to be mapped on the 1:12 000 scale field sheets, numerous other normal faults are observed over much of the study area. The western extent of the Malton gneiss often occurs as chloritized fault breccia. Although a single fault cannot be traced, the general strike and dip of a large facet at the west end of the ridge between Moonbeam Creek and Dominion Creek and a plane formed by combining outcrops of fault zone material north of Dominion Creek are

subparallel to the normal faults elsewhere. This suggests that a large normal fault bounds the west side of the Malton gneiss, and explains the drop in metamorphic grade from staurolite-kyanite to garnet (Campbell, 1968) across the North Thompson-Albreda river valley from east to west.

Malton Gneiss-Horsethief Creek Group Contact

The southern contact between the Malton gneiss and the Horsethief Creek Group lithologies is known to be a mylonite zone (Campbell, 1968; Ghent et al., 1977). This mylonite zone can be readily followed across most of the southern boundary of the study area particularly above the tree line (Campbell, 1968). The present work suggests that this contact may turn north rather than continue eastward to the Rocky Mountain Trench as proposed by Campbell (1968). Similarities in lithologies of the Malton gneiss adjacent to the south contact between Windfall Creek and Grouse Creek, at the far eastern margin of the map area, and again adjacent to the metasedimentary rocks in the northeastern extent of the study area (Fig. 1) suggest that all three areas are at the same stratigraphic level. This is further supported by the foliation attitudes that curve around the southeastern end of the large F_4 fold (Fig. 1) roughly paralleling the proposed stratigraphic level.

Conclusion

Although field work is incomplete, some tentative conclusions can be reached. A sequence of metasedimentary cover rocks is distinguished from an earlier basement complex of orthogneisses and paragneiss. This differentiation is based on the presence of two episodes of leucosome development in the probable basement lithologies and only one episode of leucosome development in the cover lithologies. Similarities between the metasedimentary sequence and the Horsethief Creek Group rocks to the immediate south in terms of lithology and structural and metamorphic history suggests the two units are correlative. The earliest episodes of deformation recognized affect both cover and basement lithologies and are responsible for the dominant planar structure in the area, that of S_{1-2} , and a northwest trending mineral lineation, L_2 . A thrust sheet

extending through most of the study area formed after F_2 as did the peak metamorphic condition responsible for the disorientated kyanite and staurolite porphyroblasts. A third phase of deformation formed tight, southeast plunging folds overturned to the northeast and a thrust. These structures dominate the western portion of the study area. A fourth phase of deformation formed an open upright fold plunging southeasterly which dominates the eastern portion of the study area. The mylonite contact between the Hadrynian cover rocks to the south and the Malton gneiss is folded by the F_4 fold and extends farther northeast than previously thought.

References

Campbell, R.B.

1968: Canoe River, British Columbia; Geological Survey of Canada, Map 15-1967.

1973: Structural cross-section and tectonic model of the southeastern Canadian Cordillera; Canadian Journal of Earth Sciences, v. 10, p. 1607-1620.

Ghent, E.D., Simony, P.S., Mitchell, W., Perry, J., Robbins, D., and Wagner, J.

1977: Structure and metamorphism in southeast Canoe River area, British Columbia; in Report of Activities, Part C, Geological Survey of Canada, Paper 77-1C, p. 13-17.

Giovannella, C.A.

1966: Structural relationships of the metamorphic rocks along the Rocky Mountain Trench at Canoe River; in Report of Activities, Part A, Geological Survey of Canada, Paper 67-1A, p. 60-62.

1967: Structural studies of the metamorphic rocks along the Rocky Mountain Trench at Canoe River, British Columbia; in Report of Activities, Part A, Geological Survey of Canada, Paper 68-1A, p. 27-30.

GROUNDHOG COAL AREA, BRITISH COLUMBIA

Project 720038

T.A. Richards¹ and R.D. Gilchrist²
Regional and Economic Geology Division

The Groundhog coal area underlies about 5000 km² in north-central British Columbia, bounded by the watersheds of the upper Skeena, Nass, Klappan and Spatzizi rivers (Fig. 1). Coal has been known from the area for some 70 years, but because of its remoteness, little of its potential has been known. Two weeks in 1978 were spent in the Groundhog area for the purposes of defining stratigraphic units, regional correlations and potential for coal prospecting. The work concentrated on the area between Nass and Panorama lakes, a distance of about 50 km. The type area of the Groundhog coal basin, the McEvoy Flats area, was not visited, hence precise correlation between the established coal region and the remainder of the basin is not presently possible.

Stratigraphy

The area investigated is underlain entirely by fluvial clastic rocks, deposited by streams that flowed south-southwest. The assemblage includes a wide spectrum of depositional environments and ranges from thick pebble-conglomerate channel facies to marly overbank facies. These two facies represent the extremes of deposition, and the subdivision into four map units used in Figure 2 is based upon the percentage of conglomeratic members within a given area. The divisions are arbitrary and are set at less than 10%, 10-30%, 30-50% and greater than 50%. The conglomeratic members within each of the subdivisions are characterized by clasts of white and grey chert; white, buff, grey and green aphanitic acidic volcanics and white, vein quartz. The similarity of conglomerate composition serves to correlate the clastic rocks of the region under one assemblage, here termed the Gunanoot assemblage (Groundhog-Gunanoot assemblage of Eisbacher 1974). The basic pattern of facies distribution is best defined between Mount Biernes and Mount Gunanoot, where, in the centre of a doubly plunging open syncline the broadest range of vertical and lateral variations can be deduced. There, the Gunanoot assemblage coarsens upwards over 1000 m and fines laterally eastward (Fig. 3). The stratigraphic boundaries are gradational with no distinctive marker horizons.

Four basic map units were defined: channel, channel-overbank, overbank-channel and overbank facies (Fig. 2). The channel facies (Fig. 5, 6) underlies the central part of the ranges between the Nass and Skeena rivers and is the highest member exposed. The dominant unit in this facies is clean, well winnowed, sorted, cliff-forming pebble conglomerate 1-10 m thick, with well rounded siliceous clasts that average 1 cm diameter (10 cm maximum). The conglomerates grade in and out of sandstones that include massive, dune rippled, ripple laminated, plane laminated and crossbedded units. Crossbedding is well developed with some foresets as much as 3 m high. Carbonized sticks and logs are widespread. Interbedded with the conglomerate-sandstone assemblage are fine sandstone, siltstone, shale and marl, all variably carbonaceous that represent overbank facies. Within the channel facies, these finer grained facies are widespread, but are distinctly lens shaped. They were probably once much more extensive than at present and have been reduced in significance by lateral erosion during deposition of the conglomeratic members. The areal extent of this conglomeratic channel facies is poorly defined. It appears to thin eastwards, where it interfingers with and is replaced by finer grained depositional

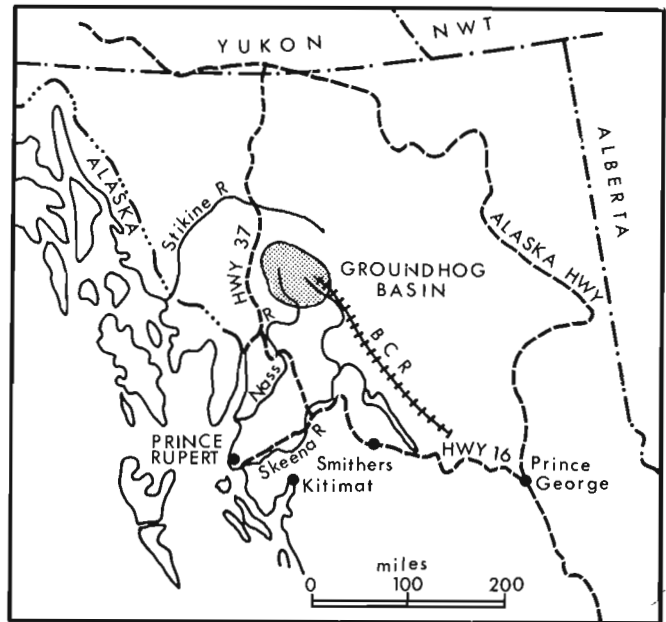


Figure 1. Location of Groundhog coal area.

assemblages. To the west, the pattern is obscured by faults, but a great abundance of conglomerate within the upper Nass Valley suggests it may have been laterally more extensive in that direction.

The overbank facies (Fig. 7) is located mainly in the western part of the area and is thought to be low in the section. It includes chert-acid volcanic-quartz pebble conglomerate and sandstone of the channel facies but is dominated by members that typify a regime of low energy deposition. Characteristic are interbedded brown marls (to 1 m), carbonaceous, plane laminated ripple laminated and massive siltstone and shale. Thin bedded (to 1 m), buff weathering festoon crossbedded, crevasse-splay type sandstone are common. Plant remains are abundant, and in most of the members they are preserved in situ with rootlets common. The subdued topography underlain by this facies reflects the recessive nature of the unit.

The two intermediate map units, the channel-overbank and overbank-channel are transitional between the above extremes and are defined by the relative proportions of coarse to fine clastics. The areal extent of these units is unknown, but appears to be very large. They occur west of the Nass Valley and extend north of the area investigated.

In places marl members comprise up to 20% of the Gunanoot assemblage. These appear to have formed in regions of very low-lying, calcareous bogs characterized by few plant remains. The strong calcareous composition of these bogs was likely a retardant to extensive plant development and may have diminished the coal potential.

Structure

Folding and related faulting are the dominant types of deformation (Fig. 4). The region is a rectilinear block defined by the northwest trending parallel valleys of the Skeena and Nass Rivers and by the major east-west valley of Panorama and Currier creeks, each of which is interpreted as being fault controlled. The Nass valley appears to be a graben-like structure within which the upper channel facies is preserved. Major faults within the block are defined by west-northwest trending valleys across which sedimentary facies change abruptly. Folding is controlled by relative rock competency

¹ Present address: Box 44, R.R. No. 1, Kispiox Valley, Hazelton, B.C.

² Ministry of Energy, Mines and Petroleum Resources, Victoria, B.C. V8V 1X4

LEGEND

Deposition facies
% conglomerate

- channel (>50)
- channel-overbank (30-50)
- overbank-channel (10-30)
- overbank (<10)

- fault
- crossbeds
- traverses



Figure 2
Depositional facies within the Gunanoot assemblage.

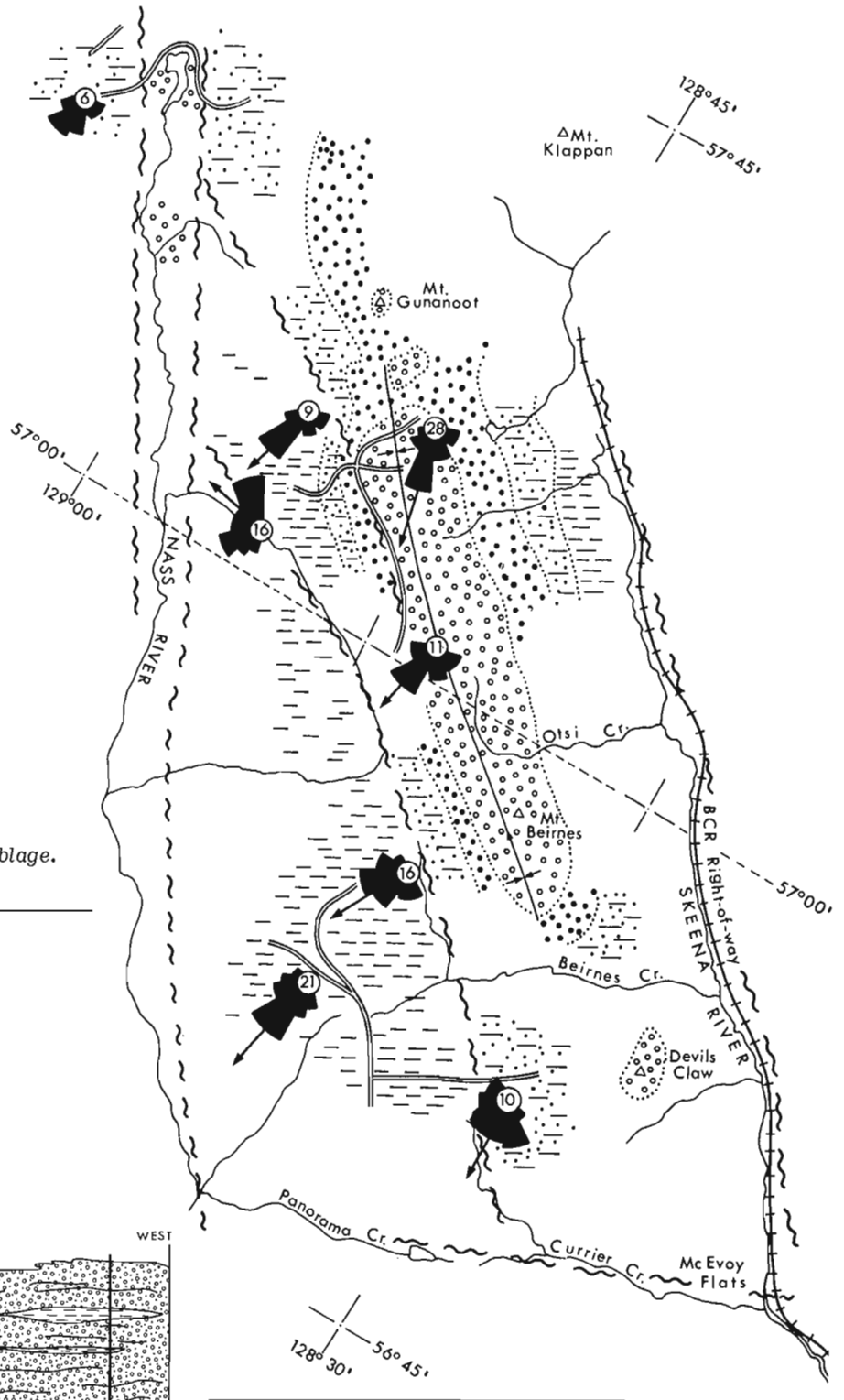
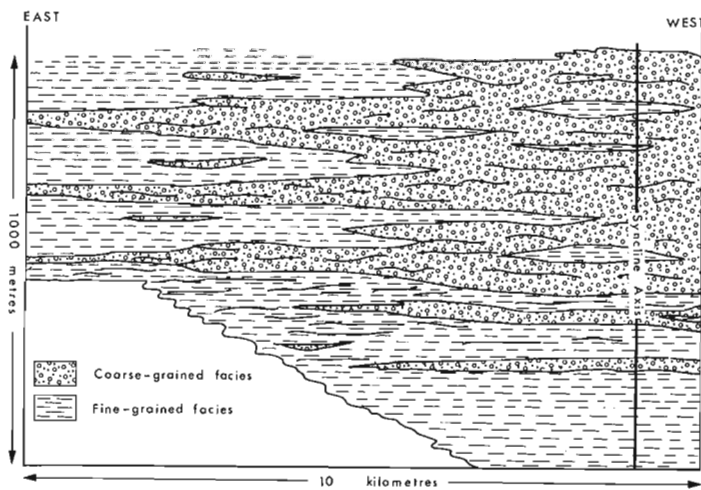


Figure 3
Generalized cross-section along line A-A' of Figure 4 showing the upward coarsening and lateral fining of the Gunanoot assemblage within and east of the Beirnes syncline.



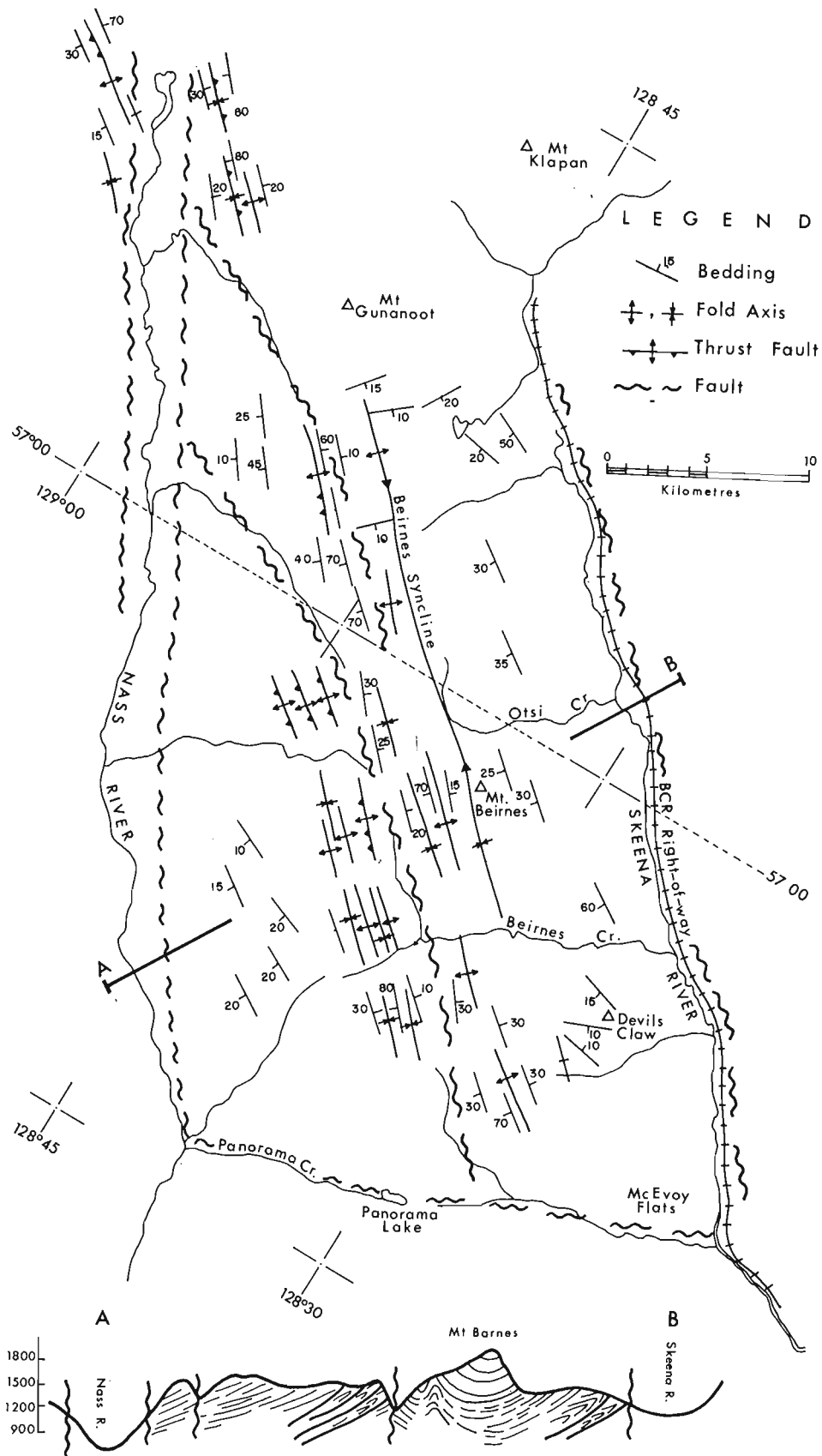


Figure 4. Structural elements of the Gunanoot-Groundhog area.

and proximity to fault boundaries. The most striking structure is the Beirnes syncline. It is a doubly plunging open, northwest trending syncline whose openness is controlled by the large percentage of conglomerate and sandstone that define it. Westward from the syncline, and near the fault valleys, the folds tighten as clast size decreases and, in the dominantly overbank assemblage to the southwest, form numerous, tight, easterly-verging low to moderate angle overthrust anticlines. In this region the zone of tight folding extends over a width of 5 km from the edge of the fault valley and to the west diminishes in intensity until the terrain is underlain by gently west dipping strata.

Most minor folds show easterly vergence. An exception is in the region flanking Nass Lake, where the vergence east of the lake is westerly and west of the lake is easterly. These folds are thought to reflect the influence of basement tectonics and are of local nature rather than reflecting some major stress from the west.

Age and Correlation

The rocks of the Gunanoot assemblage are exposed in the central part of the Bowser Basin. They are fluvialite and contain Kootenay-Blairmore floral assemblages that suggest an Upper Jurassic-Lower Cretaceous age. The conglomerate clast composition of chert, acid volcanics and quartz is markedly different from the Middle to Upper Jurassic Bowser Lake Group, which in the vicinity to the east and south comprises entirely highly varied volcanic debris. The Gunanoot assemblage must lie above the Bowser, because where seen the Bowser Lake Group rests conformably on the Hazelton Group of Lower and Middle Jurassic age. The top of the Bowser Lake Group is Kimmeridgian or younger. It is similar to the Lower and mid-Cretaceous Skeena Group in composition but lacks white mica that defines that group, although biotite is present and some (rare) pale green "phengitic" mica was noted. The base of the Skeena Group appears to be Lower Cretaceous (Hauterivian) in the Hazelton area to the south. The best guess for correlation of the Gunanoot assemblage is that it represents a separate tectono-stratigraphic assemblage between the Bowser Lake Group and the Skeena Group with strong similarities with the latter.

Discussion

The work done was of a regional reconnaissance nature, and thus few coal seams were noted. This is partly because coal, being the most recessive of all members, is the most likely to be



Figure 5.
 Unnamed 7478' mountain 15 km southeast of Nass Lake, as seen from the west. The upper 300 m consists of the channel facies.



Figure 6.
 Upper 3000 m of the mountain shown in Figure 5. Resistant light members of the channel facies are composed of pebble conglomerate and sandstone. Dark members are the overbank facies.



Figure 7.
 Dark recessive weathered overbank facies west of Beirnes Creek.

unexposed. The coaly units are most prevalent in the finer-grained facies. The full areal extent of these rocks is large but unknown. The presence of the Gunanoot assemblage west of the Nass valley implies a very extensive potential terrane for future reconnaissance prospecting.

Much of the area is dominated by tight folding that diminishes coal production potential. These areas are fault block boundaries. Areas removed from these boundaries are generally dominated by a more homoclinal structure, some of which are gently dipping. Small scale offsets in the order of 5 to 20 m are numerous.

Reference

Eisbacher, G.H.
 1974: Deltaic sedimentation in the northeastern Bowser Basin, British Columbia; Geological Survey of Canada, Paper 73-33.

BIOSTRATIGRAPHIC SIGNIFICANCE OF A LOWER CAMBRIAN TRILOBITE IN THE HAZEN FORMATION, JUDGE DALY PROMONTORY, ELLESMERE ISLAND

Ulrich Mayr
Institute of Sedimentary and Petroleum Geology, Calgary
C.D.S. de Vries
Department of Geology, University of Calgary, Calgary

During the summer of 1973 members of a field party of Sproule Associates Ltd., Calgary, headed by Mayr, found a trilobite of Early Cambrian age in scree of rocks mapped as Archer Fiord Terrane (Christie, 1964) or Ellesmere Group (Christie, 1974). The location is on Judge Daly Promontory, Ellesmere Island, at longitude 81°23.3'N and latitude 66°21.7'W (Fig. 1), about 1 km northwest of a small lake. The specimen (Fig. 2) is now part of the collection which Sproule Associates Ltd. donated to the Paleontological Collections (catalogue number 10958) at the University of Alberta and was recently reidentified by W.H. Fritz, Geological Survey of Canada. D.R. Dolphin of Norcen Energy Resources Limited, Calgary, kindly gave permission for re-examination of the specimen by the Geological Survey of Canada. W.H. Fritz states that the trilobite may belong to the genus *Wanneria* and thus indicate the medial part of the *Bonnia-Olenellus* Zone in the upper part of the Lower Cambrian.

The mapping in 1973 showed that the Archer Fiord Terrane consisted of two formations, the Grant Land Formation (Trettin, 1971) and an unnamed overlying formation of laminated, argillaceous lime-mudstone with intraformational conglomerate in the lower part. The unnamed formation overlies the Grant Land Formation with gradational contact and the top of the Grant Land Formation was drawn at the base of the first significant limestone with intraformational conglomerate. The trilobite was found on bedrock mapped as Grant Land Formation and thus included in that formation. Recent work by the Geological Survey of Canada (Trettin et al., 1979, this volume) revealed that the unnamed formation is a facies of the Hazen Formation (Trettin, 1971, 1976) and that the upper boundary of Grant Land Formation should be drawn below the first carbonate. That boundary is more than 500 m below the one mapped in 1973 and thus the trilobite, set in a Hazen limestone matrix, belongs in the lower part of that formation.

The Hazen Formation is highly diachronous and poorly fossiliferous, and the Early Cambrian age of the lower part of the formation at Ella Bay (Trettin et al., 1979) is

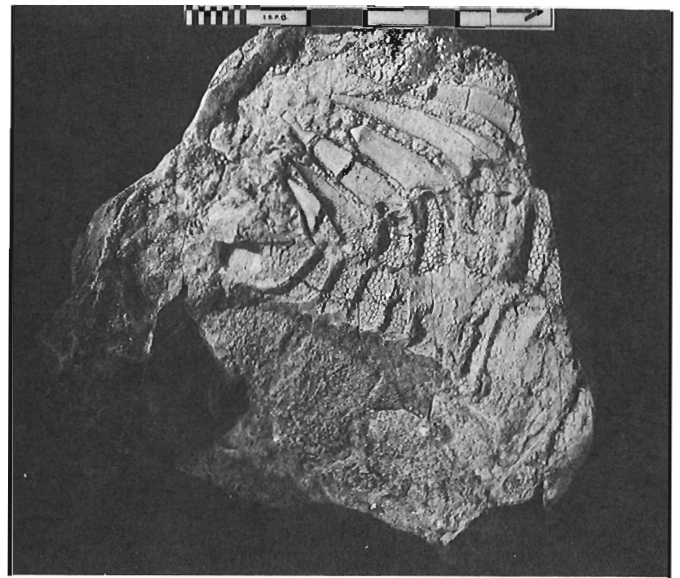


Figure 2. Posterior part of *Wanneria?* sp.
Scale in centimetres. ISPG 1223-1

corroborated by the 1973 specimen and extended northeastward along structural strike for almost the whole length of Judge Daly Promontory. A rapid increase in thickness of the Hazen Formation is also apparent. Trettin et al. (1979) reported a thickness of about 600 m from Ella Bay; the 1973 field observations at an unnamed glacier (81°15.5'N, 68°00'W) about 35 km northeast of the Ella Bay location (Fig. 1) and subsequent photogrammetric measurements at that locality by Sproule Associates Ltd., indicate a thickness in the order of 2000 m. At the 1973 locality the Hazen Formation is overlain by rocks assigned to the Copes Bay Formation. The thickness increase reflects the transition from starved basin sediments in the northwest to platform sediments in the southeast part of Judge Daly Promontory.

References

Christie, R.L.
1964: Geological reconnaissance of northeastern Ellesmere Island, District of Franklin; Geological Survey of Canada, Memoir 331.
1974: Northeastern Ellesmere Island: Lake Hazen region and Judge Daly Promontory; in Report of Activities, Part A, Geological Survey of Canada, Paper 74-1A, p. 297-299.

Trettin, H.P.
1971: Geology of lower Paleozoic formations, Hazen Plateau and southern Grant Land Mountains, Ellesmere Island, Arctic Archipelago; Geological Survey of Canada, Bulletin 203.
1976: Reconnaissance of lower Paleozoic geology, Agassiz Ice Cap to Yelverton Bay, northern Ellesmere Island; in Report of Activities, Part A, Geological Survey of Canada, Paper 76-1A, p. 431-444.

Trettin, H.P., Barnes, C.R., Kerr, J.Wm., Norford, B.S., Pedder, A.E.H., Riva, J., Tipnis, R.S., and Uyeno, T.T.
1979: Progress in lower Paleozoic stratigraphy, northern Ellesmere Island; in Current Research, Part B, Geological Survey of Canada, Paper 79-1B, report 31.

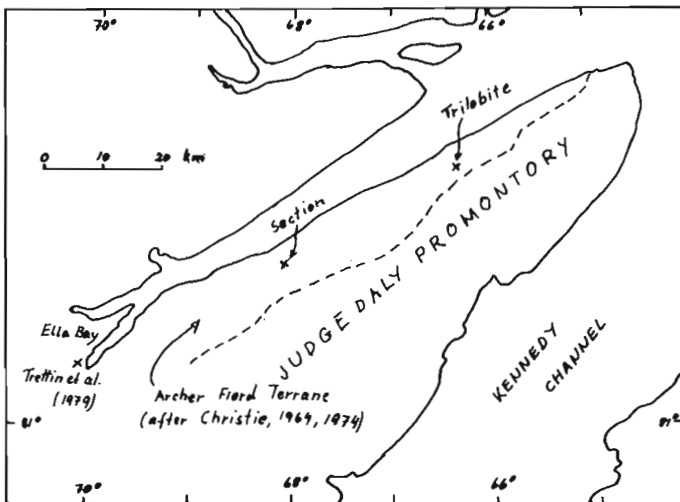


Figure 1. Index map of Judge Daly Promontory.

From: *Scientific and Technical Notes in Current Research, Part B; Geol. Surv. Can., Paper 79-1B.*

**NOTE ON A RADIOACTIVE BARITE SINTER,
BONNET PLUME MAP AREA, DISTRICT OF MACKENZIE**

Project 770044

M.P. Cecile
Institute of Sedimentary and Petroleum Geology, Calgary
L.D. Jones
Regional and Economic Geology Division

Hot and cold springs flowing from subsurface bedrock fractures are common in the North American Cordillera. These springs commonly deposit a calcareous tufa or siliceous sinter around their surface vents. In the Bonnet Plume map area (106B), however, cold springs are presently depositing barite. This is a unique occurrence and an excellent "geochemical lab" for understanding the origin of many sedimentary barites and perhaps their associated base metal deposits, common to Paleozoic rocks in the same area (Dawson, 1977 and Cecile, 1978). In addition, the barite sinter was found to be anomalously radioactive. Fist-size hand specimens give 3 to 4 times background readings on a total count scintillometer.

The springs are located at 64°18'N and 130°14'W. The sinter is very porous, grey or yellow-grey, fine grained barite. Two samples were collected, one from the edge of an active spring (39-1) and the other several metres away (39-3). In the summer of 1977, the sinter springs were expelling small quantities of water and gas. The water was clear and there was a rotten H₂S odour in the air that may have come from the gas or from the surrounding swamp. The sinter deposits cover a minimum area of 50 by 100 m, are at least 1 m thick and were deposited discordantly on a Lower to Middle Devonian dark grey, crinoidal limestone. No attempt was made to estimate the actual limits of the sinter deposits or to locate other springs in the same valley, which is mostly covered in wet tundra.

Radioactivity in the samples is due to high concentration of radium substituting for barium in the barite structure. Analysis for radium by radon emanometry (GSC, Ottawa) gave the following results. Solution of 1 g of samples 39-1 and 39-3 in a mix of nitric and hydrochloric acid gave values of 112 pCi of radium per gram (pCi Ra/g) and 79 pCi Ra/g, respectively. Solution of 1 g of samples 39-1 and 39-3 in an HF - HNO₃ mix gave 105 and 59 pCi Ra/g, respectively. Not all the sample was dissolved by the acid suggesting these are minimum radium values. Assuming 4 ppm U to be the clark of U, then the clark of radium is about 12 pCi Ra/g. Neutron activation analysis (Atomic Energy of Canada, Ottawa) gives low uranium values of <0.2 ppm (39-1) and 0.5 ppm (39-3). Gamma ray spectrometer analysis (G. Cameron, GSC, Ottawa) indicates low potassium and average thorium values (Th = 38 ppm (39-1) and 27 ppm (39-3)).

Further research is planned for the 1979 field season and will include water and gas sampling for chemical analysis, search for more springs and other mineral phases, and determination of sulphur isotope values.

References

Cecile, M.P.
1978: Report on Road River stratigraphy and the Misty Creek embayment, Bonnet Plume (106B) and surrounding map-areas, N.W.T.; in *Current Research, Part A*, Geological Survey of Canada, Paper 78-1A, p. 371-377.
Dawson, K.M.
1977: Regional metallogeny of the northern Cordillera; in *Report of Activities, Part A*, Geological Survey of Canada, Paper 77-1A, p. 1-4.

**THEORETICAL ASPECTS OF ALPHA COEFFICIENTS
USED IN X-RAY FLUORESCENCE ANALYSIS**

Gerald R. Lachance
Central Laboratories and Administrative Services Division

The comprehensive study of fundamental alpha coefficients (Lachance, 1970), held in abeyance in favour of work having a higher priority, was resumed during 1978-79. The purpose of the study is to search for systematic relations between the magnitude and algebraic sign of alpha coefficients (which many consider to be empirical) and basic X-ray theory. A joint paper is in preparation (with Prof. Fernand Claisse, Université Laval, as co-author) where it will be shown that α_{ij} in the equation

$$W_i = R_i (1 + W_j a_{ij} + \dots + W_j W_k a_{ijk})$$

is a function of

- + $W_m (\alpha_{imj} + W_m^2 \alpha_{immj})$ where
- i = analyte element
- j = matrix element, absorption or enhancement
- W = weight fraction
- R = relative intensity to pure i
- m = matrix elements j, k, . . .
- a_{ijk} = a "crossed effect" coefficient

When the interelement effect involves absorption only, the crossed coefficients are always negligible; when absorption-weak enhancement is involved, they are often negligible but they are necessary in cases of absorption-strong enhancement. All coefficients can be obtained from basic theoretical equations. Depending on specific analytical requirements, the algorithm can be used to predict when the simpler alpha models in current use are adequate.

A second paper is in preparation in which it will be shown that alpha coefficients involving absorption or absorption-weak enhancement are related (at the limit $W_i=0.0; W_1=1.0$) thus:

$$a_{ik} = (a_{ij} + 1) \left(\frac{Z_k}{Z_j} \right)^n - 1$$

where Z=atomic number
n = exponent ≈ 2.6

provided the wavelengths of the Kedge for j, k . . . are longer than the Kedge of analyte i. Similar restrictions hold for L lines - L edges, i.e. the algorithm is applicable between discontinuities except for the 5 or 6 elements having the strongest enhancement on the analyte. This α -Z relation is to be expected if one considers not the preferred power law expression to calculate mass-absorption coefficients $\mu = C \lambda^\alpha$, but the seldom used expression $\mu = C' Z^b$ (for a given wavelength). Even if not strictly quantitative, the relation has two practical implications. In cases where experimental coefficients are used, it may be preferable to proceed from one reliable alpha coefficient rather than prepare a series of alloys (of the same analyte) should that present metallurgical problems. Secondly for Z=1, whatever the analyte, the coefficients "predicted" are ≈ -0.99. It therefore follows that besides being internally concordant, tables of alpha coefficients should not contain values less than -1.0. By the same token, since α coefficient = A-1, A coefficients should not be negative.

Reference

Lachance, Gerald R.
1970: Fundamental coefficients for X-ray spectrochemical analysis; Canadian spectroscopy; v. 15, p. 64.

*From: Scientific and Technical Notes
in Current Research, Part B;
Geol. Surv. Can., Paper 79-1B.*

AN IMPROVED METHOD FOR TOTAL CARBON AND TOTAL WATER DETERMINATION IN ROCKS

J.-L. Bouvier and Sydney Abbey
Central Laboratories and Administrative Services Division

Development of a new method for these constituents (Abbey and others, 1978) awaited acquisition of a three-channel digital integrator. That apparatus was acquired late in 1978 and the new method introduced in regular analysis after a brief testing program. The procedure involves mixing the rock sample with vanadium pentoxide in a "home-made" nickel boat and heating the mixture in a stream of oxygen in a small resistance-heated tube furnace. The effluent is passed through an infrared-absorption instrument, designed to measure water content in industrial process streams. After passing through that instrument, the stream is stripped of its water vapor by a drying agent and is passed through a second infrared device, designed to measure carbon dioxide. The output signals of both infrared instruments go to the integrator which reads out integrated absorbance for both constituents. Calibrations are based on pure water and on pure barium carbonate. The output of results per man-year is of the order of three times that of existing systems, with no apparent loss in accuracy.

The third channel in the integrator is reserved for possible simultaneous determination of sulphur and a third infrared-absorption instrument has been ordered for that purpose. Even if satisfactory operating parameters cannot be found for the simultaneous determination of all three constituents, a separate determination of sulphur on these principles would be more rapid than the present chemical method and more reliable than the results now produced as part of the general X-ray fluorescence system.

Also to be investigated is a different procedure (using the same measuring technique) for separate determination of carbonate carbon dioxide, and hence noncarbonate carbon by difference. That could be achieved by merely attaching an acid-evolution train to the carbon infrared instrument, but there would then be no advantage in speed over the earlier

method (Bouvier et al., 1972). An alternative might involve use of an inert carrier gas instead of oxygen (Turek et al., 1978).

At least four other papers related to this work have appeared within the past year (Hughes and Hannaker, 1978; Din and Jones, 1978; Terashima, 1978; Turek et al., 1978). All involve some principles used in the method described herein, but none appears to feature simultaneous determination of carbon and water by infrared absorption nor is any of them comparable in terms of productivity.

References

Abbey, Sydney and others
1978: Development of analytical methods; in *Current Research, Part B, Geological Survey of Canada, Paper 78-1B*, p. 202.

Bouvier, J.-L., Sen Gupta, J.G., and Abbey, Sydney
1972: Use of an "automatic sulphur titrator" in rock and mineral analysis: Determination of sulphur, total carbon, carbonate and ferrous iron; *Geological Survey of Canada, Paper 72-31*.

Hughes, T.C. and Hannaker, P.
1978: The determination of carbon and hydrogen in geological materials by thermal decomposition; *Chemical Geology*, v. 22, p. 331-339.

Din, V.K. and Jones, G.B.
1978: The determination of total carbon and combined water in silicates using a C, H, N elemental analyser; *Chemical Geology*, v. 23, p. 347-352.

Terashima, S.
1978: The rapid determination of total carbon and sulfur in geological materials by combustion and infrared absorption photometry; *Analytica Chimica Acta*, v. 101, p. 25-31.

Turek, A., Riddle, Chris, and Talerico, Frank
1978: Determination of carbon dioxide in rock analysis by non-aqueous titration; *Chemical Geology*, v. 21, p. 351-357.

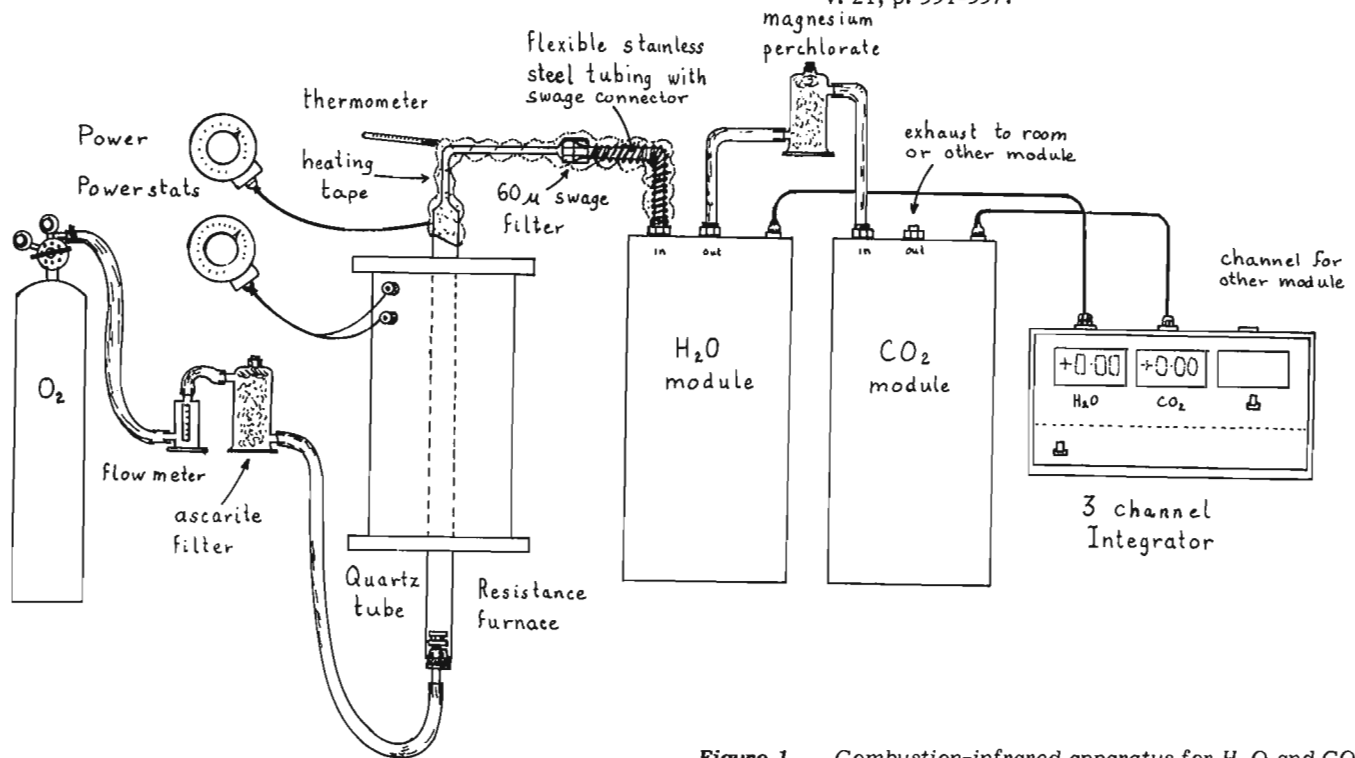


Figure 1. Combustion-infrared apparatus for H₂O and CO₂.

From: *Scientific and Technical Notes in Current Research, Part B; Geol. Surv. Can., Paper 79-1B.*

STUDIES IN REFERENCE SAMPLES OF ROCKS

Sydney Abbey and others
Central Laboratories and Administrative Services Division

Staff of the Analytical Chemistry Section are participating in the collaborative analysis of the "fourth generation" of rock reference samples distributed by the U.S. Geological Survey – a basalt, a diorite and a diabase. That involves not only "complete" analysis for all major, minor and trace constituents attainable by our regular methods, but also means working in accordance with an experimental design – two subsamples from each of three bottles of each sample, analyzed in a specified sequence.

At the suggestion of the Editor of Geostandards Newsletter, a new set of values was computed for the "USGS II" series, using the latest version of our "select laboratories" method, reported in part at Geoanalysis '78 and later published (Abbey, 1978). As a result of properties of several parameters observed in that work, a more detailed study has been undertaken on the relative merits of those parameters and others that have been suggested as measures of "best value".

Reference

Abbey, Sydney
1978: U.S.G.S. II Revisited; Geostandards Newsletter,
v. 2, p. 141-146.

THE PALEOLATITUDE AND PALEOMAGNETIC AGE
OF THE ATHABASCA FORMATION, NORTHERN
SASKATCHEWAN. DISCUSSION

M. Pagel and R.E. Openshaw
Centre de Recherches Pétrographiques et Géochimiques,
Case Officielle n° 1, 54500 – Vandoeuvre-les-Nancy, France
Manuscript received April 3, 1979

Because the paleomagnetic age of 1550 Ma (or 1700 Ma) given by Fahrig et al. (1978) for the deposition of the sediments in the Athabasca basin has important implications for the genesis of uranium deposits in Saskatchewan, we want to comment on the divergence between this age and the age of 1350 Ma found by Ramaekers and Dunn (1976) for the Athabasca Formation. We consider that the age found by Ramaekers and Dunn (1976) using Rb/Sr methods on shale horizons may only refer to a postdepositional event in the basin, most probably a diagenetic event. If, then, 1550 Ma is taken as the depositional age for the Athabasca Formation and 1350 Ma as an age of diagenesis then there is a 200 Ma time interval between the deposition and the diagenesis of the sandstones as recorded by the argillaceous fractions.

This time interval may seem to be rather long but a similar situation has been demonstrated in the Franceville basin (Gabon) where a number of detailed geochronological studies were performed because of the occurrence of natural nuclear reaction zones in the Oklo uranium deposit. An age of 1800 Ma (Bonhomme et al., 1965; Bonhomme et al., 1978) was obtained by Rb/Sr methods on illite concentrates while an age of 2000 Ma was determined for the U mineralization by U/Pb method. For the Oklo deposit, Openshaw et al. (1978) have shown that the nuclear reactions occurred after the silicification of the detritic quartz grains but before a late carbonate diagenesis. It is considered most probable that the age determined by Rb/Sr methods on the illites is related to the late carbonate diagenesis at temperatures of around 180°C. Thus, since the age of deposition for the sandstones of the Oklo deposit is at least 2000 Ma there is again a time interval of at least 200 Ma between the age of deposition and the age of the diagenetic event recorded by the argillaceous fractions.

There is a possible problem in the interpretation of the paleomagnetic data because of the uncertainty of the genesis of the hematite. Fahrig et al. (1978) consider that the dominant carrier of magnetization is hematite and note that "there is no petrographic evidence of deep burial with heating and remagnetization of the Athabasca" (p. 3). However, Pagel (1975) in a study of fluid inclusions in quartz overgrowths on detrital quartz grains, has demonstrated that the sandstones have been subjected to a deep regional diagenesis with temperatures attaining 220°C at the bottom of the Athabasca sandstones in the Carswell area and that, at that time, the overburden was three times as thick as the present maximum cover of 1525 m. In this study it was also shown that in some cases secondary hematite may have formed during silicification of the sandstones. Hoeve and Sibbald (1978) similarly concluded that the hematite in the Athabasca Formation is possibly secondary.

With respect to the relatively high temperature found by the fluid inclusions study it is noted that in the study of the Oklo deposit (Gabon) temperatures of $240 \pm 20^\circ\text{C}$ were found. These temperatures are in good agreement with those derived from studies of the crystallinity of illite and also with those derived from a study of the isotope ratios $^{176}\text{Lu}/^{175}\text{Lu}$ and $^{156}\text{Gd}/^{155}\text{Gd}$ by Hageman (1978) who found a temperature of $280 \pm 20^\circ\text{C}$.

In conclusion, we consider that the results of Fahrig et al. (1978), while indicating an earlier age for the deposition of the Athabasca Formation than that suggested by Ramaekers and Dunn (1976), are consistent with their results. The new data of Fahrig et al. (1978) reinforce the hypothesis that even if some preconcentration occurred during the weathering of the basement rocks and the subsequent sedimentation, the economic uranium mineralization in the Athabasca basin which has been dated by U/Pb methods at 1250 to 1000 Ma is related to postdepositional events in the Athabasca Formation.

References

- Bonhomme, M., Weber, F., et Favre-Mercuret, R.
1965: Age par la méthode rubidium-strontium des sédiments du bassin de Franceville (République Gabonaise); Bulletin du Service de la carte géologique d'Alsace et de Lorraine, t. 18, Fasc. 4, p. 243.
- Bonhomme, M., Leclerc, J., et Weber, F.
1978: Etude radio-chronologique complémentaire de la série du Francevillien et de son environnement; in Les réacteurs de fission naturels, A.I.E.A., Vienne 1978, p. 19-24.
- Fahrig, W.F., Christie, K.W., and Freda, G.
1978: The paleolatitude and paleomagnetic age of the Athabasca Formation, northern Saskatchewan; in Current Research, Part C, Geological Survey of Canada, Paper 78-1C, p. 1-6.
- Hageman, R.
1978: Isotopic studies relative to the Oklo natural fission reactors; in U.S. Geological Survey Open File Report 78-701, p. 157-158.
- Hoeve, J. and Sibbald, T.I.I.
1978: Uranium concentration related to the Sub-Athabasca unconformity, Northern Saskatchewan, Canada; in Short course in uranium deposits: their mineralogy and origin, editor M. Kimberley, p. 485-499.
- Openshaw, R.E., Pagel, M., et Poty, B.
1978: Phases fluides contemporaines de la diagenèse des grès, des mouvements tectoniques et du fonctionnement des réacteurs nucléaires d'Oklo (Gabon); in Les réacteurs de fission naturels, AIEA, Vienne 1978, p. 267-296.
- Pagel, M.
1975a: Cadre géologique des gisements d'uranium dans la structure Carswell (Saskatchewan, Canada). "Etude des phases fluides". Thèse de spécialité, 156 p., Nancy.
1975b: Détermination des conditions physico-chimiques de la silicification diagenétique des grès Athabasca (Canada) au moyen des inclusions fluides; Académie des Sciences Compte Rendus, t. 280, sér. D, p. 2301-2304.
- Ramaekers, P.P. and Dunn, C.G.
1976: Geology and geochemistry of the eastern margin of the Athabasca basin; in Uranium in Saskatchewan, Symposium of the Saskatchewan Geological Society (abstr.).

EDITORIAL NOTE

This communication has been read in manuscript by the authors of Fahrig et al. (1978) who are grateful for the additional information.

AUTHOR INDEX

	Page		Page
Abbey, S.	417,418	Lachance, G.R.	416
Amos, C.L.	245	Lambert, R. St J.	45
Anderson, T.W.	147	Lancaster, R.D.	223
Asprey, K.W.	245	Leatherbarrow, R.W.	319
Baadsgaard, H.	45	LeCheminant, A.N.	319
Barnes, C.R.	269	Levy, E.M.	379
Béland, J.	13	Lichti-Federovich, S.	71
Bell, K.	153	Lydon, J.W.	223
Blenkinsop, J.	153	MacLean, B.	231
Bolton, T.E.	1	Maurice, Y.T.	179
Bouvier, J-L.	417	Mayr, U.	415
Britton, J.M.	153	McConnell, J.W.	329
Cecile, M.P.	416	McGregor, D.C.	189
Chamberlain, V.E.	45	Miller, A.R.	319
Charbonneau, B.W.	207	Morris, W.A.	301
Chatterton, B.D.E.	259	Morrison, M.L.	407
Christie, R.L.	253	Morton, P.	39
Clague, J.J.	63	Norford, B.S.	269
Coker, W.B.	199	Openshaw, R.E.	419
Conaway, J.G.	27	Overton, A.	397
Dale, C.T.	357	Pagel, M.	419
Davidson, A.	153	Pedder, A.E.H.	269
de Vries, C.D.S.	415	Picklyk, D.D.	401
DiLabio, R.N.W.	199	Plant, A.G.	179
Dixon, J.	223	Raudsepp, M.	341
Dyke, A.S.	307,385	Richards, T.A.	411
Egginton, P.A.	349	Rimsaite, J.	281
Ermanovics, I.	341	Riva, J.	269
Falconer, R.K.H.	231	Shilts, W.W.	395
Ford, K.L.	207	Sinclair, A.J.	173
Fritz, W.H.	99,121	Sinha, A.K.	23
Gale, N.H.	45	Smee, B.W.	137
Gauthier, R.C.	371	Struik, L.C.	33
Gibson, H.L.	111	Tipnis, R.S.	259,269
Gilchrist, R.D.	411	Tozer, E.T.	127
Greenwood, H.J.	365	Trettin, H.P.	269
Haworth, R.T.	357	Uyeno, T.T.	269
Hill, J.	83	Vennant, G.	13
Hofmann, H.J.	83	Vincent, J-S.	301
Jones, L.D.	416	Wahlgren, R.V.	51
Karkkainen, P.	223	Watkinson, D.H.	111
Kaszycki, C.A.	395		
Kerr, J.W.	269		
Kerswill, J.A.	329		
King, A.F.	83		
Kirkham, R.V.	17		
Koop, D.J.	137		

